DEVELOPMENT OF AN INNOVATIVE EARTHQUAKE-RESILIENT REINFORCED CONCRETE CORE WALL SYSTEM

by

LISA TOBBER

B.A.Sc., The University of British Columbia, 2012

A DISSERTATION SUBMITTED IN PARTIAL FULFILLMENT OF

THE REQUIREMENTS FOR THE DEGREE OF

DOCTOR OF PHILOSOPHY

in

THE FACULTY OF GRADUATE AND POSTDOCTORAL STUDIES

(Civil Engineering)

THE UNIVERSITY OF BRITISH COLUMBIA

(Vancouver)

June 2021

The following individuals certify that they have read, and recommend to the Faculty of Graduate and Postdoctoral Studies for acceptance, the thesis entitled:

DEVELOPMENT OF AN INNOVATIVE EARTHQUAKE-RESILIENT REINFORCED CONCRETE CORE WALL SYSTEM

submitted by	Lisa Tobber	in partial fulfillment of the requirements for
the degree of	Doctor of philosophy	
in	Civil Engineering	

Examining Committee:

Tony T.Y. Yang, Professor, Department of Civil Engineering, UBC

Supervisor

Perry Adebar, Professor, Department of Civil Engineering, UBC

Supervisory Committee Member

Geoffrey Rodgers, Professor, College of Engineering, University of Canterbury

Supervisory Committee Member

Don Anderson, Professor Emeritus, Department of Civil Engineering, UBC

University examiner

Frank Lam, Professor, Department of Forestry, UBC

University examiner

Abstract

This thesis introduces an earthquake-resilient reinforced concrete core wall system, named the controlled rocking outrigger core wall (CROCW). In the CROCW system, along one principal axis is a controlled outriggered rocking wall (CORW), where an outrigger is situated at the roof and the base is designed to rock. Dampers are incorporated within the outrigger and the rocking base to give CORW added energy dissipation. Along the other principal axis is the self-centering coupled wall (SCCW). In the SCCW system, self-centering friction dampers are incorporated within the coupling beams to dissipate the earthquake energy and ensure the wall will self center. In addition, the base is design to rock, to ensure a low damage response.

The CROCW, CORW and SCCW were designed using the novel equivalent energy design procedure (EEDP). New factors were developed to modify the original EEDP to account for the dynamic responses and the different hysteretic shapes for the new systems.

Using the newly developed design procedure, four prototype buildings (two different building heights and two different building sites) were designed. The uniform hazard spectra at three hazard levels were developed using probabilistic seismic hazard analysis. Detailed nonlinear models were developed and validated using available experimental data.

Nonlinear time history analysis showed the CROCW, CORW, and SCCW can meet the design objectives, where the systems have limited damage after strong earthquake shaking. Additional studies were conducted to compare the performance of the newly proposed CROCW with conventional RC core wall system. The result shows that the CROCW has superior performance compare with conventional RC core walls.

The newly developed CROCW system will be tested using a shake table to validate the behaviour. Shake table testing will take place at the multi-function shake table array facility in Shanghai China. Due to the COVID-19 pandemic, the experimental test has been temporarily delayed. This thesis presents the specimen design, construction, planned instrumentation, and the testing plan to be implemented at a later date.

Lay Summary

Rapid urbanization is creating a demand for tall building construction globally. Many of these buildings are located in high seismic zones. To improve the resiliency of high-rise buildings under earthquake loads, this thesis proposes a novel seismic force resisting system, named the controlled rocking outriggered core wall (CROCW) system. Design procedures for the CROCW have been developed and validated using detailed numerical models, and the system performance has been compared to existing tall building systems. Additionally, a large-scale testing program was developed, where a 1/6.5 scale specimen was designed and constructed. This thesis provides background study, detailed design procedure and verification of the CROCW, which engineers and other researchers can use to design CROCW in high seismic zones.

Preface

Various parts of this thesis work have been published or are under review for publication. The following summarises each publication and the specific contributions from each author.

Published contributions

I contributed significantly to the development of the Self-centring conical friction damper (SCFD) for coupled wall systems. My role in the conceptual development and organising the experimental testing program has resulted in two patents and one journal paper. In this work, H.C. Xu was responsible for conducting the experimental testing of the SCFD. T.Y. Yang contributed to the conceptual development and writing of the paper. The design of the SCFD and implementation in a new RC coupled wall system is presented in this thesis.

The following are the publications related to the SCFD:

1. T.Y. Yang, H.C. Xu, **L. Tobber**, "Development and experimental testing of innovative self-centering conical friction damper (SCFD)," Structural Control and Health Monitoring. 27(10). https://doi.org/10.1002/stc.2609
2. T.Y. Yang, H.C. Xu, **L. Tobber**. Self-centering conical friction damper. US 62/884805A1, United States Patent and Trademark Office, filed 9 August 2019.
3. T.Y. Yang, H.C. Xu, **L. Tobber**. Self-centering conical friction damper. PCT/CA2020/051092, Canadian receiving office, filed 7 August 2020.

I led the development of a large-scale testing program, which will validate two new structural systems presented in this thesis.

This experimental testing program has been described in the following conference papers:

4. T. Y. Yang, **L. Tobber**, H.C. Xu, 2019, "Large-scale shake table testing of high-performance earthquake-resilient tall building", Proceedings of the 2019 Pacific Conference in Earthquake Engineering, New Zealand Society for Earthquake Engineering, Auckland, NZ
5. **L. Tobber**, T. Y. Yang, P. Adebar, 2018, "Development of High-Performance Earthquake Resilient Tall Buildings", Proceedings of the 11th National Conference in Earthquake Engineering, Earthquake Engineering Research Institute, Victoria, CA, USA

In these conference papers, I was the lead investigator, responsible for all major conceptual development, design, and writing. T.Y. Yang contributed to conceptual development, design, and paper edits. H.C. Xu contributed to some detailed component design calculations and drawings. P. Adebar contributed to the initial conceptual development.

Under review contributions

I was also lead investigator in four recently submitted journal papers which cover four main contributions in this thesis. In these papers, I was responsible for developing the design procedures, numerical models, and analysis of the results of the novel Controlled rocking outriggered core wall (CROCW), Controlled Outriggered Rocking Wall (CORW), and Seismic Design of Self-centering coupled wall (SCCW) systems presented in this thesis. In these papers, T.Y. Yang contributed to conceptual development and writing of the papers. H. Xu and M.A. Sadeghi contributed to some initial concept development, preparing graphs, and conducting edits.

The following show the journal publications currently under review:

6. **L. Tobber** and T. Y. Yang, "Seismic Design of Controlled Outriggered Rocking Wall (CORW) using EEDP." (Under review)
7. **L. Tobber,** T.Y. Yang, H. Xu, and M.A. Sadeghi "Seismic Design of Self-centering coupled wall (SCCW) using EEDP." (Under review)
8. **L. Tobber** and T. Y. Yang, "Bidirectional design of earthquake resilient core wall." (Under review)
9. **L. Tobber** and T. Y. Yang, "Comparison of RC core wall systems integrating new technology to increase seismic performance." (Under review)

Table of Contents

List of Tables

List of Figures

List of Abbreviations

ACI = American concrete institute

AISC = American institute of steel construction

ASCE = American society of civil engineers

ASTM = American society for testing and materials

BRB = Buckling restrained brace

CORW = Controlled rocking outriggered wall

CP = Collapse prevention

CQC = complete quadratic combination

CROCW = Controlled rocking outriggered core wall

CRW = Controlled rocking wall

CSA = Canadian standards association

CTBUH = Council of tall Buildings and urban habitat

CW = Coupled wall

DAS = Degree of axial stiffness

DBE = Design base earthquake

DCW = Damped coupled wall

DOC = Degree of coupling

EEDP = Equivalent energy-based design procedure

ELSDOF = Equivalent linear single degree-of-freedom

ENLSDOF = Equivalent nonlinear single-degree-of-freedom

EPP = Elastic perfectly plastic

FEMA = Federal emergency management administration

IO = Immediate occupancy

ISDR = Inter-story drift ratio

LDA = Linear dynamic analysis

LED = Lead extrusion dampers

LTHA = Linear time history analysis

MCE = Maximum considered earthquake

MDOF = Multi degree of freedom

MPC = Multi point constraint

MRSA = Modal response spectrum analysis

NBCC = National building code of Canada

NLTHA = Nonlinear time history analysis

OW = Outriggered wall

PEER = Pacific earthquake engineering research

PGA = Peak ground acceleration

PRESSS = Precast seismic structural system

PreWEC = Precast wall with End Columns

PSHA = Probabilistic seismic hazard analysis

PSW = Plastic hinge supported wall

PT = Post-tensioned

PVC = Polyvinyl chloride plastic

RC = Reinforced concrete

RDR = Roof drift ratio

RR = Rapid return

RSFJ = Resilient slip friction joint

SA = Spectral acceleration

SCCW = Self centering coupled wall

SCFD = Self-centering conical friction damper

SDOF = Single degree of freedom

SFRS = Seismic force resisting system

SLE = Service level earthquake

SRC = Steel reinforced concrete

SW = Shear wall

UHS = Uniform hazard spectrum

UN = United Nations

VCD = Viscoelastic coupling damper

List of Symbols

A_g = gross area of RC core wall

A_o = cross-sectional area of the exterior outrigger truss diagonals

A_c = cross-sectional area of the outrigger truss top and bottom chords

A_m = cross-sectional area of the interior outrigger truss diagonals

$A_{o,g}$ = cross-secitonal area of outrigger beam

C_n= modal particitipation of coupling beam shear force of nth mode

C_0 = factor to convert SDOF to MDOF displacements

E_c = elastic modulus of reinfroced concrete

F = base shear

F_{PR} = primary fuse system base shear

F_{SE} = secondary fuse system base shear

F_p = design base shear at the moderate hazard

$F_{p,e}$ = moderate hazard elastic base shear

F_{pt}^0 = SCFD initial post-tensioning force in the tendons

$F_{u,e}$ = high hazard elastic base shear

F_y = yield base shear

H = total building height

$I_{w,y}$ = moment of intertia of core-wall in the CORW direction

$I_{w,x}$ = moment of intertia of core-wall in the SCCW direction

K_s = system stiffness

L_{cb} = length of coupling beam

L_d = distance from edge of wall to base damper

L_f = length of wall flange

L_o = length of outrigger

L_s = span between the RC wall and the mega-column

$L_{w,y}$ = length of wall in CORW direction

$L_{w,x}$ = length of wall in SCCW direction

$M_{b,y}$ = controlled rocking yielding base moment

$M_{b,Pg}$ = overturning moment resistance provided by gravity loads

$M_{b,damp}$ = moment resistance provided by dampers

${M_t}^{dy}$ = total overturning moment from LTHA

${M_t}^{st}$ = total overturning moment from static load

M_T = base moment in “tension” wall pier in SCCW

M_C = base moment in “compression” wall pier in SCCW

M_f = base moment demand in wall piers in SCCW

$M_{T,c}$ = base moment capacity in “tension” wall pier in SCCW

$M_{C,c}$= base moment capacity in “compression” wall pier in SCCW

P_g= gravity load at wall base

P_0= SCFD initial sliding force

P_m= SCFD maximum sliding force

P_p= Coupling force in wall pier

Q = static load distribution

S_a = Spectral displacement

S_{a1} = spectral acceleration at fundemental period

S_{a2}= spectral acceleration at second mode period

S_d = spectral displacement

S_1 = shape function for first mode coupling beam shears

S_2 = shape function for second mode coupling beam shears

S_3= shape function for third mode coupling beam shears

SN = normalised shape functions for coupling beam shears

Sa_{SLE} = spectral acceleration at fundemental period for low hazard

Sa_{MH} = spectral acceleration at fundemental period for moderate hazard

Sa_{HH} = spectral acceleration at fundemental period for high hazard

$V_{P,r}$ = roof coupling beam shear

$V_{P,x}$= roof coupling beam shear at a given story x

T = fundemental structural period

$T_{n_{\alpha_f=0}}$ = fundemental period for system without outrigger

T_2 = natural period for second mode

T_3 = natural period for third mode

W = total building weight

W_{ext} = external work

W_{int} = internal work

b = system post yielding stiffness

b_c = width of outrigger column

d_o = depth of outrigger

f_o = outrigger damper force

f_b = base damper force

f_{bt} = base damper force in “tension” wall

f_{bc} = base damper force in “compression” wall

$f_{bt,min}$= minimum require base damper force in “tension” wall

$f_{bc,min}$= minimum require base damper force in “compression” wall

f_e = specimen elastic modulus scaling factor

f_l = specimen length scaling factor

f_f = specimen force scaling factor

f_M = specimen moment scaling factor

h = elevation of floor height

h_f = story height

k_o = rotational stiffness of outrigger

$k_{p,nl}$ = stiffness of nonlinear bar in coupling beam model

k_p= SCFD post-slip stiffness

k_{pt} = SCF axial stiffness of the PT tendons.

k_u = unloading stiffness of the SCFD

k_{tc}= stiffness of tension and compression only materials

f_c'= specified concrete strength

I_o = moment of inertia of outrigger beam

m = building mass

r_g = ratio between the overturning resistance from gravity($M_{b,Pg} = P_g L_w/2$)

t_f = thickness of wall flange

t_w = thickness of wall web

x_{cg} = distance from the rocking toe to the wall centroid

w = story weight

α_f = outrigger relative stiffness factor

α_c = coupled wall relative stiffness factor

β_o = force modification factor

β_x= shape factor for story shear

δ_b = deformation in base damper

δ_o = deformation in outrigger damper

γ_a = energy modification factor to relate the energy dissipated by the system under monotonic pushover as compared to the energy dissipated by dynamic load when the hazard level increases from SLE to DBE.

γ_b = energy modification factor to relate the energy dissipated by the system under monotonic pushover as compared to the energy dissipated by dynamic load when the hazard level increases from DBE to MCE.

λ_p = ratio of design DBE base shear to yield base shear ($\lambda = Fp/Fy$)

λ_x = load distribution at a given story x

μ'= friction coefficient between conical surfaces

μ= friction coefficient between the friction pad and the steel plate

μ_p = ductility the ratio of the DBE design dispalcement to the yield displacement ($\mu_p = \Delta_P/\Delta_Y$)

υ = poisson ratio

θ_b = ultimate rotation at wall base

θ_o = ultimate rotation at outrigger

θ_{pr} = plastic rotation of primary fuse system

$\theta_{critical}$ = critical angle which governs the SCFD hysteretic shape

θ_{se} = plastic rotation of secondary fuse system

Φ_s= ratio of the DBE to MCE intensity

Φ_p= ratio of the SLE to DBE intensity

Δ_p = DBE design roof displacement

Δ_u = MCE design roof displacement

$\Delta_{p,e}$ = DBE elastic roof displacement

$\Delta_{u,e}$ = MCE elastic roof displacement

Δ_y = yield roof displacement

ΔE_{E1} = incremental elastic energy from increasing intensity from SLE to DBE

ΔE_{ND1}= incremental nonlinear dynamic energy from increasing intensity from SLE to DBE

ΔE_{NM1} = monotonic nonlinear energy from increasing intensity from SLE to DBE

ΔE_{E2} = incremental elastic energy from increasing intensity from DBE to MCE

ΔE_{ND2}= incremental nonlinear dynamic energy from increasing intensity from DBE to MCE

ΔE_{NM2} = monotonic nonlinear energy from increasing intensity from DBE to MCE

Acknowledgments

There are numerous people to which I am grateful for the support throughout this incredible journey. I will forever be thankful for all the relationships formed during my graduate studies and hope to one day repay all of the support I have been given.

I want to express my sincere gratitude to my supervisor and mentor, Professor Tony Yang, for his support and guidance throughout my academic studies. Professor Yang introduced me to the world of research in the second year of my undergraduate degree. Without his support early on in my career, I would never have pursued an academic career. For this, I am eternally grateful.

I would also like to thank my supervisory committee member, Professor Perry Adebar, for his mentorship and advice throughout the development of the experimental program described in this thesis. I would particularly like to thank Professor Adebar for hours he dedicated to supporting me on the construction site. His support was vital during this time.

I am also profoundly thankful to my supervisory committee member Professor Geoffery Rodgers for his support and guidance throughout this project. I am particularly grateful for Professor Rodgers coming to China to help me there, and for his advice in the difficult decision to leave China at the onset of the Covid-19 outbreak.

Industry advice was critical to the practicality of design and construction. For this, I would like to thank Bob Neville, principal at RJC Engineers, for his invaluable guidance. I would also like to extend my appreciation to Rob Third, from George Third and Son, for his advice and generous donations in constructing the shake table specimen. Without his extreme generosity of allowing the specimen to be built on his property and providing construction support, this project would not have progressed as far as it has.

I also want to extend my gratitude to LMS reinforcing, who generously donated the reinforcing steel and placement. Their team did a fantastic job, and I am grateful for their support. I am also appreciative of Lafarge concrete for developing and donating the concrete mix. I would also like to thank Ryan Zhang, who provided construction support, carpentry, and concrete placing.

There have been several fellow graduate students who have provided instrumental support and help throughout my graduate studies. Please know that even though you are not named here, I am forever thankful for your support. I specifically want to thank Michael Fairhurst for his help with the probabilistic seismic hazard analysis provided in this thesis. I would also like to thank Henry Xu for his tireless efforts towards constructing the specimen in Canada and China. I could not have done this without you.

Last but certainly not least, I would like to thank my family. First, I would like to thank my partner Jeremy Atkinson, for his patience and support. Not only has Jeremy provided me with personal support, but his experience as a practising engineer has been a source of great technical and

practical advice. I am incredibly grateful for my children, Amelia and Levi, born during the last few years of this PhD. They accompanied me to conferences, construction sites, and to China for testing. Throughout it all, they have shown remarkable resiliency and flexibility, for which I am very proud.

To my father, James Tobber, thank you for supporting and challenging me to think critically throughout my life. Your coaching has led to my success. Additionally, I would like to thank my father for his invaluable help and support with my children, particularly during the pandemic. To my mother, thank you for teaching me to prioritise creativity in work and life. To my siblings (Ryan, Allen, Ben, Steven, and Laura), thank you so much for being a source of love, laughter, and friendship.

Dedication

I dedicate this thesis to my family: the old, the young, and the ones to come.

Chapter 1: Introduction

1.1 Background

The rapid urbanization worldwide has created significant challenges for sustainable city growth. An estimated 6.7 billion people, approximately 68% of the global population, will live in urban areas by 2050 (UN, 2019). With increased pressure for responsible use of urban land, tall buildings are a popular solution to meet high demands for housing and commercial space. Their ability to accommodate many people makes them critical to the economic, social, and cultural fabric of our growing cities.

Much of the world's high-rise construction takes place in seismically active regions. As a result, tall buildings must be designed to resist earthquake loads. One of the most prevalent seismic force-resisting systems (SFRS) in tall buildings worldwide is the reinforced concrete (RC) shear wall. In North America, RC shear walls are often integrated within a centralized core that houses elevators and stairwells, shown in Figure 1.1 (a). These RC core wall systems are advantageous due to their high strength, stiffness, and versatility for architectural expression.

RC core walls typically consist of flanged walls (shown in Figure 1.1 (b)), connected along one principal axis using diagonally reinforced coupling beams (shown in Figure 1.1 (c)). This configuration essentially consists of two distinct lateral force resisting systems along each principal axis: the coupled wall system (East-West in Figure 1.1 (b)) and the shear wall system (North-South in Figure 1.1 (b)). Depending on regional practice and layout requirement, coupled walls may be used for the SFRS along both principal axes (more common in US construction).

The use of core walls (as opposed to planar walls) as the SFRS in tall buildings is only recently gaining popularity in cities worldwide. Cities like Vancouver, Canada have been using core walls since the 1980s, but have not had a large magnitude earthquake since the 17th century. As a result, the core system remains relatively untested in the field. However, earthquake damage has been observed within planar RC walls, and it is thought that similar damage mechanisms could occur when these walls are integrated into a core.

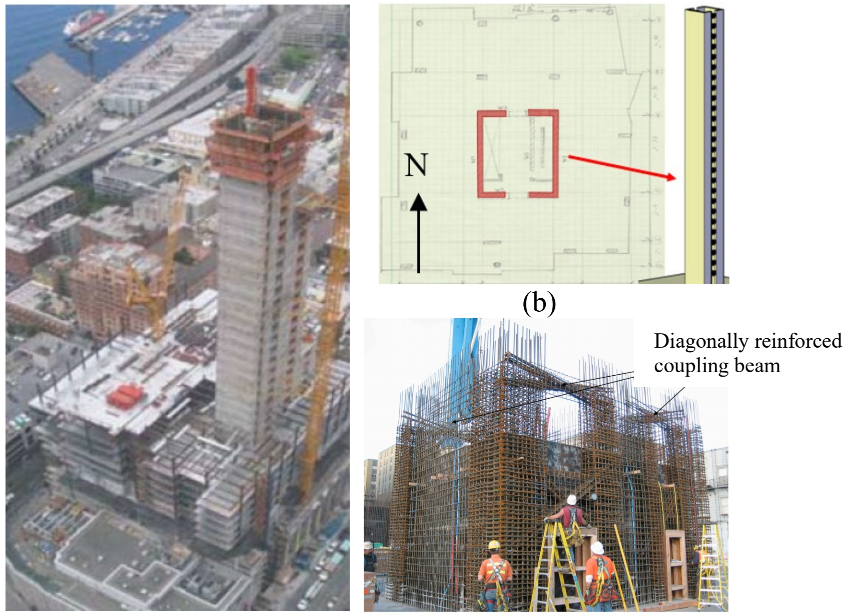

(a) (c)

Figure 1.1 Reinforced concrete core wall buildings: (a) Seattle tower (Moehle, 2007); (b) Floor layout 2-flanged wall configuration; and (c) reinforcing in RC core wall (adapted from Wallace and Naish, 2009)

Past earthquakes in Chile (February 2010) and New Zealand (February 2011) - countries that utilize modern building codes - have shown RC wall systems' adequacy to prevent collapse and achieve life-safety performance. However, in some RC wall buildings, significant damage has been observed. Specifically, earthquake damage has been observed in the RC coupling beams Figure 1.2 (a) and Figure 1.2 (c) and throughout the region near the base of the wall (shown in Figure 1.2 (a) and (b)) where axial strains are generally highest due to both gravity and overturning demands.

After the February 2011 Christchurch earthquake, numerous RC walls showed singular large cracks, and further investigation revealed that some vertical bars were fractured. Figure 1.2 (c) shows one of these walls where only one crack is observed at the far end of the wall, while Figure 1.2 (d) shows the fractured reinforcing steel within the wall. In these cases, single cracks opened and induced significant strains across a relatively short unbonded gauge length on the reinforcing steel until fracture. After the earthquake shaking, the cracks closed due to the large gravity loads, making the severity of the damage difficult to identify. Additionally, the fracturing of reinforcing steel, particularly in the critical section, is a life safety issue which will require extensive repairs or total demolition.

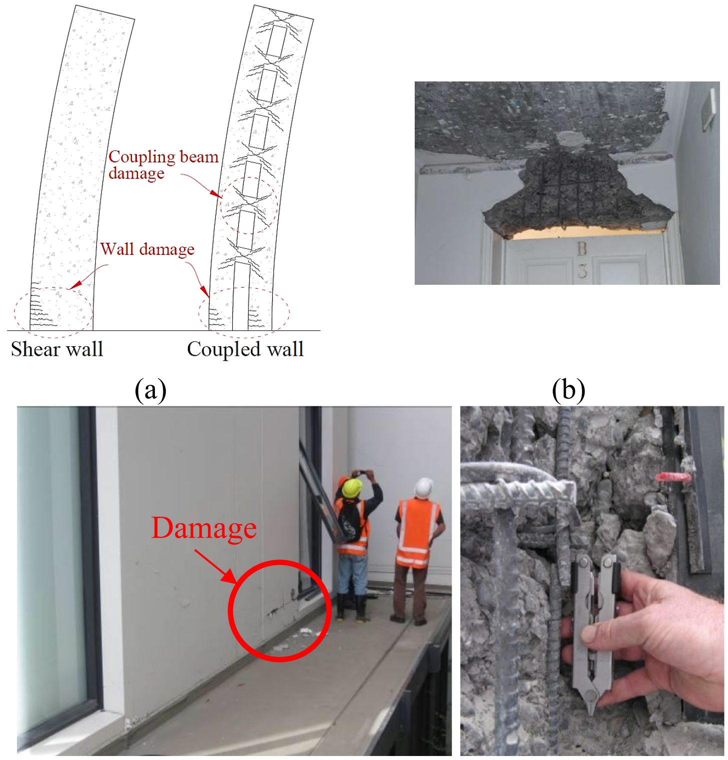

(a) (b) (c) (d)

Figure 1.2 Damage in RC wall buildings: (a) conceptual; (b) coupling beam damage from Chile, 2010 earthquake (LATBSDC, 2010); damage to tall wall Christchurch, 2011 earthquake (Buchanan et al., 2011) (d) crack at far end of wall and (d) fractured reinforcing steel

The damage exhibited in RC wall buildings may result in widespread demolition, as exemplified following the February 2011 Christchurch earthquake. The damage observed from this earthquake resulted in the demolition of over 60% of the central business district (Kim et al., 2017), an area approximately the same size as downtown Vancouver, Canada. Additionally, almost half of the total number of RC wall buildings were demolished within the central business district, despite many of the buildings meeting their design objectives (Kim et al., 2017).

The following sections describe how using innovative technology (Section 1.1.1) and improved design methods (Section 1.1.2) can increase RC core wall buildings' seismic performance and limit earthquake damage.

1.1.1 Innovative technologies

Designers may use innovative technology to enhance the performance of the RC core wall buildings. For example, damped outriggers may be used to improve performance by lowering drifts and base-moments within an RC core wall. An outrigger system consists of stiff girders or trusses that couple the RC core wall to exterior columns. An outrigger system adds rotational stiffness to the wall, reducing lateral displacements and core moment at the wall's base.

Although outriggers have been used for half a century to reduce wind displacements, they have only recently been adapted for seismic design. For example, in 2016 a 73-story building called the Wilshire Grand (Figure 1.3) was built using a large 3-story deep outrigger which incorporate Buckling Restrained Braces (BRBs). The core was extremely slender, with a height-to-width ratio of about 33. The BRBs are yielding elements which limit the force in the outrigger, protecting the core and columns from extensive damage, as well as providing energy dissipation.

(a) (b)

Figure 1.3 Wilshire Grand, Los Angeles, California: (a) building photo (LABJ,2020) and (b) outrigger concept (Photo courtesy of Prof. Geoffrey Rodgers from the University of Canterbury, NZ)

Coupling beam rotations are another important performance objective that must be met to limit damage and increase seismic performance. In situations where the typical coupling beams do not meet their performance objectives, designers may consider using damped coupling beams. Damped coupling beams utilize embedded steel beams within the RC wall and a central damper or sacrificial yielding element within the beam. The combination of using a sacrificial element to dissipate the earthquake energy can limit the damage to the RC wall, and add ductility to the coupling beam element.

Damped coupled walls are only now just beginning to be implemented around the world and applications of their use can be found in new high-rise construction projects in China. For example, the Sancai building located in Beijing, China, (Figure 1.4 (a)) is designed with coupled walls at the building perimeter. This 11-story building utilises replaceable steel links as a hysteretic damper, in lieu of RC coupling beams. China is also adapting damped coupling beams in their super-tall buildings within the core walls. For example, in Beijing, the China Zun Tower (Figure 1.4 (b)) utilizes steel fuses connected to steel embedded beams in parallel with RC coupling beams.

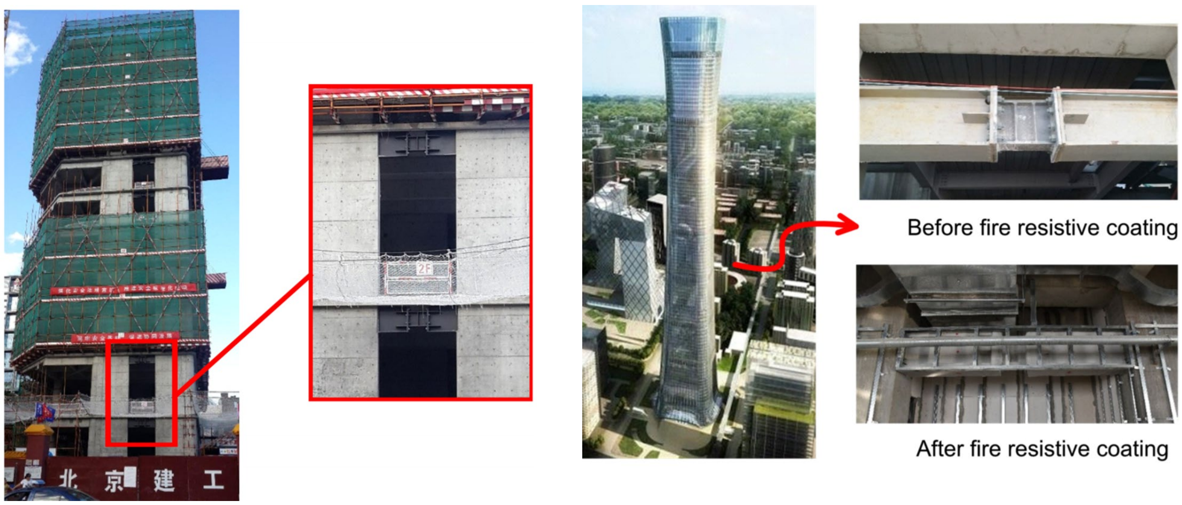

a) b)

Figure 1.4 Examples of damped coupled beam implementation: a) Sancai building adopting a hybrid coupled wall system with replaceable steel coupling beams and b) China Zun Tower (Beijing Z15 Tower) adopting replaceable steel coupling beams (Ji and Malina Hutt, 2020)

Designers can also improve performance and limit earthquake damage by reducing the vertical strains using a low-damaging wall solution, such as a controlled rocking wall. Controlled rocking is the concept of only connecting the wall vertically to the foundation with dampers. This design approach allows the wall to rock on its foundation, dissipating energy through dampers, essentially creating a damped pin at the wall's base. To the author's knowledge, controlled rocking has not been implemented in high rise RC core wall construction. However, successful implementation of these systems has been completed globally on low-rise structures.

A notable application of controlled rocking technology is the Endoscopy Consultants' Building in Christchurch, New Zealand. This low-rise building includes both controlled rocking walls and frames. The walls are coupled with U-shaped flexural plates, which are steel yielding dampers configured in a U-shape. This structure is an important example, as it survived the strong shaking and aftershocks of the February 2011 earthquakes. Figure 1.5 shows the RC walls post-earthquake. As shown, only cosmetic damage was observed on the structural elements (wall and U-dampers).

(a) (b)

Figure 1.5 Endoscopy Consultants' Building in Christchurch, New Zealand (a) wall post-earthquake and (b) U-dampers post earthquake (Buchanan et al., 2011)

Recently, new technology, such as damped outriggers, damped coupled walls, and controlled rocking walls, has been incorporated in RC wall systems to improve seismic performance. However, damped outriggers and damped coupled walls can still have damage concentrated at the wall base. Further, the controlled rocking base has not been applied to RC core walls or used in tall building applications. Therefore, there is a need for high-performance, low-damage, RC core walls for tall building applications.

1.1.2 Alternative design methods

Presently, most modern building codes use a prescriptive based design approach and do not have provisions for the latest technology developed for improving the seismic performance of RC core walls. This design approach is intended to achieve specific performance objectives, such as meeting the life-safety requirement, at a single hazard (e.g., Maximum Considered Earthquake (MCE) hazard). These design methods are based on broad classifications of building types and occupancies, and the actual performance is not assessed. As a result, the behaviour of the building after an earthquake shaking is unknown. Hence, some buildings may have higher performance than set out by the code, while others may only meet or have lower performance, even when satisfying the basic building code clauses.

The code-based design approach in Canada for normal importance buildings (i.e., typical high-rise) only considers the MCE, which corresponds to 2% probability of exceedance in 50 years, without considerations for lower hazard (more frequent) earthquakes. Since there is no requirement to check performance at different hazards, buildings may underperform - at least with regard to the general public's expectation of performance – at smaller hazards.

More recently, recognizing the issues with the code-based prescriptive design approach, some designers are adopting a performance-based design approach to understand tall buildings' seismic performance. In a performance-based design, buildings usually are required to meet strict serviceability level earthquake (SLE) requirements, in addition to the MCE required by the prescriptive design approach. While generallyit is acceptable for designers to use linear elastic analysis to design at the SLE hazard, at the MCE hazard, where inelastic action is expected, designers utilize a comprehensive nonlinear modelling approach to determine the building response. These nonlinear numerical models are peer-reviewed to ensure estimates of the response are acceptable.

A challenge with the performance-based design approach is that the building's performance is unknown until the building is designed and the nonlinear modelling is complete – the nonlinear model requires a completed preliminary design to be modelled. If the performance objectives are not met, the building must be re-designed in an iterative process. This process can be particularly problematic if the design solution is to change the geometry of structural elements when other aspects of the building design are complete (i.e., the architectural layout).

The state-of-practice to design structures to meet multiple performance objectives at different shaking intensities usually requires a nonlinear analysis performance-based design approach, which is cumbersome and involves a substantial amount of design effort and a rigorous peer-review process. To simplify this rigorous process, Yang et al. (2018) developed a simple design method called Equivalent Energy Design Procedure (EEDP). EEDP utilizes an energy-balance concept to design structures to satisfy strength and displacement limitations without iteration. Using EEDP allows engineers to design structures to achieve multiple performance objectives at different seismic hazard levels. However, the original derivation of EEDP was limited to structures that are not sensitive to higher modes and have basic elastic-perfectly-plastic hysteretic behaviour. It follows that modifications are needed to apply to RC core walls in tall buildings, which have higher mode dynamic responses.

1.2 Goals and objective

This dissertation seeks to contribute to the development of high-performance low-damage tall buildings through the creation of new technology and design methods. The overarching goals of this thesis are to develop:

1) an innovative high-performance RC core wall system which has a low-damage response under strong earthquake shaking.
2) a novel design methodology to design the proposed system for different performance objectives under different shaking intensities, in a simple non-iterative format.

These goals are accomplished through the following five objectives.

1. Conceptually develop and propose a new high-performance RC core wall system.
2. Quantify the dynamic characteristics of the new high-performance RC core wall system.
3. Develop a novel design procedure for the new high-performance RC core wall system to achieve different performance objectives at different shaking intensities.
4. Assess the seismic performance of the new high-performance RC core wall system.
5. Develop a large-scale shake table testing program which may be used to validate the behaviour of the new high-performance RC core wall system.

1.3 Methodology

In this thesis, a novel high-performance RC core wall system is proposed, named the controlled rocking outrigger core wall (CROCW) system. The CROCW system essentially consists of two unique SFRS along each principal axis. Along one principal axis is a controlled outriggered rocking wall (CORW). In the CORW system, an outrigger is situated at the roof, and the base is designed to rock. Dampers are incorporated within the outrigger and the rocking wall-base to give the system added energy dissipation. Along the other principal axis is the self-centering coupled wall (SCCW). In this system, self-centering conical friction dampers (SCFD) are incorporated within the coupling beams to dissipate energy and self-centre the wall. In addition, the base is designed to rock to ensure a low-damage response.

The novel equivalent energy design procedure (EEDP) developed by Yang et al., (2018), is modified to design the CORW and SCCW. EEDP utilizes an energy balance concept to design structures to satisfy strength and displacement limitations without iteration. Using EEDP allows engineers to design structures to achieve multiple performance objectives at different seismic hazard levels. However, the original derivation of EEDP was limited to structures which are not heavily influenced by higher modes and with basic elastic-plastic hysteretic behaviour. In this thesis, the EEDP was modified to account for these aspects and to design the CORW and SCCW.

Extensive linear and nonlinear dynamic analysis methods are used to develop and evaluate the proposed systems and design methods under earthquake loads at various hazards. The systems and design methods are thoroughly investigated using numerical modelling under both bidirectional and unidirectional earthquake shaking.

The newly developed CORW and SCCW systems will be shake table tested to validate the behaviour of these new systems. Shake table testing will take place at the Multi-function shake table array facility in Shanghai, China. This thesis provides details on the specimen design and construction, and the planned experimental programme, but not the final testing.

The outcome of this thesis is two new SFRS which can have a high-performance under different levels of shaking and new design methods so that engineers can practically implement these structural systems.

1.4 Thesis organisation

This thesis is organized into thirteen chapters with the following content.

Chapter 1: Introduction describes the background, motivation, thesis goals and objectives, methodology, and the thesis organisation.

Chapter 2: Literature review of high-performance RC wall technologies presents detailed literature review of different high performance RC wall systems and components, including energy dissipation devices (metallic yielding, friction, viscous, and viscoelastic dampers), controlled rocking walls, pin-based walls, replaceable corner walls, damped coupled walls, viscoelastic coupled walls, and outrigger systems. The merits and gaps in literature of each of these systems are presented and the need for a new high-performance RC core wall system is discussed.

Chapter 3: Mechanism and design considerations of the CROCW proposes the CORW and the SCCW as alternative systems to the RC shear wall and RC coupled wall systems, respectively.

The design objectives of the plastic mechanisms are presented in this chapter. Additionally, the unique mechanical characteristics of these systems are described, which are key in the latter chapter design and understanding of seismic response.

Chapter 4: Dynamic characteristics of proposed earthquake resilient RC core wall system presents the dynamic characteristics of the CORW and SCCW which were studied using parametric analysis. Empirical equations, developed to estimate the dynamic responses of the proposed systems, are presented in this chapter.

Chapter 5: Proposed design procedure for the proposed CROCW presents the proposed design procedure of the CORW and SCCW systems using EEDP. A step-by-step design approach for EEDP is provided. This chapter demonstrates how the empirical equations, developed in Chapter 4, are used to modify EEDP. Additionally, new energy modification factors are presented which account for the unique hysteretic shape of the CORW and SCCW systems. This chapter concludes with the detailed design of four prototype buildings.

Chapter 6: Nonlinear modelling approach presents the nonlinear modelling approach for conducting unidirectional and bidirectional nonlinear time-history analysis for the proposed CORW and SCCW systems. The experimental validation of the numerical modelling approach for each structural component is presented. Additionally, the assumptions about gravity loads, mass distribution, and damping are presented.

Chapter 7: Probabilistic seismic hazard analysis and ground motion selection and scaling describes the Probabilistic Seismic Hazard Analysis (PSHA) used to develop the uniform hazard spectra. In addition, the procedure for selecting and scaling ground motions, based on deaggregation of the hazards, is presented.

Chapter 8: Seismic performance assessment of CORW presents the unidirectional nonlinear dynamic responses of the CORW, using the four prototype buildings designed in Chapter 5, the nonlinear modelling approach from Chapter 6, and the ground motions selected in Chapter 7. The results are used to validate EEDP and study the system behaviour.

Chapter 9: Seismic performance assessment of SCCW presents the unidirectional nonlinear dynamic responses of the SCCW, using the four prototype buildings designed in Chapter 5, the nonlinear modelling approach from Chapter 6, and the ground motions selected in Chapter 7. The results are used to validate EEDP and study the system behaviour.

Chapter 10: Bidirectional performance of CROCW system presents the bidirectional nonlinear dynamic responses of the CROCW, using the four prototype buildings designed in Chapter 5, the nonlinear modelling approach from Chapter 6, and the ground motions selected in Chapter 7. The results are used to validate EEDP and study the system behaviour.

Chapter 11: Comparison between CORW and SCCW with alternative RC core wall systems presents comparisons of the seismic performance of prototype buildings designed with alternative RC wall systems. The seismic performance of the CORW and SCCW systems are compared to three alternative designs. The comparison between important parameters, such as displacements, shear forces, and moments are presented.

Chapter 12: Design and construction of shake-table testing describes the work completed towards shake table testing a large-scale specimen designed using the CORW and SCCW systems. An overview of the testing facility, specimen scaling, design, and construction is presented. In addition to the completed work, this chapter also describes the planned work for the experimental testing program. An overview of the phases of testing, instrumentation plan, and the ground motion details is provided in this chapter. A detailed numerical model is developed of the specimen, and predicted nonlinear responses are provided.

Chapter 13: Summary of work and recommendations for future work highlights some of the key contributions in this thesis and provides several recommendations for future work.

Chapter 2: Literature review of high-performance RC wall technologies

2.1 Overview

This chapter presents a literature review on different structural systems and components which can facilitate a low-damage response (i.e., higher performance) in reinforced concrete (RC) walls. The chapter begins with a brief overview of the behaviour of RC shear walls and RC coupling beams, followed by various methods of mitigating damage and improving the performance of typical RC shear walls and RC coupled walls.

Most low-damage systems use energy dissipation devices of some type. Therefore, before introducing low-damage systems, a high-level summary of various damping devices is provided. Specifically, the basic mechanics and behaviour as well as suggestions on some of the advantages and disadvantages of metallic yielding dampers, friction dampers, and viscous dampers are provided.

Following the summary of energy dissipating devices are detailed descriptions of different innovative solutions for low damage shear walls, low damage coupled walls, and damped outrigger wall buildings. A discussion on the merits of existing literature and the knowledge gaps are identified and discussed. Overall, this chapter informs the need for the development of the new systems proposed in Chapter 3.

2.2 Reinforced concrete core walls

Reinforced Concrete (RC) core wall systems are a widely used structural system to resist lateral loads in tall buildings. In these systems, a series of RC wall segments are connected by RC coupling beams to form an interconnected wall assembly. The coupling beams significantly enhance the structure's overturning resistance, stiffness, and energy dissipation as compared to isolated wall piers. The behavior of coupled walls depends strongly on the nonlinear behavior of the coupling beams joining adjacent wall segments.

The construction technique used for the beam varies, but the most common two schemes utilize either conventional beam reinforcing, shown Figure 2.1 (a), or diagonal reinforcing, shown in

Figure 2.1 (b). Compared with conventional beams, diagonally reinforced coupling beams exhibit a more ductile behavior, whereby they can sustain large inelastic rotational demands and withstand many cycles of loading without significant degradation (e.g., Paulay and Binney, 1974; Naish et al., 2013). For this reason, diagonally reinforced coupling beams are commonly used in tall buildings in seismically active regions along the West Coast of Canada and the United States

The concept of diagonally reinforced coupling beams was first tested in 1974 by Paulay and Binney (1974). They tested four coupling beam specimens with low length-to-depth ratios (between 1 - 1.29), of which three were diagonally reinforced and one was conventionally reinforced. They were able to show that diagonally reinforced coupling beams offer superior performance to conventionally reinforced beams in terms of ductility and energy dissipation.

Figure 2.1 (a) and (b) shows the hysteretic response for conventional and diagonally reinforced coupling beams, respectively. Conventionally reinforced beams exhibit much more pronounced pinching behavior than their diagonally reinforced counterparts due to crack formation and bar slippage, causing lower stiffness at high ductility demands. The diagonally reinforced coupling beam generally exhibits much less pinching behavior due to the direct transfer of shear through the diagonal. However, the beam still exhibits softening behavior due to bar slippage at the face of the walls. The confinement around the diagonal bars contributes significantly to the in-cycle and cyclic degradation, as reaffirmed by several experimental studies (Barney et al., 1980; Galano and Vignoli, 2000; Adebar et al., 2001; Naish et al, 2013; and Lim 2016).

Different damage patterns are observed in specimens with lower length-to-depth ratios when compared to specimens with higher length-to-depth ratios. Figure 2.2 shows the damage patterns of diagonally reinforced coupling beams with (a) stocky beams (i.e., length-to-depth < 2) and (b) slender beams (i.e., length-to-depth > 2). As shown, in stocky specimens, diagonal cracking formed at the same locations as the diagonal reinforcing. The concrete spalled in a diagonal pattern, and for most specimens the ultimate failure mode was buckling of the diagonal bar after the concrete spalled away. This behavior was observed in tests with length-to-depth ratios which ranged from 1-1.5 by Paulay and Binney, 1974; Galano & Vignoli, 2000; Canbolat et al., 2005.

Cyclic loading of slender beams results in several flexural cracks are observed in addition to diagonal cracking. Strength loss was eventually observed in conjunction with spalling at the wall interface, diagonal bar buckling, and concrete crushing. This behavior was exhibited in several slender diagonally reinforced coupling beam tests with length-to-depth ratios ranging from 2.4 to 3.3 by Adebar et al., 2001; Fortney et al., 2008; Naish et al., 2013; and Lim et al., 2016.

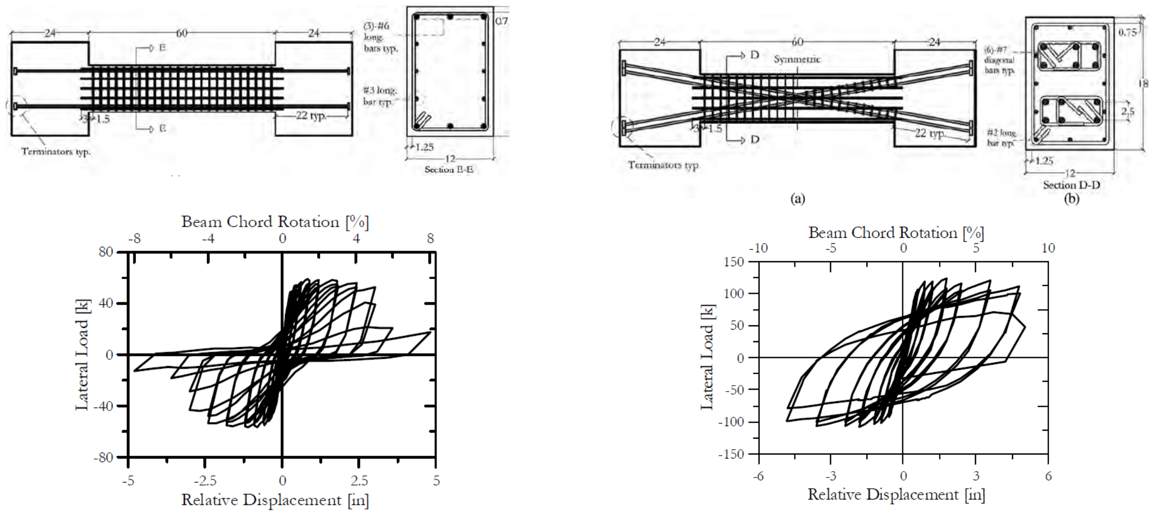

(a) (b)

Figure 2.1 Reinforcing layout of RC coupling beams: (a) longitudinally reinforced (Naish et al., 2013); and (b) diagonally reinforced (Naish et al., 2013)

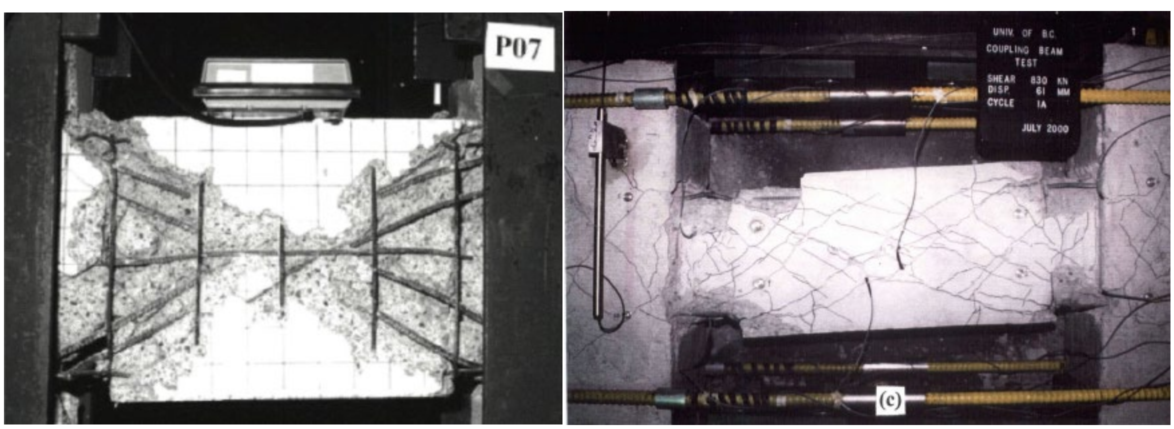

Figure 2.2: Cracking and failure pattern of (a) length-to-depth = 1.5, specimen P07 (Galano & Vignoli, 2000) and (b) length to depth = 2.74 (Adebar et al., 2001).

Damage may occur within the shear wall in addition to the coupling beams. The behavior of shear walls under cyclic loads have been studied extensively in the past half century (e.g., Massone & Wallace, 2004; Adebar et al., 2007; Dazio et al., 2009). Under high lateral loads, flexural cracks open, and vertical reinforcing yields over a region called the plastic hinge.

In typical design of shear walls the vertical reinforcing must stay constant over the plastic hinge region, to avoid concentrations of strain resulting in nonductile behaviour. The wall above the plastic hinge region is capacity designed to ensure a well predicted mechanism. Given the change in axial load over the height of the building, it is usually unnecessary to increase the reinforcement above the plastic hinge region. Reinforcement detailing varies between building codes, but generally, the requirement is to have sufficient ties within boundary elements, to avoid buckling of the vertical reinforcing.

The damage which occurs within the plastic deformations of the reinforcing steel and cracking of concrete is difficult to repair after the earthquake. Due to the large axial loads on walls in a core configuration, flexural cracks will close, and the level of yielding in the reinforcing steel may not be easily determined. Recognizing these difficulties, various alternative mechanisms have been proposed to enhance the performance of shear wall and coupled wall systems. Recent developments on the improved performance of shear wall and coupled wall systems are summarized in the following sections: *2.2 Energy dissipating devices*, *2.3 Innovative RC shear wall systems*; *2.4 Innovative RC coupled wall systems*; and *2.5 Damped outriggered RC walls*.

2.3 Energy dissipating devices

The inclusion of energy dissipation devices (or dampers) can enhance the structural performance of any building systems, including shear wall or coupled wall buildings. As dampers are such an intrinsic component to the development of earthquake resilient systems, it is worth further exploring the different damper types, behaviors, applications, and limitations.

All the methods discussed and used within this dissertation are referred to as passive damping. Passive damping, as opposed to active/semi-active, relies on the natural movement of the building to be activated, as oppose relying on computer control and/or an external power source. Generally, passive dampers are connected where the most motion will occur, maximizing energy dissipation. It is important to note that the addition of dampers often requires some degree of modification to the system. For example, adding dampers to an RC core wall using an outrigger (discussed in Section 2.6) results in both additional damping through devices incorporated within an outrigger and additional stiffness through the incorporation of the outrigger system.

Energy dissipating devices can usually be differentiated by four categories: yielding metallic dampers, friction devices, viscous fluid dampers, and viscoelastic dampers, shown in Figure 2.3. Each category has a unique set of behaviours and characteristics, which may be used for different applications, discussed in the following sections.

	Viscous fluid	Viscoelastic	Metallic	Friction
Basic construction	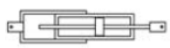	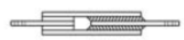	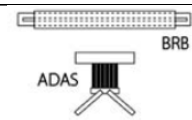	
Idealized hysteretic behaviour	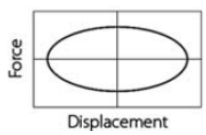	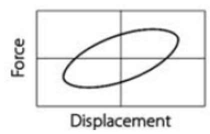	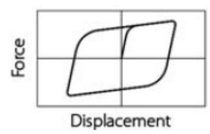	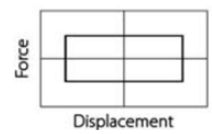
Idealized mechanical	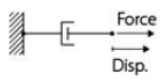	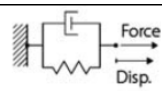	Idealisation unavailable	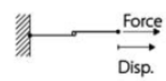
Advantages	• Activated at low displacements • Minimal restoring force • Simple modeling • Temperature - independent properties	• Activated at low displacements • Provides restoring force • Linear behaviour • Simple modeling • Strong long-term behaviour	• Stable hysteretic behaviour • Long-term reliability • Insensitive to ambient temperatures • Materials and behaviour are familiar to practicing engineers	• Sliding interfaces may change with time (reliability concern) • Strong nonlinear behaviour • Permanent deformations possible if no restoring force provided.
Disadvantages	• Possible fluid leaks (long-term reliability concern).	• Limited deformation capacity • Temperature and frequency dependant properties	• Device damaged after earthquake (may require replacement) • Nonlinear behaviour (may require nonlinear analysis)	• Large energy dissipation per cycle • Insensitivity to ambient temperature

Figure 2.3 Summary of damper characteristics (adapted from Symans et al., 2008)

2.3.1 Metallic yielding dampers

Metallic yielding dampers dissipate the earthquake energy through the plastic deformations of metals. Several metallic yielding dampers have been developed in the past, including buckling restrained braces (BRBs) (Iwata, Midorikawa, & Koyano, 2018; Xie, 2005) and plate yielding devices (Ma et al., 2011; Yang et al., 2019; Yang, Banjuradja, & Tobber, 2018).

Buckling restrained braces are typically loaded axially and consist of a steel yielding member encased by another material such as concrete. The encasing material prevents the yielding member from buckling in compression, which promotes a nearly symmetric tension and compression response. BRBs are loaded unidirectionally and can be incorporated within a variety of systems, such as braced frames and truss systems.

In some circumstances it is beneficial to have the device loaded in shear, like in the Linked column frame (Dusicka & Iwai, 2007) or H-frame structures (Etebarian, Yang & Tung, 2019). An example of a shear loaded device is the Honeycomb damper (Yang et al, 2019), shown in Figure 2.4 (a). This device consists of a steel plate with welded flanges and is loaded parallel to the flanges. The web consists of unique hole cut-out patterns designed to promote ductile yield mechanisms, while the flanges remain elastic to provide connection to the structural system.

Figure 2.4 (b) shows the hysteretic shape of the Honeycomb damper. Like most metallic yielding dampers, the hysteretic shape follows the behaviour of steel, where isotropic and kinematic hardening is observed. In the case of the Honeycomb damper, the force begins to degrade once the web undergoes inelastic buckling.

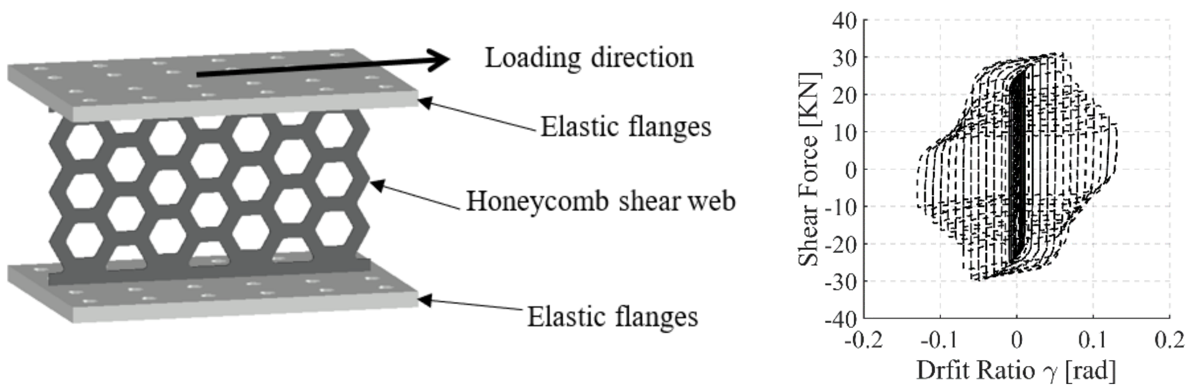

(a) (b)

Figure 2.4 Honeycomb damper: (a) conceptual view and (b) hysteretic response (Yang et al., 2019)

Metallic dampers are popular due to their simplicity in design, reliability in behaviour, and low costs. A potential drawback to these devices is the coupling of stiffness and force. For example, in the design of the Honeycomb damper, a lower desired force requires a smaller thickness of the steel plate resulting in a lower initial overall stiffness of the device. A low initial stiffness device can lead to various issues regarding the system level design, including, higher structural period of the building and higher displacement demands required to engage the device.

2.3.2 Friction dampers

Friction dampers dissipate earthquake energy through sliding contact friction. In the past researchers have investigated various configurations and loading conditions for these friction devices including the Pall friction damper (Pall & Marsh, 1982), symmetric friction damper (Gregorian et al., 1992), and the Asymmetrical Friction Connection (Rodgers, 2017). Figure 2.5 (a) shows a basic configuration of a symmetric friction damper.

In most friction dampers, plates are pretensioned together, creating a normal force. The pretensioned bolts pass through slotted hole connections to permit lateral movement, which develops the sliding friction force. Friction dampers do not begin to absorb energy until the slip force is reached, resulting in a rigid-plastic hysteretic response, shown in Figure 2.5 (b). This rigid-plastic, or stick-slip, behaviour makes friction dampers superior for energy dissipation; however, it has no self-centering tendency which may result in residual displacements when the structure no longer contains enough energy to overcome the static friction force – i.e., the device may "lock up" at some residual displacement.

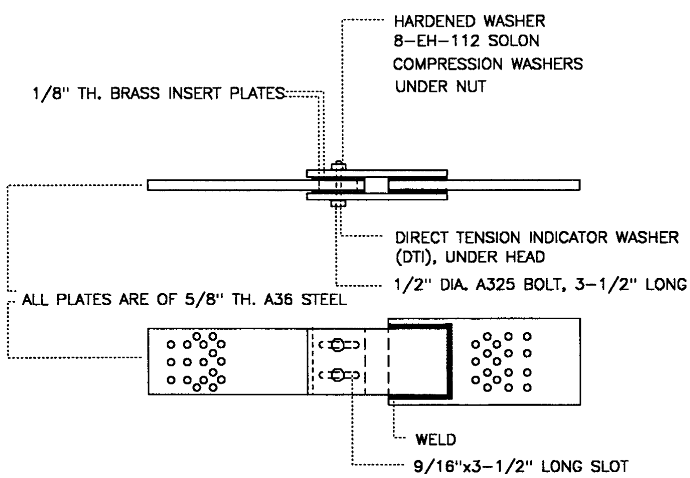

(a)

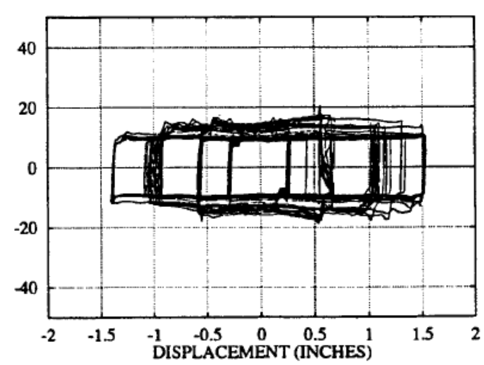

(b)

Figure 2.5 Slotted bolted connection: (a) Schematic and (b) hysteretic response (Gregorian et al., 1993)

To address these residual displacements, some researchers have proposed features to introduce self-centering behaviour, such as using sloped plates, in addition to providing sliding friction. Such devices include the Ring Spring Damper (Filiatrault et al., 2000), Resilient Slip Friction Joint (RSFJ) (Hashemi et al., 2017); and the Self-centering Conical Friction Damper (SCFD) (Yang et al., 2020). Introducing a self-centering mechanism modifies the hysteresis from a rectangular shape to a flag-shaped hysteresis. For example, the RSFJ dissipates energy through the sliding friction between sloped plates. The sliding motion results in displacements both vertically and laterally. The normal force is provided with bolts which are connected in series with low axial stiffness springs. The springs allow for vertical movement and reduces the axial forces on the bolts. The vertical movement, results in an increased clamping force, which causes a post-slip stiffness in the hysteretic response. This hysteretic behaviour results in an efficient device, which has a high post-slip stiffness and a self-centering capacity.

Overall, friction dampers are advantageous due to the high energy dissipation, and nearly rigid initial stiffness. The high initial stiffness may be particularly important for flexible structures under serviceability conditions, as the device will not be activated and initiate sliding until a specified threshold load is reached, which can help keep structural movements within acceptable limits. However, a disadvantage to friction dampers is the difficulty in preparing and maintaining a predictable sliding surface, especially over a 50 year, or more, design life.

Many proposed devices (Gregorian et al., 1993, and Tremblay, 1993) exhibit a noticeable peak in the hysteretic response before sliding initiates, due to the difference in static and dynamic friction coefficients. These peaks need to be well-defined to apply capacity design principles to the rest of the system. It has also been observed that some devices utilizing pretensioned bolts exhibit a concentration of heat generated around the bolt holes, which may degrade the sliding surfaces and change the hysteresis over time (Tremblay, 1993). There is also little research on the long-term behaviour of such devices. For reliability, they may require some level of maintenance and inspections, and special lubricants and oils to ensure the device will perform as expected. Practical issues such as fireproofing, corrosion protection, and inspection access may further complicate the maintainability of the devices.

2.3.3 Fluid viscous dampers

Fluid viscous dampers dissipate energy through the movement of viscous fluids. As a means of energy dissipation devices for earthquakes, fluid viscous dampers have been extensively studied by multiple researchers (e.g., Landi et al., 2014, and Reinhorn et al., 1995). A basic configuration of a viscous damper is shown in Figure 2.6 (a) and the hysteretic response is shown in Figure 2.6 (b). Viscous dampers dissipate energy through the movement of high viscosity fluids in or around the moving piston. The movement of the piston head results in a pressure differential between chambers, forcing the fluid through orifices and expending energy.

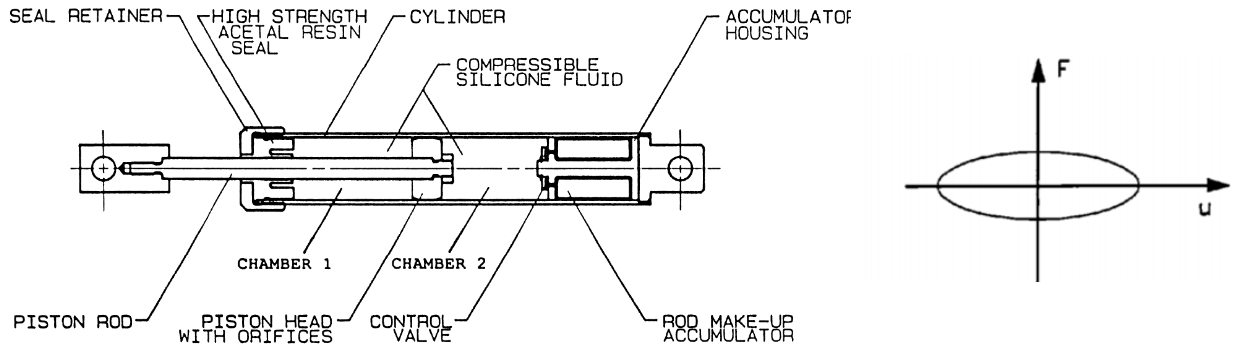

(a) (b)

Figure 2.6 Typical viscous damper (Constantinou et al., 1992)

The mechanism at work is velocity-dependant which may have implications for conventional design procedures (e.g., the design cannot be easily displacement based). Like the friction damper, the reliability of the device needs to be considered, with leaks or loss of fluid containment being of primary concern. It is worth noting, fluid damper inter-device variability is low, however, uncertainty in in-service velocity needs to be considered in overstrength factors. This is particularly important in capacity design, where the ultimate force of the damper must be accurately predicted to ensure ductile response.

2.3.4 Viscoelastic dampers

Viscoelastic dampers dissipate earthquake energy through the deformation of viscous elastic materials. Figure 2.8 (a) shows the basic configuration of Viscoelastic dampers. Viscoelastic dampers often consist of layers of viscoelastic material rigidly bonded to metal plates (Montgomery & Christopoulos, 2015). Like fluid viscous dampers, viscoelastic dampers also have velocity dependence, but the hysteresis occurs at an incline related to the elastic stiffness. The hysteretic behaviour of the viscoelastic damper is essentially a linear spring in parallel with viscous damper (Figure 2.7 (b)).

Viscoelastic dampers are advantageous due to high energy dissipation, and an initial stiffness which helps in recentering the device. However, like viscous dampers, viscoelastic dampers have a velocity dependence, which should be considered in the design procedure. The properties of the viscoelastic material may also make them sensitive to temperature changes. Experimental testing of each device at temperature and frequencies of interest should be conducted prior to implementation into the structure.

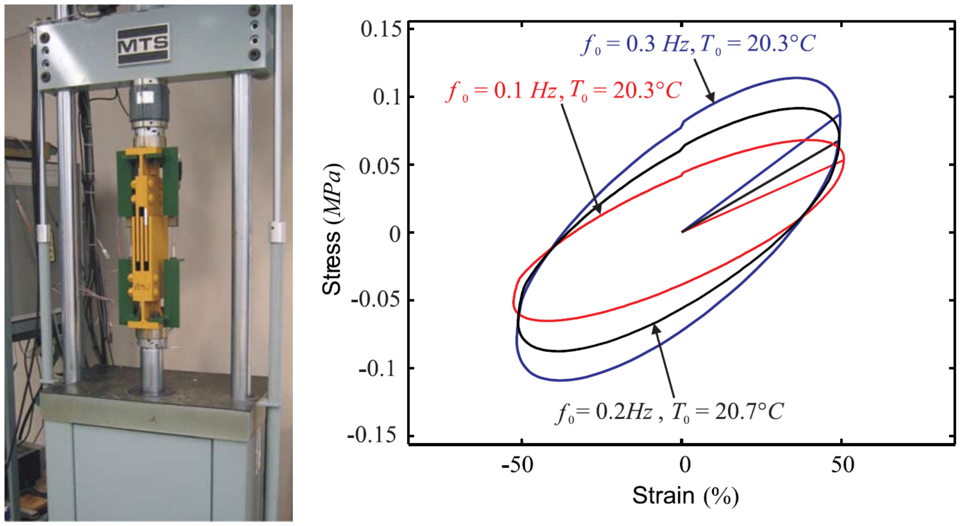

(a) (b)

Figure 2.7 Viscoelastic material: (a) basic configuration and (b) hysteretic response (Montgomery & Christopoulos, 2015)

2.4 Innovative RC shear wall systems

Researchers have investigated various methods of incorporating energy dissipation devices with RC shear walls to improve the performance. The following are some of the recent developments on innovative, low-damage RC shear wall systems.

2.4.1.1 Controlled rocking

The yielding mechanisms of typical fixed based RC walls is effective in dissipating energy, however, the damage exhibited through excessive yielding of reinforcing steel may be difficult to repair after strong earthquake shaking. To address this damage, researchers have investigated controlled rocking, which is the concept of intentionally designing the structure to be vertically separated from the foundation, such that it can freely move vertically during earthquake shaking. This movement protects the structural system from undergoing excessive strains and damage. Due to high axial loads, usually provided by PT tendons, the wall only initiates rocking at large lateral loads. Prior to the initiation of rocking the wall behaves like a fixed based wall.

PRESSS (Precast Seismic Structural System) is a US-Japan seismic research program and includes a series of experimental tests to study the behaviour of precast rocking walls (Priestley, 1991). As part of this program, Kurama et al. (1999) presented research on unbonded post-tensioned jointed precast rocking walls. This system consists of multiple precast wall panels that are connected to the foundation using unbonded post-tensioned tendons. The post-tensioned tendons provide the restoring force required for self-centering and a small level of energy dissipation through yielding at large drifts. Spiral confined reinforcing was placed within the rocking toe to mitigate damage due to pounding. Experimental testing showed excellent self-centering hysteretic behaviour with repairable damage at the rocking toe. The yielding of post-tensioned tendons limited the lateral force resulting in minimal damage in the rocking toes. A potential drawback of this system is the low energy dissipation, which can result in high displacements.

Kurama (2000) introduced joint rocking walls that included supplemental viscous dampers to dissipate energy. In their study, linear viscous fluid dampers are mounted diagonally in-plane with the walls. Nonlinear analysis demonstrated that supplemental damping results in lower drifts and accelerations compared with systems without supplemental damping. Restrepo and Rahman (2007) proposed a rocking wall system that incorporated mild steel yielding dampers. These dampers are cast in the wall and foundation. This system demonstrated excellent energy dissipation. However, extensive damage was observed on the rocking toes. Additionally, the dampers' location makes them difficult to repair or replace after a strong earthquake shaking.

Marriott et al. (2008) tested controlled rocking walls with externally mounted dampers on a shake table. They studied four unique wall designs with different damping configurations: 1) no added damping; 2) four viscous dampers; 3) four viscous dampers and two mild steel dampers; 4) two mild steel dampers. Each wall was post-tensioned such that the hysteretic backbone of each specimen was similar. Externally mounted steel plates mitigated the damage in the rocking toe. Figure 2.8 shows an example of the tested specimen. The dampers mounted near the ends of the wall, shown in Figure 2.8 (a) and Figure 2.8 (b), are the viscous dampers, while the dampers mounted in the center of the wall are the mild steel dampers.

The hysteretic response of the combined viscous and mild steel dampers, shown in Figure 2.8 (d), shows higher energy dissipation than mild steel dampers alone, shown in Figure 2.8 (c) when cycled at 0.5hz. However, when dynamically testing the walls under near-field and far-field motions, the results showed that the specimen used only mild steel dampers had lower peak displacements under lower intensity motions. In comparison, the combined viscous-mild steel damper specimen demonstrated the lowest displacements under high-intensity earthquakes. This response is due to the velocity dependence of the viscous dampers, where the lower shaking intensities result in lower overall effectiveness of the viscous damper devices. All wall specimens demonstrated low damage and negligible residual deformations. However, their study was limited to low-rise planar walls, without consideration for tall building applications.

Figure 2.8 Marriott et al. (2008) wall specimens (a) left: Unit 2 (4 viscous dampers); (b) centre: Unit 3 (4 viscous dampers and 2 TCY mild steel dampers); (c) top right: experimental response of the specimen with two mild steel dampers: (d) bottom right: experimental response of specimen with four viscous dampers and two mild steel dampers.

Sritharan et al. (2015) introduced a controlled rocking Precast Wall with End Columns (PreWEC). O-connectors, which are low-yield mild steel connectors, are mounted between the rocking wall and the end columns to dissipate the earthquake energy. Figure 2.9 shows the concept of the PreWEC system. Two specimens were constructed and experimentally tested: 1) conventional RC wall and 2) PreWEC. The result showed that the PreWEC demonstrated superior performance when compared with the conventional design in terms of residual displacements and repairable damage.

Twigden, et al. (2017) conducted a series of static cyclic tests on controlled rocking systems, including two single rocking systems and two PreWEC systems. The cyclic response of the walls using different configurations of hysteretic damping was systematically studied. The results showed that the use of O-connectors within the PReWEC system resulting in higher capacity and energy dissipation. However, the PreWEC system has higher residual displacements when compared to the controlled rocking system. This study was later expanded in by Twigden and Henry (2019), who conducted shake table testing on two PreWEC specimens and one controlled rocking specimen. The results confirmed the superior energy dissipation of the PreWEC system. An important observation from this study was the dynamic loading showed significantly lower residual drifts in the PreWEC than were observed under static cyclic loading. However, their study was limited to low-rise planar walls, without consideration for tall building applications.

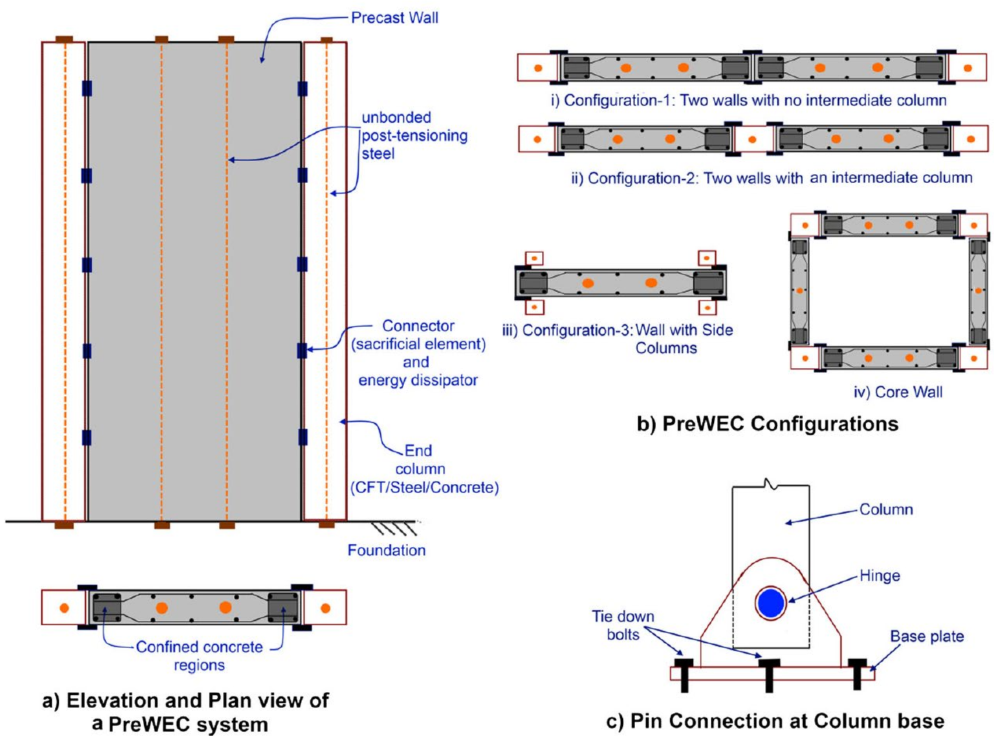

Figure 2.9 The PreWEC system including different configuration options (Sritharan et al., 2015)

2.4.1.2 Controlled rocking with tall building applications

Most research on controlled rocking walls has been limited to low-rise buildings. However, there is growing interest in applying controlled rocking mechanisms to taller buildings. For example, Wiebe and Christopoulos (2009) suggested the use of multiple rocking walls over the height of the building. They numerically investigated the seismic response of buildings from 4 stories to 20-stories using simple lump hinge modeling techniques. Their results show that including multiple rocking points throughout the building height reduces higher mode forces. This result was later verified in 2015 by Khanmohammadi and Heydari, who used more detailed distributed plasticity modeling of the controlled rocking system.

In 2015, Lu and Panagiotou studied the use of a dual system consisting of base-isolated and a controlled rocking core wall system, shown in Figure 2.10. They studied a 20-story building designed with three different systems: a) new dual system, the controlled rocking base, and a fixed base system. Their results indicated the dual system exhibited low-damage response, the controlled rocking system demonstrated minimal damage, and the fix-base structure experience significant damage at the maximum considered earthquake. However, their study was limited in the number of buildings studied, and detailed design procedures were not examined.

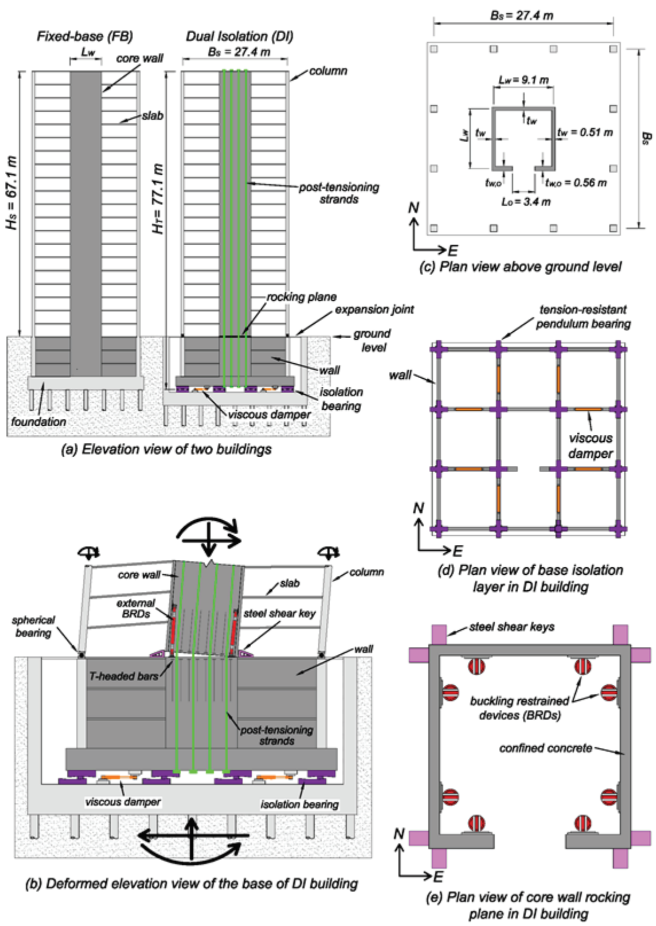

Figure 2.10 Concept of dual isolated building by Lu and Panagiotou (2015)

Tong and Christopoulos (2020) conceptualized a new dual mechanism for transferring moments and shears to the foundation. This new system, called MechRV3D transfers the overturning moments through a damped controlled rocking mechanism. The shear mechanism is a series of bracing components that allow for yielding and shear ductility. This innovative system is shown in Figure 2.11. Tong and Christopoulos (2020) show that this system could potentially reduce both shear and moment demand within the core wall. Additionally, the tall building system is essentially damage-free after strong earthquake shaking. However, their study was limited to one prototype building, and further investigations are required to develop design guidance on this novel system.

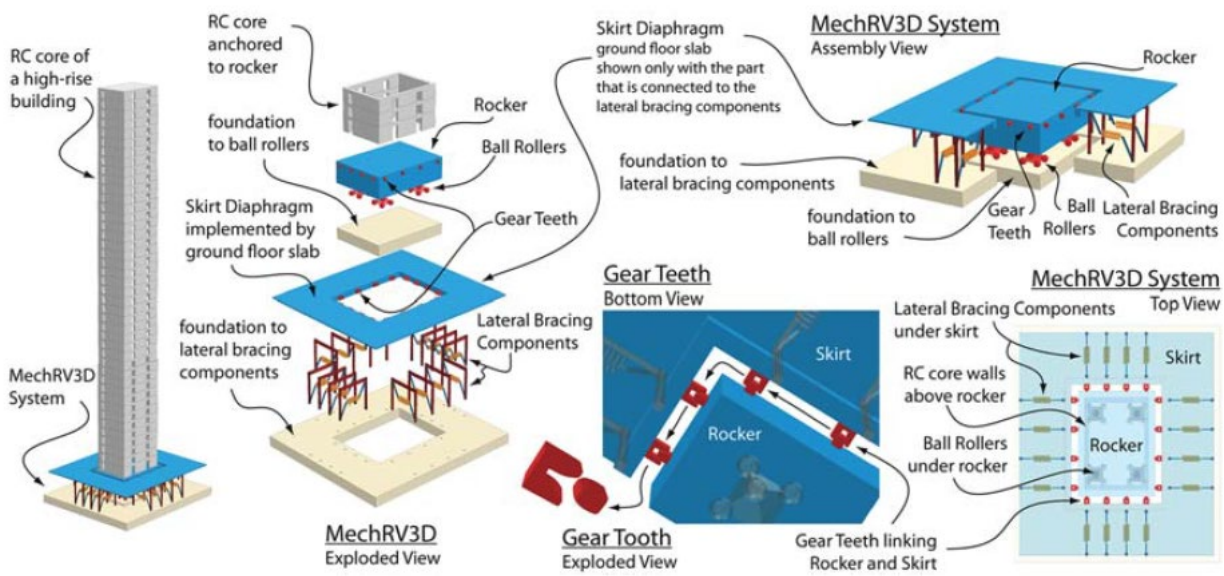

Figure 2.11 Idealized configuration of the MechRV3D system by Tong and Christopoulos (2020)

2.4.1.3 Pin-connected walls

In addition to controlled rocking, other systems have been developed as alternatives to traditional plastic hinging in RC walls. In 2012, Qu et al. proposed a RC wall with a pin support at the base connected to moment frames to retrofit existing structures. Steel shear links are situated between the shear wall and the frame to dissipated energy. Similarly, in 2017, Wada et al. developed a system which consisted of a planar wall connected to a pin at the center of the base. Either end of the wall is connected to buckling restrained braces, which dissipate the earthquake energy through the yielding of steel. Figure 2.12 shows the tested specimen. Their results showed that the damped pin could effectively transfer the shear forces while providing a stable, rapidly repairable flexural mechanism for energy dissipation.

Although effective for planar walls, these pin-connected walls can not be applied to RC core wall buildings. In RC core wall buildings, flanged walls are connected in at least one direction with coupled beams. The wall is expected high lateral loads along each axis. If the PSW were used in either the flanges or the web within an RC core wall, it would act as vertical restraint under bidirectional loading and damage the pin or the RC walls.

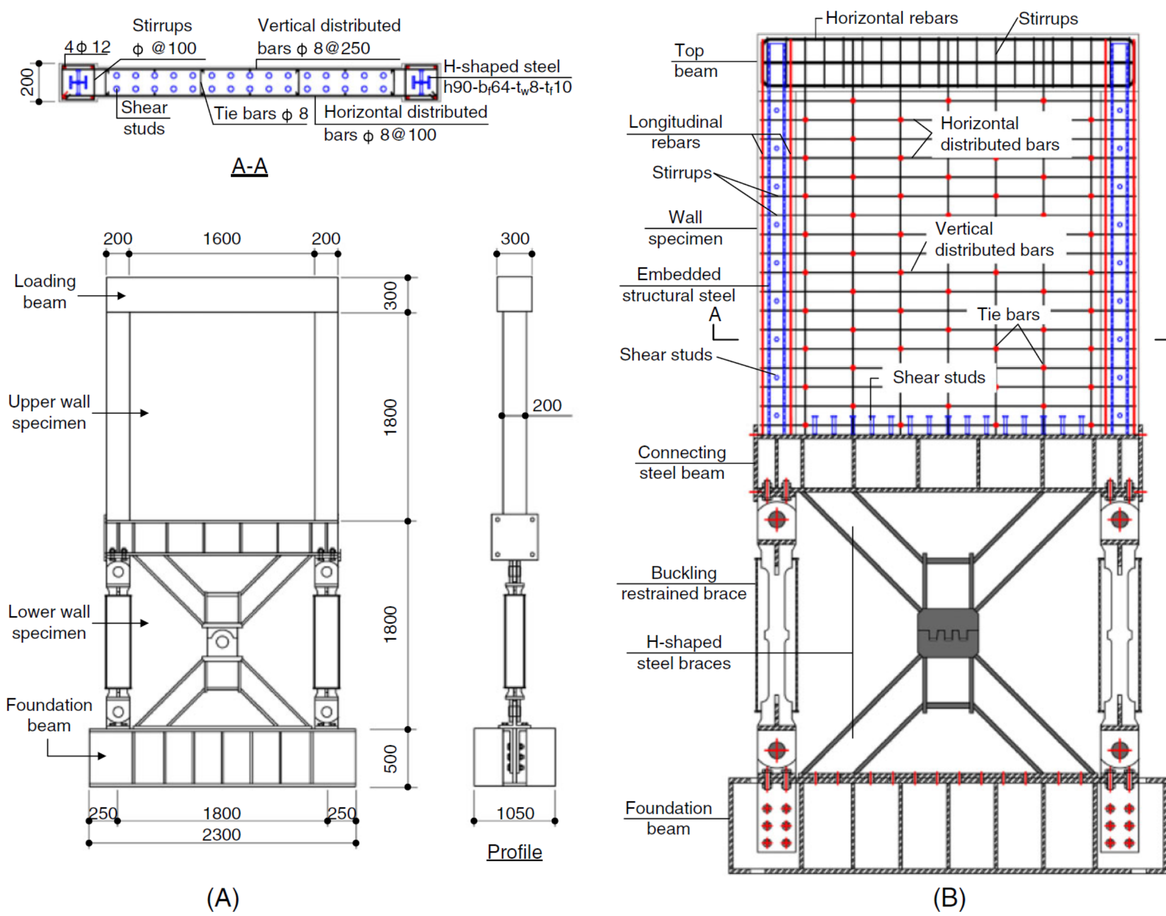

Figure 2.12 Plastic-hinge-supported wall (PSW) specimens (units: mm): (a) PSW-1: plastic hinge with gear-shaped support and (b), PSW-2: plastic hinge with pin support (Wada et al., 2017)

2.4.1.4 Replaceable cornered walls

Liu and Jiang (2017) proposed a new type of shear wall, which essentially replaces the corner of the wall with steel yielding dampers. The reduced section of the wall is strengthened in shear using steel plates. Figure 2.13 (a) shows the concept recommended by Liu and Jiang (2017). Although this system is effective in limiting damage, the walls may have some residual deformations post-disaster.

To mitigate residual displacements, Xu et al., 2018 proposed using a self-centering damper called ring springs as the energy dissipating component, shown in Figure 2.13 (b). The ring springs help in re-centering the wall after strong earthquake shaking.

Although the replaceable corner component shear walls have proven effective in reducing damage in planar shear wall systems, in their present configurations, these systems could not be integrated into a centralized core wall system. If the replaceable corner component were used in either the flanges or the web within an RC core wall, the fixed portions would act as vertical restraint under bidirectional loading and could be damaged.

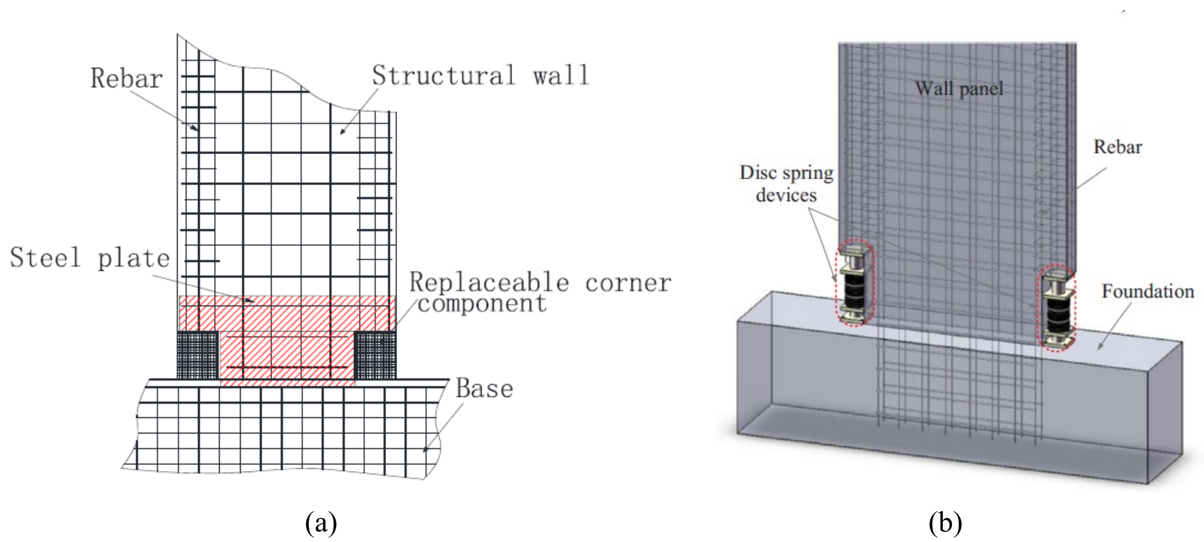

Figure 2.13 Replaceable corner component shear walls: (a) concept by Liu and Jiang, 2017 and (b) self-centering concept by Xu et al., 2018.

2.5 Innovative RC coupled wall systems

Researchers have investigated various methods of incorporating energy dissipation devices with RC coupled walls to improve the performance. The following are some of the recent developments on innovative, low-damage RC coupled wall systems.

2.5.1.1 Steel-reinforced concrete coupling beams

Steel-reinforced concrete (SRC) coupling beams, sometimes called Composite coupling beams, refer to the use of a structural steel section embedded into the boundary zones of reinforced concrete walls. These beams resist earthquake loads through the yielding of the structural steel section. Although not necessarily a low-damage component on its own, many of the damped coupling beams discussed later in the chapter utilise embedded steel beams as an important portion of the structural system. Hence, it is important to note the behavior of the SRC beams.

In the SRC beams, coupling forces are transferred to the wall through bearing of the embedded beam. The advantage of SRC beams over diagonally reinforced coupling beams is the energy dissipating capacity and ductility of the steel sections, while allowing for a small depth. Figure 2.14 shows an example SRC beam under construction in Vancouver house, Canada.

Figure 2.14 Embedded steel-reinforced concrete beams (Poh, 2020)

The behavior of the SRC beams is well established, with research extending back to 1980 (Markakis & Mitchell, 1980; Aktan & Bertero, 1984; Gong & Shahrooz, 2001; Harries et al., 1993; Motter et al., 2017) and in 2010, AISC released seismic provisions for design special walls and ordinary walls with SRC beams.

This literature describes how the performance of SRC beams is highly dependent on the embedment length. SRC beams with improper embedment length results in gaps forming in the RC wall under cyclic loading. The outcome is a highly pinched hysteresis, resulting in reduced energy dissipation (Motter et al., 2017). Figure 2.15 shows the comparison between two W310x143 SRC beams, where SRC1 (shown in Figure 2.15 (a)) has an embedment length of 32in and SRC2 (shown in Figure 2.15 (b)) has an embedment length of 24in. As shown, the longer embedment length shows superior performance in terms of both ductility and energy dissipation.

It is important to note that although the SRC beams make use of the excellent energy dissipation of structural steel sections, the stiffness of the SRC beams reported by Motter et al., 2017 demonstrated that the primary sources of deformations prior to yielding occurred due to slip and extension from the embedment regions and the overall construction of shear and flexural deformations from the steel section was relatively small.

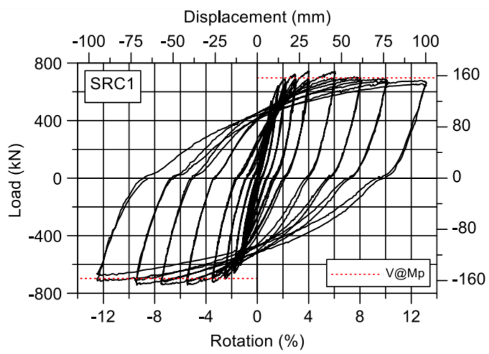

(a)

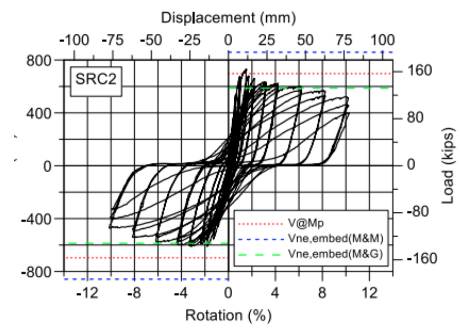

(b)

Figure 2.15 SRC beams from Motter et al. (2017): (a) specimen SRC1 (embedment length = 32”) and (b) specimen SRC2 reduced embedment length (embedment length = 24”)

2.5.1.2 Fused coupling beams

Although diagonally reinforced and SRC beams are efficient energy-dissipating components; strong earthquake shaking may still result in damage at the wall-beam interface and yielding in the wall boundary reinforcing. To mitigate this damage, researchers investigate the Fused coupled walls, which is essentially an RC core wall which utilizes dampers in place of RC coupling beams.

Fortney et al. (2007) proposed a replaceable fused steel coupling beam. In this coupling beam design, a central steel beam section, called a fuse, absorbs all the inelastic deformation and damage. Connecting the fuse to embedded steel sections through slip-critical bolted connections facilitates efficient replacement after an earthquake, leading to a more resilient coupled wall system. Chung et al. (2009) proposed a similar system, using sliding friction dampers as a fuse. Nonlinear time history analysis demonstrated that using the friction damper resulted in reduced roof displacements and overall damage.

Ahn et al. (2013) conducted large-scale quasi-static tests on a conventional longitudinally reinforced coupling beam, a coupling beam with a yielding metallic damper fuse, and a coupling beam with a friction damper fuse. The yielding metallic damper dissipates energy through the yielding of plates in parallel. The plates are cut in a specific shape to ensure that the plates endure constant curvature during bending, maximizing energy dissipation. The friction dampers dissipate energy through the sliding of two plates, which are bolted together with slotted holes. The tests showed that the coupling beams with dampers exhibited a more stable hysteretic shape, high energy dissipation, and minimal damage to the walls compared with the conventional RC beams.

Ji et al. (2016) conducted a series of quasi-static tests to study the behaviour of fused coupling beams and evaluate various end connection plates. Their tests demonstrated the high energy dissipation of the fused coupling beam and rapid repairability. In 2017, Ji et al expanded this study to include the RC slab within the component test. In this study, four types of slabs were examined: 1) a composite slab which incorporated steel studs to achieve composite action between the coupling beam and the slab; 2) a bearing slab where the RC slab was bearing on the steel coupling beam but had no mechanical connection; 3) an isolated slab where there was a gap between the coupling beam and the slab; and 4) a slotted slab where slots are inserted within the slab to allow the movement of the coupling beam. Their experimental studies concluded that the isolated floor slabs provided superior performance and limited damage when compared with the other slab connections.

Substituting the conventional RC coupling beam with rapid repairable energy dissipation devices is an effective tool in mitigating the damage within the coupling beam and the beam-wall connection. However, the use of these devices, while maintaining a fixed concrete base, can result in significant damage in the wall. For example, Cheng et al. (2017) tested a low yielding point steel damper device connected to embedded steel beams and compared it to the fixed based wall with diagonally reinforced coupling beams. The result showed more moderate damage in the wall at the coupling beam connection; however, extensive damage was observed in both wall specimens. As shown in Figure 2.16 extensive damage can be observed in the base of the wall for both systems: (a) damped coupled wall and (b) conventional coupled wall.

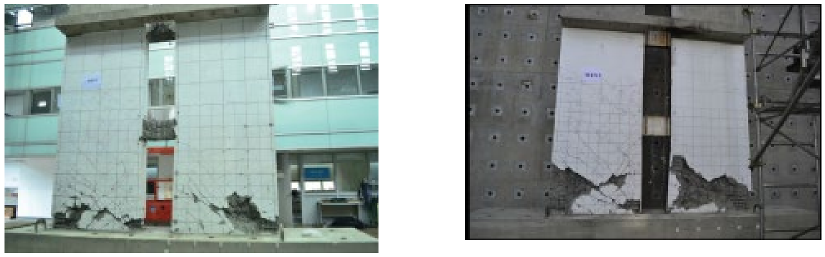

a) b)

Figure 2.16 Coupled wall testing by Cheng et al. (2017): (a) diagonally reinforced coupled wall and (b) low yield point steel coupling beams

2.5.1.3 Viscoelastic coupling damper

Christopoulos & Montgomery (2013) proposed a viscoelastic coupling damper (VCD) to enhance the coupled wall system's performance subjected to wind and moderate seismic load, shown in Figure 2.17. This device combines viscoelastic materials in addition to steel yielding beams. The VCD provides an additional velocity-dependent viscous damping to the building and increases the damping in all modes of vibration. Analysis of the system response under wind and moderate seismic load showed that using the VCD resulted in a reduction in the maximum displacement, acceleration, base shear, and base moment. Additionally, for large earthquakes, VCD is designed to yield, hence the wall is protected from damage at the coupling beam locations.

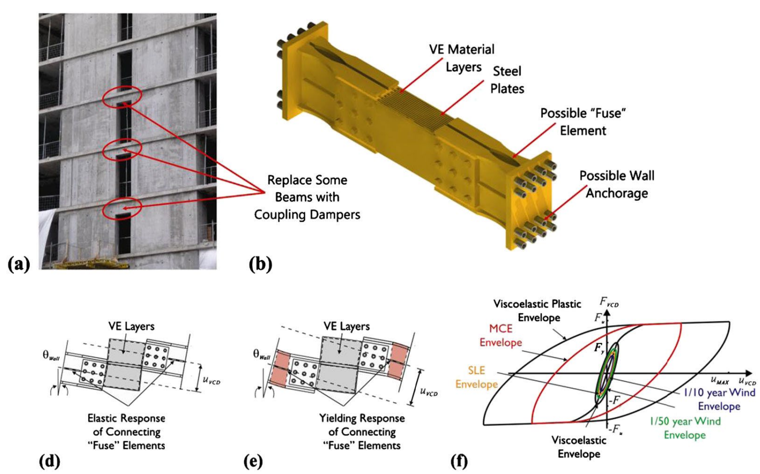

Figure 2.17 Viscoelastic coupling damper (VCD) concept from Christopoulos & Montgomery (2013): (a) reinforced concrete coupled walls in a 58-story tower in Toronto; (b) VCD; (c) exaggerated deformed shape of coupled walls; (d) exaggerated viscoelastic deformed shape; (e) exaggerated viscoelastic-plastic deformed shape; and (f) design hysteresis envelopes. VE, viscoelastic; MCE, maximum credible earthquake; SLE, service-level earthquake.

MacKay-Lyons et al. (2018) studied the nonlinear performance of tall buildings designed with VCDs using nonlinear analysis software Perform3D (Computers and Structures, 2018). Their studies showed that VCDs resulted in lower accelerations under service level earthquakes and lower interstorey drifts and base shears at moderate earthquakes, when compared to conventional RC wall buildings. Additionally, the added viscous damping provided by the viscoelastic materials in the VCD allowed for reduced wind demands. Overall, their study demonstrated that adding damping in leu of conventional RC results in improved seismic and wind performance.

Similar to fused coupled walls, coupled walls which have VCDs, are still at risk from damage near the base of the wall. Therefore, further investigations are needed to develop low damage coupled wall solutions.

2.6 Damped outriggered RC walls

An outrigger system consists of stiff girders or trusses that couple the RC core wall to exterior columns, as shown in Figure 2.18. An outrigger system adds a rotational stiffness to the RC core wall, reducing lateral displacements and core moment at the base of the wall. Outriggers can be oriented in either the shear wall direction (Figure 2.18 (a)), the coupled wall direction (Figure 2.18 (b)), or both directions in a core wall. Although outriggers have been used for half a century to reduce wind displacements, they have only recently been adapted for seismic design.

Smith and Willford (2007) proposed the use of viscous dampers in outrigger systems for tall buildings. Their study showed that the damped outrigger virtually eliminated the dynamic effects of wind, leading to 30% reduction in the quantity of concrete required and a 2% increase in floor area compared with a conventional building.

Zhou et al. (2016) compared the behaviour of a conventional buckling brace with a BRB as the energy dissipating element in an outrigger using a numerical and experimental study. Additionally, they studied the use of BRBs in high-rise buildings using nonlinear time history analysis. Their results showed that BRB elements can increase the damping on the building by 0.5% and the BRBs protects the structure from severe damage under high-intensity earthquake shaking.

Huang and Takeuchi (2017) used complex eigenvalue analysis to optimize the outrigger's location for a single-damped-outrigger building. Their results indicated that the optimal outrigger location typically falls between 50%-80% of the overall building height. They conclude that the outrigger system's governing response is mostly controlled by the first mode shape, first-mode damping ratio, and first-mode period.

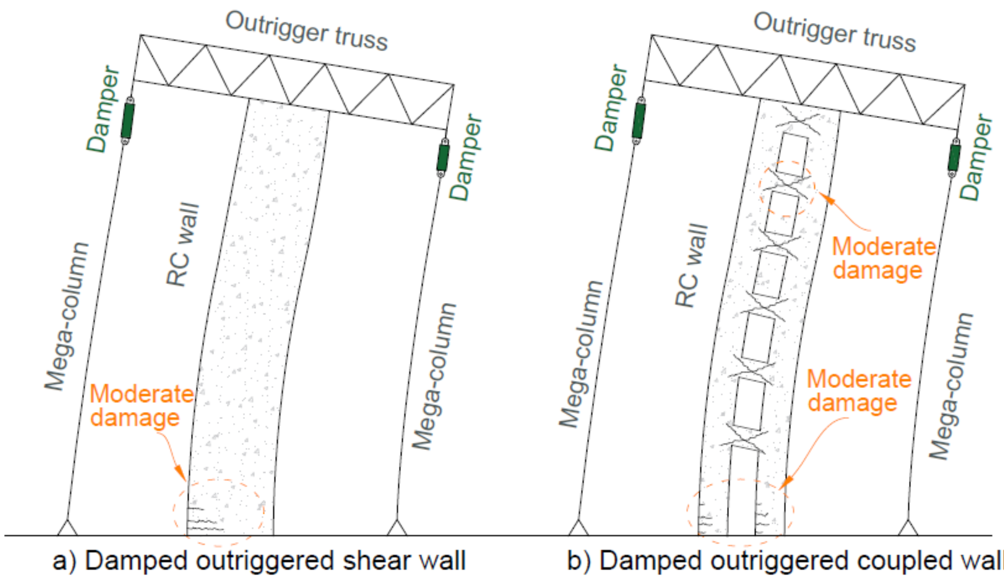

Figure 2.18 Damped outrigger system concept: (a) damped outriggered shear wall; and (b) damped outriggered coupled wall

Lin et al. (2018) investigated the influence of outrigger elevation, outrigger truss flexural stiffness, BRB axial stiffness, and perimeter column axial stiffness on roof drift and acceleration. They studied this using spectral analysis and nonlinear time history analysis. Their study indicated that the outrigger's optimum location is at 60-80% of the height of the building. According to their research, an optimal outrigger location could reduce the wall's rotation by 22%-42%, depending on the height of the building.

Lin et al. (2018) studied the use of an improved viscously damped outrigger. Their outrigger includes a top horizontal chord member on the outrigger truss preventing a break between the perimeter column and the outrigger, allowing the outrigger to maintain some degree of stiffness. They showed that structures that used this new outrigger system showed a larger damping ratio, smaller drifts, and lesser damage.

Morales-Beltran et al. (2018) investigated using multiple viscously damped outriggers. Their study showed that it is economical to use a viscously damped outrigger at 70% and 50% the building height rather than using a single damped outrigger.

Xing et al. (2018) studied using outriggers damped with both viscous dampers and BRBs. The objective of their study was to determine the optimal combination of viscous and BRB dampers. They studied the combination of viscous dampers and BRBs using small scale shake table testing and finite element analysis. The results showed that when using only two energy dissipation outriggers, combining viscous and BRB dampers provided superior performance. However, the performance decreases when more energy dissipation outriggers are used. Their studies showed that it was more beneficial to include the BRB at taller heights than the viscous dampers.

Overall, the current literature shows that the use of outriggers in tall buildings is an effective way to increase the overall performance of the structure. Generally, the optimal location for an outrigger with hysteretic dampers is at 60%-80% of the building height. However, the outrigger is often located at the roof for ease of construction and architectural purposes.

Although the outrigger system is proven to be effective in limiting roof displacements, all current literature assumes a fixed core base, where the core wall ultimately undergoes damage under strong earthquake shaking. The combination of low-damage rocking walls with a damped outrigger system has not yet been investigated.

2.7 Summary and conclusions

In this chapter, a state-of-art review of different high-performance RC wall systems was presented. This chapter demonstrated how, although several other low-damage solutions have been developed for RC walls, few tall building applications have been studied. Further, the few studies on tall buildings have been limited to a small sample size of buildings. Additionally, although some of the latest technology shows increased seismic performance, damage still occurs in wall's base and at the coupling beam wall interface. It follows that there is a gap in knowledge in the development of high-performance, low damage tall RC core wall systems. The following chapter (Chapter 3) presents a new high-performance RC wall system's conceptual development to address this gap in knowledge.

Chapter 3: Mechanism and design considerations of the CROCW

3.1 Overview

In this chapter, a novel high-performance RC core wall system is presented. This system, named the controlled rocking outrigger core wall (CROCW), essentially consists of two independent systems: the controlled outriggered rocking wall (CORW) and the self-centering coupled wall (SCCW). In this chapter, the plastic mechanisms of each system are discussed, and the critical characteristics of each system are described. Specifically, this chapter describes the behaviour of the outrigger system, the mechanics of controlled rocking wall base, and the mechanics and hysteretic behavior of the SCFDs. An essential outcome of this chapter is the derivation of the relative stiffness factor, α_f. This factor is used throughout this thesis (particularly in Chapter 4 and Chapter 5) to analyse the dynamic behaviour and the development of the design procedures for this system.

3.2 Introduction

The literature review in Chapter 2 showed the earthquake-resilient systems' effectiveness to reduce damage on low-rise RC planar walls. However, there has been minimal investigations on low-damage high-rise RC core wall buildings. For example, the experimental studies on controlled rocking systems have been limited to unidirectional loading on low-rise planar walls. Additionally, some of the mechanisms of other low damage plastic hinge walls, such as the Pin shear wall (PSW), are limited to unidirectional and would not function in the bidirectional bending mechanisms required of core walls. Damped coupled walls have demonstrated lower amounts of damage when compared with conventional coupled walls. However, the damage is still observed within the plastic hinge region of the base of the wall. Similarly, damped outrigger systems have been shown to have higher performance and limit damage than RC core walls. However, the damage was still observed within the plastic hinge region. For the aforementioned reasons there is a need for a robust earthquake-resilient tall RC core wall system which can provide limited damage in earthquakes.

This chapter proposes a novel earthquake-resilient RC core wall system that is low-damage under strong earthquake shaking. Two new systems are proposed along each axis of a centralized core wall to improve the coupled wall and shear wall systems' performance. The new system was developed in consultation with engineering practitioners familiar with designing tall buildings across Canada and the USA. Early discussions with these practitioners made evident the necessity of including the RC core wall as part of the SFRS to make the new system more adaptable to the industry. By keeping the RC core wall, these innovative buildings can use similar architectural plans as conventional buildings and the local workforce is trained to build most of the structure, with little need for specialization or re-training.

Figure 3.1 shows the proposed earthquake-resilient RC core wall's conceptual view, called the controlled rocking outrigger core wall (CROCW) system. The newly proposed system is "dual-fused," where two unique energy dissipation mechanisms (primary fuse system and secondary fuse system) act to resist earthquake shaking. In the CROCW system, along one principal axis, the Controlled outriggered rocking wall (CORW) is proposed, a novel system where the primary fuse system is a damped outrigger located at the top of an RC core wall, and the secondary fuse system is a damped controlled rocking base. Along the other principal axis, the Self-centering coupled wall (SCCW) is proposed, where novel self-centring coupling beams which utilize the self-centring conical friction dampers (SCFD), developed by Yang et al. 2020, are used as the primary fuse system, and a damped controlled rocking wall base is used as the secondary fuse system. Dampers within the outrigger and the controlled rocking base use unidirectional friction dampers to uncoupling the damper's stiffness and yield force and combining the CORW and the SCCW results in an interdependent earthquake-resilient core wall system that can resist lateral loads bi-directionally.

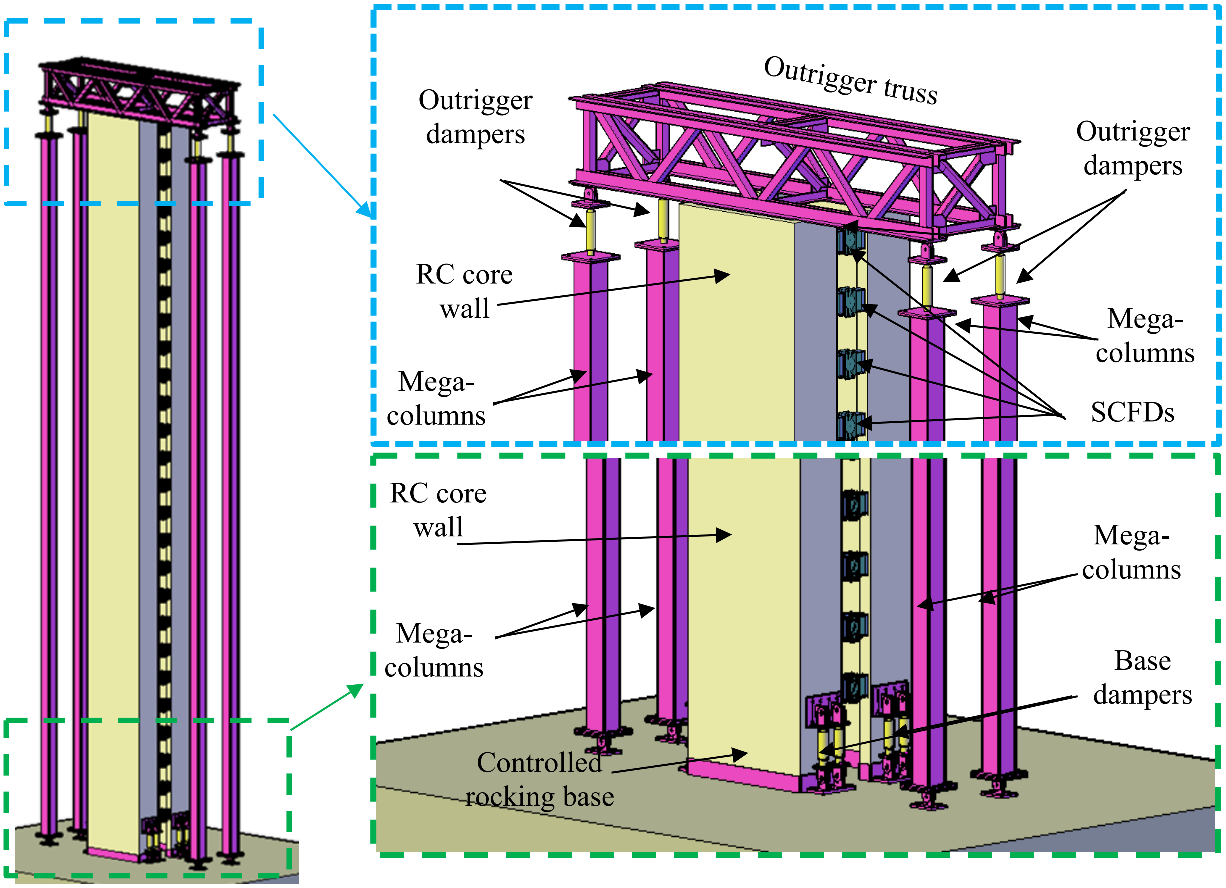

Figure 3.1 Conceptual drawing of earthquake-resilient core wall building

The proposed CROCW system utilises the conventional RC core wall, with three additional new technologies: (1) novel self-centering coupled beams (described in Section 3.3); (2) damped outrigger system (described in Section 3.4); and (3) controlled rocking base (described in Section 3.5). The following sections describe the unique energy dissipation mechanisms and some of the practical considerations in the development of the proposed CROCW system.

3.3 Self-centering coupling beams

The SCCW direction consists of self-centering coupling beams. The self-centering coupling beams are comprised of two embedded steel beams connected with Self centering conical friction dampers (SCFDs), developed by Yang et al. in 2020. Figure 3.2 shows the conceptual view of the self-centering coupling beam. In this configuration, the SCFDs are designed to dissipate the earthquake energy through sliding friction, while the embedded steel beams are designed to remain elastic.

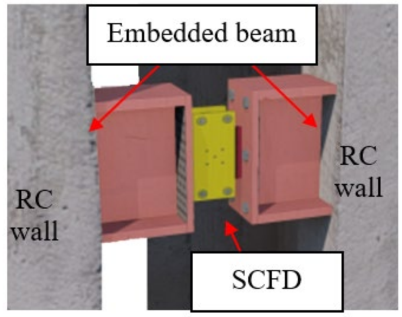

Figure 3.2 Self-centering coupling beam (image courtesy of Hamza Chaudhry)

The SCFD was explicitly developed for the SCCW with significant contributions from the author of this dissertation, however, the primary investigation of the SCFD was conducted as part of Henry Xu's thesis work (Xu, 2020).

Figure 3.3 shows the assembly view of the SCFD. As shown, the SCFD consists of an outer clamp plate A, an outer clamp plate B, and the inner plate. In the configurations presented, end plates are added at the end of clamp plate A and clamp plate B, which can be used to connect the structures. To prevent the relative in-plane rotational movement between the outer clamp plate A and outer clamp plate B, a stopper is added. In the SCFD, the energy is dissipated through sliding friction on both the cone surfaces, and the sliding of the Inner plate and the Outer clamping plate B.

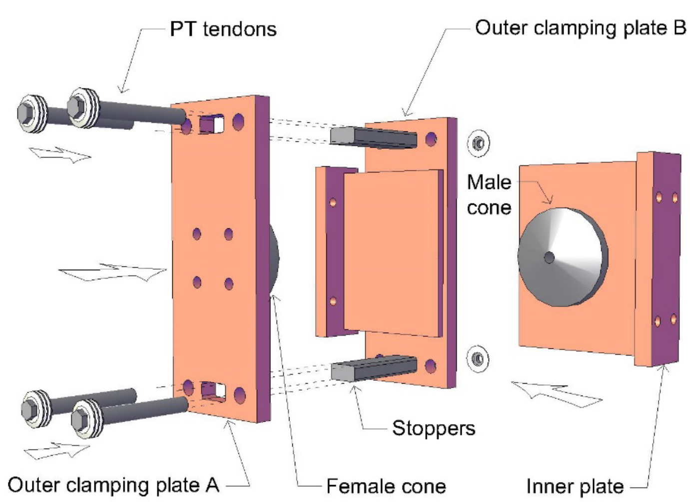

Figure 3.3 Exploded view of SCFD (Yang et al., 2020)

The mechanism of the SCFD is shown in Figure 3.4. As shown, the SCFD is permitted to move in all in-plane directions. The inner and outer plates are confined by a male cone and a female cone.

The SCFD will always self-center due to PT tendons forcing the inner and outer plates back to original position, after any translational movement. The configuration of the SCFD results in two sliding surfaces (between the inner and outer plates), which may be tuned to have different friction coefficients to obtain a desired hysteretic response.

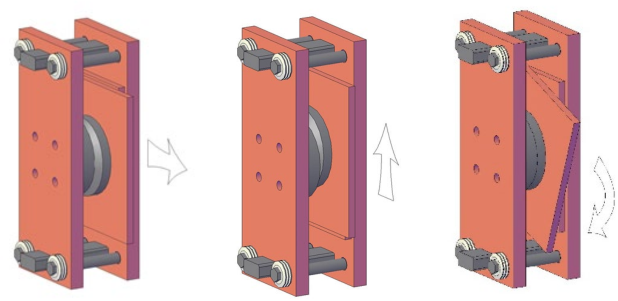

Figure 3.4 SCFD having all-direction motion (from Yang et al., 2020)

Figure 3.5 shows the hysteretic behaviour of the SCFD. The SCFD is designed to slide after the shear force exceeds the initial sliding force, P_0. After that, the SCFD is designed to move with a post-slip stiffness, k_p. When the motion reverses the direction, the SCFD is expected to drop in force to the unloading force P_u. The SCFD is designed to move back to the initial position with the unloading stiffness until it reaches zero displacement with the residual force, P_r.

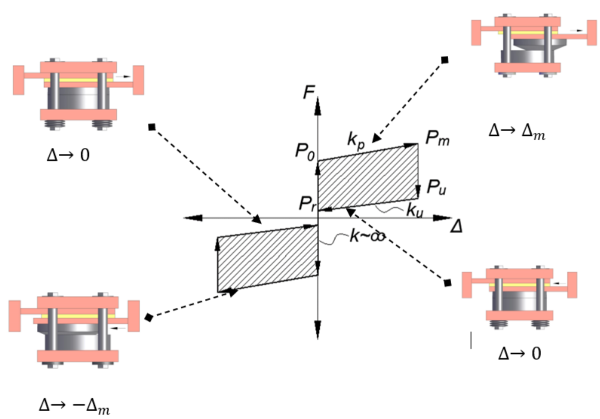

Figure 3.5 Damper movement and the corresponding hysteretic behaviour (Yang et al., 2020)

The derivation of the key hysteretic parameters can be found in Yang et al., 2020, the following is a short summary of these parameters. The initial sliding force, P_0, can be calculated using Equation 3.1. The maximum sliding force, P_m, is shown in Equation 3.2. The post sliding stiffness, k_p, is shown in Equation 3.3.

$$P_0 = F_{pt}^0 \cdot B1 \quad \text{Equation 3.1}$$

$$P_m = \left(F_{pt}^0 + k_{pt} \cdot \Delta_m \cdot tan\theta_c\right) \cdot B1 \quad \text{Equation 3.2}$$

$$k_p = \frac{P_m - P_0}{\Delta_m} = k_{pt} \cdot tan\theta_c \cdot B1 \quad \text{Equation 3.3}$$

where F_{pt}^0 is the initial post-tensioning force in the tendons; B1 relates the cone angle (θ_c), the friction coefficient between the friction pad and the steel plate (μ_f), and the friction coefficient between conical surfaces (μ'), $B1 = \left(\frac{tan\theta+\mu'}{1-\mu'\cdot tan\theta_c} + \mu_f\right)$; Δ_m is the maximum displacement of the SCFD; and k_{pt} is the axial stiffness of the PT tendons.

The unloading stiffness of the SCFD can be calculated based on the geometry and is shown in Equation 3.4.

$$k_u = k_{pt} \cdot tan\theta_c \cdot B2 \quad \text{Equation 3.4}$$

where $B2 = \left(\frac{tan\theta_c-\mu'}{1+\mu'\cdot tan\theta_c} - \mu_f\right)$.

Variables F_{pt}, k_{pt}, and $tan\theta$ must always positive, therefore, $B2$ will govern the sign of the unloading force P_u, the residual force P_r and the unloading stiffness k_u. More specifically, if $B2$ is positive, P_u, P_r, and k_u must be positive. Similarly, if B2 is negative, P_u, P_r, and k_u must be negative. The sign of B2 depends on $\theta_{critical}$, which is a function of μ and μ', and is shown in Equation 3.5. A slope of $\theta > \theta_{critical}$, will result in a positive B2 while a slope of $\theta_c < \theta_{critical}$, results in negative B2. In cases where the slope $\theta_c = \theta_{critical}$, B2 will be zero.

$$\theta_{critical} = \mathrm{atan}\left(\frac{\mu + \mu'}{1 - \mu \cdot \mu'}\right) \quad \text{Equation 3.5}$$

Figure 3.6 shows the different SCFD hysteresis types. In Figure 3.6 (a), (b), and (c) correspond to $B2$= positive, $B2$ = zero, and $B2$ = negative, respectively. Under each of these three cases the SCFD can center itself.

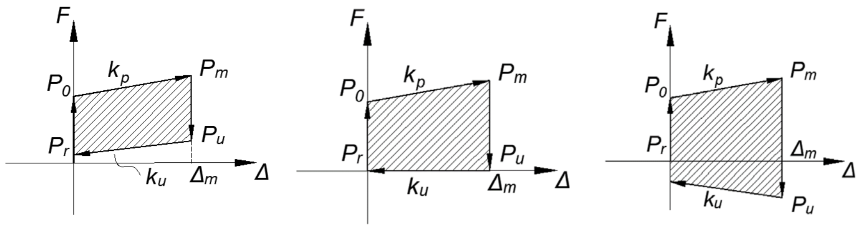

(a) (b) (c)

Figure 3.6 Three different types of hysteresis (a) Type I (b) Type II (c) Type III

3.4 Outrigger system

The outrigger system consists of mega-columns, outrigger dampers, and outrigger trusses or beams (Figure 3.7 (a)). The outrigger system provides the CORW direction with both added stiffness and added energy dissipation. The dampers within the outrigger system use symmetric friction dampers, which have an elastic-perfectly-plastic (EPP) hysteretic behaviour. The outrigger mega-column and beams are designed elastically; hence, the outrigger system has an EPP behaviour.

Mega-columns and outrigger dampers primarily resist axial loads, having a low shear resistance, and can therefore be idealized as a rotational spring (Figure 3.7 (b)). Figure 3.7 (c) shows the response of the equivalent rotational spring, where the spring rotational stiffness is k_o and the yield moment is $M_{o,y}$.

The yielding of the outrigger dampers, which are assumed to have symmetric elastic-plastic behaviour, provides the only nonlinearity in the outrigger system. The remaining outrigger columns and the beams are capacity-designed to remain elastic. Hence, the yield moment of the equivalent spring consists of the damper yield force ($f_{\mathrm{o,y}}$) multiplied by the length of the outrigger truss or beam (L_o), the result is given in Equation 3.6.

$$M_{\mathrm{o,y}} = f_{\mathrm{o,y}} L_o \qquad \text{Equation 3.6}$$

The rotational spring properties can be calculated by assuming the outrigger beam behaves as a beam connected to two springs in series (Figure 3.7 (a)). The first spring in series has the stiffness of the damper (k_d) while the other represents the stiffness of the column (k_c). The equivalent rotational stiffness (k_o) of an outrigger beam is calculated using Timoshenko Beam Theory and is shown in Equation 3.7.

$$k_o = \left[\frac{2L_s}{G_o A_v L_o} + \frac{{L_s}^2}{3E_o I_o L_o} + \frac{2}{k_{com}{L_o}^2}\right]^{-1} \quad \text{Equation 3.7}$$

where k_{com} is the axial stiffness of the column (k_c) and the damper(k_d) in series ($k_{com} = (1/k_c + 1/k_d)^{-1}$; I_o is the moment of inertia of the outrigger beam; L_s is span between the wall and the mega-column; υ is Poisson ratio of the outrigger material; E_o is the elastic modulus of the outrigger material; and L_o is the length of the outrigger beam. In these calculations, the equivalent beam is assumed to have a rectangular cross section with a shear area of $A_v = \frac{5}{6}A_{o,g}$ and a shear modulus of $G = \frac{E_o}{2(1+\upsilon)}$; where $A_{o,g}$ is the gross area of outrigger beam.

It may not always be efficient to use a beam as an outrigger system. For instance, steel beams are limited in the sizes availability, and it would be difficult to obtain the high stiffness required by outrigger systems. As an alternative, designers may use RC beams, however, the RC beams add additional weight, and utilize a significant amount of space. As such, large steel outrigger trusses may be used.

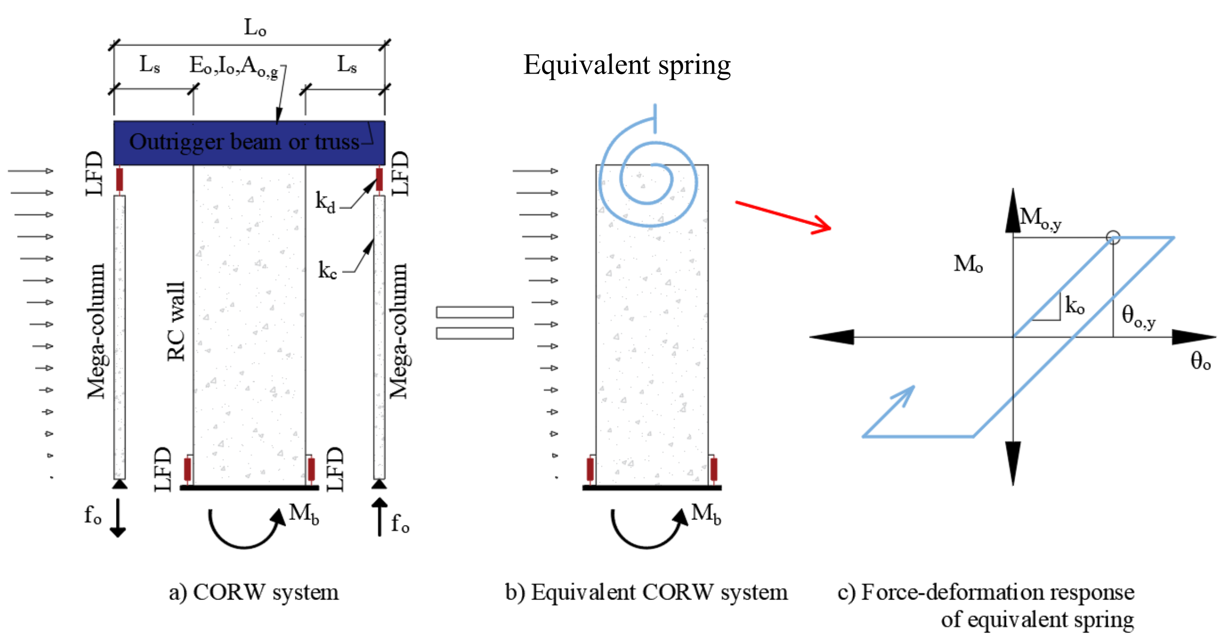

Figure 3.7 Behaviour of the outrigger system in the CORW: (a) CORW system; (b) equivalent CORW system; (c) force-deformation of equivalent outrigger spring.

In some cases, the wall may extend into the truss. This is common when the outrigger is located near mid-height of the building. In this case, the determination of the rotational stiffness assumes that wall is rigid, relative to the truss. Figure 3.8 shows the configuration where the wall extends into the truss system. Equation 3.8 shows the derived equation for a truss system with a rigid wall.

$$k_o = \left(\frac{38L_s}{3E_sA_c\,(\tan^2\theta_t){L_o}^2} + \frac{6d_o}{A_oE_s(\sin^3\theta_t){L_o}^2} + \frac{2d_o}{A_oE_s{L_o}^2} + \frac{2}{k_{com}{L_o}^2}\right)^{-1} \qquad \text{Equation 3.8}$$

where $E_s$is the elastic modulus and A_o, A_c, $\theta_t, L_s, d_o$and L_o are shown in Figure 3.8.

In Figure 3.8 A_o = area of the diagonal vertical truss, Ac = area of the top and bottom chords, Lw = length of the wall, and Ls = span from the wall edge to the centerline of the outrigger column, d_o = outrigger depth, Lo = total length of the truss, and θ_t = angle of inclination of the inside diagonal truss.

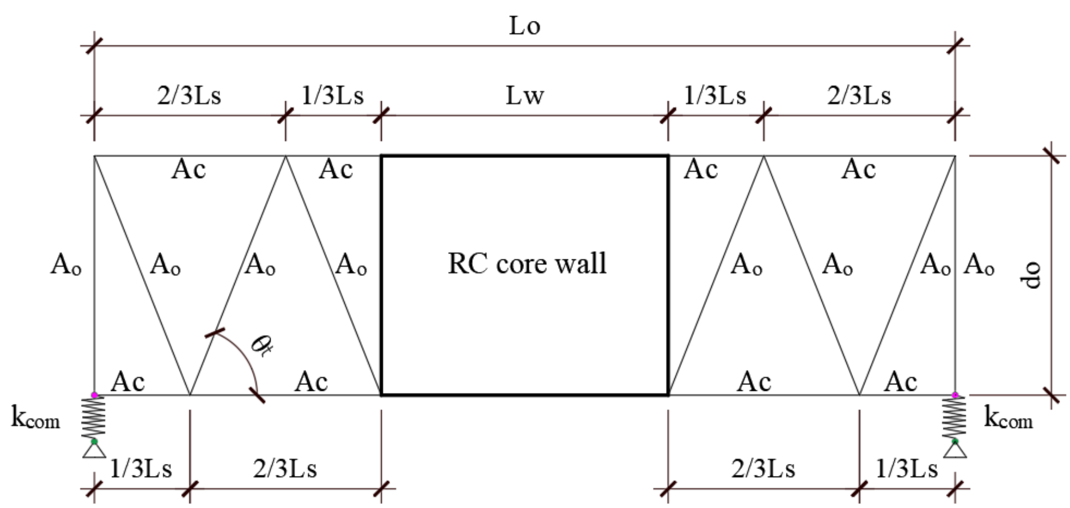

Figure 3.8 Outrigger roof truss configuration

3.4.1 Static behaviour of outrigger system

The addition of rotational stiffness provided by the outrigger system is advantageous as it provides moment resistance to the system as well as rotational stiffness, reducing drifts and displacements. The advantages of the added stiffness from outrigger systems can be exemplified by applying an inverted triangular static loading triangular loading distribution on a Euler-Bernoulli beam (representing the RC core wall) with a rotational spring (representing the outrigger). Using this simple model, the ratio of the outrigger moment (Mo) to the total overturning moment (Mt) can be derived and is shown in Equation 3.9.

$$M_o/\mathrm{M_t} = \frac{(a^3 - 6a + 8)}{8}\alpha_\mathrm{f} \qquad \text{Equation 3.9}$$

where M_o is the moment in the outrigger; M_t is the total overturning moment; a is the ratio of the elevation of the outrigger to the total elevation of the wall; and α_f is a relative stiffness parameter, which is a unitless parameter between 0-1, shown in Equation 3.10. For a cantilever wall with no outrigger, $\alpha_f = 0$. Contrastingly, for an infinitely rigid outrigger, $\alpha_f = 1$.

$$\alpha_\mathrm{f} = \left(\frac{1}{\frac{E_c I_w}{a k_o H} + 1}\right) \qquad \text{Equation 3.10}$$

where E_c is the elastic modulus of the RC wall; I_w is the moment of inertia of the core wall; H is the total height of the wall; and $k_o$is the rotational stiffness of the outrigger system described previously.

Figure 3.9 (a) shows the ratio of outrigger moment to total overturning moment for different relative stiffness factors, α_f, and outrigger locations using Equation 3.9. As shown, higher outrigger stiffness results in more significant outrigger moment resistance. Additionally, the lower the outrigger is situated on the building, the greater the resistance is provided by the outrigger.

The ratio of the outrigger building roof displacement compared with the roof displacement of a system without an outrigger ($\Delta_{\alpha_\mathrm{f}=0}$) is shown in Equation 3.11. As shown, for this theoretical model, this ratio is entirely dependant on a and α_f.

$$\Delta/\Delta_{\alpha_\mathrm{f}=0} = 1 - \frac{5}{22}\mathrm{a}\alpha_\mathrm{f}(2 - a) \qquad \text{Equation 3.11}$$

Figure 3.9 (b) graphically shows Equation 3.11 under different a and α_f . As shown, the outrigger is most effective when located near the top of the building, where a rigid outrigger ($\alpha_\mathrm{f} = 1$) gives a 70% reduction in roof displacements. Additionally, the result shows that outrigger stiffness is more sensitive at locations high in the building. Hence, there is more benefit to adding stiffness to the outrigger near the top of the building rather than at near the bottom for this model. It is important to note that these are theoretical relations under static loads, and the behavior of the outrigger system will depend on the dynamic characteristics. The dynamic characteristics are analysed in more detail in *Chapter 4: Dynamic characteristics of proposed earthquake resilient RC core wall system* of this dissertation.

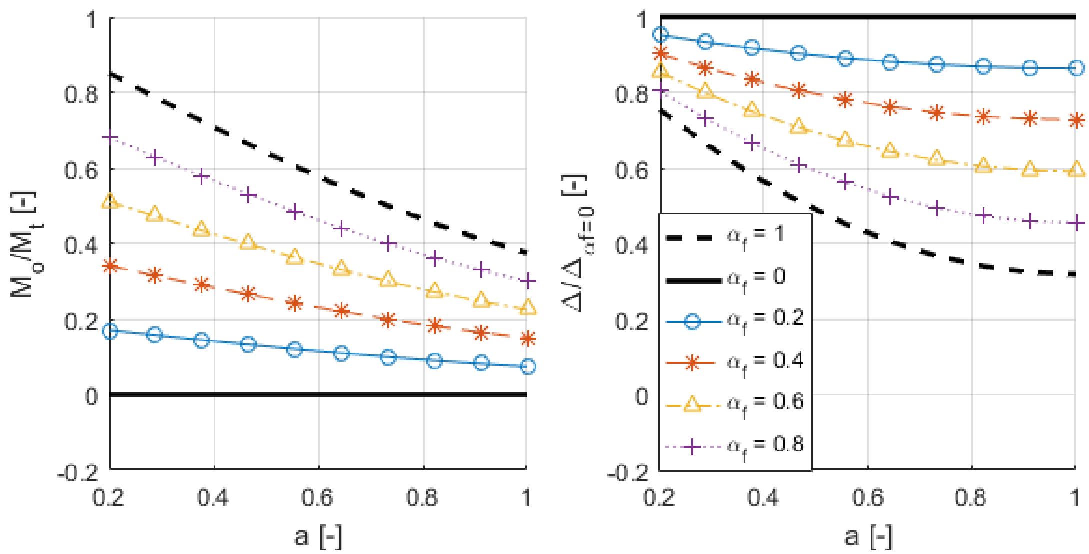

(a) (b)

Figure 3.9 Ratio of elastic static response of outrigger systems comparing the (a) outrigger moment to the total overturning moment and (b) the roof displacement compared to the displacement of a system without an outrigger (i.e., distribution of outrigger $\alpha_f = 0$)

3.5 Controlled rocking base

The controlled rocking base was selected as the CROCW's secondary fuse system to ensure a low-damage response under high intensity, bidirectional earthquake shaking. Figure 3.10 shows the conceptual view of the controlled rocking base, exemplified on a RC core wall. It is important to note that experimental studies at the time of writing this dissertation are limited to planar walls, and therefore, there are no studies on flanged walls.

Typically, research has shown that controlled rocking bases can have a good performance if the design consists of a wall-base damper, bedding layer, base armouring, and a shear key. In this study, the wall-base dampers utilise symmetric friction dampers. Friction dampers are ideally suited to the controlled rocking base, as the rigid stiffness of the dampers allow them to be near instantly engaged at the onset of rocking.

A layer of high-strength grout placed between the foundation and the rocking wall is called a bedding layer. Research has shown that bedding layers provide a flat surface makes the rocking behavior consistent and predictable, while not including bedding layers results in severe damage at the underneath contacting surface (Henry, 2011).

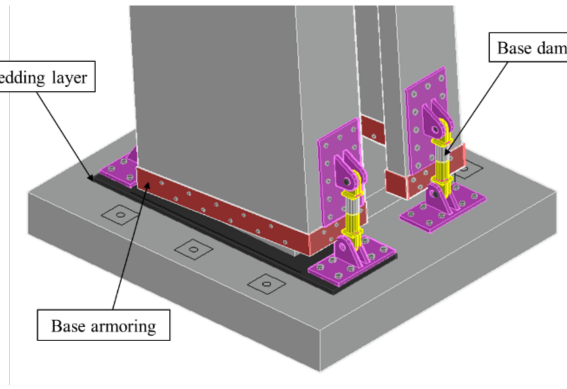

Figure 3.10 Conceptual view of controlled rocking base (courtesy of Tianyang Qiao)

Base armouring is used to protect the wall from local damage, due to concentration of compression stress on the area which the wall contacts the foundation. There are various methods to include base armouring. For example, Marriott et al. (2008) proposed and tested a rocking wall system which included confining steel channels which were welded reinforcing bars are specially designed to protect rocking toes, shown in Figure 3.11. This system resulted in minimum damage after many cycles of testing.

Figure 3.11 Base armouring specimen example (Marriott et al. (2008))

Ensuring sufficient shear restraints is also a key component of controlled rocking base design. For many controlled rocking applications, the expected sliding friction resistance is sufficient However, additional mechanical shear restraints may be provided, such as a shear key may be provided.

Figure 3.12 (a) shows the controlled rocking base in the CORW system, and Figure 3.12 (b) shows the global base moment–rotation (i.e., $\mathrm{M_b} - \theta_b$) relationship of the controlled rocking base and the local force-deformation (i.e., f_b-δ_b) relationship of the base dampers at different stages of cyclic loading. As shown in Figure 3.12, the yielding base moment ($M_{b,y}$) is a combination of the restoring force from axial load (P_g) and the yielding force of the dampers ($f_{b,y}$). The yielding base moment ($M_{b,y}$) can be estimated using Equation 3.12.

$$\mathrm{M_{b,y}} = \mathrm{f_b}(\mathrm{L_w} + 2\mathrm{L_d}) + \mathrm{P_g}\mathrm{L_w}/2 \qquad \text{Equation 3.12}$$

where $f_{b,y}$ is the yield force of the base damper; L_w is the length of the wall; L_d is the length from the edge of the wall to the damper; and P_g is the axial load in the wall.

As shown in Figure 3.12, the initial loading portion of the force-deformation relation of the controlled rocking base is governed by the wall's elastic behaviour (Segment 1, which is between the origin and point A). After Point A, the wall rocks, and the base dampers are engaged (Segment 2, which is between points A and B), and the global stiffness is controlled by a combination of the base dampers and the wall in series. If the base damper can be approximated as a rigid-perfectly plastic behaviour, then the global stiffness between Points A and B can be approximated using the elastic stiffness of the wall. However, if the damper has elastic-plastic behavior, the stiffness between point A and B will represent the elastic stiffness of the wall and the elastic stiffness of the damper in series.

After Point B, the base damper will start to yield, and the force-deformation of the controlled rocking base system plateaus (Segment 3, which is between points B and C). At Point C the loading is reversed, and the force-deformation of the controlled rocking base follows the same stiffness as in Segment 2. At point D, the damper has unloaded, such that it has zero force, but residual deformation. Between points D and E, this vertical displacement in the wall is reduced to zero, through forcing the damper into compression. At Point E the dampers have reached yielding in compression (Segment 5, which is between points E and F), at which point the force in the controlled rocking base develops a plateau. Once the wall closes the gap from rocking, the force-deformation response follows the stiffness of the wall (Segment 1).

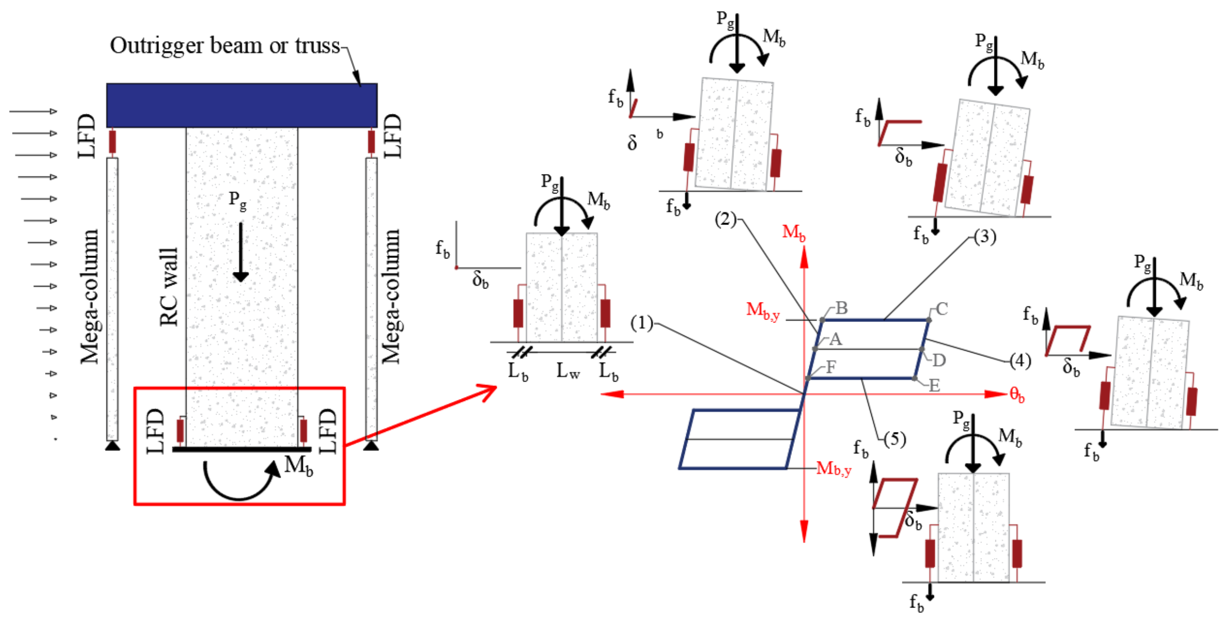

a) CORW system

b) Controlled rocking base behavior

Figure 3.12 Behaviour of the controlled rocking base: (a) CORW system and (b) Controlled rocking base behaviour

The behaviour of controlled rocking in the SCCW direction is complex when considering the interdependence of the coupling beam forces and the wall base. The yielding of coupling beams under lateral loads induces a substantial uplift force in one of wall piers, referred to as the “tension wall”, and an equal opposite compression force in the other wall pier, referred to as the “compression wall”.

The application of these tension and compression forces results in different rocking capacities at the base of each wall pier. Figure 3.13 shows an example free-body diagram of forces at the base of a SCCW wall. From the free-body diagram, the moment is derived and shown in Equation 3.13 and Equation 3.14 for tension wall pier moment ($M_{T,c}$) and compression wall pier moment ($M_{C,c}$), respectively. In Figure 3.13, B_w is the width of the wall pier; x_{cg} is the distance from the rocking toe to the wall centroid; and P_P is the contribution from the coupling beams; fdt is the damper force in the "tension wall"; f_{dc} is the damper force in the "compression" wall, and P_g is the gravity force of the wall pier

$$M_{T,c} = f_b B_w/2 + (P_g - P_p)(B_w - x_{cg}) \quad \text{Equation 3.13}$$

$$M_{C,c} = (P_g + P_p)(x_{cg}) + f_b B_w/2 \quad \text{Equation 3.14}$$

where P_g is the gravity load in one wall pier; P_P represents the coupling axial force.

In a static pushover analysis P_P would simply be the summation of the forces within all coupling beams. However, it is well established that coupling beam shears have a high mode response which results in many of the coupling beams shearing in different directions along the height of the wall. As a result, the axial force (P_p) can be lower than the summation of the yield force. These dynamic characteristics are further analysed in *Chapter 4: Dynamic characteristics of proposed earthquake resilient RC core wall system* of this dissertation.

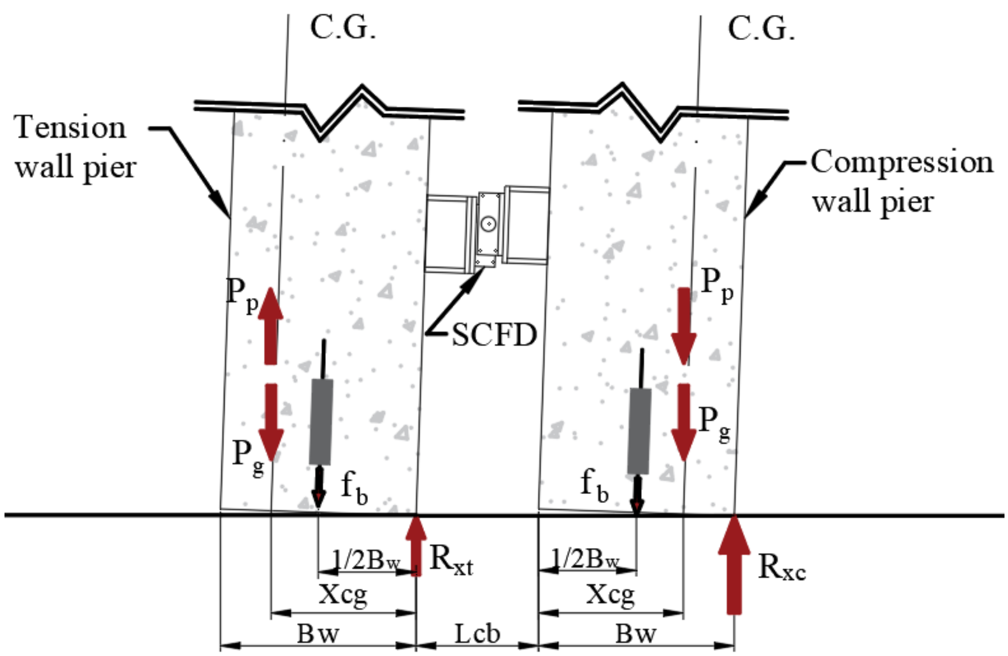

Figure 3.13 Rocking mechanism free-body diagram.

3.6 Summary

This chapter proposed two new low-damage SFRSs for tall building application: the controlled outriggered rocking wall (CORW) and the self-centring coupled wall (SCCW). Combined, these systems form a third system called the controlled rocking outrigger core wall (CROCW) system. These systems are "dual-fused" and have a primary fuse system and a secondary fuse system.

The CORW primary fuse system is a damped outrigger, and its secondary fuse system is a damped controlled rocking base. This chapter presented equations to relate the dampers to the wall moment and estimate the outrigger system's stiffness. Additionally, this chapter presented the controlled rocking base's hysteretic behaviour and equations that relate the wall base moment to the damper forces.

The SCCW system's primary fuse system consists of novel self-centring coupling beams called Self-centering conical friction dampers (SCFDs), and its secondary fuse system is a damped controlled rocking base. This chapter presented the behaviour of the SCFD and equations to estimate the hysteretic response. Additionally, this chapter presented some of the challenges of designing a controlled rocking coupled wall system. Equations that relate the wall base moment to the damper forces were presented.

Using a controlled rocking base as the secondary fuse mechanisms in the CORW and SCCW allows this system to function efficiently under bidirectional loading. This chapter's outcome is two unique systems that may be integrated into a centralised core wall to create a third unique system called the CROCW—as a low-damage solution to RC core walls.

This chapter presented plastic mechanisms and some high-level design considerations of the CROCW, CORW and SCCW systems. In the following chapter (Chapter 4), the CROCW, CORW and SCCW systems' dynamic characteristics are explored, and empirical design equations for estimating the dynamic responses are presented.

Chapter 4: Dynamic characteristics of proposed earthquake resilient RC core wall system

4.1 Overview

In this chapter, the CORW and SCCW systems' key dynamic characteristics were identified using modal response spectrum analysis. This chapter proposes new empirical equations, developed based on parametric analysis, which can estimate the dynamic response of the CORW and SCCW systems. These equations and factors are later used to modify the EEDP developed in Chapter 5.

4.2 Introduction

Understanding the dynamic characteristics of the proposed CROCW systems is critical in developing the design procedures later described in Chapter 5. In this chapter, the dynamic characteristics were studied using Linear dynamic analysis (LDA). The trends observed in LDA give insights into the seismic response of multi-degree-of-freedom (MDOF) structures. LDA is often used in performance-based design to estimate the response of structures expected to undergo minimal inelastic behaviour, such as assessing the SLE hazard (LATBSDC, 2020). Additionally, building codes have long since permitted the use of LDA to estimate seismic design demands on structures, even though these structures are expected to experience extensive inelastic behaviour (NBCC 2015 and ASCE, 2016). For these reasons, LDA, specifically, Modal response spectrum analysis (MRSA), was used in this chapter to study the seismic response of the proposed CROCW system.

MRSA was used to estimate the proposed earthquake-resilient RC core wall system's dynamic response. The MRSA was programmed using MATLAB (2016) and OpenSees (PEER, 2000). A total of 1920 archetype buildings with unique building geometry were developed. The archetype buildings were analysed using two different design spectra (Vancouver and Montreal) to understand the effect of spectral shape on the dynamic response. Empirical design equations were developed. The results showed that the recommended equations could estimate the dynamic response reasonably well.

4.3 Archetype development for parametric analysis

The archetype buildings, shown in Figure 4.1, are composed of two symmetric C-shaped walls which have an outrigger in the shear wall direction (along the X-axis) and coupled along the other (along the Y-axis). Figure 4.1 (a), (b), and (c) shows the generic X-axis elevation view, Y-axis elevation view, and the plan view of the archetype buildings, respectively. In all analyses, the thickness of the wall in the coupled direction (t_f) is assumed to be 1.3 times the thickness of the wall in the shear wall direction (t_w). The RC elastic modulus, E_c, is assumed to be 30 GPa for all buildings. A variety of parameters were studied, including: the story height (h_f), number of floors (n_f), length of coupling beam (L_{cb}), length of core in y-axis ($L_{w,y}$), length of core in x-axis direction ($L_{w,x}$), web wall thickness (t_w), flange wall thickness (t_f), and story mass (m_f). Additionally, a characteristic property unique to the CORW, called the relative stiffness factor (α_f), and a characteristic property unique to the SCCW, called the coupling beam relative stiffness factor (α_c), ranged between 0-1 were developed. Table 4.1 shows the parameters included in this study.

The relative stiffness parameter, α_f, shown in Equation 3.10 below is a unitless parameter which defines the relative stiffness of the outrigger and the RC core wall in the CORW system. The relative stiffness parameter, α_f , is a function of the rotational stiffness of the outrigger (k_o defined in Chapter 3), the elastic modulus of the concrete (E_c), the gross moment of inertia of the wall ($I_{w,y}$) and the height of the wall (H). The relative stiffness factor differentiates the CORW from a cantilever wall system: a cantilever wall without an outrigger has a relative stiffness factor of α_f = 0, while an infinitely rigid outrigger has a relative stiffness factor of $\alpha_f = 1$. The value of α_f does not influence the behaviour of the SCCW.

$$\alpha_f = \left(\frac{1}{\frac{E_c I_{w,y}}{k_o H} + 1} \right) \qquad \text{from Equation 3.10}$$

The coupling beam relative stiffness factor, α_c, shown in shown in Equation 4.1, is a unitless parameter which relates the stiffness of the coupling beams to the RC core wall stiffness in the SCCW system. A value of 1 indicates that the coupling beams are infinitely rigid, while a value of α_c = 0 indicates that the coupling beams do not provide any stiffness. Essentially, a value of α_c=1 indicates the two C-shaped walls act like a single cross section in bending, while a value of α_c= 0 indicates that the two C-shaped walls act as individual cantilever walls in bending. The value of α_c does not influence the behaviour of the CORW.

$$\alpha_c = \frac{1}{1 + \frac{\mathrm{E_c} A_w}{H \sum_{x=1}^{n_f} k_{cb,x}}} \qquad \text{Equation 4.1}$$

where $\mathrm{k_{cb,x}}$ is the shear stiffness of the coupling beam at a given floor, x.

Each archetype is analyzed for two different sites (downtown Vancouver and downtown Montreal) in Canada. The spectra are taken from the National Building Code of Canada (NBCC, 2015). These spectra were selected to provide sufficient variability in the spectra shape. Figure 4.2 shows the two response spectra normalized to the maximum spectral acceleration (max (Sa) is 0.85g and 0.45g for Vancouver and Montreal, respectively) to demonstrate the variation in spectra shape. As shown, the two spectra give suitable variations in spectral shape, where the Montreal site has a steeper drop in spectral accelerations for natural periods greater than 0.1s, when compared with Vancouver.

Systematically varying these properties, assuming the CORW and SCCW directions are analysed as individual models, results in 1920 unique building models, noting that α_f and α_c are independent of the direction, and considering the two different site spectrum results in 3840 individual MRSA.

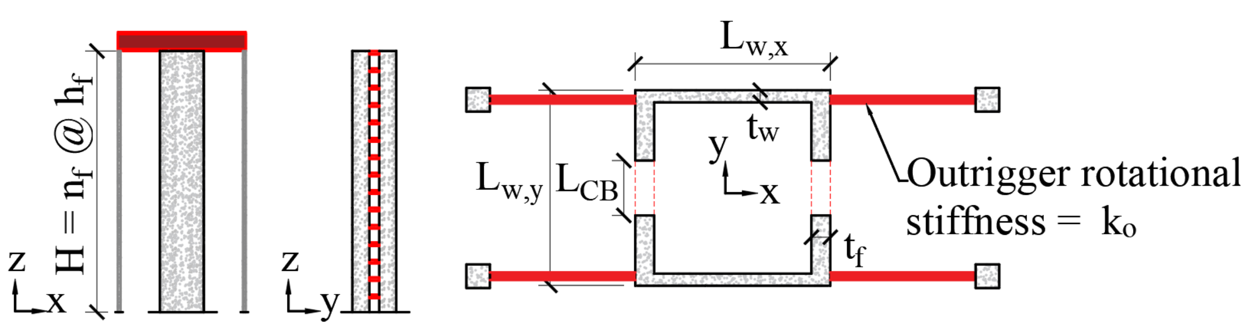

Figure 4.1 Parameters studied for earthquake-resilient core wall: (a) CORW elevation view; (b) SCCW elevation view; and (c) plan view.

Table 4.1 Summary of the prototype models used for the higher mode effect study

Property	Variable	Value	Units
Number of stories	n_f	15, 30, 45	
Floor height	h_s	3, 4	m
Mass per floor	m_f	600, 800	tonne
SCCW wall length	$L_{w,y}$	8, 12	m
CORW wall length	$L_{w,x}$	8, 12	m
Length of coupling beam	L_{CB}	1.5, 2.5	m
Thickness of wall web	t_w	0.6, 1	m
Coupling beam stiffness parameter	α_c	0.5, 0.6, 0.7, 0.8, 0.9	
Relative stiffness parameter	α_f	0.1, 0.3, 0.5, 0.7, 0.9	

Note: Total number of models = $N_{dis} x N_{nf}$ x N_{hs} x N_{mf} x $N_{Lw,y}$ x $N_{Lw,x}$ x N_{LCB} x N_{tw} x N_{α} = 2 x 3 x 2 x 2 x 2 x 2 x 2 x 2 x5 = 1920

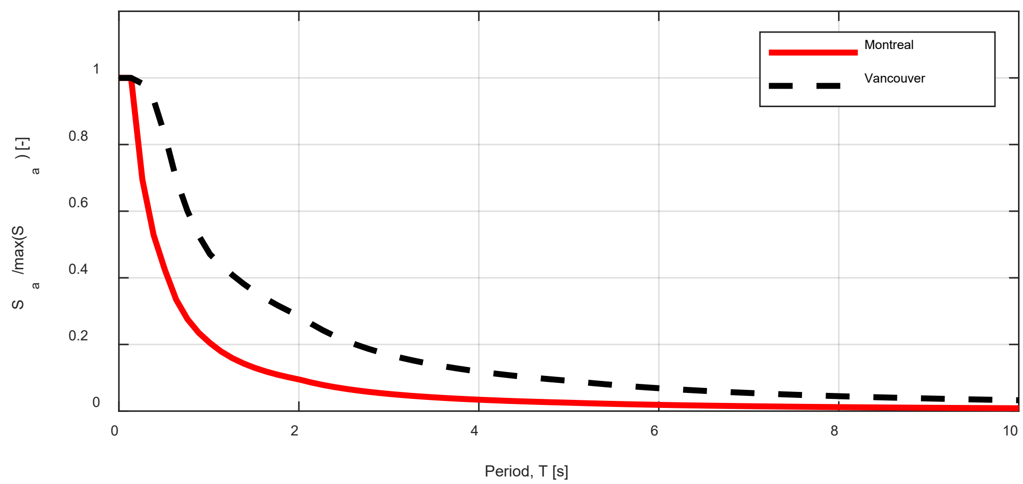

Figure 4.2 Normalized uniform hazard spectrums for Montreal and Vancouver. In this figure Sa is the spectral acceleration and T is the structural period.

4.4 Numerical models

The structural models were developed using OpenSees (PEER, 2000). For computational efficiency, the models CORW and SCCW directions are analyzed independently using 2-dimensional models. Figure 4.3 (a) and Figure 4.3 (b) shows the modeling approach for the CORW and the SCCW, respectively. Masses are considered equally distributed at each story level. The RC core walls are assumed to have a constant cross section over the building height, as a result, the inter-story stiffness is a constant value for every story. The RC core walls are modeled using *BeamColumn* elements. The coupling beams are modelled using elastic shear-springs with a stiffness, k_{cb}, centered on rigid beam elements. The outrigger is modeled using an elastic spring with a rotational stiffness, k_o. The controlled rocking base is assumed rigid until yielding is initiated, hence, in these models, the base is assumed fixed.

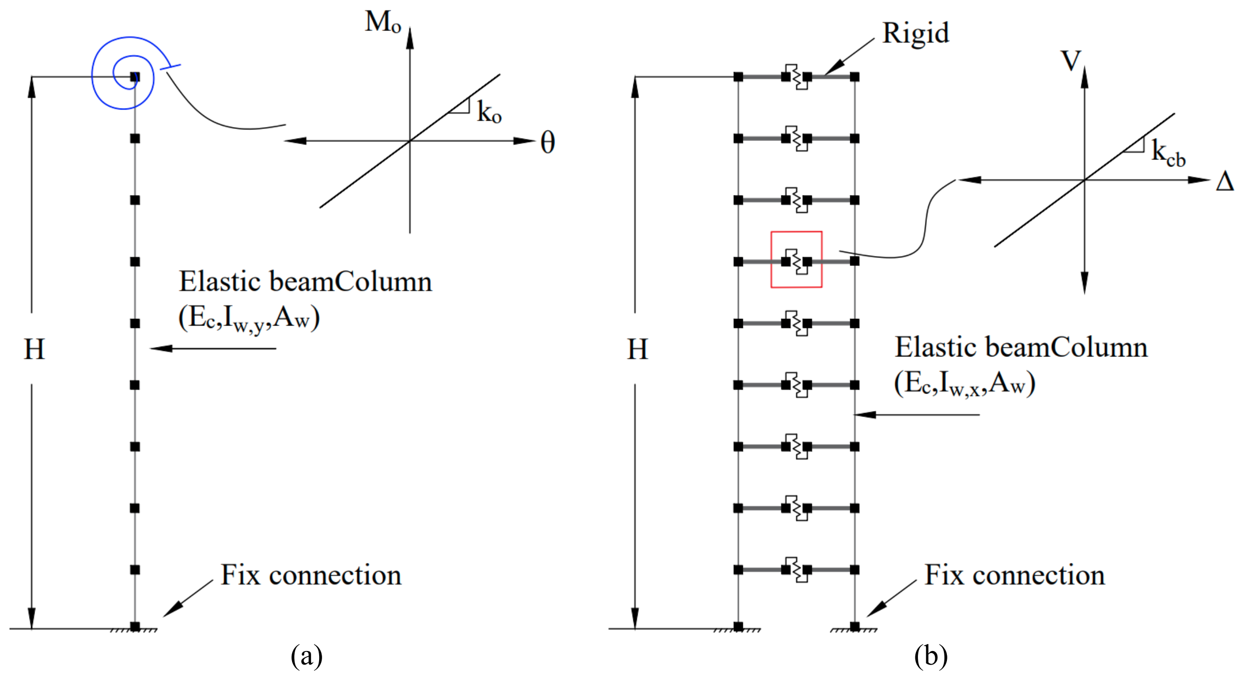

Figure 4.3 Modeling approach for higher mode effects for (a) CORW and (b) SCCW.

4.5 Linear dynamic analysis of CORW system

Eigenvalue analysis was conducted on each of the 960 unique prototype building geometry in the CORW direction and MRSA was conducted on each of the two building sites, resulting in 1920 analysis in the CORW direction. The following sections described the dynamic response of the CORW system and empirical equations used to estimate this response, the values from the analysis are tabulated in Appendix A.

4.5.1 Natural periods of vibration (T_1, T_2, T_3)

Equation 4.2, Equation 4.3, and Equation 4.4 shows empirical equations for the first, second and third modal periods of the CORW, respectively. Figure 4.4 shows comparison of the results obtained from the MRSA vs. the predicted equation. The result shows the equations provided can predict the structural period very well. In general, as α_f increases, the period decreases. But the maximum reduction is only 37%, which implies that increasing stiffness of the outrigger has a limited effect on the structural period.

$$T_1 \approx (1 - 0.37\alpha_f) T_{1_{\alpha_f=0}} \quad \text{Equation 4.2}$$

$$T_2 \approx \frac{(1 - 0.37\alpha_f)}{6} T_{1_{\alpha_f=0}} \quad \text{Equation 4.3}$$

$$T_3 \approx \frac{(1 - 0.37\alpha_f)}{16} T_{1_{\alpha_f=0}} \quad \text{Equation 4.4}$$

where α_f is the relative stiffness factor for the outrigger and $T_{1_{\alpha_f=0}}$ is the natural period of the system without an outrigger (i.e., α_f = 0) and is estimated using Equation 4.5.

$$T_{1_{\alpha_f=0}} \approx 1.86 \sqrt{\frac{WH^3}{gE_c I_{w,y}}} \quad \text{Equation 4.5}$$

where W is the total weight; H is the wall height; E_c is the modulus of elasticity of RC; g is the acceleration due to gravity (g = 9.81m/s^2) and $I_{w,y}$ is Moment of inertia of the core wall

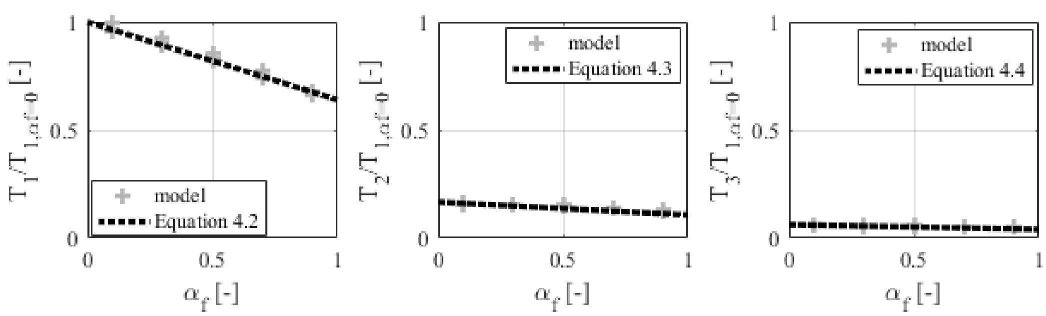

Figure 4.4 Natural frequencies using recommended equation (960 archetype models)

4.5.2 Modal mass participation

The modal mass participation factors for the first three modes are shown in the Figure 4.5. The mode mass participation is between 60-85%, 16%-20%, and 5%-9% for the first, second, and third modes, respectively.

Empirical equations for the first, second, and third modal mass participation is shown in Equation 4.6, Equation 4.7, Equation 4.8, respectively. As shown in Figure 4.5, the modal mass participation factor is dependent on α_f, where higher α_f results in increased mass participation in the first mode and decreased in the second and third modes. Hence a more rigid outrigger will result in a more significant first mode response.

$$Massparticipation(Mode1) \approx 62 + 9\alpha_f[\%] \qquad \text{Equation 4.6}$$

$$Massparticipation(Mode\ 2\ ) \approx 20 - 6\alpha_f[\%] \qquad \text{Equation 4.7}$$

$$Massparticipation(Mode\ 3\ ) \approx 7 - 2\alpha_f[\%] \qquad \text{Equation 4.8}$$

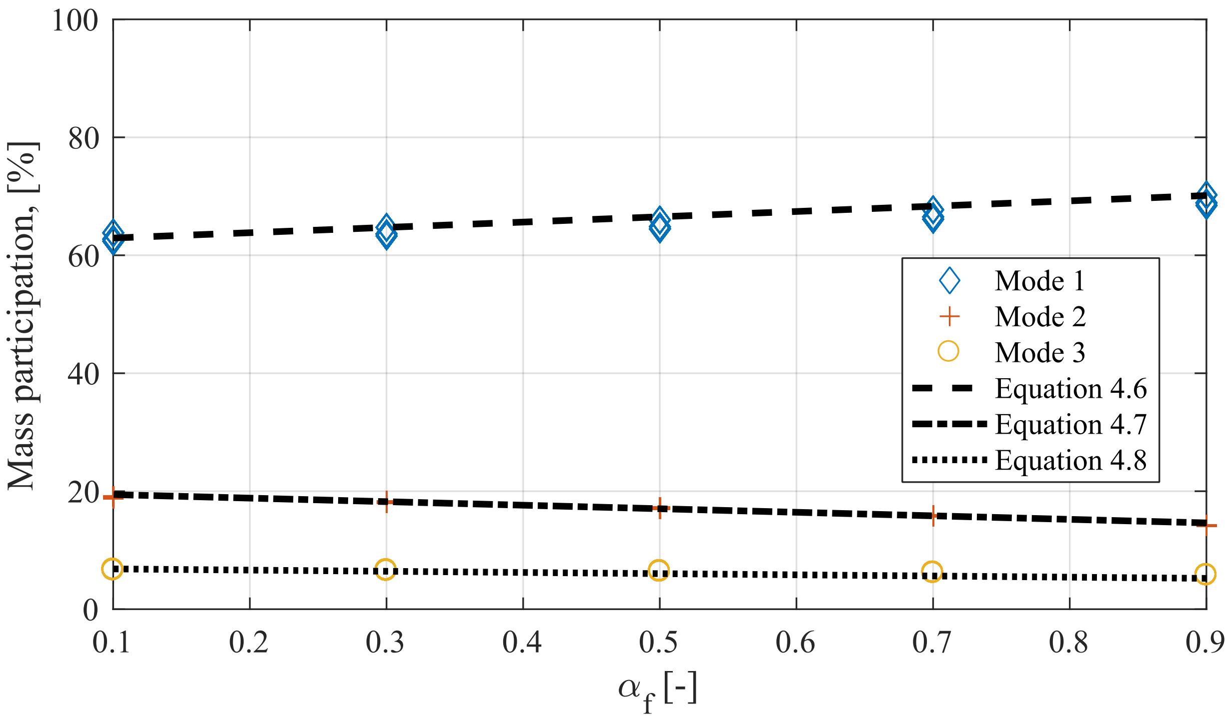

Figure 4.5 Modal mass participation factors for CORW (960 archetype models)

4.5.3 Comparison of SDOF displacement to MDOF displacements (C_0)

The C_0 factor relates the roof displacement of the MDOF system to the SDOF system. Equation 4.9 shows the C_0 factor obtained from the period data. In general, as α_f increases, the C_0 decreases. Figure 4.6 shows the comparison of the C_0 value obtained from MRSA and the Equation 4.9. The result shows Equation 4.9 can predict C_0 well.

$$C_0 = \frac{\Delta_r}{S_d} = 1.55 - \frac{0.05\alpha_f}{1.2 - \alpha_f} \qquad \text{Equation 4.9}$$

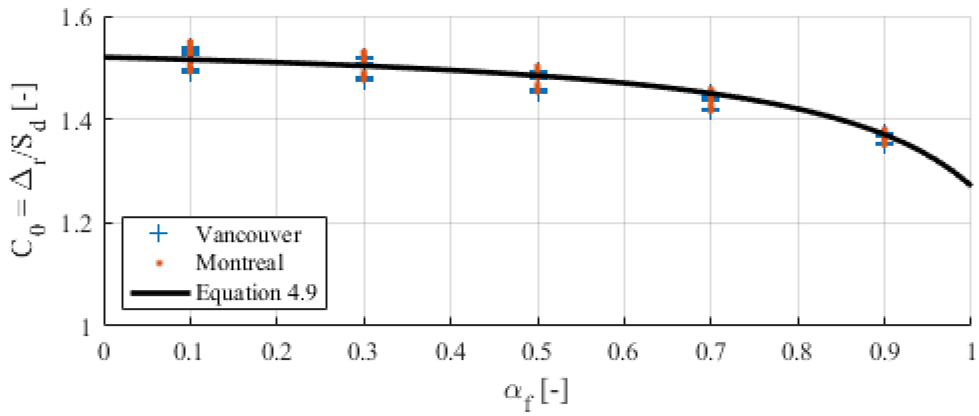

Figure 4.6 Ratio of the multi-degree-of freedom (MDOF) roof displacements to the single-degree-of-freedom (SDOF)

4.5.4 Comparison of outrigger rotation and RDR (C_θ)

Figure 4.7 shows the C_θ value, which is obtained from normalising the peak outrigger rotation (θ_o) to the peak roof drift ratio (RDR). The RDR is the ratio of the roof displacement (Δ_r) and the building height (H). RDR is often used in designs for estimating the deformation demands on structures and components. As shown, C_θ is highly dependent on α_f, where higher α_f results in a low C_θ. Based on these trends an empirical relation, shown in Equation 4.11, was developed. Equation 4.11 was developed to use for design purposes, as a result, the equation intentionally overestimates the response. As shown in Figure 4.7, the proposed Equation 4.11 gives a reasonable estimate of the model response trend.

$$C_\theta = \frac{\theta_o}{\text{RDR}} = 2 - 1.5\alpha_f \leq 1.5 \qquad \text{Equation 4.10}$$

where θ_o is the outrigger rotation and RDR is the roof drift ratio.

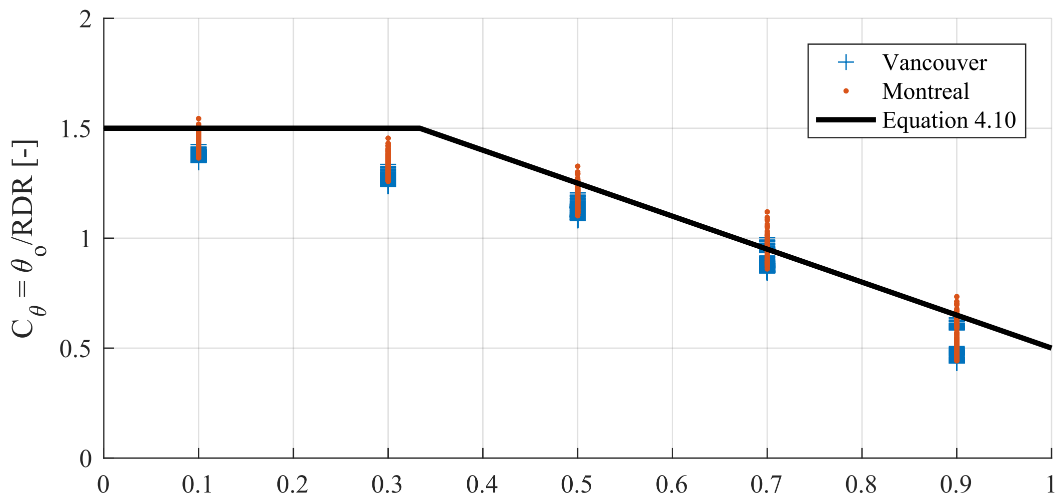

Figure 4.7 Ratio of the outrigger rotation (θ_o) and the roof drift ratio (RDR)

4.5.5 Comparison of SDOF shear to MDOF shear ($\mathbf{M_v}$)

In this section the base shear from MRSA was compared with the base shear determined by multiplying the first mode spectral acceleration with the weight of the building (W). This ratio is referred to, M_v, by the National building code of Canada (NBCC, 2015). It was observed that M_v was highly dependent on spectral shape. Figure 4.8 shows the relation between Mv and the spectral shape ratio (i.e., $S_a(T_2)/S_a(T_1)$). As shown in the figure, M_v is less than one when the spectral acceleration ratio is low (i.e., flatter spectral shape) and the M_v ratio increases in value with higher spectral acceleration ratios (i.e., steeper spectral shape).

Based on the above-mentioned trends, the following empirical relation, shown in Equation 4.11, was developed to estimate the higher mode shear response. Equation 4.11 is intended to assist with design, as a result it is conservatively limited to a minimum value of 1.

$$M_v = 0.3\frac{S_a(T_2)}{S_a(T_1)} - 0.2 \geq 1 \qquad \text{Equation 4.11}$$

where $S_a(T_2)$ is the spectral acceleration at the second mode period and $S_a(T_1)$ is the first mode period.

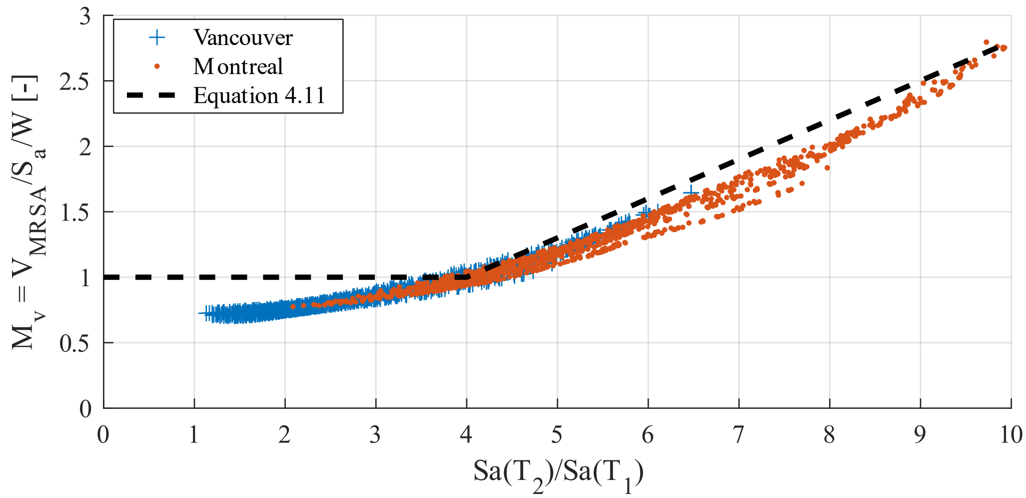

Figure 4.8 M_v ratio for CORW wall systems

4.5.6 Comparison of first mode vs the MRSA response

The MRSA responses were determined by combining the first 4 modes (over 90% modal mass participation). Figure 4.9 (a), (b), and (c) compares the ratio of first mode response to the combined response with spectral shape for roof displacements, overturning moment, and base shear, respectively.

The spectral shape is represented by the spectral shape ratio (i.e., $S_a(T_2)/S_a(T_1)$) of second mode spectral acceleration, Sa(T2), to first mode spectral accelerations, Sa(T1). A more constant spectral shape would be represented by a ratio which approaches unity (i.e., $S_a(T_2)/S_a(T_1) \rightarrow 1$), while a spectral shape which has a steeper slope is represented by a high ratio (i.e., $S_a(T_2)/S_a(T_1) \rightarrow \infty$).

Figure 4.9 (a) shows the ratio of the peak displacement from the first mode (Δ_{mode1}) to the peak displacement from MRSA (Δ_{MRSA}) compared with the spectral shape ratio (i.e., $S_a(T_2)/S_a(T_1)$). The result shows that the peak roof displacement is entirely dominated by the first mode response for all spectral shape ratios. Design spectrums often have low spectral displacements at low period, as a result, the low periods from higher modes result in smaller contributions to roof displacement. The spectral shape combined with the dominate modal mass participation of the first mode drives the observed first mode displacement response.

Figure 4.9 (b) shows the ratio of the peak moment from the first mode ($\mathrm{M_{mode1}}$) to the peak moment from MRSA (M_{MRSA}) compared with the spectral shape ratio (i.e., $S_a(T_2)/S_a(T_1)$). The result demonstrates that moment is highly influenced by the first mode response for spectral shape ratios less than 5. As the spectral shape ratio increases, the overturning moment has a more significant higher mode response, where 10%-30% of the responses are from higher modes. The Montreal site has a more significant higher mode response than the Vancouver site. This difference can be attributed to the Montreal design spectrum having a steeper spectral acceleration slope, resulting in a higher ratio of low period acceleration to high period acceleration.

Figure 4.9 (c) shows the ratio of the peak shear from the first mode (V_{mode1}) to the peak shear from MRSA (V_{MRSA}) compared with the spectral shape ratio (i.e., $S_a(T_2)/S_a(T_1)$). The result shows that the shear response is strongly governed by higher modes for spectral shape ratios greater than 1. For spectral ratios greater than 5, over 50% of the response is governed by higher modes. Like overturning moment, base shear has a more a more significant higher moment response for the Montreal spectrum.

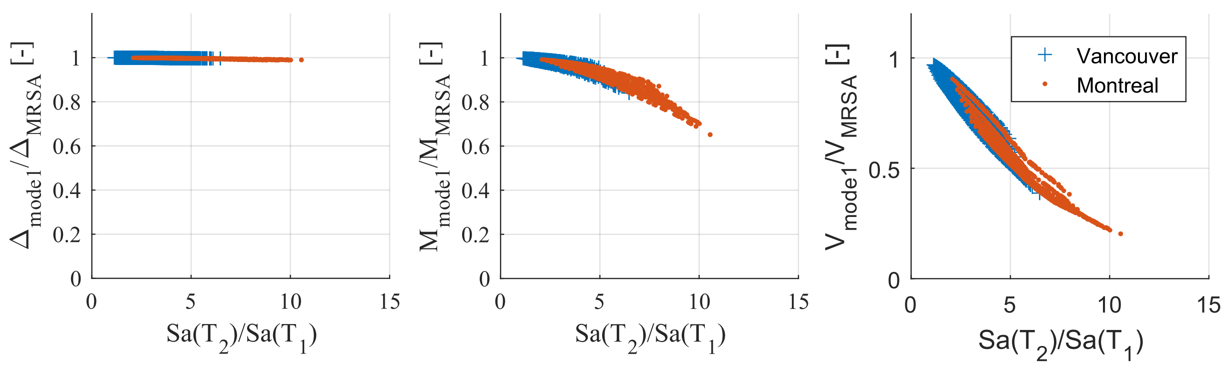

Figure 4.9 Comparison of first mode contribution to combined modes for (a) displacements, (b) moments, and (c) shears.

4.5.7 Static load distribution, λ

In many design procedures, it is desirable to apply a static load to approximate the dynamic behaviour. The appropriate static force distribution is dependent on the objective of the design. For the CORW system, the objectives are to design the outrigger and the controlled rocking base to yield and to control displacements. The following section compares a simple loading distribution, an inverted triangular distribution, to the dynamic loads and evaluates the applicability of using this loading distribution to design the CORW.

In any static load distribution, the base shear (V) is distributed over the building height. The applied static floor at any story x, is given in Equation 4.12.

$$F_x = \lambda_x V \qquad \text{Equation 4.12}$$

In Equation 4.12, V is the base shear and λ_x represents the distribution pattern where the sum is equal to 1. For an inverted triangular distribution with equal mass at each floor, λ_x, can be calculated using Equation 4.13.

$$\lambda_x = \frac{w_x h_x}{\sum_{i=1}^{n_f} w_i h_i} \qquad \text{Equation 4.13}$$

where h_x is the story elevation at story x; w_x is the xth story weight; and n_f is the total number of stories.

Figure 4.10 and Figure 4.11 shows the comparison of displaced shape between the MRSA and inverted triangular distribution, separated by design spectrum and period for α_f = 0.1 and α_f = 0.9, respectively. As shown in the figures, there is negligible differences between the responses for all cases. Hence, the triangular distribution can predict the displaced shape response well.

Figure 4.12 and Figure 4.13 shows the comparison of moments between the MRSA and inverted triangular distribution, separated by design spectrum and period for α_f= 0.1 and α_f= 0.9, respectively.

As shown in the figures, low periods tend to have similar moment response between MRSA and inverted triangular distribution. However, as periods increase higher modes begin to govern through the wall height. The MRSA results show higher moment amplitudes are observed at elevations greater than 50% for α_f= 0.1, and between 40%-60% of building heights for α_f= 0.9. The higher value of α_f results in a closer match between MRSA and inverted triangular distributions.

Inverted triangular distributions are representative of first mode behaviour. Therefore, the close match between the models and the static distribution displacements, shown in Figure 4.10 and Figure 4.11, can be attributed to the first mode dominance of displacements. Contrastingly, the large variations in moments, shown in Figure 4.12 and Figure 4.13, are attributed to higher mode contributions. This is exemplified using an example archetype building responses, shown in Figure 4.14. In this figure, the displacements from each mode, prior to combination using the complete quadratic combination (CQC) of the modes, are shown in Figure 4.14 (a); the ratio of each mode displacement to the MRSA displacements are shown in Figure 4.14 (b); the moments from each mode, prior to combination using CQC, are shown in Figure 4.14 (c); and the ratios of each mode displacement to the MRSA displacements are shown in Figure 4.14 (d). As shown, the first mode dominates the displaced shape behaviour over most of the building height, with only minor variations (within 15%) at lower levels. On the other hand, moments have a significant contribution from the second and third modes over the building height. However, the base moment and the top moments are dominated by the first mode.

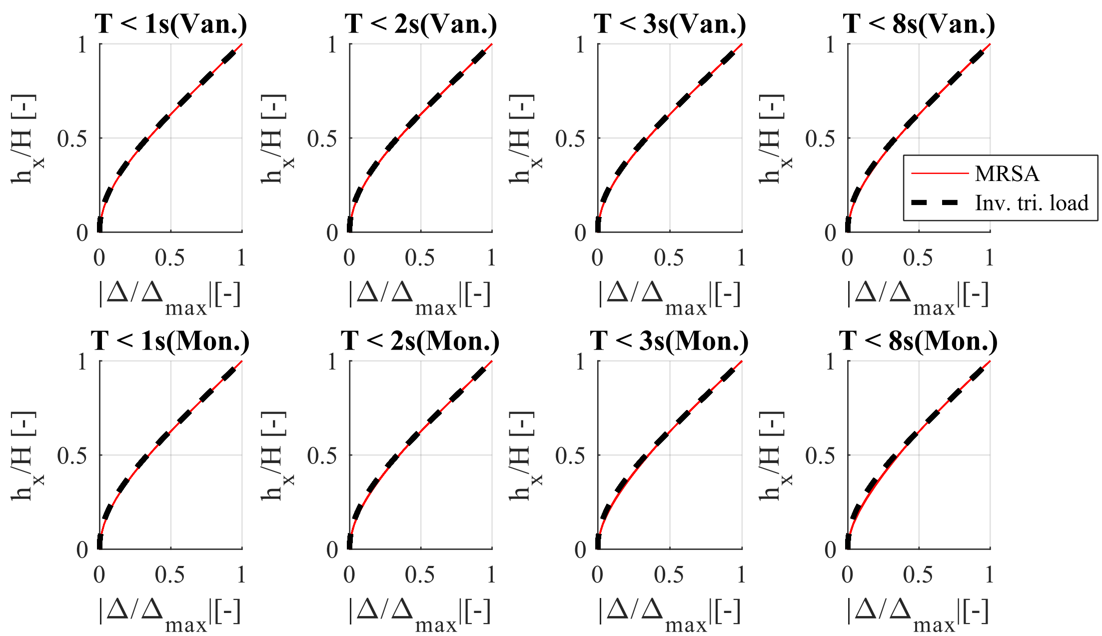

Figure 4.10 Displaced shape comparison of MRSA to inverted triangular distribution for α_f= 0.1 (192 archetypes, 384 analysis)

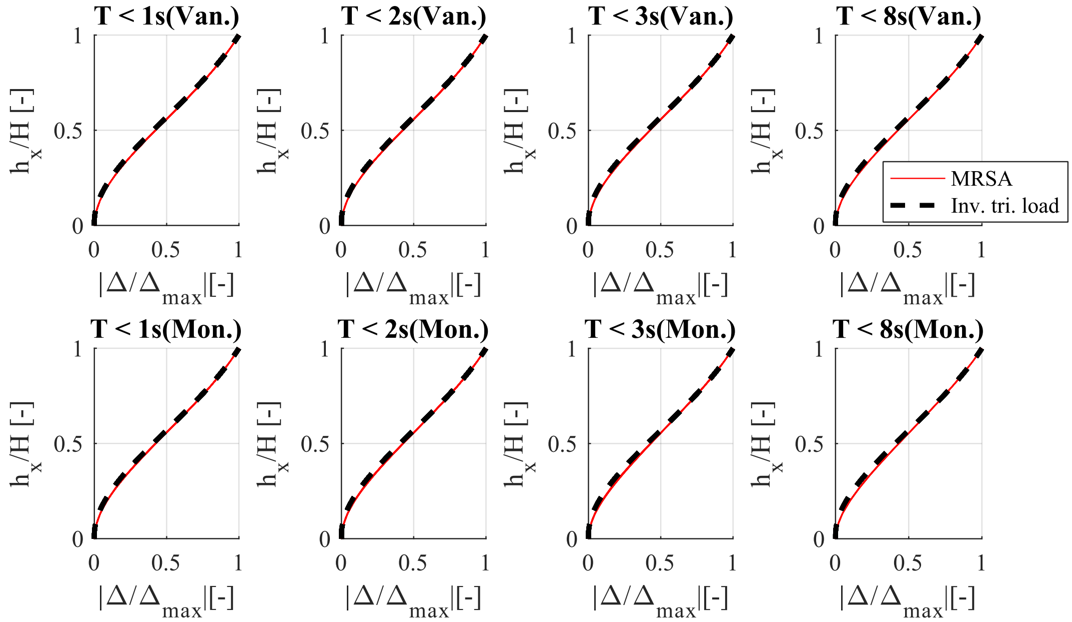

Figure 4.11 Displaced shape comparison of MRSA to inverted triangular distribution for α_f= 0.9 (192 archetypes, 384 analysis)

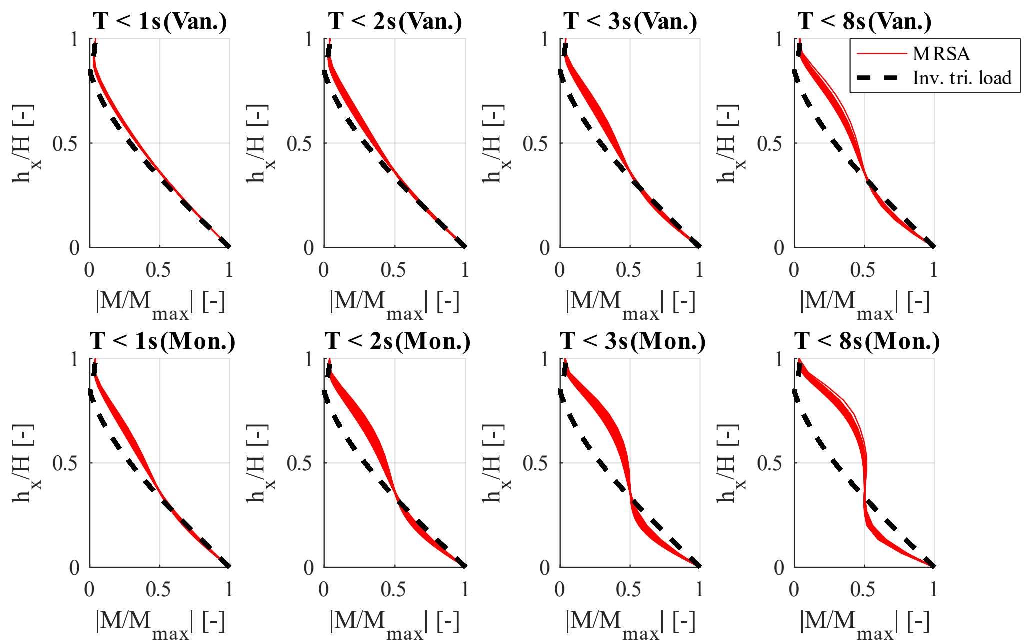

Figure 4.12 Wall moment comparison of MRSA to inverted triangular distribution for α_f= 0.1 (192 archetypes, 384 MRSA analysis)

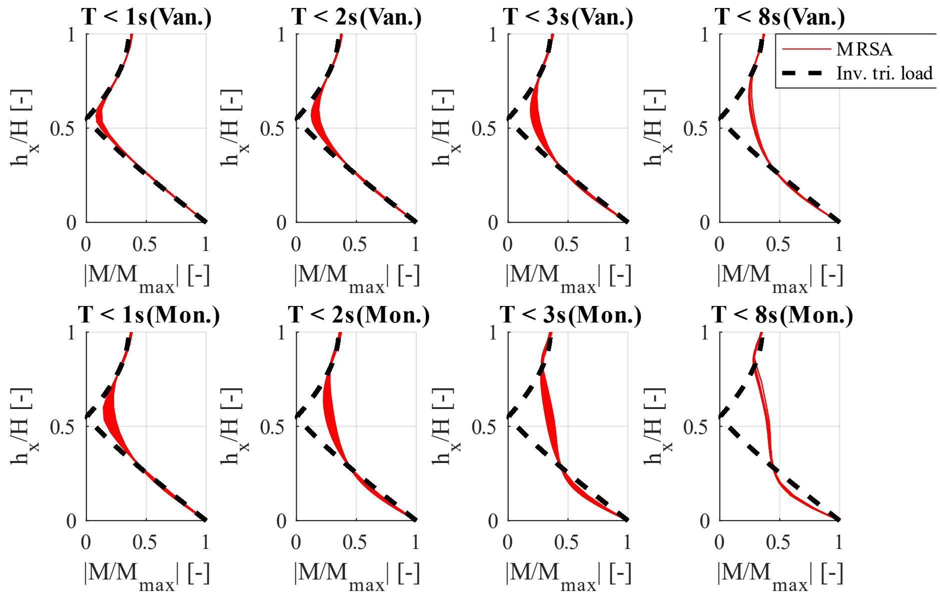

Figure 4.13 Wall moment comparison of MRSA to inverted triangular distribution for α_f = 0.9 (192 archetypes, 384 MRSA analysis)

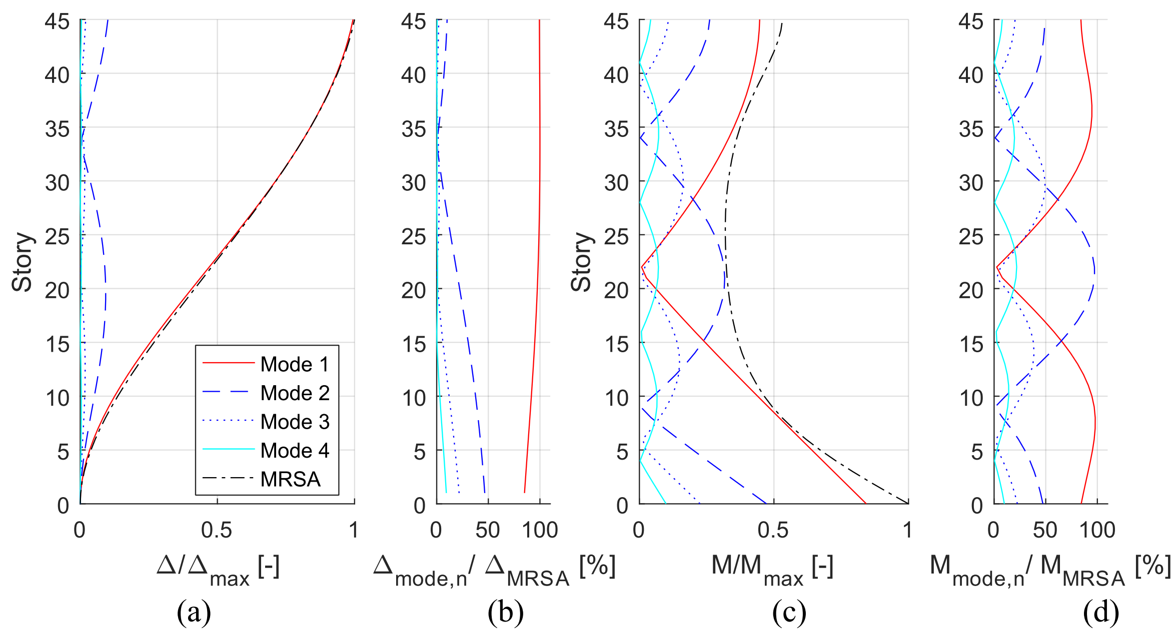

Figure 4.14 Example archetype response (Located in Montreal, T1 = 3s, α_f= 0.9): (a) displacements normalised to peak response from MRSA (Δ_{max}); (b) ratio of individual modal displacement ($\Delta_{mode,n}$) to MRSA displacement (Δ_{MRSA}); (c) ratio of moment normalised to peak moment response from MSRA (M_{max}); and (d) ratio of individual modal moment ($M_{mode,n}$) to MRSA moment (M_{MRSA});

From Figure 4.12 and Figure 4.13 it is observed that the ratio between the top and bottom moments are similar for the inverted triangular distribution and MRSA. Figure 4.15 shows the ratio of the outrigger moment to the total overturning moment for both MRSA and inverted triangular distribution. In this plot the ratio is solved theoretically using a Euler-Bernoulli beam. The ratio of a triangular distribution is shown in Equation 4.14. As shown in Figure 4.15, Equation 4.14 gives a reasonable estimate of this ratio.

$$\beta_m = \frac{M_o}{M_t} = \frac{3}{8}\alpha_f \qquad \text{Equation 4.14}$$

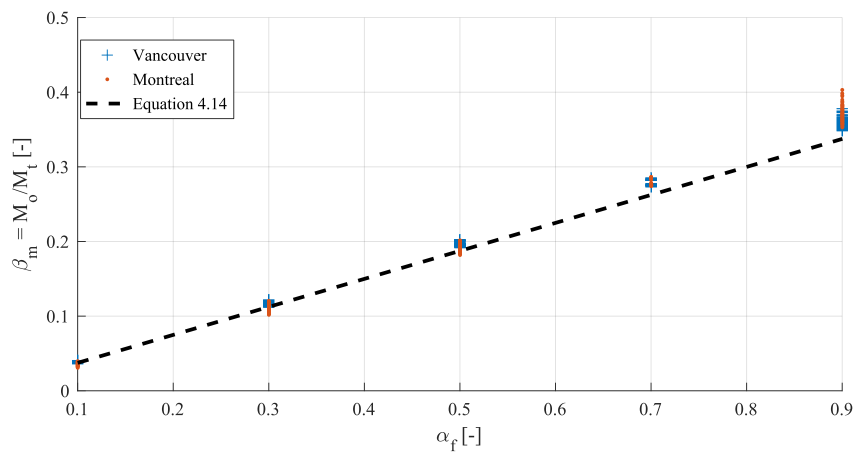

Figure 4.15 Ratio of outrigger moment to total moment (960 archetypes, 1920 MRSA)

Overall, key design parameters, such as displacements and flexural yielding (controlled rocking base and yielding outrigger), are captured well using an inverted triangular distribution. Hence, an inverted triangular distribution is a suitable static load distribution to predict these key design parameters.

4.5.8 Comparison of dynamic moment to static moment (β_o)

In this section, the dynamic force factor (β_o) of CORW defined as the ratio of the dynamic overturning moment (${M_t}^{dy}$), determined using MRSA, to the static overturning moment (${M_t}^{st}$), determined using an inverted triangular distribution, is developed. The static moment is determined by summing the moments at the base of the CORW using the SDOF base shear (V $= W * S_{a1}$) distributed in an inverted triangular pattern over the height of the building.

The analytical results are presented in the Equation 4.15. The result shows that β_o has a strong dependency on $S_a(T_2)/S_a(T_1)$. Eq. (31) is recommended to the dynamic moment. As shown in Figure 4.16, Equation 4.15 gives a reasonable estimate of the dynamic moment factor.

$$\beta_o = \frac{M_t{}^{dy}}{M_t{}^{st}} = 0.05\frac{S_{a2}}{S_{a1}} + 0.5 \geq 0.75 \qquad \text{Equation 4.15}$$

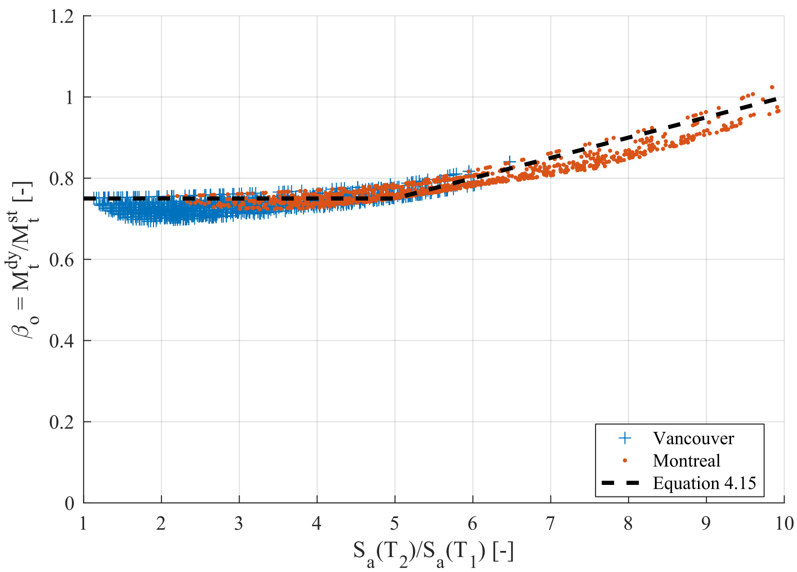

Figure 4.16 Comparison of total overturning moment using LTHA and static analysis

4.6 Linear dynamic analysis of SCCW system

Eigenvalue analysis was conducted on each of the 960 unique SCCW archetype buildings, and MRSA was conducted for each of the two building sites, resulting in 1920 analysis in the SCCW direction. The following sections describe the linear dynamic analysis of the SCCW system empirical equations to estimate these responses.

4.6.1 Natural periods of vibration (T_1, T_2, T_3)

Based on the eigen-value analysis, Equation 4.16 was developed to estimate the period of the SCCW. In Equation 4.16, the flexibility of the coupling beams is accounted for through an effective moment of inertia (I_{Te}). The effective moment of inertia is determined using parallel axis theorem, as shown in Equation 4.17 for two equally sized C-shaped walls. In Equation 4.17 an effective wall area, $A_{w,eff}$, is used to account for the increased flexibility due to coupling beam stiffness and is estimated using Equation 4.18.

$$T_1 \approx 1.85\sqrt{\frac{WH^3}{gE_cI_{Te}}} \qquad \text{Equation 4.16}$$

$$I_{Te} \approx 0.5\alpha_2 A_w {L_c}^2 + 2I_w \qquad \text{Equation 4.17}$$

$$A_{w,eff} \approx \alpha_2 A_w \qquad \text{Equation 4.18}$$

where L_c is the distance between centroids of each wall pier; I_w is the gross moment of inertia of an individual wall pier; and α_2 is a reduction factor.

In Equation 4.18, the reduction factor α_2 was determined through back-calculation of the natural periods from the eigenvalue analysis for each archetype. Figure 4.17 shows α_2 as a function of building aspect ratio (H/Lc). As shown, α_2 increases for greater values of aspect ratio and relative stiffness factors (α_c). Hence, the slenderer core wall and more rigid the coupling beams are, the more the core behaviour resembles a cantilever wall. Based on these results, Equation 4.19 was developed to estimate this behaviour. As shown in Figure 4.17, Equation 4.19 reasonably estimates this effective area reduction factor.

$$\alpha_2 = \left(0.06\frac{H}{L_c} + 0.3\right)\alpha_c \leq \alpha_c^2 \qquad \text{Equation 4.19}$$

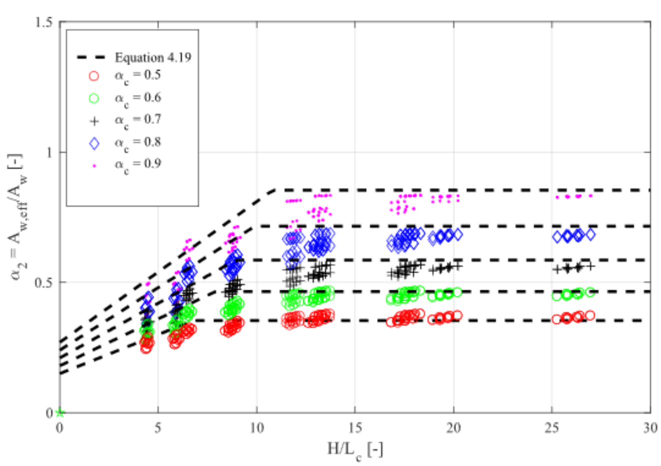

Figure 4.17 Effective area of coupled wall

Once the fundamental period is determined, Equation 4.20 and Equation 4.21 are proposed to estimate the second and third mode periods, respectively. Figure 4.18 compares the periods determined using the proposed design equations with the results of the eigen-value analysis from the models. As shown, the proposed relations estimate the modal periods well, with most of the estimates being within 5% of the model periods and all the estimated periods are within 25% of the equations for all archetypes,

$$T_2 = \frac{T_1}{4} \qquad \text{Equation 4.20}$$

$$T_3 = \frac{T_1}{8.5} \qquad \text{Equation 4.21}$$

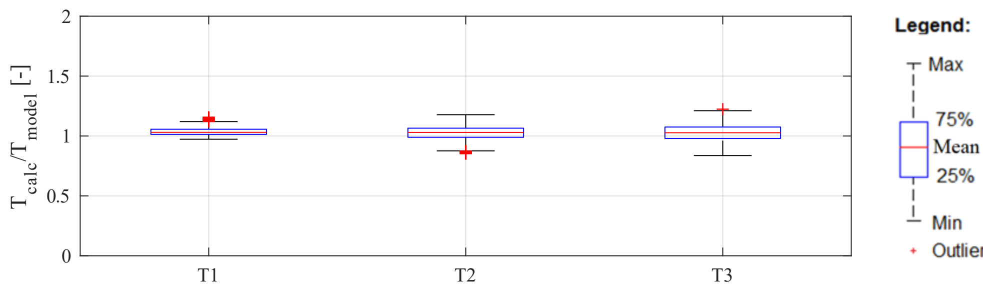

Figure 4.18 Comparison of periods estimated using Equation 4.16, Equation 4.20, and Equation 4.21

4.6.2 Modal mass participation

The modal mass participation factors for the first three modes are shown in Figure 4.19. The modal mass participation is between 63-72%, 15%-20%, and 4%-6% for the first, second, and third mode, respectively. Empirical equations for the first, second, and third modal mass participation is shown in Equation 4.25, Equation 4.26, and Equation 4.27, respectively. As shown in Figure 4.19, the modal mass participation factor is dependent on α_2, where higher α_2 results in decreased mass participation in the first mode and slightly increased in the second and third modes.

$$Mass\ participation(Mode\ 1) \approx 72 - 5\alpha_{c2}[\%] \qquad \text{Equation 4.22}$$

$$Mass\ participation(Mode\ 2) \approx 11 + 10\alpha_{c2}[\%] \qquad \text{Equation 4.23}$$

$$Mass\ participation(Mode\ 3) \approx 5 - \alpha_{c2}[\%] \qquad \text{Equation 4.24}$$

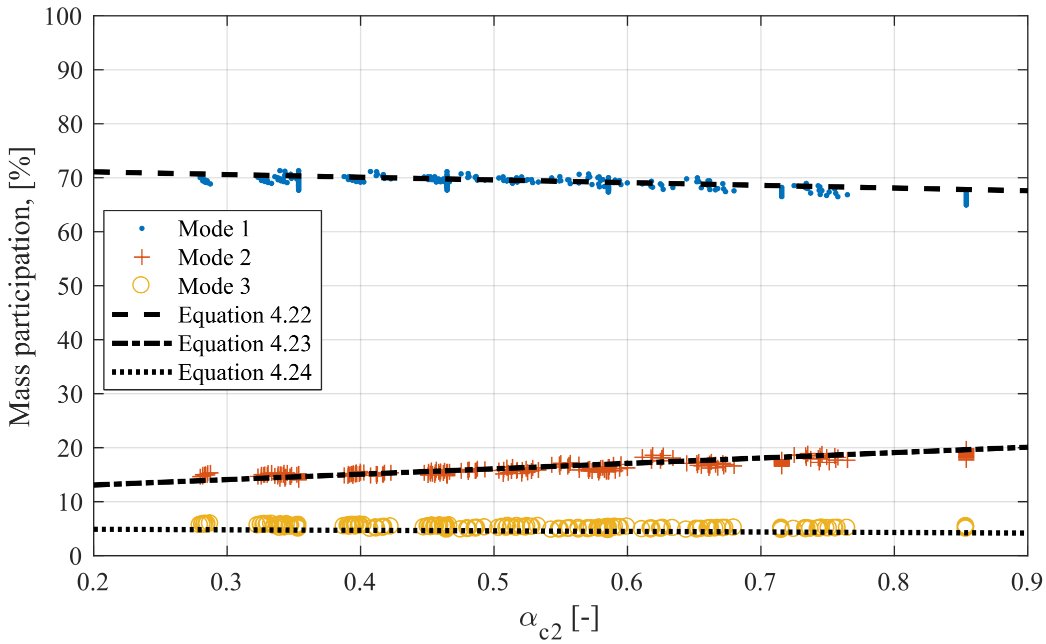

Figure 4.19 Modal mass participation of SCCW parameter study models

4.6.3 Comparison of SDOF displacement to MDOF displacements (C_0)

The C_0 factor relates the roof displacement of the MDOF system to the SDOF system. Figure 4.20 shows the C_0 value obtained from normalizing the peak roof displacement (Δ_E) of the MDOF system from MRSA with the spectral displacement from the design spectrum. From this analysis, a reasonable estimate for the SCCW is C_0 = 1.48 and is applicable for both Vancouver and Montreal spectrums.

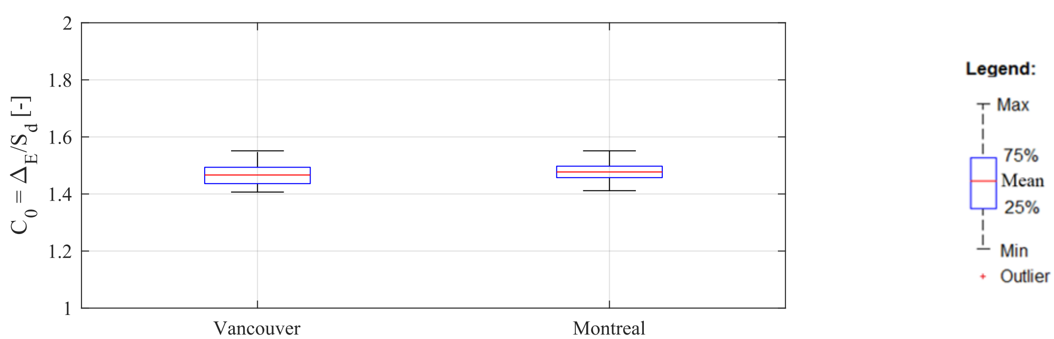

Figure 4.20 Ratio of the multi-degree-of freedom (MDOF) roof displacements to the single-degree-of-freedom (SDOF) displacement (960 archetypes, 1920 analysis)

4.6.4 Comparison of SDOF shear to MDOF shear (M_v)

To estimate the higher mode shear response, the ratio of base shear from MRSA was compared with the base shear determined by multiplying the spectral acceleration with the weight of the building. This ratio is referred to as M_v by the National building code of Canada (NBCC, 2015).

Figure 4.21 shows the relation between M_v and the ratio of the spectral acceleration at the second mode period ($S_a(T_2)$) to the spectral acceleration at the first mode period ($S_a(T_1)$). As shown, M_v is less than one when the spectral acceleration ratio is low (i.e., flatter spectral shape) and the M_v ratio increases in value with higher spectral acceleration ratios (i.e., steeper spectral shape). Based on the above-mentioned trends, the following empirical relation (Equation 4.25), was developed to estimate the higher mode shear response. This equation is intended to assist with design, as a result it is conservatively limited to a minimum value of 1.

$$M_v = 0.26\frac{S_a(T_2)}{S_a(T_1)} + 0.1 \geq 1 \qquad \text{Equation 4.25}$$

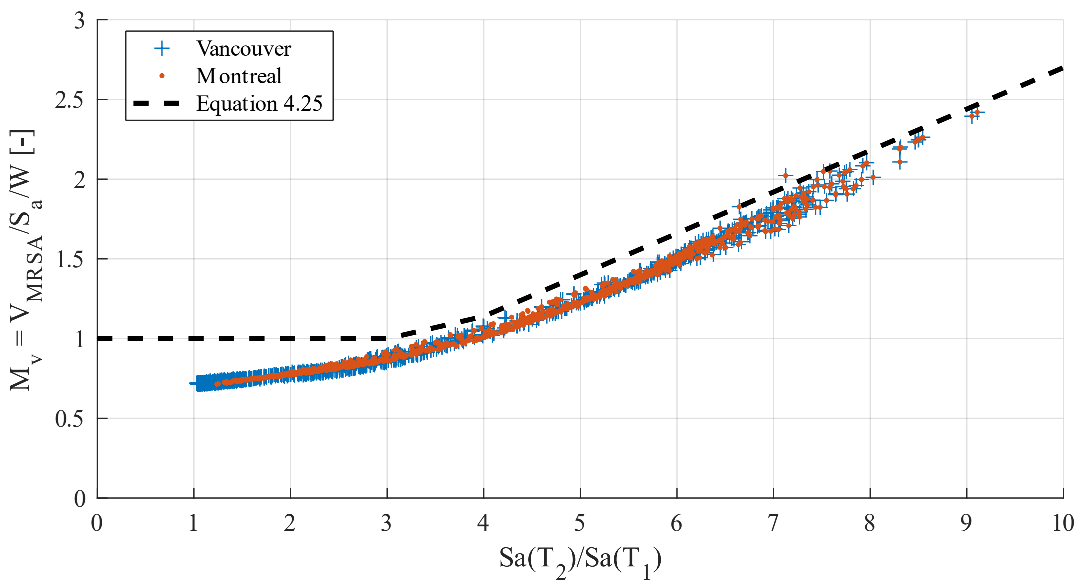

Figure 4.21 M_v ratio for SCCW wall systems (960 archetypes, 1920 analysis)

4.6.5 Degree of coupling, DOC

Coupled wall systems are often distinguished by their degree-of-coupling (DOC). The DOC is the ratio of the overturning moment resisted by the axial force couple ($P_p L_c$) to the total overturning moment (M_p), shown in Equation 4.26. The DOC helps engineers understand how significant the coupling forces in the wall are. For example, a DOC equal to 0 would indicate that the walls are two individual cantilever walls. On the other hand, a DOC equal to 1 would indicate that the walls behave as if there is a pin at the base, i.e., moment is equal to zero.

$$\mathrm{DOC} = \frac{P_p L_c}{2M_p + P_p L_c} \qquad \text{Equation 4.26}$$

where L_c is the distance between the centroid of the wall piers.

Although a useful characteristic parameter, the DOC cannot be defined prior to numerical analysis. Therefore, a new characteristic parameter, called the degree of axial stiffness (DAS), which relates the axial couple stiffness to the total flexural stiffness of the core-wall is proposed. The DAS for a symmetric core consisting of two C-shaped walls is shown in Equation 4.27.

$$\mathrm{DOC} = 0.85\frac{\alpha_2 A_w L_c^2}{2I_{Te}} \qquad \text{Equation 4.27}$$

The result of parametric MRSA analysis, as presented in Figure 4.22, shows that the DOC can be estimated as 85% of the DAS as presented in Equation 4.28. The results show that 95% of the analysis had DOC within 5% of the estimated value. Hence, Equation 4.28 can be used to predict the value of DOC effectively.

$$\mathrm{DOC\ (est.)} = 0.85DAS \qquad \text{Equation 4.28}$$

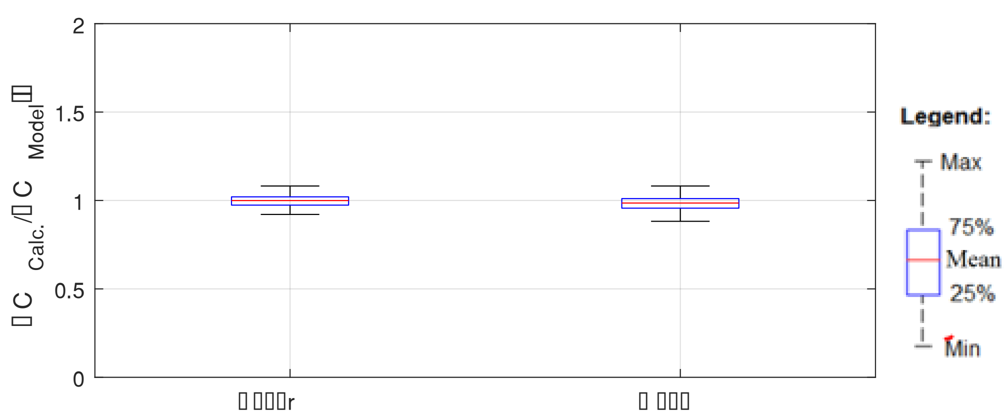

Figure 4.22 Comparison of Equation 4.28 with models (960 archetypes, 1920 analysis)

4.6.6 Comparison of first mode to combined MRSA response

MRSA was conducted on all 960 archetypes for two building sites, resulting in 1920 analysis. The responses were determined by combining the first 4 modes (over 90% modal mass participation). Figure 4.23 shows the comparison between spectral shape and the ratio of first mode response to the combination of the first 4 modes. The spectral shape is represented by the ratio of second mode spectral acceleration to first mode spectral accelerations.

Figure 4.23 (a) shows the ratio of the peak displacement from the first mode (Δ_{mode1}) to the peak displacement from MRSA (Δ_{MRSA}) compared with the spectral shape ratio (i.e., $S_a(T_2)/S_a(T_1)$). As shown in Figure 4.23 (a), the peak roof displacement is almost entirely dominated by the first mode response for all spectral shape ratios. The spectral shape combined with the dominant modal mass participation of the first mode drives the first mode displacement response. Similar to the CORW, the design spectra often have low spectral displacements at low period, as a result, the low periods from higher modes have a lower contribution to the response.

Figure 4.23 (b) shows the ratio of the peak core moment from the first mode ($\mathrm{M}_{\mathrm{t,mode1}}$) to the peak core moment from MRSA ($\mathrm{M}_{t,MRSA}$) compared with the spectral shape ratio (i.e., $S_a(T_2)/S_a(T_1)$). compares the ratio of the total overturning moment from the first mode to the combined overturning moment from all the modes with the spectral shape. Figure 4.23 (b) demonstrates that moment is highly influenced by the first mode response, where the first mode accounts for 80%-100% of the response. As the spectral shape ratio increases, the overturning moment has a more significant higher mode response.

Figure 4.23 (c) shows the ratio of the peak shear from the first mode ($\mathrm{V}_{\mathrm{mode1}}$) to the peak shear from MRSA (V_{MRSA}) compared with the spectral shape ratio (i.e., $S_a(T_2)/S_a(T_1)$). As shown, the shear response is strongly governed by higher modes for spectral shape ratios greater than 1. For spectral ratios greater than 5, over 50% of the response is governed by higher modes.

Figure 4.23 (d) shows the ratio of the peak coupling beam shear from the first mode ($\mathrm{V}_{\mathrm{CB,mode1}}$) to the peak coupling beam shear from MRSA ($\mathrm{V}_{CB,MRSA}$) compared with the spectral shape ratio (i.e., $S_a(T_2)/S_a(T_1)$). The result shows that the coupling beam shear response is strongly governed by higher modes, for spectral shape ratio greater than 8, the first mode can account for as little as 18% of the total response.

Figure 4.23 (e) shows the ratio of the peak wall pier axial load from the first mode ($P_{\text{pier,mode1}}$) to the peak pier axial load from MRSA ($P_{pier,MRSA}$) compared with the spectral shape ratio (i.e., $S_a(T_2)/S_a(T_1)$). The result shows that, similar to the total overturning moment, the wall axial load is strongly governed by the first mode, where the first mode accounts for 86-100% of the total response.

Figure 4.23 (f) shows the ratio of the peak wall pier moment from the first mode ($M_{\text{pier,mode1}}$) to the peak pier moment from MRSA ($M_{pier,MRSA}$) compared with the spectral shape ratio (i.e., $S_a(T_2)/S_a(T_1)$).The result shows that the wall pier moment is strongly governed by higher modes, where the first mode can account for as little as 40% of the response. The first mode dominance in the total moment and the axial load, demonstrate the strong influence of the axial couple.

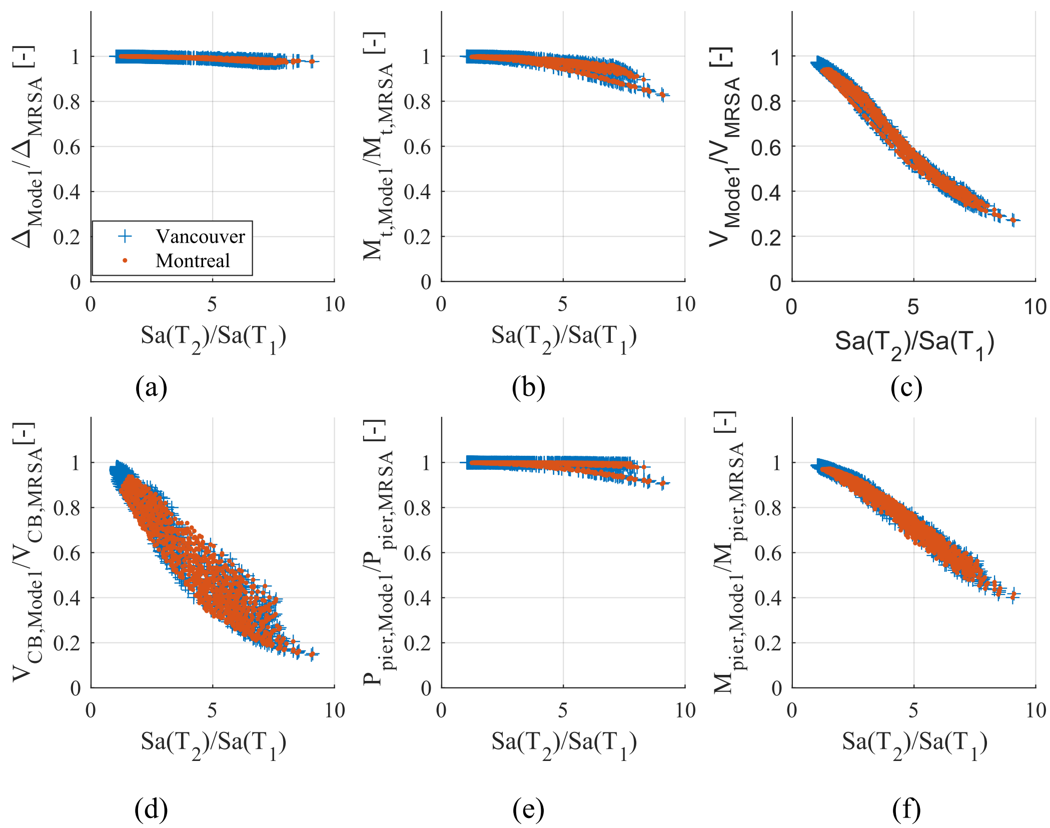

Figure 4.23 Comparison of first mode response to MRSA for (a) displacements, (b) moments, (c) shears, (d) coupling beam shear, (e) axial load, and (f) wall pier moment

4.6.7 Load distribution factor, λ

This section investigates the most effective static loading distribution for the SCCW system to accurately predict the coupling beams shear distribution. Goel et al. 2009 developed a static load distribution for link beams in eccentrically braced frames. Following the method by Goel and Chao (2008), the static loading distribution, at a given floor, x, is determined using Equation 4.29.

$$\lambda_x = (\beta_x - \beta_{x+1})\frac{1}{\beta_1} \qquad \text{Equation 4.29}$$

In Equation 4.29, β_x is the coupling beam shear ($V_{CB,x}$), at a given story x normalized to the roof coupling beam shear ($V_{CB,r}$), the relation for β is show in Equation 4.30.

$$\beta_x = \frac{V_{CB,x}}{V_{CB,r}} \qquad \text{Equation 4.30}$$

In this section, the shear distribution β is determined by first developing relations to estimate the coupling beam shears ($V_{CB,x}$). To estimate the coupling beam shear, first shape functions, $S_{n,x}$, are developed to predict the response of coupling beams at mode n and height x of the building. These shape functions are shown in Equation 4.31, Equation 4.32, and Equation 4.33 for Mode 1, Mode 2, and Mode 3, respectively. Figure 4.24 shows that the simple estimate of shear shape functions gives a reasonable estimate of the MRSA analysis.

$$S_{1,x} = \sin\left((5.65 - 2.2\alpha_c)\frac{h_x}{H} + 2.2\alpha_c - 1.25\right) + 1.5/\alpha_c \qquad \text{Equation 4.31}$$

$$S_{2,x} = \sin\left(5\frac{h_x}{H} + 0.63\right) + 0.5\alpha_c - 0.25 \qquad \text{Equation 4.32}$$

$$S_{3,x} = \sin\left(7.5\frac{h_x}{H} + 0.94\right) - 0.1\alpha_c^2 \qquad \text{Equation 4.33}$$

The value of axial couple determined at the base of the wall is lower than the summation of the coupling beam shears. This difference is due to the higher mode effects, causing some of the coupling beams to reach the peak shear in the opposite direction as others. Figure 4.25 (a), Figure 4.25 (b), and Figure 4.25 (c) show the summation of absolute coupling beam shear forces normalized by maximum axial force in the wall pier, $C_n = \frac{\Sigma|V_{CB,n}|}{\mathrm{P_p}}$, for the first, second and third mode, respectively. The first mode is the highest contributor to the pier force, $\mathrm{P_p}$. As shown in Figure 4.26 (a), Equation 4.34, Equation 4.35, and Equation 4.36 provide reasonable estimates of the contribution from the higher modes for the first, second mode and the third modes, respectively. As shown, higher values of α_c result in more contributions from the second and third modes. Hence, the higher relative stiffness of coupling beams, the more higher mode contribution.

$$C_1 = \frac{\Sigma|V_{CB,1}|}{\mathrm{P_p}} = 1.1 - 0.03\alpha_c^3 \frac{S_a(T_2)}{S_a(T_1)} \leq 1.05 \qquad \text{Equation 4.34}$$

$$C_2 = \frac{\Sigma|V_{CB,2}|}{\mathrm{P_p}} = 0.22\alpha_c \frac{S_a(T_2)}{S_a(T_1)} \qquad \text{Equation 4.35}$$

$$C_3 = \frac{\Sigma|V_{CB,3}|}{\mathrm{P_p}} = 0.055\alpha_c \frac{S_a(T_3)}{S_a(T_1)} \qquad \text{Equation 4.36}$$

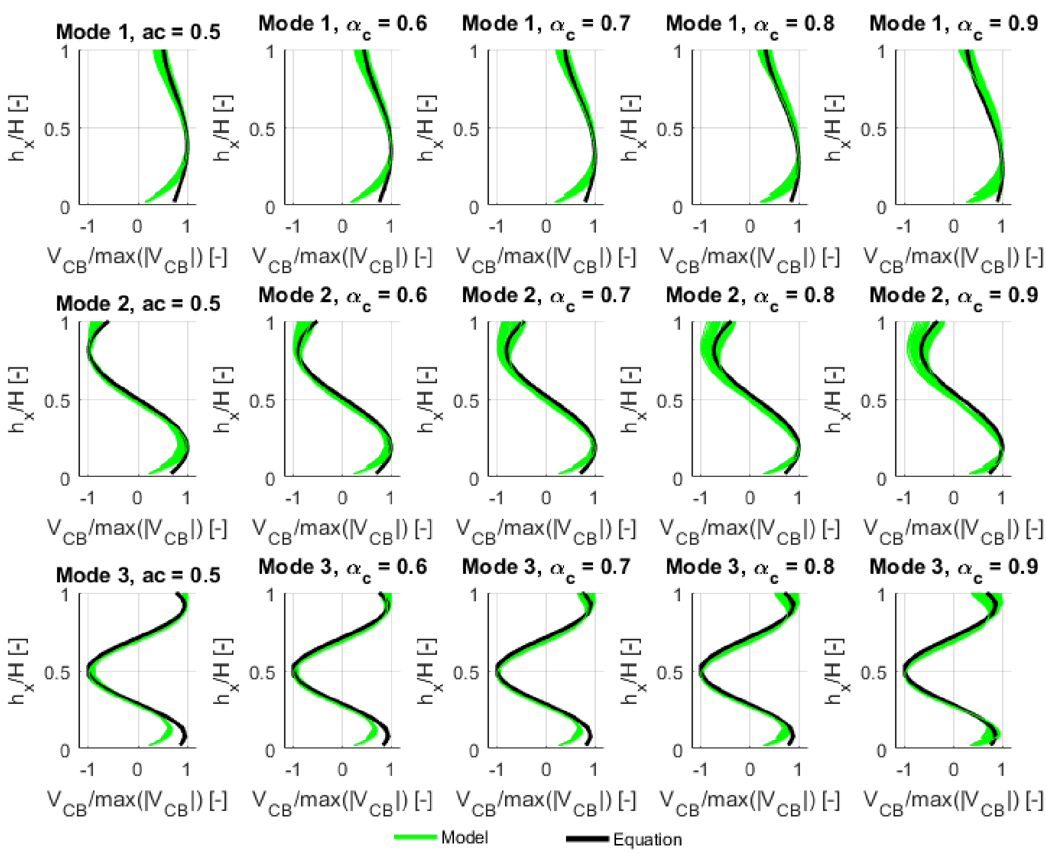

Figure 4.24 Coupling beam force shape factors (960 archetypes)

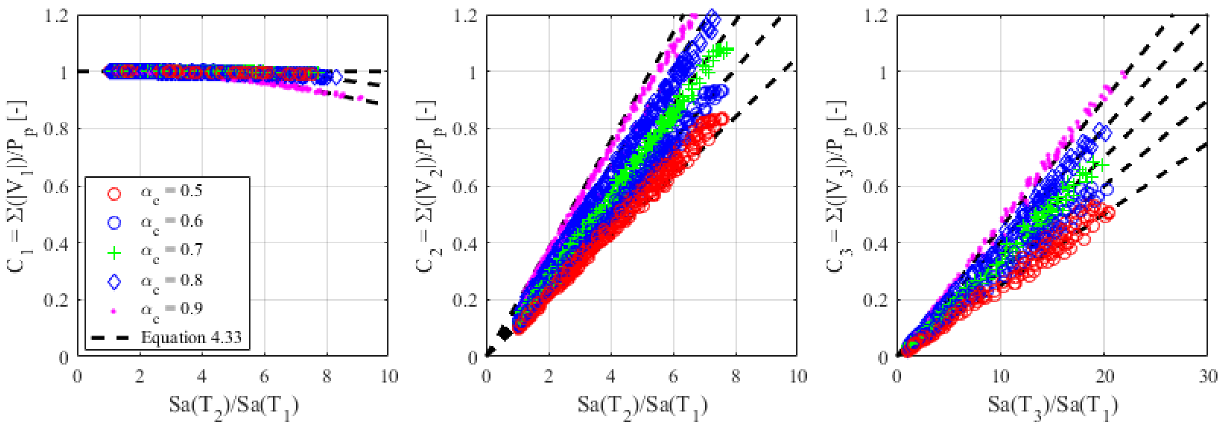

Figure 4.25 Contribution of each mode on coupling beam shears

Equation 4.37 was developed to estimate the coupling beam shear at any given story level, x. In Equation 4.37, each shape function has been normalized to the sum, $SN_{n,i} = \frac{S_{n,i}}{\Sigma|S_n|}$. Figure 4.26 shows the comparison between Equation 4.37 the MRSA results for an example 15-story, 30-story, and 45-story buildings. As shown, the recommended equation gives a reasonably good estimate of the behaviour for different building heights and locations. The equation has a less accurate prediction of the coupling beam shears at levels lower than the peak shear. However, for design purposes this equation is reasonable.

$$V_i = \mathrm{P_p} \times \sqrt{\sum_{n=1}^{3} \left(C_n * SN_{n,i}\right)^2} \qquad \text{Equation 4.37}$$

where C_n is the nth mode contribution; SN is the normalized shape function for the n mode; and $SN_{n,\mathrm{r}}$ is the shape function at the roof coupling beam for the nth mode; and i is the story number.

The static shear distribution factor, β_x, is determined by normalizing the coupling beam shear to the roof coupling beam shear using Equation 4.38.

$$\beta_x = \frac{V_i}{V_r} = \sqrt{\frac{\sum_{n=1}^{3}\left(C_n SN_{n,i}\right)^2}{\sum_{n=1}^{3}\left(C_n SN_{n,\mathrm{r}}\right)^2}} \quad \text{Equation 4.38}$$

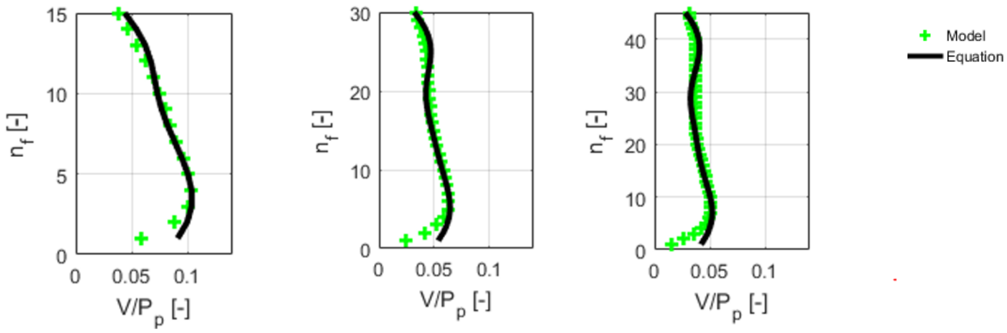

(a) 15-story (b) 30-story (c) 45-story

Figure 4.26 Estimated coupling beam shears for (a) 15-story, (b) 30-story, and (c) 45-story (Parameters = Vancouver site, ac = 0.7, Lcb = 1.5m, hf = 4m, mf = 600tonne, Lw,y =10 m, Lw,x = 10m, tw = 0.6m)

4.7 Summary

In this chapter, the dynamic characteristics of the proposed earthquake-resilient RC core wall building system are examined. The dynamic analysis was conducted using modal response spectrum analysis. A total of 960 archetypes were developed for the CORW, and 960 archetypes were developed for the SCCW. Each archetype was analysed using two different design acceleration spectrums. As a result, a total of 3840 modal response spectrum analysis were conducted.

The dynamic analyses were used to estimate the effect of the building geometry and stiffnesses on forces and deformations. Additionally, this chapter also presented new empirical equations which were developed to estimate these dynamic characteristics.

Key observations from the CORW parametric study:

1. The natural period is governed entirely by the relative stiffness factor α_f. Where an infinitely rigid outrigger (i.e., α_f = 1) would only result in about 38% reduction in fundamental period if compared to a system without an outrigger (i.e., α_f = 0).
2. The modal mass participation shows that higher relative outrigger stiffness results in a more dominate first mode response.

3. The ratio between roof displacement to spectral displacement ($C_0 = \frac{\Delta_r}{S_d}$) decreases with an increase in α_f.
4. The factor shear amplification factor, M_v, depends on spectral shape, where M_v increases with an increase in $Sa(T_2)/S_a(T_1)$.
5. Roof displacements are almost entirely governed by the first mode response regardless of spectral shape.
6. Overturning moments are dependant on spectral shape. A more constant spectral shape (i.e. $S_a(T_2)/S_a(T_1) \rightarrow 1$ results in more first mode dominate response. On the other hand, $S_a(T_2)/S_a(T_1) \rightarrow \infty$ results in significantly more higher mode response.
7. Base shear is dependant on spectral shape and have more significant higher mode contributions than overturning moments and displacements. A more constant spectral shape (i.e., $S_a(T_2)/S_a(T_1) \rightarrow 1$) results in more first mode dominate response. On the other hand, $S_a(T_2)/Sa(T_1) \rightarrow \infty$ results in significantly more higher mode response.
8. Inverted triangular static distribution gives a satisfactory estimate of the displacements and moments.
9. The ratio of the outrigger moment to the total overturning moment is similar for both the static and dynamic analysis.
10. The dynamic base moment is lower when compared to a static moment. An empirical equation is developed and presented to estimate these dynamic moments.

Key observations from the SCCW parametric study:

1. Natural period is most influenced by the relative stiffness of the coupling beams to the wall and the wall aspect ratios. Empirical equations used to estimate the response
2. First mode modal mass participation ranges between 63- 72% depending on the relative stiffness of the coupling beams.
3. The C_0, the ratio between roof displacement and S_d, can be estimated as $C_0 = 1.5$.
4. The factor shear amplification factor, M_v, depends on spectral shape, and M_v value increases with an increase in $S_a(T_2)/S_a(T_1)$.
5. Degree-of-coupling can be estimated using simple empirical equations which depend on the geometry of the wall and the stiffness of the coupling beams.

6. Roof displacement, overturning moment, and wall pier axial loads are primary first mode governed.
7. Base shear, coupling beam shear, and wall pier moments have significant higher mode responses.
8. Static load distributions, determined by estimating the coupling beam shapes of the first three modes, are proposed to estimate the shear in the coupling beams.

The elastic dynamic response of structures is a critical component in performance-based design. Practitioners often use modal response spectrum analysis to design structures at the service level earthquake hazard like used within this chapter. Additionally, building codes, such as NBCC 2020, use elastic modal response spectrum analysis to approximate the higher mode effect in structures, despite expecting them to undergo extensive nonlinear action. Therefore, this chapter is crucial in understanding the behaviour of the CORW and SCCW, particularly in the attempt to design for multiple performance objectives and different shaking intensities, which is the main objective of the following chapter (Chapter 5).

Chapter 5: Proposed design procedure for CROCW

5.1 Overview

This chapter details the development of an equivalent energy-based design procedure (EEDP) used to design the CROCW system. The methods presented in this chapter may also be applied to design the CORW and SCCW independently.

The basic theory of EEDP is described in this chapter. Afterwards, the step-by-step process for designing the CROCW system for different hazard levels (e.g., service level earthquake (SLE), design-based earthquake (DBE), and the maximum considered earthquake (MCE)) is presented. This chapter explains how the empirical equations, developed in Chapter 4, are used to modify EEDP to account for higher mode effects. Additionally, the original derivation of EEDP assumed elastic-plastic hysteresis. In the CORW and SCCW systems, the behaviour incorporates flag-shaped hysteretic behaviour. This chapter presents new energy modification factors which account for these unique combinations of hysteretic shapes. This chapter concludes with an overview of four prototype building designs which use a CROCW system following the presented EEDP is presented. This chapter only summarises the design.

5.2 Introduction

This thesis proposes a procedure to design the CROCW system to meet different performance objectives at different shaking intensities. At a service level earthquake (SLE) shaking intensity, the design objective of the CROCW is to remain essentially elastic, where no yielding occurs. At a design-based earthquake (DBE) shaking intensity, the design objective is for the CROCW primary system dampers (i.e., outrigger dampers and SCFDs) to yield and dissipate energy. At a maximum considered earthquake (MCE) shaking intensity, the design objective of the CROCW primary and secondary system dampers (i.e., outrigger dampers, SCFDs, and wall-base dampers) is to yield and dissipate the earthquake energy.

The state-of-practice in designing structures to meet multiple performance objectives at different shaking intensities usually requires a nonlinear analysis performance-based design approach (e.g., LATBSDC, 2020). This design methodology is cumbersome and involves a substantial amount of design effort and a rigorous peer review process. To simplify this procedure, Yang et al. (2018)

developed the Equivalent Energy Design Procedure (EEDP), which utilizes a balanced energy concept to design structures to satisfy strength and displacement limitations without iteration. This procedure has been used for many different seismic design applications (Yang et al. (2018); Li et al. (2018); Etebarian et al. (2019); Yang et al. (2020)). However, the original derivation of EEDP was limited to structures which are not sensitive to higher modes and which have basic Elastic-plastic hysteretic behaviour.

In this chapter, modifications to the EEDP are recommended to design the newly proposed earthquake resilient RC core wall buildings. New dynamic factors are developed and are presented within this chapter. Additionally, new energy modification factors are developed to appropriately apply EEDP to the newly proposed CROCW, CORW and SCCW systems. This chapter concludes with example design of four prototype buildings, which will be used in subsequent chapters to investigate the seismic performance of the CROCW, CORW, and SCCW systems.

5.3 Designing steps using EEDP

EEDP uses the energy balanced concept to design dual-fused structures to meet both the target displacements and forces at multiple hazard intensities. EEDP approximates the behavior of the dual-fused system with an Equivalent Nonlinear Single Degree-of-Freedom (ENSDOF) system. The energy stored in ENSDOF (elastic strain energy, E_s, plus hysteretic energy, E_h) is related to the energy dissipated by its Equivalent Linear Single Degree-of-Freedom (ELSDOF) (elastic energy, E_a). A detailed derivation of EEDP can be found in Yang et al. (2018).

Figure 5.1 shows the system global force-deformation for the ELSDOF response and the ENSDOF response of the CROCW along the CORW and SCCW axis. As the original derivation of EEDP assumes that both primary fuse system and secondary fuse systems have an Elastic-Perfectly-Plastic (EPP) hysteretic behaviour, the design procedure herein is adjusted to account for the differences in the CROCW behaviour. Specifically, new energy modification factors are developed in a subsequent section (*Section 5.4 Development of energy modification factors ($\boldsymbol{\gamma_a}$ and $\boldsymbol{\gamma_b}$)*). Additionally, the EEDP is modified to incorporate the dynamic response, using the relations developed in Chapter 4.

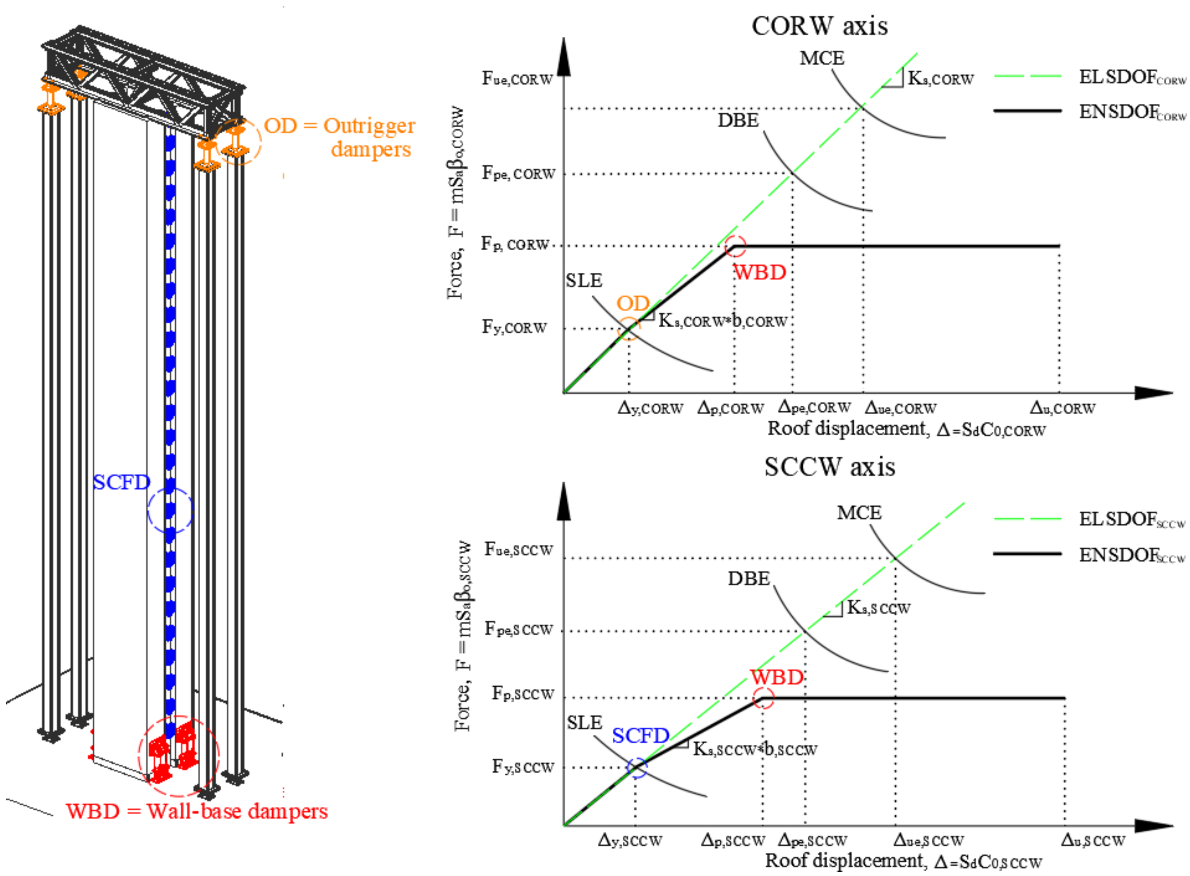

Figure 5.1 Desired nonlinear mechanisms of the CROCW

The following procedure allows engineers to design the complex behaviour of the CROCW to achieve all the desired performance objectives for the different hazards in a simple and non-iterative format. In a typical design of RCCW, the architectural constraints, such as the number of elevators, elevator and stairway sizes, and utilization of floor space, which control the geometry and mass, are often decided prior to in-depth structural design. Similarly, in the following design of the CROCW, it is assumed that the core geometry and building masses can be reasonably estimated prior to the detailed design.

Step 1: Select SLE, DBE, and MCE shaking intensities

The first step in EEDP is for the designers to work with the owners to define the demand for the CROCW system. The designer shall select SLE, DBE, and MCE hazard levels, which will be applied to both the CORW and SCCW axes. At the SLE shaking intensity, CROCW is designed to remain elastic. At the DBE shaking intensity, the outrigger dampers within the CORW and the SCFD within the SCCW is designed to yield and start to dissipate the earthquake energy, while the controlled rocking base in both systems is designed to remain elastic. At the MCE shaking intensity, the controlled rocking base in both systems is designed to yield.

Step 2: Create modified capacity design spectrum for the CORW axis

After the shaking intensities are determined, EEDP uses the capacity spectrum method concept (Freeman et al., 1975) to plot the demand and capacity curves on the same figure. In this step a modified capacity spectrum, shown in Figure 5.2, is developed for the CORW axis, where the roof displacements of the structure are estimated using the spectral displacement (S_d) multiplied by a $C_{0,\mathrm{CORW}}$ factor (shown in the equation presented below) and the base shear is determined by using the higher mode force factor, $\beta_{o,CORW}$ (shown in the equation presented below) multiplied by the spectral acceleration (S_a) of the ELSDOF and the building mass (m). Details of the development of $C_{0,CORW}$ and $\beta_{o,CORW}$ are provided in Chapter 4.

$$C_{0,CORW} = 1.52 - \frac{0.05\alpha_f}{1.2 - \alpha_f} \qquad \text{from Equation 4.9}$$

$$\beta_{o,CORW} = 0.05\frac{S_{a2}}{S_{a1}} + 0.5 \geq 0.75 \qquad \text{from Equation 4.15}$$

where S_{a2} is the spectral acceleration at the second mode period and S_{a2} is the spectral acceleration at the first mode period, and α_f is a factor which relates the stiffness of the wall to the stiffness of the outrigger as shown in Equation 3.10 (from Chapter 3).

$$\alpha_f = \frac{1}{\frac{2E_c I_{w,CORW}}{k_o H} + 1} \qquad \text{from Equation 3.10}$$

where E_c is the modulus of elasticity; $I_{w,CORW}$ is the moment of inertia of the individual wall piers in the CORW direction; ko is the rotational stiffness of the outrigger system; and H is the height of the building.

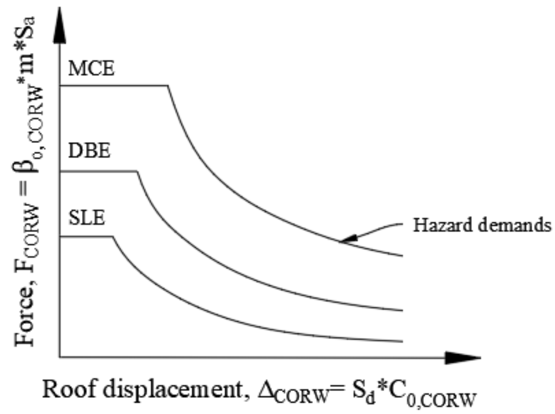

Figure 5.2 Develop modified capacity design spectrum for CORW axis

Step 3: Identify the CORW yield base shear ($F_{y,CORW}$) and yield roof displacement ($\Delta_{y,CORW}$)

In many designs, the period of the structure is usually governed by the architecture constraint. For instance, the size of the core wall and mass of the structure are usually decided based on the functionality of the structure. The CORW fundamental period governs the initial stiffness, and the selection of fundamental period will have various responses, as shown in Figure 5.3 (a). The period may be estimated using Equation 4.2 from Chapter 4, given the building geometry.

$$\mathrm{T}_{1,\mathrm{CORW}} \approx (1 - 0.37\alpha_f)1.86\sqrt{\frac{mH^3}{2E_c I_{w,CORW}}} \qquad \text{from Equation 4.2}$$

where E_c is the modulus of elasticity; $I_{w,CORW}$ is the moment of inertia of the individual wall piers in the CORW direction; ko is the rotational stiffness of the outrigger system; H is the height of the building, and α_f is a factor which relates the stiffness of the wall to the stiffness of the outrigger as shown in Equation 3.10 (from Chapter 3). .

Once the period is defined, the yield base shear ($F_{y,CORW}$) and yield displacement ($\Delta_{y,CORW}$) of the CORW system can be identified from the interaction of the constant period line with the SLE demand curve Figure 5.3 (b) shows the intersection of the yield base shear ($F_{y,CORW}$) and yield displacement ($\Delta_{y,CORW}$) of the CROCW system.

Equation 5.1, Equation 5.2 and Equation 5.3 show the relationship of initial stiffness $F_{y,CORW}$, $\Delta_{y,CORW}$, and $K_{s,CORW}$ as a function of CROCW structural properties, respectively.

$$F_{y,CORW} = S_a(\mathrm{T}_{1,\mathrm{CORW}})\beta_{o,CORW}m \qquad \text{Equation 5.1}$$

$$\Delta_{y,CORW} = S_d(\mathrm{T}_{1,\mathrm{CORW}})C_{0,CORW} \qquad \text{Equation 5.2}$$

$$K_{s,CORW} = \frac{F_{y,CORW}}{\Delta_{y,CORW}} = \frac{4\pi^2 m\beta_{o,CORW}}{\mathrm{T}_{1,\mathrm{CORW}}{}^2 C_{0,CORW}} \qquad \text{Equation 5.3}$$

where $C_{0,CORW}$ is the displacement amplification factor given in Equation 4.9; $\beta_{o,CORW}$ is the dynamic force factor given in Equation 4.15; m is the total building mass; $\mathrm{T}_{1,\mathrm{CORW}}$ is the fundamental period; and $S_a(\mathrm{T}_{1,\mathrm{CORW}})$ and $S_d(\mathrm{T}_{1,\mathrm{CORW}})$ is the spectral acceleration and displacement at the fundamental period ($\mathrm{T}_{1,\mathrm{CORW}}$), respectively.

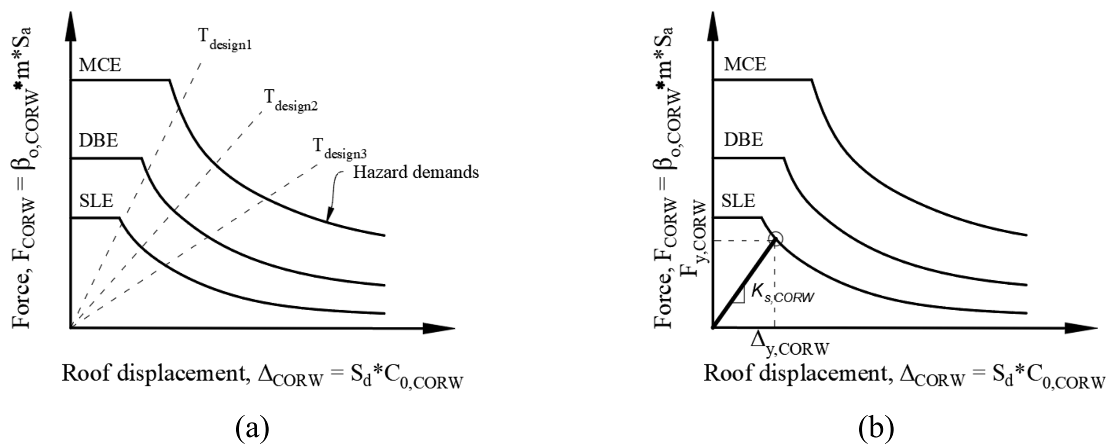

Figure 5.3 SLE performance for CORW axis: (a) period design options and (b) SLE performance point

Step 4: Design CORW at the DBE shaking intensity

In this step the performance of the CORW at the DBE shaking intensity is determined based on the designer's selection of one of following three parameters: (1) the DBE base shear ($\mathrm{F}_{p,CORW}$); (2) the DBE roof displacement ($\Delta_{p,CORW}$); or (3) the post yielding stiffness ratio (b_{CORW}). These three parameters are shown in Figure 5.4.

The post-yielding stiffness of CORW can be determined theoretically by assuming that the CORW system acts as a Euler-Bernoulli beam with a nonlinear spring (representing the controlled rocking base) at the base, and a nonlinear spring (represents the outrigger) at the roof. In this simple model, the earthquake loads are represented by an inverted triangular lateral distributed load pattern.

Equation 5.4 shows the post-yield stiffness of the, b_{CORW}, as a function of the normalized stiffness factor α_f derived in Chapter 3.

$$b_{CORW} = 1 - \frac{15}{22}\alpha_f \qquad \text{Equation 5.4}$$

Once b_{CORW} is known, EEDP uses an energy balanced concept to determine the DBE shaking intensity design base shear ($F_{p,CORW}$) and the design displacement ($\Delta_{p,CORW}$). In this process, the energy stored in an ELSDOF system is equated to that dissipated by the ENLSDOF. The incremental input energy, $\Delta E_{E1,CORW}$, shown in Figure 5.4, is determined from when the shaking intensity is increased from the SLE to the DBE shaking intensities and is given by Equation 5.5.

$$\Delta E_{E1,CORW} = \frac{1}{2}\left(F_{pe,CORW} + F_{y,CORW}\right)\left(\Delta_{pe,CORW} - \Delta_{y,CORW}\right) \qquad \text{Equation 5.5}$$

where $F_{pe,CORW}$ and $F_{y,CORW}$ are the forces in the CORW ELSDOF at the DBE and SLE hazards, respectively. $\Delta_{pe,CORW}$ and $\Delta_{y,CORW}$ are the displacement of the CORW ELSDOF at the DBE and SLE hazards, respectively.

The corresponding incremental energy dissipated by the ENLSDOF which undergoes monotonic pushover ($\Delta E_{\mathrm{NM1},CORW}$) is determined using Equation 5.6.

$$\Delta E_{\mathrm{NM1},CORW} = \frac{1}{2}\left(F_{p,CORW} + F_{y,CORW}\right)\left(\Delta_{p,CORW} - \Delta_{y,CORW}\right) \qquad \text{Equation 5.6}$$

where $F_{p,CORW}$ is the CORW axis base shear at the DBE shaking intensity and $\Delta_{p,CORW}$ is the CORW axis roof displacement at the DBE shaking intensity.

The nonlinear dynamic energy ($\Delta E_{ND1,CORW}$), determined from the ENLSDOF, is converted to the nonlinear monotonic pushover energy ($\Delta E_{\mathrm{NM1},CORW}$) using the energy modification factor $\gamma_{a,CORW}$. This process is shown in Equation 5.7.

$$\Delta E_{E1,CORW} = \Delta E_{ND1,CORW} = \gamma_{a,CORW} \Delta E_{\mathrm{NM1},CORW} \qquad \text{Equation 5.7}$$

where $\gamma_{a,CORW}$ is the energy modification, which can be calculated using Equation 5.8. Derivation of $\gamma_{a,CORW}$ is described in a subsequent section (Section 5.4 Development of energy modification factors ($\boldsymbol{\gamma_a}$ and $\boldsymbol{\gamma_b}$)).

$$\gamma_{a,CORW} = (3.5 b_{CORW} - 3)\Phi_{p,CORW} - 3.1 b_{CORW} + 3.6 \qquad \text{Equation 5.8}$$

where $\Phi_{p,CORW} = F_{y,CORW}/F_{pe,CORW}$

By substituting Equation 5.5 and Equation 5.6 in Equation 5.7, the corresponding design base shear at the DBE shaking intensity is determined by using Equation 5.9.

$$F_{p,CORW} = 2\frac{\Delta E_{E1,CORW}}{\gamma_{a,CORW}\left(\Delta_{p,CORW} - \Delta_{y,CORW}\right)} - F_{y,CORW} \qquad \text{Equation 5.9}$$

where roof displacement at the DBE intensity ($\Delta_{p,CORW}$) is calculated with Equation 5.10.

$$\Delta_{p,CORW} = \frac{F_{p,CORW} - F_{y,CORW}}{K_{s,CORW} b_{CORW}} + \Delta_{y,CORW} \qquad \text{Equation 5.10}$$

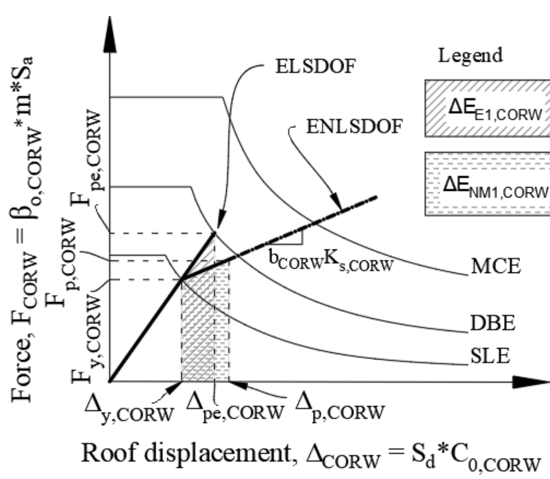

Figure 5.4 DBE performance point on CORW axis

Step 5: Determine the performance of the CORW axis system at the MCE

In this step, the performance of the CORW at the MCE, shown in Figure 5.5, is determined. EEDP assumes that the energy dissipated by the energy stored in the ELSDOF is equal to the energy dissipated by ENSDOF system. Equation 5.11 shows the incremental energy stored in the ELSDOF system when the shaking intensity changes from SLE to DBE.

$$\Delta E_{E2,CORW} = \frac{1}{2}\left(F_{ue,CORW} + F_{pe,CORW}\right)\left(\Delta_{ue,CORW} - \Delta_{pe,CORW}\right) \qquad \text{Equation 5.11}$$

where $F_{ue,CORW}$ is the elastic base shear of the CORW ELSDOF system at the MCE hazard and $\Delta_{ue,CORW}$ is the CORW elastic roof displacement of the ELSDOF system at the MCE hazard. The corresponding incremental energy dissipated from the ENLSDOF, which undergoes monotonic pushover, is determined using Equation 5.12.

$$\Delta E_{\mathrm{NM2},CORW} = F_{p,CORW}\left(\Delta_{u,CORW} - \Delta_{p,CORW}\right) \qquad \text{Equation 5.12}$$

Equation 5.13 shows the energy balanced equation.

$$\Delta E_{E2,CORW} = \Delta E_{ND2,CORW} = \gamma_{b,CORW}\Delta E_{\mathrm{NM2},CORW} \qquad \text{Equation 5.13}$$

where $\gamma_{b,CORW}$ is the energy modification factor to relate the energy dissipated by the system under monotonic pushover to that under dynamic load when the hazard level increases from DBE to MCE. Equation 5.14 shows the empirical equation for $\gamma_{b,CORW}$, developed in a subsequent section (*Section 5.4 Development of energy modification factors (*$\boldsymbol{\gamma_a}$ *and* $\boldsymbol{\gamma_b}$*)*).

$$\gamma_{b,CORW} = \left(5\lambda_{p,CORW}/\mu_{p,CORW} - 9.2\right)\Phi_{s,CORW} - 5\lambda_{p,CORW}/\mu_{p,CORW} + 8 \qquad \text{Equation 5.14}$$

where $\lambda_{p,CORW}$ is the ratio of the DBE base shear to the SLE base shear (i.e., $\lambda_{p,CORW} = F_{p,CORW}/F_{y,CORW}$); μ_p is the ratio of the DBE displacement to the SLE displacement (i.e., $\mu_{p,CORW} = \Delta_{p,CORW}/\Delta_{y,CORW}$); and $\Phi_{s,CORW}$ is the ratio of the MCE elastic base shear to the DBE elastic base shear (i.e., $\Phi_{s,CORW} = \Delta_{ue,CORW}/\Delta_{pe,CORW}$).

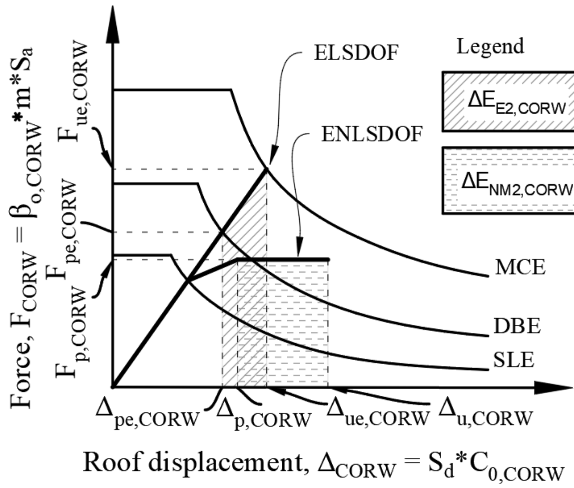

Figure 5.5 MCE performance point on CORW axis

The ultimate roof displacement ($\Delta_{u,CORW}$), can be determined by substituting Equation 5.11 and Equation 5.12 into Equation 5.13, and is shown in Equation 5.15.

$$\Delta_{u,CORW} = \frac{\Delta_{E2,CORW}}{\gamma_{b,CORW} F_{p,CORW}} + \Delta_{p,CORW} \qquad \text{Equation 5.15}$$

where $\Delta_{E2,CORW}$ is the incremental energy stored in the ELSDOF shown in Equation 5.13; $F_{P,CORW}$ is the base shear at the DBE intensity determined in Equation 5.9.

Step 6: Determine the primary and secondary system base shear in the CORW axis

In the original derivation of EEDP, the primary fuse system and secondary fuse systems are assumed to act in parallel. This results in the tri-linear system backbone to be separated into two bilinear backbones (Figure 5.6 (a)). However, the CORW system is unique due to the high contribution of elastic deformations from the core wall. As a result, the portion of force distributed to the controlled rocking base (i.e., the secondary mechanism) varies depending on the yielding force of the outrigger (i.e., primary systems). As a result, the primary system (outrigger) is a bilinear backbone, while the secondary system (controlled rocking base) has a tri-linear backbone (Figure 5.6 (b)).

The portion the demand resisted by the primary (outrigger) system, $F_{PR,CORW}$(Equation 5.16), is determined applying β_m factor, determined in Chapter 4, to the yield base shear ($F_{y,CORW}$). The part of the load resisted by the secondary (controlled rocking base) system, $F_{PR,CORW}$, can be determined by subtracting the primary force from the DBE base shear, $F_{p,CORW}$, shown in Eq. (14).

$$F_{PR,CORW} = \beta_m F_{y,CORW} \qquad \text{Equation 5.16}$$

$$F_{SC,CORW} = F_{p,CORW} - F_{PR,CORW} \qquad \text{Equation 5.17}$$

where is the ratio between the outrigger demand and the total demand determined in Chapter 4, $\beta_m = \frac{3}{8}\alpha_f$.

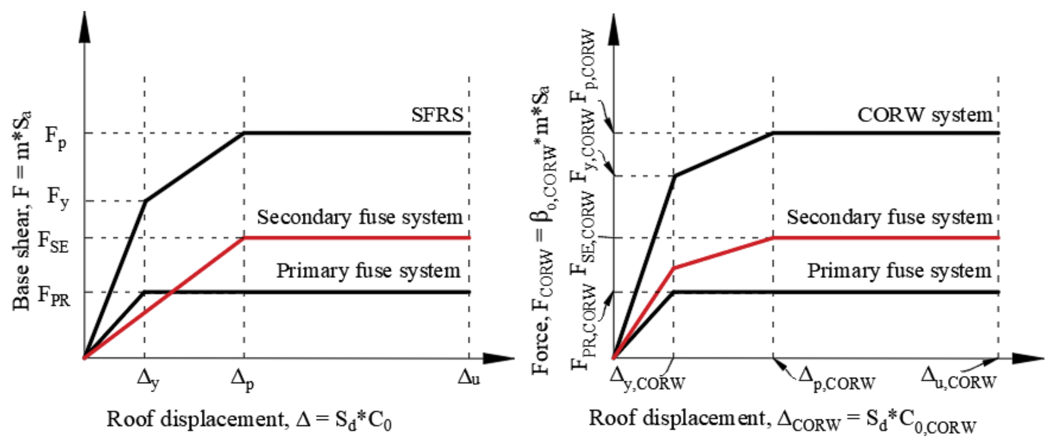

a) b)

Figure 5.6 EEDP force distribution to primary and secondary systems: (a) original EEDP force distribution and (b) CORW EEDP force distribution

Step 7: Design the primary and secondary system dampers in the CORW axis

In this step the CORW primary fuse system dampers (i.e., the outrigger dampers) and the secondary fuse system dampers (i.e., controlled rocking base) are determined. Figure 5.7 shows how the CORW mechanism (Figure 5.7 (a)) may be decomposed into the primary plastic mechanism (Figure 5.7 (b)) and secondary plastic mechanism (Figure 5.7 (c)). Equation 5.18 shows the external work done equation in the CORW primary fuse system.

$$W_{ExPr,CORW} = \theta F_{PR,CORW} \sum_{i=1}^{n} \lambda_{x,CORW} h_x \qquad \text{Equation 5.18}$$

where θ is the base rotation causing the mechanism; h_x is the elevation at a given floor, x; and $\lambda_{x,CORW}$ is the CORW force distribution, shown below. Details of the derivation of for the $\lambda_{x,CORW}$ can be identified in Chapter 4.

$$\lambda_{x,CORW} = \frac{w_x h_x}{\sum_{i=1}^{x} w_i h_i} \qquad \text{from Equation 4.13}$$

where w is the weight at each story at level x and h_x is the story elevation.

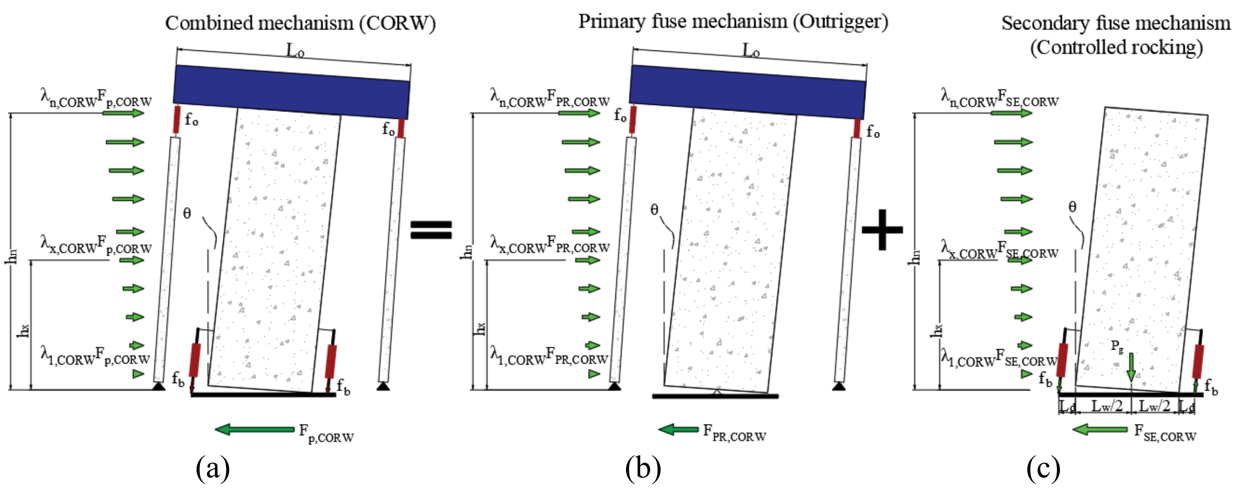

Figure 5.7 CORW axis (a) plastic mechanism, (b) primary fuse system mechanism and the (c) secondary fuse mechanism system

Equation 5.19 shows the internal work done by the primary system of the CORW.

$$W_{InPr,CORW} = \theta f_o L_o \qquad \text{Equation 5.19}$$

where $f_o$is the outrigger damper force L_o is the length of the outrigger

By equating Equation 5.18 to Equation 5.19 the forces in the outrigger are determined and shown in Equation 5.20.

$$f_o = F_{PR,CORW} \sum_{x=1}^{n} (\lambda_{x,CORW} h_x) / L_o / 2 \qquad \text{Equation 5.20}$$

The plastic mechanism of the CORW's secondary system is shown in Figure 5.7 (c). The external work for the CORW secondary fuse system is shown in Equation 5.21, while the internal work is shown in Equation 5.22.

$$W_{ExSC,CORW} = \theta F_{SC,CORW} \sum_{x=1}^{n} (\lambda_{x,CORW} h_x) - P_g(\theta L_w) \qquad \text{Equation 5.21}$$

where L_w is the length of the wall (see Figure 5.7) and P_g is the axial load in one wall pier.

$$W_{InSc,CORW} = \theta f_b (L_w + 2L_d) \qquad \text{Equation 5.22}$$

where L_d is the distance between the wall and the damper (see Figure 5.7).

The minimum design base damper force, shown in Equation 5.23, is determined by equating the internal work (Equation 5.22) and the external work (Equation 5.21).

$$f_b = \left[F_{SC,CORW} \sum_{\mathrm{x}=1}^{n} (\lambda_{x,CORW} h_x) - P_g(L_w) \right] / (L_w + 2L_d)/2 \qquad \text{Equation 5.23}$$

Step 8: Create modified capacity design spectrum for the SCCW system

Similar to Step 2, in this step the modified capacity design spectrum is developed for the SCCW axis and is shown in Figure 5.8. The SCCW roof displacements of the structure are estimated using the spectral displacement (S_d) multiplied by a $C_{0,\mathrm{SCCW}}$ factor ($C_{0,\mathrm{SCCW}} = 1.48$) and the base shear by the spectral acceleration (S_a) of the ELSDOF, the dynamic factor $\beta_{o,SCCW}$, and the building mass (m). The dynamic factor, $\beta_{o,SCCW}$, is determined using Equation 5.25, shown below.

$$\beta_{o,SCCW} = (c_1 + c_2 + c_3)^{0.5} \qquad \text{Equation 5.24}$$

where c_1, c_2, and c_3 are higher mode factors determined in Equation 4.34, Equation 4.35, and Equation 4.36, respectively.

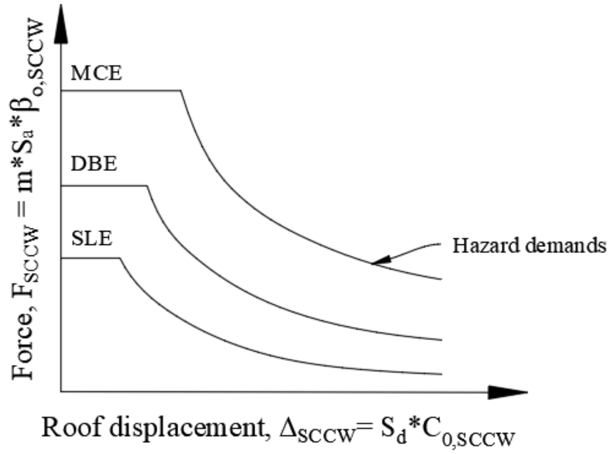

Figure 5.8 Modified capacity design spectrum for all hazards along SCCW axis

Step 9: Identify SCCW yield base shear ($F_{y,SCCW}$) and yield roof displacement ($\Delta_{y,SCCW}$)

The performance at the SLE of the SCCW is determined by selection one of the following: (1) fundamental period in the SCCW axis ($T_{1,SCCW}$); (2) the yield base shear ($F_{y,SCCW}$); or (3) the yield displacement ($\Delta_{y,SCCW}$). In this example it is assumed that the geometry of the building can be estimated early in the design process. As a result, the period may be determined using the following equation, derived in Chapter 4.

$$T_{1,SCCW} \approx 1.85\sqrt{\frac{mH^3}{E_c I_{Te}}} \qquad \text{from Equation 4.16}$$

where H is the total height of the wall; E_c is the elastic modulus of concrete; I_{Te} is the effective moment of inertia of the core, determined using parallel axis theorem which considers the moment of inertia of each wall pier and an effective area of each pier, shown in the following equation.

$$I_{Te} \approx 0.5\alpha_2 A_w L_c^{\,2} + 2I_w \qquad \text{from Equation 4.17}$$

where A_w is the cross-sectional area of a wall pier; I_w is the moment of inertia of a wall pier; d_c is the distance from the centroid of the wall pier to the centroid of the core wall; and α_2, shown in the following equation, is a stiffness factor which relates the coupling beam stiffness to the stiffness of the wall.

$$\alpha_2 = \left(0.06\frac{H}{L_c} + 0.3\right)\alpha_{\mathrm{c}} \leq \alpha_{\mathrm{c}}^2$$ from Equation 4.19

where α_{c} is relative stiffness parameter of the coupling beams to the walls developed in Chapter 4, shown in the following equation.

$$\alpha_c = \frac{1}{1 + \frac{\mathrm{E_c} A_w}{n_{\mathrm{f}} H k_{cb}}}$$ from Equation 4.1

where n_{f} is the number of stories; $\mathrm{E_c}$ is the elastic modulus of the wall; k_{cb} is the initial stiffness of the coupling beams.

The period will determine the systems initial stiffness, as shown in Figure 5.9 (a). The intersection of the SLE and a line which passes the origin and has a stiffness equal to $K_{s,SCCW}$ represents the SLE performance point, shown in Figure 5.9 (b). Equation 5.25, Equation 5.26, and Equation 5.27 shows the relationship of yield base shear ($F_{y,SCCW}$), roof displacement at yield ($\Delta_{y,SCCW}$), and initial stiffness ($K_{s,SCCW}$), respectively.

$$F_{y,SCCW} = \beta_{o,SCCW} S_a\left(\mathrm{T}_{1,SCCW}\right) m$$ Equation 5.25

$$\Delta_{y,SCCW} = S_d\left(\mathrm{T}_{1,SCCW}\right) C_{0,SCCW}$$ Equation 5.26

$$K_{s,SCCW} = \frac{F_{y,SCCW}}{\Delta_{y,SCCW}} = \frac{4\pi^2 \beta_{o,SCCW} m}{\mathrm{T}_{1,SCCW}{}^2 C_{0,\mathrm{SCCW}}}$$ Equation 5.27

where $S_a\left(\mathrm{T}_{1,SCCW}\right)$ and $S_d\left(\mathrm{T}_{1,SCCW}\right)$ is the spectral acceleration and displacement at the fundamental period($\mathrm{T}_{1,SCCW}$), respectively; m is the building mass; $C_{0,SCCW}$ is the displacement amplification factor.

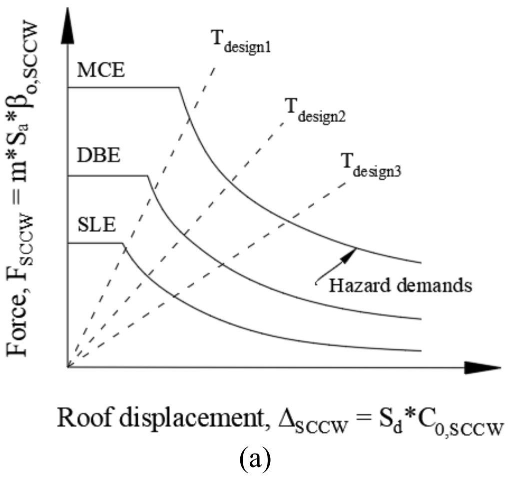

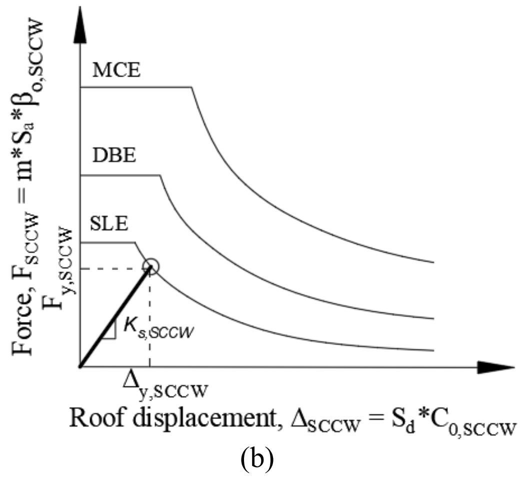

Figure 5.9 Select SLE performance for SCCW axis: (a) period options and (b) SLE performance point

Step 10: Determine relations for SCCW primary and secondary base shear

In this step the relations for the SCCW primary base shear ($F_{PR,SCCW}$) and the secondary base shear ($F_{SC,SCCW}$) are determined. In the original derivation of EEDP, the primary fuse system and secondary fuse system are assumed to act in parallel, resulting in a tri-linear system backbone to be separated into two bilinear backbones (Figure 5.10 (a)). However, in the SCCW system, a significant portion of the deformations are due to elastic deformation in the RC wall. The elastic stiffness of the core is sensitive to the boundary conditions on the wall, where, after the coupling beams yielded the elastic stiffness of the core decreases. As a result of this change in stiffness, the force-deformation relation of the secondary fuse system (i.e., the controlled rocking) shows a trilinear backbone. The primary fuse system and secondary fuse system relationship for the SCCW is shown in Figure 5.10 (b).

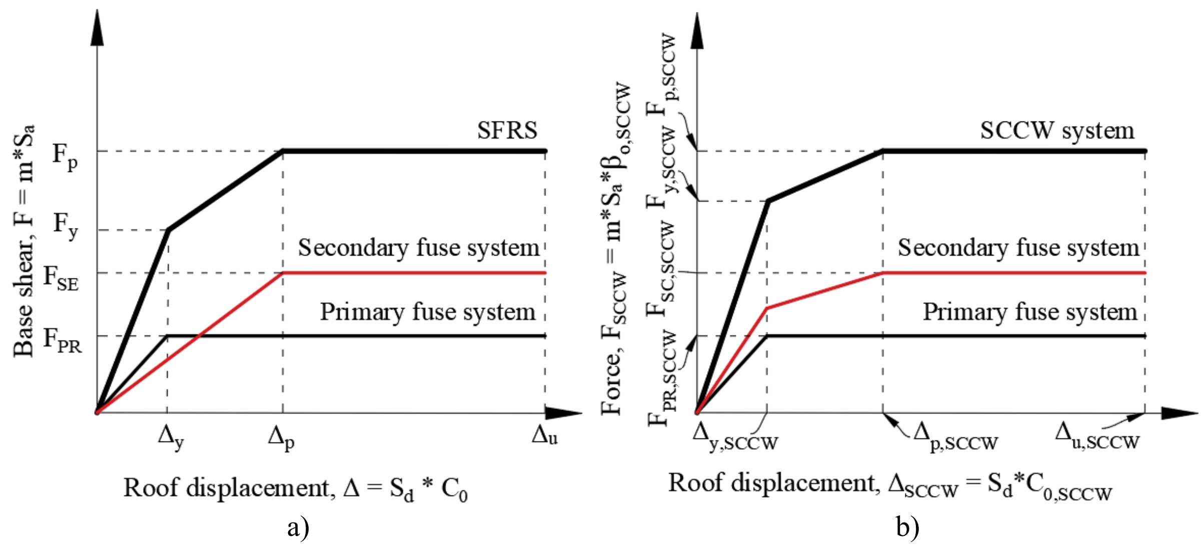

Figure 5.10 EEDP force distribution to primary fuse system and secondary fuse system: (a) original EEDP force distribution and (b) SCCW EEDP force distribution

The portion of the force resisted by the primary fuse system (i.e., $F_{PR,SCCW}$) is estimated based on the degree-of-coupling (DOC), which is defined as the ratio of the axial coupled from the coupling beams to the total overturning moment. This base shear is shown in Equation 5.28. Based on Figure 5.10 (b), the portion of the load resisted by the secondary fuse system (controlled rocking base), $F_{SC,SCCW}$, can be determined by subtracting the primary force from the DBE base shear, $F_{p,SCCW}$ as shown in Equation 5.29.

$$F_{PR,SCCW} = DOC * F_{y,SCCW} \qquad \text{Equation 5.28}$$

$$F_{SC,SCCW} = F_{p,SCCW} - F_{PR,SCCW} \qquad \text{Equation 5.29}$$

where DOC is the degree-of-coupling and can be conservatively estimated using the following equation. The development of Equation 4.28 is shown in Chapter 4.

$$\mathrm{DOC} \approx 0.85 \frac{\mathrm{A}_w {L_c}^2}{\mathrm{A}_w {L_c}^2 + 4I_w} \qquad \text{from Equation 4.28}$$

where A_w is the cross-sectional area of a wall pier; I_w is the moment of inertia of a wall pier; L_c is the distance from the centroids of the wall piers.

Step 11: Use equal work to design the SCCW primary fuse and the secondary fuse

In this step the SCCW primary fuse system dampers (i.e., the SCFDs) and the secondary fuse system base shear ($F_{SC,SCCW}$) are determined. The damper design forces are determined by first separating the primary and secondary fuse system mechanisms, shown in Figure 5.11, and applying equal work. The SCCW primary fuse system mechanism, shown in Figure 5.11 (b), assumes free rotation at the base of the walls, and all the nonlinear deformation is within the coupling beams. The SCCW secondary fuse system mechanism, as shown in Figure 5.11 (c), assumes that there is no contribution from the coupling beams, and all the plastic deformation is concentrated in the controlled rocking base. Equation 5.30 shows the expression for external work done in the SCCW primary fuse system.

$$W_{ExPr,SCCW} = \theta F_{PR,SCCW} \sum_{i=1}^{n} \lambda_{x,SCCW} h_x \qquad \text{Equation 5.30}$$

where θ is the base rotation causing the mechanism; h_x is the elevation at a given floor, x; and $\lambda_{x,SCCW}$ is the SCCW force distribution shown in the equation below. Details of the derivation of for the $\lambda_{x,SCCW}$ are shown in Chapter 4.

$$\lambda_{x,SCCW} = (\beta_x - \beta_{x+1})\frac{1}{\beta_1} \qquad \text{from Equation 4.29}$$

where β_x is the coupling beam shear distribution at a given level, x, derived in Chapter 4.

Equation 5.31 shows the internal work done by the primary system of the SCCW.

$$W_{InPr,SCCW} = \sum_{x=1}^{n} V_{P,r} \beta_x L_c \theta \qquad \text{Equation 5.31}$$

where $V_{p,r}$ is the coupling beam shear force at the top level and L_c is the distance between the centroids of the wall piers.

By equating Equation 5.31 to Equation 5.30 the forces in the coupling shear are determined and shown in Equation 5.32.

$$V_{CB,r} = \frac{F_{PR}}{2L_c}\frac{\sum_{i=1}^{n}\lambda_{x,SCCW}h_x}{\sum_{i=1}^{n}\beta_x} \qquad \text{Equation 5.32}$$

Further, the coupling beam shear at any given level x is determined using Equation 5.33.

$$V_{CB,x} = \beta_x V_{CB,r} \qquad \text{Equation 5.33}$$

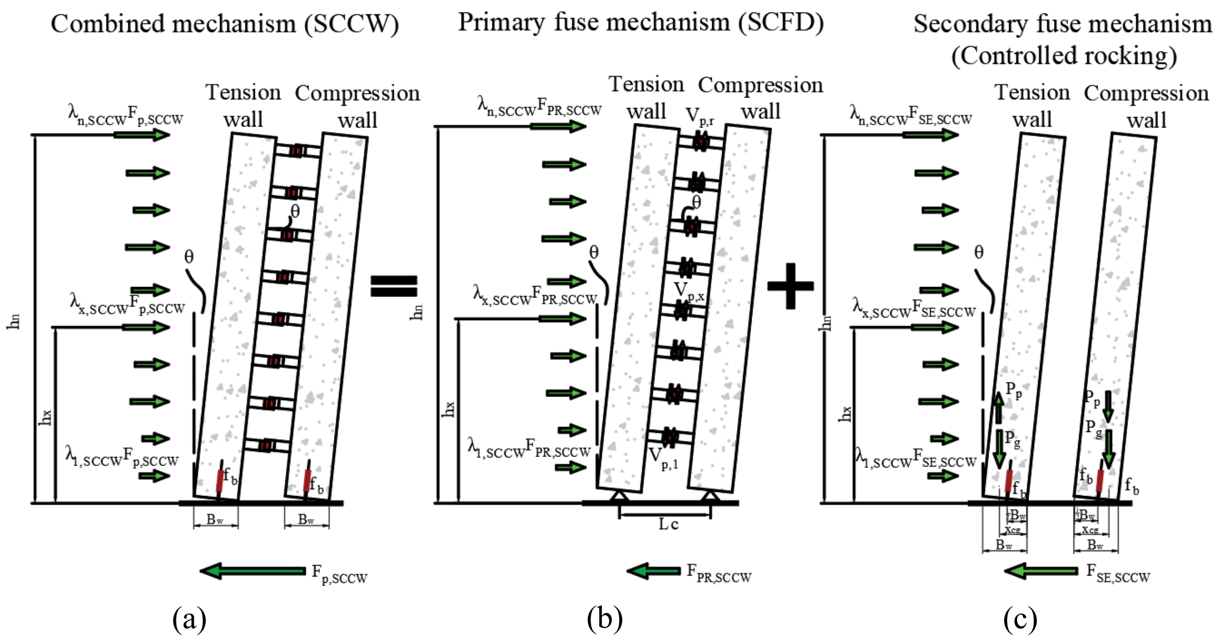

Figure 5.11 Plastic mechanisms for the SCCW system of a) the combined system; b) the primary fuse system and c) the secondary fuse system

The plastic mechanism of the SCCW's secondary system is shown in Figure 5.11 (c). The external work for the SCCW secondary fuse system is shown in Equation 5.34, while the internal work is shown in Equation 5.35.

$$W_{ExSC,SCCW} = \theta F_{SC}\sum_{x=1}^{n}(\lambda_x h_x) - \mathrm{P_g}B_W\theta + P_p(-B_W + 2x_{cg})\theta \qquad \text{Equation 5.34}$$

$$W_{InSc,CORW} = 2f_b B_W\theta \qquad \text{Equation 5.35}$$

where B_W is the length of the wall pier; x_{cg} the distance from the rocking toe of the "tension" wall to the centerline of the wall; $\mathrm{P_g}$ is the gravity load in the wall pier; and Pp is the axial couple from the coupling beams, and is estimate as the axial coupled provided by the primary fuse system, shown in Equation 5.36.

$$P_p = \frac{F_{PR}}{\beta_{o,SCCW} L_c} \sum_{x=1}^{n} (\lambda_{x,SCCW} h_x) \quad \text{Equation 5.36}$$

By equating the SCCW secondary fuse system external work (Equation 5.34) and internal work (Equation 5.35) the secondary base shear along the SCCW axis can be determined and is shown in Equation 5.37.

$$F_{SC,SCWW} = \frac{\mathrm{P_g} B_W + P_p (B_W - 2x_{cg}) + 2 f_b B_W}{\sum_{x=1}^{n} (\lambda_{x,SCCW} h_x)} \quad \text{Equation 5.37}$$

The base shear at the DBE intensity for the SCCW ($F_{p,SCCW}$), shown in Equation 5.38, may now be determined by re-arranging Equation 5.38.

$$F_{p,SCCW} = F_{SC,SCWW} + F_{PR,SCCW} \quad \text{Equation 5.38}$$

Step 12: Determine the SCCW axis DBE roof displacement and post-yielding stiffness.

In this step, the DBE base shear ($F_{p,SCCW}$), determined in Step 11, and the equal energy concept is used to determine the DBE roof displacement ($\Delta_{p,SCCW}$) and the SCCW post-yielding stiffness (b_{SCCW}).

Using the EEDP, the incremental input energy, ΔE_{E1} in the SCCW axis, shown in Figure 5.12, is determined from when the shaking intensity is increased from the SLE to the DBE shaking intensities and is given by Equation 5.39.

$$E_{E1,SCCW} = \frac{1}{2} (F_{pe,SCCW} + F_{y,SCCW})(\Delta_{pe,SCCW} - \Delta_{y,SCCW}) \quad \text{Equation 5.39}$$

where $F_{pe,SCCW}$ and $F_{y,SCCW}$ are the forces in the SCCW ELSDOF at the DBE and SLE hazards, respectively. $\Delta_{pe,SCCW}$ and $\Delta_{y,SCCW}$ are the displacement of the ELSDOF at the DBE and SLE hazards, respectively.

The corresponding incremental energy dissipated by the ENLSDOF which undergoes monotonic pushover ($\Delta E_{\mathrm{NM1},SCCW}$) is determined using Equation 5.40.

$$\Delta E_{\mathrm{NM1},SCCW} = \frac{1}{2}\left(F_{p,SCCW} + F_{y,SCCW}\right)\left(\Delta_{p,SCCW} - \Delta_{y,SCCW}\right) \quad \text{Equation 5.40}$$

where $F_{p,SCCW}$ is the base shear at the DBE shaking intensity and $\Delta_{p,SCCW}$ is the roof displacement at the DBE shaking intensity.

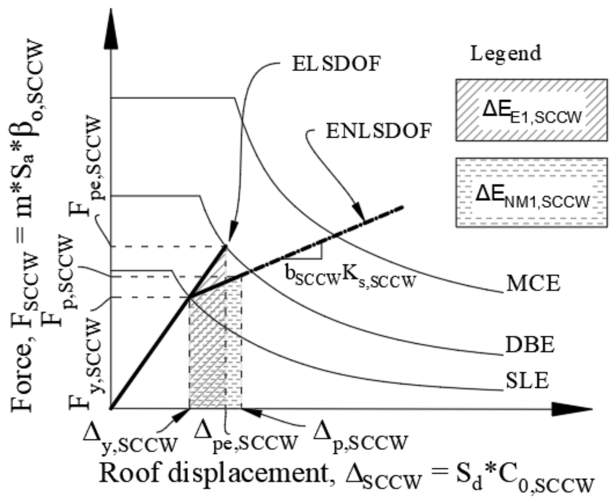

Figure 5.12 Performance of SCCW under DBE intensity

The nonlinear dynamic energy ($\Delta E_{ND1,SCCW}$), determined from the ENLSDOF, is converted to the nonlinear monotonic pushover energy ($\Delta E_{\mathrm{NM1},SCCW}$) using the energy modification factor $\gamma_{a,SCCW}$. This process is shown in Equation 5.41.

$$\Delta E_{E1,SCCW} = \Delta E_{ND1,SCCW} = \gamma_{a,SCCW}\Delta E_{\mathrm{NM1},SCCW} \quad \text{Equation 5.41}$$

where $\gamma_{a,SCCW}$ is the energy modification factor shown in Equation 5.42. Details of the derivation are shown a subsequent section (*Section 5.4 Development of energy modification factors (*$\boldsymbol{\gamma_a}$ *and* $\boldsymbol{\gamma_b}$*)*).

$$\gamma_{a,SCCW} = (3.37b_{SCCW} - 2.5)\Phi_{p,SCCW} - 2.17b_{SCCW} + 2.8 \quad \text{Equation 5.42}$$

where $\Phi_{p,SCCW} = F_{pe,SCCW}/F_{y,SCCW}$

Rearranging Equation 5.42, gives the system post yielding stiffness shown in Equation 5.43.

$$b_{SCCW} = (\gamma_{a,SCCW} - 2.8 + 2.5\Phi_{p,SCCW})/(3.37\Phi_{p,SCCW} - 2.17) \qquad \text{Equation 5.43}$$

By substituting Equation 5.39 and Equation 5.40 in Equation 5.41, the corresponding design base shear at the DBE shaking intensity is determined by using Equation 5.44.

$$F_{p,CORW} = 2\frac{\Delta E_{E1,CORW}}{\gamma_{a,CORW}\left(\Delta_{p,CORW} - \Delta_{y,CORW}\right)} - F_{y,CORW} \qquad \text{Equation 5.44}$$

Once $F_{p,SCCW}$ and b_{SCCW} are known, the SCCW roof displacement at the DBE intensity may be calculated using Equation 5.45.

$$\Delta_{p,SCCW} = \frac{F_{p,SCCW} - F_{y,SCCW}}{K_{s,SCCW}b_{SCCW}} + \Delta_{y,SCCW} \qquad \text{Equation 5.45}$$

Step 13: Determine post yielding stiffness of coupling beam

In this step, the coupling beam post yield stiffness ($k_{cb,\mathrm{p}}$) is determined. The relation between the SCCW system post yielding stiffness, b_{SCCW}, and the coupling beam post yielding stiffness $k_{p,post}$ is shown in Equation 5.46.

$$b_{SCCW} \approx \frac{\alpha_{2\mathrm{kp}}\mathrm{A}_w {L_c}^2 + 4I_w}{\alpha_2\mathrm{A}_w {L_c}^2 + 4I_w} \qquad \text{Equation 5.46}$$

where A_w is the cross-sectional area of a wall pier; I_w is the moment of inertia of a wall pier; L_c is the distance from the centroids of the wall piers; α_2, was calculated in Step 9, is a stiffness factor which relates the initial coupling beam stiffness to the stiffness of the wall; and $\alpha_{2\mathrm{kp}}$ is a stiffness factor, shown in following equation, which relates the post-yielding coupling beam stiffness to the stiffness of the wall

$$\alpha_{2\mathrm{kp}} = \left(0.06\frac{H}{L_c} + 0.3\right)\alpha_{2\mathrm{kp}} \leq \alpha_{2\mathrm{kp}}^2 \qquad \text{from Equation 4.19}$$

where $\alpha_{2\mathrm{kp}}$ is relative stiffness parameter of the coupling beams to the walls, shown in the following equation.

$$\alpha_c = \frac{1}{1 + \frac{\mathrm{E_c} A_w}{n_\mathrm{f} H k_{cb,\mathrm{p}}}} \qquad \text{from Equation 4.1}$$

where n_f is the number of stories; $\mathrm{E_c}$ is the elastic modulus of the wall; $k_{cb,\mathrm{p}}$ is the post yielding stiffness of the coupling beams.

Step 14: MCE performance point along SCCW axis

In this step, the performance of the SCCW at the MCE is determined and is shown in Figure 5.13. EEDP assumes that the energy dissipated by the energy stored in the ELSDOF is equal to the energy dissipated by ENSDOF system. Equation 5.47 shows the incremental energy stored in the ELSDOF system when the shaking intensity changes from SLE to DBE.

$$\Delta E_{E2,SCCW} = \frac{1}{2}\left(F_{ue,SCCW} + F_{pe,SCCW}\right)\left(\Delta_{ue,SCCW} - \Delta_{pe,SCCW}\right) \qquad \text{Equation 5.47}$$

where $F_{ue,SCCW}$ is the elastic base shear of the SCCW ELSDOF system at the MCE hazard and $\Delta_{ue,SCCW}$ is the SCCW elastic roof displacement of the ELSDOF system at the MCE hazard.

The corresponding incremental energy dissipated from the ENLSDOF, which undergoes monotonic pushover, is determined using Equation 5.48.

$$\Delta E_{\mathrm{NM2},SCCW} = F_{p,SCCW}\left(\Delta_{u,SCCW} - \Delta_{p,SCCW}\right) \qquad \text{Equation 5.48}$$

Equation 5.49 shows the energy balanced equation.

$$\Delta E_{E2,SCCW} = \Delta E_{ND2,SCCW} = \gamma_{b,SCCW} \Delta E_{\mathrm{NM2},SCCW} \qquad \text{Equation 5.49}$$

where $\gamma_{b,SCCW}$ is the energy modification factor to relate the energy dissipated by the system under monotonic pushover to that under dynamic load when the hazard level increases from DBE to MCE. Equation 5.50 shows the empirical equation for $\gamma_{b,SCCW}$, are shown a subsequent section (*Section 5.4 Development of energy modification factors (*$\boldsymbol{\gamma_a}$ *and* $\boldsymbol{\gamma_b}$*)*).

$$\gamma_{b,SCCW} = (5\lambda_{p,SCCW}/\mu_{p,SCCW} - 9.5)\Phi_{s,SCCW} - 5.5\lambda_{p,SCCW}/\mu_{p,SCCW} + 9 \qquad \text{Equation 5.50}$$

where $\lambda_{p,SCCW}$ is the ratio of the DBE base shear to the SLE base shear (i.e., $\lambda_{p,SCCW} = F_{p,SCCW}/F_{y,SCCW}$); μ_p is the ratio of the DBE displacement to the SLE displacement (i.e., $\mu_{p,SCCW} = \Delta_{p,SCCW}/\Delta_{y,SCCW}$); and $\Phi_{s,SCCW}$ is the ratio of the MCE elastic base shear to the DBE elastic base shear (i.e., $\Phi_{s,SCCW} = \Delta_{ue,SCCW}/\Delta_{pe,SCCW}$).

By substituting Equation 5.47 and Equation 5.48 into Equation 5.49 the ultimate roof displacement ($\Delta_{u,CORW}$) can be determined, and is shown in Equation 5.51.

$$\Delta_{u,SCCW} = \frac{\Delta_{E2,SCCW}}{\gamma_{b,SCCW} F_{p,SCCW}} + \Delta_{p,SCCW} \qquad \text{Equation 5.51}$$

where $\Delta_{E2,SCCW}$ is the incremental energy stored in the ELSDOF shown in Equation 5.49; $F_{P,SCCW}$ is the base shear at the DBE intensity determined in Equation 5.44.

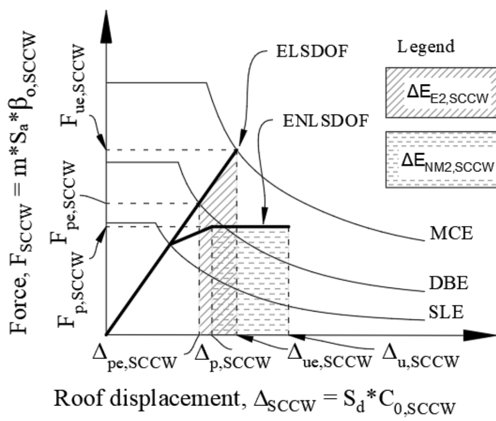

Figure 5.13 MCE performance at SCCW axis

Step 15: Capacity design of the non-yielding elements

To ensure the CROCW will achieve the performance as specified in Step 1, the non-yielding elements such as the concrete core wall, outrigger system and foundation need to be capacity designed using the maximum probable forces from the damper. It should be noted that it maybe impractical to design RC structures to be fully elastic. Hence, in this research, the RC wall reinforcement is designed to remain elastic. To ensure the yielding stays within the dampers, the connections, RC wall and foundation are designed for capacity using the maximum probable forces excreted from the dampers.

5.4 Development of energy modification factors (γ_a and γ_b)

As discussed in the previous section, EEDP assume the inelastic energy dissipated by the ENLSDOF system equals to the energy dissipated by the ELSDOF system. In 2018, Yang et al. proposed a set of γ_a and γ_b for factors to estimate the nonlinear dynamic energy dissipated by the ENLSDOF system using the nonlinear monotonic energy dissipated by the ENLSDOF system. In the original study, the system is assumed both the primary and secondary system have elastic-perfectly-plastic (EPP) force-deformation relationship. They proposed the relations for of γ_a and γ_b as a function of fundamental period and ductility factor ($\mu_p = \Delta_p/\Delta_y$). However, the CORW system utilizes the EPP hysteretic behavior for the primary system (outrigger) and flag-shaped hysteresis for the secondary system (controlled rocking base) and the SCCW utilizes the flag-shaped hysteresis for the primary system (SCFDs) and flag-shaped hysteresis for the secondary system (controlled rocking base). This unique combination requires an additional study to determine the relations for γ_a and γ_b.

To determine γ_a and γ_b factors, nonlinear time history analysis (NLTHA) was conducted on a series of SDOF systems with various parameters. The nonlinear hysteretic behavior is determined using two springs in parallel. The primary system is modelled using EPP behavior, while the secondary system utilizes a flag-shaped material following the approach proposed by Tremblay et al. (2008). In this study, a suite of 44 ground motions were adopted from the FEMA P695 study (FEMA 2009). Multiple DBE intensities ranging from 0.2, 0.4, 0.6 of the MCE level have been selected. Similarly, three additional shaking intensities ranging from 0.2, 0.4, 0.6 of the DBE hazard have been considered for SLE shaking intensity. For each combination of shaking intensities 16 nonlinear SDOF systems with 4 represented fundamental periods (T = 1, 2, 3, and 4) and 4 secondary fuse system stiffnesses of (b = 0.2, 0.4, 0.6 to 0.8) were analyzed. This results to a total of 6336 NLTHA for determining the γ_a and 6336 NLTHA for determining the γ_b.

From this analysis γ_a and γ_b factors for both the CORW and SCCW axis were developed. Equation 5.8, Equation 5.14, Equation 5.42, and Equation 5.50 shows the proposed relations for

$\gamma_{a,CORW}$, $\gamma_{b,CORW}$, $\gamma_{a,SCCW}$, and $\gamma_{b,SCCW}$, respectively. These equations were presented in the prior sections. Figure 5.14 shows the data and the equations.

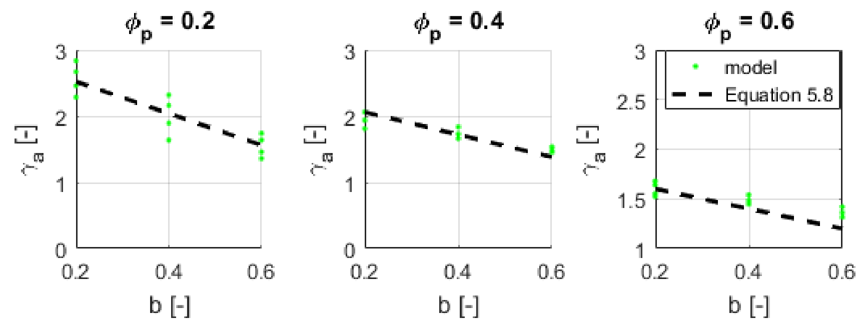

(a) $\gamma_{a,CORW}$

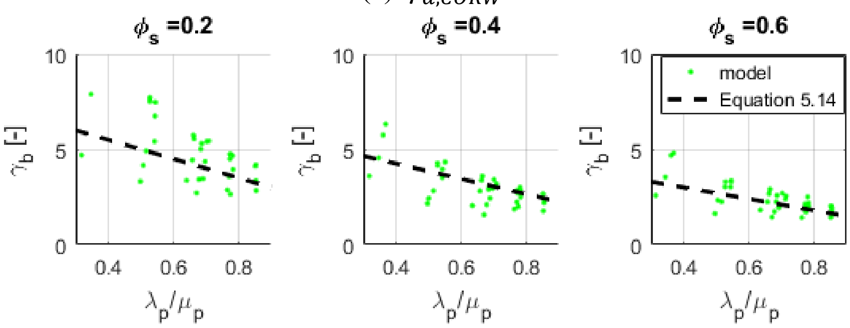

(b) $\gamma_{b,CORW}$

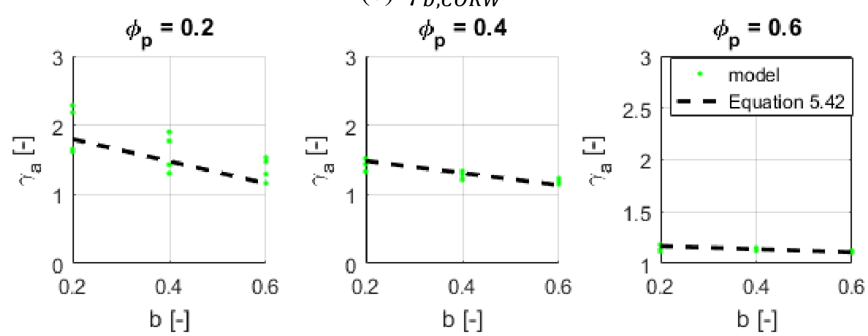

(c) $\gamma_{a,SCCW}$

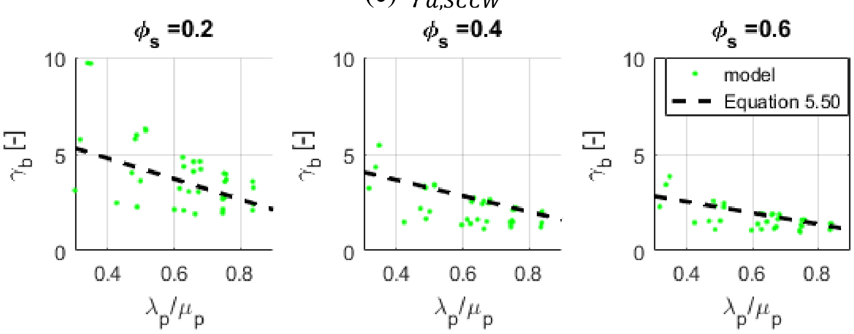

(d) $\gamma_{b,SCCW}$

Figure 5.14 Numerical response of energy modification factors (a) $\gamma_{a,CORW}$, (b) $\gamma_{b,CORW}$, (c) $\gamma_{a,SCCW}$, and (d) $\gamma_{b,SCCW}$

5.5 Prototype building designs

This section presents four prototype CROCW system buildings designed using the proposed EEDP procedure presented in Section 5.3 of this chapter. The prototype buildings were designed for two hypothetical building sites. At each site, two different buildings, differentiated by number of stories were designed: 24-stories and 40- stories. In subsequent chapters, these prototype buildings will be used to investigate the seismic performance of the novel CROCW system. The following summarises the designs.

5.5.1 Prototype building site and hazard

Both prototype building sites are in South West coast of Canada. One site is located downtown Vancouver at longitude 48.419 and latitude -123.369 and the other site is downtown Victoria at longitude 48.419 and latitude -123.369. Vancouver was selected as a prototype site as it has one of the highest tall buildings per capita in the world (CTBUH, 2019) with virtually all tall buildings use RC core walls as the primary seismic force resisting systems (Adebar et al., 2017). Hence, Vancouver is an ideal prototype site to study the performance of the novel CROCW system. Victoria was selected as the second prototype site as it has the highest seismic hazard of any large Canadian city, comparable to cities such as Los Angeles in the US. This high seismic hazard makes Victoria another excellent site to study the performance of the novel systems introduced in this dissertation.

Both sites have an assumed shear wave velocity, Vs30, of 450 m/s, which is classified as site class C according to the NBCC, 2015. In this study, the Maximum considered earthquake (MCE) represents the 2% probability of exceedance in 50 years which follows the MCE design level in the ASCE (2016) and the NBCC (2015). In Canada, there is currently no recommendation for Service Level Earthquakes (SLE), therefore, the SLE uses the 50% probability of exceedance in 30 years recommended in the US for performance-based design (LATBSDC, 2020). The Design-based earthquake (DBE), at which the base dampers to remain elastic, was selected as the 20% probability of exceedance in 50 years.

The uniform hazard spectrums (UHSs) used for the designs are presented in Figure 5.15 (a) and (b) for the Vancouver site and the Victoria sites, respectively. These UHSs were developed using probabilistic seismic hazard analysis (PSHA). The PSHA is described in further detail in a subsequent chapter (Chapter 7). As shown in Figure 5.15, spectral accelerations in the Victoria spectrum are approximately 60% greater than Vancouver values.

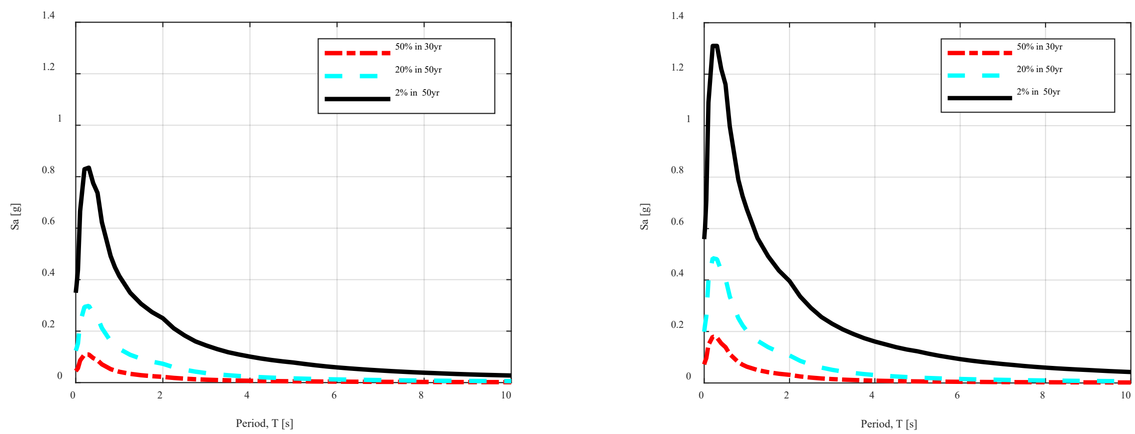

(a) (b)

Figure 5.15 Uniform hazard spectrums for (a) Vancouver site and (b) Victoria site

5.5.2 Description of prototype building geometry and materials

Four prototype core wall buildings designed using the proposed EEDP and the UHS presented in Figure 5.15. For each location, two different number of stories were designed: 24 and 40. The story height is 4 m for all buildings, resulting in building heights, excluding the height of the outrigger, of 96m and 160m for the 24 and 40, buildings, respectively.

The Seismic Force Resisting System (SFRS) utilizes a central RC core-wall. The RC core is composed of two symmetric C-shaped walls with constant thicknesses up the height of the building. The core footprint is a square shape with dimension Lw x Lw. Along one principal axis (X-axis in (b)), the SFRS consists of a controlled rocking outriggered wall (CORW). Along the other principal axis (Y-axis (b)), the SFRS consists of the self-centring coupled wall (SCCW) system.

The gravity systems consist of flat slabs connected to RC columns. All prototype buildings utilize a square flat plate floor slab (L_b x L_b) with a slab thickness of 250mm. The gravity load and seismic mass were calculated assuming the structural component self-weights with an additional distributed load of 1 kPa for finishes. Previous studies have shown that minimal interaction between the rocking wall and the gravity system can be achieved through isolated wall-to-floor connection (Henry et al., 2012). However, the performance of the gravity system was not examined in this study.

The building geometric parameters were developed in consultation with practicing engineers familiar with the design practices in the United States of America and Canada. For simplicity, only two unique building geometry are considered for each location, however, the sizes of the dampers and vertical reinforcing steel differed between buildings. Figure 5.16 (a) shows the 24-story prototype elevations, Figure 5.16 (b) shows the 40-story prototype elevations, and Figure 5.16 (c) shows the plan view. Table 5.1 summarizes the geometry and dead load for the six prototype buildings.

Table 5.1 Characteristics of prototype building designs

Name	Location	Story #	H $[m]$	L_b* $[m]$	L_w* $[m]$	B_w* $[m]$	t_w* $[m]$	t_f* $[m]$	W** [MN]	P_g*** [MN]
Van24	Vancouver	24	96	26.85	9.25	3.39	0.58	0.99	179	41
Vic24	Victoria									
Van40	Vancouver	40	160	27.6	12.00	4.77	0.50	0.80	300	75
Vic40	Victoria									

* Parameters L_w,B_w,t_w,t_f are shown in Figure 5.16; ** W is the total seismic weight of the building; *** P_g is gravity load on one C-shaped wall pier.

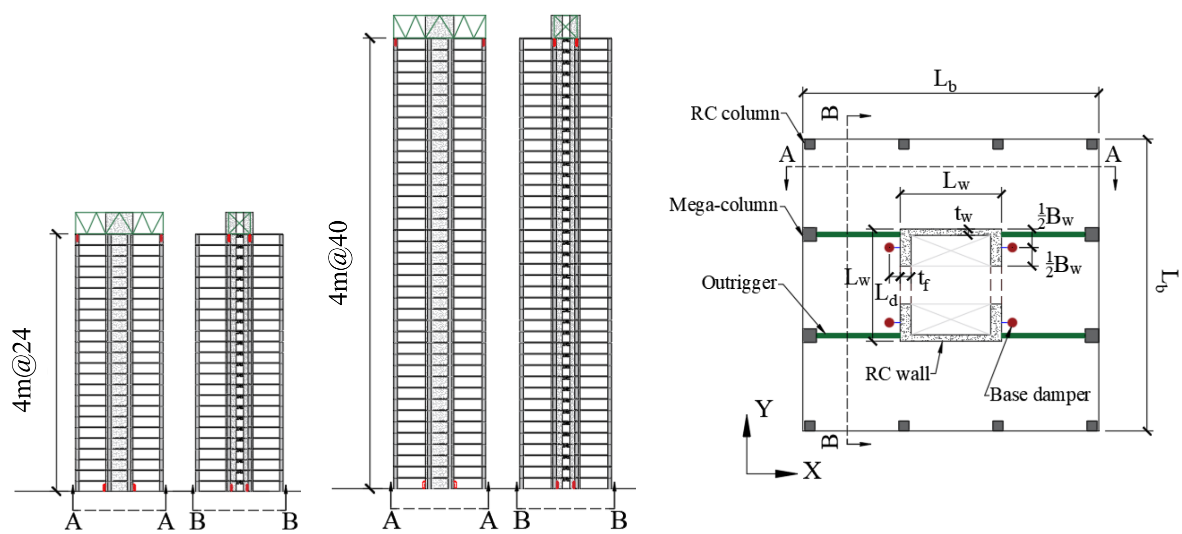

(a) (b) (c)

Figure 5.16 Prototype buildings (a) 24-story elevations; (b) 40-story elevations; and (c) plan view

The outrigger system consists of a steel truss system rigidly connected to the RC core and to exterior mega-columns. The detailed geometry of the outrigger system is shown in Figure 5.17.

The RC mega-columns are assumed to have a constant cross section of 1.2m x 1.2m over the entire height of the building. Symmetric friction dampers are fixed vertically between the mega-columns and the truss system. In these designs, the outrigger truss and columns are designed to be elastic. The outrigger system configuration used in this study are shown in Figure 5.17, however, other configurations could be equally suitable. For all prototype buildings, the outrigger depth was 8m, the top chords were W14x283 steel sections; and the Braces and Verticals were W14x426. The outrigger length is 25.75m and 26.5m for the 24-story and 40-story buildings, respectively.

The coupling beams utilize embedded steel beams connected to self-centering conical friction dampers (SCFDs). Figure 5.17 (b) shows the coupling beams embedded in the RC wall. The embedded detailing is assumed to follow the recommendations by AISC, 2016. In the prototype design, the SCFD are designed for the different force demands. However, it is assumed that all the Embedded beams are W24x335.

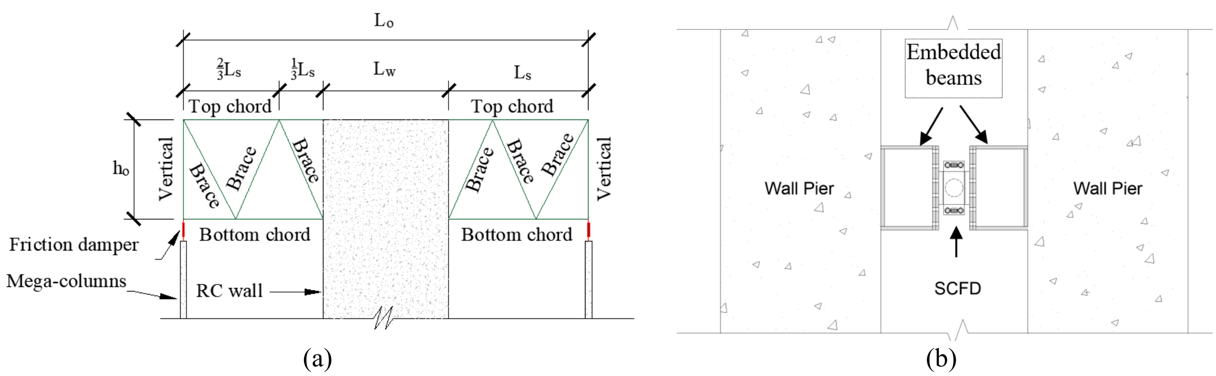

Figure 5.17 Prototype outrigger geometry

The prototype buildings were designed assuming that there were no subgrade floors. It is also assumed that the controlled rocking base is constrained from sliding either through friction or a mechanical shear key. The restoring forces for the controlled rocking base are assumed to be entirely from the gravity loads. Hence, there was no need for additional post-tensioning, typical of controlled rocking walls. The dampers within the controlled rocking base are sliding friction dampers (Rodgers et al., 2017).

All structural steel sections utilize grade ASTM A992/A992M steel, which has a yield stress of 345 MPa and a minimum tensile strength of 450MPa. All the reinforcing steel is assumed to follow CSA G30.18 Grade 400W grade reinforcing steel, which has a design yield strength of 400MPa. The elastic modulus for all steel is assumed to be Es = 200GPa. The design elastic modulus is calculated following CSA A23.3 and is shown in Equation 5.52. For a specified compressive strength at 28 days of f’c = 50MPa and f’c = 60 MPa, for the 24-story and 40 story buildings respectively.

$$E_c = 3300\sqrt{f'c} + 6900\ [MPa] \qquad \text{Equation 5.52}$$

5.5.3 Summary of design parameters

Table 5.2 shows the design EEDP base shear, roof displacements, and damper forces for each prototype building. Table 5.3 shows the damper forces for the outrigger (f_o), base dampers (f_b), roof coupling beam shear (V_{pr}), and the post yielding stiffness of the coupling beam ($k_{c,b}$). Capacity design was conducted for each prototype building. For simplicity, a constant reinforcing ratio was used throughout the height of the building, Figure 5.18 shows the designed cross section for the RC walls.

Table 5.2 EEDP design values for prototype CROCW systems, along CORW and SCCW axis

	Name	T_1 $[s]$	γ_a $[-]$	γ_b $[-]$	b [-]	Δ_y $[mm]$	Δ_p $[mm]$	Δ_u $[mm]$	F_y $[MN]$	F_p $[MN]$
CORW	Van24	2.19	1.40	2.70	0.61	40	115	435	3.38	10.75
	Vic24		1.40	2.69	0.61	60	175	680	5.42	17.20
	Van40	4.19	1.23	2.60	0.70	45	145	710	2.34	7.55
	Vic40		1.22	2.61	0.70	75	225	1130	3.74	12.07
SCCW	Van24	3.00	1.77	4.83	0.24	45	130	545	2.95	9.62
	Vic24		1.80	4.88	0.22	65	205	885	4.72	15.38
	Van40	5.23	1.58	4.63	0.41	50	155	825	2.60	8.49
	Vic40		1.80	5.20	0.23	75	255	1475	4.16	13.58

Table 5.3 Damper design values

Name	f_o $[kN]$	$f_b [kN]$	$V_{pr} [kN]$	$k_{c,b}$ [kN/mm]
Van24	920	3425	295	35
Vic24	1470	15675	465	31
Van40	800	2590	225	37
Vic40	1280	3065	360	16

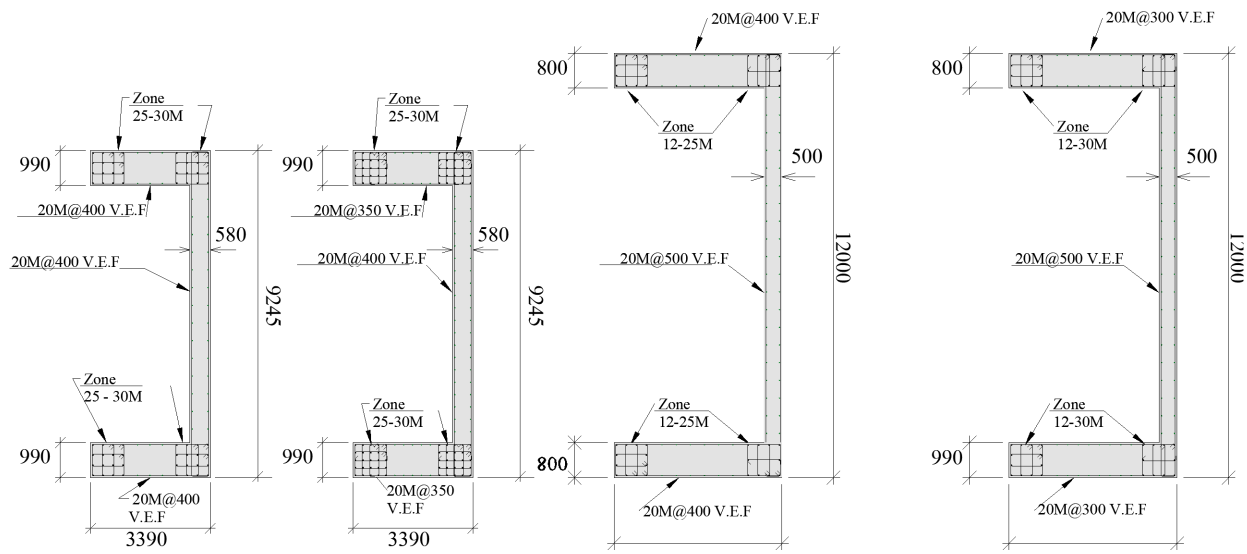

(a) Van24 (b) Vic24 (c) Van40 (d) Vic40

Figure 5.18 Reinforcing detailing for each prototype building: (a) Vancouver 24-story, (b) Victoria 24-story, (c) Vancouver 40-story, and (d) Victoria 40-story

5.6 Summary

This chapter presents a detailed EEDP for the CROCW system. While this chapter focused on designing the CROCW system, the same methods may be applied to both the SCCW and CORW systems independently. When designing independently, the governing base damper design should be used. This would result in the damper in one direction being overdesigned for the other. However, this is equally suitable, as it would be a conservative, albeit less efficient, design.

Modifications to the EEDP to account for higher mode effects are presented. Additionally, new energy modification factors are presented in this chapter, which accounts for the unique hysteretic shapes from the primary and secondary fuse systems.

The design procedure developed in this chapter is advantageous as, like other performance-based design methods, it allows the design of multiple performance objectives at different shaking intensities. However, unlike other performance-based design methods, EEDP allows for the design to be completed without iterations. This modified design process will allow for an efficient design process when implementing the novel CROCW, CORW, or SCCW systems.

This chapter concludes with the design of four prototype buildings. Two different story heights (24-story and 40-story) prototype buildings were designed for each of the two different locations

(Vancouver site and Victoria site). Buildings were designed to a Maximum considered earthquake (MCE) of 2% probability of exceedance in 50 years; a Design-based earthquake (DBE) of 20% probability of exceedance in 50 years; and a Service level earthquake (SLE) of 50% probability of exceedance in 30 years.

The next several chapters focus on investigating the nonlinear seismic performance of these systems using four prototype buildings. Chapter 6 describes the nonlinear modelling approach used for the remainder of the thesis. Chapter 7 describes the prototype site probabilistic hazard analysis, and ground motion selections for each prototype building site used throughout the remainder studies. Chapter 8, Chapter 9, and Chapter 10 investigate the seismic performance of the CORW and SCCW designed with the EEDP, which was presented in this chapter, for unidirectional loading in the CORW direction, unidirectional loading in the SCCW direction, and bidirectional loading, respectively.

Chapter 6: Nonlinear modelling approach

6.1 Overview

This chapter presents the nonlinear modelling approach, which is used in subsequent chapters to investigate the nonlinear dynamic response of the CORW and SCCW systems. Described in this chapter in the detailed 3-dimensional modelling approach for the overall structure and individual components. System-level assumptions, such as gravity loads, mass distribution, and damping are discussed. Each of the structural component numerical modelling methods, including RC wall, controlled rocking wall, SCFD, and axial friction dampers, were validated using experimental data.

6.2 System modelling

The numerical modelling utilises the commercially available software package PERFORM 3D (Computers and Structures, 2018). This software is commonly used for performance-based seismic design of tall buildings in Canada and the United States. The detailed modelling approach presented in this chapter, which uses an accessible and well-understood software, can allow for the newly proposed earthquake-resilient RC core wall system to be more easily adapted to industry.

To demonstrate the modelling approach, an example building is modelled which consists of a CORW along one principal axis (X-axis, Figure 6.1) and a SCCW along the other principal axis (Y-axis, Figure 6.1). The 3-dimensional model, shown in Figure 6.1, consists of components such as RC walls, controlled rocking base, SCFD, outrigger members and unidirectional friction dampers. The core wall utilizes 4-node *Shear Wall Elements*, situated at the centerline of the wall. The SCFDs are connected to the walls using elastic beam elements. The detailed modelling and validation of these components are discussed in Section *6.3 Component modeling.*

At typical story levels, the nodes were constrained using *Horizontal Rigid Floor* diaphragm constraint. The nodes at the base of the models were assigned restraints according to the desired fixity of degrees of freedom. Typically, vertical elements have all degrees of freedom restrained at the base. Seismic mass was calculated as 100% of the dead loads which includes self-weight of the structure and additional superimposed dead loads due to use and occupancy. The seismic mass was lumped onto a single node at the mass centroid and assigned the total lateral mass and torsional mass moment of inertia. The rigid diaphragm constraints then ensure the inertial forces are distributed out to the components of the structure.

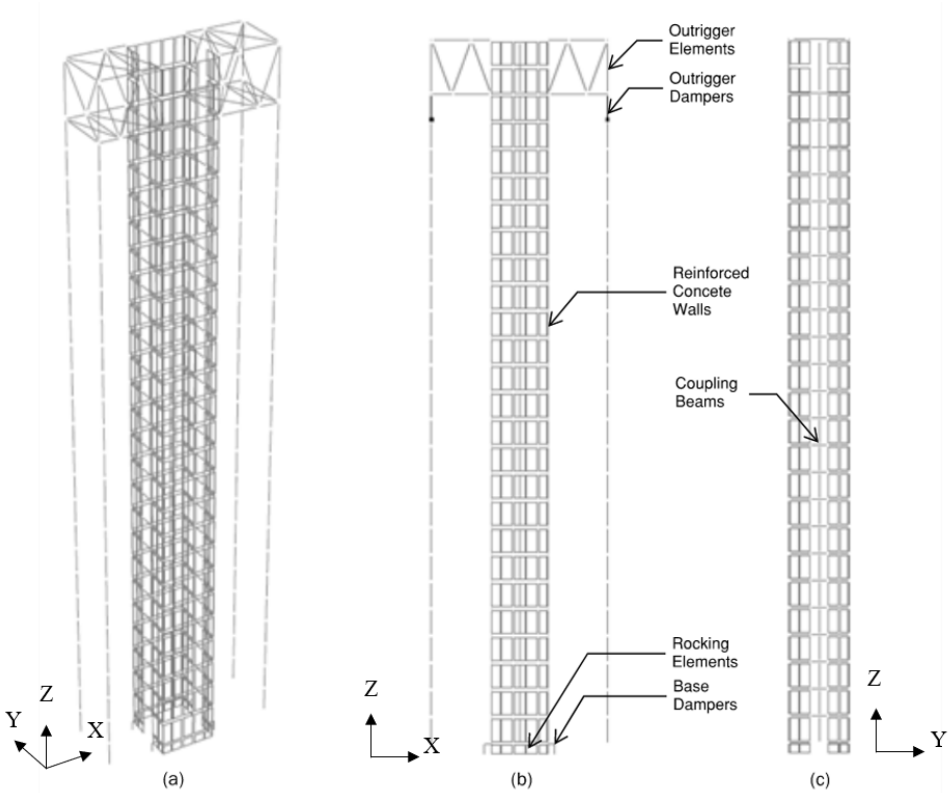

Figure 6.1 Numerical model of an example building shown in (a) 3D view, (b) Front Elevation, and (c) Side Elevation

The 3-dimensional model was developed assuming that the Seismic Force Resisting System (SFRS) resists 100% of the earthquake loads. The lateral resistance due to gravity members (i.e., slabs and columns) were excluded from analysis. However, under certain circumstances, the global stability of structures can be significantly affected by P-Delta effects (P-Δ), which refers to the second order forces induced when structures displace laterally while simultaneously being loaded with vertical (gravity) forces.

Since this research focusses on tall buildings, where both gravity loads and lateral drifts can be large, P-Δ forms an important part of the response. P-Δ effects were included in all time history analyses by using a "Leaning column" or "P-Delta column." These elements have no lateral stiffness of their own but are connected to the SFRS and will "lean" on it for stability as the structure displaces laterally. The P-Delta column is loaded with all the non-simulated gravity loads from the secondary framing system, such that the total gravity load of the structure is included in the analysis: The SFRS includes its tributary gravity loads (which are needed to properly simulate the response of fiber elements) while the remainder of the gravity loads are placed on the P-Delta column. The columns were modelled using elastic frame elements with flexural releases ("pins") at the floor levels.

The nonlinear time-history analysis uses event-to-event solution technique which provides a stable and predictable output, even with highly nonlinear structures such as rocking systems. Damping for nonlinear time history analyses employed modal damping across all significant modes of the structure, plus a small amount of Rayleigh damping. The total viscous damping ratio was set to 2.5% in line with common practice in nonlinear time history analysis (LATBSDC, 2020). Modal damping accounted for 2.4% of that damping ratio, while Rayleigh mass and stiffness proportional damping accounted for the remaining 0.1%, anchored to the periods 2.0 T_1 and 0.1 T_1. This approach is recommended to avoid some of the issues encountered with solely using Rayleigh damping or solely modal damping (Hall, 2006; Chopra & McKenna, 2016; LATBSDC, 2020).

6.3 Component modeling

The complex nonlinear behaviour of RC elements can be simulated using three broadly categorized approaches: Lumped Plasticity Models, Continuum Models, and Distributed Plasticity Models. Lumped Plasticity models are the simplest and most computationally efficient, however their simplicity often comes at the expense of missing certain phenomenon that are of interest in RC structures. For instance, a concrete element might be simulated with an elastic frame and lumped plasticity moment-hinges at each end of the element, but this model will not be able to account for the interaction between moment and axial load, nor will it provide useful information about the strain distribution in the element. For the above reasons, other modelling approaches are often chosen for simulation of vertical elements (walls, columns) in concrete structures. Continuum Models offer the most detailed modelling approach, with the ability to capture most phenomenological effects. This approach is a good candidate for simulating the detailed response of a concrete element, however this comes at the expense of computational effort, and is generally difficult to implement for full building structures. The final modelling approach, distributed plasticity models, is the one utilized in this thesis for simulating RC elements. This approach affords computational efficiency while still capturing many of the pertinent characteristics of the response of RC structures to static and dynamic loads.

PERFORM offers various component models to simulate the behaviour of structures, including both lumped plasticity and distributed plasticity components. In general, one or more structural behaviours can be defined, and then aggregated together into a compound element, which is assigned to the model geometry. For example, a shear wall fiber section can be aggregated with linear or nonlinear wall shear behaviour to form a complete shear wall compound, or nonlinear moment-rotation hinges can be aggregated with linear frame elements to form a nonlinear beam compound.

The adopted modelling approaches are discussed further in this section. The five main component types used in the numerical model are: the RC walls, the controlled rocking mechanism, the novel self-centering coupling beams spanning between wall piers, the hysteretic dampers used at the outrigger and wall-base, and the outrigger frame elements. Each component is described in the following sections, and nonlinear behaviour is validated with a previously conducted experiment.

6.3.1 Fixed base RC Walls

Nonlinear fiber elements are used to capture the hysteretic behaviour of the RC walls. In a fiber model, the material constitutive relations are assigned to discretized fibers over the cross section of the element. These elements are advantageous due to their computational efficiency and reasonable accuracy in predicting of the axial-flexural interaction. Typically, the shear behaviour is assigned as an uncoupled spring with linear elastic behaviour. The shear and flexural behaviour is decoupled; however, this simplification is common for modeling the SFRS in tall slender walls (LATBSDC, 2020).

6.3.1.1 Element formulation

Wall elements were modelled using *Shear Wall Element*. This is an engineering element, rather than a general-purpose finite element, and it is intended to capture the behaviour of RC walls without being excessively complex (Computers and Structures Inc., 2018). The shear wall element has 4 nodes and 24 degrees of freedom. Figure 6.2 shows a schematic representation of the eight in-plane deformations of the element. In this element, inelastic behaviour is modelled in the axial/bending in the vertical direction and linear shear behaviour. Other degrees of freedom are modelled with linear elastic behaviour, with reduced stiffness to account for cracking.

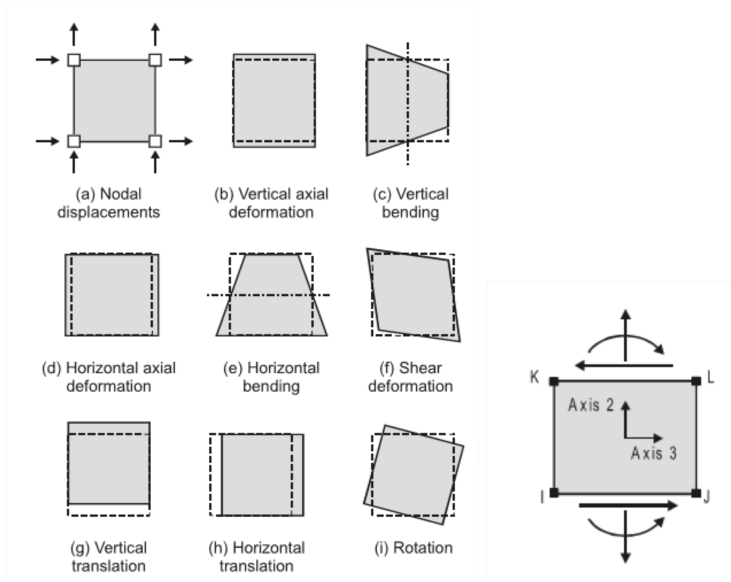

Figure 6.2 PERFORM-3D Shear Wall Element (Computers and Structures Inc., 2018)

The complex hysteretic axial-flexural behaviour of RC walls is captured by multiple nonlinear uniaxial fiber elements arranged together into a wall cross section. Each fiber is assigned material properties, cross-sectional area, and a coordinate within the overall wall cross section. The shear properties are modeled using an uncoupled elastic spring, with a cracked stiffness of $0.5GA_v$ as recommended by Los Angeles Tall Building Council (LATBSDC 2020).

6.3.1.2 Material properties

The fiber element formulation for a typical RC wall relies on at least two uniaxial material formulations: Reinforcing Steel and Concrete. The Reinforcing steel was modelled using the *Inelastic Steel Material, Non-Buckling* material. The basic backbone and cyclic behaviour are shown in Figure 6.3 (a) and (b), respectively. The steel material is described with a trilinear backbone passing through the points (0, 0), (DY, FY), (DU, FU), (DX, FX), and is symmetric in tension and compression. The yield stress, FY, is chosen based on the measured (or expected) yield stress of the steel, and the yield strain, DY, corresponds to this stress divided by the modulus of elasticity for steel, assumed to be 200,000 MPa. The next point is defined by the measured (or expected) ultimate tensile stress of the steel, and an assumed strain of 0.075, which is approximately half of the fracture strain. After this point, the stress plateaus, and the final strain is set to an assumed fracture strain of 0.15. Cyclic degradation was included in the steel material using the YX+3 option, with deformations set to (0.0025, 0.004, 0.006) and energy factors (0.7, 0.68, 0.64, 0.62, 0.60), which follows the approach in PEER Tall Building Initiative (PEER, 2012).

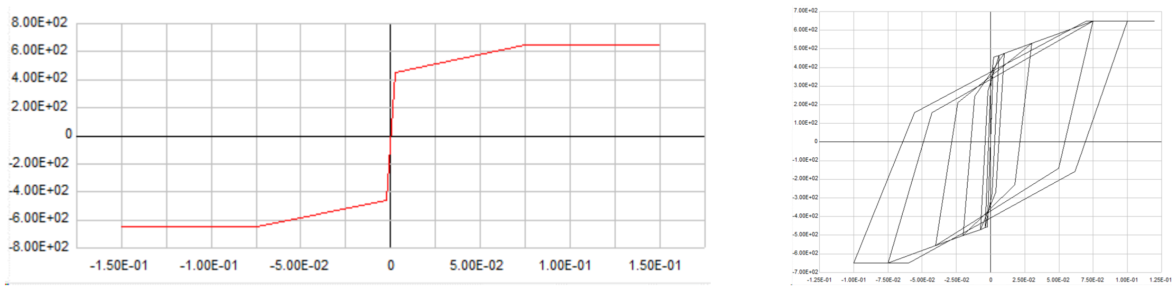

(a) (b)

Figure 6.3 Reinforcing Steel Material in units of MPa for stress and strain is unitless (a) backbone, and (b) Cyclic behaviour

In this study a single unconfined concrete material was used. The cyclic behaviour of concrete was modelled using the *Inelastic 1D Concrete Material*. In compression, the concrete material is enveloped by a trilinear backbone, followed by linear strength loss, and finally a constant residual strength. In this model, the tension stress is set to 0. The initial stiffness was determined using the equation $4500\sqrt{f_c'}$ (MPa). The compressive stress and strains at the other key points on the curve were determined by approximating the high strength concrete model described by Razvi and Saatcioglu (1999).

6.3.1.3 Description of experimental test for validation

The numerical models developed in this section are validated to a RC wall specimen tested by Adebar et al. (2007), summarized in Figure 6.4. The specimen was intended to represent a typical Vancouver high-rise building wall, constructed at ¼ scale. The specimen was 12.2 m tall and has a 1.625 m wide I-shaped cross section. The flanges and web were 203 mm and 127 mm, respectively. The reinforcing ratio in the flange was 0.65% provided by 5-10M vertical bars enclosed by #3@64mm ties. The reinforcing ratio in the web was 0.26%, provided by a single centered layer of 10M@305mm bars. Horizontal reinforcing was provided through the web and into the flanges with a single centered layer of 10M@305mm bars. The average compression strength (f'c) from the concrete cylinder tests at the day of testing was 49MPa. Tensile testing of the reinforcing showed a yield and ultimate strength of 455 and 650 MPa, respectively. A constant axial load was applied during the test with magnitude equal to $0.10f_c'A_g$ (1500 kN). Lateral load was applied 11.76m from the wall base using a hydraulic actuator using a constant displacement rate of 1mm/second. The loading protocol for the test included four cycles at each of the 13 displacement levels, which increased from ±15mm at Level 1 to ±300mm at Level 13.

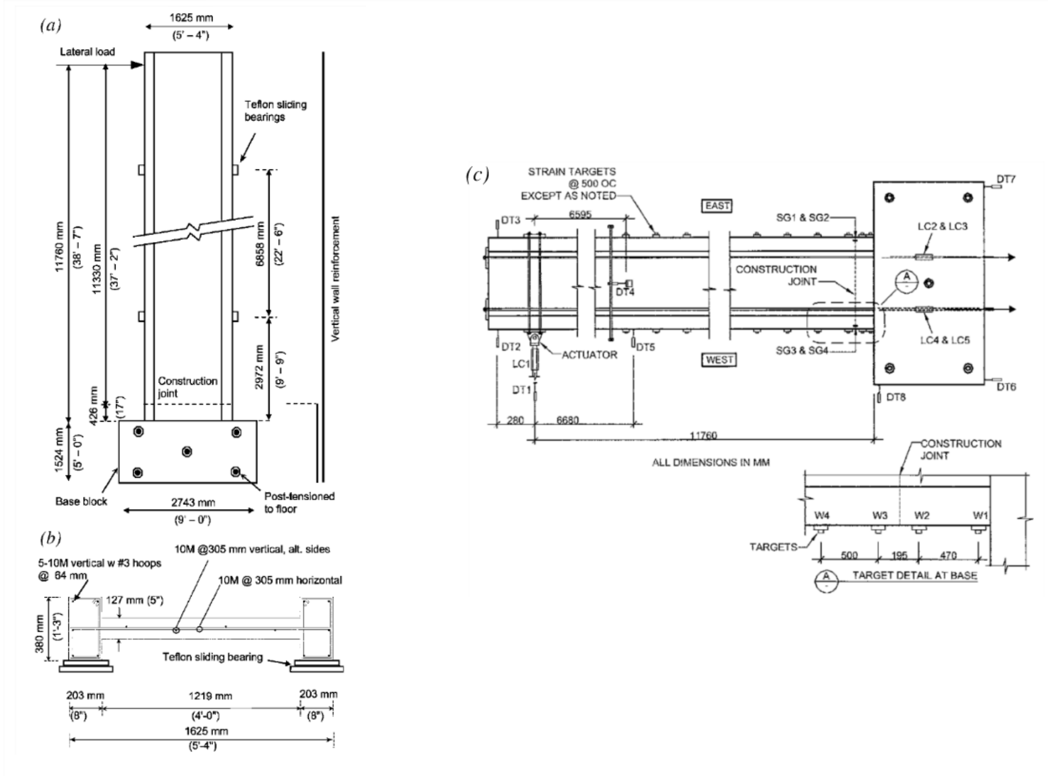

Figure 6.4 Details of test wall specimen adapted from Adebar et al. (2006): (a) elevation; (b) cross section; (c) instrumentation

6.3.1.4 Validation of model

To validate the RC wall modeling approach, the experimental test by Adebar et al. (2007) was simulated using the methods describe above (shown in Figure 6.5). Shear wall elements were defined such that the outer element on either side of the wall encompassed the entire flange, while the web was discretized into 4 elements across its length. Both flange and web had 46 elements along their height. The reinforcing ratio in the flange and wall elements were 0.65% and 0.27%, respectively. The lowermost row of elements had double the reinforcing ratio, to simulate the extra rebar across the construction joint. Wall shear behaviour was modelled linearly with an effective shear modulus of G = 6250MPa, or approximately 0.5 times the uncracked value. One additional row of elements was modeled above the point of lateral load application, like real wall geometry. Vertical gravity loads (PT loads on the real specimen) were applied to four nodes at the uppermost point on the wall, each with one quarter of the total applied PT force. The model was assumed to be fixed at the base, which coincides with the top of the foundation block in the real specimen.

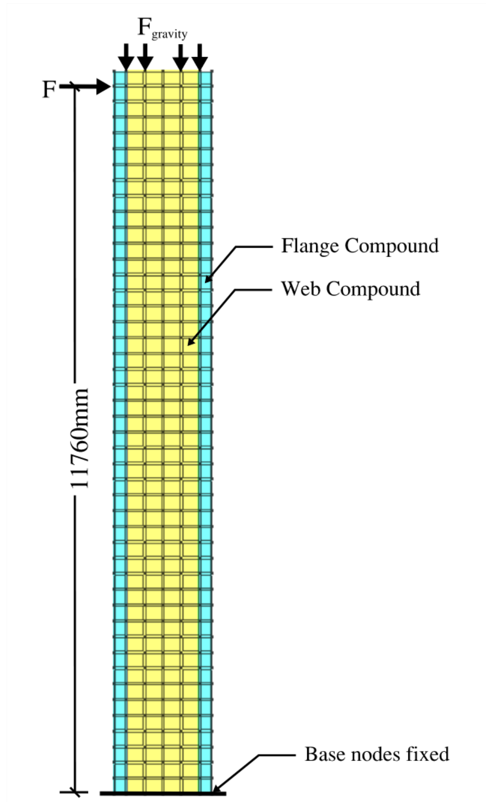

Figure 6.5 Model of experimental test of RC wall

The model was loaded to each of the recorded displacements. As shown in Figure 6.6, the simple modeling approach presented in these sections provides a reasonable match to the measured experimental behaviour. At low drifts, both the specimen and the model exhibit a prominent pinching behaviour, due to the high axial stress closing cracks upon unloading. The largest discrepancy comes from an apparent dilation of this pinched region at the largest drift cycles, likely due to deterioration of the concrete in the flexural cracks which then prevents the cracks from fully closing upon load reversal. For clarity, only the response up to 1.5% drift is shown in Figure 6.6.

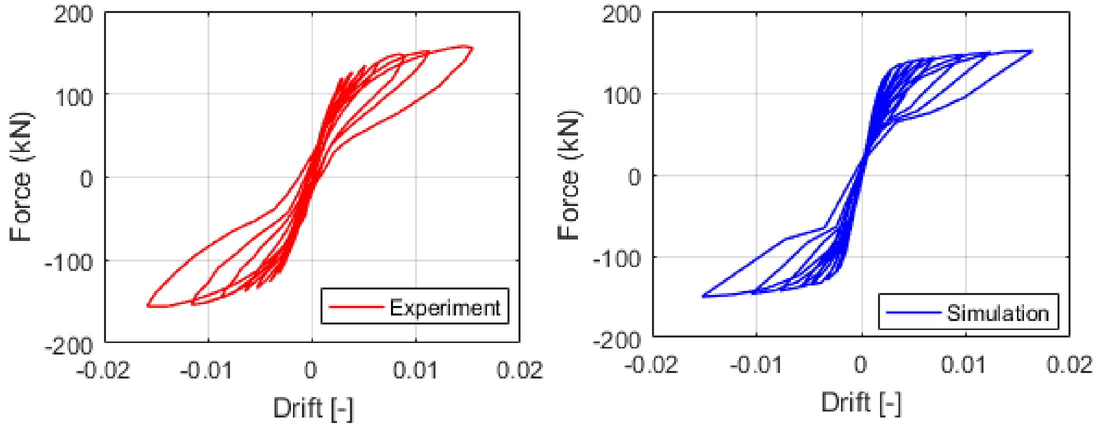

Figure 6.6 Comparison of (a) experimental from Adebar et al.(2007) and (b) numerical RC wall hysteresis

6.3.2 Controlled Rocking Base

The controlled rocking base is a critical contributor to the overall behaviour of the system. By allowing predictable rocking behaviour, the base of the structure can be engineered to be damage free, whereas conventional RC walls would see concentrated yielding and damage in this region. Nonlinear fiber elements are used to capture the behaviour of the controlled rocking base. The following summarizes the modeling approach and validation of the controlled rocking base.

6.3.2.1 Element formulation

The controlled rocking base uses the same 4-node Shear Wall elements as the RC walls. The key difference is that the rocking elements can only resist compression and shear. They do not contain any materials with tensile strength in the fiber section. The use of a 4-node element compatible with the RC walls above makes the modelling simple since the rocking based can be directly connected to the RC walls.

6.3.2.2 Material Properties

The compression resistance of the base was modelled with an Inelastic 1D Concrete Material, like the conventional RC wall elements. However, this base material can use a much simpler elastic-plastic backbone curve in compression, and zero tension response, as shown in Figure 6.7 The initial compression stiffness was assumed to be the gross concrete stiffness, determined using the equation $4500\sqrt{f_c'}$ (MPa). The compression strength was assumed to be equal to f_c' of the wall. In this study the strength loss and cyclic degradation of the base is not directly modelled, due to the presence of shielding and the base being a larger element with confining effects from the surrounding concrete. The shear response of the rocking elements was modelled elastically using the gross shear stiffness of the rocking base material.

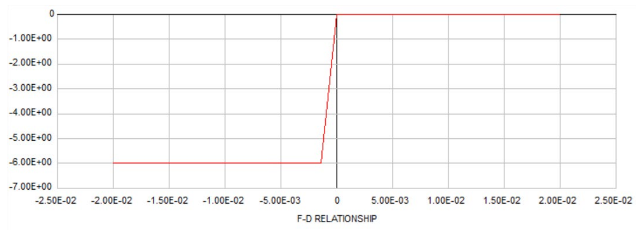

Figure 6.7 Rocking base force-deformation response

6.3.2.3 Description of experimental test for validation

The numerical model described in this section was validated against a controlled rocking wall specimen tested by Perez et al. (2007) and summarized by Figure 6.8. Several different wall panels were included as part of their testing program, but TW2 was chosen for this validation study as it most closely resembled the conditions of the prototype buildings developed later in this thesis. The TW2 specimen had a rectangular cross section with dimensions 2540 mm by 152 mm (100 in by 6 in). The specimen height between the point of lateral loading and the base joint was 7232 mm (23.73 ft), and within this height was four wall panels connected by floor joints.

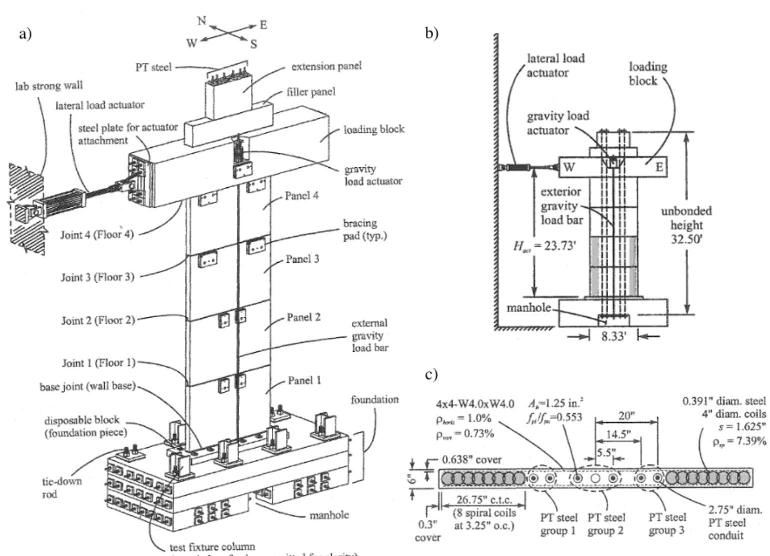

Figure 6.8 TW2 Specimen details from Perez et al. (2007): (a) Isometric View; (b) Elevation; (c) cross section

The wall was reinforced with a combination of conventional wall reinforcing and unbonded prestressing strands. In the lowermost two wall panels, each end of the wall had a 685 mm (27 in) long confined concrete region, using 8 overlapping spiral coils for the transverse reinforcing. The coils had yield and ultimate stresses of 414MPa and 614MPa (60ksi and 90ksi) respectively. The entire wall was enclosed by 4x4-W4.0xW4.0 welded wire mesh, with additional horizontal wires added in the top and bottom third of the wall panels.

Five unbonded prestressing tendons were symmetrically placed between the confined regions. Each tendon was stressed to $0.553f_{pu}$ which results in an average concrete compressive stress of 8.2 MPa (1.19 ksi) after losses, but before application of additional axial load. Additional gravity load was applied using an external PT bar on each side of the specimen midpoint, with hydraulic actuators maintaining a constant applied axial load of 531.5 kN (119.5kip) throughout the experiment.

The loading protocol for the test included three loading and unloading cycles at each of the 9 drift levels, which increased from ±0.05% to ±3.0%.

6.3.2.4 Validation of model

To validate the rocking wall modeling approach, the experimental test by Perez et al. (2007) using the component models described previously was used. Shear wall elements were defined such that the cross section had 8 elements across its length. The outermost two elements on each end of the wall were adjusted to encompass the confined regions of the wall. The concrete model described previously was adjusted to account for the level of confinement and measured material properties from the test. Both flange and web had 46 elements along their height.

The reinforcing ratio in the flange and wall elements were 0.65% and 0.27%, respectively. The lowermost row of elements had double the reinforcing ratio, to simulate the extra rebar across the construction joint. Wall shear behaviour was modelled linearly with an effective shear modulus of G = 6250MPa, or approximately 0.5 times the gross value.

One additional row of elements was modeled above the point of lateral load application, like real wall geometry. Vertical gravity loads (PT loads on the real specimen) were applied to four nodes at the uppermost point on the wall, each with one quarter of the total applied PT force. The base of the wall was modelled with full fixity, while the PT strands were pinned. The model was loaded to each of the recorded displacements by a point load positioned like the actuator.

The response of the experimental and numerical responses is shown in Figure 6.9 (a) and Figure 6.9 (b), respectively. As shown, this modeling approach adequately follows the behaviour from experimental testing. Specifically, the backbone and initial stiffness are well matched. There is some further in-cycle degradation observed in the test which is not captured within in the model. However, the model is deemed sufficiently similar for system level modeling.

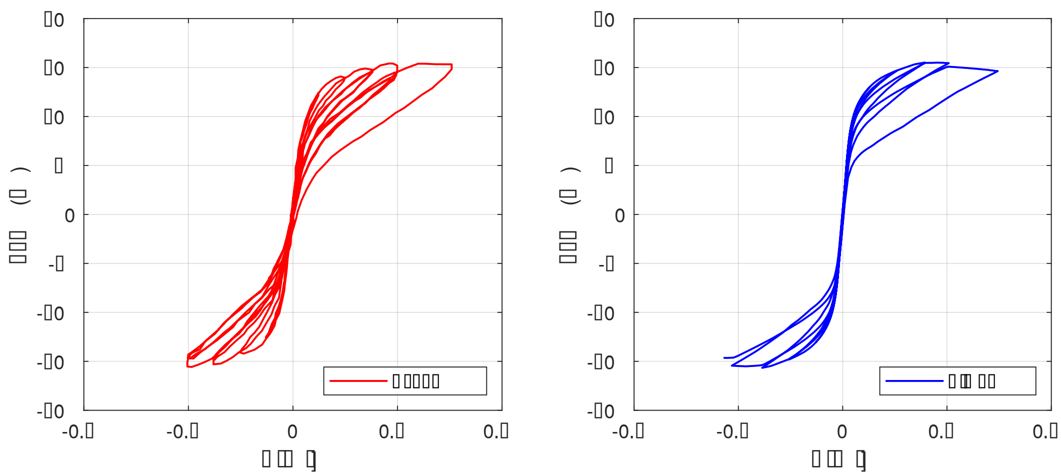

Figure 6.9 Comparison between (a) experiment from Perez et al. (2007) and (b) numerical response for controlled rocking wall

6.3.3 Self-centering coupling beams

Figure 6.10 shows the modeling approach for the coupling beam calibration model. The coupling beams are modeled assuming all the plasticity from the self-centering conical friction damper is lumped in the middle of the beam. The flexibility is modeled using elastic beams, which are connected to the wall. The wall nodes are free to rotate, therefore, a rigid beam is required to transfer the forces from the coupling beam into the walls.

There is currently no plastic hinge property within Perform3D that gives a self-centering hysteretic response. Therefore, to model the self-centering behaviour of a SCFD, an *Elastic nonlinear bar*, an *inelastic bar*, and a *tension only/compression only* bar are modeled in parallel (shown in Figure 6.11). The bars are connected to two rigid elements which connects to the elastic beams (shown in Figure 6.10).

In this model, the yield force (P_0) is taken as the sum of the yield of the inelastic bar ($P_{0,in}$) and the activation force of the nonlinear bar ($P_{0,nl}$). The hysteretic behaviour of the SCFD (shown Figure 6.11) is such that the loading stiffness (k_p) is different than the unloading stiffness ($k_{p,nl}$). In this model, the loading stiffness is taken as the sum of the Tension only/Compression only element stiffness (k_{tc}) and the stiffness of the nonlinear bar after the activation force is reached ($k_{p,nl}$). The Tension only/Compression only elements will not provide stiffness to the unloading, therefore the only stiffness from unloading is provided by the nonlinear bar stiffness ($k_{p,nl}$).

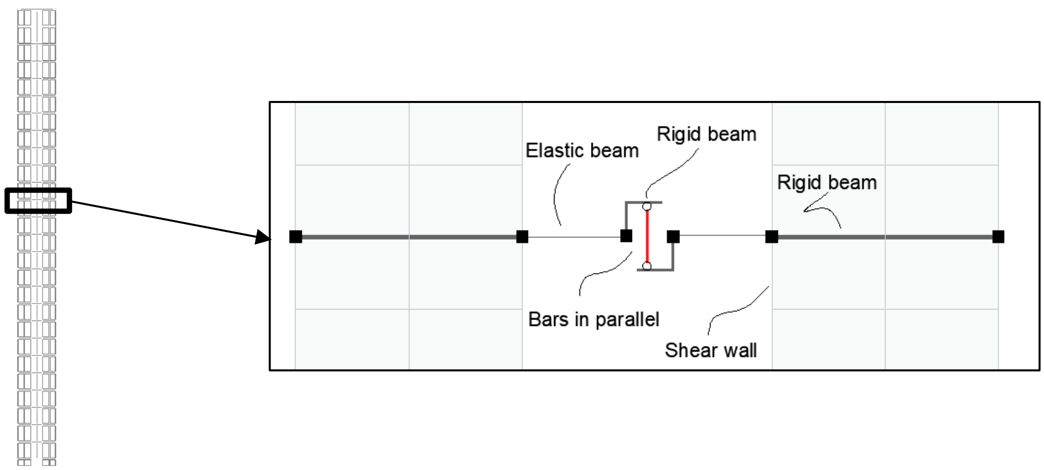

Figure 6.10 Model of SCFD coupling beam

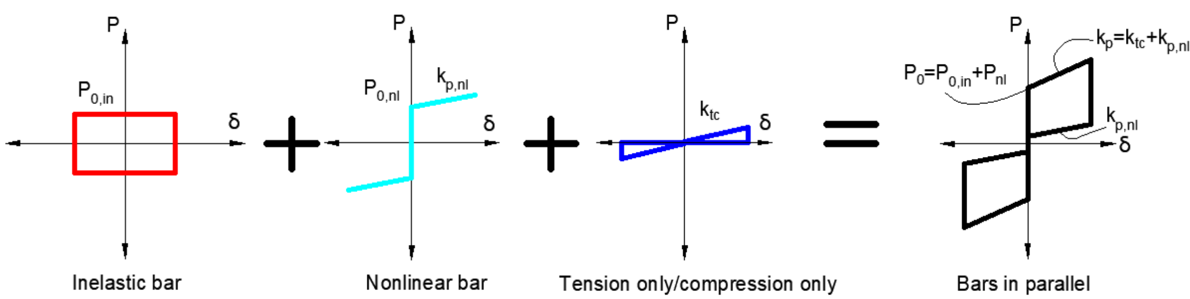

Figure 6.11 Perform3D modeling of self-centering coupling beam bars in parallel

6.3.3.1 Description of experimental test for validation

The modelling approach discussed above was validated using the experimental data from Yang et al. (2020). In their study, a 1/6.5 scale specimen was tested under quasi-static cyclic loads. Figure 6.12 shows the different components of the SCFD tested by Yang et al. (2020). The flat sliding surfaces are steel and Teflon (Figure 6.12 (a)).

The cones, shown in Figure 6.12 (b) and Figure 6.12 (d), were manufactured using stainless steel, where the friction coefficient is estimated to be μ = 0.3 and the friction coefficient between steel and Teflon is estimated as μ' = 0.03. Belleville washers (Figure 6.12c) were used as the PT tendons due to the scale of the specimen. Due to the cost of the manufacturing, only one cone with a slope angle of 22 degrees was used.

Figure 6.13 shows the test setup used for the SCFD. In this setup the SCFD is tested in shear loading. A pantograph system is used to prevent rotation of the loading beam. The actuator has a capacity of 1000kN and a stoke of +/- 150mm. The loading frame was designed to move in vertical (U1) direction. Displacements were recorded locally using LVDTs mounted across the device.

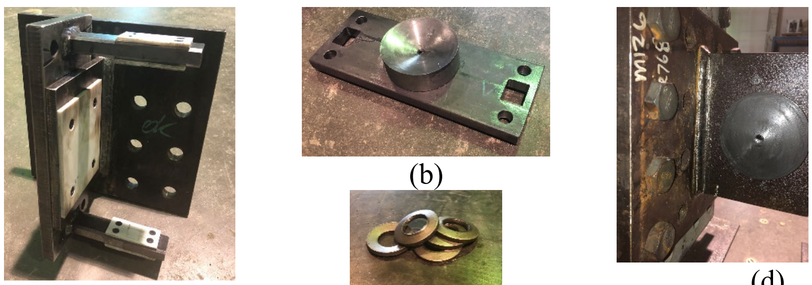

(a) (b) (c) (d)

Figure 6.12 Prototype specimen from Yang et al. (2020) (a) Clamping plate B with stoppers (b) Clamping plate A with rectangle openings and female cone (c) Belleville washers (d) Inner plate with male cone

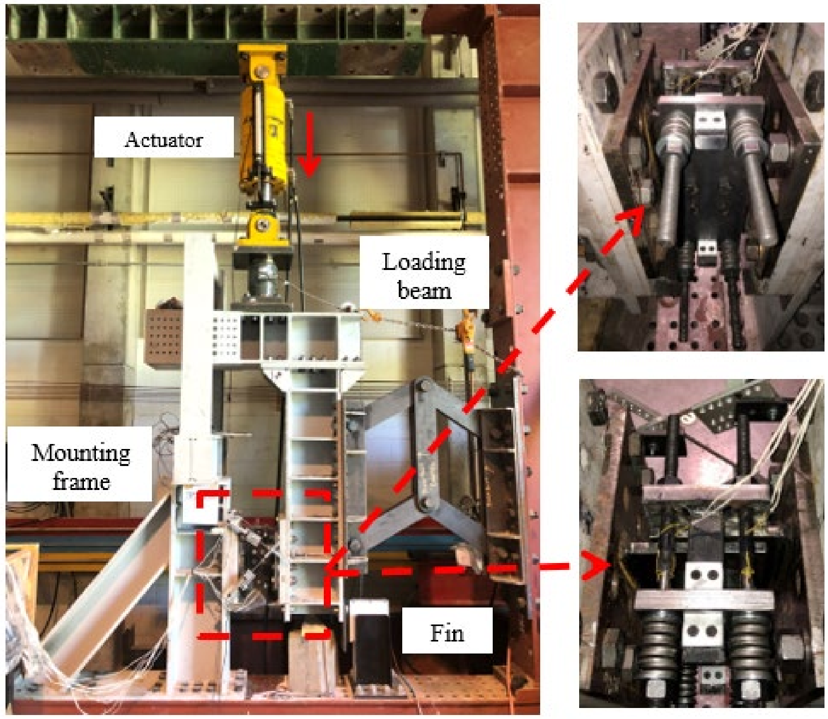

Figure 6.13 Experimental testing set-up for the SCFD from Yang et al. (2020)

6.3.3.2 Validation of model

Using the bars in parallel method described above, the experimental results of a specimen called *6P10W10*, from Yang et al., 2020, was modelled. The responses of the experimental and numerical responses are shown in Figure 6.14 (a) and Figure 6.14 (b), respectively. As shown, this modeling approach follows the behaviour from experimental testing. Specifically, the loading and unloading stiffnesses are well-matched.

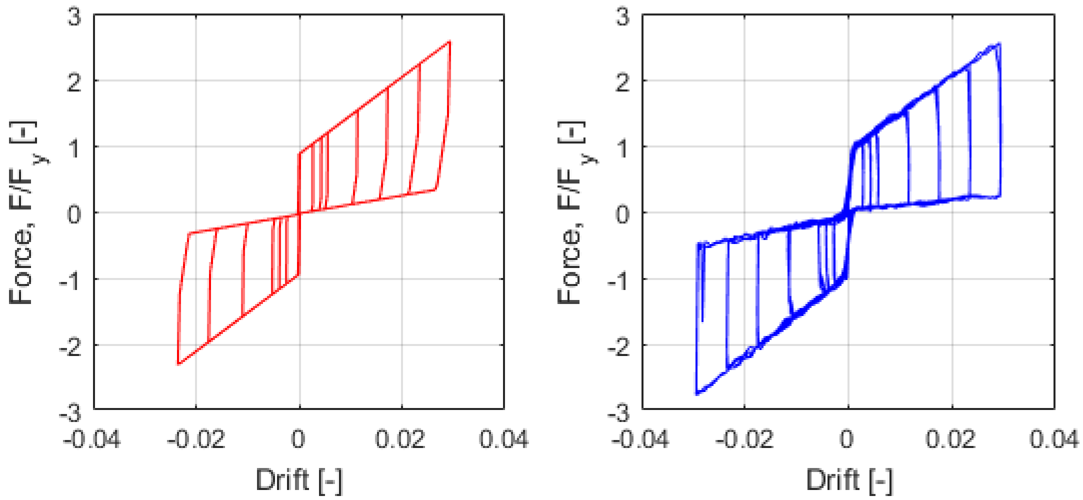

Figure 6.14 SCFD modeling comparison between (a) experimental work by Yang et al. (2020) and (b) numerical model

6.3.4 Outrigger and base dampers

Unidirectional friction dampers are used in both the controlled rocking base and the outriggers, as shown in Figure 6.15. The dampers are modeled using truss elements. In the outrigger, these trusses are simply connected from the mega-columns to the outrigger truss. In the controlled rocking base, these dampers are connected from a pin support to a rigid beam offset, which is connected to a rigid offset beam. The wall shell element nodes are free to rotate, hence, the need for rigid beams.

The hysteresis is simply modeled using an inelastic bar with elastic-plastic behaviour. The following section describe the validation of this modelling approach with experimental tests conducted by Professor Geoffrey Rodgers from the University of Canterbury New Zealand in 2019.

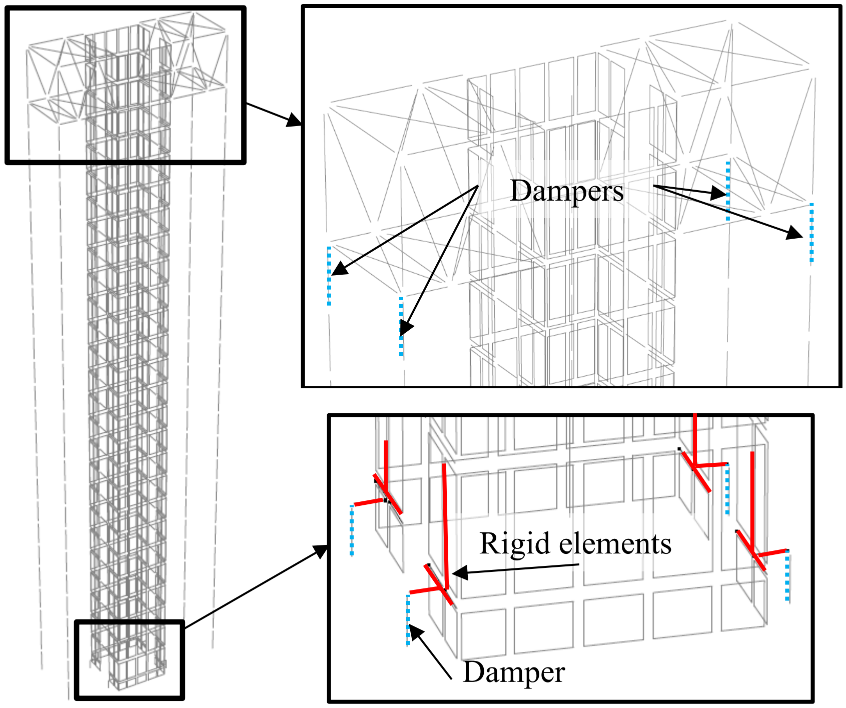

Figure 6.15 unidirectional dampers in the outrigger and the wall base.

6.3.4.1 Description of experimental test for validation

In 2019, Professor Geoffrey Rodgers from the University of Canterbury New Zealand conducted a series of axial friction damper tests. Two unique specimens were experimentally tested by Prof. Geoffrey Rodgers. One damper was designed as a scaled outrigger damper, where a symmetric force displacement response is required, while the other was a scaled controlled rocking damper, where significant ductility is required in tension, and lower ductility is required in compression. Figure 6.16 shows the specimens tested. The specimens were reverse cyclically loaded and the global force and displacement were recorded.

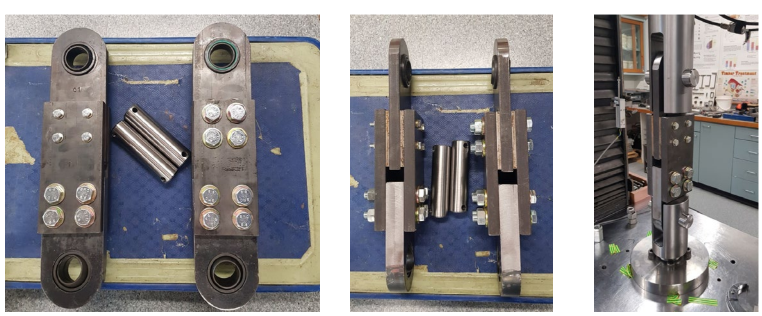
(a) (b) (c)

Figure 6.16 Friction damper experimental tests from Prof. Geoffrey Rodgers, University of Canterbury: (a) front view, (b) side view, and (c) testing set-up

6.3.4.2 Validation of model

These dampers are modeled using inelastic truss elements which have elastic-perfectly-plastic behaviour. The experimental tests by Rodgers, 2019 are used to validate the modeling approach. Figure 6.17 shows the comparison between the numerical hysteresis and the experiment.

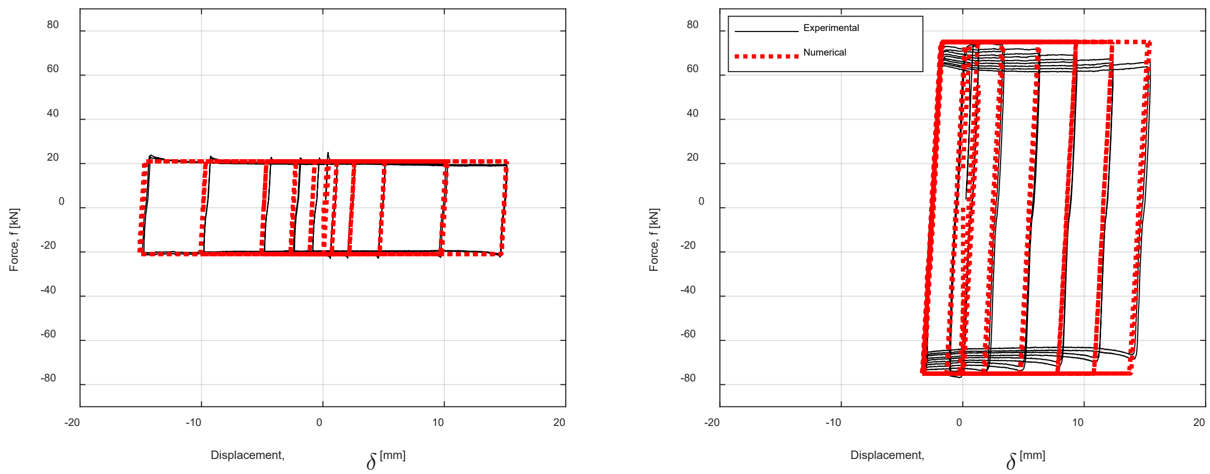

Figure 6.17 Comparison between experimental and numerical response of friction dampers for (a) outrigger damper and (b) base damper (experimental data courtesy of Rodgers, 2019)

6.3.5 Outrigger Members

The outrigger system was modelled elastically using frame elements. Nonlinearity is intended to be confined to the connected friction damper which act as fuses for the outrigger, ensuring that the outrigger members do not experience forces larger than intended. The outrigger system is checked in post-processing to ensure elastic behaviour.

6.4 Nonlinear modelling of prototype buildings

The nonlinear model was built using the methods described above and eigen-value analysis was conducted. The mode shapes for the 24 and 40 story prototype buildings are summarized Figure 6.18 show the prototype buildings first, second, and third modes are dominantly in the SCCW, CORW, and torsional, respectively.

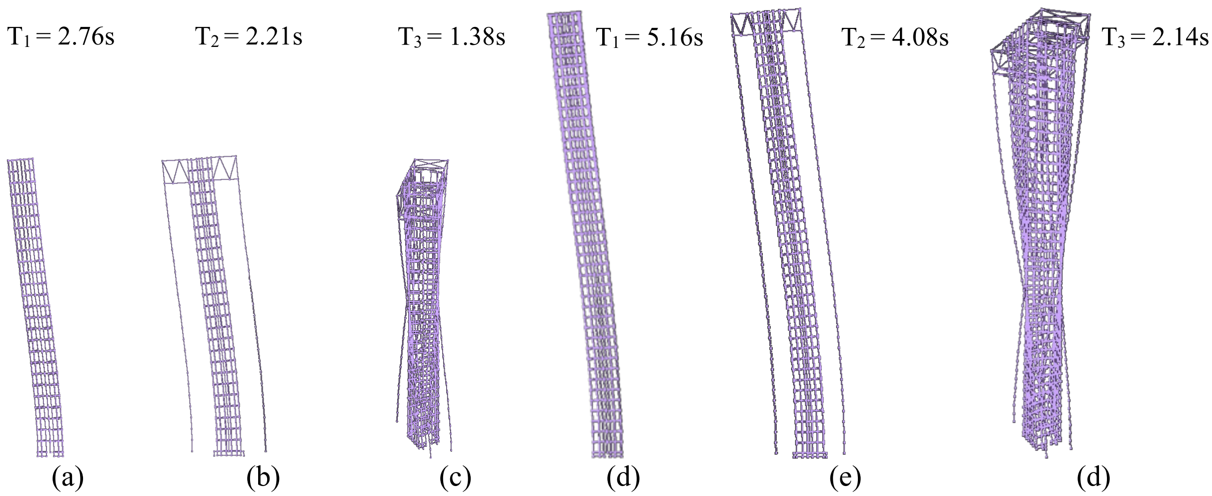

Figure 6.18 Mode shapes for each proto-type building, including: 24 story Mode 1 (a), Mode 2 (b), Mode 3 (c); 40 story Mode 1 (d), Mode 2 (e), Mode 3 (f)

6.5 Summary

This chapter presents the nonlinear modelling approach for conducting bidirectional nonlinear time-history analysis for the proposed CROCW system. The experimental validation of the numerical modelling approach for each structural component, including RC wall, controlled rocking wall, SCFD, and axial friction dampers is presented. Additionally, the assumptions about gravity loads, mass distribution, and damping are discussed.

The numerical modelling approach for the SCFD is a unique contribution within this thesis. The SCFD, only recently being developed, does not have a recommended modelling method. In this chapter, a method to model the unique characteristics of the SCFD are presented. The approach provides a reasonable estimate of the hysteretic response. Additionally, the SCFD can have different hysteretic shapes depending on the design geometry and friction coefficients. The modelling approach presented in this chapter can match well with all of these hysteretic shapes.

This chapter summarises the nonlinear modelling approach used to developed 3-dimensional numerical models of the prototype buildings designed in Chapter 5. The following chapter (Chapter 7) describes the prototype site PSHA and ground motion selection and scaling. The subsequent chapters utilise the nonlinear modelling approach and the selected ground motions to assess the seismic performance of the CORW, SCCW, and CROCW systems.

Chapter 7: Probabilistic seismic hazard analysis and ground motion selection and scaling

7.1 Overview

This chapter presents the Probabilistic Seismic Hazard Analysis (PSHA) used to develop the Uniform Hazard Spectrums (UHS) for both prototype sites (described in Chapter 5). After the presentation of the PSHA is the ground motion selection and scaling process. The selection of suitable ground motions is essential within the seismic performance assessment process. The ground motions selected within this chapter are used throughout the remainder of the thesis to study the nonlinear dynamic performance.

7.2 Introduction

This chapter describes the probabilistic seismic hazard analysis (PSHA) used to determine the uniform hazards spectrums (UHSs) and the ground motion selection and scaling. Selection of suitable ground motions is important within the performance assessment process. The selection of ground motions follows the NBCC Annexure J, where all the high contributing sources must have a unique suite of ground motions. These ground motions are used throughout the remainder of thesis to in the nonlinear modelling.

7.3 Site characteristics

Both cities are in the South West region of British Columbia which has an active seismic setting. Figure 7.1 shows a distribution of earthquake magnitudes in Canada between 1663 and 2006. As shown, the Southwestern region of Canada has some of the most powerful earthquakes in the country.

Despite the active seismic setting, there is a limited amount of data on damaging earthquakes. The first seismograph to be monitored continuously in Western Canada was situated in Victoria, British Columbia and began in 1898 (Cassidy, 2010) and the last recorded damaging earthquake was a magnitude 7.3 crustal event, which occurred in 1946 off the coast Vancouver Island. The regions near the epicenter of this historical event were sparsely populated and as such minimal damage and casualties occurred. Despite the minimal damage caused by earthquakes in recent history, there is sufficient geological and historical evidence to conclude that large magnitude earthquakes will occur in Southwest Canada in the future.

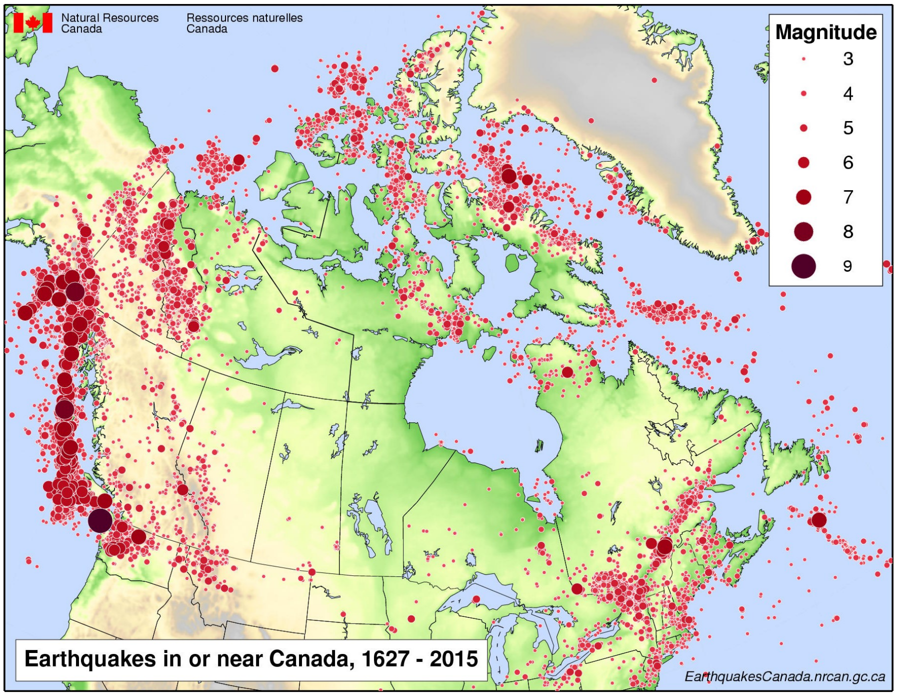

Figure 7.1 Significant earthquakes between the years 1663 – 2006 (NRCAN, 2020)

The West Coast of Canada has highly complex tectonic plate movements due to the different plates (Explorer plate, Juan de Fuca Plate, South Gorda Plate, Pacific Plate, and the North American plate) interacting with one another, shown in Figure 7.2. The tectonic setting results in three main types of earthquakes: crustal, subduction intraslab (sometimes referred to as subcrustal), and subduction interface.

Crustal earthquakes, which occur in the oceanic crust and in the continental crust, have a strike-slip and thrust fault mechanisms. The epicenter could be between 0 to 30km deep. This earthquake can produce up to about a magnitude of 7.5.

Subcrustal (also referred to as subduction intraslab) earthquakes which occur within the Juan de Fuca plate. Subcrustal earthquakes in this region have a normal fault mechanism, can produce a magnitude 7 to 7.5 earthquake, and the epicenter of this earthquake could occur between 30km to 60km deep.

Subduction earthquake (also referred to as subduction interface) which can occur between the Juan de Fuca plate and the North American plate. Subduction earthquakes in this region could rupture a zone that could be greater than a 100km long and could produce up to a magnitude 9 earthquake.

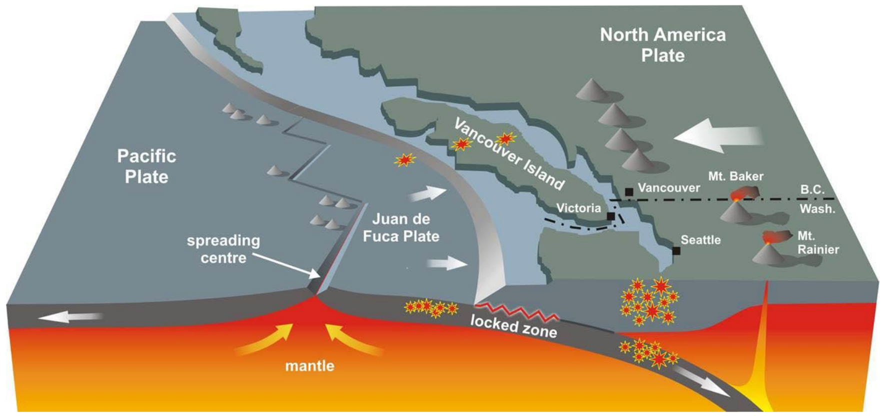

Figure 7.2 Tectonic setting of southwest British Columbia (Adapted from Rogers et al., 2015)

Each type of earthquake (i.e., crustal, subduction intraslab, and subduction interface) must be considered when developing the hazard and selecting ground motions. The following sections describe how each type of earthquake hazard is considered.

7.4 Probabilistic seismic hazard analysis

PSHA is a powerful tool which helps identify the magnitude, distances, and earthquake types which can affect a building site. The PSHA utilizes Open File 7576, (Halchuk et al, 2014), for the NBCC 2015 model. In this PSHA, seismic sources are obtained from seismic zones and faults. If there is a range of uncertainty of the earthquake's characteristics over a region, a seismic zone is used. In the case where the fault geometry and location are well understood, faults are used as sources. The seismic sources used in this PSHA are shown in Table 7.1.

Ground motion prediction equations (GMPE) are models give the spectral accelerations or PGA of a site by a given source. They are a function of magnitude, distance to site, and source type. Different sources may require different GMPEs based on the characteristics of the source. The 2015 NBCC GMPEs used are based on the recommendations from (Atkinson and Adams, 2013).

Different GMPEs may require different distances to the site. Joyner-Boore(Rjb) distance, is the closest distance to the surface projection of rupture plane. The rupture distance (Rrup) is the closest distance to fault rupture surface. The hypocentral distance (Rhypo) is the distance to the point where the fault begins to rupture. This is the location beneath the epicenter. For the Open File 7576 the Rjb is used for crustal sources, Rrup is used for subduction fault sources, and the Rhypo is used for the offshore area source and the subduction area sources. Table 7.1 shows the different distances used for each of the sources.

Table 7.1 Sources used in PSHA

Name	Type	Name	GMPE	Distance type
BRO	Area	Brooks Peninsula	Crustal	Rhypo D = 10km
CAS	Area	Cascade Mountains	Crustal	Rhypo D = 10km
CST	Area	Coastal Mountains	Crustal	Rhypo D = 10km
EXP	Area	Explorer plate bending	Crustal	Rhypo D = 10km
FHL	Area	Flathead Lake	Crustal	Rhypo D = 10km
HEC	Area	Hecate strait	Crustal	Rhypo D = 10km
JDFF	Area	Juan de Fuca plate bending, offshore	Crustal	Rhypo D = 10km
NBC	Area	Northern British Columbia	Crustal	Rhypo D = 10km
NOFR	Area	Nootka Fault	Crustal	Rhypo D = 10km
OLM	Area	Olympic Mountains	Crustal	Rhypo D = 10km
PGT	Area	Puget Sound shallow	Crustal	Rhypo D = 10km
ROCN	Area	Rocky Mountain fold/thrust belt North	Crustal	Rhypo D = 10km
SBC	Area	Southern British Columbia	Crustal	Rhypo D = 10km
VICM	Area	Vancouver Island Coast Mountains	Crustal	Rhypo D = 10km
QCFA	Area	Queen Charlotte Fault	Crustal	Rhypo D = 10km
FWFA	Area	Fairweather Fault	Crustal	Rhypo D = 10km
QCSS	Fault	Queen Charlotte Strike slip beta = 0	Crustal-Rjb	Joyner-Boore
QCSS	Fault	Queen Charlotte Strike slip beta = 1.84	Crustal-Rjb	Joyner-Boore
FWF	Fault	Fairweather Fault beta = 0	Crustal-Rjb	Joyner-Boore
FWF	Fault	Fairweather Fault beta = 1.84	Crustal-Rjb	Joyner-Boore
JDFN	Area	Juan de Fuca plate bending, onshore (deep)	Subduction inslab - D30	Rhypo D = 30km
GTP	Area	Georgia Strait/Puget Sound (deep)	Subduction inslab - D50	Rhypo D = 50km
CIS	Fault	Cascadia Interface source	Subduction Interface	Rrup
EISO	Fault	Explorer Interface outboard estimate of rupture	Subduction Interface	Rrup
EISB	Fault	Explorer Interface. Best estimate landward	Subduction Interface	Rrup
EISI	Fault	Explorer Interface. Inboard estimate of rupture	Subduction Interface	Rrup
HGT	Fault	Haida Gwaii thrust beta=0	Subduction Interface	Rrup
WIN	Fault	Winona thrust beta=0	Subduction Interface	Rrup
WIN	Fault	Winona thrust Activity Rate = 0	Subduction Interface	Rrup
OFS	Area	Offshore	Offshore crustal	Rhypo D = 10km

Figure 7.3 shows each hazard of interested in each site, separated by source contribution. As shown in the figure, the subduction interface source is not representative of the SLE UHS. Both the SLE subduction intraslab hazards and the SLE crustal hazards have minimal contribution in the high periods.

The subduction intraslab DBE hazard follows the UHS shape in low period, but drops off rapidly in the higher period. At the high-period range, all source hazards tend to have similar spectral accelerations.

As shown in the figure, the crustal hazard is least representative of the MCE UHS compared to the other sources. The subduction interface hazard follows the MCE UHS closely at periods greater in the high period range (T>1s). The subduction intraslab follows the MCE UHS closely at low periods (T<1s).

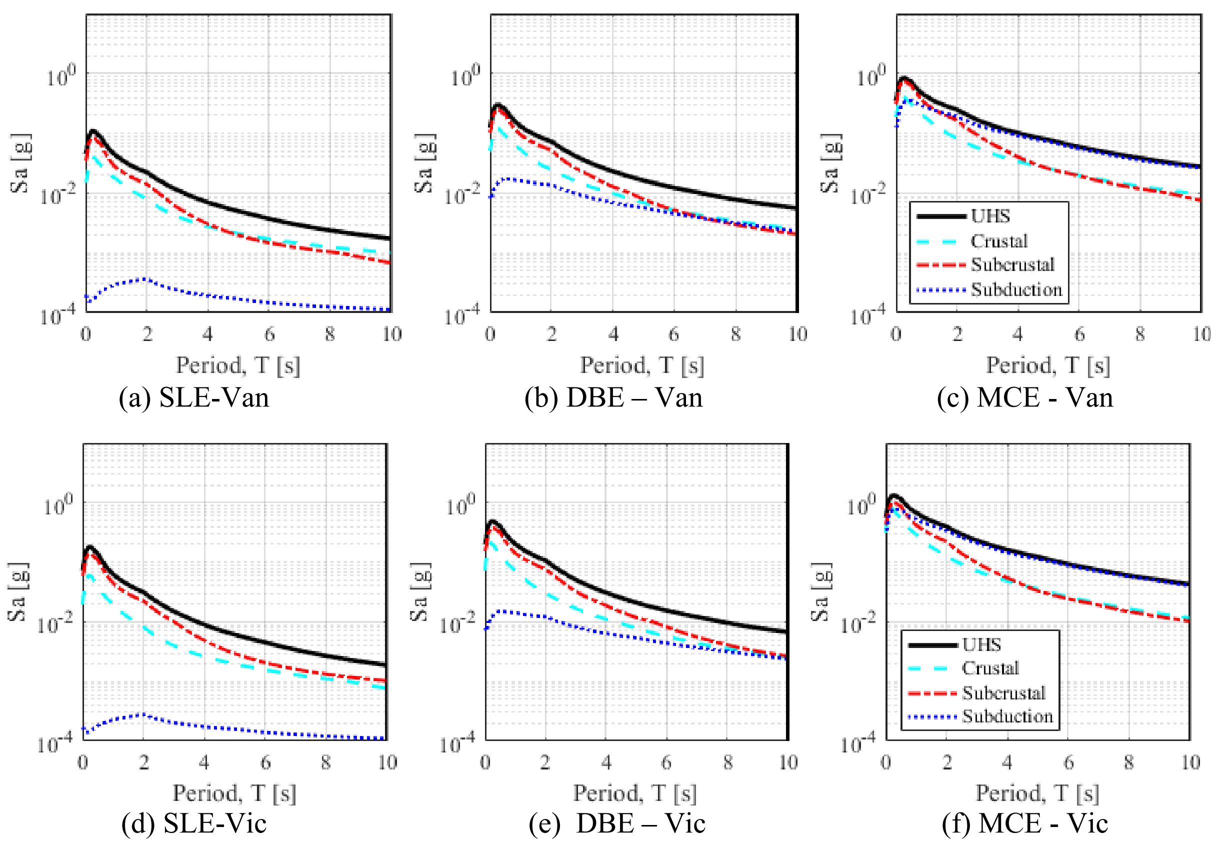

(a) SLE-Van (b) DBE – Van (c) MCE - Van

(d) SLE-Vic (e) DBE – Vic (f) MCE - Vic

Figure 7.3 Hazards by source contribution

7.5 Ground motion selection and scaling

To assess the seismic performance of the prototype buildings (which is completed in subsequent chapters) a suite of representative ground motions must be selected and scaled over an appropriate period range.

The tectonic activity near both sites consists of crustal, subduction intraslab (subcrustal), and subduction interface earthquakes. A UHS is a combination of various hazard sources, as a result it is difficult to match ground motion spectrums to the UHS over large period ranges. To address this, the NBCC 2015 permits scaling over a period range specific to the sources which have a higher contribution to the UHS (NBCC 2015, Option A in Annexure J).

The following sections discuss the source contributions to the hazard, the selected period ranges to scale the ground motions, and the highest contributing magnitudes and distances determined through deaggregation of the hazard. The chapter concludes with suites of ground motions which can be used to analyze the seismic performance of prototype buildings.

7.5.1 Period range for scaling and source contributions

NBCC 2015 suggest scaling to a lower-bound period of 0.15 times the fundamental period of the structure to capture aspects of the higher mode responses. It is also recommended that ground motions be scaled to an upper bound period of twice the fundamental period, to account for the softening of the structure from nonlinearity. To cover the range of periods, in this study the lower bound period is taken as 0.15 times the fundamental period of the 24-story building in the CORW direction, resulting in a lower bound T_{min} = 0.3s. The upper bound period at the MCE, where high degree of nonlinearity is expected, as T_{max} = 10s, as the UHS GMPEs are only reliable up to a natural period of 10s.

Ground motions are scaled following Method A in Annexure J of NBCC, 2015. This method uses one target spectrum, in this case the UHS, and scales a suite of ground motions to match a period range within the UHS. Ground motions of a particular source need only be scaled within a period range where that source is significantly contributing to the response. However, the NBCC does not have an explicit method to determine the range at which is considered “high contribution”.

In this thesis it is assumed that the sources which contribute 15% or higher to the UHS are considered in the ground motion selection and scaling. Table 7.2 shows the percent contributing from each source at periods of 0.3, 0.5, 1, 2, and 3s and the corresponding selected period range used for ground motion scaling.

As shown in Table 7.2, the SLE (50% in 30-year hazard) is almost entirely governed by the crustal and subduction interface sources for both the Vancouver and Victoria sites. As a result, the period range for crustal and subcrustal is selected as between the upper and lower bound (i.e., T_{crus} = T_{intra} =0.3s - 10s). The subduction interface source has a low contribution to the SLE hazard (i.e., less than 15% over the entire range). Hence, no subduction interface ground motions were selected for this hazard.

The DBE (20% in 50-year hazard) at the Vancouver and Victoria sites, shown in Table 7.2, respectively, are primarily governed by subduction intraslab motions over most of the period range. As a result, DBE subduction intraslab motions are scaled over the entire range (i.e., T_{intra} =0.3s-10s). The DBE crustal source has less than a 15% contribution at 0.5s and 2s, and higher contributions at all other period ranges. Since the crustal source is not showing diminishing contribution at higher periods, the entire range is also considered (i.e., T_{crus} = 0.3s - 10s). The subduction interface source has a higher than 15% contribution under most periods, except for 0.3s. However, the entire range of periods is selected for subduction interface motions (i.e., T_{inter} = 0.3s-10s).

Table 7.2 Hazard source contributions

		SLE (50% in30 year)			DBE (20% in 50 years)			MCE (2% in 50 year)		
	Period [s]	Crustal	Subduction intraslab	Subduction interface	Crustal	Subduction intraslab	Subduction interface	Crustal	Subduction intraslab	Subduction interface
Vancouver	0.3	23.2%	70.3%	6.8%	16.9%	71.4%	11.7%	20.0%	72.1%	8.0%
	0.5	22.2%	70.4%	8.0%	14.3%	70.1%	15.7%	15.6%	68.4%	16.0%
	1	29.9%	60.6%	10.4%	17.8%	57.5%	24.7%	15.2%	43.5%	41.4%
	2	26.4%	62.7%	12.4%	12.3%	56.6%	31.2%	8.4%	32.2%	59.4%
	3	33.6%	54.4%	14.5%	17.6%	44.7%	38.0%	9.0%	13.5%	77.5%
	Range	T_{crus} = 0.3s -10s	T_{intra} = 0.3s -10s	-	T_{crus} = 0.3s -10s	T_{intra} = 0.3s -10s	T_{inter} = 0.3s -10s	T_{crus} = 0.3s -1s	T_{intra} = 0.3s -3s	T_{inter} = 0.3s -10s
Victoria	0.3	22.8%	71.0%	7.4%	19.7%	60.1%	20.5%	27.4%	44.1%	28.6%
	0.5	20.6%	73.2%	7.7%	16.2%	61.4%	22.8%	20.6%	41.9%	37.7%
	1	25.4%	67.4%	9.0%	18.1%	53.1%	29.2%	17.5%	21.9%	60.7%
	2	21.4%	70.3%	10.5%	13.1%	54.2%	33.3%	9.9%	15.9%	74.3%
	3	26.0%	64.4%	12.0%	16.9%	45.6%	38.0%	10.0%	5.3%	84.7%
	Range	T_{crus} = 0.3s -10s	T_{intra} = 0.3s -10s	-	T_{crus} = 0.3s -10s	T_{intra} = 0.3s -10s	T_{inter} = 0.3s -10s	T_{crus} = 0.3s -1.5s	T_{intra} = 0.3s -2.5s	T_{inter} = 0.3s -10s

The MCE (2% in 50-year hazard) at the Vancouver and Victoria sites, shown in Table 7.2, is dominated by the subduction interface source over most of the period range. As a result, the subduction motions are scaled over the entire range (T_{inter} =0.3s-10s). In the Victoria site, the crustal and subduction intraslab sources diminish in contributions at higher periods. Less than 15%

contributions occur at a period of 2s for the crustal source and 3s for the subduction intraslab source. The Vancouver hazard has slightly higher contributions from the crustal source and slightly lower contribution from the subcrustal motions when compared o the Victoria source. As a result, the scaling period ranges are slightly different for the two sites. The Vancouver crustal motions are scaled over a range of T_{crus} = 0.3s – 1s, subduction intraslab motions are scaled over a range of T_{intra} =0.3s - 3s. Victoria motions are scaled over a range of T_{crus} = 0.3s – 1s and T_{intra} =0.3s - 3s for crustal and subduction intraslab motions, respectively.

7.5.2 De-aggregation of hazard

De-aggregation was conducted for each hazard at periods equal to 0.3s, 0.5s, 1s, 2s, and 3s. Figure 7.4 and Figure 7.5 show the result for a low period (T = 0.3s) and a high period (T = 3s), respectively. All other de-aggregation results are shown in Appendix B.

As shown in Figure 7.4, at a period of 0.3s, the SLE (50% in 30-year hazard) is dominated by magnitudes 5 -7.5 at distances between 50km to 150km for the Vancouver site and distances of 10km to 100km for Victoria for the site. These contributions are representative of the crustal and the subcrustal motions. At higher periods, the Vancouver SLE is dominated by sources which have magnitudes between 6 to 8 and between distances of 10km to 250km. The Victoria SLE is dominated by magnitudes between 5-7.5 with distances of about 50km to 200km. The subduction interface sources, identifiable from the magnitudes greater than 8.5, are shown to have a relatively low contribution at the SLE hazards.

The DBE (20% in 50 year) are dominated by magnitudes between 6 and 9 for both high and low periods and the Victoria and Vancouver sites. The Victoria hazard has the most contributions between distances of 50km – 100km, while the Vancouver hazard has the most significant contributions between 50km and 200km.

The MCE (2% in 50-year hazard) is almost entirely governed by the subduction motions at high periods. As a result, the Victoria site has high contributions at 50-100km away while the Vancouver site is of distance 100km – 150km away, this is approximately the distance of the Cascadia fault from each site. At low periods, there are contributions from the subcrustal and crustal motions, as shown by the lower magnitudes (6 – 8) at distances between 50km-140km and 50km-100km for the Vancouver and Victoria sites, respectively.

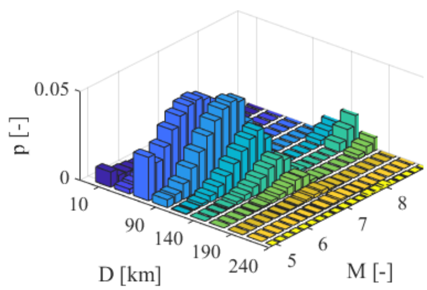

(a) Van-SLE - T = 0.3s (b) Van-DBE - T = 0.3s (c) Van-MCE - T = 0.3s

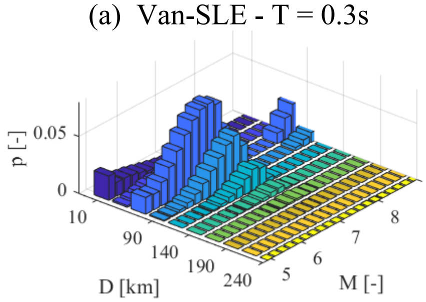

(d) Vic-SLE - T = 0.3s (e) Vic-DBE - T = 0.3s (f) Vic-MCE - T = 0.3s

Figure 7.4 Deaggregation of the site hazards for period of T = 0.3s

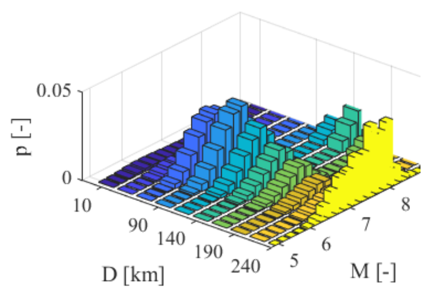

(a) Van-SLE - T = 3s (b) Van-DBE - T = 3s (c) Van-MCE - T = 3s

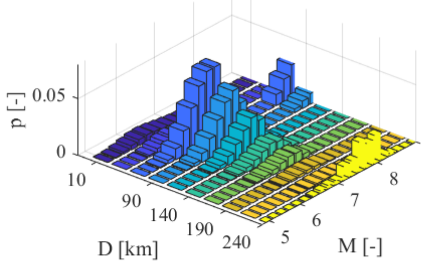

(d) Vic-SLE - T = 3s (e) Vic-DBE - T = 3s (f) Vic-MCE - T = 3s

Figure 7.5 Deaggregation of the site hazards for period of T = 3s

7.5.3 Record selection

Ground motions were selected such that they are representative of the site characteristics. Suites of 11 ground motions were selected for each source. The de-aggregation showed that the subduction motions have minimal contributions at the SLE, as a result, subduction interface motions were not selected for this hazard.

Ground motions were scaled such that the geomean of the two directions matched the UHS. Scaling factors were limited between 0.25-4. The individual ground motions were carefully selected such that the mean of all the unidirectional motions also matched the spectrums well.

Crustal ground motions were selected from the PEER West Strong motion database (PEER, 2018). Subduction motions were selected from the PEER Preliminary NGA Subduction Ground Motion Suite (UCLA, 2020). The full subduction ground motion database is not available for public use at the time of writing this dissertation. As a result, there are where a limited number of ground motions to select from. For this reason, more than two records from an individual event were selected in some cases. The individual ground motion name, year, distance, and scaling factors are shown in Table 7.3, Table 7.4, and Table 7.5 for the SLE, DBE, and MCE, respectively. Figure 7.6 show the individual, mean, and UHS response spectrums for the Vancouver and Victoria sites. Appendix C summarizes the X- and Y- component spectrums.

Table 7.3 SLE hazard ground motion properties

	Vancouver						Victoria					
	NGA	Earthquake	Year	M	Rjb [km]	SF	NGA	Earthquake	Year	M	Rjb [km]	SF
Crustal	17	Southern Calif	1952	6	73.34	1.13	13	Kern County	1952	7.36	122.6	0.70
	21	Imperial Valley-05	1955	5.4	13.78	1.24	17	Southern Calif	1952	6	73.3	1.63
	295	Irpinia, Italy-02	1980	6.2	28.69	1.39	21	Imperial Valley5	1955	5.4	13.8	1.78
	318	Westmorland	1981	5.9	19.26	0.82	295	Irpinia, Italy2	1980	6.2	28.7	2.00
	323	Coalinga-01	1983	6.36	55.05	0.6	302	Irpinia, Italy2	1980	6.2	22.7	0.56
	353	Coalinga-01	1983	6.36	40.13	0.57	318	Westmorland	1981	5.9	19.3	1.18
	4314	Umbria-03, Italy	1984	5.6	40.71	1.12	353	Coalinga1	1983	6.36	40.1	0.83
	747	Loma Prieta	1989	6.93	68.22	1.19	4314	Italy	1984	5.6	40.7	1.61
	782	Loma Prieta	1989	6.93	39.69	0.83	747	Loma Prieta	1989	6.93	68.2	1.72
	7	Northwest Calif-02	1941	6.6	91.15	1.11	782	Loma Prieta	1989	6.93	39.7	1.19
	92	San Fernando	1971	6.61	68.38	2.01	7	Northwest Calif2	1941	6.6	91.2	1.61
Subcrustal	2000007	Nisqually	2001	6.8	39	1.15	2000036	Nisqually	2001	6.8	70.2	1.06
	2000071	Nisqually	2001	6.8	79	1	2000888	Ferndale	2010	6.55	83.1	3.99
	2000888	Ferndale	2010	6.55	83	3.1	2000900	Ferndale	2010	6.55	45.3	1.38
	6001142	South America	2005	7.78	212	0.54	3000100	CA & Mexico	1992	6.51	86.5	1.08
	5001487	New Zealand	2007	6.65	162	1.96	4032628	Kushiro-oki	1993	7.59	91.2	0.75
	5001498	New Zealand	2007	6.65	149	2.41	5001497	New Zealand	2007	6.65	151.6	2.45
	2000900	Ferndale	2010	6.55	45	0.96	6001148	Tarapaca	2005	7.78	149.7	0.67
	7006355	Pingtung	2006	6.94	104	0.88	7006355	Pingtung	2006	6.94	104.1	1.27
	5001499	New Zealand	2007	6.65	149	2.67	7006358	Pingtung	2006	6.94	158.4	1.66
	4007388	Miyagi	2011	7.15	110	0.97	6001145	Tarapaca	2005	7.78	169.9	0.50
	5001497	New Zealand	2007	6.65	152	1.7	5001487	New Zealand	2007	6.65	161.6	2.83

Table 7.4 DBE hazard ground motion properties

	Vancouver						Victoria					
	NGA	Earthquake	Year	M	Rjb [km]	SF	NGA	Earthquake	Year	M	Rjb [km]	SF
Crustal	131	Friuli, Italy2	1976	5.91	41	3.58	1787	Hector Mine	1999	7.13	10.4	0.59
	164	Imperial Valley6	1979	6.53	15	0.69	285	Irpinia	1980	6.9	8.1	0.92
	187	Imperial Valley6	1979	6.53	13	0.77	285	Irpinia	1980	6.9	8.1	0.67
	285	Irpinia, Italy1	1980	6.9	8	0.54	30	Parkfield	1966	6.19	9.6	0.95
	36	Borrego Mtn	1968	6.63	45	0.68	31	Parkfield	1966	6.19	12.9	1.58
	4843	Chuetsu-oki	2007	6.8	18	0.7	353	Coalinga1	1983	6.36	40.1	2.65
	782	Loma Prieta	1989	6.93	40	2.6	4843	Chuetsu-oki	2007	6.8	18.2	1.03
	796	Loma Prieta	1989	6.93	77	0.74	4859	Chuetsu-oki	2007	6.8	11.4	0.73
	7	Northwest Calif2	1941	6.6	91	3.5	725	Superstition Hills2	1987	6.54	11.2	0.59
	832	Landers	1992	7.28	69	0.61	782	Loma Prieta	1989	6.93	39.7	3.83
	96	Managua	1972	5.2	4	0.76	796	Loma Prieta	1989	6.93	77.3	1.10
Subcrustal	1002977	Iniskin	2016	7.15	226	3	2000036	Nisqually	2001	6.8	70.2	3.42
	2000007	Nisqually	2001	6.8	39	3.62	2000049	Nisqually	2001	6.8	69.2	3.56
	2000066	Nisqually	2001	6.8	21	1.02	3000185	CA & Mexico	1982	7.31	24.4	0.59
	2000071	Nisqually	2001	6.8	79	3.14	4032462	Kushiro-oki	1993	7.59	180.1	0.98
	4007388	Miyagi	2011	7.15	110	3.05	4032652	Hokkaido	1994	8.27	115.5	0.68
	4032462	Kushiro-oki	1993	7.59	180	0.67	6001143	South America	2005	7.78	168.8	1.25
	4032463	Kushiro-oki	1993	7.59	105	0.5	6001149	South America	2005	7.78	66.6	1.37
	6001141	Tarapaca	2005	7.78	211	1.99	6001151	South America	2005	7.78	67.8	1.20
	6001143	Tarapaca	2005	7.78	169	0.85	7006078	Pingtung	2006	7.02	11.7	0.60
	6001151	Tarapaca	2005	7.78	68	0.81	7006502	Pingtung	2006	6.94	26.1	1.63
	7006502	Pingtung	2006	6.94	26	1.1	7006538	Pingtung	2006	6.94	23.3	1.78
Subduction	4000359	Tohoku	2011	9.11	126	0.73	3001962	Michoacan	1985	7.99	105.1	1.77
	4000087	Tohoku	2011	9.11	111	0.76	4000244	Tohoku	2011	9.11	23.1	1.06
	4001102	Tohoku	2011	9.11	162	0.85	4000369	Tohoku	2011	9.11	89.7	0.92
	4000684	Tohoku	2011	9.11	144	0.98	4001239	Tohoku	2011	9.11	112.6	1.00
	4028568	Tokachi-oki	2003	8.28	76	1.13	4028568	Tokachi-oki	2003	8.28	76.3	1.67
	4028609	Tokachi-oki	2003	8.28	158	1.94	6001395	Iquique	2014	8.15	96.6	2.65
	4032588	Tokachi-oki	1968	8.26	156	0.61	6001396	Iquique	2014	8.15	98.5	2.32
	6001020	South Peru	2001	8.41	201	0.61	6001800	South America	2010	8.81	120.7	0.49
	6001375	Iquique	2014	8.15	101	1.68	6001804	South America	2010	8.81	105.6	0.64
	6001396	Iquique	2014	8.15	99	1.58	6004288	Iquique	2014	8.15	56.9	1.86
	6002233	Chile	2015	8.31	111	1.78	6005357	Chile	2015	8.31	67.9	1.72

Table 7.5 MCE hazard ground motion properties

	Vancouver						Victoria					
	NGA	Earthquake	Year	M	Rjb [km]	SF	NGA	Earthquake	Year	M	Rjb [km]	SF
Crustal	164	Imperial Valley6	1979	6.53	15	1.77	138	Tabas, Iran	1978	7.35	24.1	3.99
	1787	Hector Mine	1999	7.13	10	1.29	1633	Manjil, Iran	1990	7.37	12.6	1.49
	31	Parkfield	1966	6.19	13	2.71	164	Imperial Valley6	1979	6.53	15.2	2.96
	4843	Chuetsu-oki	2007	6.8	18	1.59	1787	Hector Mine	1999	7.13	10.4	1.78
	4855	Chuetsu-oki	2007	6.8	21	2.18	20	Northern Calif3	1954	6.5	26.7	2.27
	582	Taiwan	1986	7.3	55	1.61	281	Trinidad	1980	7.2	76.1	3.99
	5837	El Mayor-Cucapah	2010	7.2	19	0.72	285	Irpinia, Italy1	1980	6.9	8.1	2.82
	68	San Fernando	1971	6.61	23	2.29	31	Parkfield	1966	6.19	12.9	3.99
	6959	Darfield	2010	7	19	0.94	3758	Landers	1992	7.28	36.9	3.97
	725	Superstition Hills2	1987	6.54	11	1.05	4843	Chuetsu-oki	2007	6.8	18.2	2.88
	832	Landers	1992	7.28	69	2.55	725	Superstition Hills2	1987	6.54	11.2	1.79
Subcrustal	2000053	Nisqually	2001	6.8	56	3.99	2001631	Ferndale	2010	6.55	34.3	3.99
	2000066	Nisqually	2001	6.8	21	3.07	3000185	CA & Mexico	1982	7.31	24.4	1.84
	2001631	Nisqually	2010	6.55	34	2.56	4032462	Kushiro-oki	1993	7.59	180.1	3.85
	4032462	Kushiro-oki	1993	7.59	180	2.33	4032479	Hokkaido	1994	8.27	218.8	1.54
	4032479	Hokkaido	1994	8.27	219	0.98	4032480	Hokkaido	1994	8.27	113.7	2.17
	4032480	Hokkaido	1994	8.27	114	1.39	6001143	Tarapaca	2005	7.78	168.8	3.91
	6001145	Tarapaca	2005	7.78	170	2.46	6001145	Tarapaca	2005	7.78	169.9	3.81
	6001149	Tarapaca	2005	7.78	67	2.74	7006504	Pingtung	2006	6.94	23.6	1.67
	7006502	Pingtung	2006	6.94	26	3.74	7006531	Pingtung	2006	6.94	23.4	2.28
	7006533	Pingtung	2006	6.94	19	1.37	7006532	Pingtung	2006	6.94	23.8	1.91
	7006538	Pingtung	2006	6.94	23	3.98	7006533	Pingtung	2006	6.94	19.0	2.22
Subduction	3001955	Michoacan	1985	7.99	8	2.42	3001955	Michoacan	1985	7.99	8.1	3.86
	4000026	Tohoku	2011	9.11	72	1.56	4000108	Tohoku	2011	9.11	5.9	1.57
	4000322	Tohoku	2011	9.11	135	3.08	4000842	Tohoku	2011	9.11	153.8	3.30
	4000836	Tohoku	2011	9.11	159	3.46	4001181	Tohoku	2011	9.11	88.2	3.98
	4032552	Tokachi-oki	2003	8.28	18	0.96	4022853	Tokachi-oki	2003	8.28	125.3	3.77
	4028567	Tokachi-oki	2003	8.28	39	2.3	4022977	Tokachi-oki	2003	8.28	140.4	2.84
	4022977	Tokachi-oki	2003	8.28	140	1.78	4028563	Tokachi-oki	2003	8.28	49.3	2.32
	4022990	Tokachi-oki	2003	8.28	71	2.73	4028574	Tokachi-oki	2003	8.28	72.9	3.38
	6001803	South America	2010	8.81	113	1.3	6001801	South America	2010	8.81	132.8	2.92
	6001804	South America	2010	8.81	106	1.53	6001804	South America	2010	8.81	105.6	2.44
	6002259	Chile	2015	8.31	106	4	6001815	South America	2010	8.81	57.5	1.85

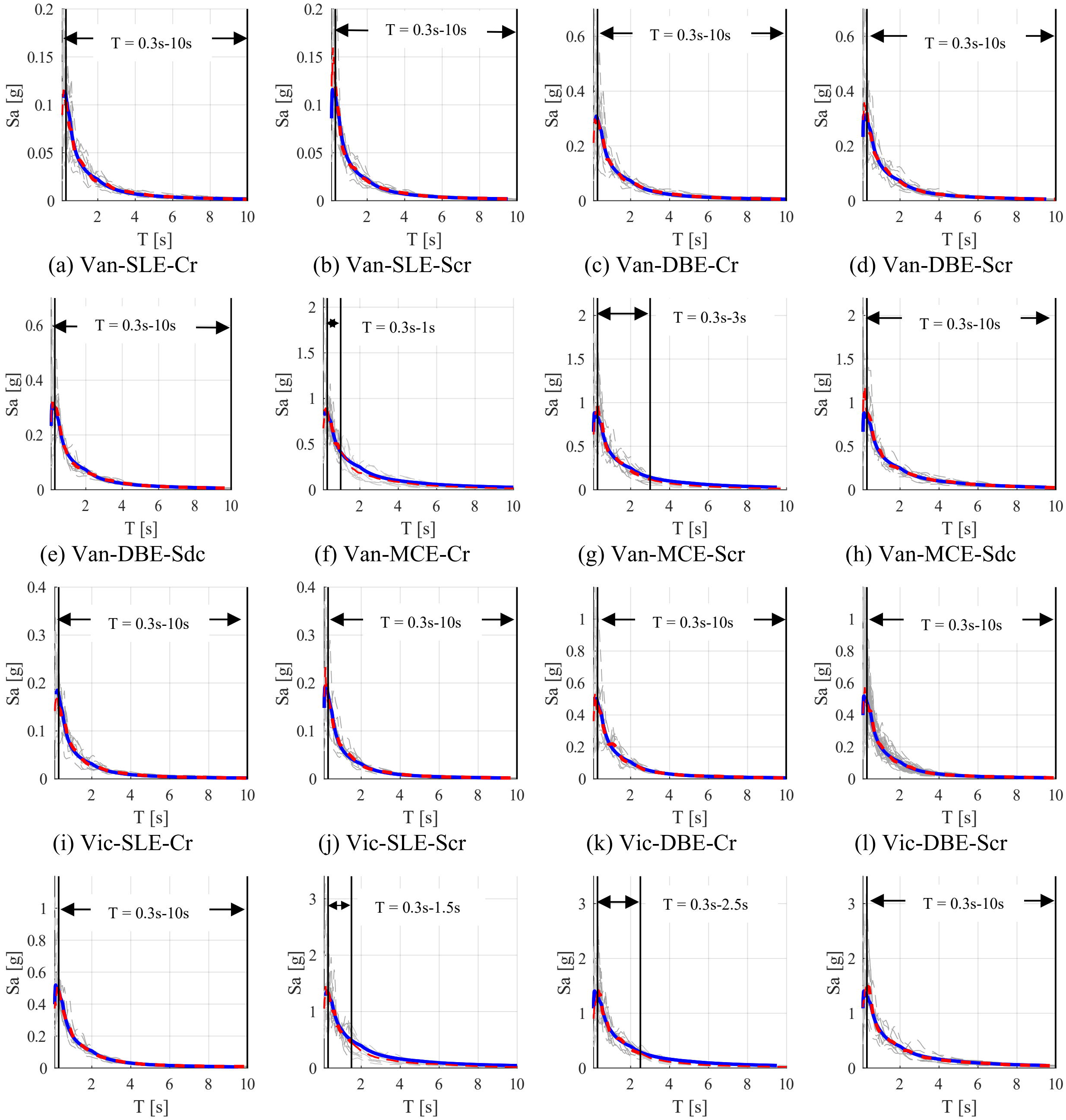

(a) Van-SLE-Cr (b) Van-SLE-Scr (c) Van-DBE-Cr (d) Van-DBE-Scr

(e) Van-DBE-Sdc (f) Van-MCE-Cr (g) Van-MCE-Scr (h) Van-MCE-Sdc

(i) Vic-SLE-Cr (j) Vic-SLE-Scr (k) Vic-DBE-Cr (l) Vic-DBE-Scr

(m) Vic-DBE-Sdc (n) Vic-MCE-Cr (o) Vic-MCE-Scr (p) Vic-MCE-Sdc

Figure 7.6 Response spectrum for ground motions for prototype sites, at all sites, at all sources

7.6 Summary

This chapter presents the prototype site probabilistic Seismic Hazard Analysis (PSHA), de-aggregation, ground motion selection and scaling for each prototype site. The South West region of Canada, where these two sites are located, have a significant seismic hazard. With Victoria having about a 60% higher hazard when compared with Vancouver. De-aggregation showed that the subduction interface seismic source has minimal contribution to the SLE. As a result, the subduction interface source is not considered in the ground motion selection of the SLE. On the other hand, the subduction interface seismic source almost entirely governs the MCE for both sites.

The following chapters utilise the selected ground motions from this chapter, the nonlinear modelling approach from Chapter 6 to assess the seismic performance of the CORW, SCCW, and CROCW systems.

Chapter 8: Seismic performance assessment of CORW

8.1 Overview

This chapter presents the nonlinear time history results of the prototype buildings designed in Chapter 5 using EEDP, under unidirectional loading in the CORW direction. This chapter presents a discussion on the peak response of displacements, interstorey drift ratios, wall moments, shear forces, shear stresses, and wall strains at each story. Additionally, a comparison between the EEDP design objectives and the nonlinear response is provided.

8.2 Introduction

Four prototype buildings, 24-story and 40-story buildings located in Vancouver and 24-story and 40-story buildings situated in Victoria, are examined in this chapter. These prototype buildings were designed for the following design hazards: Service level earthquake (SLE) of 50% in 30 years; Design-based earthquake (DBE) of 20% in 50 years; and Maximum considered earthquake (MCE) of 2% in 50 years. The detailed steps to design the prototype building designs were presented in Chapter 5.

Based on the probabilistic seismic hazard analysis (PSHA) presented in Chapter 7, a suite of 11 ground motions was selected and scaled based on the three tectonic sources near the site: crustal, subduction intraslab, and subduction interface. The SLE hazard did not contain a suite of subduction interface ground motions due to the subduction source's limited contribution. As a result, two suites of 11 ground motions at the SLE and three suites of 11 ground motions at the DBE and MCE were used to conduct the nonlinear time-history analysis- a total of 660 analysis.

The prototype buildings were analysed using three-dimensional models with the modelling approach summarized in Chapter 6. The results presented in this chapter only considers the maximum ground motions applied along the CORW direction. The nonlinear analysis results showed that the CORW can behaved as the mechanism specified by EEDP in Chapter 5.

8.3 Global displacements and ISDRs

Roof drift ratio (RDR) and interstorey drift ratios (ISDRs) were determined for each ground motion, at each story level, at each of the eight nodes on the core wall, shown in Figure 8.1.

However, all responses are essentially the same for each node under this unidirectional loading, so only the WNW node is shown herein for brevity.

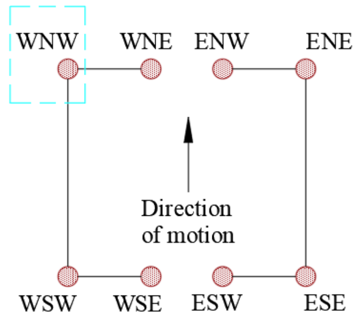

Figure 8.1 Displacement and interstorey drift post processing schematic for the CORW

8.3.1 Story displacements

Figure 8.2 shows the mean (μ) and standard deviation (σ) of the prototype building peak story displacements (Δ_s) normalised to the building height (H). The SLE peak μ roof drift ratio (RDR) is 0.046%, 0.054%, 0.035%, and 0.047% for the Van24, Vic24, Van40, and Vic40 buildings, respectively. The DBE peak RDR-μ is over double the SLE, with values of 0.14%, 0.21%, 0.10%, and 0.12% for the Van24, Vic24, Van40, and Vic40, respectively. The MCE peak RDR-μ is 0.53%, 0.85%, 0.46%, and 0.76% for the Van24, Vic24, Van40, and Vic40, respectively.

The peak RDR-σ at the SLE is 0.012%, 0.02%, 0.011%, and 0.011% for the Van24, Vic24, Van40, and Vic40, respectively. The peak RDR-σ at the DBE is 0.044%, 0.057%, 0.029%, and 0.044% for the Van24, Vic24, Van40, and Vic40, respectively. The peak for RDR- σ at the MCE is 0.28%, 0.30%, 0.18%, and 0.30% for the Van24, Vic24, Van40, and Vic40, respectively.

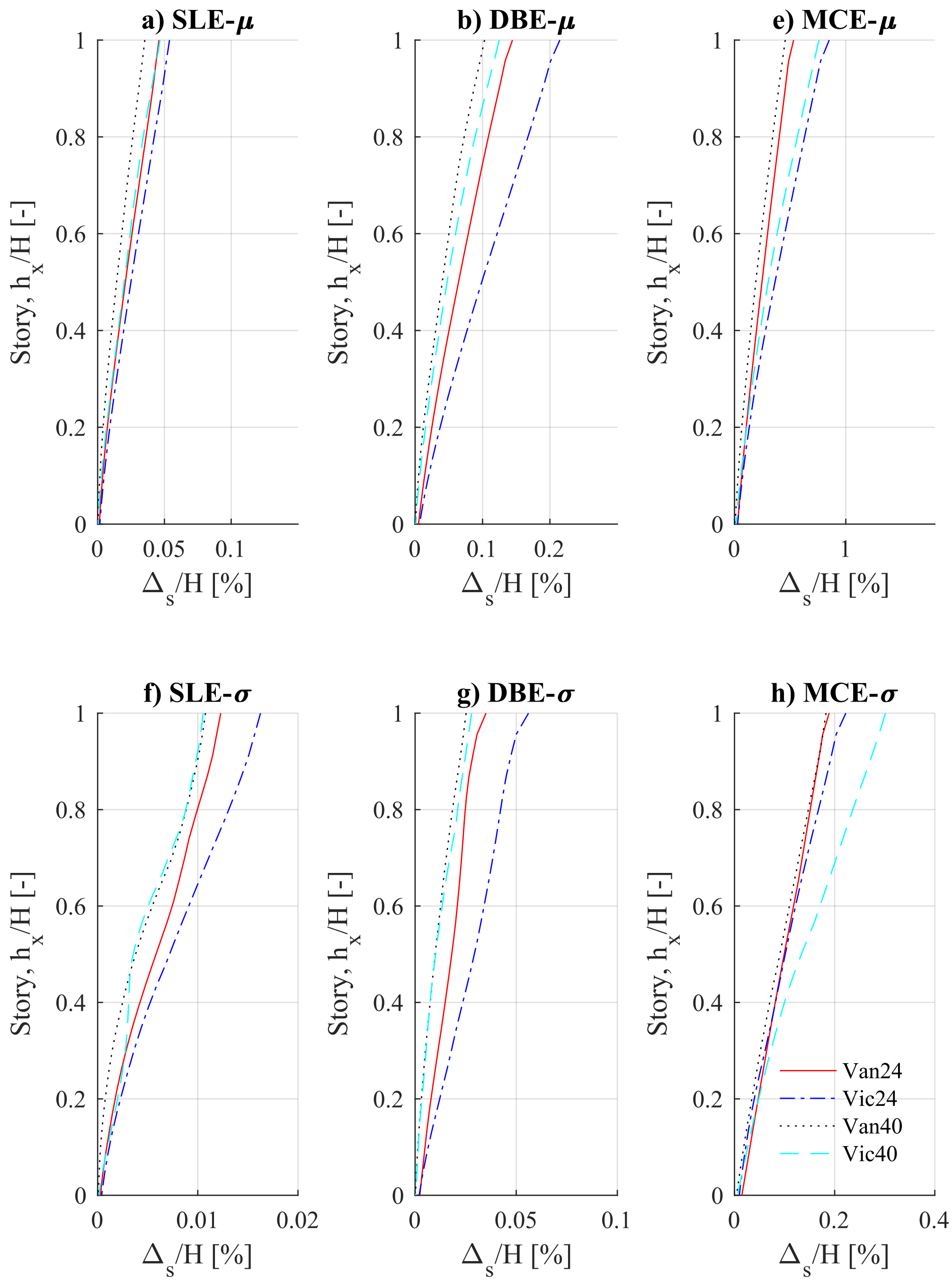

Figure 8.2 CORW unidirectional normalised displacements (governing source): (a) SLE- μ; (b) DBE- μ; (c) MCE- μ; (d) SLE- σ; (e) DBE- σ; and (f) MCE- σ

Figure 8.3 compares the ratio of the mean roof displacement from the model (Δ_r) to the EEDP design roof displacement (Δ_{EEDP}). Generally, the response matches well - demonstrating the robustness of the EEDP design procedure.

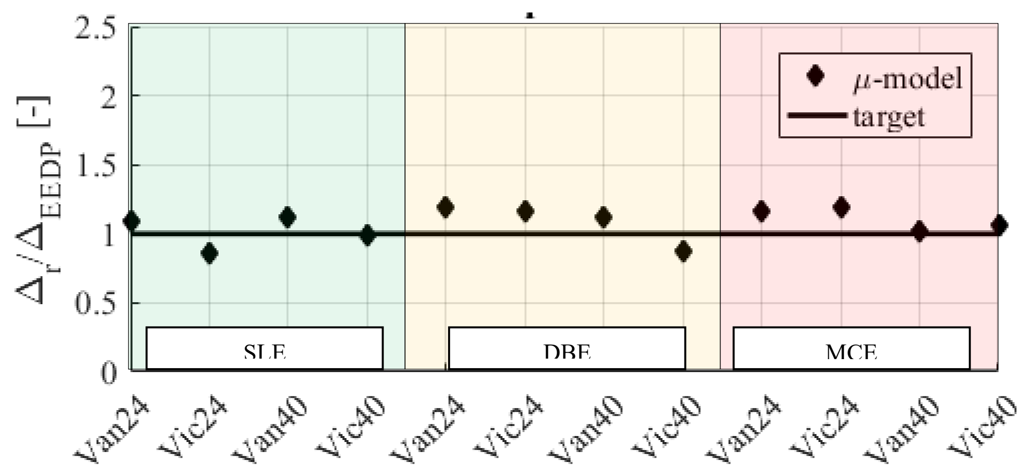

Figure 8.3 Comparison between design and numerical analysis for the CORW under unidirectional load

8.3.2 Inter-story drift ratio (ISDR)

Figure 8.4 shows the mean (μ) and standard deviation (σ) prototype building peak global ISDR over the building height. As shown in the figure, the ISDR- μ at the SLE shaking intensity is 0.060%, 0.076%, 0.051%, and 0.076% for the Van24, Vic24, Van40, and Vic40, respectively. The DBE peak ISDR- μ is 0.19%, 0.27%, 0.17%, and 0.23% for the Van24, Vic24, Van40, and Vic40, respectively. The MCE peak ISDR- μ 0.60%, 1.05%, 0.67%, and 1.10% for the Van24, Vic24, Van40, and Vic40, respectively.

The peak σ for ISDR under SLE 0.015%, 0.02%, 0.012%, and 0.019% for the Van24, Vic24, Van40, and Vic40, respectively. The peak σ for ISDR under DBE is 0.055%, 0.083%, 0.041%, and 0.060% for the Van24, Vic24, Van40, and Vic40, respectively. The peak σ for ISDR under MCE is 0.26%, 0.31%, 0.20%, and 0.33% for the Van24, Vic24, Van40, and Vic40, respectively.

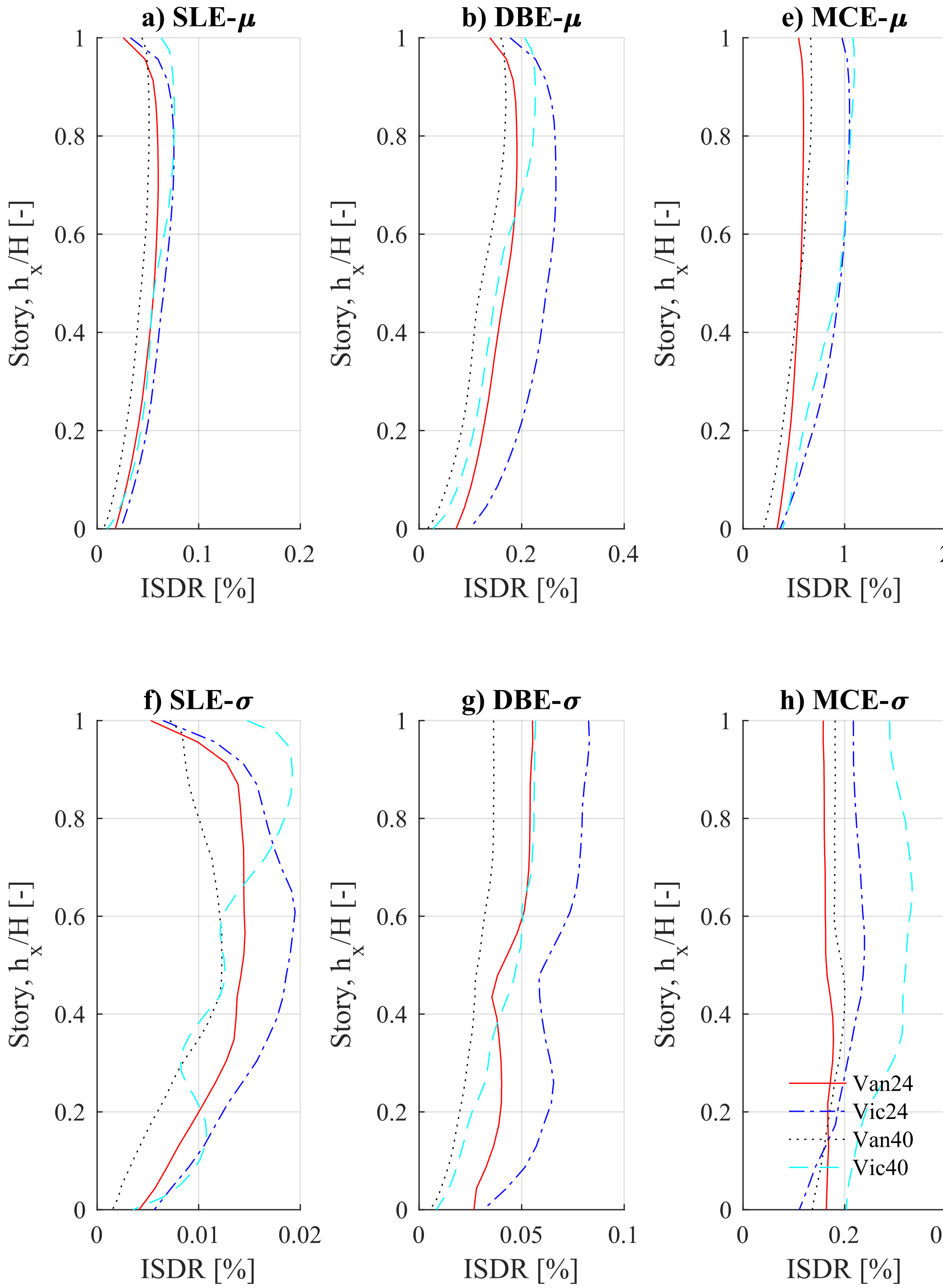

Figure 8.4 CORW unidirectional ISDR (governing source): (a) SLE- μ; (b) DBE- μ; (c) MCE- μ; (d) SLE- σ; (e) DBE- σ; and (f) MCE- σ

8.4 Outrigger dampers

Figure 8.5 compares the ratio of the mean outrigger damper force from the model (f_o) to the EEDP design yield force ($f_{o,y}$). As shown, the damper force is below yielding at the SLE. At the DBE and MCE all outrigger dampers have yielded. These observed behaviors meet the performance objectives of the EEDP, where the outrigger system is designed to remain elastic at the SLE and yield at the DBE and MCE.

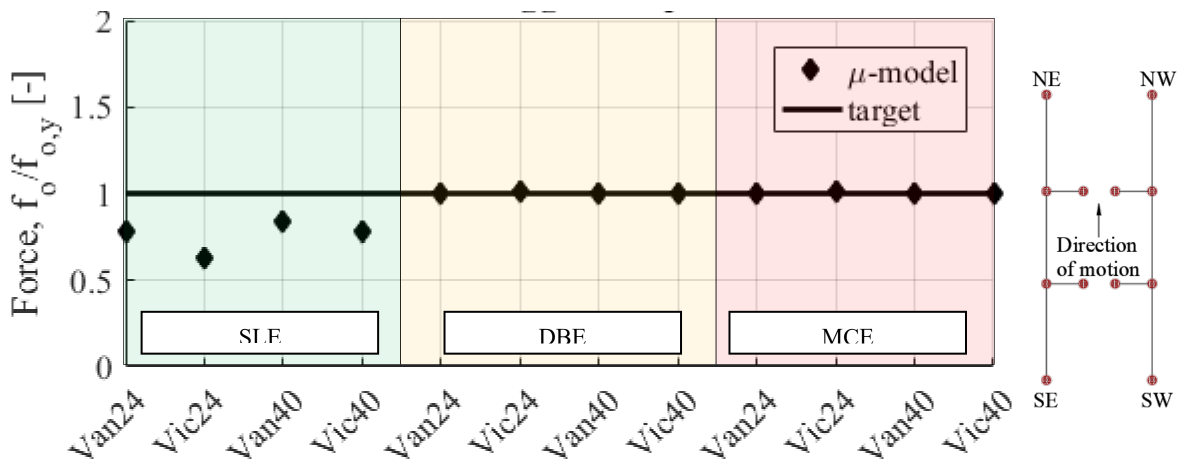

Figure 8.5 Outrigger damper force ratio for each prototype building at each hazard under unidirectional load in CORW direction.

8.5 Wall-base dampers

Figure 8.6 compares the ratio of the mean wall-base damper force from the model (f_b) to the EEDP design yield force ($f_{b,y}$). As shown, generally, the damper force is below yielding at the SLE and DBE. At the MCE all wall-base dampers have yielded. These observed behaviors meet the performance objectives of the EEDP, where the wall-base dampers are designed to remain elastic at the SLE and DBE and yield at the MCE.

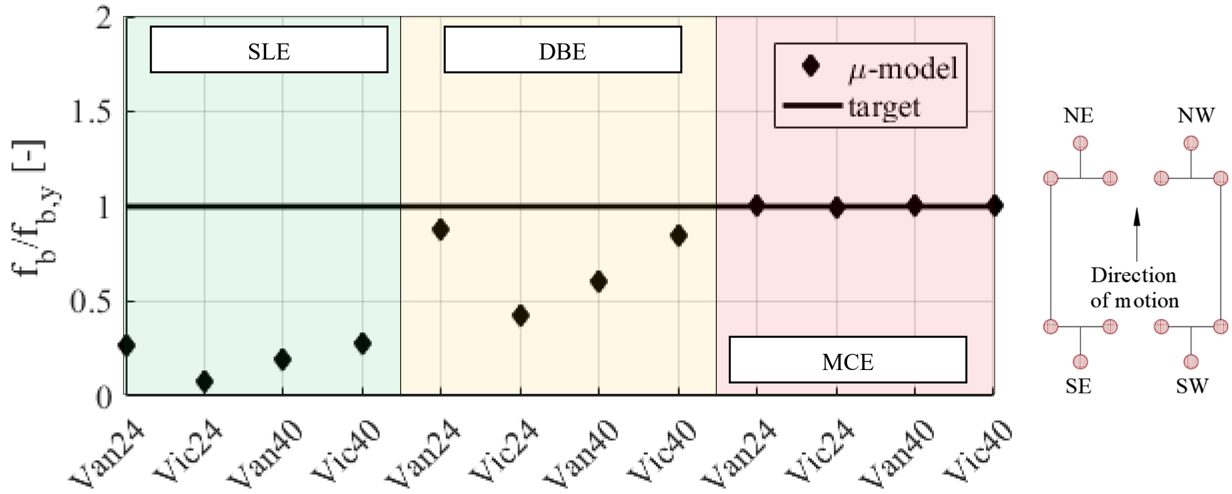

Figure 8.6 Wall-base damper force ratio under unidirectional load in CORW direction

8.6 Wall shear stress

Figure 8.7 shows the mean (μ) and standard deviation (σ) prototype building peak shear stress over the building height. The shear forces are determine using a section cut which includes only each wall web. The stress is determined by dividing this force by the wall length and the web thicknesses.

As shown in Figure 8.7, the shear stress μ at the SLE shaking intensity is 0.58 MPa, 0.81 MPa, 0.52 MPa, and 0.85 MPa for the Van24, Vic24, Van40, and Vic40, respectively. The DBE peak shear stress μ is 1.42 MPa, 1.95 MPa, 1.42 MPa, and 2.26 MPa for the Van24, Vic24, Van40, and Vic40, respectively. The MCE peak shear stress μ is 2.60 MPa, 3.69 MPa, 3.19 MPa, and 3.93 MPa for the Van24, Vic24, Van40, and Vic40, respectively.

The standard deviation (σ) of the shear stress is highest for the Vic24, under all hazards. The peak σ of the shear stress under SLE is 0.16 MPa, 0.23 MPa, 0.15 MPa, and 0.31 MPa for the Van24, Vic24, Van40, and Vic40, respectively. The peak σ of the shear stress under DBE 0.35 MPa, 0.54 MPa, 0.52 MPa, and 0.60 MPa for the Van24, Vic24, Van40, and Vic40, respectively. The peak σ of the shear stress under MCE is 0.61 MPa, 0.83 MPa, 0.63 MPa, and 0.91 MPa for the Van24, Vic24, Van40, and Vic40, respectively.

Overall, the shear stresses are low (less than 10%f’c), demonstrating this system resulting in reasonably low damage, as per the performance objective.

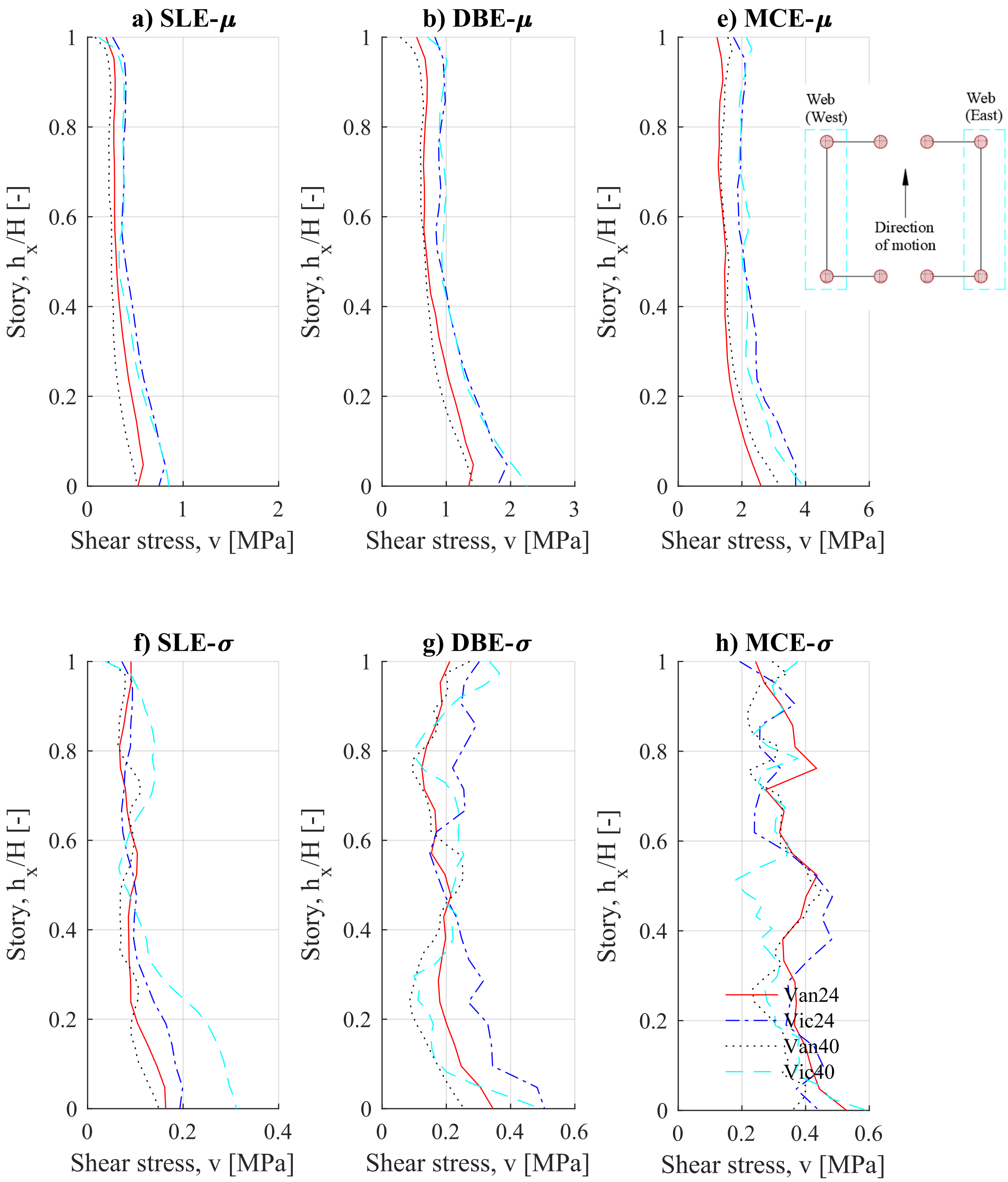

Figure 8.7 CORW unidirectional shear stress (governing source): (a) SLE- μ; (b) DBE- μ; (c) MCE- μ; (d) SLE- σ; (e) DBE- σ; and (f) MCE- σ

8.7 Wall strain

Figure 8.8 shows the mean (μ) and standard deviation (σ) prototype building peak tension strain in the wall over the building height at all hazards. At each node, strains are determined by taking the difference between the vertical displacements at each wall corner divided by the distance between the nodes. The strains are normalised to the yield strain of rebar ($\varepsilon_y = 0.002$). Strains were evaluated at each node, and the peak responses are presented in Figure 8.8.

As shown in the figure, the mean strain ratio ($\varepsilon/\varepsilon_y$ - μ) at the SLE shaking intensity is 0.10, 0.10, 0.11, and 0.12 for the Van24, Vic24, Van40, and Vic40, respectively. The DBE peak $\varepsilon/\varepsilon_y$ - μ 0.20, 0.24, 0.15, and 0.18for the Van24, Vic24, Van40, and Vic40, respectively. The MCE peak $\varepsilon/\varepsilon_y$ - μ is 0.39, 0.75, 0.45, and 0.91 for the Van24, Vic24, Van40, and Vic40, respectively.

The standard deviation (σ) of the $\varepsilon/\varepsilon_y$ is highest for the Vic24, under all hazards. The peak σ for $\varepsilon/\varepsilon_y$under SLE is 0.03, 0.03, 0.00, and 0.02 for the Van24, Vic24, Van40, and Vic40, respectively. The peak σ for $\varepsilon/\varepsilon_y$under DBE is 0.04, 0.09, 0.04, and 0.11 for the Van24, Vic24, Van40, and Vic40, respectively. The peak σ for $\varepsilon/\varepsilon_y$under MCE is 0.21, 0.31, 0.27, and 0.64for the Van24, Vic24, Van40, and Vic40, respectively.

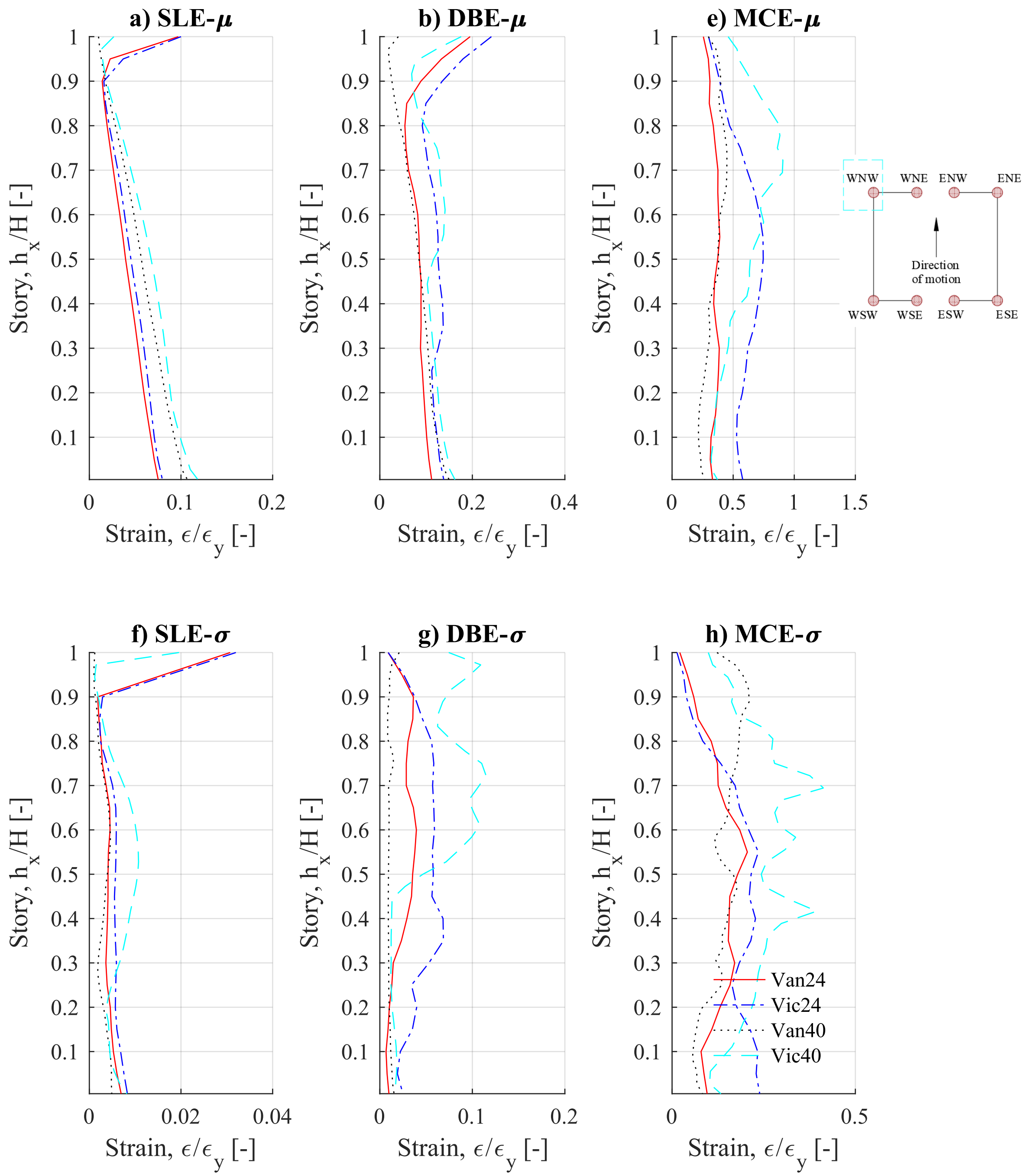

Figure 8.8 CORW unidirectional strains (governing source): (a) SLE- μ; (b) DBE- μ; (c) MCE- μ; (d) SLE- σ; (e) DBE- σ; and (f) MCE- σ

At the SLE and DBE hazard levels peak strains are observed at the top of building. This is due to the outrigger moment causing high flexural demands at the roof, where wall compression stresses are low. These strains are less prominent in the 40-story buildings, where the outrigger is less effective (i.e., lower α_f), and the higher mode moments are more prominent (i.e., more flexural strain demands are distributed over the height of the building.

At the MCE hazard, more prominent strains are observed near mid-height of the building. These high strains are more dominant in the Victoria 40-story building, where the mean of the mid-height strain is twice the mean of the base strain. The high mid-height strains are attributed to the base moment being capped by the yielding of the dampers, as a result, higher flexural demands occur over the height of the buildings.

Overall, the strains are below yielding (i.e., $\varepsilon/\varepsilon_y$<1). The strains are highest near the mid-height of the building, demonstrating the governance of higher mode moments. However, the low strains demonstrate that the EEDP performance objectives have been met.

8.8 Summary

This chapter presented the nonlinear dynamic responses of four prototype buildings: 24-story located in Victoria and Vancouver, and 40-story located in Victoria and Vancouver. Using EEDP the systems were designed to meet different performance objectives at different shaking intensities. Specifically, at the SLE shaking intensity the system remains elastic, at the DBE the outrigger dampers yield and dissipate energy, while the system remains elastic, and at the MCE intensity the outrigger and base dampers yield and dissipate energy, while the remaining wall is elastic. The nonlinear analysis conducted in this chapter demonstrates the robustness of this design procedure in meeting these performance objectives. The limited damage is demonstrated by the low shear stresses (less than 10%f'c) and the low wall strains are low (less than $\varepsilon_y = 0.002$) for all prototype buildings.

This chapter presented the seismic performance assessment of the CORW system under unidirectional loading. The following chapter (Chapter 9) presents the seismic performance assessment of the SCCW under unidirectional loading.

Chapter 9: Seismic performance assessment of SCCW

9.1 Overview

This chapter presents the nonlinear time history results of the four prototype buildings, designed in Chapter 5, under unidirectional loading in the SCCW direction. The EEDP is validated within this chapter. Additionally, this chapter presents a discussion on the peak response at every story for displacements, inter-story drift ratio (ISDR), wall moments, shear forces, shear stresses, and wall strains.

9.2 Introduction

In Chapter 3 of this thesis the SCCW was proposed as an alternative to the conventional RC coupled wall system. In Chapter 5, a EEDP is developed, to design the SCCW. Using the modified EEDP, the SCCW system can be designed to meet different performance objectives at different shaking intensities. Specifically, at the SLE shaking intensity, the system remains elastic. At the DBE intensity, the coupling beams are designed to yield and dissipate energy, while the remaining system remains elastic. At the MCE intensity, the coupling beams and wall-base dampers are designed to yield and dissipate energy, while the remaining wall is designed to remain elastic.

In this chapter, the seismic performance of the SCCW system, designed with EEDP, under different levels of earthquake shaking is studied. Four prototype buildings are investigated: a 24-story and a 40-story building located in Vancouver and a 24-story and a 40-story building located in Victoria. These buildings were designed in Chapter 5 and considered the following shaking intensities in the design process: a Service level earthquake (SLE) of 50% in 30 year; a Design-based earthquake (DBE) of 20% in 50 year; and a Maximum considered earthquake (MCE) of 2% in 50 year.

In chapter 6, detailed numerical models were developed to consider the performance of the CROCW system, where along one principal axis is the CORW and along the other principal axis is the SCCW. In this chapter, only the response along the SCCW is studied. The numerical models were subjected to a set of source-specific ground motions. The ground motion suite selection and scaling are presented in Chapter 7.

A total of 660 nonlinear time-history analyses were conducted to encompass the four prototypes, under three hazards, and the difference earthquake sources. Key engineering design parameters for each analysis are studied, including: interstorey drifts (ISDR), wall forces, damper deformations, and wall strains. Only the governing ground motion source is shown within this chapter for brevity. The following sections present the numerical results and discuss the performance of the SCCW system. The nonlinear analysis results are used to validate the EEDP design procedure and understand the seismic response of the system.

9.3 Global displacements and Interstorey drifts

Lateral displacements and interstorey drift ratios (ISDRs) were analysed at each wall node shown in Figure 9.1. Displacements and ISDR was determined through analysing the peak response for each ground motion, at each story level, at each of the eight nodes on the core wall. However, all responses are essentially the same for each node under this unidirectional loading, so only the WNW node is shown herein for brevity.

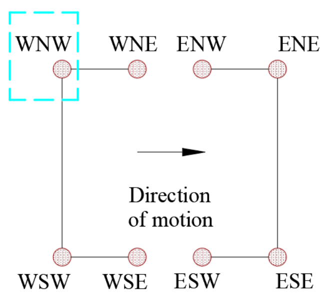

Figure 9.1 Displacement and interstorey drift post processing schematic for SCCW

9.3.1 Global displacements

Figure 9.2 shows the mean (μ) and standard deviation (σ) prototype building peak global displacements of the SCCW over the building height. As shown in the figure, the SLE peak μ roof drift ratio (RDR) is 0.053%, 0.076%, 0.035%, and 0.045% for the Van24, Vic24, Van40, and Vic40, respectively. The DBE peak RDR-μ is over double the SLE, shown as 0.14%, 0.21%, 0.12%, and 0.15% for the Van24, Vic24, Van40, and Vic40, respectively. The MCE peak RDR-μ is 0.54%, 0.97%, 0.44%, and 0.69% for the Van24, Vic24, Van40, and Vic40, respectively.

The standard deviation (σ) is highest for the Vic24, under all hazards. The peak RDR-σ under SLE is 0.015%, 0.03%, 0.008%, and 0.009% for the Van24, Vic24, Van40, and Vic40, respectively.

The peak RDR-σ under DBE is 0.051%, 0.071%, 0.046%, and 0.034% for the Van24, Vic24, Van40, and Vic40, respectively. The peak RDR-σ under MCE is 0.28%, 0.54%, 0.23%, and 0.29% for the Van24, Vic24, Van40, and Vic40, respectively.

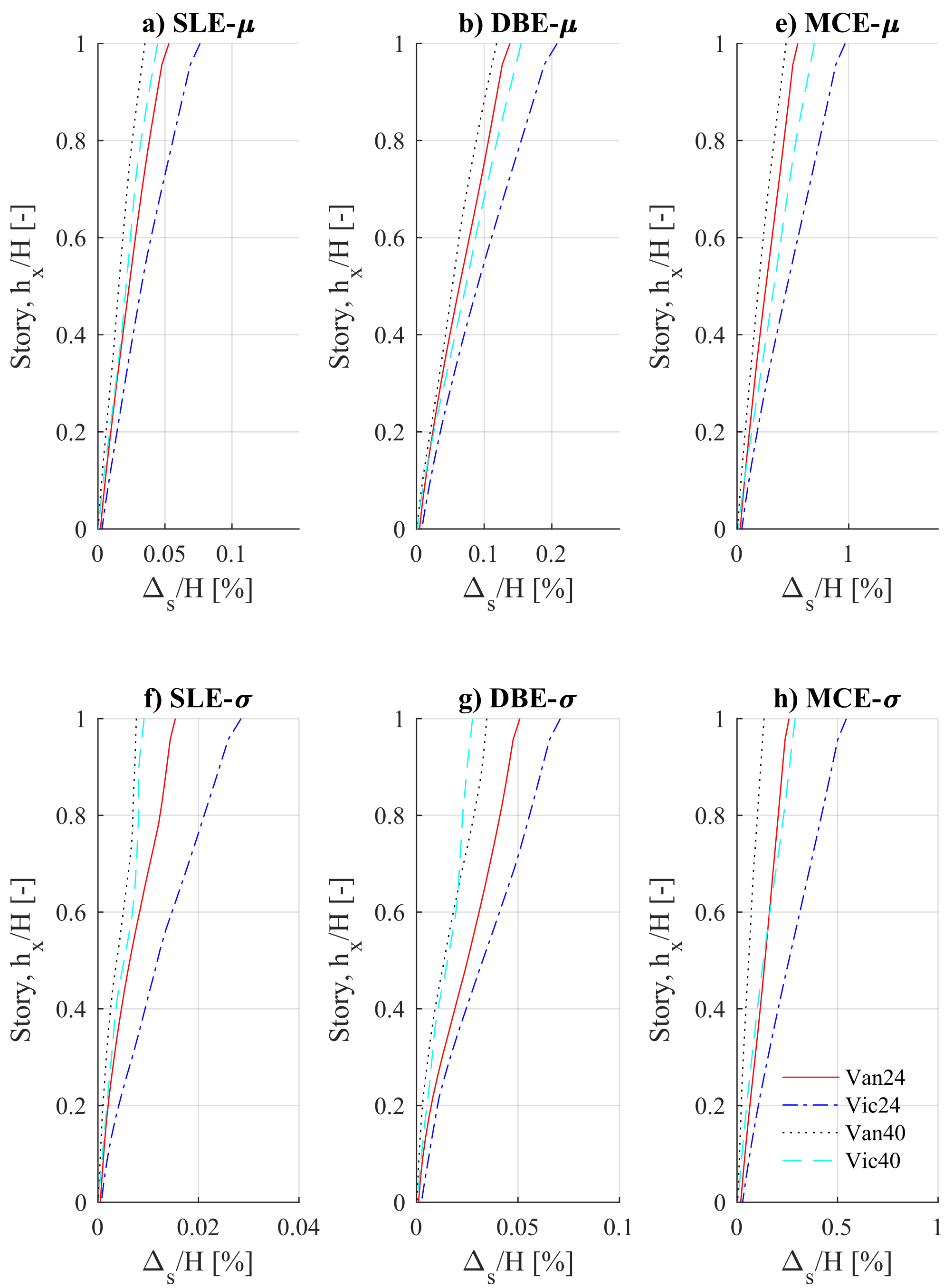

Figure 9.2 SCCW roof drift ratio (governing source): (a) SLE- μ; (b) DBE- μ; (c) MCE- μ; (d) SLE- σ; (e) DBE- σ; and (f) MCE- σ

Figure 9.3 compares the ratio of the mean roof displacement from the model (Δ_r) to the EEDP design roof displacement (Δ_{EEDP}). Generally, the response matches well - demonstrating the robustness of the EEDP design procedure.

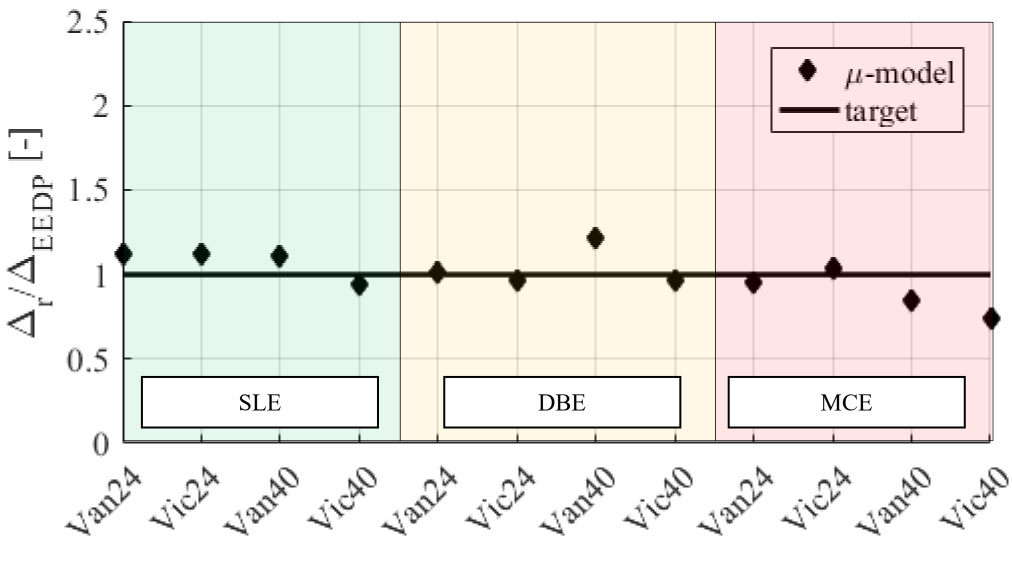

Figure 9.3 Statistical comparison between nonlinear analysis and EEDP for the SCCW

9.3.2 Inter-story drift ratio (ISDR)

Figure 9.4 shows the mean (μ) and standard deviation (σ) prototype building peak global ISDR over the building height. As shown in the figure, the ISDR-μ at the SLE shaking intensity is 0.069%, 0.102%, 0.058%, and 0.084% for the Van24, Vic24, Van40, and Vic40, respectively. The DBE peak ISDR is 0.17%, 0.27%, 0.19%, and 0.27% for the Van24, Vic24, Van40, and Vic40, respectively. The MCE peak ISDR-μ is 0.63%, 1.14%, 0.66%, and 1.01% for the Van24, Vic24, Van40, and Vic40, respectively.

The standard deviation (σ) is highest for the Vic24, under all hazards. The peak σ for ISDR under SLE is 0.016%, 0.04%, 0.011%, and 0.015% for the Van24, Vic24, Van40, and Vic40, respectively. The peak σ for ISDR under DBE is 0.060%, 0.085%, 0.053%, and 0.056% for the Van24, Vic24, Van40, and Vic40, respectively. The peak σ for ISDR under MCE is 0.31%, 0.56%, 0.30%, and 0.44% for the Van24, Vic24, Van40, and Vic40, respectively. The ISDR shown in Figure 9.4 are relatively low, compared with the allowable 2.5% drifts allowed in the National building code of Canada (NBCC, 2015) permissible for normal importance buildings. However, unlike conventional buildings, where yielding is expected over the wall height, these walls are expected to have minimal damages. Therefore, these low ISDR are to be expected.

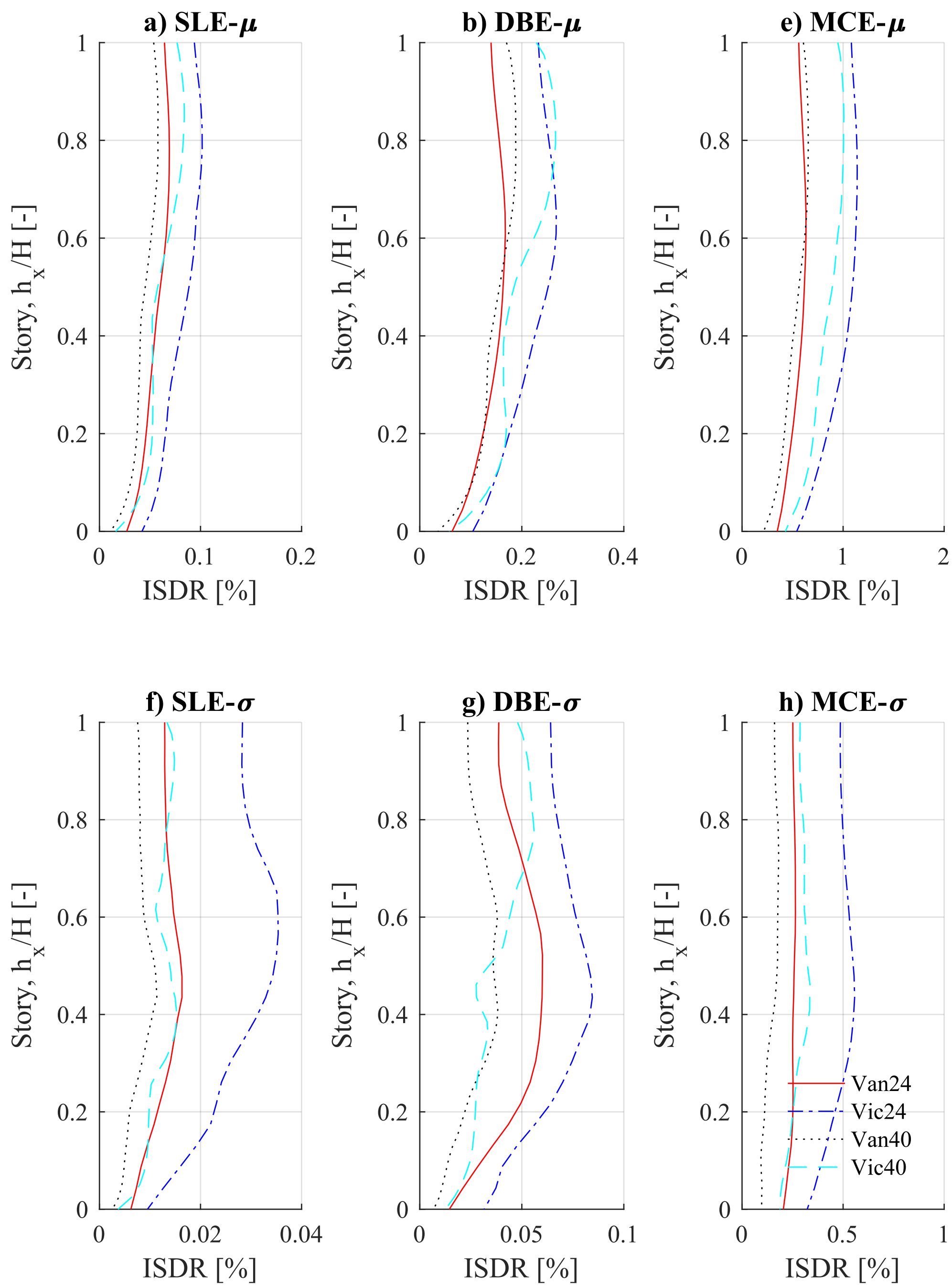

Figure 9.4 SCCW unidirectional ISDR (governing source) : (a) SLE- μ; (b) DBE- μ; (c) MCE- μ; (d) SLE- σ; (e) DBE- σ; and (f) MCE- σ

9.4 Wall-base damper

Figure 9.5 compares the ratio of the mean wall-base damper force from the model (f_b) to the EEDP design yield force ($f_{b,y}$). As shown, the damper force is below yielding at the SLE and DBE. At the MCE all wall-base dampers have yielded. These observed behaviors meet the performance objectives of the EEDP, where the wall-base dampers are designed to remain elastic at the SLE and DBE and yield at the MCE.

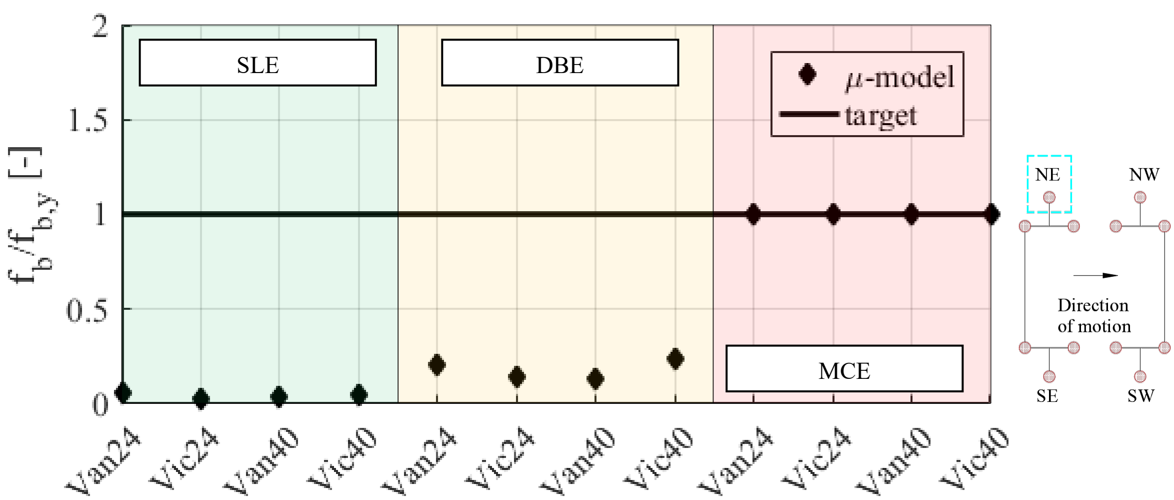

Figure 9.5 Base damper force ratio for each prototype building at each hazard under unidirectional load in SCCW direction

9.5 Coupling beam shear force

Figure 9.6 shows the mean (μ) and standard deviation (σ) of the ratio of coupling beam shear force (V_{CB}) to the yield coupling beam force ($V_{CB,y}$). The ratio $V_{CB}/V_{CB,y}$ was determined by taking the peak shear response of the North and South coupling beam at a given floor and dividing by the yield force.

As shown, generally, the coupling beam force is below yielding at the SLE. At the DBE and MCE all wall-base dampers have yielded. These observed behaviors meet the performance objectives of the EEDP, where the wall-base dampers are designed to remain elastic at the SLE and yields at the DBE and MCE.

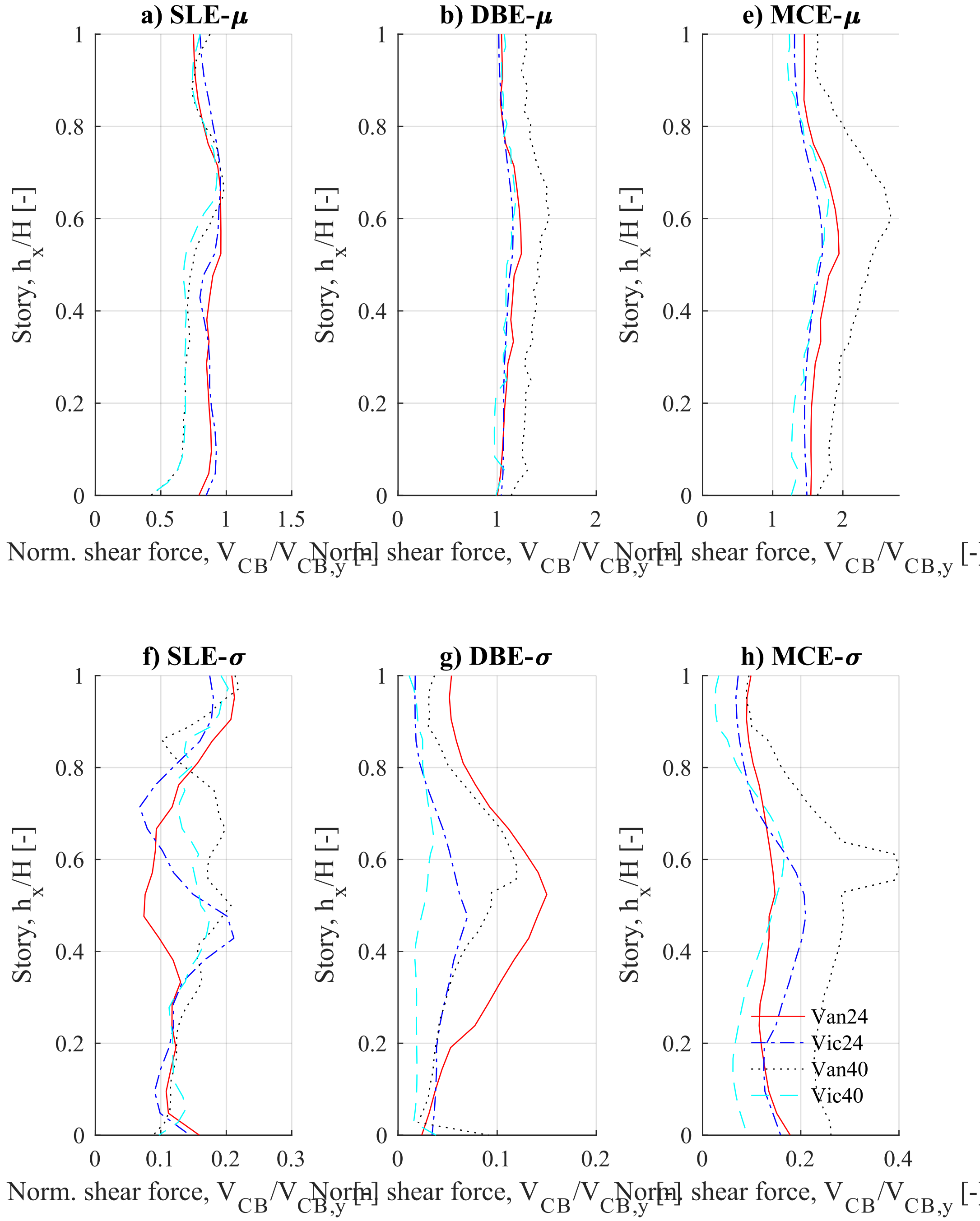

Figure 9.6 SCCW unidirectional coupling beam shear force ratio (governing source): (a) SLE- μ; (b) DBE- μ; (c) MCE- μ; (d) SLE- σ; (e) DBE- σ; and (f) MCE- σ

9.6 Wall shear stress

Figure 9.7 shows the mean (μ) and standard deviation (σ) prototype building peak shear stress over the building height. The shear forces are determine using a section cut which includes only each wall flanges. The stress is determined by dividing this force by the flange length and the flange thicknesses. Figure 9.7 shows the maximum stress of the four flanges (i.e., North-West, North-East, South-West, South-East).

As shown in the figure, the μ shear stress at the SLE shaking intensity is 0.37 MPa, 0.58 MPa, 0.31 MPa, and 0.43 MPa for the Van24, Vic24, Van40, and Vic40, respectively. The DBE peak μ shear stress is 0.65 MPa, 1.03 MPa, 0.79 MPa, and 1.07 MPa for the Van24, Vic24, Van40, and Vic40, respectively. The MCE peak μ shear stress is 1.56 MPa, 2.15 MPa, 1.82 MPa, and 2.18 MPa for the Van24, Vic24, Van40, and Vic40, respectively.

The peak σ of the shear stress under SLE is 0.09 MPa, 0.11 MPa, 0.06 MPa, and 0.11 MPa for the Van24, Vic24, Van40, and Vic40, respectively. The peak σ of the shear stress under DBE is 0.13 MPa, 0.14 MPa, 0.15 MPa, and 0.23 MPa for the Van24, Vic24, Van40, and Vic40, respectively. The peak σ of the shear stress under MCE is 0.34 MPa, 0.37 MPa, 0.38 MPa, and 0.45 MPa for the Van24, Vic24, Van40, and Vic40, respectively.

Overall, the shear stresses are low (less than 10%f'c), demonstrating this system resulting in reasonably low damage, as per the performance objective.

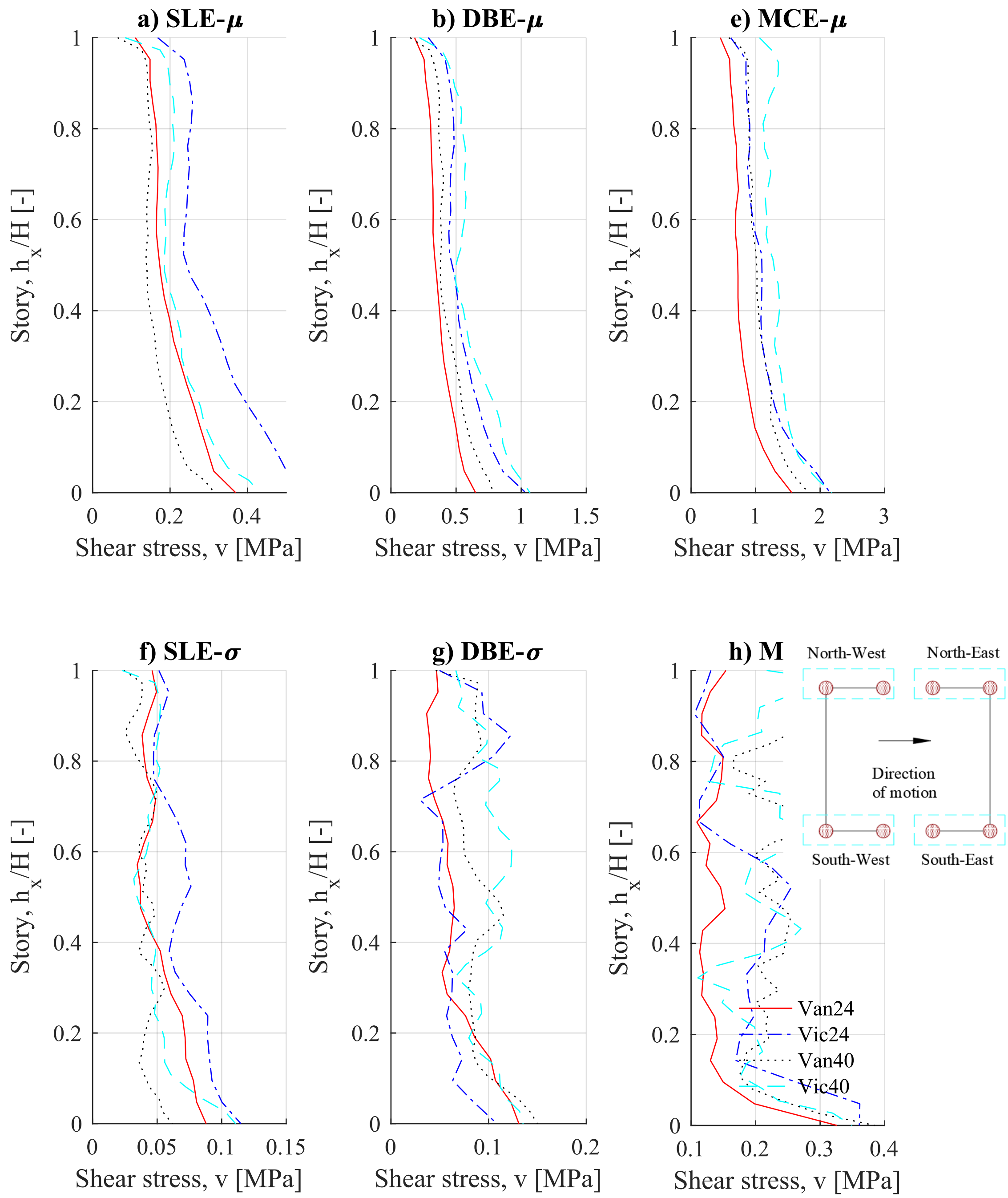

Figure 9.7 SCCW shear stress under unidirectional loading(governing source) : (a) SLE- μ; (b) DBE- μ; (c) MCE- μ; (d) SLE- σ; (e) DBE- σ; and (f) MCE- σ

9.7 Wall strains

Figure 9.8 shows the mean (μ) and standard deviation (σ) prototype building peak tension strain in the wall over the building height at all hazards. At each node, strains are determined by taking the difference between the vertical displacements at each wall corner divided by the distance between the nodes. The strains are normalised to the yield strain of the reinforcing steel ($\varepsilon_y = 0.002$). The strains are highest near the mid-height of the building, demonstrating the governance of higher mode moments. However, all strains are below yielding (i.e., $\varepsilon/\varepsilon_y$<1), demonstrating the EEDP performance objectives have been met.

As shown in the figure, the mean strain ratio ($\varepsilon/\varepsilon_y$- μ) at the SLE shaking intensity 0.072, 0.082, 0.10, and 0.11 for the Van24, Vic24, Van40, and Vic40, respectively. The DBE peak $\varepsilon/\varepsilon_y$- μ is 0.10, 0.13, 0.14, and 0.16 for the Van24, Vic24, Van40, and Vic40, respectively. The MCE peak $\varepsilon/\varepsilon_y$- μ is 0.29, 0.64, 0.31, and 0.80 for the Van24, Vic24, Van40, and Vic40, respectively.

The standard deviation (σ) of the $\varepsilon/\varepsilon_y$ is highest for the Vic24, under all hazards. The peak σ for $\varepsilon/\varepsilon_y$under SLE is 0.007, 0.012, 0.004, and 0.005 for the Van24, Vic24, Van40, and Vic40, respectively. The peak σ for $\varepsilon/\varepsilon_y$under DBE is 0.017, 0.039, 0.018, and 0.04 for the Van24, Vic24, Van40, and Vic40, respectively. The peak σ for $\varepsilon/\varepsilon_y$under MCE is 0.16, 0.28, 0.23, and 0.62 for the Van24, Vic24, Van40, and Vic40, respectively.

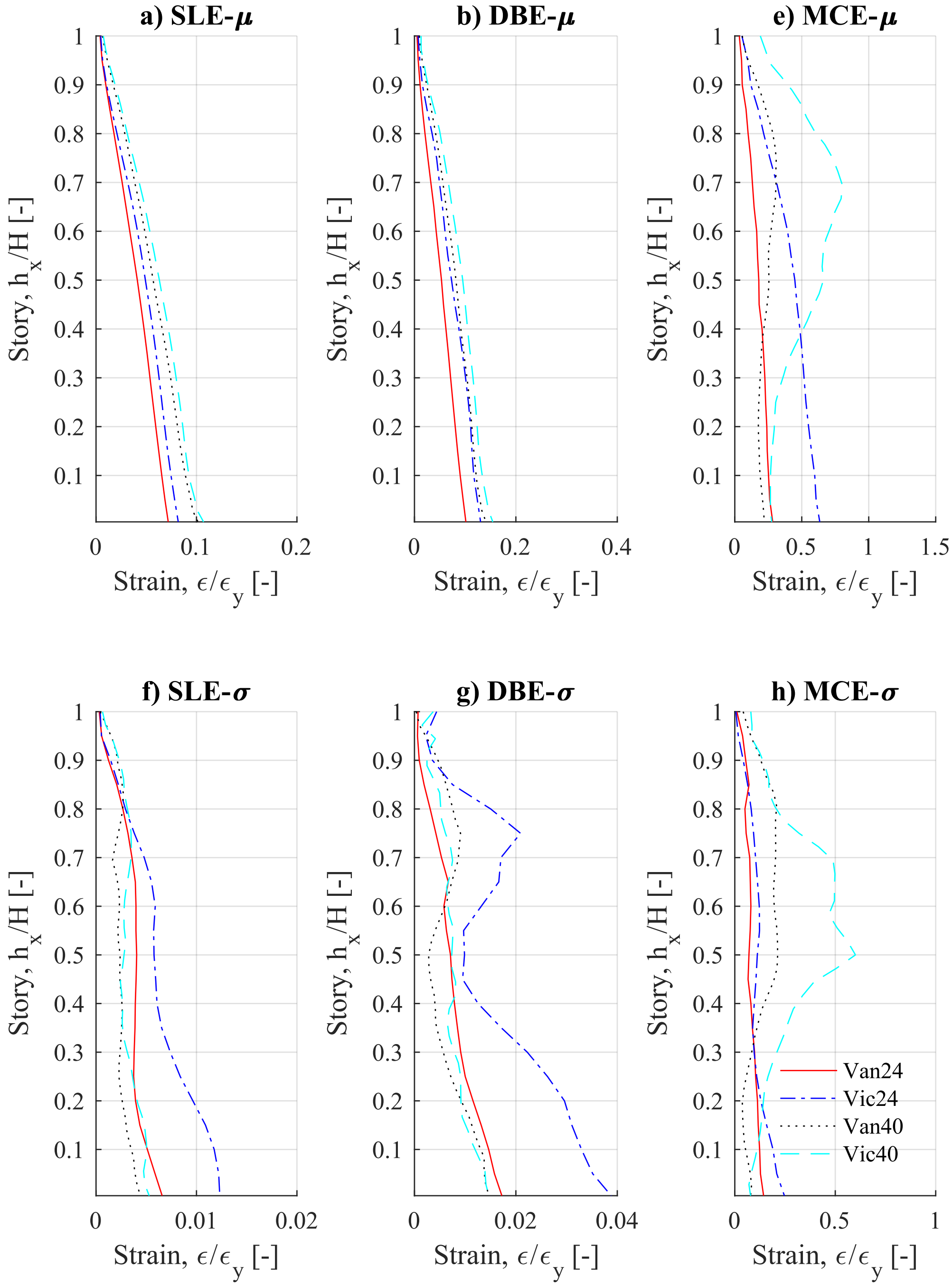

Figure 9.8 Max strain profile response for all prototype buildings under unidirectional loading in the SCCW direction at the WNE corner: (a) SLE- μ; (b) DBE- μ; (c) MCE- μ; (d) SLE- σ; (e) DBE- σ; and (f) MCE- σ

9.8 Summary

This chapter presented the nonlinear dynamic responses of four prototype buildings design with an SCCW: a 24-story located in Victoria and in Vancouver, and a 40-story located in Victoria and in Vancouver. The nonlinear analysis conducted in this chapter demonstrate the robustness of EEDP. Specifically, the performance objectives are met at the SLE shaking intensity, where the system remains elastic, at the DBE, where the SCFDs yield and dissipate energy, and at the MCE, where the SCFDs and base dampers yield and dissipate energy, while the remaining wall is elastic. The limited damage is demonstrated by the low shear stresses (less than 10%f'c) and the low wall strains are low (less than $\varepsilon_y = 0.002$) for all prototype buildings.

This chapter presented the seismic performance assessment of the SCCW system under unidirectional loading. The following chapter (Chapter 10) shows the seismic performance assessment of the CROCW, which is designed with the CORW along one axis and the SCCW along the other axis, under bidirectional loading.

Chapter 10: Bidirectional performance CROCW system

10.1 Overview

This chapter presents the seismic assessment of the CROCW system under bidirectional loading. The CROCW, which has a CORW along one principal axis and an SCCW and the other, was designed in Chapter 5. Chapter 8 and Chapter 9 validated the EEDP procedure for the CORW and SCCW, respectively. This chapter validates the design of the bidirectional CROCW system.

10.2 Introduction

The CROCW system was designed in Chapter 5 using the modified EEDP. In this procedure, the CORW and the SCCW systems were designed independently but ensuring that assuming the wall-base damper has the same design force for each direction. Chapters 8 and 9 presented the results from applying unidirectional ground motions to the CROCW system along the CORW axis and the SCCW axis– validating the EEDP. This chapter presents the response of the CROCW under bidirectional loading and compares it to the unidirectional responses (i.e., responses from Chapter 8 and 9).

A total of 660 bidirectional nonlinear time-history analysis were conducted to encompass the four prototypes, under three hazards, and the difference earthquake sources. Key engineering design parameters for each bidirectional analysis are studied, including inter-story drifts (ISDR), wall forces, damper deformations, and wall strains. Additionally, a comparison of the CROCW system under unidirectional and bidirectional loading is provided. The governing ground motion source is shown herein for brevity.

10.3 Global displacements and Interstorey drifts

Lateral displacements and interstorey drifts are determined using the North-West node of the West wall, as shown in Figure 10.1. This node was selected as it showed the highest displacements and ISDR under bidirectional loading.

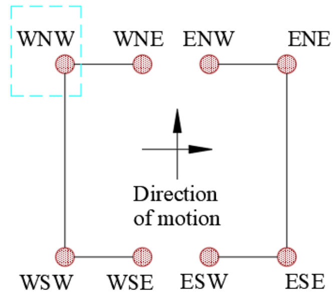

Figure 10.1 Displacement and interstorey drift post processing schematic

10.3.1 Global displacements

Figure 10.2 and Figure 10.3 shows the mean (μ) and standard deviation (σ) CROCW peak story displacements normalised to building height in the CORW direction and the SCCW direction, respectively.

As shown in Figure 10.2, the CORW direction SLE peak μ roof drift ratio (RDR) is 0.045%, 0.057%, 0.034%, and 0.049% for the Van24, Vic24, Van40, and Vic40, respectively. The CORW direction DBE peak RDR-μ is over double the SLE, shown as 0.14%, 0.21%, 0.10%, and 0.13% for the Van24, Vic24, Van40, and Vic40, respectively. The CORW direction MCE peak RDR-μ is 0.54%, 0.83%, 0.44%, and 0.75% for the Van24, Vic24, Van40, and Vic40, respectively.

The standard deviation (σ) is highest for the Vic24, under all hazards. The CORW direction peak σ for RDR under SLE is 0.013%, 0.02%, 0.010%, and 0.012% for the Van24, Vic24, Van40, and Vic40, respectively. The CORW direction peak σ for RDR under DBE is 0.041%, 0.063%, 0.028%, and 0.046% for the Van24, Vic24, Van40, and Vic40, respectively. The CORW direction peak σ for RDR under MCE is 0.26%, 0.31%, 0.17%, and 0.28% for the Van24, Vic24, Van40, and Vic40, respectively.

As shown in Figure 10.3, the SCCW direction SLE peak roof drift ratio (RDR) is 0.053%, 0.076%, 0.035%, and 0.044% for the Van24, Vic24, Van40, and Vic40, respectively. The SCCW direction DBE peak RDR is over double the SLE, shown as 0.14%, 0.21%, 0.12%, and 0.15% for the Van24, Vic24, Van40, and Vic40, respectively. The SCCW direction MCE peak RDR is 0.61%, 1.02%, 0.50%, and 0.71% for the Van24, Vic24, Van40, and Vic40, respectively.

The SCCW direction peak σ for RDR under SLE is 0.015%, 0.03%, 0.007%, and 0.009% for the Van24, Vic24, Van40, and Vic40, respectively. The SCCW direction peak σ for RDR under DBE is 0.052%, 0.073%, 0.045%, and 0.035% for the Van24, Vic24, Van40, and Vic40, respectively. The SCCW direction peak σ for RDR under MCE 0.29%, 0.58%, 0.25%, and 0.23% for the Van24, Vic24, Van40, and Vic40, respectively.

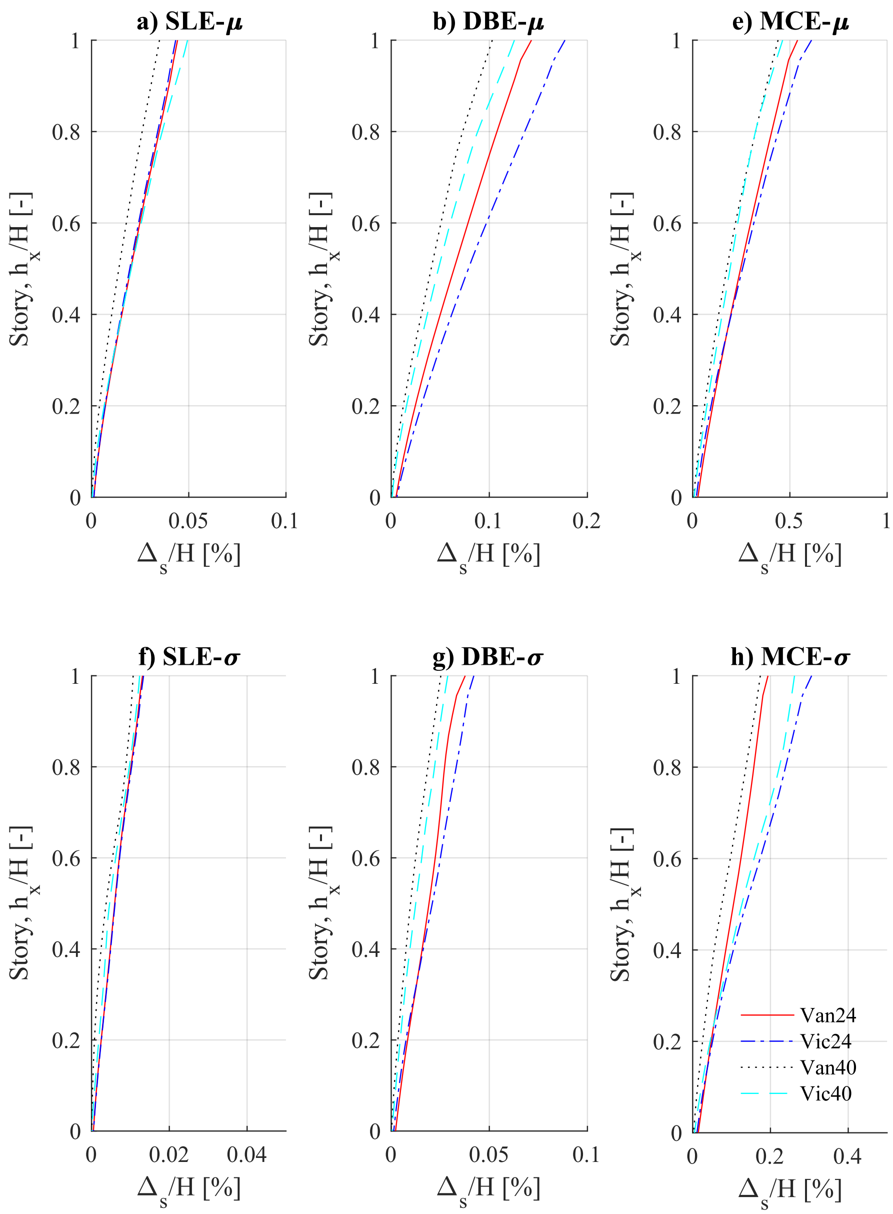

Figure 10.2 CORW bidirectional displacements (governing source): (a) SLE- μ; (b) DBE- μ; (c) MCE- μ; (d) SLE- σ; (e) DBE- σ; and (f) MCE- σ

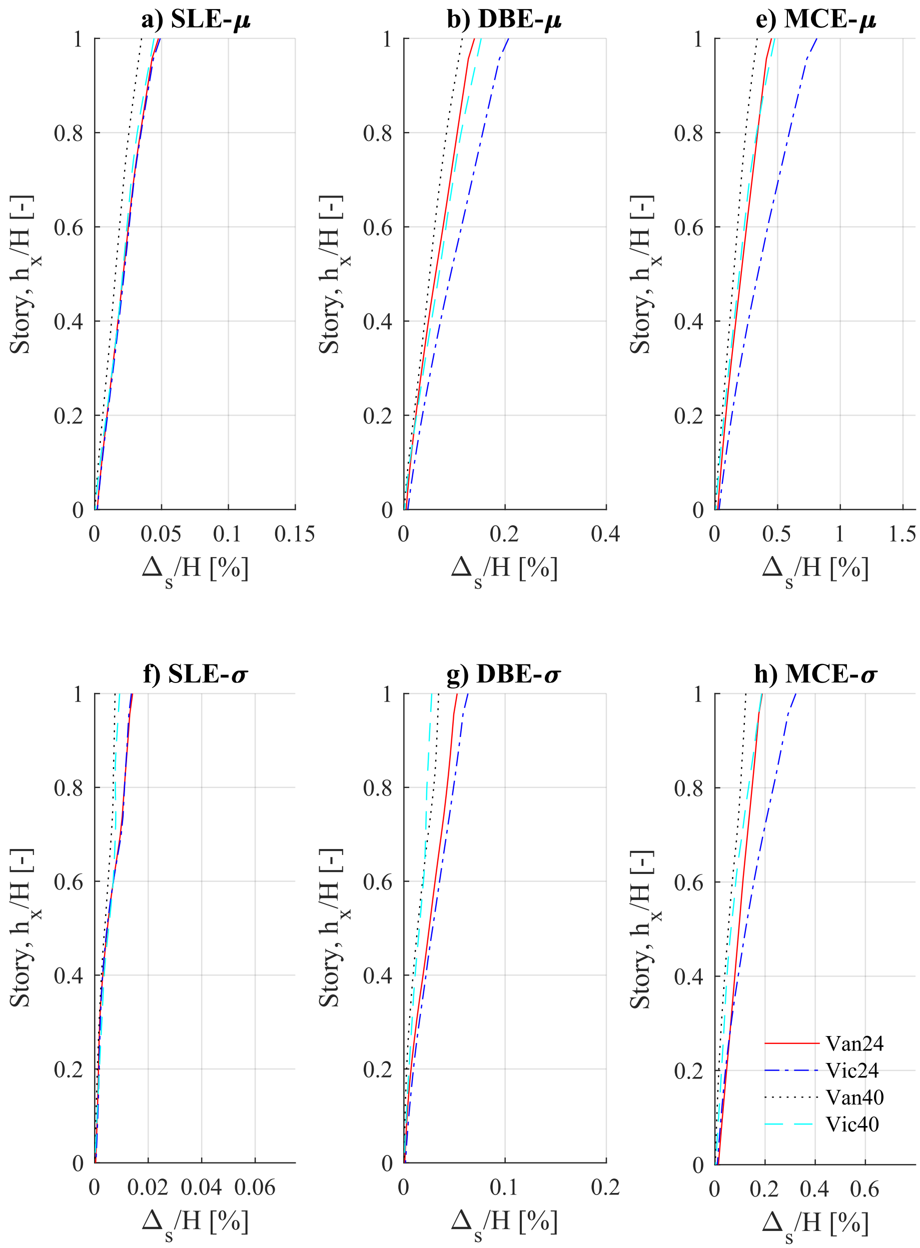

Figure 10.3 SCCW unidirectional displacements (governing source): (a) SLE- μ; (b) DBE- μ; (c) MCE- μ; (d) SLE- σ; (e) DBE- σ; and (f) MCE- σ

Figure 10.4 and Figure 10.5 compares the ratio of the mean roof displacement from the model (Δ_r) to the EEDP design roof displacement (Δ_{EEDP}) for the CORW direction and the SCCW direction of the CROCW system, respectively. Generally, the response matches well - demonstrating the robustness of the EEDP design procedure.

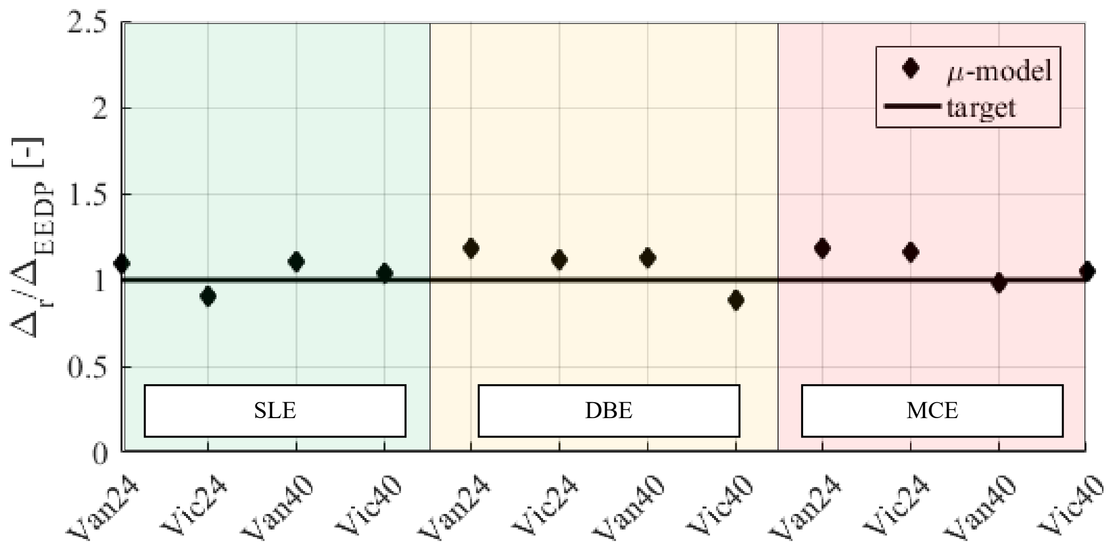

Figure 10.4 Statistical comparison between nonlinear analysis and EEDP for the CROCW in the CORW direction

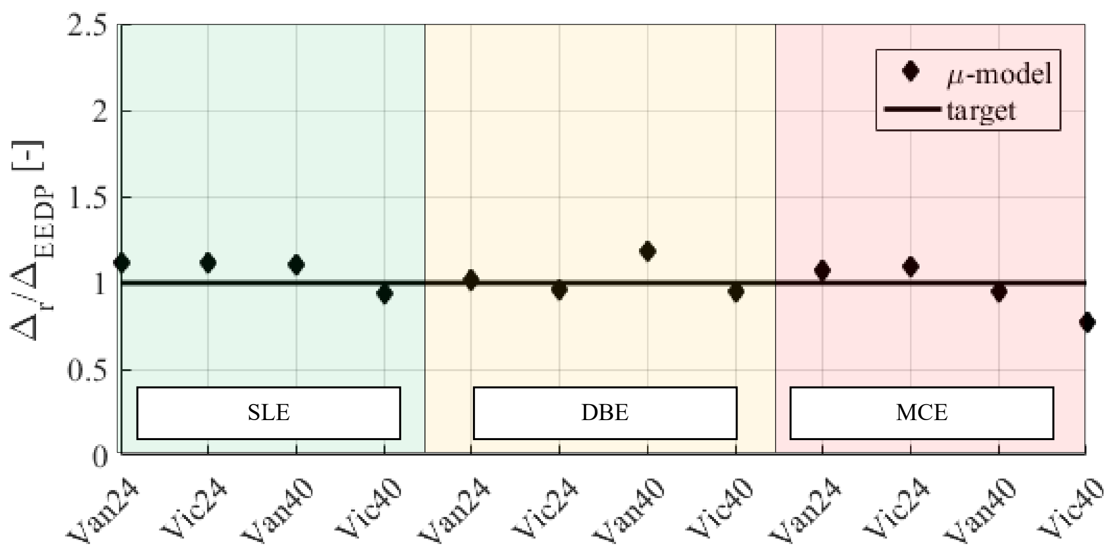

Figure 10.5 Statistical comparison between nonlinear analysis and EEDP for the CROCW in the SCCW direction

10.3.2 Inter-story drift ratio (ISDR)

Figure 10.6 and Figure 10.7 shows the mean (μ) and standard deviation (σ) prototype building peak global ISDR over the building height for the CORW and the SCCW direction, respectively.

As shown in Figure 10.6, the CORW direction ISDR- μ at the SLE shaking intensity is 0.060%, 0.079%, 0.050%, and 0.076% for the Van24, Vic24, Van40, and Vic40, respectively. The CORW direction ISDR- μ at the DBE is 0.19%, 0.26%, 0.17%, and 0.23% for the Van24, Vic24, Van40, and Vic40, respectively. The CORW direction ISDR- μ at the MCE 0.61%, 1.04%, 0.70%, and 1.21% for the Van24, Vic24, Van40, and Vic40, respectively.

The standard deviation (σ) is highest for the Vic24, under all hazards. The CORW direction peak σ for ISDR under SLE is 0.019%, 0.02%, 0.012%, and 0.018% for the Van24, Vic24, Van40, and Vic40, respectively. The CORW direction peak σ for ISDR under DBE 0.055%, 0.086%, 0.044%, and 0.066% for the Van24, Vic24, Van40, and Vic40, respectively. The CORW direction peak σ for ISDR under MCE is 0.24%, 0.32%, 0.20%, and 0.35% for the Van24, Vic24, Van40, and Vic40, respectively.

As shown in Figure 10.7, the SCCW direction ISDR at the SLE shaking intensity is 0.069%, 0.102%, 0.057%, and 0.084% for the Van24, Vic24, Van40, and Vic40, respectively. The DBE peak ISDR is 0.17%, 0.27%, 0.19%, and 0.28% for the Van24, Vic24, Van40, and Vic40, respectively. The MCE peak ISDR is 0.70%, 1.21%, 0.73%, and 1.07% for the Van24, Vic24, Van40, and Vic40, respectively.

The standard deviation (σ) is highest for the Vic24, under all hazards. The peak σ for ISDR under SLE is 0.016%, 0.04%, 0.011%, and 0.015% for the Van24, Vic24, Van40, and Vic40, respectively. The peak σ for ISDR under DBE is 0.062%, 0.091%, 0.051%, and 0.064% for the Van24, Vic24, Van40, and Vic40, respectively. The peak σ for ISDR under MCE is 0.30%, 0.58%, 0.33%, and 0.44% for the Van24, Vic24, Van40, and Vic40, respectively.

The ISDR shown are relatively low, compared with the allowable 2.5% drifts allowed in the National building code of Canada (NBCC, 2015) permissible for normal importance buildings. However, unlike conventional buildings, where yielding is expected over the wall height, these walls are expected to have minimal damages. Therefore, these low ISDR are to be expected.

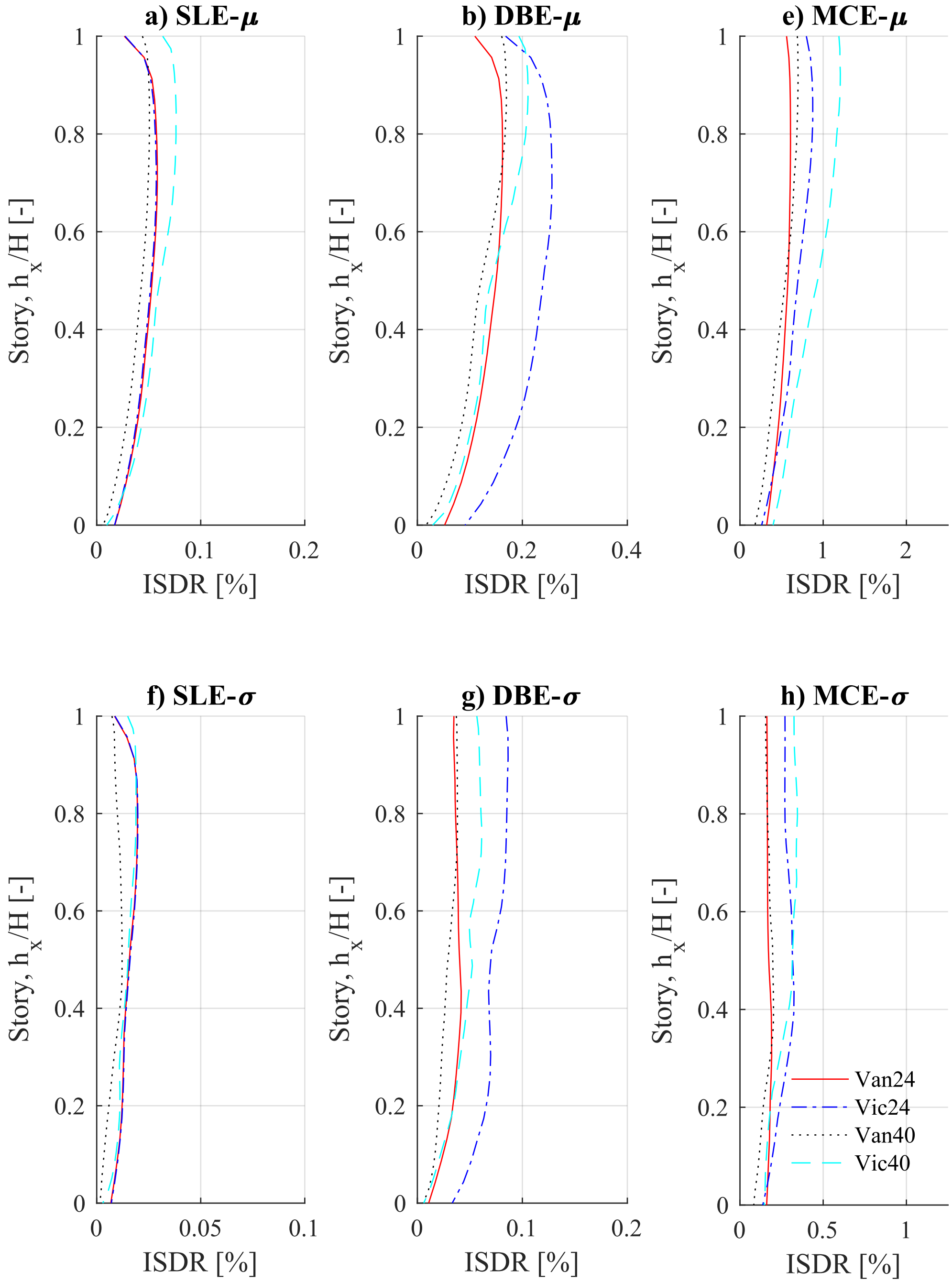

Figure 10.6 SCCW unidirectional ISDR (governing source): (a) SLE- μ; (b) DBE- μ; (c) MCE- μ; (d) SLE- σ; (e) DBE- σ; and (f) MCE- σ

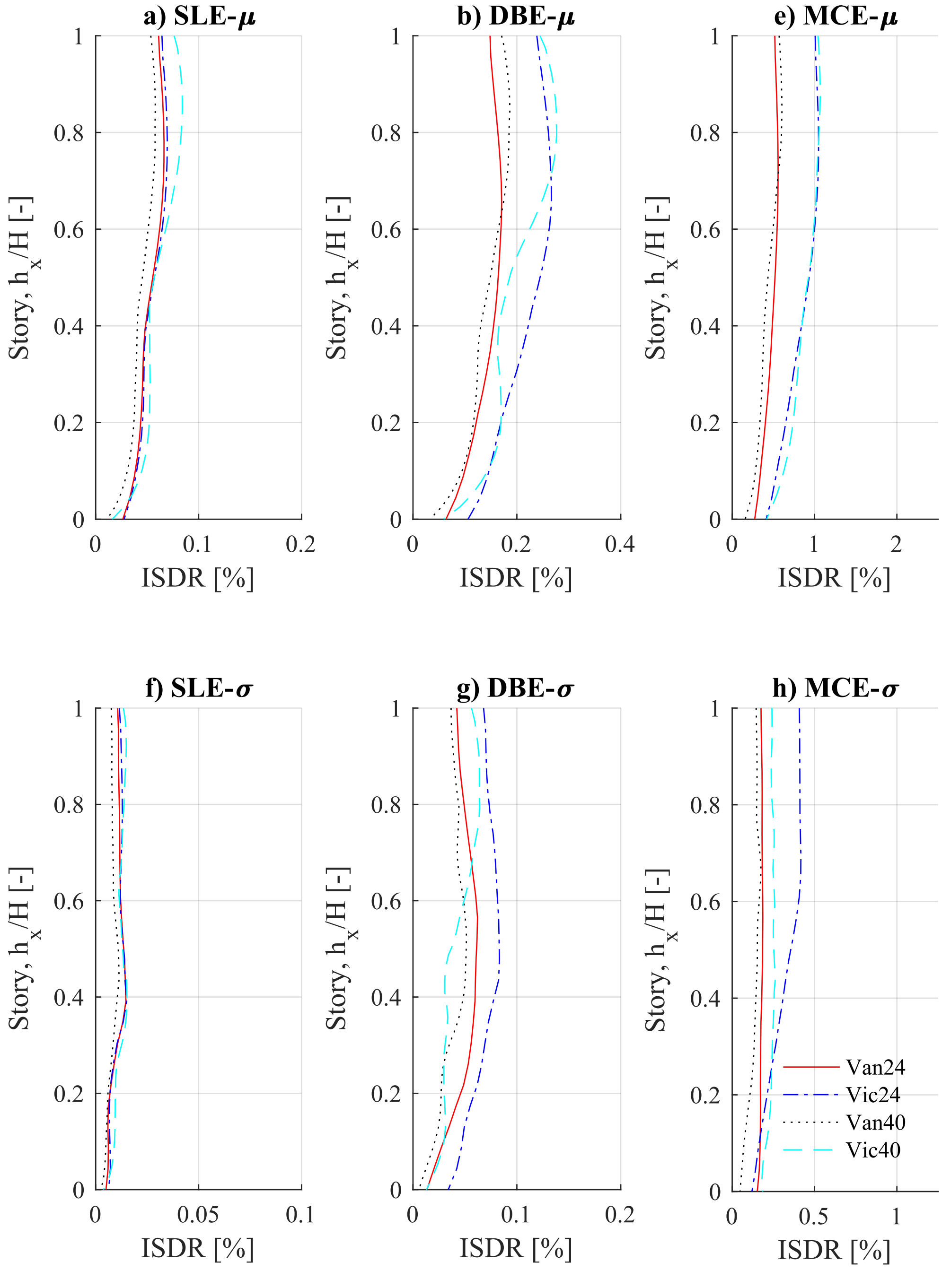

Figure 10.7 SCCW unidirectional ISDR (governing source) : (a) SLE- μ; (b) DBE- μ; (c) MCE- μ; (d) SLE- σ; (e) DBE- σ; and (f) MCE- σ

10.4 Wall-base damper

Figure 10.8 compares the ratio of the mean wall-base damper force from the model (f_b) to the EEDP design yield force ($f_{b,y}$). As shown, the damper force is below yielding at the SLE and DBE. At the MCE all wall-base dampers have yielded. These observed behaviors meet the performance objectives of the EEDP, where the wall-base dampers are designed to remain elastic at the SLE and DBE and yield at the MCE.

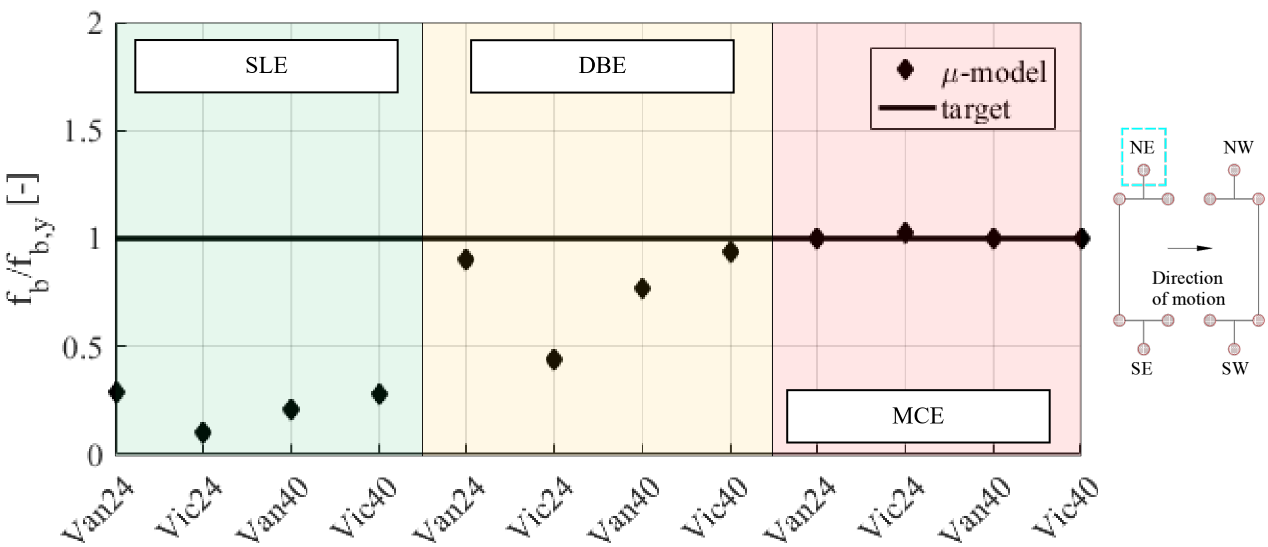

Figure 10.8 Base damper force ratio for each prototype building at each hazard under bidirectional load

10.5 Outrigger dampers

Figure 10.9 compares the ratio of the mean outrigger damper force from the model (f_o) to the EEDP design yield force ($f_{o,y}$). As shown, the damper force is below yielding at the SLE. At the DBE and MCE all outrigger dampers have yielded. These observed behaviors meet the performance objectives of the EEDP, where the outrigger system is designed to remain elastic at the SLE and yield at the DBE and MCE.

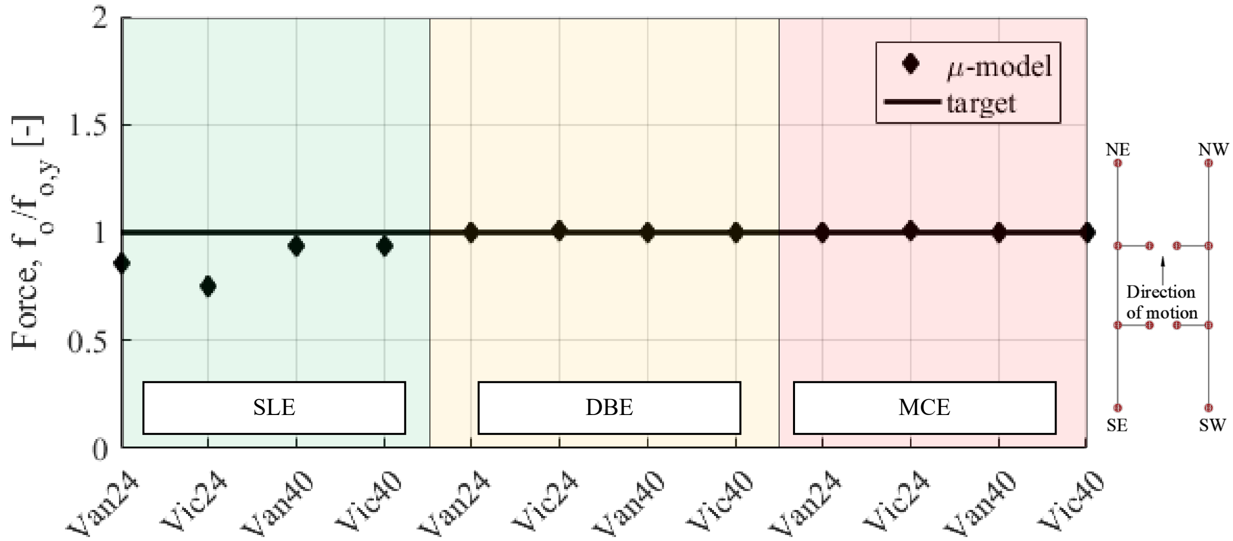

Figure 10.9 Outrigger damper force ratio for each prototype building at each hazard under bidirectional load in CORW direction.

10.6 Coupling beam shear force

Figure 10.10 shows the mean (μ) and standard deviation (σ) of the ratio of coupling beam shear force (V_{CB}) to the yield coupling beam force ($V_{CB,y}$). The ratio $V_{CB}/V_{CB,y}$ was determined by taking the peak shear response of each coupling beam at a given floor and dividing by the yield force. As shown, generally, the coupling beam force is below yielding at the SLE. At the DBE and MCE all wall-base dampers have yielded. These observed behaviors meet the performance objectives of the EEDP, where the wall-base dampers are designed to remain elastic at the SLE and yields at the DBE and MCE.

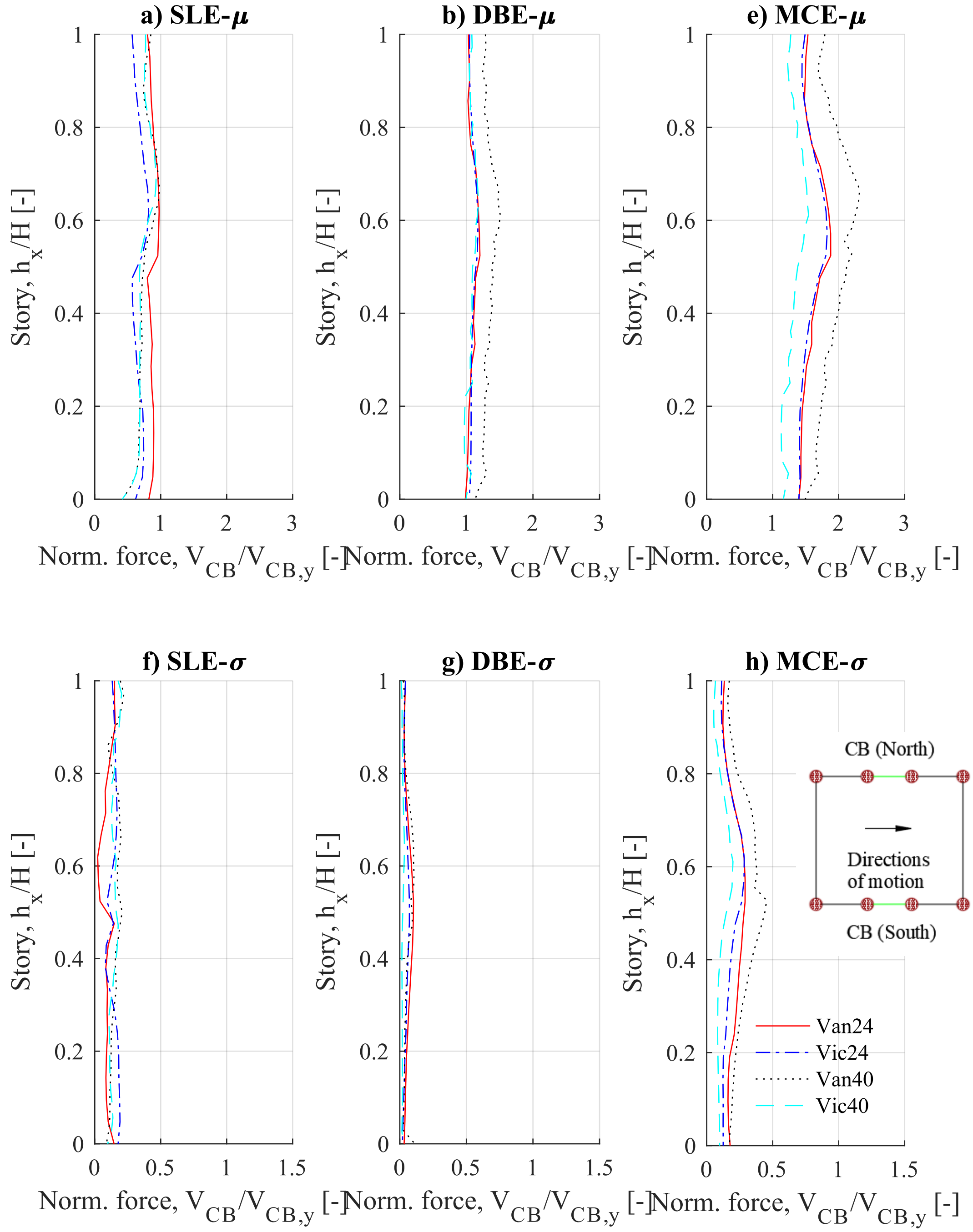

Figure 10.10 Bidirectional coupling beam shear force ratio (governing source): (a) SLE- μ; (b) DBE- μ; (c) MCE- μ; (d) SLE- σ; (e) DBE- σ; and (f) MCE- σ

10.7 Wall shear stress

Figure 10.12 shows the mean (μ) and standard deviation (σ) prototype building peak shear stress in the wall flanges. The shear forces are determine using a section cut which includes only each wall flanges. The stress is determined by dividing this force by the wall length and the flange thicknesses. Figure 9.7 shows the maximum stress of the four flanges (i.e., North-West, North-East, South-West, South-East).

As shown in the figure, the μ shear stress at the SLE shaking intensity is 0.39 MPa, 0.601 MPa, 0.35 MPa, and 0.53 MPa for the Van24, Vic24, Van40, and Vic40, respectively. The DBE peak μ shear stress is 0.70 MPa, 1.17 MPa, 0.88 MPa, and 1.28 MPa for the Van24, Vic24, Van40, and Vic40, respectively. The MCE peak μ shear stress is 3 2.29 MPa, 3.29 MPa, 2.02 MPa, and 2.57 MPa for the Van24, Vic24, Van40, and Vic40, respectively.

The peak σ of the shear stress under SLE is 0.13 MPa, 0.16 MPa, 0.066 MPa, and 0.15 MPa for the Van24, Vic24, Van40, and Vic40, respectively. The peak σ of the shear stress under DBE is 0.15 MPa, 0.22 MPa, 0.16 MPa, and 0.26 MPa for the Van24, Vic24, Van40, and Vic40, respectively. The peak σ of the shear stress under MCE is 0.70 MPa, 0.85 MPa, 0.39 MPa, and 0.53 MPa for the Van24, Vic24, Van40, and Vic40, respectively.

Overall, the shear stresses are low (less than 10%f’c), demonstrating this system resulting in reasonably low damage, as per the performance objective.

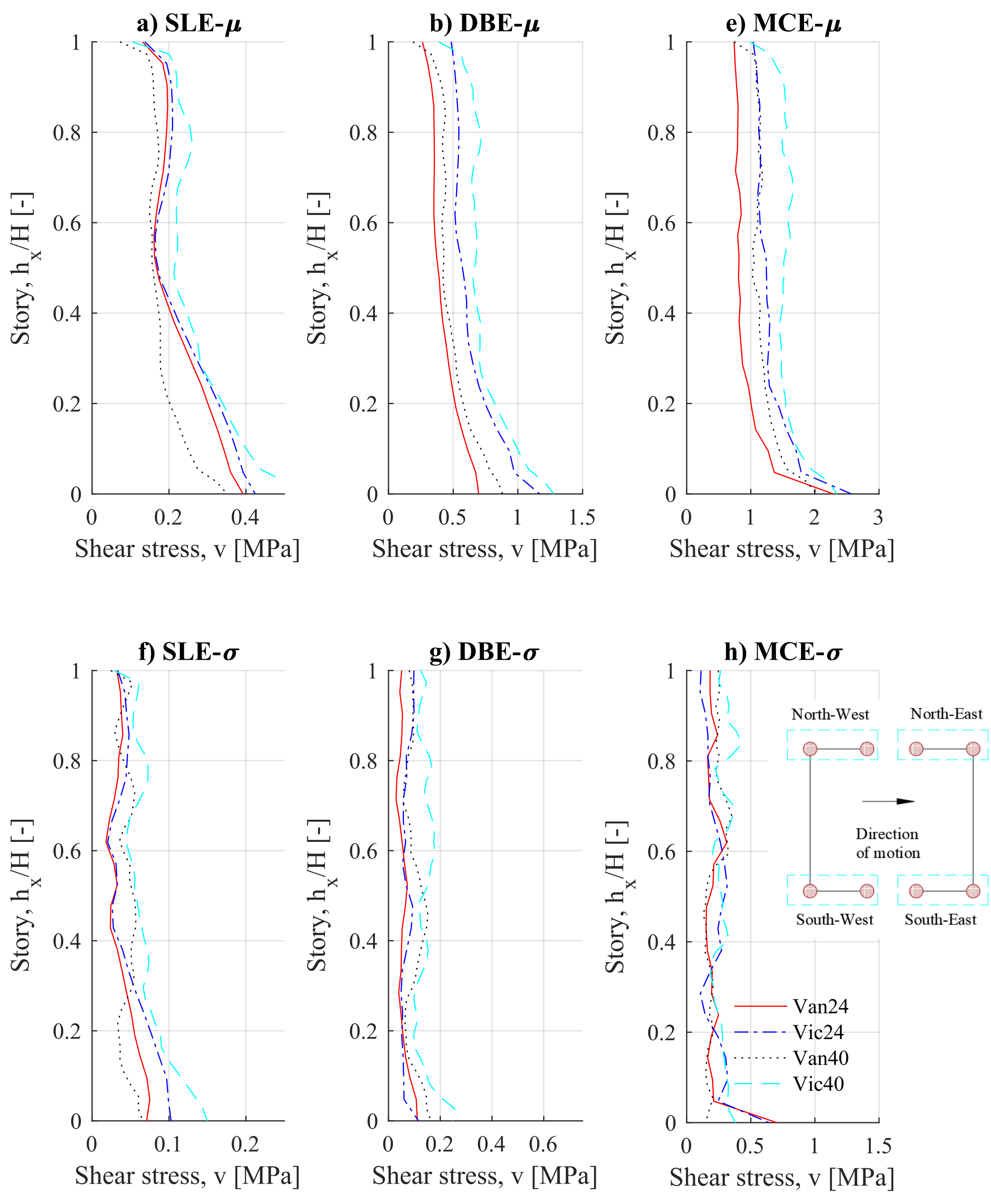

Figure 10.11 CROCW flange shear stress under unidirectional loading(governing source): (a) SLE- μ; (b) DBE- μ; (c) MCE- μ; (d) SLE- σ; (e) DBE- σ; and (f) MCE- σ

Figure 10.11 shows the mean (μ) and standard deviation (σ) prototype building peak shear stress in the web over the building height of the CROCW in the CORW direction. The shear forces are determine using a section cut which includes only each wall web. The stress is determined by dividing this force by the wall length and the web thicknesses.

As shown in the figure, the μ shear stress at the SLE shaking intensity is 0.58 MPa, 0.85 MPa, 0.52 MPa, and 0.80 MPa for the Van24, Vic24, Van40, and Vic40, respectively. The DBE peak μ shear stress is 1.34 MPa, 2.06 MPa, 1.45 MPa, and 2.04 MPa for the Van24, Vic24, Van40, and Vic40, respectively. The MCE peak μ shear stress is 3.03 MPa, 4.02 MPa, 3.26 MPa, and 4.31 MPa for the Van24, Vic24, Van40, and Vic40, respectively.

The standard deviation (σ) of the shear stress is highest for the Vic24, under all hazards. The peak σ of the shear stress under SLE is 0.23 MPa, 0.26 MPa, 0.15 MPa, and 0.23 MPa for the Van24, Vic24, Van40, and Vic40, respectively. The peak σ of the shear stress under DBE is 0.39 MPa, 0.50 MPa, 0.47 MPa, and 0.54 MPa for the Van24, Vic24, Van40, and Vic40, respectively. The peak σ of the shear stress under MCE is 0.54 MPa, 0.97 MPa, 0.70 MPa, and 0.96 MPa for the Van24, Vic24, Van40, and Vic40, respectively. Overall, the shear stresses are low (less than 10%f'c), demonstrating this system resulting in reasonably low damage, as per the performance objective.

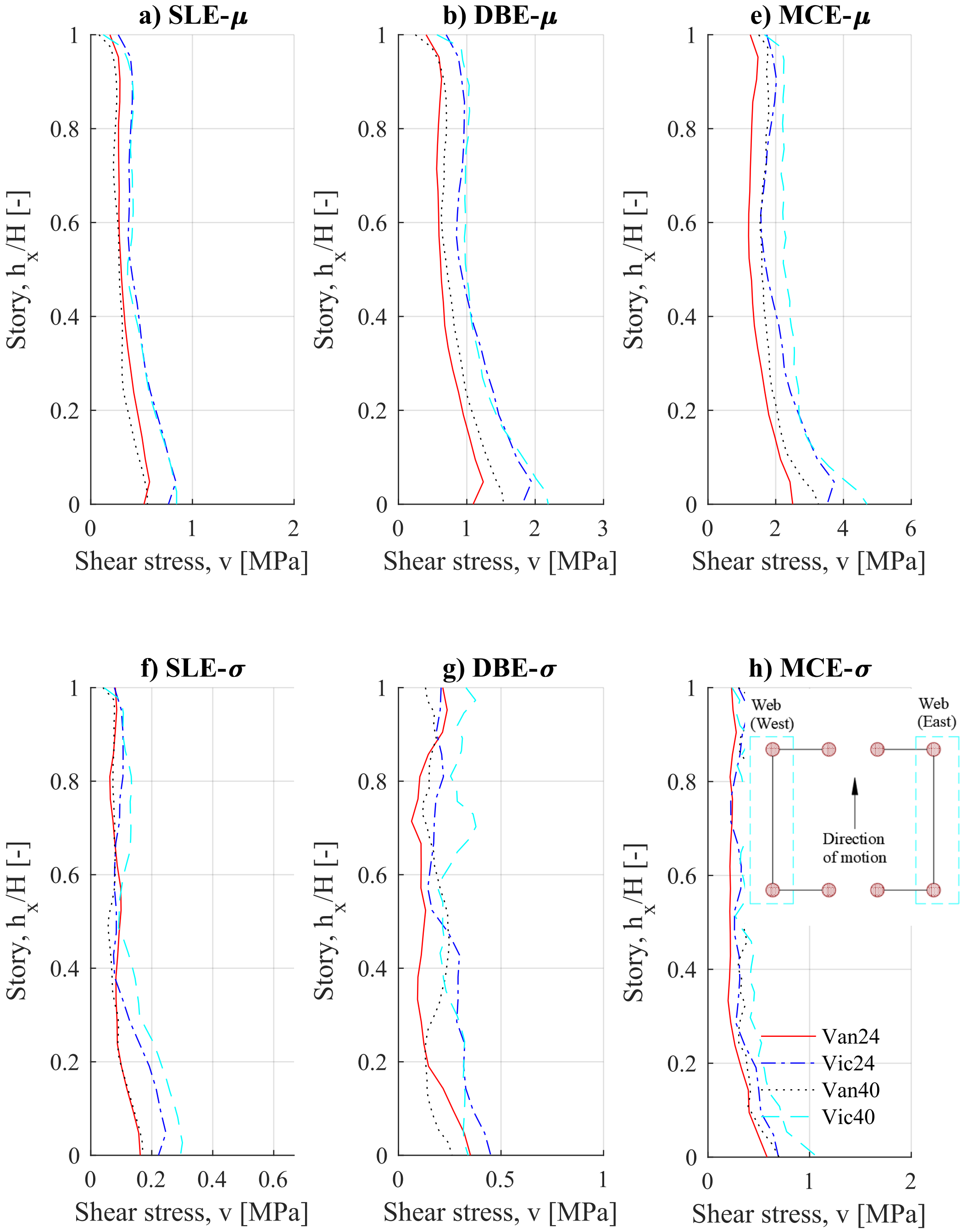

Figure 10.12 CROCW bidirectional web shear stress (governing source): (a) SLE- μ; (b) DBE- μ; (c) MCE- μ; (d) SLE- σ; (e) DBE- σ; and (f) MCE- σ

10.8 Wall strains

Figure 10.13 shows the mean (μ) and standard deviation (σ) prototype building peak tension strain in the wall over the building height at all hazards. At each node, strains are determined by taking the difference between the vertical displacements at each wall corner divided by the distance between the nodes. The tension strains are normalised to the yield strain of reinforcing steel ($\varepsilon_y = 0.002$). The strains are highest near the mid-height of the building, demonstrating the governance of higher mode moments. However, generally the strains are low, demonstrating the EEDP performance objectives have been met.

As shown in the figure, the μ strain ratio ($\varepsilon/\varepsilon_y$) at the SLE shaking intensity is 0.092, 0.099, 0.11, and 0.12 for the Van24, Vic24, Van40, and Vic40, respectively. The DBE peak $\varepsilon/\varepsilon_y$- μ is 0.18, 0.23, 0.17, and 0.19 for the Van24, Vic24, Van40, and Vic40, respectively. The MCE peak $\varepsilon/\varepsilon_y$- μ is 0.44, 0.80, 0.54, and 1.09 for the Van24, Vic24, Van40, and Vic40, respectively.

The standard deviation (σ) of the $\varepsilon/\varepsilon_y$ is highest for the Vic24, under all hazards. The peak σ for $\varepsilon/\varepsilon_y$under SLE is 0.044, 0.035, 0.005, and 0.026 for the Van24, Vic24, Van40, and Vic40, respectively. The peak σ for $\varepsilon/\varepsilon_y$under DBE is 0.034, 0.067, 0.035, and 0.12 for the Van24, Vic24, Van40, and Vic40, respectively. The peak σ for $\varepsilon/\varepsilon_y$under MCE is 0.18, 0.27, 0.26, and 0.84 for the Van24, Vic24, Van40, and Vic40, respectively.

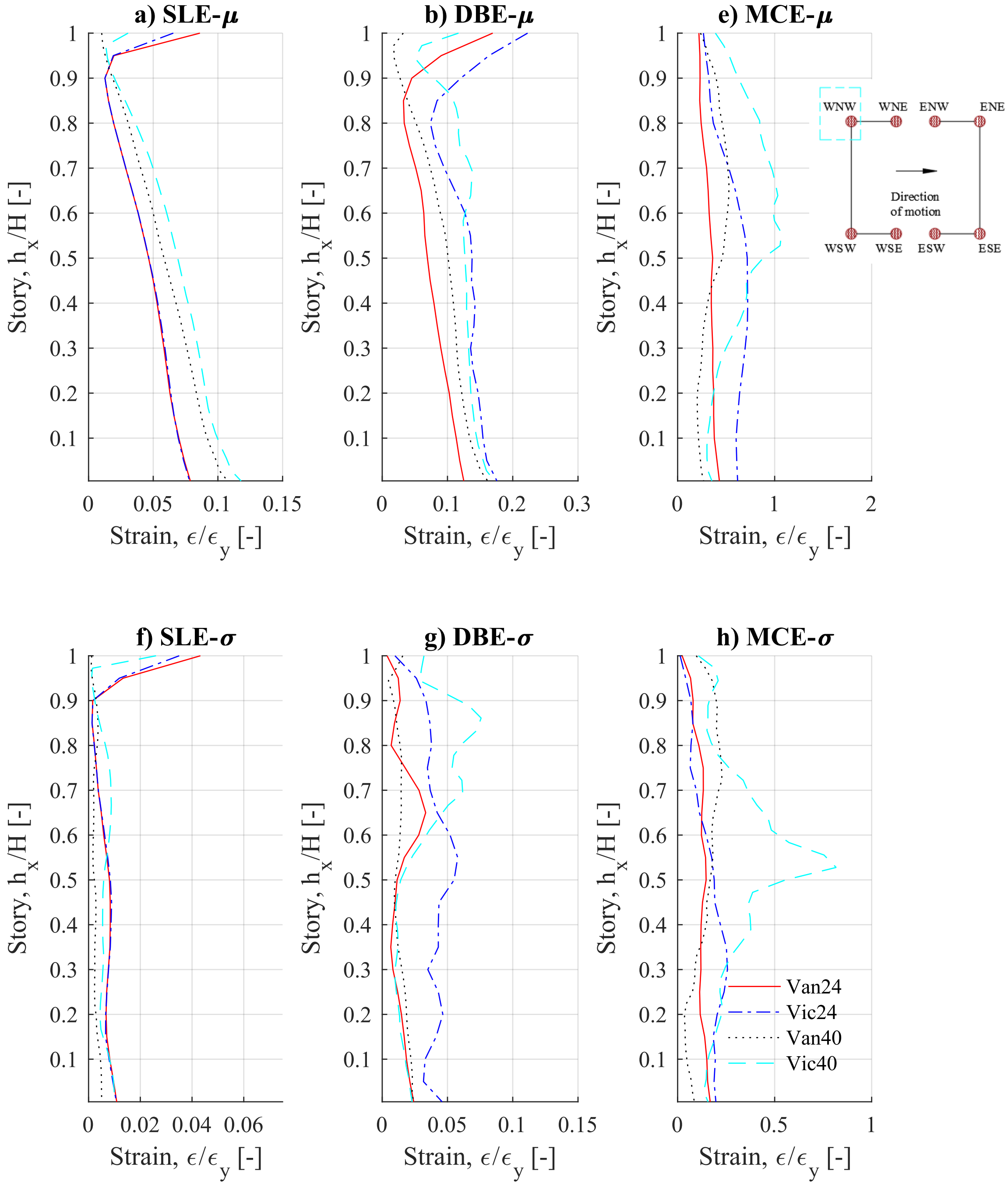

Figure 10.13 Max strain profile response for all prototype buildings under the high hazard for bidirectional loading WNW corner: (a) SLE- μ; (b) DBE- μ; (c) MCE- μ; (d) SLE- σ; (e) DBE- σ; and (f) MCE- σ

10.9 Summary

This chapter presented the bidirectional nonlinear dynamic responses of four prototype buildings: a 24-story located in Victoria and in Vancouver, and a 40-story located in Victoria and in Vancouver. Using EEDP described in Chapter 5, the CROCW were designed to meet different performance objectives at different shaking intensities.

The nonlinear analysis conducted in this chapter demonstrate the robustness of this design procedure in meeting these performance objectives. Specifically, at the SLE shaking intensity the system remains essentially elastic, at the DBE the outrigger dampers and the SCFD yield and dissipate energy, while the system remains, and at the MCE the outrigger, SCFD, and base dampers yield and dissipate energy, while the remaining wall has limited damage. The limited damage is demonstrated by the low shear stresses (less than 10%f'c) and the low wall strains are low for all prototype buildings.

Chapter 11: Comparison between CORW and SCCW with alternative RC core wall systems

11.1 Overview

The objective of this chapter is to demonstrate that the CORW and the SCCW can enhance seismic performance when compared with conventional RC wall systems. In this chapter the seismic response of the 40-story (tallest prototype) on the Victoria site (highest site hazard) is studied. The responses are discussed in detail and the end of this chapter provides some of the important conclusions from the comparisons.

11.2 Introduction

A main goal of this dissertation is to provide a novel RC core wall system which has higher seismic performance when compared to the conventional RC core wall system. To meet this goal, this thesis proposed two systems to achieve this goal: 1) the Controlled Outriggered Rocking Wall (CORW) as an alternative to the shear wall system and 2) the Self-Centering Coupled Wall (SCCW) system. Additionally, a design procedure for the proposed systems was recommended and validated using nonlinear time-history analysis. However, these studies have not yet demonstrated that the proposed systems could achieve higher performance than the conventional RC core walls. Further, the individual influence of the added technology (i.e., outrigger, controlled rocking mechanisms, and SCFDs) has yet to be examined. This chapter seeks to fill this knowledge gap through analysing and comparing different RC core wall system behavior for the shear wall and coupled wall systems.

11.3 Comparison of high-performance RC shear wall systems

This thesis has proposed the CORW system (Figure 11.1 (a)), which is an alternative system to the conventional fixed-base Shear Wall (SW), shown in Figure 11.1 (b). This chapter seeks to understand the CORW performance when compared with three alternative systems : (1) Shear Wall (SW) system (RC wall with a fixed base without an outrigger, shown in Figure 11.1 (b)); (2) Outriggered Wall (OW) system (RC wall with roof outrigger and a fixed base, shown in Figure

11.1 (c)); and (3) Controlled Rocking Wall (CRW) system (RC wall with controlled rocking base and without an outrigger, shown in Figure 11.1 (d)).

The SW system, shown in Figure 11.1 (b), consists of a fixed based shear wall which does not include an outrigger. The yielding mechanism of the SW is plastic hinging at the wall base (i.e., significant cracking of concrete and yielding of reinforcing steel). The OW, shown in Figure 11.1 (b), consists of a fixed based shear wall with a roof outrigger. Like the SW, the OW dissipates energy through plastic hinging near the wall base. However, the OW has additional energy dissipation and stiffness provided by the outrigger. The CRW, shown in Figure 11.1 (c), consists of a damped controlled rocking wall without an outrigger.

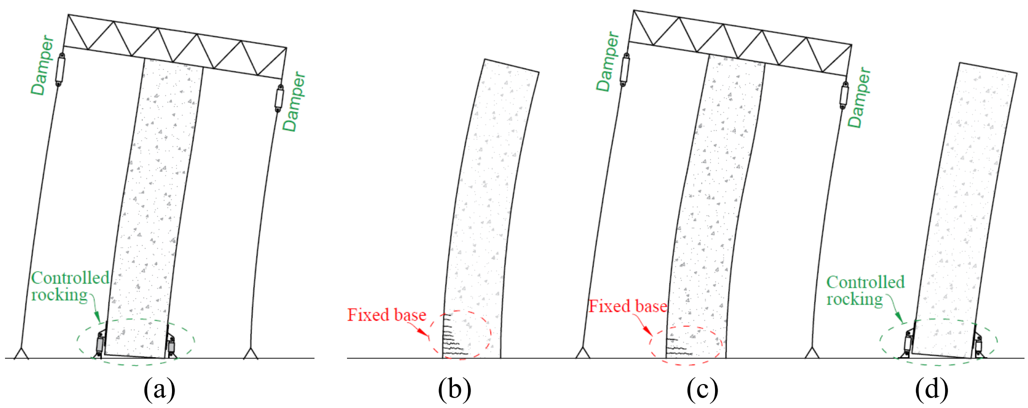

Figure 11.1 High-performance RC shear wall comparison: (a) Controlled Rocking Outriggered Wall (CORW); (b) Shear Wall (SW); (c) Outriggered Wall (OW); and (d) Controlled Rocking Wall (CRW)

To understand the differences in responses of the systems, it is important to first understand the different mechanics involved, particularly the differences between the controlled rocking and fixed base systems. The SW and the OW both form plastic hinging near the base of the wall. The plastic hinge occurs through the formation of cracks over a portion of the length of the wall. Within each open crack the rebar yields, resulting in the energy dissipation. On the other hand, the CRW and the CORW utilize controlled rocking systems at the base of the wall which essentially results in the formation of a single crack at the wall base. A large singular crack in a conventional wall would result in high localised strains and non-ductile behavior. Controlled rocking bases avoid such behaviour by not allowing rebar to cross the rocking interface, and in some cases, adding damping devices intended to withstand these high demands.

Despite the differences between the two systems' reaction mechanisms and curvatures, the global force deformation of a rocking wall system and a conventional wall system are similar when exposed to cyclic loads. For example, Figure 11.2 shows two experimental tests. Figure 11.2 (a) shows a wall test specimen design to represent a high-rise SW (Adebar et al., 2007), while Figure 11.2 (b) shows a rocking wall panel which uses post-tensioned (PT) to recenter the wall (Perez, 2013). In the SW, the energy dissipation (the enclosed hysteretic area) is primarily attributed to yielding of the wall reinforcing. Conversely, in/with the hysteretic energy dissipation/nonlinear mechanism in the rocking system, shown in Figure 11.2 (b), nonlinearity is primarily attributed to yielding of the PT tendons. For the rocking wall system, there is limited energy dissipation, and the wall behaves nonlinear elastically before the PT tendon yields.

As shown in Figure 11.2, both systems give a comparable force-deformation response. The highly pinched responses are due to the high contribution of axial load (P) to the overturning resistance in both the fixed base and rocking wall systems. As shown in Figure 11.2, hysteretic loops are essentially centered around the rocking moment ($M_{rocking} = PL_w/2$). The results exemplify the importance of axial load on the hysteretic performance of both systems.

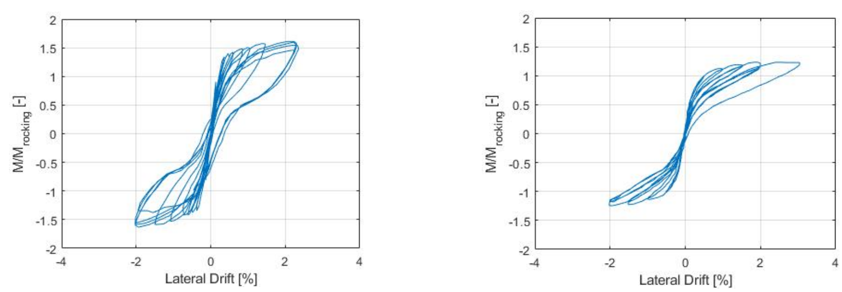

(a) (b)

Figure 11.2: Nonlinear behavior of conventional wall and rocking wall: (a) fix based wall (Adebar et al., 2007) and (b) Rocking wall (Perez, 2013)

In this chapter, a prototype building is analysed with the different SFRS systems and the systems are compared. The 40-story prototype building located in Victoria, designed in Chapter 5 and analysed in Chapter 8 and 10, is used for this comparison study. This prototype was selected due to it being the tallest building and the highest hazard.

There are numerous variations in design methods and equivalencies that could potentially occur in design practice. For simplicity, in this study, it is assumed that the reinforcing design, wall geometry, and damper forces from the 40-story building design (from Chapter 5) are the same for all configurations.

The following sections describe the numerical modelling, seismic performance, and discussion on responses of the different systems.

11.3.1 Numerical modelling

The numerical modeling approach followed the same procedure as Chapter 6. The modelling of these systems results in the fundamental periods shown in Table 11.1. As shown, the fundamental periods of the SW and CRW are greater than the CORW by about 15.4% and 17.4% respectively. The CORW is stiffer than these systems due to the inclusion of an outrigger. The fixed based boundary condition of the SW gives this system a slightly higher stiffness than the CRW. For the same reason, the OW has a slightly lower period (about 0.74% less) than the CORW.

Table 11.1 Fundamental period for comparison study

	CORW	SW	OW	CRW
T1 [s]	4.08	4.71	4.05	4.79

The same ground motions used in previous studies are used for analysing these systems. For efficiency, and clarity in the comparison, only 2-dimensional analysis is presented.

11.3.2 Nonlinear time-history analysis on different high-performance shear walls

11.3.2.1 Story displacements and ISDR

Roof drift ratio (RDR) and interstorey drift ratios (ISDRs) were determined for each ground motion, at each story level, at each of the eight nodes on the core wall, shown in Figure 8.1. However, all responses are essentially the same for each node under this unidirectional loading, so only the WNW node is shown herein for brevity.

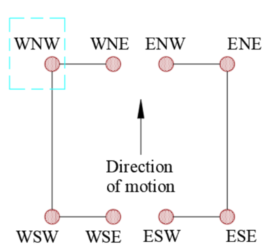

Figure 11.3 RDR and interstorey drift post processing schematic for the SW direction

11.3.2.1.1 Story displacements

Figure 11.4 (a), (b), and (c) shows the mean (μ) horizontal displacement normalised to the building height for each system (CORW, SW, OW and CRW) for the SLE, DBE, and the MCE, respectively. Figure 11.4 (d), (e), and (f) shows the standard deviation (σ) horizontal displacement normalised to the building height for each system (CORW, SW, OW and CRW) for the SLE, DBE, and the MCE, respectively.

As shown in Figure 11.4, the μ roof drift ratio (RDR) at the SLE shaking intensity is 0.047%, 0.048%, 0.047%, and 0.049% for the CORW, SW, OW and CRW, respectively. The RDR-μ at the DBE shaking intensity is 0.13%, 0.16%, 0.13%, and 0.16% for the CORW, SW, OW and CRW, respectively. The RDR-μ at the MCE shaking intensity is 0.76%, 0.93%, 0.76%, and 0.89% for the CORW, SW, OW and CRW, respectively.

The standard deviation (σ) of the RDR at the SLE shaking intensity is 0.011%, 0.02%, 0.016%, and 0.019% for the CORW, SW, OW and CRW, respectively. The σ of the RDR at the DBE shaking intensity is 0.04%, 0.06%, 0.04%, and 0.06% for the CORW, SW, OW and CRW, respectively. The RDR- σ at the MCE shaking intensity is 0.30%, 0.33%, 0.30%, and 0.33% for the CORW, SW, OW and CRW, respectively.

The SLE shaking intensity difference between the RDR-μ of the CORW to the SW, OW and CRW were 1.9%, -0.02%, and 4.3%, respectively. The DBE shaking intensity RDR-μ SW, OW and CRW has a difference of 26.8%, 0.3%, and 27.9%, respectively, compared with the CORW. The MCE shaking intensity mean RDR-μ of the SW, OW and CRW were 22.5%, 1%, and 17.4% difference compared to the CORW systems.

The SLE shaking intensity RDR- σ had a difference of 69.4%, 51.1%, and 77.9% for the of the SW, OW and CRW, respectively, compared with the CORW system. The DBE shaking intensity RDR- σ of the SW, OW and CRW had a difference of 43.9%, -0.1%, and 35.4% compared to the CORW systems. The MCE shaking intensity RDR- σ of the SW, OW and CRW had a difference of 10.3%, -0.7%, and 8.7% compared to the CORW system.

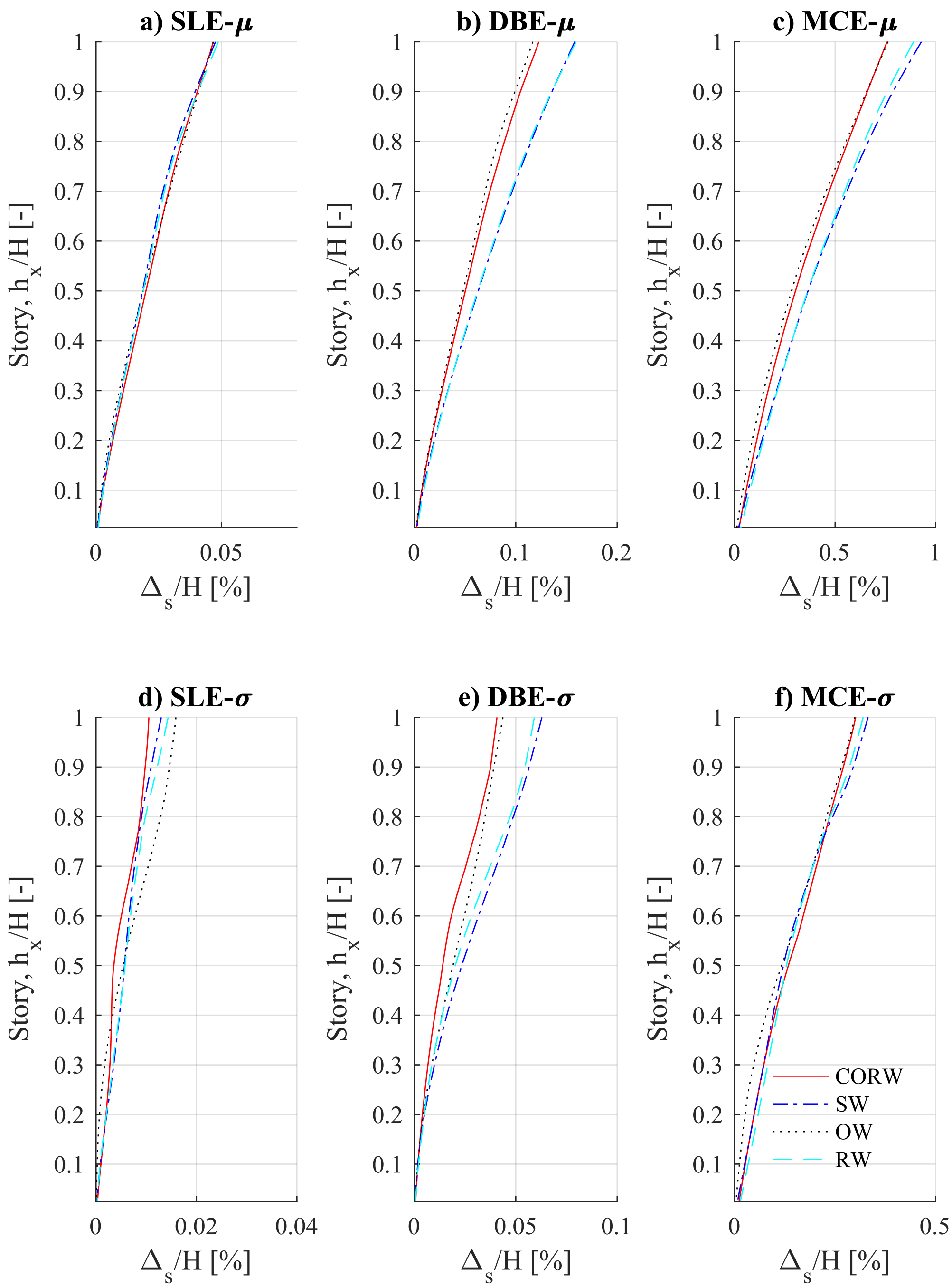

Figure 11.4 Global displacements for each RC wall system: (a) SLE- μ; (b) DBE- μ; (c) MCE- μ; (d) SLE- σ; (e) DBE- σ; and (f) MCE- σ

The higher displacements in the SW can be attributed to the higher level of cracking over the building height. The peak displacements near the roof in the OW are only slightly higher than the CORW system. This higher displacement may be attributed to the slight increase amount of cracking and wall yielding when compared to the CORW system. The CRW showed higher displacements than the CORW, which is in part due to the higher period of the CRW and the slight increase in cracking.

11.3.2.1.2 Interstorey drift ratio

Figure 11.5 (a), (b), and (c) shows the mean (μ) interstorey drift ratio (ISDR) for each system (CORW, SW, OW and CRW) for the SLE, DBE, and the MCE, respectively. Figure 11.5 (d), (e), and (f) shows the standard deviation (σ) interstorey drift ratio (ISDR) for each system (CORW, SW, OW and CRW) for the SLE, DBE, and the MCE, respectively.

As shown in Figure 11.5, the μ ISDR at the SLE shaking intensity is 0.076%, 0.090%, 0.076%, and 0.090% for the CORW, SW, OW and CRW, respectively. The peak ISDR- μ at the DBE shaking intensity is 0.23%, 0.29%, 0.22%, and 0.29% for the CORW, SW, OW and CRW, respectively. The peak ISDR-μ at the MCE shaking intensity is 1.10%, 1.67%, 1.18%, and 1.54% for the CORW, SW, OW and CRW, respectively.

The standard deviation (σ) of the ISDR at the SLE shaking intensity 0.019%, 0.03%, 0.020%, and 0.026% for the CORW, SW, OW and CRW, respectively. The σ of the ISDR at the DBE shaking intensity is 0.06%, 0.07%, 0.06%, and 0.08% for the CORW, SW, OW and CRW, respectively. The σ of the ISDR at the MCE shaking intensity is 0.33%, 0.45%, 0.37%, and 0.42% for the CORW, SW, OW and CRW, respectively.

The SLE shaking intensity ISDR-μ of the SW, OW and CRW were 18.0%, 0.001%, and 18.1% greater than the CORW systems. The DBE shaking intensity ISDR-μ of the SW, OW and CRW were 27.5%, -0.9%, and 26.0% greater than the CORW systems. The MCE shaking intensity ISDR-μ of the SW, OW and CRW were 52.1%, 8%, and 41.0% greater than the CORW systems.

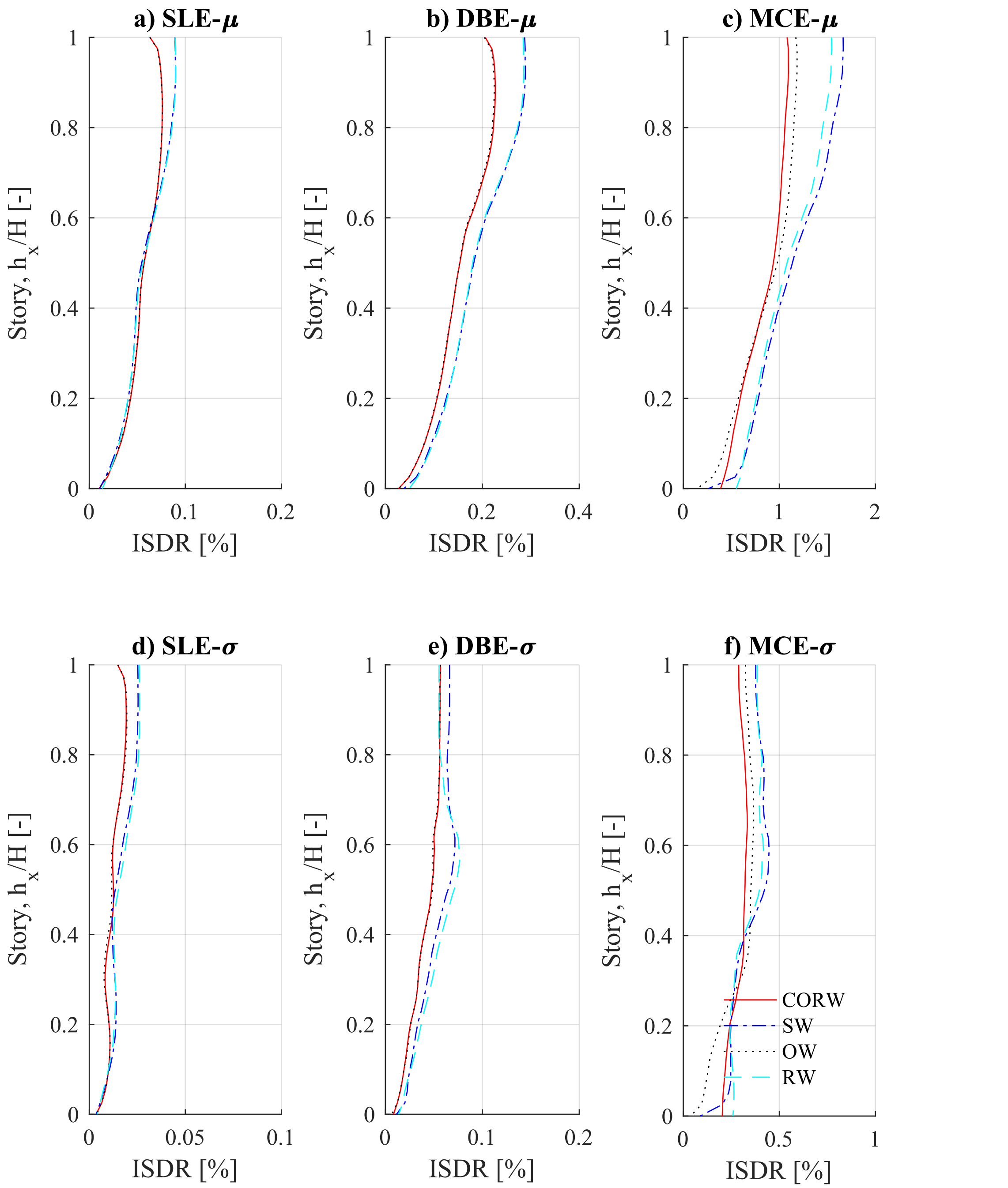

Figure 11.5 ISDR for each of the shear wall systems: (a) SLE- μ; (b) DBE- μ; (c) MCE- μ; (d) SLE- σ; (e) DBE- σ; and (f) MCE- σ

The SLE shaking intensity ISDR-σ of the SW, OW and CRW had a difference of 32.2%, 1.8%, and 36.6% difference than the CORW system, respectively. The DBE shaking intensity ISDR-σ of SW, OW and CRW had a difference of 23.1%, 2.1%, and 27.1% of the CORW system, respectively. The MCE shaking intensity ISDR-σ of SW, OW and CRW had a difference of 34.0%, 9.9%, and 25.2%, and 25.2% compared to the CORW system, respectively.

11.3.2.2 Wall shear stress

Figure 11.6 (a), (b), and (c) shows the mean (μ) shear stress for each system (CORW, SW, OW and CRW) for the SLE, DBE, and the MCE, respectively. Figure 11.5 (d), (e), and (f) shows the standard deviation (σ) shear stress, each system (CORW, SW, OW and CRW) for the SLE, DBE, and the MCE, respectively. The shear stress was determined by dividing this force by the wall length and the web thicknesses. The shear force was determine using a section cut which includes only each wall web.

As shown in Figure 11.6, the peak μ shear stress at the SLE shaking intensity is 0.85 MPa, 0.83 MPa, 0.88 MPa, and 0.82 MPa for the CORW, SW, OW and CRW, respectively. The peak μ shear stress at the DBE shaking intensity is 2.26 MPa, 2.58 MPa, 2.29 MPa, and 2.57 MPa for the CORW, SW, OW and CRW, respectively. The peak shear stress μ at the MCE shaking intensity is 3.93 MPa, 4.48 MPa, 4.25 MPa, and 4.36 MPa for the CORW, SW, OW and CRW, respectively.

The standard deviation (σ) of the shear stress at the SLE shaking intensity is 0.31 MPa, 0.29 MPa, 0.33 MPa, and 0.27 MPa for the CORW, SW, OW and CRW, respectively. The σ shear stress at the DBE shaking intensity is 0.60 MPa, 0.60 MPa, 0.63 MPa, and 0.53 MPa for the CORW, SW, OW and CRW, respectively. The σ of the shear stress at the MCE shaking intensity and 0.91 MPa, 1.02 MPa, 1.04 MPa, and 0.96 MPa for the CORW, SW, OW and CRW, respectively.

The SLE shaking intensity μ shear stress of the SW, OW and CRW had a difference of -2.3%, 3.83%, and -3.9% compared to the CORW systems. The DBE shaking intensity μ shear stress of the SW, OW and CRW had a difference of 14.1%, 1.3%, and 14.0% compared to the CORW systems. The MCE shaking intensity μ shear stress of the SW, OW and CRW were 14.0%, 8%, and 11.0% greater than the CORW systems.

The SLE shaking intensity shear stress-σ of the SW, OW and CRW had a difference of -6.1%, 6.6%, and -15.0% difference than the CORW system, respectively. The DBE shaking intensity shear stress -σ of SW, OW and CRW had a difference of -0.1%, 3.7%, and -12.4% of the CORW system, respectively. The MCE shaking intensity shear stress-σ of SW, OW and CRW had a difference of 12.1%, 14.5%, and 6.1% compared to the CORW system, respectively.

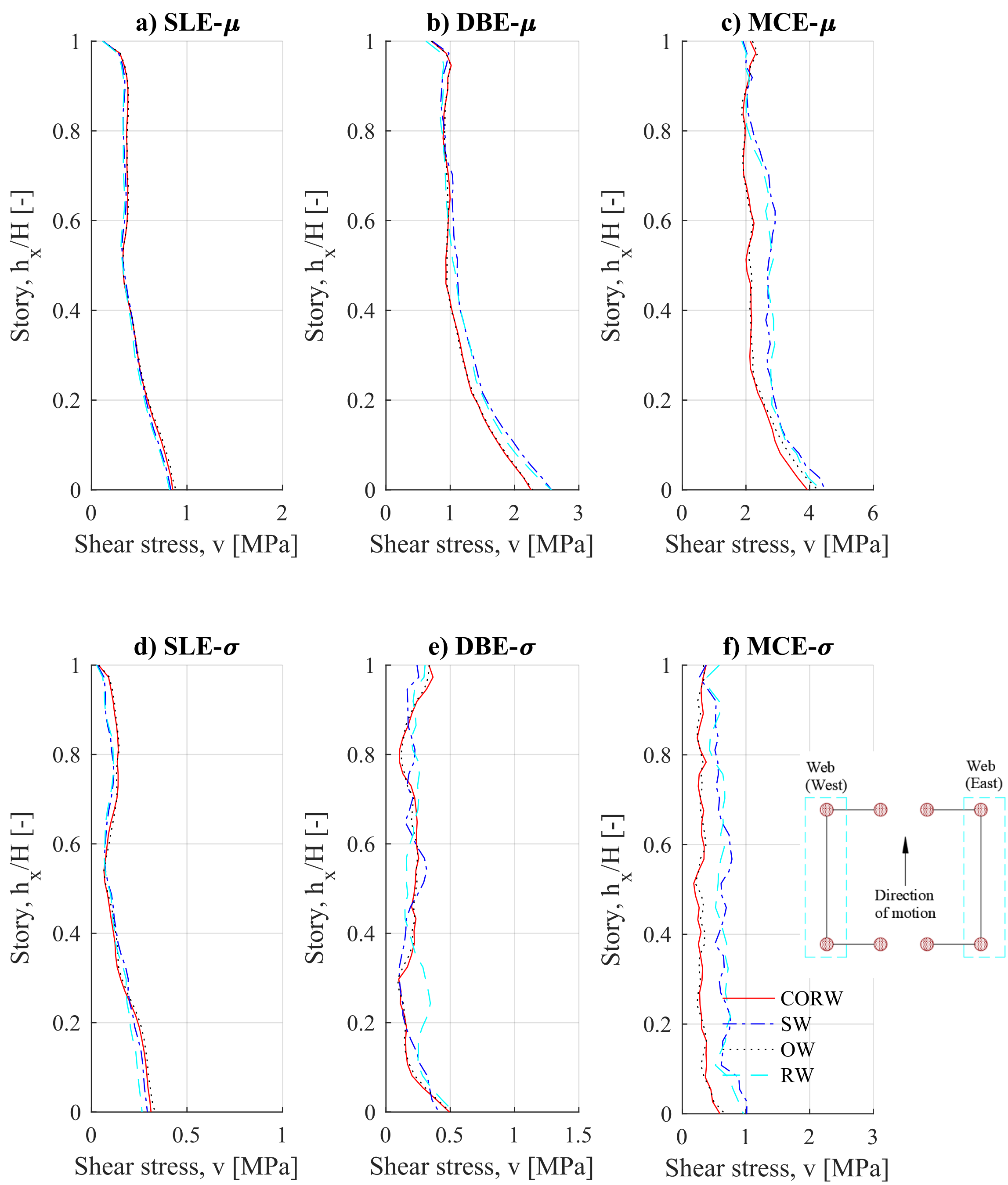

Figure 11.6 Comparison of high-performance RC wall shear force: (a) SLE- μ; (b) DBE- μ; (c) MCE- μ; (d) SLE- σ; (e) DBE- σ; and (f) MCE- σ

11.3.2.3 Vertical wall strains

Figure 11.7 (a), (b), and (c) shows the mean (μ) vertical strain for each system (CORW, SW, OW and CRW) for the SLE, DBE, and the MCE, respectively. Figure 11.7 (d), (e), and (f) shows the standard deviation (σ) vertical strain of each system (CORW, SW, OW and CRW) for the SLE, DBE, and the MCE, respectively. At each node, strains are determined by taking the difference between the vertical displacements at each wall corner divided by the distance between the nodes. The strains are normalised to the yield strain of rebar ($\varepsilon_y = 0.002$). Strains were evaluated at each node, and the peak normalised responses are presented in Figure 11.7.

As shown in Figure 11.7, the μ strain ratio ($\varepsilon/\varepsilon_y$- μ) at the SLE shaking intensity is 0.13, 0.01, 0.14, and 0.13 for the CORW, SW, OW and CRW, respectively. The peak $\varepsilon/\varepsilon_y$- μ at the DBE shaking intensity is 0.19, 0.28, 0.21, and 0.21 for the CORW, SW, OW and CRW, respectively. The peak $\varepsilon/\varepsilon_y$- μ at the MCE shaking intensity is 0.91, 5.41, 2.59, and 1.73 for the CORW, SW, OW and CRW, respectively.

The standard deviation (σ) of the $\varepsilon/\varepsilon_y$ at the SLE shaking intensity is 0.02, 0.02, 0.02, and 0.02 for the CORW, SW, OW and CRW, respectively. The σ of the $\varepsilon/\varepsilon_y$ at the DBE shaking intensity is 0.11, 0.18, 0.11, and 0.17 for the CORW, SW, OW and CRW, respectively. The σ of the $\varepsilon/\varepsilon_y$ at the MCE shaking intensity is 0.64, 2.60, 1.15, and 0.85 for the CORW, SW, OW and CRW, respectively.

The SLE shaking intensity $\varepsilon/\varepsilon_y$ - μ of the SW, OW and CRW had a difference of 1.9%, 4.20%, and -0.1% compared to the CORW system. The DBE shaking intensity $\varepsilon/\varepsilon_y$- μ of the SW, OW and CRW had a difference of 46.7%, 8.9%, and 10.4% compared to the CORW system. The MCE shaking intensity $\varepsilon/\varepsilon_y$- μ SW, OW and CRW had a difference of 497%, 186%, and 90.3% compared to the CORW system.

The SLE shaking intensity $\varepsilon/\varepsilon_y$-σ of the SW, OW and CRW had a difference of -13.2%, -1.3%, and -16.7% difference ~~than~~ of the CORW system, respectively. The DBE shaking intensity $\varepsilon/\varepsilon_y$-σ of SW, OW and CRW had a difference of 58.9%, -2.6%, and 50.6% of the CORW system, respectively. The MCE shaking intensity $\varepsilon/\varepsilon_y$-σ of SW, OW and CRW had a difference of 305%, 78.3%, and 32.5% compared to the CORW system, respectively.

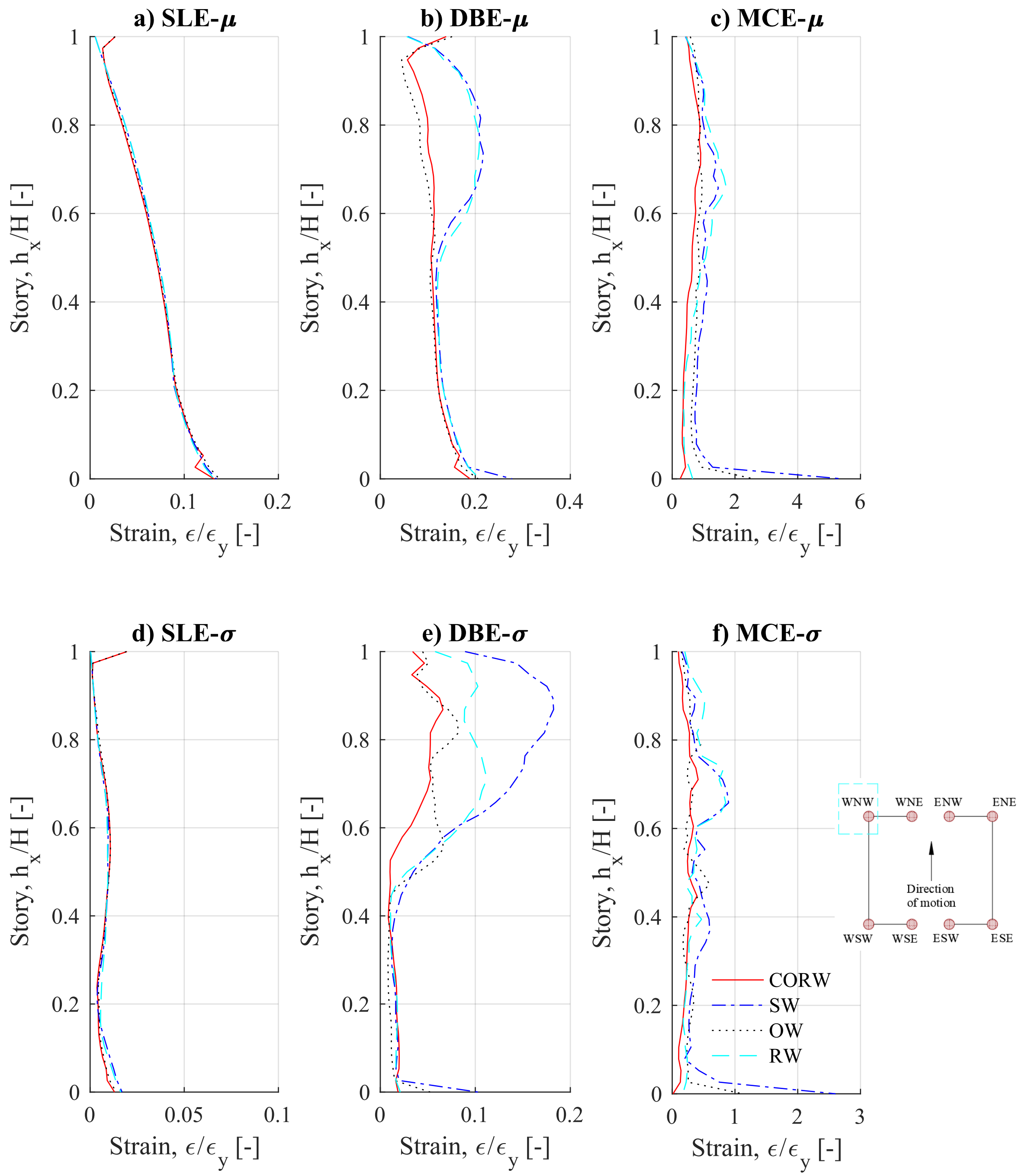

Figure 11.7 Max strain profile response for all prototype buildings under the high hazard for unidirectional loading in the CORW direction: (a) SLE- μ; (b) DBE- μ; (c) MCE- μ; (d) SLE- σ; (e) DBE- σ; and (f) MCE- σ

Figure 11.7 shows the $\varepsilon/\varepsilon_y$- μ for each system. The analysis showed the plastic hinging occurring at the base of the wall for both the SW and OW. Hence, the $\varepsilon/\varepsilon_y$- μ are higher near the base of the wall compared to the other systems. The SW has the highest strains compared to all the other systems, while the CORW has the lowest.

Lower strains are observed in the outriggered fixed base wall (OW) when compared with the conventional fixed based wall (SW). Its important to note, that although the SW and OW have the same moment capacity (i.e., same reinforcing ratio), the SW had significantly more strain. This difference is due to the outrigger adding additional damping to the system, as well as controlling the deformations of the system due to reduced cracking, and increased stiffness due to the outrigger system.

11.4 Comparison of high-performance RC coupled wall systems

In this section, the SCCW system (Figure 11.8 (a)) is compared against an additional three alternative RC coupled wall systems. Two types of coupling beams are used in this study: 1) Diagonally Reinforced Coupling Beams (DRCB) and 2) the Self-centering Conical Friction Damper (SCFD).

The three systems studied are as follows: (1) Coupled Wall (CW) system (RC coupled wall with DRCB, and a fixed base shown in Figure 11.8 (b)); (2) Damped Coupled Wall (DCW) system (RC coupled wall with new SCFD coupling beams and a fixed base shown in Figure 11.8 (c)); and (3) Controlled Rocking Coupled Wall (CRCW) system (RC coupled wall with DRCB, and a controlled rocking base shown in Figure 11.8 (d))

In this chapter, the seismic performance of the different SFRS systems for one prototype building is assessed and compared. The 40-story prototype building located in Victoria, designed in Chapter 5 and analysed in Chapter 9 and 10, is used for this comparison study. This prototype was selected due to it being the tallest building and the highest hazard.

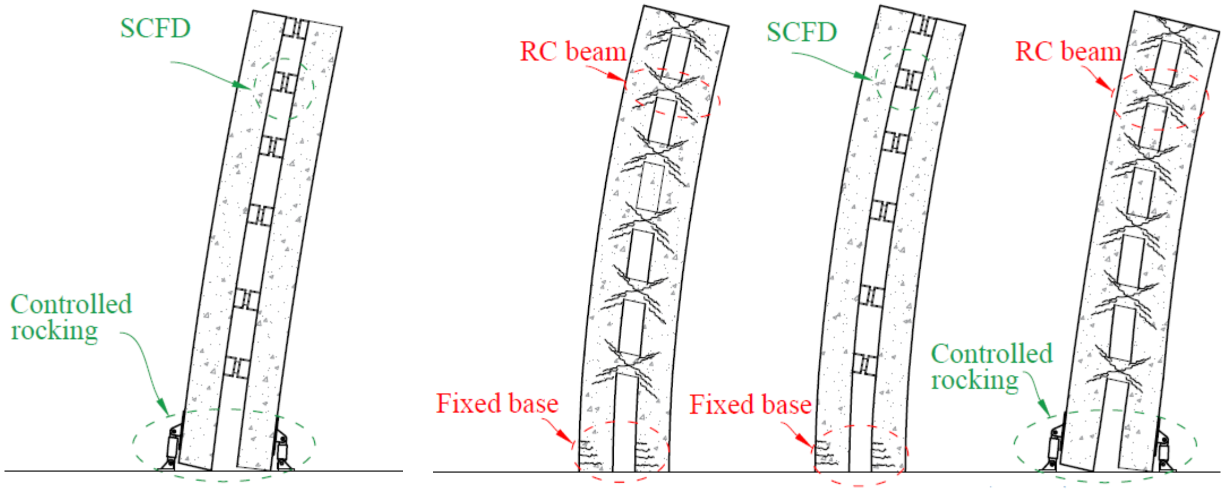

Figure 11.8 High-performance RC coupled wall comparison: (a) Self-Centering Coupled Wall (SCCW); (b) Coupled Wall (CW); (c) Damped Coupled Wall (DCW); and (d) Controlled Rocking Coupled Wall (CRCW)

There are numerous variations in design methods and equivalencies that could potentially occur in design practice. For simplicity, in this study, it is assumed that the reinforcing design, wall geometry, and damper forces from the Vic40 design are considered the same for all configurations. The yield coupling beam forces are assumed to be the same amongst the systems. However, the post-yielding stiffness of the SCFD and DRCB are expected to follow the unique characteristics of each coupling beam.

The following sections describe the numerical modelling, seismic performance, and discussion on responses of the different systems.

11.4.1 Numerical modelling

The numerical modeling approach followed the same procedure as Chapter 6. The DRCB model follow the same modelling approach as Ghodsi et al., 2010. The same ground motions used in previous analysis are used for analysing these systems. For efficiency, and clarity in the comparison, only unidirectional analysis is presented.

The modelling of these systems resulted in the fundamental periods shown in Table 11.1. As shown, the fundamental periods of the CW and CRCW are greater than the SCCW by about 14.7% and 16.4% respectively. The SCCW is stiffer than these systems due to the higher stiffness of the coupling beams. The fixed based boundary condition of the CW gives this system a slightly higher stiffness than the CRCW. For the same reason, the DCW has a slightly lower period (about 1.6% less) than the SCCW.

Table 11.2 Fundamental period for comparison study

	SCCW	CW	DCW	CRCW
T1 [s]	5.17	5.93	5.09	6.02

11.4.2 Nonlinear time-history analysis on different high-performance shear walls

11.4.2.1 Global displacements and ISDRs

Lateral displacements and interstorey drift ratios (ISDRs) were analysed at each wall node shown in Figure 9.1. Displacements and ISDRs were determined through analysing the peak response for each ground motion, at each story level, at each of the eight nodes on the core wall. However, all responses are essentially the same for each node under this unidirectional loading, so only the WNW node is shown herein for brevity.

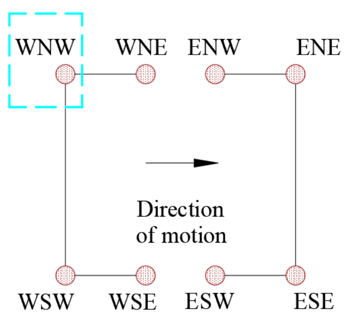

Figure 11.9 Displacement and interstorey drift post processing schematic for SCCW

11.4.2.1.1 Global displacements

Figure 11.10 (a), (b), and (c) shows the mean (μ) horizontal displacement normalised to the building height for each system (SCCW, CW, DCW and CRCW) for the SLE, DBE, and the MCE, respectively. Figure 11.10 (d), (e), and (f) shows the standard deviation (σ) horizontal displacement normalised to the building height for each system (CORW, SW, OW and CRW) for the SLE, DBE, and the MCE, respectively.

As shown in Figure 11.10, the mean (μ) roof drift ratio (RDR) at the SLE shaking intensity is 0.045%, 0.051%, 0.048%, and 0.051% for the SCCW, CW, DCW and CRCW, respectively. The

RDR-μ at the DBE shaking intensity is 0.16%, 0.17%, 0.15%, and 0.17% for the CORW, SW, OW and CRW, respectively. The RDR-μ at the MCE shaking intensity is 0.69%, 0.84%, 0.70%, and 0.86% for the SCCW, CW, DCW and CRCW, respectively.

The standard deviation (σ) of the RDR at the SLE shaking intensity is 0.009%, 0.02%, 0.014%, and 0.020% for the SCCW, CW, DCW and CRCW, respectively. The RDR-σ at the DBE shaking intensity is 0.03%, 0.07%, 0.04%, and 0.07% for the SCCW, CW, DCW and CRCW, respectively. The RDR-σ at the MCE shaking intensity is 0.29%, 0.22%, 0.31%, and 0.23% for the SCCW, CW, DCW and CRCW, respectively.

The SLE shaking intensity RDR-μ difference between the SCCW and the CW, DCW and CRCW were 15.3%, 8.34%, and 14.2%, respectively. The DBE shaking intensity RDR-μ between the SCCW of the CW, DCW and CRCW were 12.0%, -1.6%, and 12.5%, respectively. The MCE shaking intensity mean RDR of the CW, DCW and CRCW were 21.5%, 2%, and 23.7% greater than the CORW systems.

The SLE shaking intensity RDR -σ of the CW, DCW and CRCW had a difference of 110.7%, 53.0%, and 113.4% difference than the SCCW system, respectively. The DBE shaking intensity RDR -σ of CW, DCW and CRCW had a difference of 90.7%, 7.3%, and 111.5% of the SCCW system, respectively. The MCE shaking intensity RDR -σ of CW, DCW and CRCW had a difference of -22.3%, 8.3%, and -20.0% compared to the SCCW system, respectively.

High displacements result in large ductility demands on all structural components. Often the displacements govern the design of secondary gravity elements. Therefore, limiting displacements is key in creating high-performance tall buildings. The SCCW demonstrated a lower peak roof displacement compared with all other coupled wall systems in this study. Hence, the SCCW has a superior displacement performance under these design conditions.

High displacements in the CW and CRCW compared with the SCCW and the DCW can be attributed to two main factors. First, the diagonally reinforced coupling beams have lower initial stiffness when compared with the SCFD, resulting in a longer period. Secondly, the high strains in the CW soften the structure in nonlinear analysis, resulting in higher displacements.

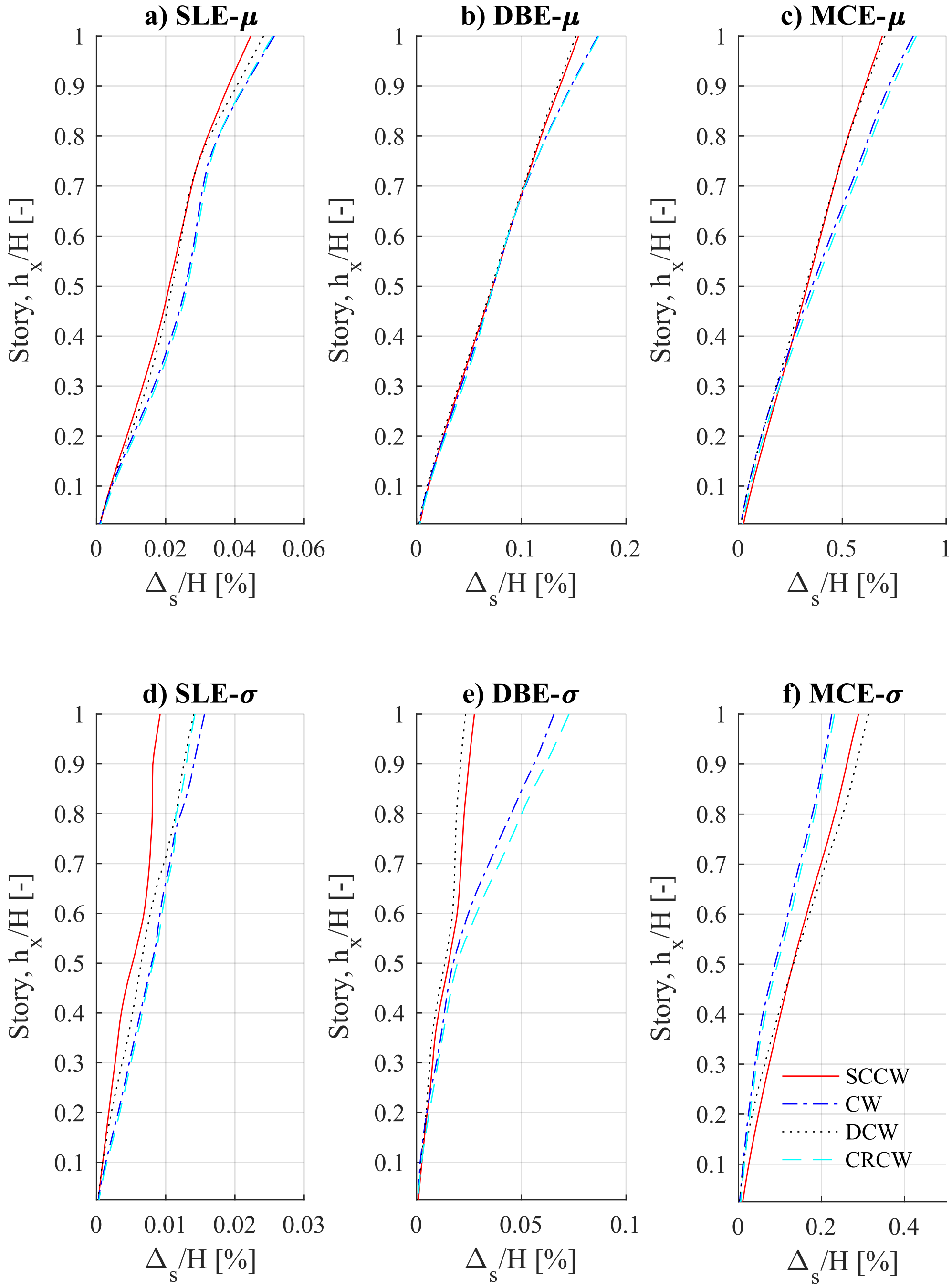

Figure 11.10 Global displacements for each RC wall system: (a) SLE- μ; (b) DBE- μ; (c) MCE- μ; (d) SLE- σ; (e) DBE- σ; and (f) MCE- σ

11.4.2.1.2 Interstorey drift ratio

Figure 11.11 (a), (b), and (c) shows the mean (μ) interstorey drift ratio (ISDR) for each system (SCCW, CW, DCW and CRCW) for the SLE, DBE, and the MCE, respectively. Figure 11.11 (d), (e), and (f) shows the standard deviation (σ) interstorey drift ratio (ISDR) for each system (SCCW, CW, DCW and CRCW) for the SLE, DBE, and the MCE, respectively.

As shown in Figure 11.11, the μ ISDR at the SLE shaking intensity is 0.084%, 0.105%, 0.094%, and 0.101% for the SCCW, CW, DCW and CRCW, respectively. The peak ISDR-μ at the DBE shaking intensity is 0.266%, 0.31%, 0.27%, and 0.30% for the SCCW, CW, DCW and CRCW respectively. The peak ISDR-μ at the MCE shaking intensity is 1.01%, 1.46%, 1.05%, and 1.45% for the SCCW, CW, DCW and CRCW, respectively.

The standard deviation (σ) of the ISDR at the SLE shaking intensity is 0.015%, 0.03%, 0.023%, and 0.033% for the SCCW, CW, DCW and CRCW, respectively. The ISDR-σ at the DBE shaking intensity is 0.06%, 0.11%, 0.05%, and 0.11% for the SCCW, CW, DCW and CRCW, respectively. The ISDR-σ at the MCE shaking intensity is 0.44%, 0.52%, 0.44%, and 0.52% for the SCCW, CW, DCW and CRCW, respectively.

The SLE shaking intensity ISDR-μ difference between the SCCW and the CW, DCW and CRCW were 24.7%, 11.62%, and 20.8%, respectively. The DBE shaking intensity ISDR-μ difference of the CW, DCW and CRCW were 15.7%, -0.3%, and 14.2% compared to the SCCW systems. The MCE shaking intensity ISDR-μ difference between the SCCW and the CW, DCW and CRCW were 44.5%, 5%, and 43.7%, respectively.

The SLE shaking intensity ISDR-σ SW, OW and CRW had a difference of 104%, 48.4%, and 117% compared to the CORW system, respectively. The DBE shaking intensity ISDR-σ of SW, OW and CRW had a difference of 93.2%, -4.1%, and 92.6% of the CORW system, respectively. The MCE shaking intensity ISDR-σ of SW, OW and CRW had a difference of 18.9%, 0.9%, and 19.2% compared to the CORW system, respectively.

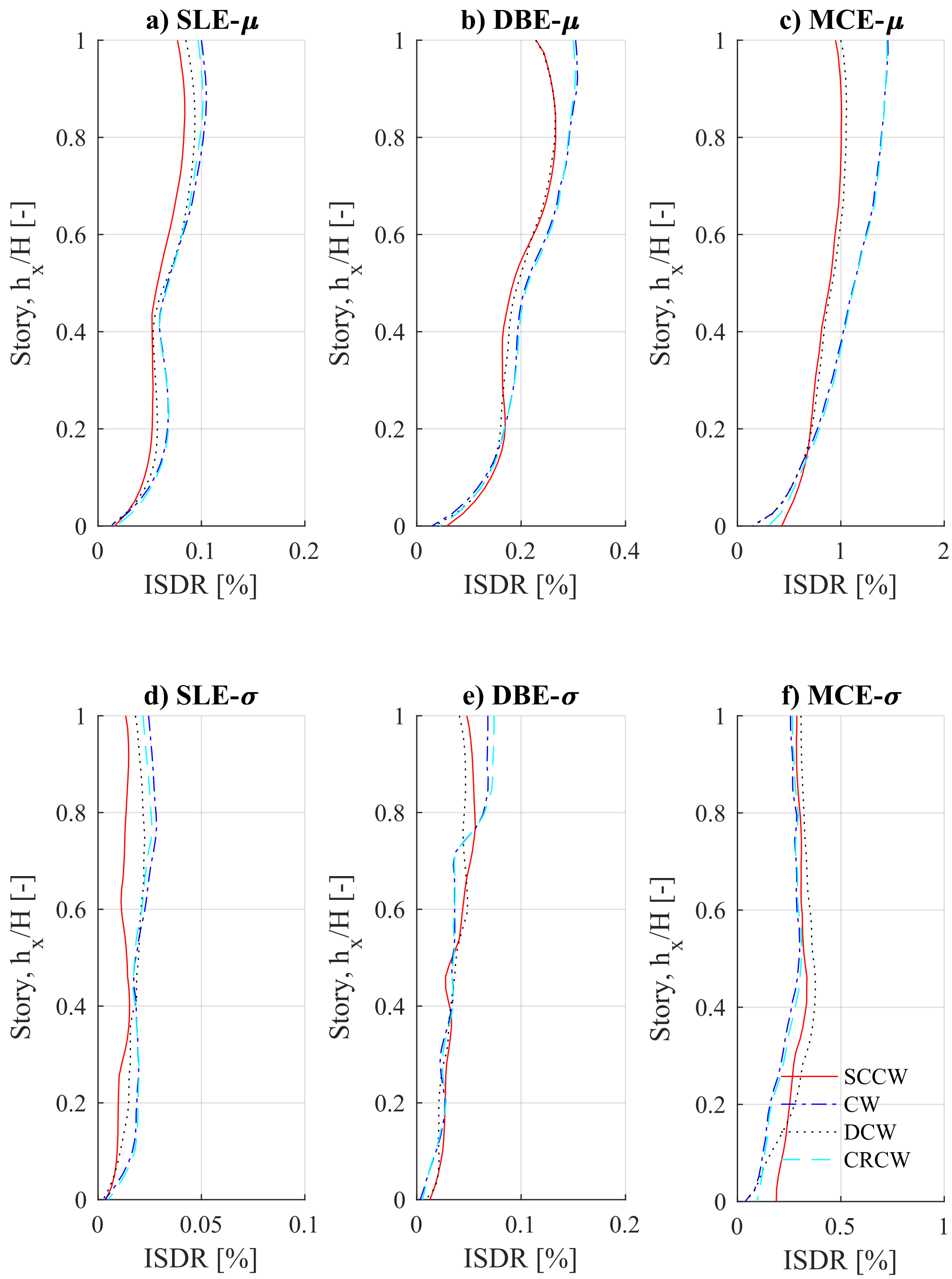

Figure 11.11 ISDR for each of the shear wall systems: (a) SLE- μ; (b) DBE- μ; (c) MCE- μ; (d) SLE- σ; (e) DBE- σ; and (f) MCE- σ

Like displacements, controlling ISDR is key in high performance structures. ISDR can control the design of secondary elements, such as the gravity system. Therefore, limiting ISDR is key in creating high-performance tall buildings. The SCCW demonstrated a lower peak ISDR when compared with all other coupled wall systems in this study.

The higher strains, natural period, and low post-yielding stiffness of the DRCB of the CW results in higher ISDR than any other system over most of the building height. Near the base of the wall, however, the SCCW and CRCW have high ISDR. This result is due to the controlled rocking wall opening at one concentrated location resulting in essentially rigid body rotation. It is important that this rotation be considered in the design of secondary elements. When compared to the DCW, the SCCW has similar ISDR over most of the building height, with the exception of the plastic hinge region. The slightly high peak ISDR in the DCW is attributed to the higher strains in the DCW system.

11.4.2.2 Shear stress

Figure 11.12 (a), (b), and (c) shows the mean (μ) shear stress for each system (SCCW, CW, DCW and CRCW) for the SLE, DBE, and the MCE, respectively. Figure 11.12 (d), (e), and (f) shows the standard deviation (σ) shear stress, each system (SCCW, CW, DCW and CRCW) for the SLE, DBE, and the MCE, respectively. The shear forces are determined using a section cut which includes only each wall flanges. The stress is determined by dividing this force by the wall length and the flange thicknesses. Figure 11.12 shows the maximum stress of the four flanges (i.e., North-West, North-East, South-West, South-East).

As shown in Figure 11.12, peak μ shear stress at the SLE shaking intensity is 0.43 MPa, 0.36 MPa, 0.41 MPa, and 0.36 MPa for the SCCW, CW, DCW and CRCW, respectively. The peak μ shear stress at the DBE shaking intensity is 1.07 MPa, 0.95 MPa, 1.10 MPa, and 0.88 MPa for the SCCW, CW, DCW and CRCW, respectively. The peak μ shear stress at the MCE shaking intensity is 2.18 MPa, 2.00 MPa, 2.44 MPa, and 1.70 MPa for the SCCW, CW, DCW and CRCW, respectively.

The standard deviation (σ) of the shear stress at the SLE shaking intensity is 0.11 MPa, 0.11 MPa, 0.10 MPa, and 0.12 MPa for the SCCW, CW, DCW and CRCW, respectively. The σ shear stress at the DBE shaking intensity is 0.23 MPa, 0.33 MPa, 0.24 MPa, and 0.27 MPa for the SCCW, CW, DCW and CRCW, respectively. The σ shear stress at the MCE shaking intensity is 0.45 MPa, 0.44 MPa, 0.52 MPa, and 0.32 MPa for the SCCW, CW, DCW and CRCW, respectively.

The SLE shaking intensity μ shear stress of the CW, DCW and CRCW were -15.6%, -5.61%, and -17.1% greater than the SCCW systems. The DBE shaking intensity μ shear stress of the CW, DCW and CRCW were -11.1%, 3.5%, and -17.2% greater than the CORW systems. The MCE shaking intensity μ shear stress of the CW, DCW and CRCW were -8.6%, 12%, and -21.9% greater than the SCCW systems.

The SLE shaking intensity shear stress-σ of the SW, OW and CRW had a difference of 3.1%, -10.8%, and 4.8% difference than the CORW system, respectively. The DBE shaking intensity shear stress -σ of SW, OW and CRW had a difference of 46.5%, 4.8%, and 19.3% of the CORW system, respectively. The MCE shaking intensity shear stress-σ of SW, OW and CRW had a difference of -4.0%, 14.6%, and -30.5% compared to the CORW system, respectively.

Figure 11.12 shows the mean responses for all the systems. As shown, the shear force in the SCCW is greater than the CW and CRCW and less than the DRCW at all building heights. However, at the base, the shear force is similar in magnitude amongst these systems, despite the CW and CRCW having lower period, and lower core moment capacity. This response can be attributed to the higher core moments observed in the SCCW and DCW systems.

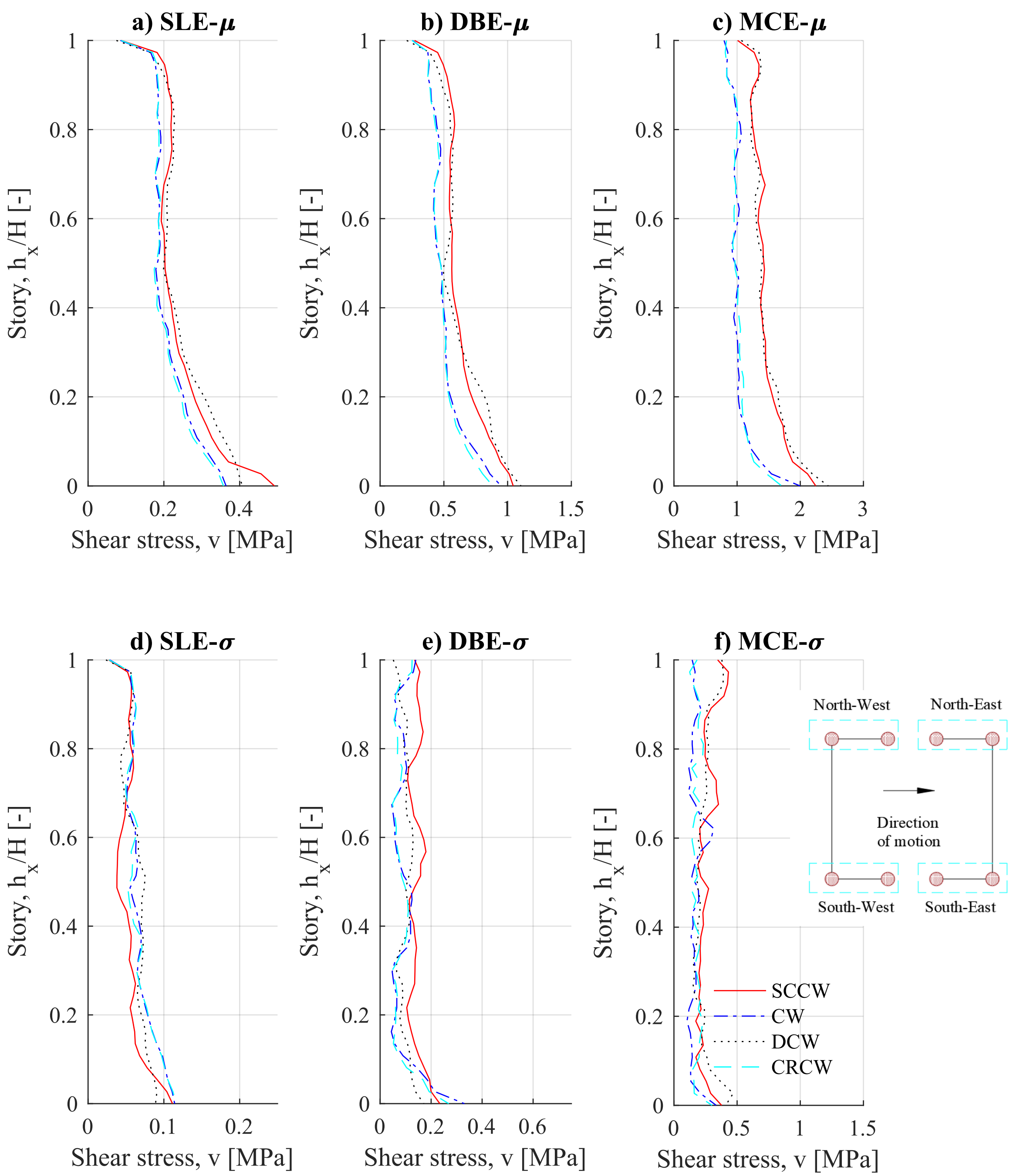

Figure 11.12 Shear stress in coupled wall flange: (a) SLE- μ; (b) DBE- μ; (c) MCE- μ; (d) SLE- σ; (e) DBE- σ; and (f) MCE- σ

11.4.2.3 Coupling forces

Figure 11.13 (a), (b), and (c) shows the mean (μ) ratio of the coupling beam shear force to the yielding shear force ($V_{CB}/V_{CB,y}$) for each system (SCCW, CW, DCW and CRCW) for the SLE, DBE, and the MCE, respectively. Figure 11.13 (d), (e), and (f) shows the standard deviation (σ) $V_{CB}/V_{CB,y}$ for each system (SCCW, CW, DCW and CRCW) for the SLE, DBE, and the MCE, respectively. The ratio $V_{CB}/V_{CB,y}$ was determined by taking the peak shear response of the North and South coupling beam at a given floor and dividing by the yield force.

As shown in Figure 11.13, the mean (μ) of the $V_{CB}/V_{CB,y}$at the SLE shaking intensity is 0.93, 0.8, 0.99, and 0.74 for the SCCW, CW, DCW and CRCW, respectively. The peak mean (μ) of the $V_{CB}/V_{CB,y}$ at the DBE shaking intensity is 1.19, 1.04, 1.19, and 1.04 for the SCCW, CW, DCW and CRCW, respectively. The peak mean (μ) ISDR at the MCE shaking intensity is 1.80, 1.31, 1.83, and 1.30 for the SCCW, CW, DCW and CRCW, respectively.

The standard deviation (σ) of the $V_{CB}/V_{CB,y}$ at the SLE shaking intensity is 0.20, 0.21, 0.23, and 0.21 for the SCCW, CW, DCW and CRCW, respectively. The σ of the $V_{CB}/V_{CB,y}$ at the DBE shaking intensity is 0.05, 0.14, 0.12, and 0.15 for the SCCW, CW, DCW and CRCW, respectively. The σ of the $V_{CB}/V_{CB,y}$ at the MCE shaking intensity is 0.17, 0.09, 0.20, and 0.09 for the SCCW, CW, DCW and CRCW, respectively.

The SLE shaking intensity $V_{CB}/V_{CB,y}$- μ of the CW, DCW and CRCW were -19.1%, 6.91%, and -20.5% greater than the SCCW systems. The DBE shaking intensity $V_{CB}/V_{CB,y}$- μ of the SW, OW and CRW were -12.3%, 0.0%, and -12.4% greater than the SCCW systems. The MCE shaking intensity $V_{CB}/V_{CB,y}$- μ of the CW, DCW and CRCW were -27.2%, 2%, and -27.4% greater than the SCCW systems.

The SLE shaking intensity $V_{CB}/V_{CB,y}$-σ of the CW, DCW and CRCW had a difference of 3.4%, 13.1%, and 5.8% difference than the SCCW system, respectively. The DBE shaking intensity $V_{CB}/V_{CB,y}$-σ of CW, DCW and CRCW had a difference of 166.3%, 114.3%, and 177.3% of the SCCW system, respectively. The MCE shaking intensity $V_{CB}/V_{CB,y}$-σ of CW, DCW and CRCW had a difference of -45.7%, 18.7%, and -46.3% compared to the SCCW system, respectively.

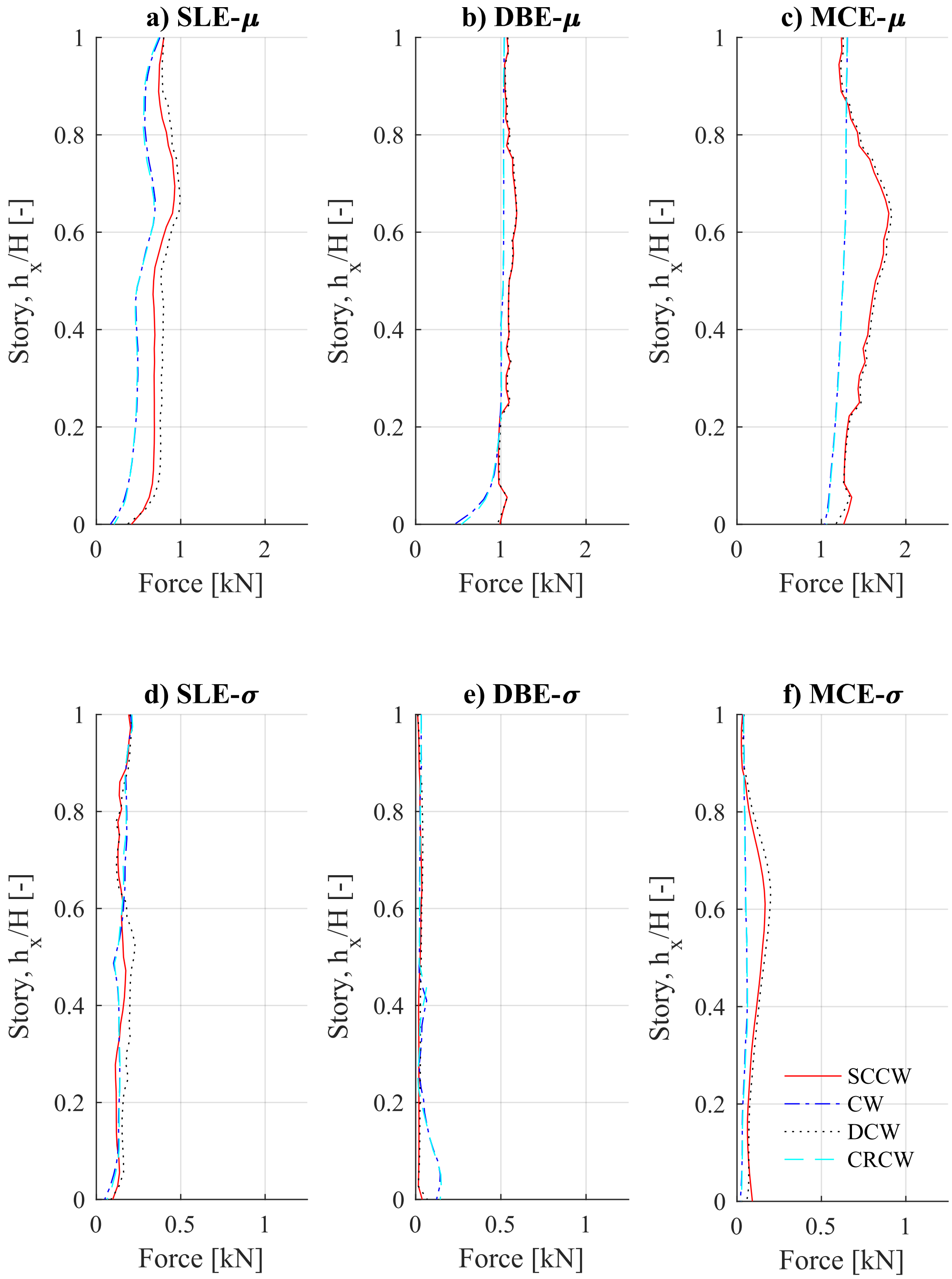

Figure 11.13 Coupling shear ratio for each RC core wall system: (a) SLE- μ; (b) DBE- μ; (c) MCE- μ; (d) SLE- σ; (e) DBE- σ; and (f) MCE- σ

11.4.2.4 Vertical wall strains

Figure 11.14 (a), (b), and (c) shows the mean (μ) vertical strain for each system (SCCW, CW, DCW and CRCW) for the SLE, DBE, and the MCE, respectively. Figure 11.14 (d), (e), and (f) shows the standard deviation (σ) vertical strain, each system (SCCW, CW, DCW and CRCW) for the SLE, DBE, and the MCE, respectively. At each node, strains are determined by taking the difference between the vertical displacements at each wall corner divided by the distance between the nodes. The tension strains are normalised to the yield strain of rebar ($\varepsilon_y = 0.002$). The strains are highest near the mid-height of the building, demonstrating the governance of higher mode moments. However, all strains are below yielding (i.e., $\varepsilon/\varepsilon_y$<1), demonstrating the EEDP performance objectives have been met.

As shown in Figure 11.14, the mean (μ) strain ratio ($\varepsilon/\varepsilon_y$) at the SLE shaking intensity is 0.12, 0.11, 0.13, and 0.12 for the SCCW, CW, DCW and CRCW, respectively. The peak $\varepsilon/\varepsilon_y$-μ at the DBE shaking intensity is 0.19, 0.18, 0.20, and 0.17 for the SCCW, CW, DCW and CRCW, respectively. The peak $\varepsilon/\varepsilon_y$-μ at the MCE shaking intensity is 0.80, 0.81, 1.05, and 0.79 for the SCCW, CW, DCW and CRCW, respectively.

The standard deviation (σ) of the $\varepsilon/\varepsilon_y$- σ at the SLE shaking intensity is 0 0.01, 0.01, 0.01, and 0.01 for the SCCW, CW, DCW and CRCW, respectively. The $\varepsilon/\varepsilon_y$- σ at the DBE shaking intensity is 0.04, 0.11, 0.04, and 0.11 for the SCCW, CW, DCW and CRCW, respectively. The $\varepsilon/\varepsilon_y$- σ at the MCE shaking intensity is 0.62, 0.63, 0.66, and 0.61 for the SCCW, CW, DCW and CRCW, respectively.

The SLE shaking intensity μ vertical strain of the CW, DCW and CRCW had a difference of 1.9%, 7.41%, and 0.001% when compared with the SCCW system. The DBE shaking intensity $\varepsilon/\varepsilon_y$-μ of the CW, DCW and CRCW were -6.5%, 5.2%, and -10.8% greater than the SCCW systems. The MCE shaking intensity $\varepsilon/\varepsilon_y$-μ difference of the CW, DCW and CRCW was 0.6%, 31%, and -1.2% compared to the SCCW system.

The SLE shaking intensity σ vertical strain of the CW, DCW and CRCW had a difference of 68.9%, 15.9%, and 62.9% when compared with the SCCW system. The DBE shaking intensity $\varepsilon/\varepsilon_y$- σ of the CW, DCW and CRCW were 148.1%, -14.2%, and 146.3% greater than the SCCW systems. The MCE shaking intensity $\varepsilon/\varepsilon_y$- σ difference of the CW, DCW and CRCW was 1.6%, 6.2%, and -1.6% compared to the SCCW system.

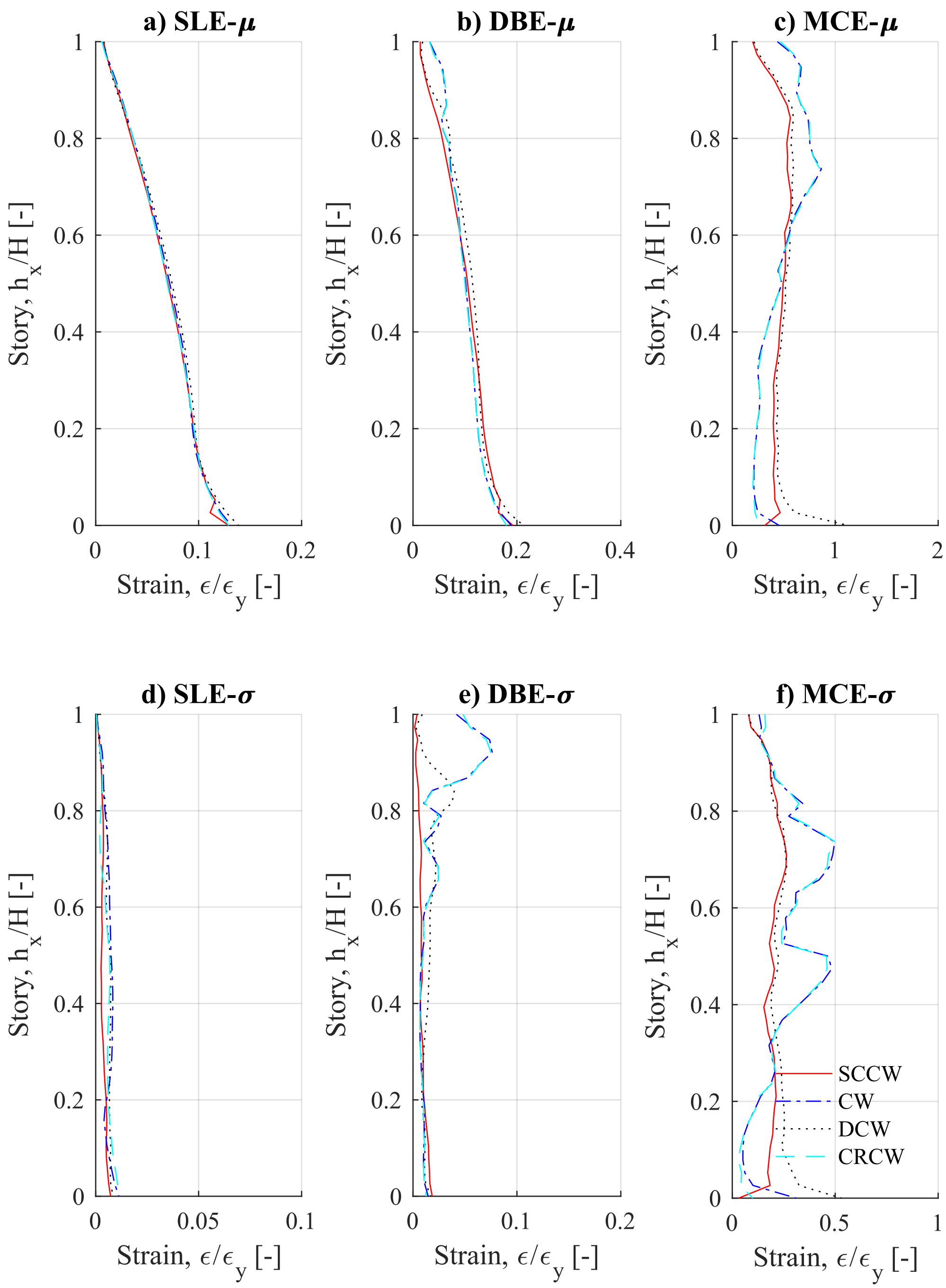

Figure 11.14 Max strain profile for each RC wall system: (a) SLE- μ; (b) DBE- μ; (c) MCE- μ; (d) SLE- σ; (e) DBE- σ; and (f) MCE- σ

11.5 Summary and conclusions

This chapter presents a comparison between alternative shear wall systems and the CORW systems and a comparison between alternative coupled wall systems and the SCCW systems. For efficiency, this comparison was completed on the 40-story (tallest prototype) on the Victoria site (highest site hazard).

The CORW was compared with three other RC wall systems: the CORW, the SW, the Outriggered Wall (OW), and the Controlled Rocking Wall (CRW).

The following are some of the important observations made in this study:

1. Displacements are 23% higher in the SW compared to the CORW
2. ISDR are 52% higher in the SW compared to the CORW
3. Shear stress in the SW is 14% higher than the CORW

The SCCW was compared with three other RC coupled wall systems: the Coupled Wall (CW), the Damped Coupled Wall (DCW), and the Controlled Rocking Coupled Wall (CRCW).

The following are some of the important observations made in this study:

1. Displacements are 22% higher in the CW compared to the SCCW
2. ISDR are 45% higher in the CW compared to the SCCW
3. Shear stress in the SW is 14% higher than the SCCW

It is important to note that this study was limited to one prototype designed using one design method. Further investigations should be completed to examine the influence of these systems on different building types. Further, this study did not investigate the influence of the design procedure on the system response. The prototype building used only the EEDP design of the SCCW. The results may vary if these systems were designed to conventional code-based methods.

These analyses demonstrate the high performance of the CORW and SCCW systems, using state of the art numerical models. However, there is limited experimental data on the dynamic behaviour of core wall buildings. The following Chapter 12 describes the work completed towards the shake-table testing of CORCW systems as well as the planned shake table testing programme.

Chapter 12: Design and construction of shake-table testing specimen.

12.1 Overview

This chapter gives the detailed design and construction of a shake-table testing program for the proposed high-performance RC core wall. This chapter begins with a description of the facility and the limitations of the shaking-table. Afterwards, a description of the specimen design simplifications and scaling is provided. Following this are the details of the specimen design and construction. This chapter also describes the planned testing phases, instrumentation plan, ground motion selection and scaling, and testing considerations. The end of this chapter describes a numerical model developed of the specimen, and the predicted results of the experimental test.

12.2 Introduction

The large scale of tall building structural systems makes them challenging to experimentally test. The only feasible way to obtain dynamic seismic response data for a full-scale tall building is through extensive instrumentation of as-built structures and analysis of the data after an earthquake occurs. This method is not practical when the objective is to immediately validate a new system; therefore, historically, researchers have tested large-scale portions of the structure, such as a wall or beam, under quasi-static cyclic loads. Although effective in examining the local behaviour, the interaction of elements and higher mode effects are not fully captured within this testing methodology.

An effective way to investigate the dynamic behavior of tall building systems is shake-table testing. However, due to the high expenses and limited availability of shake-table facilities, few low-damage RC wall systems have been experimentally tested using this method. Gavridou et al. (2017) studied a full-scale 4-story precast unbonded post-tensioned controlled rocking building. Their results demonstrated that the controlled rocking system could have minimal damage after strong dynamic shaking. Lu et al. 2018 tested a combined frame-controlled rocking wall system using 1/3 scale shaking table testing. The five-story scaled building showed negligible damage after shaking bi-directionally, demonstrating the effectiveness of this low damage system. In 2019, Henry et al. conducted a full-scale shake table test on a two-story building under unidirectional and bidirectional loading. The system consisted of planar RC walls designed for controlled rocking. Dampers were added to the edges of the walls to help dissipate the earthquake energy. Overall, the results showed minimum damage to all levels of shaking. Although these systems showed promising results for low-damage buildings, there have been limited to low-rise buildings, and the experimental response of low-damage tall buildings remains untested.

In this research, a 1/6.5 scale RC core wall specimen was built for shake table testing at the Multi-function shake table array facility in Shanghai China. The specimen is a model of the 24-Story Vancouver prototype building (Van24) designed in Chapter 5 and analyzed in Chapter 8-10. The specimen was specially designed to use materials that would be used in actual building construction. The large geometry of this specimen makes it unique; it is the largest core-wall shake table specimen ever built. The following sections describe the shake table testing facility, specimen design and scaling, and specimen construction.

12.3 Testing facility

The specimen will be tested at the Multi-Array Shaking Table Facility located on the Jiading Campus of Tongji University in Shanghai, China (Figure 12.1). The shake tables within this facility have 3-degree-of-freedom, longitudinal, lateral, and yaw. Each shake table has a dimension of 6m x 4m. In this research, two shake tables will be used, each with a payload capacity of 70 tonne. Additionally, the height to the roof crane girder is 18m. Table 12.1 shows the shake table capacities. These capacities limit the size of the specimen and the amplitude of shaking.

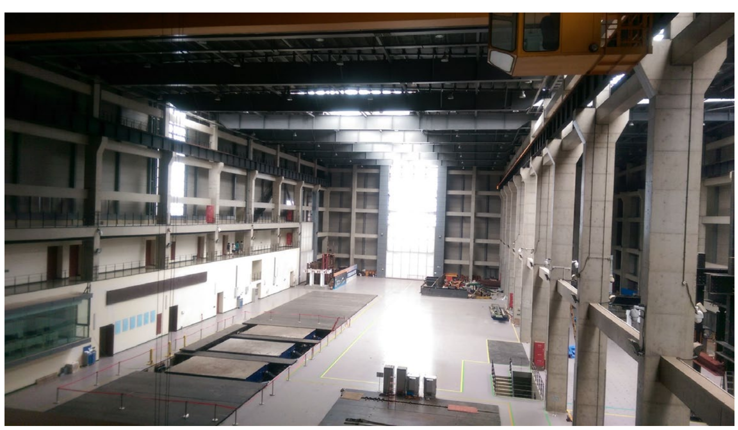

Figure 12.1 Multi-function shake table facility, Jiading, Shanghai, China

Table 12.1 Shake table capacities

Properties	Capacity (per table)
Allowable mass	70tonne
Stroke	+- 500 mm
Velocity	+- 1000 mm/s
Acceleration	+- 1.5g
Frequency of operation	0.1-50 Hz
Overturning moment	4000 kN-m

12.4 Similitude

The specimen was designed such that it represented the Vancouver 24-story prototype building presented in Chapter 5. The prototype building was scaled and simplified to facilitate experimental testing. The length scaling factor was determined based on the clearance of the crane within the laboratory (18m). The length scaling factor was selected as s_l= 1/6.5. Equation 12.1 shows the length scaling factor (s_l).

$$s_l = \frac{L_{sp}}{L_{pr}} = 6.5 \quad \text{Equation 12.1}$$

where L_{sp} is the length of any element on the specimen and L_{pr} is the corresponding element length on the prototype.

The concrete properties in the prototype building and in the specimen are assumed to be the same. Hence, the elastic modulus, stress, and strain are the same for both the prototype and specimen. Equation 12.2 shows the material scaling factor (S_e).

$$s_e = \frac{E_{sp}}{E_{pr}} = \frac{\sigma_{sp}}{\sigma_{pr}} = \frac{\varepsilon_{sp}}{\varepsilon_{pr}} = 1 \quad \text{Equation 12.2}$$

where E_{sp}, σ_{sp}, and ε_{sp} is the elastic modulus, stress, and strain, respectively, for the specimen and E_{pr}, σ_{pr}, and ε_{pr} is the elastic modulus, stress, and strain, respectively, for the prototype.

The ratio between force in the specimen to the force in the prototype is called the force scaling factor, s_f, and is shown in Equation 12.3. The force scaling factor is simplified by substituting the material scaling factor, s_e (Equation 12.2), and the length scaling factor, s_l (Equation 12.1), in Equation 12.3.

$$s_f = \frac{F_{sp}}{F_{pr}} = \frac{\sigma_{sp}A_{sp}}{\sigma_{pr}A_{pr}} = s_e s_l^2 \cong 1/43 \qquad \text{Equation 12.3}$$

where F_{sp} and A_{sp} are the specimen force and area, respectively, for the specimen and F_{pr} and A_{pr} are the specimen force and area, respectively, for the prototype.

The ratio between moment in the specimen to the moment in the prototype is called the moment scaling factor, s_m, and is shown in Equation 12.4. The moment scaling factor is simplified by substituting the material scaling factor, s_e (Equation 12.2), and the length scaling factor, s_l (Equation 12.1).

$$s_m = \frac{M_{sp}}{M_{pr}} = \frac{F_{sp}}{F_{pr}}\frac{L_{sp}}{L_{pr}} = s_e s_l^3 = 1/275 \qquad \text{Equation 12.4}$$

where M_{sp} is the specimen moment and M_{pr} is the prototype moment.

The length, material, force, and moment scaling factors can be used to scale between the prototype building properties and the specimen properties. With these factors, the prototype building geometry and capacities were scaled, and the specimen was designed. The following sections describe the detailed design of the specimens.

12.5 Specimen design

This section describes the specimen design; Appendix D shows the detailed construction drawings. In addition to the scaling factors, there were several other simplifications made for constructability and testing. Specifically, the floor masses and coupling beams were lumped at 8 levels, instead of the 24 stories of the prototype. Additionally, the gravity loads were partially simulated using unbonded PT over the height of the building. Figure 12.2, Figure 12.3 (a), and Figure 12.3 (b) shows the specimen conceptual view, CORW elevation view, and the SCCW elevation view. As shown in the figures, the scaled specimen is 15.4m tall with a core wall footprint of 1.42m x 1.42m. The outrigger beam is 4.32m long and constructed using two W14X120 steel wide flange members. The outrigger columns are made from HSS6x6x3/8 steel sections and are pin-connected at the base and outrigger. For stability, lateral supports are provided from the wall to the outrigger column at level 12 and 24. For the efficiency of construction and testing, story masses are lumped at every 3rd floor, where a total of 8 mass blocks are used. To assist with wall stability, a steel truss is bolted to the wall at every mass block level. The RC core wall was constructed in two pieces for transportation (10m wall and a 5m wall) and has a welded splice in between.

The following sections describe each component of the specimen in detail.

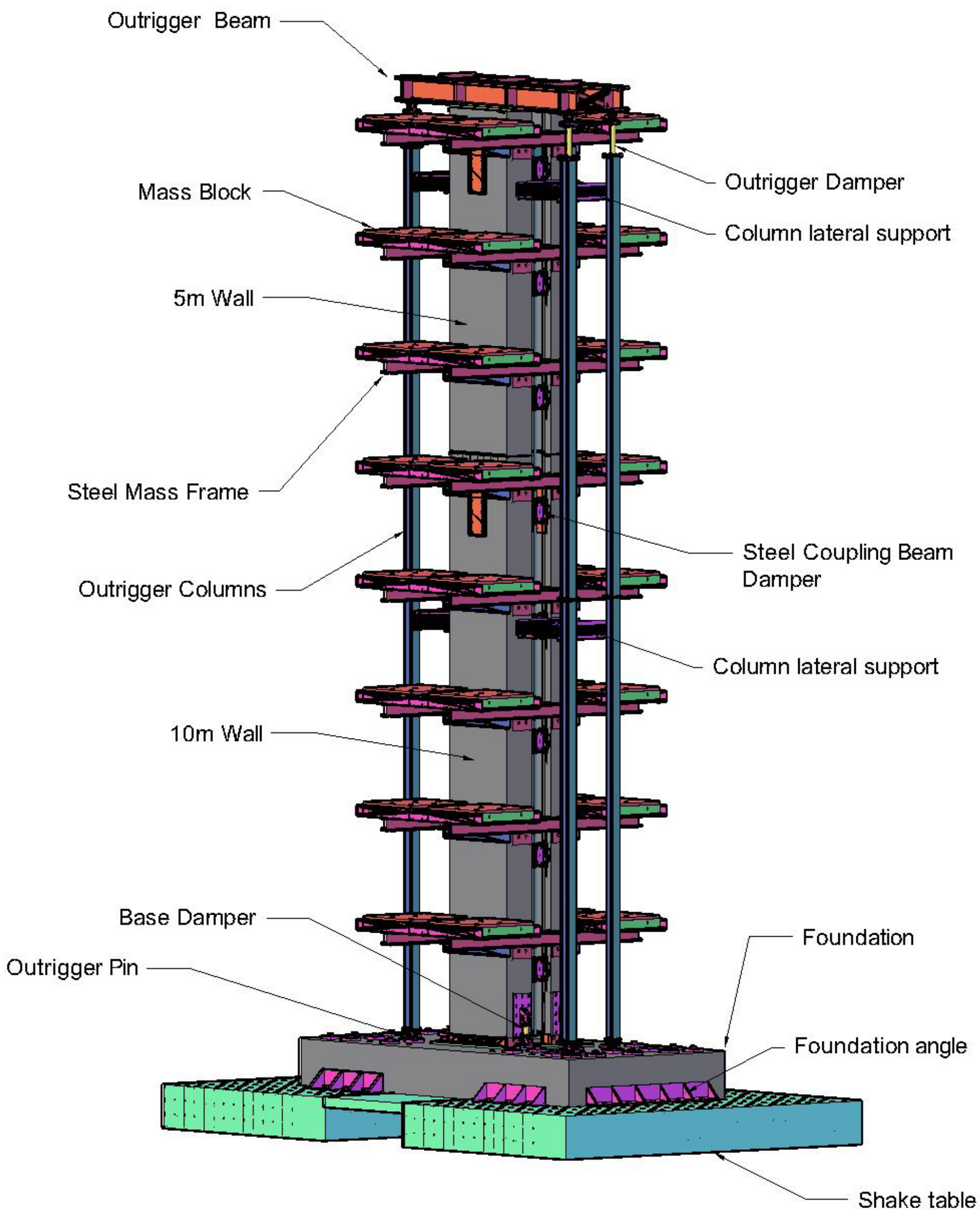

Figure 12.2 Conceptual view of specimen

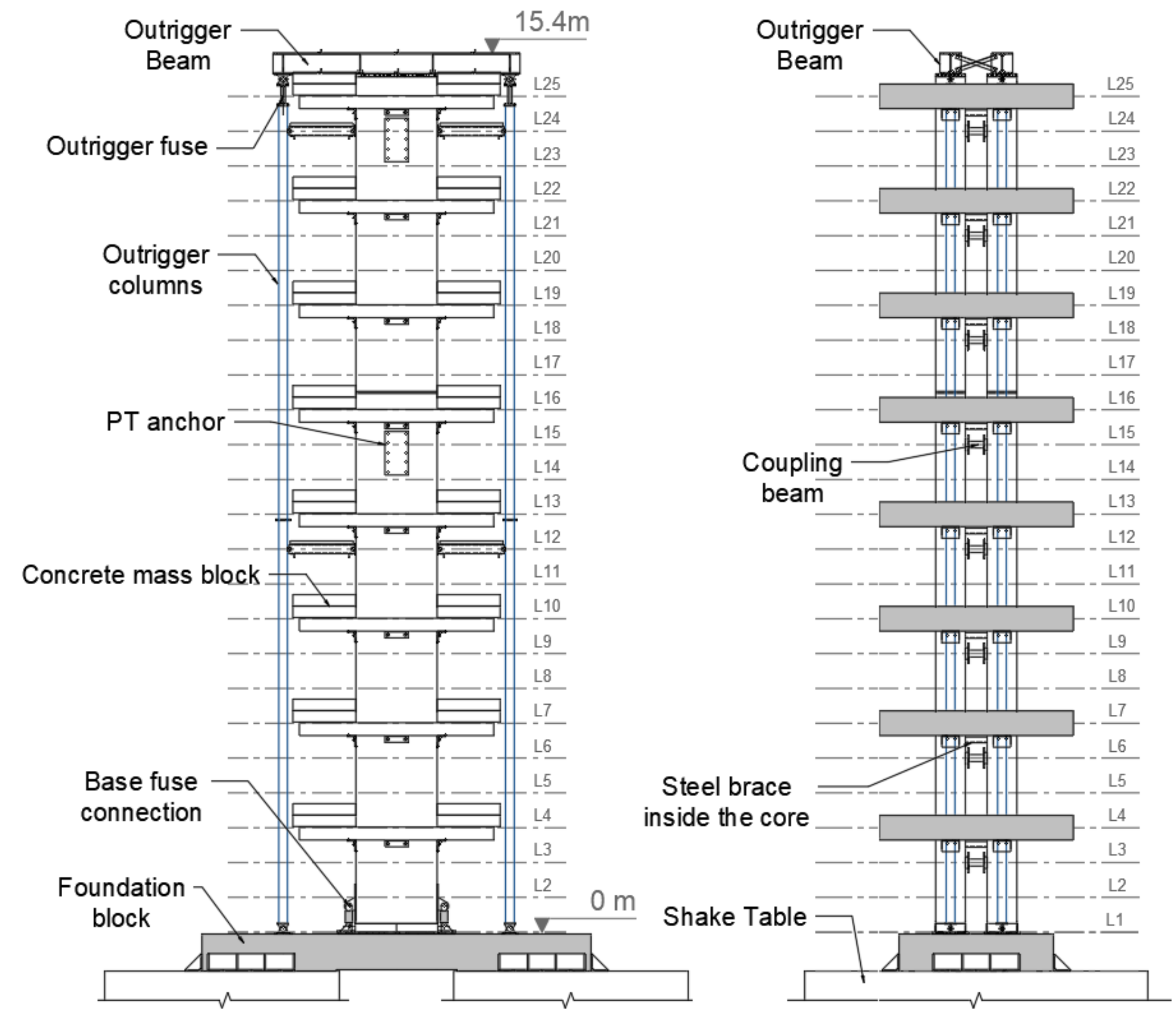

Figure 12.3 Elevation views of the specimen: (a) CORW elevation and (SCCW) elevation

12.5.1 Outrigger system

The outrigger system was approximated to match the same scaled stiffness as the prototype building. The outrigger truss and columns were approximated as two equivalent steel W14x120 beams connected to HSS6x6x3/8 columns, which are laterally braced with steel angle L2½x2½ x¼. The outrigger is connected to the wall using 16- cast in Dywidag rebar which are embedded into the wall with a 500mm embedment length. Figure 12.4 (a) presents the top view of the outrigger beams and Figure 12.4 (b) shows the side view.

The outrigger beams are pin connected to friction dampers. The HSS6x6x3/8 columns are pin connected at the top to the friction dampers and at the bottom to the foundation. The columns are constructed into two pieces and spliced between L12 and L13 with a simple 4 bolt connection. The HSS6x6x3/8 are braced to the wall at L12 and L24. The wall is brace assembly, shown in Figure 12.5 (a) (concept) and shown in Figure 12.5 (b) (plan view), and consists of W6x16 beams which use L2½x2½ x¼ cross braces for stability. The braces are pin connected to the wall. The connection plate is connected to the wall using two ½" diameter through bolts with a back plate.

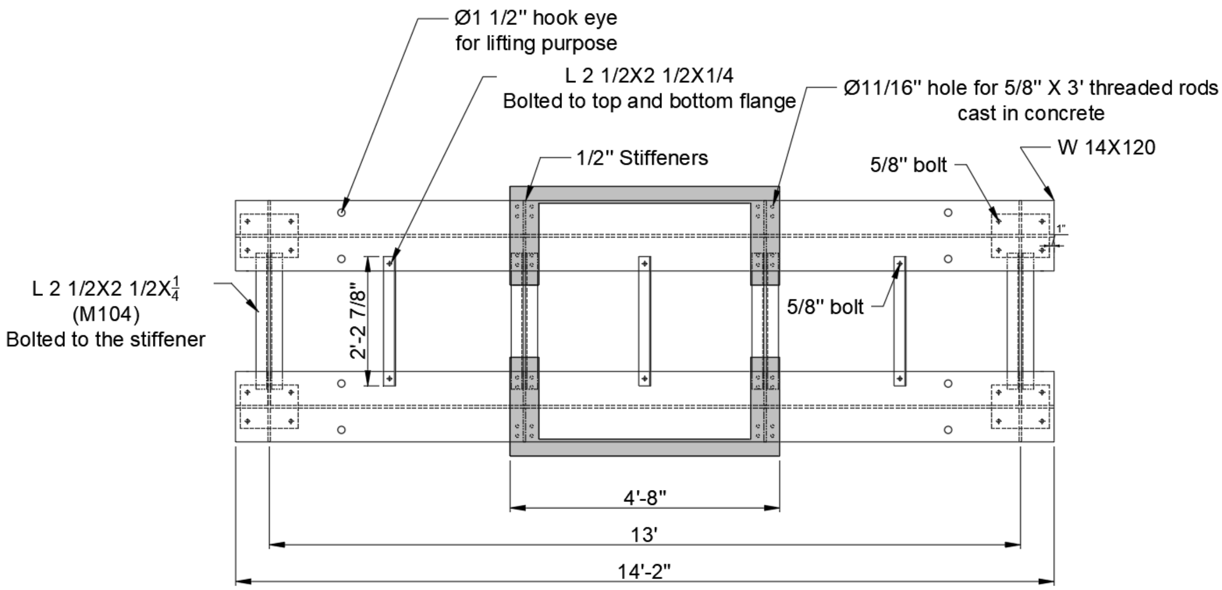

(a)

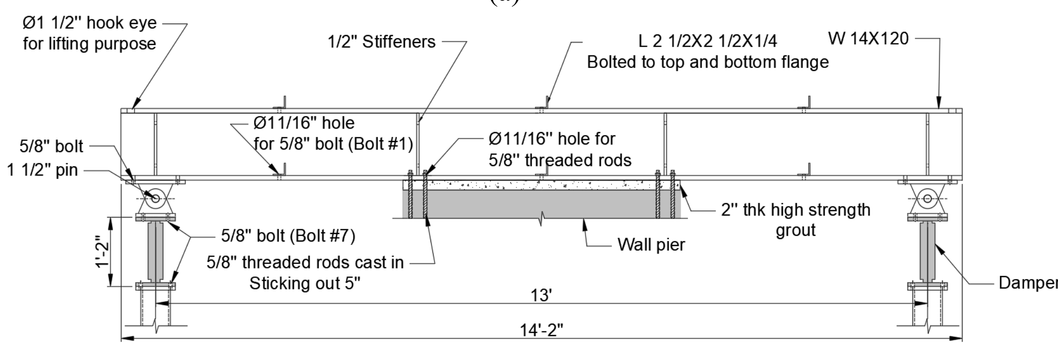

(b)

Figure 12.4 Specimen outrigger beam: (a) top view and (b) side view

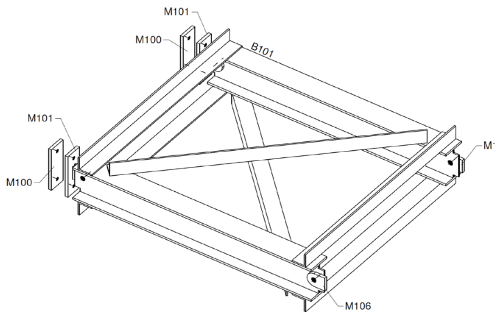

(a)

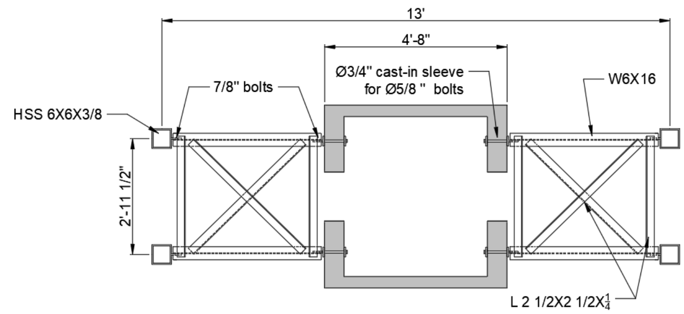

(b)

Figure 12.5 outrigger system lateral bracing: (a) top view and (b) side view

12.5.2 Post-tensioning

Due to the payload limitation of the shaking tables, gravity loads are partly simulated using post-tensioned (PT) strands anchored at level 15 and level 24. Four 0.5” diameter strands are anchored at level 15 and four 0.5” diameter strands are anchored at level 24. The strands are ASTM A 416 Grade 270 and have a specified yield strength of 1670 MPa, and ultimate strength of 1860MPa, a cross sectional area of 98.7mm^2, and a modulus of elasticity of 195,000MPa. Each strand is stressed until the design axial load taken by each PT strand is 125kN. Figure 12.6 (a) shows the elevation of the post-tensioned system, Figure 12.6 (b) shows the L24 top view PT connection, Figure 12.6 (c) shows the L15 top view PT connection, and Figure 12.6 (d) shows the top view PT connection to the foundation.

At L24 and L15 the PT strands are attached to double channel sections. The double channels have a shear key connection detailing to the wall connection plate. The connection plate and double channel assembly is shown in Figure 12.7. The connection plate has slotted holes to reduce any moment transfer into the connection. The connection plates are connected to the RC wall using through bolts and back plate. The bolts are designed to be post-tensioned, to provide a slip -critical joint between the wall connecting steel plates. Each PT strand is connected using reusable chucks (Figure 12.8), which use specially designed wedges to provide sufficient anchorage.

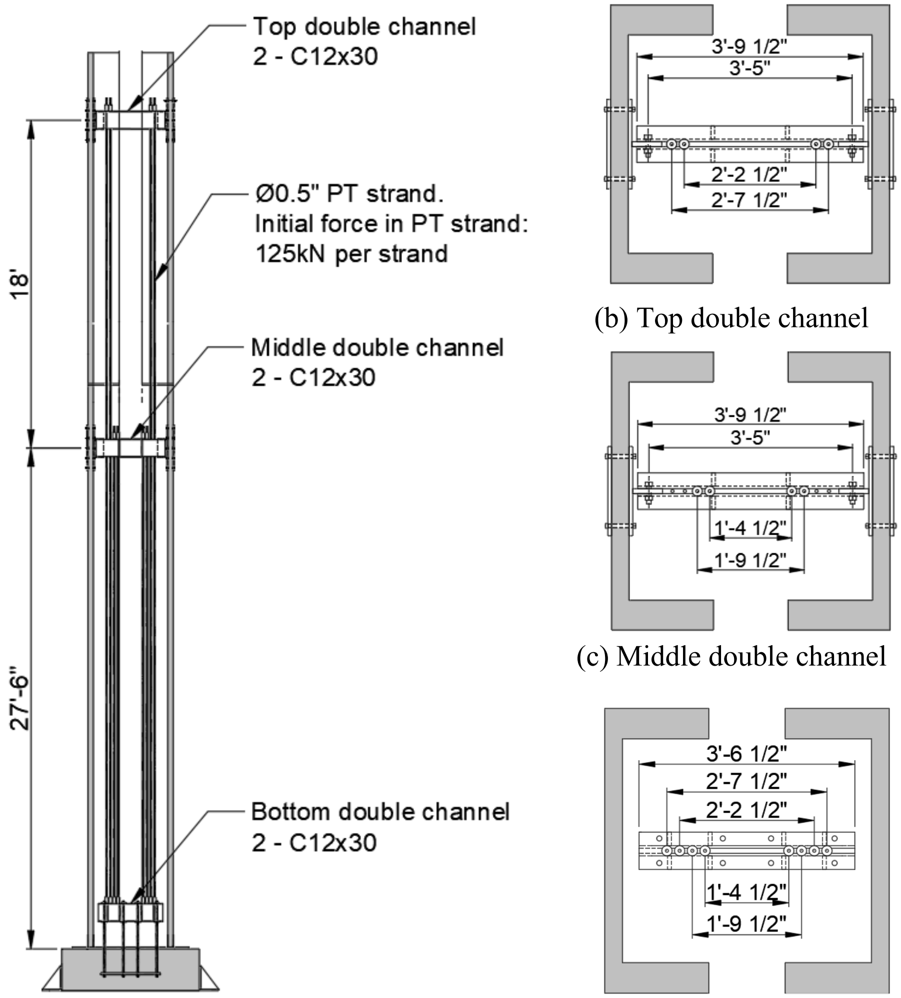

(b) Top double channel

(c) Middle double channel

(a)

(d) Bottom double channel

Figure 12.6 Post tensioned system: (a) elevation view; (b) L24 top view; (c) L 15 top view; and (d) foundation anchorage

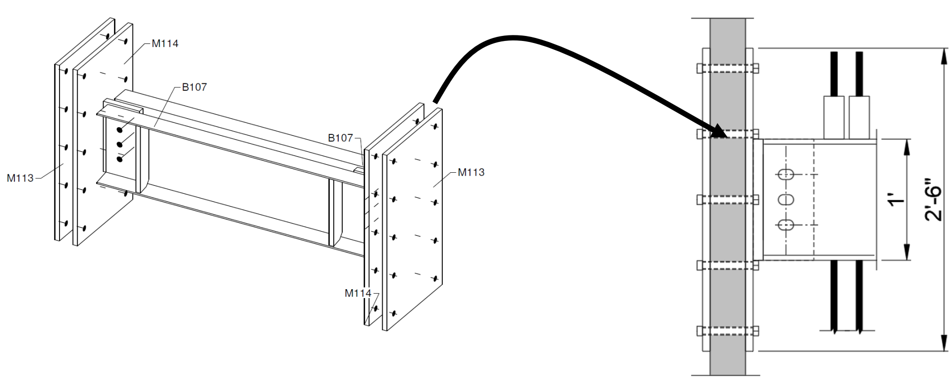

(a)

(b)

Figure 12.7 Post-tensioning anchor beam: (a) concept and (b) connection plate

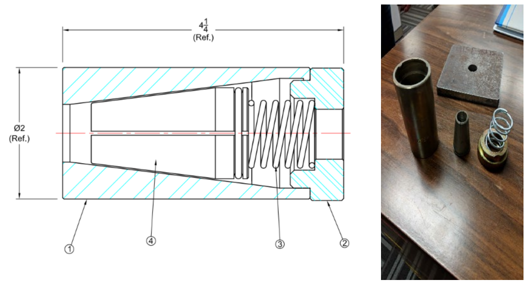

Figure 12.8 Reusable chuck for PT strand

12.5.3 RC core wall assembly

The RC core wall assembly mainly consists of two equally size C-shaped walls, shown in Figure 12.9. The C-shaped flanges are 150mm thick and 520mm long. The web is 90mm thick with a wall length of 1420mm. The reinforced core has constant cross-section reinforcing over the height of the wall. Each corner of the C-shaped walls has concentrated reinforcement, of 8-#3 bars, representative of zone reinforcing in typical RC shear walls. The flanges have distributed vertical reinforcing of #3 bars spaced at 3" at each face of the wall and horizontal reinforcing of #3 bars spaced at 6". The webs have distributed vertical reinforcing of #3 bars spaced at 5.5" at each face of the wall and horizontal reinforcing of #3 bars spaced at 6". The web horizontal bars were hooked 90 degrees within the zone for constructability, while the flange horizontal bars had 180-degree hooks on either end of the bar. All reinforcing bars are specified ASTM 706 Grade 60. The concrete is specified as 50MPa with ¼" aggregate.

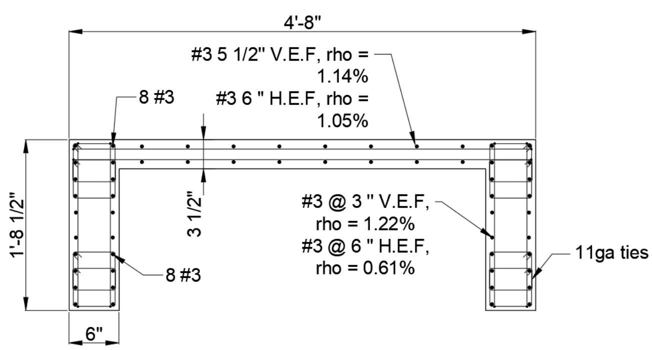

Figure 12.9 Reinforcing layout of the concrete wall. In this figure, #3 bars have a diameter of 3/8" and 10ga has a diameter of 0.1", the cover is 5/16".

The small scale limited the available reinforcing steel for ties. All ties were made from 1/8" mild steel wire. The ties around the zone are hooked 45-degrees around the vertical bar. The zone ties at the coupled wall are spaced at 2 ¼ over the entire height of the wall. The zone at the corner of the C-shape has ties spaced 2 ¼ for the first 4 levels, spaced 6” from L5-L20, and again spaced 2 1/4 “from L21 to the roof.

The coupling beam dampers are connected to W8x15 steel beams which are embedded into the wall. Figure 12.10 (a) shows the elevation of the coupling beams anchored in the wall and Figure 12.10 (b) shows the conceptual view of the coupling beam. The detailing follows AISC 2016, adjusted for scale. Each beam has four 10M transfer rebars welded to the beams. Six shear studs are welded to the tops and bottom of the embedded beams. The wide flange beam passes through the zone, which obstructs the ties. In this area, ties are placed on either side of the beam with additional ties passing through the holes, shown in Figure 12.10 (c).

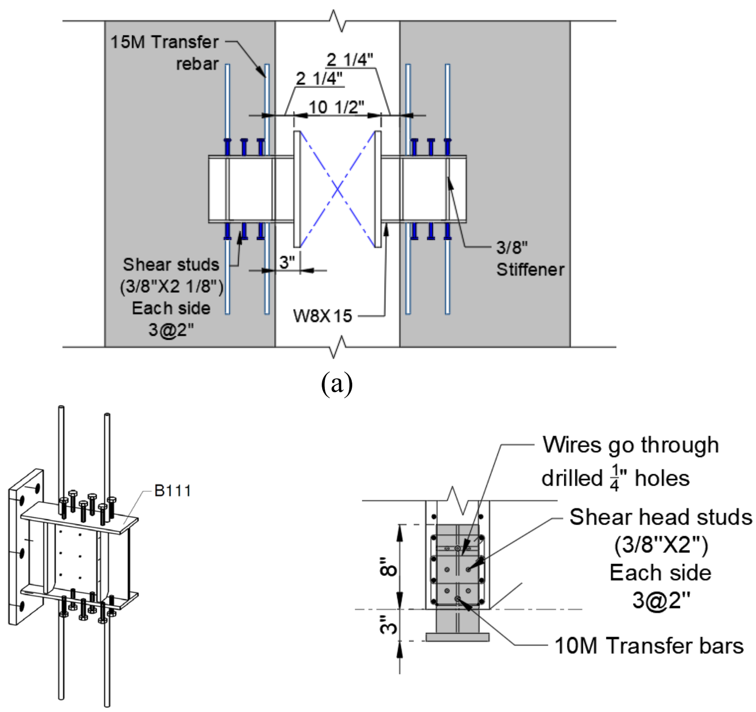

(a) (b) (c)

Figure 12.10 Anchored coupling beam details: (a) elevation view; b) concept view; and c) tie detailing.

The walls were designed to be constructed in two pieces (30’ wall and an 18’ wall), and later two wall-to-wall ½” steel plates are welded together between L16 and L17. This wall-to-wall connection plate concept is shown in Figure 12.11 (a). Cross ties are provided to hook around all the distributed vertical bars, to provide confinement for the embedded 20M bars. Figure 12.11b and Figure 12.11 (c) show the wall-to-wall connection plate located at the bottom of the 18’ wall and the top of the 30’ wall, respectively. The plate situation at the top of the 30’ wall has an additional ½” perimeter around the wall edge (Figure 12.11 (c)), to allow for a fillet weld all around. Steel tabs are welded on the sides of the plate are for positioning the wall during the construction process.

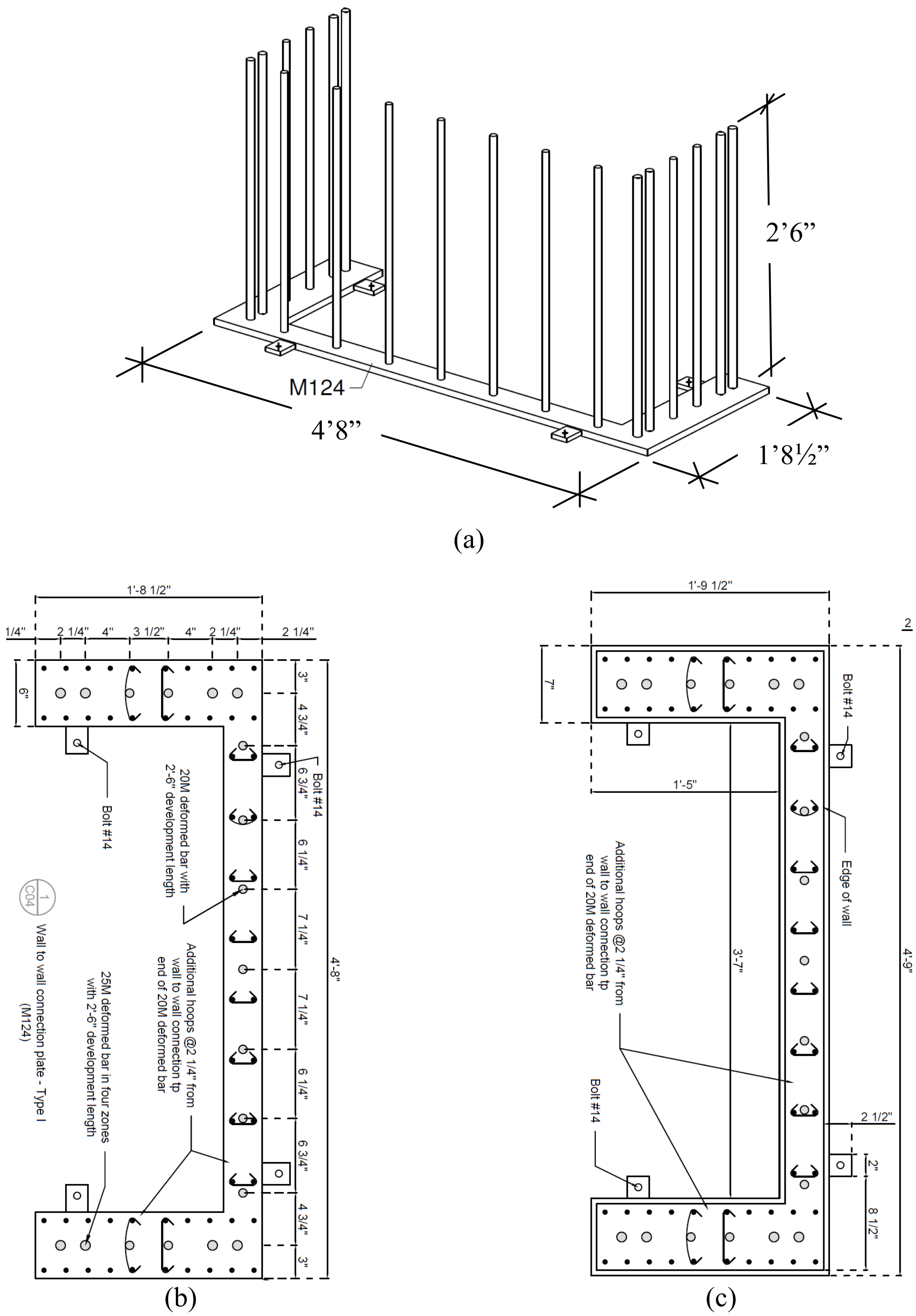

Figure 12.11 Steel welded connection plate: (a) concept view; (b) 18’ wall plate; and (c) 30’ wall plate

To endure the multiple cycles of testing, the base of the wall was confined using external steel plates call base armouring. Figure 12.12 shows base armouring: concept view (Figure 12.12 (a)); web side elevation view (Figure 12.12 (b)); flange side elevation view (Figure 12.12 (c)); and plan view (Figure 12.12 (d)). As shown, the bottom of the wall has a 6” depth of ¼” steel plate, welded at all corners. Threaded rods connected the plates together, where the rods were welded to the inside plate, and bolted to the outside plate. All vertical zone bars are welded to the flange underside of the plate.

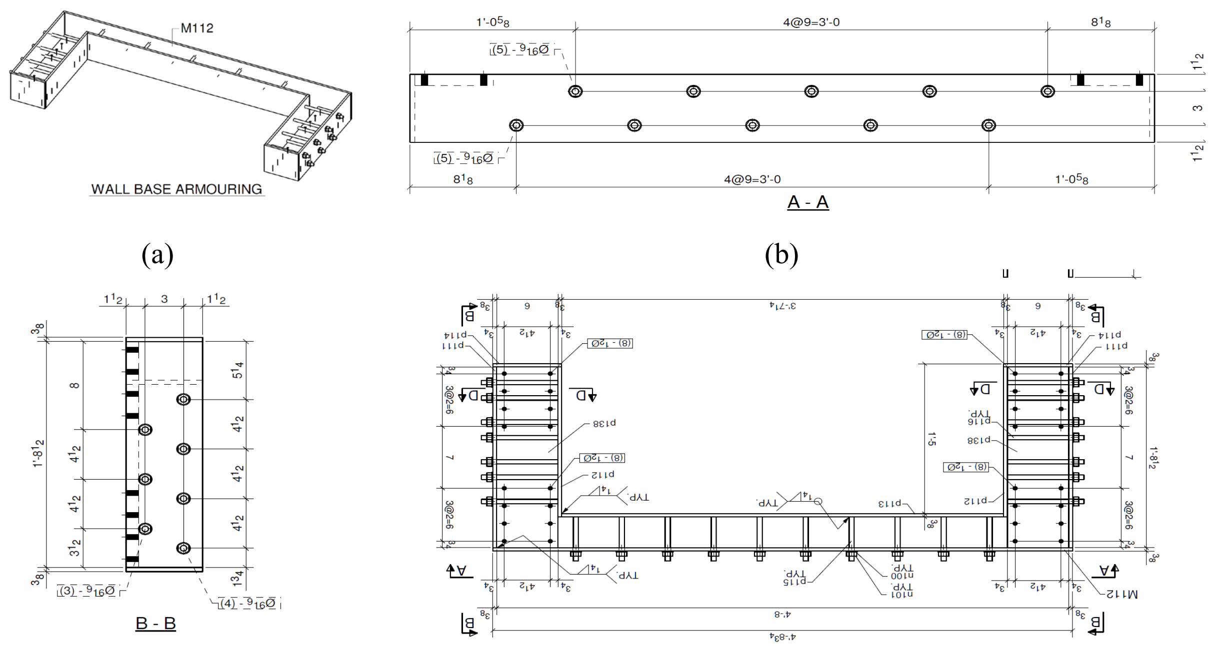

(a) (b) (c) (d)

Figure 12.12 Armoring plate: (a) concept view; (b) web side elevation view; (c) flange side elevation view; and (d) plan view,

The small-scale of the test structure results in small deformations within the base dampers, particularly for low intensity earthquakes. As a result, the connection between the base damper and the core wall needed to be constructed with high tolerances. Figure 12.13 (a) shows the cross section of the wall-base damper wall connection plate. As shown, the wall-base dampers are connected to the wall with a bolted connection. The bolts are designed to be cast-in the concrete, and post-tensioned after curing. This grout allows for a tight, slip-critical connection.

Figure 12.13 (b) and Figure 12.13 (c) show the front and side view of the base damped connection. To facilitate tight tolerances, 50mm grout layer is poured between the damper connection plate and the foundation. This allows for any differences in construction tolerances to be accommodated.

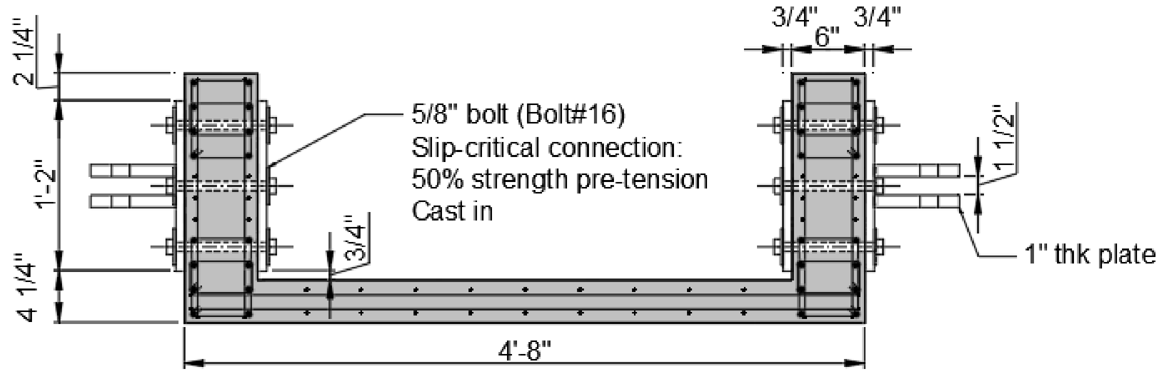

(a)

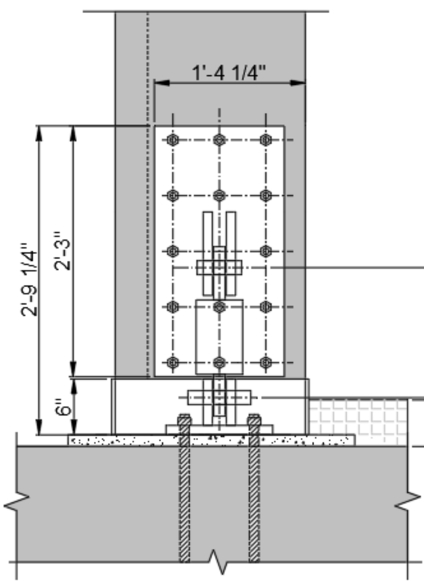

(b)

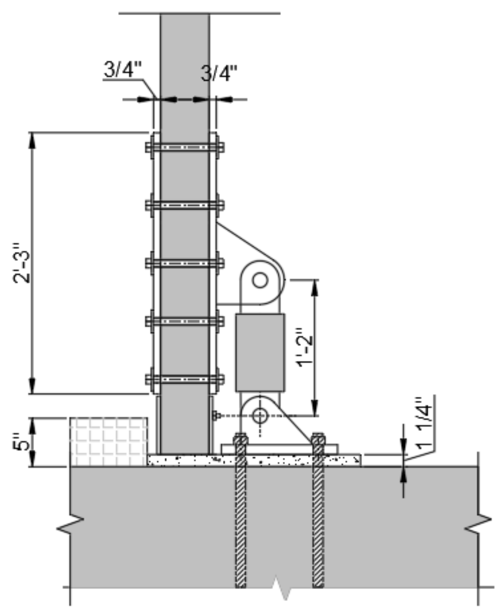

(c)

Figure 12.13 Base connection anchorage: (a) plan view; (b) front view; (c) side view

12.5.4 Mass block frame and diaphragm

The mass is provided through the self-weight of the structure, and by additional 2 tonne steel blocks provided by the Tongji lab. A steel support frame, shown in Figure 12.14, is constructed using beams and angles to support the steel blocks. The blocks are supported in gravity by two steel wide flange sections H200x200x8x10 (Chinese sizes). The blocks are prevented from sliding and movement by surrounding each block with a perimeter of L160x10 steel angle.

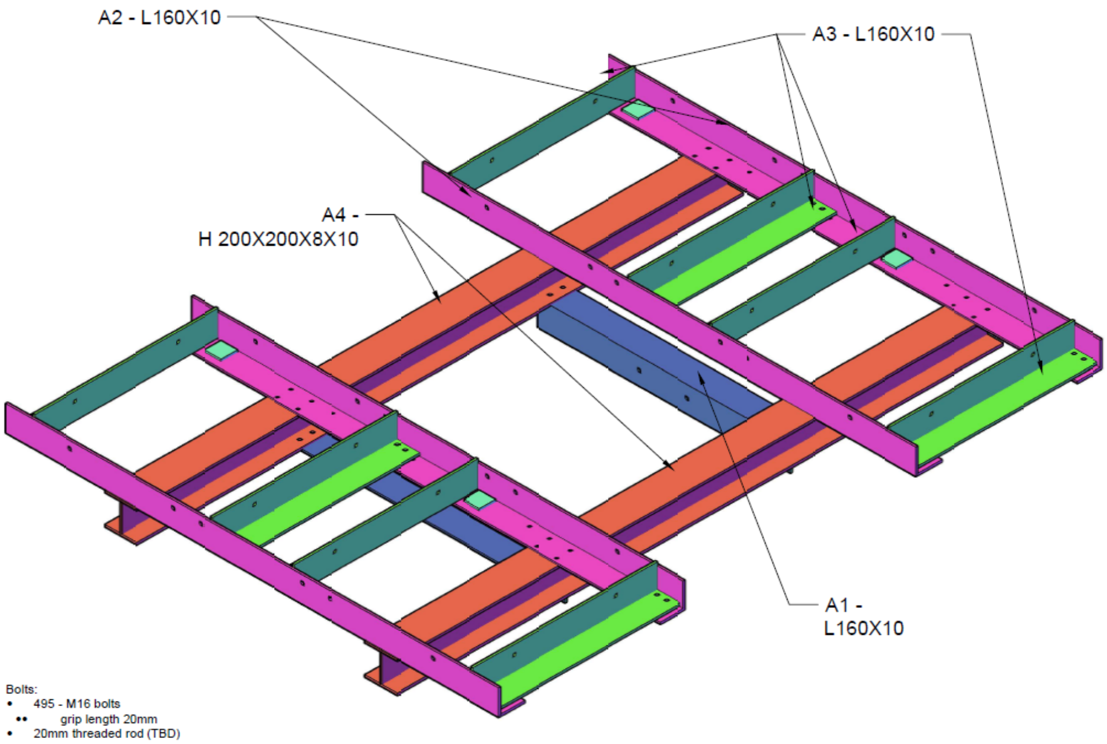

Figure 12.14 Mass block frame conceptual view

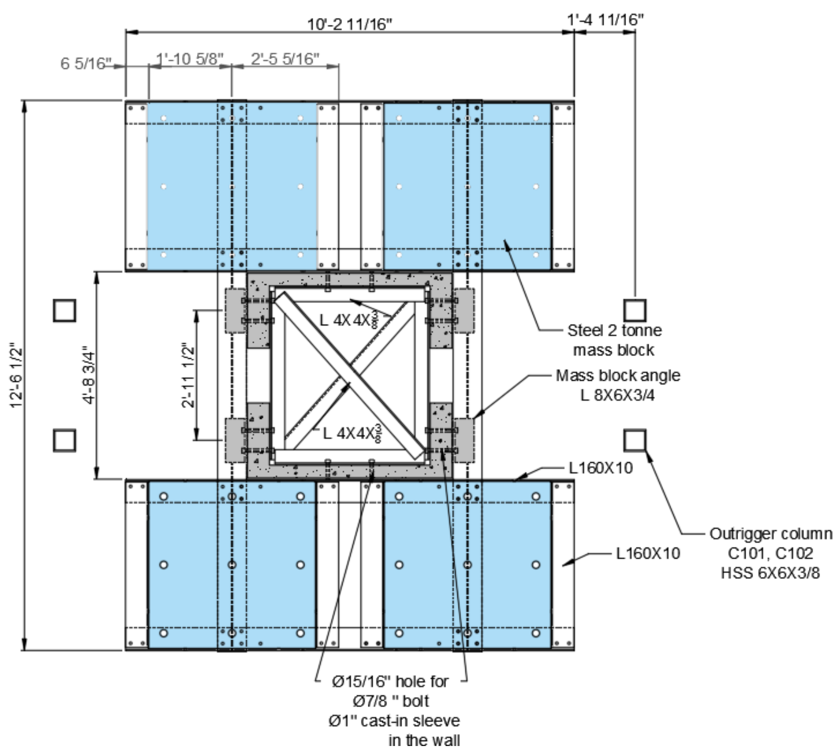

Figure 12.15 Typical floor plan view

Steel angle (L8X6X3/4) seats are bolted to the wall flanges, and the mass block frame beams sit on these angles, shown in Figure 12.15. To provide additional support, the mass block frame is connected to the wall through bolted connection in the web.

In the real building application, slabs would be providing the wall with diaphragm connection. To simulate this and ensure the wall has sufficient stability, internal bracing is provided in the wall (shown in plan, Figure 12.15). This internal bracing also provides back plates to the mass block frame connection. To ensure the bracing does not interact with the coupling beams, the steel angle is reduced to a smaller cross section.

12.5.5 Foundation

The foundation is a 2.7m x 5.5m x 0.8m RC block, shown in Figure 12.16. The foundation is prevented from sliding through the clamping force on 36mm diameter rods which are connected to the tables. Additional steel angles are provided to ensure the foundation is prevented from slipping. The foundation construction was contracted to the Chinese construction company, Best Steel.

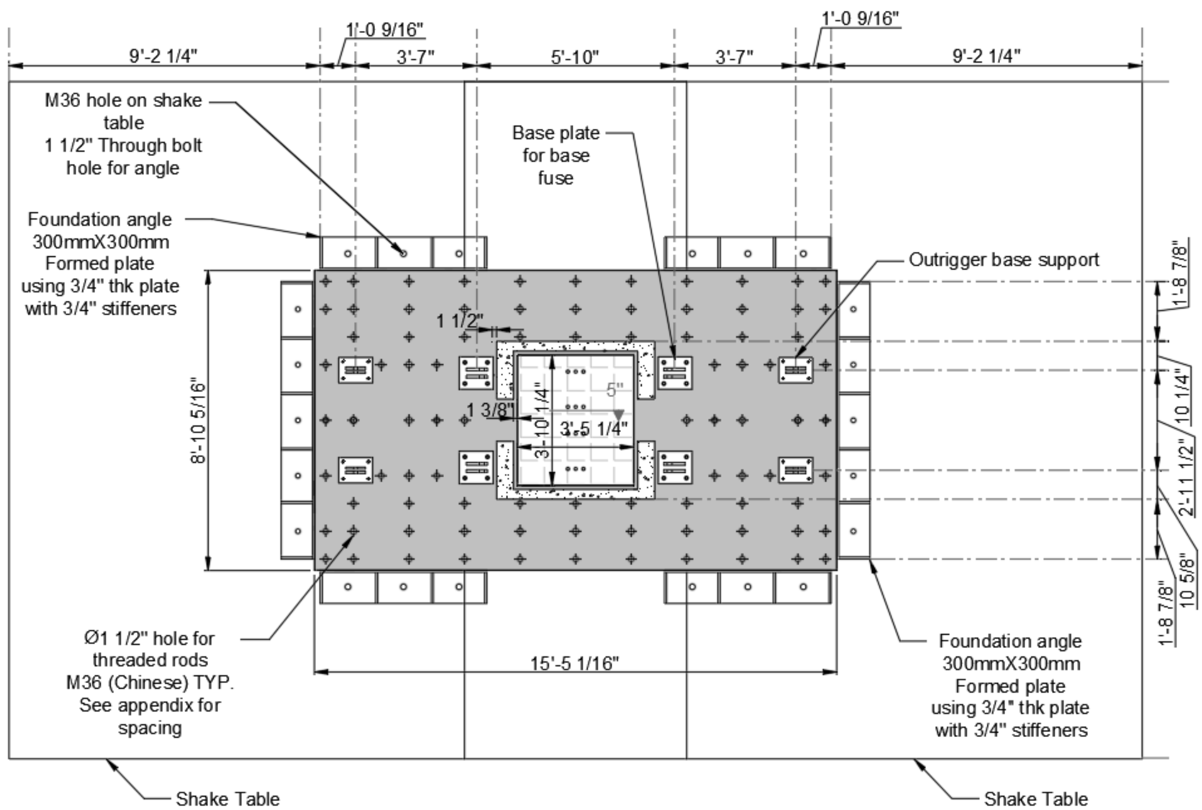

Figure 12.16 Foundation top view

12.5.6 Energy dissipation devices

The energy dissipation devices used in the outrigger and base dampers are the symmetric friction dampers designed and validated by Professor Geoffrey Rodgers. These devices are designed such that the scaled forces are the same from the Vancouver 24-story prototype building.

All of the SCFDs in the specimen are designed with the same geometry (i.e. cone slope, end plates, etc.) for manufacturing ease. The forces are adjusted by adjusting the post-tension force in the device. The SCFD had to be slightly modified from the original design due to equivalating the 24 beams to 8. Table 12.2 provides the design shear for each device the post yielding stiffness is designed to be 15kN/mm.

Table 12.2 Design SCFD specimen shear.

LVL	L4	L7	L10	L13	L16	L19	L21	L24
Design coupling beam shear, V [kN]	29	31	27	21	18	20	22	18

12.6 Specimen construction

The construction of the specimen was conducted on three continents. The RC core walls and the structural steel (except mass block) were construction in Vancouver, British Columbia, Canada. The foundation block and the mass block frames were constructed by Best Steel in Shanghai, China. The friction dampers were constructed at the University of Canterbury in New Zealand.

12.6.1 Construction at George Third and Son

All the structural steel, except for the SCFD and mass block frames, were constructed by George Third and Son, a high-quality structural steel manufacturer in Vancouver British Columbia. In addition to providing all the structural steel work, George Third and Son permitted the construction to occur in their yard, providing support for all aspects of construction.

12.6.2 RC core wall assembly

The reinforced core walls were constructed in four parts: two U-shaped walls that are 18’ long and two C-shaped walls that are 30’ walls. The U-shaped walls were constructed with the 3.5” web wall at the bottom with the two 6” flange sections pointed upward. To ensure the walls were constructed level, the formwork was built on top four large steel wide flange sections, that were levelled prior to construction, shown in Figure 12.17. The embedded steel coupling beams and the steel plates for damper connection, PT connection, Wall-wall connection, and the confinement plates were all built into the formwork. The mass block connections and the diaphragm bolt holes were constructed using PVC pipe cast in. Due to delays in reinforcement placement, the formwork was exposed the weather for weeks prior to the concrete pour. As a result, the formwork warped in some areas, resulting in small gaps at form intersections.

Figure 12.17 Formwork of wall section

12.6.3 Reinforcing steel placement

The reinforcement steel was provided and placed by LMS reinforcing steel. The intricate nature of this scaled down specimen made the construction of the steel cages a complex task. The reinforcing cage had to be built within the formwork, and could not be prefabricated and placed, as is typical construction practice. Figure 12.18 (a) shows the overview of the reinforcing steel in the specimen.

Figure 12.18 (b) shows two pre-formed steel ties stacked on top of one another. The zone ties were formed from 10ga mild steel wire. The tight tolerances were achieved using a wire forming machine. The construction resulted in the tail of the bar being slightly longer than the other. Due to the built-up construction, the #3 zone bars were tied at least five of the corners of the bar. With over 1500 zone ties this resulted in over 7500 individual wire knots. The 10ga ties are shown in Figure 12.18 (c).

(b)

(a)

(c)

Figure 12.18 Reinforcing construction: (a) overview, (b) wire tie; (c) zone detailing

12.6.4 Concrete pour and curing

The 3.5” wall web and the 6” flanges were poured on two separate days. The 3.5” web wall was poured on 8am July 1, 2019 while the 6” wall flanges were poured on 8am on July 15, 2019. A self-consolidating concrete mix, called *Agilia* was donated by Lafarge. This high cement ratio mix is sensitive to vibrations and curing. The first pour, the weather was raining; during the pour, the mix began to clump, and the Lafarge quality control added proprietary admixtures. The second pour was a clear day, the concrete was poured until it leveled with the top of the formwork. To make sure it was level between the coupling beams, the sides of the formwork near the embedded steel beams were hammered during the pour.

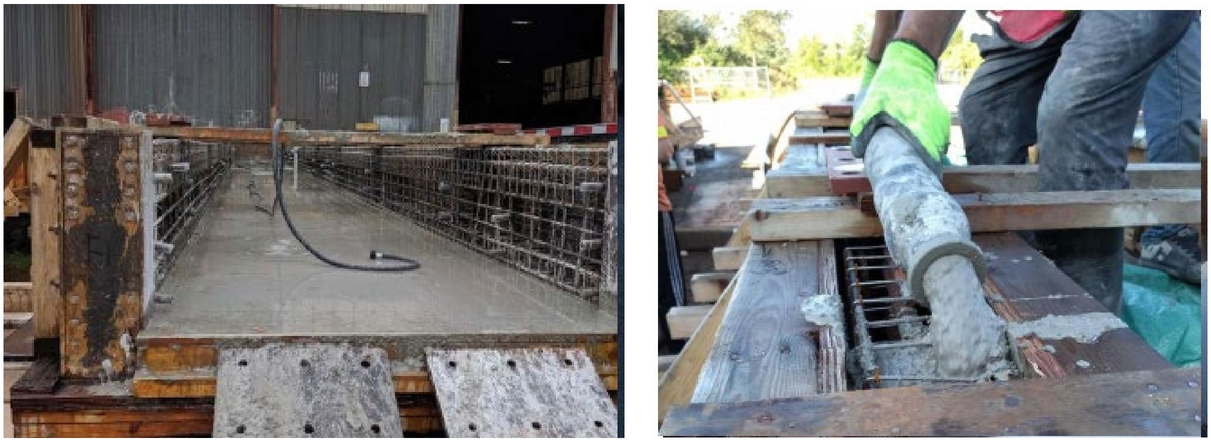

(a) (b)

Figure 12.19 concrete pour (a) pour 1 and (b) pour 2

Due to the high cement ratio of the mix, there were concerns that insufficient curing would result in large shrinkage cracks. Therefore, as soon as the concrete started to plasticize, soaker hoses were connected, and the walls were kept wet for 2 weeks for the web and 1 week for the flanges.

Concrete cylinders, with a 6in diameter, were sampled for both pours, moist cured, and tested both by UBC and by Lafarge. Table 12.3 shows the concrete strength at different testing dates. The specified design strength at 28 days was 50MPa. However, the stresses exceeded this design at both the 28 day and the 56-day strength.

Table 12.3 Concrete cylinder testing strength

	UBC		Lafarge	
Sample date	Days after pour	Concrete strength [MPa]	Days after pour	Concrete strength [MPa]
July 25, 2019 (Flanges pour)	7	48	7	36.2
	28	53.7	28	57.7
	56	62.5	56	68.6
July17, 2019 (Web pour)	11	63.6	7	42.4
	28	64.5	28	66.2
	56	74.6	56	74.1

12.6.5 Transport PT

The walls had to undergo a tremendous amount of lifting and shipment from Vancouver to Shanghai. To avoid any unexpected damage, the walls were temporarily post tensioned. A double channel was bolt connected to the backside of the base connection, and a steel angle was placed at the top of the 10m wall. Two 0.5” strands, stressed to 80% fu were used to PT the wall. Figure 12.20 shows the temporary post-tensioning for the wall.

Figure 12.20 Temporary post-tensioning for wall

12.6.6 Assembly and shipment

The walls were assembled into a core configuration in Canada. This process involved the construction of temporary lifting lugs to tilt the wall up into a C-shaped configuration, shown in Figure 12.21 (a). The walls were then aligned, and the steel X-braces were installed inside the core. To accomplish this, the steel braces were fabricated slightly smaller, lifted into the core, then turned into place. The gap between the wall and the brace was grouted in. The grouted in cross-bracing is shown in Figure 12.21 (b).

(a) (b)

Figure 12.21 Tilt up of the reinforced core wall

The core walls were then lifted into shipping containers using straps at two locations on the core wall, shown in Figure 12.22. Wood dunnage was laid out on the bottom of the container and the walls placed inside. Lateral bracing was applied to the walls to prevent them from sliding during the shipment.

Figure 12.22 Lifting into shipping container

12.6.7 Construction in China

The foundation and mass block frames were constructed by Best Steel in Shanghai China. The walls were tilted up using two cranes, as shown in Figure 12.23 (a). Both the 30' and 18' walls were erected and have been laterally secured, shown in Figure 12.23 (b). At the time of writing this dissertation, Covid-19 has resulted in global shutdowns and halted international collaborations, including this project. Therefore, final testing has not yet occurred and cannot be included within this thesis. The remaining planned steps in construction are shown in Appendix I.

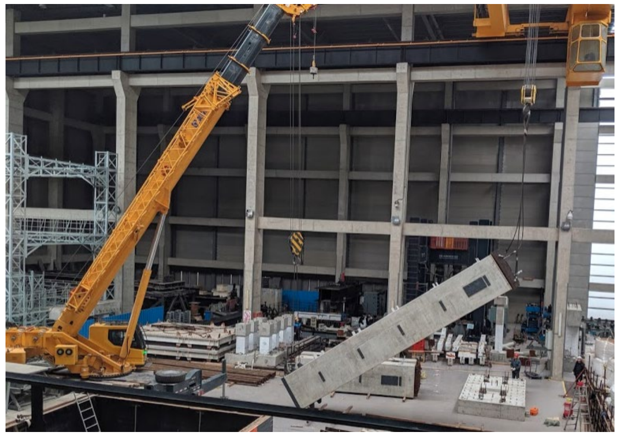

(a)

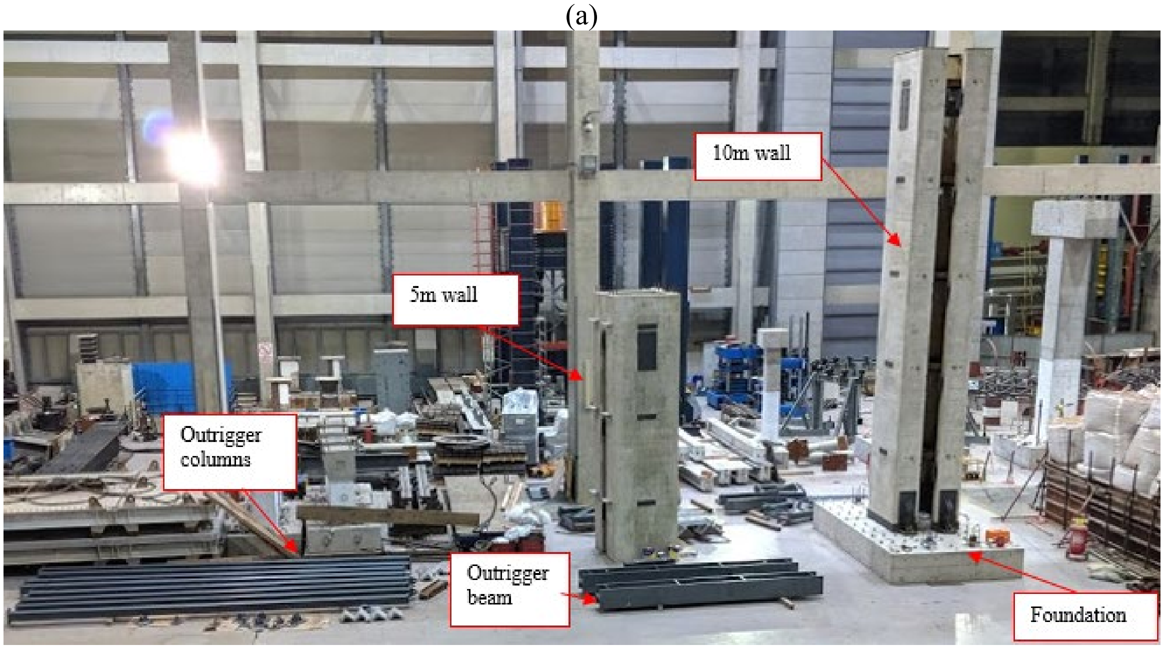

(b)

Figure 12.23 Current status of construction at Tongji University: a) tilt-up of RC wall and b) tilted up walls

12.7 Testing plan overview

To study the performance of the CORW and SCCW behaviour, the specimen designed in Chapter 12 will undergo 5 phases of shaking table tests: Phase A, Phase B, Phase C, Phase D, and Phase E. Figure 12.24 shows each of these 5 phases.

In Phase A, the proposed CORW system will be tested under unidirectional shaking. Three shaking table intensities will be tested: SLE, DBE, and MCE. At the SLE shaking intensity, no yielding is expected within the specimen. At the DBE shaking intensity level, the dampers at the top are expected to dissipate the earthquake energy, while the base of the wall is designed to remain elastic.

At the MCE shaking intensity level, the dampers at the top of outrigger columns and the base of the wall are expected to dissipate the earthquake energy to prevent the structure from collapse.

In Phase B, the proposed SCCW will be tested under unidirectional shaking under four different shaking intensities. It is anticipated that these tests will show that there is no damage under SLE shaking intensity. The SCFDs will yield and dissipate energy at the DBE shaking intensity. Finally, at the MCE shaking intensity, the dampers at the base are expected to yield and start dissipating energy.

In Phase C, the CORW and the SCCW systems will be tested under bidirectional shaking, which will validate that the system can achieve the desired performance objectives.

In Phase D, the outrigger will be removed, and the rocking wall will be tested under unidirectional shaking. The result will be used to compare the rocking wall behaviour with and without an outrigger system. In Phase E, the base of the wall will be fixed, and the conventional shear wall will be tested under unidirectional shaking.

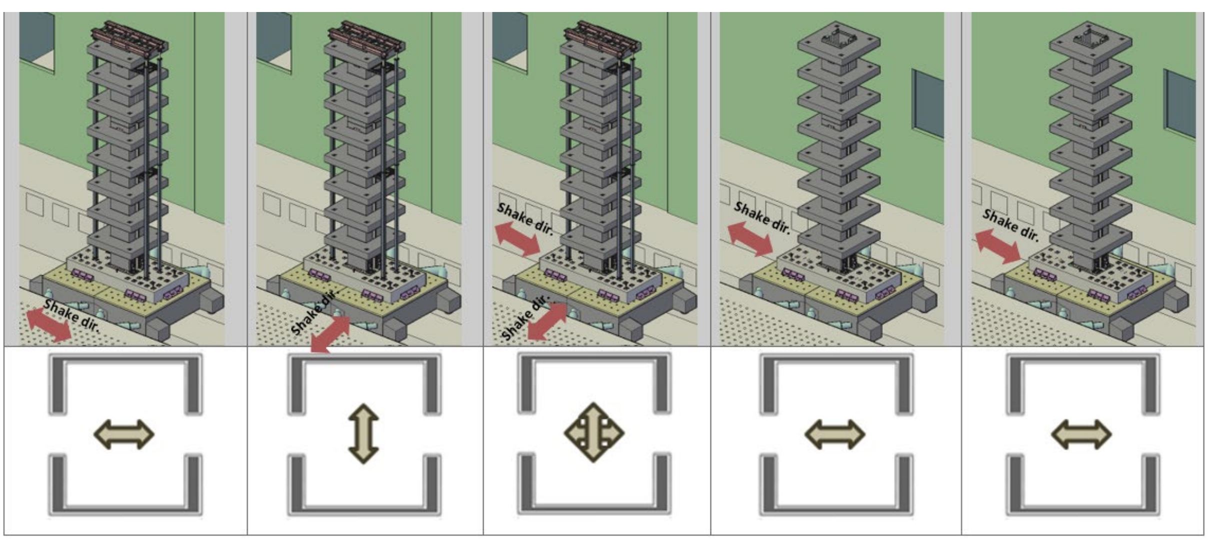

(a) CORW (b) SCCW (c) CORW (d) RW (e) SW

Figure 12.24 Shake table testing plan.

12.8 Ground motion selection and scaling

Only one ground motion is used for all phases of testing. Due to the limitations of the shaking table, only the horizontal motions are applied, and the vertical ground motion inputs are neglected. The dynamic testing of scaled specimens also requires the similitude scaling of the ground motions. The following sections discuss the methods to determine the scaling factors and the ground motion selection.

12.8.1 Similitude

The scaling factor for time and acceleration depends on the mass scaling factor. The total estimated mass of the specimen above the foundation is 97 tonnes, based on the mass of each component shown in Table 12.4. The total seismic mass in the prototype building is 17,812 tonnes. Hence, the scaling factor for mass is $s_m = \frac{1}{184}$, calculated using Equation 12.5.

$$s_m = \frac{M_{sp}}{M_{pr}} = \frac{97 \text{ tonne}}{17{,}812 \text{ tonne}} = \frac{1}{184}$$ Equation 12.5

Table 12.4 Estimate specimen masses

Mass block frame	1 tonne per floor x 8 floors = 8 tonnes
Core wall	20 tonne
Outrigger beam	1.7 tonne
Outrigger columns	2.5 tonnes
SCFDs	0.8tonne
Mass blocks	2tonne x 4 per floor x 8 floors = 64tonne
Total mass	97 tonne

With the mass and length scaling factors, the acceleration, time, and velocity scaling factors can be calculated. Acceleration scaling factor, s_A, is determined by the ratio of the specimen acceleration to the prototype acceleration. The acceleration scaling factor is derived using Equation 12.6

$$s_A = \frac{acc_{sp}}{acc_{pr}} = \frac{F_{sp}}{M_{sp}}\frac{M_{pr}}{F_{pr}} = \frac{s_l^2}{s_m} = 4.36$$ Equation 12.6

where acc_{sp}, F_{sp}, and M_{sp} is the acceleration, force, and mass, respectively, for the specimen and acc_{pr}, F_{pr}, and M_{pr} is the elastic modulus, stress, and strain, respectively, for the prototype.

The time scaling factor, s_t, is determined by the ratio of the specimen time to the prototype time. This scaling factor can be applied to any time unit used in the analysis of the specimen, such as natural period or ground motion time. The time scaling factor is derived in Equation 12.7

$$s_t = \frac{t_{sp}}{t_{pr}} = \sqrt{\frac{L_{sp}}{acc_{sp}}\frac{acc_{pr}}{L_{pr}}} = \sqrt{\frac{s_m}{s_l}} = 0.19 \qquad \text{Equation 12.7}$$

where t_{sp} is the specimen time unit and t_{pr} is the prototype time unit.

The velocity scaling factor, s_v, is determined by the ratio of the specimen velocity to the prototype velocity. This scaling factor can be applied to any velocity unit used in the analysis of the specimen, such as ground motion velocity. The velocity scaling factor is derived in Equation 12.8.

$$s_v = \frac{vel_{sp}}{vel_{pr}} = \frac{t_{sp}}{t_{pr}}\frac{acc_{sp}}{acc_{pr}} = s_t s_a = \sqrt{\frac{s_l^3}{s_m}} = 1.22 \qquad \text{Equation 12.8}$$

where vel_{sp} is the specimen velocity unit and vel_{pr} is the prototype velocity unit.

12.8.2 Ground motion selection

The ground motion was selected as the motion which is close to the uniform hazard spectrum (UHS) at the MCE, while having a low peak ground acceleration. The UHS of the prototype building located in Vancouver, Canada is used. To reduce the variabilities caused by using different ground motions for different hazards, the same ground motion was used to test the SLE, DBE, and MCE shaking levels. The SLE and DBE were estimated as 8.5% and 30% of the MCE, respectively.

The ground motion was selected to be from the 1992 Landers Earthquake, California (PEER ID: RSN 832). The selected ground motion was first scaled by factor of 0.19, 0.63, and 2.26 to match the prototype SLE, DBE, and MCE, respectively. The corresponding scaled acceleration spectrum for the North-South and West-East components, geomean, and design spectrums are shown in

Figure 12.25. In this figure $S_{a,s}$ = specimen pseudo acceleration, T_s = specimen period, S_A = acceleration scaling factor, and S_t = time scaling factor.

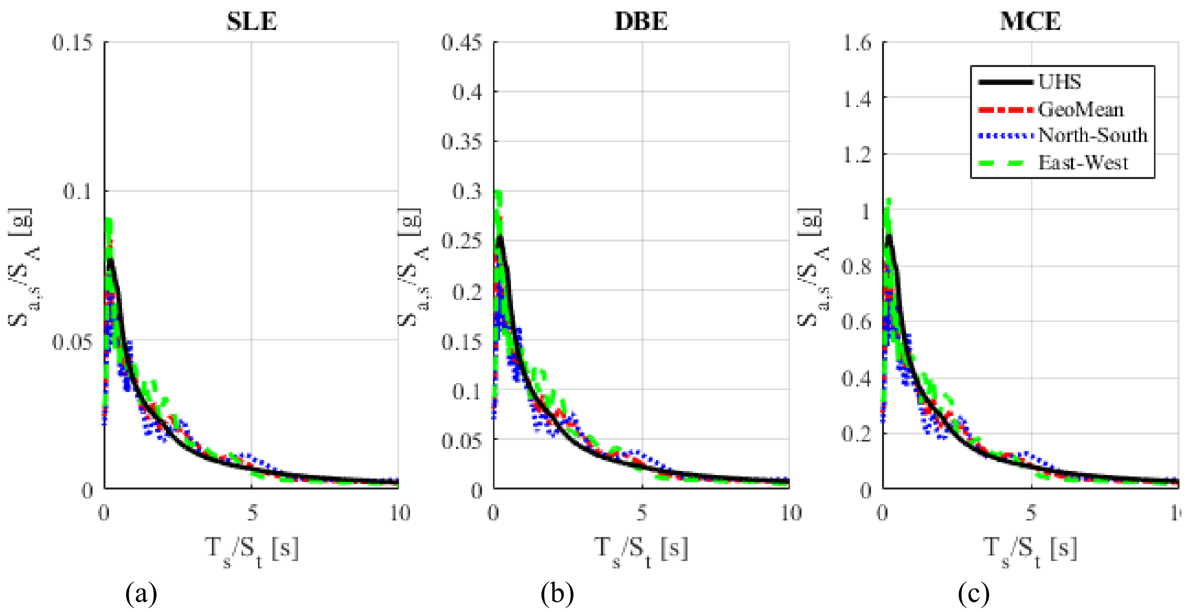

Figure 12.25 Scaled ground motion acceleration spectrums for the (a) SLE, (b) DBE, and (c) MCE hazards.

12.9 Instrumentation plan

In the proposed instrumentation there are 342 displacement gauges, 10 accelerometers, 16 load cells, and 202 strain gauges. Figure 12.26 shows the naming convention for all the planned instrumentation. Global displacements are measured using string pots which will be anchored to the walls and on to stationary frames situated off the table. Two lateral displacement measurements are recorded at three of the wall corners. In this test, it is assumed that each floor acts as a rigid diaphragm. Vertical deformations are measured using LVDTs at each corner of the core wall. Two additional vertical LVDTs are attached at the flange end. Figure 12.27 shows a typical plan view; Figure 12.28 shows the elevation view in the N-S direction; and Figure 12.29 shows the elevation view in the W-E direction.

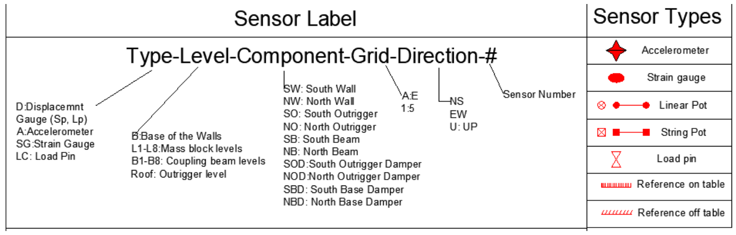

Figure 12.26 Instrumentation naming convention

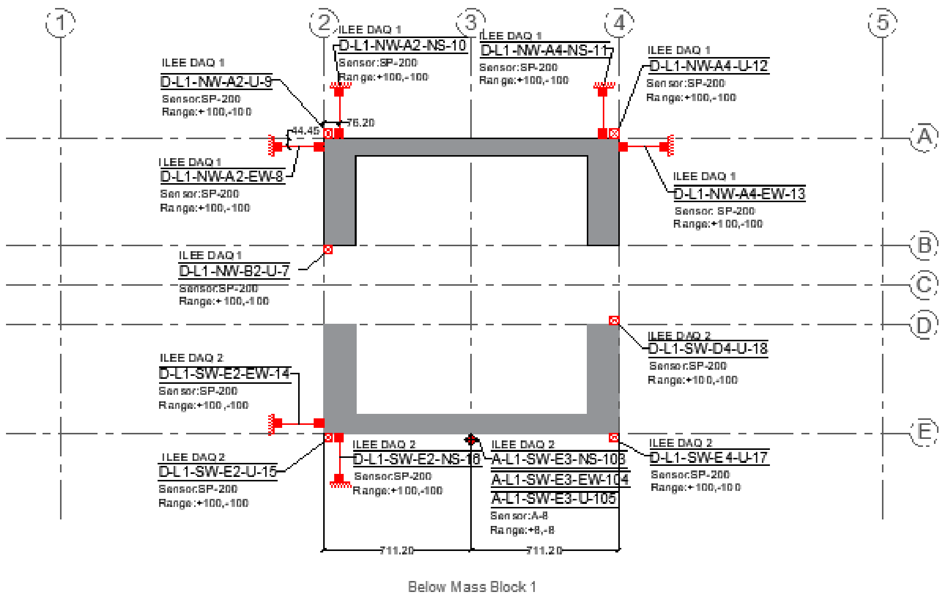

Figure 12.27 Instrumentation typical plan view

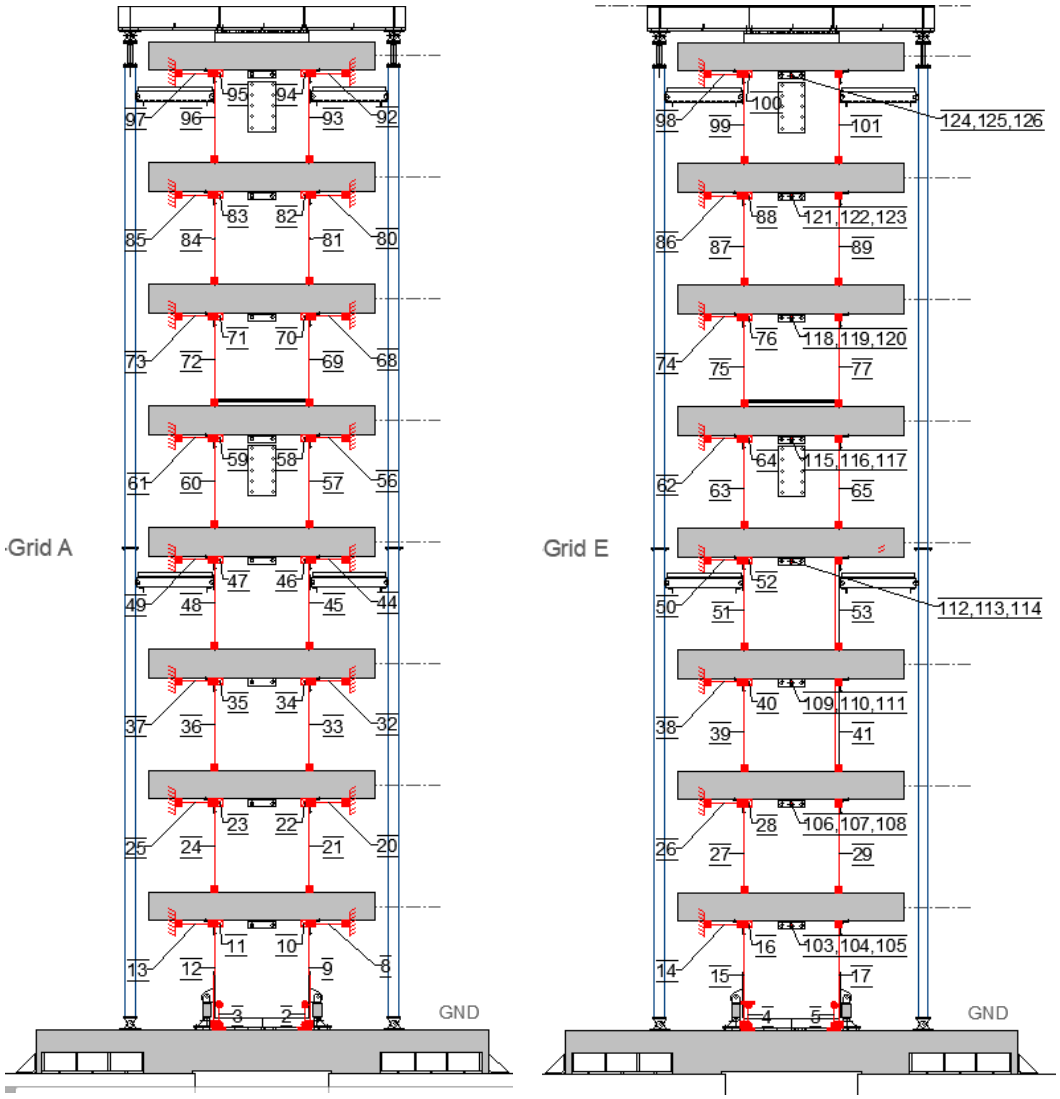

(a) (b)

Figure 12.28 Displacement transducers (North-South) views (a) Elevation- Grid A and (b) Elevation – Grid E

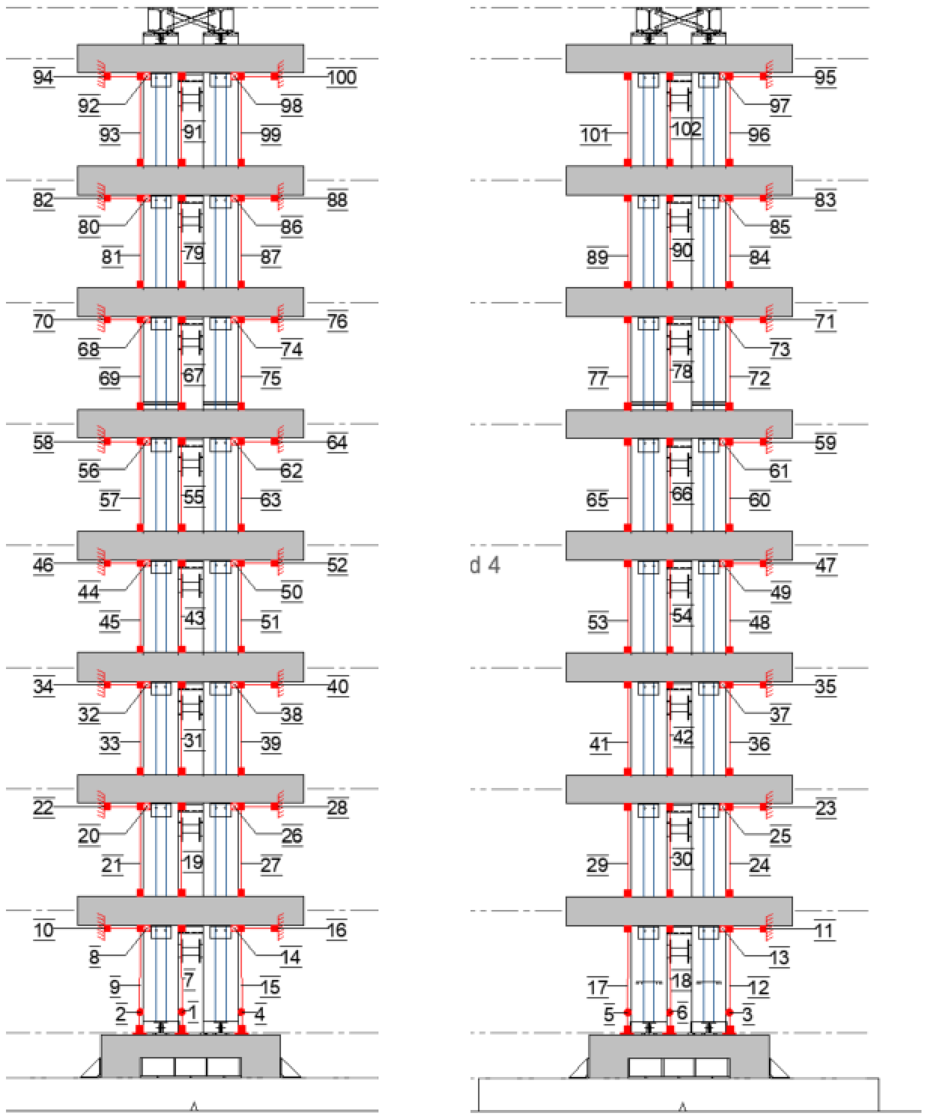

(a) (b)

Figure 12.29 Displacement transducers (East-West) views (a) Elevation- Grid A and (b) Elevation – Grid E

Strain gauges are attached to the top and bottom of two W8x15 beams on the North side of the wall. Due to limitations on instrumentation, strain gauges are attached to only one of the coupling beams on the south side. Figure 12.30 shows a typical LVDT layout each of the coupling beams. Two LVDTs are connected to estimate the shear deformation within the SCFD.

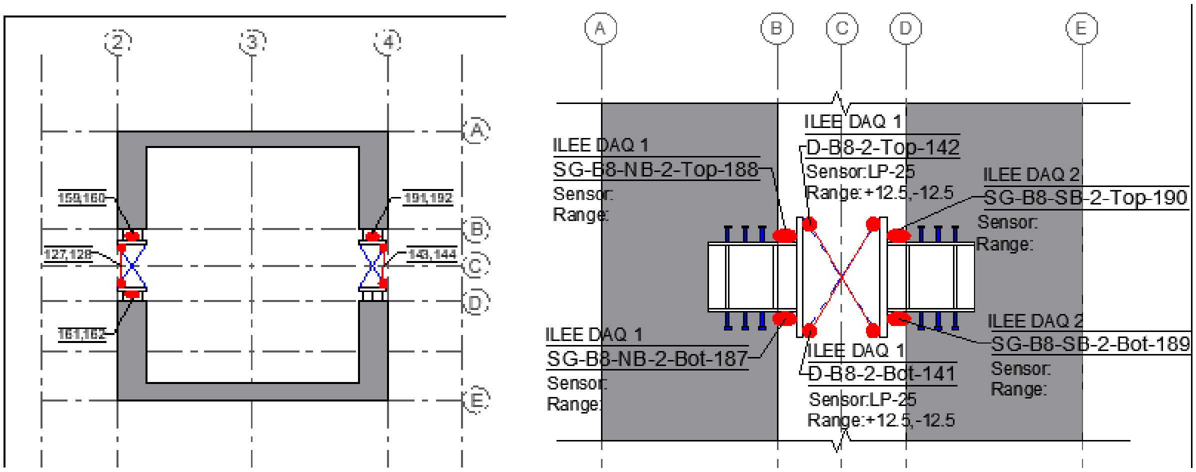

(a) (b)

Figure 12.30 Coupling beam instrumentation plan

Strain gauges are attached to the outrigger beam, shown in Figure 12.31 (a) (side view) and in Figure 12.31 (b) (front view). These gauges will later be used to estimate the elastic stresses in the beam. LVDTs will be used to measure the deformations in all both the outrigger dampers and the wall-base dampers. Load pins will be used to measure the forces within the dampers. The PT strand forces are measured using force load cells for every PT strand.

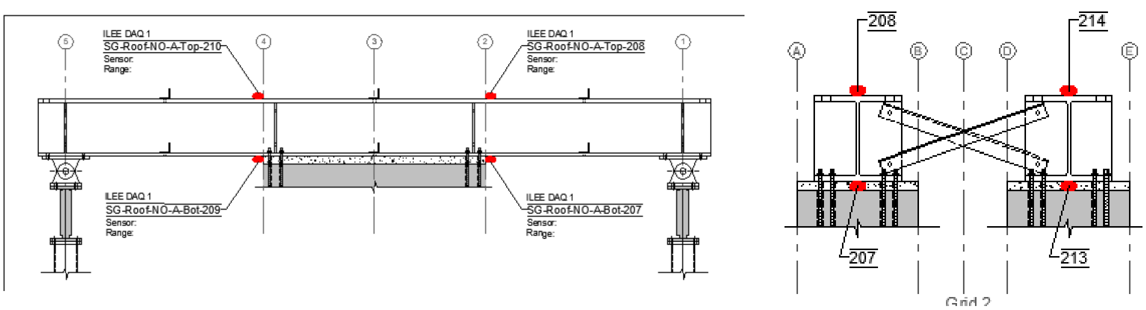

(a) (b)

Figure 12.31 Outrigger damper instrumentation

12.10 Predicted response

In this section, a detailed numerical model of the specimen is developed using Perform3D. The selected ground motion, shown in Figure 12.25 was simulated and the model, and the seismic performance evaluated.

12.10.1 Modelling approach

A detailed numerical model was developed to estimate the response of the shake table testing. The detailed model utilises the modelling approach described in Chapter 6. Like the modelling approach outlined in Chapter 6, a 3-dimensional model was developed using Perfom3D. Figure 12.32 (a) shows the model in the SCCW view, Figure 12.32 (b) shows the model in the CORW view, and Figure 12.32 (c) shows the plan view. Unlike the prototype building models, additional details unique to the specimen, such as the PT tendons, and the internal braces, were all added as elastic elements.

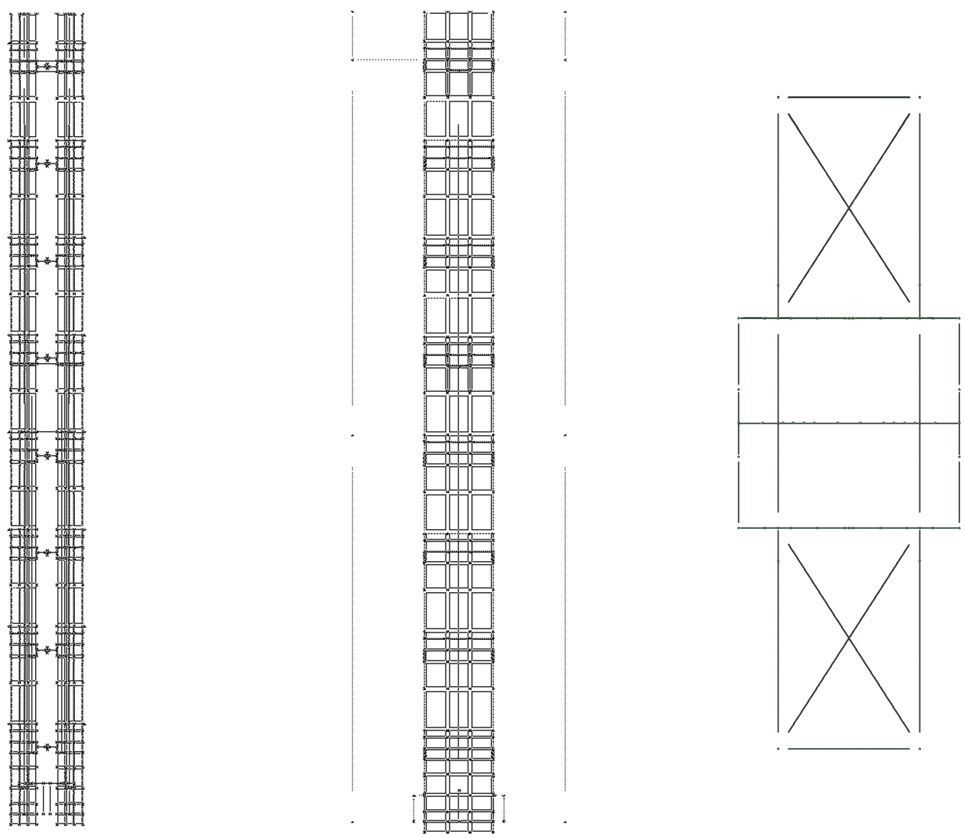

(a) (b) (c)

Figure 12.32 Numerical modelling of shake table specimen: (a) SCCW view, (b) CORW view, and (c) plan view

Eigen-value analysis was completed on the detailed model. Figure 12.33 shows the mode shapes and periods. The scaled specimen results in a scaled period of 3.10, 2.24, and 1.58 for the first, second, and third modes respectively. This is a 6.0%, 4.1%, and 3.8% difference in period with the prototype building, respectively.

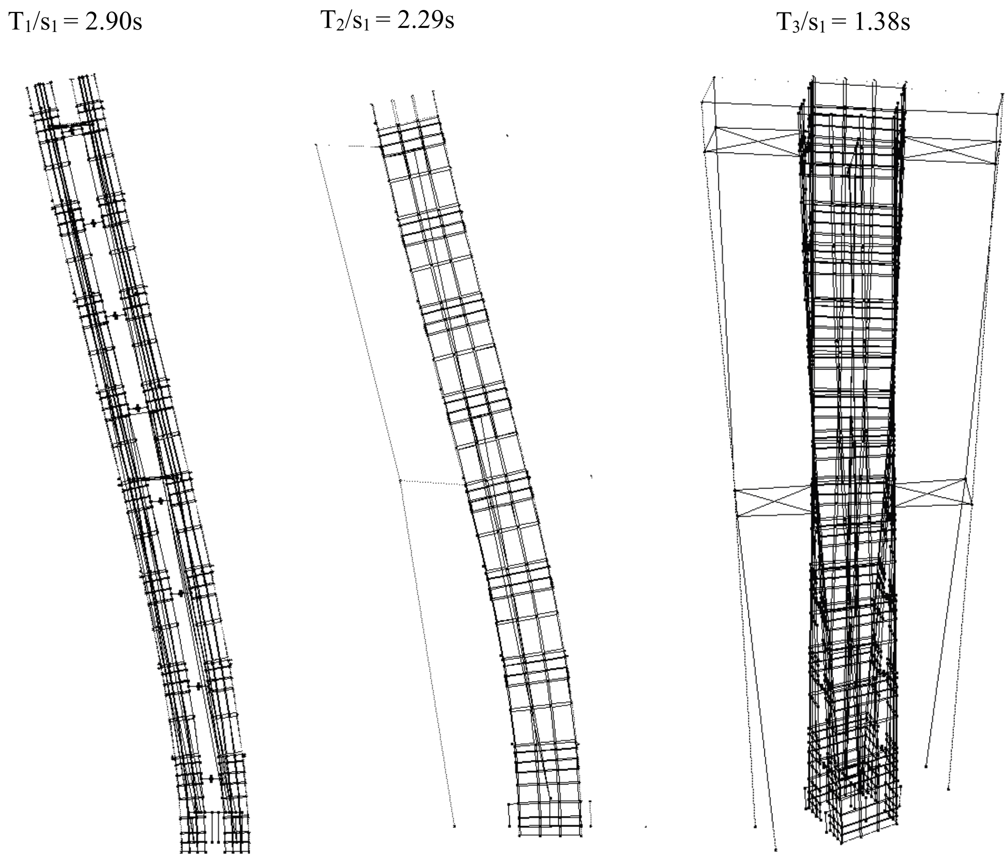

(a) (b) (c)

Figure 12.33 Mode shapes for each specimen model, including: 24 story Mode 1 (a), Mode 2 (b),

12.10.2 Nonlinear responses

The nonlinear model was subject to the ground motion selected in Section 12.8.2. The model was subjected to both unidirectional and bidirectional loading. The peak displacements were recorded at each of the four corners of the RC core-wall, at the locations of the planned instrumentation.

Figure 12.34 shows the peak story displacements (Δ_s) for each hazard, at each wall corner, normalised to the building height (H). Generally, there is a negligible difference between the displacements at each corner for unidirectional loading (i.e., no torsion is observed).

At the SLE, there is minimal differences (less than 2%) between bidirectional and unidirectional displacements, indicating that there is minimal elastic torsion in the system. However, at the DBE and MCE, more significant differences are observed between the unidirectional and bidirectional motions.

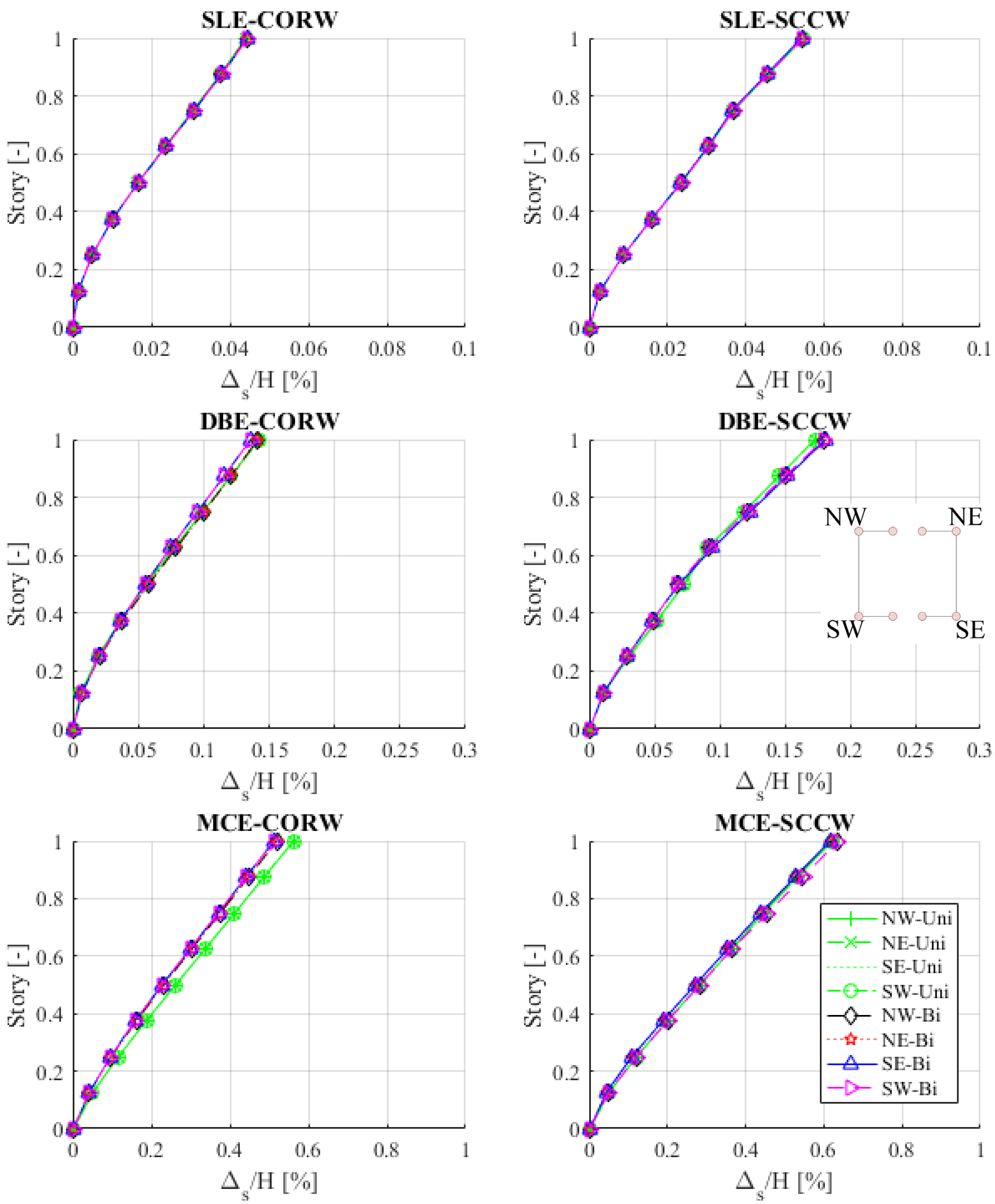

Figure 12.34 Predicted normalised story displacements: (a) SLE-CORW; (b) SLE-SCCW; (c) DBE-CORW; (d) DBE-SCCW; (e) MCE-CORW; and (f) MCE-SCCW

Figure 12.35 shows the outrigger damper forces (f_o) normalised to the yield force (f_y) in each of the four outrigger dampers at each hazard level. As shown, at the SLE f_o/f_y dampers are below yielding at the SLE, which is the performance objective at the EEDP design. At the DBE and MCE, the f_o/f_y=1 for all dampers, indicating yielding, which is the performance objective at the EEDP design.

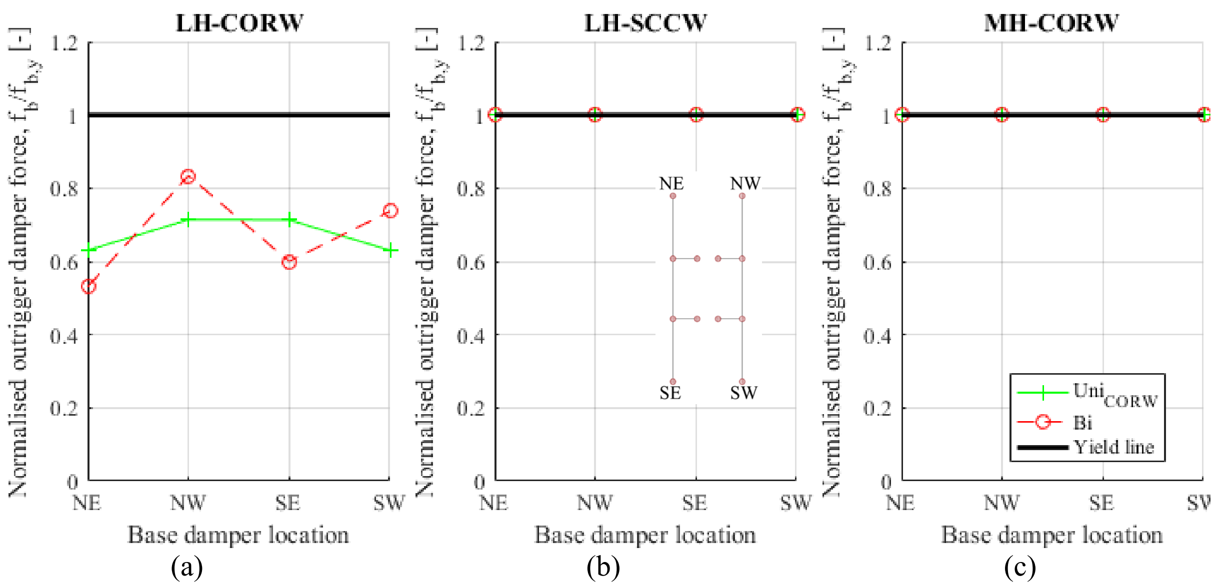

Figure 12.35 Specimen outrigger damper predicted normalised force: (a) SLE shaking intensity; (b) DBE shaking intensity; (c) MCE shaking intensity

Figure 12.36 shows the wall-base damper forces (f_b) normalised to the yield force ($f_{b,y}$) in each of the four wall-base dampers at each hazard level. As shown, at the SLE $f_b/f_{b,y}$ dampers are below yielding at the SLE and DBE, which is the performance objective at the EEDP design. At the MCE, the f_b/f_y=1 for all dampers, indicating yielding, which is the performance objective at the EEDP design.

Figure 12.37 (a), (b), and (c) shows the coupling beam forces (V_{CB}) normalised to the yield force ($V_{CB,y}$) in each of the coupling beams at the SLE, DBE, and MCE hazards, respectively. As shown, at the SLE $V_{CB}/V_{CB,y}$ dampers are below yielding at the SLE, which is the performance objective at the EEDP design. At the DBE and MCE, the $V_{CB}/V_{CB,y}$ is greater than 1 for all dampers, indicating yielding, which is the performance objective at the EEDP design. Unlike the wall-base and outrigger dampers, the ratio of the $V_{CB}/V_{CB,y}$ is greater than 1 after yielding due to the post-yielding stiffness of the dampers.

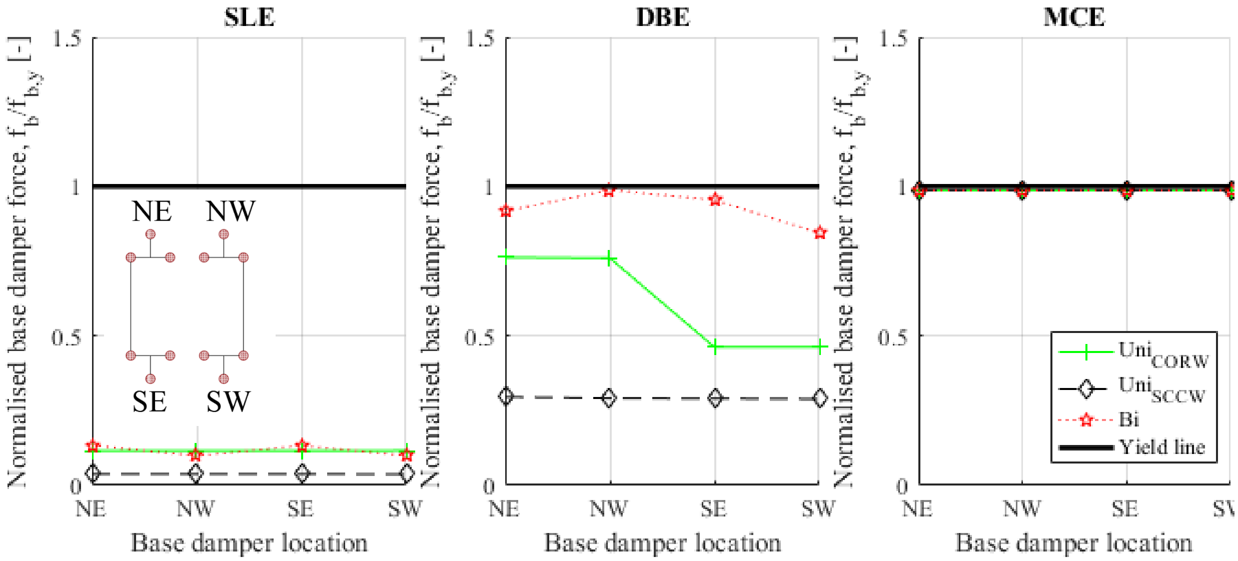

(a) (b) (c)

Figure 12.36 Wall-base normalised wall-base damper force: (a) SLE shaking intensity; (b) DBE shaking intensity; (c) MCE shaking intensity

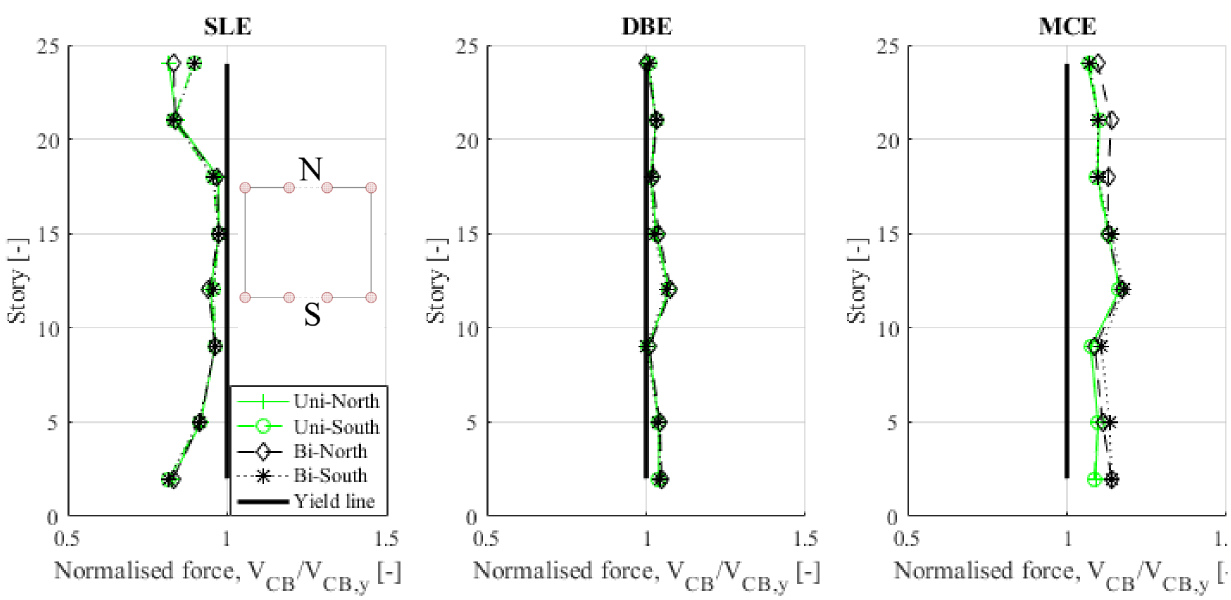

(a) (b) (c)

Figure 12.37 Specimen normalised coupling beam force: (a) SLE shaking intensity; (b) DBE shaking intensity; (c) MCE shaking intensity

Figure 12.38 shows the normalised strain for each hazard, for each direction of loading. At each node, strains are determined by taking the difference between the vertical displacements at each wall corner divided by the distance between the nodes. The tension strains are normalised to the yield strain of rebar ($\varepsilon_y = 0.002$). All strains are below yielding (i.e., $\varepsilon/\varepsilon_y$<1), demonstrating the EEDP performance objectives have been met.

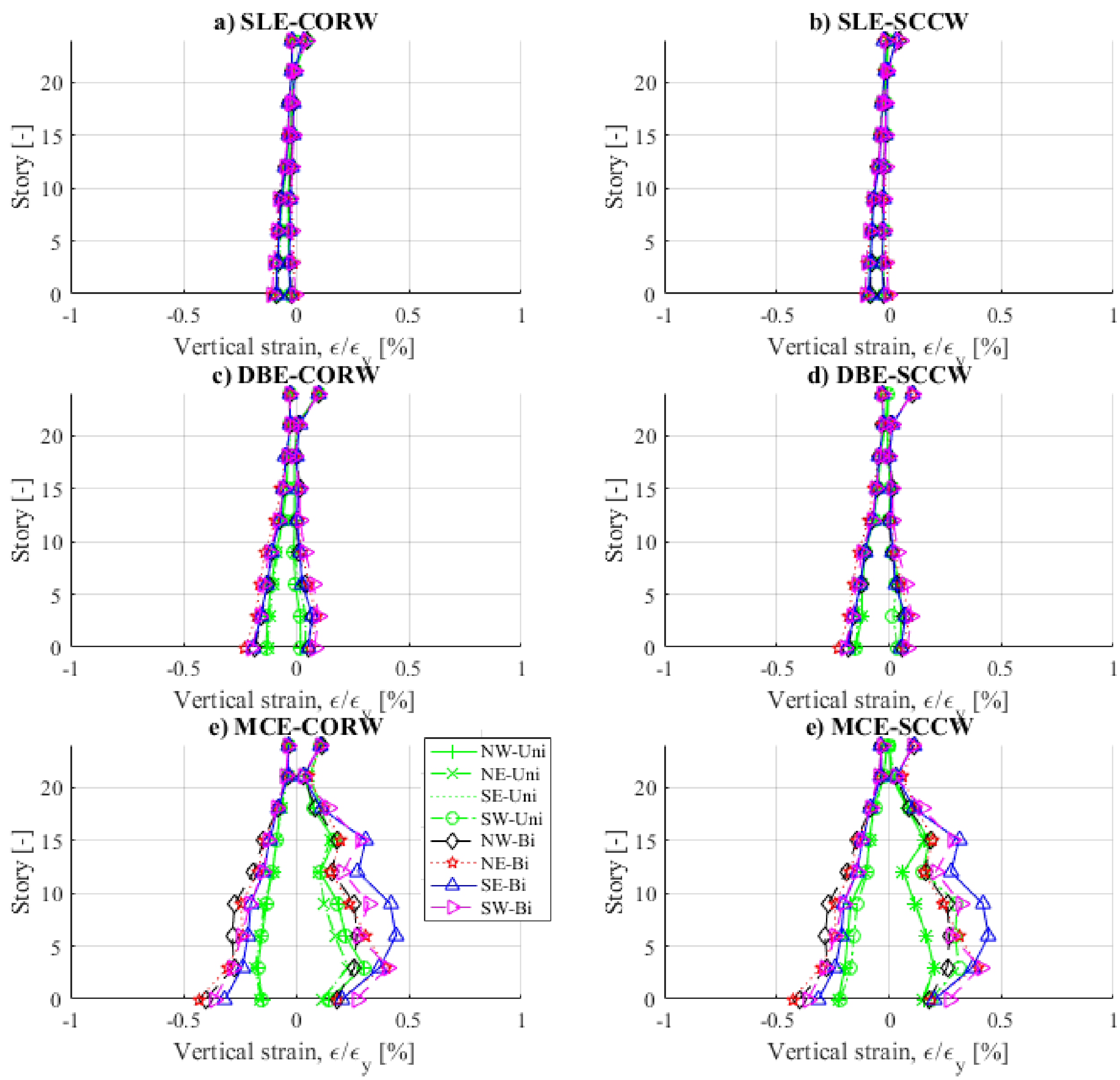

Figure 12.38 Specimen normalised vertical wall strain: (a) SLE-CORW; (b) SLE-SCCW; (c) DBE-CORW; (d) DBE-SCCW; (e) MCE-CORW; and (f) MCE-SCCW

12.11 Summary

This chapter describes the work completed towards shake-table testing of the CROCW. An overview of the testing facility, specimen scaling, design, and construction is provided. The design and construction of the testing specimen is a key contribution in this thesis. All components are currently in China, awaiting the opening of international borders at the time of writing this dissertation, such that experimental testing may continue.

This chapter also describes the testing plan which will be implemented after international borders open and research collaborations continue. A description of the testing phases and the instrumentation plan were provided. A detailed numerical model of the specimen was developed and was summarised in this chapter. The numerical model demonstrates expected high seismic performance of the proposed system.

Chapter 13: Summary of work and recommendations for future work

This thesis introduced three new seismic force resisting systems for earthquake-resilient high-rise buildings: the controlled rocking outrigger core wall (CROCW), the controlled outriggered rocking wall (CORW) and the self-centring coupled wall (SCCW). Additionally, a novel non-iterative design approach was developed, using the Equivalent energy-based design procedure (EEDP) with modifications to incorporate higher mode effects and hysteretic behaviour of the new systems. The presented EEDP is recommended to design the proposed systems for multiple performance objectives at different shaking intensities. The following describes some of the unique contributions of this work and ideas for future investigations.

13.1 Contributions

The overarching goal of this research was to provide alternative lateral force resisting systems and design methods for the RC core wall system which will result in enhanced seismic performance. The detailed contributions made towards these goals are discussed in the following sections.

13.1.1 Proposed a novel high-performance RC core wall system

This thesis provided an extensive literature review on energy dissipation devices and low-damage RC wall systems. From this review, a new RC core wall system was proposed. This new system is comprised of two unique systems along each principal axis, the CORW in the shear wall direction and the SCCW in the coupled wall direction.

Both systems are “dual-fused” and have a primary yielding mechanism and a secondary yielding mechanism. The systems are designed to remain elastic at a low hazard, yield the primary fuse system at the moderate hazard, and yield the primary fuse system and secondary fuse system at the high hazard.

The CORW primary fuse system is a damped outrigger, and its secondary fuse system is a damped controlled rocking base. This thesis details the mechanics of the primary fuse system and secondary fuse systems and provides discussion on the influence of important design parameters on the response.

The SCCW system's primary fuse system consists of novel self-centering coupling beams called Self-centering conical friction dampers (SCFD), and its secondary fuse system is a damped controlled rocking base. The author of this thesis heavily contributed to the development of the SCFD and is listed as a co-inventor on two patents and co-author on one journal paper. In this thesis, the behaviour of the SCFD and equations to estimate the hysteretic response are provided. Additionally, discussion on implementation of the SCFD in the SCCW is presented.

The use of a controlled rocking base as the secondary mechanisms in the CORW and SCCW allow this system to function efficiently under bidirectional loading. This thesis presented some of the challenges with the response of a controlled rocking base within a coupled wall system.

The outcome of this contribution is two unique systems which can be integrated into a centralised RC core wall, where the mechanical behaviour and plastic mechanisms are well understood. Hence, these systems may be used as a low-damage solution to RC core walls.

13.1.2 Quantified dynamic characteristics of the RC core wall systemS

This thesis studied the dynamic characteristics of the proposed earthquake-resilient RC core wall using linear dynamic analysis. From these studies empirical equations were developed to rapidly predict the higher mode responses of the systems.

From these analyses, it was observed that the CORW has a first mode dominant response in roof displacement, base moment, and outrigger moment. It was discovered that the CORW behaviour is highly dependent on the relative stiffness of the outrigger to the wall. This stiffness ratio was quantified using a factor α_f. Most of the empirical equations developed depend on this factor. Additionally, it was shown that the inverted triangular distribution gives a reasonable estimate of the force distribution to design the yielding mechanism for the CORW.

The dynamic analysis demonstrated that the SCCW has a significant higher mode response in the coupling beams and wall pier moments. As a result, a new static load distribution was developed to appropriately estimate the coupling beam shears.

13.1.3 Development of Equivalent Energy Based Design Procedure for earthquake resilient tall buildings

This thesis presented a design method for the proposed CROCW, CORW, and SCCW systems using EEDP with some modifications. The original derivation of EEDP assumes an elastic-plastic response for the primary fuse system and secondary fuse systems. The CORW has an elastic-plastic response for the outrigger system and a flag-shaped hysteretic response for the controlled rocking base. Therefore, new gamma factors were developed to apply EEPD to this system. Additionally, new gamma factors were developed for the SCCW, which has a self-centring hysteretic behaviour as the primary fuse system and secondary fuse system.

The original EEDP was developed for buildings which have a first mode response. The nature of tall core wall buildings is to have a dominant first mode response in displacements, but a higher mode response in terms of forces. In this study, the higher mode force response was estimated using linear dynamic models. The dynamic response was translated as factors to be incorporated with the EEDP.

The introduction of the higher mode factors and the gamma factors allows the SCCW and the CORW to be designed for multiple different performance objectives under different shaking intensities. A step-by-step guide to designing the SCCW and the CORW are provided, giving practitioners and researchers the tools to apply this procedure to design these new systems.

This thesis's design procedure has significant advantages compared with typical code-based design or other performance-based design methods. Specifically, it allows the design of multiple performance objectives at different shaking intensities. However, unlike other performance-based design methods, EEDP allows for the design to be completed without iterations. Hence, EEDP can be used as an efficient design method for the novel CORW and SCCW systems.

13.1.4 Assessed the performance of earthquake-resilient core wall buildings

A robust 3-dimensional modeling approach was developed for researchers and practitioners to use in design validation, performance-based design, and performance assessments of the CROCW system. The development of this modeling approach allows for researchers and practitioners alike to model the complex behaviour of the proposed earthquake resilient RC core wall system.

Four prototype buildings, representing different building heights and hazards, were designed and analyzed using the 3-dimensional modeling approach. Nonlinear dynamic analysis, using both unidirectional and bidirectional motions, was conducted on the four prototype buildings that were designed using the new systems.

Within this dissertation is a comparison between alternative shear wall systems and the CORW systems and alternative coupled wall systems and the SCCW systems. The CORW was compared with three other RC wall systems: the shear wall (SW), the outriggered wall (OW), and the controlled rocking wall (CRW). The SCCW was compared with three other RC coupled wall systems: the coupled wall (CW), the damped coupled wall (DCW), and the controlled rocking coupled wall (CRCW).

These comparisons demonstrated the significant higher performance when using the new technology and design methods in this thesis. For example, the CORW demonstrated 52% decrease in interstorey drifts and 22% decrease in roof displacements when compared with the conventional fixed based shear wall (SW). Similarly, the SCCW showed a 22% reduction in displacements when compared with conventional coupled wall (CW) building with the same yield force in the coupling beams. This outcome exemplifies the low damage performance of the proposed systems compared to existing technology.

13.1.5 Development of experimental program

As part of this work, a large-scale shake table specimen was designed and constructed. The objective was to design a large-scale specimen that could provide realistic local as well as global response of the system under earthquake loads. There was a significant effort to ensure the specimen was designed to meet the high-quality construction standards in typical Canadian practice. At the time of submitting this dissertation, Covid-19 travel restrictions have paused the experimental schedule.

13.2 Ongoing and Future work

This thesis presented the concept, design approach, numerical validation, and numerical comparison between the novel and conventional systems. There are several avenues for future work, particularly in experimental testing of this new system. The following describe some of the areas of future work.

The large-scale shake table testing will be completed once the Covid-19 related travel restrictions are lifted, and it is safe to continue testing. The remaining work involves specimen assembly, instrumentation, re-testing friction devices, and the shake table testing. The results from this experiment will help to validate the numerical models, developed as part of this research work. It is expected that the large-scale shake table testing will give key insight to the dynamic response of controlled rocking tall buildings.

After these shake table tests are completed, researchers can use this data to develop and calibrate numerical models of the CORW and SCCW systems. This data will allow for detailed study of the response of a range of prototype buildings, and further validate this new system. Additionally, researchers can use the data to further the understanding of coupling beam shear distribution in core wall buildings.

This thesis work focused on the response of the lateral force resisting system, while assuming the gravity system would be appropriately detailed to accommodate the deformation demands. Future research can be centered on the development of a gravity force resisting system which can work with the CORW and SCCW to ensure damage resistance.

The controlled rocking base is assumed to be on a fixed base; there was no investigation into the foundation design or the effects of podium on the response. Further investigations are required to understand the influence of the podium.

In this research, the controlled rocking base was assumed to be confined with steel plates and the sensitivity of this confinement was not examined. Future work could focus on detailed design procedures to determine appropriate rocking base design for wall systems.

The parametric analysis to quantify the higher mode effects of the system used idealized wall geometry and linear dynamic analysis. Future work could improve these design relations by conducting robust nonlinear parametric analysis using a variety of core wall geometry.

This work did not account for the wind demands within the design procedure. Wind can substantially increase the demands in high-rise building. Future work should address the consideration of wind demands.

This work did not consider the effect of vertical ground motions on the response of the controlled rocking system. Future work should include the effects of vertical ground motions on the controlled rocking tall building system.

References

Adebar P, Ibrahim A., Bryson M. (2007). Test of High-Rise Core Wall: Effective Stiffness for Seismic Analysis. ACI Structural Journal, 104(5). https://doi.org/10.14359/18857

Adebar, P., DeVall, R., and Mutrie, J. “Evolution of High-Rise Buildings in Vancouver, Canada.” Structural Engineering International, vol. 27, no. 1, Informa UK Limited, Feb. 2017, pp. 7–14. Crossref, doi:10.2749/101686617x14676303588670.

Ahn, T.-S., Kim, Y.-J., & Kim, S.-D. (2013). Large-Scale Testing of Coupled Shear Wall Structures with Damping Devices. Advances in Structural Engineering, 16(11), 1943–1955. https://doi.org/10.1260/1369-4332.16.11.1943

American Society of Civil Engineers. ASCE. (2016). Minimum Design Loads for Buildings and Other Structures (ASCE/SEI 7-16).

American institute of steel construction (AISC). (2016). Seismic Provisions for Structural Steel Buildings (ANSI/AISC 341-16).

Aktan, A. E., and Bertero, V. V. (1984). “Seismic response of R/C framewall structures.” J. Struct. Eng., 10.1061/(ASCE)0733-9445(1984) 110:8(1803), 1803–1821.

Buchanan, A., Bull, D., MacRae, G., Palermo, A., & Pampanin, S. (2011). *Base Isolation and Damage-Resistant Technologies for Improved Seismic Performance of Buildings. A report written for the Royal Commission of Inquiry into Building Failure Caused by the Canterbury Earthquakes.* Christchurch, NZ: University of Canterbury.

Canadian standards association (CSA). (2014). Design of concrete structures (CSA A23.3).

Constantinou, M.C. and Symans, M.D. (1992). Experimental and Analytical Investigation of Seismic Response of Structures with Supplemental Fluid Viscous Dampers” Technical Report NCEER-9290032, National Center for Earthquake Engineering Research, SUNY/Buffalo.

Canbolat, A., Parra-Montesinos, G. and Wight, J. (2013). Experimental Study on the Seismic Behavior of High-Performance Fiber-Reinforced Concrete Low-Rise Walls. ACI Structural Journal, vol. 110, no. 5, doi:10.14359/51685830.

Cheng, M.-Y., Fikri, R., & Chen, C.-C. (2015). Experimental study of reinforced concrete and hybrid coupled shear wall systems. Engineering Structures, 82, 214–225. https://doi.org/10.1016/j.engstruct.2014.10.039

Council on Tall Buildings and Urban Habitat (CTBUH). CTBUH Year in Review: Tall Trends of 2019. Chicago, IL: CTBUH; 2020 http://www.skyscrapercenter.com/year-in-review/2019/data. Accessed August 11, 2020.

Chopra, A. K., & McKenna, F. (2015). Modeling viscous damping in nonlinear response history analysis of buildings for earthquake excitation. Earthquake Engineering & Structural Dynamics, 45(2), 193–211. https://doi.org/10.1002/eqe.2622

Christopoulos, C., & Montgomery, M. (2013). Viscoelastic coupling dampers (VCDs) for enhanced wind and seismic performance of high-rise buildings. Earthquake Engineering and Structural Dynamics, 42(15), 2217–2233. https://doi.org/10.1002/eqe.2321

Christopoulos, C., Tremblay, R., Kim, H.-J., & Lacerte, M. (2008). Self-Centering Energy Dissipative Bracing System for the Seismic Resistance of Structures: Development and Validation. Journal of Structural Engineering, 134(1), 96–107. https://doi.org/10.1061/(asce)0733-9445(2008)134:1(96)

Chung, H.-S., Moon, B.-W., Lee, S.-K., Park, J.-H., & Min, K.-W. (2009). Seismic performance of friction dampers using flexure of rc shear wall system. The Structural Design of Tall and Special Buildings, 18(7), 807–822. https://doi.org/10.1002/tal.524

CSI Perform 3D V7. (2018). Nonlinear Analysis and Performance Assessment for 3D Structures, Computer and Structures, Inc. Berkeley, CA.

Dehghani, M., & Tremblay, R. (2017). Design and full-scale experimental evaluation of a seismically endurant steel buckling-restrained brace system. Earthquake Engineering & Structural Dynamics, 47(1), 105–129. https://doi.org/10.1002/eqe.2941

Dusicka, P., & Iwai, R. (2007, October 10). Development of Linked Column Frame System for Seismic Lateral Loads. Structural Engineering Research Frontiers. Research Frontiers at Structures Congress 2007. https://doi.org/10.1061/40944(249)63

Etebarian, H., Yang, T. Y., & Tung, D. P. (2019). Seismic Design and Performance Evaluation of Dual-Fused H-Frame System. Journal of Structural Engineering, 145(12), 04019158. https://doi.org/10.1061/(asce)st.1943-541x.0002445

Fairhurst, M., Bebamzadeh, A., & Ventura, C. E. (2019). Effect of Ground Motion Duration on Reinforced Concrete Shear Wall Buildings. Earthquake Spectra, 35(1), 311–331. https://doi.org/10.1193/101117eqs201m

Motter, C., Fields, D., Hooper, J., Klemencic, R., & Wallace, J. (2014). UCLA-SGEL - Design Recommendations for Steel-Reinforced Concrete (SRC) Coupling Beams. Los Angeles: University of California Los Angeles.

FEMA, P-695. 2009. “Quantification of Building Seismic Performance Factors.” Washington, DC.

Filiatrault, A., Tremblay, R., & Kar, R. (2000). Performance evaluation of friction spring seismic damper. Journal of Structural Engineering New York, N.Y., 126(4), 491–499. https://doi.org/10.1061/(ASCE)0733-9445(2000)126:4(491)

Fortney, P. J., Shahrooz, B. M., & Rassati, G. A. (2007). Large-Scale Testing of a Replaceable “Fuse” Steel Coupling Beam. Journal of Structural Engineering, 133(12), 1801–1807. https://doi.org/10.1061/(asce)0733-9445(2007)133:12(1801)

Fortney, P.J., Rassati G.A., Shahrooz, B.M. Investigation on Effect of Transverse Reinforcement on Performance of Diagonally Reinforced Coupling Beams. ACI Structural Journal [H.W. Wilson - AST]. 2008 November 1;105(6):781.

Gerard M. Nieblas, L., & Tran, P. (2020). STRUCTURE magazine | Wilshire Grand. Retrieved 31 December 2020, from https://www.structuremag.org/?p=8854

Goel SC, & Chao S. 2008. Performance-Based Plastic Design Earthquake-Resistant Steel Structures. International Code Council, Washington, DC.

Gong, B., and Shahrooz, B. M. (2001). “Concrete-steel composite coupling beams. I: Component testing.” J. Struct. Eng., 10.1061/(ASCE) 0733-9445(2001)127:6(625), 625–631. Gong, B., and

Gregorian, C. E., Yang, T. S., and Popov, E. P., (1992). Slotted Bolted Connection Energy Dissipators. Earthquake Engineering Research Center, Report No. UCB/EERC-9211

Galano, L. and Vignoli, A. (2000). Seismic Behavior of Short Coupling Beams with Different Reinforcement Layouts. (2000). ACI Structural Journal, 97(6). https://doi.org/10.14359/9633

Gavridou S., Wallace J.W., Nagae T., Matsumori T., Tahara K., Fukuyama K. (2017). Shake-Table Test of a Full-Scale 4-Story Precast Concrete Building. I: Overview and Experimental Results. J Struct Eng 143 (6): 04017034. doi:10.1061/(asce)st.1943-541x.0001755

Ghodsi, T., Ruiz, J.F., Massie, C., Chen, Y. (2010). PEER/ SSC tall building design case history no. 2, The Structural Design of Tall and Special Buildings, 19(1-2):197-256.

Hall, J. F. (2006). Problems encountered from the use (or misuse) of Rayleigh damping. Earthquake Engineering & Structural Dynamics, 35(5), 525–545. https://doi.org/10.1002/eqe.541

Harries, K. A., Mitchell, D., Cook, W. D., and Redwood, R. G. (1993). "Seismic response of steel beams coupling concrete walls." J. Struct. Eng., 10.1061/(ASCE)0733-9445(1993)119:12(3611), 3611–3629.

Hashemi, A., Zarnani, P., Masoudnia, R., & Quenneville, P. (2017). Seismic resistant rocking coupled walls with innovative Resilient Slip Friction (RSF) joints. Journal of Constructional Steel Research, 129, 215–226. https://doi.org/10.1016/j.jcsr.2016.11.016

Henry, R., Ingham, J., and Sritharan, S. 2012. Wall-to-Floor Interaction in Concrete Buildings with Rocking Wall Systems. New Zealand Society of Earthquake Engineering Conference, Christchurch, New Zealand.

Henry, R., Lu, Y., Elwood, K., Rodgers, G.W., Zhou, Y., Yang T.Y. 2019, "ILEE-QuakeCoRE collaboration: Low damage concrete wall building test", Proceedings of the 2019 Pacific Conference in Earthquake Engineering, New Zealand Society for Earthquake Engineering, Auckland, NZ.

Huang, B., & Takeuchi, T. (2017). Dynamic Response Evaluation of Damped-Outrigger Systems with Various Heights. Earthquake Spectra, 33(2), 665–685. https://doi.org/10.1193/051816eqs082m

Iwata, M., Midorikawa, M., & Koyano, K. (2018). Buckling-restrained brace with high structural performance. Steel Construction, 11(1), 3–10. https://doi.org/10.1002/stco.20181000

Ji, X., Wang, Y., Ma, Q., & Okazaki, T. (2017). Cyclic Behaviour of Replaceable Steel Coupling Beams. Journal of Structural Engineering, 143(2), 04016169. https://doi.org/10.1061/(asce)st.1943-541x.0001661

Ji, X., Liu, D., Sun, Y., & Molina Hutt, C. (2016). Seismic performance assessment of a hybrid coupled wall system with replaceable steel coupling beams versus traditional RC coupling beams. Earthquake Engineering & Structural Dynamics, 46(4), 517–535. https://doi.org/10.1002/eqe.2801

Ji, X., Wang, Y., Zhang, J., & Okazaki, T. (2017). Seismic behaviour and fragility curves of replaceable steel coupling beams with slabs. Engineering Structures, 150, 622–635. https://doi.org/10.1016/j.engstruct.2017.07.045

Ji, X., & Molina Hutt, C. (2020). Seismic design and application of hybrid coupled walls with replaceable steel coupling beams in high-rise buildings. The Structural Design of Tall and Special Buildings, 29(8). https://doi.org/10.1002/tal.1727

Kam WY, Pampanin S, Elwood K. Seismic performance of reinforced concrete buildings in the 22 February Christchurch (Lyttleton) earthquake. Bull NZ Soc Earthq. Eng. 2011;44(4):239-278.

Kim, J. J., Elwood, K. J., Marquis, F., & Chang, S. E. (2017). Factors Influencing Post-Earthquake Decisions on Buildings in Christchurch, New Zealand. Earthquake Spectra, 33(2), 623-640. doi:10.1193/072516eqs120m

Khanmohammadi M., Heydari S. (2015). Seismic behaviour improvement of reinforced concrete shear wall buildings using multiple rocking systems. Engineering Structures 100: 577–589. doi:10.1016/j.engstruct.2015.06.043

Kurama, Y., Sause, R., Pessiki, S., Lu, L.-W., & EI-Sheikh, M. (1999). Seismic Design and Response Evaluation of Unbonded Post-Tensioned Precast Concrete Walls. Precast/Prestressed Concrete Institute. https://doi.org/10.15554/pci.rr.seis-017

Kurama, Y. (2000). Seismic Design of Unbonded Post-Tensioned Precast Concrete Walls with Supplemental Viscous Damping. ACI Structural Journal, 97(4). https://doi.org/10.14359/7431

Landi, L., Fabbri, O., & Diotallevi, P. P. (2014). A two-step direct method for estimating the seismic response of nonlinear structures equipped with nonlinear viscous dampers. Earthquake Engineering & Structural Dynamics, 43(11), 1641–1659. https://doi.org/10.1002/eqe.2415

Lin, P.-C., Takeuchi, T., & Matsui, R. (2018). Seismic performance evaluation of single damped-outrigger system incorporating buckling-restrained braces. Earthquake Engineering & Structural Dynamics. https://doi.org/10.1002/eqe.3072

Lim, E., Hwang, S.-J., Cheng, C.-H., & Lin, P.-Y. (2016). Cyclic Tests of Reinforced Concrete Coupling Beam with Intermediate Span-to-Depth Ratio. ACI Structural Journal, 113(3). https://doi.org/10.14359/51688473

Liu, Q., & Jiang, H. (2017). Experimental study on a new type of earthquake resilient shear wall. Earthquake Engineering & Structural Dynamics, 46(14), 2479–2497. https://doi.org/10.1002/eqe.2914

Los Angeles Tall Buildings Structural Design Council (LATBSDC). (2020). An Alternative Procedure for Seismic Analysis and Design of Tall Buildings Located in the Los Angeles Region. Los Angeles Tall Building. Structural Design Council. Los Angeles, CA.

Los Angeles Tall Buildings Structural Design Council (LATBSDC). (2010). Magnitude 8.8 Chile earthquake preliminary briefing slides. Los Angeles Tall Building. Structural Design Council. Los Angeles, CA.

Los Angeles Business Journal (LABJ). (2020). Retrieved 31 December 2020, from https://labusinessjournal.com/news/2018/mar/26/whos-building-l-march-26-wilshire-grand-center/

Lu, Y., & Panagiotou, M. (2015). Earthquake Damage-Resistant Tall Buildings at Near Fault Regions Using Base Isolation and Rocking Core Walls. Structures Congress 2015. doi:10.1061/9780784479117.108

Lu X., Yang B., Zhao B. (2018). Shake-table testing of a self-centering precast reinforced concrete frame with shear walls. Earthq Eng Vib 17 (2): 221–233. doi:10.1007/s11803-018-0436-y

Ma, X., Borchers, E., Pena, A., Krawinkler, H., Billington, S., & Deierlein, G. G. (2010). Design and Behaviour of Steel Shear Plates with Openings as Energy-Dissipating Fuses. Internal Report, John A. Blume Earthquake Engineering Center, Stanford University, (17).

MacKay-Lyons, R., Christopoulos, C., & Montgomery, M. (2018). Viscoelastic Coupling Dampers for Enhanced Multiple Seismic Hazard Level Performance of High-Rise Buildings. Earthquake Spectra, 34(4), 1847–1867. https://doi.org/10.1193/091616eqs151m

Marcakis, K., and Mitchell, D. (1980). "Precast concrete connections with embedded steel members." PCI J., 25(4), 88–116.

Marriott, D., Pampanin, S., Bull, D., & Palermo, A. (2008). Dynamic testing of precast, post-tensioned rocking wall systems with alternative dissipating solutions. Bulletin of the New Zealand Society for Earthquake Engineering, 41(2), 90–103. https://doi.org/10.5459/bnzsee.41.2.90-103

MATLAB. (2016). version 7.10.0 (R2016a). Natick, Massachusetts: The MathWorks Inc.

Morales-Beltran, M., Turan, G., Dursun, O., & Nijsse, R. (2018). Energy dissipation and performance assessment of double damped outriggers in tall buildings under strong earthquakes. The Structural Design of Tall and Special Buildings, 28(1), e1554. https://doi.org/10.1002/tal.1554

Montgomery, M., & Christopoulos, C. (2015). Experimental Validation of Viscoelastic Coupling Dampers for Enhanced Dynamic Performance of High-Rise Buildings. Journal of Structural Engineering, 141(5), 04014145. https://doi.org/10.1061/(asce)st.1943-541x.0001092

Motter, C. J., Fields, D. C., Hooper, J. D., Klemencic, R., & Wallace, J. W. (2017). Steel-Reinforced Concrete Coupling Beams. I: Testing. Journal of Structural Engineering, 143(3), 04016191. https://doi.org/10.1061/(asce)st.1943-541x.0001670

Naish, D., Fry, F., Klemencic, R., and Wallace, J. (2013). Reinforced Concrete Coupling Beams—Part I: Testing. (2013). ACI Structural Journal, 110(06). https://doi.org/10.14359/51686160

National research council of Canada (NRCC). 2015. "National Building Code of Canada 2015." National Research Council of Canada, Ottawa, Ontario, Canada.

Natural Resources Canada (NRCAN). Earthquake map of Canada. Retrieved from https://earthquakescanada.nrcan.gc.ca/historic-historique/caneqmap-en.php (accessed Dec 31, 2020).

Pall, A. S., & Marsh, C. (1982). Response of friction damped brace frames. ASCE J Struct Div, 108(ST6), 1313–1323.

Paulay, T., and Binney, J. R.(1974). Diagonally Reinforced Coupling Beams of Shear Walls. Shear in Reinforced Concrete. American Concrete Institute. Farmington Hills, Mich. 579-598.

Pacific Earthquake Engineering Research Center (PEER). 2000. “Open System for Earthquake Engineering Simulation (OpenSees).” University of California, Berkeley, CA: Pacific Earthquake Engineering Research Center.

Pacific Earthquake Engineering Research Center (PEER). 2018. NGA-West 2 Peer Ground Motion Database. Available online at: https://ngawest2.berkeley.edu/site (Accessed Jan 1, 2018).

University of California Los Angeles (UCLA). 2020. NGA Subduction Database Preliminary Ground Motion Suite. Available online at: https://www.risksciences.ucla.edu/nhr3/ gmdata/preliminary-nga-subduction-records (Accessed Jan 1, 2018).

Perez, F. J., Sause, R. and Pessiki, S. (2007). Analytical and experimental lateral load behaviour of unbonded posttensioned precast concrete walls. Journal of Structural Engineering Vol. 133. No. 11: 1531-1540

Priestley, M. J. N. (1991). Overview of PRESSS Research Program. PCI Journal, 36(4), 50–57. https://doi.org/10.15554/pcij.07011991.50.57

Poh, G “Vancouver House,” STRUCTURE magazine. [Online]. Available: https://www.structuremag.org/?p=15416. [Accessed: 11-Nov-2020]

Qu Z., Wada A., Motoyui S., Sakata H., Kishiki S. (2012). Pin-supported walls for enhancing the seismic performance of building structures. Earthquake Engng Struct Dyn 41 (14): 2075–2091. doi:10.1002/eqe.2175

Razvi, S., & Saatcioglu, M. (1999). Confinement Model for High-Strength Concrete. Journal of Structural Engineering, 125(3), 281–289. https://doi.org/10.1061/(asce)0733-9445(1999)125:3(281)

Reinhorn. A. M, Li, C., and Constantinou, M. C. (1995). "Experimental and analytical investigation of seismic retrofit of structures with supplemental damping: part I-fluid viscous damping devices." NCEER Rep. 95-0028, State Univ. of New York at Buffalo, Buffalo. N.Y.

Restrepo, J. I., & Rahman, A. 2007. Seismic Performance of Self-Centering Structural Walls Incorporating Energy Dissipators. Journal of structural engineering, ASCE, 133(11), 1560-1570.

Rodgers, G. W., Chase, J. G., Causse, R., Chanchi, J., & MacRae, G. A. (2017). Performance and degradation of sliding steel friction connections: Impact of velocity, corrosion coating and shim material. Engineering Structures, 141, 292–302. https://doi.org/10.1016/j.engstruct.2017.02.070

Smith, R. J., & Willford, M. R. (2007). The Damped Outrigger Concept for Tall Buildings. Structural Design of Tall & Special Buildings, 16(4), 501-517.

Sritharan, S., Aaleti, S., Henry, R. S., Liu, K.-Y., & Tsai, K.-C. (2015). Precast concrete wall with end columns (PreWEC) for earthquake resistant design. Earthquake Engineering & Structural Dynamics, 44(12), 2075-2092. doi:10.1002/eqe.2576

Tong, F., & Christopoulos, C. (2020). Uncoupled rocking and shear base-mechanisms for resilient reinforced concrete high-rise buildings. Earthquake Engineering & Structural Dynamics, 49(10), 981–1006. https://doi.org/10.1002/eqe.3273

Tremblay, Robert. (1993). Seismic behaviour and design of friction concentrically braced frames for steel buildings. Open Collections, University of British Columbia. open.library.ubc.ca/cIRcle/collections/ubctheses/

Twigden, K. M., & Henry, R. S. (2019). Shake table testing of unbonded post-tensioned concrete walls with and without additional energy dissipation. Soil Dynamics and Earthquake Engineering, 119, 375–389. https://doi.org/10.1016/j.soildyn.2018.05.007

Twigden, K. M., Sritharan, S., & Henry, R. S. 2017. Cyclic Testing of Unbonded Post-Tensioned Concrete Wall Systems with and without Supplemental Damping. Engineering Structures, 140, 406-420.

United Nations (UN), Department of Economic and Social Affairs, Population Division. World Urbanization Prospects: The 2018 Revision (ST/ESA/SER.A/420). United Nations: New York, NY; 2019.

Wallace, J. and Naish, D. (2009). RC Core Walls – Testing And Modeling Of Coupling Beams. nees@UCLA. The George E. Brown, Jr. Network for Earthquake Engineering Simulation.

Wang X., Wang T., Qu Z. (2017). An experimental study of a damage-controllable plastic-hinge-supported wall structure. Earthquake Eng. Struct. Dyn. 47 (3): 594–612. doi:10.1002/eqe.2981

Wiebe L., & Christopoulos C. 2009. Mitigation of Higher Mode Effects in Base-Rocking Systems by Using Multiple Rocking Sections. Journal of Earthquake Engineering 13 (sup1): 83–108. doi:10.1080/13632460902813315

Xie, Q. (2005). State of the art of buckling-restrained braces in Asia. Journal of Constructional Steel Research, 61(6), 727–748. https://doi.org/10.1016/j.jcsr.2004.11.005

Xing, L., Zhou, Y., Aguaguiña. 2018. Optimal vertical configuration of combined energy dissipation outriggers. The Structural Design of Tall and Special Buildings. https:// 10.1002/tal.1579

Xu, Hengchao. “Mechanism and Experimental Validation of Innovative Self-Centering Conical Friction Damper.” Open Collections, University of British Columbia, 2020, open.library.ubc.ca/cIRcle/collections/ubctheses/24/items/1.0387456.

Xu, L., Xiao, S., & Li, Z. (2018). Hysteretic behaviour and parametric studies of a self-centering RC wall with disc spring devices. Soil Dynamics and Earthquake Engineering, 115, 476–488. https://doi.org/10.1016/j.soildyn.2018.09.017

Yang, T. Y., Banjuradja, W., & Tobber, L. (2018). Experimental Test of Welded Wide Flange Fuses. Key Engineering Materials, 763, 414–422. https://doi.org/10.4028/www.scientific.net/kem.763.414

Yang, T. Y., Li, T., Tobber, L., & Pan, X. (2019). Experimental and numerical study of honeycomb structural fuses. Engineering Structures, 109814.

Yang, T. Y., Xu, H. C., & Tobber, L. (2020). Mechanism and experimental validation of innovative self-centering conical friction damper. Structural Control and Health Monitoring, 27(10). https://doi.org/10.1002/stc.2609

Yang, T.Y., Tung, D.P., and Li, Y., 2017. Equivalent Energy Design Procedure for Earthquake Resilient Fused Structures, Earthquake Spectra, https://doi.org/10.1193/122-716EQS254M.

Yang, T. Y., Atkinson, J., Tobber, L., Tung, D. P., & Neville, B. (2020). Seismic design of outrigger systems using equivalent energy design procedure. The Structural Design of Tall and Special Buildings, 29(10). https://doi.org/10.1002/tal.1743

Zhou, Y., Zhang, C., & Lu, X. 2016. Seismic performance of a damping outrigger system for tall buildings. Structural Control and Health Monitoring,24(1). doi:10.1002/stc.1864

Appendix A: Parameter study results for all dynamic characteristic archetypes

These appendices provide the detailed numerical analysis for the LDA parametric studies provided in Chapter 4.

Name	af	nf	hf	mf	Ly	Lx	tw	Lcb	T1 [s]	T2 [s]	T3 [s]	M1 [-]	M2 [-]	M3 [-]	Sa	Sa2	Sa3	Disp [m]	ISDR [-]	Total Moment [MN-m]	Total Shear [MN]	Outrigger Moment [MN-m]	Wall Moment [MN-m]	Mode 1 Disp [m]	Mode 1 ISDR [-]	Mode 1 Moment [MN-m]	Mode 1 Shear [MN]	Mode 1 wall Moment [MN-m]
V11111111	0.1	15	3	400	8	8	0.6	1.5	0.85	0.14	0.05	0.64	0.19	0.07	0.49	0.89	0.89	0.13	0.004	618	618	25	601	0.13	0.0040	609	18	592
V11111112	0.1	15	3	400	8	8	0.6	2.5	0.93	0.15	0.05	0.64	0.19	0.07	0.45	0.89	0.89	0.14	0.004	573	573	23	558	0.14	0.0044	564	17	548
V21111111	0.3	15	3	400	8	8	0.6	1.5	0.79	0.13	0.05	0.65	0.18	0.07	0.52	0.89	0.89	0.12	0.003	661	661	80	590	0.12	0.0035	654	20	583
V21111112	0.3	15	3	400	8	8	0.6	2.5	0.86	0.15	0.05	0.65	0.18	0.07	0.48	0.89	0.89	0.13	0.004	613	613	74	548	0.13	0.0039	605	18	539
V31111111	0.5	15	3	400	8	8	0.6	1.5	0.73	0.13	0.05	0.66	0.17	0.06	0.56	0.89	0.89	0.11	0.003	717	717	145	584	0.11	0.0031	711	22	577
V31111112	0.5	15	3	400	8	8	0.6	2.5	0.79	0.14	0.05	0.66	0.17	0.06	0.52	0.89	0.89	0.12	0.003	665	665	135	542	0.12	0.0034	659	20	534
V41111111	0.7	15	3	400	8	8	0.6	1.5	0.66	0.12	0.05	0.68	0.16	0.06	0.61	0.89	0.89	0.09	0.003	789	789	222	580	0.09	0.0027	785	24	574
V41111112	0.7	15	3	400	8	8	0.6	2.5	0.72	0.13	0.05	0.68	0.16	0.06	0.56	0.89	0.89	0.10	0.003	735	735	207	540	0.10	0.0030	731	22	534
V51111111	0.9	15	3	400	8	8	0.6	1.5	0.58	0.11	0.04	0.70	0.14	0.06	0.67	0.89	0.89	0.08	0.002	892	892	320	586	0.08	0.0024	889	28	582
V51111112	0.9	15	3	400	8	8	0.6	2.5	0.63	0.12	0.05	0.70	0.14	0.06	0.62	0.89	0.89	0.08	0.003	826	826	297	543	0.08	0.0027	823	26	539
V11111121	0.1	15	3	400	8	8	1	1.5	0.73	0.12	0.04	0.64	0.19	0.07	0.55	0.89	0.89	0.11	0.003	698	698	28	679	0.11	0.0033	690	21	672
V11111122	0.1	15	3	400	8	8	1	2.5	0.81	0.13	0.05	0.64	0.19	0.07	0.51	0.89	0.89	0.12	0.004	644	644	26	627	0.12	0.0037	636	19	619
V21111121	0.3	15	3	400	8	8	1	1.5	0.68	0.12	0.04	0.65	0.18	0.07	0.59	0.89	0.89	0.10	0.003	747	747	91	668	0.10	0.0029	741	22	661
V21111122	0.3	15	3	400	8	8	1	2.5	0.75	0.13	0.05	0.65	0.18	0.07	0.54	0.89	0.89	0.11	0.003	688	688	84	615	0.11	0.0033	681	21	607
V31111121	0.5	15	3	400	8	8	1	1.5	0.63	0.11	0.04	0.66	0.17	0.06	0.63	0.89	0.89	0.09	0.003	806	806	163	656	0.09	0.0026	801	24	650
V31111122	0.5	15	3	400	8	8	1	2.5	0.69	0.12	0.05	0.66	0.17	0.06	0.58	0.89	0.89	0.10	0.003	748	748	151	609	0.10	0.0029	743	23	602
V41111121	0.7	15	3	400	8	8	1	1.5	0.57	0.11	0.04	0.68	0.16	0.06	0.68	0.89	0.89	0.08	0.002	890	890	251	653	0.08	0.0023	887	27	648
V41111122	0.7	15	3	400	8	8	1	2.5	0.63	0.12	0.04	0.68	0.16	0.06	0.63	0.89	0.89	0.09	0.003	821	821	231	603	0.09	0.0026	817	25	597
V51111121	0.9	15	3	400	8	8	1	1.5	0.50	0.09	0.04	0.70	0.14	0.06	0.74	0.89	0.89	0.06	0.002	988	988	354	648	0.06	0.0020	985	31	645
V51111122	0.9	15	3	400	8	8	1	2.5	0.55	0.10	0.04	0.70	0.14	0.06	0.70	0.89	0.89	0.07	0.002	927	927	333	609	0.07	0.0023	924	29	605
V11111211	0.1	15	3	400	8	10	0.6	1.5	2.10	0.34	0.12	0.64	0.19	0.07	0.24	0.85	0.89	0.39	0.012	315	315	12	306	0.39	0.0118	299	9	291
V11111212	0.1	15	3	400	8	10	0.6	2.5	2.32	0.38	0.14	0.64	0.19	0.07	0.21	0.83	0.89	0.42	0.013	280	280	11	272	0.42	0.0126	262	8	255
V21111211	0.3	15	3	400	8	10	0.6	1.5	1.95	0.33	0.12	0.65	0.18	0.07	0.26	0.85	0.89	0.36	0.011	340	340	41	306	0.36	0.0106	327	10	292
V21111212	0.3	15	3	400	8	10	0.6	2.5	2.15	0.37	0.13	0.65	0.18	0.07	0.23	0.84	0.89	0.39	0.012	304	304	36	274	0.39	0.0115	291	9	259
V31111211	0.5	15	3	400	8	10	0.6	1.5	1.79	0.32	0.12	0.66	0.17	0.06	0.28	0.85	0.89	0.32	0.009	366	366	74	301	0.32	0.0093	356	11	288
V31111212	0.5	15	3	400	8	10	0.6	2.5	1.98	0.35	0.13	0.66	0.17	0.06	0.26	0.84	0.89	0.36	0.011	338	338	68	278	0.36	0.0105	327	10	265
V41111211	0.7	15	3	400	8	10	0.6	1.5	1.62	0.30	0.12	0.68	0.16	0.06	0.30	0.86	0.89	0.28	0.008	399	399	113	296	0.28	0.0082	391	12	286
V41111212	0.7	15	3	400	8	10	0.6	2.5	1.79	0.33	0.13	0.68	0.16	0.06	0.28	0.85	0.89	0.32	0.009	370	370	105	275	0.32	0.0093	362	11	265
V51111211	0.9	15	3	400	8	10	0.6	1.5	1.43	0.27	0.11	0.70	0.14	0.06	0.33	0.87	0.89	0.23	0.007	445	445	162	295	0.23	0.0072	439	14	288
V51111212	0.9	15	3	400	8	10	0.6	2.5	1.58	0.30	0.12	0.70	0.14	0.06	0.31	0.86	0.89	0.26	0.008	413	413	151	275	0.26	0.0082	408	13	267
V11111221	0.1	15	3	400	8	10	1	1.5	2.02	0.33	0.12	0.64	0.19	0.07	0.25	0.85	0.89	0.38	0.012	329	329	13	319	0.38	0.0115	313	9	304
V11111222	0.1	15	3	400	8	10	1	2.5	2.24	0.36	0.13	0.64	0.19	0.07	0.22	0.84	0.89	0.41	0.013	291	291	11	282	0.41	0.0123	273	8	266
V21111221	0.3	15	3	400	8	10	1	1.5	1.88	0.32	0.12	0.65	0.18	0.07	0.27	0.85	0.89	0.35	0.010	350	350	42	314	0.35	0.0102	337	10	301
V21111222	0.3	15	3	400	8	10	1	2.5	2.09	0.36	0.13	0.65	0.18	0.07	0.24	0.84	0.89	0.39	0.011	317	317	38	286	0.39	0.0113	304	9	271
V31111221	0.5	15	3	400	8	10	1	1.5	1.73	0.31	0.12	0.66	0.17	0.06	0.29	0.86	0.89	0.31	0.009	376	376	76	309	0.31	0.0090	366	11	296
V31111222	0.5	15	3	400	8	10	1	2.5	1.92	0.34	0.13	0.66	0.17	0.06	0.26	0.85	0.89	0.35	0.010	347	347	70	286	0.35	0.0101	336	10	273
V41111221	0.7	15	3	400	8	10	1	1.5	1.57	0.29	0.11	0.68	0.16	0.06	0.31	0.86	0.89	0.27	0.008	410	410	116	304	0.27	0.0079	402	12	294
V41111222	0.7	15	3	400	8	10	1	2.5	1.73	0.32	0.12	0.68	0.16	0.06	0.29	0.85	0.89	0.30	0.009	379	379	107	282	0.30	0.0089	371	11	271
V51111221	0.9	15	3	400	8	10	1	1.5	1.38	0.26	0.10	0.70	0.14	0.06	0.34	0.88	0.89	0.22	0.007	456	456	166	302	0.22	0.0069	451	14	295
V51111222	0.9	15	3	400	8	10	1	2.5	1.53	0.29	0.12	0.70	0.14	0.06	0.32	0.87	0.89	0.25	0.008	423	423	154	281	0.25	0.0079	418	13	273
V11112111	0.1	15	3	400	10	8	0.6	1.5	1.23	0.20	0.07	0.64	0.19	0.07	0.37	0.88	0.89	0.21	0.006	473	473	19	460	0.21	0.0063	461	14	449
V11112112	0.1	15	3	400	10	8	0.6	2.5	1.52	0.25	0.09	0.64	0.19	0.07	0.32	0.88	0.89	0.27	0.008	409	409	16	398	0.27	0.0082	396	12	385
V21112111	0.3	15	3	400	10	8	0.6	1.5	1.15	0.20	0.07	0.65	0.18	0.07	0.39	0.88	0.89	0.19	0.005	498	498	60	446	0.19	0.0055	488	15	435
V21112112	0.3	15	3	400	10	8	0.6	2.5	1.41	0.24	0.09	0.65	0.18	0.07	0.34	0.88	0.89	0.25	0.007	433	433	52	388	0.25	0.0072	422	13	377
V31112111	0.5	15	3	400	10	8	0.6	1.5	1.05	0.19	0.07	0.66	0.17	0.06	0.41	0.88	0.89	0.16	0.005	529	529	107	432	0.16	0.0047	522	16	423
V31112112	0.5	15	3	400	10	8	0.6	2.5	1.30	0.23	0.09	0.66	0.17	0.06	0.36	0.88	0.89	0.22	0.006	463	463	93	379	0.22	0.0063	454	14	368
V41112111	0.7	15	3	400	10	8	0.6	1.5	0.95	0.18	0.07	0.68	0.16	0.06	0.44	0.89	0.89	0.14	0.004	579	579	164	427	0.14	0.0042	574	18	420
V41112112	0.7	15	3	400	10	8	0.6	2.5	1.17	0.22	0.08	0.68	0.16	0.06	0.38	0.88	0.89	0.19	0.005	501	501	142	371	0.19	0.0054	495	15	362
V51112111	0.9	15	3	400	10	8	0.6	1.5	0.84	0.16	0.06	0.70	0.14	0.06	0.49	0.89	0.89	0.12	0.004	656	656	237	432	0.12	0.0037	652	20	427
V51112112	0.9	15	3	400	10	8	0.6	2.5	1.04	0.19	0.08	0.70	0.14	0.06	0.41	0.88	0.89	0.15	0.005	551	551	199	364	0.15	0.0047	547	17	358
V11112121	0.1	15	3	400	10	8	1	1.5	1.12	0.18	0.07	0.64	0.19	0.07	0.39	0.88	0.89	0.18	0.006	503	503	20	489	0.18	0.0055	492	15	479
V11112122	0.1	15	3	400	10	8	1	2.5	1.46	0.24	0.08	0.64	0.19	0.07	0.33	0.88	0.89	0.26	0.008	422	422	17	410	0.26	0.0078	409	12	398
V21112121	0.3	15	3	400	10	8	1	1.5	1.04	0.18	0.06	0.65	0.18	0.07	0.41	0.89	0.89	0.16	0.005	528	528	64	473	0.16	0.0048	519	16	463
V21112122	0.3	15	3	400	10	8	1	2.5	1.35	0.23	0.08	0.65	0.18	0.07	0.35	0.88	0.89	0.23	0.007	446	446	54	400	0.23	0.0068	436	13	388
V31112121	0.5	15	3	400	10	8	1	1.5	0.96	0.17	0.06	0.66	0.17	0.06	0.44	0.89	0.89	0.15	0.004	570	570	115	465	0.15	0.0042	563	17	456
V31112122	0.5	15	3	400	10	8	1	2.5	1.24	0.22	0.08	0.66	0.17	0.06	0.37	0.88	0.89	0.21	0.006	476	476	96	389	0.21	0.0059	468	14	379
V41112121	0.7	15	3	400	10	8	1	1.5	0.86	0.16	0.06	0.68	0.16	0.06	0.48	0.89	0.89	0.13	0.004	628	628	177	463	0.13	0.0037	623	19	456
V41112122	0.7	15	3	400	10	8	1	2.5	1.13	0.21	0.08	0.68	0.16	0.06	0.39	0.88	0.89	0.18	0.005	515	515	145	380	0.18	0.0051	509	16	372
V51112121	0.9	15	3	400	10	8	1	1.5	0.76	0.14	0.06	0.70	0.14	0.06	0.53	0.89	0.89	0.10	0.003	710	710	256	467	0.10	0.0033	706	22	462
V51112122	0.9	15	3	400	10	8	1	2.5	0.99	0.19	0.07	0.70	0.14	0.06	0.43	0.88	0.89	0.14	0.004	569	569	205	376	0.14	0.0045	564	18	369
V11112211	0.1	15	3	400	10	10	0.6	1.5	3.24	0.53	0.19	0.64	0.19	0.07	0.14	0.72	0.88	0.53	0.017	191	191	7	185	0.53	0.0161	171	5	166
V11112212	0.1	15	3	400	10	10	0.6	2.5	4.29	0.70	0.25	0.64	0.19	0.07	0.10	0.58	0.88	0.66	0.021	140	140	5	136	0.66	0.0200	121	4	118
V21112211	0.3	15	3	400	10	10	0.6	1.5	3.01	0.51	0.19	0.65	0.18	0.07	0.15	0.74	0.88	0.50	0.015	205	205	24	186	0.50	0.0146	189	6	168
V21112212	0.3	15	3	400	10	10	0.6	2.5	3.99	0.68	0.25	0.65	0.18	0.07	0.11	0.59	0.88	0.62	0.019	149	149	17	136	0.62	0.0181	134	4	119
V31112211	0.5	15	3	400	10	10	0.6	1.5	2.77	0.49	0.18	0.66	0.17	0.06	0.17	0.75	0.88	0.46	0.014	226	226	45	188	0.46	0.0133	213	6	172
V31112212	0.5	15	3	400	10	10	0.6	2.5	3.66	0.65	0.24	0.66	0.17	0.06	0.12	0.61	0.88	0.57	0.017	162	162	32	136	0.57	0.0164	150	5	121
V41112211	0.7	15	3	400	10	10	0.6	1.5	2.50	0.46	0.18	0.68	0.16	0.06	0.19	0.77	0.88	0.42	0.012	256	256	73	193	0.42	0.0123	246	8	180
V41112212	0.7	15	3	400	10	10	0.6	2.5	3.31	0.61	0.24	0.68	0.16	0.06	0.13	0.64	0.88	0.52	0.015	182	182	52	139	0.51	0.0151	172	5	126
V51112211	0.9	15	3	400	10	10	0.6	1.5	2.21	0.41	0.17	0.70	0.14	0.06	0.22	0.81	0.89	0.37	0.012	303	303	112	203	0.37	0.0116	296	9	194

Name	af	nf	hf	mf	Ly	Lx	tw	Lcb	T1 [s]	T2 [s]	T3 [s]	M1 [-]	M2 [-]	M3 [-]	Sa	Sa2	Sa3	Disp [m]	ISDR [-]	Total Moment [MN-m]	Total Shear [MN]	Outrigger Moment [MN-m]	Wall Moment [MN-m]	Mode 1 Disp [m]	Mode 1 ISDR [-]	Mode 1 Moment [MN-m]	Mode 1 Shear [MN]	Mode 1 wall Moment [MN-m]
V51112212	0.9	15	3	400	10	10	0.6	2.5	2.93	0.55	0.22	0.70	0.14	0.06	0.16	0.70	0.88	0.45	0.014	213	213	80	145	0.45	0.0141	206	6	135
V11112221	0.1	15	3	400	10	10	1	1.5	3.17	0.52	0.19	0.64	0.19	0.07	0.14	0.73	0.88	0.53	0.016	196	196	7	190	0.52	0.0158	175	5	170
V11112222	0.1	15	3	400	10	10	1	2.5	4.29	0.70	0.25	0.64	0.19	0.07	0.10	0.58	0.88	0.66	0.021	140	140	5	136	0.66	0.0200	121	4	118
V21112221	0.3	15	3	400	10	10	1	1.5	2.95	0.50	0.18	0.65	0.18	0.07	0.15	0.74	0.88	0.49	0.015	210	210	25	190	0.49	0.0144	194	6	173
V21112222	0.3	15	3	400	10	10	1	2.5	3.99	0.68	0.25	0.65	0.18	0.07	0.11	0.59	0.88	0.62	0.019	149	149	17	136	0.62	0.0181	134	4	119
V31112221	0.5	15	3	400	10	10	1	1.5	2.71	0.48	0.18	0.66	0.17	0.06	0.17	0.76	0.88	0.46	0.013	231	231	46	193	0.46	0.0131	218	7	177
V31112222	0.5	15	3	400	10	10	1	2.5	3.67	0.65	0.24	0.66	0.17	0.06	0.12	0.61	0.88	0.57	0.017	162	162	32	136	0.57	0.0165	150	5	121
V41112221	0.7	15	3	400	10	10	1	1.5	2.45	0.45	0.18	0.68	0.16	0.06	0.19	0.78	0.89	0.41	0.012	262	262	75	198	0.41	0.0121	253	8	185
V41112222	0.7	15	3	400	10	10	1	2.5	3.32	0.61	0.24	0.68	0.16	0.06	0.13	0.64	0.88	0.52	0.015	182	182	52	139	0.51	0.0151	172	5	126
V51112221	0.9	15	3	400	10	10	1	1.5	2.17	0.41	0.16	0.70	0.14	0.06	0.23	0.82	0.89	0.36	0.011	310	310	114	208	0.36	0.0114	304	9	199
V51112222	0.9	15	3	400	10	10	1	2.5	2.93	0.55	0.22	0.70	0.14	0.06	0.16	0.70	0.88	0.45	0.014	213	213	80	145	0.45	0.0141	206	6	135
V11121111	0.1	15	3	600	8	8	0.6	1.5	1.04	0.17	0.06	0.64	0.19	0.07	0.41	0.89	0.89	0.17	0.005	787	787	32	765	0.17	0.0050	771	23	750
V11121112	0.1	15	3	600	8	8	0.6	2.5	1.14	0.19	0.07	0.64	0.19	0.07	0.39	0.88	0.89	0.19	0.006	745	745	30	725	0.19	0.0057	729	22	709
V21121111	0.3	15	3	600	8	8	0.6	1.5	0.97	0.17	0.06	0.65	0.18	0.07	0.44	0.89	0.89	0.15	0.004	836	836	101	748	0.15	0.0044	824	25	735
V21121112	0.3	15	3	600	8	8	0.6	2.5	1.06	0.18	0.07	0.65	0.18	0.07	0.41	0.88	0.89	0.17	0.005	784	784	95	702	0.17	0.0049	771	23	687
V31121111	0.5	15	3	600	8	8	0.6	1.5	0.89	0.16	0.06	0.66	0.17	0.06	0.47	0.89	0.89	0.13	0.004	904	904	183	737	0.13	0.0039	894	27	725
V31121112	0.5	15	3	600	8	8	0.6	2.5	0.97	0.17	0.06	0.66	0.17	0.06	0.43	0.89	0.89	0.15	0.004	841	841	170	686	0.15	0.0043	831	25	674
V41121111	0.7	15	3	600	8	8	0.6	1.5	0.81	0.15	0.06	0.68	0.16	0.06	0.51	0.89	0.89	0.12	0.003	1002	1002	283	737	0.12	0.0034	994	31	727
V41121112	0.7	15	3	600	8	8	0.6	2.5	0.88	0.16	0.06	0.68	0.16	0.06	0.47	0.89	0.89	0.13	0.004	926	926	261	682	0.13	0.0038	918	28	671
V51121111	0.9	15	3	600	8	8	0.6	1.5	0.71	0.13	0.05	0.70	0.14	0.06	0.57	0.89	0.89	0.10	0.003	1135	1135	408	746	0.10	0.0031	1130	35	739
V51121112	0.9	15	3	600	8	8	0.6	2.5	0.78	0.15	0.06	0.70	0.14	0.06	0.53	0.89	0.89	0.11	0.003	1050	1050	378	691	0.11	0.0034	1045	33	684
V11121121	0.1	15	3	600	8	8	1	1.5	0.90	0.15	0.05	0.64	0.19	0.07	0.46	0.89	0.89	0.14	0.004	883	883	36	858	0.14	0.0042	868	26	845
V11121122	0.1	15	3	600	8	8	1	2.5	0.99	0.16	0.06	0.64	0.19	0.07	0.43	0.89	0.89	0.16	0.005	815	815	33	793	0.16	0.0047	800	24	778
V21121121	0.3	15	3	600	8	8	1	1.5	0.84	0.14	0.05	0.65	0.18	0.07	0.50	0.89	0.89	0.13	0.004	947	947	115	847	0.13	0.0037	936	28	834
V21121122	0.3	15	3	600	8	8	1	2.5	0.92	0.16	0.06	0.65	0.18	0.07	0.46	0.89	0.89	0.14	0.004	871	871	106	779	0.14	0.0041	860	26	766
V31121121	0.5	15	3	600	8	8	1	1.5	0.77	0.14	0.05	0.66	0.17	0.06	0.53	0.89	0.89	0.11	0.003	1024	1024	207	834	0.11	0.0033	1015	31	823
V31121122	0.5	15	3	600	8	8	1	2.5	0.85	0.15	0.06	0.66	0.17	0.06	0.49	0.89	0.89	0.13	0.004	946	946	191	771	0.13	0.0037	936	29	759
V41121121	0.7	15	3	600	8	8	1	1.5	0.70	0.13	0.05	0.68	0.16	0.06	0.58	0.89	0.89	0.10	0.003	1134	1134	320	833	0.10	0.0029	1128	35	825
V41121122	0.7	15	3	600	8	8	1	2.5	0.77	0.14	0.05	0.68	0.16	0.06	0.53	0.89	0.89	0.11	0.003	1041	1041	294	766	0.11	0.0032	1034	32	756
V51121121	0.9	15	3	600	8	8	1	1.5	0.61	0.11	0.05	0.70	0.14	0.06	0.64	0.89	0.89	0.08	0.003	1278	1278	459	840	0.08	0.0026	1273	40	833
V51121122	0.9	15	3	600	8	8	1	2.5	0.68	0.13	0.05	0.70	0.14	0.06	0.59	0.89	0.89	0.09	0.003	1182	1182	425	777	0.09	0.0029	1177	37	770
V11121211	0.1	15	3	600	8	10	0.6	1.5	2.57	0.42	0.15	0.64	0.19	0.07	0.18	0.81	0.89	0.45	0.014	373	373	14	361	0.45	0.0136	344	10	334
V11121212	0.1	15	3	600	8	10	0.6	2.5	2.84	0.46	0.17	0.64	0.19	0.07	0.16	0.77	0.89	0.48	0.015	333	333	13	322	0.48	0.0146	302	9	294
V21121211	0.3	15	3	600	8	10	0.6	1.5	2.39	0.41	0.15	0.65	0.18	0.07	0.20	0.82	0.89	0.42	0.013	403	403	48	364	0.42	0.0123	381	12	339
V21121212	0.3	15	3	600	8	10	0.6	2.5	2.64	0.45	0.16	0.65	0.18	0.07	0.18	0.78	0.89	0.45	0.014	358	358	42	324	0.45	0.0132	335	10	298
V31121211	0.5	15	3	600	8	10	0.6	1.5	2.20	0.39	0.15	0.66	0.17	0.06	0.23	0.83	0.89	0.39	0.011	449	449	90	371	0.39	0.0113	431	13	349
V31121212	0.5	15	3	600	8	10	0.6	2.5	2.43	0.43	0.16	0.66	0.17	0.06	0.20	0.80	0.89	0.42	0.012	397	397	79	329	0.42	0.0121	378	12	307
V41121211	0.7	15	3	600	8	10	0.6	1.5	1.99	0.37	0.14	0.68	0.16	0.06	0.26	0.84	0.89	0.36	0.010	510	510	145	381	0.36	0.0104	497	15	364
V41121212	0.7	15	3	600	8	10	0.6	2.5	2.19	0.41	0.16	0.68	0.16	0.06	0.23	0.82	0.89	0.38	0.011	452	452	128	339	0.38	0.0112	439	13	321
V51121211	0.9	15	3	600	8	10	0.6	1.5	1.75	0.33	0.13	0.70	0.14	0.06	0.28	0.85	0.89	0.29	0.009	572	572	209	382	0.29	0.0093	563	18	369
V51121212	0.9	15	3	600	8	10	0.6	2.5	1.94	0.36	0.15	0.70	0.14	0.06	0.26	0.84	0.89	0.33	0.010	529	529	194	353	0.33	0.0104	519	16	340
V11121221	0.1	15	3	600	8	10	1	1.5	2.48	0.40	0.14	0.64	0.19	0.07	0.19	0.82	0.89	0.44	0.014	388	388	15	376	0.44	0.0132	359	11	350
V11121222	0.1	15	3	600	8	10	1	2.5	2.75	0.45	0.16	0.64	0.19	0.07	0.17	0.79	0.89	0.47	0.015	345	345	13	334	0.47	0.0142	315	9	307
V21121221	0.3	15	3	600	8	10	1	1.5	2.31	0.39	0.14	0.65	0.18	0.07	0.21	0.83	0.89	0.41	0.012	420	420	50	380	0.41	0.0121	399	12	356
V21121222	0.3	15	3	600	8	10	1	2.5	2.55	0.44	0.16	0.65	0.18	0.07	0.18	0.79	0.89	0.44	0.013	372	372	44	337	0.44	0.0129	349	11	311
V31121221	0.5	15	3	600	8	10	1	1.5	2.12	0.38	0.14	0.66	0.17	0.06	0.24	0.83	0.89	0.38	0.011	468	468	94	387	0.38	0.0111	451	14	366
V31121222	0.5	15	3	600	8	10	1	2.5	2.35	0.42	0.16	0.66	0.17	0.06	0.21	0.81	0.89	0.41	0.012	413	413	83	342	0.41	0.0119	395	12	320
V41121221	0.7	15	3	600	8	10	1	1.5	1.92	0.36	0.14	0.68	0.16	0.06	0.26	0.84	0.89	0.34	0.010	525	525	149	392	0.34	0.0100	513	16	375
V41121222	0.7	15	3	600	8	10	1	2.5	2.12	0.39	0.15	0.68	0.16	0.06	0.24	0.83	0.89	0.37	0.011	471	471	134	353	0.37	0.0110	458	14	335
V51121221	0.9	15	3	600	8	10	1	1.5	1.69	0.32	0.13	0.70	0.14	0.06	0.29	0.86	0.89	0.28	0.009	588	588	215	392	0.28	0.0089	580	18	379
V51121222	0.9	15	3	600	8	10	1	2.5	1.88	0.35	0.14	0.70	0.14	0.06	0.27	0.84	0.89	0.32	0.010	543	543	199	363	0.32	0.0101	534	17	349
V11122111	0.1	15	3	600	10	8	0.6	1.5	1.51	0.25	0.09	0.64	0.19	0.07	0.32	0.88	0.89	0.27	0.008	617	617	25	599	0.27	0.0081	597	18	581
V11122112	0.1	15	3	600	10	8	0.6	2.5	1.86	0.30	0.11	0.64	0.19	0.07	0.27	0.86	0.89	0.35	0.011	529	529	21	514	0.35	0.0105	507	15	493
V21122111	0.3	15	3	600	10	8	0.6	1.5	1.40	0.24	0.09	0.65	0.18	0.07	0.34	0.88	0.89	0.24	0.007	652	652	79	584	0.24	0.0071	636	19	567
V21122112	0.3	15	3	600	10	8	0.6	2.5	1.73	0.29	0.11	0.65	0.18	0.07	0.29	0.86	0.89	0.32	0.009	560	560	67	503	0.32	0.0092	542	16	483
V31122111	0.5	15	3	600	10	8	0.6	1.5	1.29	0.23	0.09	0.66	0.17	0.06	0.36	0.88	0.89	0.22	0.006	697	697	141	570	0.22	0.0062	685	21	555
V31122112	0.5	15	3	600	10	8	0.6	2.5	1.59	0.28	0.11	0.66	0.17	0.06	0.31	0.87	0.89	0.28	0.008	601	601	121	493	0.28	0.0081	587	18	476
V41122111	0.7	15	3	600	10	8	0.6	1.5	1.17	0.22	0.08	0.68	0.16	0.06	0.38	0.88	0.89	0.18	0.005	755	755	213	558	0.18	0.0054	745	23	545
V41122112	0.7	15	3	600	10	8	0.6	2.5	1.44	0.27	0.10	0.68	0.16	0.06	0.33	0.87	0.89	0.24	0.007	654	654	185	485	0.24	0.0071	643	20	471
V51122111	0.9	15	3	600	10	8	0.6	1.5	1.03	0.19	0.08	0.70	0.14	0.06	0.41	0.88	0.89	0.15	0.005	830	830	300	548	0.15	0.0047	823	26	539
V51122112	0.9	15	3	600	10	8	0.6	2.5	1.27	0.24	0.10	0.70	0.14	0.06	0.36	0.88	0.89	0.20	0.006	726	726	263	481	0.20	0.0062	718	22	470
V11122121	0.1	15	3	600	10	8	1	1.5	1.37	0.22	0.08	0.64	0.19	0.07	0.34	0.88	0.89	0.24	0.007	661	661	26	642	0.24	0.0072	642	19	625
V11122122	0.1	15	3	600	10	8	1	2.5	1.78	0.29	0.10	0.64	0.19	0.07	0.28	0.86	0.89	0.33	0.010	546	546	22	531	0.33	0.0100	524	16	510
V21122121	0.3	15	3	600	10	8	1	1.5	1.27	0.22	0.08	0.65	0.18	0.07	0.36	0.88	0.89	0.22	0.006	697	697	84	624	0.21	0.0063	682	21	608
V21122122	0.3	15	3	600	10	8	1	2.5	1.66	0.28	0.10	0.65	0.18	0.07	0.30	0.87	0.89	0.30	0.009	578	578	70	519	0.30	0.0087	560	17	500
V31122121	0.5	15	3	600	10	8	1	1.5	1.17	0.21	0.08	0.66	0.17	0.06	0.38	0.88	0.89	0.19	0.005	744	744	150	608	0.19	0.0055	732	22	593
V31122122	0.5	15	3	600	10	8	1	2.5	1.52	0.27	0.10	0.66	0.17	0.06	0.32	0.87	0.89	0.27	0.008	619	619	125	508	0.27	0.0077	606	18	491
V41122121	0.7	15	3	600	10	8	1	1.5	1.06	0.20	0.08	0.68	0.16	0.06	0.41	0.88	0.89	0.16	0.005	802	802	227	592	0.16	0.0047	793	24	580
V41122122	0.7	15	3	600	10	8	1	2.5	1.38	0.26	0.10	0.68	0.16	0.06	0.34	0.88	0.89	0.23	0.007	674	674	191	499	0.23	0.0067	663	20	485
V51122121	0.9	15	3	600	10	8	1	1.5	0.93	0.18	0.07	0.70	0.14	0.06	0.45	0.89	0.89	0.13	0.004	899	899	325	593	0.13	0.0042	893	28	585
V51122122	0.9	15	3	600	10	8	1	2.5	1.22	0.23	0.09	0.70	0.14	0.06	0.37	0.88	0.89	0.19	0.006	747	747	271	495	0.19	0.0059	740	23	484
V11122211	0.1	15	3	600	10	10	0.6	1.5	3.96	0.65	0.23	0.64	0.19	0.07	0.11	0.61	0.88	0.62	0.020	229	229	9	222	0.62	0.0188	200	6	194

Name	af	nf	hf	mf	Ly	Lx	tw	Lcb	T1 [s]	T2 [s]	T3 [s]	M1 [-]	M2 [-]	M3 [-]	Sa	Sa2	Sa3	Disp [m]	ISDR [-]	Total Moment [MN-m]	Total Shear [MN]	Outrigger Moment [MN-m]	Wall Moment [MN-m]	Mode 1 Disp [m]	Mode 1 ISDR [-]	Mode 1 Moment [MN-m]	Mode 1 Shear [MN]	Mode 1 wall Moment [MN-m]
V21122212	0.3	15	3	600	10	10	0.6	2.5	4.88	0.83	0.30	0.65	0.18	0.07	0.08	0.50	0.86	0.73	0.022	178	178	20	163	0.73	0.0213	157	5	140
V31122211	0.5	15	3	600	10	10	0.6	1.5	3.39	0.60	0.23	0.66	0.17	0.06	0.13	0.65	0.88	0.54	0.016	267	267	53	224	0.54	0.0155	247	8	201
V31122212	0.5	15	3	600	10	10	0.6	2.5	4.49	0.80	0.30	0.66	0.17	0.06	0.09	0.51	0.86	0.67	0.020	194	194	38	164	0.67	0.0193	176	5	143
V41122211	0.7	15	3	600	10	10	0.6	1.5	3.06	0.57	0.22	0.68	0.16	0.06	0.15	0.68	0.88	0.49	0.014	300	300	86	229	0.48	0.0142	285	9	208
V41122212	0.7	15	3	600	10	10	0.6	2.5	4.06	0.75	0.29	0.68	0.16	0.06	0.10	0.54	0.86	0.60	0.018	216	216	62	166	0.60	0.0177	202	6	148
V51122211	0.9	15	3	600	10	10	0.6	1.5	2.71	0.51	0.20	0.70	0.14	0.06	0.17	0.74	0.88	0.42	0.013	352	352	131	239	0.42	0.0134	341	11	223
V51122212	0.9	15	3	600	10	10	0.6	2.5	3.58	0.67	0.27	0.70	0.14	0.06	0.12	0.60	0.87	0.52	0.017	251	251	95	172	0.52	0.0165	240	7	157
V11122221	0.1	15	3	600	10	10	1	1.5	3.89	0.63	0.23	0.64	0.19	0.07	0.11	0.62	0.88	0.61	0.019	234	234	9	226	0.61	0.0185	205	6	199
V11122222	0.1	15	3	600	10	10	1	2.5	5.25	0.85	0.31	0.64	0.19	0.07	0.08	0.49	0.86	0.77	0.024	167	167	6	161	0.77	0.0232	140	4	137
V21122221	0.3	15	3	600	10	10	1	1.5	3.61	0.62	0.22	0.65	0.18	0.07	0.12	0.64	0.88	0.57	0.017	249	249	29	227	0.57	0.0167	226	7	201
V21122222	0.3	15	3	600	10	10	1	2.5	4.88	0.83	0.30	0.65	0.18	0.07	0.08	0.50	0.86	0.73	0.022	178	178	20	163	0.73	0.0213	157	5	140
V31122221	0.5	15	3	600	10	10	1	1.5	3.32	0.59	0.22	0.66	0.17	0.06	0.13	0.66	0.88	0.53	0.016	273	273	54	229	0.53	0.0153	254	8	206
V31122222	0.5	15	3	600	10	10	1	2.5	4.49	0.80	0.30	0.66	0.17	0.06	0.09	0.51	0.86	0.67	0.020	194	194	38	164	0.67	0.0193	176	5	143
V41122221	0.7	15	3	600	10	10	1	1.5	3.00	0.56	0.21	0.68	0.16	0.06	0.15	0.69	0.88	0.48	0.014	307	307	88	234	0.48	0.0140	292	9	214
V41122222	0.7	15	3	600	10	10	1	2.5	4.06	0.75	0.29	0.68	0.16	0.06	0.10	0.54	0.86	0.60	0.018	216	216	62	166	0.60	0.0177	202	6	147
V51122221	0.9	15	3	600	10	10	1	1.5	2.65	0.50	0.20	0.70	0.14	0.06	0.18	0.75	0.88	0.42	0.013	361	361	135	245	0.42	0.0132	349	11	229
V51122222	0.9	15	3	600	10	10	1	2.5	3.59	0.67	0.27	0.70	0.14	0.06	0.12	0.60	0.87	0.52	0.017	251	251	95	172	0.52	0.0165	240	7	157
V11211111	0.1	15	4	400	8	8	0.6	1.5	0.79	0.13	0.05	0.64	0.19	0.07	0.52	0.89	0.89	0.12	0.003	873	873	35	849	0.12	0.0027	862	19	838
V11211112	0.1	15	4	400	8	8	0.6	2.5	0.84	0.14	0.05	0.64	0.19	0.07	0.49	0.89	0.89	0.13	0.003	830	830	34	808	0.13	0.0029	818	18	796
V21211111	0.3	15	4	400	8	8	0.6	1.5	0.74	0.13	0.05	0.65	0.18	0.07	0.55	0.89	0.89	0.11	0.002	934	934	114	835	0.11	0.0024	925	21	825
V21211112	0.3	15	4	400	8	8	0.6	2.5	0.78	0.13	0.05	0.65	0.18	0.07	0.52	0.89	0.89	0.12	0.003	887	887	108	793	0.12	0.0026	878	20	783
V31211111	0.5	15	4	400	8	8	0.6	1.5	0.68	0.12	0.05	0.66	0.17	0.06	0.59	0.89	0.89	0.10	0.002	1013	1013	205	824	0.10	0.0021	1006	23	816
V31211112	0.5	15	4	400	8	8	0.6	2.5	0.72	0.13	0.05	0.66	0.17	0.06	0.56	0.89	0.89	0.11	0.002	964	964	195	785	0.11	0.0023	957	22	775
V41211111	0.7	15	4	400	8	8	0.6	1.5	0.61	0.11	0.04	0.68	0.16	0.06	0.64	0.89	0.89	0.09	0.002	1114	1114	314	818	0.08	0.0019	1109	26	811
V41211112	0.7	15	4	400	8	8	0.6	2.5	0.65	0.12	0.05	0.68	0.16	0.06	0.61	0.89	0.89	0.09	0.002	1059	1059	299	778	0.09	0.0020	1054	24	771
V51211111	0.9	15	4	400	8	8	0.6	1.5	0.54	0.10	0.04	0.70	0.14	0.06	0.71	0.89	0.89	0.07	0.002	1254	1254	450	823	0.07	0.0017	1250	29	818
V51211112	0.9	15	4	400	8	8	0.6	2.5	0.58	0.11	0.04	0.70	0.14	0.06	0.68	0.89	0.89	0.08	0.002	1198	1198	430	787	0.08	0.0018	1195	28	782
V11211121	0.1	15	4	400	8	8	1	1.5	0.65	0.11	0.04	0.64	0.19	0.07	0.61	0.89	0.89	0.10	0.002	1024	1024	42	996	0.10	0.0022	1014	23	987
V11211122	0.1	15	4	400	8	8	1	2.5	0.70	0.11	0.04	0.64	0.19	0.07	0.58	0.89	0.89	0.10	0.002	974	974	40	948	0.10	0.0024	964	22	938
V21211121	0.3	15	4	400	8	8	1	1.5	0.61	0.10	0.04	0.65	0.18	0.07	0.65	0.89	0.89	0.09	0.002	1096	1096	134	979	0.09	0.0019	1089	25	971
V21211122	0.3	15	4	400	8	8	1	2.5	0.65	0.11	0.04	0.65	0.18	0.07	0.61	0.89	0.89	0.09	0.002	1037	1037	126	927	0.09	0.0021	1029	23	918
V31211121	0.5	15	4	400	8	8	1	1.5	0.56	0.10	0.04	0.66	0.17	0.06	0.69	0.89	0.89	0.08	0.002	1186	1186	240	964	0.08	0.0017	1180	27	956
V31211122	0.5	15	4	400	8	8	1	2.5	0.59	0.11	0.04	0.66	0.17	0.06	0.66	0.89	0.89	0.08	0.002	1127	1127	228	916	0.08	0.0018	1120	26	908
V41211121	0.7	15	4	400	8	8	1	1.5	0.50	0.09	0.04	0.68	0.16	0.06	0.74	0.89	0.89	0.07	0.001	1287	1287	363	944	0.07	0.0015	1282	30	938
V41211122	0.7	15	4	400	8	8	1	2.5	0.54	0.10	0.04	0.68	0.16	0.06	0.71	0.89	0.89	0.07	0.002	1235	1235	348	906	0.07	0.0016	1230	28	899
V51211121	0.9	15	4	400	8	8	1	1.5	0.44	0.08	0.03	0.70	0.14	0.06	0.79	0.89	0.89	0.05	0.001	1392	1392	499	914	0.05	0.0012	1389	33	909
V51211122	0.9	15	4	400	8	8	1	2.5	0.48	0.09	0.04	0.70	0.14	0.06	0.76	0.89	0.89	0.06	0.001	1352	1352	485	887	0.06	0.0014	1348	32	883
V11211211	0.1	15	4	400	8	10	0.6	1.5	1.88	0.31	0.11	0.64	0.19	0.07	0.27	0.86	0.89	0.35	0.008	467	467	19	454	0.35	0.0079	447	10	435
V11211212	0.1	15	4	400	8	10	0.6	2.5	2.01	0.33	0.12	0.64	0.19	0.07	0.25	0.85	0.89	0.38	0.009	442	442	17	429	0.38	0.0086	421	10	410
V21211211	0.3	15	4	400	8	10	0.6	1.5	1.75	0.30	0.11	0.65	0.18	0.07	0.28	0.86	0.89	0.32	0.007	494	494	59	444	0.32	0.0070	478	11	426
V21211212	0.3	15	4	400	8	10	0.6	2.5	1.87	0.32	0.12	0.65	0.18	0.07	0.27	0.85	0.89	0.35	0.008	469	469	56	422	0.35	0.0076	453	10	404
V31211211	0.5	15	4	400	8	10	0.6	1.5	1.60	0.29	0.11	0.66	0.17	0.06	0.30	0.87	0.89	0.28	0.006	530	530	107	435	0.28	0.0061	518	12	420
V31211212	0.5	15	4	400	8	10	0.6	2.5	1.72	0.31	0.11	0.66	0.17	0.06	0.29	0.86	0.89	0.31	0.007	504	504	101	414	0.31	0.0067	491	11	398
V41211211	0.7	15	4	400	8	10	0.6	1.5	1.45	0.27	0.10	0.68	0.16	0.06	0.33	0.87	0.89	0.24	0.005	578	578	163	428	0.24	0.0054	568	13	415
V41211212	0.7	15	4	400	8	10	0.6	2.5	1.55	0.29	0.11	0.68	0.16	0.06	0.31	0.87	0.89	0.27	0.006	549	549	155	408	0.27	0.0058	539	12	395
V51211211	0.9	15	4	400	8	10	0.6	1.5	1.28	0.24	0.10	0.70	0.14	0.06	0.36	0.88	0.89	0.20	0.005	641	641	233	425	0.20	0.0047	635	15	415
V51211212	0.9	15	4	400	8	10	0.6	2.5	1.37	0.26	0.10	0.70	0.14	0.06	0.34	0.88	0.89	0.22	0.005	611	611	222	406	0.22	0.0051	605	14	396
V11211221	0.1	15	4	400	8	10	1	1.5	1.72	0.28	0.10	0.64	0.19	0.07	0.29	0.87	0.89	0.32	0.007	499	499	20	485	0.32	0.0072	480	11	467
V11211222	0.1	15	4	400	8	10	1	2.5	1.84	0.30	0.11	0.64	0.19	0.07	0.27	0.86	0.89	0.34	0.008	474	474	19	460	0.34	0.0078	453	10	441
V21211221	0.3	15	4	400	8	10	1	1.5	1.60	0.27	0.10	0.65	0.18	0.07	0.31	0.87	0.89	0.29	0.006	528	528	64	474	0.29	0.0063	513	12	457
V21211222	0.3	15	4	400	8	10	1	2.5	1.72	0.29	0.11	0.65	0.18	0.07	0.29	0.86	0.89	0.31	0.007	501	501	60	450	0.31	0.0068	485	11	433
V31211221	0.5	15	4	400	8	10	1	1.5	1.47	0.26	0.10	0.66	0.17	0.06	0.33	0.87	0.89	0.25	0.006	566	566	114	464	0.25	0.0055	554	13	449
V31211222	0.5	15	4	400	8	10	1	2.5	1.58	0.28	0.10	0.66	0.17	0.06	0.31	0.87	0.89	0.28	0.006	537	537	108	441	0.28	0.0060	525	12	425
V41211221	0.7	15	4	400	8	10	1	1.5	1.33	0.25	0.09	0.68	0.16	0.06	0.35	0.88	0.89	0.22	0.005	615	615	174	455	0.22	0.0048	606	14	443
V41211222	0.7	15	4	400	8	10	1	2.5	1.43	0.26	0.10	0.68	0.16	0.06	0.33	0.87	0.89	0.24	0.005	585	585	165	434	0.24	0.0053	575	13	421
V51211221	0.9	15	4	400	8	10	1	1.5	1.17	0.22	0.09	0.70	0.14	0.06	0.38	0.88	0.89	0.18	0.004	681	681	247	450	0.18	0.0042	674	16	441
V51211222	0.9	15	4	400	8	10	1	2.5	1.26	0.24	0.09	0.70	0.14	0.06	0.36	0.88	0.89	0.19	0.005	649	649	235	430	0.19	0.0046	642	15	420
V11212111	0.1	15	4	400	10	8	0.6	1.5	1.11	0.18	0.06	0.64	0.19	0.07	0.40	0.88	0.89	0.18	0.004	673	673	27	654	0.18	0.0041	658	15	641
V11212112	0.1	15	4	400	10	8	0.6	2.5	1.26	0.21	0.07	0.64	0.19	0.07	0.36	0.88	0.89	0.21	0.005	620	620	25	603	0.21	0.0049	604	14	588
V21212111	0.3	15	4	400	10	8	0.6	1.5	1.03	0.18	0.06	0.65	0.18	0.07	0.41	0.89	0.89	0.16	0.004	707	707	86	632	0.16	0.0036	695	16	620
V21212112	0.3	15	4	400	10	8	0.6	2.5	1.17	0.20	0.07	0.65	0.18	0.07	0.38	0.88	0.89	0.19	0.004	654	654	79	586	0.19	0.0042	641	15	572
V31212111	0.5	15	4	400	10	8	0.6	1.5	0.95	0.17	0.06	0.66	0.17	0.06	0.44	0.89	0.89	0.14	0.003	764	764	154	623	0.14	0.0031	754	17	612
V31212112	0.5	15	4	400	10	8	0.6	2.5	1.08	0.19	0.07	0.66	0.17	0.06	0.40	0.88	0.89	0.17	0.004	696	696	141	568	0.17	0.0037	686	16	556
V41212111	0.7	15	4	400	10	8	0.6	1.5	0.86	0.16	0.06	0.68	0.16	0.06	0.48	0.89	0.89	0.13	0.003	842	842	238	620	0.13	0.0028	835	19	611
V41212112	0.7	15	4	400	10	8	0.6	2.5	0.98	0.18	0.07	0.68	0.16	0.06	0.43	0.88	0.89	0.15	0.003	757	757	214	558	0.15	0.0032	749	17	548
V51212111	0.9	15	4	400	10	8	0.6	1.5	0.76	0.14	0.06	0.70	0.14	0.06	0.54	0.89	0.89	0.10	0.002	952	952	343	627	0.10	0.0025	947	22	620
V51212112	0.9	15	4	400	10	8	0.6	2.5	0.86	0.16	0.06	0.70	0.14	0.06	0.48	0.89	0.89	0.12	0.003	856	856	309	564	0.12	0.0029	851	20	557
V11212121	0.1	15	4	400	10	8	1	1.5	0.95	0.15	0.06	0.64	0.19	0.07	0.45	0.89	0.89	0.15	0.003	754	754	30	733	0.15	0.0033	741	17	721
V11212122	0.1	15	4	400	10	8	1	2.5	1.10	0.18	0.06	0.64	0.19	0.07	0.40	0.88	0.89	0.18	0.004	678	678	27	659	0.18	0.0040	663	15	645
V21212121	0.3	15	4	400	10	8	1	1.5	0.88	0.15	0.05	0.65	0.18	0.07	0.47	0.89	0.89	0.13	0.003	804	804	98	719	0.13	0.0029	793	18	707

Name	af	nf	hf	mf	Ly	Lx	tw	Lcb	T1 [s]	T2 [s]	T3 [s]	M1 [-]	M2 [-]	M3 [-]	Sa	Sa2	Sa3	Disp [m]	ISDR [-]	Total Moment [MN-m]	Total Shear [MN]	Outrigger Moment [MN-m]	Wall Moment [MN-m]	Mode 1 Disp [m]	Mode 1 ISDR [-]	Mode 1 Moment [MN-m]	Mode 1 Shear [MN]	Mode 1 wall Moment [MN-m]
V21212122	0.3	15	4	400	10	8	1	2.5	1.02	0.17	0.06	0.65	0.18	0.07	0.42	0.89	0.89	0.16	0.004	711	711	86	636	0.16	0.0035	700	16	624
V31212121	0.5	15	4	400	10	8	1	1.5	0.81	0.14	0.05	0.66	0.17	0.06	0.51	0.89	0.89	0.12	0.003	875	875	177	712	0.12	0.0026	867	20	703
V31212122	0.5	15	4	400	10	8	1	2.5	0.94	0.17	0.06	0.66	0.17	0.06	0.45	0.89	0.89	0.14	0.003	771	771	156	629	0.14	0.0031	762	17	617
V41212121	0.7	15	4	400	10	8	1	1.5	0.73	0.14	0.05	0.68	0.16	0.06	0.56	0.89	0.89	0.10	0.002	965	965	272	710	0.10	0.0023	959	22	702
V41212122	0.7	15	4	400	10	8	1	2.5	0.85	0.16	0.06	0.68	0.16	0.06	0.49	0.89	0.89	0.12	0.003	851	851	240	626	0.12	0.0027	844	19	617
V51212121	0.9	15	4	400	10	8	1	1.5	0.65	0.12	0.05	0.70	0.14	0.06	0.61	0.89	0.89	0.09	0.002	1087	1087	391	715	0.09	0.0020	1083	25	709
V51212122	0.9	15	4	400	10	8	1	2.5	0.75	0.14	0.06	0.70	0.14	0.06	0.54	0.89	0.89	0.10	0.002	962	962	346	633	0.10	0.0024	957	22	626
V11212211	0.1	15	4	400	10	10	0.6	1.5	2.78	0.45	0.16	0.64	0.19	0.07	0.17	0.78	0.89	0.48	0.011	302	302	12	293	0.48	0.0108	275	6	268
V11212212	0.1	15	4	400	10	10	0.6	2.5	3.28	0.53	0.19	0.64	0.19	0.07	0.13	0.72	0.88	0.54	0.013	252	252	10	244	0.54	0.0122	224	5	218
V21212211	0.3	15	4	400	10	10	0.6	1.5	2.59	0.44	0.16	0.65	0.18	0.07	0.18	0.79	0.89	0.45	0.010	326	326	39	295	0.45	0.0098	305	7	272
V21212212	0.3	15	4	400	10	10	0.6	2.5	3.05	0.52	0.19	0.65	0.18	0.07	0.15	0.73	0.88	0.50	0.011	269	269	32	244	0.50	0.0110	248	6	221
V31212211	0.5	15	4	400	10	10	0.6	1.5	2.38	0.42	0.16	0.66	0.17	0.06	0.20	0.80	0.89	0.42	0.009	361	361	72	299	0.41	0.0090	345	8	279
V31212212	0.5	15	4	400	10	10	0.6	2.5	2.80	0.50	0.19	0.66	0.17	0.06	0.16	0.75	0.88	0.47	0.010	296	296	59	247	0.47	0.0101	279	6	226
V41212211	0.7	15	4	400	10	10	0.6	1.5	2.15	0.40	0.15	0.68	0.16	0.06	0.23	0.82	0.89	0.38	0.008	412	412	117	309	0.38	0.0083	400	9	292
V41212212	0.7	15	4	400	10	10	0.6	2.5	2.53	0.47	0.18	0.68	0.16	0.06	0.19	0.77	0.88	0.42	0.009	336	336	95	253	0.42	0.0093	323	7	236
V51212211	0.9	15	4	400	10	10	0.6	1.5	1.90	0.36	0.14	0.70	0.14	0.06	0.27	0.84	0.89	0.32	0.008	478	478	175	319	0.32	0.0077	469	11	307
V51212212	0.9	15	4	400	10	10	0.6	2.5	2.24	0.42	0.17	0.70	0.14	0.06	0.22	0.81	0.89	0.37	0.009	397	397	147	267	0.37	0.0088	388	9	254
V11212221	0.1	15	4	400	10	10	1	1.5	2.61	0.42	0.15	0.64	0.19	0.07	0.18	0.80	0.89	0.45	0.011	326	326	13	316	0.45	0.0103	300	7	292
V11212222	0.1	15	4	400	10	10	1	2.5	3.12	0.51	0.18	0.64	0.19	0.07	0.14	0.74	0.88	0.52	0.012	266	266	10	257	0.52	0.0117	238	5	232
V21212221	0.3	15	4	400	10	10	1	1.5	2.42	0.41	0.15	0.65	0.18	0.07	0.20	0.81	0.89	0.43	0.010	352	352	42	318	0.43	0.0094	332	8	296
V21212222	0.3	15	4	400	10	10	1	2.5	2.90	0.49	0.18	0.65	0.18	0.07	0.16	0.75	0.88	0.49	0.011	285	285	33	258	0.49	0.0106	263	6	235
V31212221	0.5	15	4	400	10	10	1	1.5	2.23	0.40	0.15	0.66	0.17	0.06	0.22	0.82	0.89	0.40	0.009	392	392	79	324	0.40	0.0086	376	9	305
V31212222	0.5	15	4	400	10	10	1	2.5	2.67	0.48	0.18	0.66	0.17	0.06	0.17	0.76	0.88	0.45	0.010	314	314	63	261	0.45	0.0097	297	7	241
V41212221	0.7	15	4	400	10	10	1	1.5	2.01	0.37	0.14	0.68	0.16	0.06	0.25	0.84	0.89	0.36	0.008	448	448	127	334	0.36	0.0079	436	10	319
V41212222	0.7	15	4	400	10	10	1	2.5	2.41	0.45	0.17	0.68	0.16	0.06	0.20	0.79	0.89	0.41	0.009	357	357	101	269	0.41	0.0090	344	8	251
V51212221	0.9	15	4	400	10	10	1	1.5	1.78	0.33	0.13	0.70	0.14	0.06	0.28	0.85	0.89	0.30	0.007	503	503	184	336	0.30	0.0071	495	12	324
V51212222	0.9	15	4	400	10	10	1	2.5	2.13	0.40	0.16	0.70	0.14	0.06	0.23	0.82	0.89	0.36	0.008	422	422	155	283	0.36	0.0085	413	10	270
V11221111	0.1	15	4	600	8	8	0.6	1.5	0.97	0.16	0.06	0.64	0.19	0.07	0.44	0.89	0.89	0.15	0.003	1106	1106	45	1076	0.15	0.0034	1086	25	1057
V11221112	0.1	15	4	600	8	8	0.6	2.5	1.03	0.17	0.06	0.64	0.19	0.07	0.41	0.89	0.89	0.16	0.004	1055	1055	43	1025	0.16	0.0037	1033	23	1006
V21221111	0.3	15	4	600	8	8	0.6	1.5	0.90	0.15	0.06	0.65	0.18	0.07	0.46	0.89	0.89	0.14	0.003	1180	1180	143	1055	0.14	0.0030	1164	26	1038
V21221112	0.3	15	4	600	8	8	0.6	2.5	0.96	0.16	0.06	0.65	0.18	0.07	0.44	0.89	0.89	0.15	0.003	1124	1124	136	1006	0.15	0.0033	1108	25	987
V31221111	0.5	15	4	600	8	8	0.6	1.5	0.83	0.15	0.06	0.66	0.17	0.06	0.50	0.89	0.89	0.12	0.003	1283	1283	259	1046	0.12	0.0027	1271	29	1031
V31221112	0.5	15	4	600	8	8	0.6	2.5	0.88	0.16	0.06	0.66	0.17	0.06	0.47	0.89	0.89	0.13	0.003	1215	1215	246	990	0.13	0.0029	1202	27	974
V41221111	0.7	15	4	600	8	8	0.6	1.5	0.75	0.14	0.05	0.68	0.16	0.06	0.54	0.89	0.89	0.11	0.002	1413	1413	399	1039	0.11	0.0024	1404	32	1027
V41221112	0.7	15	4	600	8	8	0.6	2.5	0.80	0.15	0.06	0.68	0.16	0.06	0.52	0.89	0.89	0.12	0.003	1345	1345	380	990	0.12	0.0025	1336	31	977
V51221111	0.9	15	4	600	8	8	0.6	1.5	0.66	0.12	0.05	0.70	0.14	0.06	0.60	0.89	0.89	0.09	0.002	1600	1600	575	1052	0.09	0.0021	1594	37	1043
V51221112	0.9	15	4	600	8	8	0.6	2.5	0.70	0.13	0.05	0.70	0.14	0.06	0.57	0.89	0.89	0.10	0.002	1525	1525	548	1003	0.10	0.0023	1518	36	994
V11221121	0.1	15	4	600	8	8	1	1.5	0.80	0.13	0.05	0.64	0.19	0.07	0.52	0.89	0.89	0.12	0.003	1303	1303	53	1267	0.12	0.0028	1286	29	1251
V11221122	0.1	15	4	600	8	8	1	2.5	0.85	0.14	0.05	0.64	0.19	0.07	0.49	0.89	0.89	0.13	0.003	1234	1234	50	1200	0.13	0.0030	1215	27	1183
V21221121	0.3	15	4	600	8	8	1	1.5	0.74	0.13	0.05	0.65	0.18	0.07	0.55	0.89	0.89	0.11	0.002	1393	1393	169	1245	0.11	0.0024	1380	31	1230
V21221122	0.3	15	4	600	8	8	1	2.5	0.79	0.13	0.05	0.65	0.18	0.07	0.52	0.89	0.89	0.12	0.003	1319	1319	160	1179	0.12	0.0026	1305	30	1164
V31221121	0.5	15	4	600	8	8	1	1.5	0.68	0.12	0.05	0.66	0.17	0.06	0.59	0.89	0.89	0.10	0.002	1512	1512	306	1230	0.10	0.0021	1502	34	1217
V31221122	0.5	15	4	600	8	8	1	2.5	0.73	0.13	0.05	0.66	0.17	0.06	0.56	0.89	0.89	0.11	0.002	1432	1432	290	1166	0.11	0.0023	1421	32	1152
V41221121	0.7	15	4	600	8	8	1	1.5	0.62	0.11	0.04	0.68	0.16	0.06	0.64	0.89	0.89	0.09	0.002	1662	1662	469	1221	0.09	0.0019	1654	38	1210
V41221122	0.7	15	4	600	8	8	1	2.5	0.66	0.12	0.05	0.68	0.16	0.06	0.61	0.89	0.89	0.09	0.002	1576	1576	444	1158	0.09	0.0020	1568	36	1147
V51221121	0.9	15	4	600	8	8	1	1.5	0.54	0.10	0.04	0.70	0.14	0.06	0.71	0.89	0.89	0.07	0.002	1873	1873	672	1230	0.07	0.0017	1867	44	1222
V51221122	0.9	15	4	600	8	8	1	2.5	0.58	0.11	0.04	0.70	0.14	0.06	0.67	0.89	0.89	0.08	0.002	1782	1782	640	1171	0.08	0.0018	1777	42	1163
V11221211	0.1	15	4	600	8	10	0.6	1.5	2.30	0.37	0.13	0.64	0.19	0.07	0.21	0.84	0.89	0.42	0.010	565	565	22	548	0.42	0.0094	529	12	515
V11221212	0.1	15	4	600	8	10	0.6	2.5	2.46	0.40	0.14	0.64	0.19	0.07	0.19	0.82	0.89	0.44	0.010	522	522	20	506	0.44	0.0099	484	11	471
V21221211	0.3	15	4	600	8	10	0.6	1.5	2.14	0.36	0.13	0.65	0.18	0.07	0.23	0.84	0.89	0.39	0.009	615	615	73	554	0.39	0.0086	588	13	524
V21221212	0.3	15	4	600	8	10	0.6	2.5	2.29	0.39	0.14	0.65	0.18	0.07	0.21	0.83	0.89	0.41	0.009	566	566	67	511	0.41	0.0090	537	12	479
V31221211	0.5	15	4	600	8	10	0.6	1.5	1.97	0.35	0.13	0.66	0.17	0.06	0.26	0.84	0.89	0.36	0.008	680	680	137	560	0.36	0.0078	659	15	534
V31221212	0.5	15	4	600	8	10	0.6	2.5	2.10	0.37	0.14	0.66	0.17	0.06	0.24	0.84	0.89	0.38	0.008	631	631	127	521	0.38	0.0083	608	14	493
V41221211	0.7	15	4	600	8	10	0.6	1.5	1.78	0.33	0.13	0.68	0.16	0.06	0.28	0.85	0.89	0.31	0.007	744	744	211	554	0.31	0.0069	728	17	532
V41221212	0.7	15	4	600	8	10	0.6	2.5	1.90	0.35	0.14	0.68	0.16	0.06	0.27	0.84	0.89	0.34	0.007	705	705	200	526	0.34	0.0075	688	16	504
V51221211	0.9	15	4	600	8	10	0.6	1.5	1.57	0.29	0.12	0.70	0.14	0.06	0.31	0.86	0.89	0.26	0.006	831	831	303	553	0.26	0.0061	820	19	537
V51221212	0.9	15	4	600	8	10	0.6	2.5	1.68	0.31	0.13	0.70	0.14	0.06	0.29	0.86	0.89	0.28	0.007	789	789	288	526	0.28	0.0066	778	18	509
V11221221	0.1	15	4	600	8	10	1	1.5	2.10	0.34	0.12	0.64	0.19	0.07	0.24	0.85	0.89	0.39	0.009	628	628	25	610	0.39	0.0089	595	13	579
V11221222	0.1	15	4	600	8	10	1	2.5	2.26	0.37	0.13	0.64	0.19	0.07	0.22	0.84	0.89	0.41	0.009	577	577	23	560	0.41	0.0093	541	12	527
V21221221	0.3	15	4	600	8	10	1	1.5	1.96	0.33	0.12	0.65	0.18	0.07	0.26	0.85	0.89	0.36	0.008	678	678	81	610	0.36	0.0080	653	15	582
V21221222	0.3	15	4	600	8	10	1	2.5	2.10	0.36	0.13	0.65	0.18	0.07	0.24	0.84	0.89	0.39	0.009	629	629	75	566	0.39	0.0085	602	14	537
V31221221	0.5	15	4	600	8	10	1	1.5	1.80	0.32	0.12	0.66	0.17	0.06	0.28	0.85	0.89	0.33	0.007	729	729	147	600	0.33	0.0070	709	16	575
V31221222	0.5	15	4	600	8	10	1	2.5	1.93	0.34	0.13	0.66	0.17	0.06	0.26	0.85	0.89	0.35	0.008	690	690	139	568	0.35	0.0076	669	15	542
V41221221	0.7	15	4	600	8	10	1	1.5	1.63	0.30	0.12	0.68	0.16	0.06	0.30	0.86	0.89	0.28	0.006	796	796	225	591	0.28	0.0062	780	18	571
V41221222	0.7	15	4	600	8	10	1	2.5	1.75	0.32	0.12	0.68	0.16	0.06	0.28	0.85	0.89	0.31	0.007	754	754	213	561	0.31	0.0067	738	17	540
V51221221	0.9	15	4	600	8	10	1	1.5	1.44	0.27	0.11	0.70	0.14	0.06	0.33	0.87	0.89	0.23	0.005	887	887	323	589	0.23	0.0055	877	21	574
V51221222	0.9	15	4	600	8	10	1	2.5	1.54	0.29	0.12	0.70	0.14	0.06	0.31	0.87	0.89	0.25	0.006	842	842	307	560	0.25	0.0060	831	19	544
V11222111	0.1	15	4	600	10	8	0.6	1.5	1.36	0.22	0.08	0.64	0.19	0.07	0.34	0.88	0.89	0.24	0.005	885	885	35	860	0.24	0.0054	860	19	837
V11222112	0.1	15	4	600	10	8	0.6	2.5	1.54	0.25	0.09	0.64	0.19	0.07	0.31	0.88	0.89	0.28	0.006	809	809	32	786	0.28	0.0063	782	18	761
V21222111	0.3	15	4	600	10	8	0.6	1.5	1.27	0.22	0.08	0.65	0.18	0.07	0.36	0.88	0.89	0.21	0.005	933	933	113	836	0.21	0.0047	913	21	814
V21222112	0.3	15	4	600	10	8	0.6	2.5	1.44	0.24	0.09	0.65	0.18	0.07	0.33	0.88	0.89	0.25	0.006	855	855	103	767	0.25	0.0055	834	19	743
V31222111	0.5	15	4	600	10	8	0.6	1.5	1.16	0.21	0.08	0.66	0.17	0.06	0.38	0.88	0.89	0.19	0.004	995	995	201	813	0.19	0.0041	980	22	794

Name	af	nf	hf	mf	Ly	Lx	tw	Lcb	T1 [s]	T2 [s]	T3 [s]	M1 [-]	M2 [-]	M3 [-]	Sa	Sa2	Sa3	Disp [m]	ISDR [-]	Total Moment [MN-m]	Total Shear [MN]	Outrigger Moment [MN-m]	Wall Moment [MN-m]	Mode 1 Disp [m]	Mode 1 ISDR [-]	Mode 1 Moment [MN-m]	Mode 1 Shear [MN]	Mode 1 wall Moment [MN-m]
V31222112	0.5	15	4	600	10	8	0.6	2.5	1.32	0.24	0.09	0.66	0.17	0.06	0.35	0.88	0.89	0.22	0.005	915	915	185	749	0.22	0.0048	898	21	728
V41222111	0.7	15	4	600	10	8	0.6	1.5	1.05	0.19	0.08	0.68	0.16	0.06	0.41	0.88	0.89	0.16	0.004	1074	1074	303	792	0.16	0.0035	1062	24	776
V41222112	0.7	15	4	600	10	8	0.6	2.5	1.19	0.22	0.09	0.68	0.16	0.06	0.38	0.88	0.89	0.19	0.004	991	991	280	733	0.19	0.0042	978	23	716
V51222111	0.9	15	4	600	10	8	0.6	1.5	0.93	0.17	0.07	0.70	0.14	0.06	0.45	0.89	0.89	0.13	0.003	1205	1205	435	795	0.13	0.0031	1197	28	783
V51222112	0.9	15	4	600	10	8	0.6	2.5	1.06	0.20	0.08	0.70	0.14	0.06	0.41	0.88	0.89	0.15	0.004	1091	1091	395	721	0.15	0.0036	1083	25	709
V11222121	0.1	15	4	600	10	8	1	1.5	1.16	0.19	0.07	0.64	0.19	0.07	0.39	0.88	0.89	0.19	0.004	983	983	40	956	0.19	0.0043	961	22	935
V11222122	0.1	15	4	600	10	8	1	2.5	1.35	0.22	0.08	0.64	0.19	0.07	0.35	0.88	0.89	0.23	0.005	892	892	36	866	0.23	0.0053	867	20	843
V21222121	0.3	15	4	600	10	8	1	1.5	1.08	0.18	0.07	0.65	0.18	0.07	0.40	0.88	0.89	0.17	0.004	1034	1034	125	926	0.17	0.0038	1017	23	906
V21222122	0.3	15	4	600	10	8	1	2.5	1.25	0.21	0.08	0.65	0.18	0.07	0.37	0.88	0.89	0.21	0.005	940	940	114	842	0.21	0.0046	921	21	821
V31222121	0.5	15	4	600	10	8	1	1.5	0.99	0.18	0.07	0.66	0.17	0.06	0.43	0.89	0.89	0.15	0.003	1105	1105	223	901	0.15	0.0033	1090	25	884
V31222122	0.5	15	4	600	10	8	1	2.5	1.15	0.21	0.08	0.66	0.17	0.06	0.39	0.88	0.89	0.19	0.004	1002	1002	202	819	0.19	0.0040	986	23	800
V41222121	0.7	15	4	600	10	8	1	1.5	0.90	0.17	0.06	0.68	0.16	0.06	0.47	0.89	0.89	0.13	0.003	1217	1217	343	896	0.13	0.0029	1206	28	882
V41222122	0.7	15	4	600	10	8	1	2.5	1.04	0.19	0.07	0.68	0.16	0.06	0.41	0.88	0.89	0.16	0.003	1080	1080	305	797	0.16	0.0035	1069	25	782
V51222121	0.9	15	4	600	10	8	1	1.5	0.79	0.15	0.06	0.70	0.14	0.06	0.52	0.89	0.89	0.11	0.003	1381	1381	497	910	0.11	0.0026	1374	32	899
V51222122	0.9	15	4	600	10	8	1	2.5	0.92	0.17	0.07	0.70	0.14	0.06	0.46	0.89	0.89	0.13	0.003	1216	1216	439	802	0.13	0.0031	1208	28	790
V11222211	0.1	15	4	600	10	10	0.6	1.5	3.41	0.55	0.20	0.64	0.19	0.07	0.13	0.70	0.88	0.55	0.013	361	361	14	350	0.55	0.0125	320	7	312
V11222212	0.1	15	4	600	10	10	0.6	2.5	4.01	0.65	0.23	0.64	0.19	0.07	0.11	0.61	0.88	0.63	0.015	301	301	11	291	0.63	0.0142	262	6	255
V21222211	0.3	15	4	600	10	10	0.6	1.5	3.17	0.54	0.20	0.65	0.18	0.07	0.14	0.71	0.88	0.52	0.012	386	386	45	351	0.52	0.0114	354	8	316
V21222212	0.3	15	4	600	10	10	0.6	2.5	3.73	0.64	0.23	0.65	0.18	0.07	0.11	0.62	0.88	0.59	0.013	320	320	37	291	0.59	0.0129	289	7	258
V31222211	0.5	15	4	600	10	10	0.6	1.5	2.91	0.52	0.19	0.66	0.17	0.06	0.16	0.73	0.88	0.48	0.011	425	425	85	355	0.48	0.0104	398	9	323
V31222212	0.5	15	4	600	10	10	0.6	2.5	3.43	0.61	0.23	0.66	0.17	0.06	0.13	0.64	0.88	0.54	0.012	350	350	70	294	0.54	0.0117	325	7	263
V41222211	0.7	15	4	600	10	10	0.6	1.5	2.63	0.49	0.19	0.68	0.16	0.06	0.18	0.75	0.88	0.44	0.010	480	480	137	363	0.43	0.0096	460	11	337
V41222212	0.7	15	4	600	10	10	0.6	2.5	3.10	0.57	0.22	0.68	0.16	0.06	0.14	0.68	0.88	0.49	0.011	394	394	112	300	0.49	0.0108	374	9	273
V51222211	0.9	15	4	600	10	10	0.6	1.5	2.33	0.44	0.18	0.70	0.14	0.06	0.21	0.79	0.89	0.38	0.009	567	567	210	382	0.38	0.0090	553	13	362
V51222212	0.9	15	4	600	10	10	0.6	2.5	2.74	0.51	0.21	0.70	0.14	0.06	0.17	0.73	0.88	0.43	0.010	462	462	173	314	0.43	0.0101	447	10	293
V11222221	0.1	15	4	600	10	10	1	1.5	3.19	0.52	0.19	0.64	0.19	0.07	0.14	0.73	0.88	0.53	0.012	389	389	15	377	0.53	0.0119	348	8	338
V11222222	0.1	15	4	600	10	10	1	2.5	3.82	0.62	0.22	0.64	0.19	0.07	0.11	0.63	0.88	0.61	0.014	318	318	12	307	0.60	0.0137	278	6	271
V21222221	0.3	15	4	600	10	10	1	1.5	2.97	0.51	0.18	0.65	0.18	0.07	0.15	0.74	0.88	0.49	0.011	416	416	49	378	0.49	0.0108	384	9	343
V21222222	0.3	15	4	600	10	10	1	2.5	3.56	0.61	0.22	0.65	0.18	0.07	0.12	0.65	0.88	0.57	0.013	338	338	39	308	0.57	0.0124	307	7	274
V31222221	0.5	15	4	600	10	10	1	1.5	2.73	0.49	0.18	0.66	0.17	0.06	0.17	0.76	0.88	0.46	0.010	459	459	92	382	0.46	0.0099	433	10	351
V31222222	0.5	15	4	600	10	10	1	2.5	3.27	0.58	0.22	0.66	0.17	0.06	0.14	0.67	0.88	0.52	0.012	371	371	74	311	0.52	0.0113	345	8	279
V41222221	0.7	15	4	600	10	10	1	1.5	2.47	0.46	0.18	0.68	0.16	0.06	0.19	0.78	0.89	0.42	0.009	521	521	148	393	0.41	0.0091	501	12	367
V41222222	0.7	15	4	600	10	10	1	2.5	2.96	0.55	0.21	0.68	0.16	0.06	0.15	0.70	0.88	0.47	0.010	418	418	119	318	0.47	0.0104	398	9	291
V51222221	0.9	15	4	600	10	10	1	1.5	2.18	0.41	0.16	0.70	0.14	0.06	0.23	0.81	0.89	0.36	0.009	616	616	227	414	0.36	0.0086	603	14	394
V51222222	0.9	15	4	600	10	10	1	2.5	2.61	0.49	0.20	0.70	0.14	0.06	0.18	0.75	0.88	0.41	0.010	491	491	183	333	0.41	0.0098	476	11	311
V12111111	0.1	30	3	400	8	8	0.6	1.5	1.01	0.17	0.06	0.63	0.19	0.07	0.42	0.89	0.89	0.16	0.002	2077	2077	82	2005	0.16	0.0025	2041	31	1967
V12111112	0.1	30	3	400	8	8	0.6	2.5	1.05	0.17	0.06	0.63	0.19	0.07	0.41	0.89	0.89	0.17	0.003	2034	2034	80	1963	0.17	0.0026	1997	30	1925
V22111111	0.3	30	3	400	8	8	0.6	1.5	0.95	0.16	0.06	0.64	0.18	0.06	0.45	0.89	0.89	0.15	0.002	2225	2225	263	1975	0.15	0.0022	2194	33	1941
V22111112	0.3	30	3	400	8	8	0.6	2.5	0.98	0.17	0.06	0.64	0.18	0.06	0.43	0.89	0.89	0.16	0.002	2156	2156	255	1914	0.16	0.0023	2124	32	1879
V32111111	0.5	30	3	400	8	8	0.6	1.5	0.87	0.16	0.06	0.65	0.17	0.06	0.48	0.89	0.89	0.13	0.002	2405	2405	474	1948	0.13	0.0019	2380	36	1918
V32111112	0.5	30	3	400	8	8	0.6	2.5	0.90	0.16	0.06	0.65	0.17	0.06	0.46	0.89	0.89	0.14	0.002	2330	2330	459	1888	0.14	0.0020	2304	35	1857
V42111111	0.7	30	3	400	8	8	0.6	1.5	0.79	0.15	0.06	0.66	0.16	0.06	0.52	0.89	0.89	0.12	0.002	2651	2651	730	1943	0.12	0.0017	2632	41	1918
V42111112	0.7	30	3	400	8	8	0.6	2.5	0.82	0.15	0.06	0.66	0.16	0.06	0.50	0.89	0.89	0.12	0.002	2573	2573	708	1886	0.12	0.0018	2553	39	1860
V52111111	0.9	30	3	400	8	8	0.6	1.5	0.70	0.13	0.05	0.69	0.14	0.06	0.58	0.89	0.89	0.10	0.002	2993	2993	1052	1967	0.10	0.0015	2980	47	1949
V52111112	0.9	30	3	400	8	8	0.6	2.5	0.73	0.14	0.05	0.69	0.14	0.06	0.56	0.89	0.89	0.10	0.002	2900	2900	1019	1907	0.10	0.0016	2887	45	1887
V12111121	0.1	30	3	400	8	8	1	1.5	0.79	0.13	0.05	0.63	0.19	0.07	0.52	0.89	0.89	0.12	0.002	2558	2558	101	2468	0.12	0.0019	2528	38	2437
V12111122	0.1	30	3	400	8	8	1	2.5	0.82	0.13	0.05	0.63	0.19	0.07	0.50	0.89	0.89	0.13	0.002	2479	2479	98	2391	0.13	0.0019	2448	37	2359
V22111121	0.3	30	3	400	8	8	1	1.5	0.74	0.13	0.05	0.64	0.18	0.06	0.55	0.89	0.89	0.11	0.002	2736	2736	325	2426	0.11	0.0016	2711	41	2398
V22111122	0.3	30	3	400	8	8	1	2.5	0.77	0.13	0.05	0.64	0.18	0.06	0.53	0.89	0.89	0.12	0.002	2643	2643	313	2343	0.12	0.0017	2616	40	2314
V32111121	0.5	30	3	400	8	8	1	1.5	0.68	0.12	0.05	0.65	0.17	0.06	0.59	0.89	0.89	0.10	0.001	2964	2964	585	2397	0.10	0.0014	2943	45	2372
V32111122	0.5	30	3	400	8	8	1	2.5	0.71	0.13	0.05	0.65	0.17	0.06	0.57	0.89	0.89	0.11	0.002	2872	2872	567	2323	0.11	0.0015	2851	44	2297
V42111121	0.7	30	3	400	8	8	1	1.5	0.62	0.11	0.04	0.66	0.16	0.06	0.64	0.89	0.89	0.09	0.001	3250	3250	894	2377	0.09	0.0013	3234	50	2357
V42111122	0.7	30	3	400	8	8	1	2.5	0.64	0.12	0.05	0.66	0.16	0.06	0.62	0.89	0.89	0.09	0.001	3140	3140	864	2298	0.09	0.0013	3124	48	2276
V52111121	0.9	30	3	400	8	8	1	1.5	0.55	0.10	0.04	0.69	0.14	0.06	0.70	0.89	0.89	0.07	0.001	3647	3647	1279	2393	0.07	0.0011	3636	57	2377
V52111122	0.9	30	3	400	8	8	1	2.5	0.57	0.11	0.04	0.69	0.14	0.06	0.68	0.89	0.89	0.07	0.001	3543	3543	1242	2325	0.07	0.0012	3531	55	2309
V12111211	0.1	30	3	400	8	10	0.6	1.5	2.30	0.38	0.13	0.63	0.19	0.07	0.21	0.84	0.89	0.43	0.007	1094	1094	42	1059	0.43	0.0064	1032	16	994
V12111212	0.1	30	3	400	8	10	0.6	2.5	2.40	0.39	0.14	0.63	0.19	0.07	0.20	0.83	0.89	0.44	0.007	1041	1041	40	1008	0.44	0.0066	976	15	941
V22111211	0.3	30	3	400	8	10	0.6	1.5	2.15	0.37	0.13	0.64	0.18	0.06	0.23	0.84	0.89	0.40	0.006	1195	1195	139	1069	0.40	0.0058	1143	17	1011
V22111212	0.3	30	3	400	8	10	0.6	2.5	2.24	0.38	0.14	0.64	0.18	0.06	0.22	0.83	0.89	0.41	0.006	1137	1137	132	1018	0.41	0.0060	1082	16	957
V32111211	0.5	30	3	400	8	10	0.6	1.5	1.98	0.35	0.13	0.65	0.17	0.06	0.26	0.84	0.89	0.37	0.005	1322	1322	259	1082	0.37	0.0053	1280	20	1032
V32111212	0.5	30	3	400	8	10	0.6	2.5	2.06	0.37	0.14	0.65	0.17	0.06	0.25	0.84	0.89	0.38	0.006	1266	1266	248	1037	0.38	0.0055	1223	19	985
V42111211	0.7	30	3	400	8	10	0.6	1.5	1.79	0.33	0.13	0.66	0.16	0.06	0.28	0.85	0.89	0.32	0.005	1444	1444	399	1071	0.32	0.0047	1412	22	1029
V42111212	0.7	30	3	400	8	10	0.6	2.5	1.87	0.35	0.13	0.66	0.16	0.06	0.27	0.85	0.89	0.34	0.005	1398	1398	386	1038	0.34	0.0050	1365	21	995
V52111211	0.9	30	3	400	8	10	0.6	1.5	1.59	0.30	0.12	0.69	0.14	0.06	0.31	0.86	0.89	0.26	0.004	1608	1608	572	1068	0.26	0.0042	1585	25	1036
V52111212	0.9	30	3	400	8	10	0.6	2.5	1.66	0.31	0.12	0.69	0.14	0.06	0.30	0.86	0.89	0.28	0.004	1557	1557	555	1036	0.28	0.0044	1534	24	1003
V12111221	0.1	30	3	400	8	10	1	1.5	1.95	0.32	0.11	0.63	0.19	0.07	0.26	0.86	0.89	0.37	0.006	1325	1325	51	1281	0.37	0.0056	1271	19	1225
V12111222	0.1	30	3	400	8	10	1	2.5	2.03	0.33	0.12	0.63	0.19	0.07	0.25	0.85	0.89	0.39	0.006	1274	1274	49	1232	0.39	0.0059	1219	18	1174
V22111221	0.3	30	3	400	8	10	1	1.5	1.81	0.31	0.11	0.64	0.18	0.06	0.28	0.86	0.89	0.34	0.005	1408	1408	165	1256	0.34	0.0050	1362	21	1204
V22111222	0.3	30	3	400	8	10	1	2.5	1.89	0.32	0.12	0.64	0.18	0.06	0.27	0.85	0.89	0.36	0.005	1361	1361	159	1215	0.36	0.0052	1314	20	1162
V32111221	0.5	30	3	400	8	10	1	1.5	1.67	0.30	0.11	0.65	0.17	0.06	0.30	0.86	0.89	0.30	0.004	1509	1509	296	1232	0.30	0.0044	1471	23	1186
V32111222	0.5	30	3	400	8	10	1	2.5	1.74	0.31	0.12	0.65	0.17	0.06	0.29	0.86	0.89	0.32	0.005	1460	1460	287	1193	0.32	0.0046	1422	22	1146
V42111221	0.7	30	3	400	8	10	1	1.5	1.51	0.28	0.11	0.66	0.16	0.06	0.32	0.87	0.89	0.26	0.004	1640	1640	453	1213	0.26	0.0038	1611	25	1174

Name	af	nf	hf	mf	Ly	Lx	tw	Lcb	T1 [s]	T2 [s]	T3 [s]	M1 [-]	M2 [-]	M3 [-]	Sa	Sa2	Sa3	Disp [m]	ISDR [-]	Total Moment [MN-m]	Total Shear [MN]	Outrigger Moment [MN-m]	Wall Moment [MN-m]	Mode 1 Disp [m]	Mode 1 ISDR [-]	Mode 1 Moment [MN-m]	Mode 1 Shear [MN]	Mode 1 wall Moment [MN-m]
V42111222	0.7	30	3	400	8	10	1	2.5	1.58	0.29	0.11	0.66	0.16	0.06	0.31	0.86	0.89	0.28	0.004	1590	1590	439	1176	0.27	0.0040	1560	24	1137
V52111221	0.9	30	3	400	8	10	1	1.5	1.34	0.25	0.10	0.69	0.14	0.06	0.35	0.88	0.89	0.21	0.003	1819	1819	645	1205	0.21	0.0034	1799	28	1176
V52111222	0.9	30	3	400	8	10	1	2.5	1.40	0.26	0.11	0.69	0.14	0.06	0.34	0.87	0.89	0.22	0.004	1763	1763	626	1169	0.22	0.0036	1742	27	1139
V12112111	0.1	30	3	400	10	8	0.6	1.5	1.38	0.23	0.08	0.63	0.19	0.07	0.34	0.88	0.89	0.25	0.004	1705	1705	67	1647	0.25	0.0037	1662	25	1601
V12112112	0.1	30	3	400	10	8	0.6	2.5	1.48	0.24	0.09	0.63	0.19	0.07	0.32	0.88	0.89	0.27	0.004	1623	1623	64	1567	0.27	0.0041	1577	24	1520
V22112111	0.3	30	3	400	10	8	0.6	1.5	1.29	0.22	0.08	0.64	0.18	0.06	0.36	0.88	0.89	0.22	0.003	1803	1803	213	1604	0.22	0.0032	1765	27	1561
V22112112	0.3	30	3	400	10	8	0.6	2.5	1.38	0.24	0.09	0.64	0.18	0.06	0.34	0.88	0.89	0.24	0.004	1716	1716	202	1527	0.24	0.0035	1677	26	1483
V32112111	0.5	30	3	400	10	8	0.6	1.5	1.19	0.21	0.08	0.65	0.17	0.06	0.38	0.88	0.89	0.20	0.003	1922	1922	378	1562	0.20	0.0028	1891	29	1524
V32112112	0.5	30	3	400	10	8	0.6	2.5	1.27	0.23	0.08	0.65	0.17	0.06	0.36	0.88	0.89	0.22	0.003	1832	1832	361	1490	0.22	0.0031	1800	28	1451
V42112111	0.7	30	3	400	10	8	0.6	1.5	1.07	0.20	0.08	0.66	0.16	0.06	0.40	0.88	0.89	0.17	0.002	2070	2070	570	1523	0.17	0.0025	2047	32	1491
V42112112	0.7	30	3	400	10	8	0.6	2.5	1.15	0.21	0.08	0.66	0.16	0.06	0.39	0.88	0.89	0.18	0.003	1979	1979	545	1457	0.18	0.0027	1954	30	1424
V52112111	0.9	30	3	400	10	8	0.6	1.5	0.95	0.18	0.07	0.69	0.14	0.06	0.44	0.88	0.89	0.14	0.002	2303	2303	812	1519	0.14	0.0022	2287	36	1495
V52112112	0.9	30	3	400	10	8	0.6	2.5	1.02	0.19	0.08	0.69	0.14	0.06	0.42	0.88	0.89	0.15	0.002	2168	2168	765	1431	0.15	0.0023	2151	34	1406
V12112121	0.1	30	3	400	10	8	1	1.5	1.10	0.18	0.06	0.63	0.19	0.07	0.40	0.88	0.89	0.18	0.003	1978	1978	78	1909	0.18	0.0028	1940	29	1870
V12112122	0.1	30	3	400	10	8	1	2.5	1.19	0.19	0.07	0.63	0.19	0.07	0.38	0.88	0.89	0.20	0.003	1883	1883	74	1818	0.20	0.0031	1843	28	1776
V22112121	0.3	30	3	400	10	8	1	1.5	1.03	0.18	0.06	0.64	0.18	0.06	0.42	0.89	0.89	0.16	0.002	2078	2078	246	1846	0.16	0.0024	2045	31	1809
V22112122	0.3	30	3	400	10	8	1	2.5	1.11	0.19	0.07	0.64	0.18	0.06	0.40	0.88	0.89	0.18	0.003	1983	1983	234	1762	0.18	0.0027	1948	30	1723
V32112121	0.5	30	3	400	10	8	1	1.5	0.95	0.17	0.06	0.65	0.17	0.06	0.45	0.89	0.89	0.15	0.002	2246	2246	443	1821	0.15	0.0021	2219	34	1788
V32112122	0.5	30	3	400	10	8	1	2.5	1.02	0.18	0.07	0.65	0.17	0.06	0.42	0.88	0.89	0.16	0.002	2103	2103	414	1706	0.16	0.0023	2074	32	1672
V42112121	0.7	30	3	400	10	8	1	1.5	0.86	0.16	0.06	0.66	0.16	0.06	0.48	0.89	0.89	0.13	0.002	2471	2471	680	1812	0.13	0.0019	2450	38	1785
V42112122	0.7	30	3	400	10	8	1	2.5	0.93	0.17	0.07	0.66	0.16	0.06	0.45	0.89	0.89	0.14	0.002	2312	2312	637	1697	0.14	0.0021	2290	35	1669
V52112121	0.9	30	3	400	10	8	1	1.5	0.76	0.14	0.06	0.69	0.14	0.06	0.54	0.89	0.89	0.11	0.002	2779	2779	977	1828	0.11	0.0017	2765	43	1808
V52112122	0.9	30	3	400	10	8	1	2.5	0.82	0.15	0.06	0.69	0.14	0.06	0.50	0.89	0.89	0.12	0.002	2610	2610	918	1718	0.12	0.0018	2595	41	1697
V12112211	0.1	30	3	400	10	10	0.6	1.5	3.30	0.54	0.19	0.63	0.19	0.07	0.13	0.71	0.88	0.55	0.009	725	725	27	703	0.55	0.0083	653	10	629
V12112212	0.1	30	3	400	10	10	0.6	2.5	3.60	0.59	0.21	0.63	0.19	0.07	0.12	0.67	0.88	0.59	0.009	656	656	24	637	0.59	0.0089	585	9	564
V22112211	0.3	30	3	400	10	10	0.6	1.5	3.07	0.52	0.19	0.64	0.18	0.06	0.15	0.73	0.88	0.52	0.008	782	782	89	706	0.52	0.0075	720	11	637
V22112212	0.3	30	3	400	10	10	0.6	2.5	3.36	0.57	0.21	0.64	0.18	0.06	0.13	0.68	0.88	0.55	0.008	706	706	80	638	0.55	0.0080	645	10	570
V32112211	0.5	30	3	400	10	10	0.6	1.5	2.83	0.50	0.19	0.65	0.17	0.06	0.16	0.74	0.88	0.48	0.007	860	860	167	713	0.48	0.0069	809	12	652
V32112212	0.5	30	3	400	10	10	0.6	2.5	3.09	0.55	0.21	0.65	0.17	0.06	0.15	0.70	0.88	0.51	0.007	774	774	150	644	0.51	0.0074	723	11	583
V42112211	0.7	30	3	400	10	10	0.6	1.5	2.56	0.47	0.18	0.66	0.16	0.06	0.18	0.76	0.88	0.43	0.006	971	971	269	730	0.43	0.0064	932	14	679
V42112212	0.7	30	3	400	10	10	0.6	2.5	2.80	0.52	0.20	0.66	0.16	0.06	0.16	0.73	0.88	0.46	0.007	872	872	242	658	0.46	0.0068	831	13	606
V52112211	0.9	30	3	400	10	10	0.6	1.5	2.27	0.43	0.17	0.69	0.14	0.06	0.22	0.80	0.89	0.38	0.006	1140	1140	411	766	0.38	0.0060	1112	17	727
V52112212	0.9	30	3	400	10	10	0.6	2.5	2.48	0.47	0.19	0.69	0.14	0.06	0.19	0.77	0.88	0.40	0.006	1020	1020	369	689	0.40	0.0064	990	16	648
V12112221	0.1	30	3	400	10	10	1	1.5	2.85	0.46	0.17	0.63	0.19	0.07	0.16	0.77	0.89	0.50	0.008	856	856	32	830	0.49	0.0074	786	12	757
V12112222	0.1	30	3	400	10	10	1	2.5	3.14	0.51	0.18	0.63	0.19	0.07	0.14	0.74	0.88	0.53	0.008	767	767	29	744	0.53	0.0080	695	11	670
V22112221	0.3	30	3	400	10	10	1	1.5	2.65	0.45	0.17	0.64	0.18	0.06	0.18	0.78	0.89	0.46	0.007	927	927	107	834	0.46	0.0067	868	13	768
V22112222	0.3	30	3	400	10	10	1	2.5	2.92	0.50	0.18	0.64	0.18	0.06	0.16	0.75	0.88	0.50	0.007	828	828	95	747	0.50	0.0072	767	12	678
V32112221	0.5	30	3	400	10	10	1	1.5	2.44	0.43	0.16	0.65	0.17	0.06	0.20	0.79	0.89	0.43	0.006	1026	1026	200	846	0.43	0.0062	978	15	788
V32112222	0.5	30	3	400	10	10	1	2.5	2.69	0.48	0.18	0.65	0.17	0.06	0.17	0.76	0.88	0.46	0.007	912	912	178	756	0.46	0.0066	862	13	695
V42112221	0.7	30	3	400	10	10	1	1.5	2.21	0.41	0.16	0.66	0.16	0.06	0.22	0.81	0.89	0.39	0.006	1166	1166	323	871	0.39	0.0057	1130	17	823
V42112222	0.7	30	3	400	10	10	1	2.5	2.44	0.45	0.17	0.66	0.16	0.06	0.20	0.78	0.89	0.42	0.006	1033	1033	286	775	0.42	0.0061	994	15	724
V52112221	0.9	30	3	400	10	10	1	1.5	1.96	0.37	0.15	0.69	0.14	0.06	0.26	0.84	0.89	0.34	0.005	1362	1362	487	910	0.34	0.0054	1337	21	874
V52112222	0.9	30	3	400	10	10	1	2.5	2.16	0.41	0.16	0.69	0.14	0.06	0.23	0.82	0.89	0.37	0.006	1216	1216	437	815	0.36	0.0058	1188	19	777
V12121111	0.1	30	3	600	8	8	0.6	1.5	1.24	0.20	0.07	0.63	0.19	0.07	0.37	0.88	0.89	0.22	0.003	2750	2750	108	2654	0.21	0.0032	2688	41	2591
V12121112	0.1	30	3	600	8	8	0.6	2.5	1.29	0.21	0.08	0.63	0.19	0.07	0.36	0.88	0.89	0.23	0.003	2683	2683	105	2590	0.23	0.0034	2620	40	2525
V22121111	0.3	30	3	600	8	8	0.6	1.5	1.16	0.20	0.07	0.64	0.18	0.06	0.39	0.88	0.89	0.19	0.003	2899	2899	342	2577	0.19	0.0028	2846	43	2517
V22121112	0.3	30	3	600	8	8	0.6	2.5	1.20	0.20	0.07	0.64	0.18	0.06	0.38	0.88	0.89	0.20	0.003	2832	2832	334	2517	0.20	0.0030	2778	42	2457
V32121111	0.5	30	3	600	8	8	0.6	1.5	1.07	0.19	0.07	0.65	0.17	0.06	0.41	0.88	0.89	0.17	0.002	3081	3081	607	2501	0.17	0.0024	3037	47	2448
V32121112	0.5	30	3	600	8	8	0.6	2.5	1.11	0.20	0.07	0.65	0.17	0.06	0.40	0.88	0.89	0.18	0.003	3011	3011	593	2445	0.18	0.0026	2967	45	2391
V42121111	0.7	30	3	600	8	8	0.6	1.5	0.97	0.18	0.07	0.66	0.16	0.06	0.44	0.88	0.89	0.15	0.002	3352	3352	923	2463	0.15	0.0021	3319	51	2418
V42121112	0.7	30	3	600	8	8	0.6	2.5	1.00	0.19	0.07	0.66	0.16	0.06	0.42	0.88	0.89	0.15	0.002	3243	3243	893	2383	0.15	0.0022	3208	50	2338
V52121111	0.9	30	3	600	8	8	0.6	1.5	0.86	0.16	0.06	0.69	0.14	0.06	0.48	0.89	0.89	0.12	0.002	3778	3778	1330	2488	0.12	0.0019	3755	59	2455
V52121112	0.9	30	3	600	8	8	0.6	2.5	0.89	0.17	0.07	0.69	0.14	0.06	0.47	0.89	0.89	0.13	0.002	3649	3649	1286	2404	0.13	0.0020	3626	57	2371
V12121121	0.1	30	3	600	8	8	1	1.5	0.97	0.16	0.06	0.63	0.19	0.07	0.44	0.89	0.89	0.16	0.002	3240	3240	128	3126	0.16	0.0023	3187	48	3072
V12121122	0.1	30	3	600	8	8	1	2.5	1.01	0.16	0.06	0.63	0.19	0.07	0.42	0.89	0.89	0.16	0.002	3129	3129	123	3019	0.16	0.0024	3074	47	2963
V22121121	0.3	30	3	600	8	8	1	1.5	0.90	0.15	0.06	0.64	0.18	0.06	0.46	0.89	0.89	0.14	0.002	3458	3458	409	3069	0.14	0.0021	3413	52	3018
V22121122	0.3	30	3	600	8	8	1	2.5	0.94	0.16	0.06	0.64	0.18	0.06	0.45	0.89	0.89	0.15	0.002	3353	3353	397	2976	0.15	0.0022	3307	50	2924
V32121121	0.5	30	3	600	8	8	1	1.5	0.83	0.15	0.06	0.65	0.17	0.06	0.50	0.89	0.89	0.13	0.002	3754	3754	740	3040	0.13	0.0018	3718	57	2996
V32121122	0.5	30	3	600	8	8	1	2.5	0.87	0.15	0.06	0.65	0.17	0.06	0.48	0.89	0.89	0.13	0.002	3625	3625	715	2937	0.13	0.0019	3588	55	2891
V42121121	0.7	30	3	600	8	8	1	1.5	0.75	0.14	0.05	0.66	0.16	0.06	0.54	0.89	0.89	0.11	0.002	4121	4121	1134	3019	0.11	0.0016	4094	63	2983
V42121122	0.7	30	3	600	8	8	1	2.5	0.78	0.15	0.06	0.66	0.16	0.06	0.52	0.89	0.89	0.12	0.002	3994	3994	1099	2927	0.11	0.0017	3965	61	2889
V52121121	0.9	30	3	600	8	8	1	1.5	0.67	0.13	0.05	0.69	0.14	0.06	0.60	0.89	0.89	0.09	0.001	4651	4651	1633	3056	0.09	0.0014	4632	73	3029
V52121122	0.9	30	3	600	8	8	1	2.5	0.70	0.13	0.05	0.69	0.14	0.06	0.58	0.89	0.89	0.10	0.002	4510	4510	1584	2964	0.10	0.0015	4491	71	2936
V12121211	0.1	30	3	600	8	10	0.6	1.5	2.82	0.46	0.17	0.63	0.19	0.07	0.16	0.78	0.89	0.49	0.008	1295	1295	49	1256	0.49	0.0074	1191	18	1148
V12121212	0.1	30	3	600	8	10	0.6	2.5	2.94	0.48	0.17	0.63	0.19	0.07	0.15	0.76	0.89	0.51	0.008	1236	1236	47	1198	0.51	0.0076	1130	17	1089
V22121211	0.3	30	3	600	8	10	0.6	1.5	2.63	0.45	0.16	0.64	0.18	0.06	0.18	0.78	0.89	0.46	0.007	1404	1404	162	1262	0.46	0.0067	1315	20	1163
V22121212	0.3	30	3	600	8	10	0.6	2.5	2.74	0.47	0.17	0.64	0.18	0.06	0.17	0.77	0.89	0.48	0.007	1338	1338	154	1204	0.47	0.0069	1248	19	1104
V32121211	0.5	30	3	600	8	10	0.6	1.5	2.42	0.43	0.16	0.65	0.17	0.06	0.20	0.80	0.89	0.43	0.006	1554	1554	303	1281	0.43	0.0062	1482	23	1194
V32121212	0.5	30	3	600	8	10	0.6	2.5	2.52	0.45	0.17	0.65	0.17	0.06	0.19	0.78	0.89	0.44	0.006	1477	1477	288	1220	0.44	0.0063	1403	21	1131
V42121211	0.7	30	3	600	8	10	0.6	1.5	2.19	0.41	0.16	0.66	0.16	0.06	0.23	0.82	0.89	0.39	0.006	1767	1767	489	1320	0.39	0.0057	1713	26	1248
V42121212	0.7	30	3	600	8	10	0.6	2.5	2.29	0.42	0.16	0.66	0.16	0.06	0.21	0.80	0.89	0.40	0.006	1676	1676	464	1254	0.40	0.0059	1621	25	1181
V52121211	0.9	30	3	600	8	10	0.6	1.5	1.95	0.36	0.15	0.69	0.14	0.06	0.26	0.84	0.89	0.34	0.005	2057	2057	736	1373	0.33	0.0053	2019	32	1320

Name	af	nf	hf	mf	Ly	Lx	tw	Lcb	T1 [s]	T2 [s]	T3 [s]	M1 [-]	M2 [-]	M3 [-]	Sa	Sa2	Sa3	Disp [m]	ISDR [-]	Total Moment [MN-m]	Total Shear [MN]	Outrigger Moment [MN-m]	Wall Moment [MN-m]	Mode 1 Disp [m]	Mode 1 ISDR [-]	Mode 1 Moment [MN-m]	Mode 1 Shear [MN]	Mode 1 wall Moment [MN-m]
V52121212	0.9	30	3	600	8	10	0.6	2.5	2.03	0.38	0.15	0.69	0.14	0.06	0.25	0.83	0.89	0.35	0.006	1979	1979	709	1323	0.35	0.0055	1940	30	1269
V12121221	0.1	30	3	600	8	10	1	1.5	2.38	0.39	0.14	0.63	0.19	0.07	0.20	0.83	0.89	0.44	0.007	1577	1577	60	1526	0.44	0.0065	1480	22	1426
V12121222	0.1	30	3	600	8	10	1	2.5	2.49	0.41	0.15	0.63	0.19	0.07	0.19	0.82	0.89	0.45	0.007	1499	1499	57	1451	0.45	0.0067	1399	21	1349
V22121221	0.3	30	3	600	8	10	1	1.5	2.22	0.38	0.14	0.64	0.18	0.06	0.22	0.83	0.89	0.41	0.006	1722	1722	200	1542	0.41	0.0060	1641	25	1451
V22121222	0.3	30	3	600	8	10	1	2.5	2.32	0.40	0.14	0.64	0.18	0.06	0.21	0.82	0.89	0.42	0.006	1633	1633	190	1464	0.42	0.0061	1550	24	1371
V32121221	0.5	30	3	600	8	10	1	1.5	2.04	0.36	0.14	0.65	0.17	0.06	0.25	0.84	0.89	0.38	0.006	1917	1917	376	1571	0.38	0.0055	1853	28	1493
V32121222	0.5	30	3	600	8	10	1	2.5	2.13	0.38	0.14	0.65	0.17	0.06	0.23	0.83	0.89	0.39	0.006	1814	1814	355	1489	0.39	0.0056	1748	27	1408
V42121221	0.7	30	3	600	8	10	1	1.5	1.85	0.34	0.13	0.66	0.16	0.06	0.27	0.85	0.89	0.33	0.005	2110	2110	583	1567	0.33	0.0049	2062	32	1502
V42121222	0.7	30	3	600	8	10	1	2.5	1.93	0.36	0.14	0.66	0.16	0.06	0.26	0.84	0.89	0.35	0.005	2038	2038	563	1514	0.35	0.0052	1988	31	1448
V52121221	0.9	30	3	600	8	10	1	1.5	1.64	0.31	0.12	0.69	0.14	0.06	0.30	0.86	0.89	0.27	0.004	2349	2349	837	1562	0.27	0.0043	2315	36	1514
V52121222	0.9	30	3	600	8	10	1	2.5	1.72	0.32	0.13	0.69	0.14	0.06	0.29	0.85	0.89	0.29	0.005	2274	2274	811	1514	0.29	0.0046	2239	35	1464
V12122111	0.1	30	3	600	10	8	0.6	1.5	1.69	0.28	0.10	0.63	0.19	0.07	0.29	0.87	0.89	0.32	0.005	2212	2212	86	2137	0.32	0.0048	2137	32	2060
V12122112	0.1	30	3	600	10	8	0.6	2.5	1.82	0.30	0.11	0.63	0.19	0.07	0.28	0.86	0.89	0.35	0.005	2097	2097	82	2026	0.35	0.0052	2019	31	1946
V22122111	0.3	30	3	600	10	8	0.6	1.5	1.58	0.27	0.10	0.64	0.18	0.06	0.31	0.87	0.89	0.29	0.004	2344	2344	276	2089	0.29	0.0042	2280	35	2017
V22122112	0.3	30	3	600	10	8	0.6	2.5	1.69	0.29	0.11	0.64	0.18	0.06	0.29	0.87	0.89	0.31	0.005	2223	2223	261	1982	0.31	0.0046	2157	33	1908
V32122111	0.5	30	3	600	10	8	0.6	1.5	1.45	0.26	0.10	0.65	0.17	0.06	0.33	0.88	0.89	0.25	0.004	2509	2509	493	2044	0.25	0.0037	2457	38	1980
V32122112	0.5	30	3	600	10	8	0.6	2.5	1.56	0.28	0.10	0.65	0.17	0.06	0.31	0.87	0.89	0.28	0.004	2382	2382	468	1942	0.28	0.0040	2327	36	1876
V42122111	0.7	30	3	600	10	8	0.6	1.5	1.32	0.24	0.09	0.66	0.16	0.06	0.35	0.88	0.89	0.22	0.003	2721	2721	750	2007	0.22	0.0032	2680	41	1953
V42122112	0.7	30	3	600	10	8	0.6	2.5	1.41	0.26	0.10	0.66	0.16	0.06	0.34	0.87	0.89	0.24	0.004	2587	2587	713	1910	0.24	0.0035	2544	39	1854
V52122111	0.9	30	3	600	10	8	0.6	1.5	1.17	0.22	0.09	0.69	0.14	0.06	0.38	0.88	0.89	0.18	0.003	2999	2999	1061	1983	0.18	0.0028	2971	47	1942
V52122112	0.9	30	3	600	10	8	0.6	2.5	1.25	0.23	0.09	0.69	0.14	0.06	0.37	0.88	0.89	0.19	0.003	2859	2859	1012	1892	0.19	0.0031	2829	44	1850
V12122121	0.1	30	3	600	10	8	1	1.5	1.35	0.22	0.08	0.63	0.19	0.07	0.35	0.88	0.89	0.24	0.004	2600	2600	102	2510	0.24	0.0036	2535	38	2443
V12122122	0.1	30	3	600	10	8	1	2.5	1.46	0.24	0.09	0.63	0.19	0.07	0.33	0.88	0.89	0.26	0.004	2461	2461	96	2376	0.26	0.0040	2393	36	2306
V22122121	0.3	30	3	600	10	8	1	1.5	1.26	0.21	0.08	0.64	0.18	0.06	0.36	0.88	0.89	0.22	0.003	2745	2745	324	2441	0.22	0.0031	2689	41	2378
V22122122	0.3	30	3	600	10	8	1	2.5	1.36	0.23	0.08	0.64	0.18	0.06	0.34	0.88	0.89	0.24	0.004	2602	2602	307	2315	0.24	0.0035	2544	39	2250
V32122121	0.5	30	3	600	10	8	1	1.5	1.16	0.21	0.08	0.65	0.17	0.06	0.39	0.88	0.89	0.19	0.003	2924	2924	576	2376	0.19	0.0027	2879	44	2320
V32122122	0.5	30	3	600	10	8	1	2.5	1.25	0.22	0.08	0.65	0.17	0.06	0.37	0.88	0.89	0.21	0.003	2776	2776	546	2257	0.21	0.0030	2729	42	2199
V42122121	0.7	30	3	600	10	8	1	1.5	1.05	0.19	0.08	0.66	0.16	0.06	0.41	0.88	0.89	0.16	0.002	3148	3148	867	2315	0.16	0.0024	3112	48	2268
V42122122	0.7	30	3	600	10	8	1	2.5	1.14	0.21	0.08	0.66	0.16	0.06	0.39	0.88	0.89	0.18	0.003	2996	2996	826	2205	0.18	0.0027	2959	46	2156
V52122121	0.9	30	3	600	10	8	1	1.5	0.93	0.17	0.07	0.69	0.14	0.06	0.45	0.89	0.89	0.13	0.002	3520	3520	1241	2321	0.13	0.0021	3496	55	2286
V52122122	0.9	30	3	600	10	8	1	2.5	1.01	0.19	0.08	0.69	0.14	0.06	0.42	0.88	0.89	0.15	0.002	3286	3286	1160	2169	0.15	0.0023	3260	51	2132
V12122211	0.1	30	3	600	10	10	0.6	1.5	4.04	0.66	0.24	0.63	0.19	0.07	0.10	0.61	0.88	0.65	0.010	865	865	32	841	0.64	0.0097	764	12	737
V12122212	0.1	30	3	600	10	10	0.6	2.5	4.41	0.72	0.26	0.63	0.19	0.07	0.09	0.56	0.88	0.70	0.011	786	786	29	764	0.69	0.0104	687	10	662
V22122211	0.3	30	3	600	10	10	0.6	1.5	3.76	0.64	0.23	0.64	0.18	0.06	0.11	0.62	0.88	0.60	0.009	928	928	105	841	0.60	0.0088	841	13	743
V22122212	0.3	30	3	600	10	10	0.6	2.5	4.11	0.70	0.26	0.64	0.18	0.06	0.10	0.58	0.88	0.65	0.010	841	841	95	763	0.65	0.0094	755	11	668
V32122211	0.5	30	3	600	10	10	0.6	1.5	3.46	0.62	0.23	0.65	0.17	0.06	0.13	0.64	0.88	0.56	0.008	1016	1016	197	848	0.56	0.0080	942	14	759
V32122212	0.5	30	3	600	10	10	0.6	2.5	3.78	0.67	0.25	0.65	0.17	0.06	0.11	0.59	0.88	0.60	0.009	917	917	177	767	0.59	0.0086	844	13	680
V42122211	0.7	30	3	600	10	10	0.6	1.5	3.14	0.58	0.22	0.66	0.16	0.06	0.14	0.67	0.88	0.50	0.007	1140	1140	317	865	0.50	0.0074	1080	17	787
V42122212	0.7	30	3	600	10	10	0.6	2.5	3.43	0.64	0.24	0.66	0.16	0.06	0.13	0.62	0.88	0.54	0.008	1026	1026	285	780	0.54	0.0079	967	15	705
V52122211	0.9	30	3	600	10	10	0.6	1.5	2.78	0.52	0.21	0.69	0.14	0.06	0.17	0.73	0.88	0.44	0.007	1329	1329	484	902	0.44	0.0069	1283	20	839
V52122212	0.9	30	3	600	10	10	0.6	2.5	3.04	0.57	0.23	0.69	0.14	0.06	0.15	0.68	0.88	0.47	0.007	1193	1193	436	813	0.46	0.0074	1147	18	750
V12122221	0.1	30	3	600	10	10	1	1.5	3.48	0.57	0.20	0.63	0.19	0.07	0.13	0.68	0.88	0.58	0.009	1021	1021	38	991	0.57	0.0086	915	14	882
V12122222	0.1	30	3	600	10	10	1	2.5	3.84	0.63	0.22	0.63	0.19	0.07	0.11	0.63	0.88	0.62	0.010	915	915	34	889	0.62	0.0093	812	12	783
V22122221	0.3	30	3	600	10	10	1	1.5	3.25	0.55	0.20	0.64	0.18	0.06	0.14	0.70	0.88	0.54	0.008	1100	1100	126	994	0.54	0.0078	1008	15	892
V22122222	0.3	30	3	600	10	10	1	2.5	3.58	0.61	0.22	0.64	0.18	0.06	0.12	0.65	0.88	0.58	0.009	983	983	112	890	0.58	0.0084	894	14	791
V32122221	0.5	30	3	600	10	10	1	1.5	2.99	0.53	0.20	0.65	0.17	0.06	0.15	0.72	0.88	0.50	0.007	1208	1208	235	1004	0.50	0.0072	1131	17	912
V32122222	0.5	30	3	600	10	10	1	2.5	3.29	0.59	0.22	0.65	0.17	0.06	0.13	0.67	0.88	0.54	0.008	1077	1077	209	898	0.53	0.0077	1002	15	807
V42122221	0.7	30	3	600	10	10	1	1.5	2.71	0.50	0.19	0.66	0.16	0.06	0.17	0.74	0.88	0.45	0.007	1362	1362	378	1027	0.45	0.0066	1302	20	948
V42122222	0.7	30	3	600	10	10	1	2.5	2.99	0.55	0.21	0.66	0.16	0.06	0.15	0.70	0.88	0.48	0.007	1211	1211	336	917	0.48	0.0071	1150	18	838
V52122221	0.9	30	3	600	10	10	1	1.5	2.40	0.45	0.18	0.69	0.14	0.06	0.20	0.78	0.88	0.39	0.006	1595	1595	576	1075	0.39	0.0062	1551	24	1014
V52122222	0.9	30	3	600	10	10	1	2.5	2.65	0.50	0.20	0.69	0.14	0.06	0.18	0.75	0.88	0.42	0.007	1413	1413	513	957	0.42	0.0067	1367	21	894
V12211111	0.1	30	4	400	8	8	0.6	1.5	0.98	0.16	0.06	0.63	0.19	0.07	0.43	0.89	0.89	0.16	0.002	2852	2852	113	2752	0.16	0.0018	2805	32	2703
V12211112	0.1	30	4	400	8	8	0.6	2.5	1.01	0.16	0.06	0.63	0.19	0.07	0.42	0.89	0.89	0.16	0.002	2784	2784	110	2687	0.16	0.0018	2736	31	2637
V22211111	0.3	30	4	400	8	8	0.6	1.5	0.91	0.16	0.06	0.64	0.18	0.06	0.46	0.89	0.89	0.14	0.002	3047	3047	361	2705	0.14	0.0016	3007	34	2660
V22211112	0.3	30	4	400	8	8	0.6	2.5	0.94	0.16	0.06	0.64	0.18	0.06	0.45	0.89	0.89	0.15	0.002	2983	2983	353	2648	0.15	0.0016	2942	34	2602
V32211111	0.5	30	4	400	8	8	0.6	1.5	0.84	0.15	0.06	0.65	0.17	0.06	0.49	0.89	0.89	0.13	0.001	3305	3305	652	2677	0.13	0.0014	3272	38	2637
V32211112	0.5	30	4	400	8	8	0.6	2.5	0.86	0.15	0.06	0.65	0.17	0.06	0.48	0.89	0.89	0.13	0.001	3226	3226	636	2614	0.13	0.0014	3193	37	2573
V42211111	0.7	30	4	400	8	8	0.6	1.5	0.76	0.14	0.05	0.66	0.16	0.06	0.53	0.89	0.89	0.11	0.001	3626	3626	998	2657	0.11	0.0012	3601	42	2624
V42211112	0.7	30	4	400	8	8	0.6	2.5	0.78	0.15	0.06	0.66	0.16	0.06	0.52	0.89	0.89	0.11	0.001	3553	3553	978	2604	0.11	0.0013	3528	41	2571
V52211111	0.9	30	4	400	8	8	0.6	1.5	0.68	0.13	0.05	0.69	0.14	0.06	0.59	0.89	0.89	0.09	0.001	4100	4100	1440	2694	0.09	0.0011	4083	48	2669
V52211112	0.9	30	4	400	8	8	0.6	2.5	0.69	0.13	0.05	0.69	0.14	0.06	0.58	0.89	0.89	0.10	0.001	4013	4013	1410	2637	0.10	0.0011	3996	47	2613
V12211121	0.1	30	4	400	8	8	1	1.5	0.75	0.12	0.04	0.63	0.19	0.07	0.54	0.89	0.89	0.12	0.001	3579	3579	142	3452	0.12	0.0013	3541	40	3412
V12211122	0.1	30	4	400	8	8	1	2.5	0.77	0.13	0.05	0.63	0.19	0.07	0.53	0.89	0.89	0.12	0.001	3493	3493	138	3369	0.12	0.0013	3454	39	3329
V22211121	0.3	30	4	400	8	8	1	1.5	0.70	0.12	0.04	0.64	0.18	0.06	0.58	0.89	0.89	0.11	0.001	3837	3837	455	3401	0.11	0.0011	3805	43	3365
V22211122	0.3	30	4	400	8	8	1	2.5	0.72	0.12	0.04	0.64	0.18	0.06	0.57	0.89	0.89	0.11	0.001	3749	3749	445	3324	0.11	0.0012	3716	42	3287
V32211121	0.5	30	4	400	8	8	1	1.5	0.64	0.11	0.04	0.65	0.17	0.06	0.62	0.89	0.89	0.09	0.001	4127	4127	815	3337	0.09	0.0010	4101	47	3305
V32211122	0.5	30	4	400	8	8	1	2.5	0.66	0.12	0.04	0.65	0.17	0.06	0.60	0.89	0.89	0.10	0.001	4046	4046	798	3271	0.10	0.0010	4019	46	3239
V42211121	0.7	30	4	400	8	8	1	1.5	0.58	0.11	0.04	0.66	0.16	0.06	0.67	0.89	0.89	0.08	0.001	4553	4553	1252	3329	0.08	0.0009	4533	53	3303
V42211122	0.7	30	4	400	8	8	1	2.5	0.60	0.11	0.04	0.66	0.16	0.06	0.66	0.89	0.89	0.08	0.001	4451	4451	1224	3255	0.08	0.0009	4430	51	3228
V52211121	0.9	30	4	400	8	8	1	1.5	0.52	0.10	0.04	0.69	0.14	0.06	0.73	0.89	0.89	0.07	0.001	5061	5061	1774	3320	0.07	0.0008	5047	59	3300
V52211122	0.9	30	4	400	8	8	1	2.5	0.53	0.10	0.04	0.69	0.14	0.06	0.72	0.89	0.89	0.07	0.001	4969	4969	1742	3260	0.07	0.0008	4954	58	3240
V12211211	0.1	30	4	400	8	10	0.6	1.5	2.18	0.36	0.13	0.63	0.19	0.07	0.23	0.84	0.89	0.41	0.005	1556	1556	60	1505	0.41	0.0046	1477	17	1423

Name	af	nf	hf	mf	Ly	Lx	tw	Lcb	T1 [s]	T2 [s]	T3 [s]	M1 [-]	M2 [-]	M3 [-]	Sa	Sa2	Sa3	Disp [m]	ISDR [-]	Total Moment [MN-m]	Total Shear [MN]	Outrigger Moment [MN-m]	Wall Moment [MN-m]	Mode 1 Disp [m]	Mode 1 ISDR [-]	Mode 1 Moment [MN-m]	Mode 1 Shear [MN]	Mode 1 wall Moment [MN-m]
V12211212	0.1	30	4	400	8	10	0.6	2.5	2.25	0.37	0.13	0.63	0.19	0.07	0.22	0.84	0.89	0.42	0.005	1501	1501	58	1452	0.42	0.0047	1419	16	1368
V22211211	0.3	30	4	400	8	10	0.6	1.5	2.03	0.35	0.13	0.64	0.18	0.06	0.25	0.85	0.89	0.39	0.004	1704	1704	199	1522	0.39	0.0042	1638	19	1449
V22211212	0.3	30	4	400	8	10	0.6	2.5	2.10	0.36	0.13	0.64	0.18	0.06	0.24	0.84	0.89	0.39	0.004	1643	1643	192	1469	0.39	0.0043	1575	18	1393
V32211211	0.5	30	4	400	8	10	0.6	1.5	1.87	0.33	0.12	0.65	0.17	0.06	0.27	0.85	0.89	0.35	0.004	1842	1842	361	1506	0.35	0.0038	1788	21	1441
V32211212	0.5	30	4	400	8	10	0.6	2.5	1.93	0.34	0.13	0.65	0.17	0.06	0.26	0.85	0.89	0.36	0.004	1798	1798	353	1472	0.36	0.0039	1744	20	1405
V42211211	0.7	30	4	400	8	10	0.6	1.5	1.70	0.31	0.12	0.66	0.16	0.06	0.29	0.86	0.89	0.30	0.003	2007	2007	554	1487	0.30	0.0033	1966	23	1432
V42211212	0.7	30	4	400	8	10	0.6	2.5	1.75	0.32	0.12	0.66	0.16	0.06	0.28	0.85	0.89	0.31	0.003	1961	1961	542	1454	0.31	0.0034	1919	22	1398
V52211211	0.9	30	4	400	8	10	0.6	1.5	1.51	0.28	0.11	0.69	0.14	0.06	0.32	0.87	0.89	0.25	0.003	2231	2231	793	1481	0.25	0.0029	2201	26	1439
V52211212	0.9	30	4	400	8	10	0.6	2.5	1.55	0.29	0.12	0.69	0.14	0.06	0.31	0.86	0.89	0.26	0.003	2183	2183	776	1450	0.26	0.0030	2153	25	1408
V12211221	0.1	30	4	400	8	10	1	1.5	1.76	0.29	0.10	0.63	0.19	0.07	0.28	0.87	0.89	0.33	0.004	1906	1906	74	1841	0.33	0.0037	1838	21	1771
V12211222	0.1	30	4	400	8	10	1	2.5	1.82	0.30	0.11	0.63	0.19	0.07	0.28	0.86	0.89	0.35	0.004	1863	1863	73	1800	0.35	0.0039	1794	20	1729
V22211221	0.3	30	4	400	8	10	1	1.5	1.64	0.28	0.10	0.64	0.18	0.06	0.30	0.87	0.89	0.30	0.003	2020	2020	237	1801	0.30	0.0033	1962	22	1735
V22211222	0.3	30	4	400	8	10	1	2.5	1.69	0.29	0.11	0.64	0.18	0.06	0.29	0.87	0.89	0.31	0.003	1976	1976	232	1761	0.31	0.0034	1917	22	1695
V32211221	0.5	30	4	400	8	10	1	1.5	1.51	0.27	0.10	0.65	0.17	0.06	0.32	0.87	0.89	0.27	0.003	2164	2164	425	1763	0.27	0.0029	2116	24	1705
V32211222	0.5	30	4	400	8	10	1	2.5	1.56	0.28	0.10	0.65	0.17	0.06	0.31	0.87	0.89	0.28	0.003	2117	2117	416	1726	0.28	0.0030	2068	24	1667
V42211221	0.7	30	4	400	8	10	1	1.5	1.37	0.25	0.10	0.66	0.16	0.06	0.34	0.88	0.89	0.23	0.003	2349	2349	648	1734	0.23	0.0025	2312	27	1685
V42211222	0.7	30	4	400	8	10	1	2.5	1.41	0.26	0.10	0.66	0.16	0.06	0.34	0.87	0.89	0.24	0.003	2299	2299	634	1697	0.24	0.0026	2261	26	1647
V52211221	0.9	30	4	400	8	10	1	1.5	1.22	0.23	0.09	0.69	0.14	0.06	0.37	0.88	0.89	0.19	0.002	2596	2596	919	1717	0.19	0.0022	2570	30	1680
V52211222	0.9	30	4	400	8	10	1	2.5	1.25	0.24	0.09	0.69	0.14	0.06	0.37	0.88	0.89	0.19	0.002	2541	2541	900	1681	0.19	0.0023	2514	30	1644
V12212111	0.1	30	4	400	10	8	0.6	1.5	1.32	0.22	0.08	0.63	0.19	0.07	0.35	0.88	0.89	0.23	0.003	2349	2349	92	2268	0.23	0.0026	2292	26	2209
V12212112	0.1	30	4	400	10	8	0.6	2.5	1.39	0.23	0.08	0.63	0.19	0.07	0.34	0.88	0.89	0.25	0.003	2268	2268	89	2190	0.25	0.0028	2210	25	2130
V22212111	0.3	30	4	400	10	8	0.6	1.5	1.23	0.21	0.08	0.64	0.18	0.06	0.37	0.88	0.89	0.21	0.002	2480	2480	293	2205	0.21	0.0023	2431	28	2150
V22212112	0.3	30	4	400	10	8	0.6	2.5	1.29	0.22	0.08	0.64	0.18	0.06	0.36	0.88	0.89	0.22	0.002	2399	2399	283	2133	0.22	0.0024	2348	27	2077
V32212111	0.5	30	4	400	10	8	0.6	1.5	1.13	0.20	0.08	0.65	0.17	0.06	0.39	0.88	0.89	0.18	0.002	2638	2638	519	2142	0.18	0.0020	2598	30	2093
V32212112	0.5	30	4	400	10	8	0.6	2.5	1.19	0.21	0.08	0.65	0.17	0.06	0.38	0.88	0.89	0.20	0.002	2557	2557	503	2078	0.20	0.0021	2516	29	2028
V42212111	0.7	30	4	400	10	8	0.6	1.5	1.03	0.19	0.07	0.66	0.16	0.06	0.42	0.88	0.89	0.16	0.002	2836	2836	781	2085	0.16	0.0017	2805	33	2044
V42212112	0.7	30	4	400	10	8	0.6	2.5	1.08	0.20	0.08	0.66	0.16	0.06	0.40	0.88	0.89	0.17	0.002	2755	2755	759	2026	0.17	0.0019	2723	32	1984
V52212111	0.9	30	4	400	10	8	0.6	1.5	0.91	0.17	0.07	0.69	0.14	0.06	0.46	0.89	0.89	0.13	0.002	3188	3188	1123	2101	0.13	0.0015	3167	37	2071
V52212112	0.9	30	4	400	10	8	0.6	2.5	0.96	0.18	0.07	0.69	0.14	0.06	0.44	0.88	0.89	0.14	0.002	3062	3062	1080	2019	0.14	0.0016	3040	36	1988
V12212121	0.1	30	4	400	10	8	1	1.5	1.02	0.17	0.06	0.63	0.19	0.07	0.42	0.89	0.89	0.16	0.002	2761	2761	109	2665	0.16	0.0019	2712	31	2614
V12212122	0.1	30	4	400	10	8	1	2.5	1.08	0.18	0.06	0.63	0.19	0.07	0.40	0.89	0.89	0.18	0.002	2678	2678	105	2584	0.18	0.0020	2628	30	2532
V22212121	0.3	30	4	400	10	8	1	1.5	0.95	0.16	0.06	0.64	0.18	0.06	0.44	0.89	0.89	0.15	0.002	2953	2953	350	2622	0.15	0.0016	2912	33	2575
V22212122	0.3	30	4	400	10	8	1	2.5	1.00	0.17	0.06	0.64	0.18	0.06	0.42	0.89	0.89	0.16	0.002	2819	2819	333	2504	0.16	0.0017	2776	32	2455
V32212121	0.5	30	4	400	10	8	1	1.5	0.88	0.16	0.06	0.65	0.17	0.06	0.48	0.89	0.89	0.13	0.001	3189	3189	629	2584	0.13	0.0014	3156	36	2543
V32212122	0.5	30	4	400	10	8	1	2.5	0.92	0.16	0.06	0.65	0.17	0.06	0.45	0.89	0.89	0.14	0.002	3054	3054	602	2476	0.14	0.0015	3019	35	2433
V42212121	0.7	30	4	400	10	8	1	1.5	0.79	0.15	0.06	0.66	0.16	0.06	0.52	0.89	0.89	0.12	0.001	3519	3519	969	2580	0.12	0.0013	3494	41	2546
V42212122	0.7	30	4	400	10	8	1	2.5	0.84	0.15	0.06	0.66	0.16	0.06	0.50	0.89	0.89	0.12	0.001	3367	3367	927	2469	0.12	0.0014	3341	39	2434
V52212121	0.9	30	4	400	10	8	1	1.5	0.70	0.13	0.05	0.69	0.14	0.06	0.57	0.89	0.89	0.10	0.001	3973	3973	1396	2611	0.10	0.0011	3955	47	2586
V52212122	0.9	30	4	400	10	8	1	2.5	0.74	0.14	0.06	0.69	0.14	0.06	0.55	0.89	0.89	0.10	0.001	3792	3792	1333	2493	0.10	0.0012	3774	44	2468
V12212211	0.1	30	4	400	10	10	0.6	1.5	3.07	0.50	0.18	0.63	0.19	0.07	0.15	0.74	0.88	0.52	0.006	1046	1046	39	1015	0.52	0.0059	950	11	916
V12212212	0.1	30	4	400	10	10	0.6	2.5	3.27	0.53	0.19	0.63	0.19	0.07	0.14	0.72	0.88	0.55	0.006	976	976	36	947	0.55	0.0062	880	10	849
V22212211	0.3	30	4	400	10	10	0.6	1.5	2.86	0.49	0.18	0.64	0.18	0.06	0.16	0.75	0.88	0.49	0.005	1130	1130	130	1018	0.49	0.0054	1049	12	928
V22212212	0.3	30	4	400	10	10	0.6	2.5	3.04	0.52	0.19	0.64	0.18	0.06	0.15	0.73	0.88	0.51	0.006	1054	1054	121	951	0.51	0.0056	972	11	859
V32212211	0.5	30	4	400	10	10	0.6	1.5	2.64	0.47	0.18	0.65	0.17	0.06	0.18	0.77	0.89	0.45	0.005	1245	1245	243	1030	0.45	0.0049	1179	14	950
V32212212	0.5	30	4	400	10	10	0.6	2.5	2.80	0.50	0.19	0.65	0.17	0.06	0.16	0.75	0.88	0.48	0.005	1159	1159	226	961	0.47	0.0051	1091	13	880
V42212211	0.7	30	4	400	10	10	0.6	1.5	2.39	0.44	0.17	0.66	0.16	0.06	0.20	0.79	0.89	0.41	0.005	1410	1410	391	1057	0.41	0.0045	1359	16	991
V42212212	0.7	30	4	400	10	10	0.6	2.5	2.54	0.47	0.18	0.66	0.16	0.06	0.19	0.77	0.88	0.43	0.005	1309	1309	363	984	0.43	0.0047	1257	15	916
V52212211	0.9	30	4	400	10	10	0.6	1.5	2.12	0.40	0.16	0.69	0.14	0.06	0.24	0.82	0.89	0.36	0.004	1663	1663	597	1114	0.36	0.0043	1627	19	1064
V52212212	0.9	30	4	400	10	10	0.6	2.5	2.25	0.42	0.17	0.69	0.14	0.06	0.22	0.80	0.89	0.38	0.004	1538	1538	554	1034	0.37	0.0045	1501	18	981
V12212221	0.1	30	4	400	10	10	1	1.5	2.53	0.41	0.15	0.63	0.19	0.07	0.19	0.81	0.89	0.45	0.005	1309	1309	50	1268	0.45	0.0051	1220	14	1176
V12212222	0.1	30	4	400	10	10	1	2.5	2.70	0.44	0.16	0.63	0.19	0.07	0.17	0.79	0.89	0.48	0.005	1214	1214	46	1176	0.48	0.0054	1122	13	1082
V22212221	0.3	30	4	400	10	10	1	1.5	2.35	0.40	0.15	0.64	0.18	0.06	0.21	0.82	0.89	0.43	0.005	1426	1426	166	1279	0.43	0.0047	1352	15	1195
V22212222	0.3	30	4	400	10	10	1	2.5	2.51	0.43	0.16	0.64	0.18	0.06	0.19	0.80	0.89	0.45	0.005	1317	1317	152	1183	0.45	0.0049	1240	14	1097
V32212221	0.5	30	4	400	10	10	1	1.5	2.17	0.39	0.14	0.65	0.17	0.06	0.23	0.83	0.89	0.40	0.004	1585	1585	310	1302	0.40	0.0043	1525	18	1229
V32212222	0.5	30	4	400	10	10	1	2.5	2.31	0.41	0.15	0.65	0.17	0.06	0.21	0.81	0.89	0.41	0.005	1461	1461	286	1203	0.41	0.0045	1399	16	1127
V42212221	0.7	30	4	400	10	10	1	1.5	1.96	0.36	0.14	0.66	0.16	0.06	0.26	0.84	0.89	0.36	0.004	1789	1789	494	1330	0.36	0.0039	1744	20	1271
V42212222	0.7	30	4	400	10	10	1	2.5	2.10	0.39	0.15	0.66	0.16	0.06	0.24	0.83	0.89	0.38	0.004	1665	1665	461	1241	0.38	0.0042	1618	19	1179
V52212221	0.9	30	4	400	10	10	1	1.5	1.74	0.33	0.13	0.69	0.14	0.06	0.29	0.85	0.89	0.29	0.003	1998	1998	712	1331	0.29	0.0035	1966	23	1286
V52212222	0.9	30	4	400	10	10	1	2.5	1.86	0.35	0.14	0.69	0.14	0.06	0.27	0.84	0.89	0.32	0.004	1899	1899	678	1266	0.32	0.0038	1866	22	1220
V12221111	0.1	30	4	600	8	8	0.6	1.5	1.20	0.20	0.07	0.63	0.19	0.07	0.38	0.88	0.89	0.21	0.002	3749	3749	147	3619	0.21	0.0023	3668	42	3536
V12221112	0.1	30	4	600	8	8	0.6	2.5	1.23	0.20	0.07	0.63	0.19	0.07	0.37	0.88	0.89	0.21	0.002	3683	3683	145	3555	0.21	0.0024	3601	41	3471
V22221111	0.3	30	4	600	8	8	0.6	1.5	1.12	0.19	0.07	0.64	0.18	0.06	0.39	0.88	0.89	0.18	0.002	3948	3948	466	3508	0.18	0.0020	3879	44	3430
V22221112	0.3	30	4	600	8	8	0.6	2.5	1.15	0.20	0.07	0.64	0.18	0.06	0.39	0.88	0.89	0.19	0.002	3881	3881	458	3450	0.19	0.0021	3811	43	3371
V32221111	0.5	30	4	600	8	8	0.6	1.5	1.03	0.18	0.07	0.65	0.17	0.06	0.41	0.88	0.89	0.16	0.002	4189	4189	825	3399	0.16	0.0018	4132	47	3329
V32221112	0.5	30	4	600	8	8	0.6	2.5	1.06	0.19	0.07	0.65	0.17	0.06	0.41	0.88	0.89	0.17	0.002	4124	4124	812	3348	0.17	0.0018	4066	47	3277
V42221111	0.7	30	4	600	8	8	0.6	1.5	0.93	0.17	0.07	0.66	0.16	0.06	0.45	0.89	0.89	0.14	0.002	4597	4597	1266	3376	0.14	0.0016	4554	53	3318
V42221112	0.7	30	4	600	8	8	0.6	2.5	0.96	0.18	0.07	0.66	0.16	0.06	0.44	0.88	0.89	0.14	0.002	4496	4496	1238	3302	0.14	0.0016	4451	52	3243
V52221111	0.9	30	4	600	8	8	0.6	1.5	0.83	0.16	0.06	0.69	0.14	0.06	0.50	0.89	0.89	0.12	0.001	5189	5189	1826	3416	0.12	0.0014	5159	61	3373
V52221112	0.9	30	4	600	8	8	0.6	2.5	0.85	0.16	0.06	0.69	0.14	0.06	0.49	0.89	0.89	0.12	0.001	5068	5068	1784	3337	0.12	0.0014	5038	59	3294
V12221121	0.1	30	4	600	8	8	1	1.5	0.92	0.15	0.05	0.63	0.19	0.07	0.46	0.89	0.89	0.15	0.002	4532	4532	179	4373	0.15	0.0016	4465	51	4303
V12221122	0.1	30	4	600	8	8	1	2.5	0.94	0.15	0.06	0.63	0.19	0.07	0.45	0.89	0.89	0.15	0.002	4433	4433	175	4278	0.15	0.0017	4365	50	4207
V22221121	0.3	30	4	600	8	8	1	1.5	0.85	0.15	0.05	0.64	0.18	0.06	0.49	0.89	0.89	0.13	0.001	4852	4852	575	4305	0.13	0.0014	4796	55	4241

Name	af	nf	hf	mf	Ly	Lx	tw	Lcb	T1 [s]	T2 [s]	T3 [s]	M1 [-]	M2 [-]	M3 [-]	Sa	Sa2	Sa3	Disp [m]	ISDR [-]	Total Moment [MN-m]	Total Shear [MN]	Outrigger Moment [MN-m]	Wall Moment [MN-m]	Mode 1 Disp [m]	Mode 1 ISDR [-]	Mode 1 Moment [MN-m]	Mode 1 Shear [MN]	Mode 1 wall Moment [MN-m]
V22221122	0.3	30	4	600	8	8	1	2.5	0.88	0.15	0.05	0.64	0.18	0.06	0.47	0.89	0.89	0.14	0.001	4730	4730	560	4197	0.14	0.0015	4672	53	4132
V32221121	0.5	30	4	600	8	8	1	1.5	0.78	0.14	0.05	0.65	0.17	0.06	0.52	0.89	0.89	0.12	0.001	5251	5251	1036	4251	0.12	0.0013	5205	60	4194
V32221122	0.5	30	4	600	8	8	1	2.5	0.81	0.14	0.05	0.65	0.17	0.06	0.51	0.89	0.89	0.12	0.001	5137	5137	1013	4159	0.12	0.0013	5090	58	4101
V42221121	0.7	30	4	600	8	8	1	1.5	0.71	0.13	0.05	0.66	0.16	0.06	0.57	0.89	0.89	0.10	0.001	5792	5792	1594	4241	0.10	0.0011	5757	67	4195
V42221122	0.7	30	4	600	8	8	1	2.5	0.73	0.14	0.05	0.66	0.16	0.06	0.56	0.89	0.89	0.11	0.001	5654	5654	1556	4141	0.11	0.0012	5618	65	4093
V52221121	0.9	30	4	600	8	8	1	1.5	0.63	0.12	0.05	0.69	0.14	0.06	0.63	0.89	0.89	0.08	0.001	6486	6486	2276	4259	0.08	0.0010	6461	76	4225
V52221122	0.9	30	4	600	8	8	1	2.5	0.65	0.12	0.05	0.69	0.14	0.06	0.61	0.89	0.89	0.09	0.001	6346	6346	2228	4168	0.09	0.0010	6321	74	4133
V12221211	0.1	30	4	600	8	10	0.6	1.5	2.67	0.44	0.16	0.63	0.19	0.07	0.17	0.79	0.89	0.47	0.005	1837	1837	70	1780	0.47	0.0053	1700	19	1639
V12221212	0.1	30	4	600	8	10	0.6	2.5	2.76	0.45	0.16	0.63	0.19	0.07	0.17	0.78	0.89	0.48	0.006	1775	1775	67	1720	0.48	0.0054	1636	19	1577
V22221211	0.3	30	4	600	8	10	0.6	1.5	2.49	0.42	0.16	0.64	0.18	0.06	0.19	0.80	0.89	0.44	0.005	1996	1996	231	1792	0.44	0.0048	1881	21	1663
V22221212	0.3	30	4	600	8	10	0.6	2.5	2.57	0.44	0.16	0.64	0.18	0.06	0.18	0.79	0.89	0.45	0.005	1927	1927	223	1732	0.45	0.0050	1810	21	1601
V32221211	0.5	30	4	600	8	10	0.6	1.5	2.29	0.41	0.15	0.65	0.17	0.06	0.21	0.81	0.89	0.41	0.004	2213	2213	433	1821	0.41	0.0045	2120	24	1708
V32221212	0.5	30	4	600	8	10	0.6	2.5	2.36	0.42	0.16	0.65	0.17	0.06	0.20	0.81	0.89	0.42	0.005	2133	2133	417	1758	0.42	0.0045	2039	23	1643
V42221211	0.7	30	4	600	8	10	0.6	1.5	2.08	0.38	0.15	0.66	0.16	0.06	0.24	0.83	0.89	0.38	0.004	2524	2524	698	1880	0.37	0.0041	2453	28	1788
V42221212	0.7	30	4	600	8	10	0.6	2.5	2.14	0.40	0.15	0.66	0.16	0.06	0.23	0.82	0.89	0.38	0.004	2426	2426	671	1810	0.38	0.0042	2355	27	1716
V52221211	0.9	30	4	600	8	10	0.6	1.5	1.84	0.35	0.14	0.69	0.14	0.06	0.27	0.85	0.89	0.31	0.004	2867	2867	1024	1911	0.31	0.0037	2817	33	1842
V52221212	0.9	30	4	600	8	10	0.6	2.5	1.90	0.36	0.14	0.69	0.14	0.06	0.27	0.84	0.89	0.33	0.004	2798	2798	1000	1867	0.33	0.0039	2748	32	1797
V12221221	0.1	30	4	600	8	10	1	1.5	2.16	0.35	0.13	0.63	0.19	0.07	0.23	0.84	0.89	0.41	0.005	2365	2365	91	2288	0.41	0.0046	2247	26	2166
V12221222	0.1	30	4	600	8	10	1	2.5	2.23	0.36	0.13	0.63	0.19	0.07	0.22	0.84	0.89	0.42	0.005	2280	2280	88	2206	0.42	0.0047	2158	24	2080
V22221221	0.3	30	4	600	8	10	1	1.5	2.01	0.34	0.13	0.64	0.18	0.06	0.25	0.85	0.89	0.38	0.004	2588	2588	303	2312	0.38	0.0042	2490	28	2203
V22221222	0.3	30	4	600	8	10	1	2.5	2.07	0.35	0.13	0.64	0.18	0.06	0.24	0.84	0.89	0.39	0.004	2495	2495	291	2231	0.39	0.0043	2395	27	2118
V32221221	0.5	30	4	600	8	10	1	1.5	1.85	0.33	0.12	0.65	0.17	0.06	0.27	0.85	0.89	0.34	0.004	2788	2788	547	2279	0.34	0.0037	2708	31	2182
V32221222	0.5	30	4	600	8	10	1	2.5	1.91	0.34	0.13	0.65	0.17	0.06	0.26	0.85	0.89	0.36	0.004	2720	2720	534	2225	0.36	0.0038	2639	30	2126
V42221221	0.7	30	4	600	8	10	1	1.5	1.68	0.31	0.12	0.66	0.16	0.06	0.29	0.86	0.89	0.30	0.003	3036	3036	838	2249	0.30	0.0033	2975	35	2168
V42221222	0.7	30	4	600	8	10	1	2.5	1.73	0.32	0.12	0.66	0.16	0.06	0.29	0.85	0.89	0.31	0.003	2966	2966	819	2198	0.31	0.0034	2903	34	2115
V52221221	0.9	30	4	600	8	10	1	1.5	1.49	0.28	0.11	0.69	0.14	0.06	0.32	0.87	0.89	0.24	0.003	3375	3375	1199	2240	0.24	0.0029	3331	39	2178
V52221222	0.9	30	4	600	8	10	1	2.5	1.53	0.29	0.12	0.69	0.14	0.06	0.32	0.87	0.89	0.25	0.003	3298	3298	1172	2190	0.25	0.0030	3254	38	2127
V12222111	0.1	30	4	600	10	8	0.6	1.5	1.62	0.26	0.09	0.63	0.19	0.07	0.30	0.87	0.89	0.30	0.003	3051	3051	119	2947	0.30	0.0034	2954	34	2847
V12222112	0.1	30	4	600	10	8	0.6	2.5	1.70	0.28	0.10	0.63	0.19	0.07	0.29	0.87	0.89	0.32	0.004	2942	2942	115	2842	0.32	0.0036	2842	32	2739
V22222111	0.3	30	4	600	10	8	0.6	1.5	1.51	0.26	0.09	0.64	0.18	0.06	0.32	0.88	0.89	0.27	0.003	3231	3231	380	2877	0.27	0.0030	3148	36	2784
V22222112	0.3	30	4	600	10	8	0.6	2.5	1.58	0.27	0.10	0.64	0.18	0.06	0.31	0.87	0.89	0.29	0.003	3118	3118	367	2778	0.29	0.0032	3033	35	2682
V32222111	0.5	30	4	600	10	8	0.6	1.5	1.39	0.25	0.09	0.65	0.17	0.06	0.34	0.88	0.89	0.24	0.003	3454	3454	679	2812	0.24	0.0026	3386	39	2729
V32222112	0.5	30	4	600	10	8	0.6	2.5	1.46	0.26	0.10	0.65	0.17	0.06	0.33	0.87	0.89	0.26	0.003	3338	3338	656	2719	0.26	0.0028	3267	38	2633
V42222111	0.7	30	4	600	10	8	0.6	1.5	1.26	0.23	0.09	0.66	0.16	0.06	0.36	0.88	0.89	0.21	0.002	3741	3741	1031	2757	0.21	0.0023	3689	43	2688
V42222112	0.7	30	4	600	10	8	0.6	2.5	1.32	0.24	0.09	0.66	0.16	0.06	0.35	0.88	0.89	0.22	0.002	3619	3619	998	2669	0.22	0.0024	3565	41	2598
V52222111	0.9	30	4	600	10	8	0.6	1.5	1.11	0.21	0.08	0.69	0.14	0.06	0.40	0.88	0.89	0.17	0.002	4118	4118	1455	2721	0.17	0.0020	4081	48	2669
V52222112	0.9	30	4	600	10	8	0.6	2.5	1.17	0.22	0.09	0.69	0.14	0.06	0.38	0.88	0.89	0.18	0.002	3990	3990	1411	2638	0.18	0.0021	3952	47	2584
V12222121	0.1	30	4	600	10	8	1	1.5	1.25	0.20	0.07	0.63	0.19	0.07	0.37	0.88	0.89	0.22	0.002	3652	3652	143	3526	0.22	0.0024	3570	41	3440
V12222122	0.1	30	4	600	10	8	1	2.5	1.32	0.21	0.08	0.63	0.19	0.07	0.35	0.88	0.89	0.23	0.003	3526	3526	138	3404	0.23	0.0026	3441	39	3316
V22222121	0.3	30	4	600	10	8	1	1.5	1.16	0.20	0.07	0.64	0.18	0.06	0.38	0.88	0.89	0.19	0.002	3852	3852	455	3424	0.19	0.0021	3782	43	3344
V22222122	0.3	30	4	600	10	8	1	2.5	1.23	0.21	0.08	0.64	0.18	0.06	0.37	0.88	0.89	0.21	0.002	3722	3722	439	3309	0.21	0.0023	3649	42	3227
V32222121	0.5	30	4	600	10	8	1	1.5	1.07	0.19	0.07	0.65	0.17	0.06	0.40	0.88	0.89	0.17	0.002	4094	4094	806	3323	0.17	0.0019	4036	46	3252
V32222122	0.5	30	4	600	10	8	1	2.5	1.13	0.20	0.08	0.65	0.17	0.06	0.39	0.88	0.89	0.18	0.002	3959	3959	780	3216	0.18	0.0020	3899	45	3142
V42222121	0.7	30	4	600	10	8	1	1.5	0.97	0.18	0.07	0.66	0.16	0.06	0.44	0.88	0.89	0.15	0.002	4448	4448	1225	3268	0.15	0.0016	4403	51	3208
V42222122	0.7	30	4	600	10	8	1	2.5	1.02	0.19	0.07	0.66	0.16	0.06	0.42	0.88	0.89	0.16	0.002	4257	4257	1173	3130	0.16	0.0017	4210	49	3068
V52222121	0.9	30	4	600	10	8	1	1.5	0.86	0.16	0.06	0.69	0.14	0.06	0.48	0.89	0.89	0.12	0.001	5011	5011	1765	3300	0.12	0.0014	4981	59	3257
V52222122	0.9	30	4	600	10	8	1	2.5	0.91	0.17	0.07	0.69	0.14	0.06	0.46	0.89	0.89	0.13	0.002	4786	4786	1686	3154	0.13	0.0015	4754	56	3108
V12222211	0.1	30	4	600	10	10	0.6	1.5	3.76	0.61	0.22	0.63	0.19	0.07	0.11	0.64	0.88	0.61	0.007	1247	1247	46	1212	0.61	0.0069	1109	13	1069
V12222212	0.1	30	4	600	10	10	0.6	2.5	4.00	0.65	0.23	0.63	0.19	0.07	0.11	0.61	0.88	0.64	0.008	1166	1166	43	1133	0.64	0.0072	1031	12	993
V22222211	0.3	30	4	600	10	10	0.6	1.5	3.51	0.60	0.22	0.64	0.18	0.06	0.12	0.66	0.88	0.57	0.006	1341	1341	153	1214	0.57	0.0062	1221	14	1080
V22222212	0.3	30	4	600	10	10	0.6	2.5	3.73	0.64	0.23	0.64	0.18	0.06	0.12	0.62	0.88	0.60	0.007	1251	1251	142	1133	0.60	0.0065	1134	13	1003
V32222211	0.5	30	4	600	10	10	0.6	1.5	3.23	0.58	0.22	0.65	0.17	0.06	0.14	0.68	0.88	0.53	0.006	1470	1470	285	1225	0.53	0.0057	1369	16	1103
V32222212	0.5	30	4	600	10	10	0.6	2.5	3.43	0.61	0.23	0.65	0.17	0.06	0.13	0.64	0.88	0.55	0.006	1369	1369	265	1143	0.55	0.0060	1270	15	1023
V42222211	0.7	30	4	600	10	10	0.6	1.5	2.93	0.54	0.21	0.66	0.16	0.06	0.16	0.71	0.88	0.48	0.005	1654	1654	459	1251	0.48	0.0053	1573	18	1146
V42222212	0.7	30	4	600	10	10	0.6	2.5	3.11	0.58	0.22	0.66	0.16	0.06	0.14	0.68	0.88	0.50	0.006	1537	1537	427	1166	0.50	0.0055	1457	17	1062
V52222211	0.9	30	4	600	10	10	0.6	1.5	2.59	0.49	0.20	0.69	0.14	0.06	0.18	0.76	0.88	0.42	0.005	1932	1932	701	1307	0.41	0.0049	1872	22	1224
V52222212	0.9	30	4	600	10	10	0.6	2.5	2.76	0.52	0.21	0.69	0.14	0.06	0.17	0.73	0.88	0.43	0.005	1792	1792	653	1216	0.43	0.0051	1731	20	1132
V12222221	0.1	30	4	600	10	10	1	1.5	3.09	0.50	0.18	0.63	0.19	0.07	0.14	0.74	0.88	0.53	0.006	1558	1558	58	1511	0.53	0.0059	1414	16	1363
V12222222	0.1	30	4	600	10	10	1	2.5	3.30	0.54	0.19	0.63	0.19	0.07	0.13	0.71	0.88	0.55	0.006	1447	1447	54	1404	0.55	0.0062	1303	15	1256
V22222221	0.3	30	4	600	10	10	1	1.5	2.88	0.49	0.18	0.64	0.18	0.06	0.16	0.75	0.88	0.49	0.006	1683	1683	193	1517	0.49	0.0054	1561	18	1380
V22222222	0.3	30	4	600	10	10	1	2.5	3.08	0.52	0.19	0.64	0.18	0.06	0.15	0.72	0.88	0.52	0.006	1561	1561	179	1409	0.52	0.0056	1438	16	1272
V32222221	0.5	30	4	600	10	10	1	1.5	2.65	0.47	0.18	0.65	0.17	0.06	0.18	0.77	0.89	0.46	0.005	1854	1854	362	1535	0.46	0.0049	1755	20	1414
V32222222	0.5	30	4	600	10	10	1	2.5	2.83	0.50	0.19	0.65	0.17	0.06	0.16	0.74	0.88	0.48	0.005	1716	1716	334	1424	0.48	0.0052	1615	19	1301
V42222221	0.7	30	4	600	10	10	1	1.5	2.40	0.45	0.17	0.66	0.16	0.06	0.20	0.79	0.89	0.41	0.005	2100	2100	582	1575	0.41	0.0046	2023	23	1474
V42222222	0.7	30	4	600	10	10	1	2.5	2.57	0.48	0.18	0.66	0.16	0.06	0.18	0.76	0.88	0.43	0.005	1938	1938	537	1458	0.43	0.0048	1860	22	1355
V52222221	0.9	30	4	600	10	10	1	1.5	2.13	0.40	0.16	0.69	0.14	0.06	0.23	0.82	0.89	0.36	0.004	2474	2474	888	1658	0.36	0.0043	2419	28	1582
V52222222	0.9	30	4	600	10	10	1	2.5	2.28	0.43	0.17	0.69	0.14	0.06	0.21	0.80	0.89	0.38	0.005	2275	2275	820	1530	0.38	0.0045	2219	26	1451
V13111111	0.1	45	3	400	8	8	0.6	1.5	1.18	0.19	0.07	0.62	0.19	0.07	0.38	0.88	0.89	0.20	0.002	4238	4238	165	4084	0.20	0.0020	4150	42	3992
V13111112	0.1	45	3	400	8	8	0.6	2.5	1.20	0.20	0.07	0.62	0.19	0.07	0.38	0.88	0.89	0.21	0.002	4175	4175	163	4023	0.21	0.0021	4085	41	3930
V23111111	0.3	45	3	400	8	8	0.6	1.5	1.10	0.19	0.07	0.63	0.18	0.06	0.40	0.88	0.89	0.18	0.002	4460	4460	523	3958	0.18	0.0018	4385	45	3873
V23111112	0.3	45	3	400	8	8	0.6	2.5	1.12	0.19	0.07	0.63	0.18	0.06	0.39	0.88	0.89	0.19	0.002	4395	4395	515	3900	0.19	0.0018	4318	44	3814
V33111111	0.5	45	3	400	8	8	0.6	1.5	1.01	0.18	0.07	0.64	0.17	0.06	0.42	0.88	0.89	0.16	0.002	4728	4728	925	3834	0.16	0.0015	4665	48	3757

Name	af	nf	hf	mf	Ly	Lx	tw	Lcb	T1 [s]	T2 [s]	T3 [s]	M1 [-]	M2 [-]	M3 [-]	Sa	Sa2	Sa3	Disp [m]	ISDR [-]	Total Moment [MN-m]	Total Shear [MN]	Outrigger Moment [MN-m]	Wall Moment [MN-m]	Mode 1 Disp [m]	Mode 1 ISDR [-]	Mode 1 Moment [MN-m]	Mode 1 Shear [MN]	Mode 1 wall Moment [MN-m]
V33111112	0.5	45	3	400	8	8	0.6	2.5	1.03	0.18	0.07	0.64	0.17	0.06	0.41	0.88	0.89	0.16	0.002	4662	4662	912	3781	0.16	0.0016	4598	47	3703
V43111111	0.7	45	3	400	8	8	0.6	1.5	0.92	0.17	0.07	0.66	0.16	0.06	0.46	0.89	0.89	0.14	0.001	5206	5206	1423	3822	0.14	0.0014	5158	53	3758
V43111112	0.7	45	3	400	8	8	0.6	2.5	0.94	0.17	0.07	0.66	0.16	0.06	0.45	0.89	0.89	0.14	0.001	5109	5109	1397	3752	0.14	0.0014	5060	52	3687
V53111111	0.9	45	3	400	8	8	0.6	1.5	0.81	0.15	0.06	0.68	0.14	0.06	0.51	0.89	0.89	0.11	0.001	5873	5873	2052	3869	0.11	0.0012	5840	61	3822
V53111112	0.9	45	3	400	8	8	0.6	2.5	0.83	0.16	0.06	0.68	0.14	0.06	0.50	0.89	0.89	0.12	0.001	5757	5757	2012	3794	0.12	0.0012	5724	60	3746
V13111121	0.1	45	3	400	8	8	1	1.5	0.89	0.14	0.05	0.62	0.19	0.07	0.47	0.89	0.89	0.14	0.001	5169	5169	203	4979	0.14	0.0014	5096	52	4903
V13111122	0.1	45	3	400	8	8	1	2.5	0.91	0.15	0.05	0.62	0.19	0.07	0.46	0.89	0.89	0.15	0.001	5076	5076	199	4889	0.15	0.0015	5001	51	4812
V23111121	0.3	45	3	400	8	8	1	1.5	0.83	0.14	0.05	0.63	0.18	0.06	0.50	0.89	0.89	0.13	0.001	5551	5551	653	4919	0.13	0.0013	5490	56	4849
V23111122	0.3	45	3	400	8	8	1	2.5	0.85	0.14	0.05	0.63	0.18	0.06	0.49	0.89	0.89	0.13	0.001	5436	5436	639	4817	0.13	0.0013	5373	55	4746
V33111121	0.5	45	3	400	8	8	1	1.5	0.76	0.14	0.05	0.64	0.17	0.06	0.53	0.89	0.89	0.11	0.001	5983	5983	1172	4840	0.11	0.0011	5933	61	4778
V33111122	0.5	45	3	400	8	8	1	2.5	0.78	0.14	0.05	0.64	0.17	0.06	0.52	0.89	0.89	0.12	0.001	5875	5875	1151	4753	0.12	0.0011	5824	60	4690
V43111121	0.7	45	3	400	8	8	1	1.5	0.69	0.13	0.05	0.66	0.16	0.06	0.58	0.89	0.89	0.10	0.001	6608	6608	1805	4838	0.10	0.0010	6570	68	4788
V43111122	0.7	45	3	400	8	8	1	2.5	0.71	0.13	0.05	0.66	0.16	0.06	0.57	0.89	0.89	0.10	0.001	6477	6477	1770	4743	0.10	0.0010	6438	67	4692
V53111121	0.9	45	3	400	8	8	1	1.5	0.61	0.12	0.05	0.68	0.14	0.06	0.64	0.89	0.89	0.08	0.001	7405	7405	2581	4867	0.08	0.0009	7379	77	4829
V53111122	0.9	45	3	400	8	8	1	2.5	0.63	0.12	0.05	0.68	0.14	0.06	0.63	0.89	0.89	0.08	0.001	7245	7245	2525	4762	0.08	0.0009	7217	76	4724
V13111211	0.1	45	3	400	8	10	0.6	1.5	2.60	0.42	0.15	0.62	0.19	0.07	0.18	0.80	0.89	0.47	0.005	2117	2117	80	2047	0.47	0.0047	1967	20	1892
V13111212	0.1	45	3	400	8	10	0.6	2.5	2.67	0.44	0.16	0.62	0.19	0.07	0.17	0.79	0.89	0.48	0.005	2053	2053	77	1986	0.47	0.0047	1901	19	1829
V23111211	0.3	45	3	400	8	10	0.6	1.5	2.42	0.41	0.15	0.63	0.18	0.06	0.20	0.81	0.89	0.44	0.004	2301	2301	265	2063	0.44	0.0042	2175	22	1921
V23111212	0.3	45	3	400	8	10	0.6	2.5	2.49	0.42	0.15	0.63	0.18	0.06	0.19	0.80	0.89	0.45	0.004	2231	2231	256	2000	0.45	0.0043	2102	21	1857
V33111211	0.5	45	3	400	8	10	0.6	1.5	2.23	0.40	0.15	0.64	0.17	0.06	0.22	0.82	0.89	0.41	0.004	2553	2553	496	2098	0.41	0.0039	2450	25	1973
V33111212	0.5	45	3	400	8	10	0.6	2.5	2.29	0.41	0.15	0.64	0.17	0.06	0.21	0.81	0.89	0.41	0.004	2471	2471	480	2032	0.41	0.0040	2367	24	1906
V43111211	0.7	45	3	400	8	10	0.6	1.5	2.02	0.37	0.14	0.66	0.16	0.06	0.25	0.84	0.89	0.37	0.004	2907	2907	798	2163	0.37	0.0036	2830	29	2062
V43111212	0.7	45	3	400	8	10	0.6	2.5	2.08	0.38	0.15	0.66	0.16	0.06	0.24	0.83	0.89	0.38	0.004	2815	2815	773	2097	0.38	0.0037	2736	28	1994
V53111211	0.9	45	3	400	8	10	0.6	1.5	1.80	0.34	0.14	0.68	0.14	0.06	0.28	0.85	0.89	0.31	0.003	3258	3258	1154	2173	0.31	0.0032	3203	34	2097
V53111212	0.9	45	3	400	8	10	0.6	2.5	1.84	0.35	0.14	0.68	0.14	0.06	0.27	0.85	0.89	0.32	0.003	3192	3192	1132	2131	0.32	0.0033	3137	33	2053
V13111221	0.1	45	3	400	8	10	1	1.5	2.07	0.34	0.12	0.62	0.19	0.07	0.24	0.85	0.89	0.40	0.004	2782	2782	107	2686	0.40	0.0040	2657	27	2556
V13111222	0.1	45	3	400	8	10	1	2.5	2.12	0.35	0.12	0.62	0.19	0.07	0.24	0.85	0.89	0.41	0.004	2690	2690	103	2598	0.41	0.0041	2561	26	2464
V23111221	0.3	45	3	400	8	10	1	1.5	1.93	0.33	0.12	0.63	0.18	0.06	0.26	0.85	0.89	0.37	0.004	2992	2992	348	2668	0.37	0.0036	2886	29	2549
V23111222	0.3	45	3	400	8	10	1	2.5	1.98	0.34	0.12	0.63	0.18	0.06	0.26	0.85	0.89	0.38	0.004	2926	2926	340	2610	0.38	0.0037	2818	29	2489
V33111221	0.5	45	3	400	8	10	1	1.5	1.77	0.32	0.12	0.64	0.17	0.06	0.28	0.86	0.89	0.33	0.003	3210	3210	626	2621	0.33	0.0031	3123	32	2515
V33111222	0.5	45	3	400	8	10	1	2.5	1.82	0.32	0.12	0.64	0.17	0.06	0.28	0.85	0.89	0.34	0.003	3146	3146	613	2570	0.34	0.0033	3057	31	2462
V43111221	0.7	45	3	400	8	10	1	1.5	1.61	0.30	0.11	0.66	0.16	0.06	0.30	0.86	0.89	0.28	0.003	3493	3493	957	2585	0.28	0.0028	3425	35	2496
V43111222	0.7	45	3	400	8	10	1	2.5	1.65	0.31	0.12	0.66	0.16	0.06	0.30	0.86	0.89	0.29	0.003	3421	3421	938	2534	0.29	0.0029	3353	35	2443
V53111221	0.9	45	3	400	8	10	1	1.5	1.43	0.27	0.11	0.68	0.14	0.06	0.33	0.87	0.89	0.23	0.002	3874	3874	1365	2572	0.23	0.0025	3826	40	2504
V53111222	0.9	45	3	400	8	10	1	2.5	1.47	0.28	0.11	0.68	0.14	0.06	0.33	0.87	0.89	0.24	0.003	3799	3799	1340	2523	0.24	0.0025	3750	39	2454
V13112111	0.1	45	3	400	10	8	0.6	1.5	1.58	0.26	0.09	0.62	0.19	0.07	0.31	0.88	0.89	0.29	0.003	3467	3467	135	3343	0.29	0.0029	3361	34	3233
V13112112	0.1	45	3	400	10	8	0.6	2.5	1.64	0.27	0.10	0.62	0.19	0.07	0.30	0.87	0.89	0.31	0.003	3357	3357	130	3238	0.31	0.0031	3248	33	3125
V23112111	0.3	45	3	400	10	8	0.6	1.5	1.47	0.25	0.09	0.63	0.18	0.06	0.33	0.88	0.89	0.26	0.003	3670	3670	429	3263	0.26	0.0026	3579	36	3161
V23112112	0.3	45	3	400	10	8	0.6	2.5	1.53	0.26	0.10	0.63	0.18	0.06	0.32	0.87	0.89	0.28	0.003	3557	3557	415	3164	0.28	0.0027	3463	35	3059
V33112111	0.5	45	3	400	10	8	0.6	1.5	1.35	0.24	0.09	0.64	0.17	0.06	0.35	0.88	0.89	0.23	0.002	3921	3921	766	3188	0.23	0.0023	3846	39	3097
V33112112	0.5	45	3	400	10	8	0.6	2.5	1.41	0.25	0.09	0.64	0.17	0.06	0.34	0.88	0.89	0.25	0.002	3803	3803	743	3095	0.25	0.0024	3726	38	3001
V43112111	0.7	45	3	400	10	8	0.6	1.5	1.23	0.23	0.09	0.66	0.16	0.06	0.37	0.88	0.89	0.20	0.002	4240	4240	1160	3124	0.20	0.0020	4182	43	3047
V43112112	0.7	45	3	400	10	8	0.6	2.5	1.28	0.24	0.09	0.66	0.16	0.06	0.36	0.88	0.89	0.21	0.002	4117	4117	1127	3035	0.21	0.0021	4058	42	2957
V53112111	0.9	45	3	400	10	8	0.6	1.5	1.09	0.20	0.08	0.68	0.14	0.06	0.40	0.88	0.89	0.16	0.002	4655	4655	1633	3078	0.16	0.0017	4614	48	3020
V53112112	0.9	45	3	400	10	8	0.6	2.5	1.14	0.21	0.09	0.68	0.14	0.06	0.39	0.88	0.89	0.17	0.002	4528	4528	1590	2995	0.17	0.0018	4486	47	2936
V13112121	0.1	45	3	400	10	8	1	1.5	1.21	0.20	0.07	0.62	0.19	0.07	0.38	0.88	0.89	0.21	0.002	4171	4171	163	4020	0.21	0.0021	4082	41	3927
V13112122	0.1	45	3	400	10	8	1	2.5	1.26	0.21	0.07	0.62	0.19	0.07	0.36	0.88	0.89	0.22	0.002	4044	4044	158	3898	0.22	0.0022	3952	40	3802
V23112121	0.3	45	3	400	10	8	1	1.5	1.12	0.19	0.07	0.63	0.18	0.06	0.39	0.88	0.89	0.19	0.002	4391	4391	515	3897	0.19	0.0018	4314	44	3811
V23112122	0.3	45	3	400	10	8	1	2.5	1.18	0.20	0.07	0.63	0.18	0.06	0.38	0.88	0.89	0.20	0.002	4268	4268	500	3789	0.20	0.0019	4189	43	3700
V33112121	0.5	45	3	400	10	8	1	1.5	1.04	0.18	0.07	0.64	0.17	0.06	0.41	0.88	0.89	0.16	0.002	4659	4659	911	3778	0.16	0.0016	4595	47	3700
V33112122	0.5	45	3	400	10	8	1	2.5	1.08	0.19	0.07	0.64	0.17	0.06	0.40	0.88	0.89	0.17	0.002	4534	4534	887	3679	0.17	0.0017	4469	46	3599
V43112121	0.7	45	3	400	10	8	1	1.5	0.94	0.17	0.07	0.66	0.16	0.06	0.45	0.89	0.89	0.14	0.001	5104	5104	1395	3748	0.14	0.0014	5055	52	3683
V43112122	0.7	45	3	400	10	8	1	2.5	0.98	0.18	0.07	0.66	0.16	0.06	0.43	0.88	0.89	0.15	0.001	4908	4908	1342	3606	0.15	0.0015	4857	50	3539
V53112121	0.9	45	3	400	10	8	1	1.5	0.83	0.16	0.06	0.68	0.14	0.06	0.50	0.89	0.89	0.12	0.001	5751	5751	2010	3790	0.12	0.0012	5718	60	3742
V53112122	0.9	45	3	400	10	8	1	2.5	0.87	0.16	0.07	0.68	0.14	0.06	0.48	0.89	0.89	0.12	0.001	5518	5518	1930	3638	0.12	0.0013	5483	58	3588
V13112211	0.1	45	3	400	10	10	0.6	1.5	3.64	0.59	0.21	0.62	0.19	0.07	0.12	0.66	0.88	0.60	0.006	1444	1444	53	1400	0.60	0.0060	1289	13	1240
V13112212	0.1	45	3	400	10	10	0.6	2.5	3.84	0.63	0.22	0.62	0.19	0.07	0.11	0.63	0.88	0.63	0.006	1361	1361	50	1320	0.62	0.0062	1209	12	1163
V23112211	0.3	45	3	400	10	10	0.6	1.5	3.39	0.58	0.21	0.63	0.18	0.06	0.13	0.67	0.88	0.56	0.006	1554	1554	176	1403	0.56	0.0054	1418	14	1253
V23112212	0.3	45	3	400	10	10	0.6	2.5	3.57	0.61	0.22	0.63	0.18	0.06	0.12	0.65	0.88	0.59	0.006	1463	1463	165	1323	0.58	0.0057	1330	14	1175
V33112211	0.5	45	3	400	10	10	0.6	1.5	3.12	0.56	0.21	0.64	0.17	0.06	0.14	0.69	0.88	0.52	0.005	1703	1703	328	1417	0.52	0.0050	1589	16	1280
V33112212	0.5	45	3	400	10	10	0.6	2.5	3.29	0.59	0.22	0.64	0.17	0.06	0.13	0.67	0.88	0.54	0.005	1601	1601	308	1334	0.54	0.0052	1489	15	1199
V43112211	0.7	45	3	400	10	10	0.6	1.5	2.83	0.52	0.20	0.66	0.16	0.06	0.16	0.72	0.88	0.47	0.005	1916	1916	528	1448	0.47	0.0046	1825	19	1330
V43112212	0.7	45	3	400	10	10	0.6	2.5	2.99	0.55	0.21	0.66	0.16	0.06	0.15	0.70	0.88	0.49	0.005	1798	1798	496	1362	0.49	0.0048	1708	18	1244
V53112211	0.9	45	3	400	10	10	0.6	1.5	2.52	0.47	0.19	0.68	0.14	0.06	0.19	0.77	0.88	0.41	0.004	2235	2235	804	1511	0.41	0.0043	2168	23	1419
V53112212	0.9	45	3	400	10	10	0.6	2.5	2.65	0.50	0.20	0.68	0.14	0.06	0.18	0.75	0.88	0.42	0.004	2095	2095	756	1420	0.42	0.0045	2027	21	1327
V13112221	0.1	45	3	400	10	10	1	1.5	2.94	0.48	0.17	0.62	0.19	0.07	0.15	0.76	0.89	0.51	0.005	1838	1838	69	1779	0.51	0.0051	1680	17	1617
V13112222	0.1	45	3	400	10	10	1	2.5	3.11	0.51	0.18	0.62	0.19	0.07	0.14	0.74	0.88	0.53	0.005	1725	1725	64	1671	0.53	0.0053	1566	16	1506
V23112221	0.3	45	3	400	10	10	1	1.5	2.74	0.47	0.17	0.63	0.18	0.06	0.17	0.77	0.89	0.48	0.005	1989	1989	227	1788	0.48	0.0046	1855	19	1638
V23112222	0.3	45	3	400	10	10	1	2.5	2.90	0.49	0.18	0.63	0.18	0.06	0.16	0.75	0.88	0.50	0.005	1863	1863	212	1677	0.50	0.0048	1727	18	1525
V33112221	0.5	45	3	400	10	10	1	1.5	2.52	0.45	0.17	0.64	0.17	0.06	0.19	0.78	0.89	0.44	0.004	2194	2194	425	1811	0.44	0.0043	2085	21	1679
V33112222	0.5	45	3	400	10	10	1	2.5	2.67	0.48	0.18	0.64	0.17	0.06	0.17	0.76	0.88	0.46	0.004	2052	2052	397	1697	0.46	0.0044	1940	20	1562
V43112221	0.7	45	3	400	10	10	1	1.5	2.29	0.42	0.16	0.66	0.16	0.06	0.21	0.80	0.89	0.40	0.004	2488	2488	684	1861	0.40	0.0039	2404	25	1752

Name	af	nf	hf	mf	Ly	Lx	tw	Lcb	T1 [s]	T2 [s]	T3 [s]	M1 [-]	M2 [-]	M3 [-]	Sa	Sa2	Sa3	Disp [m]	ISDR [-]	Total Moment [MN-m]	Total Shear [MN]	Outrigger Moment [MN-m]	Wall Moment [MN-m]	Mode 1 Disp [m]	Mode 1 ISDR [-]	Mode 1 Moment [MN-m]	Mode 1 Shear [MN]	Mode 1 wall Moment [MN-m]
V43112222	0.7	45	3	400	10	10	1	2.5	2.42	0.45	0.17	0.66	0.16	0.06	0.20	0.78	0.89	0.42	0.004	2320	2320	638	1741	0.42	0.0041	2234	23	1628
V53112221	0.9	45	3	400	10	10	1	1.5	2.03	0.38	0.15	0.68	0.14	0.06	0.25	0.83	0.89	0.35	0.004	2932	2932	1043	1962	0.35	0.0037	2873	30	1880
V53112222	0.9	45	3	400	10	10	1	2.5	2.15	0.40	0.16	0.68	0.14	0.06	0.23	0.82	0.89	0.37	0.004	2726	2726	972	1830	0.36	0.0039	2665	28	1744
V13121111	0.1	45	3	600	8	8	0.6	1.5	1.44	0.23	0.08	0.62	0.19	0.07	0.33	0.88	0.89	0.26	0.003	5544	5544	216	5345	0.26	0.0026	5394	55	5189
V13121112	0.1	45	3	600	8	8	0.6	2.5	1.48	0.24	0.09	0.62	0.19	0.07	0.32	0.88	0.89	0.27	0.003	5452	5452	212	5256	0.27	0.0027	5300	54	5099
V23121111	0.3	45	3	600	8	8	0.6	1.5	1.34	0.23	0.08	0.63	0.18	0.06	0.35	0.88	0.89	0.24	0.002	5861	5861	686	5208	0.24	0.0023	5732	58	5063
V23121112	0.3	45	3	600	8	8	0.6	2.5	1.37	0.23	0.09	0.63	0.18	0.06	0.34	0.88	0.89	0.24	0.002	5764	5764	674	5122	0.24	0.0024	5633	57	4976
V33121111	0.5	45	3	600	8	8	0.6	1.5	1.24	0.22	0.08	0.64	0.17	0.06	0.37	0.88	0.89	0.21	0.002	6249	6249	1221	5076	0.21	0.0020	6143	63	4947
V33121112	0.5	45	3	600	8	8	0.6	2.5	1.27	0.23	0.08	0.64	0.17	0.06	0.36	0.88	0.89	0.22	0.002	6148	6148	1201	4996	0.21	0.0021	6041	62	4865
V43121111	0.7	45	3	600	8	8	0.6	1.5	1.12	0.21	0.08	0.66	0.16	0.06	0.39	0.88	0.89	0.18	0.002	6736	6736	1843	4957	0.18	0.0017	6654	69	4849
V43121112	0.7	45	3	600	8	8	0.6	2.5	1.15	0.21	0.08	0.66	0.16	0.06	0.39	0.88	0.89	0.18	0.002	6636	6636	1816	4885	0.18	0.0018	6552	68	4775
V53121111	0.9	45	3	600	8	8	0.6	1.5	1.00	0.19	0.07	0.68	0.14	0.06	0.43	0.88	0.89	0.14	0.002	7402	7402	2594	4889	0.14	0.0015	7344	77	4806
V53121112	0.9	45	3	600	8	8	0.6	2.5	1.02	0.19	0.08	0.68	0.14	0.06	0.42	0.88	0.89	0.15	0.002	7261	7261	2545	4797	0.15	0.0016	7201	76	4713
V13121121	0.1	45	3	600	8	8	1	1.5	1.09	0.18	0.06	0.62	0.19	0.07	0.40	0.88	0.89	0.18	0.002	6675	6675	261	6431	0.18	0.0018	6548	66	6300
V13121122	0.1	45	3	600	8	8	1	2.5	1.11	0.18	0.07	0.62	0.19	0.07	0.40	0.88	0.89	0.19	0.002	6574	6574	257	6335	0.19	0.0019	6446	65	6202
V23121121	0.3	45	3	600	8	8	1	1.5	1.01	0.17	0.06	0.63	0.18	0.06	0.42	0.89	0.89	0.16	0.002	7004	7004	822	6213	0.16	0.0016	6895	70	6090
V23121122	0.3	45	3	600	8	8	1	2.5	1.04	0.18	0.06	0.63	0.18	0.06	0.41	0.89	0.89	0.17	0.002	6909	6909	811	6130	0.17	0.0016	6799	69	6005
V33121121	0.5	45	3	600	8	8	1	1.5	0.93	0.17	0.06	0.64	0.17	0.06	0.45	0.89	0.89	0.15	0.001	7591	7591	1485	6150	0.15	0.0014	7502	77	6042
V33121122	0.5	45	3	600	8	8	1	2.5	0.96	0.17	0.06	0.64	0.17	0.06	0.44	0.89	0.89	0.15	0.001	7440	7440	1456	6029	0.15	0.0014	7350	75	5919
V43121121	0.7	45	3	600	8	8	1	1.5	0.85	0.16	0.06	0.66	0.16	0.06	0.49	0.89	0.89	0.13	0.001	8353	8353	2283	6127	0.13	0.0012	8286	86	6038
V43121122	0.7	45	3	600	8	8	1	2.5	0.87	0.16	0.06	0.66	0.16	0.06	0.48	0.89	0.89	0.13	0.001	8170	8170	2233	5995	0.13	0.0013	8101	84	5904
V53121121	0.9	45	3	600	8	8	1	1.5	0.75	0.14	0.06	0.68	0.14	0.06	0.54	0.89	0.89	0.10	0.001	9388	9388	3278	6180	0.10	0.0011	9341	98	6113
V53121122	0.9	45	3	600	8	8	1	2.5	0.77	0.14	0.06	0.68	0.14	0.06	0.53	0.89	0.89	0.11	0.001	9194	9194	3211	6053	0.11	0.0011	9146	96	5986
V13121211	0.1	45	3	600	8	10	0.6	1.5	3.18	0.52	0.19	0.62	0.19	0.07	0.14	0.73	0.88	0.54	0.006	2521	2521	94	2442	0.54	0.0054	2281	23	2195
V13121212	0.1	45	3	600	8	10	0.6	2.5	3.27	0.53	0.19	0.62	0.19	0.07	0.14	0.72	0.88	0.55	0.006	2446	2446	91	2371	0.55	0.0055	2207	22	2124
V23121211	0.3	45	3	600	8	10	0.6	1.5	2.97	0.51	0.18	0.63	0.18	0.06	0.15	0.74	0.88	0.51	0.005	2721	2721	310	2451	0.51	0.0049	2516	26	2222
V23121212	0.3	45	3	600	8	10	0.6	2.5	3.05	0.52	0.19	0.63	0.18	0.06	0.15	0.73	0.88	0.52	0.005	2640	2640	300	2380	0.52	0.0050	2434	25	2150
V33121211	0.5	45	3	600	8	10	0.6	1.5	2.73	0.49	0.18	0.64	0.17	0.06	0.17	0.76	0.88	0.47	0.005	2993	2993	579	2478	0.47	0.0045	2824	29	2275
V33121212	0.5	45	3	600	8	10	0.6	2.5	2.81	0.50	0.19	0.64	0.17	0.06	0.16	0.75	0.88	0.48	0.005	2902	2902	561	2405	0.48	0.0046	2732	28	2200
V43121211	0.7	45	3	600	8	10	0.6	1.5	2.48	0.46	0.18	0.66	0.16	0.06	0.19	0.78	0.89	0.43	0.004	3382	3382	930	2540	0.42	0.0042	3251	34	2369
V43121212	0.7	45	3	600	8	10	0.6	2.5	2.55	0.47	0.18	0.66	0.16	0.06	0.19	0.77	0.88	0.43	0.004	3275	3275	901	2462	0.43	0.0042	3143	33	2290
V53121211	0.9	45	3	600	8	10	0.6	1.5	2.20	0.41	0.17	0.68	0.14	0.06	0.22	0.81	0.89	0.37	0.004	3972	3972	1418	2668	0.37	0.0039	3879	41	2539
V53121212	0.9	45	3	600	8	10	0.6	2.5	2.26	0.42	0.17	0.68	0.14	0.06	0.22	0.80	0.89	0.38	0.004	3839	3839	1373	2582	0.38	0.0040	3744	39	2450
V13121221	0.1	45	3	600	8	10	1	1.5	2.53	0.41	0.15	0.62	0.19	0.07	0.19	0.81	0.89	0.46	0.005	3273	3273	124	3165	0.46	0.0046	3050	31	2935
V13121222	0.1	45	3	600	8	10	1	2.5	2.60	0.42	0.15	0.62	0.19	0.07	0.18	0.80	0.89	0.47	0.005	3172	3172	120	3069	0.47	0.0047	2947	30	2836
V23121221	0.3	45	3	600	8	10	1	1.5	2.36	0.40	0.15	0.63	0.18	0.06	0.21	0.82	0.89	0.43	0.004	3564	3564	411	3192	0.43	0.0042	3376	34	2982
V23121222	0.3	45	3	600	8	10	1	2.5	2.42	0.41	0.15	0.63	0.18	0.06	0.20	0.81	0.89	0.44	0.004	3450	3450	397	3092	0.44	0.0043	3260	33	2879
V33121221	0.5	45	3	600	8	10	1	1.5	2.17	0.39	0.14	0.64	0.17	0.06	0.23	0.83	0.89	0.40	0.004	3957	3957	769	3248	0.40	0.0038	3806	39	3065
V33121222	0.5	45	3	600	8	10	1	2.5	2.23	0.40	0.15	0.64	0.17	0.06	0.22	0.82	0.89	0.41	0.004	3826	3826	743	3144	0.41	0.0039	3672	38	2958
V43121221	0.7	45	3	600	8	10	1	1.5	1.97	0.36	0.14	0.66	0.16	0.06	0.26	0.84	0.89	0.36	0.004	4469	4469	1226	3323	0.36	0.0035	4356	45	3174
V43121222	0.7	45	3	600	8	10	1	2.5	2.03	0.37	0.14	0.66	0.16	0.06	0.25	0.84	0.89	0.37	0.004	4357	4357	1196	3243	0.37	0.0036	4242	44	3091
V53121221	0.9	45	3	600	8	10	1	1.5	1.75	0.33	0.13	0.68	0.14	0.06	0.28	0.85	0.89	0.30	0.003	4987	4987	1766	3324	0.30	0.0031	4906	52	3211
V53121222	0.9	45	3	600	8	10	1	2.5	1.80	0.34	0.14	0.68	0.14	0.06	0.28	0.85	0.89	0.31	0.003	4885	4885	1731	3258	0.31	0.0032	4803	50	3143
V13122111	0.1	45	3	600	10	8	0.6	1.5	1.93	0.31	0.11	0.62	0.19	0.07	0.26	0.86	0.89	0.37	0.004	4462	4462	172	4306	0.37	0.0037	4283	43	4121
V13122112	0.1	45	3	600	10	8	0.6	2.5	2.01	0.33	0.12	0.62	0.19	0.07	0.25	0.85	0.89	0.39	0.004	4305	4305	166	4155	0.39	0.0039	4121	42	3965
V23122111	0.3	45	3	600	10	8	0.6	1.5	1.80	0.31	0.11	0.63	0.18	0.06	0.28	0.86	0.89	0.34	0.003	4736	4736	551	4220	0.34	0.0033	4584	47	4049
V23122112	0.3	45	3	600	10	8	0.6	2.5	1.88	0.32	0.12	0.63	0.18	0.06	0.27	0.85	0.89	0.36	0.003	4582	4582	533	4085	0.36	0.0035	4426	45	3909
V33122111	0.5	45	3	600	10	8	0.6	1.5	1.66	0.30	0.11	0.64	0.17	0.06	0.30	0.86	0.89	0.30	0.003	5075	5075	990	4139	0.30	0.0029	4949	51	3985
V33122112	0.5	45	3	600	10	8	0.6	2.5	1.73	0.31	0.12	0.64	0.17	0.06	0.29	0.86	0.89	0.32	0.003	4914	4914	958	4010	0.32	0.0031	4785	49	3853
V43122111	0.7	45	3	600	10	8	0.6	1.5	1.50	0.28	0.11	0.66	0.16	0.06	0.32	0.87	0.89	0.26	0.003	5513	5513	1510	4076	0.26	0.0025	5416	56	3946
V43122112	0.7	45	3	600	10	8	0.6	2.5	1.57	0.29	0.11	0.66	0.16	0.06	0.31	0.86	0.89	0.27	0.003	5344	5344	1464	3953	0.27	0.0027	5244	54	3821
V53122111	0.9	45	3	600	10	8	0.6	1.5	1.33	0.25	0.10	0.68	0.14	0.06	0.35	0.88	0.89	0.21	0.002	6106	6106	2149	4049	0.21	0.0022	6036	63	3951
V53122112	0.9	45	3	600	10	8	0.6	2.5	1.39	0.26	0.10	0.68	0.14	0.06	0.34	0.87	0.89	0.22	0.002	5918	5918	2085	3927	0.22	0.0024	5847	61	3827
V13122121	0.1	45	3	600	10	8	1	1.5	1.48	0.24	0.09	0.62	0.19	0.07	0.32	0.88	0.89	0.27	0.003	5447	5447	212	5252	0.27	0.0027	5295	54	5094
V13122122	0.1	45	3	600	10	8	1	2.5	1.55	0.25	0.09	0.62	0.19	0.07	0.31	0.88	0.89	0.29	0.003	5271	5271	205	5083	0.29	0.0029	5114	52	4920
V23122121	0.3	45	3	600	10	8	1	1.5	1.38	0.23	0.09	0.63	0.18	0.06	0.34	0.88	0.89	0.24	0.002	5759	5759	674	5118	0.24	0.0024	5628	57	4971
V23122122	0.3	45	3	600	10	8	1	2.5	1.44	0.25	0.09	0.63	0.18	0.06	0.33	0.88	0.89	0.26	0.003	5579	5579	652	4960	0.26	0.0025	5445	55	4809
V33122121	0.5	45	3	600	10	8	1	1.5	1.27	0.23	0.08	0.64	0.17	0.06	0.36	0.88	0.89	0.22	0.002	6143	6143	1200	4992	0.22	0.0021	6036	62	4861
V33122122	0.5	45	3	600	10	8	1	2.5	1.33	0.24	0.09	0.64	0.17	0.06	0.35	0.88	0.89	0.23	0.002	5959	5959	1164	4845	0.23	0.0022	5849	60	4710
V43122121	0.7	45	3	600	10	8	1	1.5	1.15	0.21	0.08	0.66	0.16	0.06	0.39	0.88	0.89	0.18	0.002	6631	6631	1814	4882	0.18	0.0018	6548	68	4771
V43122122	0.7	45	3	600	10	8	1	2.5	1.20	0.22	0.09	0.66	0.16	0.06	0.38	0.88	0.89	0.20	0.002	6441	6441	1763	4744	0.20	0.0019	6355	66	4631
V53122121	0.9	45	3	600	10	8	1	1.5	1.02	0.19	0.08	0.68	0.14	0.06	0.42	0.88	0.89	0.15	0.002	7256	7256	2544	4794	0.15	0.0016	7196	76	4710
V53122122	0.9	45	3	600	10	8	1	2.5	1.07	0.20	0.08	0.68	0.14	0.06	0.41	0.88	0.89	0.16	0.002	7065	7065	2478	4670	0.16	0.0017	7004	74	4584
V13122211	0.1	45	3	600	10	10	0.6	1.5	4.46	0.73	0.26	0.62	0.19	0.07	0.09	0.56	0.87	0.71	0.007	1731	1731	63	1681	0.70	0.0070	1514	15	1456
V13122212	0.1	45	3	600	10	10	0.6	2.5	4.70	0.77	0.28	0.62	0.19	0.07	0.09	0.53	0.87	0.74	0.008	1635	1635	59	1587	0.73	0.0073	1423	14	1369
V23122211	0.3	45	3	600	10	10	0.6	1.5	4.15	0.71	0.26	0.63	0.18	0.06	0.10	0.57	0.88	0.66	0.007	1853	1853	208	1680	0.66	0.0064	1662	17	1468
V23122212	0.3	45	3	600	10	10	0.6	2.5	4.38	0.75	0.27	0.63	0.18	0.06	0.09	0.55	0.87	0.69	0.007	1748	1748	195	1586	0.68	0.0066	1561	16	1379
V33122211	0.5	45	3	600	10	10	0.6	1.5	3.83	0.68	0.25	0.64	0.17	0.06	0.11	0.59	0.88	0.61	0.006	2020	2020	387	1689	0.60	0.0058	1857	19	1496
V33122212	0.5	45	3	600	10	10	0.6	2.5	4.03	0.72	0.27	0.64	0.17	0.06	0.10	0.56	0.87	0.63	0.006	1903	1903	364	1594	0.63	0.0060	1743	18	1403
V43122211	0.7	45	3	600	10	10	0.6	1.5	3.47	0.64	0.25	0.66	0.16	0.06	0.13	0.62	0.88	0.55	0.005	2256	2256	622	1717	0.54	0.0053	2124	22	1548
V43122212	0.7	45	3	600	10	10	0.6	2.5	3.66	0.68	0.26	0.66	0.16	0.06	0.12	0.59	0.87	0.57	0.006	2123	2123	585	1619	0.57	0.0056	1991	21	1451
V53122211	0.9	45	3	600	10	10	0.6	1.5	3.08	0.58	0.23	0.68	0.14	0.06	0.15	0.67	0.88	0.47	0.005	2618	2618	950	1786	0.47	0.0050	2514	26	1645

Name	af	nf	hf	mf	Ly	Lx	tw	Lcb	T1 [s]	T2 [s]	T3 [s]	M1 [-]	M2 [-]	M3 [-]	Sa	Sa2	Sa3	Disp [m]	ISDR [-]	Total Moment [MN-m]	Total Shear [MN]	Outrigger Moment [MN-m]	Wall Moment [MN-m]	Mode 1 Disp [m]	Mode 1 ISDR [-]	Mode 1 Moment [MN-m]	Mode 1 Shear [MN]	Mode 1 wall Moment [MN-m]
V53122212	0.9	45	3	600	10	10	0.6	2.5	3.25	0.61	0.24	0.68	0.14	0.06	0.14	0.65	0.88	0.49	0.005	2458	2458	893	1679	0.49	0.0052	2354	25	1540
V13122221	0.1	45	3	600	10	10	1	1.5	3.60	0.59	0.21	0.62	0.19	0.07	0.12	0.67	0.88	0.60	0.006	2193	2193	81	2126	0.59	0.0059	1959	20	1884
V13122222	0.1	45	3	600	10	10	1	2.5	3.81	0.62	0.22	0.62	0.19	0.07	0.11	0.63	0.88	0.62	0.006	2058	2058	76	1996	0.62	0.0062	1829	19	1760
V23122221	0.3	45	3	600	10	10	1	1.5	3.36	0.57	0.21	0.63	0.18	0.06	0.13	0.68	0.88	0.56	0.006	2360	2360	267	2131	0.56	0.0054	2156	22	1905
V23122222	0.3	45	3	600	10	10	1	2.5	3.55	0.61	0.22	0.63	0.18	0.06	0.12	0.65	0.88	0.58	0.006	2212	2212	250	2000	0.58	0.0056	2012	20	1777
V33122221	0.5	45	3	600	10	10	1	1.5	3.09	0.55	0.21	0.64	0.17	0.06	0.15	0.70	0.88	0.51	0.005	2587	2587	499	2151	0.51	0.0049	2417	25	1946
V33122222	0.5	45	3	600	10	10	1	2.5	3.27	0.58	0.22	0.64	0.17	0.06	0.14	0.67	0.88	0.54	0.005	2421	2421	466	2017	0.53	0.0051	2252	23	1814
V43122221	0.7	45	3	600	10	10	1	1.5	2.81	0.52	0.20	0.66	0.16	0.06	0.16	0.73	0.88	0.46	0.005	2911	2911	802	2199	0.46	0.0046	2775	29	2022
V43122222	0.7	45	3	600	10	10	1	2.5	2.97	0.55	0.21	0.66	0.16	0.06	0.15	0.70	0.88	0.48	0.005	2721	2721	750	2060	0.48	0.0047	2585	27	1883
V53122221	0.9	45	3	600	10	10	1	1.5	2.49	0.47	0.19	0.68	0.14	0.06	0.19	0.77	0.88	0.40	0.004	3399	3399	1222	2297	0.40	0.0043	3299	35	2159
V53122222	0.9	45	3	600	10	10	1	2.5	2.63	0.49	0.20	0.68	0.14	0.06	0.18	0.75	0.88	0.42	0.004	3170	3170	1143	2148	0.42	0.0044	3067	32	2008
V13211111	0.1	45	4	400	8	8	0.6	1.5	1.15	0.19	0.07	0.62	0.19	0.07	0.39	0.88	0.89	0.20	0.001	5727	5727	224	5519	0.20	0.0015	5611	43	5398
V13211112	0.1	45	4	400	8	8	0.6	2.5	1.17	0.19	0.07	0.62	0.19	0.07	0.38	0.88	0.89	0.20	0.002	5667	5667	221	5461	0.20	0.0015	5550	42	5340
V23211111	0.3	45	4	400	8	8	0.6	1.5	1.07	0.18	0.07	0.63	0.18	0.06	0.40	0.88	0.89	0.18	0.001	6028	6028	707	5348	0.18	0.0013	5928	45	5236
V23211112	0.3	45	4	400	8	8	0.6	2.5	1.09	0.19	0.07	0.63	0.18	0.06	0.40	0.88	0.89	0.18	0.001	5965	5965	700	5293	0.18	0.0013	5864	45	5180
V33211111	0.5	45	4	400	8	8	0.6	1.5	0.99	0.18	0.07	0.64	0.17	0.06	0.43	0.89	0.89	0.15	0.001	6432	6432	1258	5214	0.15	0.0011	6349	49	5113
V33211112	0.5	45	4	400	8	8	0.6	2.5	1.01	0.18	0.07	0.64	0.17	0.06	0.42	0.88	0.89	0.16	0.001	6332	6332	1239	5134	0.16	0.0011	6248	48	5032
V43211111	0.7	45	4	400	8	8	0.6	1.5	0.90	0.17	0.06	0.66	0.16	0.06	0.47	0.89	0.89	0.13	0.001	7059	7059	1930	5181	0.13	0.0010	6996	54	5098
V43211112	0.7	45	4	400	8	8	0.6	2.5	0.91	0.17	0.07	0.66	0.16	0.06	0.46	0.89	0.89	0.14	0.001	6967	6967	1905	5115	0.14	0.0010	6903	54	5030
V53211111	0.9	45	4	400	8	8	0.6	1.5	0.80	0.15	0.06	0.68	0.14	0.06	0.52	0.89	0.89	0.11	0.001	7972	7972	2785	5250	0.11	0.0009	7928	62	5189
V53211112	0.9	45	4	400	8	8	0.6	2.5	0.81	0.15	0.06	0.68	0.14	0.06	0.51	0.89	0.89	0.11	0.001	7862	7862	2747	5179	0.11	0.0009	7818	62	5117
V13211121	0.1	45	4	400	8	8	1	1.5	0.85	0.14	0.05	0.62	0.19	0.07	0.49	0.89	0.89	0.14	0.001	7142	7142	280	6879	0.14	0.0010	7048	54	6781
V13211122	0.1	45	4	400	8	8	1	2.5	0.87	0.14	0.05	0.62	0.19	0.07	0.48	0.89	0.89	0.14	0.001	7029	7029	276	6769	0.14	0.0010	6933	53	6670
V23211121	0.3	45	4	400	8	8	1	1.5	0.80	0.14	0.05	0.63	0.18	0.06	0.52	0.89	0.89	0.12	0.001	7640	7640	899	6768	0.12	0.0009	7560	58	6678
V23211122	0.3	45	4	400	8	8	1	2.5	0.81	0.14	0.05	0.63	0.18	0.06	0.51	0.89	0.89	0.13	0.001	7533	7533	887	6673	0.13	0.0009	7452	57	6582
V33211121	0.5	45	4	400	8	8	1	1.5	0.73	0.13	0.05	0.64	0.17	0.06	0.55	0.89	0.89	0.11	0.001	8267	8267	1619	6685	0.11	0.0008	8202	63	6606
V33211122	0.5	45	4	400	8	8	1	2.5	0.75	0.13	0.05	0.64	0.17	0.06	0.54	0.89	0.89	0.11	0.001	8136	8136	1593	6580	0.11	0.0008	8070	62	6499
V43211121	0.7	45	4	400	8	8	1	1.5	0.67	0.12	0.05	0.66	0.16	0.06	0.60	0.89	0.89	0.10	0.001	9080	9080	2480	6646	0.10	0.0007	9030	70	6580
V43211122	0.7	45	4	400	8	8	1	2.5	0.68	0.13	0.05	0.66	0.16	0.06	0.59	0.89	0.89	0.10	0.001	8959	8959	2447	6558	0.10	0.0007	8908	69	6492
V53211121	0.9	45	4	400	8	8	1	1.5	0.59	0.11	0.04	0.68	0.14	0.06	0.66	0.89	0.89	0.08	0.001	10204	10204	3555	6704	0.08	0.0006	10169	80	6656
V53211122	0.9	45	4	400	8	8	1	2.5	0.60	0.11	0.05	0.68	0.14	0.06	0.65	0.89	0.89	0.08	0.001	10055	10055	3504	6607	0.08	0.0006	10020	79	6558
V13211211	0.1	45	4	400	8	10	0.6	1.5	2.51	0.41	0.15	0.62	0.19	0.07	0.19	0.81	0.89	0.46	0.003	2939	2939	111	2842	0.45	0.0034	2743	21	2639
V13211212	0.1	45	4	400	8	10	0.6	2.5	2.56	0.42	0.15	0.62	0.19	0.07	0.18	0.81	0.89	0.46	0.004	2876	2876	109	2782	0.46	0.0035	2678	20	2576
V23211211	0.3	45	4	400	8	10	0.6	1.5	2.34	0.40	0.15	0.63	0.18	0.06	0.21	0.82	0.89	0.43	0.003	3203	3203	369	2868	0.43	0.0031	3037	23	2683
V23211212	0.3	45	4	400	8	10	0.6	2.5	2.38	0.41	0.15	0.63	0.18	0.06	0.20	0.82	0.89	0.43	0.003	3128	3128	360	2802	0.43	0.0031	2960	23	2615
V33211211	0.5	45	4	400	8	10	0.6	1.5	2.15	0.38	0.14	0.64	0.17	0.06	0.23	0.83	0.89	0.40	0.003	3555	3555	691	2917	0.40	0.0029	3422	26	2756
V33211212	0.5	45	4	400	8	10	0.6	2.5	2.20	0.39	0.15	0.64	0.17	0.06	0.23	0.83	0.89	0.40	0.003	3474	3474	675	2853	0.40	0.0029	3339	26	2689
V43211211	0.7	45	4	400	8	10	0.6	1.5	1.95	0.36	0.14	0.66	0.16	0.06	0.26	0.84	0.89	0.36	0.003	4003	4003	1098	2976	0.36	0.0026	3903	30	2844
V43211212	0.7	45	4	400	8	10	0.6	2.5	1.99	0.37	0.14	0.66	0.16	0.06	0.26	0.84	0.89	0.36	0.003	3938	3938	1081	2929	0.36	0.0027	3837	30	2796
V53211211	0.9	45	4	400	8	10	0.6	1.5	1.73	0.33	0.13	0.68	0.14	0.06	0.29	0.85	0.89	0.29	0.002	4465	4465	1581	2976	0.29	0.0023	4393	35	2876
V53211212	0.9	45	4	400	8	10	0.6	2.5	1.77	0.33	0.13	0.68	0.14	0.06	0.28	0.85	0.89	0.30	0.002	4398	4398	1557	2932	0.30	0.0024	4325	34	2831
V13211221	0.1	45	4	400	8	10	1	1.5	1.94	0.32	0.11	0.62	0.19	0.07	0.26	0.86	0.89	0.37	0.003	3954	3954	152	3816	0.37	0.0028	3795	29	3651
V13211222	0.1	45	4	400	8	10	1	2.5	1.97	0.32	0.12	0.62	0.19	0.07	0.26	0.85	0.89	0.38	0.003	3891	3891	150	3755	0.38	0.0029	3730	28	3589
V23211221	0.3	45	4	400	8	10	1	1.5	1.80	0.31	0.11	0.63	0.18	0.06	0.28	0.86	0.89	0.34	0.003	4198	4198	489	3741	0.34	0.0025	4062	31	3588
V23211222	0.3	45	4	400	8	10	1	2.5	1.84	0.31	0.11	0.63	0.18	0.06	0.27	0.86	0.89	0.35	0.003	4137	4137	481	3687	0.35	0.0025	3999	31	3532
V33211221	0.5	45	4	400	8	10	1	1.5	1.66	0.30	0.11	0.64	0.17	0.06	0.30	0.86	0.89	0.30	0.002	4498	4498	877	3669	0.30	0.0022	4386	34	3532
V33211222	0.5	45	4	400	8	10	1	2.5	1.70	0.30	0.11	0.64	0.17	0.06	0.29	0.86	0.89	0.31	0.002	4434	4434	865	3618	0.31	0.0022	4321	33	3480
V43211221	0.7	45	4	400	8	10	1	1.5	1.51	0.28	0.11	0.66	0.16	0.06	0.32	0.87	0.89	0.26	0.002	4886	4886	1339	3612	0.26	0.0019	4799	37	3497
V43211222	0.7	45	4	400	8	10	1	2.5	1.54	0.28	0.11	0.66	0.16	0.06	0.31	0.87	0.89	0.27	0.002	4819	4819	1320	3563	0.27	0.0020	4731	37	3447
V53211221	0.9	45	4	400	8	10	1	1.5	1.34	0.25	0.10	0.68	0.14	0.06	0.35	0.88	0.89	0.21	0.002	5413	5413	1905	3589	0.21	0.0017	5351	42	3502
V53211222	0.9	45	4	400	8	10	1	2.5	1.37	0.26	0.10	0.68	0.14	0.06	0.34	0.88	0.89	0.22	0.002	5337	5337	1879	3540	0.22	0.0017	5274	42	3452
V13212111	0.1	45	4	400	10	8	0.6	1.5	1.53	0.25	0.09	0.62	0.19	0.07	0.32	0.88	0.89	0.28	0.002	4721	4721	183	4552	0.28	0.0021	4582	35	4408
V13212112	0.1	45	4	400	10	8	0.6	2.5	1.58	0.26	0.09	0.62	0.19	0.07	0.31	0.88	0.89	0.29	0.002	4619	4619	179	4454	0.29	0.0022	4477	34	4308
V23212111	0.3	45	4	400	10	8	0.6	1.5	1.42	0.24	0.09	0.63	0.18	0.06	0.33	0.88	0.89	0.26	0.002	4997	4997	584	4442	0.25	0.0019	4878	37	4309
V23212112	0.3	45	4	400	10	8	0.6	2.5	1.47	0.25	0.09	0.63	0.18	0.06	0.33	0.88	0.89	0.27	0.002	4889	4889	571	4348	0.26	0.0019	4768	36	4212
V33212111	0.5	45	4	400	10	8	0.6	1.5	1.31	0.23	0.09	0.64	0.17	0.06	0.35	0.88	0.89	0.23	0.002	5337	5337	1042	4338	0.23	0.0016	5239	40	4219
V33212112	0.5	45	4	400	10	8	0.6	2.5	1.35	0.24	0.09	0.64	0.17	0.06	0.35	0.88	0.89	0.23	0.002	5224	5224	1020	4248	0.23	0.0017	5124	39	4127
V43212111	0.7	45	4	400	10	8	0.6	1.5	1.19	0.22	0.08	0.66	0.16	0.06	0.38	0.88	0.89	0.19	0.001	5766	5766	1578	4246	0.19	0.0014	5690	44	4146
V43212112	0.7	45	4	400	10	8	0.6	2.5	1.23	0.23	0.09	0.66	0.16	0.06	0.37	0.88	0.89	0.20	0.001	5649	5649	1546	4162	0.20	0.0015	5572	43	4060
V53212111	0.9	45	4	400	10	8	0.6	1.5	1.06	0.20	0.08	0.68	0.14	0.06	0.41	0.88	0.89	0.16	0.001	6321	6321	2217	4177	0.16	0.0012	6267	49	4102
V53212112	0.9	45	4	400	10	8	0.6	2.5	1.09	0.20	0.08	0.68	0.14	0.06	0.40	0.88	0.89	0.16	0.001	6203	6203	2176	4101	0.16	0.0013	6148	48	4024
V13212121	0.1	45	4	400	10	8	1	1.5	1.15	0.19	0.07	0.62	0.19	0.07	0.39	0.88	0.89	0.19	0.001	5739	5739	224	5530	0.19	0.0015	5624	43	5410
V13212122	0.1	45	4	400	10	8	1	2.5	1.18	0.19	0.07	0.62	0.19	0.07	0.38	0.88	0.89	0.20	0.002	5627	5627	220	5422	0.20	0.0015	5509	42	5300
V23212121	0.3	45	4	400	10	8	1	1.5	1.07	0.18	0.07	0.63	0.18	0.06	0.41	0.88	0.89	0.17	0.001	6040	6040	709	5359	0.17	0.0013	5941	45	5247
V23212122	0.3	45	4	400	10	8	1	2.5	1.10	0.19	0.07	0.63	0.18	0.06	0.40	0.88	0.89	0.18	0.001	5923	5923	695	5256	0.18	0.0013	5821	44	5142
V33212121	0.5	45	4	400	10	8	1	1.5	0.98	0.18	0.07	0.64	0.17	0.06	0.43	0.89	0.89	0.15	0.001	6452	6452	1262	5230	0.15	0.0011	6370	49	5130
V33212122	0.5	45	4	400	10	8	1	2.5	1.02	0.18	0.07	0.64	0.17	0.06	0.42	0.88	0.89	0.16	0.001	6275	6275	1227	5088	0.16	0.0012	6191	48	4985
V43212121	0.7	45	4	400	10	8	1	1.5	0.89	0.17	0.06	0.66	0.16	0.06	0.47	0.89	0.89	0.13	0.001	7078	7078	1935	5195	0.13	0.0010	7015	54	5112
V43212122	0.7	45	4	400	10	8	1	2.5	0.92	0.17	0.07	0.66	0.16	0.06	0.45	0.89	0.89	0.14	0.001	6904	6904	1888	5069	0.14	0.0010	6840	53	4985
V53212121	0.9	45	4	400	10	8	1	1.5	0.79	0.15	0.06	0.68	0.14	0.06	0.52	0.89	0.89	0.11	0.001	7994	7994	2793	5265	0.11	0.0009	7951	63	5204
V53212122	0.9	45	4	400	10	8	1	2.5	0.82	0.15	0.06	0.68	0.14	0.06	0.50	0.89	0.89	0.12	0.001	7787	7787	2721	5130	0.12	0.0009	7743	61	5068
V13212211	0.1	45	4	400	10	10	0.6	1.5	3.48	0.57	0.20	0.62	0.19	0.07	0.13	0.68	0.88	0.58	0.005	2027	2027	75	1965	0.58	0.0043	1817	14	1748

Name	af	nf	hf	mf	Ly	Lx	tw	Lcb	T1 [s]	T2 [s]	T3 [s]	M1 [-]	M2 [-]	M3 [-]	Sa	Sa2	Sa3	Disp [m]	ISDR [-]	Total Moment [MN-m]	Total Shear [MN]	Outrigger Moment [MN-m]	Wall Moment [MN-m]	Mode 1 Disp [m]	Mode 1 ISDR [-]	Mode 1 Moment [MN-m]	Mode 1 Shear [MN]	Mode 1 wall Moment [MN-m]
V13212212	0.1	45	4	400	10	10	0.6	2.5	3.61	0.59	0.21	0.62	0.19	0.07	0.12	0.66	0.88	0.60	0.005	1944	1944	72	1885	0.60	0.0045	1736	13	1670
V23212211	0.3	45	4	400	10	10	0.6	1.5	3.24	0.55	0.20	0.63	0.18	0.06	0.14	0.70	0.88	0.54	0.004	2183	2183	247	1970	0.54	0.0039	2001	15	1768
V23212212	0.3	45	4	400	10	10	0.6	2.5	3.36	0.57	0.21	0.63	0.18	0.06	0.13	0.68	0.88	0.56	0.004	2092	2092	237	1889	0.56	0.0040	1911	15	1688
V33212211	0.5	45	4	400	10	10	0.6	1.5	2.99	0.53	0.20	0.64	0.17	0.06	0.15	0.72	0.88	0.50	0.004	2396	2396	462	1990	0.50	0.0036	2244	17	1807
V33212212	0.5	45	4	400	10	10	0.6	2.5	3.10	0.55	0.21	0.64	0.17	0.06	0.14	0.70	0.88	0.52	0.004	2293	2293	442	1907	0.51	0.0037	2142	16	1725
V43212211	0.7	45	4	400	10	10	0.6	1.5	2.71	0.50	0.19	0.66	0.16	0.06	0.17	0.74	0.88	0.45	0.003	2699	2699	743	2035	0.45	0.0033	2579	20	1879
V43212212	0.7	45	4	400	10	10	0.6	2.5	2.81	0.52	0.20	0.66	0.16	0.06	0.16	0.73	0.88	0.47	0.003	2580	2580	711	1949	0.46	0.0034	2459	19	1792
V53212211	0.9	45	4	400	10	10	0.6	1.5	2.40	0.45	0.18	0.68	0.14	0.06	0.20	0.78	0.88	0.39	0.003	3154	3154	1132	2128	0.39	0.0031	3067	24	2007
V53212212	0.9	45	4	400	10	10	0.6	2.5	2.50	0.47	0.19	0.68	0.14	0.06	0.19	0.77	0.88	0.41	0.003	3012	3012	1083	2035	0.40	0.0032	2923	23	1913
V13212221	0.1	45	4	400	10	10	1	1.5	2.72	0.44	0.16	0.62	0.19	0.07	0.17	0.79	0.89	0.48	0.004	2682	2682	101	2595	0.48	0.0036	2478	19	2384
V13212222	0.1	45	4	400	10	10	1	2.5	2.83	0.46	0.17	0.62	0.19	0.07	0.16	0.78	0.89	0.50	0.004	2565	2565	96	2482	0.49	0.0037	2358	18	2268
V23212221	0.3	45	4	400	10	10	1	1.5	2.53	0.43	0.16	0.63	0.18	0.06	0.19	0.80	0.89	0.45	0.003	2910	2910	334	2611	0.45	0.0033	2738	21	2418
V23212222	0.3	45	4	400	10	10	1	2.5	2.63	0.45	0.16	0.63	0.18	0.06	0.18	0.78	0.89	0.47	0.003	2778	2778	318	2495	0.46	0.0034	2603	20	2299
V33212221	0.5	45	4	400	10	10	1	1.5	2.33	0.42	0.16	0.64	0.17	0.06	0.21	0.81	0.89	0.42	0.003	3224	3224	626	2653	0.42	0.0030	3084	24	2484
V33212222	0.5	45	4	400	10	10	1	2.5	2.43	0.43	0.16	0.64	0.17	0.06	0.20	0.80	0.89	0.43	0.003	3072	3072	596	2532	0.43	0.0031	2930	23	2359
V43212221	0.7	45	4	400	10	10	1	1.5	2.12	0.39	0.15	0.66	0.16	0.06	0.24	0.83	0.89	0.38	0.003	3666	3666	1007	2734	0.38	0.0028	3560	28	2594
V43212222	0.7	45	4	400	10	10	1	2.5	2.20	0.41	0.16	0.66	0.16	0.06	0.22	0.82	0.89	0.39	0.003	3490	3490	959	2607	0.39	0.0029	3381	26	2464
V53212221	0.9	45	4	400	10	10	1	1.5	1.88	0.35	0.14	0.68	0.14	0.06	0.27	0.84	0.89	0.32	0.003	4195	4195	1488	2801	0.32	0.0026	4120	32	2697
V53212222	0.9	45	4	400	10	10	1	2.5	1.95	0.37	0.15	0.68	0.14	0.06	0.26	0.84	0.89	0.34	0.003	4061	4061	1442	2715	0.34	0.0027	3985	31	2608
V13221111	0.1	45	4	600	8	8	0.6	1.5	1.41	0.23	0.08	0.62	0.19	0.07	0.34	0.88	0.89	0.25	0.002	7504	7504	292	7234	0.25	0.0019	7307	55	7030
V13221112	0.1	45	4	600	8	8	0.6	2.5	1.43	0.23	0.08	0.62	0.19	0.07	0.33	0.88	0.89	0.26	0.002	7416	7416	288	7150	0.26	0.0020	7217	55	6943
V23221111	0.3	45	4	600	8	8	0.6	1.5	1.31	0.22	0.08	0.63	0.18	0.06	0.35	0.88	0.89	0.23	0.002	7933	7933	929	7048	0.23	0.0017	7764	59	6858
V23221112	0.3	45	4	600	8	8	0.6	2.5	1.34	0.23	0.08	0.63	0.18	0.06	0.35	0.88	0.89	0.24	0.002	7841	7841	918	6967	0.23	0.0017	7670	59	6775
V33221111	0.5	45	4	600	8	8	0.6	1.5	1.21	0.22	0.08	0.64	0.17	0.06	0.37	0.88	0.89	0.20	0.001	8456	8456	1653	6868	0.20	0.0015	8317	64	6698
V33221112	0.5	45	4	600	8	8	0.6	2.5	1.23	0.22	0.08	0.64	0.17	0.06	0.37	0.88	0.89	0.21	0.002	8359	8359	1634	6790	0.21	0.0015	8218	63	6618
V43221111	0.7	45	4	600	8	8	0.6	1.5	1.10	0.20	0.08	0.66	0.16	0.06	0.40	0.88	0.89	0.17	0.001	9108	9108	2492	6702	0.17	0.0013	9000	70	6558
V43221112	0.7	45	4	600	8	8	0.6	2.5	1.12	0.21	0.08	0.66	0.16	0.06	0.39	0.88	0.89	0.18	0.001	9009	9009	2465	6630	0.18	0.0013	8900	69	6485
V53221111	0.9	45	4	600	8	8	0.6	1.5	0.97	0.18	0.07	0.68	0.14	0.06	0.43	0.88	0.89	0.14	0.001	10066	10066	3526	6646	0.14	0.0011	9990	79	6538
V53221112	0.9	45	4	600	8	8	0.6	2.5	0.99	0.19	0.07	0.68	0.14	0.06	0.43	0.88	0.89	0.14	0.001	9913	9913	3474	6546	0.14	0.0011	9835	77	6437
V13221121	0.1	45	4	600	8	8	1	1.5	1.05	0.17	0.06	0.62	0.19	0.07	0.41	0.89	0.89	0.17	0.001	9106	9106	356	8773	0.17	0.0013	8941	68	8602
V13221122	0.1	45	4	600	8	8	1	2.5	1.07	0.17	0.06	0.62	0.19	0.07	0.41	0.89	0.89	0.18	0.001	9013	9013	353	8684	0.18	0.0013	8847	67	8511
V23221121	0.3	45	4	600	8	8	1	1.5	0.98	0.17	0.06	0.63	0.18	0.06	0.43	0.89	0.89	0.16	0.001	9666	9666	1135	8572	0.16	0.0011	9525	73	8413
V23221122	0.3	45	4	600	8	8	1	2.5	0.99	0.17	0.06	0.63	0.18	0.06	0.43	0.89	0.89	0.16	0.001	9516	9516	1118	8440	0.16	0.0012	9373	72	8279
V33221121	0.5	45	4	600	8	8	1	1.5	0.90	0.16	0.06	0.64	0.17	0.06	0.46	0.89	0.89	0.14	0.001	10432	10432	2042	8449	0.14	0.0010	10317	79	8308
V33221122	0.5	45	4	600	8	8	1	2.5	0.91	0.16	0.06	0.64	0.17	0.06	0.46	0.89	0.89	0.14	0.001	10292	10292	2014	8337	0.14	0.0010	10175	78	8195
V43221121	0.7	45	4	600	8	8	1	1.5	0.82	0.15	0.06	0.66	0.16	0.06	0.51	0.89	0.89	0.12	0.001	11514	11514	3147	8442	0.12	0.0009	11427	89	8327
V43221122	0.7	45	4	600	8	8	1	2.5	0.83	0.15	0.06	0.66	0.16	0.06	0.50	0.89	0.89	0.12	0.001	11345	11345	3101	8319	0.12	0.0009	11256	87	8202
V53221121	0.9	45	4	600	8	8	1	1.5	0.72	0.14	0.05	0.68	0.14	0.06	0.56	0.89	0.89	0.10	0.001	12964	12964	4524	8531	0.10	0.0008	12904	102	8446
V53221122	0.9	45	4	600	8	8	1	2.5	0.74	0.14	0.06	0.68	0.14	0.06	0.55	0.89	0.89	0.10	0.001	12763	12763	4455	8399	0.10	0.0008	12701	100	8313
V13221211	0.1	45	4	600	8	10	0.6	1.5	3.07	0.50	0.18	0.62	0.19	0.07	0.15	0.74	0.88	0.53	0.004	3497	3497	130	3388	0.53	0.0039	3179	24	3059
V13221212	0.1	45	4	600	8	10	0.6	2.5	3.13	0.51	0.18	0.62	0.19	0.07	0.14	0.74	0.88	0.54	0.004	3422	3422	127	3316	0.53	0.0040	3103	24	2985
V23221211	0.3	45	4	600	8	10	0.6	1.5	2.86	0.49	0.18	0.63	0.18	0.06	0.16	0.75	0.88	0.49	0.004	3778	3778	431	3400	0.49	0.0036	3507	27	3098
V23221212	0.3	45	4	600	8	10	0.6	2.5	2.92	0.50	0.18	0.63	0.18	0.06	0.16	0.75	0.88	0.50	0.004	3696	3696	421	3328	0.50	0.0036	3423	26	3024
V33221211	0.5	45	4	600	8	10	0.6	1.5	2.64	0.47	0.18	0.64	0.17	0.06	0.18	0.77	0.89	0.46	0.003	4160	4160	805	3440	0.46	0.0033	3938	30	3171
V33221212	0.5	45	4	600	8	10	0.6	2.5	2.69	0.48	0.18	0.64	0.17	0.06	0.17	0.76	0.88	0.46	0.003	4069	4069	787	3367	0.46	0.0033	3846	30	3097
V43221211	0.7	45	4	600	8	10	0.6	1.5	2.39	0.44	0.17	0.66	0.16	0.06	0.20	0.79	0.89	0.41	0.003	4706	4706	1294	3529	0.41	0.0030	4535	35	3305
V43221212	0.7	45	4	600	8	10	0.6	2.5	2.44	0.45	0.17	0.66	0.16	0.06	0.20	0.78	0.89	0.42	0.003	4601	4601	1265	3452	0.42	0.0031	4428	34	3227
V53221211	0.9	45	4	600	8	10	0.6	1.5	2.12	0.40	0.16	0.68	0.14	0.06	0.24	0.82	0.89	0.36	0.003	5538	5538	1974	3714	0.36	0.0029	5416	43	3545
V53221212	0.9	45	4	600	8	10	0.6	2.5	2.17	0.41	0.16	0.68	0.14	0.06	0.23	0.82	0.89	0.37	0.003	5405	5405	1929	3628	0.37	0.0029	5282	42	3457
V13221221	0.1	45	4	600	8	10	1	1.5	2.37	0.39	0.14	0.62	0.19	0.07	0.20	0.83	0.89	0.44	0.003	4715	4715	179	4557	0.44	0.0033	4429	34	4261
V13221222	0.1	45	4	600	8	10	1	2.5	2.42	0.39	0.14	0.62	0.19	0.07	0.20	0.83	0.89	0.44	0.003	4607	4607	175	4454	0.44	0.0033	4318	33	4154
V23221221	0.3	45	4	600	8	10	1	1.5	2.21	0.38	0.14	0.63	0.18	0.06	0.22	0.83	0.89	0.41	0.003	5146	5146	595	4602	0.41	0.0030	4908	37	4335
V23221222	0.3	45	4	600	8	10	1	2.5	2.25	0.38	0.14	0.63	0.18	0.06	0.22	0.83	0.89	0.42	0.003	5022	5022	580	4493	0.42	0.0030	4779	36	4221
V33221221	0.5	45	4	600	8	10	1	1.5	2.04	0.36	0.14	0.64	0.17	0.06	0.25	0.84	0.89	0.38	0.003	5724	5724	1114	4687	0.38	0.0028	5535	43	4458
V33221222	0.5	45	4	600	8	10	1	2.5	2.08	0.37	0.14	0.64	0.17	0.06	0.24	0.84	0.89	0.39	0.003	5589	5589	1087	4580	0.39	0.0028	5396	41	4346
V43221221	0.7	45	4	600	8	10	1	1.5	1.85	0.34	0.13	0.66	0.16	0.06	0.27	0.85	0.89	0.33	0.002	6288	6288	1725	4668	0.33	0.0025	6143	48	4476
V43221222	0.7	45	4	600	8	10	1	2.5	1.88	0.35	0.13	0.66	0.16	0.06	0.27	0.84	0.89	0.34	0.003	6190	6190	1698	4597	0.34	0.0025	6043	47	4403
V53221221	0.9	45	4	600	8	10	1	1.5	1.64	0.31	0.12	0.68	0.14	0.06	0.30	0.86	0.89	0.27	0.002	6990	6990	2471	4653	0.27	0.0022	6886	54	4507
V53221222	0.9	45	4	600	8	10	1	2.5	1.67	0.31	0.13	0.68	0.14	0.06	0.29	0.86	0.89	0.28	0.002	6891	6891	2437	4589	0.28	0.0022	6786	53	4441
V13222111	0.1	45	4	600	10	8	0.6	1.5	1.87	0.31	0.11	0.62	0.19	0.07	0.27	0.86	0.89	0.36	0.003	6091	6091	235	5877	0.36	0.0027	5857	44	5635
V13222112	0.1	45	4	600	10	8	0.6	2.5	1.93	0.31	0.11	0.62	0.19	0.07	0.26	0.86	0.89	0.37	0.003	5944	5944	229	5737	0.37	0.0028	5706	43	5490
V23222111	0.3	45	4	600	10	8	0.6	1.5	1.75	0.30	0.11	0.63	0.18	0.06	0.28	0.86	0.89	0.33	0.002	6458	6458	752	5752	0.33	0.0024	6257	48	5527
V23222112	0.3	45	4	600	10	8	0.6	2.5	1.80	0.31	0.11	0.63	0.18	0.06	0.28	0.86	0.89	0.34	0.002	6311	6311	735	5623	0.34	0.0025	6107	47	5394
V33222111	0.5	45	4	600	10	8	0.6	1.5	1.61	0.29	0.11	0.64	0.17	0.06	0.30	0.87	0.89	0.29	0.002	6920	6920	1350	5641	0.29	0.0021	6755	52	5440
V33222112	0.5	45	4	600	10	8	0.6	2.5	1.66	0.30	0.11	0.64	0.17	0.06	0.30	0.86	0.89	0.30	0.002	6761	6761	1319	5514	0.30	0.0022	6593	51	5310
V43222111	0.7	45	4	600	10	8	0.6	1.5	1.46	0.27	0.10	0.66	0.16	0.06	0.33	0.87	0.89	0.25	0.002	7517	7517	2059	5553	0.25	0.0018	7388	57	5384
V43222112	0.7	45	4	600	10	8	0.6	2.5	1.50	0.28	0.11	0.66	0.16	0.06	0.32	0.87	0.89	0.26	0.002	7345	7345	2012	5430	0.26	0.0019	7215	56	5258
V53222111	0.9	45	4	600	10	8	0.6	1.5	1.29	0.24	0.10	0.68	0.14	0.06	0.36	0.88	0.89	0.20	0.002	8309	8309	2923	5507	0.20	0.0016	8218	65	5379
V53222112	0.9	45	4	600	10	8	0.6	2.5	1.33	0.25	0.10	0.68	0.14	0.06	0.35	0.88	0.89	0.21	0.002	8135	8135	2864	5394	0.21	0.0017	8042	63	5264
V13222121	0.1	45	4	600	10	8	1	1.5	1.40	0.23	0.08	0.62	0.19	0.07	0.34	0.88	0.89	0.25	0.002	7522	7522	293	7251	0.25	0.0019	7325	56	7047
V13222122	0.1	45	4	600	10	8	1	2.5	1.45	0.24	0.08	0.62	0.19	0.07	0.33	0.88	0.89	0.26	0.002	7357	7357	286	7093	0.26	0.0020	7156	54	6885
V23222121	0.3	45	4	600	10	8	1	1.5	1.31	0.22	0.08	0.63	0.18	0.06	0.35	0.88	0.89	0.23	0.002	7953	7953	931	7065	0.23	0.0017	7784	59	6875

Name	af	nf	hf	mf	Ly	Lx	tw	Lcb	T1 [s]	T2 [s]	T3 [s]	M1 [-]	M2 [-]	M3 [-]	Sa	Sa2	Sa3	Disp [m]	ISDR [-]	Total Moment [MN-m]	Total Shear [MN]	Outrigger Moment [MN-m]	Wall Moment [MN-m]	Mode 1 Disp [m]	Mode 1 ISDR [-]	Mode 1 Moment [MN-m]	Mode 1 Shear [MN]	Mode 1 wall Moment [MN-m]
V23222122	0.3	45	4	600	10	8	1	2.5	1.35	0.23	0.08	0.63	0.18	0.06	0.35	0.88	0.89	0.24	0.002	7778	7778	910	6912	0.24	0.0017	7606	58	6718
V33222121	0.5	45	4	600	10	8	1	1.5	1.21	0.21	0.08	0.64	0.17	0.06	0.38	0.88	0.89	0.20	0.001	8476	8476	1657	6884	0.20	0.0015	8337	64	6714
V33222122	0.5	45	4	600	10	8	1	2.5	1.25	0.22	0.08	0.64	0.17	0.06	0.37	0.88	0.89	0.21	0.002	8294	8294	1621	6738	0.21	0.0015	8152	63	6565
V43222121	0.7	45	4	600	10	8	1	1.5	1.09	0.20	0.08	0.66	0.16	0.06	0.40	0.88	0.89	0.17	0.001	9129	9129	2497	6717	0.17	0.0013	9021	70	6573
V43222122	0.7	45	4	600	10	8	1	2.5	1.13	0.21	0.08	0.66	0.16	0.06	0.39	0.88	0.89	0.18	0.001	8942	8942	2447	6582	0.18	0.0013	8832	69	6436
V53222121	0.9	45	4	600	10	8	1	1.5	0.97	0.18	0.07	0.68	0.14	0.06	0.44	0.88	0.89	0.14	0.001	10098	10098	3537	6667	0.14	0.0011	10022	79	6559
V53222122	0.9	45	4	600	10	8	1	2.5	1.00	0.19	0.08	0.68	0.14	0.06	0.42	0.88	0.89	0.14	0.001	9809	9809	3438	6479	0.14	0.0012	9731	77	6369
V13222211	0.1	45	4	600	10	10	0.6	1.5	4.26	0.69	0.25	0.62	0.19	0.07	0.10	0.58	0.88	0.68	0.005	2426	2426	88	2355	0.68	0.0051	2130	16	2050
V13222212	0.1	45	4	600	10	10	0.6	2.5	4.42	0.72	0.26	0.62	0.19	0.07	0.09	0.56	0.88	0.70	0.005	2329	2329	85	2261	0.70	0.0052	2038	15	1961
V23222211	0.3	45	4	600	10	10	0.6	1.5	3.97	0.68	0.25	0.63	0.18	0.06	0.11	0.59	0.88	0.64	0.005	2599	2599	292	2354	0.63	0.0046	2341	18	2068
V23222212	0.3	45	4	600	10	10	0.6	2.5	4.12	0.70	0.26	0.63	0.18	0.06	0.10	0.58	0.88	0.65	0.005	2493	2493	279	2260	0.65	0.0047	2238	17	1977
V33222211	0.5	45	4	600	10	10	0.6	1.5	3.66	0.65	0.24	0.64	0.17	0.06	0.12	0.61	0.88	0.58	0.004	2834	2834	544	2368	0.58	0.0042	2616	20	2107
V33222212	0.5	45	4	600	10	10	0.6	2.5	3.80	0.68	0.25	0.64	0.17	0.06	0.11	0.59	0.88	0.60	0.004	2718	2718	521	2273	0.60	0.0043	2501	19	2014
V43222211	0.7	45	4	600	10	10	0.6	1.5	3.32	0.61	0.24	0.66	0.16	0.06	0.13	0.64	0.88	0.53	0.004	3174	3174	875	2412	0.53	0.0039	2996	23	2183
V43222212	0.7	45	4	600	10	10	0.6	2.5	3.44	0.64	0.25	0.66	0.16	0.06	0.13	0.62	0.88	0.54	0.004	3037	3037	837	2310	0.54	0.0040	2861	22	2085
V53222211	0.9	45	4	600	10	10	0.6	1.5	2.94	0.55	0.22	0.68	0.14	0.06	0.15	0.70	0.88	0.46	0.004	3688	3688	1336	2511	0.46	0.0036	3548	28	2322
V53222212	0.9	45	4	600	10	10	0.6	2.5	3.06	0.57	0.23	0.68	0.14	0.06	0.15	0.68	0.88	0.47	0.004	3525	3525	1279	2404	0.47	0.0037	3386	27	2216
V13222221	0.1	45	4	600	10	10	1	1.5	3.33	0.54	0.19	0.62	0.19	0.07	0.13	0.71	0.88	0.56	0.004	3198	3198	118	3099	0.56	0.0042	2880	22	2771
V13222222	0.1	45	4	600	10	10	1	2.5	3.46	0.56	0.20	0.62	0.19	0.07	0.13	0.69	0.88	0.58	0.004	3059	3059	113	2966	0.58	0.0043	2744	21	2640
V23222221	0.3	45	4	600	10	10	1	1.5	3.10	0.53	0.19	0.63	0.18	0.06	0.14	0.72	0.88	0.52	0.004	3448	3448	392	3109	0.52	0.0038	3174	24	2803
V23222222	0.3	45	4	600	10	10	1	2.5	3.22	0.55	0.20	0.63	0.18	0.06	0.14	0.70	0.88	0.54	0.004	3296	3296	374	2974	0.54	0.0039	3022	23	2670
V33222221	0.5	45	4	600	10	10	1	1.5	2.86	0.51	0.19	0.64	0.17	0.06	0.16	0.74	0.88	0.49	0.004	3789	3789	732	3142	0.48	0.0035	3561	27	2868
V33222222	0.5	45	4	600	10	10	1	2.5	2.97	0.53	0.20	0.64	0.17	0.06	0.15	0.72	0.88	0.50	0.004	3617	3617	698	3004	0.50	0.0036	3389	26	2729
V43222221	0.7	45	4	600	10	10	1	1.5	2.59	0.48	0.18	0.66	0.16	0.06	0.18	0.76	0.88	0.44	0.003	4273	4273	1176	3215	0.44	0.0032	4095	32	2984
V43222222	0.7	45	4	600	10	10	1	2.5	2.69	0.50	0.19	0.66	0.16	0.06	0.17	0.75	0.88	0.45	0.003	4074	4074	1122	3072	0.45	0.0033	3895	30	2838
V53222221	0.9	45	4	600	10	10	1	1.5	2.30	0.43	0.17	0.68	0.14	0.06	0.21	0.80	0.89	0.38	0.003	5007	5007	1792	3370	0.38	0.0030	4879	38	3193
V53222222	0.9	45	4	600	10	10	1	2.5	2.39	0.45	0.18	0.68	0.14	0.06	0.20	0.78	0.88	0.39	0.003	4762	4762	1708	3212	0.39	0.0031	4631	36	3031
M11111111	0.1	15	3	400	8	8	0.6	1.5	0.85	0.14	0.05	0.64	0.19	0.07	0.18	0.71	0.71	0.05	0.001	235	235	9	228	0.05	0.0014	220	7	214
M11111112	0.1	15	3	400	8	8	0.6	2.5	0.93	0.15	0.05	0.64	0.19	0.07	0.16	0.69	0.71	0.05	0.002	216	216	8	209	0.05	0.0016	200	6	195
M21111111	0.3	15	3	400	8	8	0.6	1.5	0.79	0.13	0.05	0.65	0.18	0.07	0.19	0.71	0.71	0.04	0.001	251	251	30	227	0.04	0.0013	240	7	214
M21111112	0.3	15	3	400	8	8	0.6	2.5	0.86	0.15	0.05	0.65	0.18	0.07	0.17	0.69	0.71	0.05	0.001	230	230	27	208	0.05	0.0014	218	7	194
M31111111	0.5	15	3	400	8	8	0.6	1.5	0.73	0.13	0.05	0.66	0.17	0.06	0.21	0.71	0.71	0.04	0.001	275	275	55	227	0.04	0.0012	266	8	216
M31111112	0.5	15	3	400	8	8	0.6	2.5	0.79	0.14	0.05	0.66	0.17	0.06	0.19	0.70	0.71	0.04	0.001	251	251	50	208	0.04	0.0012	241	7	196
M41111111	0.7	15	3	400	8	8	0.6	1.5	0.66	0.12	0.05	0.68	0.16	0.06	0.23	0.71	0.71	0.04	0.001	307	307	87	229	0.04	0.0010	300	9	220
M41111112	0.7	15	3	400	8	8	0.6	2.5	0.72	0.13	0.05	0.68	0.16	0.06	0.21	0.71	0.71	0.04	0.001	281	281	80	210	0.04	0.0011	274	8	200
M51111111	0.9	15	3	400	8	8	0.6	1.5	0.58	0.11	0.04	0.70	0.14	0.06	0.27	0.71	0.71	0.03	0.001	358	358	130	238	0.03	0.0010	354	11	231
M51111112	0.9	15	3	400	8	8	0.6	2.5	0.63	0.12	0.05	0.70	0.14	0.06	0.24	0.71	0.71	0.03	0.001	322	322	118	215	0.03	0.0010	317	10	208
M11111121	0.1	15	3	400	8	8	1	1.5	0.73	0.12	0.04	0.64	0.19	0.07	0.21	0.71	0.71	0.04	0.001	271	271	11	263	0.04	0.0012	257	8	250
M11111122	0.1	15	3	400	8	8	1	2.5	0.81	0.13	0.05	0.64	0.19	0.07	0.19	0.71	0.71	0.05	0.001	247	247	10	240	0.05	0.0014	232	7	226
M21111121	0.3	15	3	400	8	8	1	1.5	0.68	0.12	0.04	0.65	0.18	0.07	0.22	0.71	0.71	0.04	0.001	292	292	35	262	0.04	0.0011	281	9	251
M21111122	0.3	15	3	400	8	8	1	2.5	0.75	0.13	0.05	0.65	0.18	0.07	0.20	0.71	0.71	0.04	0.001	263	263	31	237	0.04	0.0012	252	8	225
M31111121	0.5	15	3	400	8	8	1	1.5	0.63	0.11	0.04	0.66	0.17	0.06	0.24	0.71	0.71	0.03	0.001	318	318	64	261	0.03	0.0010	310	9	251
M31111122	0.5	15	3	400	8	8	1	2.5	0.69	0.12	0.05	0.66	0.17	0.06	0.22	0.71	0.71	0.04	0.001	290	290	58	239	0.04	0.0011	281	9	228
M41111121	0.7	15	3	400	8	8	1	1.5	0.57	0.11	0.04	0.68	0.16	0.06	0.27	0.71	0.71	0.03	0.001	361	361	102	267	0.03	0.0009	355	11	260
M41111122	0.7	15	3	400	8	8	1	2.5	0.63	0.12	0.04	0.68	0.16	0.06	0.24	0.71	0.71	0.03	0.001	323	323	91	240	0.03	0.0010	317	10	232
M51111121	0.9	15	3	400	8	8	1	1.5	0.50	0.09	0.04	0.70	0.14	0.06	0.31	0.71	0.71	0.03	0.001	412	412	149	273	0.03	0.0008	408	13	267
M51111122	0.9	15	3	400	8	8	1	2.5	0.55	0.10	0.04	0.70	0.14	0.06	0.28	0.71	0.71	0.03	0.001	377	377	137	250	0.03	0.0009	373	12	244
M11111211	0.1	15	3	400	8	10	0.6	1.5	2.10	0.34	0.12	0.64	0.19	0.07	0.06	0.42	0.71	0.10	0.003	94	94	3	91	0.10	0.0031	79	2	77
M11111212	0.1	15	3	400	8	10	0.6	2.5	2.32	0.38	0.14	0.64	0.19	0.07	0.05	0.39	0.71	0.11	0.003	83	83	3	80	0.11	0.0033	68	2	66
M21111211	0.3	15	3	400	8	10	0.6	1.5	1.95	0.33	0.12	0.65	0.18	0.07	0.07	0.43	0.71	0.10	0.003	100	100	11	92	0.10	0.0028	88	3	78
M21111212	0.3	15	3	400	8	10	0.6	2.5	2.15	0.37	0.13	0.65	0.18	0.07	0.06	0.40	0.71	0.10	0.003	89	89	10	81	0.10	0.0030	76	2	68
M31111211	0.5	15	3	400	8	10	0.6	1.5	1.79	0.32	0.12	0.66	0.17	0.06	0.08	0.44	0.71	0.09	0.003	108	108	21	91	0.09	0.0026	98	3	79
M31111212	0.5	15	3	400	8	10	0.6	2.5	1.98	0.35	0.13	0.66	0.17	0.06	0.07	0.41	0.71	0.10	0.003	98	98	19	83	0.10	0.0028	87	3	71
M41111211	0.7	15	3	400	8	10	0.6	1.5	1.62	0.30	0.12	0.68	0.16	0.06	0.09	0.46	0.71	0.08	0.002	119	119	34	92	0.08	0.0023	111	3	81
M41111212	0.7	15	3	400	8	10	0.6	2.5	1.79	0.33	0.13	0.68	0.16	0.06	0.08	0.43	0.71	0.09	0.003	108	108	31	83	0.09	0.0025	99	3	73
M51111211	0.9	15	3	400	8	10	0.6	1.5	1.43	0.27	0.11	0.70	0.14	0.06	0.10	0.49	0.71	0.07	0.002	136	136	52	94	0.07	0.0021	130	4	85
M51111212	0.9	15	3	400	8	10	0.6	2.5	1.58	0.30	0.12	0.70	0.14	0.06	0.09	0.46	0.71	0.07	0.002	123	123	47	85	0.07	0.0023	117	4	76
M11111221	0.1	15	3	400	8	10	1	1.5	2.02	0.33	0.12	0.64	0.19	0.07	0.07	0.43	0.71	0.10	0.003	99	99	4	95	0.10	0.0031	83	3	81
M11111222	0.1	15	3	400	8	10	1	2.5	2.24	0.36	0.13	0.64	0.19	0.07	0.06	0.40	0.71	0.11	0.003	87	87	3	84	0.11	0.0032	71	2	69
M21111221	0.3	15	3	400	8	10	1	1.5	1.88	0.32	0.12	0.65	0.18	0.07	0.07	0.44	0.71	0.09	0.003	104	104	12	95	0.09	0.0028	91	3	82
M21111222	0.3	15	3	400	8	10	1	2.5	2.09	0.36	0.13	0.65	0.18	0.07	0.06	0.41	0.71	0.10	0.003	93	93	11	85	0.10	0.0030	80	2	72
M31111221	0.5	15	3	400	8	10	1	1.5	1.73	0.31	0.12	0.66	0.17	0.06	0.08	0.45	0.71	0.09	0.003	112	112	22	95	0.09	0.0025	102	3	82
M31111222	0.5	15	3	400	8	10	1	2.5	1.92	0.34	0.13	0.66	0.17	0.06	0.07	0.42	0.71	0.09	0.003	101	101	20	86	0.09	0.0027	91	3	74
M41111221	0.7	15	3	400	8	10	1	1.5	1.57	0.29	0.11	0.68	0.16	0.06	0.09	0.47	0.71	0.08	0.002	124	124	35	95	0.08	0.0023	115	4	84
M41111222	0.7	15	3	400	8	10	1	2.5	1.73	0.32	0.12	0.68	0.16	0.06	0.08	0.44	0.71	0.08	0.003	111	111	32	86	0.08	0.0025	103	3	75
M51111221	0.9	15	3	400	8	10	1	1.5	1.38	0.26	0.10	0.70	0.14	0.06	0.10	0.50	0.71	0.07	0.002	141	141	53	97	0.07	0.0021	135	4	89
M51111222	0.9	15	3	400	8	10	1	2.5	1.53	0.29	0.12	0.70	0.14	0.06	0.09	0.47	0.71	0.07	0.002	127	127	48	88	0.07	0.0023	121	4	79
M11112111	0.1	15	3	400	10	8	0.6	1.5	1.23	0.20	0.07	0.64	0.19	0.07	0.12	0.60	0.71	0.07	0.002	162	162	6	157	0.07	0.0020	146	4	142
M11112112	0.1	15	3	400	10	8	0.6	2.5	1.52	0.25	0.09	0.64	0.19	0.07	0.09	0.52	0.71	0.08	0.002	131	131	5	127	0.08	0.0024	115	3	112
M21112111	0.3	15	3	400	10	8	0.6	1.5	1.15	0.20	0.07	0.65	0.18	0.07	0.13	0.61	0.71	0.06	0.002	172	172	20	157	0.06	0.0018	159	5	142
M21112112	0.3	15	3	400	10	8	0.6	2.5	1.41	0.24	0.09	0.65	0.18	0.07	0.10	0.53	0.71	0.07	0.002	139	139	16	126	0.07	0.0021	126	4	112
M31112111	0.5	15	3	400	10	8	0.6	1.5	1.05	0.19	0.07	0.66	0.17	0.06	0.14	0.62	0.71	0.06	0.002	189	189	38	157	0.06	0.0016	178	5	145

Name	af	nf	hf	mf	Ly	Lx	tw	Lcb	T1 [s]	T2 [s]	T3 [s]	M1 [-]	M2 [-]	M3 [-]	Sa	Sa2	Sa3	Disp [m]	ISDR [-]	Total Moment [MN-m]	Total Shear [MN]	Outrigger Moment [MN-m]	Wall Moment [MN-m]	Mode 1 Disp [m]	Mode 1 ISDR [-]	Mode 1 Moment [MN-m]	Mode 1 Shear [MN]	Mode 1 wall Moment [MN-m]
M31112112	0.5	15	3	400	10	8	0.6	2.5	1.30	0.23	0.09	0.66	0.17	0.06	0.11	0.55	0.71	0.07	0.002	151	151	30	126	0.07	0.0019	140	4	114
M41112111	0.7	15	3	400	10	8	0.6	1.5	0.95	0.18	0.07	0.68	0.16	0.06	0.16	0.64	0.71	0.05	0.001	211	211	60	159	0.05	0.0015	203	6	148
M41112112	0.7	15	3	400	10	8	0.6	2.5	1.17	0.22	0.08	0.68	0.16	0.06	0.12	0.57	0.71	0.06	0.002	168	168	48	128	0.06	0.0018	160	5	117
M51112111	0.9	15	3	400	10	8	0.6	1.5	0.84	0.16	0.06	0.70	0.14	0.06	0.18	0.68	0.71	0.04	0.001	242	242	90	163	0.04	0.0013	236	7	155
M51112112	0.9	15	3	400	10	8	0.6	2.5	1.04	0.19	0.08	0.70	0.14	0.06	0.14	0.61	0.71	0.05	0.002	195	195	73	132	0.05	0.0016	188	6	123
M11112121	0.1	15	3	400	10	8	1	1.5	1.12	0.18	0.07	0.64	0.19	0.07	0.13	0.63	0.71	0.06	0.002	179	179	7	174	0.06	0.0018	163	5	158
M11112122	0.1	15	3	400	10	8	1	2.5	1.46	0.24	0.08	0.64	0.19	0.07	0.10	0.54	0.71	0.08	0.002	137	137	5	133	0.08	0.0023	121	4	117
M21112121	0.3	15	3	400	10	8	1	1.5	1.04	0.18	0.06	0.65	0.18	0.07	0.14	0.64	0.71	0.06	0.002	192	192	23	174	0.06	0.0016	179	5	159
M21112122	0.3	15	3	400	10	8	1	2.5	1.35	0.23	0.08	0.65	0.18	0.07	0.10	0.55	0.71	0.07	0.002	145	145	17	132	0.07	0.0021	132	4	118
M31112121	0.5	15	3	400	10	8	1	1.5	0.96	0.17	0.06	0.66	0.17	0.06	0.16	0.65	0.71	0.05	0.002	209	209	42	174	0.05	0.0015	199	6	161
M31112122	0.5	15	3	400	10	8	1	2.5	1.24	0.22	0.08	0.66	0.17	0.06	0.12	0.56	0.71	0.06	0.002	158	158	31	132	0.06	0.0019	147	4	119
M41112121	0.7	15	3	400	10	8	1	1.5	0.86	0.16	0.06	0.68	0.16	0.06	0.17	0.67	0.71	0.05	0.001	232	232	66	175	0.05	0.0013	224	7	164
M41112122	0.7	15	3	400	10	8	1	2.5	1.13	0.21	0.08	0.68	0.16	0.06	0.13	0.59	0.71	0.06	0.002	176	176	50	134	0.06	0.0017	168	5	123
M51112121	0.9	15	3	400	10	8	1	1.5	0.76	0.14	0.06	0.70	0.14	0.06	0.20	0.70	0.71	0.04	0.001	266	266	98	179	0.04	0.0012	260	8	170
M51112122	0.9	15	3	400	10	8	1	2.5	0.99	0.19	0.07	0.70	0.14	0.06	0.15	0.63	0.71	0.05	0.002	204	204	76	138	0.05	0.0016	197	6	129
M11112211	0.1	15	3	400	10	10	0.6	1.5	3.24	0.53	0.19	0.64	0.19	0.07	0.03	0.29	0.62	0.13	0.004	56	56	2	54	0.13	0.0039	41	1	40
M11112212	0.1	15	3	400	10	10	0.6	2.5	4.29	0.70	0.25	0.64	0.19	0.07	0.02	0.22	0.51	0.15	0.005	40	40	1	38	0.15	0.0046	28	1	27
M21112211	0.3	15	3	400	10	10	0.6	1.5	3.01	0.51	0.19	0.65	0.18	0.07	0.04	0.30	0.62	0.12	0.004	58	58	6	54	0.12	0.0036	46	1	41
M21112212	0.3	15	3	400	10	10	0.6	2.5	3.99	0.68	0.25	0.65	0.18	0.07	0.02	0.22	0.52	0.14	0.005	41	41	4	38	0.14	0.0042	31	1	28
M31112211	0.5	15	3	400	10	10	0.6	1.5	2.77	0.49	0.18	0.66	0.17	0.06	0.04	0.31	0.63	0.12	0.003	63	63	12	55	0.11	0.0033	53	2	43
M31112212	0.5	15	3	400	10	10	0.6	2.5	3.66	0.65	0.24	0.66	0.17	0.06	0.03	0.23	0.53	0.14	0.004	44	44	8	39	0.13	0.0039	35	1	29
M41112211	0.7	15	3	400	10	10	0.6	1.5	2.50	0.46	0.18	0.68	0.16	0.06	0.05	0.33	0.64	0.11	0.003	70	70	20	56	0.11	0.0031	62	2	46
M41112212	0.7	15	3	400	10	10	0.6	2.5	3.31	0.61	0.24	0.68	0.16	0.06	0.03	0.25	0.54	0.12	0.004	49	49	14	39	0.12	0.0036	41	1	30
M51112211	0.9	15	3	400	10	10	0.6	1.5	2.21	0.41	0.17	0.70	0.14	0.06	0.06	0.36	0.66	0.10	0.003	83	83	32	59	0.10	0.0030	77	2	51
M51112212	0.9	15	3	400	10	10	0.6	2.5	2.93	0.55	0.22	0.70	0.14	0.06	0.04	0.28	0.57	0.11	0.004	57	57	23	41	0.11	0.0035	51	2	33
M11112221	0.1	15	3	400	10	10	1	1.5	3.17	0.52	0.19	0.64	0.19	0.07	0.03	0.30	0.63	0.13	0.004	57	57	2	55	0.13	0.0038	42	1	41
M11112222	0.1	15	3	400	10	10	1	2.5	4.29	0.70	0.25	0.64	0.19	0.07	0.02	0.22	0.51	0.15	0.005	40	40	1	38	0.15	0.0046	28	1	27
M21112221	0.3	15	3	400	10	10	1	1.5	2.95	0.50	0.18	0.65	0.18	0.07	0.04	0.31	0.63	0.12	0.004	60	60	6	55	0.12	0.0035	48	1	42
M21112222	0.3	15	3	400	10	10	1	2.5	3.99	0.68	0.25	0.65	0.18	0.07	0.02	0.22	0.52	0.14	0.005	41	41	4	38	0.14	0.0042	31	1	28
M31112221	0.5	15	3	400	10	10	1	1.5	2.71	0.48	0.18	0.66	0.17	0.06	0.04	0.32	0.64	0.11	0.003	65	65	12	56	0.11	0.0033	55	2	44
M31112222	0.5	15	3	400	10	10	1	2.5	3.67	0.65	0.24	0.66	0.17	0.06	0.03	0.23	0.52	0.14	0.004	44	44	8	39	0.13	0.0039	35	1	29
M41112221	0.7	15	3	400	10	10	1	1.5	2.45	0.45	0.18	0.68	0.16	0.06	0.05	0.34	0.64	0.11	0.003	72	72	21	57	0.11	0.0031	64	2	47
M41112222	0.7	15	3	400	10	10	1	2.5	3.32	0.61	0.24	0.68	0.16	0.06	0.03	0.25	0.54	0.12	0.004	49	49	14	39	0.12	0.0036	41	1	30
M51112221	0.9	15	3	400	10	10	1	1.5	2.17	0.41	0.16	0.70	0.14	0.06	0.06	0.37	0.67	0.10	0.003	86	86	33	60	0.09	0.0030	80	2	52
M51112222	0.9	15	3	400	10	10	1	2.5	2.93	0.55	0.22	0.70	0.14	0.06	0.04	0.28	0.57	0.11	0.004	57	57	23	41	0.11	0.0035	51	2	33
M11121111	0.1	15	3	600	8	8	0.6	1.5	1.04	0.17	0.06	0.64	0.19	0.07	0.14	0.65	0.71	0.06	0.002	289	289	11	281	0.06	0.0017	265	8	258
M11121112	0.1	15	3	600	8	8	0.6	2.5	1.14	0.19	0.07	0.64	0.19	0.07	0.13	0.63	0.71	0.06	0.002	263	263	10	255	0.06	0.0018	238	7	232
M21121111	0.3	15	3	600	8	8	0.6	1.5	0.97	0.17	0.06	0.65	0.18	0.07	0.15	0.66	0.71	0.05	0.002	309	309	37	279	0.05	0.0015	290	9	258
M21121112	0.3	15	3	600	8	8	0.6	2.5	1.06	0.18	0.07	0.65	0.18	0.07	0.14	0.64	0.71	0.06	0.002	282	282	33	256	0.06	0.0017	263	8	234
M31121111	0.5	15	3	600	8	8	0.6	1.5	0.89	0.16	0.06	0.66	0.17	0.06	0.17	0.67	0.71	0.05	0.001	335	335	67	278	0.05	0.0014	320	10	259
M31121112	0.5	15	3	600	8	8	0.6	2.5	0.97	0.17	0.06	0.66	0.17	0.06	0.15	0.65	0.71	0.05	0.002	308	308	62	256	0.05	0.0015	292	9	237
M41121111	0.7	15	3	600	8	8	0.6	1.5	0.81	0.15	0.06	0.68	0.16	0.06	0.19	0.69	0.71	0.04	0.001	375	375	106	281	0.04	0.0013	363	11	266
M41121112	0.7	15	3	600	8	8	0.6	2.5	0.88	0.16	0.06	0.68	0.16	0.06	0.17	0.67	0.71	0.05	0.001	341	341	97	257	0.05	0.0014	329	10	241
M51121111	0.9	15	3	600	8	8	0.6	1.5	0.71	0.13	0.05	0.70	0.14	0.06	0.21	0.71	0.71	0.04	0.001	433	433	159	290	0.04	0.0012	425	13	278
M51121112	0.9	15	3	600	8	8	0.6	2.5	0.78	0.15	0.06	0.70	0.14	0.06	0.19	0.70	0.71	0.04	0.001	393	393	145	264	0.04	0.0012	384	12	251
M11121121	0.1	15	3	600	8	8	1	1.5	0.90	0.15	0.05	0.64	0.19	0.07	0.17	0.69	0.71	0.05	0.002	334	334	13	324	0.05	0.0015	310	9	302
M11121122	0.1	15	3	600	8	8	1	2.5	0.99	0.16	0.06	0.64	0.19	0.07	0.15	0.67	0.71	0.05	0.002	304	304	12	295	0.05	0.0016	280	8	272
M21121121	0.3	15	3	600	8	8	1	1.5	0.84	0.14	0.05	0.65	0.18	0.07	0.18	0.70	0.71	0.05	0.001	358	358	43	323	0.05	0.0013	339	10	303
M21121122	0.3	15	3	600	8	8	1	2.5	0.92	0.16	0.06	0.65	0.18	0.07	0.16	0.68	0.71	0.05	0.002	324	324	38	293	0.05	0.0015	306	9	272
M31121121	0.5	15	3	600	8	8	1	1.5	0.77	0.14	0.05	0.66	0.17	0.06	0.20	0.71	0.71	0.04	0.001	389	389	78	321	0.04	0.0012	374	11	303
M31121122	0.5	15	3	600	8	8	1	2.5	0.85	0.15	0.06	0.66	0.17	0.06	0.18	0.69	0.71	0.05	0.001	354	354	71	293	0.05	0.0013	339	10	275
M41121121	0.7	15	3	600	8	8	1	1.5	0.70	0.13	0.05	0.68	0.16	0.06	0.22	0.71	0.71	0.04	0.001	437	437	124	326	0.04	0.0011	426	13	312
M41121122	0.7	15	3	600	8	8	1	2.5	0.77	0.14	0.05	0.68	0.16	0.06	0.20	0.70	0.71	0.04	0.001	393	393	111	294	0.04	0.0012	381	12	279
M51121121	0.9	15	3	600	8	8	1	1.5	0.61	0.11	0.05	0.70	0.14	0.06	0.25	0.71	0.71	0.03	0.001	504	504	184	335	0.03	0.0010	497	16	325
M51121122	0.9	15	3	600	8	8	1	2.5	0.68	0.13	0.05	0.70	0.14	0.06	0.23	0.71	0.71	0.03	0.001	455	455	167	304	0.03	0.0011	448	14	293
M11121211	0.1	15	3	600	8	10	0.6	1.5	2.57	0.42	0.15	0.64	0.19	0.07	0.05	0.36	0.69	0.11	0.004	110	110	4	106	0.11	0.0034	87	3	84
M11121212	0.1	15	3	600	8	10	0.6	2.5	2.84	0.46	0.17	0.64	0.19	0.07	0.04	0.33	0.66	0.12	0.004	98	98	3	94	0.12	0.0036	75	2	73
M21121211	0.3	15	3	600	8	10	0.6	1.5	2.39	0.41	0.15	0.65	0.18	0.07	0.05	0.36	0.69	0.11	0.003	116	116	13	107	0.11	0.0032	98	3	87
M21121212	0.3	15	3	600	8	10	0.6	2.5	2.64	0.45	0.16	0.65	0.18	0.07	0.04	0.34	0.66	0.11	0.004	103	103	11	95	0.11	0.0033	84	3	75
M31121211	0.5	15	3	600	8	10	0.6	1.5	2.20	0.39	0.15	0.66	0.17	0.06	0.06	0.37	0.70	0.10	0.003	128	128	25	109	0.10	0.0030	113	3	91
M31121212	0.5	15	3	600	8	10	0.6	2.5	2.43	0.43	0.16	0.66	0.17	0.06	0.05	0.35	0.67	0.11	0.003	112	112	22	96	0.11	0.0031	97	3	78
M41121211	0.7	15	3	600	8	10	0.6	1.5	1.99	0.37	0.14	0.68	0.16	0.06	0.07	0.39	0.70	0.10	0.003	145	145	41	112	0.09	0.0028	133	4	97
M41121212	0.7	15	3	600	8	10	0.6	2.5	2.19	0.41	0.16	0.68	0.16	0.06	0.06	0.37	0.68	0.10	0.003	126	126	36	99	0.10	0.0029	115	4	84
M51121211	0.9	15	3	600	8	10	0.6	1.5	1.75	0.33	0.13	0.70	0.14	0.06	0.08	0.43	0.71	0.08	0.003	165	165	63	115	0.08	0.0026	156	5	102
M51121212	0.9	15	3	600	8	10	0.6	2.5	1.94	0.36	0.15	0.70	0.14	0.06	0.07	0.40	0.70	0.09	0.003	149	149	57	104	0.09	0.0028	140	4	91
M11121221	0.1	15	3	600	8	10	1	1.5	2.48	0.40	0.14	0.64	0.19	0.07	0.05	0.37	0.70	0.11	0.004	115	115	4	111	0.11	0.0034	91	3	89
M11121222	0.1	15	3	600	8	10	1	2.5	2.75	0.45	0.16	0.64	0.19	0.07	0.04	0.34	0.67	0.12	0.004	102	102	4	98	0.12	0.0035	78	2	76
M21121221	0.3	15	3	600	8	10	1	1.5	2.31	0.39	0.14	0.65	0.18	0.07	0.05	0.37	0.70	0.11	0.003	121	121	14	112	0.11	0.0031	103	3	92
M21121222	0.3	15	3	600	8	10	1	2.5	2.55	0.44	0.16	0.65	0.18	0.07	0.05	0.35	0.67	0.11	0.003	107	107	12	99	0.11	0.0033	88	3	79
M31121221	0.5	15	3	600	8	10	1	1.5	2.12	0.38	0.14	0.66	0.17	0.06	0.06	0.38	0.70	0.10	0.003	134	134	26	114	0.10	0.0029	119	4	96
M31121222	0.5	15	3	600	8	10	1	2.5	2.35	0.42	0.16	0.66	0.17	0.06	0.05	0.36	0.68	0.11	0.003	117	117	23	100	0.11	0.0031	102	3	82
M41121221	0.7	15	3	600	8	10	1	1.5	1.92	0.36	0.14	0.68	0.16	0.06	0.07	0.41	0.71	0.09	0.003	150	150	43	117	0.09	0.0027	138	4	101

Name	af	nf	hf	mf	Ly	Lx	tw	Lcb	T1 [s]	T2 [s]	T3 [s]	M1 [-]	M2 [-]	M3 [-]	Sa	Sa2	Sa3	Disp [m]	ISDR [-]	Total Moment [MN-m]	Total Shear [MN]	Outrigger Moment [MN-m]	Wall Moment [MN-m]	Mode 1 Disp [m]	Mode 1 ISDR [-]	Mode 1 Moment [MN-m]	Mode 1 Shear [MN]	Mode 1 wall Moment [MN-m]
M41121222	0.7	15	3	600	8	10	1	2.5	2.12	0.39	0.15	0.68	0.16	0.06	0.06	0.37	0.69	0.10	0.003	132	132	38	103	0.10	0.0029	120	4	88
M51121221	0.9	15	3	600	8	10	1	1.5	1.69	0.32	0.13	0.70	0.14	0.06	0.08	0.44	0.71	0.08	0.002	172	172	65	119	0.08	0.0025	162	5	106
M51121222	0.9	15	3	600	8	10	1	2.5	1.88	0.35	0.14	0.70	0.14	0.06	0.07	0.41	0.70	0.09	0.003	154	154	59	107	0.09	0.0027	145	5	95
M11122111	0.1	15	3	600	10	8	0.6	1.5	1.51	0.25	0.09	0.64	0.19	0.07	0.09	0.52	0.71	0.08	0.002	198	198	7	191	0.08	0.0024	174	5	169
M11122112	0.1	15	3	600	10	8	0.6	2.5	1.86	0.30	0.11	0.64	0.19	0.07	0.07	0.46	0.71	0.09	0.003	161	161	6	156	0.09	0.0029	138	4	134
M21122111	0.3	15	3	600	10	8	0.6	1.5	1.40	0.24	0.09	0.65	0.18	0.07	0.10	0.53	0.71	0.07	0.002	209	209	24	190	0.07	0.0021	190	6	169
M21122112	0.3	15	3	600	10	8	0.6	2.5	1.73	0.29	0.11	0.65	0.18	0.07	0.08	0.46	0.71	0.09	0.003	169	169	20	155	0.09	0.0026	151	5	134
M31122111	0.5	15	3	600	10	8	0.6	1.5	1.29	0.23	0.09	0.66	0.17	0.06	0.11	0.55	0.71	0.07	0.002	228	228	45	191	0.07	0.0019	212	6	172
M31122112	0.5	15	3	600	10	8	0.6	2.5	1.59	0.28	0.11	0.66	0.17	0.06	0.09	0.47	0.71	0.08	0.002	183	183	36	154	0.08	0.0023	168	5	136
M41122111	0.7	15	3	600	10	8	0.6	1.5	1.17	0.22	0.08	0.68	0.16	0.06	0.12	0.57	0.71	0.06	0.002	254	254	72	193	0.06	0.0017	241	7	177
M41122112	0.7	15	3	600	10	8	0.6	2.5	1.44	0.27	0.10	0.68	0.16	0.06	0.10	0.49	0.71	0.07	0.002	203	203	58	155	0.07	0.0021	191	6	139
M51122111	0.9	15	3	600	10	8	0.6	1.5	1.03	0.19	0.08	0.70	0.14	0.06	0.14	0.61	0.71	0.05	0.002	294	294	110	199	0.05	0.0016	284	9	186
M51122112	0.9	15	3	600	10	8	0.6	2.5	1.27	0.24	0.10	0.70	0.14	0.06	0.11	0.54	0.71	0.06	0.002	233	233	88	159	0.06	0.0019	224	7	146
M11122121	0.1	15	3	600	10	8	1	1.5	1.37	0.22	0.08	0.64	0.19	0.07	0.10	0.56	0.71	0.07	0.002	219	219	8	212	0.07	0.0022	194	6	189
M11122122	0.1	15	3	600	10	8	1	2.5	1.78	0.29	0.10	0.64	0.19	0.07	0.08	0.47	0.71	0.09	0.003	168	168	6	162	0.09	0.0027	144	4	140
M21122121	0.3	15	3	600	10	8	1	1.5	1.27	0.22	0.08	0.65	0.18	0.07	0.11	0.57	0.71	0.07	0.002	232	232	27	211	0.07	0.0020	212	6	189
M21122122	0.3	15	3	600	10	8	1	2.5	1.66	0.28	0.10	0.65	0.18	0.07	0.08	0.48	0.71	0.08	0.003	176	176	20	161	0.08	0.0025	158	5	141
M31122121	0.5	15	3	600	10	8	1	1.5	1.17	0.21	0.08	0.66	0.17	0.06	0.12	0.59	0.71	0.06	0.002	253	253	50	211	0.06	0.0018	237	7	192
M31122122	0.5	15	3	600	10	8	1	2.5	1.52	0.27	0.10	0.66	0.17	0.06	0.09	0.49	0.71	0.08	0.002	191	191	38	161	0.08	0.0022	175	5	142
M41122121	0.7	15	3	600	10	8	1	1.5	1.06	0.20	0.08	0.68	0.16	0.06	0.14	0.61	0.71	0.06	0.002	283	283	81	214	0.05	0.0016	270	8	198
M41122122	0.7	15	3	600	10	8	1	2.5	1.38	0.26	0.10	0.68	0.16	0.06	0.10	0.51	0.71	0.07	0.002	212	212	60	162	0.07	0.0020	200	6	146
M51122121	0.9	15	3	600	10	8	1	1.5	0.93	0.18	0.07	0.70	0.14	0.06	0.16	0.64	0.71	0.05	0.001	326	326	121	220	0.05	0.0015	317	10	207
M51122122	0.9	15	3	600	10	8	1	2.5	1.22	0.23	0.09	0.70	0.14	0.06	0.12	0.55	0.71	0.06	0.002	245	245	92	167	0.06	0.0019	235	7	154
M11122211	0.1	15	3	600	10	10	0.6	1.5	3.96	0.65	0.23	0.64	0.19	0.07	0.02	0.24	0.55	0.15	0.005	66	66	2	63	0.14	0.0044	46	1	45
M11122212	0.1	15	3	600	10	10	0.6	2.5	5.25	0.85	0.31	0.64	0.19	0.07	0.02	0.18	0.45	0.17	0.006	48	48	1	45	0.17	0.0051	31	1	30
M21122211	0.3	15	3	600	10	10	0.6	1.5	3.69	0.63	0.23	0.65	0.18	0.07	0.03	0.24	0.55	0.14	0.004	68	68	7	63	0.14	0.0040	52	2	46
M21122212	0.3	15	3	600	10	10	0.6	2.5	4.88	0.83	0.30	0.65	0.18	0.07	0.02	0.18	0.46	0.16	0.005	49	49	5	46	0.16	0.0048	35	1	31
M31122211	0.5	15	3	600	10	10	0.6	1.5	3.39	0.60	0.23	0.66	0.17	0.06	0.03	0.26	0.56	0.13	0.004	73	73	14	64	0.13	0.0037	59	2	48
M31122212	0.5	15	3	600	10	10	0.6	2.5	4.49	0.80	0.30	0.66	0.17	0.06	0.02	0.19	0.46	0.15	0.005	52	52	10	46	0.15	0.0044	40	1	32
M41122211	0.7	15	3	600	10	10	0.6	1.5	3.06	0.57	0.22	0.68	0.16	0.06	0.04	0.27	0.57	0.12	0.004	81	81	23	65	0.12	0.0035	69	2	51
M41122212	0.7	15	3	600	10	10	0.6	2.5	4.06	0.75	0.29	0.68	0.16	0.06	0.02	0.20	0.47	0.14	0.004	56	56	16	46	0.14	0.0041	47	1	34
M51122211	0.9	15	3	600	10	10	0.6	1.5	2.71	0.51	0.20	0.70	0.14	0.06	0.04	0.31	0.60	0.11	0.003	94	94	37	68	0.11	0.0033	85	3	56
M51122212	0.9	15	3	600	10	10	0.6	2.5	3.58	0.67	0.27	0.70	0.14	0.06	0.03	0.23	0.49	0.12	0.004	65	65	26	47	0.12	0.0039	57	2	37
M11122221	0.1	15	3	600	10	10	1	1.5	3.89	0.63	0.23	0.64	0.19	0.07	0.03	0.24	0.55	0.14	0.005	67	67	2	65	0.14	0.0043	48	1	46
M11122222	0.1	15	3	600	10	10	1	2.5	5.25	0.85	0.31	0.64	0.19	0.07	0.02	0.18	0.45	0.17	0.006	48	48	1	45	0.17	0.0051	31	1	30
M21122221	0.3	15	3	600	10	10	1	1.5	3.61	0.62	0.22	0.65	0.18	0.07	0.03	0.25	0.56	0.14	0.004	70	70	7	65	0.14	0.0039	53	2	47
M21122222	0.3	15	3	600	10	10	1	2.5	4.88	0.83	0.30	0.65	0.18	0.07	0.02	0.18	0.46	0.16	0.005	49	49	5	46	0.16	0.0048	35	1	31
M31122221	0.5	15	3	600	10	10	1	1.5	3.32	0.59	0.22	0.66	0.17	0.06	0.03	0.26	0.56	0.13	0.004	75	75	14	65	0.13	0.0037	61	2	49
M31122222	0.5	15	3	600	10	10	1	2.5	4.49	0.80	0.30	0.66	0.17	0.06	0.02	0.19	0.46	0.15	0.005	52	52	10	46	0.15	0.0044	40	1	32
M41122221	0.7	15	3	600	10	10	1	1.5	3.00	0.56	0.21	0.68	0.16	0.06	0.04	0.28	0.58	0.12	0.004	83	83	24	67	0.12	0.0034	71	2	52
M41122222	0.7	15	3	600	10	10	1	2.5	4.06	0.75	0.29	0.68	0.16	0.06	0.02	0.20	0.47	0.14	0.004	56	56	16	46	0.14	0.0041	46	1	34
M51122221	0.9	15	3	600	10	10	1	1.5	2.65	0.50	0.20	0.70	0.14	0.06	0.04	0.31	0.60	0.10	0.003	97	97	38	69	0.10	0.0033	88	3	57
M51122222	0.9	15	3	600	10	10	1	2.5	3.59	0.67	0.27	0.70	0.14	0.06	0.03	0.23	0.49	0.12	0.004	65	65	26	47	0.12	0.0039	57	2	37
M11211111	0.1	15	4	400	8	8	0.6	1.5	0.79	0.13	0.05	0.64	0.19	0.07	0.19	0.71	0.71	0.04	0.001	335	335	13	325	0.04	0.0010	316	7	307
M11211112	0.1	15	4	400	8	8	0.6	2.5	0.84	0.14	0.05	0.64	0.19	0.07	0.18	0.71	0.71	0.05	0.001	317	317	12	307	0.05	0.0011	296	7	288
M21211111	0.3	15	4	400	8	8	0.6	1.5	0.74	0.13	0.05	0.65	0.18	0.07	0.21	0.71	0.71	0.04	0.001	359	359	43	323	0.04	0.0009	344	8	307
M21211112	0.3	15	4	400	8	8	0.6	2.5	0.78	0.13	0.05	0.65	0.18	0.07	0.19	0.71	0.71	0.04	0.001	338	338	40	305	0.04	0.0009	322	7	287
M31211111	0.5	15	4	400	8	8	0.6	1.5	0.68	0.12	0.05	0.66	0.17	0.06	0.23	0.71	0.71	0.04	0.001	394	394	79	324	0.04	0.0008	382	9	310
M31211112	0.5	15	4	400	8	8	0.6	2.5	0.72	0.13	0.05	0.66	0.17	0.06	0.21	0.71	0.71	0.04	0.001	371	371	75	306	0.04	0.0009	358	8	291
M41211111	0.7	15	4	400	8	8	0.6	1.5	0.61	0.11	0.04	0.68	0.16	0.06	0.25	0.71	0.71	0.03	0.001	441	441	125	328	0.03	0.0007	433	10	317
M41211112	0.7	15	4	400	8	8	0.6	2.5	0.65	0.12	0.05	0.68	0.16	0.06	0.23	0.71	0.71	0.03	0.001	413	413	117	307	0.03	0.0008	404	9	295
M51211111	0.9	15	4	400	8	8	0.6	1.5	0.54	0.10	0.04	0.70	0.14	0.06	0.29	0.71	0.71	0.03	0.001	512	512	186	340	0.03	0.0007	507	12	332
M51211112	0.9	15	4	400	8	8	0.6	2.5	0.58	0.11	0.04	0.70	0.14	0.06	0.27	0.71	0.71	0.03	0.001	482	482	175	320	0.03	0.0007	476	11	312
M11211121	0.1	15	4	400	8	8	1	1.5	0.65	0.11	0.04	0.64	0.19	0.07	0.23	0.71	0.71	0.04	0.001	405	405	16	393	0.04	0.0008	389	9	378
M11211122	0.1	15	4	400	8	8	1	2.5	0.70	0.11	0.04	0.64	0.19	0.07	0.22	0.71	0.71	0.04	0.001	381	381	15	370	0.04	0.0009	364	8	355
M21211121	0.3	15	4	400	8	8	1	1.5	0.61	0.10	0.04	0.65	0.18	0.07	0.25	0.71	0.71	0.03	0.001	439	439	53	394	0.03	0.0008	427	10	381
M21211122	0.3	15	4	400	8	8	1	2.5	0.65	0.11	0.04	0.65	0.18	0.07	0.24	0.71	0.71	0.04	0.001	408	408	49	367	0.04	0.0008	395	9	352
M31211121	0.5	15	4	400	8	8	1	1.5	0.56	0.10	0.04	0.66	0.17	0.06	0.28	0.71	0.71	0.03	0.001	484	484	98	396	0.03	0.0007	475	11	385
M31211122	0.5	15	4	400	8	8	1	2.5	0.59	0.11	0.04	0.66	0.17	0.06	0.26	0.71	0.71	0.03	0.001	452	452	91	371	0.03	0.0007	442	10	358
M41211121	0.7	15	4	400	8	8	1	1.5	0.50	0.09	0.04	0.68	0.16	0.06	0.31	0.71	0.71	0.03	0.001	537	537	152	397	0.03	0.0006	530	12	388
M41211122	0.7	15	4	400	8	8	1	2.5	0.54	0.10	0.04	0.68	0.16	0.06	0.29	0.71	0.71	0.03	0.001	507	507	143	375	0.03	0.0006	499	12	365
M51211121	0.9	15	4	400	8	8	1	1.5	0.44	0.08	0.03	0.70	0.14	0.06	0.34	0.71	0.71	0.02	0.001	608	608	220	402	0.02	0.0005	604	14	395
M51211122	0.9	15	4	400	8	8	1	2.5	0.48	0.09	0.04	0.70	0.14	0.06	0.32	0.71	0.71	0.02	0.001	577	577	209	381	0.02	0.0006	572	13	374
M11211211	0.1	15	4	400	8	10	0.6	1.5	1.88	0.31	0.11	0.64	0.19	0.07	0.07	0.45	0.71	0.10	0.002	142	142	5	137	0.10	0.0022	121	3	118
M11211212	0.1	15	4	400	8	10	0.6	2.5	2.01	0.33	0.12	0.64	0.19	0.07	0.07	0.43	0.71	0.10	0.002	133	133	5	128	0.10	0.0023	112	3	109
M21211211	0.3	15	4	400	8	10	0.6	1.5	1.75	0.30	0.11	0.65	0.18	0.07	0.08	0.46	0.71	0.09	0.002	149	149	17	136	0.09	0.0019	133	3	118
M21211212	0.3	15	4	400	8	10	0.6	2.5	1.87	0.32	0.12	0.65	0.18	0.07	0.07	0.44	0.71	0.09	0.002	139	139	16	128	0.09	0.0021	123	3	110
M31211211	0.5	15	4	400	8	10	0.6	1.5	1.60	0.29	0.11	0.66	0.17	0.06	0.09	0.47	0.71	0.08	0.002	161	161	32	136	0.08	0.0017	147	3	120
M31211212	0.5	15	4	400	8	10	0.6	2.5	1.72	0.31	0.11	0.66	0.17	0.06	0.08	0.45	0.71	0.09	0.002	150	150	30	127	0.09	0.0019	137	3	111
M41211211	0.7	15	4	400	8	10	0.6	1.5	1.45	0.27	0.10	0.68	0.16	0.06	0.10	0.49	0.71	0.07	0.002	178	178	51	137	0.07	0.0016	168	4	123
M41211212	0.7	15	4	400	8	10	0.6	2.5	1.55	0.29	0.11	0.68	0.16	0.06	0.09	0.47	0.71	0.08	0.002	166	166	47	128	0.08	0.0017	155	4	114
M51211211	0.9	15	4	400	8	10	0.6	1.5	1.28	0.24	0.10	0.70	0.14	0.06	0.11	0.53	0.71	0.06	0.001	205	205	77	140	0.06	0.0015	197	5	129

Name	af	nf	hf	mf	Ly	Lx	tw	Lcb	T1 [s]	T2 [s]	T3 [s]	M1 [-]	M2 [-]	M3 [-]	Sa	Sa2	Sa3	Disp [m]	ISDR [-]	Total Moment [MN-m]	Total Shear [MN]	Outrigger Moment [MN-m]	Wall Moment [MN-m]	Mode 1 Disp [m]	Mode 1 ISDR [-]	Mode 1 Moment [MN-m]	Mode 1 Shear [MN]	Mode 1 wall Moment [MN-m]
M51211212	0.9	15	4	400	8	10	0.6	2.5	1.37	0.26	0.10	0.70	0.14	0.06	0.10	0.50	0.71	0.07	0.002	190	190	72	131	0.07	0.0015	182	4	119
M11211221	0.1	15	4	400	8	10	1	1.5	1.72	0.28	0.10	0.64	0.19	0.07	0.08	0.48	0.71	0.09	0.002	155	155	6	150	0.09	0.0020	134	3	130
M11211222	0.1	15	4	400	8	10	1	2.5	1.84	0.30	0.11	0.64	0.19	0.07	0.07	0.46	0.71	0.09	0.002	145	145	5	140	0.09	0.0021	124	3	120
M21211221	0.3	15	4	400	8	10	1	1.5	1.60	0.27	0.10	0.65	0.18	0.07	0.09	0.49	0.71	0.08	0.002	163	163	19	148	0.08	0.0018	146	3	130
M21211222	0.3	15	4	400	8	10	1	2.5	1.72	0.29	0.11	0.65	0.18	0.07	0.08	0.47	0.71	0.09	0.002	152	152	17	139	0.09	0.0019	135	3	121
M31211221	0.5	15	4	400	8	10	1	1.5	1.47	0.26	0.10	0.66	0.17	0.06	0.10	0.50	0.71	0.07	0.002	176	176	35	148	0.07	0.0016	163	4	132
M31211222	0.5	15	4	400	8	10	1	2.5	1.58	0.28	0.10	0.66	0.17	0.06	0.09	0.48	0.71	0.08	0.002	164	164	32	138	0.08	0.0017	150	3	122
M41211221	0.7	15	4	400	8	10	1	1.5	1.33	0.25	0.09	0.68	0.16	0.06	0.11	0.52	0.71	0.07	0.001	196	196	56	150	0.07	0.0015	185	4	135
M41211222	0.7	15	4	400	8	10	1	2.5	1.43	0.26	0.10	0.68	0.16	0.06	0.10	0.49	0.71	0.07	0.002	182	182	52	139	0.07	0.0016	171	4	125
M51211221	0.9	15	4	400	8	10	1	1.5	1.17	0.22	0.09	0.70	0.14	0.06	0.12	0.57	0.71	0.06	0.001	226	226	85	154	0.06	0.0014	218	5	143
M51211222	0.9	15	4	400	8	10	1	2.5	1.26	0.24	0.09	0.70	0.14	0.06	0.11	0.54	0.71	0.06	0.001	209	209	79	143	0.06	0.0014	201	5	131
M11212111	0.1	15	4	400	10	8	0.6	1.5	1.11	0.18	0.06	0.64	0.19	0.07	0.13	0.64	0.71	0.06	0.001	241	241	9	233	0.06	0.0014	219	5	213
M11212112	0.1	15	4	400	10	8	0.6	2.5	1.26	0.21	0.07	0.64	0.19	0.07	0.11	0.59	0.71	0.07	0.002	211	211	8	204	0.07	0.0015	189	4	183
M21212111	0.3	15	4	400	10	8	0.6	1.5	1.03	0.18	0.06	0.65	0.18	0.07	0.14	0.64	0.71	0.06	0.001	257	257	30	233	0.06	0.0012	240	5	214
M21212112	0.3	15	4	400	10	8	0.6	2.5	1.17	0.20	0.07	0.65	0.18	0.07	0.12	0.60	0.71	0.06	0.001	225	225	26	204	0.06	0.0014	207	5	185
M31212111	0.5	15	4	400	10	8	0.6	1.5	0.95	0.17	0.06	0.66	0.17	0.06	0.16	0.66	0.71	0.05	0.001	281	281	56	233	0.05	0.0011	267	6	216
M31212112	0.5	15	4	400	10	8	0.6	2.5	1.08	0.19	0.07	0.66	0.17	0.06	0.14	0.62	0.71	0.06	0.001	246	246	49	205	0.06	0.0012	231	5	188
M41212111	0.7	15	4	400	10	8	0.6	1.5	0.86	0.16	0.06	0.68	0.16	0.06	0.17	0.67	0.71	0.05	0.001	312	312	89	235	0.05	0.0010	301	7	220
M41212112	0.7	15	4	400	10	8	0.6	2.5	0.98	0.18	0.07	0.68	0.16	0.06	0.15	0.64	0.71	0.05	0.001	274	274	78	207	0.05	0.0011	263	6	193
M51212111	0.9	15	4	400	10	8	0.6	1.5	0.76	0.14	0.06	0.70	0.14	0.06	0.20	0.70	0.71	0.04	0.001	357	357	132	240	0.04	0.0009	350	8	229
M51212112	0.9	15	4	400	10	8	0.6	2.5	0.86	0.16	0.06	0.70	0.14	0.06	0.17	0.67	0.71	0.04	0.001	315	315	117	212	0.04	0.0010	307	7	201
M11212121	0.1	15	4	400	10	8	1	1.5	0.95	0.15	0.06	0.64	0.19	0.07	0.16	0.68	0.71	0.05	0.001	283	283	11	275	0.05	0.0012	262	6	255
M11212122	0.1	15	4	400	10	8	1	2.5	1.10	0.18	0.06	0.64	0.19	0.07	0.13	0.64	0.71	0.06	0.001	244	244	9	236	0.06	0.0014	222	5	216
M21212121	0.3	15	4	400	10	8	1	1.5	0.88	0.15	0.05	0.65	0.18	0.07	0.17	0.69	0.71	0.05	0.001	301	301	36	272	0.05	0.0011	285	6	254
M21212122	0.3	15	4	400	10	8	1	2.5	1.02	0.17	0.06	0.65	0.18	0.07	0.14	0.65	0.71	0.06	0.001	260	260	31	235	0.06	0.0012	243	6	216
M31212121	0.5	15	4	400	10	8	1	1.5	0.81	0.14	0.05	0.66	0.17	0.06	0.19	0.70	0.71	0.04	0.001	330	330	66	273	0.04	0.0010	316	7	257
M31212122	0.5	15	4	400	10	8	1	2.5	0.94	0.17	0.06	0.66	0.17	0.06	0.16	0.66	0.71	0.05	0.001	284	284	57	236	0.05	0.0011	270	6	219
M41212121	0.7	15	4	400	10	8	1	1.5	0.73	0.14	0.05	0.68	0.16	0.06	0.21	0.71	0.71	0.04	0.001	368	368	104	275	0.04	0.0009	358	8	262
M41212122	0.7	15	4	400	10	8	1	2.5	0.85	0.16	0.06	0.68	0.16	0.06	0.18	0.68	0.71	0.04	0.001	316	316	90	237	0.04	0.0010	305	7	223
M51212121	0.9	15	4	400	10	8	1	1.5	0.65	0.12	0.05	0.70	0.14	0.06	0.24	0.71	0.71	0.03	0.001	422	422	154	282	0.03	0.0008	416	10	272
M51212122	0.9	15	4	400	10	8	1	2.5	0.75	0.14	0.06	0.70	0.14	0.06	0.20	0.71	0.71	0.04	0.001	362	362	133	243	0.04	0.0009	355	8	232
M11212211	0.1	15	4	400	10	10	0.6	1.5	2.78	0.45	0.16	0.64	0.19	0.07	0.04	0.34	0.67	0.12	0.003	89	89	3	86	0.12	0.0027	68	2	67
M11212212	0.1	15	4	400	10	10	0.6	2.5	3.28	0.53	0.19	0.64	0.19	0.07	0.03	0.29	0.62	0.13	0.003	73	73	2	71	0.13	0.0029	54	1	52
M21212211	0.3	15	4	400	10	10	0.6	1.5	2.59	0.44	0.16	0.65	0.18	0.07	0.05	0.34	0.67	0.11	0.003	93	93	10	86	0.11	0.0025	77	2	69
M21212212	0.3	15	4	400	10	10	0.6	2.5	3.05	0.52	0.19	0.65	0.18	0.07	0.04	0.30	0.62	0.12	0.003	76	76	8	71	0.12	0.0027	60	1	54
M31212211	0.5	15	4	400	10	10	0.6	1.5	2.38	0.42	0.16	0.66	0.17	0.06	0.05	0.35	0.67	0.11	0.002	102	102	20	88	0.11	0.0023	88	2	72
M31212212	0.5	15	4	400	10	10	0.6	2.5	2.80	0.50	0.19	0.66	0.17	0.06	0.04	0.31	0.62	0.12	0.003	83	83	16	72	0.12	0.0025	69	2	56
M41212211	0.7	15	4	400	10	10	0.6	1.5	2.15	0.40	0.15	0.68	0.16	0.06	0.06	0.37	0.68	0.10	0.002	115	115	33	90	0.10	0.0022	105	2	77
M41212212	0.7	15	4	400	10	10	0.6	2.5	2.53	0.47	0.18	0.68	0.16	0.06	0.05	0.33	0.63	0.11	0.002	92	92	26	73	0.11	0.0024	82	2	60
M51212211	0.9	15	4	400	10	10	0.6	1.5	1.90	0.36	0.14	0.70	0.14	0.06	0.07	0.41	0.70	0.09	0.002	135	135	52	94	0.09	0.0021	127	3	83
M51212212	0.9	15	4	400	10	10	0.6	2.5	2.24	0.42	0.17	0.70	0.14	0.06	0.06	0.36	0.66	0.10	0.002	109	109	42	77	0.10	0.0023	101	2	66
M11212221	0.1	15	4	400	10	10	1	1.5	2.61	0.42	0.15	0.64	0.19	0.07	0.05	0.35	0.68	0.11	0.003	96	96	3	93	0.11	0.0026	75	2	73
M11212222	0.1	15	4	400	10	10	1	2.5	3.12	0.51	0.18	0.64	0.19	0.07	0.03	0.30	0.63	0.13	0.003	78	78	3	75	0.13	0.0028	58	1	56
M21212221	0.3	15	4	400	10	10	1	1.5	2.42	0.41	0.15	0.65	0.18	0.07	0.05	0.36	0.69	0.11	0.003	101	101	11	93	0.11	0.0024	85	2	76
M21212222	0.3	15	4	400	10	10	1	2.5	2.90	0.49	0.18	0.65	0.18	0.07	0.04	0.31	0.64	0.12	0.003	81	81	9	75	0.12	0.0026	65	1	58
M31212221	0.5	15	4	400	10	10	1	1.5	2.23	0.40	0.15	0.66	0.17	0.06	0.06	0.37	0.69	0.10	0.002	111	111	22	95	0.10	0.0022	98	2	79
M31212222	0.5	15	4	400	10	10	1	2.5	2.67	0.48	0.18	0.66	0.17	0.06	0.04	0.32	0.64	0.11	0.003	88	88	17	76	0.11	0.0024	74	2	60
M41212221	0.7	15	4	400	10	10	1	1.5	2.01	0.37	0.14	0.68	0.16	0.06	0.07	0.39	0.70	0.10	0.002	126	126	36	98	0.10	0.0021	116	3	85
M41212222	0.7	15	4	400	10	10	1	2.5	2.41	0.45	0.17	0.68	0.16	0.06	0.05	0.34	0.65	0.11	0.002	99	99	28	78	0.10	0.0023	88	2	64
M51212221	0.9	15	4	400	10	10	1	1.5	1.78	0.33	0.13	0.70	0.14	0.06	0.08	0.43	0.71	0.08	0.002	145	145	55	101	0.08	0.0020	136	3	89
M51212222	0.9	15	4	400	10	10	1	2.5	2.13	0.40	0.16	0.70	0.14	0.06	0.06	0.37	0.67	0.09	0.002	117	117	45	82	0.09	0.0022	109	3	71
M11221111	0.1	15	4	600	8	8	0.6	1.5	0.97	0.16	0.06	0.64	0.19	0.07	0.15	0.67	0.71	0.05	0.001	414	414	16	401	0.05	0.0012	382	9	372
M11221112	0.1	15	4	600	8	8	0.6	2.5	1.03	0.17	0.06	0.64	0.19	0.07	0.14	0.66	0.71	0.06	0.001	389	389	15	377	0.06	0.0013	357	8	347
M21221111	0.3	15	4	600	8	8	0.6	1.5	0.90	0.15	0.06	0.65	0.18	0.07	0.17	0.68	0.71	0.05	0.001	440	440	52	398	0.05	0.0011	415	9	370
M21221112	0.3	15	4	600	8	8	0.6	2.5	0.96	0.16	0.06	0.65	0.18	0.07	0.16	0.67	0.71	0.05	0.001	416	416	49	376	0.05	0.0011	391	9	348
M31221111	0.5	15	4	600	8	8	0.6	1.5	0.83	0.15	0.06	0.66	0.17	0.06	0.18	0.69	0.71	0.05	0.001	482	482	97	399	0.05	0.0010	462	11	374
M31221112	0.5	15	4	600	8	8	0.6	2.5	0.88	0.16	0.06	0.66	0.17	0.06	0.17	0.68	0.71	0.05	0.001	451	451	90	374	0.05	0.0010	431	10	349
M41221111	0.7	15	4	600	8	8	0.6	1.5	0.75	0.14	0.05	0.68	0.16	0.06	0.20	0.71	0.71	0.04	0.001	536	536	152	401	0.04	0.0009	520	12	380
M41221112	0.7	15	4	600	8	8	0.6	2.5	0.80	0.15	0.06	0.68	0.16	0.06	0.19	0.69	0.71	0.04	0.001	505	505	143	378	0.04	0.0009	489	11	358
M51221111	0.9	15	4	600	8	8	0.6	1.5	0.66	0.12	0.05	0.70	0.14	0.06	0.23	0.71	0.71	0.03	0.001	619	619	226	413	0.03	0.0008	609	14	398
M51221112	0.9	15	4	600	8	8	0.6	2.5	0.70	0.13	0.05	0.70	0.14	0.06	0.22	0.71	0.71	0.04	0.001	583	583	214	390	0.04	0.0009	572	13	374
M11221121	0.1	15	4	600	8	8	1	1.5	0.80	0.13	0.05	0.64	0.19	0.07	0.19	0.71	0.71	0.04	0.001	500	500	20	485	0.04	0.0010	471	11	458
M11221122	0.1	15	4	600	8	8	1	2.5	0.85	0.14	0.05	0.64	0.19	0.07	0.18	0.71	0.71	0.05	0.001	470	470	18	456	0.05	0.0011	439	10	427
M21221121	0.3	15	4	600	8	8	1	1.5	0.74	0.13	0.05	0.65	0.18	0.07	0.20	0.71	0.71	0.04	0.001	535	535	64	482	0.04	0.0009	513	12	457
M21221122	0.3	15	4	600	8	8	1	2.5	0.79	0.13	0.05	0.65	0.18	0.07	0.19	0.71	0.71	0.04	0.001	502	502	60	453	0.04	0.0010	478	11	427
M31221121	0.5	15	4	600	8	8	1	1.5	0.68	0.12	0.05	0.66	0.17	0.06	0.22	0.71	0.71	0.04	0.001	588	588	118	483	0.04	0.0008	570	13	462
M31221122	0.5	15	4	600	8	8	1	2.5	0.73	0.13	0.05	0.66	0.17	0.06	0.21	0.71	0.71	0.04	0.001	550	550	110	453	0.04	0.0009	531	12	430
M41221121	0.7	15	4	600	8	8	1	1.5	0.62	0.11	0.04	0.68	0.16	0.06	0.25	0.71	0.71	0.03	0.001	657	657	186	488	0.03	0.0007	645	15	471
M41221122	0.7	15	4	600	8	8	1	2.5	0.66	0.12	0.05	0.68	0.16	0.06	0.23	0.71	0.71	0.04	0.001	613	613	174	457	0.04	0.0008	600	14	439
M51221121	0.9	15	4	600	8	8	1	1.5	0.54	0.10	0.04	0.70	0.14	0.06	0.29	0.71	0.71	0.03	0.001	764	764	277	506	0.03	0.0007	756	18	495
M51221122	0.9	15	4	600	8	8	1	2.5	0.58	0.11	0.04	0.70	0.14	0.06	0.27	0.71	0.71	0.03	0.001	715	715	260	475	0.03	0.0007	706	17	462
M11221211	0.1	15	4	600	8	10	0.6	1.5	2.30	0.37	0.13	0.64	0.19	0.07	0.05	0.39	0.71	0.11	0.003	168	168	6	162	0.11	0.0024	137	3	133

Name	af	nf	hf	mf	Ly	Lx	tw	Lcb	T1 [s]	T2 [s]	T3 [s]	M1 [-]	M2 [-]	M3 [-]	Sa	Sa2	Sa3	Disp [m]	ISDR [-]	Total Moment [MN-m]	Total Shear [MN]	Outrigger Moment [MN-m]	Wall Moment [MN-m]	Mode 1 Disp [m]	Mode 1 ISDR [-]	Mode 1 Moment [MN-m]	Mode 1 Shear [MN]	Mode 1 wall Moment [MN-m]
M11221212	0.1	15	4	600	8	10	0.6	2.5	2.46	0.40	0.14	0.64	0.19	0.07	0.05	0.37	0.70	0.11	0.003	154	154	5	149	0.11	0.0025	124	3	120
M21221211	0.3	15	4	600	8	10	0.6	1.5	2.14	0.36	0.13	0.65	0.18	0.07	0.06	0.40	0.71	0.10	0.002	179	179	20	164	0.10	0.0023	154	4	138
M21221212	0.3	15	4	600	8	10	0.6	2.5	2.29	0.39	0.14	0.65	0.18	0.07	0.06	0.37	0.70	0.11	0.002	163	163	18	150	0.11	0.0023	139	3	124
M31221211	0.5	15	4	600	8	10	0.6	1.5	1.97	0.35	0.13	0.66	0.17	0.06	0.07	0.41	0.71	0.10	0.002	197	197	39	167	0.10	0.0021	177	4	143
M31221212	0.5	15	4	600	8	10	0.6	2.5	2.10	0.37	0.14	0.66	0.17	0.06	0.06	0.39	0.71	0.10	0.002	180	180	35	154	0.10	0.0022	161	4	130
M41221211	0.7	15	4	600	8	10	0.6	1.5	1.78	0.33	0.13	0.68	0.16	0.06	0.08	0.43	0.71	0.09	0.002	217	217	62	168	0.09	0.0019	201	5	147
M41221212	0.7	15	4	600	8	10	0.6	2.5	1.90	0.35	0.14	0.68	0.16	0.06	0.07	0.41	0.71	0.09	0.002	202	202	58	157	0.09	0.0020	186	4	136
M51221211	0.9	15	4	600	8	10	0.6	1.5	1.57	0.29	0.12	0.70	0.14	0.06	0.09	0.46	0.71	0.07	0.002	248	248	94	171	0.07	0.0017	235	6	154
M51221212	0.9	15	4	600	8	10	0.6	2.5	1.68	0.31	0.13	0.70	0.14	0.06	0.08	0.44	0.71	0.08	0.002	231	231	88	160	0.08	0.0019	218	5	143
M11221221	0.1	15	4	600	8	10	1	1.5	2.10	0.34	0.12	0.64	0.19	0.07	0.06	0.42	0.71	0.10	0.002	188	188	7	182	0.10	0.0023	157	4	153
M11221222	0.1	15	4	600	8	10	1	2.5	2.26	0.37	0.13	0.64	0.19	0.07	0.06	0.39	0.71	0.11	0.003	172	172	6	166	0.11	0.0024	141	3	137
M21221221	0.3	15	4	600	8	10	1	1.5	1.96	0.33	0.12	0.65	0.18	0.07	0.07	0.43	0.71	0.10	0.002	200	200	23	183	0.10	0.0021	175	4	156
M21221222	0.3	15	4	600	8	10	1	2.5	2.10	0.36	0.13	0.65	0.18	0.07	0.06	0.40	0.71	0.10	0.002	183	183	21	168	0.10	0.0022	159	4	142
M31221221	0.5	15	4	600	8	10	1	1.5	1.80	0.32	0.12	0.66	0.17	0.06	0.08	0.44	0.71	0.09	0.002	215	215	42	182	0.09	0.0019	195	4	158
M31221222	0.5	15	4	600	8	10	1	2.5	1.93	0.34	0.13	0.66	0.17	0.06	0.07	0.42	0.71	0.10	0.002	200	200	39	170	0.10	0.0021	180	4	146
M41221221	0.7	15	4	600	8	10	1	1.5	1.63	0.30	0.12	0.68	0.16	0.06	0.09	0.46	0.71	0.08	0.002	237	237	68	183	0.08	0.0018	221	5	162
M41221222	0.7	15	4	600	8	10	1	2.5	1.75	0.32	0.12	0.68	0.16	0.06	0.08	0.44	0.71	0.09	0.002	221	221	63	171	0.08	0.0019	205	5	150
M51221221	0.9	15	4	600	8	10	1	1.5	1.44	0.27	0.11	0.70	0.14	0.06	0.10	0.49	0.71	0.07	0.002	272	272	103	187	0.07	0.0016	260	6	170
M51221222	0.9	15	4	600	8	10	1	2.5	1.54	0.29	0.12	0.70	0.14	0.06	0.09	0.47	0.71	0.07	0.002	252	252	96	174	0.07	0.0017	240	6	157
M11222111	0.1	15	4	600	10	8	0.6	1.5	1.36	0.22	0.08	0.64	0.19	0.07	0.10	0.56	0.71	0.07	0.002	293	293	11	284	0.07	0.0016	260	6	253
M11222112	0.1	15	4	600	10	8	0.6	2.5	1.54	0.25	0.09	0.64	0.19	0.07	0.09	0.51	0.71	0.08	0.002	257	257	10	249	0.08	0.0018	226	5	220
M21222111	0.3	15	4	600	10	8	0.6	1.5	1.27	0.22	0.08	0.65	0.18	0.07	0.11	0.57	0.71	0.07	0.001	311	311	36	282	0.07	0.0015	285	6	254
M21222112	0.3	15	4	600	10	8	0.6	2.5	1.44	0.24	0.09	0.65	0.18	0.07	0.10	0.52	0.71	0.07	0.002	272	272	32	248	0.07	0.0016	247	6	220
M31222111	0.5	15	4	600	10	8	0.6	1.5	1.16	0.21	0.08	0.66	0.17	0.06	0.12	0.59	0.71	0.06	0.001	339	339	68	283	0.06	0.0013	318	7	258
M31222112	0.5	15	4	600	10	8	0.6	2.5	1.32	0.24	0.09	0.66	0.17	0.06	0.11	0.54	0.71	0.07	0.002	296	296	59	248	0.07	0.0015	275	6	223
M41222111	0.7	15	4	600	10	8	0.6	1.5	1.05	0.19	0.08	0.68	0.16	0.06	0.14	0.61	0.71	0.05	0.001	380	380	108	288	0.05	0.0012	363	8	265
M41222112	0.7	15	4	600	10	8	0.6	2.5	1.19	0.22	0.09	0.68	0.16	0.06	0.12	0.56	0.71	0.06	0.001	330	330	94	251	0.06	0.0013	314	7	229
M51222111	0.9	15	4	600	10	8	0.6	1.5	0.93	0.17	0.07	0.70	0.14	0.06	0.16	0.65	0.71	0.05	0.001	437	437	162	295	0.05	0.0011	425	10	278
M51222112	0.9	15	4	600	10	8	0.6	2.5	1.06	0.20	0.08	0.70	0.14	0.06	0.14	0.61	0.71	0.05	0.001	382	382	143	259	0.05	0.0012	370	9	242
M11222121	0.1	15	4	600	10	8	1	1.5	1.16	0.19	0.07	0.64	0.19	0.07	0.13	0.62	0.71	0.06	0.001	346	346	13	335	0.06	0.0014	312	7	304
M11222122	0.1	15	4	600	10	8	1	2.5	1.35	0.22	0.08	0.64	0.19	0.07	0.11	0.57	0.71	0.07	0.002	297	297	11	287	0.07	0.0016	264	6	257
M21222121	0.3	15	4	600	10	8	1	1.5	1.08	0.18	0.07	0.65	0.18	0.07	0.14	0.63	0.71	0.06	0.001	369	369	44	335	0.06	0.0013	343	8	306
M21222122	0.3	15	4	600	10	8	1	2.5	1.25	0.21	0.08	0.65	0.18	0.07	0.11	0.58	0.71	0.07	0.001	314	314	37	286	0.07	0.0014	288	7	257
M31222121	0.5	15	4	600	10	8	1	1.5	0.99	0.18	0.07	0.66	0.17	0.06	0.15	0.64	0.71	0.05	0.001	403	403	81	335	0.05	0.0011	382	9	309
M31222122	0.5	15	4	600	10	8	1	2.5	1.15	0.21	0.08	0.66	0.17	0.06	0.13	0.59	0.71	0.06	0.001	343	343	68	287	0.06	0.0013	321	7	261
M41222121	0.7	15	4	600	10	8	1	1.5	0.90	0.17	0.06	0.68	0.16	0.06	0.17	0.66	0.71	0.05	0.001	447	447	127	337	0.05	0.0010	431	10	315
M41222122	0.7	15	4	600	10	8	1	2.5	1.04	0.19	0.07	0.68	0.16	0.06	0.14	0.61	0.71	0.05	0.001	384	384	109	291	0.05	0.0012	367	8	269
M51222121	0.9	15	4	600	10	8	1	1.5	0.79	0.15	0.06	0.70	0.14	0.06	0.19	0.69	0.71	0.04	0.001	515	515	190	346	0.04	0.0009	504	12	330
M51222122	0.9	15	4	600	10	8	1	2.5	0.92	0.17	0.07	0.70	0.14	0.06	0.16	0.65	0.71	0.05	0.001	442	442	164	298	0.05	0.0011	430	10	281
M11222211	0.1	15	4	600	10	10	0.6	1.5	3.41	0.55	0.20	0.64	0.19	0.07	0.03	0.28	0.60	0.13	0.003	105	105	3	101	0.13	0.0030	76	2	74
M11222212	0.1	15	4	600	10	10	0.6	2.5	4.01	0.65	0.23	0.64	0.19	0.07	0.02	0.23	0.54	0.15	0.004	86	86	3	83	0.15	0.0033	61	1	59
M21222211	0.3	15	4	600	10	10	0.6	1.5	3.17	0.54	0.20	0.65	0.18	0.07	0.03	0.29	0.61	0.13	0.003	109	109	12	102	0.13	0.0027	86	2	76
M21222212	0.3	15	4	600	10	10	0.6	2.5	3.73	0.64	0.23	0.65	0.18	0.07	0.03	0.24	0.55	0.14	0.003	89	89	9	83	0.14	0.0030	68	2	60
M31222211	0.5	15	4	600	10	10	0.6	1.5	2.91	0.52	0.19	0.66	0.17	0.06	0.04	0.30	0.61	0.12	0.003	118	118	23	102	0.12	0.0026	98	2	79
M31222212	0.5	15	4	600	10	10	0.6	2.5	3.43	0.61	0.23	0.66	0.17	0.06	0.03	0.25	0.55	0.13	0.003	96	96	18	84	0.13	0.0028	77	2	63
M41222211	0.7	15	4	600	10	10	0.6	1.5	2.63	0.49	0.19	0.68	0.16	0.06	0.04	0.32	0.62	0.11	0.002	131	131	38	105	0.11	0.0024	116	3	85
M41222212	0.7	15	4	600	10	10	0.6	2.5	3.10	0.57	0.22	0.68	0.16	0.06	0.04	0.27	0.56	0.12	0.003	106	106	30	85	0.12	0.0026	91	2	66
M51222211	0.9	15	4	600	10	10	0.6	1.5	2.33	0.44	0.18	0.70	0.14	0.06	0.05	0.35	0.64	0.10	0.002	155	155	61	110	0.10	0.0023	143	3	93
M51222212	0.9	15	4	600	10	10	0.6	2.5	2.74	0.51	0.21	0.70	0.14	0.06	0.04	0.30	0.59	0.11	0.003	124	124	49	89	0.11	0.0025	111	3	73
M11222221	0.1	15	4	600	10	10	1	1.5	3.19	0.52	0.19	0.64	0.19	0.07	0.03	0.30	0.63	0.13	0.003	114	114	4	109	0.13	0.0029	84	2	82
M11222222	0.1	15	4	600	10	10	1	2.5	3.82	0.62	0.22	0.64	0.19	0.07	0.03	0.25	0.56	0.14	0.004	92	92	3	88	0.14	0.0032	65	1	63
M21222221	0.3	15	4	600	10	10	1	1.5	2.97	0.51	0.18	0.65	0.18	0.07	0.04	0.31	0.63	0.12	0.003	118	118	13	110	0.12	0.0027	94	2	84
M21222222	0.3	15	4	600	10	10	1	2.5	3.56	0.61	0.22	0.65	0.18	0.07	0.03	0.25	0.56	0.13	0.003	95	95	10	88	0.13	0.0029	73	2	65
M31222221	0.5	15	4	600	10	10	1	1.5	2.73	0.49	0.18	0.66	0.17	0.06	0.04	0.32	0.63	0.11	0.003	128	128	25	111	0.11	0.0025	108	2	88
M31222222	0.5	15	4	600	10	10	1	2.5	3.27	0.58	0.22	0.66	0.17	0.06	0.03	0.27	0.57	0.13	0.003	102	102	19	89	0.13	0.0027	83	2	67
M41222221	0.7	15	4	600	10	10	1	1.5	2.47	0.46	0.18	0.68	0.16	0.06	0.05	0.33	0.64	0.11	0.002	144	144	41	114	0.11	0.0023	128	3	93
M41222222	0.7	15	4	600	10	10	1	2.5	2.96	0.55	0.21	0.68	0.16	0.06	0.04	0.28	0.58	0.12	0.003	113	113	32	91	0.12	0.0026	98	2	71
M51222221	0.9	15	4	600	10	10	1	1.5	2.18	0.41	0.16	0.70	0.14	0.06	0.06	0.36	0.66	0.10	0.002	170	170	66	119	0.10	0.0023	158	4	103
M51222222	0.9	15	4	600	10	10	1	2.5	2.61	0.49	0.20	0.70	0.14	0.06	0.05	0.32	0.61	0.10	0.002	132	132	52	95	0.10	0.0025	120	3	78
M12111111	0.1	30	3	400	8	8	0.6	1.5	1.01	0.17	0.06	0.63	0.19	0.07	0.15	0.66	0.71	0.06	0.001	767	767	29	743	0.06	0.0009	710	11	684
M12111112	0.1	30	3	400	8	8	0.6	2.5	1.05	0.17	0.06	0.63	0.19	0.07	0.14	0.65	0.71	0.06	0.001	739	739	28	717	0.06	0.0009	682	10	658
M22111111	0.3	30	3	400	8	8	0.6	1.5	0.95	0.16	0.06	0.64	0.18	0.06	0.16	0.67	0.71	0.05	0.001	825	825	95	741	0.05	0.0008	776	12	686
M22111112	0.3	30	3	400	8	8	0.6	2.5	0.98	0.17	0.06	0.64	0.18	0.06	0.15	0.66	0.71	0.05	0.001	794	794	92	714	0.05	0.0008	745	11	659
M32111111	0.5	30	3	400	8	8	0.6	1.5	0.87	0.16	0.06	0.65	0.17	0.06	0.17	0.68	0.71	0.05	0.001	896	896	175	738	0.05	0.0007	856	13	690
M32111112	0.5	30	3	400	8	8	0.6	2.5	0.90	0.16	0.06	0.65	0.17	0.06	0.16	0.67	0.71	0.05	0.001	862	862	168	711	0.05	0.0007	822	13	662
M42111111	0.7	30	3	400	8	8	0.6	1.5	0.79	0.15	0.06	0.66	0.16	0.06	0.19	0.70	0.71	0.04	0.001	996	996	276	744	0.04	0.0006	965	15	703
M42111112	0.7	30	3	400	8	8	0.6	2.5	0.82	0.15	0.06	0.66	0.16	0.06	0.18	0.69	0.71	0.04	0.001	961	961	266	719	0.04	0.0006	930	14	678
M52111111	0.9	30	3	400	8	8	0.6	1.5	0.70	0.13	0.05	0.69	0.14	0.06	0.22	0.71	0.71	0.04	0.001	1147	1147	410	766	0.04	0.0006	1125	18	736
M52111112	0.9	30	3	400	8	8	0.6	2.5	0.73	0.14	0.05	0.69	0.14	0.06	0.21	0.71	0.71	0.04	0.001	1102	1102	395	738	0.04	0.0006	1080	17	706
M12111121	0.1	30	3	400	8	8	1	1.5	0.79	0.13	0.05	0.63	0.19	0.07	0.19	0.71	0.71	0.05	0.001	977	977	38	946	0.05	0.0007	927	14	893
M12111122	0.1	30	3	400	8	8	1	2.5	0.82	0.13	0.05	0.63	0.19	0.07	0.18	0.71	0.71	0.05	0.001	943	943	36	913	0.05	0.0007	890	13	858
M22111121	0.3	30	3	400	8	8	1	1.5	0.74	0.13	0.05	0.64	0.18	0.06	0.20	0.71	0.71	0.04	0.001	1052	1052	123	940	0.04	0.0006	1009	15	893

Name	af	nf	hf	mf	Ly	Lx	tw	Lcb	T1 [s]	T2 [s]	T3 [s]	M1 [-]	M2 [-]	M3 [-]	Sa	Sa2	Sa3	Disp [m]	ISDR [-]	Total Moment [MN-m]	Total Shear [MN]	Outrigger Moment [MN-m]	Wall Moment [MN-m]	Mode 1 Disp [m]	Mode 1 ISDR [-]	Mode 1 Moment [MN-m]	Mode 1 Shear [MN]	Mode 1 wall Moment [MN-m]
M22111122	0.3	30	3	400	8	8	1	2.5	0.77	0.13	0.05	0.64	0.18	0.06	0.20	0.71	0.71	0.04	0.001	1008	1008	118	902	0.04	0.0006	964	15	852
M32111121	0.5	30	3	400	8	8	1	1.5	0.68	0.12	0.05	0.65	0.17	0.06	0.22	0.71	0.71	0.04	0.001	1152	1152	226	942	0.04	0.0005	1118	17	901
M32111122	0.5	30	3	400	8	8	1	2.5	0.71	0.13	0.05	0.65	0.17	0.06	0.22	0.71	0.71	0.04	0.001	1108	1108	217	908	0.04	0.0006	1073	16	865
M42111121	0.7	30	3	400	8	8	1	1.5	0.62	0.11	0.04	0.66	0.16	0.06	0.25	0.71	0.71	0.03	0.000	1286	1286	355	952	0.03	0.0005	1261	20	919
M42111122	0.7	30	3	400	8	8	1	2.5	0.64	0.12	0.05	0.66	0.16	0.06	0.24	0.71	0.71	0.03	0.001	1227	1227	339	910	0.03	0.0005	1201	19	875
M52111121	0.9	30	3	400	8	8	1	1.5	0.55	0.10	0.04	0.69	0.14	0.06	0.28	0.71	0.71	0.03	0.000	1487	1487	527	985	0.03	0.0005	1470	23	961
M52111122	0.9	30	3	400	8	8	1	2.5	0.57	0.11	0.04	0.69	0.14	0.06	0.27	0.71	0.71	0.03	0.000	1430	1430	508	949	0.03	0.0005	1413	22	924
M12111211	0.1	30	3	400	8	10	0.6	1.5	2.30	0.38	0.13	0.63	0.19	0.07	0.05	0.39	0.71	0.11	0.002	321	321	11	313	0.11	0.0017	267	4	257
M12111212	0.1	30	3	400	8	10	0.6	2.5	2.40	0.39	0.14	0.63	0.19	0.07	0.05	0.37	0.70	0.11	0.002	304	304	11	297	0.11	0.0017	250	4	241
M22111211	0.3	30	3	400	8	10	0.6	1.5	2.15	0.37	0.13	0.64	0.18	0.06	0.06	0.40	0.71	0.11	0.002	347	347	38	317	0.11	0.0015	300	5	265
M22111212	0.3	30	3	400	8	10	0.6	2.5	2.24	0.38	0.14	0.64	0.18	0.06	0.06	0.38	0.71	0.11	0.002	328	328	36	300	0.11	0.0016	282	4	249
M32111211	0.5	30	3	400	8	10	0.6	1.5	1.98	0.35	0.13	0.65	0.17	0.06	0.07	0.41	0.71	0.10	0.001	382	382	73	323	0.10	0.0014	343	5	276
M32111212	0.5	30	3	400	8	10	0.6	2.5	2.06	0.37	0.14	0.65	0.17	0.06	0.07	0.40	0.71	0.10	0.002	363	363	69	307	0.10	0.0015	324	5	261
M42111211	0.7	30	3	400	8	10	0.6	1.5	1.79	0.33	0.13	0.66	0.16	0.06	0.08	0.43	0.71	0.09	0.001	421	421	117	324	0.09	0.0013	388	6	283
M42111212	0.7	30	3	400	8	10	0.6	2.5	1.87	0.35	0.13	0.66	0.16	0.06	0.07	0.42	0.71	0.09	0.001	403	403	112	311	0.09	0.0013	371	6	270
M52111211	0.9	30	3	400	8	10	0.6	1.5	1.59	0.30	0.12	0.69	0.14	0.06	0.09	0.46	0.71	0.08	0.001	479	479	177	330	0.08	0.0012	453	7	296
M52111212	0.9	30	3	400	8	10	0.6	2.5	1.66	0.31	0.12	0.69	0.14	0.06	0.08	0.45	0.71	0.08	0.001	458	458	170	316	0.08	0.0012	432	7	283
M12111221	0.1	30	3	400	8	10	1	1.5	1.95	0.32	0.11	0.63	0.19	0.07	0.07	0.44	0.71	0.10	0.002	396	396	14	385	0.10	0.0015	342	5	329
M12111222	0.1	30	3	400	8	10	1	2.5	2.03	0.33	0.12	0.63	0.19	0.07	0.07	0.43	0.71	0.10	0.002	378	378	14	368	0.10	0.0016	324	5	312
M22111221	0.3	30	3	400	8	10	1	1.5	1.81	0.31	0.11	0.64	0.18	0.06	0.08	0.45	0.71	0.09	0.001	421	421	47	383	0.09	0.0014	373	6	330
M22111222	0.3	30	3	400	8	10	1	2.5	1.89	0.32	0.12	0.64	0.18	0.06	0.07	0.44	0.71	0.10	0.001	403	403	45	367	0.10	0.0014	356	5	314
M32111221	0.5	30	3	400	8	10	1	1.5	1.67	0.30	0.11	0.65	0.17	0.06	0.08	0.46	0.71	0.09	0.001	454	454	87	381	0.09	0.0012	414	6	333
M32111222	0.5	30	3	400	8	10	1	2.5	1.74	0.31	0.12	0.65	0.17	0.06	0.08	0.45	0.71	0.09	0.001	434	434	84	365	0.09	0.0013	394	6	318
M42111221	0.7	30	3	400	8	10	1	1.5	1.51	0.28	0.11	0.66	0.16	0.06	0.09	0.48	0.71	0.08	0.001	500	500	139	382	0.08	0.0011	468	7	341
M42111222	0.7	30	3	400	8	10	1	2.5	1.58	0.29	0.11	0.66	0.16	0.06	0.09	0.47	0.71	0.08	0.001	479	479	133	367	0.08	0.0012	447	7	325
M52111221	0.9	30	3	400	8	10	1	1.5	1.34	0.25	0.10	0.69	0.14	0.06	0.11	0.51	0.71	0.06	0.001	573	573	210	392	0.06	0.0010	548	9	358
M52111222	0.9	30	3	400	8	10	1	2.5	1.40	0.26	0.11	0.69	0.14	0.06	0.10	0.49	0.71	0.07	0.001	546	546	201	374	0.07	0.0011	521	8	341
M12112111	0.1	30	3	400	10	8	0.6	1.5	1.38	0.23	0.08	0.63	0.19	0.07	0.10	0.56	0.71	0.07	0.001	557	557	21	541	0.07	0.0011	499	8	481
M12112112	0.1	30	3	400	10	8	0.6	2.5	1.48	0.24	0.09	0.63	0.19	0.07	0.09	0.53	0.71	0.08	0.001	518	518	19	503	0.08	0.0012	461	7	445
M22112111	0.3	30	3	400	10	8	0.6	1.5	1.29	0.22	0.08	0.64	0.18	0.06	0.11	0.57	0.71	0.07	0.001	596	596	68	539	0.07	0.0010	547	8	483
M22112112	0.3	30	3	400	10	8	0.6	2.5	1.38	0.24	0.09	0.64	0.18	0.06	0.10	0.54	0.71	0.07	0.001	553	553	63	500	0.07	0.0011	504	8	446
M32112111	0.5	30	3	400	10	8	0.6	1.5	1.19	0.21	0.08	0.65	0.17	0.06	0.12	0.58	0.71	0.06	0.001	650	650	126	541	0.06	0.0009	608	9	490
M32112112	0.5	30	3	400	10	8	0.6	2.5	1.27	0.23	0.08	0.65	0.17	0.06	0.11	0.55	0.71	0.07	0.001	601	601	117	501	0.07	0.0010	560	9	451
M42112111	0.7	30	3	400	10	8	0.6	1.5	1.07	0.20	0.08	0.66	0.16	0.06	0.14	0.60	0.71	0.06	0.001	725	725	201	548	0.06	0.0008	692	11	504
M42112112	0.7	30	3	400	10	8	0.6	2.5	1.15	0.21	0.08	0.66	0.16	0.06	0.13	0.58	0.71	0.06	0.001	669	669	186	507	0.06	0.0009	636	10	463
M52112111	0.9	30	3	400	10	8	0.6	1.5	0.95	0.18	0.07	0.69	0.14	0.06	0.16	0.64	0.71	0.05	0.001	832	832	302	562	0.05	0.0008	808	13	528
M52112112	0.9	30	3	400	10	8	0.6	2.5	1.02	0.19	0.08	0.69	0.14	0.06	0.14	0.62	0.71	0.05	0.001	771	771	280	522	0.05	0.0008	745	12	487
M12112121	0.1	30	3	400	10	8	1	1.5	1.10	0.18	0.06	0.63	0.19	0.07	0.13	0.64	0.71	0.06	0.001	704	704	27	683	0.06	0.0009	647	10	623
M12112122	0.1	30	3	400	10	8	1	2.5	1.19	0.19	0.07	0.63	0.19	0.07	0.12	0.61	0.71	0.07	0.001	649	649	24	630	0.07	0.0010	591	9	570
M22112121	0.3	30	3	400	10	8	1	1.5	1.03	0.18	0.06	0.64	0.18	0.06	0.14	0.64	0.71	0.06	0.001	757	757	87	681	0.06	0.0008	707	11	626
M22112122	0.3	30	3	400	10	8	1	2.5	1.11	0.19	0.07	0.64	0.18	0.06	0.13	0.62	0.71	0.06	0.001	696	696	80	628	0.06	0.0009	647	10	572
M32112121	0.5	30	3	400	10	8	1	1.5	0.95	0.17	0.06	0.65	0.17	0.06	0.16	0.66	0.71	0.05	0.001	825	825	161	682	0.05	0.0007	785	12	632
M32112122	0.5	30	3	400	10	8	1	2.5	1.02	0.18	0.07	0.65	0.17	0.06	0.14	0.63	0.71	0.06	0.001	760	760	148	629	0.06	0.0008	719	11	579
M42112121	0.7	30	3	400	10	8	1	1.5	0.86	0.16	0.06	0.66	0.16	0.06	0.17	0.67	0.71	0.05	0.001	916	916	254	686	0.05	0.0007	884	14	644
M42112122	0.7	30	3	400	10	8	1	2.5	0.93	0.17	0.07	0.66	0.16	0.06	0.16	0.65	0.71	0.05	0.001	845	845	234	635	0.05	0.0007	813	13	592
M52112121	0.9	30	3	400	10	8	1	1.5	0.76	0.14	0.06	0.69	0.14	0.06	0.20	0.70	0.71	0.04	0.001	1044	1044	375	700	0.04	0.0006	1021	16	667
M52112122	0.9	30	3	400	10	8	1	2.5	0.82	0.15	0.06	0.69	0.14	0.06	0.18	0.68	0.71	0.04	0.001	968	968	349	651	0.04	0.0007	944	15	618
M12112211	0.1	30	3	400	10	10	0.6	1.5	3.30	0.54	0.19	0.63	0.19	0.07	0.03	0.29	0.61	0.13	0.002	208	208	7	204	0.13	0.0020	157	2	151
M12112212	0.1	30	3	400	10	10	0.6	2.5	3.60	0.59	0.21	0.63	0.19	0.07	0.03	0.26	0.58	0.14	0.002	187	187	6	183	0.14	0.0021	138	2	133
M22112211	0.3	30	3	400	10	10	0.6	1.5	3.07	0.52	0.19	0.64	0.18	0.06	0.04	0.30	0.62	0.13	0.002	220	220	23	204	0.13	0.0018	175	3	155
M22112212	0.3	30	3	400	10	10	0.6	2.5	3.36	0.57	0.21	0.64	0.18	0.06	0.03	0.27	0.59	0.13	0.002	198	198	21	184	0.13	0.0019	154	2	136
M32112211	0.5	30	3	400	10	10	0.6	1.5	2.83	0.50	0.19	0.65	0.17	0.06	0.04	0.31	0.62	0.12	0.002	239	239	45	207	0.12	0.0017	200	3	161
M32112212	0.5	30	3	400	10	10	0.6	2.5	3.09	0.55	0.21	0.65	0.17	0.06	0.04	0.28	0.59	0.12	0.002	213	213	40	185	0.12	0.0018	176	3	142
M42112211	0.7	30	3	400	10	10	0.6	1.5	2.56	0.47	0.18	0.66	0.16	0.06	0.05	0.32	0.63	0.11	0.002	268	268	74	211	0.11	0.0016	235	4	172
M42112212	0.7	30	3	400	10	10	0.6	2.5	2.80	0.52	0.20	0.66	0.16	0.06	0.04	0.30	0.60	0.12	0.002	238	238	66	189	0.11	0.0017	206	3	150
M52112211	0.9	30	3	400	10	10	0.6	1.5	2.27	0.43	0.17	0.69	0.14	0.06	0.06	0.35	0.65	0.10	0.002	314	314	118	221	0.10	0.0016	288	5	189
M52112212	0.9	30	3	400	10	10	0.6	2.5	2.48	0.47	0.19	0.69	0.14	0.06	0.05	0.33	0.62	0.10	0.002	278	278	106	197	0.10	0.0016	252	4	165
M12112221	0.1	30	3	400	10	10	1	1.5	2.85	0.46	0.17	0.63	0.19	0.07	0.04	0.33	0.66	0.12	0.002	248	248	8	243	0.12	0.0018	194	3	187
M12112222	0.1	30	3	400	10	10	1	2.5	3.14	0.51	0.18	0.63	0.19	0.07	0.03	0.30	0.63	0.13	0.002	221	221	7	216	0.13	0.0019	168	3	162
M22112221	0.3	30	3	400	10	10	1	1.5	2.65	0.45	0.17	0.64	0.18	0.06	0.04	0.34	0.66	0.12	0.002	265	265	29	244	0.12	0.0017	218	3	193
M22112222	0.3	30	3	400	10	10	1	2.5	2.92	0.50	0.18	0.64	0.18	0.06	0.04	0.31	0.63	0.12	0.002	234	234	25	217	0.12	0.0018	189	3	167
M32112221	0.5	30	3	400	10	10	1	1.5	2.44	0.43	0.16	0.65	0.17	0.06	0.05	0.35	0.67	0.11	0.002	289	289	55	248	0.11	0.0016	250	4	201
M32112222	0.5	30	3	400	10	10	1	2.5	2.69	0.48	0.18	0.65	0.17	0.06	0.04	0.32	0.64	0.12	0.002	255	255	48	220	0.12	0.0017	216	3	174
M42112221	0.7	30	3	400	10	10	1	1.5	2.21	0.41	0.16	0.66	0.16	0.06	0.06	0.36	0.67	0.10	0.002	327	327	91	254	0.10	0.0015	295	5	215
M42112222	0.7	30	3	400	10	10	1	2.5	2.44	0.45	0.17	0.66	0.16	0.06	0.05	0.34	0.65	0.11	0.002	286	286	80	225	0.11	0.0016	254	4	185
M52112221	0.9	30	3	400	10	10	1	1.5	1.96	0.37	0.15	0.69	0.14	0.06	0.07	0.39	0.69	0.09	0.001	384	384	143	266	0.09	0.0014	359	6	234
M52112222	0.9	30	3	400	10	10	1	2.5	2.16	0.41	0.16	0.69	0.14	0.06	0.06	0.37	0.67	0.10	0.002	337	337	126	236	0.10	0.0015	312	5	204
M12121111	0.1	30	3	600	8	8	0.6	1.5	1.24	0.20	0.07	0.63	0.19	0.07	0.12	0.60	0.71	0.07	0.001	932	932	35	905	0.07	0.0010	845	13	815
M12121112	0.1	30	3	600	8	8	0.6	2.5	1.29	0.21	0.08	0.63	0.19	0.07	0.11	0.58	0.71	0.07	0.001	897	897	34	871	0.07	0.0010	810	12	781
M22121111	0.3	30	3	600	8	8	0.6	1.5	1.16	0.20	0.07	0.64	0.18	0.06	0.13	0.61	0.71	0.06	0.001	1000	1000	115	902	0.06	0.0009	925	14	818
M22121112	0.3	30	3	600	8	8	0.6	2.5	1.20	0.20	0.07	0.64	0.18	0.06	0.12	0.59	0.71	0.07	0.001	963	963	110	869	0.06	0.0009	888	14	785
M32121111	0.5	30	3	600	8	8	0.6	1.5	1.07	0.19	0.07	0.65	0.17	0.06	0.14	0.62	0.71	0.06	0.001	1094	1094	213	906	0.06	0.0008	1032	16	831

Name	af	nf	hf	mf	Ly	Lx	tw	Lcb	T1 [s]	T2 [s]	T3 [s]	M1 [-]	M2 [-]	M3 [-]	Sa	Sa2	Sa3	Disp [m]	ISDR [-]	Total Moment [MN-m]	Total Shear [MN]	Outrigger Moment [MN-m]	Wall Moment [MN-m]	Mode 1 Disp [m]	Mode 1 ISDR [-]	Mode 1 Moment [MN-m]	Mode 1 Shear [MN]	Mode 1 wall Moment [MN-m]
M32121112	0.5	30	3	600	8	8	0.6	2.5	1.11	0.20	0.07	0.65	0.17	0.06	0.13	0.61	0.71	0.06	0.001	1050	1050	204	871	0.06	0.0009	987	15	796
M42121111	0.7	30	3	600	8	8	0.6	1.5	0.97	0.18	0.07	0.66	0.16	0.06	0.15	0.64	0.71	0.05	0.001	1217	1217	338	916	0.05	0.0008	1169	18	851
M42121112	0.7	30	3	600	8	8	0.6	2.5	1.00	0.19	0.07	0.66	0.16	0.06	0.15	0.63	0.71	0.05	0.001	1169	1169	324	880	0.05	0.0008	1120	17	816
M52121111	0.9	30	3	600	8	8	0.6	1.5	0.86	0.16	0.06	0.69	0.14	0.06	0.17	0.67	0.71	0.04	0.001	1391	1391	502	936	0.04	0.0007	1355	21	886
M52121112	0.9	30	3	600	8	8	0.6	2.5	0.89	0.17	0.07	0.69	0.14	0.06	0.17	0.66	0.71	0.05	0.001	1334	1334	482	899	0.04	0.0007	1297	20	848
M12121121	0.1	30	3	600	8	8	1	1.5	0.97	0.16	0.06	0.63	0.19	0.07	0.15	0.67	0.71	0.05	0.001	1205	1205	46	1167	0.05	0.0008	1121	17	1080
M12121122	0.1	30	3	600	8	8	1	2.5	1.01	0.16	0.06	0.63	0.19	0.07	0.15	0.66	0.71	0.06	0.001	1156	1156	44	1120	0.06	0.0008	1071	16	1032
M22121121	0.3	30	3	600	8	8	1	1.5	0.90	0.15	0.06	0.64	0.18	0.06	0.16	0.68	0.71	0.05	0.001	1289	1289	149	1157	0.05	0.0007	1218	19	1077
M22121122	0.3	30	3	600	8	8	1	2.5	0.94	0.16	0.06	0.64	0.18	0.06	0.16	0.67	0.71	0.05	0.001	1243	1243	144	1117	0.05	0.0008	1171	18	1036
M32121121	0.5	30	3	600	8	8	1	1.5	0.83	0.15	0.06	0.65	0.17	0.06	0.18	0.69	0.71	0.05	0.001	1409	1409	276	1159	0.05	0.0007	1350	21	1088
M32121122	0.5	30	3	600	8	8	1	2.5	0.87	0.15	0.06	0.65	0.17	0.06	0.17	0.68	0.71	0.05	0.001	1351	1351	264	1113	0.05	0.0007	1292	20	1041
M42121121	0.7	30	3	600	8	8	1	1.5	0.75	0.14	0.05	0.66	0.16	0.06	0.20	0.71	0.71	0.04	0.001	1560	1560	432	1164	0.04	0.0006	1514	23	1103
M42121122	0.7	30	3	600	8	8	1	2.5	0.78	0.15	0.06	0.66	0.16	0.06	0.19	0.70	0.71	0.04	0.001	1502	1502	416	1122	0.04	0.0006	1456	23	1061
M52121121	0.9	30	3	600	8	8	1	1.5	0.67	0.13	0.05	0.69	0.14	0.06	0.23	0.71	0.71	0.03	0.001	1797	1797	642	1199	0.03	0.0005	1766	28	1155
M52121122	0.9	30	3	600	8	8	1	2.5	0.70	0.13	0.05	0.69	0.14	0.06	0.22	0.71	0.71	0.04	0.001	1729	1729	619	1155	0.04	0.0006	1697	27	1110
M12121211	0.1	30	3	600	8	10	0.6	1.5	2.82	0.46	0.17	0.63	0.19	0.07	0.04	0.33	0.66	0.12	0.002	376	376	13	367	0.12	0.0018	295	4	284
M12121212	0.1	30	3	600	8	10	0.6	2.5	2.94	0.48	0.17	0.63	0.19	0.07	0.04	0.32	0.65	0.13	0.002	358	358	12	350	0.12	0.0019	277	4	267
M22121211	0.3	30	3	600	8	10	0.6	1.5	2.63	0.45	0.16	0.64	0.18	0.06	0.04	0.34	0.66	0.12	0.002	401	401	43	370	0.12	0.0017	331	5	292
M22121212	0.3	30	3	600	8	10	0.6	2.5	2.74	0.47	0.17	0.64	0.18	0.06	0.04	0.33	0.65	0.12	0.002	381	381	41	352	0.12	0.0017	311	5	275
M32121211	0.5	30	3	600	8	10	0.6	1.5	2.42	0.43	0.16	0.65	0.17	0.06	0.05	0.35	0.67	0.11	0.002	438	438	83	375	0.11	0.0016	379	6	305
M32121212	0.5	30	3	600	8	10	0.6	2.5	2.52	0.45	0.17	0.65	0.17	0.06	0.05	0.34	0.66	0.11	0.002	415	415	78	356	0.11	0.0016	356	5	287
M42121211	0.7	30	3	600	8	10	0.6	1.5	2.19	0.41	0.16	0.66	0.16	0.06	0.06	0.37	0.68	0.10	0.002	495	495	138	385	0.10	0.0015	448	7	326
M42121212	0.7	30	3	600	8	10	0.6	2.5	2.29	0.42	0.16	0.66	0.16	0.06	0.06	0.35	0.67	0.10	0.002	468	468	130	365	0.10	0.0015	420	6	306
M52121211	0.9	30	3	600	8	10	0.6	1.5	1.95	0.36	0.15	0.69	0.14	0.06	0.07	0.40	0.69	0.09	0.001	581	581	216	403	0.09	0.0014	543	9	355
M52121212	0.9	30	3	600	8	10	0.6	2.5	2.03	0.38	0.15	0.69	0.14	0.06	0.07	0.38	0.68	0.09	0.001	554	554	206	385	0.09	0.0015	516	8	337
M12121221	0.1	30	3	600	8	10	1	1.5	2.38	0.39	0.14	0.63	0.19	0.07	0.05	0.38	0.71	0.11	0.002	461	461	16	449	0.11	0.0017	380	6	366
M12121222	0.1	30	3	600	8	10	1	2.5	2.49	0.41	0.15	0.63	0.19	0.07	0.05	0.37	0.70	0.11	0.002	437	437	15	426	0.11	0.0017	356	5	343
M22121221	0.3	30	3	600	8	10	1	1.5	2.22	0.38	0.14	0.64	0.18	0.06	0.06	0.38	0.71	0.11	0.002	497	497	55	455	0.11	0.0016	428	7	378
M22121222	0.3	30	3	600	8	10	1	2.5	2.32	0.40	0.14	0.64	0.18	0.06	0.05	0.37	0.70	0.11	0.002	470	470	52	431	0.11	0.0016	400	6	354
M32121221	0.5	30	3	600	8	10	1	1.5	2.04	0.36	0.14	0.65	0.17	0.06	0.07	0.40	0.71	0.10	0.002	550	550	105	466	0.10	0.0015	492	8	396
M32121222	0.5	30	3	600	8	10	1	2.5	2.13	0.38	0.14	0.65	0.17	0.06	0.06	0.38	0.70	0.10	0.002	517	517	99	439	0.10	0.0015	459	7	370
M42121221	0.7	30	3	600	8	10	1	1.5	1.85	0.34	0.13	0.66	0.16	0.06	0.07	0.42	0.71	0.09	0.001	610	610	169	470	0.09	0.0013	562	9	409
M42121222	0.7	30	3	600	8	10	1	2.5	1.93	0.36	0.14	0.66	0.16	0.06	0.07	0.40	0.71	0.09	0.001	583	583	162	450	0.09	0.0014	535	8	390
M52121221	0.9	30	3	600	8	10	1	1.5	1.64	0.31	0.12	0.69	0.14	0.06	0.08	0.45	0.71	0.08	0.001	692	692	256	478	0.08	0.0012	654	10	427
M52121222	0.9	30	3	600	8	10	1	2.5	1.72	0.32	0.13	0.69	0.14	0.06	0.08	0.44	0.71	0.08	0.001	663	663	246	458	0.08	0.0013	624	10	408
M12122111	0.1	30	3	600	10	8	0.6	1.5	1.69	0.28	0.10	0.63	0.19	0.07	0.08	0.48	0.71	0.09	0.001	680	680	25	661	0.09	0.0013	598	9	577
M12122112	0.1	30	3	600	10	8	0.6	2.5	1.82	0.30	0.11	0.63	0.19	0.07	0.08	0.46	0.71	0.09	0.001	635	635	23	617	0.09	0.0014	553	8	533
M22122111	0.3	30	3	600	10	8	0.6	1.5	1.58	0.27	0.10	0.64	0.18	0.06	0.09	0.49	0.71	0.08	0.001	724	724	82	657	0.08	0.0012	653	10	578
M22122112	0.3	30	3	600	10	8	0.6	2.5	1.69	0.29	0.11	0.64	0.18	0.06	0.08	0.47	0.71	0.09	0.001	675	675	76	613	0.09	0.0013	604	9	534
M32122111	0.5	30	3	600	10	8	0.6	1.5	1.45	0.26	0.10	0.65	0.17	0.06	0.10	0.50	0.71	0.08	0.001	785	785	152	656	0.08	0.0011	725	11	584
M32122112	0.5	30	3	600	10	8	0.6	2.5	1.56	0.28	0.10	0.65	0.17	0.06	0.09	0.48	0.71	0.08	0.001	729	729	141	611	0.08	0.0012	669	10	539
M42122111	0.7	30	3	600	10	8	0.6	1.5	1.32	0.24	0.09	0.66	0.16	0.06	0.11	0.53	0.71	0.07	0.001	871	871	242	663	0.07	0.0010	823	13	599
M42122112	0.7	30	3	600	10	8	0.6	2.5	1.41	0.26	0.10	0.66	0.16	0.06	0.10	0.50	0.71	0.07	0.001	806	806	224	614	0.07	0.0010	758	12	553
M52122111	0.9	30	3	600	10	8	0.6	1.5	1.17	0.22	0.09	0.69	0.14	0.06	0.12	0.57	0.71	0.06	0.001	1000	1000	366	681	0.06	0.0009	962	15	629
M52122112	0.9	30	3	600	10	8	0.6	2.5	1.25	0.23	0.09	0.69	0.14	0.06	0.11	0.54	0.71	0.06	0.001	924	924	339	631	0.06	0.0010	886	14	579
M12122121	0.1	30	3	600	10	8	1	1.5	1.35	0.22	0.08	0.63	0.19	0.07	0.11	0.57	0.71	0.07	0.001	856	856	32	831	0.07	0.0011	769	12	742
M12122122	0.1	30	3	600	10	8	1	2.5	1.46	0.24	0.09	0.63	0.19	0.07	0.10	0.54	0.71	0.08	0.001	789	789	29	766	0.08	0.0012	704	11	679
M22122121	0.3	30	3	600	10	8	1	1.5	1.26	0.21	0.08	0.64	0.18	0.06	0.11	0.58	0.71	0.07	0.001	915	915	105	827	0.07	0.0010	840	13	743
M22122122	0.3	30	3	600	10	8	1	2.5	1.36	0.23	0.08	0.64	0.18	0.06	0.10	0.55	0.71	0.07	0.001	843	843	96	763	0.07	0.0011	770	12	681
M32122121	0.5	30	3	600	10	8	1	1.5	1.16	0.21	0.08	0.65	0.17	0.06	0.13	0.59	0.71	0.06	0.001	998	998	194	829	0.06	0.0009	935	14	754
M32122122	0.5	30	3	600	10	8	1	2.5	1.25	0.22	0.08	0.65	0.17	0.06	0.11	0.56	0.71	0.07	0.001	916	916	178	763	0.07	0.0010	854	13	688
M42122121	0.7	30	3	600	10	8	1	1.5	1.05	0.19	0.08	0.66	0.16	0.06	0.14	0.61	0.71	0.06	0.001	1114	1114	309	841	0.06	0.0008	1065	16	776
M42122122	0.7	30	3	600	10	8	1	2.5	1.14	0.21	0.08	0.66	0.16	0.06	0.13	0.58	0.71	0.06	0.001	1019	1019	283	771	0.06	0.0009	969	15	706
M52122121	0.9	30	3	600	10	8	1	1.5	0.93	0.17	0.07	0.69	0.14	0.06	0.16	0.65	0.71	0.05	0.001	1277	1277	462	862	0.05	0.0007	1240	19	811
M52122122	0.9	30	3	600	10	8	1	2.5	1.01	0.19	0.08	0.69	0.14	0.06	0.15	0.62	0.71	0.05	0.001	1174	1174	427	795	0.05	0.0008	1137	18	743
M12122211	0.1	30	3	600	10	10	0.6	1.5	4.04	0.66	0.24	0.63	0.19	0.07	0.02	0.23	0.54	0.15	0.003	244	244	8	239	0.15	0.0022	176	3	170
M12122212	0.1	30	3	600	10	10	0.6	2.5	4.41	0.72	0.26	0.63	0.19	0.07	0.02	0.21	0.50	0.16	0.003	220	220	7	216	0.16	0.0024	156	2	150
M22122211	0.3	30	3	600	10	10	0.6	1.5	3.76	0.64	0.23	0.64	0.18	0.06	0.03	0.24	0.54	0.14	0.002	256	256	27	239	0.14	0.0021	197	3	174
M22122212	0.3	30	3	600	10	10	0.6	2.5	4.11	0.70	0.26	0.64	0.18	0.06	0.02	0.22	0.50	0.15	0.002	231	231	24	216	0.15	0.0022	174	3	154
M32122211	0.5	30	3	600	10	10	0.6	1.5	3.46	0.62	0.23	0.65	0.17	0.06	0.03	0.25	0.55	0.13	0.002	276	276	51	241	0.13	0.0019	224	3	180
M32122212	0.5	30	3	600	10	10	0.6	2.5	3.78	0.67	0.25	0.65	0.17	0.06	0.03	0.23	0.51	0.14	0.002	247	247	46	217	0.14	0.0020	197	3	159
M42122211	0.7	30	3	600	10	10	0.6	1.5	3.14	0.58	0.22	0.66	0.16	0.06	0.03	0.27	0.56	0.12	0.002	307	307	85	246	0.12	0.0018	262	4	191
M42122212	0.7	30	3	600	10	10	0.6	2.5	3.43	0.64	0.24	0.66	0.16	0.06	0.03	0.24	0.52	0.13	0.002	273	273	76	219	0.13	0.0019	230	4	168
M52122211	0.9	30	3	600	10	10	0.6	1.5	2.78	0.52	0.21	0.69	0.14	0.06	0.04	0.30	0.59	0.11	0.002	357	357	137	255	0.11	0.0017	319	5	208
M52122212	0.9	30	3	600	10	10	0.6	2.5	3.04	0.57	0.23	0.69	0.14	0.06	0.04	0.27	0.55	0.11	0.002	317	317	122	228	0.11	0.0018	280	4	183
M12122221	0.1	30	3	600	10	10	1	1.5	3.48	0.57	0.20	0.63	0.19	0.07	0.03	0.27	0.59	0.14	0.002	292	292	10	286	0.14	0.0020	217	3	209
M12122222	0.1	30	3	600	10	10	1	2.5	3.84	0.63	0.22	0.63	0.19	0.07	0.03	0.24	0.56	0.15	0.002	259	259	8	254	0.14	0.0022	189	3	182
M22122221	0.3	30	3	600	10	10	1	1.5	3.25	0.55	0.20	0.64	0.18	0.06	0.03	0.28	0.60	0.13	0.002	309	309	33	287	0.13	0.0019	243	4	215
M22122222	0.3	30	3	600	10	10	1	2.5	3.58	0.61	0.22	0.64	0.18	0.06	0.03	0.25	0.56	0.14	0.002	273	273	29	255	0.14	0.0020	211	3	187
M32122221	0.5	30	3	600	10	10	1	1.5	2.99	0.53	0.20	0.65	0.17	0.06	0.04	0.29	0.60	0.12	0.002	334	334	62	290	0.12	0.0018	277	4	223
M32122222	0.5	30	3	600	10	10	1	2.5	3.29	0.59	0.22	0.65	0.17	0.06	0.03	0.26	0.57	0.13	0.002	295	295	55	257	0.13	0.0019	240	4	194
M42122221	0.7	30	3	600	10	10	1	1.5	2.71	0.50	0.19	0.66	0.16	0.06	0.04	0.31	0.61	0.11	0.002	373	373	104	295	0.11	0.0017	325	5	237

Name	af	nf	hf	mf	Ly	Lx	tw	Lcb	T1 [s]	T2 [s]	T3 [s]	M1 [-]	M2 [-]	M3 [-]	Sa	Sa2	Sa3	Disp [m]	ISDR [-]	Total Moment [MN-m]	Total Shear [MN]	Outrigger Moment [MN-m]	Wall Moment [MN-m]	Mode 1 Disp [m]	Mode 1 ISDR [-]	Mode 1 Moment [MN-m]	Mode 1 Shear [MN]	Mode 1 wall Moment [MN-m]
M42122222	0.7	30	3	600	10	10	1	2.5	2.99	0.55	0.21	0.66	0.16	0.06	0.04	0.28	0.58	0.12	0.002	328	328	91	262	0.12	0.0017	282	4	205
M52122221	0.9	30	3	600	10	10	1	1.5	2.40	0.45	0.18	0.69	0.14	0.06	0.05	0.34	0.64	0.10	0.002	437	437	165	308	0.10	0.0016	397	6	260
M52122222	0.9	30	3	600	10	10	1	2.5	2.65	0.50	0.20	0.69	0.14	0.06	0.04	0.31	0.60	0.11	0.002	382	382	146	272	0.11	0.0017	343	5	224
M12211111	0.1	30	4	400	8	8	0.6	1.5	0.98	0.16	0.06	0.63	0.19	0.07	0.15	0.67	0.71	0.06	0.001	1059	1059	40	1026	0.06	0.0006	984	11	948
M12211112	0.1	30	4	400	8	8	0.6	2.5	1.01	0.16	0.06	0.63	0.19	0.07	0.15	0.66	0.71	0.06	0.001	1029	1029	39	997	0.06	0.0006	954	11	919
M22211111	0.3	30	4	400	8	8	0.6	1.5	0.91	0.16	0.06	0.64	0.18	0.06	0.16	0.68	0.71	0.05	0.001	1135	1135	131	1019	0.05	0.0006	1071	12	947
M22211112	0.3	30	4	400	8	8	0.6	2.5	0.94	0.16	0.06	0.64	0.18	0.06	0.16	0.67	0.71	0.05	0.001	1106	1106	128	994	0.05	0.0006	1042	12	922
M32211111	0.5	30	4	400	8	8	0.6	1.5	0.84	0.15	0.06	0.65	0.17	0.06	0.18	0.69	0.71	0.05	0.001	1238	1238	242	1019	0.05	0.0005	1185	14	955
M32211112	0.5	30	4	400	8	8	0.6	2.5	0.86	0.15	0.06	0.65	0.17	0.06	0.17	0.68	0.71	0.05	0.001	1203	1203	235	991	0.05	0.0005	1150	13	927
M42211111	0.7	30	4	400	8	8	0.6	1.5	0.76	0.14	0.05	0.66	0.16	0.06	0.20	0.70	0.71	0.04	0.000	1369	1369	379	1022	0.04	0.0005	1328	15	968
M42211112	0.7	30	4	400	8	8	0.6	2.5	0.78	0.15	0.06	0.66	0.16	0.06	0.19	0.70	0.71	0.04	0.000	1337	1337	370	998	0.04	0.0005	1295	15	944
M52211111	0.9	30	4	400	8	8	0.6	1.5	0.68	0.13	0.05	0.69	0.14	0.06	0.23	0.71	0.71	0.04	0.000	1581	1581	565	1055	0.04	0.0004	1553	18	1015
M52211112	0.9	30	4	400	8	8	0.6	2.5	0.69	0.13	0.05	0.69	0.14	0.06	0.22	0.71	0.71	0.04	0.000	1539	1539	551	1028	0.04	0.0004	1511	18	988
M12211121	0.1	30	4	400	8	8	1	1.5	0.75	0.12	0.04	0.63	0.19	0.07	0.20	0.71	0.71	0.04	0.000	1378	1378	53	1332	0.04	0.0005	1314	15	1266
M12211122	0.1	30	4	400	8	8	1	2.5	0.77	0.13	0.05	0.63	0.19	0.07	0.20	0.71	0.71	0.04	0.001	1338	1338	52	1294	0.04	0.0005	1272	14	1226
M22211121	0.3	30	4	400	8	8	1	1.5	0.70	0.12	0.04	0.64	0.18	0.06	0.22	0.71	0.71	0.04	0.000	1491	1491	175	1331	0.04	0.0004	1438	16	1272
M22211122	0.3	30	4	400	8	8	1	2.5	0.72	0.12	0.04	0.64	0.18	0.06	0.21	0.71	0.71	0.04	0.000	1450	1450	170	1295	0.04	0.0004	1395	16	1234
M32211121	0.5	30	4	400	8	8	1	1.5	0.64	0.11	0.04	0.65	0.17	0.06	0.24	0.71	0.71	0.04	0.000	1619	1619	318	1323	0.04	0.0004	1577	18	1271
M32211122	0.5	30	4	400	8	8	1	2.5	0.66	0.12	0.04	0.65	0.17	0.06	0.23	0.71	0.71	0.04	0.000	1581	1581	310	1292	0.04	0.0004	1537	18	1238
M42211121	0.7	30	4	400	8	8	1	1.5	0.58	0.11	0.04	0.66	0.16	0.06	0.27	0.71	0.71	0.03	0.000	1833	1833	506	1354	0.03	0.0004	1802	21	1313
M42211122	0.7	30	4	400	8	8	1	2.5	0.60	0.11	0.04	0.66	0.16	0.06	0.26	0.71	0.71	0.03	0.000	1778	1778	491	1315	0.03	0.0004	1746	20	1272
M52211121	0.9	30	4	400	8	8	1	1.5	0.52	0.10	0.04	0.69	0.14	0.06	0.30	0.71	0.71	0.03	0.000	2091	2091	740	1383	0.03	0.0003	2070	24	1354
M52211122	0.9	30	4	400	8	8	1	2.5	0.53	0.10	0.04	0.69	0.14	0.06	0.29	0.71	0.71	0.03	0.000	2041	2041	723	1351	0.03	0.0003	2019	24	1320
M12211211	0.1	30	4	400	8	10	0.6	1.5	2.18	0.36	0.13	0.63	0.19	0.07	0.06	0.41	0.71	0.11	0.001	459	459	16	447	0.11	0.0012	386	4	372
M12211212	0.1	30	4	400	8	10	0.6	2.5	2.25	0.37	0.13	0.63	0.19	0.07	0.06	0.40	0.71	0.11	0.001	441	441	16	430	0.11	0.0012	369	4	355
M22211211	0.3	30	4	400	8	10	0.6	1.5	2.03	0.35	0.13	0.64	0.18	0.06	0.07	0.41	0.71	0.10	0.001	497	497	55	454	0.10	0.0011	435	5	385
M22211212	0.3	30	4	400	8	10	0.6	2.5	2.10	0.36	0.13	0.64	0.18	0.06	0.06	0.40	0.71	0.10	0.001	478	478	53	436	0.10	0.0011	416	5	368
M32211211	0.5	30	4	400	8	10	0.6	1.5	1.87	0.33	0.12	0.65	0.17	0.06	0.07	0.43	0.71	0.09	0.001	538	538	103	454	0.09	0.0010	486	6	391
M32211212	0.5	30	4	400	8	10	0.6	2.5	1.93	0.34	0.13	0.65	0.17	0.06	0.07	0.42	0.71	0.10	0.001	522	522	100	441	0.10	0.0010	470	5	379
M42211211	0.7	30	4	400	8	10	0.6	1.5	1.70	0.31	0.12	0.66	0.16	0.06	0.08	0.45	0.71	0.08	0.001	593	593	165	456	0.08	0.0009	550	6	401
M42211212	0.7	30	4	400	8	10	0.6	2.5	1.75	0.32	0.12	0.66	0.16	0.06	0.08	0.44	0.71	0.09	0.001	575	575	160	442	0.09	0.0010	532	6	387
M52211211	0.9	30	4	400	8	10	0.6	1.5	1.51	0.28	0.11	0.69	0.14	0.06	0.09	0.48	0.71	0.07	0.001	674	674	249	463	0.07	0.0009	641	8	419
M52211212	0.9	30	4	400	8	10	0.6	2.5	1.55	0.29	0.12	0.69	0.14	0.06	0.09	0.47	0.71	0.07	0.001	654	654	242	450	0.07	0.0009	620	7	406
M12211221	0.1	30	4	400	8	10	1	1.5	1.76	0.29	0.10	0.63	0.19	0.07	0.08	0.47	0.71	0.09	0.001	581	581	21	564	0.09	0.0010	508	6	489
M12211222	0.1	30	4	400	8	10	1	2.5	1.82	0.30	0.11	0.63	0.19	0.07	0.08	0.46	0.71	0.09	0.001	564	564	21	549	0.09	0.0011	491	6	474
M22211221	0.3	30	4	400	8	10	1	1.5	1.64	0.28	0.10	0.64	0.18	0.06	0.08	0.48	0.71	0.09	0.001	617	617	70	560	0.09	0.0009	554	6	490
M22211222	0.3	30	4	400	8	10	1	2.5	1.69	0.29	0.11	0.64	0.18	0.06	0.08	0.47	0.71	0.09	0.001	600	600	68	545	0.09	0.0010	536	6	474
M32211221	0.5	30	4	400	8	10	1	1.5	1.51	0.27	0.10	0.65	0.17	0.06	0.09	0.49	0.71	0.08	0.001	667	667	129	559	0.08	0.0008	615	7	495
M32211222	0.5	30	4	400	8	10	1	2.5	1.56	0.28	0.10	0.65	0.17	0.06	0.09	0.48	0.71	0.08	0.001	648	648	125	543	0.08	0.0009	595	7	479
M42211221	0.7	30	4	400	8	10	1	1.5	1.37	0.25	0.10	0.66	0.16	0.06	0.10	0.51	0.71	0.07	0.001	740	740	206	563	0.07	0.0008	697	8	508
M42211222	0.7	30	4	400	8	10	1	2.5	1.41	0.26	0.10	0.66	0.16	0.06	0.10	0.50	0.71	0.07	0.001	716	716	199	546	0.07	0.0008	674	8	491
M52211221	0.9	30	4	400	8	10	1	1.5	1.22	0.23	0.09	0.69	0.14	0.06	0.12	0.55	0.71	0.06	0.001	851	851	311	580	0.06	0.0007	817	10	534
M52211222	0.9	30	4	400	8	10	1	2.5	1.25	0.24	0.09	0.69	0.14	0.06	0.11	0.54	0.71	0.06	0.001	821	821	301	560	0.06	0.0007	787	9	515
M12212111	0.1	30	4	400	10	8	0.6	1.5	1.32	0.22	0.08	0.63	0.19	0.07	0.11	0.58	0.71	0.07	0.001	780	780	29	757	0.07	0.0008	703	8	677
M12212112	0.1	30	4	400	10	8	0.6	2.5	1.39	0.23	0.08	0.63	0.19	0.07	0.10	0.56	0.71	0.07	0.001	740	740	28	718	0.07	0.0008	663	8	639
M22212111	0.3	30	4	400	10	8	0.6	1.5	1.23	0.21	0.08	0.64	0.18	0.06	0.12	0.59	0.71	0.07	0.001	835	835	96	754	0.07	0.0007	769	9	680
M22212112	0.3	30	4	400	10	8	0.6	2.5	1.29	0.22	0.08	0.64	0.18	0.06	0.11	0.57	0.71	0.07	0.001	793	793	90	716	0.07	0.0008	726	8	642
M32212111	0.5	30	4	400	10	8	0.6	1.5	1.13	0.20	0.08	0.65	0.17	0.06	0.13	0.60	0.71	0.06	0.001	909	909	177	755	0.06	0.0007	853	10	687
M32212112	0.5	30	4	400	10	8	0.6	2.5	1.19	0.21	0.08	0.65	0.17	0.06	0.12	0.58	0.71	0.06	0.001	864	864	168	718	0.06	0.0007	808	9	651
M42212111	0.7	30	4	400	10	8	0.6	1.5	1.03	0.19	0.07	0.66	0.16	0.06	0.14	0.62	0.71	0.05	0.001	1015	1015	282	765	0.05	0.0006	971	11	707
M42212112	0.7	30	4	400	10	8	0.6	2.5	1.08	0.20	0.08	0.66	0.16	0.06	0.14	0.60	0.71	0.06	0.001	963	963	267	727	0.06	0.0006	919	11	670
M52212111	0.9	30	4	400	10	8	0.6	1.5	0.91	0.17	0.07	0.69	0.14	0.06	0.16	0.65	0.71	0.05	0.001	1161	1161	420	783	0.05	0.0005	1129	13	738
M52212112	0.9	30	4	400	10	8	0.6	2.5	0.96	0.18	0.07	0.69	0.14	0.06	0.16	0.64	0.71	0.05	0.001	1106	1106	401	747	0.05	0.0006	1073	13	702
M12212121	0.1	30	4	400	10	8	1	1.5	1.02	0.17	0.06	0.63	0.19	0.07	0.14	0.66	0.71	0.06	0.001	1017	1017	39	985	0.06	0.0006	941	11	907
M12212122	0.1	30	4	400	10	8	1	2.5	1.08	0.18	0.06	0.63	0.19	0.07	0.14	0.64	0.71	0.06	0.001	964	964	36	935	0.06	0.0007	888	10	856
M22212121	0.3	30	4	400	10	8	1	1.5	0.95	0.16	0.06	0.64	0.18	0.06	0.16	0.67	0.71	0.05	0.001	1093	1093	126	982	0.05	0.0006	1029	12	910
M22212122	0.3	30	4	400	10	8	1	2.5	1.00	0.17	0.06	0.64	0.18	0.06	0.15	0.65	0.71	0.06	0.001	1034	1034	119	930	0.06	0.0006	969	11	857
M32212121	0.5	30	4	400	10	8	1	1.5	0.88	0.16	0.06	0.65	0.17	0.06	0.17	0.68	0.71	0.05	0.001	1186	1186	232	978	0.05	0.0005	1133	13	913
M32212122	0.5	30	4	400	10	8	1	2.5	0.92	0.16	0.06	0.65	0.17	0.06	0.16	0.66	0.71	0.05	0.001	1127	1127	220	930	0.05	0.0005	1073	12	865
M42212121	0.7	30	4	400	10	8	1	1.5	0.79	0.15	0.06	0.66	0.16	0.06	0.19	0.69	0.71	0.04	0.000	1321	1321	366	987	0.04	0.0005	1280	15	933
M42212122	0.7	30	4	400	10	8	1	2.5	0.84	0.15	0.06	0.66	0.16	0.06	0.18	0.68	0.71	0.05	0.000	1254	1254	347	938	0.04	0.0005	1212	14	883
M52212121	0.9	30	4	400	10	8	1	1.5	0.70	0.13	0.05	0.69	0.14	0.06	0.22	0.71	0.71	0.04	0.000	1520	1520	544	1016	0.04	0.0004	1491	18	975
M52212122	0.9	30	4	400	10	8	1	2.5	0.74	0.14	0.06	0.69	0.14	0.06	0.20	0.71	0.71	0.04	0.000	1433	1433	515	960	0.04	0.0005	1403	17	917
M12212211	0.1	30	4	400	10	10	0.6	1.5	3.07	0.50	0.18	0.63	0.19	0.07	0.04	0.31	0.64	0.13	0.002	302	302	10	295	0.13	0.0014	231	3	223
M12212212	0.1	30	4	400	10	10	0.6	2.5	3.27	0.53	0.19	0.63	0.19	0.07	0.03	0.29	0.62	0.13	0.002	281	281	9	274	0.13	0.0015	212	2	204
M22212211	0.3	30	4	400	10	10	0.6	1.5	2.86	0.49	0.18	0.64	0.18	0.06	0.04	0.32	0.64	0.12	0.001	321	321	34	297	0.12	0.0013	259	3	229
M22212212	0.3	30	4	400	10	10	0.6	2.5	3.04	0.52	0.19	0.64	0.18	0.06	0.04	0.30	0.62	0.13	0.001	297	297	32	276	0.12	0.0014	237	3	210
M32212211	0.5	30	4	400	10	10	0.6	1.5	2.64	0.47	0.18	0.65	0.17	0.06	0.04	0.33	0.64	0.11	0.001	349	349	66	300	0.11	0.0012	296	3	239
M32212212	0.5	30	4	400	10	10	0.6	2.5	2.80	0.50	0.19	0.65	0.17	0.06	0.04	0.31	0.62	0.12	0.001	322	322	61	279	0.12	0.0013	271	3	218
M42212211	0.7	30	4	400	10	10	0.6	1.5	2.39	0.44	0.17	0.66	0.16	0.06	0.05	0.34	0.65	0.11	0.001	392	392	109	307	0.11	0.0012	349	4	254
M42212212	0.7	30	4	400	10	10	0.6	2.5	2.54	0.47	0.18	0.66	0.16	0.06	0.05	0.33	0.63	0.11	0.001	361	361	100	285	0.11	0.0012	318	4	232
M52212211	0.9	30	4	400	10	10	0.6	1.5	2.12	0.40	0.16	0.69	0.14	0.06	0.06	0.37	0.67	0.10	0.001	462	462	173	323	0.09	0.0011	429	5	280

Name	af	nf	hf	mf	Ly	Lx	tw	Lcb	T1 [s]	T2 [s]	T3 [s]	M1 [-]	M2 [-]	M3 [-]	Sa	Sa2	Sa3	Disp [m]	ISDR [-]	Total Moment [MN-m]	Total Shear [MN]	Outrigger Moment [MN-m]	Wall Moment [MN-m]	Mode 1 Disp [m]	Mode 1 ISDR [-]	Mode 1 Moment [MN-m]	Mode 1 Shear [MN]	Mode 1 wall Moment [MN-m]
M52212212	0.9	30	4	400	10	10	0.6	2.5	2.25	0.42	0.17	0.69	0.14	0.06	0.06	0.36	0.65	0.10	0.001	425	425	160	298	0.10	0.0012	390	5	255
M12212221	0.1	30	4	400	10	10	1	1.5	2.53	0.41	0.15	0.63	0.19	0.07	0.05	0.36	0.69	0.12	0.001	382	382	13	372	0.11	0.0013	309	4	298
M12212222	0.1	30	4	400	10	10	1	2.5	2.70	0.44	0.16	0.63	0.19	0.07	0.04	0.35	0.67	0.12	0.001	353	353	12	345	0.12	0.0013	281	3	270
M22212221	0.3	30	4	400	10	10	1	1.5	2.35	0.40	0.15	0.64	0.18	0.06	0.05	0.37	0.69	0.11	0.001	410	410	45	376	0.11	0.0012	348	4	308
M22212222	0.3	30	4	400	10	10	1	2.5	2.51	0.43	0.16	0.64	0.18	0.06	0.05	0.35	0.68	0.11	0.001	377	377	41	347	0.11	0.0012	315	4	278
M32212221	0.5	30	4	400	10	10	1	1.5	2.17	0.39	0.14	0.65	0.17	0.06	0.06	0.38	0.70	0.10	0.001	451	451	86	383	0.10	0.0011	400	5	322
M32212222	0.5	30	4	400	10	10	1	2.5	2.31	0.41	0.15	0.65	0.17	0.06	0.05	0.36	0.68	0.11	0.001	414	414	79	353	0.11	0.0012	361	4	291
M42212221	0.7	30	4	400	10	10	1	1.5	1.96	0.36	0.14	0.66	0.16	0.06	0.07	0.40	0.71	0.10	0.001	510	510	142	394	0.10	0.0011	468	5	341
M42212222	0.7	30	4	400	10	10	1	2.5	2.10	0.39	0.15	0.66	0.16	0.06	0.06	0.38	0.69	0.10	0.001	469	469	130	363	0.10	0.0011	427	5	311
M52212221	0.9	30	4	400	10	10	1	1.5	1.74	0.33	0.13	0.69	0.14	0.06	0.08	0.43	0.71	0.08	0.001	580	580	215	401	0.08	0.0010	546	6	357
M52212222	0.9	30	4	400	10	10	1	2.5	1.86	0.35	0.14	0.69	0.14	0.06	0.07	0.41	0.71	0.09	0.001	542	542	202	376	0.09	0.0010	508	6	332
M12221111	0.1	30	4	600	8	8	0.6	1.5	1.20	0.20	0.07	0.63	0.19	0.07	0.12	0.61	0.71	0.07	0.001	1289	1289	48	1250	0.07	0.0007	1172	13	1130
M12221112	0.1	30	4	600	8	8	0.6	2.5	1.23	0.20	0.07	0.63	0.19	0.07	0.12	0.60	0.71	0.07	0.001	1252	1252	47	1215	0.07	0.0008	1136	13	1095
M22221111	0.3	30	4	600	8	8	0.6	1.5	1.12	0.19	0.07	0.64	0.18	0.06	0.13	0.62	0.71	0.06	0.001	1382	1382	159	1245	0.06	0.0007	1282	15	1134
M22221112	0.3	30	4	600	8	8	0.6	2.5	1.15	0.20	0.07	0.64	0.18	0.06	0.13	0.61	0.71	0.06	0.001	1342	1342	154	1210	0.06	0.0007	1242	14	1098
M32221111	0.5	30	4	600	8	8	0.6	1.5	1.03	0.18	0.07	0.65	0.17	0.06	0.14	0.63	0.71	0.06	0.001	1509	1509	294	1250	0.06	0.0006	1427	16	1150
M32221112	0.5	30	4	600	8	8	0.6	2.5	1.06	0.19	0.07	0.65	0.17	0.06	0.14	0.62	0.71	0.06	0.001	1469	1469	286	1217	0.06	0.0006	1386	16	1117
M42221111	0.7	30	4	600	8	8	0.6	1.5	0.93	0.17	0.07	0.66	0.16	0.06	0.16	0.65	0.71	0.05	0.001	1679	1679	465	1261	0.05	0.0005	1614	19	1176
M42221112	0.7	30	4	600	8	8	0.6	2.5	0.96	0.18	0.07	0.66	0.16	0.06	0.16	0.64	0.71	0.05	0.001	1634	1634	453	1229	0.05	0.0006	1569	18	1144
M52221111	0.9	30	4	600	8	8	0.6	1.5	0.83	0.16	0.06	0.69	0.14	0.06	0.18	0.68	0.71	0.04	0.001	1922	1922	693	1292	0.04	0.0005	1875	22	1226
M52221112	0.9	30	4	600	8	8	0.6	2.5	0.85	0.16	0.06	0.69	0.14	0.06	0.18	0.67	0.71	0.04	0.001	1868	1868	674	1257	0.04	0.0005	1821	21	1190
M12221121	0.1	30	4	600	8	8	1	1.5	0.92	0.15	0.05	0.63	0.19	0.07	0.16	0.69	0.71	0.05	0.001	1700	1700	65	1646	0.05	0.0006	1589	18	1532
M12221122	0.1	30	4	600	8	8	1	2.5	0.94	0.15	0.06	0.63	0.19	0.07	0.16	0.68	0.71	0.05	0.001	1656	1656	63	1604	0.05	0.0006	1545	18	1489
M22221121	0.3	30	4	600	8	8	1	1.5	0.85	0.15	0.05	0.64	0.18	0.06	0.18	0.70	0.71	0.05	0.001	1826	1826	212	1637	0.05	0.0005	1732	20	1532
M22221122	0.3	30	4	600	8	8	1	2.5	0.88	0.15	0.05	0.64	0.18	0.06	0.17	0.69	0.71	0.05	0.001	1772	1772	206	1590	0.05	0.0005	1677	19	1483
M32221121	0.5	30	4	600	8	8	1	1.5	0.78	0.14	0.05	0.65	0.17	0.06	0.19	0.71	0.71	0.04	0.000	1988	1988	389	1633	0.04	0.0005	1911	22	1540
M32221122	0.5	30	4	600	8	8	1	2.5	0.81	0.14	0.05	0.65	0.17	0.06	0.19	0.70	0.71	0.04	0.000	1937	1937	379	1592	0.04	0.0005	1859	21	1498
M42221121	0.7	30	4	600	8	8	1	1.5	0.71	0.13	0.05	0.66	0.16	0.06	0.21	0.71	0.71	0.04	0.000	2222	2222	614	1654	0.04	0.0004	2164	25	1577
M42221122	0.7	30	4	600	8	8	1	2.5	0.73	0.14	0.05	0.66	0.16	0.06	0.21	0.71	0.71	0.04	0.000	2156	2156	597	1607	0.04	0.0004	2097	24	1528
M52221121	0.9	30	4	600	8	8	1	1.5	0.63	0.12	0.05	0.69	0.14	0.06	0.24	0.71	0.71	0.03	0.000	2535	2535	904	1688	0.03	0.0004	2496	29	1632
M52221122	0.9	30	4	600	8	8	1	2.5	0.65	0.12	0.05	0.69	0.14	0.06	0.23	0.71	0.71	0.03	0.000	2465	2465	880	1642	0.03	0.0004	2425	29	1585
M12221211	0.1	30	4	600	8	10	0.6	1.5	2.67	0.44	0.16	0.63	0.19	0.07	0.04	0.35	0.68	0.12	0.001	535	535	18	522	0.12	0.0013	426	5	410
M12221212	0.1	30	4	600	8	10	0.6	2.5	2.76	0.45	0.16	0.63	0.19	0.07	0.04	0.34	0.67	0.12	0.001	516	516	18	504	0.12	0.0014	407	5	392
M22221211	0.3	30	4	600	8	10	0.6	1.5	2.49	0.42	0.16	0.64	0.18	0.06	0.05	0.35	0.68	0.11	0.001	572	572	62	526	0.11	0.0012	478	5	423
M22221212	0.3	30	4	600	8	10	0.6	2.5	2.57	0.44	0.16	0.64	0.18	0.06	0.05	0.35	0.67	0.12	0.001	551	551	60	508	0.11	0.0013	457	5	405
M32221211	0.5	30	4	600	8	10	0.6	1.5	2.29	0.41	0.15	0.65	0.17	0.06	0.06	0.36	0.68	0.11	0.001	627	627	119	534	0.11	0.0012	549	6	442
M32221212	0.5	30	4	600	8	10	0.6	2.5	2.36	0.42	0.16	0.65	0.17	0.06	0.05	0.36	0.68	0.11	0.001	603	603	114	515	0.11	0.0012	524	6	423
M42221211	0.7	30	4	600	8	10	0.6	1.5	2.08	0.38	0.15	0.66	0.16	0.06	0.06	0.38	0.69	0.10	0.001	711	711	198	551	0.10	0.0011	649	8	473
M42221212	0.7	30	4	600	8	10	0.6	2.5	2.14	0.40	0.15	0.66	0.16	0.06	0.06	0.37	0.68	0.10	0.001	681	681	189	529	0.10	0.0011	619	7	451
M52221211	0.9	30	4	600	8	10	0.6	1.5	1.84	0.35	0.14	0.69	0.14	0.06	0.07	0.42	0.71	0.09	0.001	820	820	305	568	0.09	0.0010	769	9	503
M52221212	0.9	30	4	600	8	10	0.6	2.5	1.90	0.36	0.14	0.69	0.14	0.06	0.07	0.41	0.70	0.09	0.001	794	794	296	551	0.09	0.0010	743	9	486
M12221221	0.1	30	4	600	8	10	1	1.5	2.16	0.35	0.13	0.63	0.19	0.07	0.06	0.41	0.71	0.11	0.001	698	698	25	680	0.11	0.0012	589	7	568
M12221222	0.1	30	4	600	8	10	1	2.5	2.23	0.36	0.13	0.63	0.19	0.07	0.06	0.40	0.71	0.11	0.001	671	671	24	654	0.11	0.0012	562	6	542
M22221221	0.3	30	4	600	8	10	1	1.5	2.01	0.34	0.13	0.64	0.18	0.06	0.07	0.42	0.71	0.10	0.001	756	756	84	690	0.10	0.0011	663	8	587
M22221222	0.3	30	4	600	8	10	1	2.5	2.07	0.35	0.13	0.64	0.18	0.06	0.06	0.41	0.71	0.10	0.001	727	727	81	663	0.10	0.0011	634	7	561
M32221221	0.5	30	4	600	8	10	1	1.5	1.85	0.33	0.12	0.65	0.17	0.06	0.07	0.43	0.71	0.09	0.001	817	817	157	689	0.09	0.0010	738	8	595
M32221222	0.5	30	4	600	8	10	1	2.5	1.91	0.34	0.13	0.65	0.17	0.06	0.07	0.42	0.71	0.10	0.001	791	791	152	668	0.10	0.0010	713	8	574
M42221221	0.7	30	4	600	8	10	1	1.5	1.68	0.31	0.12	0.66	0.16	0.06	0.08	0.45	0.71	0.08	0.001	900	900	250	691	0.08	0.0009	835	10	608
M42221222	0.7	30	4	600	8	10	1	2.5	1.73	0.32	0.12	0.66	0.16	0.06	0.08	0.44	0.71	0.09	0.001	872	872	242	670	0.09	0.0009	807	9	588
M52221221	0.9	30	4	600	8	10	1	1.5	1.49	0.28	0.11	0.69	0.14	0.06	0.09	0.48	0.71	0.07	0.001	1024	1024	378	703	0.07	0.0008	974	11	637
M52221222	0.9	30	4	600	8	10	1	2.5	1.53	0.29	0.12	0.69	0.14	0.06	0.09	0.47	0.71	0.07	0.001	992	992	366	682	0.07	0.0009	941	11	615
M12222111	0.1	30	4	600	10	8	0.6	1.5	1.62	0.26	0.09	0.63	0.19	0.07	0.09	0.49	0.71	0.09	0.001	948	948	35	921	0.09	0.0010	839	10	809
M12222112	0.1	30	4	600	10	8	0.6	2.5	1.70	0.28	0.10	0.63	0.19	0.07	0.08	0.48	0.71	0.09	0.001	904	904	33	879	0.09	0.0010	795	9	766
M22222111	0.3	30	4	600	10	8	0.6	1.5	1.51	0.26	0.09	0.64	0.18	0.06	0.09	0.50	0.71	0.08	0.001	1011	1011	115	916	0.08	0.0009	916	10	810
M22222112	0.3	30	4	600	10	8	0.6	2.5	1.58	0.27	0.10	0.64	0.18	0.06	0.09	0.49	0.71	0.08	0.001	962	962	109	873	0.08	0.0009	868	10	768
M32222111	0.5	30	4	600	10	8	0.6	1.5	1.39	0.25	0.09	0.65	0.17	0.06	0.10	0.52	0.71	0.07	0.001	1097	1097	213	916	0.07	0.0008	1016	12	819
M32222112	0.5	30	4	600	10	8	0.6	2.5	1.46	0.26	0.10	0.65	0.17	0.06	0.10	0.50	0.71	0.08	0.001	1042	1042	202	871	0.08	0.0008	963	11	776
M42222111	0.7	30	4	600	10	8	0.6	1.5	1.26	0.23	0.09	0.66	0.16	0.06	0.11	0.54	0.71	0.06	0.001	1219	1219	339	926	0.06	0.0007	1153	13	840
M42222112	0.7	30	4	600	10	8	0.6	2.5	1.32	0.24	0.09	0.66	0.16	0.06	0.11	0.52	0.71	0.07	0.001	1158	1158	322	880	0.07	0.0007	1093	13	796
M52222111	0.9	30	4	600	10	8	0.6	1.5	1.11	0.21	0.08	0.69	0.14	0.06	0.13	0.59	0.71	0.06	0.001	1404	1404	512	954	0.06	0.0007	1353	16	885
M52222112	0.9	30	4	600	10	8	0.6	2.5	1.17	0.22	0.09	0.69	0.14	0.06	0.12	0.57	0.71	0.06	0.001	1329	1329	486	905	0.06	0.0007	1278	15	836
M12222121	0.1	30	4	600	10	8	1	1.5	1.25	0.20	0.07	0.63	0.19	0.07	0.11	0.60	0.71	0.07	0.001	1236	1236	46	1199	0.07	0.0008	1119	13	1078
M12222122	0.1	30	4	600	10	8	1	2.5	1.32	0.21	0.08	0.63	0.19	0.07	0.11	0.58	0.71	0.07	0.001	1171	1171	44	1137	0.07	0.0008	1055	12	1017
M22222121	0.3	30	4	600	10	8	1	1.5	1.16	0.20	0.07	0.64	0.18	0.06	0.12	0.60	0.71	0.06	0.001	1326	1326	152	1196	0.06	0.0007	1226	14	1084
M22222122	0.3	30	4	600	10	8	1	2.5	1.23	0.21	0.08	0.64	0.18	0.06	0.12	0.59	0.71	0.07	0.001	1254	1254	143	1133	0.07	0.0007	1154	13	1021
M32222121	0.5	30	4	600	10	8	1	1.5	1.07	0.19	0.07	0.65	0.17	0.06	0.14	0.62	0.71	0.06	0.001	1450	1450	282	1202	0.06	0.0006	1367	16	1101
M32222122	0.5	30	4	600	10	8	1	2.5	1.13	0.20	0.08	0.65	0.17	0.06	0.13	0.60	0.71	0.06	0.001	1365	1365	265	1133	0.06	0.0007	1281	15	1032
M42222121	0.7	30	4	600	10	8	1	1.5	0.97	0.18	0.07	0.66	0.16	0.06	0.15	0.64	0.71	0.05	0.001	1614	1614	447	1214	0.05	0.0006	1548	18	1128
M42222122	0.7	30	4	600	10	8	1	2.5	1.02	0.19	0.07	0.66	0.16	0.06	0.14	0.62	0.71	0.05	0.001	1524	1524	423	1148	0.05	0.0006	1458	17	1062
M52222121	0.9	30	4	600	10	8	1	1.5	0.86	0.16	0.06	0.69	0.14	0.06	0.17	0.67	0.71	0.04	0.001	1843	1843	665	1241	0.04	0.0005	1795	21	1174
M52222122	0.9	30	4	600	10	8	1	2.5	0.91	0.17	0.07	0.69	0.14	0.06	0.16	0.65	0.71	0.05	0.001	1743	1743	631	1176	0.05	0.0005	1694	20	1108
M12222211	0.1	30	4	600	10	10	0.6	1.5	3.76	0.61	0.22	0.63	0.19	0.07	0.03	0.25	0.57	0.14	0.002	354	354	12	347	0.14	0.0016	259	3	250

Name	af	nf	hf	mf	Ly	Lx	tw	Lcb	T1 [s]	T2 [s]	T3 [s]	M1 [-]	M2 [-]	M3 [-]	Sa	Sa2	Sa3	Disp [m]	ISDR [-]	Total Moment [MN-m]	Total Shear [MN]	Outrigger Moment [MN-m]	Wall Moment [MN-m]	Mode 1 Disp [m]	Mode 1 ISDR [-]	Mode 1 Moment [MN-m]	Mode 1 Shear [MN]	Mode 1 wall Moment [MN-m]
M12222212	0.1	30	4	600	10	10	0.6	2.5	4.00	0.65	0.23	0.63	0.19	0.07	0.02	0.23	0.54	0.15	0.002	329	329	11	322	0.15	0.0017	238	3	230
M22222211	0.3	30	4	600	10	10	0.6	1.5	3.51	0.60	0.22	0.64	0.18	0.06	0.03	0.26	0.57	0.14	0.002	374	374	39	348	0.14	0.0015	290	3	256
M22222212	0.3	30	4	600	10	10	0.6	2.5	3.73	0.64	0.23	0.64	0.18	0.06	0.03	0.24	0.55	0.14	0.002	346	346	36	322	0.14	0.0015	266	3	235
M32222211	0.5	30	4	600	10	10	0.6	1.5	3.23	0.58	0.22	0.65	0.17	0.06	0.03	0.27	0.58	0.13	0.001	404	404	75	351	0.13	0.0014	330	4	266
M32222212	0.5	30	4	600	10	10	0.6	2.5	3.43	0.61	0.23	0.65	0.17	0.06	0.03	0.25	0.55	0.13	0.002	373	373	69	326	0.13	0.0014	302	3	244
M42222211	0.7	30	4	600	10	10	0.6	1.5	2.93	0.54	0.21	0.66	0.16	0.06	0.04	0.29	0.59	0.12	0.001	449	449	125	358	0.12	0.0013	387	4	282
M42222212	0.7	30	4	600	10	10	0.6	2.5	3.11	0.58	0.22	0.66	0.16	0.06	0.03	0.27	0.56	0.12	0.001	415	415	115	332	0.12	0.0013	354	4	258
M52222211	0.9	30	4	600	10	10	0.6	1.5	2.59	0.49	0.20	0.69	0.14	0.06	0.05	0.32	0.61	0.11	0.001	524	524	200	372	0.10	0.0012	472	6	309
M52222212	0.9	30	4	600	10	10	0.6	2.5	2.76	0.52	0.21	0.69	0.14	0.06	0.04	0.30	0.59	0.11	0.001	482	482	185	344	0.11	0.0013	431	5	282
M12222221	0.1	30	4	600	10	10	1	1.5	3.09	0.50	0.18	0.63	0.19	0.07	0.04	0.31	0.63	0.13	0.002	449	449	15	439	0.13	0.0014	344	4	331
M12222222	0.1	30	4	600	10	10	1	2.5	3.30	0.54	0.19	0.63	0.19	0.07	0.03	0.29	0.61	0.13	0.002	416	416	14	407	0.13	0.0015	313	4	301
M22222221	0.3	30	4	600	10	10	1	1.5	2.88	0.49	0.18	0.64	0.18	0.06	0.04	0.31	0.64	0.12	0.001	477	477	51	441	0.12	0.0013	385	4	340
M22222222	0.3	30	4	600	10	10	1	2.5	3.08	0.52	0.19	0.64	0.18	0.06	0.04	0.30	0.62	0.13	0.001	440	440	47	408	0.13	0.0014	350	4	309
M32222221	0.5	30	4	600	10	10	1	1.5	2.65	0.47	0.18	0.65	0.17	0.06	0.04	0.33	0.64	0.12	0.001	519	519	98	447	0.11	0.0012	440	5	355
M32222222	0.5	30	4	600	10	10	1	2.5	2.83	0.50	0.19	0.65	0.17	0.06	0.04	0.31	0.62	0.12	0.001	477	477	90	412	0.12	0.0013	400	5	322
M42222221	0.7	30	4	600	10	10	1	1.5	2.40	0.45	0.17	0.66	0.16	0.06	0.05	0.34	0.65	0.11	0.001	583	583	162	457	0.11	0.0012	518	6	378
M42222222	0.7	30	4	600	10	10	1	2.5	2.57	0.48	0.18	0.66	0.16	0.06	0.05	0.32	0.63	0.11	0.001	534	534	148	421	0.11	0.0012	470	5	342
M52222221	0.9	30	4	600	10	10	1	1.5	2.13	0.40	0.16	0.69	0.14	0.06	0.06	0.37	0.67	0.10	0.001	687	687	257	480	0.10	0.0011	636	7	416
M52222222	0.9	30	4	600	10	10	1	2.5	2.28	0.43	0.17	0.69	0.14	0.06	0.06	0.35	0.65	0.10	0.001	627	627	236	440	0.10	0.0012	575	7	376
M13111111	0.1	45	3	400	8	8	0.6	1.5	1.18	0.19	0.07	0.62	0.19	0.07	0.12	0.62	0.71	0.07	0.001	1468	1468	55	1422	0.06	0.0006	1339	14	1288
M13111112	0.1	45	3	400	8	8	0.6	2.5	1.20	0.20	0.07	0.62	0.19	0.07	0.12	0.61	0.71	0.07	0.001	1434	1434	53	1389	0.07	0.0007	1305	13	1255
M23111111	0.3	45	3	400	8	8	0.6	1.5	1.10	0.19	0.07	0.63	0.18	0.06	0.13	0.62	0.71	0.06	0.001	1578	1578	180	1420	0.06	0.0006	1467	15	1296
M23111112	0.3	45	3	400	8	8	0.6	2.5	1.12	0.19	0.07	0.63	0.18	0.06	0.13	0.62	0.71	0.06	0.001	1536	1536	175	1383	0.06	0.0006	1425	15	1259
M33111111	0.5	45	3	400	8	8	0.6	1.5	1.01	0.18	0.07	0.64	0.17	0.06	0.15	0.64	0.71	0.06	0.001	1718	1718	332	1420	0.06	0.0005	1626	17	1309
M33111112	0.5	45	3	400	8	8	0.6	2.5	1.03	0.18	0.07	0.64	0.17	0.06	0.14	0.63	0.71	0.06	0.001	1678	1678	325	1388	0.06	0.0005	1586	16	1277
M43111111	0.7	45	3	400	8	8	0.6	1.5	0.92	0.17	0.07	0.66	0.16	0.06	0.16	0.65	0.71	0.05	0.000	1908	1908	525	1432	0.05	0.0005	1836	19	1338
M43111112	0.7	45	3	400	8	8	0.6	2.5	0.94	0.17	0.07	0.66	0.16	0.06	0.16	0.65	0.71	0.05	0.000	1865	1865	513	1401	0.05	0.0005	1793	19	1306
M53111111	0.9	45	3	400	8	8	0.6	1.5	0.81	0.15	0.06	0.68	0.14	0.06	0.19	0.68	0.71	0.04	0.000	2183	2183	781	1468	0.04	0.0004	2130	22	1394
M53111112	0.9	45	3	400	8	8	0.6	2.5	0.83	0.16	0.06	0.68	0.14	0.06	0.18	0.68	0.71	0.04	0.000	2132	2132	763	1435	0.04	0.0005	2078	22	1360
M13111121	0.1	45	3	400	8	8	1	1.5	0.89	0.14	0.05	0.62	0.19	0.07	0.17	0.70	0.71	0.05	0.001	1945	1945	74	1881	0.05	0.0005	1824	18	1755
M13111122	0.1	45	3	400	8	8	1	2.5	0.91	0.15	0.05	0.62	0.19	0.07	0.16	0.69	0.71	0.05	0.001	1904	1904	72	1841	0.05	0.0005	1782	18	1715
M23111121	0.3	45	3	400	8	8	1	1.5	0.83	0.14	0.05	0.63	0.18	0.06	0.18	0.70	0.71	0.05	0.000	2099	2099	242	1878	0.05	0.0005	1995	20	1763
M23111122	0.3	45	3	400	8	8	1	2.5	0.85	0.14	0.05	0.63	0.18	0.06	0.18	0.70	0.71	0.05	0.000	2048	2048	236	1833	0.05	0.0005	1943	20	1716
M33111121	0.5	45	3	400	8	8	1	1.5	0.76	0.14	0.05	0.64	0.17	0.06	0.20	0.71	0.71	0.04	0.000	2274	2274	442	1866	0.04	0.0004	2188	22	1762
M33111122	0.5	45	3	400	8	8	1	2.5	0.78	0.14	0.05	0.64	0.17	0.06	0.19	0.71	0.71	0.04	0.000	2225	2225	433	1827	0.04	0.0004	2140	22	1723
M43111121	0.7	45	3	400	8	8	1	1.5	0.69	0.13	0.05	0.66	0.16	0.06	0.22	0.71	0.71	0.04	0.000	2550	2550	700	1895	0.04	0.0004	2486	26	1812
M43111122	0.7	45	3	400	8	8	1	2.5	0.71	0.13	0.05	0.66	0.16	0.06	0.21	0.71	0.71	0.04	0.000	2487	2487	683	1851	0.04	0.0004	2423	25	1765
M53111121	0.9	45	3	400	8	8	1	1.5	0.61	0.12	0.05	0.68	0.14	0.06	0.25	0.71	0.71	0.03	0.000	2922	2922	1033	1945	0.03	0.0003	2880	30	1885
M53111122	0.9	45	3	400	8	8	1	2.5	0.63	0.12	0.05	0.68	0.14	0.06	0.24	0.71	0.71	0.03	0.000	2835	2835	1003	1889	0.03	0.0003	2791	29	1827
M13111211	0.1	45	3	400	8	10	0.6	1.5	2.60	0.42	0.15	0.62	0.19	0.07	0.05	0.35	0.68	0.12	0.001	616	616	21	601	0.12	0.0012	496	5	477
M13111212	0.1	45	3	400	8	10	0.6	2.5	2.67	0.44	0.16	0.62	0.19	0.07	0.04	0.35	0.68	0.12	0.001	597	597	21	583	0.12	0.0012	476	5	458
M23111211	0.3	45	3	400	8	10	0.6	1.5	2.42	0.41	0.15	0.63	0.18	0.06	0.05	0.36	0.69	0.11	0.001	661	661	72	606	0.11	0.0011	556	6	491
M23111212	0.3	45	3	400	8	10	0.6	2.5	2.49	0.42	0.15	0.63	0.18	0.06	0.05	0.35	0.68	0.11	0.001	639	639	69	587	0.11	0.0011	535	5	472
M33111211	0.5	45	3	400	8	10	0.6	1.5	2.23	0.40	0.15	0.64	0.17	0.06	0.06	0.37	0.69	0.11	0.001	725	725	137	616	0.11	0.0010	638	7	514
M33111212	0.5	45	3	400	8	10	0.6	2.5	2.29	0.41	0.15	0.64	0.17	0.06	0.06	0.36	0.68	0.11	0.001	701	701	132	596	0.11	0.0010	613	6	494
M43111211	0.7	45	3	400	8	10	0.6	1.5	2.02	0.37	0.14	0.66	0.16	0.06	0.07	0.39	0.70	0.10	0.001	823	823	227	636	0.10	0.0010	753	8	549
M43111212	0.7	45	3	400	8	10	0.6	2.5	2.08	0.38	0.15	0.66	0.16	0.06	0.06	0.38	0.69	0.10	0.001	794	794	219	615	0.10	0.0010	724	7	527
M53111211	0.9	45	3	400	8	10	0.6	1.5	1.80	0.34	0.14	0.68	0.14	0.06	0.08	0.42	0.71	0.08	0.001	939	939	346	650	0.08	0.0009	880	9	576
M53111212	0.9	45	3	400	8	10	0.6	2.5	1.84	0.35	0.14	0.68	0.14	0.06	0.07	0.42	0.71	0.09	0.001	914	914	337	634	0.09	0.0009	856	9	560
M13111221	0.1	45	3	400	8	10	1	1.5	2.07	0.34	0.12	0.62	0.19	0.07	0.06	0.42	0.71	0.11	0.001	824	824	29	801	0.11	0.0011	704	7	677
M13111222	0.1	45	3	400	8	10	1	2.5	2.12	0.35	0.12	0.62	0.19	0.07	0.06	0.41	0.71	0.11	0.001	795	795	28	773	0.11	0.0011	674	7	649
M23111221	0.3	45	3	400	8	10	1	1.5	1.93	0.33	0.12	0.63	0.18	0.06	0.07	0.43	0.71	0.10	0.001	882	882	98	803	0.10	0.0010	778	8	687
M23111222	0.3	45	3	400	8	10	1	2.5	1.98	0.34	0.12	0.63	0.18	0.06	0.07	0.42	0.71	0.10	0.001	858	858	95	781	0.10	0.0010	754	8	666
M33111221	0.5	45	3	400	8	10	1	1.5	1.77	0.32	0.12	0.64	0.17	0.06	0.08	0.44	0.71	0.09	0.001	950	950	181	799	0.09	0.0009	861	9	693
M33111222	0.5	45	3	400	8	10	1	2.5	1.82	0.32	0.12	0.64	0.17	0.06	0.08	0.44	0.71	0.09	0.001	926	926	177	779	0.09	0.0009	837	9	674
M43111221	0.7	45	3	400	8	10	1	1.5	1.61	0.30	0.11	0.66	0.16	0.06	0.09	0.46	0.71	0.08	0.001	1047	1047	289	802	0.08	0.0008	974	10	710
M43111222	0.7	45	3	400	8	10	1	2.5	1.65	0.31	0.12	0.66	0.16	0.06	0.08	0.45	0.71	0.08	0.001	1018	1018	281	781	0.08	0.0008	945	10	689
M53111221	0.9	45	3	400	8	10	1	1.5	1.43	0.27	0.11	0.68	0.14	0.06	0.10	0.49	0.71	0.07	0.001	1192	1192	435	818	0.07	0.0007	1136	12	743
M53111222	0.9	45	3	400	8	10	1	2.5	1.47	0.28	0.11	0.68	0.14	0.06	0.10	0.48	0.71	0.07	0.001	1159	1159	424	796	0.07	0.0007	1102	12	721
M13112111	0.1	45	3	400	10	8	0.6	1.5	1.58	0.26	0.09	0.62	0.19	0.07	0.09	0.50	0.71	0.08	0.001	1085	1085	40	1052	0.08	0.0008	963	10	927
M13112112	0.1	45	3	400	10	8	0.6	2.5	1.64	0.27	0.10	0.62	0.19	0.07	0.08	0.49	0.71	0.09	0.001	1038	1038	38	1008	0.09	0.0009	917	9	882
M23112111	0.3	45	3	400	10	8	0.6	1.5	1.47	0.25	0.09	0.63	0.18	0.06	0.10	0.51	0.71	0.08	0.001	1159	1159	131	1048	0.08	0.0008	1052	11	929
M23112112	0.3	45	3	400	10	8	0.6	2.5	1.53	0.26	0.10	0.63	0.18	0.06	0.09	0.50	0.71	0.08	0.001	1107	1107	125	1001	0.08	0.0008	1002	10	885
M33112111	0.5	45	3	400	10	8	0.6	1.5	1.35	0.24	0.09	0.64	0.17	0.06	0.11	0.53	0.71	0.07	0.001	1258	1258	242	1049	0.07	0.0007	1167	12	940
M33112112	0.5	45	3	400	10	8	0.6	2.5	1.41	0.25	0.09	0.64	0.17	0.06	0.10	0.51	0.71	0.07	0.001	1201	1201	231	1002	0.07	0.0007	1111	11	895
M43112111	0.7	45	3	400	10	8	0.6	1.5	1.23	0.23	0.09	0.66	0.16	0.06	0.12	0.55	0.71	0.06	0.001	1398	1398	385	1060	0.06	0.0006	1323	14	964
M43112112	0.7	45	3	400	10	8	0.6	2.5	1.28	0.24	0.09	0.66	0.16	0.06	0.11	0.54	0.71	0.07	0.001	1332	1332	367	1012	0.07	0.0006	1259	13	917
M53112111	0.9	45	3	400	10	8	0.6	1.5	1.09	0.20	0.08	0.68	0.14	0.06	0.13	0.59	0.71	0.05	0.001	1606	1606	581	1092	0.05	0.0006	1550	16	1014
M53112112	0.9	45	3	400	10	8	0.6	2.5	1.14	0.21	0.09	0.68	0.14	0.06	0.13	0.58	0.71	0.06	0.001	1526	1526	553	1039	0.06	0.0006	1469	15	961
M13112121	0.1	45	3	400	10	8	1	1.5	1.21	0.20	0.07	0.62	0.19	0.07	0.12	0.61	0.71	0.07	0.001	1432	1432	53	1387	0.07	0.0007	1303	13	1253
M13112122	0.1	45	3	400	10	8	1	2.5	1.26	0.21	0.07	0.62	0.19	0.07	0.11	0.59	0.71	0.07	0.001	1362	1362	51	1320	0.07	0.0007	1233	12	1186
M23112121	0.3	45	3	400	10	8	1	1.5	1.12	0.19	0.07	0.63	0.18	0.06	0.13	0.62	0.71	0.06	0.001	1534	1534	175	1381	0.06	0.0006	1423	14	1257

Name	af	nf	hf	mf	Ly	Lx	tw	Lcb	T1 [s]	T2 [s]	T3 [s]	M1 [-]	M2 [-]	M3 [-]	Sa	Sa2	Sa3	Disp [m]	ISDR [-]	Total Moment [MN-m]	Total Shear [MN]	Outrigger Moment [MN-m]	Wall Moment [MN-m]	Mode 1 Disp [m]	Mode 1 ISDR [-]	Mode 1 Moment [MN-m]	Mode 1 Shear [MN]	Mode 1 wall Moment [MN-m]
M23112122	0.3	45	3	400	10	8	1	2.5	1.18	0.20	0.07	0.63	0.18	0.06	0.12	0.60	0.71	0.06	0.001	1464	1464	167	1319	0.06	0.0006	1352	14	1194
M33112121	0.5	45	3	400	10	8	1	1.5	1.04	0.18	0.07	0.64	0.17	0.06	0.14	0.63	0.71	0.06	0.001	1676	1676	324	1387	0.06	0.0005	1584	16	1275
M33112122	0.5	45	3	400	10	8	1	2.5	1.08	0.19	0.07	0.64	0.17	0.06	0.14	0.61	0.71	0.06	0.001	1598	1598	309	1324	0.06	0.0006	1505	15	1212
M43112121	0.7	45	3	400	10	8	1	1.5	0.94	0.17	0.07	0.66	0.16	0.06	0.16	0.65	0.71	0.05	0.000	1863	1863	513	1400	0.05	0.0005	1790	19	1305
M43112122	0.7	45	3	400	10	8	1	2.5	0.98	0.18	0.07	0.66	0.16	0.06	0.15	0.63	0.71	0.05	0.001	1777	1777	489	1337	0.05	0.0005	1704	18	1241
M53112121	0.9	45	3	400	10	8	1	1.5	0.83	0.16	0.06	0.68	0.14	0.06	0.18	0.68	0.71	0.04	0.000	2129	2129	762	1433	0.04	0.0005	2075	22	1358
M53112122	0.9	45	3	400	10	8	1	2.5	0.87	0.16	0.07	0.68	0.14	0.06	0.17	0.66	0.71	0.04	0.000	2025	2025	726	1365	0.04	0.0005	1970	21	1290
M13112211	0.1	45	3	400	10	10	0.6	1.5	3.64	0.59	0.21	0.62	0.19	0.07	0.03	0.26	0.58	0.14	0.002	411	411	13	402	0.14	0.0014	303	3	292
M13112212	0.1	45	3	400	10	10	0.6	2.5	3.84	0.63	0.22	0.62	0.19	0.07	0.03	0.24	0.56	0.15	0.002	385	385	13	377	0.15	0.0015	282	3	271
M23112211	0.3	45	3	400	10	10	0.6	1.5	3.39	0.58	0.21	0.63	0.18	0.06	0.03	0.27	0.58	0.13	0.001	435	435	45	404	0.13	0.0013	338	3	299
M23112212	0.3	45	3	400	10	10	0.6	2.5	3.57	0.61	0.22	0.63	0.18	0.06	0.03	0.25	0.56	0.14	0.001	407	407	42	379	0.14	0.0013	314	3	278
M33112211	0.5	45	3	400	10	10	0.6	1.5	3.12	0.56	0.21	0.64	0.17	0.06	0.03	0.28	0.59	0.13	0.001	470	470	87	407	0.13	0.0012	385	4	310
M33112212	0.5	45	3	400	10	10	0.6	2.5	3.29	0.59	0.22	0.64	0.17	0.06	0.03	0.26	0.57	0.13	0.001	439	439	81	382	0.13	0.0012	357	4	288
M43112211	0.7	45	3	400	10	10	0.6	1.5	2.83	0.52	0.20	0.66	0.16	0.06	0.04	0.30	0.60	0.12	0.001	523	523	144	415	0.12	0.0011	452	5	329
M43112212	0.7	45	3	400	10	10	0.6	2.5	2.99	0.55	0.21	0.66	0.16	0.06	0.04	0.28	0.58	0.12	0.001	488	488	134	389	0.12	0.0012	418	4	305
M53112211	0.9	45	3	400	10	10	0.6	1.5	2.52	0.47	0.19	0.68	0.14	0.06	0.05	0.33	0.62	0.10	0.001	609	609	230	432	0.10	0.0011	550	6	360
M53112212	0.9	45	3	400	10	10	0.6	2.5	2.65	0.50	0.20	0.68	0.14	0.06	0.04	0.31	0.60	0.11	0.001	567	567	215	404	0.11	0.0011	509	5	333
M13112221	0.1	45	3	400	10	10	1	1.5	2.94	0.48	0.17	0.62	0.19	0.07	0.04	0.32	0.65	0.13	0.001	532	532	18	519	0.13	0.0013	413	4	397
M13112222	0.1	45	3	400	10	10	1	2.5	3.11	0.51	0.18	0.62	0.19	0.07	0.03	0.31	0.63	0.13	0.001	497	497	17	485	0.13	0.0013	380	4	366
M23112221	0.3	45	3	400	10	10	1	1.5	2.74	0.47	0.17	0.63	0.18	0.06	0.04	0.33	0.65	0.12	0.001	566	566	61	522	0.12	0.0012	462	5	408
M23112222	0.3	45	3	400	10	10	1	2.5	2.90	0.49	0.18	0.63	0.18	0.06	0.04	0.31	0.64	0.12	0.001	528	528	56	488	0.12	0.0012	425	4	376
M33112221	0.5	45	3	400	10	10	1	1.5	2.52	0.45	0.17	0.64	0.17	0.06	0.05	0.34	0.66	0.11	0.001	617	617	116	529	0.11	0.0011	528	5	426
M33112222	0.5	45	3	400	10	10	1	2.5	2.67	0.48	0.18	0.64	0.17	0.06	0.04	0.32	0.64	0.12	0.001	574	574	107	494	0.12	0.0011	486	5	391
M43112221	0.7	45	3	400	10	10	1	1.5	2.29	0.42	0.16	0.66	0.16	0.06	0.06	0.35	0.67	0.10	0.001	695	695	191	542	0.10	0.0010	622	6	454
M43112222	0.7	45	3	400	10	10	1	2.5	2.42	0.45	0.17	0.66	0.16	0.06	0.05	0.34	0.65	0.11	0.001	644	644	178	505	0.11	0.0010	572	6	416
M53112221	0.9	45	3	400	10	10	1	1.5	2.03	0.38	0.15	0.68	0.14	0.06	0.07	0.38	0.68	0.09	0.001	820	820	303	570	0.09	0.0010	763	8	500
M53112222	0.9	45	3	400	10	10	1	2.5	2.15	0.40	0.16	0.68	0.14	0.06	0.06	0.37	0.67	0.10	0.001	757	757	281	529	0.10	0.0010	700	7	458
M13121111	0.1	45	3	600	8	8	0.6	1.5	1.44	0.23	0.08	0.62	0.19	0.07	0.10	0.54	0.71	0.08	0.001	1786	1786	66	1732	0.08	0.0008	1597	16	1536
M13121112	0.1	45	3	600	8	8	0.6	2.5	1.48	0.24	0.09	0.62	0.19	0.07	0.10	0.53	0.71	0.08	0.001	1743	1743	64	1690	0.08	0.0008	1555	16	1496
M23121111	0.3	45	3	600	8	8	0.6	1.5	1.34	0.23	0.08	0.63	0.18	0.06	0.11	0.55	0.71	0.07	0.001	1910	1910	216	1725	0.07	0.0007	1745	18	1541
M23121112	0.3	45	3	600	8	8	0.6	2.5	1.37	0.23	0.09	0.63	0.18	0.06	0.10	0.54	0.71	0.07	0.001	1861	1861	210	1682	0.07	0.0007	1697	17	1499
M33121111	0.5	45	3	600	8	8	0.6	1.5	1.24	0.22	0.08	0.64	0.17	0.06	0.12	0.57	0.71	0.07	0.001	2076	2076	400	1727	0.07	0.0006	1936	20	1559
M33121112	0.5	45	3	600	8	8	0.6	2.5	1.27	0.23	0.08	0.64	0.17	0.06	0.11	0.56	0.71	0.07	0.001	2021	2021	389	1682	0.07	0.0006	1882	19	1515
M43121111	0.7	45	3	600	8	8	0.6	1.5	1.12	0.21	0.08	0.66	0.16	0.06	0.13	0.59	0.71	0.06	0.001	2308	2308	636	1745	0.06	0.0006	2196	23	1600
M43121112	0.7	45	3	600	8	8	0.6	2.5	1.15	0.21	0.08	0.66	0.16	0.06	0.13	0.58	0.71	0.06	0.001	2248	2248	619	1702	0.06	0.0006	2136	22	1557
M53121111	0.9	45	3	600	8	8	0.6	1.5	1.00	0.19	0.07	0.68	0.14	0.06	0.15	0.62	0.71	0.05	0.001	2652	2652	956	1796	0.05	0.0005	2568	27	1681
M53121112	0.9	45	3	600	8	8	0.6	2.5	1.02	0.19	0.08	0.68	0.14	0.06	0.14	0.62	0.71	0.05	0.001	2584	2584	932	1752	0.05	0.0005	2500	26	1636
M13121121	0.1	45	3	600	8	8	1	1.5	1.09	0.18	0.06	0.62	0.19	0.07	0.13	0.64	0.71	0.06	0.001	2392	2392	90	2315	0.06	0.0006	2200	22	2117
M13121122	0.1	45	3	600	8	8	1	2.5	1.11	0.18	0.07	0.62	0.19	0.07	0.13	0.63	0.71	0.06	0.001	2329	2329	87	2254	0.06	0.0006	2136	22	2055
M23121121	0.3	45	3	600	8	8	1	1.5	1.01	0.17	0.06	0.63	0.18	0.06	0.15	0.65	0.71	0.06	0.001	2564	2564	294	2303	0.06	0.0005	2400	24	2120
M23121122	0.3	45	3	600	8	8	1	2.5	1.04	0.18	0.06	0.63	0.18	0.06	0.14	0.64	0.71	0.06	0.001	2504	2504	287	2251	0.06	0.0006	2340	24	2067
M33121121	0.5	45	3	600	8	8	1	1.5	0.93	0.17	0.06	0.64	0.17	0.06	0.16	0.66	0.71	0.05	0.001	2796	2796	542	2307	0.05	0.0005	2660	27	2142
M33121122	0.5	45	3	600	8	8	1	2.5	0.96	0.17	0.06	0.64	0.17	0.06	0.16	0.65	0.71	0.05	0.001	2730	2730	529	2253	0.05	0.0005	2593	27	2088
M43121121	0.7	45	3	600	8	8	1	1.5	0.85	0.16	0.06	0.66	0.16	0.06	0.18	0.68	0.71	0.05	0.000	3104	3104	853	2324	0.05	0.0004	2997	31	2184
M43121122	0.7	45	3	600	8	8	1	2.5	0.87	0.16	0.06	0.66	0.16	0.06	0.17	0.67	0.71	0.05	0.000	3022	3022	831	2265	0.05	0.0005	2915	30	2124
M53121121	0.9	45	3	600	8	8	1	1.5	0.75	0.14	0.06	0.68	0.14	0.06	0.20	0.70	0.71	0.04	0.000	3536	3536	1261	2372	0.04	0.0004	3459	36	2264
M53121122	0.9	45	3	600	8	8	1	2.5	0.77	0.14	0.06	0.68	0.14	0.06	0.20	0.70	0.71	0.04	0.000	3446	3446	1230	2314	0.04	0.0004	3368	35	2204
M13121211	0.1	45	3	600	8	10	0.6	1.5	3.18	0.52	0.19	0.62	0.19	0.07	0.03	0.30	0.62	0.13	0.001	725	725	24	708	0.13	0.0013	551	6	530
M13121212	0.1	45	3	600	8	10	0.6	2.5	3.27	0.53	0.19	0.62	0.19	0.07	0.03	0.29	0.62	0.13	0.001	702	702	23	687	0.13	0.0013	530	5	510
M23121211	0.3	45	3	600	8	10	0.6	1.5	2.97	0.51	0.18	0.63	0.18	0.06	0.04	0.31	0.63	0.13	0.001	769	769	81	712	0.12	0.0012	617	6	545
M23121212	0.3	45	3	600	8	10	0.6	2.5	3.05	0.52	0.19	0.63	0.18	0.06	0.04	0.30	0.62	0.13	0.001	745	745	79	690	0.13	0.0012	593	6	524
M33121211	0.5	45	3	600	8	10	0.6	1.5	2.73	0.49	0.18	0.64	0.17	0.06	0.04	0.32	0.63	0.12	0.001	836	836	156	720	0.12	0.0011	704	7	567
M33121212	0.5	45	3	600	8	10	0.6	2.5	2.81	0.50	0.19	0.64	0.17	0.06	0.04	0.31	0.62	0.12	0.001	808	808	150	697	0.12	0.0011	678	7	546
M43121211	0.7	45	3	600	8	10	0.6	1.5	2.48	0.46	0.18	0.66	0.16	0.06	0.05	0.33	0.64	0.11	0.001	936	936	258	736	0.11	0.0011	828	9	603
M43121212	0.7	45	3	600	8	10	0.6	2.5	2.55	0.47	0.18	0.66	0.16	0.06	0.05	0.33	0.63	0.11	0.001	904	904	249	712	0.11	0.0011	795	8	580
M53121211	0.9	45	3	600	8	10	0.6	1.5	2.20	0.41	0.17	0.68	0.14	0.06	0.06	0.36	0.66	0.10	0.001	1100	1100	410	771	0.10	0.0010	1013	11	663
M53121212	0.9	45	3	600	8	10	0.6	2.5	2.26	0.42	0.17	0.68	0.14	0.06	0.06	0.35	0.65	0.10	0.001	1060	1060	396	744	0.10	0.0010	972	10	636
M13121221	0.1	45	3	600	8	10	1	1.5	2.53	0.41	0.15	0.62	0.19	0.07	0.05	0.36	0.69	0.12	0.001	954	954	33	930	0.12	0.0012	773	8	744
M13121222	0.1	45	3	600	8	10	1	2.5	2.60	0.42	0.15	0.62	0.19	0.07	0.05	0.35	0.68	0.12	0.001	924	924	32	901	0.12	0.0012	743	8	714
M23121221	0.3	45	3	600	8	10	1	1.5	2.36	0.40	0.15	0.63	0.18	0.06	0.05	0.37	0.69	0.11	0.001	1024	1024	112	939	0.11	0.0011	869	9	767
M23121222	0.3	45	3	600	8	10	1	2.5	2.42	0.41	0.15	0.63	0.18	0.06	0.05	0.36	0.69	0.11	0.001	990	990	107	908	0.11	0.0011	834	8	736
M33121221	0.5	45	3	600	8	10	1	1.5	2.17	0.39	0.14	0.64	0.17	0.06	0.06	0.38	0.70	0.11	0.001	1127	1127	213	955	0.10	0.0010	997	10	803
M33121222	0.5	45	3	600	8	10	1	2.5	2.23	0.40	0.15	0.64	0.17	0.06	0.06	0.37	0.69	0.11	0.001	1087	1087	205	924	0.11	0.0010	956	10	770
M43121221	0.7	45	3	600	8	10	1	1.5	1.97	0.36	0.14	0.66	0.16	0.06	0.07	0.40	0.70	0.10	0.001	1273	1273	351	983	0.10	0.0009	1167	12	850
M43121222	0.7	45	3	600	8	10	1	2.5	2.03	0.37	0.14	0.66	0.16	0.06	0.07	0.39	0.70	0.10	0.001	1234	1234	340	954	0.10	0.0010	1128	12	822
M53121221	0.9	45	3	600	8	10	1	1.5	1.75	0.33	0.13	0.68	0.14	0.06	0.08	0.43	0.71	0.08	0.001	1447	1447	533	1001	0.08	0.0009	1359	14	889
M53121222	0.9	45	3	600	8	10	1	2.5	1.80	0.34	0.14	0.68	0.14	0.06	0.08	0.42	0.71	0.08	0.001	1408	1408	519	975	0.08	0.0009	1320	14	864
M13122111	0.1	45	3	600	10	8	0.6	1.5	1.93	0.31	0.11	0.62	0.19	0.07	0.07	0.45	0.71	0.10	0.001	1335	1335	48	1297	0.10	0.0010	1154	12	1110
M13122112	0.1	45	3	600	10	8	0.6	2.5	2.01	0.33	0.12	0.62	0.19	0.07	0.07	0.43	0.71	0.10	0.001	1277	1277	46	1242	0.10	0.0010	1097	11	1056
M23122111	0.3	45	3	600	10	8	0.6	1.5	1.80	0.31	0.11	0.63	0.18	0.06	0.08	0.45	0.71	0.09	0.001	1418	1418	158	1288	0.09	0.0009	1260	13	1113
M23122112	0.3	45	3	600	10	8	0.6	2.5	1.88	0.32	0.12	0.63	0.18	0.06	0.07	0.44	0.71	0.10	0.001	1359	1359	151	1235	0.10	0.0009	1201	12	1061
M33122111	0.5	45	3	600	10	8	0.6	1.5	1.66	0.30	0.11	0.64	0.17	0.06	0.08	0.46	0.71	0.09	0.001	1529	1529	293	1283	0.08	0.0008	1394	14	1123

Name	af	nf	hf	mf	Ly	Lx	tw	Lcb	T1 [s]	T2 [s]	T3 [s]	M1 [-]	M2 [-]	M3 [-]	Sa	Sa2	Sa3	Disp [m]	ISDR [-]	Total Moment [MN-m]	Total Shear [MN]	Outrigger Moment [MN-m]	Wall Moment [MN-m]	Mode 1 Disp [m]	Mode 1 ISDR [-]	Mode 1 Moment [MN-m]	Mode 1 Shear [MN]	Mode 1 wall Moment [MN-m]
M33122112	0.5	45	3	600	10	8	0.6	2.5	1.73	0.31	0.12	0.64	0.17	0.06	0.08	0.45	0.71	0.09	0.001	1465	1465	280	1231	0.09	0.0008	1331	14	1071
M43122111	0.7	45	3	600	10	8	0.6	1.5	1.50	0.28	0.11	0.66	0.16	0.06	0.09	0.48	0.71	0.08	0.001	1686	1686	465	1288	0.08	0.0007	1577	16	1149
M43122112	0.7	45	3	600	10	8	0.6	2.5	1.57	0.29	0.11	0.66	0.16	0.06	0.09	0.47	0.71	0.08	0.001	1614	1614	445	1235	0.08	0.0008	1505	16	1097
M53122111	0.9	45	3	600	10	8	0.6	1.5	1.33	0.25	0.10	0.68	0.14	0.06	0.11	0.51	0.71	0.06	0.001	1928	1928	702	1319	0.06	0.0007	1843	19	1206
M53122112	0.9	45	3	600	10	8	0.6	2.5	1.39	0.26	0.10	0.68	0.14	0.06	0.10	0.50	0.71	0.07	0.001	1836	1836	669	1257	0.07	0.0007	1751	18	1146
M13122121	0.1	45	3	600	10	8	1	1.5	1.48	0.24	0.09	0.62	0.19	0.07	0.10	0.53	0.71	0.08	0.001	1740	1740	64	1688	0.08	0.0008	1553	16	1494
M13122122	0.1	45	3	600	10	8	1	2.5	1.55	0.25	0.09	0.62	0.19	0.07	0.09	0.51	0.71	0.08	0.001	1659	1659	61	1609	0.08	0.0008	1475	15	1419
M23122121	0.3	45	3	600	10	8	1	1.5	1.38	0.23	0.09	0.63	0.18	0.06	0.10	0.54	0.71	0.07	0.001	1859	1859	210	1680	0.07	0.0007	1694	17	1497
M23122122	0.3	45	3	600	10	8	1	2.5	1.44	0.25	0.09	0.63	0.18	0.06	0.10	0.52	0.71	0.08	0.001	1773	1773	200	1603	0.08	0.0007	1612	16	1424
M33122121	0.5	45	3	600	10	8	1	1.5	1.27	0.23	0.08	0.64	0.17	0.06	0.11	0.56	0.71	0.07	0.001	2018	2018	389	1681	0.07	0.0006	1879	19	1513
M33122122	0.5	45	3	600	10	8	1	2.5	1.33	0.24	0.09	0.64	0.17	0.06	0.11	0.54	0.71	0.07	0.001	1926	1926	371	1605	0.07	0.0007	1789	18	1441
M43122121	0.7	45	3	600	10	8	1	1.5	1.15	0.21	0.08	0.66	0.16	0.06	0.13	0.58	0.71	0.06	0.001	2245	2245	619	1700	0.06	0.0006	2134	22	1555
M43122122	0.7	45	3	600	10	8	1	2.5	1.20	0.22	0.09	0.66	0.16	0.06	0.12	0.56	0.71	0.06	0.001	2141	2141	590	1623	0.06	0.0006	2030	21	1479
M53122121	0.9	45	3	600	10	8	1	1.5	1.02	0.19	0.08	0.68	0.14	0.06	0.14	0.62	0.71	0.05	0.001	2581	2581	931	1750	0.05	0.0005	2497	26	1634
M53122122	0.9	45	3	600	10	8	1	2.5	1.07	0.20	0.08	0.68	0.14	0.06	0.14	0.60	0.71	0.05	0.001	2461	2461	889	1671	0.05	0.0006	2376	25	1555
M13122211	0.1	45	3	600	10	10	0.6	1.5	4.46	0.73	0.26	0.62	0.19	0.07	0.02	0.21	0.50	0.16	0.002	484	484	15	474	0.16	0.0016	343	3	330
M13122212	0.1	45	3	600	10	10	0.6	2.5	4.70	0.77	0.28	0.62	0.19	0.07	0.02	0.20	0.48	0.17	0.002	455	455	14	446	0.16	0.0016	320	3	307
M23122211	0.3	45	3	600	10	10	0.6	1.5	4.15	0.71	0.26	0.63	0.18	0.06	0.02	0.22	0.50	0.15	0.002	508	508	52	474	0.15	0.0015	382	4	337
M23122212	0.3	45	3	600	10	10	0.6	2.5	4.38	0.75	0.27	0.63	0.18	0.06	0.02	0.20	0.48	0.16	0.002	477	477	49	446	0.16	0.0015	355	4	314
M33122211	0.5	45	3	600	10	10	0.6	1.5	3.83	0.68	0.25	0.64	0.17	0.06	0.03	0.22	0.51	0.14	0.001	545	545	99	477	0.14	0.0014	433	4	349
M33122212	0.5	45	3	600	10	10	0.6	2.5	4.03	0.72	0.27	0.64	0.17	0.06	0.02	0.21	0.49	0.15	0.002	511	511	93	448	0.15	0.0014	402	4	324
M43122211	0.7	45	3	600	10	10	0.6	1.5	3.47	0.64	0.25	0.66	0.16	0.06	0.03	0.24	0.52	0.13	0.001	600	600	165	482	0.13	0.0013	505	5	368
M43122212	0.7	45	3	600	10	10	0.6	2.5	3.66	0.68	0.26	0.66	0.16	0.06	0.03	0.23	0.50	0.13	0.001	562	562	154	453	0.13	0.0013	468	5	341
M53122211	0.9	45	3	600	10	10	0.6	1.5	3.08	0.58	0.23	0.68	0.14	0.06	0.04	0.27	0.55	0.12	0.001	696	696	266	501	0.11	0.0012	611	6	400
M53122212	0.9	45	3	600	10	10	0.6	2.5	3.25	0.61	0.24	0.68	0.14	0.06	0.03	0.25	0.52	0.12	0.001	649	649	248	468	0.12	0.0012	566	6	371
M13122221	0.1	45	3	600	10	10	1	1.5	3.60	0.59	0.21	0.62	0.19	0.07	0.03	0.26	0.58	0.14	0.002	625	625	20	612	0.14	0.0014	462	5	444
M13122222	0.1	45	3	600	10	10	1	2.5	3.81	0.62	0.22	0.62	0.19	0.07	0.03	0.25	0.56	0.15	0.002	583	583	19	571	0.14	0.0014	427	4	411
M23122221	0.3	45	3	600	10	10	1	1.5	3.36	0.57	0.21	0.63	0.18	0.06	0.03	0.27	0.59	0.13	0.001	661	661	69	614	0.13	0.0013	516	5	455
M23122222	0.3	45	3	600	10	10	1	2.5	3.55	0.61	0.22	0.63	0.18	0.06	0.03	0.25	0.56	0.14	0.001	616	616	64	573	0.14	0.0013	476	5	420
M33122221	0.5	45	3	600	10	10	1	1.5	3.09	0.55	0.21	0.64	0.17	0.06	0.04	0.28	0.59	0.13	0.001	714	714	132	619	0.12	0.0012	587	6	473
M33122222	0.5	45	3	600	10	10	1	2.5	3.27	0.58	0.22	0.64	0.17	0.06	0.03	0.27	0.57	0.13	0.001	665	665	122	578	0.13	0.0012	541	6	436
M43122221	0.7	45	3	600	10	10	1	1.5	2.81	0.52	0.20	0.66	0.16	0.06	0.04	0.30	0.60	0.12	0.001	795	795	219	631	0.11	0.0011	688	7	501
M43122222	0.7	45	3	600	10	10	1	2.5	2.97	0.55	0.21	0.66	0.16	0.06	0.04	0.28	0.58	0.12	0.001	739	739	203	588	0.12	0.0012	634	7	462
M53122221	0.9	45	3	600	10	10	1	1.5	2.49	0.47	0.19	0.68	0.14	0.06	0.05	0.33	0.62	0.10	0.001	928	928	349	657	0.10	0.0011	839	9	549
M53122222	0.9	45	3	600	10	10	1	2.5	2.63	0.49	0.20	0.68	0.14	0.06	0.04	0.31	0.60	0.11	0.001	859	859	325	611	0.11	0.0011	771	8	504
M13211111	0.1	45	4	400	8	8	0.6	1.5	1.15	0.19	0.07	0.62	0.19	0.07	0.13	0.62	0.71	0.06	0.000	2000	2000	75	1937	0.06	0.0005	1828	14	1759
M13211112	0.1	45	4	400	8	8	0.6	2.5	1.17	0.19	0.07	0.62	0.19	0.07	0.12	0.62	0.71	0.06	0.001	1967	1967	73	1905	0.06	0.0005	1795	14	1727
M23211111	0.3	45	4	400	8	8	0.6	1.5	1.07	0.18	0.07	0.63	0.18	0.06	0.14	0.63	0.71	0.06	0.000	2154	2154	246	1937	0.06	0.0004	2007	15	1773
M23211112	0.3	45	4	400	8	8	0.6	2.5	1.09	0.19	0.07	0.63	0.18	0.06	0.13	0.63	0.71	0.06	0.000	2115	2115	241	1903	0.06	0.0004	1967	15	1738
M33211111	0.5	45	4	400	8	8	0.6	1.5	0.99	0.18	0.07	0.64	0.17	0.06	0.15	0.64	0.71	0.05	0.000	2346	2346	454	1939	0.05	0.0004	2224	17	1791
M33211112	0.5	45	4	400	8	8	0.6	2.5	1.01	0.18	0.07	0.64	0.17	0.06	0.15	0.64	0.71	0.06	0.000	2302	2302	446	1904	0.05	0.0004	2180	17	1756
M43211111	0.7	45	4	400	8	8	0.6	1.5	0.90	0.17	0.06	0.66	0.16	0.06	0.17	0.66	0.71	0.05	0.000	2596	2596	714	1948	0.05	0.0004	2500	19	1822
M43211112	0.7	45	4	400	8	8	0.6	2.5	0.91	0.17	0.07	0.66	0.16	0.06	0.16	0.66	0.71	0.05	0.000	2555	2555	703	1918	0.05	0.0004	2459	19	1792
M53211111	0.9	45	4	400	8	8	0.6	1.5	0.80	0.15	0.06	0.68	0.14	0.06	0.19	0.69	0.71	0.04	0.000	2974	2974	1062	1998	0.04	0.0003	2903	23	1900
M53211112	0.9	45	4	400	8	8	0.6	2.5	0.81	0.15	0.06	0.68	0.14	0.06	0.19	0.69	0.71	0.04	0.000	2925	2925	1046	1966	0.04	0.0003	2854	22	1868
M13211121	0.1	45	4	400	8	8	1	1.5	0.85	0.14	0.05	0.62	0.19	0.07	0.18	0.71	0.71	0.05	0.000	2704	2704	103	2613	0.05	0.0004	2545	19	2448
M13211122	0.1	45	4	400	8	8	1	2.5	0.87	0.14	0.05	0.62	0.19	0.07	0.17	0.70	0.71	0.05	0.000	2654	2654	101	2565	0.05	0.0004	2493	19	2399
M23211121	0.3	45	4	400	8	8	1	1.5	0.80	0.14	0.05	0.63	0.18	0.06	0.19	0.71	0.71	0.05	0.000	2904	2904	336	2597	0.05	0.0003	2768	21	2445
M23211122	0.3	45	4	400	8	8	1	2.5	0.81	0.14	0.05	0.63	0.18	0.06	0.19	0.71	0.71	0.05	0.000	2856	2856	330	2556	0.05	0.0003	2720	21	2402
M33211121	0.5	45	4	400	8	8	1	1.5	0.73	0.13	0.05	0.64	0.17	0.06	0.21	0.71	0.71	0.04	0.000	3168	3168	616	2596	0.04	0.0003	3059	24	2463
M33211122	0.5	45	4	400	8	8	1	2.5	0.75	0.13	0.05	0.64	0.17	0.06	0.20	0.71	0.71	0.04	0.000	3106	3106	604	2547	0.04	0.0003	2995	23	2412
M43211121	0.7	45	4	400	8	8	1	1.5	0.67	0.12	0.05	0.66	0.16	0.06	0.23	0.71	0.71	0.04	0.000	3527	3527	968	2619	0.04	0.0003	3446	27	2511
M43211122	0.7	45	4	400	8	8	1	2.5	0.68	0.13	0.05	0.66	0.16	0.06	0.23	0.71	0.71	0.04	0.000	3470	3470	952	2577	0.04	0.0003	3387	26	2468
M53211121	0.9	45	4	400	8	8	1	1.5	0.59	0.11	0.04	0.68	0.14	0.06	0.26	0.71	0.71	0.03	0.000	4076	4076	1438	2709	0.03	0.0002	4021	32	2632
M53211122	0.9	45	4	400	8	8	1	2.5	0.60	0.11	0.05	0.68	0.14	0.06	0.26	0.71	0.71	0.03	0.000	3995	3995	1411	2657	0.03	0.0003	3939	31	2578
M13211211	0.1	45	4	400	8	10	0.6	1.5	2.51	0.41	0.15	0.62	0.19	0.07	0.05	0.36	0.69	0.12	0.001	857	857	30	835	0.12	0.0009	696	5	670
M13211212	0.1	45	4	400	8	10	0.6	2.5	2.56	0.42	0.15	0.62	0.19	0.07	0.05	0.36	0.69	0.12	0.001	838	838	29	817	0.12	0.0009	677	5	651
M23211211	0.3	45	4	400	8	10	0.6	1.5	2.34	0.40	0.15	0.63	0.18	0.06	0.05	0.37	0.70	0.11	0.001	921	921	100	844	0.11	0.0008	783	6	692
M23211212	0.3	45	4	400	8	10	0.6	2.5	2.38	0.41	0.15	0.63	0.18	0.06	0.05	0.37	0.69	0.11	0.001	899	899	98	824	0.11	0.0008	760	6	671
M33211211	0.5	45	4	400	8	10	0.6	1.5	2.15	0.38	0.14	0.64	0.17	0.06	0.06	0.38	0.70	0.10	0.001	1013	1013	192	859	0.10	0.0008	898	7	723
M33211212	0.5	45	4	400	8	10	0.6	2.5	2.20	0.39	0.15	0.64	0.17	0.06	0.06	0.37	0.70	0.11	0.001	988	988	187	839	0.11	0.0008	873	7	703
M43211211	0.7	45	4	400	8	10	0.6	1.5	1.95	0.36	0.14	0.66	0.16	0.06	0.07	0.40	0.71	0.10	0.001	1143	1143	315	882	0.10	0.0007	1048	8	764
M43211212	0.7	45	4	400	8	10	0.6	2.5	1.99	0.37	0.14	0.66	0.16	0.06	0.07	0.39	0.70	0.10	0.001	1119	1119	308	865	0.10	0.0007	1025	8	747
M53211211	0.9	45	4	400	8	10	0.6	1.5	1.73	0.33	0.13	0.68	0.14	0.06	0.08	0.43	0.71	0.08	0.001	1298	1298	478	898	0.08	0.0006	1220	10	799
M53211212	0.9	45	4	400	8	10	0.6	2.5	1.77	0.33	0.13	0.68	0.14	0.06	0.08	0.43	0.71	0.08	0.001	1272	1272	468	881	0.08	0.0007	1194	9	781
M13211221	0.1	45	4	400	8	10	1	1.5	1.94	0.32	0.11	0.62	0.19	0.07	0.07	0.44	0.71	0.10	0.001	1182	1182	43	1149	0.10	0.0008	1021	8	983
M13211222	0.1	45	4	400	8	10	1	2.5	1.97	0.32	0.12	0.62	0.19	0.07	0.07	0.44	0.71	0.10	0.001	1159	1159	42	1126	0.10	0.0008	999	8	961
M23211221	0.3	45	4	400	8	10	1	1.5	1.80	0.31	0.11	0.63	0.18	0.06	0.08	0.45	0.71	0.09	0.001	1256	1256	140	1141	0.09	0.0007	1115	9	985
M23211222	0.3	45	4	400	8	10	1	2.5	1.84	0.31	0.11	0.63	0.18	0.06	0.07	0.45	0.71	0.10	0.001	1232	1232	137	1120	0.10	0.0007	1092	8	964
M33211221	0.5	45	4	400	8	10	1	1.5	1.66	0.30	0.11	0.64	0.17	0.06	0.08	0.46	0.71	0.09	0.001	1354	1354	259	1136	0.09	0.0006	1234	9	994
M33211222	0.5	45	4	400	8	10	1	2.5	1.70	0.30	0.11	0.64	0.17	0.06	0.08	0.46	0.71	0.09	0.001	1328	1328	254	1115	0.09	0.0006	1209	9	974
M43211221	0.7	45	4	400	8	10	1	1.5	1.51	0.28	0.11	0.66	0.16	0.06	0.09	0.48	0.71	0.08	0.001	1492	1492	411	1140	0.08	0.0006	1395	11	1017

Name	af	nf	hf	mf	Ly	Lx	tw	Lcb	T1 [s]	T2 [s]	T3 [s]	M1 [-]	M2 [-]	M3 [-]	Sa	Sa2	Sa3	Disp [m]	ISDR [-]	Total Moment [MN-m]	Total Shear [MN]	Outrigger Moment [MN-m]	Wall Moment [MN-m]	Mode 1 Disp [m]	Mode 1 ISDR [-]	Mode 1 Moment [MN-m]	Mode 1 Shear [MN]	Mode 1 wall Moment [MN-m]
M43211222	0.7	45	4	400	8	10	1	2.5	1.54	0.28	0.11	0.66	0.16	0.06	0.09	0.47	0.71	0.08	0.001	1464	1464	403	1119	0.08	0.0006	1367	11	996
M53211221	0.9	45	4	400	8	10	1	1.5	1.34	0.25	0.10	0.68	0.14	0.06	0.11	0.51	0.71	0.07	0.001	1706	1706	621	1167	0.06	0.0005	1631	13	1067
M53211222	0.9	45	4	400	8	10	1	2.5	1.37	0.26	0.10	0.68	0.14	0.06	0.10	0.50	0.71	0.07	0.001	1669	1669	608	1142	0.07	0.0005	1594	13	1043
M13212111	0.1	45	4	400	10	8	0.6	1.5	1.53	0.25	0.09	0.62	0.19	0.07	0.09	0.52	0.71	0.08	0.001	1491	1491	55	1446	0.08	0.0006	1326	10	1276
M13212112	0.1	45	4	400	10	8	0.6	2.5	1.58	0.26	0.09	0.62	0.19	0.07	0.09	0.50	0.71	0.08	0.001	1445	1445	53	1402	0.08	0.0006	1283	10	1234
M23212111	0.3	45	4	400	10	8	0.6	1.5	1.42	0.24	0.09	0.63	0.18	0.06	0.10	0.53	0.71	0.08	0.001	1594	1594	180	1441	0.08	0.0006	1450	11	1280
M23212112	0.3	45	4	400	10	8	0.6	2.5	1.47	0.25	0.09	0.63	0.18	0.06	0.10	0.51	0.71	0.08	0.001	1543	1543	174	1396	0.08	0.0006	1401	11	1237
M33212111	0.5	45	4	400	10	8	0.6	1.5	1.31	0.23	0.09	0.64	0.17	0.06	0.11	0.54	0.71	0.07	0.001	1732	1732	333	1443	0.07	0.0005	1610	12	1296
M33212112	0.5	45	4	400	10	8	0.6	2.5	1.35	0.24	0.09	0.64	0.17	0.06	0.10	0.53	0.71	0.07	0.001	1676	1676	322	1397	0.07	0.0005	1554	12	1252
M43212111	0.7	45	4	400	10	8	0.6	1.5	1.19	0.22	0.08	0.66	0.16	0.06	0.12	0.57	0.71	0.06	0.000	1925	1925	531	1459	0.06	0.0005	1826	14	1331
M43212112	0.7	45	4	400	10	8	0.6	2.5	1.23	0.23	0.09	0.66	0.16	0.06	0.12	0.55	0.71	0.06	0.000	1861	1861	513	1412	0.06	0.0005	1763	14	1284
M53212111	0.9	45	4	400	10	8	0.6	1.5	1.06	0.20	0.08	0.68	0.14	0.06	0.14	0.60	0.71	0.05	0.000	2213	2213	799	1502	0.05	0.0004	2138	17	1399
M53212112	0.9	45	4	400	10	8	0.6	2.5	1.09	0.20	0.08	0.68	0.14	0.06	0.13	0.59	0.71	0.05	0.000	2140	2140	774	1454	0.05	0.0004	2064	16	1351
M13212121	0.1	45	4	400	10	8	1	1.5	1.15	0.19	0.07	0.62	0.19	0.07	0.13	0.62	0.71	0.06	0.000	2007	2007	75	1943	0.06	0.0005	1835	14	1765
M13212122	0.1	45	4	400	10	8	1	2.5	1.18	0.19	0.07	0.62	0.19	0.07	0.12	0.61	0.71	0.07	0.001	1945	1945	73	1883	0.07	0.0005	1773	13	1705
M23212121	0.3	45	4	400	10	8	1	1.5	1.07	0.18	0.07	0.63	0.18	0.06	0.14	0.63	0.71	0.06	0.000	2162	2162	247	1944	0.06	0.0004	2015	15	1780
M23212122	0.3	45	4	400	10	8	1	2.5	1.10	0.19	0.07	0.63	0.18	0.06	0.13	0.62	0.71	0.06	0.000	2088	2088	238	1879	0.06	0.0004	1940	15	1714
M33212121	0.5	45	4	400	10	8	1	1.5	0.98	0.18	0.07	0.64	0.17	0.06	0.15	0.64	0.71	0.05	0.000	2355	2355	456	1946	0.05	0.0004	2233	17	1799
M33212122	0.5	45	4	400	10	8	1	2.5	1.02	0.18	0.07	0.64	0.17	0.06	0.15	0.63	0.71	0.06	0.000	2275	2275	440	1881	0.06	0.0004	2152	17	1733
M43212121	0.7	45	4	400	10	8	1	1.5	0.89	0.17	0.06	0.66	0.16	0.06	0.17	0.66	0.71	0.05	0.000	2604	2604	716	1954	0.05	0.0004	2508	19	1828
M43212122	0.7	45	4	400	10	8	1	2.5	0.92	0.17	0.07	0.66	0.16	0.06	0.16	0.65	0.71	0.05	0.000	2528	2528	696	1898	0.05	0.0004	2431	19	1772
M53212121	0.9	45	4	400	10	8	1	1.5	0.79	0.15	0.06	0.68	0.14	0.06	0.19	0.69	0.71	0.04	0.000	2984	2984	1066	2005	0.04	0.0003	2914	23	1907
M53212122	0.9	45	4	400	10	8	1	2.5	0.82	0.15	0.06	0.68	0.14	0.06	0.18	0.68	0.71	0.04	0.000	2891	2891	1034	1945	0.04	0.0003	2821	22	1846
M13212211	0.1	45	4	400	10	10	0.6	1.5	3.48	0.57	0.20	0.62	0.19	0.07	0.03	0.27	0.59	0.14	0.001	580	580	19	567	0.14	0.0010	431	3	415
M13212212	0.1	45	4	400	10	10	0.6	2.5	3.61	0.59	0.21	0.62	0.19	0.07	0.03	0.26	0.58	0.14	0.001	554	554	18	542	0.14	0.0011	409	3	394
M23212211	0.3	45	4	400	10	10	0.6	1.5	3.24	0.55	0.20	0.63	0.18	0.06	0.03	0.28	0.60	0.13	0.001	613	613	64	569	0.13	0.0009	482	4	426
M23212212	0.3	45	4	400	10	10	0.6	2.5	3.36	0.57	0.21	0.63	0.18	0.06	0.03	0.27	0.59	0.13	0.001	586	586	61	544	0.13	0.0010	457	3	403
M33212211	0.5	45	4	400	10	10	0.6	1.5	2.99	0.53	0.20	0.64	0.17	0.06	0.04	0.29	0.60	0.12	0.001	663	663	123	574	0.12	0.0009	549	4	442
M33212212	0.5	45	4	400	10	10	0.6	2.5	3.10	0.55	0.21	0.64	0.17	0.06	0.04	0.28	0.59	0.13	0.001	633	633	117	549	0.12	0.0009	520	4	419
M43212211	0.7	45	4	400	10	10	0.6	1.5	2.71	0.50	0.19	0.66	0.16	0.06	0.04	0.31	0.61	0.11	0.001	740	740	204	585	0.11	0.0008	644	5	469
M43212212	0.7	45	4	400	10	10	0.6	2.5	2.81	0.52	0.20	0.66	0.16	0.06	0.04	0.30	0.60	0.12	0.001	704	704	194	559	0.12	0.0008	609	5	444
M53212211	0.9	45	4	400	10	10	0.6	1.5	2.40	0.45	0.18	0.68	0.14	0.06	0.05	0.34	0.63	0.10	0.001	865	865	325	610	0.10	0.0008	786	6	514
M53212212	0.9	45	4	400	10	10	0.6	2.5	2.50	0.47	0.19	0.68	0.14	0.06	0.05	0.33	0.62	0.10	0.001	822	822	309	582	0.10	0.0008	743	6	486
M13212221	0.1	45	4	400	10	10	1	1.5	2.72	0.44	0.16	0.62	0.19	0.07	0.04	0.34	0.67	0.12	0.001	779	779	27	761	0.12	0.0009	619	5	595
M13212222	0.1	45	4	400	10	10	1	2.5	2.83	0.46	0.17	0.62	0.19	0.07	0.04	0.33	0.66	0.12	0.001	744	744	25	726	0.12	0.0009	584	4	562
M23212221	0.3	45	4	400	10	10	1	1.5	2.53	0.43	0.16	0.63	0.18	0.06	0.05	0.35	0.68	0.12	0.001	833	833	90	766	0.11	0.0008	694	5	613
M23212222	0.3	45	4	400	10	10	1	2.5	2.63	0.45	0.16	0.63	0.18	0.06	0.04	0.34	0.66	0.12	0.001	794	794	85	731	0.12	0.0008	654	5	578
M33212221	0.5	45	4	400	10	10	1	1.5	2.33	0.42	0.16	0.64	0.17	0.06	0.05	0.36	0.68	0.11	0.001	913	913	172	778	0.11	0.0008	796	6	641
M33212222	0.5	45	4	400	10	10	1	2.5	2.43	0.43	0.16	0.64	0.17	0.06	0.05	0.35	0.67	0.11	0.001	867	867	163	741	0.11	0.0008	749	6	603
M43212221	0.7	45	4	400	10	10	1	1.5	2.12	0.39	0.15	0.66	0.16	0.06	0.06	0.37	0.69	0.10	0.001	1032	1032	284	800	0.10	0.0007	938	7	683
M43212222	0.7	45	4	400	10	10	1	2.5	2.20	0.41	0.16	0.66	0.16	0.06	0.06	0.36	0.68	0.10	0.001	979	979	270	761	0.10	0.0008	883	7	644
M53212221	0.9	45	4	400	10	10	1	1.5	1.88	0.35	0.14	0.68	0.14	0.06	0.07	0.41	0.70	0.09	0.001	1195	1195	441	829	0.09	0.0007	1118	9	732
M53212222	0.9	45	4	400	10	10	1	2.5	1.95	0.37	0.15	0.68	0.14	0.06	0.07	0.40	0.69	0.09	0.001	1147	1147	423	796	0.09	0.0007	1070	8	700
M13221111	0.1	45	4	600	8	8	0.6	1.5	1.41	0.23	0.08	0.62	0.19	0.07	0.10	0.55	0.71	0.08	0.001	2434	2434	90	2360	0.08	0.0006	2180	17	2097
M13221112	0.1	45	4	600	8	8	0.6	2.5	1.43	0.23	0.08	0.62	0.19	0.07	0.10	0.54	0.71	0.08	0.001	2393	2393	88	2320	0.08	0.0006	2140	16	2059
M23221111	0.3	45	4	600	8	8	0.6	1.5	1.31	0.22	0.08	0.63	0.18	0.06	0.11	0.56	0.71	0.07	0.001	2606	2606	295	2353	0.07	0.0005	2385	18	2107
M23221112	0.3	45	4	600	8	8	0.6	2.5	1.34	0.23	0.08	0.63	0.18	0.06	0.11	0.55	0.71	0.07	0.001	2560	2560	290	2312	0.07	0.0005	2339	18	2066
M33221111	0.5	45	4	600	8	8	0.6	1.5	1.21	0.22	0.08	0.64	0.17	0.06	0.12	0.57	0.71	0.06	0.000	2836	2836	547	2358	0.06	0.0005	2650	20	2134
M33221112	0.5	45	4	600	8	8	0.6	2.5	1.23	0.22	0.08	0.64	0.17	0.06	0.12	0.57	0.71	0.07	0.000	2783	2783	536	2315	0.07	0.0005	2597	20	2091
M43221111	0.7	45	4	600	8	8	0.6	1.5	1.10	0.20	0.08	0.66	0.16	0.06	0.13	0.60	0.71	0.06	0.000	3157	3157	870	2386	0.06	0.0004	3009	23	2193
M43221112	0.7	45	4	600	8	8	0.6	2.5	1.12	0.21	0.08	0.66	0.16	0.06	0.13	0.59	0.71	0.06	0.000	3095	3095	853	2340	0.06	0.0004	2946	23	2147
M53221111	0.9	45	4	600	8	8	0.6	1.5	0.97	0.18	0.07	0.68	0.14	0.06	0.15	0.63	0.71	0.05	0.000	3622	3622	1304	2452	0.05	0.0004	3511	28	2298
M53221112	0.9	45	4	600	8	8	0.6	2.5	0.99	0.19	0.07	0.68	0.14	0.06	0.15	0.63	0.71	0.05	0.000	3555	3555	1281	2408	0.05	0.0004	3443	27	2253
M13221121	0.1	45	4	600	8	8	1	1.5	1.05	0.17	0.06	0.62	0.19	0.07	0.14	0.65	0.71	0.06	0.000	3318	3318	125	3211	0.06	0.0004	3065	23	2949
M13221122	0.1	45	4	600	8	8	1	2.5	1.07	0.17	0.06	0.62	0.19	0.07	0.14	0.65	0.71	0.06	0.000	3260	3260	123	3155	0.06	0.0004	3006	23	2892
M23221121	0.3	45	4	600	8	8	1	1.5	0.98	0.17	0.06	0.63	0.18	0.06	0.15	0.66	0.71	0.05	0.000	3564	3564	409	3199	0.05	0.0004	3347	26	2956
M23221122	0.3	45	4	600	8	8	1	2.5	0.99	0.17	0.06	0.63	0.18	0.06	0.15	0.66	0.71	0.06	0.000	3498	3498	401	3141	0.06	0.0004	3280	25	2897
M33221121	0.5	45	4	600	8	8	1	1.5	0.90	0.16	0.06	0.64	0.17	0.06	0.17	0.67	0.71	0.05	0.000	3865	3865	750	3185	0.05	0.0004	3685	28	2967
M33221122	0.5	45	4	600	8	8	1	2.5	0.91	0.16	0.06	0.64	0.17	0.06	0.16	0.67	0.71	0.05	0.000	3803	3803	737	3136	0.05	0.0004	3623	28	2917
M43221121	0.7	45	4	600	8	8	1	1.5	0.82	0.15	0.06	0.66	0.16	0.06	0.18	0.69	0.71	0.04	0.000	4306	4306	1183	3220	0.04	0.0003	4166	32	3036
M43221122	0.7	45	4	600	8	8	1	2.5	0.83	0.15	0.06	0.66	0.16	0.06	0.18	0.68	0.71	0.04	0.000	4230	4230	1163	3165	0.04	0.0003	4090	32	2980
M53221121	0.9	45	4	600	8	8	1	1.5	0.72	0.14	0.05	0.68	0.14	0.06	0.21	0.71	0.71	0.04	0.000	4931	4931	1756	3303	0.04	0.0003	4830	38	3161
M53221122	0.9	45	4	600	8	8	1	2.5	0.74	0.14	0.06	0.68	0.14	0.06	0.21	0.71	0.71	0.04	0.000	4834	4834	1722	3240	0.04	0.0003	4732	37	3097
M13221211	0.1	45	4	600	8	10	0.6	1.5	3.07	0.50	0.18	0.62	0.19	0.07	0.04	0.31	0.64	0.13	0.001	1008	1008	34	985	0.13	0.0010	774	6	744
M13221212	0.1	45	4	600	8	10	0.6	2.5	3.13	0.51	0.18	0.62	0.19	0.07	0.03	0.30	0.63	0.13	0.001	984	984	33	962	0.13	0.0010	752	6	724
M23221211	0.3	45	4	600	8	10	0.6	1.5	2.86	0.49	0.18	0.63	0.18	0.06	0.04	0.32	0.64	0.12	0.001	1072	1072	114	990	0.12	0.0009	866	7	765
M23221212	0.3	45	4	600	8	10	0.6	2.5	2.92	0.50	0.18	0.63	0.18	0.06	0.04	0.31	0.63	0.12	0.001	1047	1047	111	968	0.12	0.0009	842	6	744
M33221211	0.5	45	4	600	8	10	0.6	1.5	2.64	0.47	0.18	0.64	0.17	0.06	0.04	0.33	0.64	0.12	0.001	1166	1166	218	1002	0.11	0.0008	989	8	796
M33221212	0.5	45	4	600	8	10	0.6	2.5	2.69	0.48	0.18	0.64	0.17	0.06	0.04	0.32	0.64	0.12	0.001	1138	1138	212	979	0.12	0.0008	962	7	775
M43221211	0.7	45	4	600	8	10	0.6	1.5	2.39	0.44	0.17	0.66	0.16	0.06	0.05	0.34	0.65	0.11	0.001	1308	1308	360	1025	0.11	0.0008	1163	9	847
M43221212	0.7	45	4	600	8	10	0.6	2.5	2.44	0.45	0.17	0.66	0.16	0.06	0.05	0.34	0.65	0.11	0.001	1276	1276	352	1002	0.11	0.0008	1131	9	824
M53221211	0.9	45	4	600	8	10	0.6	1.5	2.12	0.40	0.16	0.68	0.14	0.06	0.06	0.37	0.67	0.10	0.001	1540	1540	572	1075	0.10	0.0008	1425	11	933

Name	af	nf	hf	mf	Ly	Lx	tw	Lcb	T1 [s]	T2 [s]	T3 [s]	M1 [-]	M2 [-]	M3 [-]	Sa	Sa2	Sa3	Disp [m]	ISDR [-]	Total Moment [MN-m]	Total Shear [MN]	Outrigger Moment [MN-m]	Wall Moment [MN-m]	Mode 1 Disp [m]	Mode 1 ISDR [-]	Mode 1 Moment [MN-m]	Mode 1 Shear [MN]	Mode 1 wall Moment [MN-m]
M53221212	0.9	45	4	600	8	10	0.6	2.5	2.17	0.41	0.16	0.68	0.14	0.06	0.06	0.37	0.67	0.10	0.001	1500	1500	558	1049	0.10	0.0008	1385	11	906
M13221221	0.1	45	4	600	8	10	1	1.5	2.37	0.39	0.14	0.62	0.19	0.07	0.05	0.38	0.71	0.11	0.001	1376	1376	48	1341	0.11	0.0008	1138	9	1095
M13221222	0.1	45	4	600	8	10	1	2.5	2.42	0.39	0.14	0.62	0.19	0.07	0.05	0.37	0.70	0.11	0.001	1344	1344	47	1310	0.11	0.0008	1105	8	1063
M23221221	0.3	45	4	600	8	10	1	1.5	2.21	0.38	0.14	0.63	0.18	0.06	0.06	0.39	0.71	0.11	0.001	1488	1488	163	1359	0.11	0.0008	1281	10	1131
M23221222	0.3	45	4	600	8	10	1	2.5	2.25	0.38	0.14	0.63	0.18	0.06	0.06	0.38	0.71	0.11	0.001	1448	1448	158	1324	0.11	0.0008	1242	9	1097
M33221221	0.5	45	4	600	8	10	1	1.5	2.04	0.36	0.14	0.64	0.17	0.06	0.07	0.40	0.71	0.10	0.001	1645	1645	313	1390	0.10	0.0007	1471	11	1184
M33221222	0.5	45	4	600	8	10	1	2.5	2.08	0.37	0.14	0.64	0.17	0.06	0.06	0.39	0.71	0.10	0.001	1602	1602	304	1355	0.10	0.0007	1428	11	1150
M43221221	0.7	45	4	600	8	10	1	1.5	1.85	0.34	0.13	0.66	0.16	0.06	0.07	0.42	0.71	0.09	0.001	1820	1820	502	1402	0.09	0.0007	1675	13	1220
M43221222	0.7	45	4	600	8	10	1	2.5	1.88	0.35	0.13	0.66	0.16	0.06	0.07	0.41	0.71	0.09	0.001	1782	1782	491	1374	0.09	0.0007	1638	13	1194
M53221221	0.9	45	4	600	8	10	1	1.5	1.64	0.31	0.12	0.68	0.14	0.06	0.08	0.45	0.71	0.08	0.001	2062	2062	757	1423	0.08	0.0006	1946	15	1274
M53221222	0.9	45	4	600	8	10	1	2.5	1.67	0.31	0.13	0.68	0.14	0.06	0.08	0.45	0.71	0.08	0.001	2023	2023	744	1397	0.08	0.0006	1907	15	1248
M13222111	0.1	45	4	600	10	8	0.6	1.5	1.87	0.31	0.11	0.62	0.19	0.07	0.07	0.45	0.71	0.10	0.001	1832	1832	66	1780	0.10	0.0007	1590	12	1530
M13222112	0.1	45	4	600	10	8	0.6	2.5	1.93	0.31	0.11	0.62	0.19	0.07	0.07	0.44	0.71	0.10	0.001	1778	1778	64	1728	0.10	0.0008	1537	12	1478
M23222111	0.3	45	4	600	10	8	0.6	1.5	1.75	0.30	0.11	0.63	0.18	0.06	0.08	0.46	0.71	0.09	0.001	1946	1946	217	1767	0.09	0.0007	1735	13	1532
M23222112	0.3	45	4	600	10	8	0.6	2.5	1.80	0.31	0.11	0.63	0.18	0.06	0.08	0.45	0.71	0.09	0.001	1889	1889	211	1716	0.09	0.0007	1678	13	1482
M33222111	0.5	45	4	600	10	8	0.6	1.5	1.61	0.29	0.11	0.64	0.17	0.06	0.09	0.47	0.71	0.08	0.001	2101	2101	402	1761	0.08	0.0006	1922	15	1548
M33222112	0.5	45	4	600	10	8	0.6	2.5	1.66	0.30	0.11	0.64	0.17	0.06	0.08	0.46	0.71	0.09	0.001	2036	2036	390	1709	0.08	0.0006	1857	14	1496
M43222111	0.7	45	4	600	10	8	0.6	1.5	1.46	0.27	0.10	0.66	0.16	0.06	0.10	0.49	0.71	0.07	0.001	2321	2321	640	1770	0.07	0.0005	2177	17	1586
M43222112	0.7	45	4	600	10	8	0.6	2.5	1.50	0.28	0.11	0.66	0.16	0.06	0.09	0.48	0.71	0.08	0.001	2245	2245	619	1715	0.08	0.0006	2100	16	1530
M53222111	0.9	45	4	600	10	8	0.6	1.5	1.29	0.24	0.10	0.68	0.14	0.06	0.11	0.53	0.71	0.06	0.001	2653	2653	965	1813	0.06	0.0005	2539	20	1662
M53222112	0.9	45	4	600	10	8	0.6	2.5	1.33	0.25	0.10	0.68	0.14	0.06	0.11	0.51	0.71	0.06	0.001	2567	2567	935	1756	0.06	0.0005	2454	19	1606
M13222121	0.1	45	4	600	10	8	1	1.5	1.40	0.23	0.08	0.62	0.19	0.07	0.10	0.55	0.71	0.08	0.001	2442	2442	90	2368	0.08	0.0006	2188	17	2105
M13222122	0.1	45	4	600	10	8	1	2.5	1.45	0.24	0.08	0.62	0.19	0.07	0.10	0.54	0.71	0.08	0.001	2365	2365	87	2293	0.08	0.0006	2113	16	2033
M23222121	0.3	45	4	600	10	8	1	1.5	1.31	0.22	0.08	0.63	0.18	0.06	0.11	0.56	0.71	0.07	0.001	2616	2616	296	2362	0.07	0.0005	2394	18	2115
M23222122	0.3	45	4	600	10	8	1	2.5	1.35	0.23	0.08	0.63	0.18	0.06	0.11	0.55	0.71	0.07	0.001	2528	2528	286	2284	0.07	0.0005	2309	18	2039
M33222121	0.5	45	4	600	10	8	1	1.5	1.21	0.21	0.08	0.64	0.17	0.06	0.12	0.58	0.71	0.06	0.000	2847	2847	549	2367	0.06	0.0005	2661	20	2143
M33222122	0.5	45	4	600	10	8	1	2.5	1.25	0.22	0.08	0.64	0.17	0.06	0.12	0.56	0.71	0.07	0.000	2746	2746	529	2285	0.07	0.0005	2561	20	2062
M43222121	0.7	45	4	600	10	8	1	1.5	1.09	0.20	0.08	0.66	0.16	0.06	0.13	0.60	0.71	0.06	0.000	3170	3170	873	2395	0.06	0.0004	3022	23	2202
M43222122	0.7	45	4	600	10	8	1	2.5	1.13	0.21	0.08	0.66	0.16	0.06	0.13	0.59	0.71	0.06	0.000	3053	3053	841	2309	0.06	0.0004	2904	23	2116
M53222121	0.9	45	4	600	10	8	1	1.5	0.97	0.18	0.07	0.68	0.14	0.06	0.15	0.63	0.71	0.05	0.000	3636	3636	1309	2461	0.05	0.0004	3525	28	2307
M53222122	0.9	45	4	600	10	8	1	2.5	1.00	0.19	0.08	0.68	0.14	0.06	0.15	0.62	0.71	0.05	0.000	3509	3509	1265	2378	0.05	0.0004	3397	27	2223
M13222211	0.1	45	4	600	10	10	0.6	1.5	4.26	0.69	0.25	0.62	0.19	0.07	0.02	0.22	0.52	0.16	0.001	681	681	22	667	0.15	0.0012	487	4	468
M13222212	0.1	45	4	600	10	10	0.6	2.5	4.42	0.72	0.26	0.62	0.19	0.07	0.02	0.21	0.50	0.16	0.001	652	652	21	639	0.16	0.0012	463	4	445
M23222211	0.3	45	4	600	10	10	0.6	1.5	3.97	0.68	0.25	0.63	0.18	0.06	0.02	0.23	0.52	0.15	0.001	716	716	74	667	0.15	0.0011	542	4	479
M23222212	0.3	45	4	600	10	10	0.6	2.5	4.12	0.70	0.26	0.63	0.18	0.06	0.02	0.22	0.50	0.15	0.001	685	685	70	639	0.15	0.0011	515	4	455
M33222211	0.5	45	4	600	10	10	0.6	1.5	3.66	0.65	0.24	0.64	0.17	0.06	0.03	0.23	0.53	0.14	0.001	768	768	140	670	0.14	0.0010	615	5	495
M33222212	0.5	45	4	600	10	10	0.6	2.5	3.80	0.68	0.25	0.64	0.17	0.06	0.03	0.23	0.51	0.14	0.001	734	734	134	641	0.14	0.0010	584	4	470
M43222211	0.7	45	4	600	10	10	0.6	1.5	3.32	0.61	0.24	0.66	0.16	0.06	0.03	0.25	0.54	0.13	0.001	850	850	233	681	0.13	0.0009	718	6	523
M43222212	0.7	45	4	600	10	10	0.6	2.5	3.44	0.64	0.25	0.66	0.16	0.06	0.03	0.24	0.52	0.13	0.001	809	809	222	649	0.13	0.0009	681	5	496
M53222211	0.9	45	4	600	10	10	0.6	1.5	2.94	0.55	0.22	0.68	0.14	0.06	0.04	0.28	0.56	0.11	0.001	986	986	376	707	0.11	0.0009	871	7	570
M53222212	0.9	45	4	600	10	10	0.6	2.5	3.06	0.57	0.23	0.68	0.14	0.06	0.04	0.27	0.55	0.11	0.001	939	939	358	675	0.11	0.0009	825	6	540
M13222221	0.1	45	4	600	10	10	1	1.5	3.33	0.54	0.19	0.62	0.19	0.07	0.03	0.29	0.61	0.14	0.001	917	917	30	897	0.13	0.0010	690	5	664
M13222222	0.1	45	4	600	10	10	1	2.5	3.46	0.56	0.20	0.62	0.19	0.07	0.03	0.28	0.60	0.14	0.001	875	875	29	856	0.14	0.0010	652	5	627
M23222221	0.3	45	4	600	10	10	1	1.5	3.10	0.53	0.19	0.63	0.18	0.06	0.04	0.29	0.61	0.13	0.001	972	972	102	900	0.13	0.0009	771	6	681
M23222222	0.3	45	4	600	10	10	1	2.5	3.22	0.55	0.20	0.63	0.18	0.06	0.03	0.28	0.60	0.13	0.001	926	926	97	859	0.13	0.0009	728	6	643
M33222221	0.5	45	4	600	10	10	1	1.5	2.86	0.51	0.19	0.64	0.17	0.06	0.04	0.30	0.62	0.12	0.001	1053	1053	196	909	0.12	0.0009	880	7	708
M33222222	0.5	45	4	600	10	10	1	2.5	2.97	0.53	0.20	0.64	0.17	0.06	0.04	0.29	0.61	0.12	0.001	1002	1002	186	867	0.12	0.0009	831	6	669
M43222221	0.7	45	4	600	10	10	1	1.5	2.59	0.48	0.18	0.66	0.16	0.06	0.05	0.32	0.63	0.11	0.001	1177	1177	324	929	0.11	0.0008	1033	8	753
M43222222	0.7	45	4	600	10	10	1	2.5	2.69	0.50	0.19	0.66	0.16	0.06	0.04	0.31	0.62	0.11	0.001	1118	1118	308	884	0.11	0.0008	974	8	710
M53222221	0.9	45	4	600	10	10	1	1.5	2.30	0.43	0.17	0.68	0.14	0.06	0.05	0.35	0.65	0.10	0.001	1380	1380	516	970	0.10	0.0008	1262	10	826
M53222222	0.9	45	4	600	10	10	1	2.5	2.39	0.45	0.18	0.68	0.14	0.06	0.05	0.34	0.64	0.10	0.001	1306	1306	490	922	0.10	0.0008	1188	9	777

Name	T1 [s]	Sa(T1) [g]	Sa(T2) [g]	Sa(T3) [g]	DOC [-]	Disp [m]	ISDR [-]	Total Moment [MN-m]	Total Shear [MN]	Max CB Shear [MN]	Max Pp [MN]	Max wall moment [MN-m]	Disp [m]2	ISDR [-]3	Total Moment [MN-m]4	Total Shear [MN]5	Max CB Shear [MN]6	Max Pp [MN]2	Max wall moment [MN-m]8	C1 [-]	C2 [-]	C3 [-]	Mdy/ Mst [-]
V11111111	0.73	0.55	0.88	0.89	0.70	0.11	0.0029	1111	1111	10	115	168	0.11	0.0029	1109	34	10	115	164	1.00	0.18	0.04	0.49
V11111112	0.77	0.53	0.88	0.89	0.74	0.11	0.0031	1073	1073	11	115	141	0.11	0.0031	1072	33	10	115	136	1.00	0.19	0.05	0.49
V21111111	0.68	0.59	0.89	0.89	0.74	0.10	0.0026	1192	1192	12	129	160	0.10	0.0026	1190	37	12	129	155	1.00	0.18	0.04	0.52
V21111112	0.70	0.57	0.88	0.89	0.78	0.10	0.0028	1161	1161	12	129	134	0.10	0.0027	1159	36	12	129	129	1.00	0.19	0.05	0.52
V31111111	0.62	0.63	0.89	0.89	0.77	0.09	0.0024	1265	1265	13	143	149	0.09	0.0024	1263	39	13	143	145	1.00	0.19	0.05	0.56
V31111112	0.65	0.61	0.89	0.89	0.80	0.09	0.0025	1234	1234	14	142	124	0.09	0.0025	1232	38	13	142	120	1.00	0.20	0.05	0.56
V41111111	0.58	0.67	0.89	0.89	0.80	0.08	0.0022	1342	1342	15	157	138	0.08	0.0022	1339	41	15	157	134	1.00	0.20	0.05	0.60
V41111112	0.60	0.66	0.89	0.89	0.83	0.08	0.0023	1313	1313	15	156	115	0.08	0.0023	1311	40	15	156	111	1.00	0.21	0.05	0.61
V51111111	0.54	0.71	0.89	0.89	0.83	0.08	0.0021	1406	1406	17	171	124	0.07	0.0021	1402	43	16	170	121	1.00	0.21	0.05	0.65
V51111112	0.55	0.70	0.89	0.89	0.85	0.08	0.0021	1382	1382	17	169	103	0.08	0.0021	1379	42	16	169	100	1.00	0.22	0.06	0.65
V11111121	0.60	0.65	0.89	0.89	0.70	0.08	0.0023	1306	1306	12	136	203	0.08	0.0023	1304	40	12	136	198	1.00	0.15	0.03	0.49
V11111122	0.63	0.62	0.89	0.89	0.74	0.09	0.0024	1259	1259	12	136	169	0.09	0.0024	1258	39	12	136	165	1.00	0.16	0.04	0.49
V21111121	0.56	0.69	0.89	0.89	0.73	0.08	0.0021	1393	1393	14	152	192	0.08	0.0021	1391	43	14	152	188	1.00	0.15	0.03	0.52
V21111122	0.58	0.67	0.89	0.89	0.77	0.08	0.0022	1356	1356	14	152	161	0.08	0.0022	1355	42	14	152	157	1.00	0.16	0.04	0.52
V31111121	0.52	0.73	0.89	0.89	0.76	0.07	0.0019	1465	1465	16	166	179	0.07	0.0019	1463	45	15	166	176	1.00	0.16	0.04	0.56
V31111122	0.54	0.71	0.89	0.89	0.79	0.07	0.0020	1435	1435	16	167	150	0.07	0.0020	1433	44	16	167	147	1.00	0.17	0.04	0.56
V41111121	0.48	0.76	0.89	0.89	0.79	0.06	0.0017	1514	1514	17	178	164	0.06	0.0017	1512	46	17	178	160	1.00	0.17	0.04	0.61
V41111122	0.50	0.75	0.89	0.89	0.82	0.07	0.0018	1495	1495	17	179	138	0.07	0.0018	1493	46	17	179	134	1.00	0.18	0.04	0.61
V51111121	0.45	0.78	0.89	0.89	0.81	0.06	0.0016	1552	1552	18	189	147	0.06	0.0016	1548	47	18	189	143	1.00	0.18	0.04	0.65
V51111122	0.46	0.77	0.89	0.89	0.84	0.06	0.0016	1536	1536	18	189	123	0.06	0.0016	1533	47	18	189	120	1.00	0.19	0.05	0.66
V11111211	0.66	0.61	0.89	0.89	0.73	0.09	0.0026	1221	1221	11	127	170	0.09	0.0026	1220	38	11	127	166	1.00	0.16	0.04	0.49
V11111212	0.68	0.59	0.88	0.89	0.77	0.10	0.0027	1192	1192	12	128	143	0.10	0.0027	1191	37	12	128	139	1.00	0.18	0.04	0.49
V21111211	0.60	0.65	0.89	0.89	0.76	0.08	0.0023	1310	1310	13	142	161	0.08	0.0023	1309	40	13	142	157	1.00	0.17	0.04	0.52
V21111212	0.63	0.63	0.89	0.89	0.79	0.09	0.0024	1278	1278	14	142	135	0.09	0.0024	1276	40	13	142	131	1.00	0.18	0.04	0.53
V31111211	0.56	0.69	0.89	0.89	0.79	0.08	0.0021	1392	1392	15	157	151	0.08	0.0021	1391	43	15	157	148	1.00	0.17	0.04	0.56
V31111212	0.58	0.68	0.89	0.89	0.82	0.08	0.0022	1366	1366	15	157	126	0.08	0.0021	1365	42	15	157	123	1.00	0.18	0.05	0.57
V41111211	0.52	0.73	0.89	0.89	0.81	0.07	0.0019	1460	1460	16	170	139	0.07	0.0019	1458	45	16	170	136	1.00	0.18	0.04	0.61
V41111212	0.53	0.72	0.89	0.89	0.84	0.07	0.0020	1439	1439	17	170	116	0.07	0.0020	1437	44	16	170	113	1.00	0.19	0.05	0.61
V51111211	0.48	0.76	0.89	0.89	0.84	0.06	0.0017	1505	1505	18	180	124	0.06	0.0017	1502	46	17	180	121	1.00	0.19	0.05	0.65
V51111212	0.49	0.75	0.89	0.89	0.86	0.07	0.0018	1492	1492	18	181	104	0.07	0.0018	1489	46	17	181	101	1.00	0.20	0.05	0.66
V11111221	0.54	0.71	0.89	0.89	0.72	0.07	0.0020	1431	1431	13	150	205	0.07	0.0020	1430	44	13	150	201	1.00	0.14	0.03	0.49
V11111222	0.56	0.69	0.89	0.89	0.76	0.08	0.0021	1398	1398	14	152	173	0.08	0.0021	1397	43	14	151	170	1.00	0.15	0.04	0.49
V21111221	0.50	0.75	0.89	0.89	0.75	0.07	0.0018	1505	1505	15	164	192	0.07	0.0018	1504	46	15	164	188	1.00	0.14	0.03	0.52
V21111222	0.52	0.73	0.89	0.89	0.78	0.07	0.0019	1483	1483	16	167	162	0.07	0.0019	1482	46	16	167	159	1.00	0.15	0.04	0.53
V31111221	0.46	0.77	0.89	0.89	0.78	0.06	0.0016	1556	1556	17	176	177	0.06	0.0016	1555	48	16	176	174	1.00	0.15	0.04	0.56
V31111222	0.48	0.76	0.89	0.89	0.81	0.06	0.0017	1540	1540	17	178	150	0.06	0.0017	1539	48	17	178	147	1.00	0.16	0.04	0.57
V41111221	0.43	0.80	0.89	0.89	0.80	0.05	0.0014	1597	1597	18	187	162	0.05	0.0014	1595	49	18	187	159	1.00	0.16	0.04	0.61
V41111222	0.44	0.79	0.89	0.89	0.83	0.06	0.0015	1584	1584	18	188	137	0.06	0.0015	1583	49	18	188	134	1.00	0.17	0.04	0.61
V51111221	0.40	0.82	0.89	0.89	0.82	0.05	0.0013	1629	1629	19	196	146	0.05	0.0013	1627	50	19	196	143	1.00	0.17	0.04	0.66
V51111222	0.41	0.81	0.89	0.89	0.85	0.05	0.0014	1619	1619	19	197	123	0.05	0.0013	1616	50	19	197	120	1.00	0.18	0.04	0.66
V11112111	0.45	0.79	0.89	0.89	0.65	0.06	0.0015	1566	1566	9	102	280	0.06	0.0015	1565	48	9	101	277	1.00	0.11	0.02	0.49
V11112112	0.46	0.77	0.89	0.89	0.68	0.06	0.0016	1550	1550	9	103	255	0.06	0.0016	1548	48	9	103	251	1.00	0.12	0.03	0.49
V21112111	0.42	0.81	0.89	0.89	0.68	0.05	0.0014	1611	1611	10	109	263	0.05	0.0014	1610	49	10	109	260	1.00	0.12	0.03	0.52
V21112112	0.43	0.80	0.89	0.89	0.70	0.05	0.0015	1598	1598	10	111	239	0.05	0.0015	1596	49	10	111	235	1.00	0.12	0.03	0.52
V31112111	0.40	0.82	0.89	0.89	0.70	0.05	0.0013	1647	1647	10	116	247	0.05	0.0013	1645	50	10	116	244	1.00	0.12	0.03	0.56
V31112112	0.41	0.82	0.89	0.89	0.73	0.05	0.0013	1636	1636	11	118	224	0.05	0.0013	1634	50	11	118	221	1.00	0.13	0.03	0.56
V41112111	0.38	0.84	0.89	0.89	0.73	0.04	0.0011	1667	1667	11	121	231	0.04	0.0011	1666	51	11	121	228	1.00	0.13	0.03	0.61
V41112112	0.39	0.83	0.89	0.89	0.75	0.04	0.0012	1667	1667	11	123	210	0.04	0.0012	1665	51	11	123	206	1.00	0.14	0.03	0.61
V51112111	0.36	0.84	0.89	0.89	0.75	0.04	0.0011	1677	1677	12	126	214	0.04	0.0011	1675	51	12	126	211	1.00	0.14	0.03	0.66
V51112112	0.37	0.84	0.89	0.89	0.77	0.04	0.0011	1676	1676	12	127	194	0.04	0.0011	1674	51	12	127	191	1.00	0.14	0.03	0.66
V11112121	0.37	0.84	0.89	0.89	0.63	0.04	0.0011	1666	1666	9	106	313	0.04	0.0011	1664	51	9	106	310	1.00	0.10	0.02	0.48
V11112122	0.38	0.83	0.89	0.89	0.66	0.04	0.0012	1664	1664	9	109	288	0.04	0.0012	1663	51	9	109	284	1.00	0.11	0.02	0.49
V21112121	0.35	0.84	0.89	0.89	0.65	0.04	0.0010	1683	1683	10	112	293	0.04	0.0010	1682	52	10	112	290	1.00	0.11	0.02	0.52
V21112122	0.36	0.84	0.89	0.89	0.68	0.04	0.0011	1683	1683	10	115	268	0.04	0.0011	1681	52	10	115	265	1.00	0.11	0.02	0.52
V31112121	0.33	0.85	0.89	0.89	0.68	0.03	0.0009	1697	1697	10	117	276	0.03	0.0009	1695	52	10	117	272	1.00	0.11	0.02	0.56
V31112122	0.34	0.85	0.89	0.89	0.71	0.04	0.0010	1696	1696	11	120	252	0.04	0.0010	1695	52	11	120	248	1.00	0.12	0.03	0.56
V41112121	0.32	0.85	0.89	0.89	0.70	0.03	0.0009	1707	1707	11	121	260	0.03	0.0008	1705	52	11	121	257	1.00	0.12	0.03	0.61
V41112122	0.33	0.85	0.89	0.89	0.73	0.03	0.0009	1707	1707	11	124	237	0.03	0.0009	1705	52	11	124	234	1.00	0.12	0.03	0.61
V51112121	0.31	0.86	0.89	0.89	0.72	0.03	0.0008	1714	1714	11	125	246	0.03	0.0008	1713	52	11	125	243	1.00	0.13	0.03	0.66
V51112122	0.32	0.86	0.89	0.89	0.74	0.03	0.0008	1715	1715	12	127	224	0.03	0.0008	1713	53	12	127	220	1.00	0.13	0.03	0.66
V11112211	0.41	0.81	0.89	0.89	0.66	0.05	0.0014	1621	1621	9	104	279	0.05	0.0014	1619	50	9	104	276	1.00	0.11	0.02	0.49
V11112212	0.43	0.80	0.89	0.89	0.69	0.05	0.0014	1608	1608	9	106	254	0.05	0.0014	1606	49	9	106	250	1.00	0.11	0.02	0.49
V21112211	0.39	0.83	0.89	0.89	0.69	0.04	0.0012	1661	1661	10	111	263	0.04	0.0012	1660	51	10	111	259	1.00	0.11	0.02	0.52
V21112212	0.40	0.82	0.89	0.89	0.71	0.05	0.0013	1651	1651	10	113	238	0.05	0.0013	1650	51	10	113	235	1.00	0.12	0.03	0.52
V31112211	0.37	0.84	0.89	0.89	0.71	0.04	0.0011	1679	1679	10	116	245	0.04	0.0011	1677	52	10	116	242	1.00	0.12	0.03	0.56
V31112212	0.38	0.83	0.89	0.89	0.74	0.04	0.0012	1679	1679	11	119	223	0.04	0.0012	1677	52	11	119	220	1.00	0.12	0.03	0.56
V41112211	0.35	0.84	0.89	0.89	0.73	0.04	0.0010	1690	1690	11	121	230	0.04	0.0010	1688	52	11	121	227	1.00	0.13	0.03	0.61
V41112212	0.36	0.84	0.89	0.89	0.76	0.04	0.0011	1690	1690	11	123	209	0.04	0.0011	1689	52	11	123	206	1.00	0.13	0.03	0.61
V51112211	0.34	0.85	0.89	0.89	0.75	0.03	0.0009	1698	1698	12	124	215	0.03	0.0009	1697	52	11	124	212	1.00	0.13	0.03	0.66
V51112212	0.34	0.85	0.89	0.89	0.77	0.04	0.0010	1699	1699	12	126	195	0.04	0.0010	1698	52	12	126	192	1.00	0.14	0.03	0.66
V11112221	0.34	0.85	0.89	0.89	0.64	0.04	0.0010	1688	1688	9	107	308	0.04	0.0010	1686	52	9	107	305	1.00	0.10	0.02	0.49
V11112222	0.36	0.84	0.89	0.89	0.67	0.04	0.0011	1688	1688	10	110	283	0.04	0.0011	1687	52	10	110	279	1.00	0.10	0.02	0.49
V21112221	0.33	0.85	0.89	0.89	0.66	0.03	0.0009	1704	1704	10	112	290	0.03	0.0009	1702	52	10	112	286	1.00	0.11	0.02	0.52
V21112222	0.34	0.85	0.89	0.89	0.69	0.03	0.0009	1704	1704	10	115	265	0.03	0.0009	1703	52	10	115	262	1.00	0.11	0.02	0.52
V31112221	0.31	0.86	0.89	0.89	0.68	0.03	0.0008	1715	1715	10	116	274	0.03	0.0008	1714	53	10	116	271	1.00	0.11	0.02	0.56
V31112222	0.32	0.85	0.89	0.89	0.71	0.03	0.0009	1716	1716	11	119	250	0.03	0.0009	1715	53	11	119	247	1.00	0.11	0.03	0.56
V41112221	0.30	0.86	0.89	0.89	0.70	0.03	0.0008	1725	1725	11	120	261	0.03	0.0008	1723	53	11	120	257	1.00	0.11	0.03	0.61
V41112222	0.31	0.86	0.89	0.89	0.73	0.03	0.0008	1726	1726	11	122	238	0.03	0.0008	1725	53	11	122	235	1.00	0.12	0.03	0.61
V51112221	0.29	0.86	0.89	0.89	0.72	0.03	0.0007	1732	1732	11	123	249	0.03	0.0007	1730	53	11	123	246	1.00	0.12	0.03	0.66
V51112222	0.30	0.86	0.89	0.89	0.74	0.03	0.0007	1733	1733	11	125	226	0.03	0.0007	1732	53	11	125	223	1.00	0.12	0.03	0.66
V11121111	0.85	0.49	0.88	0.89	0.70	0.12	0.0035	1310	1310	12	135	200	0.12	0.0034	1307	40	12	135	193	1.00	0.20	0.04	0.49
V11121112	0.89	0.47	0.88	0.89	0.74	0.13	0.0036	1264	1264	12	135	167	0.13	0.0036	1262	39	12	135	161	1.00	0.21	0.05	0.49
V21121111	0.78	0.52	0.88	0.89	0.74	0.11	0.0031	1406	1406	14	152	189	0.11	0.0031	1403	43	14	152	183	1.00	0.20	0.05	0.52
V21121112	0.81	0.51	0.88	0.89	0.78	0.12	0.0032	1369	1369	14	152	159	0.12	0.0032	1367	42	14	152	153	1.00	0.22	0.05	0.53
V31121111	0.72	0.56	0.88	0.89	0.77	0.10	0.0028	1502	1502	16	170	178	0.10	0.0028	1499	46	16	170	172	1.00	0.21	0.05	0.56
V31121112	0.75	0.54	0.88	0.89	0.80	0.11	0.0029	1462	1462	16	168	148	0.11	0.0029	1459	45	16	168	143	1.00	0.22	0.06	0.56
V41121111	0.67	0.60	0.89	0.89	0.80	0.10	0.0026	1590	1590	18	186	165	0.10	0.0026	1586	49	18	186	159	1.00	0.22	0.05	0.61
V41121112	0.69	0.58	0.89	0.89	0.83	0.10	0.0027	1557	1557	18	185	137	0.10	0.0027	1554	48	18	185	132	1.00	0.23	0.06	0.61
V51121111	0.62	0.63	0.89	0.89	0.83	0.09	0.0025	1672	1672	20	203	149	0.09	0.0024	1667	51	19	203	143	1.00	0.24	0.06	0.65
V51121112	0.64	0.62	0.89	0.89	0.85	0.09	0.0025	1636	1636	20	200	123	0.09	0.0025	1630	50	19	200	118	1.00	0.25	0.06	0.65
V11121121	0.70	0.58	0.88	0.89	0.69	0.10	0.0028	1549	1549	14	161	241	0.10	0.0028	1546	48	14	161	235	1.00	0.16	0.04	0.49
V11121122	0.73	0.56	0.88	0.89	0.74	0.10	0.0029	1496	1496	15	161	202	0.10	0.0029	1494	46	15	161	196	1.00	0.18	0.04	0.49
V21121121	0.64	0.62	0.89	0.89	0.73	0.09	0.0025	1648	1648	16	180	228	0.09	0.0025	1646	51	16	180	222	1.00	0.17	0.04	0.52
V21121122	0.67	0.60	0.88	0.89	0.77	0.09	0.0026	1606	1606	17	180	192	0.09	0.0026	1604	50	17	180	186	1.00	0.18	0.04	0.52
V31121121	0.60	0.66	0.89	0.89	0.76	0.08	0.0023	1755	1755	19	199	216	0.08	0.0023	1752	54	18	199	210	1.00	0.18	0.04	0.56
V31121122	0.62	0.64	0.89	0.89	0.79	0.09	0.0024	1706	1706	19	198	180	0.09	0.0024	1704	53	19	198	175	1.00	0.19	0.05	0.56
V41121121	0.56	0.70	0.89	0.89	0.79	0.08	0.0021	1849	1849	21	218	201	0.08	0.0021	1845	56	20	218	196	1.00	0.18	0.04	0.61
V41121122	0.58	0.68	0.89	0.89	0.82	0.08	0.0022	1809	1809	21	217	167	0.08	0.0022	1806	55	21	217	162	1.00	0.20	0.05	0.61
V51121121	0.52	0.73	0.89	0.89	0.81	0.07	0.0020	1926	1926	23	235	183	0.07	0.0019	1922	59	22	235	178	1.00	0.20	0.05	0.65
V51121122	0.54	0.71	0.89	0.89	0.84	0.07	0.0020	1893	1893	23	233	152	0.07	0.0020	1889	58	22	233	147	1.00	0.21	0.05	0.66
V11121211	0.76	0.54	0.88	0.89	0.73	0.11	0.0030	1441	1441	14	150	202	0.11	0.0030	1439	44	14	150	196	1.00	0.18	0.04	0.49

Name	T1 [s]	Sa(T1) [g]	Sa(T2) [g]	Sa(T3) [g]	DOC [-]	Disp [m]	ISDR [-]	Total Moment [MN-m]	Total Shear [MN]	Max CB Shear [MN]	Max Pp [MN]	Max wall moment [MN-m]	Disp [m]2	ISDR [-]3	Total Moment [MN-m]4	Total Shear [MN]5	Max CB Shear [MN]6	Max Pp [MN]2	Max wall moment [MN-m]8	C1 [-]	C2 [-]	C3 [-]	Mdy/ Mst [-]
V21121211	0.70	0.58	0.88	0.89	0.76	0.10	0.0027	1554	1554	16	169	192	0.10	0.0027	1552	48	16	169	187	1.00	0.19	0.05	0.52
V21121212	0.72	0.56	0.88	0.89	0.79	0.10	0.0028	1517	1517	16	169	161	0.10	0.0028	1516	47	16	169	156	1.00	0.20	0.05	0.53
V31121211	0.65	0.61	0.89	0.89	0.79	0.09	0.0025	1648	1648	18	185	180	0.09	0.0025	1645	51	17	185	175	1.00	0.19	0.05	0.56
V31121212	0.67	0.60	0.88	0.89	0.82	0.09	0.0025	1618	1618	18	186	151	0.09	0.0025	1616	50	18	186	146	1.00	0.20	0.05	0.57
V41121211	0.60	0.66	0.89	0.89	0.81	0.08	0.0023	1749	1749	20	203	168	0.08	0.0023	1745	54	19	203	163	1.00	0.20	0.05	0.61
V41121212	0.62	0.64	0.89	0.89	0.84	0.09	0.0023	1714	1714	20	202	140	0.09	0.0023	1711	53	19	202	135	1.00	0.21	0.05	0.61
V51121211	0.56	0.69	0.89	0.89	0.84	0.08	0.0021	1837	1837	21	220	152	0.08	0.0021	1833	56	21	220	148	1.00	0.21	0.05	0.65
V51121212	0.57	0.68	0.89	0.89	0.86	0.08	0.0022	1809	1809	22	219	127	0.08	0.0022	1805	55	21	219	123	1.00	0.22	0.06	0.66
V11121221	0.62	0.63	0.89	0.89	0.72	0.09	0.0024	1701	1701	16	178	245	0.09	0.0024	1699	52	16	178	239	1.00	0.15	0.04	0.49
V11121222	0.65	0.61	0.89	0.89	0.76	0.09	0.0025	1654	1654	17	179	206	0.09	0.0025	1653	51	16	179	201	1.00	0.17	0.04	0.49
V21121221	0.57	0.68	0.89	0.89	0.75	0.08	0.0022	1821	1821	18	199	233	0.08	0.0022	1819	56	18	199	228	1.00	0.16	0.04	0.52
V21121222	0.60	0.66	0.89	0.89	0.78	0.08	0.0023	1778	1778	19	200	195	0.08	0.0023	1776	55	19	200	191	1.00	0.17	0.04	0.53
V31121221	0.53	0.72	0.89	0.89	0.78	0.07	0.0020	1920	1920	20	217	219	0.07	0.0020	1917	59	20	217	214	1.00	0.16	0.04	0.56
V31121222	0.55	0.70	0.89	0.89	0.81	0.08	0.0020	1885	1885	21	218	184	0.08	0.0020	1883	58	21	218	179	1.00	0.17	0.04	0.57
V41121221	0.50	0.75	0.89	0.89	0.80	0.07	0.0018	1995	1995	22	233	202	0.07	0.0018	1992	61	22	233	198	1.00	0.17	0.04	0.61
V41121222	0.51	0.73	0.89	0.89	0.83	0.07	0.0019	1972	1972	23	234	170	0.07	0.0019	1970	61	22	234	166	1.00	0.18	0.04	0.61
V51121221	0.47	0.77	0.89	0.89	0.82	0.06	0.0016	2047	2047	24	246	184	0.06	0.0016	2043	62	23	246	179	1.00	0.18	0.04	0.66
V51121222	0.48	0.76	0.89	0.89	0.85	0.06	0.0017	2029	2029	24	247	154	0.06	0.0017	2026	62	24	247	150	1.00	0.19	0.05	0.66
V11122111	0.52	0.73	0.89	0.89	0.65	0.07	0.0019	1948	1948	11	126	349	0.07	0.0019	1945	60	11	126	344	1.00	0.12	0.02	0.49
V11122112	0.53	0.72	0.89	0.89	0.68	0.07	0.0020	1912	1912	11	127	315	0.07	0.0020	1910	59	11	127	310	1.00	0.13	0.03	0.49
V21122111	0.48	0.76	0.89	0.89	0.68	0.06	0.0017	2018	2018	12	137	330	0.06	0.0017	2015	62	12	137	325	1.00	0.13	0.03	0.52
V21122112	0.50	0.75	0.89	0.89	0.70	0.07	0.0018	1995	1995	12	139	299	0.07	0.0018	1993	61	12	139	294	1.00	0.13	0.03	0.52
V31122111	0.46	0.78	0.89	0.89	0.70	0.06	0.0016	2073	2073	13	146	312	0.06	0.0016	2070	63	13	146	307	1.00	0.13	0.03	0.56
V31122112	0.47	0.77	0.89	0.89	0.73	0.06	0.0017	2054	2054	13	148	282	0.06	0.0017	2052	63	13	148	277	1.00	0.14	0.03	0.56
V41122111	0.43	0.80	0.89	0.89	0.73	0.05	0.0015	2118	2118	14	154	294	0.05	0.0015	2115	65	14	154	289	1.00	0.14	0.03	0.61
V41122112	0.45	0.79	0.89	0.89	0.75	0.06	0.0015	2102	2102	14	156	265	0.06	0.0015	2099	65	14	156	260	1.00	0.14	0.03	0.61
V51122111	0.41	0.81	0.89	0.89	0.75	0.05	0.0014	2155	2155	15	162	276	0.05	0.0014	2152	66	15	162	271	1.00	0.15	0.03	0.66
V51122112	0.42	0.80	0.89	0.89	0.77	0.05	0.0014	2141	2141	15	163	248	0.05	0.0014	2138	66	15	163	244	1.00	0.15	0.04	0.66
V11122121	0.43	0.80	0.89	0.89	0.63	0.05	0.0014	2124	2124	12	136	400	0.05	0.0014	2121	65	12	136	395	1.00	0.11	0.02	0.48
V11122122	0.44	0.79	0.89	0.89	0.66	0.06	0.0015	2101	2101	12	138	364	0.05	0.0015	2099	64	12	138	359	1.00	0.11	0.02	0.49
V21122121	0.40	0.82	0.89	0.89	0.65	0.05	0.0013	2175	2175	13	145	379	0.05	0.0013	2173	67	13	145	374	1.00	0.11	0.02	0.52
V21122122	0.42	0.81	0.89	0.89	0.68	0.05	0.0014	2157	2157	13	148	344	0.05	0.0014	2155	66	13	148	340	1.00	0.12	0.03	0.52
V31122121	0.38	0.83	0.89	0.89	0.68	0.04	0.0012	2215	2215	14	153	360	0.04	0.0012	2213	68	13	153	355	1.00	0.12	0.02	0.56
V31122122	0.40	0.82	0.89	0.89	0.71	0.05	0.0013	2201	2201	14	155	327	0.05	0.0013	2199	68	14	155	322	1.00	0.12	0.03	0.56
V41122121	0.37	0.84	0.89	0.89	0.70	0.04	0.0011	2230	2230	14	159	340	0.04	0.0011	2228	68	14	159	335	1.00	0.12	0.03	0.61
V41122122	0.38	0.83	0.89	0.89	0.73	0.04	0.0012	2229	2229	15	162	310	0.04	0.0012	2227	68	15	162	305	1.00	0.13	0.03	0.61
V51122121	0.35	0.84	0.89	0.89	0.72	0.04	0.0010	2242	2242	15	163	322	0.04	0.0010	2240	69	15	163	317	1.00	0.13	0.03	0.66
V51122122	0.36	0.84	0.89	0.89	0.74	0.04	0.0011	2242	2242	15	166	292	0.04	0.0011	2239	69	15	166	288	1.00	0.13	0.03	0.66
V11122211	0.48	0.76	0.89	0.89	0.66	0.06	0.0017	2032	2032	11	131	350	0.06	0.0017	2029	62	11	131	345	1.00	0.12	0.02	0.49
V11122212	0.49	0.75	0.89	0.89	0.69	0.06	0.0018	2010	2010	12	133	318	0.06	0.0018	2008	62	12	133	313	1.00	0.12	0.03	0.49
V21122211	0.45	0.78	0.89	0.89	0.69	0.06	0.0015	2093	2093	12	140	331	0.06	0.0015	2091	64	12	140	327	1.00	0.12	0.03	0.52
V21122212	0.46	0.77	0.89	0.89	0.71	0.06	0.0016	2075	2075	13	143	300	0.06	0.0016	2073	64	13	143	295	1.00	0.13	0.03	0.52
V31122211	0.43	0.80	0.89	0.89	0.71	0.05	0.0014	2142	2142	13	149	314	0.05	0.0014	2140	66	13	149	309	1.00	0.13	0.03	0.56
V31122212	0.44	0.79	0.89	0.89	0.74	0.05	0.0015	2127	2127	14	151	284	0.05	0.0015	2125	66	14	151	279	1.00	0.13	0.03	0.56
V41122211	0.41	0.82	0.89	0.89	0.73	0.05	0.0013	2182	2182	14	156	297	0.05	0.0013	2180	67	14	156	293	1.00	0.13	0.03	0.61
V41122212	0.42	0.81	0.89	0.89	0.76	0.05	0.0014	2169	2169	15	158	268	0.05	0.0014	2168	67	15	158	264	1.00	0.14	0.03	0.61
V51122211	0.39	0.83	0.89	0.89	0.75	0.04	0.0012	2215	2215	15	162	281	0.04	0.0012	2213	68	15	162	277	1.00	0.14	0.03	0.66
V51122212	0.40	0.82	0.89	0.89	0.77	0.05	0.0013	2204	2204	15	164	253	0.05	0.0013	2202	68	15	164	249	1.00	0.14	0.03	0.66
V11122221	0.40	0.82	0.89	0.89	0.64	0.05	0.0013	2189	2189	12	138	400	0.05	0.0013	2187	67	12	138	395	1.00	0.10	0.02	0.49
V11122222	0.41	0.81	0.89	0.89	0.67	0.05	0.0014	2171	2171	12	141	364	0.05	0.0014	2169	67	12	141	359	1.00	0.11	0.02	0.49
V21122221	0.38	0.83	0.89	0.89	0.66	0.04	0.0012	2225	2225	13	146	379	0.04	0.0012	2223	68	13	146	374	1.00	0.11	0.02	0.52
V21122222	0.39	0.83	0.89	0.89	0.69	0.04	0.0012	2220	2220	13	150	346	0.04	0.0012	2218	68	13	150	341	1.00	0.11	0.02	0.52
V31122221	0.36	0.84	0.89	0.89	0.68	0.04	0.0011	2243	2243	13	152	359	0.04	0.0011	2241	69	13	152	354	1.00	0.11	0.02	0.56
V31122222	0.37	0.84	0.89	0.89	0.71	0.04	0.0011	2243	2243	14	155	327	0.04	0.0011	2241	69	14	155	323	1.00	0.12	0.03	0.56
V41122221	0.35	0.85	0.89	0.89	0.70	0.04	0.0010	2257	2257	14	157	341	0.04	0.0010	2255	69	14	157	337	1.00	0.12	0.03	0.61
V41122222	0.36	0.84	0.89	0.89	0.73	0.04	0.0010	2257	2257	14	160	311	0.04	0.0010	2256	70	14	160	307	1.00	0.12	0.03	0.61
V51122221	0.33	0.85	0.89	0.89	0.72	0.03	0.0009	2268	2268	15	161	326	0.03	0.0009	2266	70	14	161	322	1.00	0.12	0.03	0.66
V51122222	0.34	0.85	0.89	0.89	0.74	0.04	0.0010	2269	2269	15	164	296	0.04	0.0010	2267	70	15	164	292	1.00	0.13	0.03	0.66
V11211111	1.13	0.39	0.86	0.89	0.71	0.18	0.0037	1052	1052	10	109	162	0.18	0.0037	1049	24	10	109	154	1.00	0.24	0.06	0.49
V11211112	1.18	0.38	0.86	0.89	0.75	0.19	0.0039	1029	1029	10	110	137	0.19	0.0039	1026	24	10	110	130	1.00	0.26	0.06	0.50
V21211111	1.03	0.41	0.87	0.89	0.74	0.16	0.0032	1110	1110	11	121	151	0.16	0.0032	1107	26	11	121	143	1.00	0.26	0.06	0.52
V21211112	1.08	0.40	0.87	0.89	0.78	0.17	0.0034	1090	1090	12	122	127	0.17	0.0034	1087	25	11	122	120	1.00	0.27	0.07	0.53
V31211111	0.95	0.44	0.88	0.89	0.77	0.14	0.0029	1183	1183	13	134	141	0.14	0.0029	1179	27	12	134	133	1.00	0.27	0.07	0.56
V31211112	0.99	0.43	0.87	0.89	0.81	0.15	0.0030	1152	1152	13	133	118	0.15	0.0030	1149	27	13	133	111	1.00	0.29	0.07	0.57
V41211111	0.88	0.47	0.88	0.89	0.80	0.13	0.0027	1253	1253	14	147	130	0.13	0.0027	1248	29	14	147	123	1.00	0.28	0.07	0.61
V41211112	0.91	0.46	0.88	0.89	0.83	0.14	0.0028	1227	1227	15	146	108	0.14	0.0028	1222	28	14	146	102	1.00	0.30	0.08	0.61
V51211111	0.82	0.51	0.88	0.89	0.83	0.12	0.0026	1332	1332	16	162	117	0.12	0.0025	1325	30	15	162	110	1.00	0.30	0.08	0.65
V51211112	0.84	0.49	0.88	0.89	0.86	0.13	0.0026	1304	1304	16	160	97	0.13	0.0026	1297	30	15	160	91	1.00	0.31	0.08	0.65
V11211121	0.92	0.45	0.88	0.89	0.70	0.14	0.0028	1218	1218	11	127	191	0.14	0.0028	1214	28	11	127	183	1.00	0.21	0.05	0.49
V11211122	0.97	0.44	0.88	0.89	0.74	0.14	0.0030	1177	1177	12	127	160	0.14	0.0030	1175	27	12	127	153	1.00	0.23	0.05	0.49
V21211121	0.85	0.49	0.88	0.89	0.73	0.13	0.0026	1308	1308	13	143	181	0.13	0.0026	1305	30	13	143	174	1.00	0.22	0.05	0.52
V21211122	0.89	0.47	0.88	0.89	0.77	0.13	0.0027	1264	1264	13	142	151	0.13	0.0027	1262	29	13	142	144	1.00	0.23	0.06	0.53
V31211121	0.79	0.52	0.88	0.89	0.76	0.12	0.0024	1393	1393	15	159	170	0.12	0.0023	1390	32	15	159	164	1.00	0.22	0.05	0.56
V31211122	0.82	0.51	0.88	0.89	0.80	0.12	0.0024	1358	1358	15	159	142	0.12	0.0024	1355	31	15	159	136	1.00	0.24	0.06	0.56
V41211121	0.73	0.56	0.88	0.89	0.79	0.11	0.0022	1478	1478	17	175	158	0.11	0.0022	1474	34	16	175	152	1.00	0.23	0.06	0.61
V41211122	0.76	0.54	0.88	0.89	0.82	0.11	0.0022	1438	1438	17	173	131	0.11	0.0022	1435	33	16	173	125	1.00	0.25	0.06	0.61
V51211121	0.68	0.59	0.89	0.89	0.82	0.10	0.0021	1559	1559	19	191	144	0.10	0.0020	1553	35	18	191	138	1.00	0.25	0.06	0.65
V51211122	0.70	0.58	0.89	0.89	0.85	0.10	0.0021	1526	1526	19	189	119	0.10	0.0021	1520	35	18	189	114	1.00	0.26	0.07	0.65
V11211211	1.01	0.42	0.87	0.89	0.73	0.15	0.0031	1134	1134	11	118	160	0.15	0.0031	1132	26	11	118	153	1.00	0.23	0.05	0.49
V11211212	1.05	0.41	0.87	0.89	0.77	0.16	0.0033	1113	1113	11	120	136	0.16	0.0033	1111	26	11	120	129	1.00	0.25	0.06	0.50
V21211211	0.92	0.45	0.88	0.89	0.76	0.14	0.0028	1223	1223	13	133	152	0.14	0.0028	1221	28	12	133	145	1.00	0.24	0.06	0.53
V21211212	0.95	0.44	0.87	0.89	0.80	0.14	0.0029	1195	1195	13	134	127	0.14	0.0029	1193	28	13	134	121	1.00	0.25	0.06	0.53
V31211211	0.85	0.49	0.88	0.89	0.79	0.13	0.0026	1309	1309	14	148	143	0.13	0.0025	1306	30	14	148	136	1.00	0.25	0.06	0.56
V31211212	0.88	0.47	0.88	0.89	0.82	0.13	0.0026	1278	1278	14	147	119	0.13	0.0026	1276	30	14	147	113	1.00	0.26	0.07	0.57
V41211211	0.79	0.52	0.88	0.89	0.82	0.12	0.0024	1390	1390	16	162	132	0.12	0.0023	1386	32	15	162	126	1.00	0.26	0.06	0.61
V41211212	0.81	0.51	0.88	0.89	0.84	0.12	0.0024	1366	1366	16	162	110	0.12	0.0024	1362	31	15	162	104	1.00	0.27	0.07	0.61
V51211211	0.73	0.56	0.89	0.89	0.84	0.11	0.0022	1471	1471	18	177	119	0.11	0.0022	1466	33	17	177	114	1.00	0.27	0.07	0.65
V51211212	0.75	0.54	0.88	0.89	0.87	0.11	0.0023	1444	1444	18	176	99	0.11	0.0022	1438	33	17	176	94	1.00	0.28	0.07	0.66
V11211221	0.82	0.50	0.88	0.89	0.72	0.12	0.0025	1352	1352	13	142	194	0.12	0.0025	1349	31	13	142	187	1.00	0.19	0.04	0.49
V11211222	0.86	0.48	0.88	0.89	0.76	0.12	0.0026	1311	1311	13	143	163	0.12	0.0026	1310	30	13	143	157	1.00	0.21	0.05	0.50
V21211221	0.76	0.54	0.88	0.89	0.75	0.11	0.0022	1446	1446	15	159	184	0.11	0.0022	1444	33	15	159	178	1.00	0.20	0.05	0.52
V21211222	0.78	0.52	0.88	0.89	0.79	0.11	0.0023	1413	1413	15	160	154	0.11	0.0023	1411	33	15	159	149	1.00	0.21	0.05	0.53
V31211221	0.70	0.58	0.88	0.89	0.78	0.10	0.0021	1546	1546	17	176	174	0.10	0.0020	1543	36	16	176	168	1.00	0.20	0.05	0.56
V31211222	0.72	0.56	0.88	0.89	0.81	0.10	0.0021	1511	1511	17	176	145	0.10	0.0021	1509	35	17	176	140	1.00	0.22	0.05	0.57
V41211221	0.65	0.61	0.89	0.89	0.81	0.09	0.0019	1629	1629	18	192	161	0.09	0.0019	1626	37	18	192	156	1.00	0.21	0.05	0.61
V41211222	0.67	0.60	0.89	0.89	0.84	0.10	0.0019	1601	1601	19	192	135	0.10	0.0019	1598	37	18	192	130	1.00	0.22	0.06	0.61
V51211221	0.61	0.65	0.89	0.89	0.83	0.09	0.0018	1717	1717	20	208	148	0.09	0.0018	1712	39	20	208	143	1.00	0.22	0.06	0.65
V51211222	0.62	0.63	0.89	0.89	0.86	0.09	0.0018	1683	1683	20	207	123	0.09	0.0018	1679	39	20	207	118	1.00	0.23	0.06	0.66
V11212111	0.68	0.59	0.89	0.89	0.65	0.10	0.0020	1578	1578	9	103	279	0.10	0.0020	1575	36	9	103	272	1.00	0.15	0.03	0.49
V11212112	0.70	0.58	0.88	0.89	0.68	0.10	0.0021	1543	1543	9	104	250	0.10	0.0021	1540	36	9	104	244	1.00	0.16	0.03	0.49
V21212111	0.63	0.63	0.89	0.89	0.69	0.09	0.0018	1666	1666	10	115	266	0.09	0.0018	1663	38	10	115	260	1.00	0.16	0.03	0.52
V21212112	0.65	0.61	0.89	0.89	0.71	0.09	0.0019	1634	1634	10	115	239	0.09	0.0019	1631	38	10	115	233	1.00	0.16	0.04	0.52
V31212111	0.59	0.66	0.89	0.89	0.71	0.08	0.0017	1760	1760	11	126	256	0.08	0.0017	1757	40	11	126	250	1.00	0.16	0.04	0.56

Name	T1 [s]	Sa(T1) [g]	Sa(T2) [g]	Sa(T3) [g]	DOC [-]	Disp [m]	ISDR [-]	Total Moment [MN-m]	Total Shear [MN]	Max CB Shear [MN]	Max Pp [MN]	Max wall moment [MN-m]	Disp [m]2	ISDR [-]3	Total Moment [MN-m]4	Total Shear [MN]5	Max CB Shear [MN]6	Max Pp [MN]2	Max wall moment [MN-m]8	C1 [-]	C2 [-]	C3 [-]	Mdy/ Mst [-]
V31212112	0.61	0.64	0.89	0.89	0.74	0.09	0.0018	1724	1724	12	126	228	0.09	0.0017	1722	40	11	126	223	1.00	0.17	0.04	0.56
V41212111	0.56	0.69	0.89	0.89	0.74	0.08	0.0016	1838	1838	13	136	244	0.08	0.0016	1835	42	13	136	238	1.00	0.17	0.04	0.61
V41212112	0.57	0.68	0.89	0.89	0.76	0.08	0.0016	1808	1808	13	136	217	0.08	0.0016	1806	42	13	136	212	1.00	0.17	0.04	0.61
V51212111	0.53	0.72	0.89	0.89	0.76	0.07	0.0015	1905	1905	14	146	230	0.07	0.0015	1902	44	14	146	224	1.00	0.17	0.04	0.66
V51212112	0.54	0.71	0.89	0.89	0.79	0.08	0.0015	1879	1879	14	146	205	0.07	0.0015	1876	43	14	146	200	1.00	0.18	0.04	0.66
V11212121	0.56	0.69	0.89	0.89	0.64	0.08	0.0016	1844	1844	10	120	338	0.08	0.0016	1841	42	10	120	333	1.00	0.12	0.03	0.49
V11212122	0.58	0.67	0.89	0.89	0.67	0.08	0.0017	1802	1802	10	120	304	0.08	0.0017	1799	41	10	120	298	1.00	0.13	0.03	0.49
V21212121	0.52	0.73	0.89	0.89	0.67	0.07	0.0015	1930	1930	12	131	325	0.07	0.0015	1927	44	11	131	319	1.00	0.13	0.03	0.52
V21212122	0.54	0.71	0.89	0.89	0.70	0.07	0.0015	1894	1894	12	132	292	0.07	0.0015	1892	44	12	132	286	1.00	0.14	0.03	0.52
V31212121	0.50	0.75	0.89	0.89	0.69	0.07	0.0014	1993	1993	13	141	309	0.07	0.0013	1990	46	13	141	304	1.00	0.13	0.03	0.56
V31212122	0.51	0.74	0.89	0.89	0.72	0.07	0.0014	1969	1969	13	142	279	0.07	0.0014	1967	45	13	142	274	1.00	0.14	0.03	0.56
V41212121	0.47	0.77	0.89	0.89	0.72	0.06	0.0013	2040	2040	13	149	294	0.06	0.0013	2037	47	13	149	289	1.00	0.14	0.03	0.61
V41212122	0.49	0.76	0.89	0.89	0.74	0.06	0.0013	2020	2020	14	150	264	0.06	0.0013	2017	46	14	150	259	1.00	0.15	0.03	0.61
V51212121	0.45	0.78	0.89	0.89	0.74	0.06	0.0012	2079	2079	14	156	278	0.06	0.0012	2076	48	14	156	273	1.00	0.15	0.03	0.66
V51212122	0.46	0.77	0.89	0.89	0.76	0.06	0.0012	2061	2061	15	157	250	0.06	0.0012	2059	47	15	157	245	1.00	0.15	0.04	0.66
V11212211	0.62	0.63	0.89	0.89	0.67	0.09	0.0018	1687	1687	10	110	285	0.09	0.0018	1684	39	10	110	279	1.00	0.14	0.03	0.49
V11212212	0.64	0.62	0.89	0.89	0.70	0.09	0.0019	1650	1650	10	111	255	0.09	0.0019	1648	38	10	110	249	1.00	0.15	0.03	0.49
V21212211	0.58	0.67	0.89	0.89	0.70	0.08	0.0017	1789	1789	11	122	274	0.08	0.0017	1787	41	11	122	269	1.00	0.15	0.03	0.52
V21212212	0.60	0.65	0.89	0.89	0.73	0.08	0.0017	1755	1755	11	122	246	0.08	0.0017	1753	41	11	122	240	1.00	0.15	0.04	0.52
V31212211	0.55	0.70	0.89	0.89	0.72	0.08	0.0015	1873	1873	12	132	263	0.08	0.0015	1871	43	12	132	258	1.00	0.15	0.03	0.56
V31212212	0.56	0.69	0.89	0.89	0.75	0.08	0.0016	1844	1844	12	133	235	0.08	0.0016	1842	43	12	133	230	1.00	0.16	0.04	0.56
V41212211	0.52	0.73	0.89	0.89	0.75	0.07	0.0014	1943	1943	13	142	250	0.07	0.0014	1940	45	13	142	245	1.00	0.16	0.04	0.61
V41212212	0.53	0.72	0.89	0.89	0.77	0.07	0.0015	1918	1918	13	142	224	0.07	0.0015	1916	44	13	142	219	1.00	0.16	0.04	0.61
V51212211	0.50	0.75	0.89	0.89	0.77	0.07	0.0013	1994	1994	14	149	236	0.07	0.0013	1992	46	14	149	231	1.00	0.16	0.04	0.66
V51212212	0.51	0.74	0.89	0.89	0.79	0.07	0.0014	1978	1978	14	150	212	0.07	0.0014	1976	46	14	150	207	1.00	0.17	0.04	0.66
V11212221	0.52	0.73	0.89	0.89	0.65	0.07	0.0014	1951	1951	11	126	345	0.07	0.0014	1949	45	11	126	339	1.00	0.12	0.02	0.49
V11212222	0.53	0.72	0.89	0.89	0.68	0.07	0.0015	1917	1917	11	127	310	0.07	0.0015	1915	44	11	127	305	1.00	0.13	0.03	0.49
V21212221	0.49	0.76	0.89	0.89	0.68	0.06	0.0013	2016	2016	12	135	328	0.06	0.0013	2014	46	12	135	323	1.00	0.12	0.03	0.52
V21212222	0.50	0.74	0.89	0.89	0.71	0.07	0.0014	1995	1995	12	137	297	0.07	0.0014	1993	46	12	137	292	1.00	0.13	0.03	0.52
V31212221	0.46	0.77	0.89	0.89	0.70	0.06	0.0012	2067	2067	13	143	313	0.06	0.0012	2065	48	13	143	308	1.00	0.13	0.03	0.56
V31212222	0.48	0.76	0.89	0.89	0.73	0.06	0.0013	2048	2048	13	145	283	0.06	0.0013	2047	47	13	145	278	1.00	0.13	0.03	0.56
V41212221	0.44	0.79	0.89	0.89	0.72	0.05	0.0011	2109	2109	14	150	298	0.05	0.0011	2106	49	14	150	294	1.00	0.13	0.03	0.61
V41212222	0.45	0.78	0.89	0.89	0.75	0.06	0.0012	2092	2092	14	152	269	0.06	0.0012	2091	48	14	152	265	1.00	0.14	0.03	0.61
V51212221	0.42	0.80	0.89	0.89	0.74	0.05	0.0011	2143	2143	14	156	285	0.05	0.0011	2141	49	14	156	280	1.00	0.14	0.03	0.66
V51212222	0.43	0.79	0.89	0.89	0.76	0.05	0.0011	2129	2129	15	158	257	0.05	0.0011	2127	49	15	158	252	1.00	0.14	0.03	0.66
V11221111	1.30	0.36	0.85	0.89	0.70	0.21	0.0044	1274	1274	12	132	198	0.21	0.0044	1270	29	12	132	186	1.00	0.26	0.06	0.49
V11221112	1.36	0.34	0.84	0.89	0.75	0.22	0.0047	1241	1241	12	133	167	0.22	0.0047	1238	29	12	133	156	1.00	0.28	0.07	0.50
V21221111	1.19	0.38	0.86	0.89	0.74	0.19	0.0039	1352	1352	14	147	185	0.19	0.0039	1347	31	13	147	174	1.00	0.28	0.07	0.52
V21221112	1.24	0.37	0.85	0.89	0.78	0.20	0.0041	1322	1322	14	147	156	0.20	0.0041	1318	31	14	147	146	1.00	0.29	0.07	0.53
V31221111	1.10	0.40	0.87	0.89	0.77	0.17	0.0035	1421	1421	15	161	171	0.17	0.0035	1415	33	15	161	160	1.00	0.29	0.07	0.56
V31221112	1.14	0.39	0.86	0.89	0.80	0.18	0.0037	1394	1394	16	161	144	0.18	0.0036	1390	32	15	161	134	1.00	0.31	0.08	0.57
V41221111	1.02	0.42	0.88	0.89	0.80	0.16	0.0032	1482	1482	17	174	155	0.16	0.0032	1474	34	16	174	145	1.00	0.32	0.08	0.61
V41221112	1.05	0.41	0.87	0.89	0.83	0.16	0.0033	1460	1460	18	174	130	0.16	0.0033	1454	33	17	174	121	1.00	0.33	0.08	0.61
V51221111	0.94	0.45	0.88	0.89	0.83	0.15	0.0030	1571	1571	19	191	139	0.14	0.0030	1560	36	18	191	130	1.00	0.34	0.09	0.65
V51221112	0.97	0.44	0.88	0.89	0.86	0.15	0.0031	1538	1538	20	189	116	0.15	0.0031	1527	35	18	188	107	1.00	0.35	0.09	0.65
V11221121	1.07	0.41	0.87	0.89	0.70	0.16	0.0034	1452	1452	14	152	229	0.16	0.0034	1448	33	13	152	218	1.00	0.23	0.05	0.49
V11221122	1.12	0.39	0.86	0.89	0.74	0.17	0.0036	1418	1418	14	153	194	0.17	0.0036	1415	33	14	153	184	1.00	0.25	0.06	0.49
V21221121	0.98	0.43	0.88	0.89	0.73	0.15	0.0030	1541	1541	16	169	215	0.15	0.0030	1537	35	15	169	205	1.00	0.24	0.06	0.52
V21221122	1.02	0.42	0.87	0.89	0.77	0.15	0.0032	1496	1496	16	169	180	0.15	0.0032	1493	35	16	168	171	1.00	0.26	0.06	0.53
V31221121	0.91	0.46	0.88	0.89	0.76	0.14	0.0028	1641	1641	18	187	202	0.14	0.0028	1636	38	17	187	193	1.00	0.25	0.06	0.56
V31221122	0.94	0.45	0.88	0.89	0.80	0.14	0.0029	1600	1600	18	187	169	0.14	0.0029	1595	37	18	187	160	1.00	0.27	0.07	0.57
V41221121	0.84	0.49	0.88	0.89	0.79	0.13	0.0026	1744	1744	20	207	188	0.13	0.0026	1738	40	19	207	179	1.00	0.26	0.06	0.61
V41221122	0.87	0.48	0.88	0.89	0.82	0.13	0.0027	1698	1698	20	204	157	0.13	0.0026	1692	39	19	204	148	1.00	0.28	0.07	0.61
V51221121	0.78	0.52	0.88	0.89	0.82	0.12	0.0024	1840	1840	22	226	171	0.12	0.0024	1831	42	21	226	163	1.00	0.28	0.07	0.65
V51221122	0.81	0.51	0.88	0.89	0.85	0.12	0.0025	1801	1801	22	223	142	0.12	0.0025	1793	41	21	223	134	1.00	0.29	0.07	0.65
V11221211	1.16	0.38	0.86	0.89	0.73	0.18	0.0038	1380	1380	13	144	197	0.18	0.0038	1377	32	13	144	186	1.00	0.25	0.06	0.49
V11221212	1.21	0.37	0.85	0.89	0.77	0.19	0.0040	1353	1353	14	146	166	0.19	0.0040	1351	31	13	146	156	1.00	0.27	0.07	0.50
V21221211	1.06	0.41	0.87	0.89	0.76	0.16	0.0034	1459	1459	15	159	183	0.16	0.0034	1455	34	15	159	173	1.00	0.26	0.06	0.53
V21221212	1.10	0.40	0.86	0.89	0.80	0.17	0.0035	1435	1435	15	160	154	0.17	0.0035	1432	33	15	160	145	1.00	0.28	0.07	0.53
V31221211	0.98	0.43	0.88	0.89	0.79	0.15	0.0030	1542	1542	17	174	170	0.15	0.0030	1538	36	16	174	160	1.00	0.28	0.07	0.57
V31221212	1.01	0.42	0.87	0.89	0.82	0.15	0.0031	1506	1506	17	174	142	0.15	0.0031	1502	35	16	174	133	1.00	0.29	0.08	0.57
V41221211	0.91	0.46	0.88	0.89	0.82	0.14	0.0028	1638	1638	19	191	157	0.14	0.0028	1632	38	18	191	148	1.00	0.29	0.07	0.61
V41221212	0.93	0.45	0.88	0.89	0.84	0.14	0.0029	1609	1609	19	191	131	0.14	0.0028	1604	37	18	191	123	1.00	0.30	0.08	0.61
V51221211	0.84	0.49	0.88	0.89	0.84	0.13	0.0026	1737	1737	21	209	142	0.13	0.0026	1728	39	20	209	134	1.00	0.30	0.08	0.65
V51221212	0.86	0.48	0.88	0.89	0.87	0.13	0.0027	1704	1704	21	207	119	0.13	0.0027	1696	39	20	207	111	1.00	0.32	0.08	0.66
V11221221	0.95	0.44	0.88	0.89	0.72	0.14	0.0029	1592	1592	15	168	231	0.14	0.0029	1589	37	15	167	221	1.00	0.22	0.05	0.49
V11221222	0.99	0.43	0.87	0.89	0.76	0.15	0.0031	1545	1545	16	168	194	0.15	0.0031	1542	36	15	168	185	1.00	0.24	0.06	0.50
V21221221	0.87	0.48	0.88	0.89	0.75	0.13	0.0026	1707	1707	17	187	219	0.13	0.0026	1703	39	17	187	209	1.00	0.22	0.05	0.52
V21221222	0.91	0.46	0.88	0.89	0.79	0.13	0.0027	1663	1663	18	188	183	0.13	0.0027	1661	39	18	188	175	1.00	0.24	0.06	0.53
V31221221	0.81	0.51	0.88	0.89	0.78	0.12	0.0024	1824	1824	20	208	207	0.12	0.0024	1820	42	19	208	198	1.00	0.23	0.06	0.56
V31221222	0.84	0.50	0.88	0.89	0.81	0.12	0.0025	1783	1783	20	208	173	0.12	0.0025	1780	41	20	208	165	1.00	0.24	0.06	0.57
V41221221	0.75	0.54	0.88	0.89	0.81	0.11	0.0022	1928	1928	22	227	192	0.11	0.0022	1923	44	21	227	184	1.00	0.24	0.06	0.61
V41221222	0.77	0.53	0.88	0.89	0.84	0.11	0.0023	1888	1888	22	226	161	0.11	0.0023	1884	44	22	226	153	1.00	0.25	0.06	0.61
V51221221	0.70	0.58	0.89	0.89	0.83	0.10	0.0021	2038	2038	24	247	177	0.10	0.0021	2031	46	23	247	170	1.00	0.25	0.06	0.65
V51221222	0.72	0.56	0.88	0.89	0.86	0.11	0.0022	2000	2000	24	245	148	0.11	0.0021	1993	46	23	245	141	1.00	0.26	0.07	0.66
V11222111	0.78	0.52	0.88	0.89	0.65	0.11	0.0024	1862	1862	11	122	331	0.11	0.0024	1857	43	11	122	321	1.00	0.17	0.04	0.49
V11222112	0.81	0.51	0.88	0.89	0.68	0.12	0.0025	1820	1820	11	122	297	0.12	0.0025	1816	42	11	122	288	1.00	0.18	0.04	0.49
V21222111	0.73	0.56	0.88	0.89	0.69	0.11	0.0022	1980	1980	12	136	318	0.11	0.0022	1976	45	12	136	309	1.00	0.17	0.04	0.52
V21222112	0.75	0.54	0.88	0.89	0.71	0.11	0.0022	1932	1932	12	136	284	0.11	0.0022	1929	44	12	136	276	1.00	0.18	0.04	0.52
V31222111	0.69	0.59	0.89	0.89	0.71	0.10	0.0020	2086	2086	14	149	305	0.10	0.0020	2082	48	13	149	297	1.00	0.18	0.04	0.56
V31222112	0.70	0.57	0.88	0.89	0.74	0.10	0.0021	2046	2046	14	149	273	0.10	0.0021	2043	47	14	149	265	1.00	0.19	0.04	0.56
V41222111	0.65	0.61	0.89	0.89	0.74	0.09	0.0019	2176	2176	15	161	290	0.09	0.0019	2171	50	15	161	282	1.00	0.19	0.04	0.61
V41222112	0.66	0.60	0.89	0.89	0.76	0.09	0.0019	2142	2142	15	161	259	0.09	0.0019	2138	49	15	161	251	1.00	0.20	0.05	0.61
V51222111	0.61	0.64	0.89	0.89	0.76	0.09	0.0018	2272	2272	16	174	275	0.09	0.0018	2266	52	16	174	268	1.00	0.19	0.05	0.66
V51222112	0.63	0.63	0.89	0.89	0.79	0.09	0.0018	2230	2230	16	173	244	0.09	0.0018	2225	51	16	173	237	1.00	0.20	0.05	0.66
V11222121	0.64	0.62	0.89	0.89	0.64	0.09	0.0019	2182	2182	12	142	402	0.09	0.0019	2177	50	12	142	393	1.00	0.14	0.03	0.49
V11222122	0.67	0.60	0.89	0.89	0.67	0.09	0.0020	2134	2134	12	143	361	0.09	0.0020	2131	49	12	142	353	1.00	0.15	0.03	0.49
V21222121	0.60	0.65	0.89	0.89	0.67	0.08	0.0018	2307	2307	14	157	389	0.08	0.0017	2303	53	14	157	381	1.00	0.14	0.03	0.52
V21222122	0.63	0.63	0.89	0.89	0.70	0.09	0.0018	2249	2249	14	157	348	0.09	0.0018	2246	52	14	157	340	1.00	0.15	0.03	0.52
V31222121	0.57	0.68	0.89	0.89	0.69	0.08	0.0016	2414	2414	15	170	376	0.08	0.0016	2410	55	15	170	368	1.00	0.15	0.03	0.56
V31222122	0.59	0.66	0.89	0.89	0.72	0.08	0.0017	2364	2364	15	170	336	0.08	0.0017	2361	54	15	170	329	1.00	0.16	0.04	0.56
V41222121	0.55	0.71	0.89	0.89	0.72	0.07	0.0015	2503	2503	17	182	361	0.07	0.0015	2500	57	16	182	354	1.00	0.15	0.03	0.61
V41222122	0.56	0.69	0.89	0.89	0.74	0.08	0.0016	2460	2460	17	183	323	0.08	0.0016	2457	57	17	182	316	1.00	0.16	0.04	0.61
V51222121	0.52	0.73	0.89	0.89	0.74	0.07	0.0014	2579	2579	18	193	346	0.07	0.0014	2575	59	18	193	339	1.00	0.16	0.04	0.66
V51222122	0.54	0.71	0.89	0.89	0.76	0.07	0.0015	2541	2541	18	193	309	0.07	0.0015	2538	58	18	193	302	1.00	0.16	0.04	0.66
V11222211	0.72	0.56	0.88	0.89	0.67	0.10	0.0022	2003	2003	11	131	340	0.10	0.0022	2000	46	11	131	331	1.00	0.16	0.03	0.49
V11222212	0.74	0.55	0.88	0.89	0.70	0.11	0.0022	1956	1956	12	131	304	0.11	0.0022	1953	45	12	131	295	1.00	0.17	0.04	0.49
V21222211	0.67	0.59	0.89	0.89	0.70	0.10	0.0020	2120	2120	13	144	327	0.10	0.0020	2117	49	13	144	319	1.00	0.16	0.04	0.52
V21222212	0.69	0.58	0.88	0.89	0.72	0.10	0.0020	2081	2081	13	145	293	0.10	0.0020	2079	48	13	145	285	1.00	0.17	0.04	0.52
V31222211	0.63	0.62	0.89	0.89	0.72	0.09	0.0018	2217	2217	14	157	313	0.09	0.0018	2214	51	14	157	305	1.00	0.17	0.04	0.56
V31222212	0.65	0.61	0.89	0.89	0.75	0.09	0.0019	2183	2183	15	157	280	0.09	0.0019	2180	50	14	157	273	1.00	0.18	0.04	0.56
V41222211	0.60	0.65	0.89	0.89	0.75	0.08	0.0017	2325	2325	16	169	301	0.08	0.0017	2322	53	16	169	294	1.00	0.17	0.04	0.61
V41222212	0.62	0.64	0.89	0.89	0.77	0.09	0.0018	2285	2285	16	169	268	0.09	0.0018	2282	53	16	169	261	1.00	0.18	0.04	0.61
V51222211	0.57	0.68	0.89	0.89	0.77	0.08	0.0016	2417	2417	17	181	287	0.08	0.0016	2413	55	17	181	280	1.00	0.18	0.04	0.66

Name	T1 [s]	Sa(T1) [g]	Sa(T2) [g]	Sa(T3) [g]	DOC [-]	Disp [m]	ISDR [-]	Total Moment [MN-m]	Total Shear [MN]	Max CB Shear [MN]	Max Pp [MN]	Max wall moment [MN-m]	Disp [m]2	ISDR [-]3	Total Moment [MN-m]4	Total Shear [MN]5	Max CB Shear [MN]6	Max Pp [MN]2	Max wall moment [MN-m]8	C1 [-]	C2 [-]	C3 [-]	Mdy/ Mst [-]
V51222212	0.58	0.67	0.89	0.89	0.79	0.08	0.0017	2382	2382	17	181	256	0.08	0.0017	2379	55	17	181	250	1.00	0.18	0.04	0.66
V11222221	0.60	0.66	0.89	0.89	0.65	0.08	0.0017	2339	2339	13	151	414	0.08	0.0017	2335	54	13	151	407	1.00	0.13	0.03	0.49
V11222222	0.62	0.64	0.89	0.89	0.68	0.09	0.0018	2283	2283	13	151	371	0.09	0.0018	2280	53	13	151	363	1.00	0.14	0.03	0.49
V21222221	0.56	0.69	0.89	0.89	0.68	0.08	0.0016	2456	2456	15	165	401	0.08	0.0016	2453	56	14	165	394	1.00	0.13	0.03	0.52
V21222222	0.58	0.67	0.89	0.89	0.71	0.08	0.0017	2408	2408	15	166	359	0.08	0.0017	2406	56	15	166	352	1.00	0.14	0.03	0.52
V31222221	0.53	0.72	0.89	0.89	0.70	0.07	0.0015	2550	2550	16	177	387	0.07	0.0015	2547	59	16	177	380	1.00	0.14	0.03	0.56
V31222222	0.55	0.70	0.89	0.89	0.73	0.07	0.0015	2509	2509	16	178	347	0.07	0.0015	2506	58	16	178	340	1.00	0.15	0.03	0.56
V41222221	0.51	0.74	0.89	0.89	0.72	0.07	0.0014	2627	2627	17	187	373	0.07	0.0014	2624	60	17	187	366	1.00	0.14	0.03	0.61
V41222222	0.52	0.72	0.89	0.89	0.75	0.07	0.0015	2592	2592	17	188	334	0.07	0.0014	2590	60	17	188	328	1.00	0.15	0.03	0.61
V51222221	0.49	0.75	0.89	0.89	0.74	0.06	0.0013	2680	2680	18	196	357	0.06	0.0013	2677	62	18	196	350	1.00	0.15	0.03	0.66
V51222222	0.50	0.74	0.89	0.89	0.76	0.07	0.0014	2656	2656	18	197	321	0.07	0.0014	2653	61	18	197	315	1.00	0.15	0.04	0.66
V12111111	2.82	0.16	0.56	0.85	0.71	0.47	0.0065	1277	1277	6	132	209	0.47	0.0064	1265	20	6	132	183	1.00	0.38	0.13	0.45
V12111112	2.95	0.15	0.52	0.84	0.75	0.48	0.0067	1214	1214	6	130	172	0.48	0.0066	1205	19	6	130	150	1.00	0.39	0.15	0.46
V22111111	2.58	0.18	0.60	0.86	0.74	0.44	0.0061	1432	1432	8	156	204	0.44	0.0060	1420	22	7	156	179	1.00	0.40	0.14	0.48
V22111112	2.68	0.17	0.57	0.85	0.78	0.45	0.0062	1369	1369	8	153	168	0.45	0.0061	1360	21	7	153	146	1.00	0.42	0.15	0.48
V32111111	2.36	0.20	0.65	0.87	0.78	0.42	0.0058	1597	1597	9	182	198	0.42	0.0056	1582	25	9	182	172	1.00	0.44	0.14	0.52
V32111112	2.44	0.20	0.62	0.86	0.81	0.43	0.0059	1535	1535	9	179	162	0.42	0.0057	1523	24	9	178	140	1.00	0.45	0.16	0.52
V42111111	2.17	0.23	0.72	0.88	0.81	0.40	0.0056	1778	1778	11	211	188	0.40	0.0054	1755	27	10	210	162	1.00	0.49	0.15	0.55
V42111112	2.23	0.22	0.69	0.87	0.84	0.41	0.0056	1717	1717	12	207	154	0.40	0.0054	1697	26	10	206	130	1.00	0.51	0.16	0.56
V52111111	1.99	0.26	0.78	0.88	0.84	0.38	0.0054	1970	1970	14	243	169	0.38	0.0053	1930	30	12	241	144	0.99	0.56	0.16	0.60
V52111112	2.04	0.25	0.77	0.88	0.87	0.39	0.0055	1921	1921	14	239	138	0.39	0.0054	1882	29	11	237	115	0.99	0.57	0.17	0.60
V12111121	2.30	0.21	0.66	0.87	0.70	0.41	0.0056	1655	1655	8	174	270	0.40	0.0056	1643	26	8	173	243	1.00	0.34	0.10	0.45
V12111122	2.41	0.20	0.62	0.86	0.74	0.42	0.0058	1566	1566	8	170	221	0.41	0.0057	1557	24	8	170	198	1.00	0.36	0.12	0.45
V22111121	2.11	0.24	0.71	0.88	0.74	0.38	0.0053	1860	1860	10	205	265	0.38	0.0052	1848	29	10	205	239	1.00	0.36	0.10	0.48
V22111122	2.19	0.23	0.67	0.87	0.78	0.39	0.0054	1772	1772	10	201	217	0.39	0.0053	1762	28	9	201	194	1.00	0.38	0.12	0.48
V32111121	1.94	0.26	0.75	0.88	0.77	0.36	0.0049	2039	2039	12	235	253	0.36	0.0048	2024	32	11	235	227	1.00	0.39	0.11	0.51
V32111122	2.01	0.25	0.72	0.88	0.81	0.37	0.0051	1983	1983	12	234	210	0.37	0.0050	1971	31	11	234	186	1.00	0.41	0.12	0.52
V42111121	1.78	0.28	0.79	0.88	0.80	0.33	0.0045	2174	2174	14	261	231	0.33	0.0044	2152	33	12	261	205	1.00	0.44	0.12	0.55
V42111122	1.84	0.27	0.77	0.88	0.83	0.34	0.0047	2127	2127	14	260	192	0.34	0.0046	2108	33	12	259	168	1.00	0.45	0.13	0.56
V52111121	1.64	0.30	0.84	0.89	0.84	0.30	0.0043	2306	2306	16	289	202	0.30	0.0042	2269	35	14	287	176	0.99	0.50	0.13	0.60
V52111122	1.68	0.29	0.83	0.88	0.86	0.31	0.0044	2264	2264	16	286	166	0.31	0.0043	2228	34	14	284	143	0.99	0.51	0.14	0.60
V12111211	2.51	0.19	0.60	0.86	0.73	0.43	0.0060	1484	1484	7	155	219	0.43	0.0059	1474	23	7	155	195	1.00	0.36	0.12	0.45
V12111212	2.61	0.18	0.57	0.85	0.77	0.44	0.0061	1421	1421	7	154	180	0.43	0.0060	1414	22	7	154	160	1.00	0.37	0.14	0.46
V22111211	2.29	0.21	0.65	0.87	0.77	0.40	0.0056	1674	1674	9	184	215	0.40	0.0055	1664	26	9	183	191	1.00	0.38	0.12	0.48
V22111212	2.36	0.20	0.62	0.86	0.80	0.41	0.0056	1612	1612	9	182	176	0.41	0.0056	1604	25	9	181	156	1.00	0.39	0.14	0.48
V32111211	2.09	0.24	0.71	0.88	0.80	0.38	0.0053	1878	1878	11	214	208	0.38	0.0052	1865	29	10	214	184	1.00	0.41	0.13	0.52
V32111212	2.15	0.23	0.68	0.87	0.83	0.39	0.0053	1815	1815	11	211	171	0.39	0.0052	1804	28	10	211	150	1.00	0.43	0.14	0.52
V42111211	1.92	0.26	0.76	0.88	0.83	0.36	0.0050	2050	2050	13	242	193	0.36	0.0048	2030	32	12	242	169	1.00	0.46	0.13	0.55
V42111212	1.97	0.26	0.74	0.88	0.86	0.37	0.0051	2014	2014	13	242	160	0.37	0.0049	1996	31	12	241	138	1.00	0.47	0.14	0.56
V52111211	1.76	0.28	0.82	0.88	0.86	0.33	0.0047	2185	2185	15	268	168	0.33	0.0045	2148	33	13	266	144	0.99	0.52	0.15	0.60
V52111212	1.80	0.28	0.81	0.88	0.88	0.34	0.0048	2155	2155	16	267	139	0.33	0.0046	2120	33	13	265	117	0.99	0.53	0.15	0.60
V12111221	2.04	0.25	0.71	0.88	0.73	0.37	0.0052	1949	1949	10	207	287	0.37	0.0051	1939	30	9	207	262	1.00	0.32	0.09	0.45
V12111222	2.12	0.24	0.68	0.87	0.77	0.38	0.0053	1859	1859	10	204	236	0.38	0.0052	1852	29	10	204	214	1.00	0.34	0.11	0.45
V22111221	1.86	0.27	0.75	0.88	0.76	0.34	0.0046	2119	2119	11	236	273	0.34	0.0046	2109	33	11	235	248	1.00	0.35	0.10	0.48
V22111222	1.92	0.26	0.73	0.88	0.80	0.35	0.0048	2069	2069	12	236	228	0.35	0.0048	2061	32	11	236	206	1.00	0.36	0.11	0.48
V32111221	1.71	0.29	0.79	0.88	0.79	0.31	0.0042	2266	2266	13	262	254	0.31	0.0041	2252	35	12	262	229	1.00	0.38	0.10	0.51
V32111222	1.76	0.28	0.77	0.88	0.82	0.32	0.0043	2221	2221	14	262	211	0.32	0.0043	2210	35	13	262	189	1.00	0.39	0.11	0.52
V42111221	1.57	0.31	0.83	0.88	0.82	0.28	0.0039	2408	2408	15	289	231	0.28	0.0038	2388	37	14	288	206	1.00	0.42	0.11	0.55
V42111222	1.61	0.30	0.81	0.88	0.85	0.29	0.0040	2368	2368	15	288	192	0.29	0.0039	2350	37	14	288	169	1.00	0.43	0.12	0.56
V52111221	1.44	0.33	0.85	0.89	0.85	0.26	0.0036	2545	2545	17	317	200	0.26	0.0035	2513	39	15	315	177	0.99	0.46	0.12	0.60
V52111222	1.47	0.33	0.85	0.89	0.88	0.26	0.0037	2509	2509	18	315	166	0.26	0.0036	2478	38	15	313	145	0.99	0.47	0.13	0.60
V12112111	1.65	0.30	0.81	0.88	0.67	0.29	0.0041	2313	2313	7	155	409	0.29	0.0041	2298	36	7	155	379	1.00	0.28	0.07	0.45
V12112112	1.71	0.29	0.79	0.88	0.70	0.30	0.0042	2264	2264	7	155	367	0.30	0.0042	2253	35	7	155	339	1.00	0.30	0.07	0.45
V22112111	1.52	0.32	0.83	0.89	0.70	0.27	0.0037	2462	2462	8	174	386	0.27	0.0037	2448	38	8	174	358	1.00	0.30	0.07	0.48
V22112112	1.57	0.31	0.82	0.88	0.73	0.28	0.0038	2418	2418	8	174	346	0.27	0.0038	2407	38	8	174	319	1.00	0.32	0.08	0.48
V32112111	1.41	0.34	0.84	0.89	0.74	0.24	0.0033	2603	2603	9	193	361	0.24	0.0033	2587	40	9	193	334	1.00	0.32	0.08	0.51
V32112112	1.45	0.33	0.84	0.89	0.76	0.25	0.0034	2563	2563	9	193	323	0.25	0.0034	2549	40	9	193	297	1.00	0.34	0.08	0.51
V42112111	1.31	0.35	0.85	0.89	0.77	0.22	0.0031	2736	2736	11	211	332	0.22	0.0030	2716	42	10	211	306	1.00	0.35	0.09	0.55
V42112112	1.34	0.35	0.85	0.89	0.79	0.23	0.0032	2699	2699	11	211	296	0.23	0.0031	2681	42	10	211	271	1.00	0.36	0.09	0.55
V52112111	1.22	0.37	0.87	0.89	0.80	0.21	0.0029	2860	2860	12	230	297	0.21	0.0028	2833	44	11	230	273	1.00	0.38	0.10	0.60
V52112112	1.24	0.37	0.86	0.89	0.82	0.21	0.0029	2826	2826	12	229	264	0.21	0.0029	2800	43	11	229	240	1.00	0.39	0.10	0.60
V12112121	1.34	0.35	0.85	0.89	0.66	0.23	0.0031	2702	2702	8	181	483	0.23	0.0031	2689	42	8	181	454	1.00	0.25	0.05	0.45
V12112122	1.39	0.34	0.84	0.89	0.69	0.24	0.0033	2645	2645	8	182	434	0.23	0.0033	2634	41	8	182	406	1.00	0.26	0.06	0.45
V22112121	1.24	0.37	0.86	0.89	0.70	0.21	0.0028	2854	2854	9	202	455	0.21	0.0028	2841	44	9	202	428	1.00	0.26	0.06	0.47
V22112122	1.28	0.36	0.85	0.89	0.72	0.21	0.0029	2804	2804	9	203	408	0.21	0.0029	2793	44	9	203	382	1.00	0.28	0.07	0.48
V32112121	1.16	0.39	0.86	0.89	0.73	0.19	0.0026	2992	2992	10	222	425	0.19	0.0026	2978	46	10	222	400	1.00	0.28	0.07	0.51
V32112122	1.19	0.38	0.86	0.89	0.75	0.19	0.0027	2949	2949	11	222	381	0.19	0.0026	2937	46	10	222	356	1.00	0.29	0.07	0.51
V42112121	1.08	0.40	0.87	0.89	0.76	0.17	0.0024	3118	3118	12	241	393	0.17	0.0023	3102	48	11	241	369	1.00	0.30	0.07	0.55
V42112122	1.11	0.40	0.87	0.89	0.78	0.18	0.0024	3079	3079	12	241	351	0.18	0.0024	3064	48	11	241	327	1.00	0.31	0.08	0.55
V52112121	1.01	0.42	0.88	0.89	0.79	0.16	0.0022	3232	3232	13	259	356	0.16	0.0022	3210	50	12	259	333	1.00	0.33	0.08	0.60
V52112122	1.03	0.41	0.88	0.89	0.81	0.16	0.0022	3195	3195	13	259	316	0.16	0.0022	3175	49	12	259	294	1.00	0.34	0.08	0.60
V12112211	1.51	0.32	0.83	0.89	0.69	0.26	0.0036	2485	2485	8	166	413	0.26	0.0036	2473	39	7	166	385	1.00	0.28	0.06	0.45
V12112212	1.55	0.31	0.82	0.88	0.71	0.27	0.0038	2442	2442	8	168	371	0.27	0.0037	2432	38	8	168	344	1.00	0.29	0.07	0.45
V22112211	1.39	0.34	0.84	0.89	0.72	0.24	0.0033	2641	2641	9	186	389	0.24	0.0032	2629	41	9	186	362	1.00	0.29	0.07	0.48
V22112212	1.43	0.33	0.84	0.89	0.75	0.24	0.0034	2603	2603	9	187	349	0.24	0.0033	2593	41	9	187	324	1.00	0.30	0.08	0.48
V32112211	1.29	0.36	0.85	0.89	0.75	0.22	0.0030	2786	2786	10	205	363	0.22	0.0029	2773	43	10	205	338	1.00	0.31	0.08	0.51
V32112212	1.32	0.35	0.85	0.89	0.78	0.22	0.0030	2751	2751	10	206	325	0.22	0.0030	2740	43	10	206	301	1.00	0.32	0.08	0.51
V42112211	1.20	0.38	0.86	0.89	0.78	0.20	0.0027	2920	2920	11	223	334	0.20	0.0027	2904	45	11	223	310	1.00	0.33	0.08	0.55
V42112212	1.22	0.37	0.86	0.89	0.80	0.20	0.0028	2888	2888	11	223	298	0.20	0.0027	2873	45	11	223	275	1.00	0.34	0.09	0.56
V52112211	1.12	0.39	0.87	0.89	0.81	0.18	0.0025	3041	3041	12	241	300	0.18	0.0025	3018	47	12	240	277	1.00	0.36	0.09	0.60
V52112212	1.13	0.39	0.87	0.89	0.83	0.19	0.0026	3012	3012	13	241	267	0.19	0.0025	2990	46	12	240	245	1.00	0.37	0.09	0.60
V12112221	1.22	0.37	0.86	0.89	0.68	0.20	0.0028	2888	2888	9	194	486	0.20	0.0028	2876	45	9	194	459	1.00	0.24	0.05	0.45
V12112222	1.26	0.36	0.85	0.89	0.71	0.21	0.0029	2837	2837	9	196	436	0.21	0.0029	2828	44	9	195	411	1.00	0.25	0.06	0.45
V22112221	1.13	0.39	0.86	0.89	0.71	0.18	0.0025	3040	3040	10	214	457	0.18	0.0025	3029	47	10	214	432	1.00	0.25	0.06	0.48
V22112222	1.16	0.38	0.86	0.89	0.74	0.19	0.0026	2999	2999	10	216	410	0.19	0.0026	2990	47	10	216	386	1.00	0.26	0.06	0.48
V32112221	1.06	0.41	0.87	0.89	0.74	0.17	0.0023	3178	3178	11	234	427	0.16	0.0023	3166	49	11	234	404	1.00	0.27	0.06	0.51
V32112222	1.08	0.40	0.87	0.89	0.77	0.17	0.0023	3141	3141	11	235	382	0.17	0.0023	3131	49	11	235	360	1.00	0.28	0.07	0.51
V42112221	0.99	0.43	0.88	0.89	0.77	0.15	0.0021	3325	3325	12	253	398	0.15	0.0021	3312	52	12	253	376	1.00	0.28	0.07	0.55
V42112222	1.01	0.42	0.88	0.89	0.79	0.16	0.0021	3268	3268	12	253	353	0.16	0.0021	3256	51	12	253	332	1.00	0.29	0.07	0.56
V52112221	0.93	0.45	0.88	0.89	0.80	0.14	0.0020	3499	3499	14	276	369	0.14	0.0019	3482	54	13	276	348	1.00	0.30	0.07	0.60
V52112222	0.94	0.45	0.88	0.89	0.82	0.15	0.0020	3452	3452	14	275	327	0.15	0.0020	3436	53	13	275	307	1.00	0.31	0.08	0.60
V12121111	3.26	0.14	0.49	0.84	0.70	0.52	0.0073	1423	1423	7	147	237	0.52	0.0072	1407	22	7	147	204	1.00	0.40	0.15	0.46
V12121112	3.40	0.13	0.46	0.81	0.75	0.53	0.0075	1353	1353	7	145	195	0.53	0.0074	1342	21	7	145	167	1.00	0.41	0.17	0.46
V22121111	2.98	0.15	0.53	0.84	0.74	0.49	0.0068	1591	1591	9	173	231	0.49	0.0067	1576	25	8	173	199	1.00	0.43	0.16	0.48
V22121112	3.09	0.15	0.50	0.83	0.78	0.50	0.0069	1523	1523	9	171	190	0.50	0.0068	1511	24	8	170	162	1.00	0.44	0.18	0.48
V32121111	2.73	0.17	0.58	0.85	0.77	0.46	0.0064	1771	1771	10	201	224	0.46	0.0062	1751	27	10	201	191	1.00	0.47	0.17	0.52
V32121112	2.82	0.16	0.55	0.85	0.81	0.47	0.0065	1704	1704	11	198	183	0.47	0.0063	1688	26	9	198	155	1.00	0.48	0.18	0.52
V42121111	2.51	0.19	0.64	0.87	0.81	0.44	0.0062	1967	1967	13	233	212	0.44	0.0059	1937	30	11	232	178	1.00	0.53	0.18	0.56
V42121112	2.58	0.18	0.61	0.86	0.84	0.45	0.0063	1901	1901	13	228	174	0.45	0.0060	1875	29	11	228	144	1.00	0.54	0.19	0.56
V52121111	2.30	0.21	0.73	0.88	0.84	0.42	0.0061	2194	2194	17	270	194	0.42	0.0058	2138	33	13	267	159	0.99	0.62	0.19	0.60
V52121112	2.36	0.21	0.71	0.88	0.87	0.43	0.0062	2127	2127	17	264	158	0.43	0.0059	2075	32	13	261	127	0.99	0.64	0.20	0.60
V12121121	2.66	0.18	0.59	0.86	0.70	0.45	0.0062	1833	1833	9	192	304	0.45	0.0062	1817	28	9	192	269	1.00	0.37	0.12	0.45
V12121122	2.78	0.17	0.55	0.85	0.74	0.46	0.0064	1737	1737	9	189	250	0.46	0.0064	1725	27	9	188	219	1.00	0.38	0.14	0.46
V22121121	2.43	0.20	0.63	0.87	0.74	0.42	0.0058	2055	2055	11	227	298	0.42	0.0058	2039	32	10	226	263	1.00	0.39	0.12	0.48

Name	T1 [s]	Sa(T1) [g]	Sa(T2) [g]	Sa(T3) [g]	DOC [-]	Disp [m]	ISDR [-]	Total Moment [MN-m]	Total Shear [MN]	Max CB Shear [MN]	Max Pp [MN]	Max wall moment [MN-m]	Disp [m]2	ISDR [-]3	Total Moment [MN-m]4	Total Shear [MN]5	Max CB Shear [MN]6	Max Pp [MN]2	Max wall moment [MN-m]8	C1 [-]	C2 [-]	C3 [-]	Mdy/ Mst [-]
V32121121	2.23	0.22	0.68	0.87	0.77	0.40	0.0055	2290	2290	13	264	289	0.40	0.0054	2270	35	12	264	254	1.00	0.42	0.13	0.51
V32121122	2.32	0.21	0.65	0.87	0.81	0.41	0.0056	2194	2194	13	259	237	0.41	0.0055	2178	34	12	258	206	1.00	0.44	0.14	0.52
V42121121	2.06	0.25	0.74	0.88	0.80	0.38	0.0053	2546	2546	16	306	275	0.38	0.0052	2516	39	15	305	240	1.00	0.47	0.14	0.55
V42121122	2.12	0.24	0.72	0.88	0.83	0.39	0.0054	2449	2449	16	299	225	0.39	0.0053	2423	38	14	298	193	1.00	0.49	0.15	0.56
V52121121	1.89	0.27	0.80	0.88	0.84	0.36	0.0051	2747	2747	20	344	244	0.36	0.0049	2697	41	16	341	210	0.99	0.53	0.15	0.60
V52121122	1.94	0.26	0.79	0.88	0.86	0.37	0.0052	2690	2690	20	340	201	0.37	0.0051	2642	41	16	337	170	0.99	0.55	0.16	0.60
V12121211	2.90	0.16	0.53	0.85	0.73	0.47	0.0066	1648	1648	8	172	247	0.47	0.0066	1635	26	8	172	216	1.00	0.39	0.14	0.46
V12121212	3.01	0.15	0.50	0.83	0.77	0.48	0.0068	1579	1579	8	171	204	0.48	0.0067	1569	25	8	171	177	1.00	0.40	0.16	0.46
V22121211	2.64	0.18	0.58	0.85	0.77	0.45	0.0062	1853	1853	10	203	242	0.44	0.0061	1840	29	10	203	211	1.00	0.41	0.15	0.48
V22121212	2.73	0.17	0.55	0.84	0.80	0.45	0.0063	1786	1786	10	201	199	0.45	0.0062	1776	28	10	201	172	1.00	0.42	0.16	0.48
V32121211	2.42	0.20	0.63	0.86	0.80	0.42	0.0058	2073	2073	12	236	234	0.42	0.0057	2056	32	11	236	203	1.00	0.45	0.15	0.52
V32121212	2.48	0.19	0.60	0.86	0.83	0.43	0.0059	2007	2007	12	233	192	0.43	0.0058	1993	31	11	233	165	1.00	0.46	0.16	0.52
V42121211	2.22	0.22	0.70	0.88	0.83	0.40	0.0056	2313	2313	15	273	223	0.40	0.0054	2286	35	13	273	190	1.00	0.50	0.16	0.56
V42121212	2.27	0.22	0.67	0.87	0.85	0.41	0.0057	2245	2245	15	269	183	0.41	0.0055	2221	35	13	269	154	1.00	0.51	0.17	0.56
V52121211	2.03	0.25	0.77	0.88	0.86	0.39	0.0055	2578	2578	19	316	202	0.38	0.0053	2529	39	15	313	170	0.99	0.56	0.16	0.60
V52121212	2.07	0.24	0.76	0.88	0.88	0.39	0.0056	2517	2517	19	311	165	0.39	0.0054	2469	38	15	308	137	0.99	0.57	0.17	0.60
V12121221	2.35	0.21	0.64	0.87	0.73	0.41	0.0057	2150	2150	11	228	322	0.41	0.0057	2138	34	10	228	289	1.00	0.35	0.11	0.45
V12121222	2.45	0.20	0.60	0.86	0.77	0.42	0.0058	2053	2053	11	225	265	0.42	0.0058	2044	32	11	225	237	1.00	0.36	0.13	0.46
V22121221	2.15	0.23	0.69	0.87	0.76	0.39	0.0053	2422	2422	13	269	316	0.38	0.0053	2408	38	13	269	283	1.00	0.37	0.11	0.48
V22121222	2.22	0.22	0.65	0.87	0.80	0.39	0.0054	2328	2328	13	266	260	0.39	0.0054	2317	36	13	266	231	1.00	0.38	0.13	0.48
V32121221	1.97	0.26	0.74	0.88	0.79	0.36	0.0050	2684	2684	16	310	304	0.36	0.0049	2667	42	15	310	271	1.00	0.40	0.12	0.51
V32121222	2.03	0.25	0.71	0.88	0.82	0.37	0.0051	2617	2617	16	309	252	0.37	0.0050	2603	41	15	309	223	1.00	0.41	0.13	0.52
V42121221	1.81	0.28	0.78	0.88	0.82	0.33	0.0046	2869	2869	18	344	278	0.33	0.0045	2842	44	16	343	245	1.00	0.44	0.12	0.55
V42121222	1.86	0.27	0.76	0.88	0.85	0.34	0.0047	2818	2818	19	343	231	0.34	0.0046	2795	44	17	342	202	1.00	0.45	0.13	0.56
V52121221	1.66	0.30	0.83	0.89	0.85	0.31	0.0043	3046	3046	21	378	244	0.30	0.0042	3000	46	18	376	212	0.99	0.50	0.14	0.60
V52121222	1.70	0.29	0.82	0.88	0.88	0.31	0.0044	3001	3001	22	377	202	0.31	0.0043	2957	46	18	374	172	0.99	0.51	0.14	0.60
V12122111	1.91	0.27	0.76	0.88	0.67	0.35	0.0048	2749	2749	8	184	490	0.35	0.0048	2730	42	8	184	450	1.00	0.30	0.07	0.45
V12122112	1.97	0.26	0.74	0.88	0.70	0.36	0.0050	2683	2683	8	184	438	0.36	0.0050	2667	42	8	184	401	1.00	0.31	0.08	0.45
V22122111	1.76	0.28	0.79	0.88	0.70	0.32	0.0044	2936	2936	10	207	465	0.32	0.0044	2917	45	9	207	426	1.00	0.32	0.08	0.48
V22122112	1.81	0.28	0.77	0.88	0.73	0.33	0.0045	2880	2880	10	208	416	0.33	0.0045	2864	45	10	208	380	1.00	0.33	0.09	0.48
V32122111	1.63	0.30	0.81	0.88	0.74	0.29	0.0040	3113	3113	11	230	437	0.29	0.0040	3092	48	11	230	399	1.00	0.35	0.09	0.51
V32122112	1.67	0.29	0.80	0.88	0.76	0.30	0.0041	3062	3062	11	230	390	0.30	0.0041	3043	47	11	230	354	1.00	0.36	0.09	0.51
V42122111	1.52	0.32	0.84	0.89	0.77	0.27	0.0037	3283	3283	13	253	404	0.27	0.0036	3255	50	12	253	367	1.00	0.38	0.10	0.55
V42122112	1.55	0.31	0.83	0.89	0.79	0.28	0.0038	3237	3237	13	253	360	0.27	0.0037	3212	50	12	253	325	1.00	0.39	0.10	0.55
V52122111	1.41	0.34	0.85	0.89	0.80	0.25	0.0035	3448	3448	15	277	363	0.25	0.0034	3410	53	13	276	328	1.00	0.42	0.11	0.60
V52122112	1.44	0.33	0.85	0.89	0.82	0.25	0.0035	3405	3405	15	276	322	0.25	0.0035	3369	52	13	275	289	1.00	0.43	0.11	0.60
V12122121	1.55	0.31	0.83	0.89	0.66	0.27	0.0038	3240	3240	10	217	584	0.27	0.0037	3221	50	10	217	544	1.00	0.27	0.06	0.45
V12122122	1.60	0.31	0.81	0.88	0.69	0.28	0.0039	3169	3169	10	218	524	0.28	0.0039	3153	49	10	218	487	1.00	0.28	0.07	0.45
V22122121	1.43	0.33	0.84	0.89	0.70	0.25	0.0034	3436	3436	11	243	553	0.25	0.0034	3418	53	11	243	515	1.00	0.29	0.07	0.48
V22122122	1.48	0.32	0.83	0.89	0.72	0.26	0.0035	3371	3371	11	244	496	0.26	0.0035	3356	52	11	244	460	1.00	0.30	0.07	0.48
V32122121	1.33	0.35	0.85	0.89	0.73	0.23	0.0031	3617	3617	13	268	519	0.23	0.0031	3598	56	12	268	483	1.00	0.31	0.07	0.51
V32122122	1.37	0.34	0.84	0.89	0.75	0.23	0.0032	3557	3557	13	268	464	0.23	0.0032	3539	55	13	268	430	1.00	0.32	0.08	0.51
V42122121	1.25	0.37	0.86	0.89	0.76	0.21	0.0029	3783	3783	14	292	481	0.21	0.0028	3760	58	14	292	447	1.00	0.33	0.08	0.55
V42122122	1.28	0.36	0.85	0.89	0.78	0.21	0.0029	3730	3730	15	292	429	0.21	0.0029	3708	58	14	292	396	1.00	0.34	0.08	0.55
V52122121	1.17	0.38	0.87	0.89	0.79	0.19	0.0027	3940	3940	16	316	438	0.19	0.0026	3909	60	15	315	406	1.00	0.35	0.09	0.60
V52122122	1.19	0.38	0.87	0.89	0.81	0.20	0.0027	3893	3893	16	315	389	0.20	0.0027	3864	60	15	315	358	1.00	0.36	0.09	0.60
V12122211	1.74	0.29	0.79	0.88	0.69	0.31	0.0043	2966	2966	9	199	497	0.31	0.0043	2949	46	9	198	459	1.00	0.29	0.07	0.45
V12122212	1.79	0.28	0.77	0.88	0.71	0.32	0.0045	2909	2909	9	200	445	0.32	0.0045	2895	45	9	199	410	1.00	0.30	0.08	0.45
V22122211	1.60	0.30	0.81	0.88	0.72	0.28	0.0039	3164	3164	10	223	470	0.28	0.0039	3147	49	10	223	434	1.00	0.31	0.08	0.48
V22122212	1.65	0.30	0.80	0.88	0.75	0.29	0.0040	3110	3110	11	224	421	0.29	0.0040	3096	48	10	223	386	1.00	0.32	0.08	0.48
V32122211	1.49	0.32	0.83	0.89	0.75	0.26	0.0036	3348	3348	12	246	441	0.26	0.0035	3329	52	11	246	405	1.00	0.34	0.08	0.51
V32122212	1.52	0.32	0.82	0.88	0.78	0.27	0.0036	3299	3299	12	246	394	0.27	0.0036	3283	51	12	246	360	1.00	0.35	0.09	0.51
V42122211	1.38	0.34	0.85	0.89	0.78	0.24	0.0033	3520	3520	13	269	407	0.24	0.0032	3496	54	13	268	373	1.00	0.36	0.09	0.55
V42122212	1.41	0.34	0.84	0.89	0.80	0.24	0.0033	3479	3479	14	269	363	0.24	0.0033	3458	54	13	269	331	1.00	0.37	0.10	0.56
V52122211	1.29	0.36	0.86	0.89	0.81	0.22	0.0031	3685	3685	15	292	368	0.22	0.0030	3653	56	14	291	335	1.00	0.39	0.10	0.60
V52122212	1.31	0.35	0.86	0.89	0.83	0.22	0.0031	3648	3648	15	291	327	0.22	0.0031	3618	56	14	291	296	1.00	0.40	0.10	0.60
V12122221	1.41	0.34	0.84	0.89	0.68	0.24	0.0033	3477	3477	10	233	590	0.24	0.0033	3461	54	10	233	553	1.00	0.26	0.06	0.45
V12122222	1.46	0.33	0.83	0.89	0.71	0.25	0.0035	3414	3414	11	235	530	0.25	0.0035	3401	53	11	235	495	1.00	0.28	0.07	0.45
V22122221	1.31	0.35	0.85	0.89	0.71	0.22	0.0030	3680	3680	12	259	558	0.22	0.0030	3665	57	12	259	523	1.00	0.27	0.06	0.48
V22122222	1.34	0.35	0.84	0.89	0.74	0.23	0.0031	3623	3623	12	261	500	0.23	0.0031	3610	57	12	261	467	1.00	0.29	0.07	0.48
V32122221	1.22	0.37	0.86	0.89	0.74	0.20	0.0028	3862	3862	14	284	523	0.20	0.0027	3846	60	13	284	490	1.00	0.29	0.07	0.51
V32122222	1.25	0.37	0.85	0.89	0.77	0.21	0.0028	3809	3809	14	285	468	0.21	0.0028	3795	59	13	285	436	1.00	0.30	0.07	0.51
V42122221	1.14	0.39	0.87	0.89	0.77	0.18	0.0025	4025	4025	15	307	486	0.18	0.0025	4005	62	14	307	454	1.00	0.31	0.08	0.55
V42122222	1.16	0.38	0.86	0.89	0.79	0.19	0.0026	3982	3982	15	308	434	0.19	0.0026	3964	62	15	308	404	1.00	0.32	0.08	0.56
V52122221	1.07	0.41	0.87	0.89	0.80	0.17	0.0023	4178	4178	17	329	446	0.17	0.0023	4153	64	16	329	415	1.00	0.33	0.08	0.60
V52122222	1.09	0.40	0.87	0.89	0.82	0.17	0.0024	4137	4137	17	330	397	0.17	0.0024	4114	64	16	329	367	1.00	0.34	0.09	0.60
V12211111	4.34	0.10	0.39	0.75	0.70	0.65	0.0069	1008	1008	5	104	174	0.65	0.0067	993	12	5	104	143	1.00	0.45	0.19	0.46
V12211112	4.53	0.09	0.37	0.69	0.75	0.67	0.0071	960	960	5	103	144	0.67	0.0069	949	11	5	102	118	1.00	0.48	0.21	0.46
V22211111	3.96	0.11	0.42	0.77	0.74	0.61	0.0064	1122	1122	6	122	169	0.60	0.0062	1107	13	6	122	139	1.00	0.48	0.21	0.49
V22211112	4.11	0.10	0.40	0.74	0.78	0.62	0.0065	1076	1076	6	120	140	0.62	0.0064	1064	13	6	120	114	1.00	0.50	0.23	0.49
V32211111	3.63	0.12	0.45	0.80	0.77	0.57	0.0060	1244	1244	8	141	163	0.57	0.0058	1225	14	7	141	133	1.00	0.53	0.23	0.52
V32211112	3.75	0.11	0.43	0.77	0.81	0.59	0.0061	1198	1198	8	139	134	0.58	0.0059	1183	14	7	139	108	1.00	0.54	0.24	0.52
V42211111	3.33	0.13	0.51	0.84	0.80	0.54	0.0058	1379	1379	9	163	155	0.54	0.0055	1351	16	8	162	124	1.00	0.60	0.25	0.56
V42211112	3.43	0.13	0.48	0.82	0.84	0.55	0.0059	1333	1333	10	160	127	0.55	0.0056	1309	15	8	159	100	1.00	0.61	0.26	0.56
V52211111	3.06	0.15	0.59	0.86	0.84	0.52	0.0057	1538	1538	12	189	142	0.51	0.0054	1484	17	9	186	109	0.98	0.72	0.27	0.60
V52211112	3.13	0.14	0.57	0.85	0.86	0.52	0.0058	1492	1492	12	185	116	0.52	0.0055	1442	17	9	182	87	0.98	0.73	0.29	0.60
V12211121	3.54	0.12	0.46	0.82	0.70	0.56	0.0058	1286	1286	6	134	220	0.55	0.0057	1269	15	6	134	187	1.00	0.41	0.16	0.46
V12211122	3.70	0.12	0.43	0.78	0.74	0.57	0.0060	1220	1220	6	132	181	0.57	0.0059	1209	14	6	132	153	1.00	0.43	0.18	0.46
V22211121	3.23	0.14	0.50	0.84	0.73	0.52	0.0054	1434	1434	8	158	215	0.52	0.0053	1418	17	7	158	182	1.00	0.44	0.17	0.48
V22211122	3.37	0.13	0.47	0.81	0.77	0.53	0.0056	1369	1369	8	155	176	0.53	0.0054	1357	16	7	155	149	1.00	0.46	0.19	0.49
V32211121	2.97	0.15	0.54	0.85	0.77	0.49	0.0051	1592	1592	10	183	207	0.49	0.0050	1572	18	9	183	175	1.00	0.49	0.18	0.52
V32211122	3.08	0.15	0.51	0.84	0.80	0.50	0.0052	1528	1528	10	180	171	0.50	0.0051	1512	18	9	180	142	1.00	0.50	0.20	0.52
V42211121	2.73	0.17	0.60	0.86	0.80	0.47	0.0049	1766	1766	12	212	198	0.47	0.0047	1736	20	10	211	164	1.00	0.55	0.19	0.56
V42211122	2.82	0.16	0.57	0.85	0.83	0.48	0.0050	1702	1702	12	207	162	0.48	0.0048	1676	20	10	207	132	1.00	0.56	0.21	0.56
V52211121	2.51	0.19	0.69	0.88	0.83	0.45	0.0049	1965	1965	15	245	181	0.44	0.0046	1910	22	12	242	146	0.99	0.65	0.21	0.60
V52211122	2.58	0.18	0.67	0.87	0.86	0.45	0.0049	1902	1902	15	240	148	0.45	0.0047	1850	21	11	237	117	0.99	0.66	0.23	0.60
V12211211	3.86	0.11	0.42	0.77	0.73	0.59	0.0062	1161	1161	6	121	180	0.59	0.0061	1148	14	6	121	151	1.00	0.43	0.19	0.46
V12211212	4.01	0.11	0.40	0.74	0.77	0.61	0.0064	1113	1113	6	120	149	0.60	0.0063	1104	13	6	120	124	1.00	0.45	0.20	0.46
V22211211	3.51	0.12	0.45	0.80	0.76	0.55	0.0058	1299	1299	7	142	175	0.55	0.0056	1286	15	7	142	147	1.00	0.46	0.20	0.49
V22211212	3.63	0.12	0.43	0.77	0.80	0.56	0.0059	1253	1253	7	141	145	0.56	0.0057	1243	15	7	141	120	1.00	0.47	0.21	0.49
V32211211	3.21	0.14	0.50	0.83	0.79	0.52	0.0054	1448	1448	9	165	169	0.52	0.0052	1431	17	8	164	140	1.00	0.51	0.21	0.52
V32211212	3.30	0.13	0.47	0.81	0.83	0.53	0.0055	1402	1402	9	163	139	0.53	0.0053	1389	16	8	163	114	1.00	0.52	0.22	0.52
V42211211	2.94	0.15	0.55	0.85	0.82	0.49	0.0052	1610	1610	11	190	161	0.49	0.0050	1583	18	9	189	131	1.00	0.57	0.22	0.56
V42211212	3.01	0.15	0.53	0.84	0.85	0.50	0.0053	1565	1565	11	187	132	0.50	0.0050	1542	18	9	187	106	1.00	0.58	0.23	0.56
V52211211	2.69	0.17	0.64	0.87	0.85	0.47	0.0051	1798	1798	14	220	147	0.47	0.0049	1746	20	10	217	115	0.99	0.68	0.24	0.60
V52211212	2.75	0.17	0.62	0.86	0.88	0.48	0.0052	1753	1753	14	216	121	0.47	0.0049	1705	20	10	213	93	0.99	0.68	0.25	0.60
V12211221	3.13	0.14	0.50	0.84	0.73	0.50	0.0053	1497	1497	8	159	231	0.50	0.0052	1484	17	7	158	200	1.00	0.40	0.15	0.46
V12211222	3.26	0.14	0.47	0.81	0.77	0.51	0.0054	1432	1432	8	157	190	0.51	0.0053	1422	17	7	157	164	1.00	0.41	0.17	0.46
V22211221	2.85	0.16	0.54	0.85	0.76	0.47	0.0049	1680	1680	9	186	225	0.47	0.0048	1666	20	9	186	195	1.00	0.42	0.16	0.48
V22211222	2.95	0.15	0.51	0.83	0.80	0.48	0.0050	1616	1616	9	184	186	0.48	0.0049	1606	19	9	184	159	1.00	0.44	0.18	0.48
V32211221	2.61	0.18	0.59	0.86	0.79	0.45	0.0046	1874	1874	11	216	218	0.44	0.0045	1856	22	10	216	187	1.00	0.46	0.16	0.52
V32211222	2.69	0.17	0.57	0.85	0.82	0.45	0.0047	1811	1811	11	214	180	0.45	0.0046	1797	21	10	214	153	1.00	0.47	0.18	0.52
V42211221	2.40	0.20	0.66	0.87	0.82	0.43	0.0045	2084	2084	14	250	208	0.42	0.0043	2057	24	12	249	175	1.00	0.52	0.17	0.56

Name	T1 [s]	Sa(T1) [g]	Sa(T2) [g]	Sa(T3) [g]	DOC [-]	Disp [m]	ISDR [-]	Total Moment [MN-m]	Total Shear [MN]	Max CB Shear [MN]	Max Pp [MN]	Max wall moment [MN-m]	Disp [m]2	ISDR [-]3	Total Moment [MN-m]4	Total Shear [MN]5	Max CB Shear [MN]6	Max Pp [MN]2	Max wall moment [MN-m]8	C1 [-]	C2 [-]	C3 [-]	Mdy/ Mst [-]
V52211221	2.20	0.22	0.74	0.88	0.85	0.41	0.0044	2324	2324	17	289	190	0.41	0.0042	2274	26	14	286	157	0.99	0.59	0.18	0.60
V52211222	2.25	0.22	0.73	0.88	0.88	0.41	0.0044	2262	2262	17	284	156	0.41	0.0043	2214	26	13	281	126	0.99	0.61	0.19	0.60
V12212111	2.53	0.19	0.62	0.87	0.67	0.44	0.0045	1946	1946	6	130	354	0.43	0.0045	1927	22	6	130	315	1.00	0.35	0.10	0.45
V12212112	2.61	0.18	0.60	0.86	0.70	0.44	0.0046	1874	1874	6	129	313	0.44	0.0046	1858	22	6	128	278	1.00	0.36	0.12	0.45
V22212111	2.33	0.21	0.66	0.87	0.70	0.41	0.0043	2167	2167	7	153	348	0.41	0.0042	2148	25	7	153	311	1.00	0.37	0.11	0.48
V22212112	2.40	0.20	0.64	0.87	0.73	0.42	0.0043	2093	2093	7	151	307	0.42	0.0043	2077	24	7	151	273	1.00	0.38	0.12	0.48
V32212111	2.16	0.23	0.71	0.88	0.74	0.39	0.0041	2396	2396	9	178	339	0.39	0.0040	2373	28	8	178	302	1.00	0.40	0.12	0.51
V32212112	2.21	0.22	0.69	0.88	0.76	0.40	0.0041	2325	2325	9	175	299	0.40	0.0040	2306	27	8	175	264	1.00	0.41	0.13	0.51
V42212111	2.00	0.25	0.75	0.88	0.77	0.37	0.0039	2631	2631	11	204	324	0.37	0.0038	2601	30	10	203	287	1.00	0.44	0.12	0.55
V42212112	2.04	0.25	0.74	0.88	0.79	0.38	0.0040	2571	2571	11	202	287	0.38	0.0039	2545	30	10	201	252	1.00	0.45	0.13	0.55
V52212111	1.85	0.27	0.80	0.88	0.80	0.35	0.0037	2796	2796	12	226	293	0.35	0.0036	2751	32	11	225	256	1.00	0.50	0.14	0.60
V52212112	1.89	0.27	0.79	0.88	0.83	0.36	0.0038	2755	2755	13	224	259	0.35	0.0037	2712	31	11	223	224	1.00	0.51	0.14	0.60
V12212121	2.05	0.25	0.73	0.88	0.66	0.38	0.0039	2562	2562	8	173	465	0.38	0.0039	2542	30	8	172	425	1.00	0.31	0.08	0.45
V12212122	2.12	0.24	0.71	0.88	0.69	0.38	0.0040	2458	2458	8	170	410	0.38	0.0040	2442	29	8	170	373	1.00	0.32	0.09	0.45
V22212121	1.89	0.27	0.76	0.88	0.70	0.35	0.0036	2767	2767	9	197	447	0.35	0.0036	2748	32	9	197	408	1.00	0.33	0.08	0.48
V22212122	1.95	0.26	0.74	0.88	0.73	0.36	0.0037	2706	2706	9	197	399	0.36	0.0037	2690	32	9	196	363	1.00	0.34	0.09	0.48
V32212121	1.76	0.28	0.79	0.88	0.73	0.32	0.0033	2936	2936	11	219	422	0.32	0.0033	2914	34	10	219	383	1.00	0.36	0.09	0.51
V32212122	1.80	0.28	0.77	0.88	0.76	0.33	0.0034	2883	2883	11	218	376	0.33	0.0033	2864	33	10	218	340	1.00	0.37	0.10	0.51
V42212121	1.64	0.30	0.82	0.88	0.76	0.29	0.0031	3098	3098	12	241	392	0.29	0.0030	3070	36	11	240	354	1.00	0.39	0.10	0.55
V42212122	1.67	0.29	0.81	0.88	0.79	0.30	0.0031	3049	3049	12	240	349	0.30	0.0031	3025	35	11	240	313	1.00	0.40	0.11	0.55
V52212121	1.52	0.32	0.84	0.89	0.79	0.27	0.0029	3256	3256	14	263	356	0.27	0.0028	3218	37	13	263	319	1.00	0.43	0.11	0.60
V52212122	1.56	0.31	0.84	0.89	0.82	0.28	0.0029	3212	3212	14	262	316	0.28	0.0029	3175	37	13	261	281	1.00	0.44	0.12	0.60
V12212211	2.31	0.21	0.66	0.88	0.69	0.41	0.0042	2199	2199	7	148	374	0.40	0.0042	2182	26	7	147	336	1.00	0.34	0.10	0.45
V12212212	2.37	0.20	0.63	0.87	0.72	0.41	0.0043	2124	2124	7	146	330	0.41	0.0043	2110	25	7	146	296	1.00	0.35	0.11	0.45
V22212211	2.12	0.24	0.71	0.88	0.72	0.38	0.0040	2454	2454	8	173	368	0.38	0.0039	2437	29	8	173	331	1.00	0.36	0.10	0.48
V22212212	2.18	0.23	0.68	0.87	0.75	0.39	0.0040	2381	2381	8	172	325	0.39	0.0040	2367	28	8	172	291	1.00	0.37	0.11	0.48
V32212211	1.96	0.26	0.75	0.88	0.76	0.36	0.0037	2687	2687	10	198	355	0.36	0.0037	2668	31	9	198	319	1.00	0.38	0.11	0.51
V32212212	2.01	0.25	0.73	0.88	0.78	0.37	0.0038	2641	2641	10	198	315	0.37	0.0038	2624	31	9	198	282	1.00	0.39	0.11	0.51
V42212211	1.82	0.28	0.78	0.88	0.79	0.34	0.0035	2855	2855	11	219	330	0.33	0.0034	2829	33	10	219	294	1.00	0.42	0.11	0.55
V42212212	1.85	0.27	0.77	0.88	0.81	0.34	0.0035	2817	2817	11	219	293	0.34	0.0035	2793	33	10	219	260	1.00	0.43	0.12	0.56
V52212211	1.69	0.29	0.82	0.88	0.82	0.31	0.0033	3016	3016	13	240	298	0.31	0.0032	2976	34	11	239	262	1.00	0.47	0.13	0.60
V52212212	1.72	0.29	0.81	0.88	0.84	0.32	0.0033	2981	2981	13	240	264	0.31	0.0032	2943	34	11	239	231	1.00	0.48	0.13	0.60
V12212221	1.87	0.27	0.76	0.88	0.68	0.34	0.0035	2805	2805	9	189	478	0.34	0.0035	2788	33	8	189	439	1.00	0.30	0.07	0.45
V12212222	1.92	0.26	0.74	0.88	0.71	0.35	0.0036	2745	2745	9	190	427	0.35	0.0036	2731	32	9	190	392	1.00	0.31	0.08	0.45
V22212221	1.72	0.29	0.79	0.88	0.72	0.31	0.0032	2993	2993	10	212	454	0.31	0.0032	2976	35	10	212	417	1.00	0.32	0.08	0.48
V22212222	1.77	0.28	0.77	0.88	0.74	0.32	0.0033	2938	2938	10	213	405	0.32	0.0033	2924	34	10	213	371	1.00	0.33	0.09	0.48
V32212221	1.60	0.31	0.81	0.88	0.75	0.28	0.0029	3169	3169	11	234	427	0.28	0.0029	3150	37	11	234	391	1.00	0.34	0.09	0.51
V32212222	1.64	0.30	0.80	0.88	0.77	0.29	0.0030	3118	3118	12	235	381	0.29	0.0030	3102	36	11	235	347	1.00	0.35	0.09	0.51
V42212221	1.49	0.32	0.84	0.89	0.78	0.26	0.0027	3335	3335	13	256	398	0.26	0.0027	3312	39	12	256	362	1.00	0.37	0.09	0.55
V42212222	1.52	0.32	0.83	0.88	0.80	0.27	0.0028	3290	3290	13	256	354	0.27	0.0027	3269	38	12	256	320	1.00	0.38	0.10	0.56
V52212221	1.39	0.34	0.85	0.89	0.80	0.24	0.0025	3491	3491	14	278	362	0.24	0.0025	3460	40	13	277	328	1.00	0.40	0.10	0.60
V52212222	1.42	0.33	0.85	0.89	0.83	0.25	0.0026	3453	3453	15	278	322	0.25	0.0025	3423	40	13	277	289	1.00	0.41	0.11	0.60
V12221111	5.01	0.08	0.36	0.68	0.70	0.73	0.0078	1135	1135	6	117	201	0.73	0.0075	1115	13	5	116	161	1.00	0.49	0.21	0.46
V12221112	5.23	0.08	0.34	0.62	0.74	0.74	0.0079	1064	1064	6	114	165	0.74	0.0077	1050	12	5	113	130	1.00	0.52	0.22	0.46
V22221111	4.57	0.09	0.38	0.71	0.74	0.68	0.0072	1263	1263	7	137	195	0.68	0.0070	1242	15	6	137	156	1.00	0.52	0.23	0.49
V22221112	4.75	0.09	0.36	0.66	0.78	0.70	0.0074	1210	1210	7	135	161	0.70	0.0071	1195	14	6	135	128	1.00	0.54	0.24	0.49
V32221111	4.19	0.10	0.41	0.75	0.77	0.64	0.0068	1397	1397	9	158	187	0.64	0.0065	1372	16	7	158	149	1.00	0.56	0.25	0.52
V32221112	4.33	0.10	0.39	0.72	0.81	0.66	0.0070	1346	1346	9	156	155	0.65	0.0066	1326	16	7	156	121	1.00	0.58	0.27	0.52
V42221111	3.85	0.11	0.45	0.80	0.80	0.61	0.0065	1545	1545	11	182	178	0.60	0.0061	1510	18	9	181	138	1.00	0.64	0.28	0.56
V42221112	3.96	0.11	0.43	0.77	0.83	0.62	0.0066	1495	1495	11	179	146	0.62	0.0062	1464	17	9	178	112	1.00	0.65	0.29	0.56
V52221111	3.53	0.12	0.52	0.84	0.83	0.58	0.0064	1722	1722	14	211	163	0.57	0.0060	1654	19	10	207	122	0.98	0.76	0.32	0.60
V52221112	3.62	0.12	0.50	0.84	0.86	0.59	0.0065	1673	1673	14	207	134	0.58	0.0061	1609	19	10	203	97	0.98	0.77	0.34	0.60
V12221121	4.08	0.10	0.41	0.77	0.70	0.62	0.0065	1443	1443	7	150	252	0.62	0.0064	1421	17	7	150	210	1.00	0.44	0.18	0.46
V12221122	4.28	0.10	0.39	0.73	0.74	0.64	0.0068	1370	1370	7	148	208	0.64	0.0066	1354	16	7	148	172	1.00	0.46	0.20	0.46
V22221121	3.73	0.11	0.44	0.79	0.73	0.58	0.0061	1605	1605	9	176	245	0.58	0.0059	1583	19	8	176	204	1.00	0.47	0.20	0.49
V22221122	3.89	0.11	0.41	0.76	0.77	0.60	0.0062	1533	1533	9	173	202	0.59	0.0061	1516	18	8	173	166	1.00	0.48	0.22	0.49
V32221121	3.43	0.13	0.48	0.82	0.77	0.55	0.0058	1778	1778	11	204	236	0.55	0.0055	1752	20	10	204	195	1.00	0.51	0.21	0.52
V32221122	3.55	0.12	0.45	0.80	0.80	0.56	0.0059	1707	1707	11	200	195	0.56	0.0056	1686	20	10	200	158	1.00	0.53	0.23	0.52
V42221121	3.15	0.14	0.53	0.84	0.80	0.52	0.0055	1967	1967	13	235	225	0.52	0.0053	1929	22	11	234	182	1.00	0.58	0.23	0.56
V42221122	3.25	0.14	0.51	0.83	0.83	0.53	0.0056	1897	1897	14	231	185	0.53	0.0054	1864	22	11	230	147	1.00	0.60	0.25	0.56
V52221121	2.90	0.16	0.61	0.86	0.83	0.49	0.0054	2188	2188	18	272	207	0.49	0.0051	2118	24	13	269	162	0.99	0.69	0.25	0.60
V52221122	2.98	0.15	0.59	0.86	0.86	0.50	0.0055	2119	2119	18	266	169	0.50	0.0052	2053	24	13	263	130	0.99	0.71	0.27	0.60
V12221211	4.45	0.09	0.38	0.72	0.73	0.66	0.0070	1305	1305	7	136	208	0.66	0.0069	1288	15	6	136	170	1.00	0.47	0.20	0.46
V12221212	4.63	0.09	0.36	0.66	0.77	0.68	0.0072	1251	1251	7	135	172	0.67	0.0070	1239	15	6	135	139	1.00	0.49	0.22	0.46
V22221211	4.03	0.02	0.14	0.32	0.75	0.14	0.0016	346	346	2	37	57	0.14	0.0014	335	4	2	37	38	1.00	0.73	0.40	0.51
V22221212	4.16	0.02	0.13	0.29	0.79	0.15	0.0016	330	330	2	37	47	0.14	0.0015	323	4	2	37	31	1.00	0.73	0.42	0.50
V32221211	3.67	0.03	0.16	0.34	0.78	0.14	0.0016	393	393	3	44	56	0.13	0.0014	380	4	2	44	37	1.00	0.81	0.44	0.54
V32221212	3.77	0.03	0.15	0.32	0.82	0.14	0.0016	378	378	3	43	46	0.14	0.0014	367	4	2	43	30	1.00	0.82	0.46	0.54
V42221211	3.35	0.03	0.18	0.38	0.81	0.13	0.0015	449	449	4	52	55	0.13	0.0013	428	5	2	51	34	0.99	0.94	0.49	0.58
V42221212	3.43	0.03	0.17	0.36	0.84	0.13	0.0015	434	434	4	51	46	0.13	0.0013	415	5	2	51	28	0.99	0.95	0.51	0.57
V52221211	3.06	0.04	0.23	0.45	0.83	0.13	0.0015	528	528	6	63	53	0.13	0.0013	481	6	3	60	30	0.95	1.14	0.60	0.63
V52221212	3.12	0.03	0.22	0.44	0.86	0.13	0.0015	512	512	6	62	44	0.13	0.0013	468	5	3	59	24	0.95	1.15	0.62	0.63
V12221221	3.59	0.03	0.16	0.35	0.72	0.13	0.0015	407	407	2	43	75	0.13	0.0014	395	5	2	42	52	0.99	0.63	0.33	0.48
V12221222	3.73	0.03	0.15	0.33	0.76	0.14	0.0015	385	385	2	42	61	0.13	0.0014	376	4	2	42	43	0.99	0.64	0.35	0.47
V22221221	3.26	0.03	0.17	0.37	0.75	0.13	0.0014	464	464	3	51	74	0.12	0.0013	452	5	2	51	52	1.00	0.68	0.35	0.50
V22221222	3.37	0.03	0.16	0.35	0.79	0.13	0.0014	442	442	3	50	61	0.13	0.0013	433	5	2	50	42	1.00	0.69	0.37	0.50
V32221221	2.98	0.04	0.20	0.41	0.78	0.12	0.0013	529	529	4	60	73	0.12	0.0012	514	6	3	60	50	1.00	0.75	0.38	0.53
V32221222	3.06	0.04	0.19	0.38	0.82	0.12	0.0014	507	507	4	59	60	0.12	0.0012	495	6	3	59	41	1.00	0.76	0.39	0.53
V42221221	2.72	0.04	0.23	0.45	0.81	0.12	0.0013	606	606	5	72	72	0.12	0.0012	581	7	3	71	48	0.99	0.86	0.43	0.57
V42221222	2.79	0.04	0.22	0.43	0.84	0.12	0.0013	584	584	5	70	60	0.12	0.0012	563	7	3	70	38	0.99	0.88	0.44	0.57
V52221221	2.48	0.05	0.28	0.52	0.84	0.11	0.0013	710	710	7	87	69	0.11	0.0012	656	8	4	83	42	0.96	1.06	0.51	0.62
V52221222	2.53	0.05	0.27	0.50	0.86	0.11	0.0013	688	688	8	85	57	0.11	0.0012	637	7	4	82	34	0.96	1.07	0.52	0.62
V12222111	2.88	0.04	0.21	0.44	0.66	0.12	0.0013	557	557	2	37	117	0.12	0.0012	538	6	2	37	86	1.00	0.57	0.26	0.47
V12222112	2.97	0.04	0.20	0.42	0.69	0.12	0.0013	532	532	2	36	103	0.12	0.0012	516	6	2	36	75	1.00	0.58	0.28	0.47
V22222111	2.64	0.04	0.23	0.46	0.70	0.11	0.0012	631	631	2	44	116	0.11	0.0012	612	7	2	44	86	1.00	0.62	0.28	0.50
V22222112	2.71	0.04	0.22	0.44	0.73	0.11	0.0012	607	607	2	44	103	0.11	0.0012	591	7	2	43	75	1.00	0.63	0.30	0.50
V32222111	2.42	0.05	0.26	0.49	0.73	0.11	0.0012	716	716	3	53	115	0.11	0.0011	693	8	2	53	84	1.00	0.69	0.31	0.53
V32222112	2.48	0.05	0.24	0.47	0.76	0.11	0.0012	690	690	3	52	101	0.11	0.0011	671	8	2	52	73	1.00	0.69	0.32	0.53
V42222111	2.23	0.06	0.29	0.53	0.77	0.11	0.0012	815	815	4	63	113	0.11	0.0011	782	9	3	62	80	0.99	0.79	0.35	0.57
V42222112	2.27	0.06	0.28	0.51	0.79	0.11	0.0012	789	789	4	62	100	0.11	0.0011	759	9	3	61	69	0.99	0.80	0.36	0.57
V52222111	2.04	0.07	0.34	0.61	0.81	0.10	0.0012	943	943	6	76	106	0.10	0.0011	881	10	4	74	72	0.97	0.94	0.43	0.61
V52222112	2.08	0.06	0.34	0.59	0.83	0.10	0.0012	918	918	6	75	94	0.10	0.0011	859	10	3	72	62	0.97	0.95	0.44	0.61
V12222121	2.31	0.05	0.27	0.51	0.66	0.11	0.0011	767	767	2	52	156	0.11	0.0011	746	9	2	51	121	1.00	0.52	0.21	0.46
V12222122	2.39	0.05	0.25	0.49	0.69	0.11	0.0011	729	729	2	50	136	0.11	0.0011	713	8	2	50	105	1.00	0.53	0.23	0.46
V22222121	2.12	0.06	0.29	0.54	0.70	0.10	0.0011	874	874	3	62	156	0.10	0.0010	853	10	3	62	121	1.00	0.56	0.23	0.49
V22222122	2.18	0.06	0.28	0.51	0.73	0.10	0.0011	837	837	3	61	137	0.10	0.0010	820	10	3	61	105	1.00	0.57	0.25	0.49
V32222121	1.95	0.07	0.32	0.57	0.74	0.10	0.0011	981	981	4	74	152	0.10	0.0010	956	11	3	73	117	1.00	0.62	0.26	0.52
V32222122	2.00	0.07	0.31	0.55	0.76	0.10	0.0011	953	953	4	73	135	0.10	0.0010	932	11	3	73	103	1.00	0.63	0.27	0.52
V42222121	1.79	0.08	0.35	0.61	0.77	0.09	0.0010	1077	1077	5	84	144	0.09	0.0009	1041	12	4	84	108	0.99	0.72	0.30	0.56
V42222122	1.83	0.07	0.34	0.60	0.79	0.09	0.0010	1052	1052	5	84	128	0.09	0.0009	1020	12	4	83	94	0.99	0.73	0.31	0.56
V52222121	1.65	0.08	0.41	0.67	0.81	0.09	0.0010	1194	1194	7	98	131	0.09	0.0009	1128	13	5	96	94	0.98	0.87	0.37	0.61
V52222122	1.68	0.08	0.40	0.66	0.83	0.09	0.0010	1171	1171	7	97	115	0.09	0.0009	1107	13	5	94	81	0.97	0.87	0.38	0.61
V12222211	2.61	0.05	0.23	0.46	0.68	0.11	0.0012	641	641	2	43	124	0.11	0.0012	624	7	2	43	93	1.00	0.55	0.25	0.47

Name	T1 [s]	Sa(T1) [g]	Sa(T2) [g]	Sa(T3) [g]	DOC [-]	Disp [m]	ISDR [-]	Total Moment [MN-m]	Total Shear [MN]	Max CB Shear [MN]	Max Pp [MN]	Max wall moment [MN-m]	Disp [m]2	ISDR [-]3	Total Moment [MN-m]4	Total Shear [MN]5	Max CB Shear [MN]6	Max Pp [MN]2	Max wall moment [MN-m]8	C1 [-]	C2 [-]	C3 [-]	Mdy/ Mst [-]
V22222211	2.38	0.05	0.25	0.48	0.72	0.11	0.0012	732	732	3	52	123	0.11	0.0011	714	8	2	52	93	1.00	0.60	0.26	0.49
V22222212	2.44	0.05	0.24	0.47	0.75	0.11	0.0012	706	706	3	51	108	0.11	0.0011	692	8	2	51	81	1.00	0.60	0.28	0.49
V32222211	2.19	0.06	0.28	0.51	0.76	0.10	0.0011	835	835	4	62	122	0.10	0.0011	814	9	3	62	91	1.00	0.66	0.29	0.53
V32222212	2.23	0.06	0.27	0.49	0.78	0.11	0.0011	809	809	4	61	108	0.10	0.0011	791	9	3	61	80	1.00	0.67	0.30	0.53
V42222211	2.01	0.07	0.32	0.57	0.79	0.10	0.0011	952	952	5	73	119	0.10	0.0010	920	11	3	73	87	0.99	0.75	0.32	0.56
V42222212	2.04	0.07	0.31	0.55	0.81	0.10	0.0011	929	929	5	72	105	0.10	0.0010	900	10	3	72	76	0.99	0.76	0.33	0.56
V52222211	1.84	0.07	0.37	0.64	0.82	0.09	0.0011	1063	1063	6	86	108	0.09	0.0010	1002	12	4	83	75	0.97	0.90	0.40	0.61
V52222212	1.86	0.07	0.36	0.63	0.84	0.10	0.0011	1046	1046	6	85	96	0.10	0.0010	987	11	4	82	65	0.97	0.90	0.41	0.61
V12222221	2.09	0.06	0.29	0.54	0.69	0.10	0.0011	894	894	3	61	166	0.10	0.0010	876	10	3	61	132	1.00	0.50	0.20	0.46
V12222222	2.15	0.06	0.28	0.51	0.72	0.10	0.0011	855	855	3	60	146	0.10	0.0010	840	10	3	59	115	1.00	0.51	0.22	0.46
V22222221	1.91	0.07	0.32	0.57	0.72	0.10	0.0010	1003	1003	4	72	163	0.09	0.0010	984	12	3	72	129	1.00	0.54	0.22	0.49
V22222222	1.96	0.07	0.30	0.54	0.75	0.10	0.0010	977	977	4	72	145	0.10	0.0010	961	11	3	71	114	1.00	0.55	0.23	0.49
V32222221	1.75	0.08	0.34	0.60	0.76	0.09	0.0009	1102	1102	5	83	157	0.09	0.0009	1079	13	4	83	122	1.00	0.61	0.25	0.52
V32222222	1.79	0.08	0.33	0.58	0.78	0.09	0.0010	1078	1078	5	82	139	0.09	0.0009	1058	12	4	82	107	1.00	0.62	0.26	0.52
V42222221	1.61	0.09	0.38	0.64	0.79	0.08	0.0009	1212	1212	6	95	148	0.08	0.0008	1178	14	5	94	112	0.99	0.69	0.29	0.56
V42222222	1.64	0.08	0.37	0.63	0.81	0.08	0.0009	1187	1187	6	94	131	0.08	0.0009	1155	13	4	93	98	0.99	0.70	0.30	0.56
V52222221	1.47	0.10	0.44	0.70	0.83	0.08	0.0009	1348	1348	8	110	133	0.08	0.0008	1280	15	5	108	97	0.98	0.84	0.35	0.60
V52222222	1.49	0.09	0.43	0.69	0.84	0.08	0.0009	1324	1324	8	109	118	0.08	0.0008	1259	14	5	106	84	0.98	0.85	0.36	0.61
V13111111	6.26	0.01	0.09	0.21	0.68	0.18	0.0019	229	229	1	23	51	0.18	0.0016	216	2	1	23	31	0.99	0.76	0.42	0.47
V13111112	6.54	0.01	0.08	0.19	0.73	0.18	0.0019	213	213	1	22	42	0.18	0.0017	203	2	1	22	25	0.99	0.78	0.44	0.47
V23111111	5.71	0.01	0.10	0.23	0.72	0.18	0.0018	264	264	1	28	51	0.17	0.0016	251	3	1	28	31	1.00	0.81	0.46	0.49
V23111112	5.92	0.01	0.09	0.21	0.76	0.18	0.0018	247	247	1	27	42	0.17	0.0016	238	2	1	27	25	1.00	0.83	0.48	0.49
V33111111	5.22	0.02	0.11	0.25	0.75	0.17	0.0018	304	304	1	33	51	0.17	0.0015	289	3	1	33	31	1.00	0.89	0.51	0.52
V33111112	5.39	0.02	0.10	0.23	0.79	0.17	0.0018	287	287	2	32	42	0.17	0.0015	275	3	1	32	25	1.00	0.91	0.52	0.52
V43111111	4.78	0.02	0.12	0.29	0.78	0.16	0.0017	350	350	2	40	51	0.16	0.0015	326	3	1	39	29	0.99	1.03	0.60	0.56
V43111112	4.91	0.02	0.12	0.27	0.81	0.17	0.0018	335	335	2	39	42	0.16	0.0015	316	3	1	39	23	0.99	1.04	0.61	0.56
V53111111	4.36	0.02	0.16	0.35	0.81	0.16	0.0017	412	412	3	49	49	0.16	0.0015	363	4	1	46	26	0.94	1.27	0.75	0.61
V53111112	4.47	0.02	0.15	0.34	0.84	0.16	0.0017	397	397	3	48	41	0.16	0.0015	353	4	1	45	20	0.94	1.28	0.77	0.61
V13111121	5.10	0.02	0.11	0.27	0.68	0.17	0.0017	317	317	1	32	68	0.16	0.0015	301	3	1	32	44	0.99	0.68	0.37	0.47
V13111122	5.33	0.02	0.10	0.23	0.73	0.17	0.0017	292	292	1	31	55	0.17	0.0015	282	3	1	31	35	0.99	0.71	0.39	0.46
V23111121	4.65	0.02	0.12	0.29	0.72	0.16	0.0016	358	358	1	38	68	0.16	0.0014	343	4	1	38	44	1.00	0.75	0.42	0.49
V23111122	4.84	0.02	0.11	0.26	0.76	0.16	0.0016	338	338	1	38	55	0.16	0.0014	327	3	1	37	35	1.00	0.76	0.43	0.49
V33111121	4.26	0.02	0.14	0.31	0.75	0.15	0.0016	404	404	2	45	67	0.15	0.0013	385	4	1	45	42	1.00	0.84	0.47	0.52
V33111122	4.41	0.02	0.13	0.29	0.79	0.15	0.0016	383	383	2	44	55	0.15	0.0014	369	4	1	44	34	1.00	0.85	0.48	0.52
V43111121	3.90	0.03	0.16	0.35	0.78	0.14	0.0015	459	459	3	53	66	0.14	0.0013	431	4	2	53	39	0.99	0.98	0.54	0.55
V43111122	4.02	0.02	0.15	0.33	0.81	0.15	0.0015	439	439	3	52	54	0.14	0.0013	415	4	2	52	32	0.99	0.99	0.56	0.55
V53111121	3.56	0.03	0.19	0.41	0.81	0.14	0.0015	538	538	4	65	63	0.14	0.0013	482	5	2	62	35	0.95	1.20	0.66	0.60
V53111122	3.66	0.03	0.19	0.39	0.84	0.14	0.0015	518	518	4	64	52	0.14	0.0013	466	5	2	60	27	0.95	1.21	0.68	0.60
V13111211	5.56	0.02	0.10	0.23	0.71	0.17	0.0018	274	274	1	28	54	0.17	0.0016	263	3	1	28	34	0.99	0.72	0.40	0.47
V13111212	5.77	0.01	0.09	0.21	0.76	0.17	0.0018	257	257	1	27	44	0.17	0.0016	249	3	1	27	28	0.99	0.74	0.42	0.46
V23111211	5.05	0.02	0.11	0.25	0.75	0.17	0.0017	319	319	1	34	54	0.16	0.0015	307	3	1	34	35	1.00	0.77	0.43	0.49
V23111212	5.21	0.02	0.10	0.23	0.79	0.17	0.0017	302	302	1	33	44	0.16	0.0015	293	3	1	33	28	1.00	0.78	0.45	0.49
V33111211	4.60	0.02	0.12	0.28	0.78	0.16	0.0016	362	362	2	40	54	0.16	0.0014	347	4	1	40	33	1.00	0.86	0.49	0.52
V33111212	4.73	0.02	0.11	0.26	0.81	0.16	0.0017	348	348	2	40	44	0.16	0.0014	337	4	1	40	27	1.00	0.87	0.50	0.52
V43111211	4.20	0.02	0.14	0.32	0.80	0.15	0.0016	413	413	2	47	53	0.15	0.0013	390	4	2	47	31	0.99	1.01	0.57	0.55
V43111212	4.30	0.02	0.14	0.30	0.84	0.15	0.0016	399	399	3	47	44	0.15	0.0014	379	4	1	46	25	0.99	1.01	0.58	0.55
V53111211	3.83	0.03	0.18	0.38	0.83	0.15	0.0016	488	488	4	58	51	0.14	0.0013	436	4	2	55	27	0.94	1.23	0.69	0.61
V53111212	3.90	0.03	0.17	0.37	0.86	0.15	0.0016	473	473	4	57	42	0.14	0.0014	426	4	2	54	22	0.94	1.23	0.71	0.60
V13111221	4.50	0.02	0.12	0.29	0.71	0.15	0.0015	374	374	1	39	72	0.15	0.0014	360	4	1	39	48	0.99	0.67	0.37	0.46
V13111222	4.68	0.02	0.11	0.26	0.76	0.16	0.0016	353	353	1	38	59	0.15	0.0014	344	4	1	38	39	0.99	0.67	0.38	0.46
V23111221	4.09	0.02	0.14	0.31	0.75	0.15	0.0015	425	425	2	46	71	0.14	0.0013	411	4	1	46	47	1.00	0.73	0.40	0.48
V23111222	4.23	0.02	0.13	0.29	0.79	0.15	0.0015	405	405	2	46	58	0.15	0.0013	394	4	1	45	38	1.00	0.74	0.42	0.48
V33111221	3.73	0.03	0.15	0.34	0.78	0.14	0.0014	482	482	2	55	70	0.14	0.0012	465	5	2	55	46	1.00	0.82	0.44	0.51
V33111222	3.84	0.03	0.15	0.32	0.81	0.14	0.0014	462	462	2	54	58	0.14	0.0012	449	5	2	54	37	1.00	0.83	0.46	0.51
V43111221	3.41	0.03	0.18	0.38	0.80	0.13	0.0014	551	551	3	65	69	0.13	0.0012	524	5	2	64	43	0.99	0.94	0.49	0.55
V43111222	3.49	0.03	0.17	0.36	0.84	0.14	0.0014	531	531	3	64	57	0.13	0.0012	508	5	2	63	34	0.99	0.95	0.51	0.55
V53111221	3.11	0.04	0.22	0.45	0.83	0.13	0.0014	648	648	5	79	66	0.13	0.0012	589	6	2	75	37	0.95	1.15	0.61	0.60
V53111222	3.17	0.03	0.22	0.44	0.86	0.13	0.0014	628	628	5	77	54	0.13	0.0012	573	6	2	73	30	0.95	1.16	0.62	0.60
V13112111	3.61	0.03	0.16	0.37	0.65	0.14	0.0013	507	507	1	33	112	0.13	0.0012	485	5	1	33	78	0.99	0.62	0.30	0.46
V13112112	3.73	0.03	0.15	0.35	0.68	0.14	0.0014	484	484	1	33	99	0.14	0.0012	466	5	1	33	68	0.99	0.63	0.32	0.46
V23112111	3.31	0.03	0.18	0.39	0.69	0.13	0.0013	572	572	1	40	111	0.13	0.0012	550	6	1	40	77	1.00	0.67	0.33	0.48
V23112112	3.40	0.03	0.17	0.37	0.72	0.13	0.0013	549	549	1	39	97	0.13	0.0012	531	6	1	39	67	1.00	0.68	0.35	0.48
V33112111	3.04	0.04	0.20	0.42	0.73	0.12	0.0012	645	645	2	47	109	0.12	0.0011	620	6	1	47	75	1.00	0.75	0.37	0.51
V33112112	3.11	0.03	0.19	0.40	0.76	0.13	0.0012	622	622	2	46	96	0.12	0.0011	601	6	1	46	65	1.00	0.76	0.38	0.51
V43112111	2.79	0.04	0.23	0.46	0.76	0.12	0.0012	733	733	3	56	107	0.12	0.0011	696	7	2	56	71	0.99	0.87	0.42	0.55
V43112112	2.85	0.04	0.22	0.44	0.79	0.12	0.0012	711	711	3	55	94	0.12	0.0011	677	7	2	55	62	0.99	0.88	0.43	0.55
V53112111	2.56	0.05	0.28	0.52	0.80	0.12	0.0012	854	854	4	68	102	0.12	0.0011	782	8	2	66	64	0.96	1.07	0.51	0.59
V53112112	2.60	0.05	0.27	0.50	0.82	0.12	0.0012	831	831	4	67	90	0.12	0.0011	762	8	2	64	55	0.96	1.08	0.52	0.59
V13112121	2.90	0.04	0.21	0.44	0.65	0.12	0.0012	689	689	1	46	147	0.12	0.0011	664	7	1	46	108	1.00	0.57	0.26	0.45
V13112122	3.00	0.04	0.19	0.42	0.69	0.12	0.0012	656	656	1	45	129	0.12	0.0011	636	7	1	45	94	1.00	0.58	0.28	0.45
V23112121	2.66	0.04	0.23	0.46	0.69	0.11	0.0011	781	781	2	55	146	0.11	0.0010	756	8	2	55	107	1.00	0.62	0.28	0.48
V23112122	2.74	0.04	0.22	0.44	0.72	0.12	0.0011	748	748	2	54	128	0.11	0.0010	728	8	2	54	93	1.00	0.63	0.30	0.48
V33112121	2.45	0.05	0.25	0.48	0.73	0.11	0.0011	885	885	3	66	144	0.11	0.0010	856	9	2	66	105	1.00	0.69	0.31	0.51
V33112122	2.51	0.05	0.24	0.47	0.76	0.11	0.0011	851	851	3	64	126	0.11	0.0010	827	9	2	64	91	1.00	0.69	0.32	0.51
V43112121	2.25	0.06	0.29	0.53	0.77	0.11	0.0011	1007	1007	3	78	141	0.11	0.0010	965	10	2	78	100	0.99	0.79	0.35	0.54
V43112122	2.30	0.05	0.28	0.51	0.79	0.11	0.0011	974	974	3	77	124	0.11	0.0010	937	10	2	76	87	0.99	0.81	0.36	0.54
V53112121	2.06	0.06	0.34	0.60	0.80	0.10	0.0011	1166	1166	5	95	132	0.10	0.0010	1089	11	3	93	90	0.97	0.94	0.43	0.59
V53112122	2.10	0.06	0.33	0.59	0.82	0.11	0.0011	1134	1134	5	93	116	0.10	0.0010	1059	11	3	90	77	0.97	0.96	0.44	0.59
V13112211	3.28	0.03	0.18	0.39	0.68	0.13	0.0012	579	579	1	38	118	0.13	0.0012	559	6	1	38	84	1.00	0.60	0.29	0.46
V13112212	3.37	0.03	0.17	0.37	0.71	0.13	0.0013	556	556	1	38	103	0.13	0.0012	540	6	1	38	74	1.00	0.61	0.31	0.45
V23112211	2.99	0.04	0.20	0.42	0.72	0.12	0.0012	658	658	2	46	116	0.12	0.0011	638	7	1	46	83	1.00	0.65	0.32	0.48
V23112212	3.06	0.04	0.19	0.39	0.75	0.12	0.0012	635	635	2	46	103	0.12	0.0011	618	6	1	45	73	1.00	0.66	0.33	0.48
V33112211	2.80	0.04	0.21	0.44	0.74	0.12	0.0012	724	724	2	53	116	0.12	0.0011	701	7	2	52	82	1.00	0.70	0.34	0.51
V33112212	2.80	0.04	0.21	0.43	0.78	0.12	0.0012	724	724	2	54	102	0.12	0.0011	704	7	2	54	71	1.00	0.73	0.36	0.51
V43112211	2.51	0.05	0.25	0.48	0.78	0.11	0.0011	852	852	3	65	113	0.11	0.0010	816	8	2	65	77	0.99	0.84	0.39	0.54
V43112212	2.56	0.05	0.24	0.47	0.81	0.11	0.0011	830	830	3	64	99	0.11	0.0010	798	8	2	64	67	0.99	0.84	0.40	0.54
V53112211	2.30	0.05	0.31	0.56	0.82	0.11	0.0011	995	995	4	79	107	0.11	0.0010	921	9	2	77	68	0.96	1.01	0.48	0.59
V53112212	2.33	0.05	0.30	0.55	0.84	0.11	0.0011	973	973	4	78	94	0.11	0.0010	903	9	2	75	59	0.96	1.02	0.49	0.59
V13112221	2.62	0.04	0.23	0.46	0.68	0.11	0.0011	797	797	2	54	155	0.11	0.0010	775	8	2	53	117	1.00	0.55	0.25	0.45
V13112222	2.70	0.04	0.22	0.44	0.71	0.11	0.0011	764	764	2	53	137	0.11	0.0010	746	8	2	53	102	1.00	0.56	0.26	0.45
V23112221	2.40	0.05	0.25	0.48	0.72	0.11	0.0010	909	909	2	65	155	0.11	0.0010	887	9	2	65	117	1.00	0.59	0.26	0.47
V23112222	2.46	0.05	0.24	0.46	0.75	0.11	0.0010	877	877	2	64	136	0.11	0.0010	859	9	2	64	102	1.00	0.60	0.28	0.47
V33112221	2.27	0.06	0.27	0.50	0.74	0.11	0.0010	987	987	3	72	154	0.11	0.0010	963	10	2	72	115	1.00	0.63	0.28	0.50
V33112222	2.32	0.05	0.26	0.48	0.77	0.11	0.0010	955	955	3	71	135	0.11	0.0010	934	10	2	71	101	1.00	0.64	0.29	0.50
V43112221	2.10	0.06	0.30	0.54	0.77	0.10	0.0010	1112	1112	3	85	152	0.10	0.0009	1080	11	3	85	112	1.00	0.70	0.30	0.54
V43112222	2.14	0.06	0.29	0.52	0.80	0.10	0.0010	1077	1077	3	83	133	0.10	0.0009	1049	11	3	83	97	1.00	0.71	0.31	0.54
V53112221	1.95	0.07	0.34	0.59	0.80	0.10	0.0010	1237	1237	4	98	145	0.10	0.0009	1187	12	3	97	104	0.99	0.80	0.35	0.58
V53112222	1.98	0.07	0.33	0.57	0.82	0.10	0.0010	1213	1213	4	97	128	0.10	0.0009	1166	12	3	96	91	0.99	0.81	0.36	0.58
V13121111	7.24	0.01	0.07	0.18	0.67	0.19	0.0021	245	245	1	24	57	0.19	0.0017	229	2	1	24	33	0.99	0.81	0.45	0.48
V13121112	7.57	0.01	0.07	0.16	0.72	0.20	0.0021	227	227	1	24	46	0.19	0.0018	216	2	1	23	27	0.99	0.83	0.47	0.47
V23121111	6.61	0.01	0.08	0.19	0.71	0.19	0.0020	280	280	1	29	57	0.18	0.0017	265	3	1	29	33	1.00	0.87	0.49	0.50
V23121112	6.86	0.01	0.07	0.18	0.76	0.19	0.0020	262	262	1	28	46	0.18	0.0017	251	3	1	28	27	1.00	0.89	0.51	0.50
V33121111	6.03	0.01	0.09	0.22	0.74	0.18	0.0019	324	324	2	35	57	0.18	0.0016	305	3	1	35	33	1.00	0.96	0.55	0.53

Name	T1 [s]	Sa(T1) [g]	Sa(T2) [g]	Sa(T3) [g]	DOC [-]	Disp [m]	ISDR [-]	Total Moment [MN-m]	Total Shear [MN]	Max CB Shear [MN]	Max Pp [MN]	Max wall moment [MN-m]	Disp [m]2	ISDR [-]3	Total Moment [MN-m]4	Total Shear [MN]5	Max CB Shear [MN]6	Max Pp [MN]2	Max wall moment [MN-m]8	C1 [-]	C2 [-]	C3 [-]	Mdy/ Mst [-]
V43121111	5.52	0.02	0.11	0.25	0.77	0.18	0.0019	377	377	2	43	57	0.17	0.0016	349	4	1	42	31	0.99	1.09	0.64	0.56
V43121112	5.67	0.01	0.10	0.23	0.81	0.18	0.0019	358	358	2	42	47	0.17	0.0016	335	3	1	41	25	0.98	1.11	0.65	0.56
V53121111	5.04	0.02	0.13	0.31	0.80	0.17	0.0019	455	455	4	54	56	0.17	0.0016	398	4	2	50	28	0.94	1.31	0.80	0.62
V53121112	5.16	0.02	0.13	0.30	0.83	0.17	0.0019	436	436	4	52	46	0.17	0.0016	383	4	2	49	22	0.93	1.32	0.82	0.61
V13121121	5.88	0.01	0.09	0.23	0.67	0.18	0.0019	337	337	1	34	75	0.17	0.0016	318	3	1	34	47	0.99	0.73	0.40	0.47
V13121122	6.16	0.01	0.08	0.20	0.72	0.18	0.0019	311	311	1	33	61	0.17	0.0016	298	3	1	33	37	0.99	0.76	0.42	0.47
V23121121	5.37	0.02	0.10	0.24	0.71	0.17	0.0018	387	387	2	41	75	0.17	0.0015	369	4	1	41	47	1.00	0.79	0.44	0.49
V23121122	5.59	0.02	0.09	0.22	0.76	0.17	0.0018	361	361	2	40	61	0.17	0.0015	348	4	1	40	38	1.00	0.81	0.46	0.49
V33121121	4.91	0.02	0.12	0.27	0.74	0.17	0.0017	444	444	2	50	75	0.16	0.0015	422	4	2	49	46	1.00	0.87	0.49	0.52
V33121122	5.09	0.02	0.11	0.25	0.79	0.17	0.0017	420	420	2	48	61	0.17	0.0015	403	4	2	48	37	1.00	0.88	0.50	0.52
V43121121	4.50	0.02	0.13	0.31	0.77	0.16	0.0017	505	505	3	58	74	0.16	0.0014	472	5	2	58	43	0.99	1.02	0.58	0.56
V43121122	4.64	0.02	0.13	0.29	0.81	0.16	0.0017	482	482	3	57	61	0.16	0.0014	455	5	2	56	35	0.99	1.03	0.59	0.56
V53121121	4.16	0.02	0.16	0.36	0.80	0.15	0.0016	580	580	4	69	72	0.15	0.0014	519	5	2	66	39	0.95	1.22	0.70	0.61
V53121122	4.27	0.02	0.15	0.35	0.83	0.16	0.0017	558	558	4	68	59	0.15	0.0014	502	5	2	64	31	0.95	1.23	0.72	0.60
V13121211	6.44	0.01	0.08	0.19	0.71	0.18	0.0019	291	291	1	29	60	0.18	0.0016	277	3	1	29	36	0.99	0.77	0.43	0.47
V13121212	6.69	0.01	0.08	0.18	0.75	0.18	0.0019	272	272	1	29	49	0.18	0.0017	263	3	1	29	29	0.99	0.79	0.45	0.47
V23121211	5.86	0.01	0.09	0.21	0.74	0.18	0.0018	336	336	1	36	60	0.17	0.0016	322	3	1	36	37	1.00	0.82	0.47	0.49
V23121212	6.05	0.01	0.08	0.19	0.78	0.18	0.0019	318	318	1	35	49	0.17	0.0016	308	3	1	35	30	1.00	0.84	0.48	0.49
V33121211	5.35	0.02	0.10	0.24	0.77	0.17	0.0018	388	388	2	43	60	0.17	0.0015	371	4	1	43	36	1.00	0.90	0.51	0.52
V33121212	5.49	0.02	0.10	0.22	0.81	0.17	0.0018	370	370	2	42	49	0.17	0.0015	357	4	1	42	29	1.00	0.91	0.53	0.52
V43121211	4.89	0.02	0.12	0.28	0.80	0.17	0.0018	450	450	3	51	60	0.16	0.0015	423	4	2	51	34	0.99	1.02	0.59	0.56
V43121212	5.00	0.02	0.11	0.26	0.83	0.17	0.0018	434	434	3	51	49	0.17	0.0015	411	4	2	50	28	0.99	1.03	0.60	0.55
V53121211	4.47	0.02	0.15	0.34	0.82	0.16	0.0017	527	527	4	62	59	0.16	0.0015	471	5	2	59	30	0.95	1.25	0.74	0.61
V53121212	4.55	0.02	0.14	0.32	0.85	0.16	0.0018	511	511	4	61	49	0.16	0.0015	460	5	2	58	24	0.95	1.25	0.75	0.60
V13121221	5.22	0.02	0.10	0.25	0.71	0.17	0.0017	404	404	1	42	80	0.16	0.0015	388	4	1	41	52	0.99	0.69	0.38	0.46
V13121222	5.43	0.02	0.10	0.22	0.75	0.17	0.0017	378	378	1	41	65	0.17	0.0015	367	4	1	40	42	0.99	0.71	0.40	0.46
V23121221	4.72	0.02	0.12	0.27	0.74	0.16	0.0016	466	466	2	51	80	0.16	0.0014	450	5	2	51	52	1.00	0.75	0.43	0.49
V23121222	4.88	0.02	0.11	0.25	0.79	0.16	0.0016	444	444	2	50	65	0.16	0.0015	432	5	2	50	42	1.00	0.76	0.43	0.48
V33121221	4.31	0.02	0.13	0.30	0.77	0.15	0.0016	528	528	3	60	79	0.15	0.0013	507	5	2	59	50	1.00	0.85	0.48	0.52
V33121222	4.43	0.02	0.12	0.28	0.81	0.15	0.0016	506	506	3	59	65	0.15	0.0014	490	5	2	59	40	1.00	0.86	0.49	0.52
V43121221	3.93	0.03	0.15	0.34	0.80	0.15	0.0015	603	603	4	70	78	0.14	0.0013	570	6	2	70	46	0.99	0.99	0.55	0.55
V43121222	4.03	0.02	0.15	0.32	0.83	0.15	0.0015	581	581	4	69	64	0.15	0.0013	553	6	2	68	37	0.99	1.00	0.56	0.55
V53121221	3.58	0.03	0.19	0.40	0.83	0.14	0.0015	710	710	6	86	75	0.14	0.0013	638	7	3	81	40	0.95	1.20	0.67	0.60
V53121222	3.66	0.03	0.18	0.39	0.86	0.14	0.0015	689	689	6	84	62	0.14	0.0013	621	6	3	80	32	0.94	1.21	0.68	0.60
V13122111	4.17	0.02	0.14	0.34	0.65	0.15	0.0015	556	556	1	36	126	0.15	0.0013	528	6	1	36	85	0.99	0.65	0.33	0.47
V13122112	4.30	0.02	0.13	0.31	0.68	0.15	0.0015	531	531	1	36	111	0.15	0.0014	509	5	1	35	74	0.99	0.66	0.35	0.46
V23122111	3.82	0.03	0.15	0.35	0.69	0.14	0.0014	625	625	2	43	125	0.14	0.0013	598	6	1	43	84	1.00	0.71	0.37	0.49
V23122112	3.92	0.03	0.15	0.33	0.72	0.14	0.0014	600	600	2	43	110	0.14	0.0013	577	6	1	42	73	1.00	0.72	0.38	0.49
V33122111	3.51	0.03	0.17	0.37	0.72	0.13	0.0014	703	703	2	51	123	0.13	0.0012	671	7	2	51	81	1.00	0.79	0.41	0.52
V33122112	3.59	0.03	0.16	0.36	0.75	0.14	0.0014	678	678	2	50	108	0.13	0.0012	651	7	2	50	71	1.00	0.80	0.42	0.52
V43122111	3.29	0.03	0.19	0.40	0.75	0.13	0.0013	771	771	3	58	121	0.13	0.0012	731	8	2	58	78	0.99	0.88	0.45	0.55
V43122112	3.36	0.03	0.18	0.38	0.77	0.13	0.0014	747	747	3	57	107	0.13	0.0012	711	7	2	57	68	0.99	0.89	0.46	0.55
V53122111	3.04	0.04	0.22	0.45	0.78	0.13	0.0013	881	881	4	69	117	0.13	0.0012	812	8	2	67	72	0.97	1.05	0.53	0.59
V53122112	3.10	0.04	0.22	0.44	0.80	0.13	0.0013	856	856	4	68	104	0.13	0.0012	792	8	2	66	62	0.97	1.06	0.55	0.59
V13122121	3.40	0.03	0.18	0.39	0.64	0.13	0.0013	736	736	2	48	165	0.13	0.0012	704	7	1	48	117	0.99	0.60	0.28	0.46
V13122122	3.51	0.03	0.17	0.37	0.68	0.13	0.0013	700	700	2	47	145	0.13	0.0012	675	7	1	47	102	0.99	0.61	0.30	0.46
V23122121	3.13	0.03	0.19	0.41	0.68	0.13	0.0012	825	825	2	57	163	0.12	0.0011	794	8	2	57	116	1.00	0.64	0.31	0.48
V23122122	3.22	0.03	0.18	0.39	0.71	0.13	0.0012	790	790	2	56	144	0.12	0.0011	765	8	2	56	101	1.00	0.65	0.32	0.48
V33122121	2.89	0.04	0.21	0.44	0.72	0.12	0.0012	922	922	3	67	162	0.12	0.0011	888	9	2	67	114	1.00	0.71	0.34	0.51
V33122122	2.97	0.04	0.20	0.42	0.75	0.12	0.0012	887	887	3	66	142	0.12	0.0011	859	9	2	66	99	1.00	0.71	0.35	0.51
V43122121	2.68	0.04	0.23	0.46	0.75	0.12	0.0012	1034	1034	3	79	159	0.12	0.0010	991	10	2	78	110	1.00	0.79	0.38	0.55
V43122122	2.74	0.04	0.22	0.45	0.77	0.12	0.0012	999	999	3	77	140	0.12	0.0011	960	10	2	77	95	1.00	0.80	0.39	0.54
V53122121	2.48	0.05	0.27	0.50	0.78	0.11	0.0012	1172	1172	5	93	155	0.11	0.0010	1101	11	3	91	102	0.98	0.94	0.43	0.58
V53122122	2.42	0.05	0.29	0.54	0.82	0.11	0.0012	1228	1228	6	101	132	0.11	0.0011	1133	12	3	97	82	0.96	1.04	0.50	0.59
V13122211	3.78	0.03	0.15	0.35	0.68	0.14	0.0014	633	633	1	42	132	0.14	0.0013	607	6	1	42	91	0.99	0.63	0.32	0.46
V13122212	3.89	0.03	0.14	0.33	0.71	0.14	0.0014	607	607	1	41	116	0.14	0.0013	587	6	1	41	80	0.99	0.64	0.34	0.46
V23122211	3.45	0.03	0.17	0.37	0.71	0.13	0.0013	716	716	2	50	131	0.13	0.0012	691	7	2	50	90	1.00	0.68	0.35	0.48
V23122212	3.54	0.03	0.16	0.35	0.74	0.13	0.0013	691	691	2	49	115	0.13	0.0012	670	7	2	49	79	1.00	0.70	0.37	0.48
V33122211	3.16	0.03	0.19	0.40	0.75	0.13	0.0013	810	810	2	59	129	0.12	0.0011	780	8	2	59	88	1.00	0.77	0.39	0.51
V33122212	3.23	0.03	0.18	0.38	0.77	0.13	0.0013	786	786	2	58	114	0.13	0.0011	760	8	2	58	76	1.00	0.78	0.40	0.51
V43122211	2.90	0.04	0.22	0.44	0.78	0.12	0.0012	924	924	3	70	127	0.12	0.0011	879	9	2	70	83	0.99	0.89	0.44	0.55
V43122212	2.95	0.04	0.21	0.43	0.80	0.12	0.0012	900	900	3	69	112	0.12	0.0011	859	9	2	69	72	0.99	0.89	0.45	0.55
V53122211	2.65	0.04	0.27	0.50	0.81	0.12	0.0012	1080	1080	5	86	121	0.12	0.0011	988	10	3	82	73	0.96	1.09	0.53	0.60
V53122212	2.69	0.04	0.26	0.49	0.83	0.12	0.0012	1056	1056	5	85	106	0.12	0.0011	968	10	3	81	63	0.96	1.09	0.54	0.59
V13122221	3.03	0.04	0.19	0.42	0.68	0.12	0.0012	863	863	2	58	173	0.12	0.0011	835	9	2	58	126	1.00	0.58	0.28	0.45
V13122222	3.12	0.03	0.18	0.40	0.71	0.12	0.0012	827	827	2	57	153	0.12	0.0011	804	8	2	57	110	1.00	0.60	0.29	0.45
V23122221	2.84	0.04	0.21	0.44	0.71	0.12	0.0011	948	948	2	66	173	0.12	0.0011	920	10	2	66	126	1.00	0.62	0.29	0.48
V23122222	2.91	0.04	0.20	0.41	0.74	0.12	0.0012	912	912	2	65	152	0.12	0.0011	889	9	2	65	110	1.00	0.62	0.31	0.48
V33122221	2.62	0.05	0.23	0.46	0.74	0.11	0.0011	1063	1063	3	78	171	0.11	0.0010	1033	11	2	78	124	1.00	0.67	0.32	0.51
V33122222	2.68	0.04	0.22	0.44	0.77	0.12	0.0011	1028	1028	3	77	151	0.11	0.0010	1002	10	2	77	108	1.00	0.68	0.33	0.51
V43122221	2.43	0.05	0.26	0.48	0.77	0.11	0.0011	1194	1194	4	91	169	0.11	0.0010	1154	12	3	90	120	1.00	0.75	0.34	0.54
V43122222	2.47	0.05	0.25	0.47	0.79	0.11	0.0011	1158	1158	4	89	148	0.11	0.0010	1123	12	3	89	104	1.00	0.75	0.36	0.54
V53122221	2.25	0.06	0.29	0.53	0.80	0.11	0.0011	1348	1348	5	106	164	0.11	0.0010	1284	13	3	105	112	0.99	0.86	0.39	0.58
V53122222	2.29	0.06	0.29	0.52	0.82	0.11	0.0011	1313	1313	5	105	145	0.11	0.0010	1253	13	3	103	97	0.99	0.88	0.40	0.58
V13211111	9.64	0.01	0.05	0.13	0.66	0.22	0.0019	161	161	1	16	39	0.22	0.0015	149	1	0	16	21	0.99	0.83	0.51	0.49
V13211112	10.06	0.01	0.04	0.12	0.72	0.23	0.0019	149	149	1	15	31	0.22	0.0015	141	1	0	15	17	0.99	0.82	0.53	0.48
V23211111	8.78	0.01	0.06	0.14	0.70	0.21	0.0018	183	183	1	19	39	0.21	0.0014	170	1	1	19	21	1.00	0.93	0.56	0.51
V23211112	9.12	0.01	0.05	0.13	0.75	0.22	0.0018	171	171	1	18	31	0.21	0.0014	162	1	1	18	17	1.00	0.93	0.58	0.50
V33211111	8.04	0.01	0.07	0.16	0.73	0.21	0.0018	210	210	1	23	40	0.20	0.0014	194	2	1	22	21	1.00	1.08	0.63	0.54
V33211112	8.30	0.01	0.06	0.15	0.78	0.21	0.0018	197	197	1	22	32	0.20	0.0014	186	1	1	22	17	1.00	1.07	0.65	0.53
V43211111	7.36	0.01	0.08	0.18	0.76	0.20	0.0017	244	244	2	27	40	0.19	0.0013	221	2	1	27	20	0.98	1.25	0.73	0.58
V43211112	7.56	0.01	0.07	0.17	0.80	0.20	0.0017	232	232	2	26	33	0.20	0.0013	212	2	1	26	16	0.98	1.26	0.75	0.57
V53211111	6.72	0.01	0.10	0.23	0.79	0.19	0.0017	298	298	3	34	40	0.19	0.0013	250	2	1	32	18	0.92	1.48	0.93	0.64
V53211112	6.88	0.01	0.09	0.22	0.82	0.20	0.0017	285	285	3	34	33	0.19	0.0013	242	2	1	31	14	0.91	1.49	0.94	0.64
V13211121	7.85	0.01	0.07	0.17	0.66	0.20	0.0017	218	218	1	22	53	0.20	0.0014	202	2	1	21	30	0.99	0.83	0.46	0.48
V13211122	8.21	0.01	0.06	0.15	0.71	0.20	0.0017	201	201	1	21	42	0.20	0.0014	190	2	1	21	24	0.99	0.83	0.49	0.48
V23211121	7.16	0.01	0.07	0.18	0.70	0.19	0.0016	249	249	1	26	53	0.19	0.0013	233	2	1	26	30	1.00	0.90	0.51	0.50
V23211122	7.45	0.01	0.07	0.16	0.75	0.20	0.0016	232	232	1	25	43	0.19	0.0013	221	2	1	25	24	1.00	0.92	0.53	0.50
V33211121	6.55	0.01	0.08	0.20	0.73	0.19	0.0015	285	285	1	31	53	0.18	0.0012	267	2	1	31	29	1.00	1.00	0.57	0.53
V33211122	6.78	0.01	0.08	0.18	0.78	0.19	0.0016	268	268	2	30	43	0.18	0.0012	254	2	1	30	23	1.00	1.02	0.59	0.53
V43211121	6.00	0.01	0.10	0.23	0.76	0.18	0.0015	331	331	2	38	52	0.18	0.0012	304	2	1	37	28	0.98	1.14	0.66	0.57
V43211122	6.18	0.01	0.09	0.21	0.80	0.18	0.0015	314	314	2	37	43	0.18	0.0012	291	2	1	36	22	0.98	1.15	0.68	0.56
V53211121	5.49	0.02	0.12	0.29	0.79	0.18	0.0015	401	401	3	48	52	0.18	0.0012	346	3	1	44	25	0.93	1.36	0.85	0.62
V53211122	5.63	0.01	0.12	0.27	0.83	0.18	0.0015	383	383	3	46	42	0.18	0.0012	333	3	1	43	20	0.93	1.37	0.86	0.62
V13211211	8.56	0.01	0.06	0.14	0.70	0.21	0.0017	190	190	1	19	41	0.20	0.0014	178	1	1	19	23	0.99	0.83	0.49	0.48
V13211212	8.89	0.01	0.05	0.13	0.75	0.21	0.0017	177	177	1	19	33	0.20	0.0014	170	1	1	18	19	0.99	0.82	0.51	0.47
V23211211	7.77	0.01	0.07	0.16	0.73	0.20	0.0017	218	218	1	23	42	0.19	0.0013	206	2	1	23	23	1.00	0.93	0.54	0.50
V23211212	8.02	0.01	0.06	0.14	0.78	0.20	0.0017	206	206	1	23	34	0.20	0.0013	197	2	1	22	19	1.00	0.92	0.56	0.50
V33211211	7.09	0.01	0.07	0.18	0.76	0.19	0.0016	251	251	1	27	42	0.19	0.0013	237	2	1	27	23	1.00	1.04	0.60	0.53
V33211212	7.28	0.01	0.07	0.16	0.80	0.20	0.0016	239	239	1	27	35	0.19	0.0013	228	2	1	27	18	1.00	1.05	0.61	0.53
V43211211	6.47	0.01	0.09	0.20	0.79	0.19	0.0016	294	294	2	33	42	0.18	0.0012	271	2	1	33	22	0.98	1.18	0.69	0.57
V43211212	6.62	0.01	0.08	0.19	0.82	0.19	0.0016	282	282	2	33	35	0.19	0.0013	262	2	1	32	17	0.98	1.19	0.70	0.56
V53211211	5.89	0.01	0.11	0.26	0.81	0.18	0.0016	358	358	3	42	42	0.18	0.0013	309	2	1	39	19	0.93	1.40	0.88	0.63

Name	T1 [s]	Sa(T1) [g]	Sa(T2) [g]	Sa(T3) [g]	DOC [-]	Disp [m]	ISDR [-]	Total Moment [MN-m]	Total Shear [MN]	Max CB Shear [MN]	Max Pp [MN]	Max wall moment [MN-m]	Disp [m]2	ISDR [-]3	Total Moment [MN-m]4	Total Shear [MN]5	Max CB Shear [MN]6	Max Pp [MN]2	Max wall moment [MN-m]8	C1 [-]	C2 [-]	C3 [-]	Mdy/ Mst [-]
V13211221	6.93	0.01	0.08	0.18	0.70	0.19	0.0015	261	261	1	27	56	0.18	0.0013	247	2	1	26	33	0.99	0.80	0.45	0.47
V13211222	7.20	0.01	0.07	0.16	0.75	0.19	0.0015	244	244	1	26	45	0.19	0.0013	234	2	1	26	27	0.99	0.82	0.47	0.47
V23211221	6.29	0.01	0.08	0.20	0.74	0.18	0.0015	301	301	1	32	56	0.18	0.0012	287	2	1	32	33	1.00	0.85	0.48	0.50
V23211222	6.51	0.01	0.08	0.18	0.78	0.18	0.0015	284	284	1	32	45	0.18	0.0012	273	2	1	32	27	1.00	0.87	0.50	0.49
V33211221	5.74	0.01	0.09	0.22	0.77	0.18	0.0014	347	347	2	39	56	0.17	0.0012	330	3	1	39	32	1.00	0.94	0.54	0.52
V33211222	5.91	0.01	0.09	0.20	0.80	0.18	0.0014	330	330	2	38	46	0.17	0.0012	317	2	1	38	26	1.00	0.95	0.55	0.52
V43211221	5.24	0.02	0.11	0.26	0.79	0.17	0.0014	406	406	3	47	56	0.17	0.0011	379	3	1	46	31	0.99	1.07	0.62	0.56
V43211222	5.37	0.02	0.11	0.24	0.83	0.17	0.0014	389	389	3	46	46	0.17	0.0012	366	3	1	45	25	0.98	1.08	0.63	0.56
V53211221	4.78	0.02	0.14	0.32	0.82	0.17	0.0014	487	487	4	58	55	0.16	0.0012	428	3	2	55	27	0.94	1.30	0.79	0.61
V53211222	4.88	0.02	0.13	0.31	0.85	0.17	0.0014	472	472	4	57	45	0.17	0.0012	418	3	2	54	22	0.93	1.30	0.80	0.61
V13212111	5.56	0.02	0.10	0.25	0.64	0.17	0.0014	371	371	1	24	89	0.17	0.0012	347	3	1	24	56	0.99	0.71	0.38	0.47
V13212112	5.74	0.01	0.09	0.23	0.67	0.18	0.0014	350	350	1	23	78	0.17	0.0012	332	3	1	23	49	0.99	0.73	0.40	0.47
V23212111	5.09	0.02	0.11	0.27	0.68	0.17	0.0013	424	424	1	29	89	0.17	0.0011	401	3	1	29	56	1.00	0.76	0.42	0.50
V23212112	5.23	0.02	0.11	0.25	0.71	0.17	0.0013	403	403	1	28	78	0.17	0.0011	385	3	1	28	49	1.00	0.78	0.43	0.49
V33212111	4.68	0.02	0.12	0.30	0.72	0.16	0.0013	476	476	1	34	88	0.16	0.0011	450	4	1	34	55	1.00	0.86	0.48	0.52
V33212112	4.79	0.02	0.12	0.28	0.75	0.16	0.0013	460	460	1	34	78	0.16	0.0011	437	3	1	34	48	1.00	0.87	0.49	0.52
V43212111	4.30	0.02	0.14	0.33	0.75	0.15	0.0012	539	539	2	40	87	0.15	0.0010	501	4	1	40	51	0.99	1.01	0.56	0.56
V43212112	4.39	0.02	0.14	0.32	0.77	0.16	0.0012	522	522	2	40	77	0.15	0.0010	488	4	1	39	45	0.99	1.02	0.57	0.56
V53212111	3.94	0.02	0.18	0.38	0.78	0.15	0.0012	630	630	3	49	83	0.15	0.0010	557	4	1	47	45	0.95	1.23	0.69	0.61
V53212112	4.01	0.02	0.17	0.37	0.80	0.15	0.0012	613	613	3	49	73	0.15	0.0010	545	4	1	46	39	0.95	1.24	0.71	0.61
V13212121	4.47	0.02	0.13	0.32	0.64	0.16	0.0012	507	507	1	33	117	0.15	0.0011	480	4	1	33	78	0.99	0.66	0.34	0.47
V13212122	4.62	0.02	0.12	0.30	0.68	0.16	0.0012	483	483	1	33	103	0.15	0.0011	461	4	1	32	68	0.99	0.67	0.36	0.47
V23212121	4.10	0.02	0.14	0.34	0.68	0.15	0.0011	569	569	1	40	116	0.14	0.0010	542	4	1	40	77	1.00	0.72	0.38	0.49
V23212122	4.21	0.02	0.14	0.32	0.71	0.15	0.0011	545	545	1	39	102	0.15	0.0010	523	4	1	39	67	1.00	0.73	0.40	0.49
V33212121	3.76	0.03	0.16	0.36	0.72	0.14	0.0011	638	638	2	47	115	0.14	0.0009	607	5	1	47	75	1.00	0.81	0.43	0.52
V33212122	3.86	0.03	0.15	0.34	0.75	0.14	0.0011	615	615	2	46	101	0.14	0.0009	589	5	1	46	65	1.00	0.82	0.44	0.52
V43212121	3.46	0.03	0.18	0.39	0.75	0.14	0.0010	723	723	3	55	112	0.13	0.0009	679	5	2	55	70	0.99	0.94	0.49	0.55
V43212122	3.54	0.03	0.17	0.37	0.78	0.14	0.0011	699	699	3	54	99	0.13	0.0009	660	5	2	54	61	0.99	0.95	0.50	0.55
V53212121	3.17	0.03	0.22	0.45	0.79	0.13	0.0010	843	843	4	68	107	0.13	0.0009	758	6	2	64	63	0.95	1.15	0.61	0.60
V53212122	3.23	0.03	0.22	0.44	0.81	0.13	0.0010	820	820	4	66	95	0.13	0.0009	739	6	2	63	54	0.95	1.16	0.62	0.60
V13212211	5.04	0.02	0.11	0.27	0.67	0.17	0.0013	430	430	1	28	94	0.16	0.0011	408	3	1	28	61	0.99	0.68	0.37	0.47
V13212212	5.19	0.02	0.10	0.25	0.70	0.17	0.0013	409	409	1	28	82	0.16	0.0011	392	3	1	27	53	0.99	0.69	0.38	0.47
V23212211	4.61	0.02	0.12	0.29	0.71	0.16	0.0012	484	484	1	33	93	0.15	0.0011	462	4	1	33	60	1.00	0.75	0.41	0.49
V23212212	4.72	0.02	0.12	0.27	0.74	0.16	0.0012	467	467	1	33	82	0.16	0.0011	449	4	1	33	53	1.00	0.75	0.42	0.49
V33212211	4.22	0.02	0.14	0.32	0.74	0.15	0.0012	545	545	2	39	92	0.15	0.0010	519	4	1	39	58	1.00	0.84	0.46	0.52
V33212212	4.31	0.02	0.13	0.30	0.77	0.15	0.0012	528	528	2	39	81	0.15	0.0010	507	4	1	39	51	1.00	0.85	0.47	0.52
V43212211	3.87	0.03	0.16	0.35	0.77	0.14	0.0011	619	619	2	47	91	0.14	0.0010	581	5	1	46	55	0.99	0.98	0.53	0.56
V43212212	3.94	0.02	0.15	0.34	0.79	0.15	0.0011	603	603	2	46	80	0.14	0.0010	569	4	1	46	48	0.99	0.99	0.55	0.55
V53212211	3.54	0.03	0.19	0.42	0.80	0.14	0.0011	725	725	4	57	87	0.14	0.0010	649	5	2	54	48	0.95	1.19	0.66	0.60
V53212212	3.59	0.03	0.19	0.40	0.82	0.14	0.0011	709	709	4	56	77	0.14	0.0010	637	5	2	53	42	0.95	1.20	0.67	0.60
V13212221	4.04	0.02	0.14	0.34	0.67	0.14	0.0011	579	579	1	38	123	0.14	0.0010	554	4	1	38	84	0.99	0.65	0.33	0.46
V13212222	4.16	0.02	0.13	0.32	0.70	0.15	0.0011	555	555	1	38	108	0.14	0.0010	535	4	1	38	73	0.99	0.65	0.35	0.46
V23212221	3.69	0.03	0.16	0.35	0.71	0.14	0.0010	654	654	2	46	122	0.14	0.0009	629	5	1	46	83	1.00	0.70	0.37	0.48
V23212222	3.78	0.03	0.15	0.34	0.74	0.14	0.0010	630	630	2	45	107	0.14	0.0009	609	5	1	45	72	1.00	0.71	0.38	0.48
V33212221	3.38	0.03	0.18	0.38	0.74	0.13	0.0010	738	738	2	54	120	0.13	0.0009	709	6	2	54	80	1.00	0.78	0.40	0.51
V33212222	3.45	0.03	0.17	0.36	0.77	0.13	0.0010	715	715	2	54	106	0.13	0.0009	690	5	2	54	70	1.00	0.79	0.42	0.51
V43212221	3.10	0.04	0.20	0.42	0.78	0.13	0.0010	840	840	3	64	118	0.13	0.0009	797	6	2	64	76	0.99	0.90	0.46	0.55
V43212222	3.16	0.03	0.19	0.40	0.80	0.13	0.0010	817	817	3	64	104	0.13	0.0009	778	6	2	63	66	0.99	0.91	0.47	0.55
V53212221	2.84	0.04	0.25	0.48	0.81	0.12	0.0010	982	982	5	79	112	0.12	0.0009	894	7	2	75	67	0.96	1.11	0.56	0.60
V53212222	2.88	0.04	0.24	0.47	0.83	0.12	0.0010	958	958	5	77	99	0.12	0.0009	875	7	2	74	58	0.96	1.11	0.57	0.60
V13221111	11.13	0.01	0.04	0.11	0.67	0.25	0.0021	182	182	1	18	43	0.25	0.0017	168	1	1	18	24	0.99	0.79	0.50	0.49
V13221112	11.62	0.01	0.03	0.10	0.72	0.26	0.0021	172	172	1	18	35	0.25	0.0018	162	1	1	18	20	0.99	0.77	0.52	0.48
V23221111	10.14	0.01	0.04	0.12	0.70	0.23	0.0020	199	199	1	20	43	0.22	0.0015	185	1	1	20	23	1.00	0.92	0.59	0.51
V23221112	10.53	0.01	0.04	0.11	0.75	0.24	0.0020	189	189	1	20	35	0.23	0.0016	179	1	1	20	19	1.00	0.90	0.59	0.50
V33221111	9.28	0.01	0.05	0.14	0.73	0.22	0.0019	226	226	1	24	44	0.21	0.0015	208	2	1	24	22	1.00	1.08	0.67	0.54
V33221112	9.58	0.01	0.05	0.12	0.77	0.22	0.0019	213	213	1	24	35	0.22	0.0015	200	2	1	24	18	1.00	1.07	0.68	0.53
V43221111	8.49	0.01	0.06	0.16	0.75	0.21	0.0019	264	264	2	29	45	0.21	0.0014	236	2	1	28	21	0.98	1.31	0.78	0.58
V43221112	8.73	0.01	0.06	0.15	0.79	0.22	0.0019	250	250	2	28	36	0.21	0.0014	227	2	1	28	17	0.98	1.30	0.80	0.58
V53221111	7.76	0.01	0.08	0.20	0.78	0.21	0.0018	324	324	3	37	45	0.20	0.0014	267	2	1	34	19	0.91	1.56	0.98	0.65
V53221112	7.94	0.01	0.08	0.19	0.81	0.21	0.0019	310	310	3	36	37	0.21	0.0014	258	2	1	33	15	0.91	1.57	1.00	0.65
V13221121	9.06	0.01	0.05	0.14	0.66	0.22	0.0018	235	235	1	23	58	0.21	0.0014	217	2	1	23	32	0.99	0.83	0.49	0.49
V13221122	9.48	0.01	0.05	0.13	0.71	0.22	0.0018	217	217	1	23	46	0.21	0.0015	204	2	1	22	26	0.99	0.83	0.51	0.48
V23221121	8.26	0.01	0.06	0.15	0.70	0.21	0.0017	268	268	1	28	58	0.20	0.0014	249	2	1	28	32	1.00	0.93	0.55	0.51
V23221122	8.60	0.01	0.06	0.14	0.75	0.21	0.0017	249	249	1	27	47	0.20	0.0014	236	2	1	27	26	1.00	0.93	0.57	0.50
V33221121	7.57	0.01	0.07	0.17	0.73	0.20	0.0017	307	307	2	33	59	0.19	0.0013	284	2	1	33	31	1.00	1.06	0.61	0.54
V33221122	7.83	0.01	0.07	0.16	0.77	0.20	0.0017	288	288	2	32	48	0.20	0.0013	271	2	1	32	25	1.00	1.08	0.63	0.53
V43221121	6.93	0.01	0.08	0.20	0.75	0.19	0.0016	356	356	2	40	59	0.19	0.0013	323	3	1	40	30	0.98	1.21	0.71	0.57
V43221122	7.14	0.01	0.08	0.18	0.79	0.20	0.0017	337	337	2	39	48	0.19	0.0013	309	2	1	38	24	0.98	1.23	0.73	0.57
V53221121	6.33	0.01	0.10	0.25	0.79	0.19	0.0016	432	432	4	51	58	0.19	0.0013	366	3	2	47	26	0.92	1.44	0.90	0.63
V53221122	6.50	0.01	0.10	0.23	0.82	0.19	0.0016	413	413	4	50	48	0.19	0.0013	352	3	1	45	21	0.92	1.46	0.91	0.63
V13221211	9.88	0.01	0.05	0.12	0.70	0.22	0.0019	205	205	1	20	45	0.22	0.0015	192	2	1	20	25	0.99	0.83	0.52	0.48
V13221212	10.26	0.01	0.04	0.11	0.75	0.23	0.0019	194	194	1	20	36	0.22	0.0016	185	1	1	20	21	0.99	0.81	0.53	0.48
V23221211	8.97	0.01	0.05	0.13	0.73	0.21	0.0018	235	235	1	25	46	0.21	0.0014	221	2	1	24	25	1.00	0.93	0.57	0.51
V23221212	9.27	0.01	0.05	0.12	0.78	0.22	0.0018	221	221	1	24	37	0.21	0.0014	212	2	1	24	20	1.00	0.92	0.59	0.50
V33221211	8.18	0.01	0.06	0.15	0.76	0.21	0.0018	270	270	2	29	47	0.20	0.0014	253	2	1	29	24	1.00	1.08	0.64	0.53
V33221212	8.41	0.01	0.06	0.14	0.80	0.21	0.0018	257	257	2	29	38	0.20	0.0014	244	2	1	29	20	1.00	1.07	0.66	0.53
V43221211	7.47	0.01	0.07	0.18	0.78	0.20	0.0017	316	316	2	35	48	0.20	0.0013	288	2	1	35	23	0.98	1.26	0.74	0.57
V43221212	7.64	0.01	0.07	0.16	0.82	0.20	0.0017	303	303	2	35	39	0.20	0.0013	279	2	1	34	18	0.98	1.27	0.75	0.57
V53221211	6.81	0.01	0.09	0.22	0.81	0.20	0.0017	387	387	4	45	47	0.19	0.0013	328	3	1	41	20	0.92	1.48	0.94	0.64
V53221212	6.94	0.01	0.09	0.21	0.84	0.20	0.0017	374	374	4	44	39	0.19	0.0013	319	2	1	40	16	0.91	1.49	0.94	0.63
V13221221	8.00	0.01	0.06	0.16	0.70	0.20	0.0017	280	280	1	28	62	0.20	0.0014	263	2	1	28	35	0.99	0.83	0.48	0.48
V13221222	8.31	0.01	0.06	0.14	0.75	0.20	0.0017	261	261	1	28	50	0.20	0.0014	250	2	1	28	28	0.99	0.82	0.50	0.47
V23221221	7.27	0.01	0.07	0.17	0.73	0.19	0.0016	322	322	1	34	62	0.19	0.0013	305	2	1	34	35	1.00	0.91	0.52	0.50
V23221222	7.51	0.01	0.07	0.16	0.78	0.20	0.0016	304	304	2	34	51	0.19	0.0013	291	2	1	34	28	1.00	0.93	0.54	0.50
V33221221	6.63	0.01	0.08	0.19	0.76	0.19	0.0015	371	371	2	41	62	0.18	0.0012	350	3	1	41	34	1.00	1.01	0.58	0.53
V33221222	6.82	0.01	0.08	0.18	0.80	0.19	0.0016	353	353	2	40	51	0.18	0.0012	337	3	1	40	28	1.00	1.02	0.59	0.53
V43221221	6.06	0.01	0.09	0.22	0.79	0.18	0.0015	433	433	3	50	62	0.18	0.0012	401	3	2	49	33	0.98	1.14	0.67	0.57
V43221222	6.20	0.01	0.09	0.21	0.82	0.18	0.0015	415	415	3	49	51	0.18	0.0012	387	3	2	48	26	0.98	1.16	0.68	0.56
V53221221	5.52	0.02	0.12	0.28	0.81	0.18	0.0015	527	527	5	63	62	0.18	0.0012	457	4	2	58	29	0.93	1.36	0.85	0.62
V53221222	5.63	0.01	0.11	0.27	0.84	0.18	0.0015	508	508	5	61	51	0.18	0.0012	444	3	2	57	23	0.93	1.37	0.86	0.62
V13222111	6.42	0.01	0.09	0.22	0.63	0.18	0.0015	396	396	1	25	99	0.18	0.0012	367	3	1	25	59	0.99	0.76	0.41	0.48
V13222112	6.62	0.01	0.08	0.20	0.67	0.19	0.0015	375	375	1	25	86	0.18	0.0013	351	3	1	25	51	0.99	0.78	0.43	0.48
V23222111	5.88	0.01	0.09	0.23	0.68	0.18	0.0014	451	451	1	31	98	0.17	0.0012	423	3	1	31	59	1.00	0.82	0.45	0.50
V23222112	6.04	0.01	0.09	0.22	0.71	0.18	0.0014	430	430	1	30	86	0.18	0.0012	406	3	1	30	52	1.00	0.83	0.47	0.50
V33222111	5.40	0.02	0.11	0.25	0.71	0.17	0.0014	515	515	2	37	98	0.17	0.0012	483	4	1	37	59	1.00	0.90	0.51	0.53
V33222112	5.53	0.02	0.10	0.24	0.74	0.17	0.0014	493	493	2	36	86	0.17	0.0012	467	4	1	36	51	1.00	0.92	0.52	0.53
V43222111	4.96	0.02	0.12	0.29	0.74	0.17	0.0014	594	594	2	44	98	0.17	0.0011	549	4	1	44	56	0.99	1.04	0.60	0.56
V43222112	5.07	0.02	0.12	0.28	0.77	0.17	0.0014	574	574	2	44	86	0.17	0.0011	534	4	1	43	49	0.99	1.05	0.61	0.56
V53222111	4.55	0.02	0.15	0.35	0.78	0.16	0.0013	697	697	4	54	95	0.16	0.0011	609	5	2	51	50	0.94	1.28	0.76	0.62
V53222112	4.63	0.02	0.15	0.34	0.80	0.16	0.0013	678	678	4	54	84	0.16	0.0011	596	5	2	50	43	0.94	1.29	0.77	0.61
V13222121	5.16	0.02	0.11	0.28	0.64	0.17	0.0013	556	556	1	36	132	0.17	0.0011	522	4	1	36	85	0.99	0.68	0.37	0.47
V13222122	5.33	0.02	0.10	0.25	0.67	0.17	0.0013	524	524	1	35	115	0.17	0.0012	497	4	1	35	74	0.99	0.70	0.38	0.47
V23222121	4.73	0.02	0.12	0.29	0.68	0.16	0.0012	626	626	2	43	131	0.16	0.0011	593	5	1	43	84	1.00	0.75	0.41	0.49

Name	T1 [s]	Sa(T1) [g]	Sa(T2) [g]	Sa(T3) [g]	DOC [-]	Disp [m]	ISDR [-]	Total Moment [MN-m]	Total Shear [MN]	Max CB Shear [MN]	Max Pp [MN]	Max wall moment [MN-m]	Disp [m]2	ISDR [-]3	Total Moment [MN-m]4	Total Shear [MN]5	Max CB Shear [MN]6	Max Pp [MN]2	Max wall moment [MN-m]8	C1 [-]	C2 [-]	C3 [-]	Mdy/ Mst [-]
V33222121	4.35	0.02	0.14	0.32	0.72	0.15	0.0012	701	701	2	51	129	0.15	0.0010	663	5	2	51	81	1.00	0.85	0.46	0.52
V33222122	4.46	0.02	0.13	0.30	0.74	0.16	0.0012	675	675	2	50	114	0.15	0.0010	643	5	2	50	71	1.00	0.85	0.48	0.52
V43222121	4.00	0.02	0.16	0.35	0.75	0.15	0.0012	793	793	3	60	127	0.15	0.0010	739	6	2	60	77	0.99	0.99	0.54	0.56
V43222122	4.08	0.02	0.15	0.34	0.77	0.15	0.0012	767	767	3	59	112	0.15	0.0010	719	6	2	59	67	0.99	1.00	0.55	0.56
V53222121	3.66	0.03	0.19	0.41	0.78	0.14	0.0011	925	925	5	74	122	0.14	0.0010	823	6	2	70	68	0.95	1.21	0.67	0.61
V53222122	3.73	0.03	0.18	0.40	0.80	0.14	0.0012	900	900	5	72	107	0.14	0.0010	803	6	2	69	58	0.95	1.22	0.68	0.61
V13222211	5.82	0.01	0.09	0.23	0.66	0.18	0.0014	457	457	1	30	104	0.17	0.0012	431	3	1	29	65	0.99	0.73	0.40	0.47
V13222212	5.99	0.01	0.09	0.22	0.70	0.18	0.0014	435	435	1	29	91	0.17	0.0012	414	3	1	29	56	0.99	0.74	0.41	0.47
V23222211	5.32	0.02	0.10	0.25	0.70	0.17	0.0013	525	525	1	36	104	0.17	0.0011	499	4	1	36	65	1.00	0.78	0.44	0.49
V23222212	5.45	0.02	0.10	0.23	0.73	0.17	0.0013	503	503	1	36	91	0.17	0.0011	482	4	1	35	57	1.00	0.79	0.45	0.49
V33222211	4.87	0.02	0.12	0.28	0.74	0.17	0.0013	600	600	2	43	104	0.16	0.0011	569	4	1	43	64	1.00	0.87	0.49	0.52
V33222212	4.97	0.02	0.11	0.26	0.77	0.17	0.0013	581	581	2	43	92	0.16	0.0011	555	4	1	43	56	1.00	0.87	0.50	0.52
V43222211	4.47	0.02	0.14	0.31	0.77	0.16	0.0013	681	681	3	51	103	0.16	0.0011	635	5	2	50	60	0.99	1.02	0.58	0.56
V43222212	4.55	0.02	0.13	0.30	0.79	0.16	0.0013	662	662	3	50	91	0.16	0.0011	622	5	2	50	52	0.99	1.02	0.59	0.56
V53222211	4.09	0.02	0.17	0.37	0.80	0.15	0.0012	798	798	4	62	98	0.15	0.0010	707	5	2	59	53	0.95	1.24	0.71	0.61
V53222212	4.15	0.02	0.16	0.36	0.82	0.15	0.0012	781	781	4	61	87	0.15	0.0011	694	5	2	58	45	0.94	1.25	0.73	0.61
V13222221	4.66	0.02	0.12	0.30	0.67	0.16	0.0012	637	637	1	42	139	0.16	0.0011	606	5	1	42	92	0.99	0.67	0.36	0.47
V13222222	4.80	0.02	0.11	0.28	0.70	0.16	0.0012	610	610	1	42	122	0.16	0.0011	586	5	1	41	80	0.99	0.67	0.37	0.46
V23222221	4.26	0.02	0.13	0.32	0.71	0.15	0.0011	717	717	2	50	138	0.15	0.0010	686	5	2	50	90	1.00	0.73	0.40	0.49
V23222222	4.37	0.02	0.13	0.30	0.74	0.15	0.0011	690	690	2	50	121	0.15	0.0010	665	5	2	49	79	1.00	0.74	0.41	0.49
V33222221	3.91	0.03	0.15	0.34	0.74	0.14	0.0011	807	807	3	59	136	0.14	0.0010	771	6	2	59	87	1.00	0.82	0.44	0.52
V33222222	3.99	0.02	0.14	0.33	0.77	0.15	0.0011	782	782	3	58	120	0.14	0.0010	751	6	2	58	76	1.00	0.83	0.46	0.52
V43222221	3.58	0.03	0.17	0.37	0.77	0.14	0.0011	917	917	3	70	133	0.14	0.0009	864	7	2	69	82	0.99	0.95	0.50	0.55
V43222222	3.65	0.03	0.17	0.36	0.80	0.14	0.0011	891	891	3	69	117	0.14	0.0009	844	7	2	68	71	0.99	0.96	0.52	0.55
V53222221	3.28	0.03	0.21	0.44	0.80	0.13	0.0011	1073	1073	5	85	127	0.13	0.0009	966	7	3	81	73	0.95	1.17	0.63	0.60
V53222222	3.33	0.03	0.21	0.43	0.82	0.13	0.0011	1048	1048	5	84	112	0.13	0.0009	947	7	3	80	63	0.95	1.17	0.64	0.60
M11111111	0.72	0.21	0.63	0.71	0.71	0.04	0.0011	426	426	4	44	67	0.04	0.0011	423	13	4	44	61	1.00	0.33	0.09	0.50
M11111112	0.75	0.20	0.60	0.71	0.75	0.04	0.0011	406	406	4	44	55	0.04	0.0011	404	13	4	44	50	1.00	0.35	0.10	0.50
M21111111	0.66	0.23	0.65	0.71	0.75	0.04	0.0010	467	467	5	51	64	0.04	0.0010	464	14	5	51	58	1.00	0.35	0.09	0.53
M21111112	0.68	0.22	0.63	0.71	0.78	0.04	0.0010	452	452	5	51	53	0.04	0.0010	450	14	5	51	48	1.00	0.37	0.10	0.53
M31111111	0.60	0.26	0.68	0.71	0.78	0.03	0.0009	514	514	6	59	61	0.03	0.0009	510	16	6	59	55	1.00	0.38	0.09	0.57
M31111112	0.62	0.25	0.67	0.71	0.81	0.03	0.0009	495	495	6	58	50	0.03	0.0009	492	15	5	58	45	1.00	0.39	0.10	0.57
M41111111	0.55	0.28	0.71	0.71	0.81	0.03	0.0009	561	561	7	67	57	0.03	0.0008	556	17	6	67	51	1.00	0.41	0.10	0.61
M41111112	0.57	0.27	0.70	0.71	0.84	0.03	0.0009	545	545	7	66	47	0.03	0.0009	541	17	6	66	42	1.00	0.42	0.11	0.61
M51111111	0.51	0.30	0.71	0.71	0.85	0.03	0.0008	601	601	8	75	49	0.03	0.0008	593	18	7	74	44	0.99	0.43	0.11	0.65
M51111112	0.52	0.30	0.71	0.71	0.87	0.03	0.0008	589	589	8	73	41	0.03	0.0008	581	18	7	73	36	0.99	0.45	0.12	0.65
M11111121	0.59	0.26	0.69	0.71	0.71	0.03	0.0009	532	532	5	56	83	0.03	0.0009	530	16	5	56	77	1.00	0.29	0.07	0.49
M11111122	0.61	0.25	0.66	0.71	0.75	0.03	0.0009	507	507	5	55	69	0.03	0.0009	505	16	5	55	64	1.00	0.31	0.08	0.50
M21111121	0.54	0.29	0.71	0.71	0.74	0.03	0.0008	583	583	6	65	80	0.03	0.0008	581	18	6	65	74	1.00	0.30	0.07	0.53
M21111122	0.56	0.28	0.69	0.71	0.78	0.03	0.0008	563	563	6	64	66	0.03	0.0008	561	17	6	64	61	1.00	0.32	0.08	0.53
M31111121	0.49	0.31	0.71	0.71	0.78	0.03	0.0007	630	630	7	73	74	0.03	0.0007	627	19	7	73	69	1.00	0.32	0.08	0.56
M31111122	0.51	0.30	0.71	0.71	0.81	0.03	0.0008	611	611	7	72	62	0.03	0.0008	608	19	7	72	57	1.00	0.34	0.08	0.57
M41111121	0.45	0.34	0.71	0.71	0.81	0.03	0.0007	673	673	8	81	67	0.03	0.0007	668	20	8	81	63	1.00	0.34	0.08	0.61
M41111122	0.47	0.33	0.71	0.71	0.84	0.03	0.0007	658	658	8	81	56	0.03	0.0007	654	20	8	81	52	1.00	0.35	0.09	0.61
M51111121	0.41	0.36	0.71	0.71	0.84	0.02	0.0006	708	708	9	90	57	0.02	0.0006	702	21	8	89	53	1.00	0.37	0.09	0.65
M51111122	0.43	0.35	0.71	0.71	0.87	0.02	0.0007	696	696	9	88	48	0.02	0.0007	690	21	8	88	44	1.00	0.38	0.10	0.65
M11111211	0.64	0.24	0.66	0.71	0.74	0.03	0.0010	481	481	5	51	68	0.03	0.0009	479	15	5	51	63	1.00	0.32	0.08	0.50
M11111212	0.66	0.23	0.63	0.71	0.77	0.04	0.0010	466	466	5	51	57	0.04	0.0010	465	14	5	51	52	1.00	0.33	0.09	0.50
M21111211	0.58	0.27	0.68	0.71	0.77	0.03	0.0009	538	538	6	59	66	0.03	0.0009	536	17	6	59	61	1.00	0.33	0.08	0.53
M21111212	0.60	0.26	0.67	0.71	0.80	0.03	0.0009	520	520	6	59	55	0.03	0.0009	519	16	6	59	50	1.00	0.34	0.09	0.53
M31111211	0.53	0.29	0.71	0.71	0.80	0.03	0.0008	587	587	7	67	62	0.03	0.0008	584	18	6	67	57	1.00	0.35	0.09	0.57
M31111212	0.55	0.28	0.70	0.71	0.83	0.03	0.0008	573	573	7	67	52	0.03	0.0008	571	18	6	67	47	1.00	0.36	0.09	0.57
M41111211	0.49	0.32	0.71	0.71	0.83	0.03	0.0008	632	632	8	75	57	0.03	0.0007	628	19	7	75	52	1.00	0.37	0.09	0.61
M41111212	0.50	0.31	0.71	0.71	0.86	0.03	0.0008	619	619	8	74	47	0.03	0.0008	616	19	7	74	43	1.00	0.38	0.10	0.61
M51111211	0.45	0.34	0.71	0.71	0.86	0.02	0.0007	673	673	9	83	49	0.02	0.0007	666	20	8	83	44	1.00	0.39	0.10	0.65
M51111212	0.46	0.34	0.71	0.71	0.88	0.03	0.0007	663	663	9	82	41	0.03	0.0007	656	20	8	82	37	1.00	0.40	0.11	0.65
M11111221	0.52	0.30	0.71	0.71	0.73	0.03	0.0008	604	604	6	65	85	0.03	0.0008	602	19	6	65	80	1.00	0.27	0.06	0.49
M11111222	0.54	0.29	0.69	0.71	0.77	0.03	0.0008	586	586	6	65	72	0.03	0.0008	585	18	6	65	67	1.00	0.29	0.07	0.50
M21111221	0.47	0.33	0.71	0.71	0.77	0.03	0.0007	658	658	7	74	81	0.03	0.0007	656	20	7	74	76	1.00	0.28	0.07	0.53
M21111222	0.49	0.32	0.71	0.71	0.80	0.03	0.0007	641	641	7	74	68	0.03	0.0007	640	20	7	74	63	1.00	0.30	0.07	0.53
M31111221	0.43	0.35	0.71	0.71	0.80	0.02	0.0006	703	703	8	82	74	0.02	0.0006	701	22	8	82	70	1.00	0.29	0.07	0.56
M31111222	0.44	0.34	0.71	0.71	0.83	0.02	0.0007	690	690	8	82	62	0.02	0.0006	688	21	8	82	58	1.00	0.31	0.08	0.57
M41111221	0.40	0.37	0.71	0.71	0.83	0.02	0.0006	741	741	9	90	66	0.02	0.0006	737	22	8	89	62	1.00	0.31	0.08	0.61
M41111222	0.41	0.37	0.71	0.71	0.85	0.02	0.0006	731	731	9	89	56	0.02	0.0006	727	22	9	89	52	1.00	0.32	0.08	0.61
M51111221	0.36	0.40	0.71	0.71	0.86	0.02	0.0005	787	787	10	99	57	0.02	0.0005	781	24	9	98	53	1.00	0.33	0.09	0.65
M51111222	0.37	0.39	0.71	0.71	0.88	0.02	0.0006	773	773	10	98	48	0.02	0.0006	767	23	9	97	44	1.00	0.34	0.09	0.65
M11112111	0.42	0.36	0.71	0.71	0.68	0.02	0.0006	720	720	4	49	120	0.02	0.0006	717	22	4	49	115	1.00	0.21	0.05	0.49
M11112112	0.43	0.35	0.71	0.71	0.71	0.02	0.0006	707	707	4	49	108	0.02	0.0006	705	22	4	49	103	1.00	0.23	0.05	0.49
M21112111	0.38	0.38	0.71	0.71	0.72	0.02	0.0005	764	764	5	55	111	0.02	0.0005	762	23	5	55	107	1.00	0.23	0.05	0.52
M21112112	0.39	0.37	0.71	0.71	0.74	0.02	0.0006	751	751	5	55	100	0.02	0.0006	748	23	5	55	95	1.00	0.24	0.06	0.52
M31112111	0.35	0.41	0.71	0.71	0.75	0.02	0.0005	819	819	6	62	104	0.02	0.0005	816	25	6	62	99	1.00	0.24	0.06	0.56
M31112112	0.36	0.40	0.71	0.71	0.78	0.02	0.0005	805	805	6	62	92	0.02	0.0005	802	25	6	62	88	1.00	0.25	0.06	0.56
M41112111	0.32	0.44	0.71	0.71	0.79	0.02	0.0005	865	865	7	69	93	0.02	0.0005	862	26	6	68	90	1.00	0.26	0.06	0.60
M41112112	0.33	0.43	0.71	0.71	0.81	0.02	0.0005	854	854	7	68	83	0.02	0.0005	851	26	6	68	79	1.00	0.27	0.07	0.60
M51112111	0.30	0.46	0.71	0.71	0.83	0.02	0.0004	903	903	7	75	80	0.01	0.0004	898	27	7	75	76	1.00	0.28	0.07	0.64
M51112112	0.30	0.46	0.71	0.71	0.85	0.02	0.0004	894	894	7	75	71	0.02	0.0004	889	27	7	74	67	1.00	0.29	0.08	0.65
M11112121	0.33	0.43	0.71	0.71	0.68	0.02	0.0005	852	852	5	59	142	0.02	0.0005	850	26	5	59	137	1.00	0.18	0.04	0.49
M11112122	0.35	0.42	0.71	0.71	0.70	0.02	0.0005	835	835	5	59	127	0.02	0.0005	833	26	5	59	123	1.00	0.19	0.04	0.49
M21112121	0.31	0.45	0.71	0.71	0.72	0.02	0.0004	904	904	6	66	132	0.02	0.0004	902	28	6	66	128	1.00	0.19	0.04	0.52
M21112122	0.32	0.44	0.71	0.71	0.74	0.02	0.0004	891	891	6	66	118	0.02	0.0004	889	27	6	66	114	1.00	0.20	0.05	0.52
M31112121	0.28	0.48	0.71	0.71	0.75	0.01	0.0004	947	947	7	72	120	0.01	0.0004	945	29	7	72	117	1.00	0.20	0.05	0.56
M31112122	0.29	0.47	0.71	0.71	0.78	0.01	0.0004	937	937	7	73	108	0.01	0.0004	934	29	7	73	104	1.00	0.21	0.05	0.56
M41112121	0.26	0.50	0.71	0.71	0.79	0.01	0.0003	983	983	8	79	107	0.01	0.0003	980	30	7	79	103	1.00	0.22	0.05	0.60
M41112122	0.27	0.49	0.71	0.71	0.81	0.01	0.0003	974	974	8	79	95	0.01	0.0003	971	30	7	79	92	1.00	0.23	0.06	0.60
M51112121	0.24	0.53	0.71	0.71	0.83	0.01	0.0003	1041	1041	9	88	92	0.01	0.0003	1037	31	8	87	89	1.00	0.24	0.06	0.64
M51112122	0.24	0.52	0.71	0.71	0.84	0.01	0.0003	1027	1027	9	87	81	0.01	0.0003	1022	31	8	87	78	1.00	0.25	0.07	0.64
M11112211	0.38	0.39	0.71	0.71	0.70	0.02	0.0005	774	774	5	53	120	0.02	0.0005	772	24	5	53	115	1.00	0.20	0.05	0.49
M11112212	0.39	0.38	0.71	0.71	0.73	0.02	0.0006	758	758	5	53	107	0.02	0.0006	756	23	5	53	103	1.00	0.22	0.05	0.49
M21112211	0.34	0.42	0.71	0.71	0.74	0.02	0.0005	835	835	6	60	113	0.02	0.0005	833	26	5	60	109	1.00	0.21	0.05	0.52
M21112212	0.35	0.41	0.71	0.71	0.76	0.02	0.0005	821	821	6	60	101	0.02	0.0005	820	25	6	60	97	1.00	0.22	0.05	0.52
M31112211	0.32	0.44	0.71	0.71	0.77	0.02	0.0004	885	885	6	67	104	0.02	0.0004	883	27	6	67	100	1.00	0.22	0.05	0.56
M31112212	0.32	0.44	0.71	0.71	0.79	0.02	0.0004	875	875	6	67	93	0.02	0.0004	873	27	6	67	89	1.00	0.23	0.06	0.56
M41112211	0.29	0.47	0.71	0.71	0.81	0.01	0.0004	927	927	7	73	92	0.01	0.0004	923	28	7	73	89	1.00	0.24	0.06	0.60
M41112212	0.30	0.46	0.71	0.71	0.83	0.01	0.0004	919	919	7	73	82	0.01	0.0004	916	28	7	73	79	1.00	0.25	0.06	0.60
M51112211	0.27	0.49	0.71	0.71	0.84	0.01	0.0004	959	959	8	79	78	0.01	0.0004	954	29	7	79	75	1.00	0.27	0.07	0.65
M51112212	0.27	0.49	0.71	0.71	0.86	0.01	0.0004	953	953	8	79	69	0.01	0.0004	948	29	7	78	66	1.00	0.27	0.07	0.65
M11112221	0.30	0.46	0.71	0.71	0.70	0.01	0.0004	916	916	6	63	142	0.01	0.0004	914	28	6	63	138	1.00	0.17	0.04	0.49
M11112222	0.31	0.45	0.71	0.71	0.73	0.02	0.0004	903	903	6	64	127	0.02	0.0004	902	28	6	64	124	1.00	0.18	0.04	0.49
M21112221	0.28	0.48	0.71	0.71	0.74	0.01	0.0004	964	964	6	70	130	0.01	0.0004	963	30	6	70	127	1.00	0.18	0.04	0.52
M21112222	0.28	0.47	0.71	0.71	0.76	0.01	0.0004	955	955	7	71	117	0.01	0.0004	953	29	7	71	114	1.00	0.19	0.05	0.52
M31112221	0.25	0.51	0.71	0.71	0.77	0.01	0.0003	1014	1014	7	77	119	0.01	0.0003	1012	31	7	77	115	1.00	0.20	0.05	0.56
M31112222	0.26	0.50	0.71	0.71	0.79	0.01	0.0003	998	998	7	77	106	0.01	0.0003	996	31	7	77	102	1.00	0.20	0.05	0.56
M41112221	0.23	0.54	0.71	0.71	0.80	0.01	0.0003	1077	1077	8	86	107	0.01	0.0003	1074	33	8	86	104	1.00	0.21	0.05	0.60

Name	T1 [s]	Sa(T1) [g]	Sa(T2) [g]	Sa(T3) [g]	DOC [-]	Disp [m]	ISDR [-]	Total Moment [MN-m]	Total Shear [MN]	Max CB Shear [MN]	Max Pp [MN]	Max wall moment [MN-m]	Disp [m]2	ISDR [-]3	Total Moment [MN-m]4	Total Shear [MN]5	Max CB Shear [MN]6	Max Pp [MN]2	Max wall moment [MN-m]8	C1 [-]	C2 [-]	C3 [-]	Mdy/ Mst [-]
M51112221	0.21	0.58	0.71	0.71	0.84	0.01	0.0003	1128	1128	9	94	91	0.01	0.0003	1123	34	9	94	89	1.00	0.23	0.06	0.64
M51112222	0.22	0.57	0.71	0.71	0.86	0.01	0.0003	1117	1117	9	93	81	0.01	0.0003	1113	34	9	93	78	1.00	0.23	0.06	0.65
M11121111	0.83	0.18	0.58	0.71	0.71	0.04	0.0012	487	487	5	51	77	0.04	0.0012	483	15	5	51	69	1.00	0.36	0.10	0.50
M11121112	0.87	0.17	0.54	0.71	0.75	0.05	0.0013	466	466	5	50	64	0.05	0.0013	463	14	5	50	57	1.00	0.37	0.12	0.50
M21121111	0.76	0.20	0.61	0.71	0.75	0.04	0.0011	532	532	6	58	74	0.04	0.0011	529	16	5	58	66	1.00	0.38	0.11	0.53
M21121112	0.79	0.19	0.58	0.71	0.78	0.04	0.0012	515	515	6	58	62	0.04	0.0011	513	16	5	58	55	1.00	0.40	0.12	0.53
M31121111	0.70	0.22	0.64	0.71	0.78	0.04	0.0011	587	587	7	67	71	0.04	0.0010	582	18	6	67	63	1.00	0.41	0.11	0.57
M31121112	0.72	0.21	0.62	0.71	0.81	0.04	0.0011	568	568	7	66	59	0.04	0.0011	564	17	6	66	52	1.00	0.43	0.12	0.57
M41121111	0.64	0.24	0.68	0.71	0.81	0.04	0.0010	634	634	8	75	65	0.04	0.0010	627	19	7	75	57	1.00	0.46	0.12	0.61
M41121112	0.66	0.23	0.66	0.71	0.84	0.04	0.0010	619	619	8	75	55	0.04	0.0010	613	19	7	74	47	1.00	0.47	0.13	0.61
M51121111	0.59	0.26	0.71	0.71	0.84	0.03	0.0010	698	698	10	86	58	0.03	0.0009	687	21	8	86	51	0.99	0.50	0.13	0.65
M51121112	0.60	0.26	0.71	0.71	0.87	0.03	0.0010	679	679	10	85	49	0.03	0.0010	667	20	8	84	42	0.99	0.52	0.14	0.66
M11121121	0.68	0.23	0.65	0.71	0.70	0.04	0.0010	605	605	6	64	96	0.04	0.0010	602	19	6	64	88	1.00	0.32	0.08	0.49
M11121122	0.71	0.21	0.62	0.71	0.75	0.04	0.0011	580	580	6	63	80	0.04	0.0011	577	18	6	63	73	1.00	0.34	0.09	0.50
M21121121	0.62	0.25	0.67	0.71	0.74	0.03	0.0009	665	665	7	74	92	0.03	0.0009	661	20	7	74	84	1.00	0.34	0.08	0.53
M21121122	0.64	0.24	0.65	0.71	0.78	0.03	0.0010	637	637	7	73	76	0.03	0.0009	634	20	7	73	69	1.00	0.36	0.10	0.53
M31121121	0.57	0.27	0.70	0.71	0.77	0.03	0.0009	732	732	8	85	88	0.03	0.0009	728	22	8	85	80	1.00	0.36	0.09	0.57
M31121122	0.62	0.25	0.66	0.71	0.79	0.03	0.0009	666	666	8	77	75	0.03	0.0009	663	20	7	77	68	1.00	0.36	0.10	0.57
M41121121	0.56	0.28	0.71	0.71	0.78	0.03	0.0009	748	748	9	88	86	0.03	0.0008	743	23	8	88	79	1.00	0.36	0.09	0.61
M41121122	0.58	0.27	0.69	0.71	0.82	0.03	0.0009	724	724	9	86	72	0.03	0.0009	720	22	8	86	65	1.00	0.38	0.10	0.61
M51121121	0.52	0.30	0.71	0.71	0.81	0.03	0.0008	793	793	10	96	80	0.03	0.0008	787	24	9	96	73	1.00	0.38	0.09	0.66
M51121122	0.54	0.29	0.71	0.71	0.84	0.03	0.0008	774	774	10	95	67	0.03	0.0008	768	23	9	95	60	1.00	0.41	0.10	0.66
M11121211	0.76	0.20	0.60	0.71	0.73	0.04	0.0011	534	534	5	55	80	0.04	0.0011	531	16	5	55	72	1.00	0.34	0.09	0.50
M11121212	0.79	0.19	0.57	0.71	0.76	0.04	0.0012	517	517	5	55	67	0.04	0.0012	515	16	5	55	60	1.00	0.35	0.11	0.50
M21121211	0.70	0.22	0.63	0.71	0.76	0.04	0.0010	589	589	6	64	78	0.04	0.0010	586	18	6	64	71	1.00	0.35	0.10	0.53
M21121212	0.72	0.21	0.61	0.71	0.79	0.04	0.0011	570	570	6	63	65	0.04	0.0011	567	18	6	63	58	1.00	0.37	0.11	0.53
M31121211	0.61	0.25	0.67	0.71	0.80	0.03	0.0009	671	671	8	77	72	0.03	0.0009	667	20	7	77	65	1.00	0.39	0.10	0.57
M31121212	0.63	0.24	0.66	0.71	0.83	0.03	0.0009	649	649	8	76	60	0.03	0.0009	645	20	7	76	53	1.00	0.40	0.11	0.57
M41121211	0.56	0.28	0.71	0.71	0.83	0.03	0.0009	736	736	9	87	67	0.03	0.0009	730	22	8	87	60	1.00	0.42	0.10	0.61
M41121212	0.58	0.27	0.70	0.71	0.86	0.03	0.0009	719	719	9	86	56	0.03	0.0009	714	22	8	86	50	1.00	0.43	0.11	0.61
M51121211	0.52	0.30	0.71	0.71	0.86	0.03	0.0008	792	792	11	98	58	0.03	0.0008	782	24	9	97	52	0.99	0.44	0.12	0.65
M51121212	0.53	0.29	0.71	0.71	0.88	0.03	0.0009	779	779	11	96	49	0.03	0.0008	769	23	9	96	43	0.99	0.46	0.12	0.65
M11121221	0.60	0.26	0.68	0.71	0.73	0.03	0.0009	696	696	7	74	100	0.03	0.0009	694	21	7	74	92	1.00	0.30	0.07	0.50
M11121222	0.62	0.25	0.66	0.71	0.77	0.03	0.0009	667	667	7	74	83	0.03	0.0009	665	21	7	73	76	1.00	0.32	0.08	0.50
M21121221	0.54	0.29	0.70	0.71	0.77	0.03	0.0008	768	768	8	86	95	0.03	0.0008	766	24	8	86	88	1.00	0.31	0.08	0.53
M21121222	0.56	0.28	0.68	0.71	0.80	0.03	0.0008	746	746	8	86	80	0.03	0.0008	744	23	8	86	73	1.00	0.33	0.09	0.53
M31121221	0.50	0.31	0.71	0.71	0.80	0.03	0.0008	832	832	10	97	89	0.03	0.0007	828	25	9	97	82	1.00	0.33	0.08	0.57
M31121222	0.51	0.30	0.71	0.71	0.83	0.03	0.0008	811	811	10	96	75	0.03	0.0008	808	25	9	96	68	1.00	0.35	0.09	0.57
M41121221	0.46	0.34	0.71	0.71	0.83	0.03	0.0007	892	892	11	108	81	0.03	0.0007	886	27	10	108	74	1.00	0.35	0.09	0.61
M41121222	0.47	0.33	0.71	0.71	0.85	0.03	0.0007	875	875	11	107	68	0.03	0.0007	870	27	10	107	62	1.00	0.36	0.09	0.61
M51121221	0.42	0.36	0.71	0.71	0.86	0.02	0.0007	941	941	12	118	69	0.02	0.0006	932	28	11	118	63	1.00	0.37	0.10	0.65
M51121222	0.43	0.35	0.71	0.71	0.88	0.02	0.0007	928	928	12	117	58	0.02	0.0007	919	28	11	117	53	1.00	0.38	0.10	0.65
M11122111	0.48	0.32	0.71	0.71	0.68	0.03	0.0007	858	858	5	58	144	0.03	0.0007	855	26	5	58	136	1.00	0.24	0.05	0.49
M11122112	0.50	0.31	0.71	0.71	0.71	0.03	0.0008	837	837	5	58	129	0.03	0.0007	834	26	5	58	122	1.00	0.25	0.06	0.49
M21122111	0.44	0.34	0.71	0.71	0.72	0.02	0.0007	921	921	6	66	135	0.02	0.0007	917	28	6	66	128	1.00	0.25	0.06	0.52
M21122112	0.45	0.34	0.71	0.71	0.74	0.02	0.0007	905	905	6	66	121	0.02	0.0007	902	28	6	66	115	1.00	0.26	0.06	0.52
M31122111	0.41	0.37	0.71	0.71	0.75	0.02	0.0006	973	973	7	74	124	0.02	0.0006	970	30	7	74	118	1.00	0.27	0.06	0.56
M31122112	0.47	0.33	0.71	0.71	0.73	0.03	0.0007	877	877	6	63	125	0.03	0.0007	874	27	6	63	118	1.00	0.26	0.06	0.57
M41122111	0.37	0.39	0.71	0.71	0.79	0.02	0.0005	1029	1029	8	81	112	0.02	0.0005	1024	31	8	81	106	1.00	0.29	0.07	0.60
M41122112	0.38	0.38	0.71	0.71	0.81	0.02	0.0006	1011	1011	8	81	100	0.02	0.0005	1006	31	8	81	94	1.00	0.30	0.07	0.60
M51122111	0.34	0.42	0.71	0.71	0.83	0.02	0.0005	1091	1091	9	91	97	0.02	0.0005	1083	33	9	90	92	1.00	0.31	0.08	0.65
M51122112	0.35	0.41	0.71	0.71	0.84	0.02	0.0005	1077	1077	9	90	86	0.02	0.0005	1069	32	8	89	81	1.00	0.32	0.08	0.65
M11122121	0.39	0.38	0.71	0.71	0.68	0.02	0.0006	1006	1006	6	69	168	0.02	0.0006	1003	31	6	69	162	1.00	0.20	0.04	0.49
M11122122	0.40	0.37	0.71	0.71	0.70	0.02	0.0006	990	990	6	70	152	0.02	0.0006	988	30	6	70	145	1.00	0.21	0.05	0.49
M21122121	0.35	0.41	0.71	0.71	0.71	0.02	0.0005	1087	1087	7	79	159	0.02	0.0005	1084	33	7	79	153	1.00	0.21	0.05	0.52
M21122122	0.36	0.40	0.71	0.71	0.74	0.02	0.0005	1064	1064	7	79	142	0.02	0.0005	1062	33	7	79	137	1.00	0.22	0.05	0.52
M31122121	0.33	0.43	0.71	0.71	0.75	0.02	0.0005	1154	1154	8	88	147	0.02	0.0005	1150	35	8	88	142	1.00	0.22	0.05	0.56
M31122122	0.33	0.43	0.71	0.71	0.78	0.02	0.0005	1136	1136	8	88	131	0.02	0.0005	1133	35	8	88	126	1.00	0.23	0.06	0.56
M41122121	0.30	0.46	0.71	0.71	0.79	0.02	0.0004	1210	1210	9	97	132	0.02	0.0004	1205	37	9	97	127	1.00	0.24	0.06	0.60
M41122122	0.31	0.45	0.71	0.71	0.81	0.02	0.0004	1196	1196	9	97	117	0.02	0.0004	1191	36	9	97	113	1.00	0.25	0.06	0.60
M51122121	0.28	0.48	0.71	0.71	0.83	0.01	0.0004	1255	1255	10	105	112	0.01	0.0004	1248	38	10	105	107	1.00	0.27	0.07	0.64
M51122122	0.28	0.48	0.71	0.71	0.84	0.01	0.0004	1243	1243	10	105	99	0.01	0.0004	1236	37	10	105	95	1.00	0.28	0.07	0.65
M11122211	0.44	0.35	0.71	0.71	0.70	0.02	0.0006	931	931	6	64	145	0.02	0.0006	928	29	6	64	139	1.00	0.23	0.05	0.49
M11122212	0.45	0.34	0.71	0.71	0.73	0.02	0.0007	915	915	6	64	131	0.02	0.0007	913	28	6	64	124	1.00	0.24	0.05	0.49
M21122211	0.40	0.37	0.71	0.71	0.74	0.02	0.0006	990	990	7	71	135	0.02	0.0006	987	30	6	71	129	1.00	0.24	0.06	0.52
M21122212	0.41	0.36	0.71	0.71	0.76	0.02	0.0006	977	977	7	72	121	0.02	0.0006	975	30	7	72	115	1.00	0.25	0.06	0.52
M31122211	0.37	0.40	0.71	0.71	0.77	0.02	0.0005	1057	1057	8	80	125	0.02	0.0005	1053	32	7	80	119	1.00	0.25	0.06	0.56
M31122212	0.37	0.39	0.71	0.71	0.79	0.02	0.0005	1040	1040	8	79	111	0.02	0.0005	1037	32	7	79	106	1.00	0.26	0.06	0.56
M41122211	0.34	0.42	0.71	0.71	0.81	0.02	0.0005	1123	1123	9	88	113	0.02	0.0005	1119	34	8	88	107	1.00	0.27	0.07	0.60
M41122212	0.34	0.42	0.71	0.71	0.82	0.02	0.0005	1110	1110	9	88	100	0.02	0.0005	1106	34	8	88	95	1.00	0.28	0.07	0.60
M51122211	0.39	0.38	0.71	0.71	0.75	0.02	0.0006	1005	1005	7	73	131	0.02	0.0005	1002	31	7	73	125	1.00	0.24	0.06	0.66
M51122212	0.31	0.45	0.71	0.71	0.86	0.02	0.0005	1167	1167	10	96	85	0.02	0.0005	1160	35	9	96	81	1.00	0.30	0.08	0.65
M11122221	0.35	0.41	0.71	0.71	0.70	0.02	0.0005	1103	1103	7	76	171	0.02	0.0005	1101	34	7	76	166	1.00	0.19	0.04	0.49
M11122222	0.36	0.40	0.71	0.71	0.72	0.02	0.0005	1082	1082	7	76	153	0.02	0.0005	1080	33	7	76	148	1.00	0.20	0.05	0.49
M21122221	0.32	0.44	0.71	0.71	0.74	0.02	0.0004	1178	1178	8	86	160	0.02	0.0004	1175	36	8	86	155	1.00	0.20	0.05	0.52
M21122222	0.33	0.43	0.71	0.71	0.76	0.02	0.0004	1161	1161	8	86	143	0.02	0.0004	1159	36	8	86	138	1.00	0.21	0.05	0.52
M31122221	0.29	0.47	0.71	0.71	0.77	0.01	0.0004	1239	1239	9	94	146	0.01	0.0004	1236	38	9	94	141	1.00	0.21	0.05	0.56
M31122222	0.30	0.46	0.71	0.71	0.79	0.01	0.0004	1227	1227	9	95	131	0.01	0.0004	1224	38	9	95	126	1.00	0.22	0.05	0.56
M41122221	0.27	0.49	0.71	0.71	0.80	0.01	0.0004	1289	1289	10	103	129	0.01	0.0004	1285	39	10	103	125	1.00	0.23	0.06	0.60
M41122222	0.27	0.48	0.71	0.71	0.82	0.01	0.0004	1279	1279	10	103	115	0.01	0.0004	1275	39	10	103	111	1.00	0.24	0.06	0.60
M51122221	0.25	0.52	0.71	0.71	0.84	0.01	0.0003	1354	1354	11	113	110	0.01	0.0003	1348	41	11	112	106	1.00	0.25	0.07	0.64
M51122222	0.25	0.51	0.71	0.71	0.86	0.01	0.0003	1337	1337	11	112	98	0.01	0.0003	1331	40	11	111	94	1.00	0.26	0.07	0.65
M11211111	1.11	0.13	0.47	0.71	0.71	0.06	0.0012	356	356	3	37	58	0.06	0.0012	352	8	3	37	51	1.00	0.40	0.14	0.50
M11211112	1.16	0.13	0.45	0.70	0.75	0.06	0.0012	339	339	3	36	48	0.06	0.0012	337	8	3	36	42	1.00	0.42	0.16	0.50
M21211111	1.01	0.15	0.50	0.71	0.74	0.05	0.0011	393	393	4	43	56	0.05	0.0011	390	9	4	43	49	1.00	0.42	0.14	0.53
M21211112	1.05	0.14	0.48	0.71	0.78	0.06	0.0011	379	379	4	43	47	0.05	0.0011	376	9	4	42	40	1.00	0.44	0.16	0.54
M31211111	0.93	0.16	0.54	0.71	0.78	0.05	0.0010	432	432	5	49	54	0.05	0.0010	427	10	5	49	46	1.00	0.47	0.15	0.57
M31211112	0.96	0.15	0.51	0.71	0.81	0.05	0.0011	418	418	5	49	45	0.05	0.0010	414	10	5	49	38	1.00	0.48	0.17	0.57
M41211111	0.85	0.18	0.59	0.71	0.81	0.05	0.0010	471	471	6	56	51	0.05	0.0009	464	11	5	56	43	1.00	0.54	0.16	0.62
M41211112	0.88	0.17	0.57	0.71	0.84	0.05	0.0010	456	456	6	55	42	0.05	0.0010	450	10	5	55	35	1.00	0.55	0.17	0.62
M51211111	0.78	0.19	0.65	0.71	0.84	0.04	0.0009	513	513	8	63	45	0.04	0.0009	500	11	6	62	37	0.99	0.62	0.18	0.66
M51211112	0.80	0.19	0.64	0.71	0.86	0.04	0.0010	501	501	8	62	38	0.04	0.0009	488	11	6	61	30	0.99	0.63	0.19	0.66
M11211121	0.90	0.17	0.54	0.71	0.70	0.05	0.0010	445	445	4	47	73	0.05	0.0010	441	10	4	47	64	1.00	0.37	0.11	0.50
M11211122	0.95	0.16	0.51	0.71	0.74	0.05	0.0010	427	427	4	47	60	0.05	0.0010	424	10	4	46	53	1.00	0.38	0.12	0.50
M21211121	0.83	0.18	0.58	0.71	0.74	0.04	0.0009	491	491	5	54	70	0.04	0.0009	487	11	5	54	62	1.00	0.40	0.11	0.53
M21211122	0.86	0.17	0.55	0.71	0.78	0.05	0.0009	471	471	5	54	58	0.05	0.0009	468	11	5	54	51	1.00	0.41	0.13	0.53
M31211121	0.76	0.20	0.62	0.71	0.77	0.04	0.0008	533	533	6	62	66	0.04	0.0008	528	12	6	62	58	1.00	0.43	0.12	0.57
M31211122	0.78	0.19	0.59	0.71	0.81	0.04	0.0009	516	516	6	61	55	0.04	0.0009	512	12	6	61	48	1.00	0.45	0.13	0.57
M41211121	0.70	0.22	0.66	0.71	0.80	0.04	0.0008	585	585	8	71	62	0.04	0.0008	578	13	7	70	54	1.00	0.48	0.13	0.61
M41211122	0.76	0.20	0.61	0.71	0.82	0.04	0.0008	535	535	7	64	54	0.04	0.0008	530	12	6	64	46	1.00	0.47	0.14	0.62
M51211121	0.64	0.24	0.71	0.71	0.84	0.04	0.0008	632	632	9	79	55	0.04	0.0008	619	14	7	79	47	0.99	0.54	0.14	0.66
M51211122	0.66	0.23	0.69	0.71	0.86	0.04	0.0008	617	617	9	78	46	0.04	0.0008	604	14	7	77	39	0.99	0.56	0.15	0.66
M11211211	0.99	0.15	0.50	0.71	0.73	0.05	0.0011	407	407	4	43	60	0.05	0.0011	405	9	4	43	53	1.00	0.38	0.13	0.50

Name	T1 [s]	Sa(T1) [g]	Sa(T2) [g]	Sa(T3) [g]	DOC [-]	Disp [m]	ISDR [-]	Total Moment [MN-m]	Total Shear [MN]	Max CB Shear [MN]	Max Pp [MN]	Max wall moment [MN-m]	Disp [m]2	ISDR [-]3	Total Moment [MN-m]4	Total Shear [MN]5	Max CB Shear [MN]6	Max Pp [MN]2	Max wall moment [MN-m]8	C1 [-]	C2 [-]	C3 [-]	Mdy/ Mst [-]
M21211211	0.90	0.17	0.54	0.71	0.77	0.05	0.0010	449	449	5	49	58	0.05	0.0010	446	10	5	49	51	1.00	0.41	0.13	0.53
M21211212	0.93	0.16	0.51	0.71	0.80	0.05	0.0010	436	436	5	49	48	0.05	0.0010	434	10	5	49	42	1.00	0.42	0.15	0.54
M31211211	0.82	0.18	0.58	0.71	0.80	0.04	0.0009	494	494	6	56	55	0.04	0.0009	490	11	5	56	48	1.00	0.45	0.14	0.57
M31211212	0.84	0.18	0.56	0.71	0.83	0.05	0.0009	481	481	6	56	46	0.05	0.0009	477	11	5	56	40	1.00	0.46	0.15	0.57
M41211211	0.75	0.20	0.63	0.71	0.83	0.04	0.0009	538	538	7	64	51	0.04	0.0008	531	12	6	63	44	1.00	0.51	0.14	0.61
M41211212	0.77	0.20	0.61	0.71	0.85	0.04	0.0009	524	524	7	63	43	0.04	0.0008	518	12	6	63	36	1.00	0.52	0.15	0.62
M51211211	0.69	0.22	0.68	0.71	0.86	0.04	0.0008	590	590	9	72	46	0.04	0.0008	578	13	7	72	39	0.99	0.57	0.16	0.66
M51211212	0.70	0.22	0.67	0.71	0.88	0.04	0.0009	577	577	9	71	39	0.04	0.0008	566	13	7	70	32	0.99	0.58	0.16	0.66
M11211221	0.80	0.19	0.58	0.71	0.73	0.04	0.0009	510	510	5	54	75	0.04	0.0009	507	12	5	54	67	1.00	0.35	0.10	0.50
M11211222	0.83	0.18	0.56	0.71	0.77	0.04	0.0009	492	492	5	54	63	0.04	0.0009	490	11	5	54	56	1.00	0.37	0.11	0.50
M21211221	0.73	0.21	0.62	0.71	0.77	0.04	0.0008	563	563	6	63	72	0.04	0.0008	560	13	6	63	65	1.00	0.38	0.10	0.53
M21211222	0.75	0.20	0.60	0.71	0.80	0.04	0.0008	543	543	6	62	60	0.04	0.0008	541	13	6	62	53	1.00	0.39	0.12	0.53
M31211221	0.66	0.23	0.65	0.71	0.80	0.04	0.0007	617	617	7	72	68	0.04	0.0007	613	14	7	72	61	1.00	0.41	0.11	0.57
M31211222	0.68	0.22	0.63	0.71	0.83	0.04	0.0008	601	601	7	71	57	0.04	0.0007	597	14	7	71	50	1.00	0.42	0.12	0.57
M41211221	0.61	0.25	0.69	0.71	0.83	0.03	0.0007	675	675	9	81	64	0.03	0.0007	669	15	8	81	56	1.00	0.44	0.11	0.61
M41211222	0.62	0.24	0.68	0.71	0.85	0.03	0.0007	655	655	9	80	53	0.03	0.0007	649	15	8	80	46	1.00	0.46	0.12	0.61
M51211221	0.56	0.28	0.71	0.71	0.86	0.03	0.0007	737	737	10	92	56	0.03	0.0007	727	16	9	92	49	0.99	0.48	0.12	0.65
M51211222	0.57	0.27	0.71	0.71	0.88	0.03	0.0007	721	721	10	91	47	0.03	0.0007	711	16	9	90	41	0.99	0.49	0.13	0.65
M11212111	0.64	0.24	0.67	0.71	0.68	0.03	0.0007	636	636	4	43	110	0.03	0.0007	632	15	4	43	101	1.00	0.30	0.07	0.49
M11212112	0.66	0.23	0.65	0.71	0.71	0.04	0.0007	620	620	4	43	98	0.04	0.0007	617	14	4	43	90	1.00	0.32	0.08	0.49
M21212111	0.59	0.26	0.69	0.71	0.72	0.03	0.0007	707	707	5	51	107	0.03	0.0007	702	16	5	51	98	1.00	0.32	0.07	0.52
M21212112	0.60	0.26	0.68	0.71	0.74	0.03	0.0007	686	686	5	50	95	0.03	0.0007	683	16	5	50	87	1.00	0.33	0.08	0.53
M31212111	0.54	0.29	0.71	0.71	0.75	0.03	0.0006	768	768	6	58	101	0.03	0.0006	763	17	5	58	93	1.00	0.34	0.08	0.56
M31212112	0.55	0.28	0.71	0.71	0.78	0.03	0.0006	752	752	6	57	90	0.03	0.0006	747	17	5	57	82	1.00	0.35	0.09	0.57
M41212111	0.50	0.31	0.71	0.71	0.79	0.03	0.0006	823	823	7	65	92	0.03	0.0006	817	19	6	65	85	1.00	0.36	0.09	0.61
M41212112	0.51	0.30	0.71	0.71	0.81	0.03	0.0006	808	808	7	64	82	0.03	0.0006	802	18	6	64	75	1.00	0.37	0.09	0.61
M51212111	0.46	0.33	0.71	0.71	0.82	0.03	0.0006	877	877	8	73	80	0.03	0.0005	867	20	7	72	74	1.00	0.39	0.10	0.65
M51212112	0.47	0.33	0.71	0.71	0.84	0.03	0.0006	865	865	8	72	71	0.03	0.0006	855	19	7	72	65	1.00	0.40	0.10	0.65
M11212121	0.51	0.30	0.71	0.71	0.67	0.03	0.0006	804	804	5	55	137	0.03	0.0006	800	18	5	55	129	1.00	0.26	0.05	0.49
M11212122	0.53	0.29	0.71	0.71	0.70	0.03	0.0006	784	784	5	55	123	0.03	0.0006	781	18	5	55	115	1.00	0.27	0.06	0.49
M21212121	0.47	0.33	0.71	0.71	0.71	0.03	0.0005	870	870	6	63	130	0.03	0.0005	867	20	6	63	123	1.00	0.26	0.06	0.52
M21212122	0.49	0.32	0.71	0.71	0.74	0.03	0.0005	851	851	6	63	116	0.03	0.0005	848	20	6	63	109	1.00	0.28	0.06	0.52
M31212121	0.50	0.31	0.71	0.71	0.69	0.03	0.0006	833	833	5	59	134	0.03	0.0006	829	19	5	59	127	1.00	0.26	0.06	0.56
M31212122	0.45	0.34	0.71	0.71	0.77	0.02	0.0005	912	912	7	71	108	0.02	0.0005	908	21	7	71	101	1.00	0.29	0.07	0.56
M41212121	0.40	0.37	0.71	0.71	0.79	0.02	0.0004	975	975	8	78	108	0.02	0.0004	969	22	7	78	102	1.00	0.30	0.07	0.60
M41212122	0.41	0.36	0.71	0.71	0.81	0.02	0.0005	963	963	8	78	96	0.02	0.0005	957	22	7	78	90	1.00	0.31	0.08	0.60
M51212121	0.37	0.39	0.71	0.71	0.82	0.02	0.0004	1029	1029	9	86	93	0.02	0.0004	1021	23	8	86	88	1.00	0.33	0.08	0.65
M51212122	0.38	0.39	0.71	0.71	0.84	0.02	0.0004	1013	1013	9	85	82	0.02	0.0004	1004	23	8	85	77	1.00	0.34	0.09	0.65
M11212211	0.58	0.27	0.69	0.71	0.70	0.03	0.0007	717	717	4	49	115	0.03	0.0007	714	16	4	49	107	1.00	0.29	0.07	0.49
M11212212	0.60	0.26	0.68	0.71	0.73	0.03	0.0007	697	697	4	49	102	0.03	0.0007	694	16	4	49	94	1.00	0.30	0.07	0.49
M21212211	0.53	0.29	0.71	0.71	0.74	0.03	0.0006	784	784	5	56	109	0.03	0.0006	780	18	5	56	102	1.00	0.30	0.07	0.52
M21212212	0.54	0.29	0.70	0.71	0.76	0.03	0.0006	769	769	5	56	98	0.03	0.0006	766	18	5	56	91	1.00	0.31	0.08	0.53
M31212211	0.49	0.32	0.71	0.71	0.77	0.03	0.0006	846	846	6	64	102	0.03	0.0005	841	19	6	64	95	1.00	0.31	0.07	0.56
M31212212	0.50	0.31	0.71	0.71	0.79	0.03	0.0006	831	831	6	63	91	0.03	0.0006	828	19	6	63	84	1.00	0.33	0.08	0.56
M41212211	0.45	0.34	0.71	0.71	0.80	0.02	0.0005	902	902	7	71	93	0.02	0.0005	896	20	7	71	86	1.00	0.33	0.08	0.61
M41212212	0.46	0.34	0.71	0.71	0.82	0.03	0.0005	891	891	7	71	83	0.03	0.0005	885	20	7	70	76	1.00	0.34	0.09	0.61
M51212211	0.41	0.36	0.71	0.71	0.84	0.02	0.0005	949	949	8	78	79	0.02	0.0005	940	21	7	77	73	1.00	0.36	0.09	0.65
M51212212	0.42	0.36	0.71	0.71	0.86	0.02	0.0005	940	940	8	77	70	0.02	0.0005	931	21	7	77	65	1.00	0.37	0.10	0.65
M11212221	0.46	0.33	0.71	0.71	0.70	0.03	0.0005	884	884	5	61	140	0.03	0.0005	881	20	5	61	133	1.00	0.24	0.05	0.49
M11212222	0.48	0.32	0.71	0.71	0.72	0.03	0.0005	866	866	6	61	125	0.03	0.0005	863	20	6	61	118	1.00	0.25	0.06	0.49
M21212221	0.43	0.35	0.71	0.71	0.73	0.02	0.0005	946	946	6	69	131	0.02	0.0005	943	22	6	69	124	1.00	0.25	0.06	0.52
M21212222	0.44	0.35	0.71	0.71	0.76	0.02	0.0005	932	932	7	69	117	0.02	0.0005	930	21	6	69	111	1.00	0.26	0.06	0.52
M31212221	0.39	0.37	0.71	0.71	0.77	0.02	0.0004	998	998	7	76	119	0.02	0.0004	995	23	7	76	113	1.00	0.26	0.06	0.56
M31212222	0.40	0.37	0.71	0.71	0.79	0.02	0.0004	987	987	7	76	107	0.02	0.0004	984	23	7	76	101	1.00	0.27	0.07	0.56
M41212221	0.36	0.40	0.71	0.71	0.80	0.02	0.0004	1066	1066	8	85	108	0.02	0.0004	1061	24	8	85	103	1.00	0.28	0.07	0.60
M41212222	0.37	0.40	0.71	0.71	0.82	0.02	0.0004	1050	1050	8	84	96	0.02	0.0004	1046	24	8	84	91	1.00	0.29	0.07	0.60
M51212221	0.33	0.43	0.71	0.71	0.84	0.02	0.0004	1125	1125	9	93	93	0.02	0.0004	1118	25	9	93	88	1.00	0.31	0.08	0.65
M51212222	0.34	0.42	0.71	0.71	0.86	0.02	0.0004	1113	1113	9	93	82	0.02	0.0004	1106	25	9	93	78	1.00	0.31	0.08	0.65
M11221111	1.28	0.11	0.43	0.69	0.71	0.07	0.0014	403	403	4	42	67	0.06	0.0013	398	9	4	42	57	1.00	0.43	0.16	0.50
M11221112	1.34	0.11	0.40	0.66	0.75	0.07	0.0014	385	385	4	41	56	0.07	0.0014	382	9	4	41	47	1.00	0.44	0.17	0.51
M21221111	1.17	0.12	0.46	0.71	0.74	0.06	0.0013	446	446	5	49	65	0.06	0.0012	441	10	4	49	55	1.00	0.46	0.17	0.54
M21221112	1.22	0.12	0.44	0.69	0.78	0.06	0.0013	429	429	5	48	54	0.06	0.0013	425	10	4	48	45	1.00	0.48	0.18	0.54
M31221111	1.07	0.14	0.48	0.71	0.77	0.06	0.0012	492	492	6	56	63	0.06	0.0011	486	11	5	56	53	1.00	0.50	0.18	0.57
M31221112	1.11	0.13	0.47	0.71	0.81	0.06	0.0012	475	475	6	55	52	0.06	0.0012	470	11	5	55	43	1.00	0.52	0.19	0.58
M41221111	0.98	0.15	0.53	0.71	0.80	0.05	0.0011	540	540	7	64	59	0.05	0.0011	530	12	6	64	49	1.00	0.56	0.19	0.62
M41221112	1.01	0.15	0.51	0.71	0.83	0.05	0.0012	522	522	7	63	49	0.05	0.0011	514	12	6	62	40	1.00	0.57	0.20	0.62
M51221111	0.90	0.16	0.60	0.71	0.84	0.05	0.0011	590	590	9	72	53	0.05	0.0010	572	13	7	71	42	0.99	0.67	0.21	0.66
M51221112	0.93	0.16	0.59	0.71	0.86	0.05	0.0011	575	575	9	71	45	0.05	0.0011	559	13	7	70	35	0.99	0.68	0.22	0.67
M11221121	1.04	0.14	0.49	0.71	0.70	0.05	0.0011	509	509	5	54	84	0.05	0.0011	504	12	5	53	74	1.00	0.38	0.13	0.50
M11221122	1.09	0.13	0.47	0.71	0.74	0.06	0.0012	485	485	5	53	70	0.06	0.0012	482	11	5	53	61	1.00	0.40	0.15	0.50
M21221121	0.95	0.16	0.52	0.71	0.74	0.05	0.0011	561	561	6	62	81	0.05	0.0010	556	13	6	62	71	1.00	0.42	0.13	0.53
M21221122	0.99	0.15	0.49	0.71	0.78	0.05	0.0011	539	539	6	61	67	0.05	0.0011	535	12	6	61	58	1.00	0.43	0.15	0.53
M31221121	0.87	0.17	0.56	0.71	0.77	0.05	0.0010	612	612	7	71	77	0.05	0.0010	606	14	7	71	67	1.00	0.46	0.14	0.57
M31221122	0.91	0.16	0.54	0.71	0.81	0.05	0.0010	591	591	7	70	64	0.05	0.0010	586	14	7	70	55	1.00	0.47	0.16	0.57
M41221121	0.80	0.19	0.61	0.71	0.80	0.04	0.0009	669	669	9	80	73	0.04	0.0009	659	15	8	80	62	1.00	0.52	0.15	0.61
M41221122	0.87	0.17	0.56	0.71	0.82	0.05	0.0010	614	614	8	74	63	0.05	0.0009	608	14	7	73	53	1.00	0.50	0.16	0.62
M51221121	0.74	0.21	0.67	0.71	0.84	0.04	0.0009	729	729	11	91	65	0.04	0.0009	711	16	9	90	54	0.99	0.60	0.17	0.66
M51221122	0.76	0.20	0.65	0.71	0.86	0.04	0.0009	705	705	11	89	54	0.04	0.0009	689	16	8	88	44	0.99	0.61	0.18	0.66
M11221211	1.14	0.13	0.46	0.71	0.73	0.06	0.0012	461	461	5	48	69	0.06	0.0012	457	11	4	48	60	1.00	0.41	0.15	0.50
M11221212	1.18	0.12	0.44	0.69	0.77	0.06	0.0013	444	444	5	48	58	0.06	0.0012	441	10	4	48	50	1.00	0.43	0.17	0.51
M21221211	1.04	0.14	0.48	0.71	0.77	0.05	0.0011	514	514	6	56	67	0.05	0.0011	510	12	5	56	58	1.00	0.44	0.15	0.54
M21221212	1.07	0.14	0.47	0.71	0.80	0.06	0.0012	497	497	6	56	56	0.06	0.0011	494	11	5	56	48	1.00	0.45	0.17	0.54
M31221211	0.95	0.16	0.52	0.71	0.80	0.05	0.0011	566	566	7	64	64	0.05	0.0010	560	13	6	64	55	1.00	0.48	0.16	0.57
M31221212	0.97	0.15	0.50	0.71	0.83	0.05	0.0011	550	550	7	64	53	0.05	0.0010	546	13	6	64	45	1.00	0.48	0.17	0.58
M41221211	0.87	0.17	0.58	0.71	0.83	0.05	0.0010	617	617	8	73	60	0.05	0.0010	608	14	7	73	50	1.00	0.54	0.17	0.62
M41221212	0.89	0.17	0.56	0.71	0.85	0.05	0.0010	601	601	8	72	50	0.05	0.0010	593	14	7	72	41	1.00	0.55	0.18	0.62
M51221211	0.79	0.19	0.64	0.71	0.85	0.04	0.0010	676	676	10	83	54	0.04	0.0009	658	15	8	82	44	0.99	0.63	0.18	0.66
M51221212	0.81	0.19	0.63	0.71	0.88	0.04	0.0010	662	662	10	81	46	0.04	0.0009	646	15	8	80	36	0.99	0.63	0.19	0.66
M11221221	0.92	0.16	0.53	0.71	0.73	0.05	0.0010	583	583	6	62	87	0.05	0.0010	580	13	6	62	77	1.00	0.37	0.12	0.50
M11221222	0.96	0.16	0.50	0.71	0.77	0.05	0.0010	563	563	6	62	72	0.05	0.0010	560	13	6	62	64	1.00	0.38	0.13	0.50
M21221221	0.84	0.18	0.57	0.71	0.76	0.04	0.0009	645	645	7	72	84	0.04	0.0009	641	15	7	72	74	1.00	0.40	0.12	0.53
M21221222	0.87	0.17	0.54	0.71	0.80	0.05	0.0009	623	623	7	71	70	0.05	0.0009	620	14	7	71	61	1.00	0.41	0.14	0.53
M31221221	0.77	0.20	0.61	0.71	0.79	0.04	0.0009	703	703	8	82	79	0.04	0.0008	697	16	8	81	69	1.00	0.44	0.13	0.57
M31221222	0.79	0.19	0.59	0.71	0.83	0.04	0.0009	685	685	8	81	66	0.04	0.0009	681	16	8	81	58	1.00	0.45	0.14	0.57
M41221221	0.70	0.22	0.65	0.71	0.82	0.04	0.0008	773	773	10	93	74	0.04	0.0008	764	17	9	93	64	1.00	0.48	0.13	0.61
M41221222	0.72	0.21	0.63	0.71	0.85	0.04	0.0008	753	753	10	92	62	0.04	0.0008	745	17	9	92	53	1.00	0.50	0.14	0.61
M51221221	0.64	0.24	0.70	0.71	0.85	0.04	0.0008	837	837	12	104	66	0.04	0.0008	821	19	10	103	56	0.99	0.55	0.15	0.66
M51221222	0.66	0.23	0.69	0.71	0.88	0.04	0.0008	821	821	12	103	56	0.04	0.0008	805	18	10	102	46	0.99	0.56	0.15	0.66
M11222111	0.74	0.20	0.63	0.71	0.68	0.04	0.0008	732	732	4	50	128	0.04	0.0008	726	17	4	50	116	1.00	0.33	0.08	0.49
M11222112	0.76	0.20	0.61	0.71	0.70	0.04	0.0008	707	707	4	49	113	0.04	0.0008	702	16	4	49	102	1.00	0.34	0.09	0.50
M21222111	0.68	0.23	0.65	0.71	0.71	0.04	0.0008	804	804	5	58	123	0.04	0.0008	798	18	5	58	112	1.00	0.35	0.09	0.53
M21222112	0.70	0.22	0.64	0.71	0.74	0.04	0.0008	784	784	5	57	110	0.04	0.0008	779	18	5	57	99	1.00	0.36	0.09	0.53
M31222111	0.62	0.25	0.68	0.71	0.75	0.03	0.0007	874	874	6	66	117	0.03	0.0007	867	20	6	66	106	1.00	0.38	0.09	0.57

Name	T1 [s]	Sa(T1) [g]	Sa(T2) [g]	Sa(T3) [g]	DOC [-]	Disp [m]	ISDR [-]	Total Moment [MN-m]	Total Shear [MN]	Max CB Shear [MN]	Max Pp [MN]	Max wall moment [MN-m]	Disp [m]2	ISDR [-]3	Total Moment [MN-m]4	Total Shear [MN]5	Max CB Shear [MN]6	Max Pp [MN]2	Max wall moment [MN-m]8	C1 [-]	C2 [-]	C3 [-]	Mdy/ Mst [-]
M41222111	0.57	0.27	0.71	0.71	0.79	0.03	0.0007	957	957	8	75	109	0.03	0.0007	948	22	7	75	98	1.00	0.41	0.10	0.61
M41222112	0.59	0.26	0.70	0.71	0.81	0.03	0.0007	937	937	8	75	97	0.03	0.0007	928	21	7	74	87	1.00	0.42	0.11	0.61
M51222111	0.53	0.29	0.71	0.71	0.82	0.03	0.0007	1030	1030	9	85	95	0.03	0.0006	1016	23	8	85	86	0.99	0.44	0.11	0.65
M51222112	0.54	0.29	0.71	0.71	0.84	0.03	0.0007	1014	1014	9	84	85	0.03	0.0006	1000	23	8	84	76	0.99	0.46	0.12	0.65
M11222121	0.59	0.26	0.69	0.71	0.67	0.03	0.0007	929	929	6	64	160	0.03	0.0007	923	21	6	64	149	1.00	0.28	0.06	0.49
M11222122	0.61	0.25	0.68	0.71	0.70	0.03	0.0007	896	896	6	63	142	0.03	0.0007	892	21	6	63	131	1.00	0.30	0.07	0.49
M21222121	0.54	0.29	0.71	0.71	0.71	0.03	0.0006	1017	1017	7	74	154	0.03	0.0006	1012	23	7	74	143	1.00	0.30	0.07	0.52
M21222122	0.56	0.28	0.70	0.71	0.74	0.03	0.0006	991	991	7	73	137	0.03	0.0006	987	23	7	73	127	1.00	0.31	0.07	0.53
M31222121	0.50	0.31	0.71	0.71	0.75	0.03	0.0006	1095	1095	8	84	144	0.03	0.0006	1089	25	8	83	134	1.00	0.32	0.07	0.56
M31222122	0.51	0.30	0.71	0.71	0.77	0.03	0.0006	1072	1072	8	83	128	0.03	0.0006	1066	24	8	83	119	1.00	0.33	0.08	0.56
M41222121	0.46	0.33	0.71	0.71	0.78	0.03	0.0005	1171	1171	9	94	131	0.03	0.0005	1162	27	9	93	122	1.00	0.34	0.08	0.60
M41222122	0.47	0.33	0.71	0.71	0.81	0.03	0.0005	1151	1151	9	93	117	0.03	0.0005	1143	26	9	93	108	1.00	0.35	0.09	0.61
M51222121	0.43	0.35	0.71	0.71	0.82	0.02	0.0005	1235	1235	11	104	113	0.02	0.0005	1223	28	10	103	105	1.00	0.37	0.09	0.65
M51222122	0.43	0.35	0.71	0.71	0.84	0.02	0.0005	1219	1219	11	103	100	0.02	0.0005	1207	27	10	102	93	1.00	0.38	0.10	0.65
M11222211	0.67	0.23	0.65	0.71	0.70	0.04	0.0008	815	815	5	55	132	0.04	0.0008	810	19	5	55	121	1.00	0.32	0.08	0.49
M11222212	0.69	0.22	0.64	0.71	0.73	0.04	0.0008	795	795	5	55	118	0.04	0.0008	791	18	5	55	108	1.00	0.33	0.08	0.50
M21222211	0.61	0.25	0.68	0.71	0.74	0.03	0.0007	897	897	6	64	127	0.03	0.0007	892	21	6	64	116	1.00	0.33	0.08	0.53
M21222212	0.63	0.24	0.66	0.71	0.76	0.03	0.0007	872	872	6	64	113	0.03	0.0007	868	20	6	64	103	1.00	0.35	0.09	0.53
M31222211	0.56	0.28	0.70	0.71	0.77	0.03	0.0006	985	985	7	74	121	0.03	0.0006	979	22	7	74	111	1.00	0.35	0.09	0.56
M31222212	0.58	0.27	0.69	0.71	0.79	0.03	0.0007	965	965	7	73	108	0.03	0.0006	960	22	7	73	98	1.00	0.36	0.09	0.57
M41222211	0.52	0.30	0.71	0.71	0.80	0.03	0.0006	1060	1060	8	83	111	0.03	0.0006	1052	24	8	83	101	1.00	0.38	0.09	0.61
M41222212	0.53	0.29	0.71	0.71	0.82	0.03	0.0006	1045	1045	9	83	99	0.03	0.0006	1037	24	8	83	89	1.00	0.39	0.10	0.61
M51222211	0.48	0.32	0.71	0.71	0.84	0.03	0.0006	1135	1135	10	93	96	0.03	0.0006	1122	25	9	92	88	1.00	0.41	0.10	0.65
M51222212	0.48	0.32	0.71	0.71	0.85	0.03	0.0006	1121	1121	10	92	85	0.03	0.0006	1108	25	9	92	77	0.99	0.42	0.11	0.65
M11222221	0.54	0.29	0.71	0.71	0.70	0.03	0.0006	1035	1035	6	71	166	0.03	0.0006	1030	24	6	71	155	1.00	0.27	0.06	0.49
M11222222	0.55	0.28	0.70	0.71	0.72	0.03	0.0006	1010	1010	7	71	148	0.03	0.0006	1006	23	6	71	138	1.00	0.28	0.07	0.49
M21222221	0.49	0.31	0.71	0.71	0.73	0.03	0.0006	1123	1123	8	82	157	0.03	0.0006	1118	26	7	82	147	1.00	0.28	0.06	0.52
M21222222	0.50	0.31	0.71	0.71	0.76	0.03	0.0006	1100	1100	8	81	140	0.03	0.0006	1096	25	8	81	131	1.00	0.29	0.07	0.53
M31222221	0.45	0.34	0.71	0.71	0.77	0.02	0.0005	1204	1204	9	92	146	0.02	0.0005	1199	28	9	92	137	1.00	0.29	0.07	0.56
M31222222	0.46	0.33	0.71	0.71	0.79	0.03	0.0005	1186	1186	9	91	130	0.03	0.0005	1181	27	9	91	121	1.00	0.31	0.07	0.56
M41222221	0.41	0.36	0.71	0.71	0.80	0.02	0.0005	1272	1272	10	101	131	0.02	0.0005	1265	29	10	101	123	1.00	0.31	0.08	0.60
M41222222	0.52	0.30	0.71	0.71	0.74	0.03	0.0006	1062	1062	7	77	143	0.03	0.0006	1058	24	7	77	134	1.00	0.29	0.07	0.61
M51222221	0.38	0.38	0.71	0.71	0.84	0.02	0.0004	1334	1334	11	111	111	0.02	0.0004	1322	30	10	110	104	1.00	0.34	0.09	0.65
M51222222	0.39	0.38	0.71	0.71	0.86	0.02	0.0004	1316	1316	11	110	99	0.02	0.0004	1305	30	10	109	92	1.00	0.35	0.09	0.65
M12111111	2.81	0.04	0.21	0.44	0.70	0.12	0.0017	324	324	2	33	61	0.11	0.0016	316	5	1	33	45	1.00	0.57	0.27	0.47
M12111112	2.93	0.04	0.19	0.40	0.74	0.12	0.0017	304	304	2	32	50	0.12	0.0016	298	5	1	32	37	1.00	0.59	0.29	0.47
M22111111	2.56	0.05	0.23	0.46	0.73	0.11	0.0016	371	371	2	40	61	0.11	0.0015	362	6	2	40	45	1.00	0.61	0.29	0.50
M22111112	2.66	0.04	0.21	0.43	0.77	0.11	0.0016	351	351	2	39	50	0.11	0.0015	344	5	2	39	36	1.00	0.63	0.31	0.50
M32111111	2.34	0.05	0.26	0.48	0.77	0.11	0.0016	423	423	3	48	60	0.11	0.0014	412	6	2	48	44	1.00	0.68	0.31	0.53
M32111112	2.42	0.05	0.24	0.46	0.80	0.11	0.0016	403	403	3	46	49	0.11	0.0015	394	6	2	46	36	1.00	0.69	0.33	0.53
M42111111	2.15	0.06	0.30	0.53	0.80	0.10	0.0015	484	484	4	57	59	0.10	0.0014	467	7	3	56	42	0.99	0.78	0.34	0.57
M42111112	2.21	0.06	0.28	0.50	0.83	0.11	0.0016	464	464	4	55	48	0.10	0.0014	450	7	3	55	34	0.99	0.79	0.36	0.57
M52111111	1.96	0.07	0.35	0.61	0.83	0.10	0.0015	557	557	5	68	55	0.10	0.0014	523	8	3	66	37	0.97	0.92	0.42	0.61
M52111112	2.01	0.07	0.34	0.60	0.86	0.10	0.0016	541	541	5	67	45	0.10	0.0014	510	8	3	65	30	0.97	0.93	0.43	0.61
M12111121	2.28	0.06	0.26	0.50	0.69	0.11	0.0015	439	439	2	46	81	0.10	0.0014	430	7	2	46	63	1.00	0.53	0.22	0.46
M12111122	2.39	0.05	0.24	0.47	0.74	0.11	0.0015	410	410	2	44	66	0.11	0.0015	403	6	2	44	51	1.00	0.53	0.25	0.46
M22111121	2.08	0.06	0.29	0.53	0.73	0.10	0.0014	505	505	3	55	81	0.10	0.0014	495	8	3	55	63	1.00	0.56	0.24	0.49
M22111122	2.17	0.06	0.27	0.49	0.77	0.10	0.0015	475	475	3	54	66	0.10	0.0014	468	7	3	54	51	1.00	0.58	0.26	0.49
M32111121	1.91	0.07	0.32	0.56	0.77	0.10	0.0014	565	565	4	65	79	0.09	0.0013	552	9	3	65	60	1.00	0.62	0.26	0.52
M32111122	1.98	0.07	0.30	0.53	0.80	0.10	0.0014	543	543	4	64	65	0.10	0.0013	534	8	3	64	49	1.00	0.63	0.28	0.52
M42111121	1.75	0.08	0.35	0.61	0.80	0.09	0.0013	622	622	5	74	74	0.09	0.0012	603	9	4	74	55	0.99	0.72	0.30	0.56
M42111122	1.80	0.08	0.34	0.59	0.83	0.09	0.0013	602	602	5	73	61	0.09	0.0012	586	9	3	73	45	0.99	0.73	0.32	0.56
M52111121	1.60	0.09	0.41	0.68	0.83	0.08	0.0013	692	692	6	86	67	0.08	0.0012	656	10	4	84	48	0.97	0.86	0.37	0.61
M52111122	1.64	0.08	0.40	0.66	0.86	0.09	0.0013	672	672	6	84	55	0.09	0.0012	637	10	4	82	38	0.97	0.87	0.38	0.61
M12111211	2.49	0.05	0.23	0.46	0.73	0.11	0.0016	386	386	2	40	65	0.11	0.0015	379	6	2	40	50	1.00	0.55	0.25	0.47
M12111212	2.59	0.05	0.22	0.43	0.77	0.11	0.0016	366	366	2	39	53	0.11	0.0015	360	6	2	39	40	1.00	0.56	0.28	0.47
M22111211	2.26	0.06	0.26	0.48	0.76	0.10	0.0015	445	445	3	48	65	0.10	0.0014	437	7	2	48	49	1.00	0.59	0.26	0.49
M22111212	2.34	0.05	0.24	0.46	0.80	0.11	0.0015	425	425	3	48	53	0.10	0.0014	419	7	2	48	40	1.00	0.59	0.28	0.49
M32111211	2.07	0.06	0.29	0.52	0.79	0.10	0.0015	512	512	3	58	64	0.10	0.0014	502	8	3	58	48	1.00	0.64	0.28	0.52
M32111212	2.12	0.06	0.28	0.49	0.83	0.10	0.0015	491	491	3	57	53	0.10	0.0014	483	8	3	57	39	1.00	0.66	0.30	0.53
M42111211	1.89	0.07	0.33	0.57	0.82	0.10	0.0014	573	573	4	67	62	0.09	0.0013	556	9	3	67	45	0.99	0.74	0.32	0.56
M42111212	1.93	0.07	0.32	0.55	0.85	0.10	0.0014	559	559	4	67	51	0.10	0.0013	545	8	3	66	36	0.99	0.75	0.33	0.56
M52111211	1.72	0.08	0.38	0.65	0.85	0.09	0.0013	640	640	6	78	55	0.09	0.0012	606	9	4	76	38	0.97	0.88	0.39	0.61
M52111212	1.75	0.08	0.37	0.64	0.88	0.09	0.0014	626	626	6	77	46	0.09	0.0013	594	9	4	75	31	0.97	0.89	0.40	0.61
M12111221	2.02	0.07	0.29	0.53	0.73	0.10	0.0014	531	531	3	56	87	0.10	0.0014	523	8	3	56	70	1.00	0.50	0.21	0.46
M12111222	2.10	0.06	0.27	0.49	0.77	0.10	0.0014	502	502	3	55	71	0.10	0.0014	497	8	3	55	57	1.00	0.51	0.23	0.46
M22111221	1.83	0.07	0.32	0.56	0.76	0.09	0.0013	591	591	3	66	84	0.09	0.0012	583	9	3	66	67	1.00	0.54	0.23	0.49
M22111222	1.90	0.07	0.30	0.53	0.80	0.09	0.0013	571	571	3	65	70	0.09	0.0013	565	9	3	65	55	1.00	0.55	0.24	0.49
M32111221	1.67	0.08	0.35	0.60	0.79	0.08	0.0012	652	652	4	75	81	0.08	0.0011	641	10	4	75	63	1.00	0.60	0.25	0.52
M32111222	1.72	0.08	0.34	0.57	0.82	0.09	0.0012	634	634	4	75	67	0.09	0.0012	625	10	4	75	52	1.00	0.62	0.27	0.52
M42111221	1.53	0.09	0.39	0.65	0.82	0.08	0.0011	720	720	5	86	76	0.08	0.0011	702	11	4	86	57	0.99	0.68	0.29	0.56
M42111222	1.57	0.09	0.37	0.63	0.85	0.08	0.0012	702	702	5	85	63	0.08	0.0011	686	11	4	85	47	0.99	0.69	0.30	0.56
M52111221	1.40	0.10	0.45	0.71	0.85	0.07	0.0011	801	801	7	100	68	0.07	0.0010	764	12	5	97	49	0.98	0.82	0.34	0.60
M52111222	1.42	0.10	0.44	0.70	0.88	0.08	0.0011	784	784	7	98	57	0.08	0.0011	749	12	5	96	40	0.98	0.83	0.35	0.60
M12112111	1.62	0.09	0.36	0.64	0.67	0.08	0.0012	676	676	2	45	129	0.08	0.0011	663	10	2	45	106	1.00	0.45	0.17	0.46
M12112112	1.67	0.08	0.35	0.62	0.70	0.08	0.0012	654	654	2	45	115	0.08	0.0011	644	10	2	45	94	1.00	0.47	0.18	0.46
M22112111	1.48	0.09	0.39	0.66	0.71	0.08	0.0011	744	744	3	53	125	0.08	0.0010	731	11	2	53	102	1.00	0.49	0.19	0.49
M22112112	1.52	0.09	0.37	0.64	0.74	0.08	0.0011	722	722	3	52	110	0.08	0.0011	712	11	2	52	90	1.00	0.50	0.20	0.49
M32112111	1.36	0.10	0.42	0.68	0.74	0.07	0.0010	817	817	3	61	120	0.07	0.0010	801	12	3	61	97	1.00	0.55	0.21	0.52
M32112112	1.40	0.10	0.41	0.67	0.77	0.07	0.0010	795	795	3	60	106	0.07	0.0010	782	12	3	60	85	1.00	0.56	0.22	0.52
M42112111	1.25	0.11	0.46	0.71	0.78	0.07	0.0010	896	896	4	70	112	0.07	0.0009	873	13	3	70	89	1.00	0.63	0.24	0.56
M42112112	1.28	0.11	0.45	0.70	0.80	0.07	0.0010	876	876	4	69	100	0.07	0.0009	856	13	3	69	78	1.00	0.64	0.25	0.56
M52112111	1.15	0.13	0.52	0.71	0.82	0.06	0.0009	990	990	5	81	100	0.06	0.0009	950	15	4	80	78	0.98	0.74	0.26	0.60
M52112112	1.17	0.12	0.50	0.71	0.84	0.06	0.0009	972	972	5	80	88	0.06	0.0009	934	14	4	79	68	0.98	0.75	0.28	0.60
M12112121	1.30	0.11	0.43	0.70	0.67	0.07	0.0009	860	860	3	58	162	0.07	0.0009	847	13	3	58	137	1.00	0.42	0.15	0.46
M12112122	1.34	0.11	0.42	0.68	0.70	0.07	0.0010	831	831	3	58	143	0.07	0.0010	821	13	3	58	121	1.00	0.43	0.16	0.46
M22112121	1.19	0.12	0.46	0.71	0.71	0.06	0.0009	950	950	3	68	156	0.06	0.0009	936	15	3	68	133	1.00	0.45	0.16	0.48
M22112122	1.23	0.12	0.44	0.70	0.73	0.06	0.0009	921	921	3	68	139	0.06	0.0009	909	14	3	68	117	1.00	0.47	0.17	0.48
M32112121	1.10	0.13	0.48	0.71	0.74	0.06	0.0008	1043	1043	4	79	149	0.06	0.0008	1028	16	4	79	126	1.00	0.49	0.17	0.52
M32112122	1.12	0.13	0.47	0.71	0.77	0.06	0.0008	1014	1014	4	78	132	0.06	0.0008	1000	16	4	78	110	1.00	0.51	0.18	0.52
M42112121	1.01	0.15	0.53	0.71	0.78	0.06	0.0008	1142	1142	5	91	140	0.06	0.0008	1119	17	4	90	116	1.00	0.57	0.18	0.56
M42112122	1.03	0.14	0.52	0.71	0.80	0.06	0.0008	1117	1117	5	90	123	0.06	0.0008	1096	17	4	89	102	1.00	0.57	0.20	0.56
M52112121	0.93	0.16	0.60	0.71	0.82	0.05	0.0008	1255	1255	7	105	124	0.05	0.0007	1213	19	5	103	101	0.99	0.68	0.21	0.60
M52112122	0.94	0.16	0.59	0.71	0.84	0.05	0.0008	1232	1232	7	103	110	0.05	0.0007	1191	18	5	102	87	0.98	0.69	0.22	0.60
M12112211	1.47	0.10	0.39	0.66	0.69	0.07	0.0010	753	753	2	51	133	0.07	0.0010	742	12	2	51	111	1.00	0.44	0.17	0.46
M12112212	1.51	0.09	0.37	0.64	0.72	0.08	0.0011	731	731	2	51	118	0.08	0.0010	722	11	2	50	98	1.00	0.45	0.18	0.46
M22112211	1.34	0.11	0.42	0.68	0.73	0.07	0.0010	833	833	3	59	129	0.07	0.0009	822	13	3	59	107	1.00	0.48	0.18	0.48
M22112212	1.37	0.10	0.40	0.66	0.76	0.07	0.0010	811	811	3	59	114	0.07	0.0010	802	13	3	59	94	1.00	0.49	0.19	0.49
M32112211	1.23	0.12	0.45	0.70	0.76	0.06	0.0009	917	917	4	68	123	0.06	0.0009	903	14	3	68	101	1.00	0.53	0.20	0.52
M32112212	1.26	0.11	0.44	0.69	0.79	0.07	0.0009	896	896	4	68	109	0.07	0.0009	883	14	3	68	89	1.00	0.54	0.21	0.52
M42112211	1.13	0.13	0.48	0.71	0.80	0.06	0.0009	1008	1008	5	78	115	0.06	0.0008	987	15	4	78	93	1.00	0.60	0.22	0.56
M42112212	1.15	0.13	0.48	0.71	0.82	0.06	0.0009	989	989	5	78	102	0.06	0.0008	970	15	4	78	81	1.00	0.61	0.23	0.56
M52112211	1.03	0.14	0.56	0.71	0.83	0.06	0.0008	1118	1118	6	91	103	0.06	0.0008	1077	17	4	89	81	0.98	0.72	0.24	0.60

Name	T1 [s]	Sa(T1) [g]	Sa(T2) [g]	Sa(T3) [g]	DOC [-]	Disp [m]	ISDR [-]	Total Moment [MN-m]	Total Shear [MN]	Max CB Shear [MN]	Max Pp [MN]	Max wall moment [MN-m]	Disp [m]2	ISDR [-]3	Total Moment [MN-m]4	Total Shear [MN]5	Max CB Shear [MN]6	Max Pp [MN]2	Max wall moment [MN-m]8	C1 [-]	C2 [-]	C3 [-]	Mdy/ Mst [-]
M12112221	1.18	0.12	0.46	0.71	0.69	0.06	0.0009	966	966	3	66	167	0.06	0.0008	954	15	3	66	144	1.00	0.41	0.14	0.45
M12112222	1.21	0.12	0.44	0.70	0.72	0.06	0.0009	937	937	3	66	149	0.06	0.0009	928	15	3	66	127	1.00	0.42	0.15	0.46
M22112221	1.07	0.14	0.48	0.71	0.73	0.06	0.0008	1071	1071	4	77	161	0.06	0.0008	1059	17	4	77	139	1.00	0.43	0.15	0.48
M22112222	1.10	0.13	0.47	0.71	0.76	0.06	0.0008	1043	1043	4	77	143	0.06	0.0008	1033	16	4	77	122	1.00	0.45	0.16	0.48
M32112221	0.99	0.15	0.52	0.71	0.76	0.05	0.0007	1176	1176	5	89	154	0.05	0.0007	1162	18	4	89	132	1.00	0.48	0.16	0.52
M32112222	1.01	0.15	0.50	0.71	0.79	0.05	0.0008	1149	1149	5	88	136	0.05	0.0007	1137	18	4	88	115	1.00	0.48	0.17	0.52
M42112221	0.90	0.16	0.57	0.71	0.80	0.05	0.0007	1284	1284	6	101	143	0.05	0.0007	1262	20	5	101	120	1.00	0.55	0.17	0.55
M42112222	0.92	0.16	0.56	0.71	0.82	0.05	0.0007	1262	1262	6	101	127	0.05	0.0007	1242	19	5	101	105	1.00	0.56	0.18	0.56
M52112221	0.83	0.18	0.64	0.71	0.84	0.05	0.0007	1410	1410	7	117	126	0.05	0.0007	1369	21	5	115	103	0.99	0.64	0.19	0.60
M52112222	0.84	0.18	0.63	0.71	0.85	0.05	0.0007	1388	1388	7	116	111	0.05	0.0007	1348	21	5	114	90	0.99	0.65	0.19	0.60
M12121111	3.24	0.03	0.18	0.39	0.69	0.13	0.0018	352	352	2	36	68	0.12	0.0017	341	5	2	36	49	1.00	0.60	0.29	0.47
M12121112	3.38	0.03	0.16	0.36	0.74	0.13	0.0019	330	330	2	35	56	0.13	0.0018	323	5	2	35	40	1.00	0.62	0.32	0.47
M22121111	2.95	0.04	0.20	0.41	0.73	0.12	0.0018	401	401	2	43	68	0.12	0.0016	390	6	2	43	49	1.00	0.65	0.32	0.50
M22121112	3.07	0.04	0.18	0.38	0.77	0.12	0.0018	379	379	2	42	55	0.12	0.0016	371	6	2	42	39	1.00	0.67	0.34	0.50
M32121111	2.70	0.04	0.22	0.44	0.76	0.12	0.0017	456	456	3	51	67	0.11	0.0015	443	7	2	51	47	1.00	0.72	0.35	0.53
M32121112	2.79	0.04	0.21	0.42	0.80	0.12	0.0017	434	434	3	50	55	0.12	0.0016	424	7	2	50	38	1.00	0.74	0.37	0.53
M42121111	2.48	0.05	0.26	0.48	0.79	0.11	0.0017	522	522	4	61	66	0.11	0.0015	501	8	3	60	45	0.99	0.83	0.39	0.57
M42121112	2.55	0.05	0.24	0.46	0.83	0.11	0.0017	499	499	4	59	54	0.11	0.0015	482	7	3	59	36	0.99	0.84	0.41	0.57
M52121111	2.27	0.06	0.31	0.56	0.83	0.11	0.0017	608	608	6	74	63	0.11	0.0015	564	9	3	71	40	0.97	1.01	0.47	0.62
M52121112	2.32	0.05	0.30	0.54	0.85	0.11	0.0017	586	586	6	72	52	0.11	0.0015	546	8	3	69	32	0.96	1.02	0.49	0.62
M12121121	2.64	0.04	0.22	0.46	0.69	0.11	0.0016	473	473	2	49	90	0.11	0.0015	461	7	2	49	67	1.00	0.56	0.25	0.47
M12121122	2.76	0.04	0.21	0.42	0.74	0.11	0.0016	442	442	2	48	73	0.11	0.0016	433	7	2	47	54	1.00	0.57	0.28	0.47
M22121121	2.41	0.05	0.25	0.48	0.73	0.11	0.0016	541	541	3	59	89	0.11	0.0015	529	8	3	59	67	1.00	0.60	0.27	0.49
M22121122	2.51	0.05	0.23	0.45	0.77	0.11	0.0016	510	510	3	58	73	0.11	0.0015	501	8	3	57	54	1.00	0.61	0.29	0.49
M32121121	2.21	0.06	0.28	0.51	0.76	0.10	0.0015	618	618	4	71	89	0.10	0.0014	603	9	3	71	66	1.00	0.66	0.29	0.53
M32121122	2.28	0.06	0.26	0.48	0.80	0.11	0.0015	586	586	4	69	72	0.10	0.0014	574	9	3	69	53	1.00	0.68	0.31	0.53
M42121121	2.02	0.07	0.32	0.56	0.79	0.10	0.0015	707	707	5	84	86	0.10	0.0014	683	11	4	84	63	0.99	0.75	0.33	0.56
M42121122	2.08	0.06	0.30	0.53	0.83	0.10	0.0015	676	676	5	82	71	0.10	0.0014	655	10	4	81	50	0.99	0.77	0.34	0.56
M52121121	1.85	0.07	0.37	0.63	0.83	0.10	0.0014	791	791	7	98	78	0.09	0.0013	746	11	5	96	54	0.97	0.90	0.40	0.61
M52121122	1.90	0.07	0.36	0.62	0.86	0.10	0.0015	769	769	8	96	65	0.10	0.0014	725	11	4	94	43	0.97	0.91	0.42	0.61
M12121211	2.88	0.04	0.20	0.42	0.72	0.12	0.0017	417	417	2	43	72	0.12	0.0016	407	6	2	43	53	1.00	0.58	0.28	0.47
M12121212	2.99	0.04	0.18	0.38	0.77	0.12	0.0017	395	395	2	43	59	0.12	0.0016	388	6	2	42	43	1.00	0.59	0.30	0.47
M22121211	2.61	0.05	0.22	0.44	0.76	0.11	0.0016	479	479	3	52	72	0.11	0.0015	469	7	2	52	53	1.00	0.62	0.30	0.50
M22121212	2.70	0.04	0.21	0.41	0.80	0.11	0.0016	457	457	3	51	59	0.11	0.0015	450	7	2	51	43	1.00	0.63	0.32	0.50
M32121211	2.39	0.05	0.25	0.47	0.79	0.11	0.0016	548	548	4	62	71	0.11	0.0014	536	8	3	62	52	1.00	0.69	0.32	0.53
M32121212	2.45	0.05	0.23	0.45	0.82	0.11	0.0016	527	527	4	61	58	0.11	0.0015	517	8	3	61	42	1.00	0.69	0.34	0.53
M42121211	2.18	0.06	0.29	0.52	0.82	0.11	0.0016	631	631	5	74	70	0.10	0.0014	610	9	4	73	49	0.99	0.79	0.35	0.57
M42121212	2.23	0.06	0.28	0.49	0.85	0.11	0.0016	609	609	5	73	57	0.11	0.0014	591	9	3	72	39	0.99	0.80	0.36	0.57
M52121211	1.99	0.07	0.35	0.60	0.85	0.10	0.0015	731	731	7	89	65	0.10	0.0014	688	11	4	86	43	0.97	0.93	0.43	0.61
M52121212	2.03	0.07	0.34	0.59	0.87	0.10	0.0016	713	713	7	88	54	0.10	0.0014	673	10	4	85	35	0.97	0.94	0.44	0.61
M12121221	2.33	0.05	0.25	0.48	0.72	0.11	0.0015	570	570	3	60	96	0.10	0.0014	559	9	3	60	74	1.00	0.53	0.24	0.46
M12121222	2.42	0.05	0.23	0.45	0.76	0.11	0.0015	538	538	3	59	78	0.11	0.0015	531	8	3	59	60	1.00	0.54	0.26	0.47
M22121221	2.12	0.06	0.28	0.50	0.76	0.10	0.0014	657	657	4	73	96	0.10	0.0014	647	10	3	73	74	1.00	0.57	0.25	0.49
M22121222	2.19	0.06	0.26	0.48	0.80	0.10	0.0015	626	626	4	71	78	0.10	0.0014	618	10	3	71	60	1.00	0.58	0.27	0.49
M32121221	1.93	0.07	0.31	0.55	0.79	0.10	0.0014	743	743	5	86	94	0.10	0.0013	729	11	4	86	72	1.00	0.63	0.27	0.52
M32121222	1.99	0.07	0.30	0.52	0.82	0.10	0.0014	720	720	5	85	77	0.10	0.0013	709	11	4	85	59	1.00	0.64	0.28	0.52
M42121221	1.77	0.08	0.35	0.60	0.82	0.09	0.0013	820	820	6	98	89	0.09	0.0012	797	12	5	97	65	0.99	0.72	0.31	0.56
M42121222	1.81	0.08	0.34	0.58	0.85	0.09	0.0013	800	800	6	97	74	0.09	0.0012	780	12	5	96	53	0.99	0.73	0.32	0.56
M52121221	1.61	0.09	0.41	0.67	0.85	0.08	0.0013	916	916	8	114	80	0.08	0.0012	869	13	5	111	56	0.97	0.87	0.38	0.61
M52121222	1.65	0.08	0.39	0.66	0.87	0.09	0.0013	894	894	9	112	66	0.09	0.0012	850	13	5	109	45	0.97	0.87	0.39	0.61
M12122111	1.87	0.07	0.33	0.59	0.67	0.09	0.0013	771	771	2	52	149	0.09	0.0013	755	12	2	51	121	1.00	0.48	0.19	0.46
M12122112	1.93	0.07	0.31	0.57	0.70	0.10	0.0013	745	745	2	51	133	0.09	0.0013	732	11	2	51	107	1.00	0.49	0.20	0.46
M22122111	1.71	0.08	0.35	0.62	0.71	0.09	0.0012	848	848	3	60	145	0.09	0.0012	831	13	3	60	116	1.00	0.52	0.21	0.49
M22122112	1.76	0.08	0.34	0.59	0.73	0.09	0.0012	823	823	3	60	128	0.09	0.0012	809	13	3	60	103	1.00	0.53	0.22	0.49
M32122111	1.57	0.09	0.37	0.64	0.74	0.08	0.0011	929	929	4	69	138	0.08	0.0011	910	14	3	69	110	1.00	0.57	0.23	0.52
M32122112	1.61	0.09	0.36	0.62	0.77	0.08	0.0012	906	906	4	69	123	0.08	0.0011	889	14	3	69	97	1.00	0.59	0.24	0.52
M42122111	1.45	0.10	0.42	0.68	0.78	0.08	0.0011	1021	1021	5	80	131	0.08	0.0010	992	15	4	79	102	1.00	0.67	0.26	0.56
M42122112	1.48	0.10	0.40	0.66	0.80	0.08	0.0011	998	998	5	79	116	0.08	0.0010	971	15	4	78	89	1.00	0.68	0.27	0.56
M52122111	1.33	0.11	0.47	0.71	0.81	0.07	0.0011	1130	1130	6	92	117	0.07	0.0010	1078	16	4	90	88	0.98	0.79	0.31	0.60
M52122112	1.35	0.11	0.46	0.71	0.83	0.07	0.0011	1108	1108	6	91	104	0.07	0.0010	1057	16	4	89	77	0.98	0.81	0.32	0.60
M12122121	1.50	0.09	0.39	0.66	0.67	0.08	0.0011	977	977	3	66	186	0.08	0.0011	960	15	3	66	155	1.00	0.44	0.16	0.46
M12122122	1.55	0.09	0.37	0.64	0.70	0.08	0.0011	945	945	3	66	166	0.08	0.0011	931	15	3	66	137	1.00	0.45	0.17	0.46
M22122121	1.38	0.10	0.41	0.68	0.71	0.07	0.0010	1076	1076	4	77	181	0.07	0.0010	1058	16	4	77	150	1.00	0.48	0.18	0.48
M22122122	1.42	0.10	0.40	0.66	0.73	0.07	0.0010	1044	1044	4	77	160	0.07	0.0010	1030	16	4	77	132	1.00	0.49	0.19	0.49
M32122121	1.27	0.11	0.44	0.70	0.74	0.07	0.0009	1180	1180	5	89	173	0.07	0.0009	1159	18	4	89	142	1.00	0.54	0.20	0.52
M32122122	1.30	0.11	0.43	0.69	0.77	0.07	0.0010	1151	1151	5	88	154	0.07	0.0009	1132	18	4	88	125	1.00	0.55	0.21	0.52
M42122121	1.17	0.12	0.48	0.71	0.78	0.06	0.0009	1297	1297	6	103	162	0.06	0.0009	1267	20	5	102	131	1.00	0.60	0.22	0.56
M42122122	1.19	0.12	0.47	0.71	0.80	0.06	0.0009	1268	1268	6	101	144	0.06	0.0009	1241	19	5	101	115	1.00	0.61	0.23	0.56
M52122121	1.07	0.14	0.55	0.71	0.82	0.06	0.0009	1436	1436	8	119	145	0.06	0.0008	1381	21	6	117	115	0.98	0.72	0.24	0.60
M52122122	1.09	0.13	0.54	0.71	0.84	0.06	0.0009	1406	1406	8	118	128	0.06	0.0008	1353	21	6	115	99	0.98	0.73	0.25	0.60
M12122211	1.70	0.08	0.35	0.62	0.69	0.09	0.0012	858	858	3	58	154	0.08	0.0012	843	13	3	58	126	1.00	0.47	0.18	0.46
M12122212	1.74	0.08	0.33	0.59	0.72	0.09	0.0012	833	833	3	58	137	0.09	0.0012	821	13	3	57	112	1.00	0.48	0.19	0.46
M22122211	1.55	0.09	0.37	0.64	0.73	0.08	0.0011	947	947	3	67	149	0.08	0.0011	932	15	3	67	121	1.00	0.51	0.20	0.49
M22122212	1.59	0.09	0.36	0.62	0.76	0.08	0.0011	924	924	3	67	132	0.08	0.0011	911	14	3	67	107	1.00	0.52	0.21	0.49
M32122211	1.42	0.10	0.40	0.67	0.76	0.07	0.0010	1041	1041	4	77	143	0.07	0.0010	1023	16	4	77	115	1.00	0.56	0.22	0.52
M32122212	1.45	0.10	0.39	0.65	0.79	0.07	0.0011	1019	1019	4	77	127	0.07	0.0010	1008	16	4	77	101	1.00	0.57	0.23	0.52
M42122211	1.38	0.10	0.42	0.68	0.77	0.07	0.0010	1071	1071	5	81	140	0.07	0.0010	1050	16	4	81	112	1.00	0.59	0.23	0.56
M42122212	1.41	0.10	0.40	0.66	0.80	0.07	0.0010	1049	1049	5	80	125	0.07	0.0010	1031	16	4	80	99	1.00	0.59	0.24	0.56
M52122211	1.19	0.12	0.50	0.71	0.83	0.06	0.0010	1270	1270	7	103	119	0.06	0.0009	1219	19	5	101	91	0.98	0.75	0.28	0.60
M52122212	1.31	0.11	0.44	0.69	0.82	0.07	0.0010	1140	1140	6	90	118	0.07	0.0009	1112	17	4	89	91	0.99	0.67	0.26	0.60
M12122221	1.36	0.10	0.41	0.68	0.69	0.07	0.0010	1095	1095	4	75	193	0.07	0.0010	1080	17	3	75	163	1.00	0.43	0.16	0.46
M12122222	1.46	0.10	0.38	0.66	0.70	0.07	0.0010	1015	1015	3	69	174	0.07	0.0010	1003	16	3	69	146	1.00	0.43	0.16	0.46
M22122221	1.31	0.11	0.43	0.69	0.71	0.07	0.0009	1143	1143	4	80	191	0.07	0.0009	1128	18	4	80	161	1.00	0.45	0.16	0.48
M22122222	1.27	0.11	0.43	0.69	0.75	0.07	0.0009	1178	1178	4	87	166	0.07	0.0009	1165	18	4	87	138	1.00	0.48	0.18	0.48
M32122221	1.22	0.12	0.45	0.71	0.74	0.06	0.0009	1238	1238	5	90	185	0.06	0.0009	1221	19	4	90	156	1.00	0.48	0.17	0.52
M32122222	1.25	0.11	0.43	0.69	0.76	0.07	0.0009	1204	1204	5	89	164	0.06	0.0009	1191	19	4	89	137	1.00	0.49	0.19	0.52
M42122221	1.04	0.14	0.51	0.71	0.80	0.06	0.0008	1469	1469	7	116	167	0.06	0.0008	1441	22	6	116	137	1.00	0.57	0.20	0.56
M42122222	1.16	0.12	0.46	0.71	0.79	0.06	0.0009	1302	1302	5	100	158	0.06	0.0008	1285	20	5	100	131	1.00	0.52	0.20	0.56
M52122221	0.96	0.16	0.59	0.71	0.83	0.05	0.0008	1620	1620	9	134	148	0.05	0.0008	1566	24	6	132	118	0.98	0.69	0.22	0.60
M52122222	1.09	0.13	0.49	0.71	0.81	0.06	0.0008	1404	1404	6	111	151	0.06	0.0008	1381	21	5	111	123	1.00	0.56	0.20	0.60
M12211111	4.32	0.02	0.13	0.31	0.69	0.15	0.0017	237	237	1	24	49	0.15	0.0015	227	3	1	24	33	0.99	0.66	0.35	0.48
M12211112	4.51	0.02	0.12	0.28	0.73	0.15	0.0017	223	223	1	23	40	0.15	0.0016	216	3	1	23	27	0.99	0.67	0.37	0.48
M22211111	3.94	0.02	0.14	0.33	0.72	0.14	0.0016	268	268	2	29	48	0.14	0.0014	258	3	1	28	32	1.00	0.72	0.39	0.51
M22211112	4.09	0.02	0.13	0.30	0.77	0.14	0.0016	254	254	2	28	39	0.14	0.0015	246	3	1	28	26	1.00	0.73	0.41	0.51
M32211111	3.61	0.03	0.16	0.36	0.76	0.14	0.0015	303	303	2	34	48	0.13	0.0014	291	3	2	34	31	1.00	0.81	0.43	0.54
M32211112	3.72	0.03	0.15	0.34	0.80	0.14	0.0016	289	289	2	33	39	0.14	0.0014	280	3	2	33	25	1.00	0.82	0.45	0.54
M42211111	3.30	0.03	0.19	0.39	0.79	0.13	0.0015	345	345	3	40	47	0.13	0.0013	327	4	2	39	29	0.99	0.93	0.48	0.58
M42211112	3.40	0.03	0.18	0.37	0.82	0.13	0.0015	331	331	3	39	38	0.13	0.0013	315	4	2	39	24	0.99	0.94	0.50	0.58
M52211111	3.02	0.04	0.23	0.46	0.82	0.13	0.0015	404	404	4	48	45	0.12	0.0013	367	4	2	46	26	0.96	1.13	0.59	0.63
M52211112	3.09	0.04	0.22	0.45	0.85	0.13	0.0015	389	389	4	47	37	0.13	0.0013	355	4	2	45	21	0.95	1.14	0.61	0.63
M12211121	3.52	0.03	0.16	0.37	0.69	0.13	0.0015	314	314	2	32	63	0.13	0.0013	303	4	1	32	44	0.99	0.62	0.31	0.48
M12211122	3.68	0.03	0.15	0.34	0.73	0.13	0.0015	294	294	2	31	52	0.13	0.0014	286	3	1	31	36	0.99	0.64	0.34	0.48
M22211121	3.21	0.03	0.18	0.39	0.72	0.13	0.0014	356	356	2	39	63	0.12	0.0013	345	4	2	39	44	1.00	0.67	0.34	0.50

Name	T1 [s]	Sa(T1) [g]	Sa(T2) [g]	Sa(T3) [g]	DOC [-]	Disp [m]	ISDR [-]	Total Moment [MN-m]	Total Shear [MN]	Max CB Shear [MN]	Max Pp [MN]	Max wall moment [MN-m]	Disp [m]2	ISDR [-]3	Total Moment [MN-m]4	Total Shear [MN]5	Max CB Shear [MN]6	Max Pp [MN]2	Max wall moment [MN-m]8	C1 [-]	C2 [-]	C3 [-]	Mdy/ Mst [-]
M32211121	2.94	0.04	0.20	0.42	0.76	0.12	0.0013	404	404	3	46	62	0.12	0.0012	391	5	2	46	43	1.00	0.74	0.37	0.53
M32211122	3.04	0.04	0.19	0.39	0.79	0.12	0.0014	384	384	3	45	51	0.12	0.0012	373	4	2	45	34	1.00	0.76	0.39	0.53
M42211121	2.69	0.04	0.23	0.46	0.79	0.12	0.0013	461	461	4	54	61	0.12	0.0012	441	5	3	54	40	0.99	0.86	0.42	0.57
M42211122	2.82	0.04	0.22	0.43	0.82	0.12	0.0013	431	431	4	52	50	0.12	0.0012	415	5	2	51	33	0.99	0.85	0.43	0.57
M52211121	2.47	0.05	0.29	0.53	0.82	0.11	0.0013	539	539	6	66	58	0.11	0.0012	496	6	3	64	36	0.96	1.05	0.50	0.62
M52211122	2.53	0.05	0.28	0.51	0.85	0.11	0.0013	517	517	6	64	48	0.11	0.0012	478	5	3	62	29	0.96	1.07	0.51	0.62
M12211211	3.86	0.03	0.14	0.33	0.72	0.14	0.0015	276	276	1	28	51	0.14	0.0014	267	3	1	28	35	0.99	0.64	0.34	0.48
M12211212	3.98	0.02	0.13	0.30	0.76	0.14	0.0016	263	263	2	28	42	0.14	0.0014	257	3	1	28	29	0.99	0.65	0.36	0.48
M22211211	3.51	0.03	0.16	0.35	0.75	0.13	0.0015	313	313	2	34	51	0.13	0.0013	305	4	2	34	35	1.00	0.69	0.37	0.50
M22211212	3.63	0.03	0.15	0.33	0.79	0.13	0.0015	299	299	2	33	41	0.13	0.0014	293	3	2	33	28	1.00	0.70	0.39	0.50
M32211211	3.18	0.03	0.18	0.38	0.78	0.13	0.0014	361	361	3	40	50	0.12	0.0013	350	4	2	40	34	1.00	0.77	0.40	0.53
M32211212	3.30	0.03	0.17	0.36	0.82	0.13	0.0014	341	341	3	39	41	0.13	0.0013	333	4	2	39	27	1.00	0.77	0.41	0.53
M42211211	2.91	0.04	0.21	0.43	0.81	0.12	0.0014	413	413	3	48	49	0.12	0.0012	395	5	2	47	32	0.99	0.89	0.45	0.57
M42211212	2.97	0.04	0.20	0.41	0.84	0.12	0.0014	399	399	3	47	40	0.12	0.0012	384	4	2	47	26	0.99	0.90	0.46	0.57
M52211211	2.69	0.04	0.25	0.48	0.83	0.12	0.0014	469	469	5	56	48	0.12	0.0012	437	5	3	54	29	0.97	1.04	0.51	0.62
M52211212	2.70	0.04	0.25	0.48	0.87	0.12	0.0014	470	470	5	57	39	0.12	0.0012	434	5	3	55	22	0.96	1.09	0.55	0.62
M12211221	3.10	0.04	0.18	0.39	0.72	0.12	0.0013	374	374	2	39	67	0.12	0.0013	364	4	2	39	48	1.00	0.60	0.29	0.47
M12211222	3.26	0.03	0.17	0.36	0.76	0.12	0.0014	349	349	2	38	55	0.12	0.0013	342	4	2	38	39	0.99	0.60	0.32	0.47
M22211221	2.82	0.04	0.20	0.42	0.75	0.12	0.0013	428	428	3	47	66	0.12	0.0012	418	5	2	47	48	1.00	0.64	0.32	0.50
M22211222	2.92	0.04	0.19	0.39	0.79	0.12	0.0013	408	408	3	46	54	0.12	0.0012	400	5	2	46	39	1.00	0.65	0.33	0.50
M32211221	2.61	0.05	0.23	0.45	0.78	0.11	0.0012	479	479	3	55	66	0.11	0.0011	467	5	3	54	47	1.00	0.70	0.34	0.53
M32211222	2.65	0.04	0.22	0.43	0.82	0.11	0.0012	469	469	3	55	54	0.11	0.0011	459	5	3	55	38	1.00	0.72	0.36	0.53
M42211221	2.36	0.05	0.27	0.49	0.81	0.11	0.0012	562	562	5	67	65	0.11	0.0011	541	6	3	66	44	0.99	0.82	0.37	0.57
M42211222	2.46	0.05	0.24	0.46	0.84	0.11	0.0012	525	525	4	63	53	0.11	0.0011	510	6	3	63	36	0.99	0.80	0.38	0.57
M52211221	2.15	0.06	0.32	0.58	0.84	0.11	0.0012	655	655	7	81	61	0.11	0.0011	613	7	4	78	39	0.97	0.98	0.46	0.61
M52211222	2.25	0.06	0.30	0.53	0.86	0.11	0.0012	607	607	6	75	52	0.11	0.0011	575	7	4	73	33	0.98	0.94	0.44	0.61
M12212111	2.53	0.05	0.24	0.48	0.66	0.11	0.0012	503	503	2	33	105	0.11	0.0011	488	6	1	33	80	1.00	0.53	0.23	0.47
M12212112	2.57	0.05	0.23	0.46	0.69	0.11	0.0012	492	492	2	34	92	0.11	0.0011	479	6	2	33	70	1.00	0.55	0.25	0.47
M22212111	2.33	0.05	0.26	0.50	0.69	0.11	0.0012	569	569	2	40	105	0.11	0.0011	554	6	2	40	80	1.00	0.57	0.24	0.49
M22212112	2.40	0.05	0.25	0.48	0.72	0.11	0.0012	545	545	2	39	92	0.11	0.0011	532	6	2	39	70	1.00	0.58	0.26	0.49
M32212111	2.10	0.06	0.30	0.54	0.74	0.10	0.0011	667	667	3	49	104	0.10	0.0010	649	8	2	49	79	1.00	0.64	0.27	0.53
M32212112	2.21	0.06	0.28	0.50	0.75	0.10	0.0011	616	616	3	46	92	0.10	0.0011	602	7	2	46	69	1.00	0.63	0.27	0.53
M42212111	2.00	0.07	0.32	0.57	0.76	0.10	0.0011	716	716	3	54	102	0.10	0.0010	694	8	3	54	77	1.00	0.69	0.29	0.56
M42212112	1.97	0.07	0.32	0.57	0.80	0.10	0.0011	729	729	4	57	89	0.10	0.0010	705	8	3	57	65	0.99	0.74	0.32	0.56
M52212111	1.85	0.07	0.35	0.61	0.79	0.10	0.0011	783	783	4	62	96	0.09	0.0010	749	9	3	61	70	0.99	0.80	0.34	0.60
M52212112	1.89	0.07	0.34	0.60	0.81	0.10	0.0011	766	766	4	61	85	0.10	0.0010	734	8	3	60	61	0.99	0.81	0.35	0.60
M12212121	2.00	0.07	0.31	0.57	0.66	0.10	0.0011	713	713	2	48	141	0.10	0.0010	697	8	2	48	113	1.00	0.48	0.19	0.46
M12212122	2.12	0.06	0.29	0.53	0.68	0.10	0.0011	657	657	2	45	124	0.10	0.0010	643	8	2	45	98	1.00	0.49	0.20	0.46
M22212121	1.89	0.07	0.32	0.58	0.69	0.09	0.0010	760	760	3	53	138	0.09	0.0010	744	9	2	53	110	1.00	0.51	0.21	0.49
M22212122	1.89	0.07	0.32	0.57	0.73	0.09	0.0010	762	762	3	56	121	0.09	0.0010	748	9	3	56	96	1.00	0.54	0.23	0.49
M32212121	1.76	0.08	0.34	0.61	0.72	0.09	0.0009	824	824	3	60	134	0.09	0.0009	806	9	3	60	106	1.00	0.56	0.23	0.52
M32212122	1.80	0.08	0.33	0.59	0.75	0.09	0.0010	801	801	3	60	119	0.09	0.0009	786	9	3	60	93	1.00	0.57	0.24	0.52
M42212121	1.55	0.09	0.39	0.66	0.77	0.08	0.0009	944	944	4	74	124	0.08	0.0008	916	11	4	74	95	1.00	0.68	0.28	0.56
M42212122	1.59	0.09	0.38	0.64	0.80	0.08	0.0009	921	921	5	73	109	0.08	0.0008	896	10	3	73	83	0.99	0.68	0.29	0.56
M52212121	1.52	0.09	0.40	0.67	0.78	0.08	0.0009	964	964	5	77	122	0.08	0.0008	932	11	4	76	93	0.99	0.71	0.29	0.60
M52212122	1.45	0.10	0.44	0.70	0.83	0.08	0.0009	1025	1025	6	85	99	0.08	0.0008	975	11	4	83	72	0.98	0.83	0.34	0.60
M12212211	2.26	0.06	0.27	0.51	0.69	0.10	0.0011	595	595	2	40	112	0.10	0.0011	581	7	2	40	87	1.00	0.52	0.22	0.46
M12212212	2.37	0.05	0.25	0.48	0.71	0.11	0.0011	553	553	2	38	98	0.11	0.0011	542	6	2	37	76	1.00	0.52	0.23	0.46
M22212211	2.07	0.06	0.29	0.54	0.73	0.10	0.0011	683	683	2	48	112	0.10	0.0010	669	8	2	48	87	1.00	0.56	0.23	0.49
M22212212	2.12	0.06	0.28	0.51	0.75	0.10	0.0011	658	658	3	48	98	0.10	0.0010	647	8	2	48	76	1.00	0.57	0.25	0.49
M32212211	1.96	0.07	0.31	0.56	0.75	0.10	0.0010	731	731	3	53	110	0.10	0.0010	716	8	2	53	86	1.00	0.59	0.25	0.52
M32212212	1.93	0.07	0.31	0.55	0.78	0.10	0.0010	743	743	3	56	96	0.10	0.0010	728	9	3	56	73	1.00	0.63	0.27	0.52
M42212211	1.74	0.08	0.36	0.62	0.79	0.09	0.0010	836	836	4	65	102	0.09	0.0009	811	9	3	64	76	0.99	0.71	0.30	0.56
M42212212	1.85	0.07	0.33	0.57	0.80	0.09	0.0010	778	778	4	60	94	0.09	0.0009	761	9	3	60	71	1.00	0.67	0.29	0.56
M52212211	1.69	0.08	0.37	0.63	0.80	0.09	0.0010	864	864	4	68	100	0.09	0.0009	834	10	3	67	73	0.99	0.75	0.32	0.60
M52212212	1.61	0.09	0.41	0.67	0.85	0.08	0.0010	915	915	6	74	82	0.08	0.0009	867	10	3	72	57	0.97	0.87	0.37	0.61
M12212221	1.81	0.08	0.33	0.59	0.69	0.09	0.0010	798	798	3	54	146	0.09	0.0009	784	9	2	54	118	1.00	0.48	0.19	0.46
M12212222	1.92	0.07	0.31	0.56	0.70	0.09	0.0010	748	748	2	51	130	0.09	0.0010	736	9	2	51	106	1.00	0.47	0.19	0.46
M22212221	1.65	0.08	0.35	0.62	0.73	0.08	0.0009	880	880	3	63	141	0.08	0.0009	865	10	3	63	114	1.00	0.52	0.21	0.49
M22212222	1.70	0.08	0.34	0.60	0.75	0.09	0.0009	858	858	3	63	125	0.08	0.0009	846	10	3	63	100	1.00	0.53	0.22	0.49
M32212221	1.60	0.09	0.36	0.63	0.74	0.08	0.0009	914	914	3	67	139	0.08	0.0008	898	11	3	67	112	1.00	0.54	0.22	0.52
M32212222	1.55	0.09	0.37	0.63	0.78	0.08	0.0008	945	945	4	72	119	0.08	0.0008	930	11	3	72	95	1.00	0.58	0.24	0.52
M42212221	1.39	0.10	0.42	0.68	0.79	0.07	0.0008	1063	1063	5	83	127	0.07	0.0007	1036	12	4	83	99	1.00	0.66	0.26	0.56
M42212222	1.52	0.09	0.38	0.64	0.79	0.08	0.0008	964	964	4	74	118	0.08	0.0008	948	11	4	74	93	1.00	0.60	0.25	0.56
M52212221	1.39	0.10	0.43	0.68	0.79	0.07	0.0008	1065	1065	5	84	127	0.07	0.0007	1037	12	4	83	98	1.00	0.66	0.26	0.60
M52212222	1.29	0.11	0.47	0.71	0.85	0.07	0.0008	1160	1160	7	96	100	0.07	0.0007	1110	13	4	94	74	0.98	0.79	0.31	0.60
M12221111	4.99	0.02	0.11	0.27	0.68	0.16	0.0019	261	261	1	26	55	0.16	0.0017	249	3	1	26	36	0.99	0.68	0.37	0.49
M12221112	5.23	0.02	0.10	0.24	0.73	0.17	0.0019	241	241	1	25	44	0.16	0.0017	232	3	1	25	29	0.99	0.70	0.39	0.48
M22221111	4.55	0.02	0.12	0.29	0.72	0.16	0.0018	294	294	2	31	54	0.15	0.0016	282	3	1	31	35	1.00	0.75	0.41	0.51
M22221112	4.72	0.02	0.11	0.26	0.77	0.16	0.0018	278	278	2	31	44	0.16	0.0016	270	3	1	31	29	1.00	0.75	0.43	0.51
M32221111	4.19	0.02	0.14	0.32	0.75	0.15	0.0017	329	329	2	36	54	0.15	0.0015	315	4	2	36	34	1.00	0.83	0.46	0.54
M32221112	4.33	0.02	0.13	0.29	0.79	0.15	0.0017	313	313	2	36	44	0.15	0.0015	302	4	2	35	28	1.00	0.84	0.48	0.54
M42221111	3.81	0.03	0.16	0.35	0.78	0.14	0.0017	378	378	3	43	53	0.14	0.0014	356	4	2	43	32	0.99	0.98	0.53	0.58
M42221112	3.92	0.03	0.15	0.34	0.82	0.14	0.0017	362	362	3	42	44	0.14	0.0014	343	4	2	42	26	0.99	0.99	0.55	0.58
M52221111	3.53	0.03	0.19	0.41	0.81	0.14	0.0016	432	432	5	51	51	0.14	0.0014	392	5	2	49	29	0.96	1.15	0.63	0.63
M52221112	3.57	0.03	0.19	0.40	0.84	0.14	0.0017	426	426	5	51	42	0.14	0.0014	385	4	2	49	22	0.95	1.20	0.67	0.63
M12221121	4.06	0.02	0.14	0.33	0.68	0.14	0.0016	344	344	2	35	71	0.14	0.0015	330	4	2	35	48	0.99	0.65	0.34	0.48
M12221122	4.28	0.02	0.13	0.30	0.73	0.15	0.0016	319	319	2	34	58	0.15	0.0015	309	4	2	34	39	0.99	0.66	0.36	0.48
M22221121	3.73	0.03	0.15	0.35	0.72	0.14	0.0015	385	385	2	41	71	0.14	0.0014	371	4	2	41	48	1.00	0.70	0.37	0.51
M22221122	3.86	0.03	0.14	0.32	0.76	0.14	0.0016	367	367	2	41	58	0.14	0.0014	356	4	2	41	39	1.00	0.72	0.40	0.50
M32221121	3.39	0.03	0.17	0.37	0.75	0.13	0.0015	439	439	3	50	69	0.13	0.0013	423	5	2	49	46	1.00	0.79	0.41	0.54
M32221122	3.55	0.03	0.16	0.35	0.79	0.13	0.0015	411	411	3	47	57	0.13	0.0013	399	5	2	47	37	1.00	0.79	0.43	0.54
M42221121	3.15	0.03	0.19	0.41	0.78	0.13	0.0015	490	490	4	57	68	0.13	0.0013	467	5	3	57	44	0.99	0.88	0.45	0.57
M42221122	3.21	0.03	0.19	0.39	0.82	0.13	0.0015	478	478	4	57	56	0.13	0.0013	457	5	3	57	35	0.99	0.92	0.48	0.57
M52221121	2.85	0.04	0.25	0.48	0.81	0.12	0.0014	585	585	6	71	65	0.12	0.0013	533	6	3	68	39	0.96	1.11	0.56	0.63
M52221122	2.98	0.04	0.22	0.45	0.84	0.12	0.0015	543	543	6	67	55	0.12	0.0013	503	6	3	64	32	0.97	1.07	0.56	0.62
M12221211	4.43	0.02	0.12	0.29	0.72	0.15	0.0017	305	305	2	31	57	0.15	0.0015	294	3	1	31	38	0.99	0.67	0.37	0.48
M12221212	4.60	0.02	0.11	0.26	0.76	0.15	0.0017	289	289	2	31	47	0.15	0.0016	281	3	1	31	31	0.99	0.67	0.38	0.48
M22221211	4.03	0.02	0.14	0.32	0.75	0.14	0.0016	346	346	2	37	57	0.14	0.0014	335	4	2	37	38	1.00	0.73	0.40	0.51
M22221212	4.19	0.02	0.13	0.29	0.79	0.15	0.0016	327	327	2	36	47	0.14	0.0015	319	4	2	36	31	1.00	0.73	0.41	0.50
M32221211	3.67	0.03	0.16	0.34	0.78	0.14	0.0016	393	393	3	44	56	0.13	0.0014	379	4	2	44	37	1.00	0.81	0.44	0.54
M32221212	3.77	0.03	0.15	0.32	0.82	0.14	0.0016	378	378	3	43	46	0.14	0.0014	367	4	2	43	30	1.00	0.82	0.46	0.54
M42221211	3.35	0.03	0.18	0.38	0.81	0.13	0.0015	449	449	4	52	55	0.13	0.0013	428	5	2	51	34	0.99	0.94	0.49	0.58
M42221212	3.48	0.03	0.17	0.36	0.84	0.13	0.0015	425	425	4	50	46	0.13	0.0013	408	5	2	49	28	0.99	0.92	0.50	0.57
M52221211	3.06	0.04	0.23	0.45	0.83	0.13	0.0015	528	528	6	63	53	0.13	0.0013	481	6	3	60	30	0.95	1.14	0.60	0.63
M52221212	3.12	0.03	0.22	0.44	0.86	0.13	0.0015	512	512	6	62	44	0.13	0.0013	468	5	3	59	24	0.95	1.15	0.62	0.63
M12221221	3.59	0.03	0.16	0.35	0.72	0.13	0.0015	407	407	2	43	75	0.13	0.0014	395	5	2	42	52	0.99	0.63	0.33	0.48
M12221222	3.76	0.03	0.14	0.32	0.76	0.14	0.0015	380	380	2	41	61	0.13	0.0014	372	4	2	41	43	0.99	0.64	0.35	0.47
M22221221	3.26	0.03	0.17	0.37	0.75	0.13	0.0014	464	464	3	51	74	0.12	0.0013	452	5	2	51	52	1.00	0.68	0.35	0.50
M22221222	3.37	0.03	0.16	0.35	0.79	0.13	0.0014	442	442	3	50	61	0.13	0.0013	433	5	2	50	42	1.00	0.69	0.37	0.50
M32221221	2.98	0.04	0.20	0.41	0.78	0.12	0.0013	529	529	4	60	73	0.12	0.0012	514	6	3	60	50	1.00	0.75	0.38	0.53
M32221222	3.11	0.03	0.18	0.37	0.81	0.12	0.0014	496	496	4	58	61	0.12	0.0012	485	6	3	58	41	1.00	0.75	0.39	0.53
M42221221	2.72	0.04	0.23	0.45	0.81	0.12	0.0013	606	606	5	72	72	0.12	0.0012	581	7	3	71	48	0.99	0.86	0.43	0.57

Name	T1 [s]	Sa(T1) [g]	Sa(T2) [g]	Sa(T3) [g]	DOC [-]	Disp [m]	ISDR [-]	Total Moment [MN-m]	Total Shear [MN]	Max CB Shear [MN]	Max Pp [MN]	Max wall moment [MN-m]	Disp [m]2	ISDR [-]3	Total Moment [MN-m]4	Total Shear [MN]5	Max CB Shear [MN]6	Max Pp [MN]2	Max wall moment [MN-m]8	C1 [-]	C2 [-]	C3 [-]	Mdy/ Mst [-]
M52221221	2.48	0.05	0.28	0.52	0.84	0.11	0.0013	710	710	7	87	69	0.11	0.0012	656	8	4	83	42	0.96	1.06	0.51	0.62
M52221222	2.60	0.05	0.26	0.48	0.86	0.12	0.0013	656	656	7	81	58	0.11	0.0012	617	7	4	78	35	0.97	1.00	0.49	0.61
M12222111	2.92	0.04	0.21	0.44	0.65	0.12	0.0013	545	545	2	36	117	0.12	0.0012	526	6	2	35	86	1.00	0.57	0.26	0.47
M12222112	2.97	0.04	0.20	0.42	0.69	0.12	0.0013	532	532	2	36	103	0.12	0.0012	516	6	2	36	75	1.00	0.58	0.28	0.47
M22222111	2.64	0.04	0.23	0.46	0.70	0.11	0.0012	631	631	2	44	116	0.11	0.0012	612	7	2	44	86	1.00	0.62	0.28	0.50
M22222112	2.77	0.04	0.21	0.44	0.72	0.12	0.0013	588	588	2	42	103	0.11	0.0012	572	7	2	42	75	1.00	0.62	0.29	0.50
M32222111	2.49	0.05	0.24	0.48	0.72	0.11	0.0012	687	687	3	50	116	0.11	0.0011	666	8	2	50	85	1.00	0.66	0.30	0.53
M32222112	2.48	0.05	0.24	0.47	0.76	0.11	0.0012	690	690	3	52	101	0.11	0.0011	671	8	2	52	73	1.00	0.69	0.32	0.53
M42222111	2.23	0.06	0.29	0.53	0.77	0.11	0.0012	815	815	4	63	113	0.11	0.0011	782	9	3	62	80	0.99	0.79	0.35	0.57
M42222112	2.28	0.06	0.28	0.51	0.79	0.11	0.0012	789	789	4	62	100	0.11	0.0011	759	9	3	61	69	0.99	0.80	0.36	0.57
M52222111	2.14	0.06	0.31	0.56	0.78	0.11	0.0012	870	870	5	68	111	0.10	0.0011	827	10	3	68	77	0.99	0.85	0.38	0.61
M52222112	2.08	0.06	0.34	0.59	0.83	0.10	0.0012	917	917	6	75	94	0.10	0.0011	858	10	3	72	62	0.97	0.95	0.44	0.61
M12222121	2.31	0.05	0.27	0.51	0.66	0.11	0.0011	767	767	2	52	156	0.11	0.0011	746	9	2	51	121	1.00	0.52	0.21	0.46
M12222122	2.39	0.05	0.25	0.49	0.69	0.11	0.0011	729	729	2	50	136	0.11	0.0011	713	8	2	50	105	1.00	0.53	0.23	0.46
M22222121	2.19	0.06	0.28	0.53	0.69	0.10	0.0011	836	836	3	58	156	0.10	0.0011	815	10	3	58	121	1.00	0.55	0.23	0.49
M22222122	2.25	0.06	0.27	0.50	0.72	0.10	0.0011	798	798	3	57	137	0.10	0.0011	781	9	3	57	105	1.00	0.56	0.24	0.49
M32222121	1.95	0.07	0.32	0.57	0.74	0.10	0.0011	981	981	4	74	152	0.10	0.0010	956	11	3	73	117	1.00	0.62	0.26	0.52
M32222122	2.00	0.07	0.31	0.55	0.76	0.10	0.0011	953	953	4	73	135	0.10	0.0010	932	11	3	73	103	1.00	0.63	0.27	0.52
M42222121	1.79	0.08	0.35	0.61	0.77	0.09	0.0010	1076	1076	5	84	144	0.09	0.0009	1041	12	4	84	108	0.99	0.71	0.30	0.56
M42222122	1.93	0.07	0.32	0.57	0.77	0.10	0.0011	990	990	4	77	133	0.10	0.0010	966	11	4	77	100	1.00	0.66	0.28	0.56
M52222121	1.76	0.08	0.36	0.63	0.78	0.09	0.0010	1100	1100	6	87	142	0.09	0.0009	1060	12	4	86	105	0.99	0.74	0.31	0.60
M52222122	1.68	0.08	0.40	0.66	0.83	0.09	0.0010	1171	1171	7	97	115	0.09	0.0009	1107	13	5	94	81	0.97	0.87	0.38	0.61
M12222211	2.61	0.05	0.23	0.46	0.68	0.11	0.0012	641	641	2	43	124	0.11	0.0012	624	7	2	43	93	1.00	0.55	0.25	0.47
M12222212	2.74	0.04	0.21	0.44	0.71	0.11	0.0012	596	596	2	40	109	0.11	0.0012	582	7	2	40	82	1.00	0.56	0.26	0.47
M22222211	2.45	0.05	0.24	0.48	0.71	0.11	0.0012	704	704	2	49	123	0.11	0.0011	687	8	2	49	93	1.00	0.58	0.26	0.49
M22222212	2.44	0.05	0.24	0.47	0.75	0.11	0.0012	706	706	3	51	108	0.11	0.0011	692	8	2	51	81	1.00	0.60	0.28	0.49
M32222211	2.19	0.06	0.28	0.51	0.76	0.10	0.0011	835	835	4	62	122	0.10	0.0011	814	9	3	62	91	1.00	0.66	0.29	0.53
M32222212	2.23	0.06	0.27	0.49	0.78	0.11	0.0011	809	809	4	61	108	0.10	0.0011	791	9	3	61	80	1.00	0.67	0.30	0.53
M42222211	2.10	0.06	0.30	0.54	0.77	0.10	0.0011	888	888	4	67	121	0.10	0.0010	864	10	3	67	90	1.00	0.69	0.30	0.56
M42222212	2.14	0.06	0.29	0.51	0.80	0.10	0.0011	861	861	4	66	107	0.10	0.0010	839	10	3	66	78	1.00	0.71	0.31	0.56
M52222211	1.84	0.07	0.37	0.64	0.82	0.09	0.0011	1063	1063	6	86	108	0.09	0.0010	1002	12	4	83	75	0.97	0.90	0.40	0.61
M52222212	1.86	0.07	0.36	0.63	0.84	0.10	0.0011	1046	1046	6	85	96	0.10	0.0010	987	11	4	82	65	0.97	0.90	0.41	0.61
M12222221	2.09	0.06	0.29	0.54	0.69	0.10	0.0011	894	894	3	61	166	0.10	0.0010	875	10	3	60	132	1.00	0.50	0.20	0.46
M12222222	2.22	0.06	0.27	0.50	0.70	0.10	0.0011	816	816	3	56	146	0.10	0.0011	801	9	3	56	115	1.00	0.50	0.21	0.46
M22222221	1.99	0.07	0.30	0.55	0.71	0.10	0.0010	959	959	3	67	165	0.10	0.0010	941	11	3	67	132	1.00	0.52	0.21	0.49
M22222222	1.96	0.07	0.30	0.54	0.75	0.10	0.0010	977	977	4	72	145	0.10	0.0010	961	11	3	71	114	1.00	0.55	0.23	0.49
M32222221	1.75	0.08	0.34	0.60	0.76	0.09	0.0009	1102	1102	5	83	157	0.09	0.0009	1079	13	4	83	122	1.00	0.61	0.25	0.52
M32222222	1.79	0.08	0.33	0.58	0.78	0.09	0.0010	1077	1077	5	82	139	0.09	0.0009	1057	12	4	82	107	1.00	0.61	0.26	0.52
M42222221	1.72	0.08	0.35	0.61	0.76	0.09	0.0009	1125	1125	5	85	155	0.09	0.0009	1100	13	4	85	120	1.00	0.62	0.26	0.56
M42222222	1.76	0.08	0.34	0.59	0.79	0.09	0.0010	1099	1099	5	85	138	0.09	0.0009	1078	13	4	84	106	1.00	0.63	0.27	0.56
M52222221	1.47	0.10	0.44	0.70	0.83	0.08	0.0009	1348	1348	8	110	133	0.08	0.0008	1280	15	5	108	97	0.98	0.84	0.35	0.60
M52222222	1.49	0.09	0.43	0.69	0.84	0.08	0.0009	1324	1324	8	109	118	0.08	0.0008	1259	14	5	106	84	0.98	0.85	0.36	0.61
M13111111	6.26	0.01	0.09	0.21	0.68	0.18	0.0019	229	229	1	23	51	0.18	0.0016	216	2	1	23	31	0.99	0.76	0.42	0.47
M13111112	6.54	0.01	0.08	0.19	0.73	0.18	0.0019	213	213	1	22	42	0.18	0.0017	203	2	1	22	25	0.99	0.78	0.44	0.47
M23111111	5.71	0.01	0.10	0.23	0.72	0.18	0.0018	264	264	1	28	51	0.17	0.0016	251	3	1	28	31	1.00	0.81	0.46	0.49
M23111112	5.92	0.01	0.09	0.21	0.76	0.18	0.0018	247	247	1	27	42	0.17	0.0016	238	2	1	27	25	1.00	0.83	0.48	0.49
M33111111	5.22	0.02	0.11	0.25	0.75	0.17	0.0018	304	304	1	33	51	0.17	0.0015	289	3	1	33	31	1.00	0.89	0.51	0.52
M33111112	5.39	0.02	0.10	0.23	0.79	0.17	0.0018	287	287	2	32	42	0.17	0.0015	275	3	1	32	25	1.00	0.91	0.52	0.52
M43111111	4.78	0.02	0.12	0.29	0.78	0.16	0.0017	350	350	2	40	51	0.16	0.0015	326	3	1	39	29	0.99	1.03	0.60	0.56
M43111112	4.91	0.02	0.12	0.27	0.81	0.17	0.0018	335	335	2	39	42	0.16	0.0015	316	3	1	39	23	0.99	1.04	0.61	0.56
M53111111	4.36	0.02	0.16	0.35	0.81	0.16	0.0017	412	412	3	49	49	0.16	0.0015	363	4	1	46	26	0.94	1.27	0.75	0.61
M53111112	4.47	0.02	0.15	0.34	0.84	0.16	0.0017	397	397	3	48	41	0.16	0.0015	353	4	1	45	20	0.94	1.28	0.77	0.61
M13111121	5.10	0.02	0.11	0.27	0.68	0.17	0.0017	317	317	1	32	68	0.16	0.0015	301	3	1	32	44	0.99	0.68	0.37	0.47
M13111122	5.33	0.02	0.10	0.23	0.73	0.17	0.0017	292	292	1	31	55	0.17	0.0015	282	3	1	31	35	0.99	0.71	0.39	0.46
M23111121	4.65	0.02	0.12	0.29	0.72	0.16	0.0016	358	358	1	38	68	0.16	0.0014	343	4	1	38	44	1.00	0.75	0.42	0.49
M23111122	4.84	0.02	0.11	0.26	0.76	0.16	0.0016	338	338	1	38	55	0.16	0.0014	327	3	1	37	35	1.00	0.76	0.43	0.49
M33111121	4.26	0.02	0.14	0.31	0.75	0.15	0.0016	404	404	2	45	67	0.15	0.0013	385	4	1	45	42	1.00	0.84	0.47	0.52
M33111122	4.41	0.02	0.13	0.29	0.79	0.15	0.0016	383	383	2	44	55	0.15	0.0014	369	4	1	44	34	1.00	0.85	0.48	0.52
M43111121	3.90	0.03	0.16	0.35	0.78	0.14	0.0015	459	459	3	53	66	0.14	0.0013	431	4	2	53	39	0.99	0.98	0.54	0.55
M43111122	4.02	0.02	0.15	0.33	0.81	0.15	0.0015	439	439	3	52	54	0.14	0.0013	415	4	2	52	32	0.99	0.99	0.56	0.55
M53111121	3.56	0.03	0.19	0.41	0.81	0.14	0.0015	538	538	4	65	63	0.14	0.0013	482	5	2	62	35	0.95	1.20	0.66	0.60
M53111122	3.66	0.03	0.19	0.39	0.84	0.14	0.0015	518	518	4	64	52	0.14	0.0013	466	5	2	60	27	0.95	1.21	0.68	0.60
M13111211	5.56	0.02	0.10	0.23	0.71	0.17	0.0018	274	274	1	28	54	0.17	0.0016	263	3	1	28	34	0.99	0.72	0.40	0.47
M13111212	5.77	0.01	0.09	0.21	0.76	0.17	0.0018	257	257	1	27	44	0.17	0.0016	249	3	1	27	28	0.99	0.74	0.42	0.46
M23111211	5.05	0.02	0.11	0.25	0.75	0.17	0.0017	319	319	1	34	54	0.16	0.0015	307	3	1	34	35	1.00	0.77	0.43	0.49
M23111212	5.21	0.02	0.10	0.23	0.79	0.17	0.0017	302	302	1	33	44	0.16	0.0015	293	3	1	33	28	1.00	0.78	0.45	0.49
M33111211	4.60	0.02	0.12	0.28	0.78	0.16	0.0016	362	362	2	40	54	0.16	0.0014	347	4	1	40	33	1.00	0.86	0.49	0.52
M33111212	4.73	0.02	0.11	0.26	0.81	0.16	0.0017	348	348	2	40	44	0.16	0.0014	337	4	1	40	27	1.00	0.87	0.50	0.52
M43111211	4.20	0.02	0.14	0.32	0.80	0.15	0.0016	413	413	2	47	53	0.15	0.0013	390	4	2	47	31	0.99	1.01	0.57	0.55
M43111212	4.30	0.02	0.14	0.30	0.84	0.15	0.0016	399	399	3	47	44	0.15	0.0014	379	4	1	46	25	0.99	1.01	0.58	0.55
M53111211	3.83	0.03	0.18	0.38	0.83	0.15	0.0016	488	488	4	58	51	0.14	0.0013	436	4	2	55	27	0.94	1.23	0.69	0.61
M53111212	3.90	0.03	0.17	0.37	0.86	0.15	0.0016	473	473	4	57	42	0.14	0.0014	426	4	2	54	22	0.94	1.23	0.71	0.60
M13111221	4.50	0.02	0.12	0.29	0.71	0.15	0.0015	374	374	1	39	72	0.15	0.0014	360	4	1	39	48	0.99	0.67	0.37	0.46
M13111222	4.68	0.02	0.11	0.26	0.76	0.16	0.0016	353	353	1	38	59	0.15	0.0014	344	4	1	38	39	0.99	0.67	0.38	0.46
M23111221	4.09	0.02	0.14	0.31	0.75	0.15	0.0015	425	425	2	46	71	0.14	0.0013	411	4	1	46	47	1.00	0.73	0.40	0.48
M23111222	4.23	0.02	0.13	0.29	0.79	0.15	0.0015	405	405	2	46	58	0.15	0.0013	394	4	1	45	38	1.00	0.74	0.42	0.48
M33111221	3.73	0.03	0.15	0.34	0.78	0.14	0.0014	482	482	2	55	70	0.14	0.0012	465	5	2	55	46	1.00	0.82	0.44	0.51
M33111222	3.84	0.03	0.15	0.32	0.81	0.14	0.0014	462	462	2	54	58	0.14	0.0012	449	5	2	54	37	1.00	0.83	0.46	0.51
M43111221	3.41	0.03	0.18	0.38	0.80	0.13	0.0014	551	551	3	65	69	0.13	0.0012	524	5	2	64	43	0.99	0.94	0.49	0.55
M43111222	3.49	0.03	0.17	0.36	0.84	0.14	0.0014	531	531	3	64	57	0.13	0.0012	508	5	2	63	34	0.99	0.95	0.51	0.55
M53111221	3.11	0.04	0.22	0.45	0.83	0.13	0.0014	648	648	5	79	66	0.13	0.0012	589	6	2	75	37	0.95	1.15	0.61	0.60
M53111222	3.17	0.03	0.22	0.44	0.86	0.13	0.0014	628	628	5	77	54	0.13	0.0012	573	6	2	73	30	0.95	1.16	0.62	0.60
M13112111	3.61	0.03	0.16	0.37	0.65	0.14	0.0013	507	507	1	33	112	0.13	0.0012	485	5	1	33	78	0.99	0.62	0.30	0.46
M13112112	3.73	0.03	0.15	0.35	0.68	0.14	0.0014	484	484	1	33	99	0.14	0.0012	466	5	1	33	68	0.99	0.63	0.32	0.46
M23112111	3.31	0.03	0.18	0.39	0.69	0.13	0.0013	572	572	1	40	111	0.13	0.0012	550	6	1	40	77	1.00	0.67	0.33	0.48
M23112112	3.40	0.03	0.17	0.37	0.72	0.13	0.0013	549	549	1	39	97	0.13	0.0012	531	6	1	39	67	1.00	0.68	0.35	0.48
M33112111	3.04	0.04	0.20	0.42	0.73	0.12	0.0012	645	645	2	47	109	0.12	0.0011	620	6	1	47	75	1.00	0.75	0.37	0.51
M33112112	3.11	0.03	0.19	0.40	0.76	0.13	0.0012	622	622	2	46	96	0.12	0.0011	601	6	1	46	65	1.00	0.76	0.38	0.51
M43112111	2.79	0.04	0.23	0.46	0.76	0.12	0.0012	733	733	3	56	107	0.12	0.0011	696	7	2	56	71	0.99	0.87	0.42	0.55
M43112112	2.85	0.04	0.22	0.44	0.79	0.12	0.0012	711	711	3	55	94	0.12	0.0011	677	7	2	55	62	0.99	0.88	0.43	0.55
M53112111	2.56	0.05	0.28	0.52	0.80	0.12	0.0012	854	854	4	68	102	0.12	0.0011	782	8	2	66	64	0.96	1.07	0.51	0.59
M53112112	2.60	0.05	0.27	0.50	0.82	0.12	0.0012	831	831	4	67	90	0.12	0.0011	762	8	2	64	55	0.96	1.08	0.52	0.59
M13112121	2.90	0.04	0.21	0.44	0.65	0.12	0.0012	689	689	1	46	147	0.12	0.0011	664	7	1	46	108	1.00	0.57	0.26	0.45
M13112122	3.00	0.04	0.19	0.42	0.69	0.12	0.0012	656	656	1	45	129	0.12	0.0011	636	7	1	45	94	1.00	0.58	0.28	0.45
M23112121	2.66	0.04	0.23	0.46	0.69	0.11	0.0011	781	781	2	55	146	0.11	0.0010	756	8	2	55	107	1.00	0.62	0.28	0.48
M23112122	2.74	0.04	0.22	0.44	0.72	0.12	0.0011	748	748	2	54	128	0.11	0.0010	728	8	2	54	93	1.00	0.63	0.30	0.48
M33112121	2.45	0.05	0.25	0.48	0.73	0.11	0.0011	885	885	3	66	144	0.11	0.0010	856	9	2	66	105	1.00	0.69	0.31	0.51
M33112122	2.51	0.05	0.24	0.47	0.76	0.11	0.0011	851	851	3	64	126	0.11	0.0010	827	9	2	64	91	1.00	0.69	0.32	0.51
M43112121	2.25	0.06	0.29	0.53	0.77	0.11	0.0011	1007	1007	3	78	141	0.11	0.0010	965	10	2	78	100	0.99	0.79	0.35	0.54
M43112122	2.30	0.05	0.28	0.51	0.79	0.11	0.0011	974	974	3	77	124	0.11	0.0010	937	10	2	76	87	0.99	0.81	0.36	0.54
M53112121	2.06	0.06	0.34	0.60	0.80	0.10	0.0011	1166	1166	5	95	132	0.10	0.0010	1089	11	3	93	90	0.97	0.94	0.43	0.59
M53112122	2.10	0.06	0.33	0.59	0.82	0.11	0.0011	1134	1134	5	93	116	0.10	0.0010	1059	11	3	90	77	0.97	0.96	0.44	0.59
M13112211	3.28	0.03	0.18	0.39	0.68	0.13	0.0012	579	579	1	38	118	0.13	0.0012	559	6	1	38	84	1.00	0.60	0.29	0.46

Name	T1 [s]	Sa(T1) [g]	Sa(T2) [g]	Sa(T3) [g]	DOC [-]	Disp [m]	ISDR [-]	Total Moment [MN-m]	Total Shear [MN]	Max CB Shear [MN]	Max Pp [MN]	Max wall moment [MN-m]	Disp [m]2	ISDR [-]3	Total Moment [MN-m]4	Total Shear [MN]5	Max CB Shear [MN]6	Max Pp [MN]2	Max wall moment [MN-m]8	C1 [-]	C2 [-]	C3 [-]	Mdy/ Mst [-]
M23112211	2.99	0.04	0.20	0.42	0.72	0.12	0.0012	658	658	2	46	116	0.12	0.0011	638	7	1	46	83	1.00	0.65	0.32	0.48
M23112212	3.06	0.04	0.19	0.39	0.75	0.12	0.0012	635	635	2	46	103	0.12	0.0011	618	6	1	45	73	1.00	0.66	0.33	0.48
M33112211	2.74	0.04	0.22	0.44	0.75	0.12	0.0012	747	747	2	55	115	0.12	0.0010	723	8	2	55	81	1.00	0.72	0.35	0.51
M33112212	2.80	0.04	0.21	0.43	0.78	0.12	0.0012	724	724	2	54	102	0.12	0.0011	704	7	2	54	71	1.00	0.73	0.36	0.51
M43112211	2.51	0.05	0.25	0.48	0.78	0.11	0.0011	852	852	3	65	113	0.11	0.0010	816	8	2	65	77	0.99	0.84	0.39	0.54
M43112212	2.56	0.05	0.24	0.47	0.81	0.11	0.0011	830	830	3	64	99	0.11	0.0010	798	8	2	64	67	0.99	0.84	0.40	0.54
M53112211	2.30	0.05	0.31	0.56	0.82	0.11	0.0011	994	994	4	79	107	0.11	0.0010	921	9	2	77	68	0.96	1.01	0.48	0.59
M53112212	2.33	0.05	0.30	0.55	0.84	0.11	0.0011	972	972	4	78	94	0.11	0.0010	902	9	2	75	59	0.96	1.02	0.48	0.59
M13112221	2.62	0.04	0.23	0.46	0.68	0.11	0.0011	796	796	2	54	155	0.11	0.0010	774	8	2	53	117	1.00	0.55	0.25	0.45
M13112222	2.70	0.04	0.22	0.44	0.71	0.11	0.0011	763	763	2	53	137	0.11	0.0010	746	8	2	53	102	1.00	0.56	0.26	0.45
M23112221	2.40	0.05	0.25	0.48	0.72	0.11	0.0010	909	909	2	65	155	0.11	0.0010	887	9	2	65	117	1.00	0.59	0.26	0.47
M23112222	2.46	0.05	0.24	0.46	0.75	0.11	0.0010	877	877	2	64	136	0.11	0.0010	859	9	2	64	102	1.00	0.60	0.28	0.47
M33112221	2.20	0.06	0.28	0.51	0.75	0.11	0.0010	1038	1038	3	77	154	0.10	0.0009	1011	11	2	77	115	1.00	0.66	0.29	0.50
M33112222	2.24	0.06	0.27	0.49	0.78	0.11	0.0010	1004	1004	3	76	135	0.10	0.0009	981	10	2	76	100	1.00	0.67	0.30	0.50
M43112221	2.01	0.07	0.32	0.56	0.79	0.10	0.0010	1185	1185	4	92	149	0.10	0.0009	1145	12	3	92	109	0.99	0.75	0.32	0.54
M43112222	2.05	0.07	0.31	0.55	0.81	0.10	0.0010	1154	1154	4	91	131	0.10	0.0009	1118	12	3	90	95	0.99	0.76	0.33	0.54
M53112221	1.84	0.07	0.37	0.64	0.82	0.10	0.0010	1325	1325	5	108	135	0.10	0.0009	1249	13	3	105	94	0.97	0.90	0.40	0.58
M53112222	1.87	0.07	0.36	0.63	0.84	0.10	0.0010	1303	1303	6	107	119	0.10	0.0009	1229	13	3	104	81	0.97	0.91	0.41	0.58
M13121111	7.23	0.01	0.07	0.18	0.67	0.19	0.0021	246	246	1	24	57	0.19	0.0017	230	2	1	24	33	0.99	0.81	0.45	0.48
M13121112	7.55	0.01	0.07	0.16	0.72	0.20	0.0021	228	228	1	24	46	0.19	0.0018	217	2	1	23	27	0.99	0.83	0.47	0.47
M23121111	6.59	0.01	0.08	0.19	0.71	0.19	0.0020	282	282	1	29	57	0.18	0.0017	266	3	1	29	33	1.00	0.87	0.49	0.50
M23121112	6.84	0.01	0.08	0.18	0.76	0.19	0.0020	264	264	1	29	46	0.18	0.0017	252	3	1	29	27	1.00	0.89	0.51	0.50
M33121111	6.03	0.01	0.09	0.22	0.74	0.18	0.0019	324	324	2	35	57	0.18	0.0016	305	3	1	35	33	1.00	0.96	0.55	0.53
M33121112	6.22	0.01	0.09	0.20	0.78	0.18	0.0020	305	305	2	34	46	0.18	0.0016	291	3	1	34	26	1.00	0.98	0.56	0.52
M43121111	5.52	0.02	0.11	0.25	0.77	0.18	0.0019	376	376	2	43	57	0.17	0.0016	349	4	1	42	31	0.99	1.09	0.64	0.56
M43121112	5.67	0.01	0.10	0.23	0.81	0.18	0.0019	358	358	2	42	47	0.17	0.0016	335	3	1	41	25	0.98	1.11	0.65	0.56
M53121111	5.04	0.02	0.13	0.31	0.80	0.17	0.0019	455	455	4	54	56	0.17	0.0016	398	4	2	50	28	0.94	1.31	0.80	0.62
M53121112	5.16	0.02	0.13	0.30	0.83	0.17	0.0019	436	436	4	52	46	0.17	0.0016	383	4	2	49	22	0.93	1.32	0.82	0.61
M13121121	5.88	0.01	0.09	0.23	0.67	0.18	0.0019	337	337	1	34	75	0.17	0.0016	318	3	1	34	47	0.99	0.73	0.40	0.47
M13121122	6.16	0.01	0.08	0.20	0.72	0.18	0.0019	311	311	1	33	61	0.17	0.0016	298	3	1	33	37	0.99	0.76	0.42	0.47
M23121121	5.37	0.02	0.10	0.24	0.71	0.17	0.0018	387	387	2	41	75	0.17	0.0015	369	4	1	41	47	1.00	0.79	0.44	0.49
M23121122	5.59	0.02	0.09	0.22	0.76	0.17	0.0018	361	361	2	40	61	0.17	0.0015	348	4	1	40	38	1.00	0.81	0.46	0.49
M33121121	4.91	0.02	0.11	0.27	0.74	0.17	0.0017	444	444	2	50	75	0.16	0.0015	422	4	2	49	46	1.00	0.87	0.49	0.52
M33121122	5.09	0.02	0.11	0.25	0.79	0.17	0.0017	420	420	2	48	61	0.17	0.0015	403	4	2	48	37	1.00	0.88	0.50	0.52
M43121121	4.50	0.02	0.13	0.31	0.77	0.16	0.0017	505	505	3	58	74	0.16	0.0014	472	5	2	58	43	0.99	1.02	0.58	0.56
M43121122	4.64	0.02	0.13	0.29	0.81	0.16	0.0017	482	482	3	57	61	0.16	0.0014	454	5	2	56	35	0.99	1.03	0.59	0.56
M53121121	4.11	0.02	0.17	0.37	0.80	0.15	0.0016	593	593	5	71	71	0.15	0.0014	525	5	2	67	38	0.94	1.25	0.72	0.61
M53121122	4.22	0.02	0.16	0.35	0.83	0.15	0.0017	571	571	5	70	59	0.15	0.0014	508	5	2	66	30	0.94	1.26	0.74	0.61
M13121211	6.42	0.01	0.08	0.20	0.71	0.18	0.0019	292	292	1	30	60	0.18	0.0016	278	3	1	29	36	0.99	0.77	0.43	0.47
M13121212	6.66	0.01	0.08	0.18	0.76	0.18	0.0019	274	274	1	29	49	0.18	0.0017	264	3	1	29	29	0.99	0.79	0.45	0.47
M23121211	5.83	0.01	0.09	0.21	0.74	0.18	0.0018	339	339	1	36	60	0.17	0.0016	324	3	1	36	37	1.00	0.82	0.47	0.49
M23121212	6.02	0.01	0.08	0.19	0.79	0.18	0.0019	320	320	1	35	49	0.17	0.0016	310	3	1	35	30	1.00	0.84	0.48	0.49
M33121211	5.32	0.02	0.10	0.24	0.77	0.17	0.0018	392	392	2	43	60	0.17	0.0015	375	4	1	43	36	1.00	0.90	0.51	0.52
M33121212	5.46	0.02	0.10	0.22	0.81	0.17	0.0018	374	374	2	43	49	0.17	0.0015	360	4	1	42	29	1.00	0.92	0.53	0.52
M43121211	4.85	0.02	0.12	0.28	0.80	0.17	0.0018	455	455	3	52	60	0.16	0.0015	427	4	2	51	34	0.99	1.04	0.60	0.56
M43121212	4.96	0.02	0.11	0.26	0.83	0.17	0.0018	439	439	3	51	49	0.17	0.0015	416	4	2	51	27	0.99	1.04	0.61	0.55
M53121211	4.42	0.02	0.15	0.34	0.83	0.16	0.0017	538	538	4	64	59	0.16	0.0015	477	5	2	60	30	0.94	1.28	0.76	0.61
M53121212	4.50	0.02	0.15	0.33	0.85	0.16	0.0018	523	523	4	63	48	0.16	0.0015	465	5	2	59	24	0.94	1.28	0.77	0.61
M13121221	5.19	0.02	0.10	0.25	0.71	0.17	0.0017	407	407	1	42	80	0.16	0.0015	391	4	1	42	52	0.99	0.69	0.38	0.46
M13121222	5.40	0.02	0.10	0.22	0.75	0.17	0.0017	381	381	2	41	65	0.17	0.0015	370	4	1	41	42	0.99	0.71	0.41	0.46
M23121221	4.72	0.02	0.12	0.27	0.74	0.16	0.0016	466	466	2	51	80	0.16	0.0014	449	5	2	51	52	1.00	0.75	0.43	0.49
M23121222	4.88	0.02	0.11	0.25	0.79	0.16	0.0016	444	444	2	50	65	0.16	0.0015	432	5	2	50	42	1.00	0.76	0.43	0.48
M33121221	4.31	0.02	0.13	0.30	0.77	0.15	0.0016	528	528	3	60	79	0.15	0.0013	507	5	2	59	50	1.00	0.85	0.48	0.52
M33121222	4.43	0.02	0.12	0.28	0.81	0.15	0.0016	506	506	3	59	65	0.15	0.0014	490	5	2	59	40	1.00	0.86	0.49	0.52
M43121221	3.93	0.03	0.15	0.34	0.80	0.15	0.0015	603	603	4	70	78	0.14	0.0013	570	6	2	70	46	0.99	0.99	0.55	0.55
M43121222	4.03	0.02	0.15	0.32	0.83	0.15	0.0015	581	581	4	69	64	0.15	0.0013	553	6	2	68	37	0.99	1.00	0.56	0.55
M53121221	3.59	0.03	0.19	0.40	0.83	0.14	0.0015	710	710	6	86	75	0.14	0.0013	638	7	3	81	40	0.95	1.20	0.67	0.60
M53121222	3.66	0.03	0.18	0.39	0.86	0.14	0.0015	688	688	6	84	62	0.14	0.0013	621	6	3	80	32	0.94	1.21	0.68	0.60
M13122111	4.17	0.02	0.14	0.34	0.65	0.15	0.0015	556	556	1	36	126	0.15	0.0013	528	6	1	36	85	0.99	0.65	0.33	0.47
M13122112	4.30	0.02	0.13	0.31	0.68	0.15	0.0015	531	531	1	36	111	0.15	0.0014	509	5	1	35	74	0.99	0.66	0.35	0.46
M23122111	3.82	0.03	0.15	0.35	0.69	0.14	0.0014	625	625	2	43	125	0.14	0.0013	597	6	1	43	84	1.00	0.71	0.37	0.49
M23122112	3.92	0.03	0.15	0.33	0.72	0.14	0.0014	600	600	2	43	110	0.14	0.0013	577	6	1	42	73	1.00	0.72	0.38	0.49
M33122111	3.51	0.03	0.17	0.37	0.72	0.13	0.0014	703	703	2	51	123	0.13	0.0012	671	7	2	51	81	1.00	0.79	0.40	0.52
M33122112	3.59	0.03	0.16	0.36	0.75	0.14	0.0014	678	678	2	50	108	0.13	0.0012	651	7	2	50	71	1.00	0.80	0.42	0.52
M43122111	3.22	0.03	0.19	0.41	0.76	0.13	0.0013	797	797	3	61	120	0.13	0.0012	752	8	2	60	77	0.99	0.91	0.47	0.55
M43122112	3.29	0.03	0.19	0.40	0.78	0.13	0.0013	773	773	3	60	106	0.13	0.0012	732	8	2	59	67	0.99	0.93	0.48	0.55
M53122111	2.96	0.04	0.24	0.47	0.79	0.13	0.0013	929	929	4	74	114	0.12	0.0012	842	9	2	71	68	0.96	1.12	0.57	0.60
M53122112	3.01	0.04	0.23	0.46	0.81	0.13	0.0013	904	904	4	73	101	0.13	0.0012	821	8	2	69	59	0.96	1.13	0.59	0.60
M13122121	3.35	0.03	0.18	0.40	0.65	0.13	0.0013	750	750	2	50	165	0.13	0.0012	718	7	1	49	117	1.00	0.60	0.29	0.46
M13122122	3.46	0.03	0.17	0.37	0.68	0.13	0.0013	714	714	2	49	144	0.13	0.0012	689	7	1	49	102	1.00	0.61	0.30	0.46
M23122121	3.07	0.04	0.19	0.42	0.69	0.12	0.0012	847	847	2	60	163	0.12	0.0011	816	9	2	59	116	1.00	0.65	0.32	0.48
M23122122	3.16	0.03	0.18	0.40	0.72	0.13	0.0012	811	811	2	58	143	0.12	0.0011	785	8	2	58	101	1.00	0.67	0.33	0.48
M33122121	2.82	0.04	0.22	0.44	0.73	0.12	0.0012	956	956	3	71	161	0.12	0.0011	920	10	2	71	113	1.00	0.73	0.35	0.51
M33122122	2.89	0.04	0.21	0.43	0.75	0.12	0.0012	920	920	3	69	142	0.12	0.0011	889	9	2	69	98	1.00	0.74	0.37	0.51
M43122121	2.60	0.05	0.25	0.48	0.76	0.12	0.0012	1086	1086	4	84	158	0.11	0.0010	1035	11	3	84	107	0.99	0.84	0.39	0.55
M43122122	2.65	0.04	0.24	0.46	0.79	0.12	0.0012	1050	1050	4	82	138	0.12	0.0010	1004	10	3	82	93	0.99	0.85	0.41	0.55
M53122121	2.38	0.05	0.30	0.55	0.80	0.11	0.0012	1262	1262	6	102	150	0.11	0.0010	1162	12	3	99	96	0.96	1.03	0.48	0.59
M53122122	2.43	0.05	0.29	0.54	0.82	0.11	0.0012	1227	1227	6	100	132	0.11	0.0011	1132	12	3	97	83	0.96	1.04	0.50	0.59
M13122211	3.78	0.03	0.15	0.35	0.68	0.14	0.0014	633	633	1	42	132	0.14	0.0013	607	6	1	41	91	0.99	0.63	0.32	0.46
M13122212	3.89	0.03	0.14	0.33	0.71	0.14	0.0014	607	607	1	41	116	0.14	0.0013	587	6	1	41	80	0.99	0.64	0.34	0.46
M23122211	3.45	0.03	0.17	0.37	0.71	0.13	0.0013	716	716	2	50	131	0.13	0.0012	691	7	2	50	90	1.00	0.68	0.35	0.48
M23122212	3.54	0.03	0.16	0.35	0.74	0.13	0.0013	691	691	2	49	115	0.13	0.0012	670	7	2	49	79	1.00	0.70	0.37	0.48
M33122211	3.17	0.03	0.19	0.40	0.75	0.13	0.0013	810	810	2	59	129	0.12	0.0011	780	8	2	59	88	1.00	0.76	0.39	0.51
M33122212	3.23	0.03	0.18	0.38	0.77	0.13	0.0013	785	785	2	58	114	0.13	0.0011	760	8	2	58	77	1.00	0.78	0.40	0.51
M43122211	2.90	0.04	0.22	0.44	0.78	0.12	0.0012	923	923	3	70	127	0.12	0.0011	878	9	2	70	83	0.99	0.89	0.44	0.55
M43122212	2.95	0.04	0.21	0.43	0.80	0.12	0.0012	899	899	3	69	112	0.12	0.0011	859	9	2	69	72	0.99	0.89	0.45	0.55
M53122211	2.65	0.04	0.27	0.50	0.81	0.12	0.0012	1079	1079	5	86	121	0.12	0.0011	987	10	3	82	73	0.96	1.09	0.52	0.60
M53122212	2.69	0.04	0.26	0.49	0.83	0.12	0.0012	1055	1055	5	84	106	0.12	0.0011	968	10	3	81	63	0.96	1.09	0.54	0.59
M13122221	3.03	0.04	0.19	0.42	0.68	0.12	0.0012	863	863	2	58	173	0.12	0.0011	835	9	2	58	126	1.00	0.58	0.28	0.45
M13122222	3.12	0.03	0.18	0.40	0.71	0.12	0.0012	827	827	2	57	153	0.12	0.0011	804	8	2	57	110	1.00	0.60	0.29	0.45
M23122221	2.77	0.04	0.21	0.44	0.72	0.12	0.0011	981	981	2	70	173	0.12	0.0011	953	10	2	70	125	1.00	0.63	0.30	0.48
M23122222	2.84	0.04	0.20	0.42	0.75	0.12	0.0011	946	946	3	69	152	0.12	0.0011	923	10	2	69	110	1.00	0.64	0.32	0.48
M33122221	2.54	0.05	0.24	0.47	0.75	0.11	0.0011	1115	1115	3	83	170	0.11	0.0010	1082	11	3	83	123	1.00	0.69	0.33	0.51
M33122222	2.59	0.05	0.23	0.45	0.78	0.11	0.0011	1080	1080	3	82	150	0.11	0.0010	1052	11	3	82	107	1.00	0.71	0.34	0.51
M43122221	2.33	0.05	0.28	0.50	0.78	0.11	0.0011	1275	1275	4	99	167	0.11	0.0010	1224	13	3	98	116	0.99	0.81	0.36	0.54
M43122222	2.37	0.05	0.27	0.49	0.81	0.11	0.0011	1239	1239	4	97	147	0.11	0.0010	1193	12	3	97	101	0.99	0.82	0.37	0.54
M53122221	2.13	0.06	0.33	0.59	0.82	0.11	0.0011	1481	1481	6	120	157	0.11	0.0010	1381	14	4	116	104	0.97	0.97	0.45	0.59
M53122222	2.16	0.06	0.32	0.58	0.84	0.11	0.0011	1447	1447	6	118	138	0.11	0.0010	1351	14	4	114	89	0.97	0.98	0.46	0.59
M13211111	9.64	0.01	0.05	0.13	0.66	0.22	0.0019	161	161	1	16	39	0.22	0.0015	149	1	0	16	21	0.99	0.83	0.51	0.49
M13211112	10.06	0.01	0.04	0.12	0.72	0.23	0.0019	149	149	1	15	31	0.22	0.0015	141	1	0	15	17	0.99	0.82	0.53	0.48
M23211111	8.78	0.01	0.06	0.14	0.70	0.21	0.0018	183	183	1	19	39	0.21	0.0014	170	1	1	19	21	1.00	0.93	0.56	0.51
M23211112	9.12	0.01	0.05	0.13	0.75	0.22	0.0018	171	171	1	18	31	0.21	0.0014	162	1	1	18	17	1.00	0.93	0.58	0.50
M33211111	8.04	0.01	0.07	0.16	0.73	0.21	0.0018	210	210	1	23	40	0.20	0.0014	194	2	1	22	21	1.00	1.08	0.63	0.54

Name	T1 [s]	Sa(T1) [g]	Sa(T2) [g]	Sa(T3) [g]	DOC [-]	Disp [m]	ISDR [-]	Total Moment [MN-m]	Total Shear [MN]	Max CB Shear [MN]	Max Pp [MN]	Max wall moment [MN-m]	Disp [m]2	ISDR [-]3	Total Moment [MN-m]4	Total Shear [MN]5	Max CB Shear [MN]6	Max Pp [MN]2	Max wall moment [MN-m]8	C1 [-]	C2 [-]	C3 [-]	Mdy/ Mst [-]
M43211111	7.36	0.01	0.08	0.18	0.76	0.20	0.0017	244	244	2	27	40	0.19	0.0013	221	2	1	27	20	0.98	1.25	0.73	0.58
M43211112	7.56	0.01	0.07	0.17	0.80	0.20	0.0017	232	232	2	26	33	0.20	0.0013	212	2	1	26	16	0.98	1.26	0.75	0.57
M53211111	6.72	0.01	0.10	0.23	0.79	0.19	0.0017	298	298	3	34	40	0.19	0.0013	250	2	1	32	18	0.92	1.48	0.93	0.64
M53211112	6.88	0.01	0.09	0.22	0.82	0.20	0.0017	285	285	3	34	33	0.19	0.0013	242	2	1	31	14	0.91	1.49	0.94	0.64
M13211121	7.85	0.01	0.07	0.17	0.66	0.20	0.0017	218	218	1	22	53	0.20	0.0014	202	2	1	21	30	0.99	0.83	0.46	0.48
M13211122	8.21	0.01	0.06	0.15	0.71	0.20	0.0017	201	201	1	21	42	0.20	0.0014	190	2	1	21	24	0.99	0.83	0.49	0.48
M23211121	7.16	0.01	0.07	0.18	0.70	0.19	0.0016	249	249	1	26	53	0.19	0.0013	233	2	1	26	30	1.00	0.90	0.51	0.50
M23211122	7.45	0.01	0.07	0.16	0.75	0.20	0.0016	232	232	1	25	43	0.19	0.0013	221	2	1	25	24	1.00	0.92	0.53	0.50
M33211121	6.55	0.01	0.08	0.20	0.73	0.19	0.0015	285	285	1	31	53	0.18	0.0012	267	2	1	31	29	1.00	1.00	0.57	0.53
M33211122	6.78	0.01	0.08	0.18	0.78	0.19	0.0016	268	268	2	30	43	0.18	0.0012	254	2	1	30	23	1.00	1.02	0.59	0.53
M43211121	6.00	0.01	0.10	0.23	0.76	0.18	0.0015	331	331	2	38	52	0.18	0.0012	304	2	1	37	28	0.98	1.14	0.66	0.57
M43211122	6.18	0.01	0.09	0.21	0.80	0.18	0.0015	314	314	2	37	43	0.18	0.0012	291	2	1	36	22	0.98	1.15	0.68	0.56
M53211121	5.49	0.02	0.12	0.29	0.79	0.18	0.0015	401	401	3	48	52	0.18	0.0012	346	3	1	44	25	0.93	1.36	0.85	0.62
M53211122	5.63	0.01	0.12	0.27	0.83	0.18	0.0015	383	383	3	46	42	0.18	0.0012	333	3	1	43	20	0.93	1.37	0.86	0.62
M13211211	8.56	0.01	0.06	0.14	0.70	0.21	0.0017	190	190	1	19	41	0.20	0.0014	178	1	1	19	23	0.99	0.83	0.49	0.48
M13211212	8.89	0.01	0.05	0.13	0.75	0.21	0.0017	177	177	1	19	33	0.20	0.0014	170	1	1	18	19	0.99	0.82	0.51	0.47
M23211211	7.77	0.01	0.07	0.16	0.73	0.20	0.0017	218	218	1	23	42	0.19	0.0013	206	2	1	23	23	1.00	0.93	0.54	0.50
M23211212	8.02	0.01	0.06	0.14	0.78	0.20	0.0017	206	206	1	23	34	0.20	0.0013	197	2	1	22	19	1.00	0.92	0.56	0.50
M33211211	7.09	0.01	0.07	0.18	0.76	0.19	0.0016	251	251	1	27	42	0.19	0.0013	237	2	1	27	23	1.00	1.04	0.60	0.53
M33211212	7.28	0.01	0.07	0.16	0.80	0.20	0.0016	239	239	1	27	35	0.19	0.0013	228	2	1	27	18	1.00	1.05	0.61	0.53
M43211211	6.47	0.01	0.09	0.20	0.79	0.19	0.0016	294	294	2	33	42	0.18	0.0012	271	2	1	33	22	0.98	1.18	0.69	0.57
M43211212	6.62	0.01	0.08	0.19	0.82	0.19	0.0016	282	282	2	33	35	0.19	0.0013	262	2	1	32	17	0.98	1.19	0.70	0.56
M53211211	5.89	0.01	0.11	0.26	0.81	0.18	0.0016	358	358	3	42	42	0.18	0.0013	309	2	1	39	19	0.93	1.40	0.88	0.63
M53211212	6.01	0.01	0.11	0.25	0.84	0.19	0.0016	346	346	3	41	34	0.18	0.0013	300	2	1	38	15	0.92	1.41	0.89	0.62
M13211221	6.93	0.01	0.08	0.18	0.70	0.19	0.0015	261	261	1	27	56	0.18	0.0013	247	2	1	26	33	0.99	0.80	0.45	0.47
M13211222	7.20	0.01	0.07	0.16	0.75	0.19	0.0015	244	244	1	26	45	0.19	0.0013	234	2	1	26	27	0.99	0.82	0.47	0.47
M23211221	6.29	0.01	0.08	0.20	0.74	0.18	0.0015	301	301	1	32	56	0.18	0.0012	287	2	1	32	33	1.00	0.85	0.48	0.50
M23211222	6.51	0.01	0.08	0.18	0.78	0.18	0.0015	284	284	1	32	45	0.18	0.0012	273	2	1	32	27	1.00	0.87	0.50	0.49
M33211221	5.74	0.01	0.09	0.22	0.77	0.18	0.0014	347	347	2	39	56	0.17	0.0012	330	3	1	39	32	1.00	0.94	0.54	0.52
M33211222	5.91	0.01	0.09	0.20	0.80	0.18	0.0014	330	330	2	38	46	0.17	0.0012	317	2	1	38	26	1.00	0.95	0.55	0.52
M43211221	5.24	0.02	0.11	0.26	0.79	0.17	0.0014	406	406	3	47	56	0.17	0.0011	379	3	1	46	31	0.99	1.07	0.62	0.56
M43211222	5.37	0.02	0.11	0.24	0.83	0.17	0.0014	389	389	3	46	46	0.17	0.0012	366	3	1	45	25	0.98	1.08	0.63	0.56
M53211221	4.78	0.02	0.14	0.32	0.82	0.17	0.0014	487	487	4	58	55	0.16	0.0012	428	3	2	55	27	0.94	1.30	0.79	0.61
M53211222	4.88	0.02	0.13	0.31	0.85	0.17	0.0014	472	472	4	57	45	0.17	0.0012	418	3	2	54	22	0.93	1.30	0.80	0.61
M13212111	5.56	0.02	0.10	0.25	0.64	0.17	0.0014	371	371	1	24	89	0.17	0.0012	347	3	1	24	56	0.99	0.71	0.38	0.47
M13212112	5.74	0.01	0.09	0.23	0.67	0.18	0.0014	350	350	1	23	78	0.17	0.0012	332	3	1	23	49	0.99	0.73	0.40	0.47
M23212111	5.09	0.02	0.11	0.27	0.68	0.17	0.0013	424	424	1	29	89	0.17	0.0011	401	3	1	29	56	1.00	0.76	0.42	0.50
M23212112	5.23	0.02	0.11	0.25	0.71	0.17	0.0013	403	403	1	28	78	0.17	0.0011	385	3	1	28	49	1.00	0.78	0.43	0.49
M33212111	4.68	0.02	0.12	0.30	0.72	0.16	0.0013	476	476	1	34	88	0.16	0.0011	450	4	1	34	55	1.00	0.86	0.48	0.52
M33212112	4.79	0.02	0.12	0.28	0.75	0.16	0.0013	460	460	1	34	78	0.16	0.0011	437	3	1	34	48	1.00	0.87	0.49	0.52
M43212111	4.30	0.02	0.14	0.33	0.75	0.15	0.0012	539	539	2	40	87	0.15	0.0010	501	4	1	40	51	0.99	1.01	0.56	0.56
M43212112	4.39	0.02	0.14	0.32	0.77	0.16	0.0012	522	522	2	40	77	0.15	0.0010	488	4	1	39	45	0.99	1.02	0.57	0.56
M53212111	3.94	0.02	0.18	0.38	0.78	0.15	0.0012	630	630	3	49	83	0.15	0.0010	557	4	1	47	45	0.95	1.23	0.69	0.61
M53212112	4.01	0.02	0.17	0.37	0.80	0.15	0.0012	613	613	3	49	73	0.15	0.0010	545	4	1	46	39	0.95	1.24	0.71	0.61
M13212121	4.47	0.02	0.13	0.32	0.64	0.16	0.0012	507	507	1	33	117	0.15	0.0011	480	4	1	33	78	0.99	0.66	0.34	0.47
M13212122	4.62	0.02	0.12	0.30	0.68	0.16	0.0012	483	483	1	33	103	0.15	0.0011	461	4	1	32	68	0.99	0.67	0.36	0.47
M23212121	4.10	0.02	0.14	0.34	0.68	0.15	0.0011	569	569	1	40	116	0.14	0.0010	542	4	1	40	77	1.00	0.72	0.38	0.49
M23212122	4.21	0.02	0.14	0.32	0.71	0.15	0.0011	545	545	1	39	102	0.15	0.0010	523	4	1	39	67	1.00	0.73	0.40	0.49
M33212121	3.76	0.03	0.16	0.36	0.72	0.14	0.0011	638	638	2	47	115	0.14	0.0009	607	5	1	47	75	1.00	0.81	0.43	0.52
M33212122	3.86	0.03	0.15	0.34	0.75	0.14	0.0011	615	615	2	46	101	0.14	0.0009	589	5	1	46	65	1.00	0.82	0.44	0.52
M43212121	3.46	0.03	0.18	0.39	0.75	0.14	0.0010	723	723	3	55	112	0.13	0.0009	679	5	2	55	70	0.99	0.94	0.49	0.55
M43212122	3.54	0.03	0.17	0.37	0.78	0.14	0.0011	699	699	3	54	99	0.13	0.0009	660	5	2	54	61	0.99	0.95	0.50	0.55
M53212121	3.17	0.03	0.22	0.45	0.79	0.13	0.0010	843	843	4	68	107	0.13	0.0009	758	6	2	64	63	0.95	1.15	0.61	0.60
M53212122	3.23	0.03	0.22	0.44	0.81	0.13	0.0010	820	820	4	66	95	0.13	0.0009	739	6	2	63	54	0.95	1.16	0.62	0.60
M13212211	5.04	0.02	0.11	0.27	0.67	0.17	0.0013	430	430	1	28	94	0.16	0.0011	408	3	1	28	61	0.99	0.68	0.37	0.47
M13212212	5.19	0.02	0.10	0.25	0.70	0.17	0.0013	409	409	1	28	82	0.16	0.0011	392	3	1	27	53	0.99	0.69	0.38	0.47
M23212211	4.61	0.02	0.12	0.29	0.71	0.16	0.0012	484	484	1	33	93	0.15	0.0011	462	4	1	33	60	1.00	0.75	0.41	0.49
M23212212	4.72	0.02	0.12	0.27	0.74	0.16	0.0012	467	467	1	33	82	0.16	0.0011	449	4	1	33	53	1.00	0.75	0.42	0.49
M33212211	4.22	0.02	0.14	0.32	0.74	0.15	0.0012	545	545	2	39	92	0.15	0.0010	519	4	1	39	58	1.00	0.84	0.46	0.52
M33212212	4.31	0.02	0.13	0.30	0.77	0.15	0.0012	528	528	2	39	81	0.15	0.0010	507	4	1	39	51	1.00	0.85	0.47	0.52
M43212211	3.87	0.03	0.16	0.35	0.77	0.14	0.0011	619	619	2	47	91	0.14	0.0010	581	5	1	46	55	0.99	0.98	0.53	0.56
M43212212	3.94	0.02	0.15	0.34	0.79	0.15	0.0011	603	603	2	46	80	0.14	0.0010	569	4	1	46	48	0.99	0.99	0.55	0.55
M53212211	3.54	0.03	0.19	0.42	0.80	0.14	0.0011	725	725	4	57	87	0.14	0.0010	649	5	2	54	48	0.95	1.19	0.66	0.60
M53212212	3.59	0.03	0.19	0.40	0.82	0.14	0.0011	709	709	4	56	77	0.14	0.0010	637	5	2	53	42	0.95	1.20	0.67	0.60
M13212221	4.04	0.02	0.14	0.34	0.67	0.14	0.0011	579	579	1	38	123	0.14	0.0010	554	4	1	38	84	0.99	0.65	0.33	0.46
M13212222	4.16	0.02	0.13	0.32	0.70	0.15	0.0011	555	555	1	38	108	0.14	0.0010	535	4	1	38	73	0.99	0.65	0.35	0.46
M23212221	3.69	0.03	0.16	0.35	0.71	0.14	0.0010	654	654	2	46	122	0.14	0.0009	629	5	1	46	83	1.00	0.70	0.37	0.48
M23212222	3.78	0.03	0.15	0.34	0.74	0.14	0.0010	630	630	2	45	107	0.14	0.0009	609	5	1	45	72	1.00	0.71	0.38	0.48
M33212221	3.38	0.03	0.18	0.38	0.74	0.13	0.0010	738	738	2	54	120	0.13	0.0009	709	6	2	54	80	1.00	0.78	0.40	0.51
M33212222	3.45	0.03	0.17	0.36	0.77	0.13	0.0010	715	715	2	54	106	0.13	0.0009	690	5	2	54	70	1.00	0.79	0.42	0.51
M43212221	3.10	0.04	0.20	0.42	0.78	0.13	0.0010	840	840	3	64	118	0.13	0.0009	797	6	2	64	76	0.99	0.90	0.46	0.55
M43212222	3.16	0.03	0.19	0.40	0.80	0.13	0.0010	817	817	3	64	104	0.13	0.0009	778	6	2	63	66	0.99	0.91	0.47	0.55
M53212221	2.84	0.04	0.25	0.48	0.81	0.12	0.0010	982	982	5	79	112	0.12	0.0009	894	7	2	75	67	0.96	1.11	0.56	0.60
M53212222	2.88	0.04	0.24	0.47	0.83	0.12	0.0010	958	958	5	77	99	0.12	0.0009	875	7	2	74	58	0.96	1.11	0.57	0.60
M13221111	11.13	0.01	0.04	0.11	0.67	0.25	0.0021	182	182	1	18	43	0.25	0.0017	168	1	1	18	24	0.99	0.79	0.50	0.49
M13221112	11.62	0.01	0.03	0.10	0.72	0.26	0.0021	172	172	1	18	35	0.25	0.0018	162	1	1	18	20	0.99	0.77	0.52	0.48
M23221111	10.14	0.01	0.04	0.12	0.70	0.23	0.0020	199	199	1	20	43	0.22	0.0015	185	1	1	20	23	1.00	0.92	0.59	0.51
M23221112	10.53	0.01	0.04	0.11	0.75	0.24	0.0020	189	189	1	20	35	0.23	0.0016	179	1	1	20	19	1.00	0.90	0.59	0.50
M33221111	9.28	0.01	0.05	0.14	0.73	0.22	0.0019	226	226	1	24	44	0.21	0.0015	208	2	1	24	22	1.00	1.08	0.67	0.54
M33221112	9.58	0.01	0.05	0.12	0.77	0.22	0.0019	213	213	1	24	35	0.22	0.0015	200	2	1	24	18	1.00	1.07	0.68	0.53
M43221111	8.49	0.01	0.06	0.16	0.75	0.21	0.0019	264	264	2	29	45	0.21	0.0014	236	2	1	28	21	0.98	1.31	0.78	0.58
M43221112	8.73	0.01	0.06	0.15	0.79	0.22	0.0019	250	250	2	28	36	0.21	0.0014	227	2	1	28	17	0.98	1.30	0.80	0.58
M53221111	7.76	0.01	0.08	0.20	0.78	0.21	0.0018	324	324	3	37	45	0.20	0.0014	267	2	1	34	19	0.91	1.56	0.98	0.65
M53221112	7.94	0.01	0.08	0.19	0.81	0.21	0.0019	310	310	3	36	37	0.21	0.0014	258	2	1	33	15	0.91	1.57	1.00	0.65
M13221121	9.06	0.01	0.05	0.14	0.66	0.22	0.0018	235	235	1	23	58	0.21	0.0014	217	2	1	23	32	0.99	0.83	0.49	0.49
M13221122	9.48	0.01	0.05	0.13	0.71	0.22	0.0018	217	217	1	23	46	0.21	0.0015	204	2	1	22	26	0.99	0.83	0.51	0.48
M23221121	8.26	0.01	0.06	0.15	0.70	0.21	0.0017	268	268	1	28	58	0.20	0.0014	249	2	1	28	32	1.00	0.93	0.55	0.51
M23221122	8.60	0.01	0.06	0.14	0.75	0.21	0.0017	249	249	1	27	47	0.20	0.0014	236	2	1	27	26	1.00	0.93	0.57	0.50
M33221121	7.57	0.01	0.07	0.17	0.73	0.20	0.0017	307	307	2	33	59	0.19	0.0013	284	2	1	33	31	1.00	1.06	0.61	0.54
M33221122	7.83	0.01	0.07	0.16	0.77	0.20	0.0017	288	288	2	32	48	0.20	0.0013	271	2	1	32	25	1.00	1.08	0.63	0.53
M43221121	6.93	0.01	0.08	0.20	0.75	0.19	0.0016	356	356	2	40	59	0.19	0.0013	323	3	1	40	30	0.98	1.21	0.71	0.57
M43221122	7.14	0.01	0.08	0.18	0.79	0.20	0.0017	337	337	2	39	48	0.19	0.0013	309	2	1	38	24	0.98	1.23	0.73	0.57
M53221121	6.33	0.01	0.10	0.25	0.79	0.19	0.0016	432	432	4	51	58	0.19	0.0013	366	3	2	47	26	0.92	1.44	0.90	0.63
M53221122	6.50	0.01	0.10	0.23	0.82	0.19	0.0016	413	413	4	50	48	0.19	0.0013	352	3	1	45	21	0.92	1.46	0.91	0.63
M13221211	9.88	0.01	0.05	0.12	0.70	0.22	0.0019	205	205	1	20	45	0.22	0.0015	192	2	1	20	25	0.99	0.83	0.52	0.48
M13221212	10.26	0.01	0.04	0.11	0.75	0.23	0.0019	194	194	1	20	36	0.22	0.0016	185	1	1	20	21	0.99	0.81	0.53	0.48
M23221211	8.97	0.01	0.05	0.13	0.73	0.21	0.0018	235	235	1	25	46	0.21	0.0014	221	2	1	24	25	1.00	0.93	0.57	0.51
M23221212	9.27	0.01	0.05	0.12	0.78	0.22	0.0018	221	221	1	24	37	0.21	0.0014	212	2	1	24	20	1.00	0.92	0.59	0.50
M33221211	8.18	0.01	0.06	0.15	0.76	0.21	0.0018	270	270	2	29	47	0.20	0.0014	253	2	1	29	24	1.00	1.08	0.64	0.53
M33221212	8.41	0.01	0.06	0.14	0.80	0.21	0.0018	257	257	2	29	38	0.20	0.0014	244	2	1	29	20	1.00	1.07	0.66	0.53
M43221211	7.47	0.01	0.07	0.18	0.78	0.20	0.0017	316	316	2	35	48	0.20	0.0013	288	2	1	35	23	0.98	1.26	0.74	0.57
M43221212	7.64	0.01	0.07	0.16	0.82	0.20	0.0017	303	303	2	35	39	0.20	0.0013	279	2	1	34	18	0.98	1.27	0.75	0.57
M53221211	6.81	0.01	0.09	0.22	0.81	0.20	0.0017	387	387	4	45	47	0.19	0.0013	328	3	1	41	20	0.92	1.48	0.94	0.64

Name	T1 [s]	Sa(T1) [g]	Sa(T2) [g]	Sa(T3) [g]	DOC [-]	Disp [m]	ISDR [-]	Total Moment [MN-m]	Total Shear [MN]	Max CB Shear [MN]	Max Pp [MN]	Max wall moment [MN-m]	Disp [m]2	ISDR [-]3	Total Moment [MN-m]4	Total Shear [MN]5	Max CB Shear [MN]6	Max Pp [MN]2	Max wall moment [MN-m]8	C1 [-]	C2 [-]	C3 [-]	Mdy/ Mst [-]
M13221221	8.00	0.01	0.06	0.16	0.70	0.20	0.0017	280	280	1	28	62	0.20	0.0014	263	2	1	28	35	0.99	0.83	0.48	0.48
M13221222	8.31	0.01	0.06	0.14	0.75	0.20	0.0017	261	261	1	28	50	0.20	0.0014	250	2	1	28	28	0.99	0.82	0.50	0.47
M23221221	7.27	0.01	0.07	0.17	0.73	0.19	0.0016	322	322	1	34	62	0.19	0.0013	305	2	1	34	35	1.00	0.91	0.52	0.50
M23221222	7.51	0.01	0.07	0.16	0.78	0.20	0.0016	304	304	2	34	51	0.19	0.0013	291	2	1	34	28	1.00	0.93	0.54	0.50
M33221221	6.63	0.01	0.08	0.19	0.76	0.19	0.0015	371	371	2	41	62	0.18	0.0012	350	3	1	41	34	1.00	1.01	0.58	0.53
M33221222	6.82	0.01	0.08	0.18	0.80	0.19	0.0016	353	353	2	40	51	0.18	0.0012	337	3	1	40	28	1.00	1.02	0.59	0.53
M43221221	6.06	0.01	0.09	0.22	0.79	0.18	0.0015	433	433	3	50	62	0.18	0.0012	401	3	2	49	33	0.98	1.14	0.67	0.57
M43221222	6.20	0.01	0.09	0.21	0.82	0.18	0.0015	415	415	3	49	51	0.18	0.0012	387	3	2	48	26	0.98	1.16	0.68	0.56
M53221221	5.52	0.02	0.12	0.28	0.81	0.18	0.0015	527	527	5	63	62	0.18	0.0012	457	4	2	58	29	0.93	1.36	0.85	0.62
M53221222	5.63	0.01	0.11	0.27	0.84	0.18	0.0015	508	508	5	61	51	0.18	0.0012	444	3	2	57	23	0.93	1.37	0.86	0.62
M13222111	6.42	0.01	0.09	0.22	0.63	0.18	0.0015	396	396	1	25	99	0.18	0.0012	367	3	1	25	59	0.99	0.76	0.41	0.48
M13222112	6.62	0.01	0.08	0.20	0.67	0.19	0.0015	375	375	1	25	86	0.18	0.0013	351	3	1	25	51	0.99	0.78	0.43	0.48
M23222111	5.88	0.01	0.09	0.23	0.68	0.18	0.0014	451	451	1	31	98	0.17	0.0012	423	3	1	31	59	1.00	0.82	0.45	0.50
M23222112	6.04	0.01	0.09	0.22	0.71	0.18	0.0014	430	430	1	30	86	0.18	0.0012	406	3	1	30	52	1.00	0.83	0.47	0.50
M33222111	5.40	0.02	0.11	0.25	0.71	0.17	0.0014	515	515	2	37	98	0.17	0.0012	483	4	1	37	59	1.00	0.90	0.51	0.53
M33222112	5.53	0.02	0.10	0.24	0.74	0.17	0.0014	493	493	2	36	86	0.17	0.0012	467	4	1	36	51	1.00	0.92	0.52	0.53
M43222111	4.96	0.02	0.12	0.29	0.74	0.17	0.0014	594	594	2	44	98	0.17	0.0011	549	4	1	44	56	0.99	1.04	0.60	0.56
M43222112	5.07	0.02	0.12	0.28	0.77	0.17	0.0014	574	574	2	44	86	0.17	0.0011	534	4	1	43	49	0.99	1.05	0.61	0.56
M53222111	4.55	0.02	0.15	0.35	0.78	0.16	0.0013	697	697	4	54	95	0.16	0.0011	609	5	2	51	50	0.94	1.28	0.76	0.62
M53222112	4.63	0.02	0.15	0.34	0.80	0.16	0.0013	678	678	4	54	84	0.16	0.0011	596	5	2	50	43	0.94	1.29	0.77	0.61
M13222121	5.16	0.02	0.11	0.28	0.64	0.17	0.0013	556	556	1	36	132	0.17	0.0011	522	4	1	36	85	0.99	0.68	0.37	0.47
M13222122	5.33	0.02	0.10	0.25	0.67	0.17	0.0013	524	524	1	35	115	0.17	0.0012	497	4	1	35	74	0.99	0.70	0.38	0.47
M23222121	4.73	0.02	0.12	0.29	0.68	0.16	0.0012	626	626	2	43	131	0.16	0.0011	593	5	1	43	84	1.00	0.75	0.41	0.49
M23222122	4.87	0.02	0.11	0.28	0.71	0.16	0.0013	600	600	2	43	115	0.16	0.0011	573	4	1	43	74	1.00	0.75	0.42	0.49
M33222121	4.35	0.02	0.14	0.32	0.72	0.15	0.0012	701	701	2	51	129	0.15	0.0010	663	5	2	51	81	1.00	0.85	0.46	0.52
M33222122	4.46	0.02	0.13	0.30	0.74	0.16	0.0012	675	675	2	50	114	0.15	0.0010	643	5	2	50	71	1.00	0.85	0.48	0.52
M43222121	4.00	0.02	0.16	0.35	0.75	0.15	0.0012	793	793	3	60	127	0.15	0.0010	739	6	2	60	77	0.99	0.99	0.54	0.56
M43222122	4.08	0.02	0.15	0.34	0.77	0.15	0.0012	767	767	3	59	112	0.15	0.0010	719	6	2	59	67	0.99	1.00	0.55	0.56
M53222121	3.66	0.03	0.19	0.41	0.78	0.14	0.0011	925	925	5	74	122	0.14	0.0010	823	6	2	70	68	0.95	1.21	0.67	0.61
M53222122	3.73	0.03	0.18	0.40	0.80	0.14	0.0012	900	900	5	72	107	0.14	0.0010	803	6	2	69	58	0.95	1.22	0.68	0.61
M13222211	5.82	0.01	0.09	0.23	0.66	0.18	0.0014	457	457	1	30	104	0.17	0.0012	431	3	1	29	65	0.99	0.73	0.40	0.47
M13222212	5.99	0.01	0.09	0.22	0.70	0.18	0.0014	435	435	1	29	91	0.17	0.0012	414	3	1	29	56	0.99	0.74	0.41	0.47
M23222211	5.32	0.02	0.10	0.25	0.70	0.17	0.0013	525	525	1	36	104	0.17	0.0011	499	4	1	36	65	1.00	0.78	0.44	0.49
M23222212	5.45	0.02	0.10	0.23	0.73	0.17	0.0013	503	503	1	36	91	0.17	0.0011	482	4	1	35	57	1.00	0.79	0.45	0.49
M33222211	4.87	0.02	0.12	0.28	0.74	0.17	0.0013	600	600	2	43	104	0.16	0.0011	569	4	1	43	64	1.00	0.87	0.49	0.52
M33222212	4.97	0.02	0.11	0.26	0.77	0.17	0.0013	581	581	2	43	92	0.16	0.0011	555	4	1	43	56	1.00	0.87	0.50	0.52
M43222211	4.47	0.02	0.14	0.31	0.77	0.16	0.0013	681	681	3	51	103	0.16	0.0011	635	5	2	50	60	0.99	1.02	0.58	0.56
M43222212	4.55	0.02	0.13	0.30	0.79	0.16	0.0013	662	662	3	50	91	0.16	0.0011	622	5	2	50	52	0.99	1.02	0.59	0.56
M53222211	4.09	0.02	0.17	0.37	0.80	0.15	0.0012	798	798	4	62	98	0.15	0.0010	707	5	2	59	53	0.95	1.24	0.71	0.61
M53222212	4.15	0.02	0.16	0.36	0.82	0.15	0.0012	781	781	4	61	87	0.15	0.0011	694	5	2	58	45	0.94	1.25	0.73	0.61
M13222221	4.66	0.02	0.12	0.30	0.67	0.16	0.0012	637	637	1	42	139	0.16	0.0011	606	5	1	42	92	0.99	0.67	0.36	0.47
M13222222	4.80	0.02	0.11	0.28	0.70	0.16	0.0012	610	610	1	42	122	0.16	0.0011	586	5	1	41	80	0.99	0.67	0.37	0.46
M23222221	4.26	0.02	0.13	0.32	0.71	0.15	0.0011	717	717	2	50	138	0.15	0.0010	686	5	2	50	90	1.00	0.73	0.40	0.49
M23222222	4.37	0.02	0.13	0.30	0.74	0.15	0.0011	690	690	2	50	121	0.15	0.0010	665	5	2	49	79	1.00	0.74	0.41	0.49
M33222221	3.91	0.03	0.15	0.34	0.74	0.14	0.0011	807	807	3	59	136	0.14	0.0010	771	6	2	59	87	1.00	0.82	0.44	0.52
M33222222	3.99	0.02	0.14	0.33	0.77	0.15	0.0011	782	782	3	58	120	0.14	0.0010	751	6	2	58	76	1.00	0.83	0.46	0.52
M43222221	3.58	0.03	0.17	0.37	0.77	0.14	0.0011	917	917	3	70	133	0.14	0.0009	864	7	2	69	82	0.99	0.95	0.50	0.55
M43222222	3.65	0.03	0.17	0.36	0.80	0.14	0.0011	891	891	3	69	117	0.14	0.0009	844	7	2	68	71	0.99	0.96	0.52	0.55
M53222221	3.28	0.03	0.21	0.44	0.80	0.13	0.0011	1073	1073	5	85	127	0.13	0.0009	966	7	3	81	73	0.95	1.17	0.63	0.60
M53222222	3.33	0.03	0.21	0.43	0.82	0.13	0.0011	1048	1048	5	84	112	0.13	0.0009	947	7	3	80	63	0.95	1.17	0.64	0.60

Appendix B: Ground motion de-aggregation

The following figure shows the De-aggregation for the Vancouver site for the 50% in 30 year hazard.

B.1 - Vancouver LH

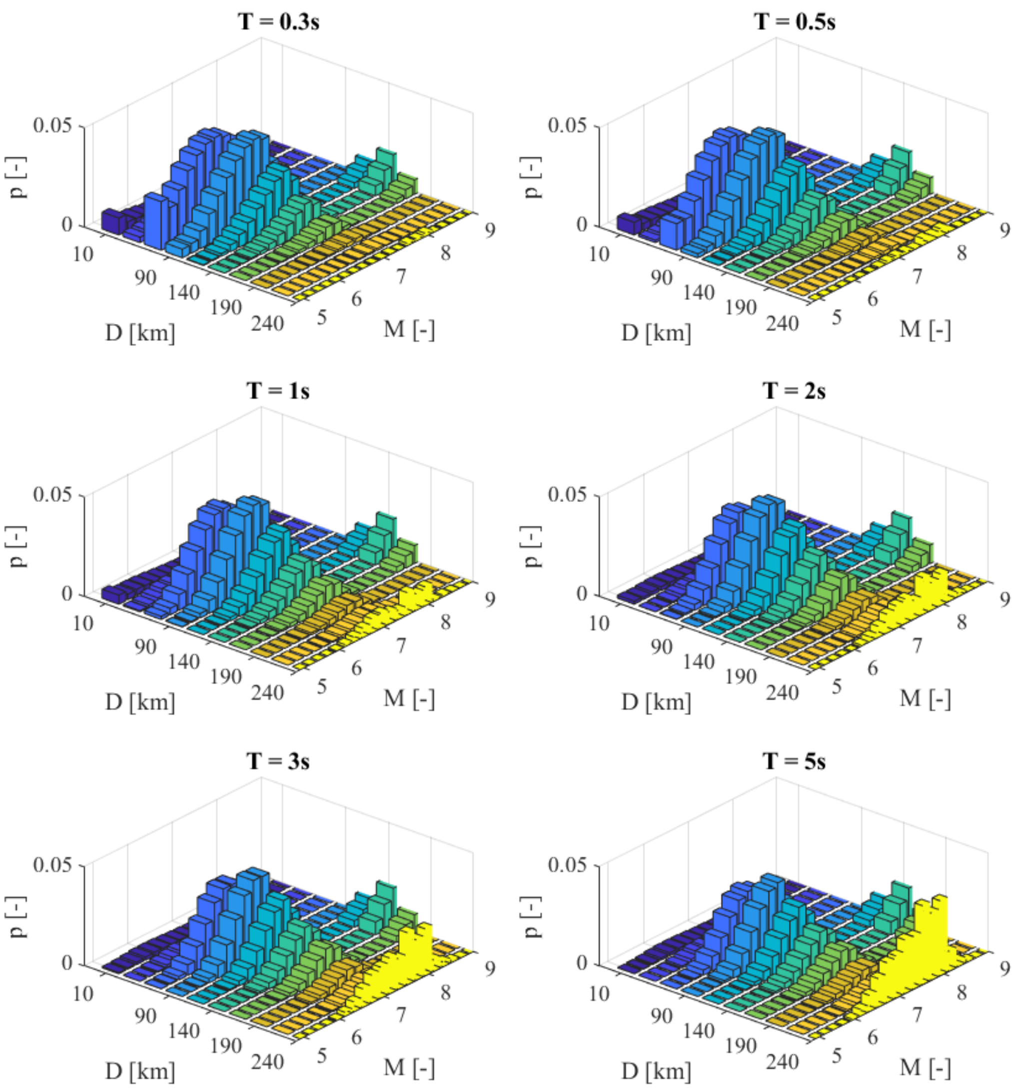

Figure: De-aggregation for Vancouver 50% in 30 year hazard: (a) T = 0.3s; (b) T = 0.5s; (c) T = 1s; (d) T = 2s; (e) T = 3s; (f) and T = 5s

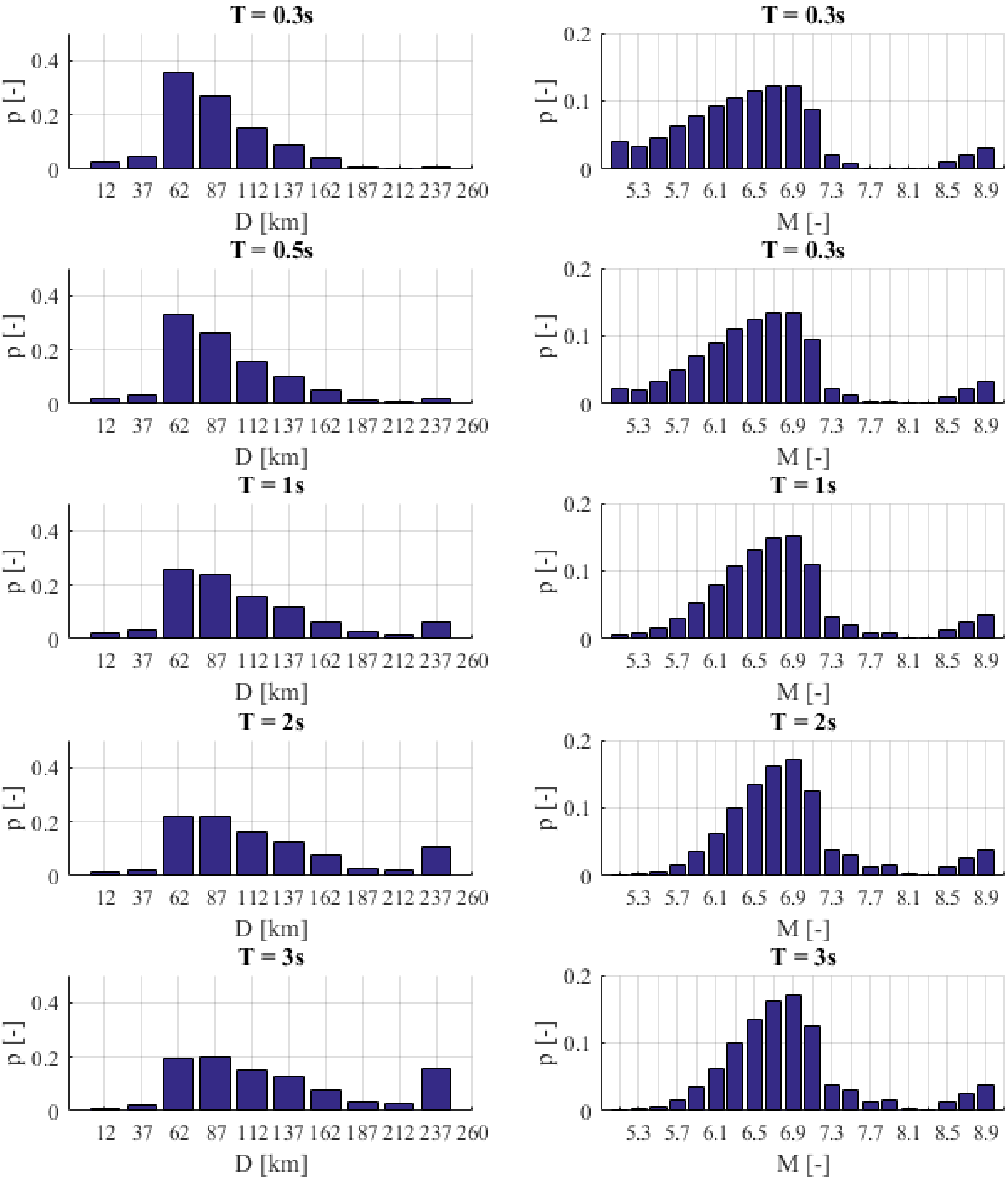

Figure: De-aggregation for Vancouver 50% in 30 year hazard

B.2 - Vancouver MH

The following figure shows the De-aggregation for the Vancouver site for the 20% in 50 year hazard.

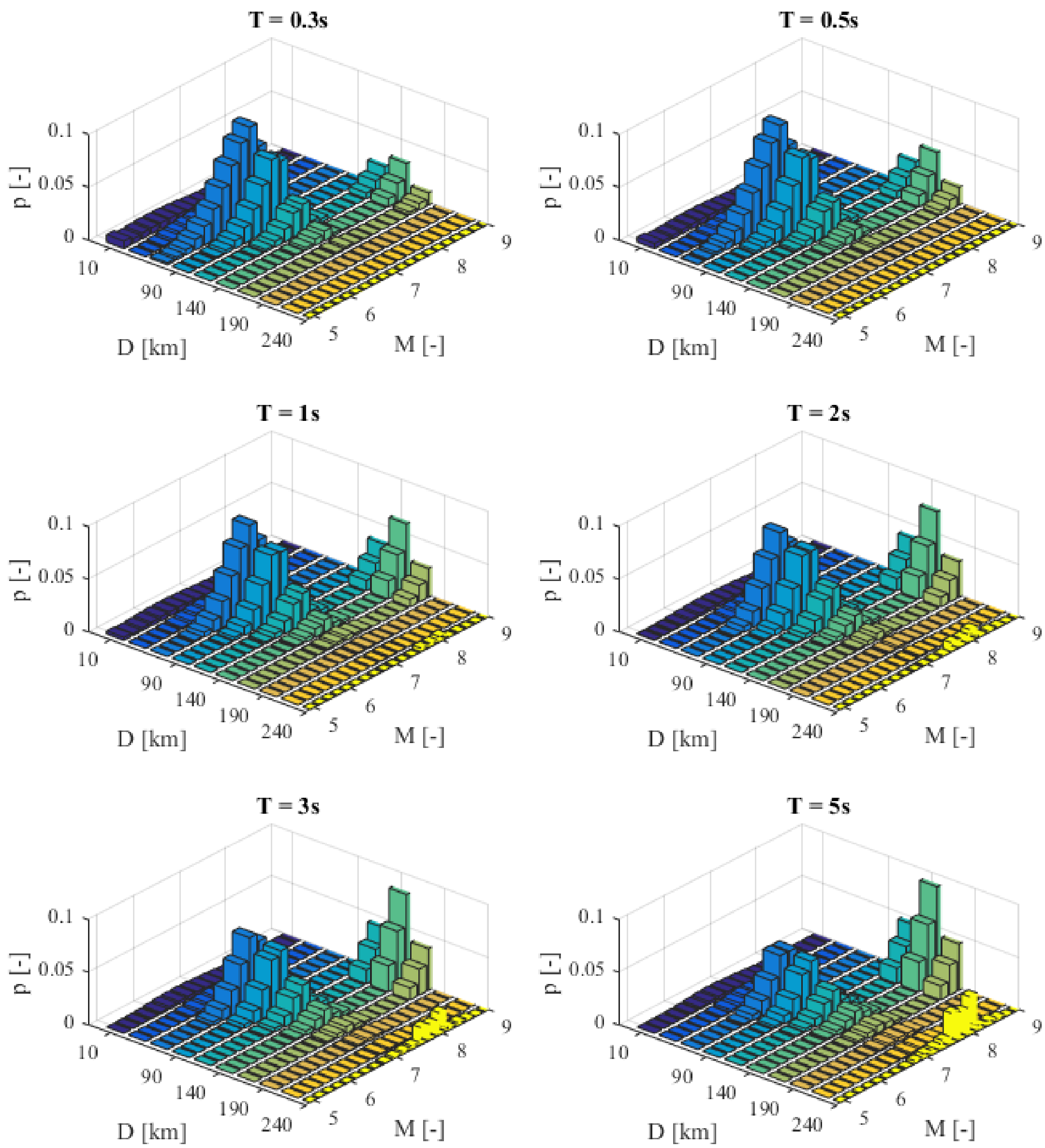

Figure: De-aggregation for Vancouver 20% in 50 year hazard: (a) T = 0.3s; (b) T = 0.5s; (c) T = 1s; (d) T = 2s; (e) T = 3s; (f) and T = 5s

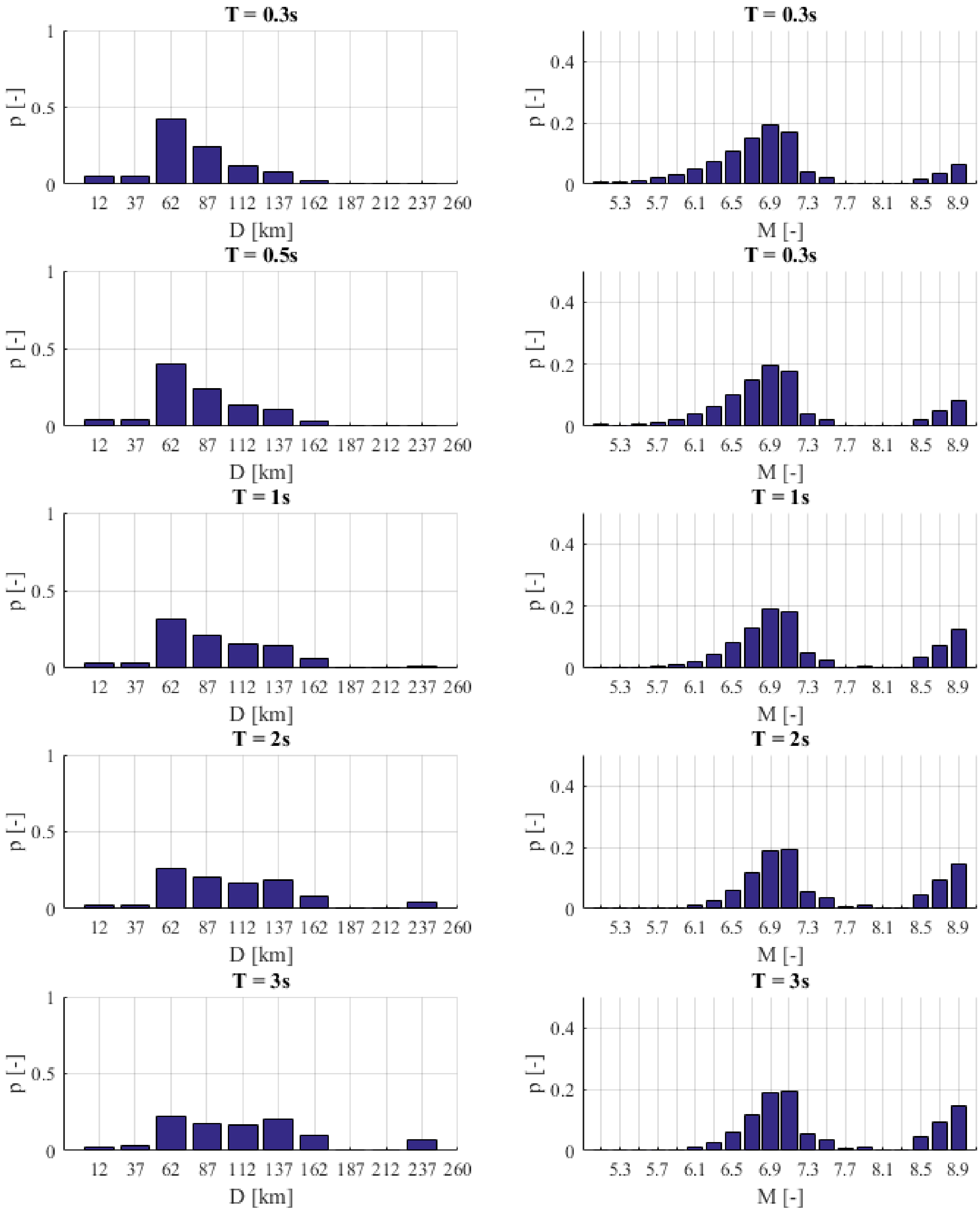

Figure: De-aggregation for Vancouver 20% in 50 year hazard

B.3 - Vancouver HH

The following figure shows the De-aggregation for the Vancouver site for the 2% in 50 year hazard.

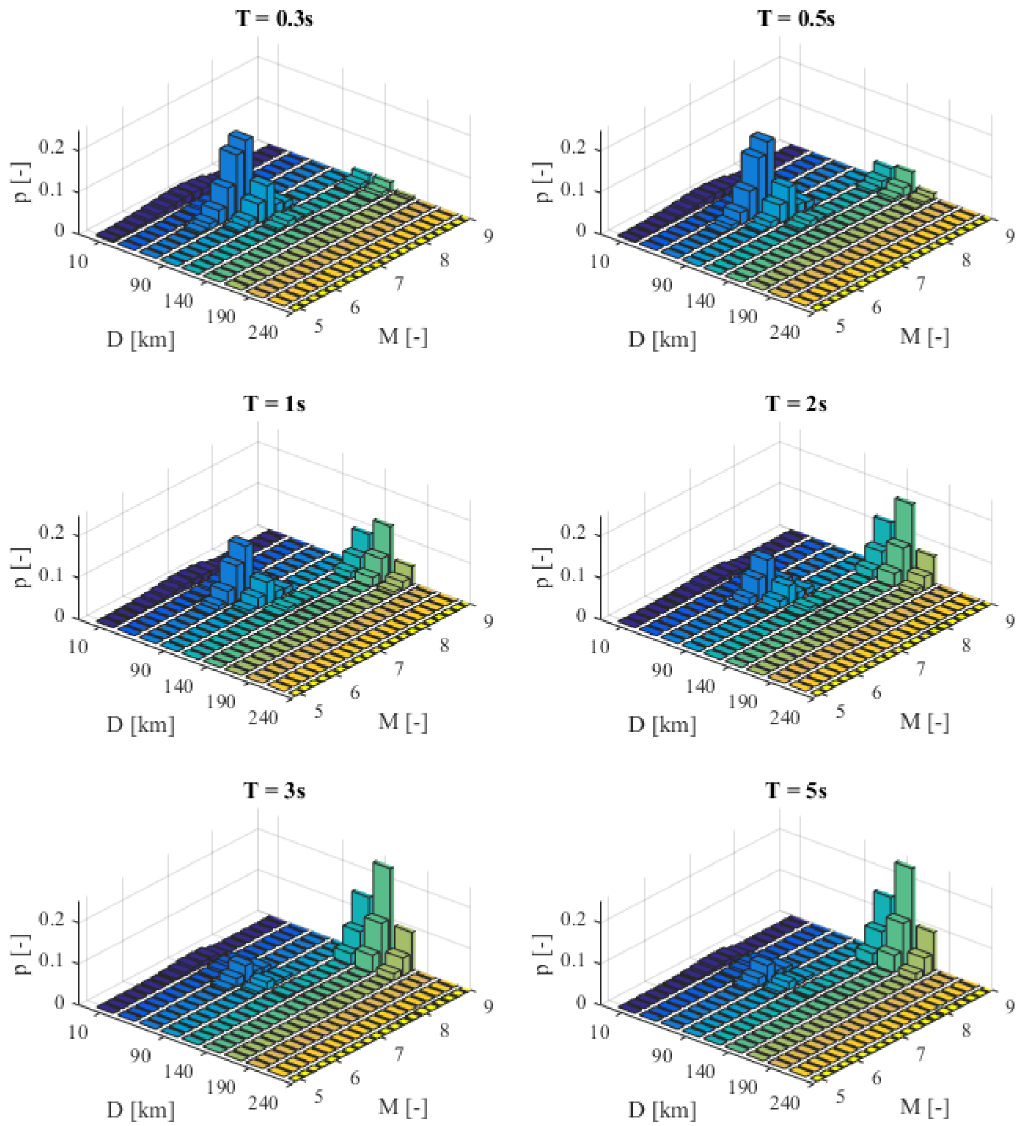

Figure: De-aggregation for Vancouver 2% in 50 year hazard

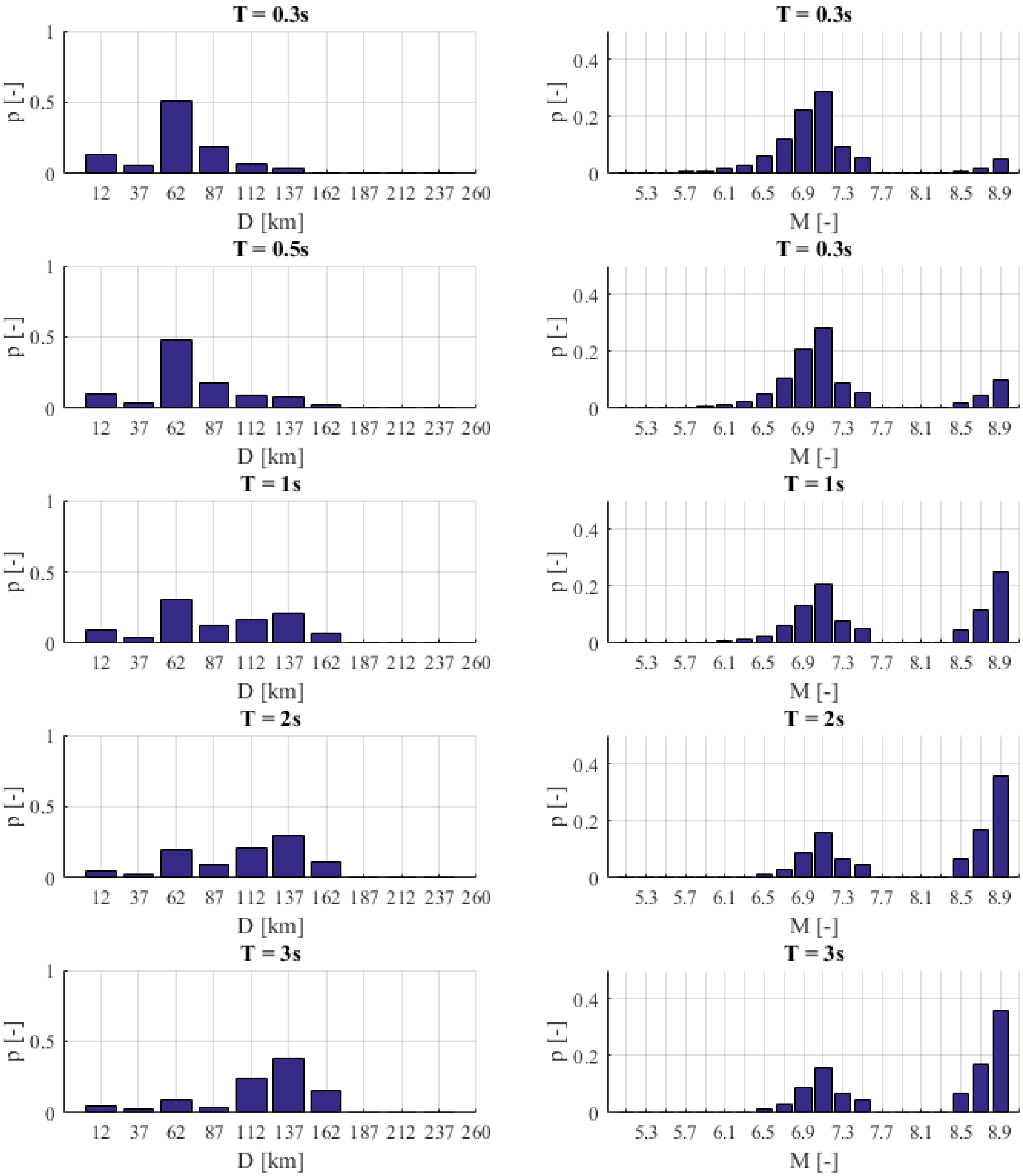

Figure: De-aggregation for Vancouver 2% in 50 year hazard

B.4 - Victoria LH

The following figure shows the De-aggregation for the Victoria site for the 50% in 30 year hazard.

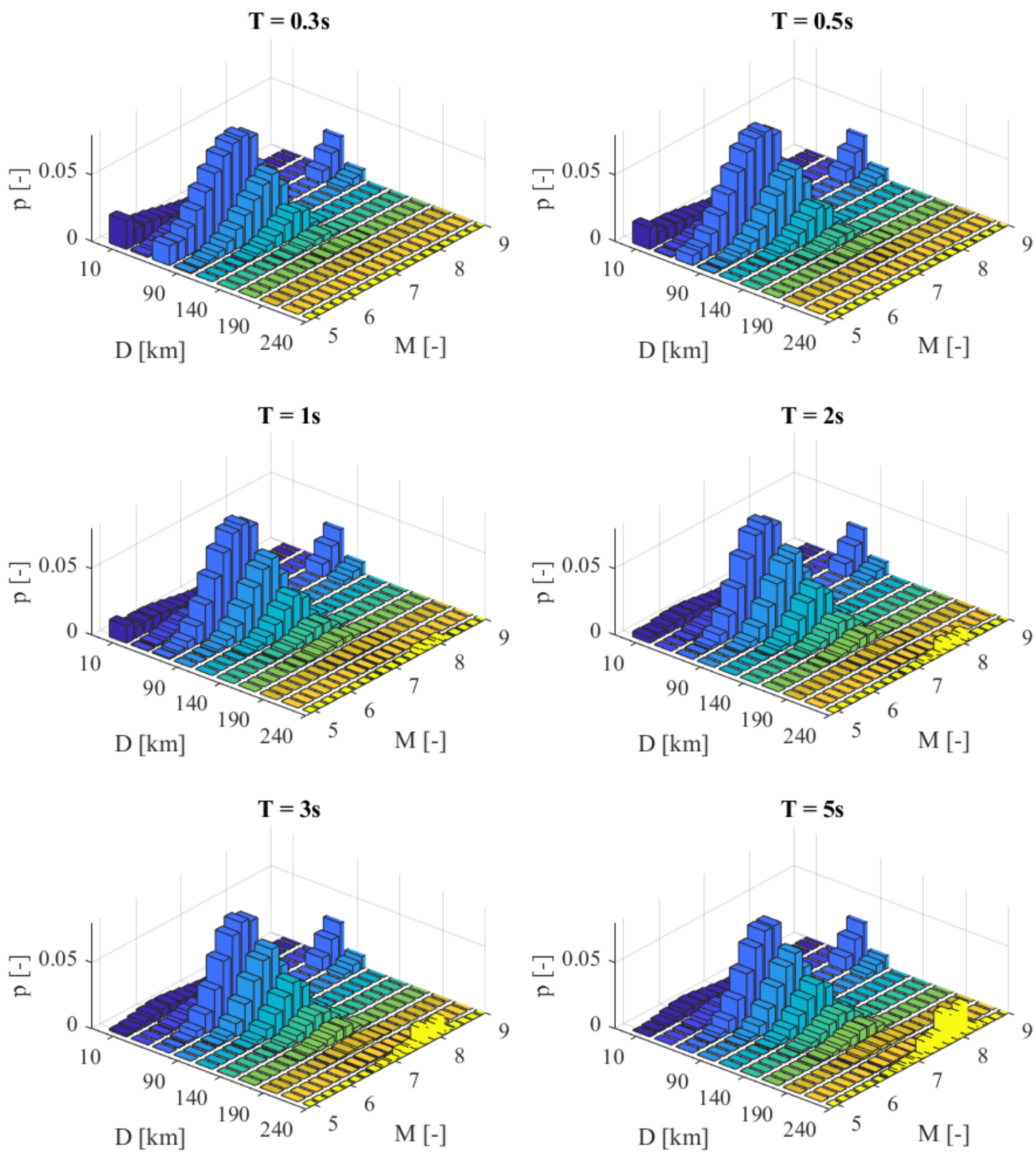

Figure: De-aggregation for Victoria 50% in 30 year hazard: (a) T = 0.3s; (b) T = 0.5s; (c) T = 1s; (d) T = 2s; (e) T = 3s; (f) and T = 5s

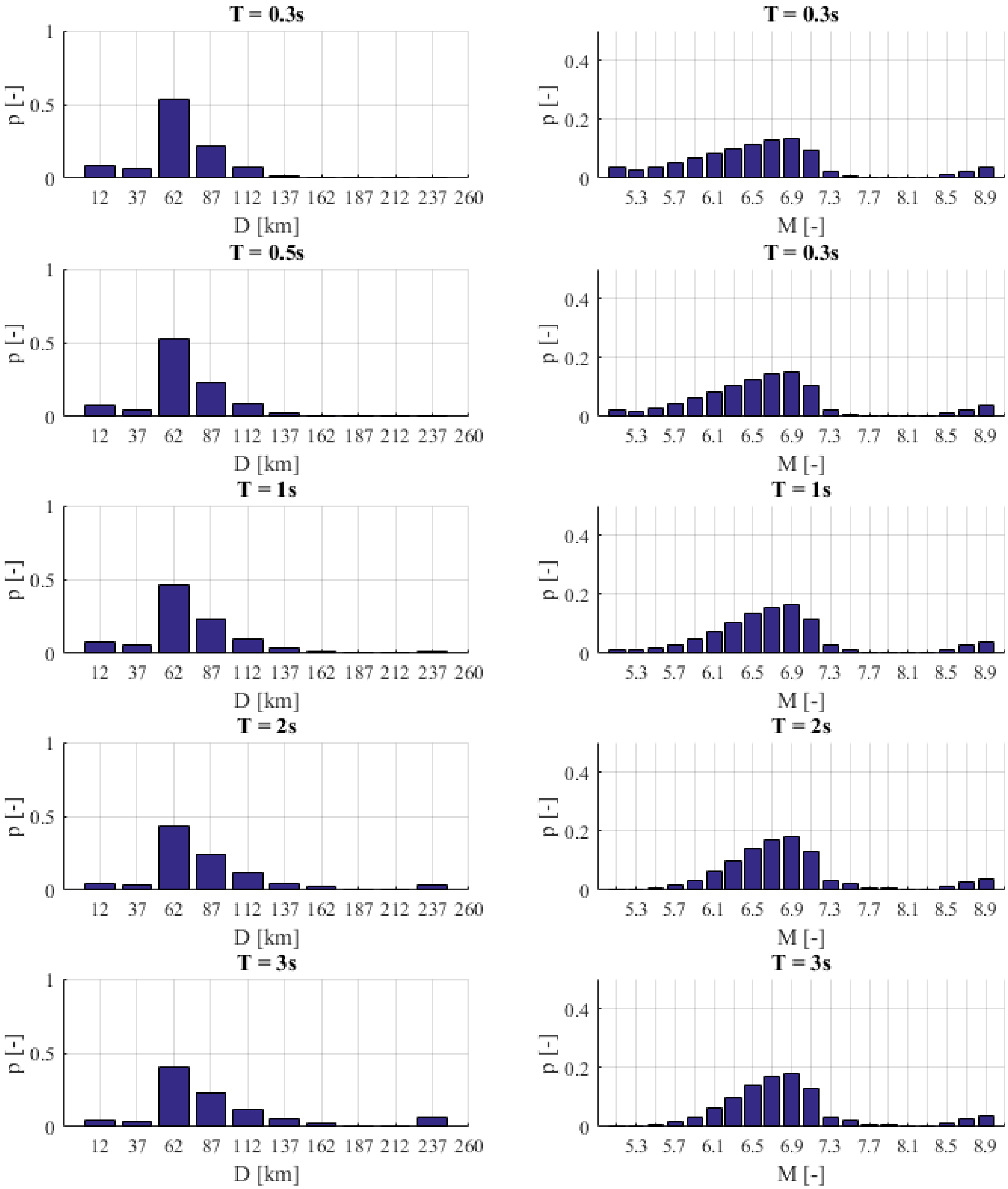

Figure: De-aggregation for Victoria 50% in 30 year hazard

B.5 - Victoria MH

The following figure shows the De-aggregation for the Victoria site for the 20% in 50 year hazard.

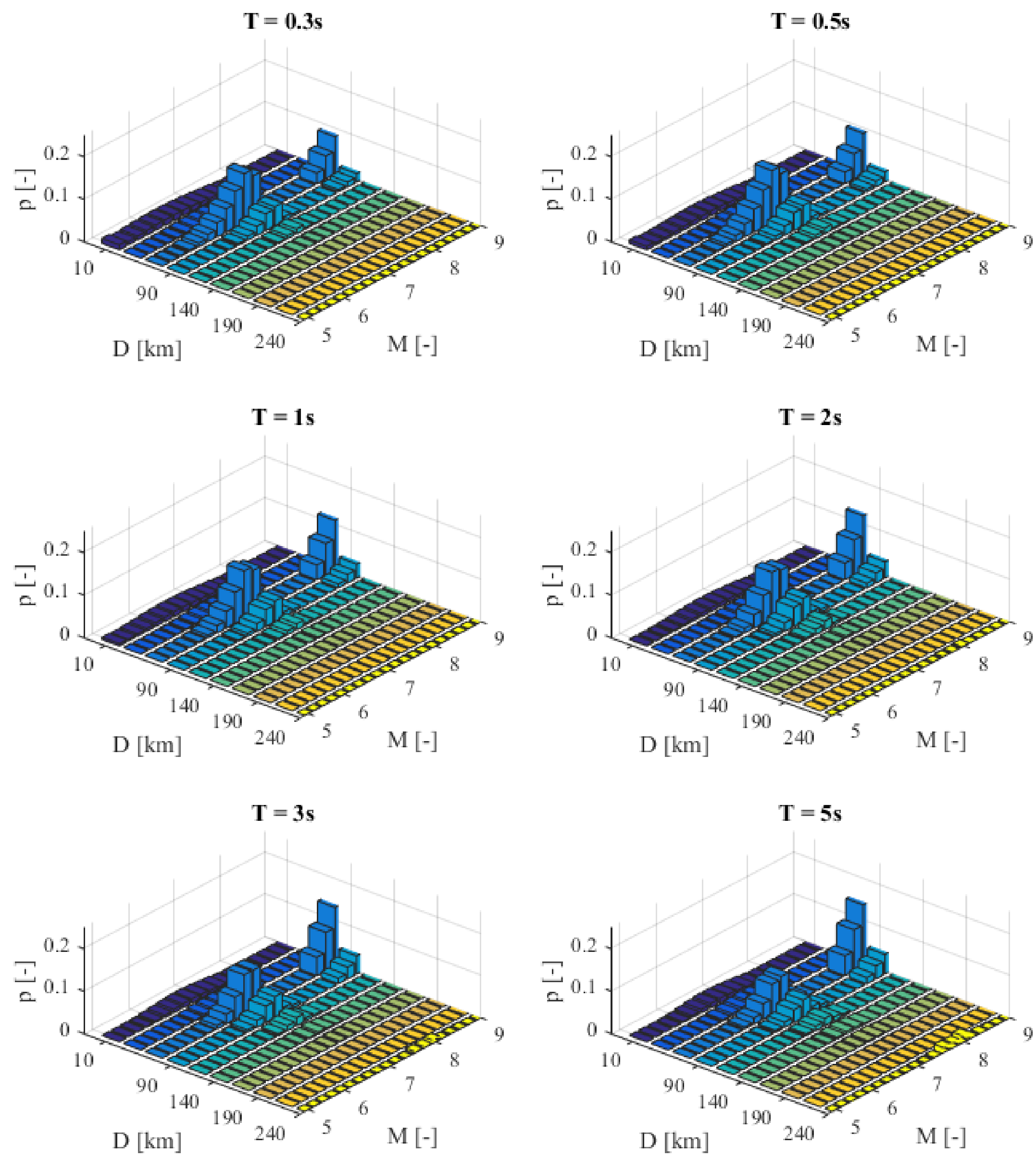

Figure: De-aggregation for Victoria 20% in 50 year hazard: (a) T = 0.3s; (b) T = 0.5s; (c) T = 1s; (d) T = 2s; (e) T = 3s; (f) and T = 5s

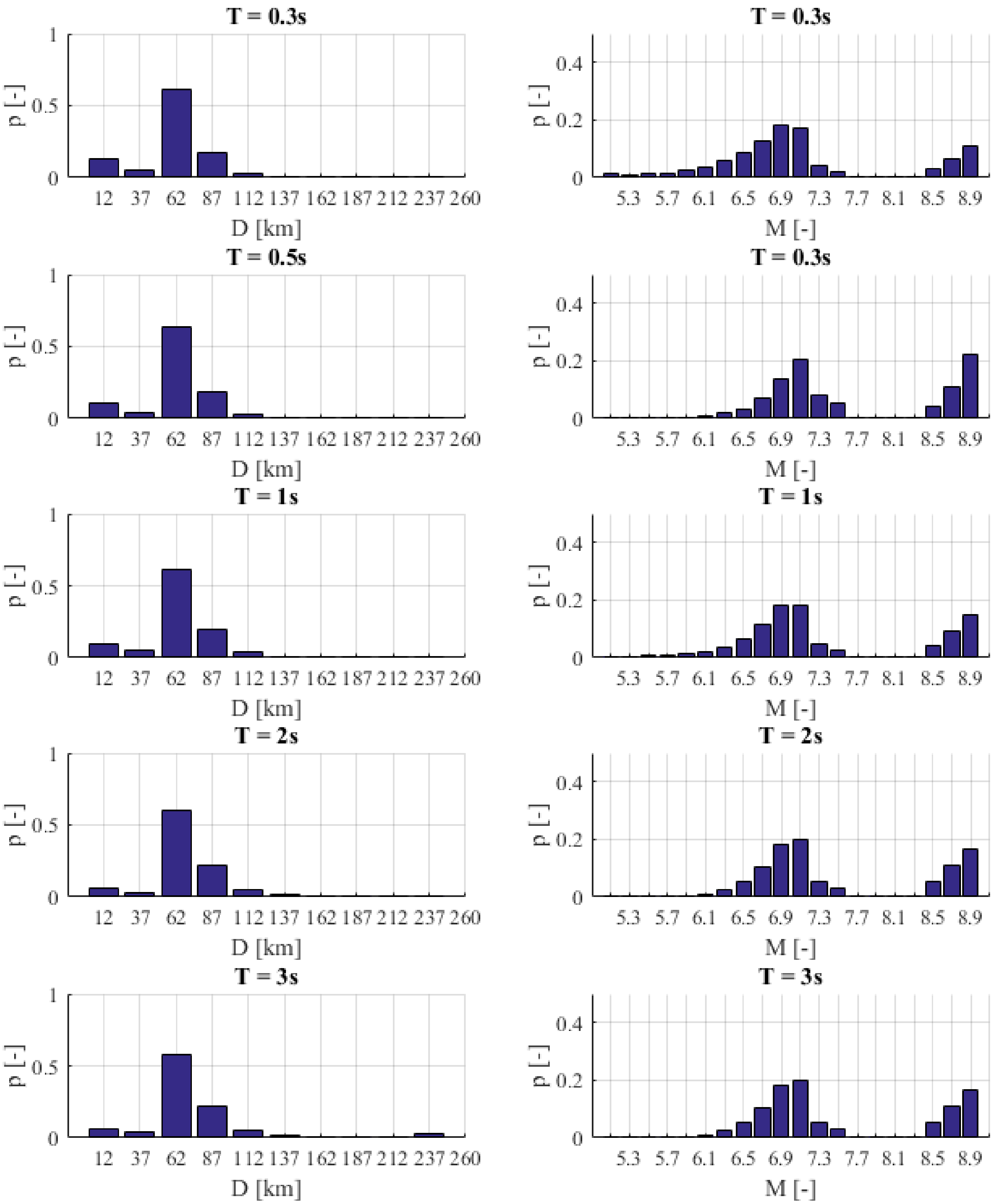

Figure: De-aggregation for Victoria 20% in 50 year hazard

B.5 - Victoria HH

The following figure shows the De-aggregation for the Victoria site for the 2% in 50 year hazard.

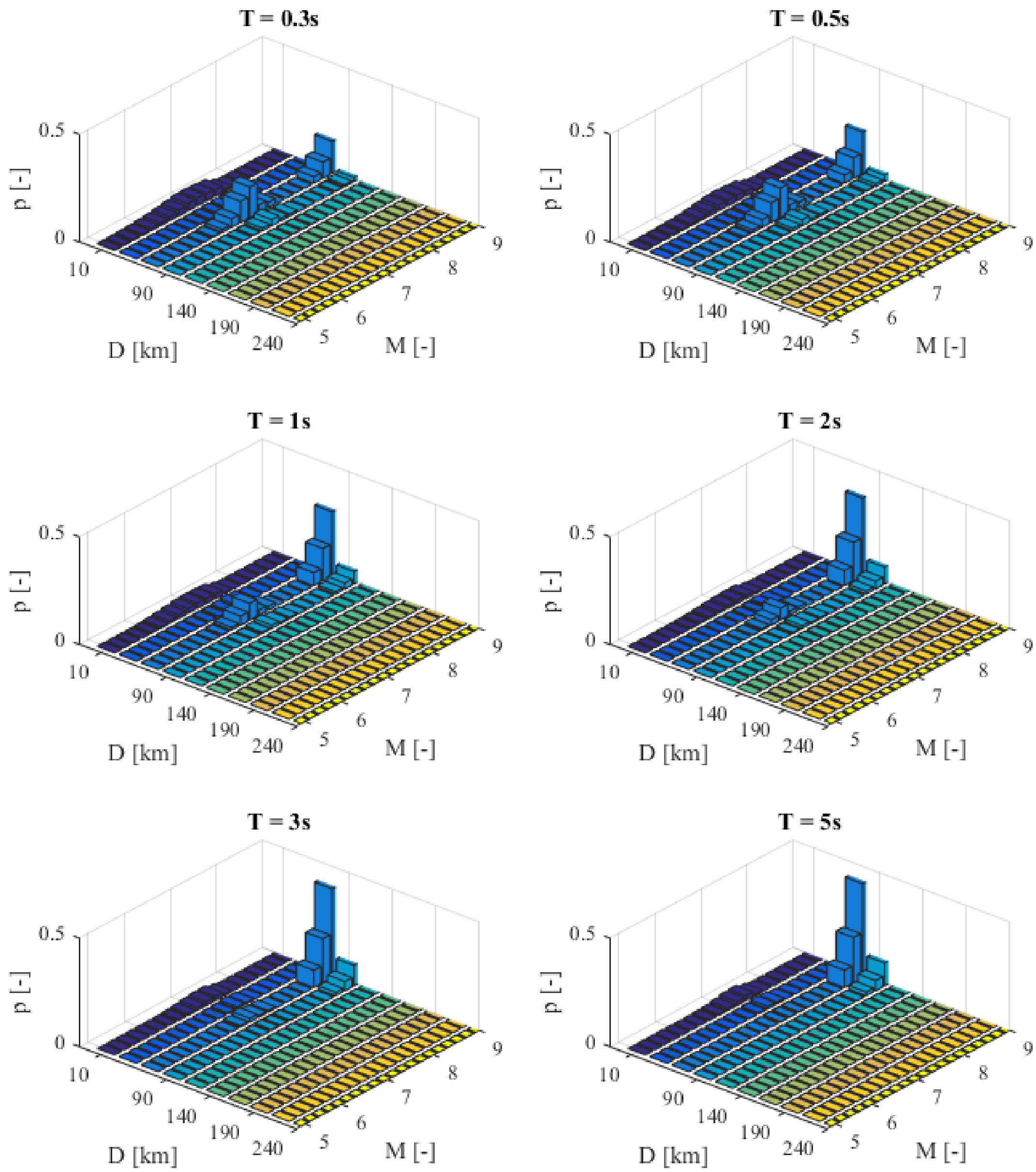

Figure: De-aggregation for Victoria 2% in 50 year hazard: (a) T = 0.3s; (b) T = 0.5s; (c) T = 1s; (d) T = 2s; (e) T = 3s; (f) and T = 5s

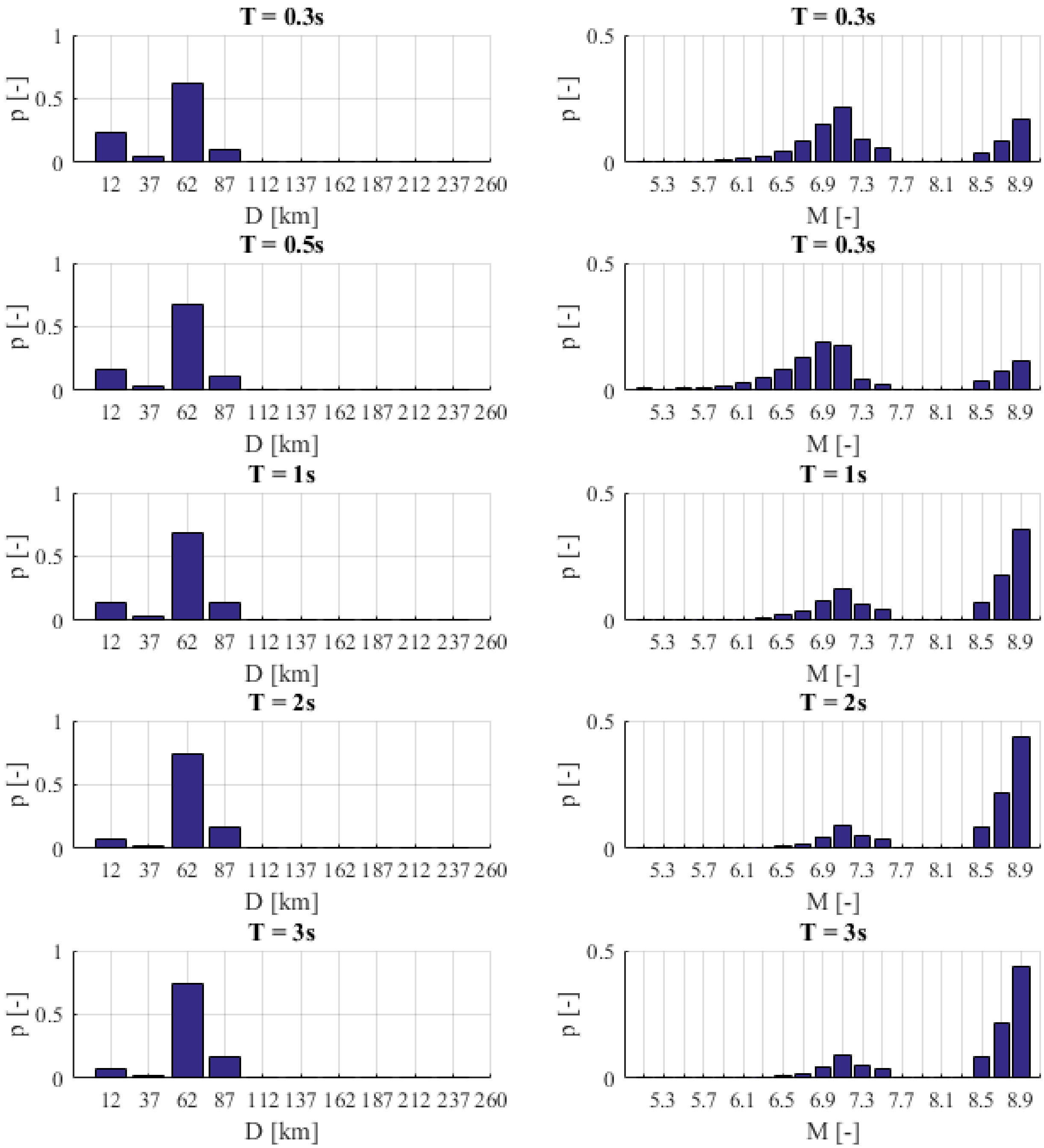

Figure: 2D De-aggregation for Victoria 2% in 50 year hazard

Appendix C: Ground motion scaling for unidirectional

C.1 - Vancouver LH

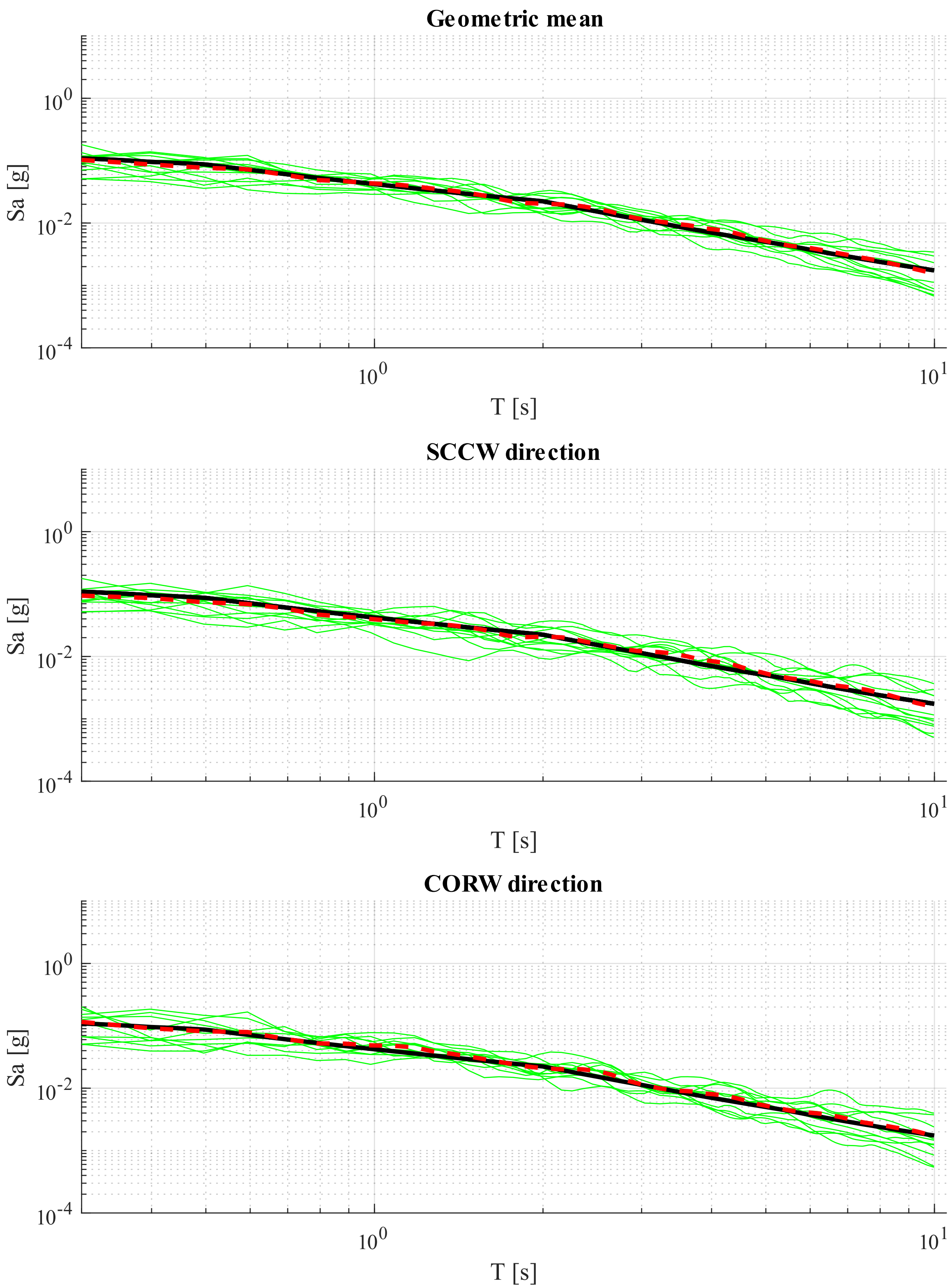

Figure: Crustal LH Vancouver

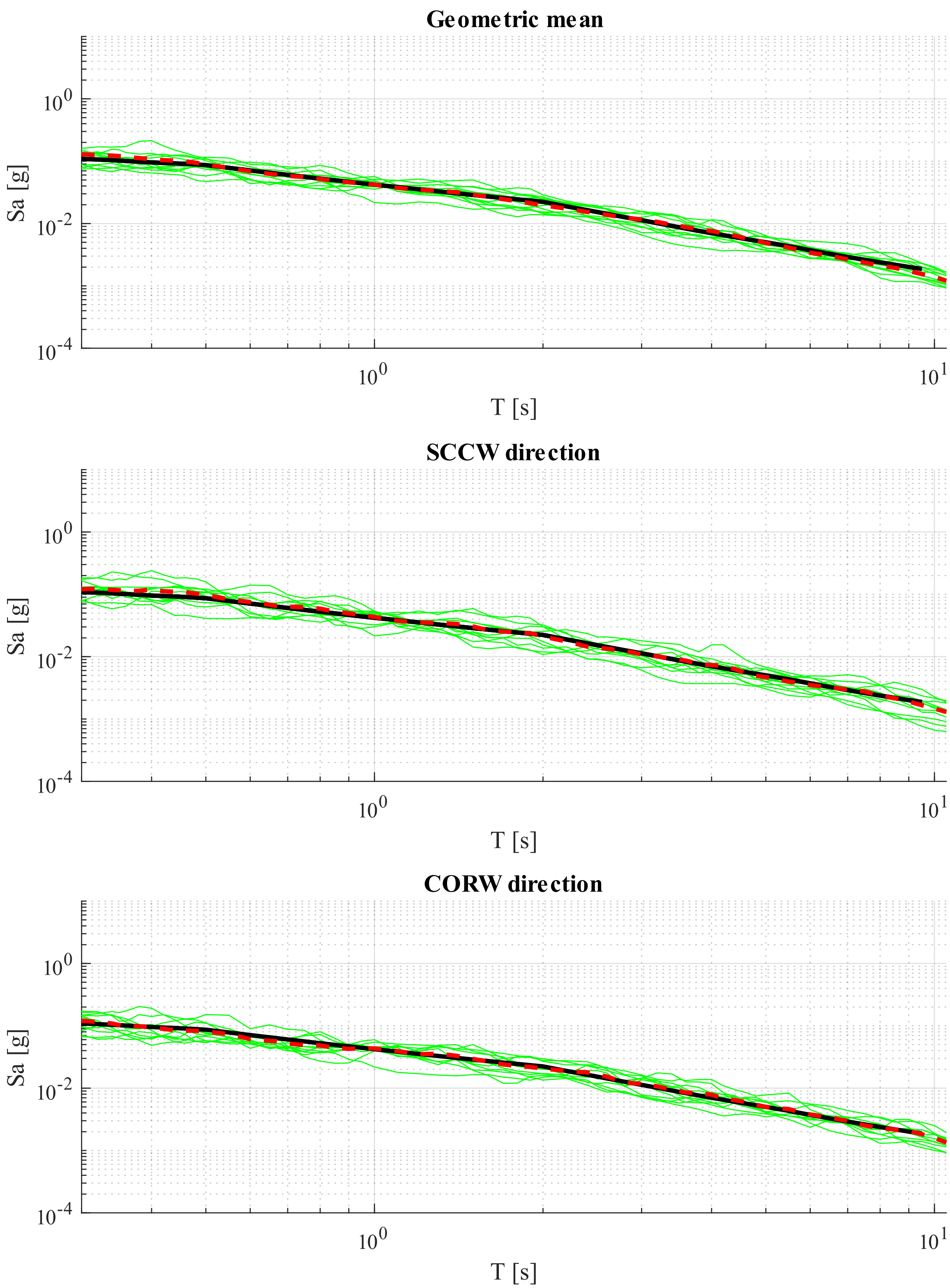

Figure: Subcrustal LH Vancouver

C.2 - Vancouver MH

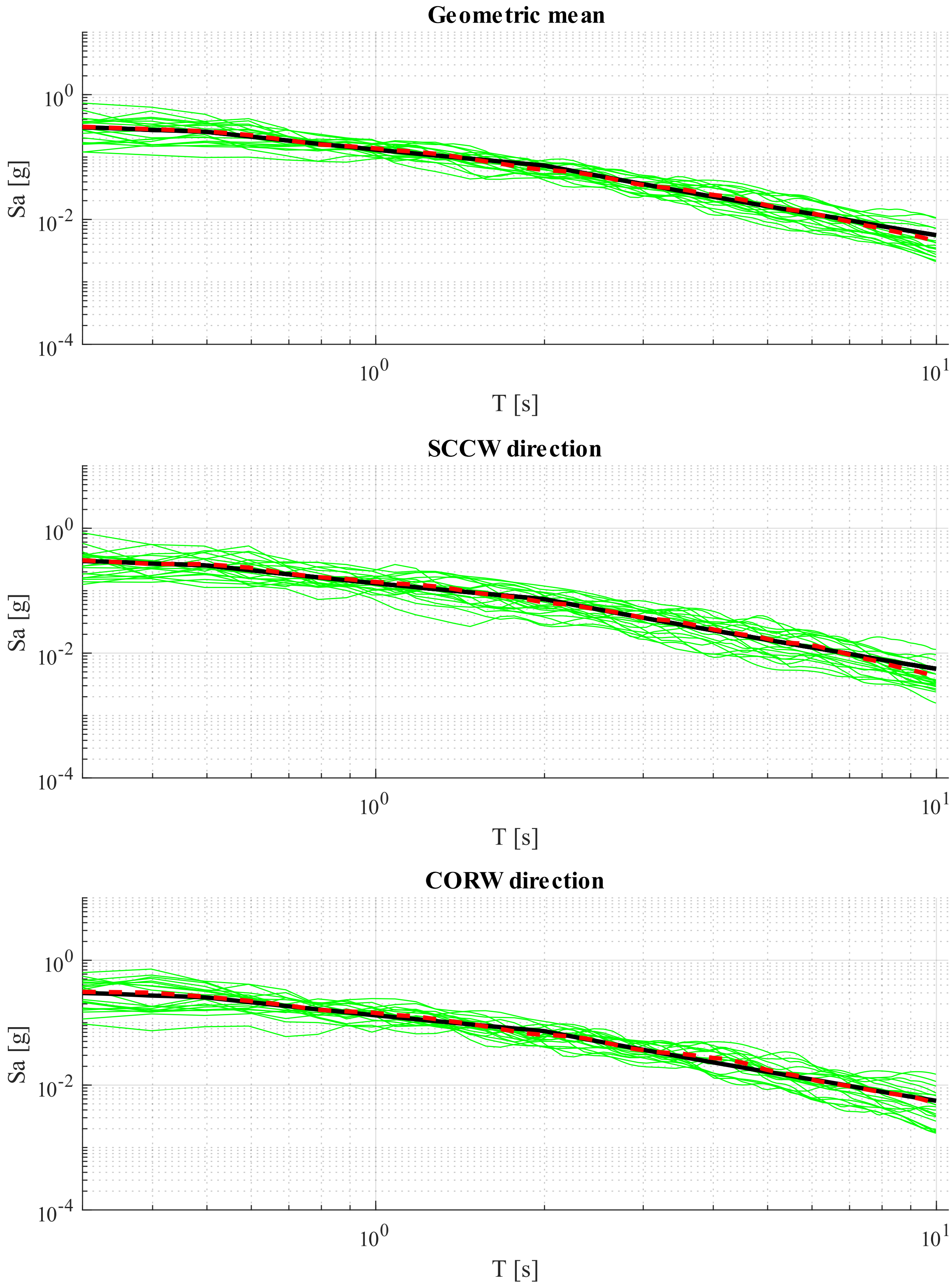

Figure: Crustal MH Vancouver

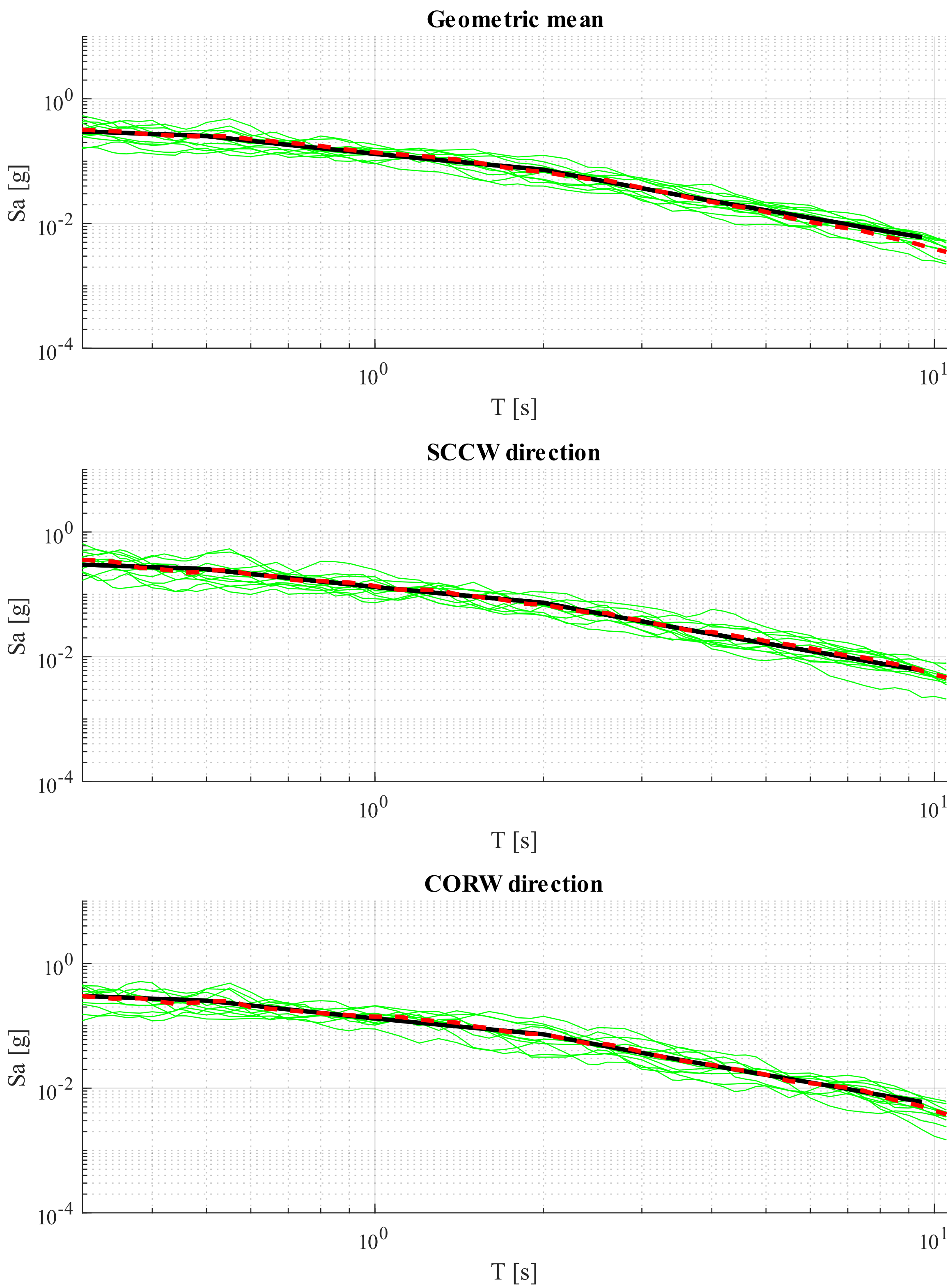

Figure: Subduction intraslab MH Vancouver

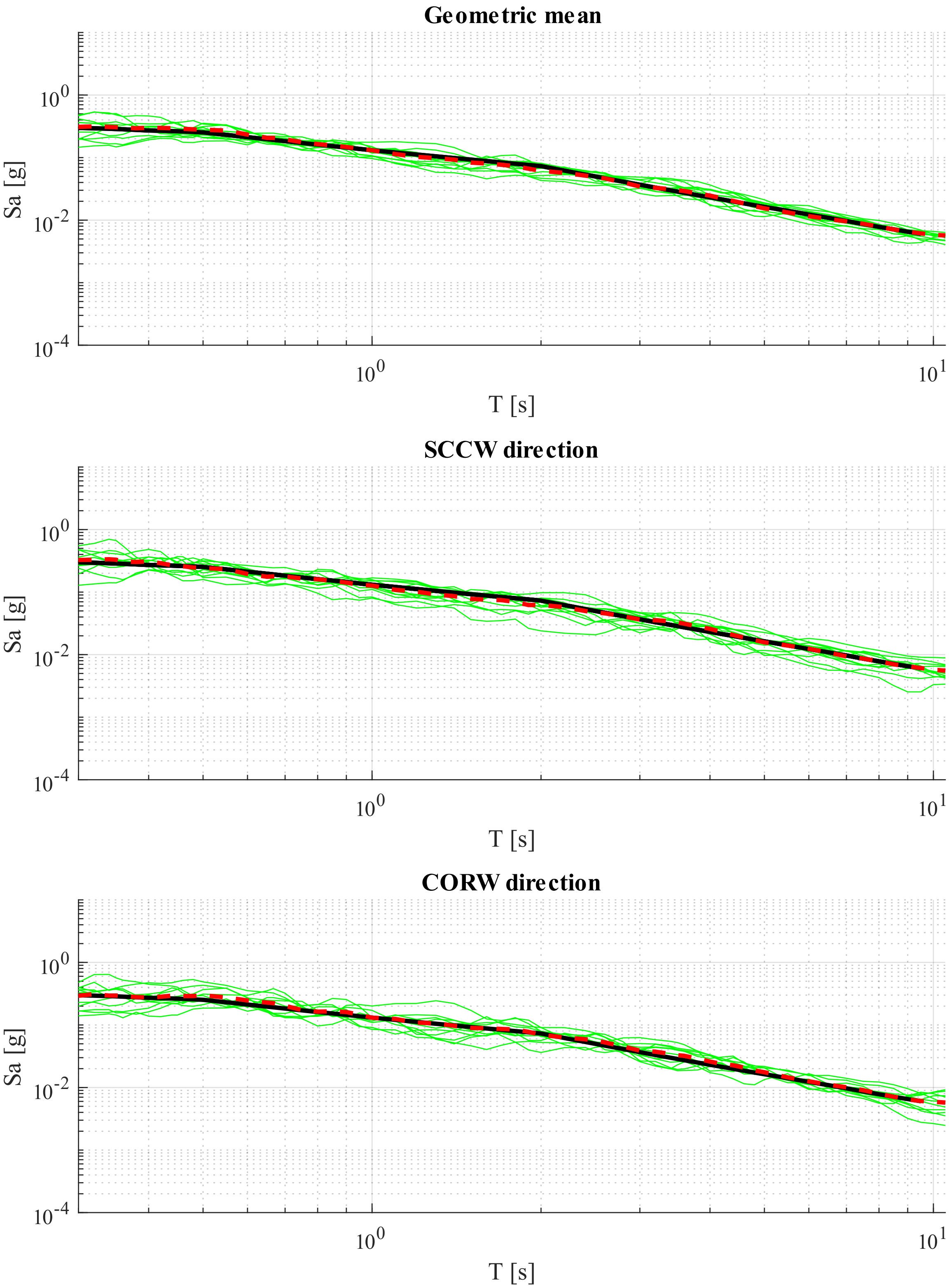

Figure: Subduction interface MH Vancouver

C.3 - Vancouver HH

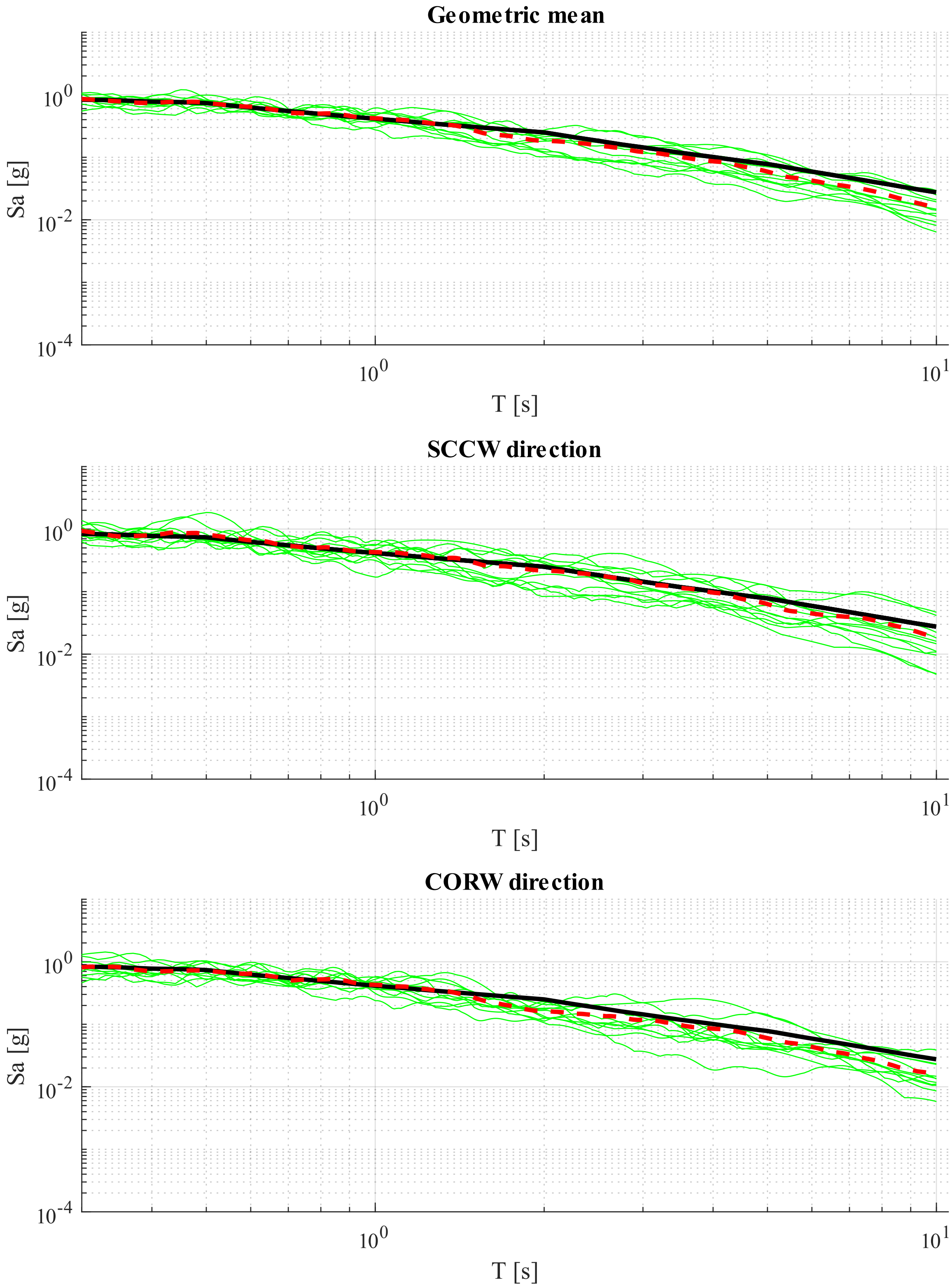

Figure: Crustal HH Vancouver

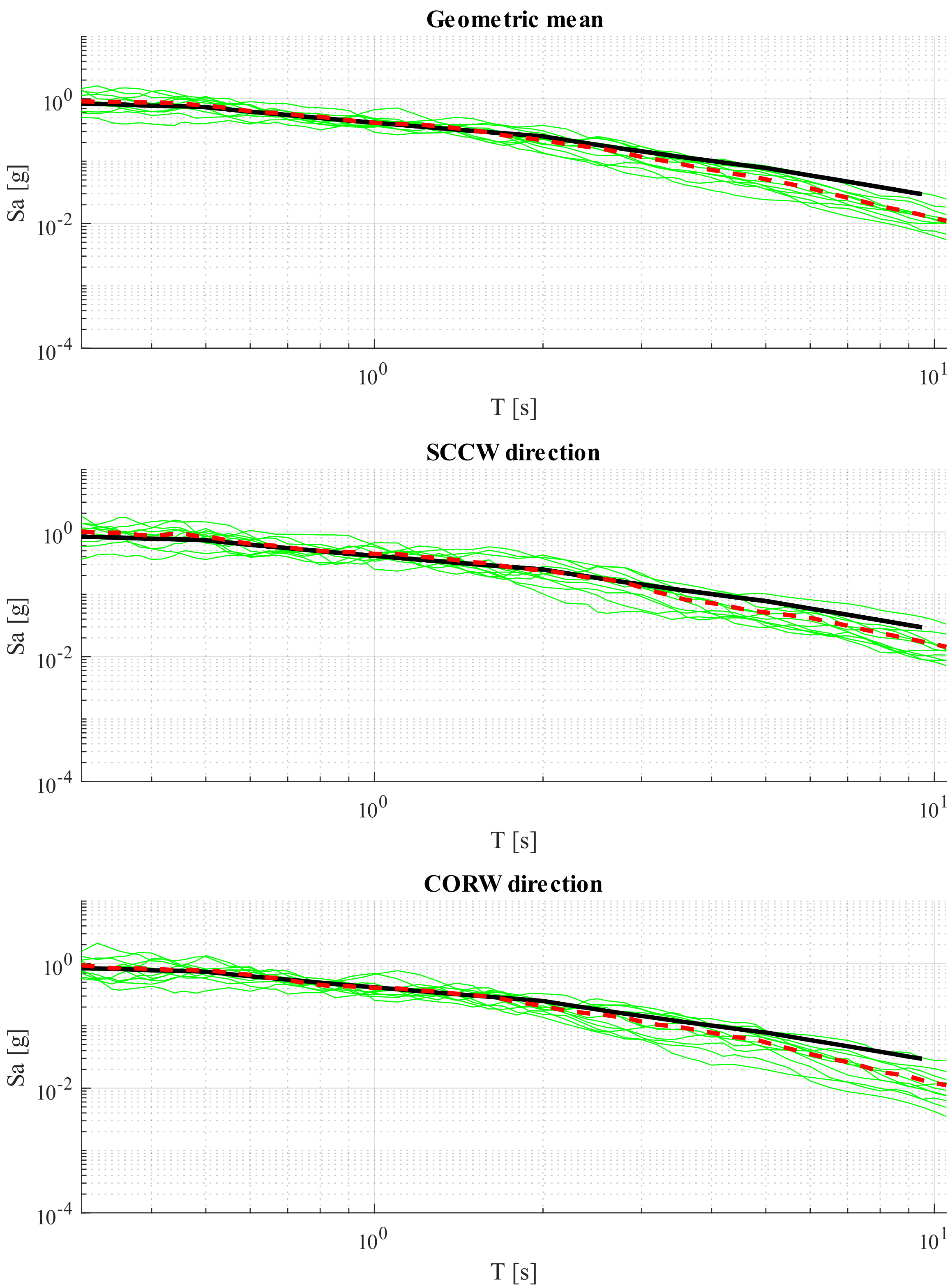

Figure: Subduction intraslab HH Vancouver

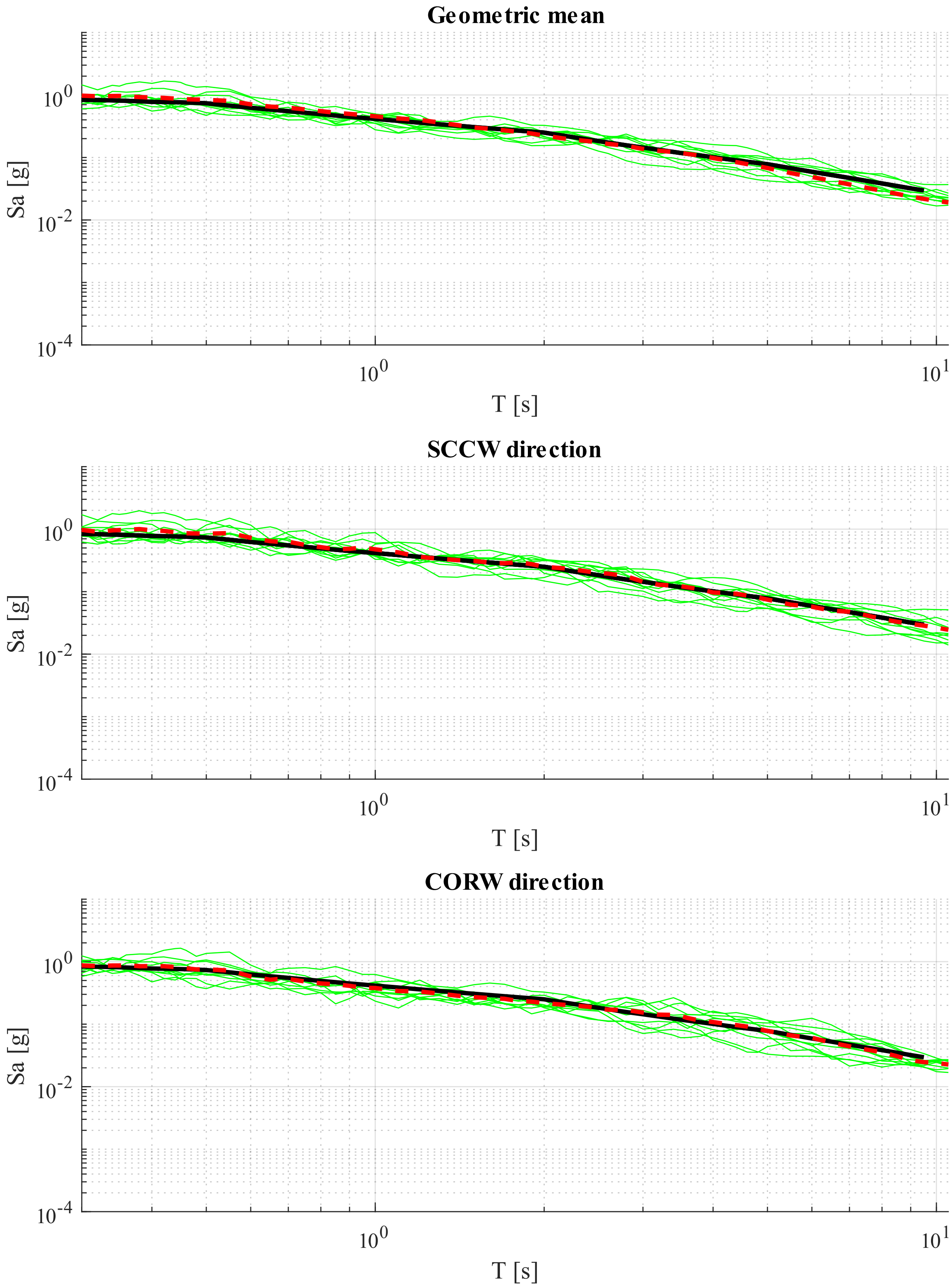

Figure: Subduction interface HH Vancouver

C.1 - Victoria LH

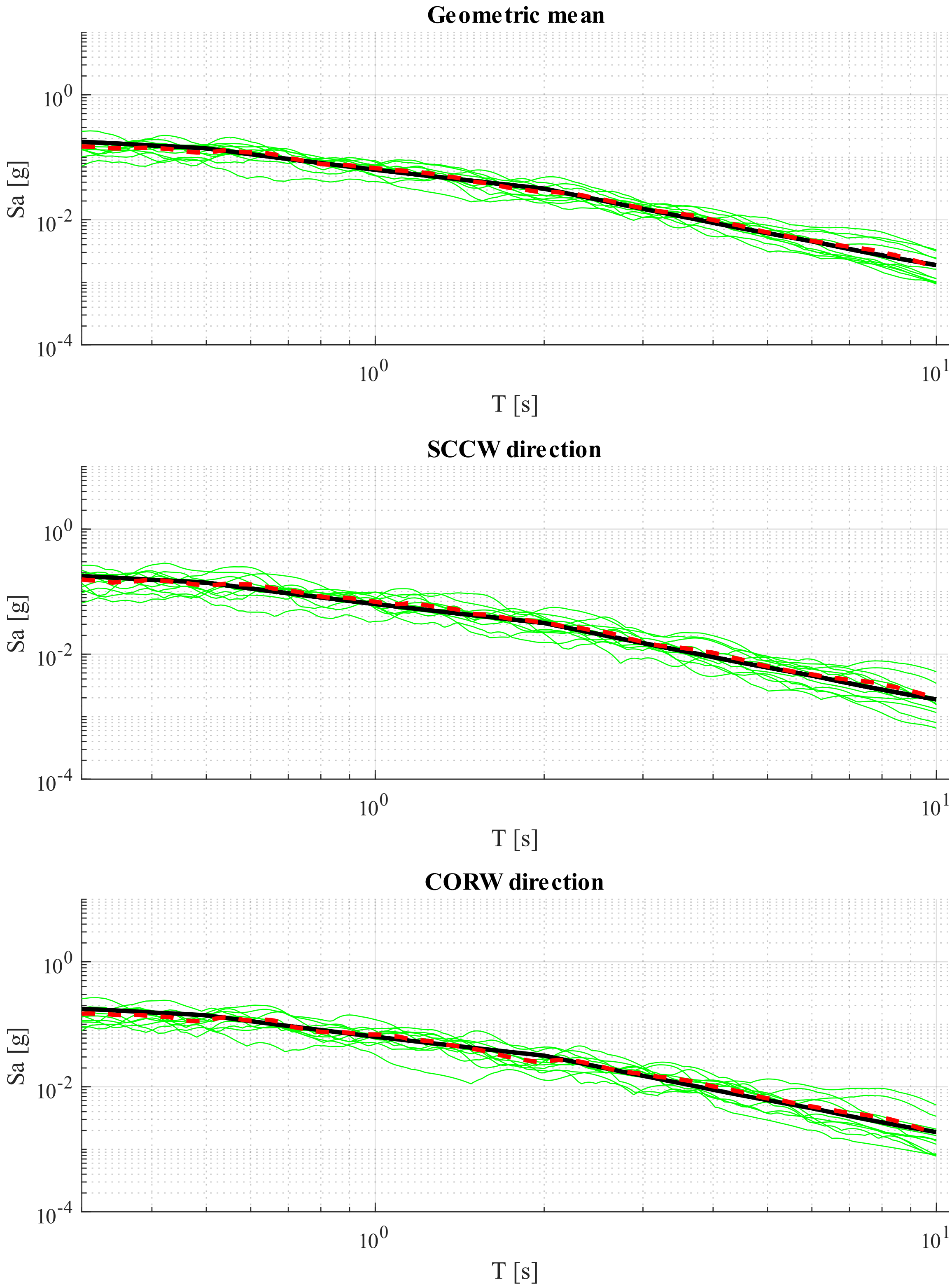

Figure: Crustal LH Victoria

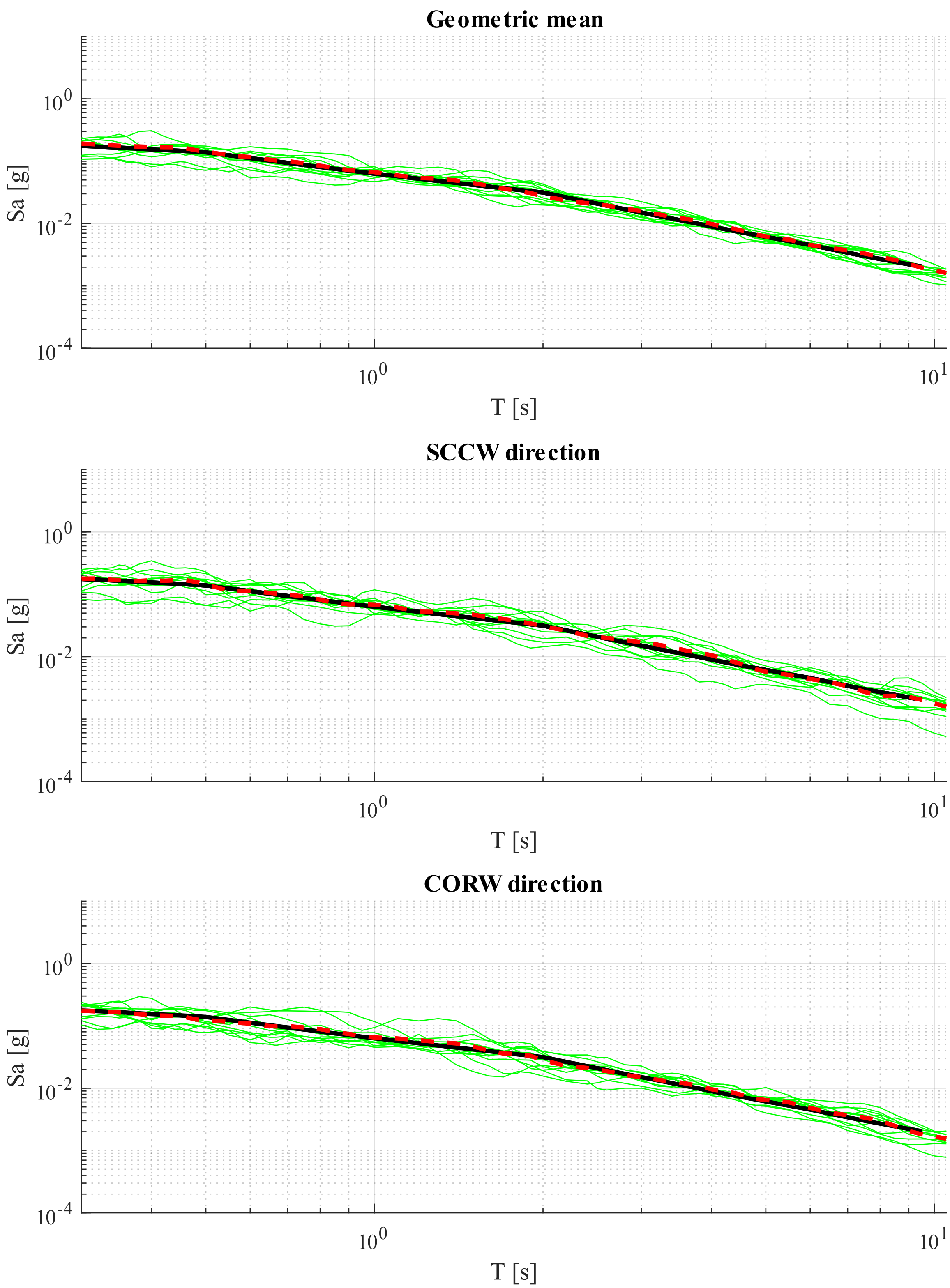

Figure: Subcrustal LH Victoria

C.2 - Victoria MH

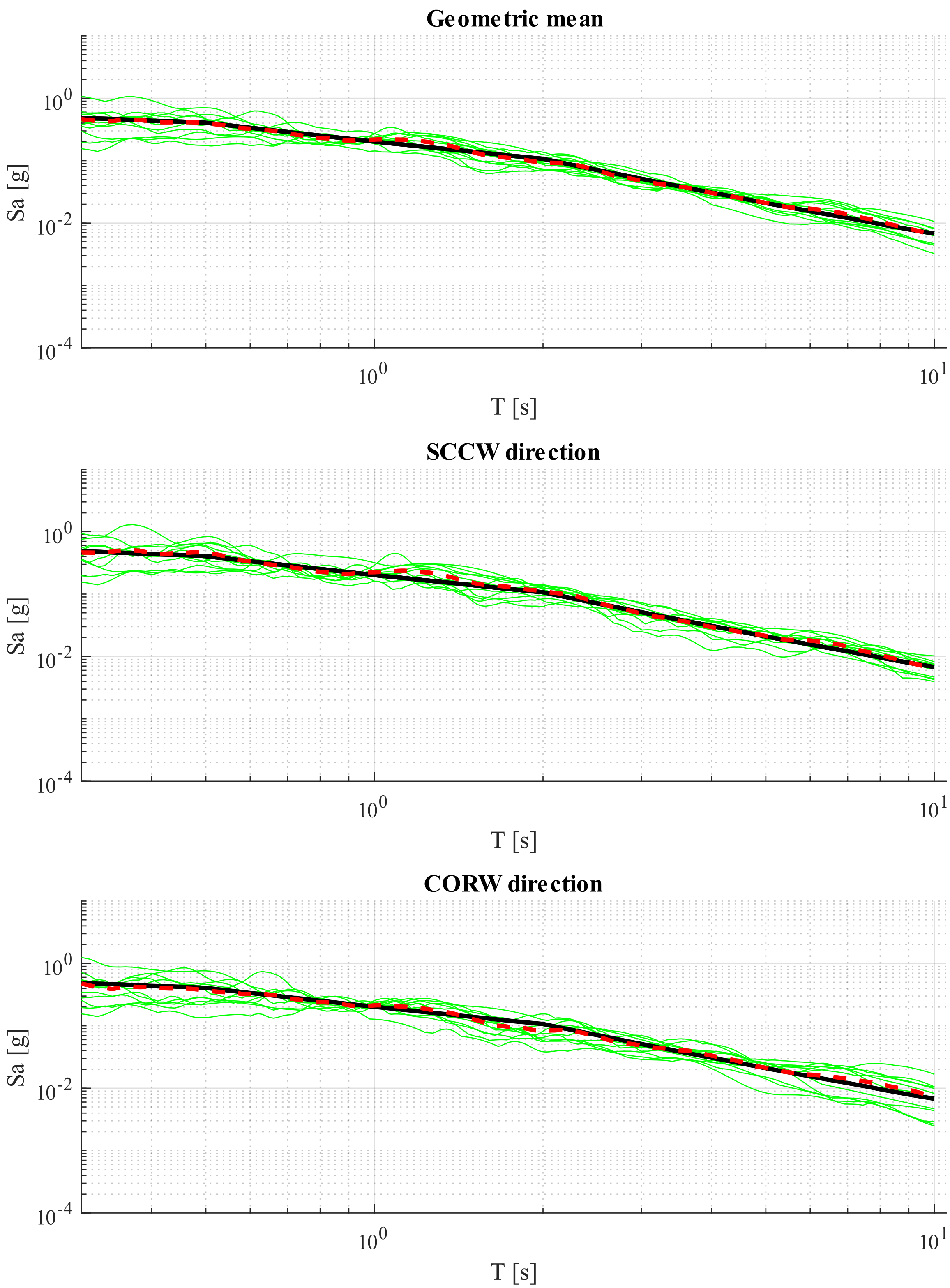

Figure: Crustal MH Victoria

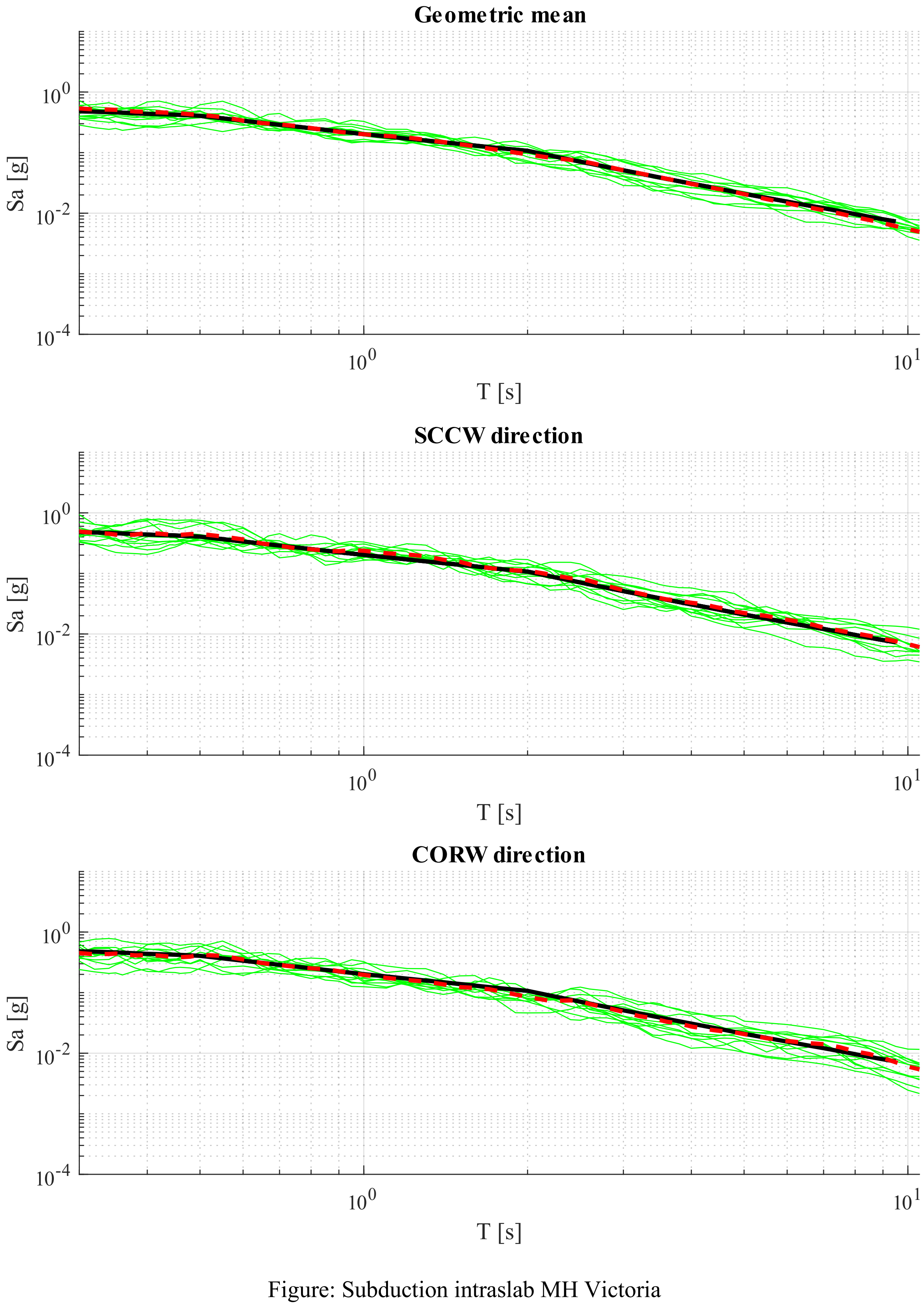

Figure: Subduction intraslab MH Victoria

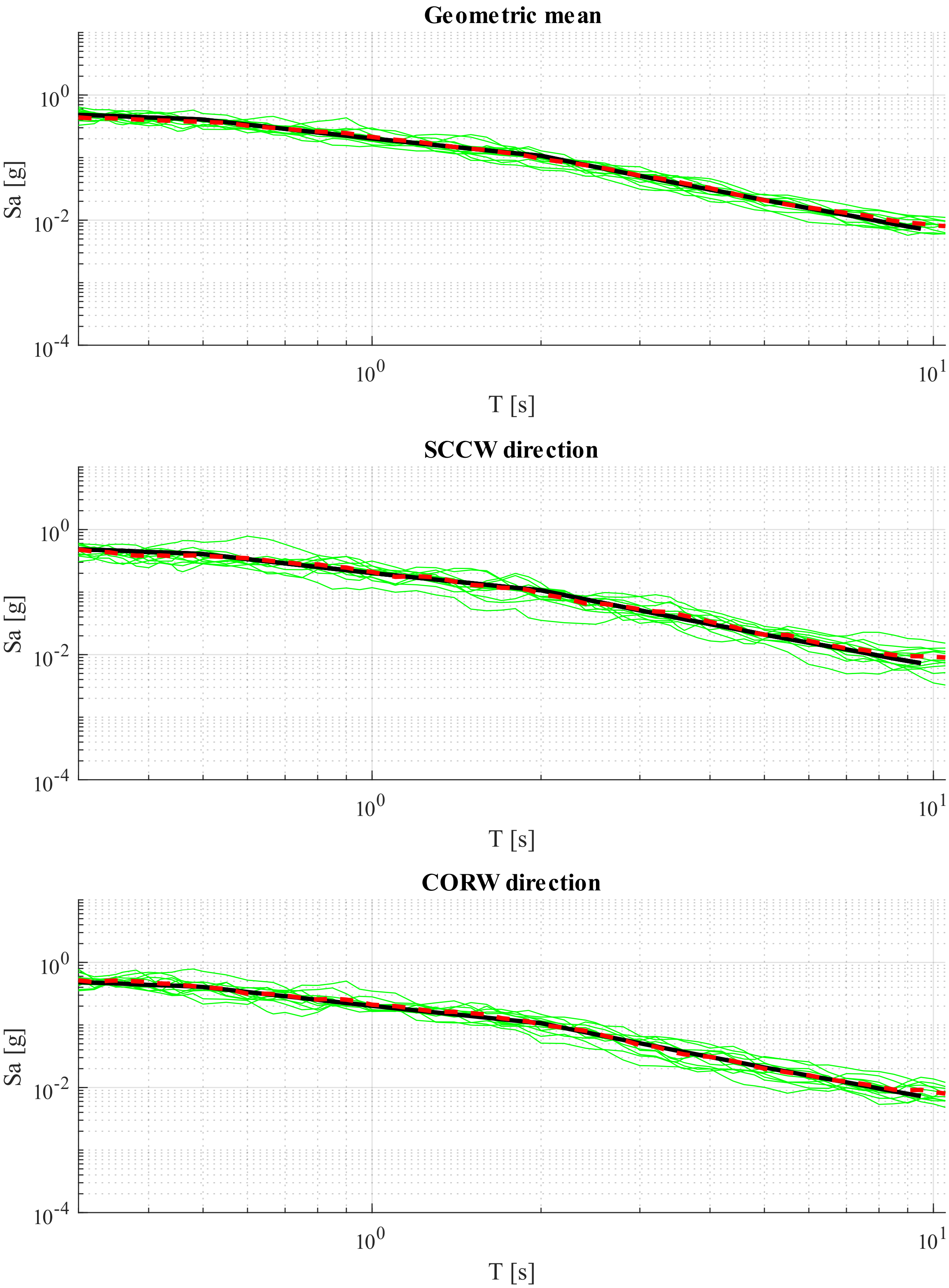

Figure: Subduction interface MH Victoria

C.3 - Victoria HH

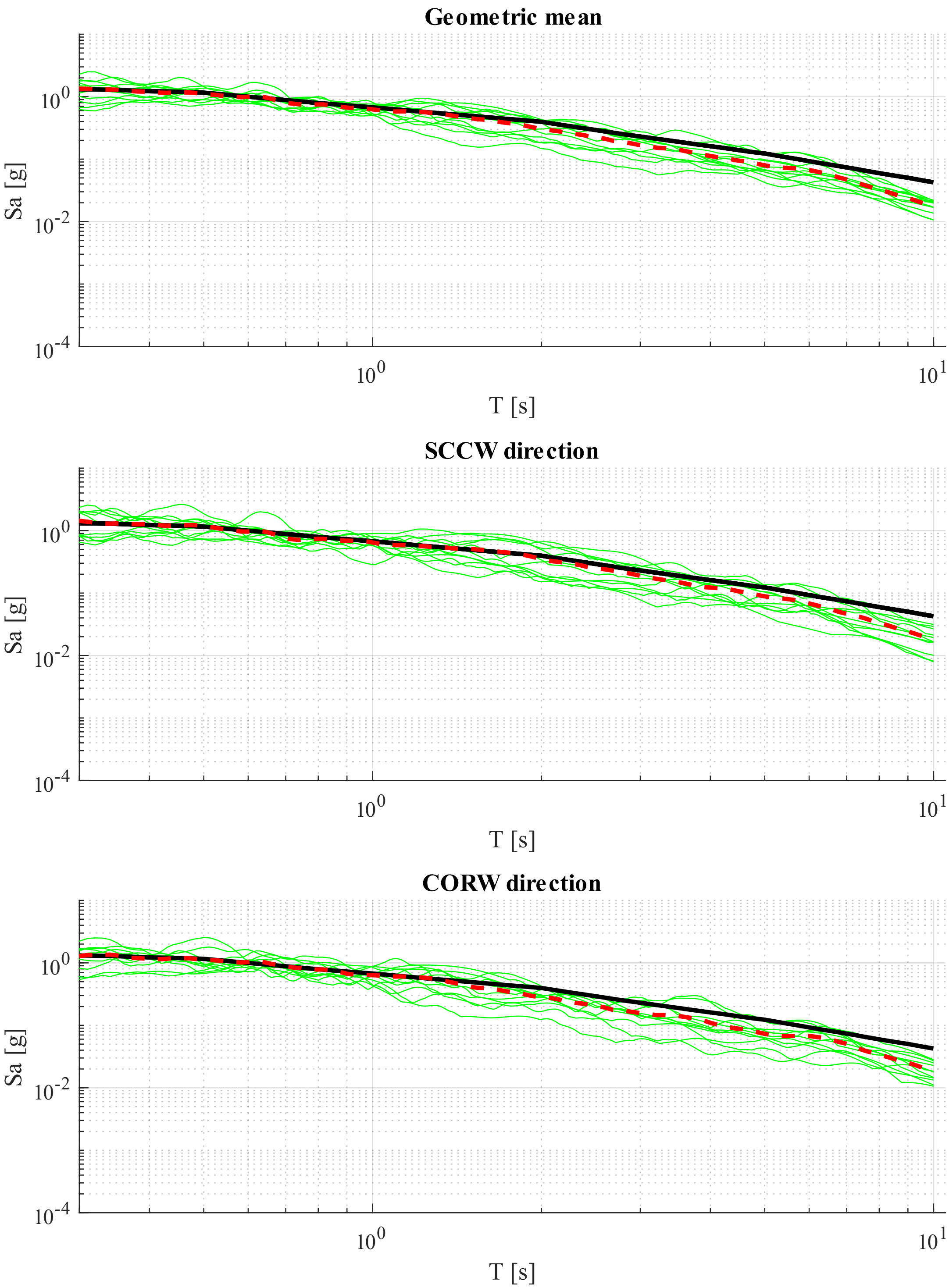

Figure: Crustal HH Victoria

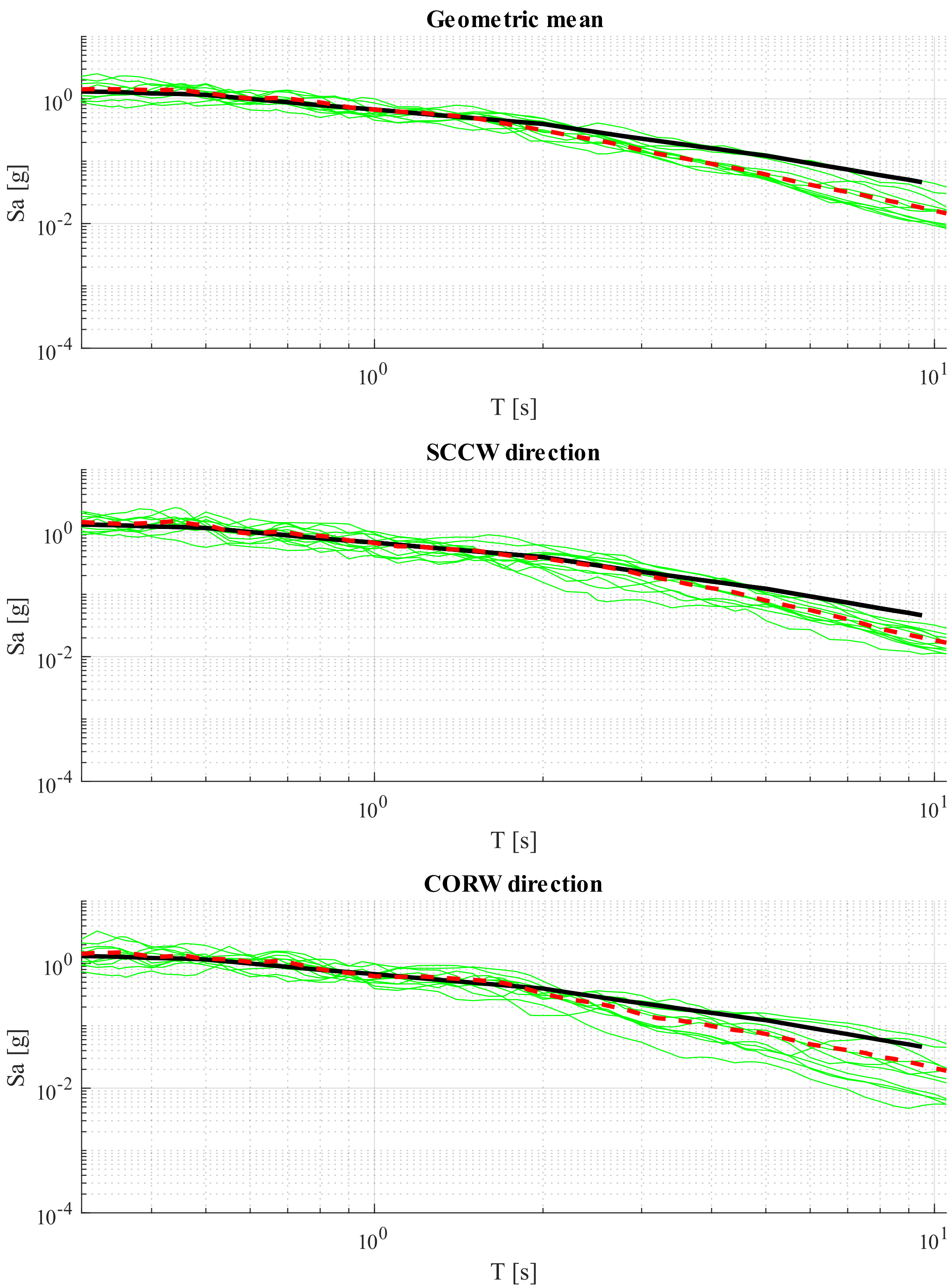

Figure: Subduction intraslab HH Victoria

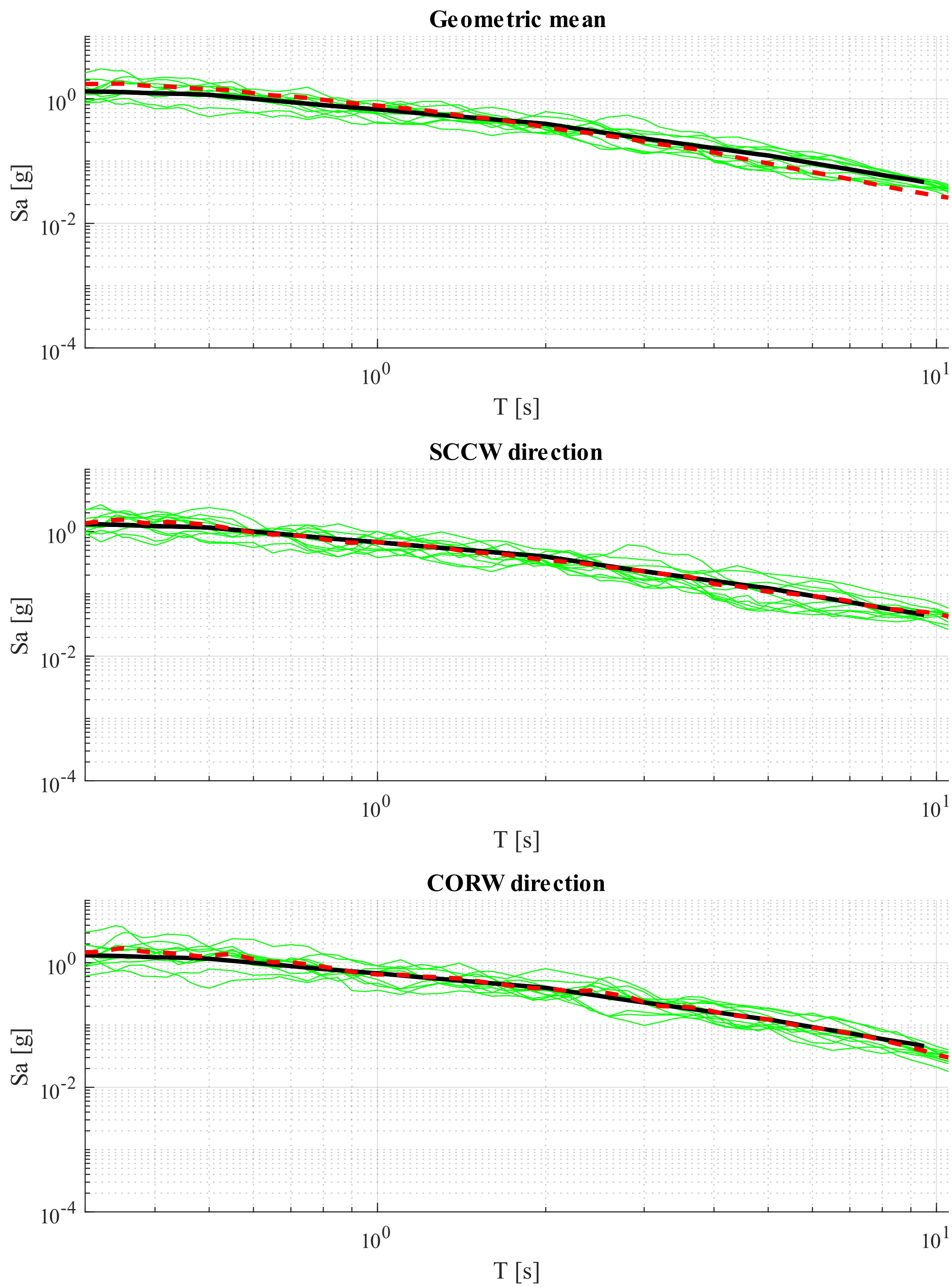

Figure: Subduction interface HH Victoria

Appendix D: Detailed construction drawings

The following shows the detailed construction drawings for the experimental set-up.

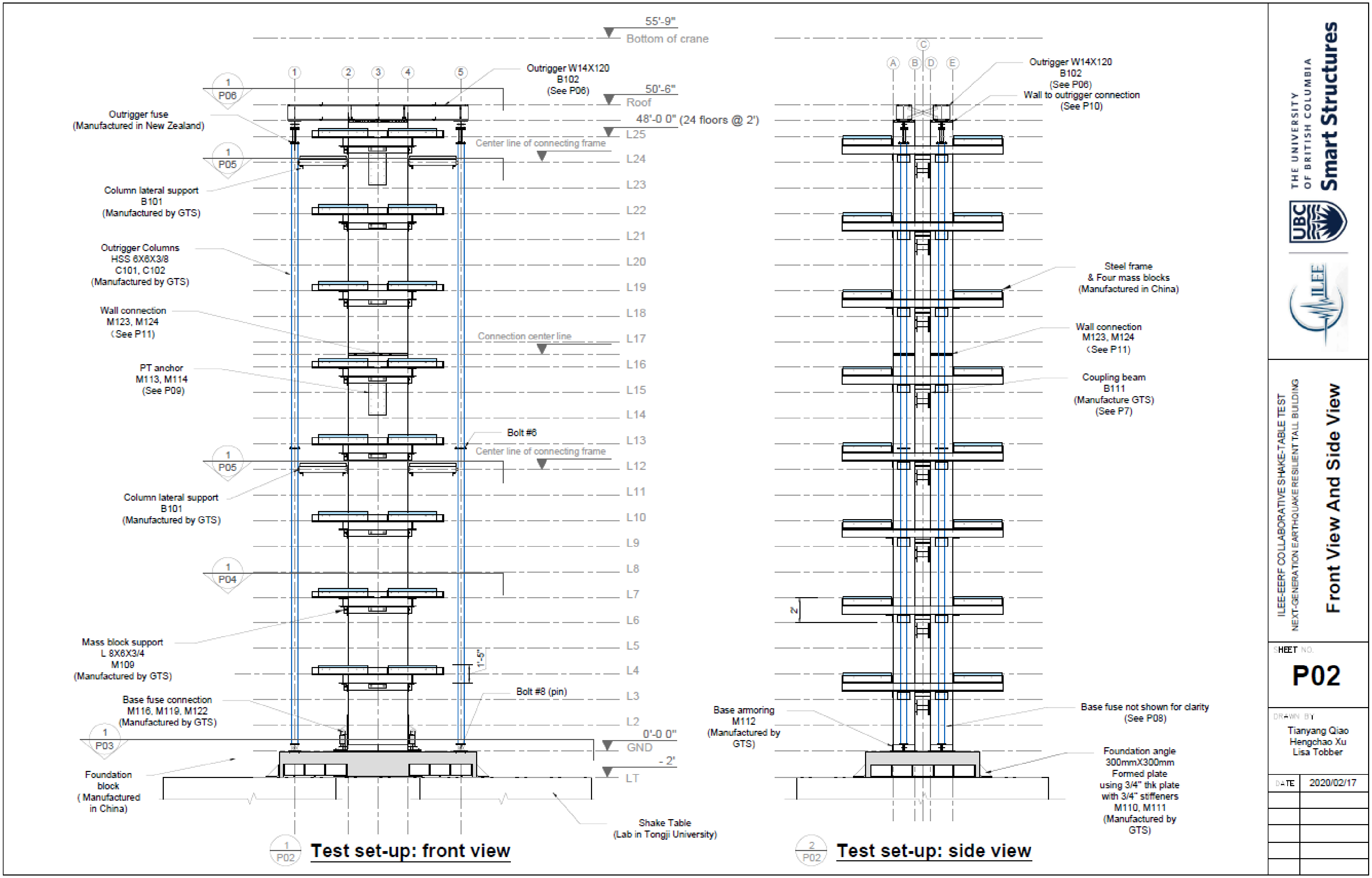

55'-9"
Bottom of crane
50'-6"
Roof
48'-0 0" (24 floors @ 2')
Outrigger W14X120
B102
(See P06)
Outrigger fuse
(Manufactured in New Zealand)
Center line of connecting frame
Column lateral support
B101
(Manufactured by GTS)
Outrigger Columns
HSS 6X6X3/8
C101, C102
(Manufactured by GTS)
Wall connection
M123, M124
(See P11)
Connection center line
PT anchor
M113, M114
(See P09)
Bolt #8
Mass block support
L 8X6X3/4
M109
(Manufactured by GTS)
Base fuse connection
M116, M119, M122
(Manufactured by GTS)
Bolt #8 (pin)
0'-0 0"
GND
- 2'
LT
Foundation
block
(Manufactured
in China)
Shake Table
(Lab in Tongji University)
Test set-up: front view
Wall to outrigger connection
(See P10)
Steel frame
& Four mass blocks
(Manufactured in China)
Coupling beam
B111
(Manufacture GTS)
(See P7)
Base armoring
M112
(Manufactured by
GTS)
Base fuse not shown for clarity
(See P08)
Foundation angle
300mmX300mm
Formed plate
using 3/4" thk plate
with 3/4" stiffeners
M110, M111
(Manufactured by
GTS)
Test set-up: side view
THE UNIVERSITY OF BRITISH COLUMBIA
Smart Structures
ILEE-EERF COLLABORATIVE SHAKE-TABLE TEST
NEXT-GENERATION EARTHQUAKE RESILIENT TALL BUILDING
Front View And Side View
SHEET NO.
P02
DRAWN BY
Tianyang Qiao
Hengchao Xu
Lisa Tobber
DATE
2020/02/17

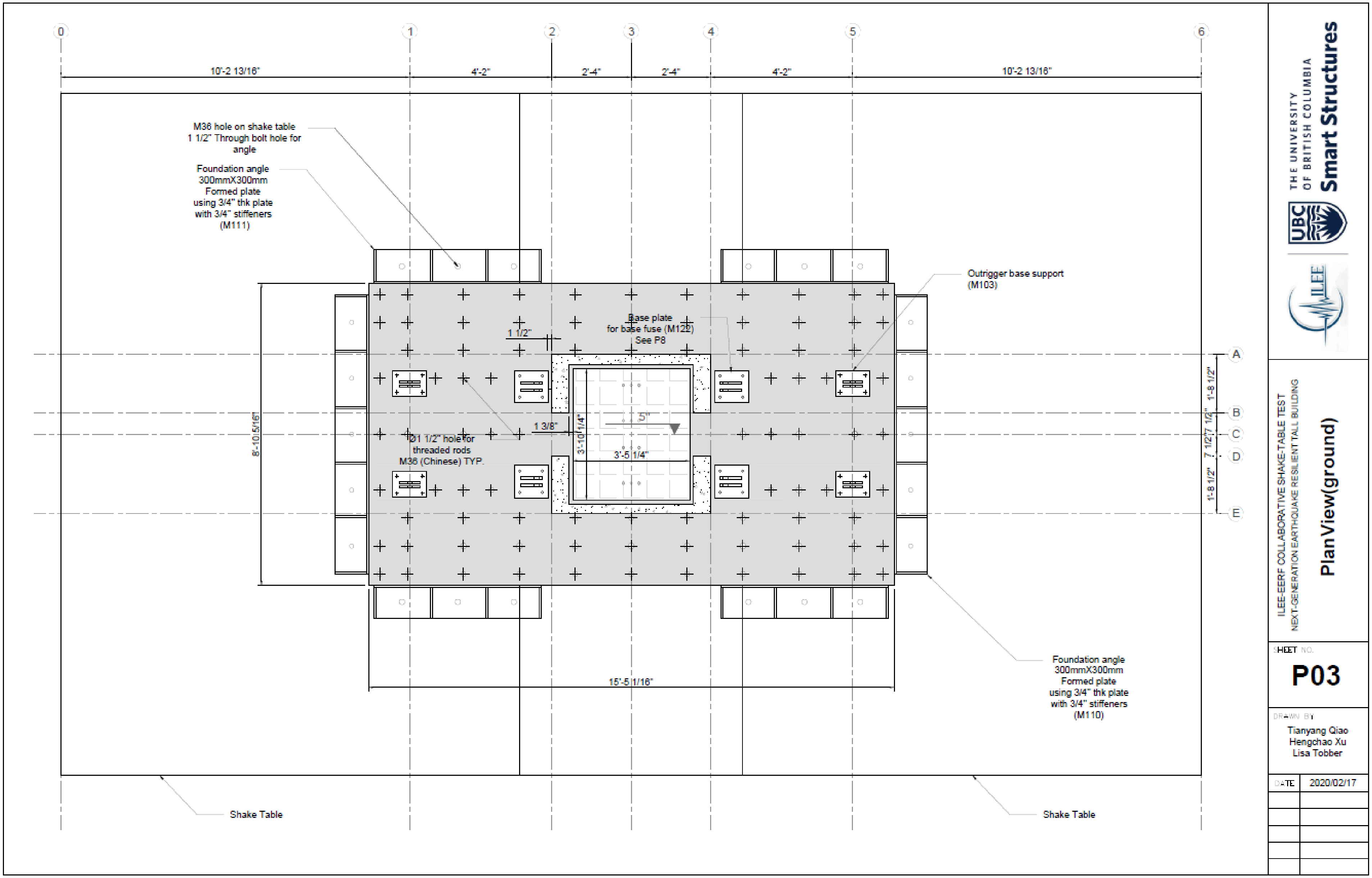
10'-2 13/16"
4'-2"
2'-4"
2'-4"
4'-2"
10'-2 13/16"
M36 hole on shake table
1 1/2" Through bolt hole for angle
Foundation angle 300mmX300mm Formed plate using 3/4" thk plate with 3/4" stiffeners (M111)
Outrigger base support (M103)
Base plate for base fuse (M122) See P8
1 1/2"
1 3/8"
Ø1 1/2" hole for threaded rods M36 (Chinese) TYP.
3'-10 1/4"
3'-5 1/4"
8'-10 5/16"
1'-8 1/2"
7 1/2"
7 1/2"
1'-8 1/2"
15'-5 1/16"
Foundation angle 300mmX300mm Formed plate using 3/4" thk plate with 3/4" stiffeners (M110)
Shake Table
Shake Table
THE UNIVERSITY OF BRITISH COLUMBIA
Smart Structures
ILEE-EERF COLLABORATIVE SHAKE-TABLE TEST
NEXT-GENERATION EARTHQUAKE RESILIENT TALL BUILDING
Plan View(ground)
SHEET NO.
P03
DRAWN BY
Tianyang Qiao
Hengchao Xu
Lisa Tobber
DATE
2020/02/17

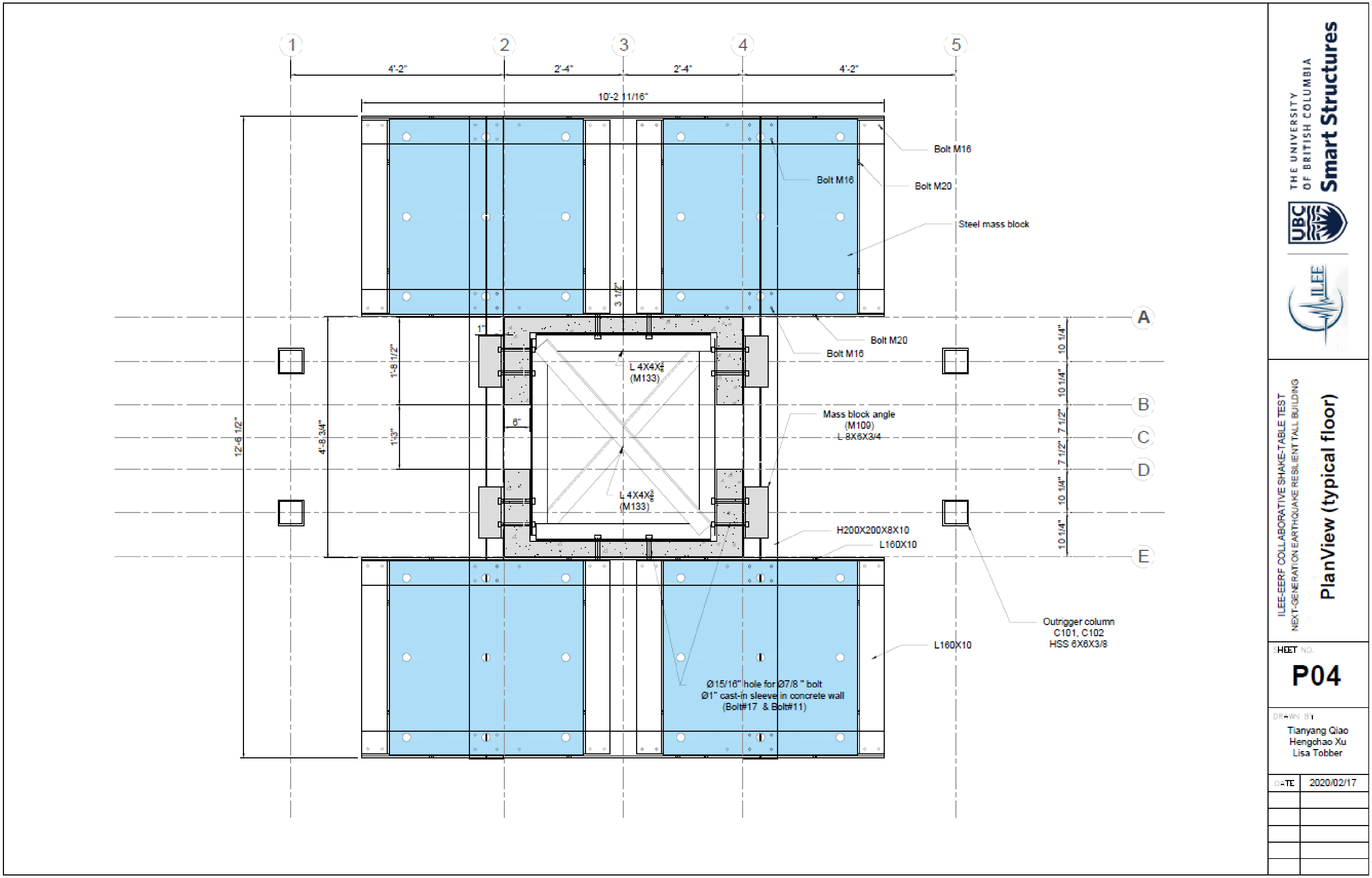
1
2
3
4
5
4'-2"
2'-4"
2'-4"
4'-2"
10'-2 11/16"
Bolt M16
Bolt M16
Bolt M20
Steel mass block
Bolt M20
Bolt M16
A
B
C
D
E
12'-8 1/2"
4'-8 3/4"
1'-8 1/2"
1'-3"
1"
6"
3 1/2"
L 4X4X3/8
(M133)
L 4X4X3/8
(M133)
Mass block angle
(M109)
L 8X6X3/4
10 1/4"
10 1/4"
7 1/2"
7 1/2"
10 1/4"
10 1/4"
H200X200X8X10
L160X10
Outrigger column
C101, C102
HSS 6X6X3/8
L160X10
Ø15/16" hole for Ø7/8 " bolt
Ø1" cast-in sleeve in concrete wall
(Bolt#17 & Bolt#11)
THE UNIVERSITY OF BRITISH COLUMBIA
Smart Structures
UBC
ILEE
ILEE-EERF COLLABORATIVE SHAKE-TABLE TEST
NEXT-GENERATION EARTHQUAKE RESILIENT TALL BUILDING
PlanView (typical floor)
SHEET NO.
P04
DRAWN BY
Tianyang Qiao
Hengchao Xu
Lisa Tobber
DATE
2020/02/17

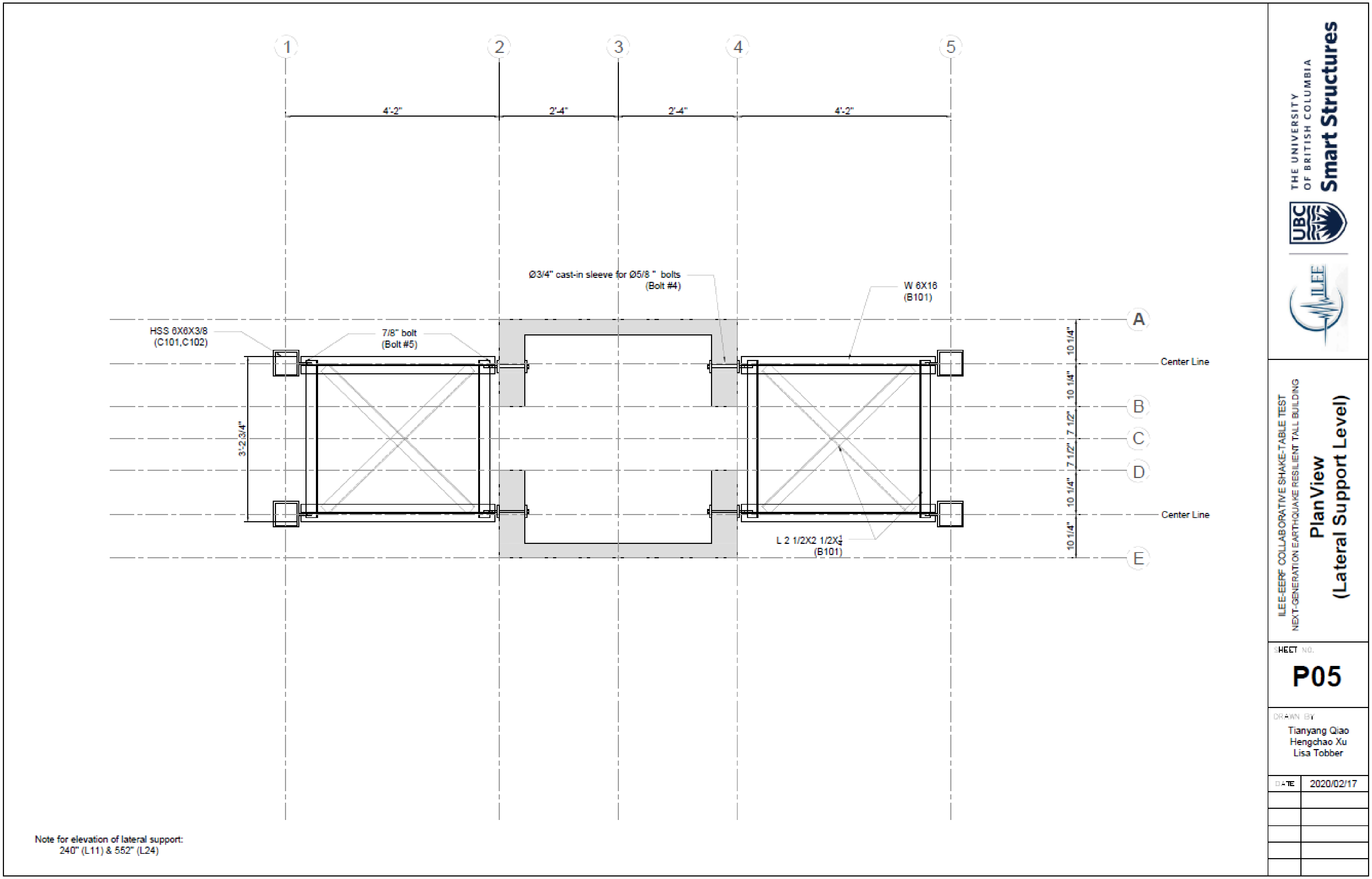

1
2
3
4
5
4'-2"
2'-4"
2'-4"
4'-2"
Ø3/4" cast-in sleeve for Ø5/8 " bolts (Bolt #4)
W 6X16 (B101)
HSS 6X6X3/8 (C101,C102)
7/8" bolt (Bolt #5)
A
B
C
D
E
Center Line
Center Line
3'-2 3/4"
10 1/4"
10 1/4"
7 1/2"
7 1/2"
10 1/4"
10 1/4"
L 2 1/2X2 1/2X¼ (B101)
Note for elevation of lateral support: 240" (L11) & 552" (L24)
THE UNIVERSITY OF BRITISH COLUMBIA
Smart Structures
ILEE-EERF COLLABORATIVE SHAKE-TABLE TEST
NEXT-GENERATION EARTHQUAKE RESILIENT TALL BUILDING
Plan View (Lateral Support Level)
SHEET NO.
P05
DRAWN BY
Tianyang Qiao
Hengchao Xu
Lisa Tobber
DATE
2020/02/17

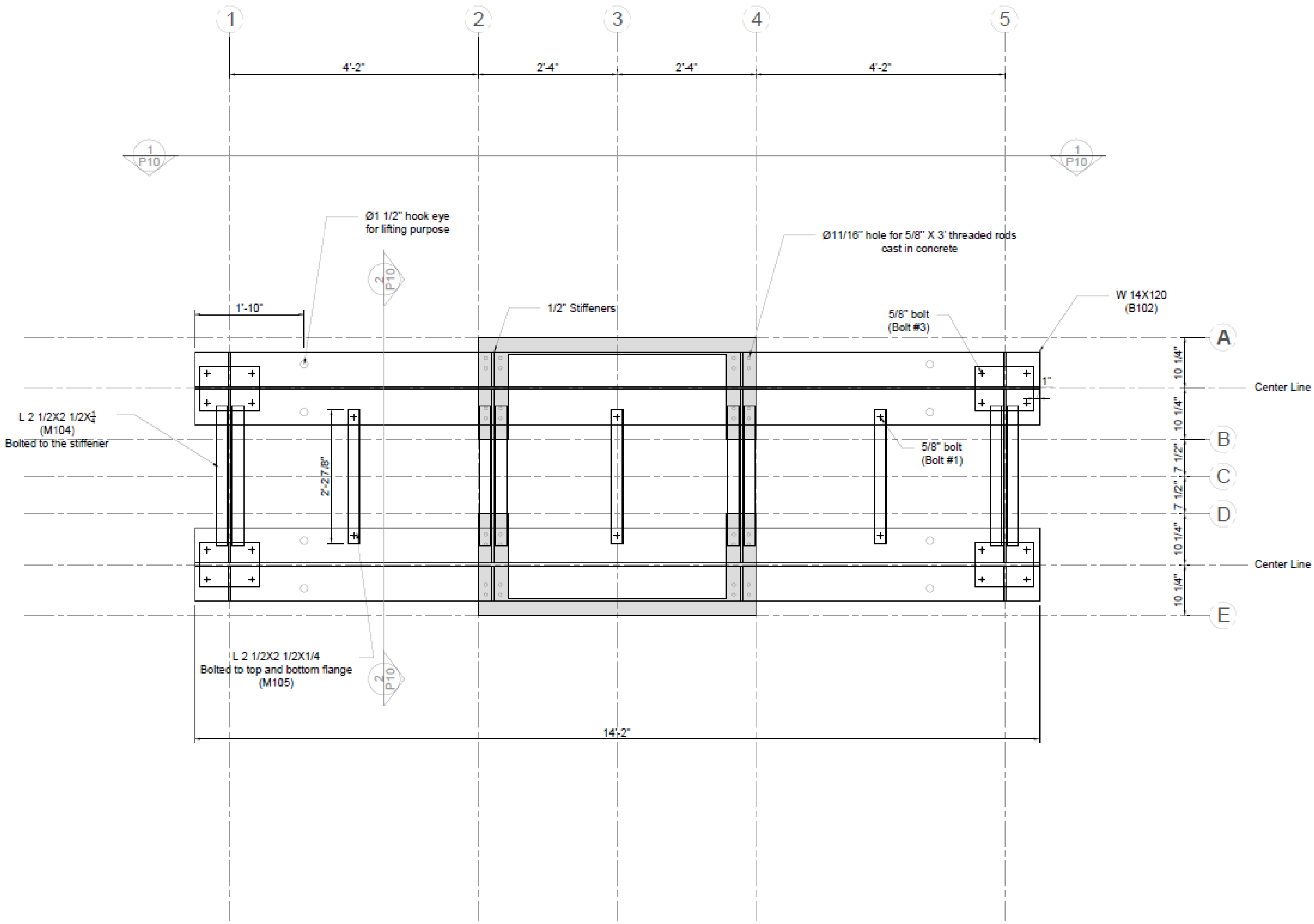

THE UNIVERSITY OF BRITISH COLUMBIA

Smart Structures

ILEE-EERF COLLABORATIVE SHAKE-TABLE TEST

NEXT-GENERATION EARTHQUAKE RESILIENT TALL BUILDING

PlanView(RoofBeam)

SHEET NO.

P06

DRAWN BY

Tianyang Qiao
Hengchao Xu
Lisa Tobber

DATE 2020/02/17

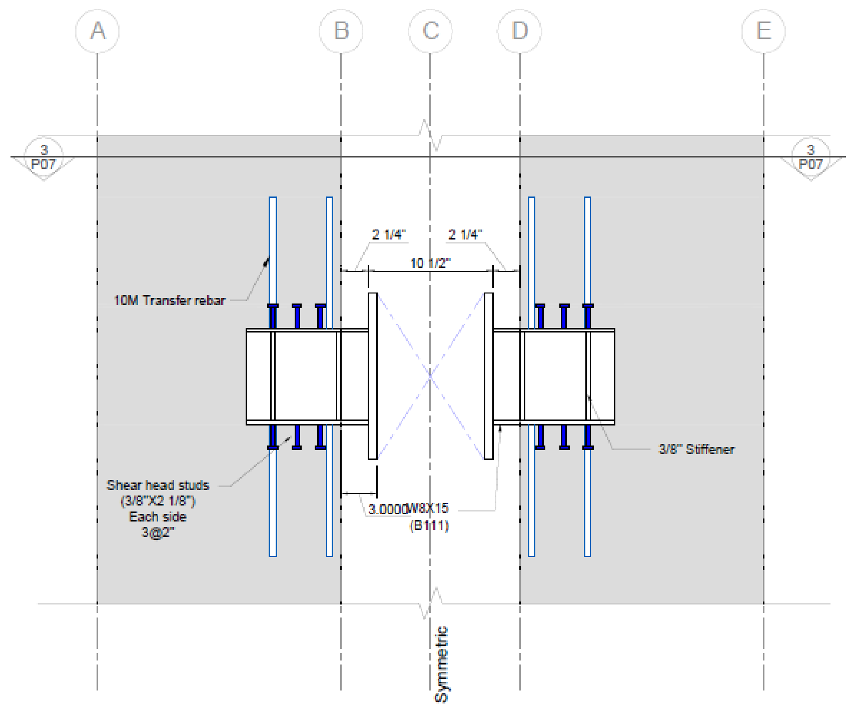

1 P07 B111

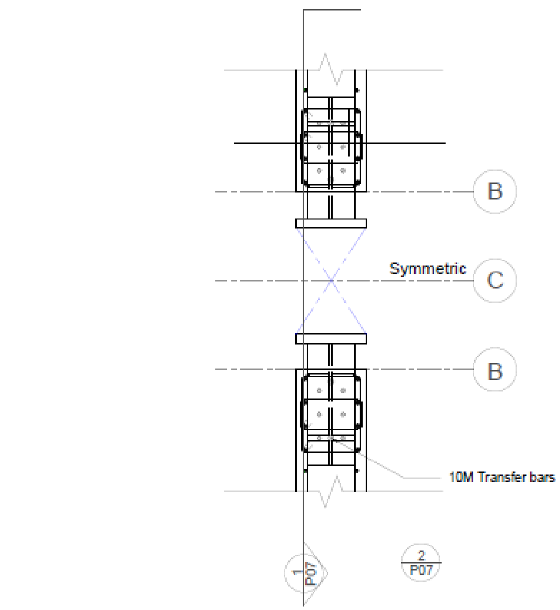

2 P07

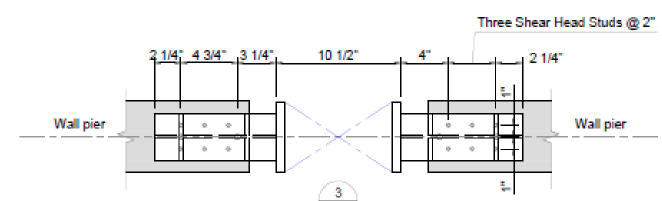

3 P07

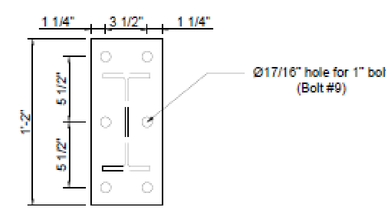

4 P07 End plate, thk 3/4"

THE UNIVERSITY OF BRITISH COLUMBIA
Smart Structures

ILEE-EERF COLLABORATIVE SHAKE-TABLE TEST
NEXT-GENERATION EARTHQUAKE RESILIENT TALL BUILDING

Coupling Beam Detail

SHEET NO.	**P07**
DRAWN BY	Tianyang Qiao Hengchao Xu Lisa Tobber
DATE	2020/02/17

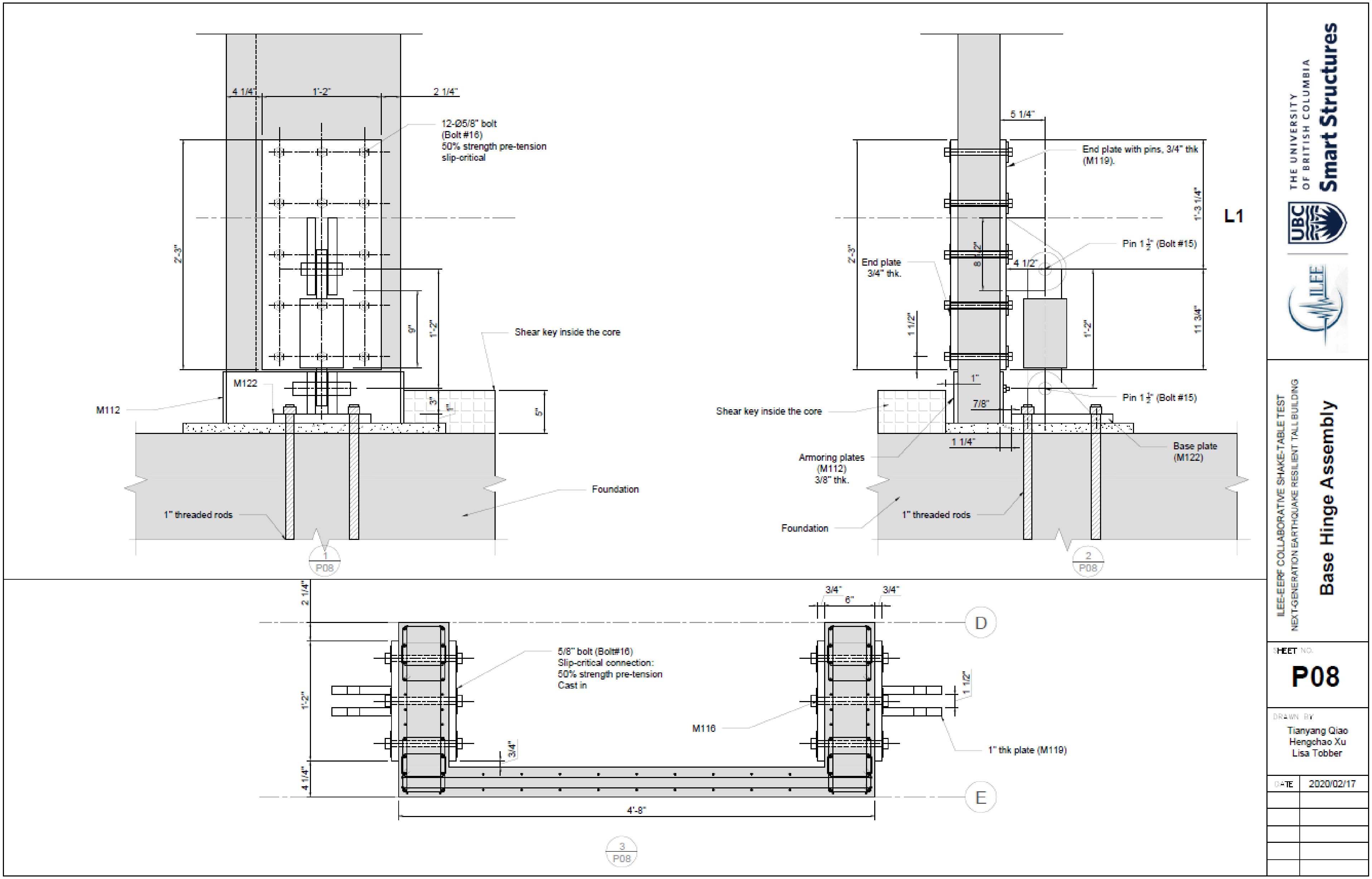

4 1/4"
1'-2"
2 1/4"
12-Ø5/8" bolt
(Bolt #16)
50% strength pre-tension
slip-critical
2'-3"
9"
1'-2"
Shear key inside the core
M122
M112
3"
1"
5"
1" threaded rods
Foundation
1
P08
5 1/4"
End plate with pins, 3/4" thk
(M119).
1'-3 1/4"
L1
Pin 1 1/2" (Bolt #15)
End plate
3/4" thk.
8 1/2"
4 1/2"
11 3/4"
1 1/2"
1'-2"
1"
7/8"
Shear key inside the core
Base plate
(M122)
1 1/4"
Armoring plates
(M112)
3/8" thk.
1" threaded rods
Foundation
2
P08
2 1/4"
3/4"
6"
3/4"
D
5/8" bolt (Bolt#16)
Slip-critical connection:
50% strength pre-tension
Cast in
1'-2"
1 1/2"
M116
1" thk plate (M119)
3/4"
4 1/4"
E
4'-8"
3
P08
THE UNIVERSITY OF BRITISH COLUMBIA
Smart Structures
UBC
ILEE
ILEE-EERF COLLABORATIVE SHAKE-TABLE TEST
NEXT-GENERATION EARTHQUAKE RESILIENT TALL BUILDING
Base Hinge Assembly
SHEET NO.
P08
DRAWN BY
Tianyang Qiao
Hengchao Xu
Lisa Tobber
DATE
2020/02/17

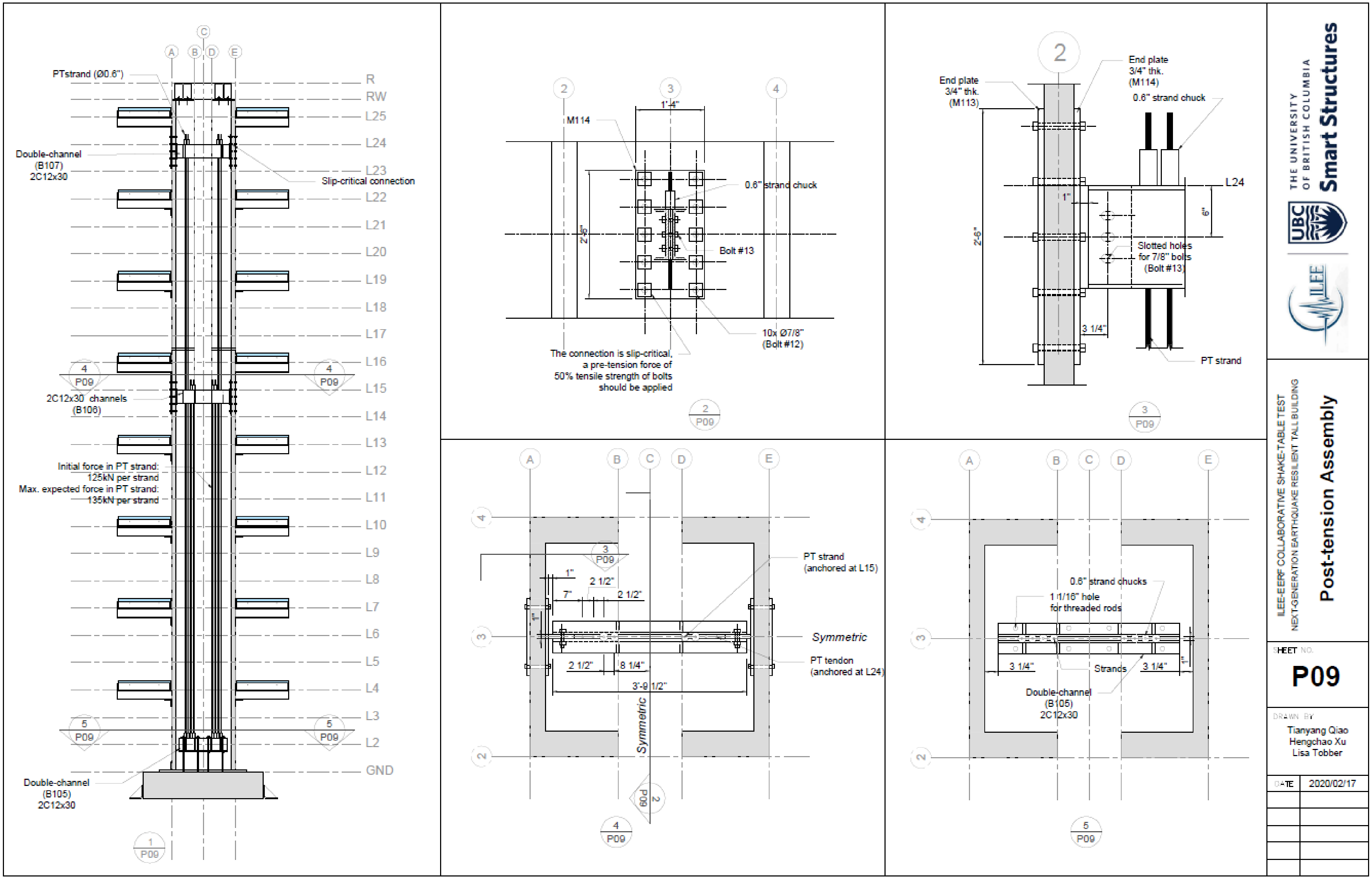
PTstrand (Ø0.6")
Double-channel (B107) 2C12x30
Slip-critical connection
2C12x30 channels (B106)
Initial force in PT strand: 125kN per strand
Max. expected force in PT strand: 135kN per strand
Double-channel (B105) 2C12x30
R
RW
L25
L24
L23
L22
L21
L20
L19
L18
L17
L16
L15
L14
L13
L12
L11
L10
L9
L8
L7
L6
L5
L4
L3
L2
GND
M114
1'-4"
0.6" strand chuck
Bolt #13
2'-6"
10x Ø7/8" (Bolt #12)
The connection is slip-critical, a pre-tension force of 50% tensile strength of bolts should be applied
End plate 3/4" thk. (M113)
End plate 3/4" thk. (M114)
0.6" strand chuck
L24
Slotted holes for 7/8" bolts (Bolt #13)
3 1/4"
PT strand
PT strand (anchored at L15)
Symmetric
PT tendon (anchored at L24)
2 1/2"
8 1/4"
3'-9 1/2"
0.6" strand chucks
1 1/16" hole for threaded rods
3 1/4"
Strands
Double-channel (B105) 2C12x30
THE UNIVERSITY OF BRITISH COLUMBIA
Smart Structures
ILEE-EERF COLLABORATIVE SHAKE-TABLE TEST
NEXT-GENERATION EARTHQUAKE RESILIENT TALL BUILDING
Post-tension Assembly
SHEET NO.
P09
DRAWN BY
Tianyang Qiao
Hengchao Xu
Lisa Tobber
DATE 2020/02/17

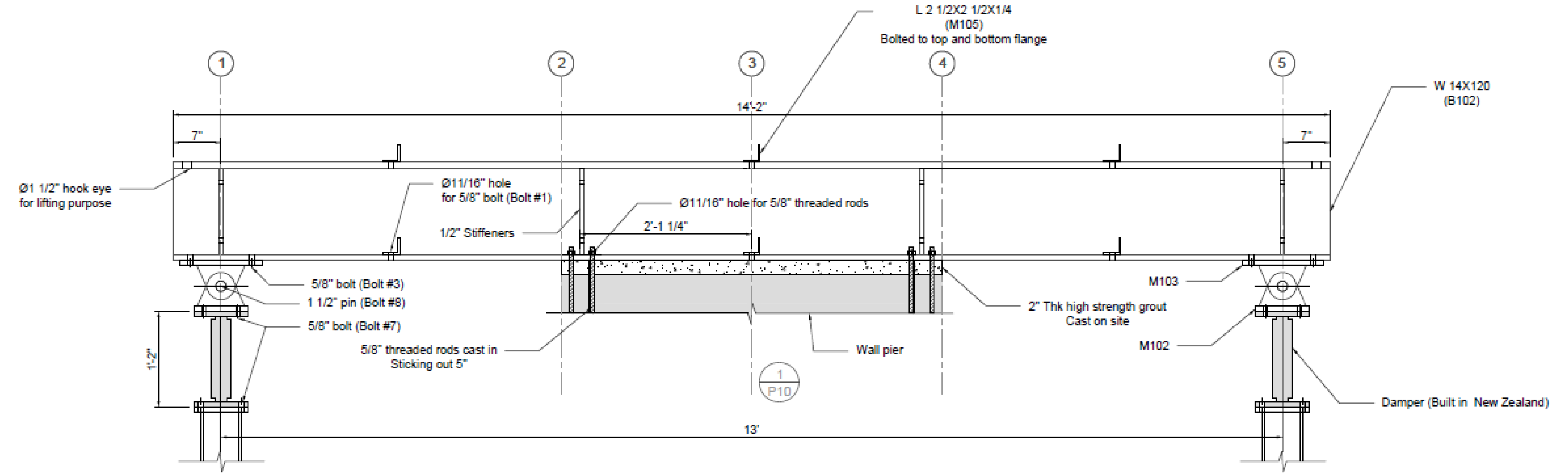

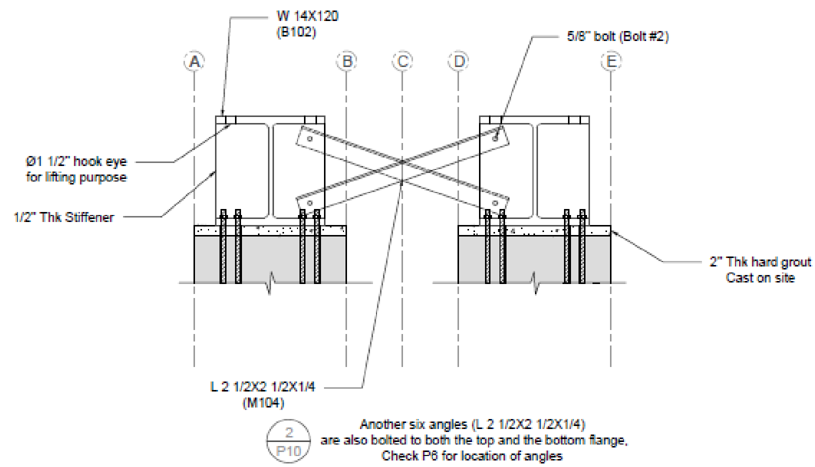

THE UNIVERSITY OF BRITISH COLUMBIA
Smart Structures

ILEE-EERF COLLABORATIVE SHAKE-TABLE TEST
NEXT-GENERATION EARTHQUAKE RESILIENT TALL BUILDING

Wall Top Connection Detail

SHEET NO.
P10

DRAWN BY
Tianyang Qiao
Hengchao Xu
Lisa Tobber

DATE 2020/02/17

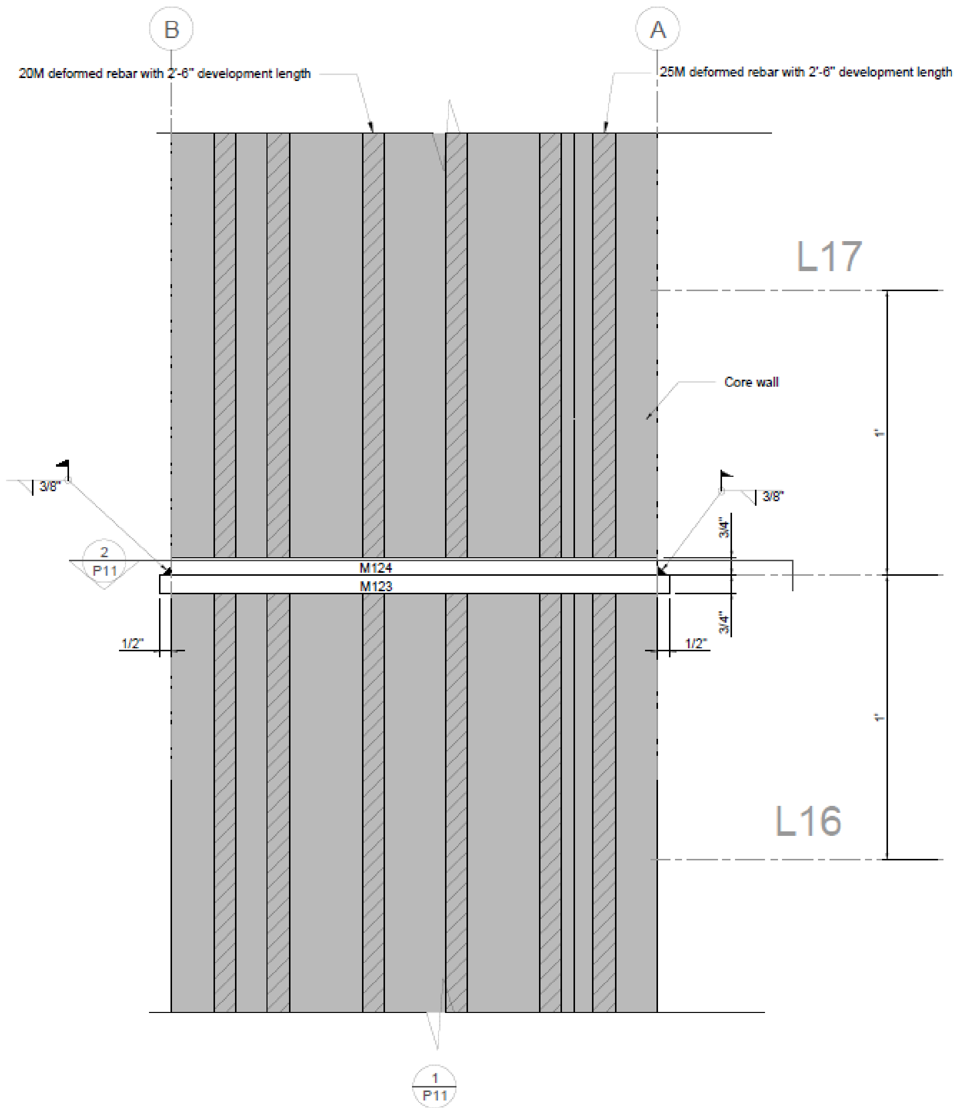

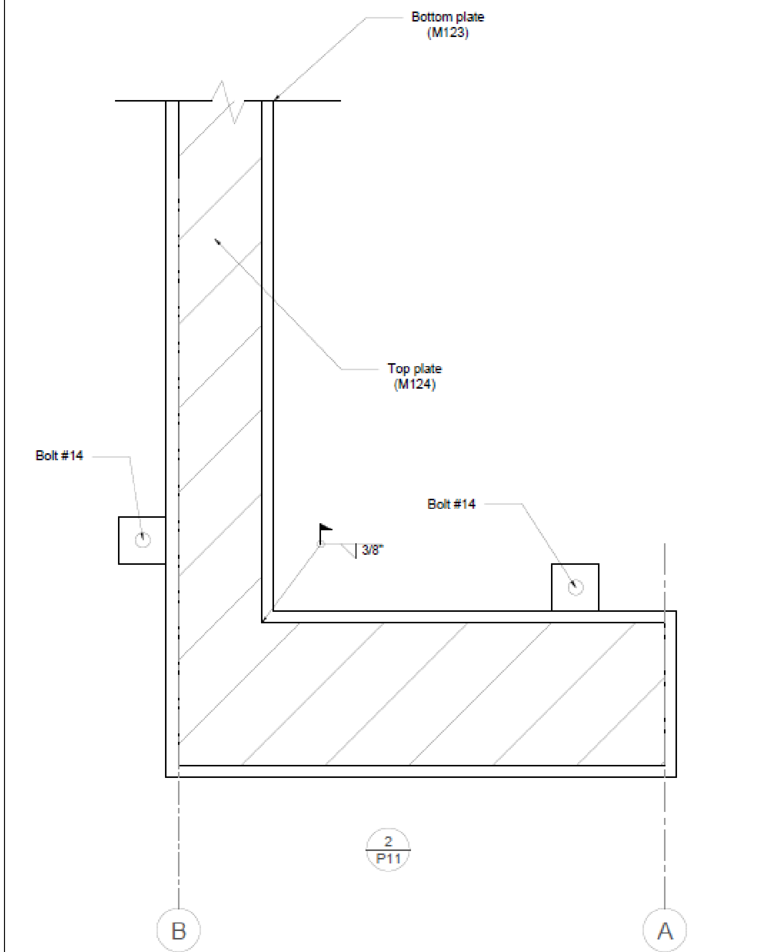

THE UNIVERSITY OF BRITISH COLUMBIA
Smart Structures

ILEE-EERF COLLABORATIVE SHAKE-TABLE TEST
NEXT-GENERATION EARTHQUAKE RESILIENT TALL BUILDING

Mid-Wall Connection Detail

SHEET NO.
P11

DRAWN BY
Tianyang Qiao
Hengchao Xu
Lisa Tobber

DATE 2020/02/17

Appendix E: Remaining construction steps

The specimen is currently partially assembled in the laboratory in the Tongji University. The following describes the steps required to prepare the specimen for shake-table testing.

Step 1: Secure and level the 10m wall to the foundation

We will level and grout the 10m wall to the foundation. The 10m wall should be vertically straight prior to grouting. A rigid non-yielding “dummy damper” will be placed in lieu of the damper at this stage.

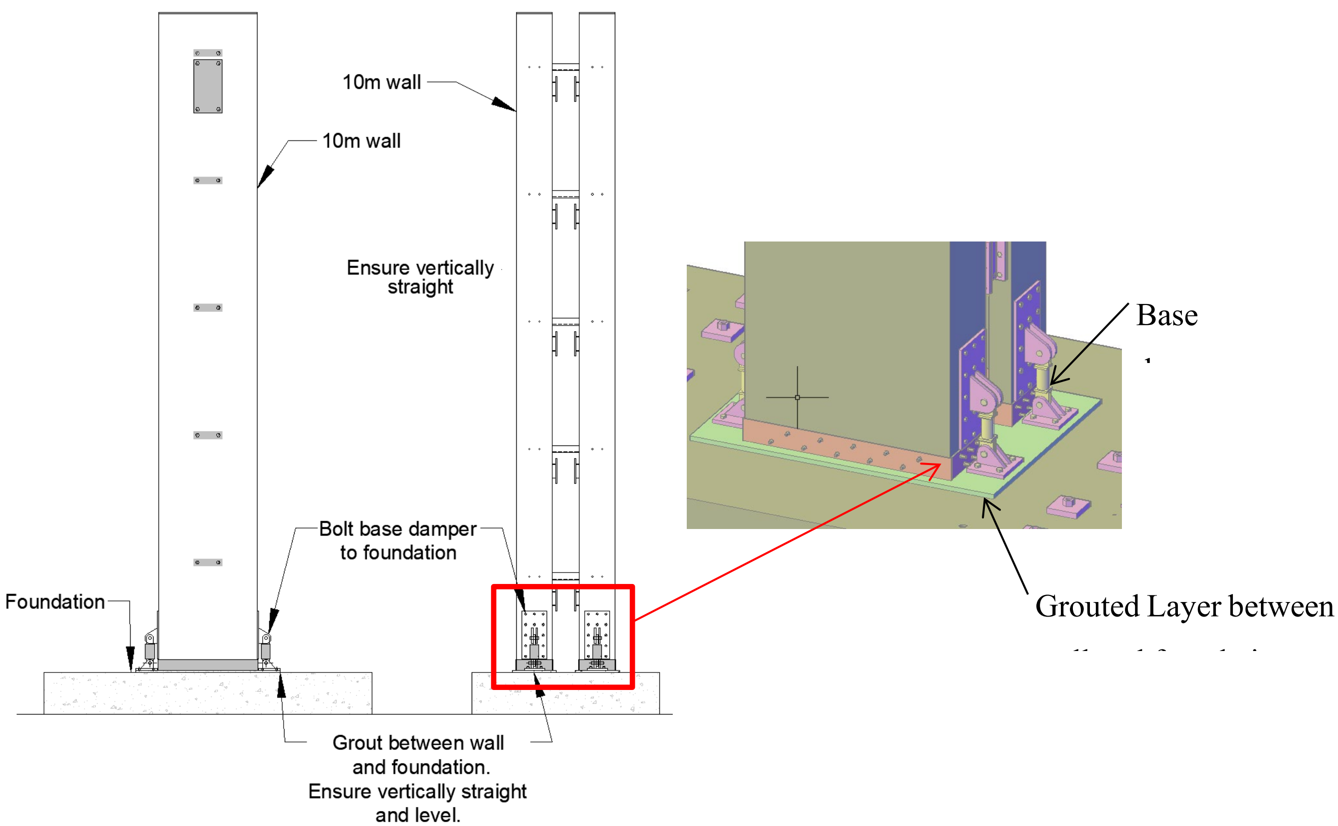

Step 2: Secure the outrigger beam on the 5m wall as shown in the figure below.

Secure the outrigger beam to the 5m wall through bolt connection using 32 embedded rods. Approximately 50mm of grout between the wall and the outrigger beam. We will ensure beam is level and adjust any necessary misalignments.

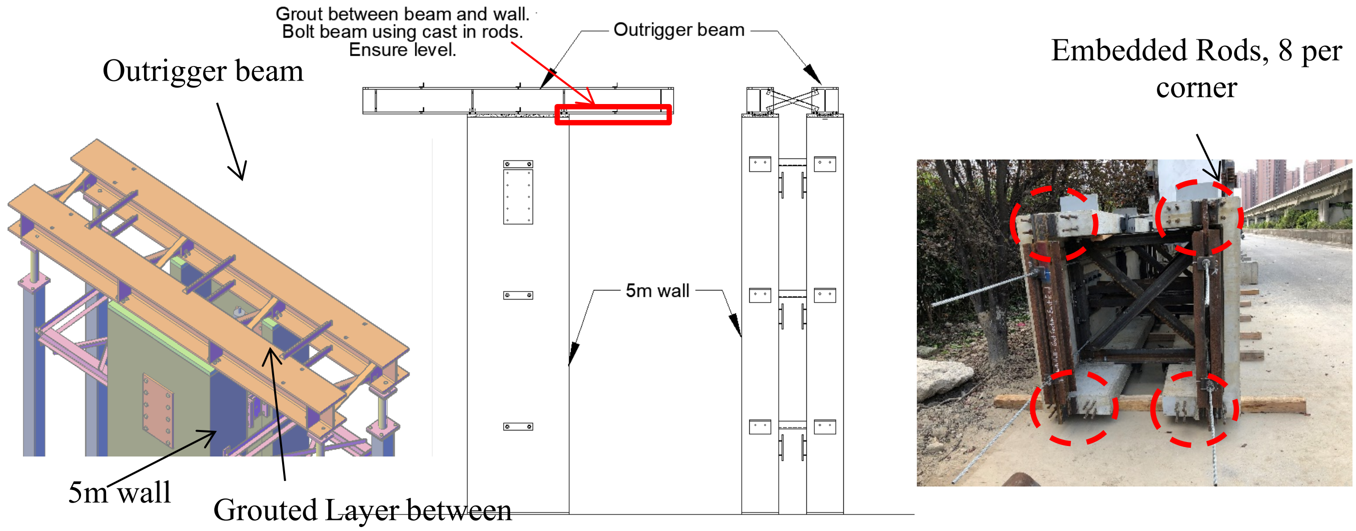

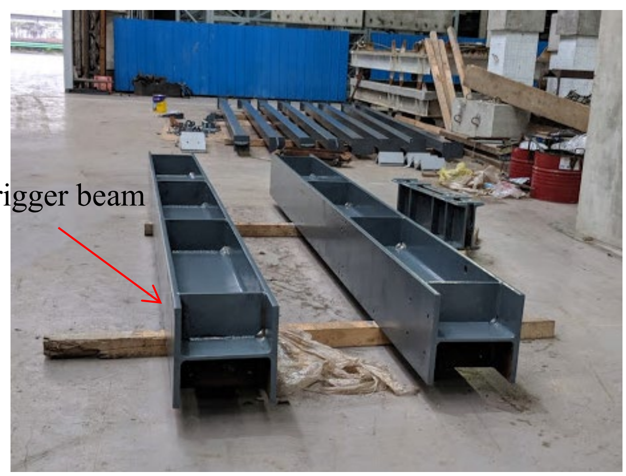

Step 3: Connect the 5m wall onto the 10m wall

We will line up the 5m wall to the 10m wall. The bolt connection can be used to align the wall segments. Make sure the wall segments are fully aligned. Welded the 5 m and 10 m wall segment together using a 19mm first-grade fillet weld.

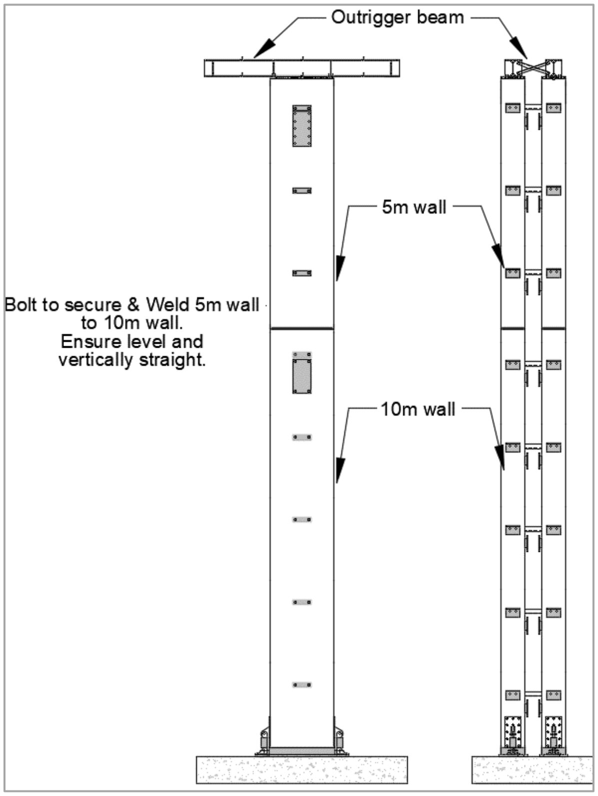

Bolt connection to line up the wall

Weld around the steel plate

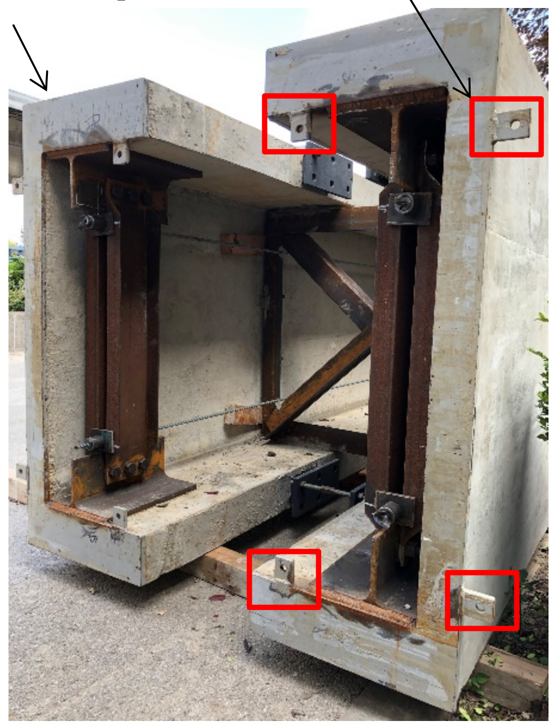

Step 4: Cut out section of steel braces

The steel braces within the wall must be cut out as the drawing shows. A total of 32 cuts are needed.

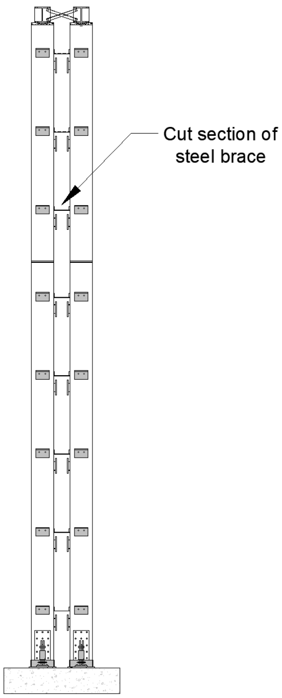

Step 5: Install the steel coupling beam dampers

We will assemble and install the coupling beams to the specimen. It should be noted that the damper-to-beam connections are slip critical connections. All bolts need to be pretensioned. Operation should be supervised by research team.

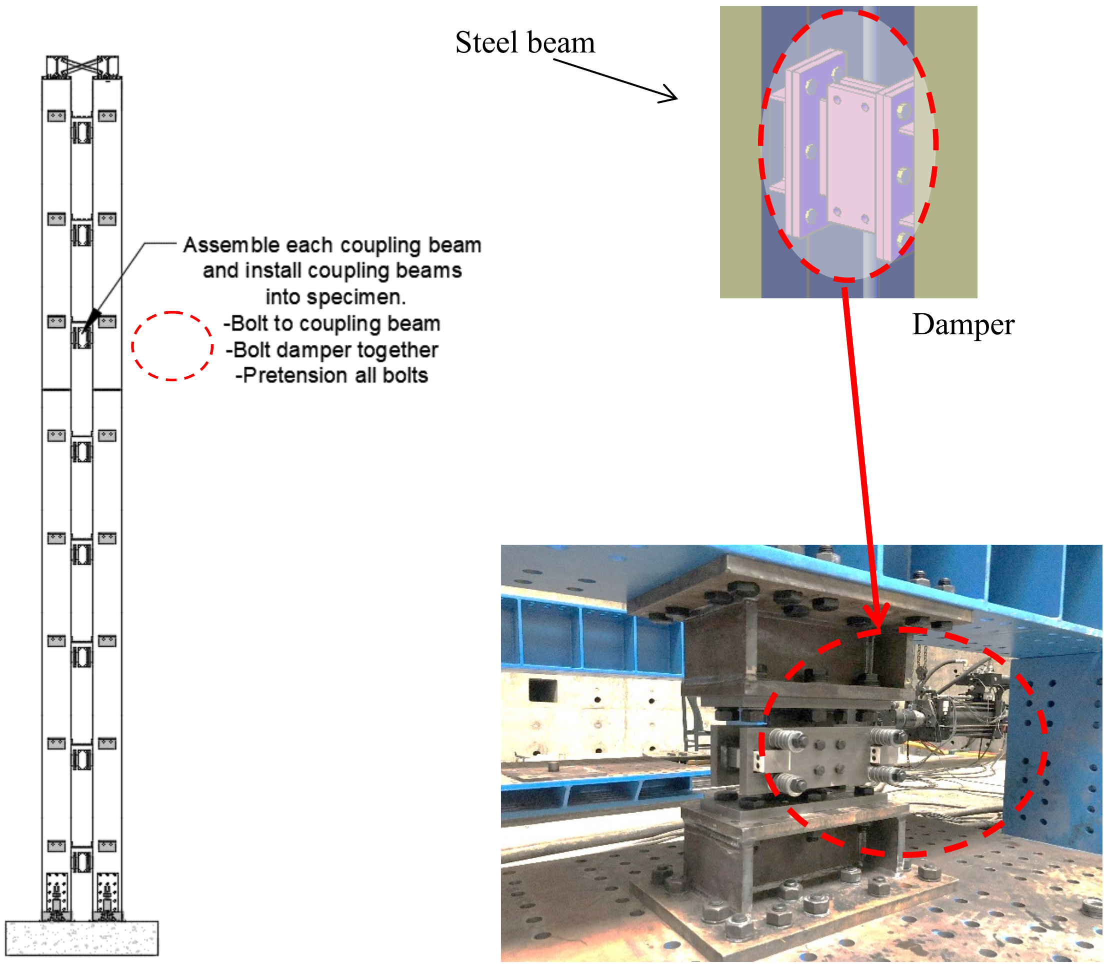

Step 6: Install the steel mass frames

We will assemble and install all 8 mass block frames. We will make sure they are leveled. Any gaps between frame and wall should be filled with grout.

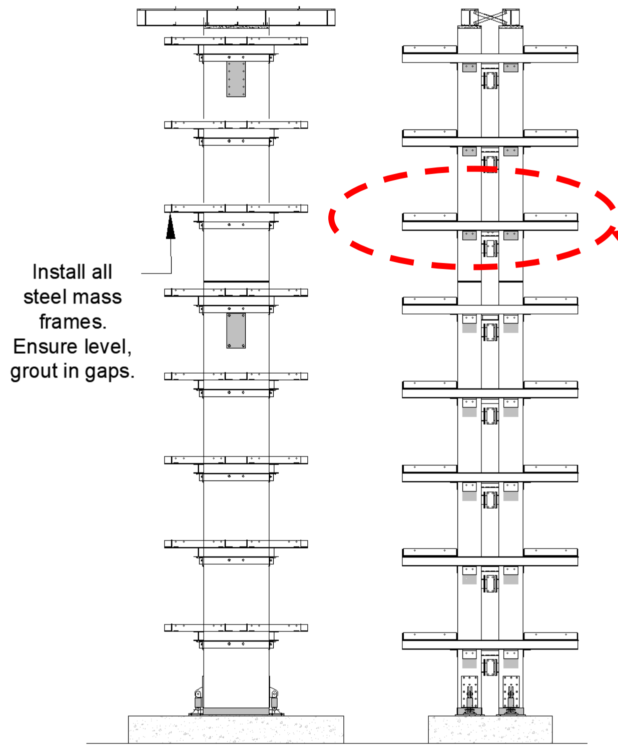

Step 7: Post-tension tendons

Post-tension the wall segments using the 8 tendons provided. Each tendon need to be tensioned to a force of 150kN. Please see drawings in Appendix D for location of PT tendon.

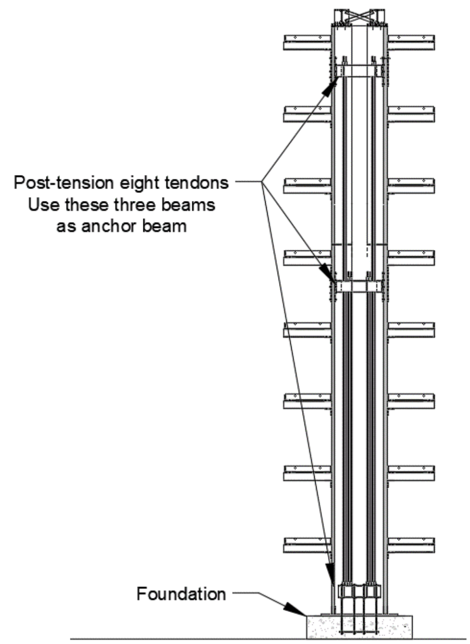

Step 8: Install the outrigger columns, dampers, column lateral support

We will install the outrigger columns, and column lateral supports. The columns will be bolted together and connected to outrigger beams, outrigger pins. The column lateral supports should connect the outrigger columns to the concrete wall. There are four assembled lateral supports.

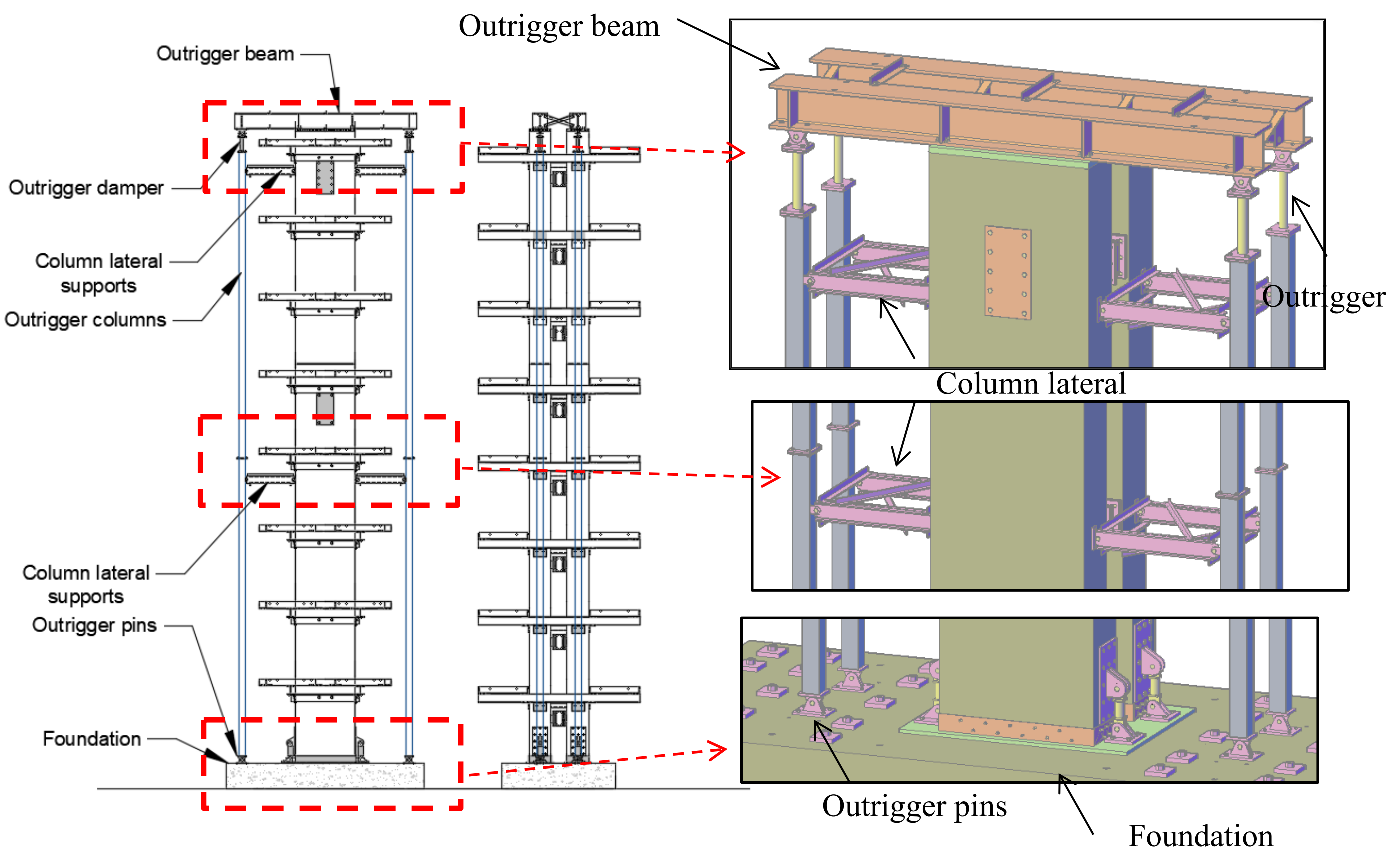

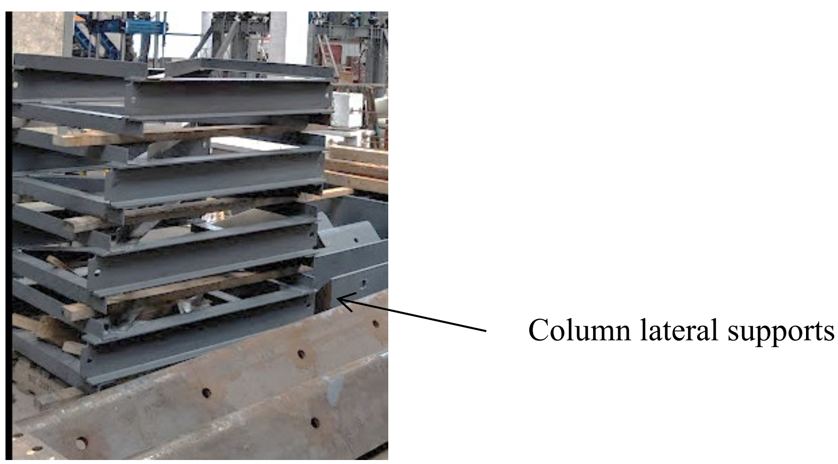

Step 9: Clean and paint wall white

We will sand off any significant bumps or marks. Also, we will paint with whitewash paint.

Step 10: Install specimen on shaking table

We will lift and bolt the specimen to the shaking table. Make sure the specimen are vertically aligned.

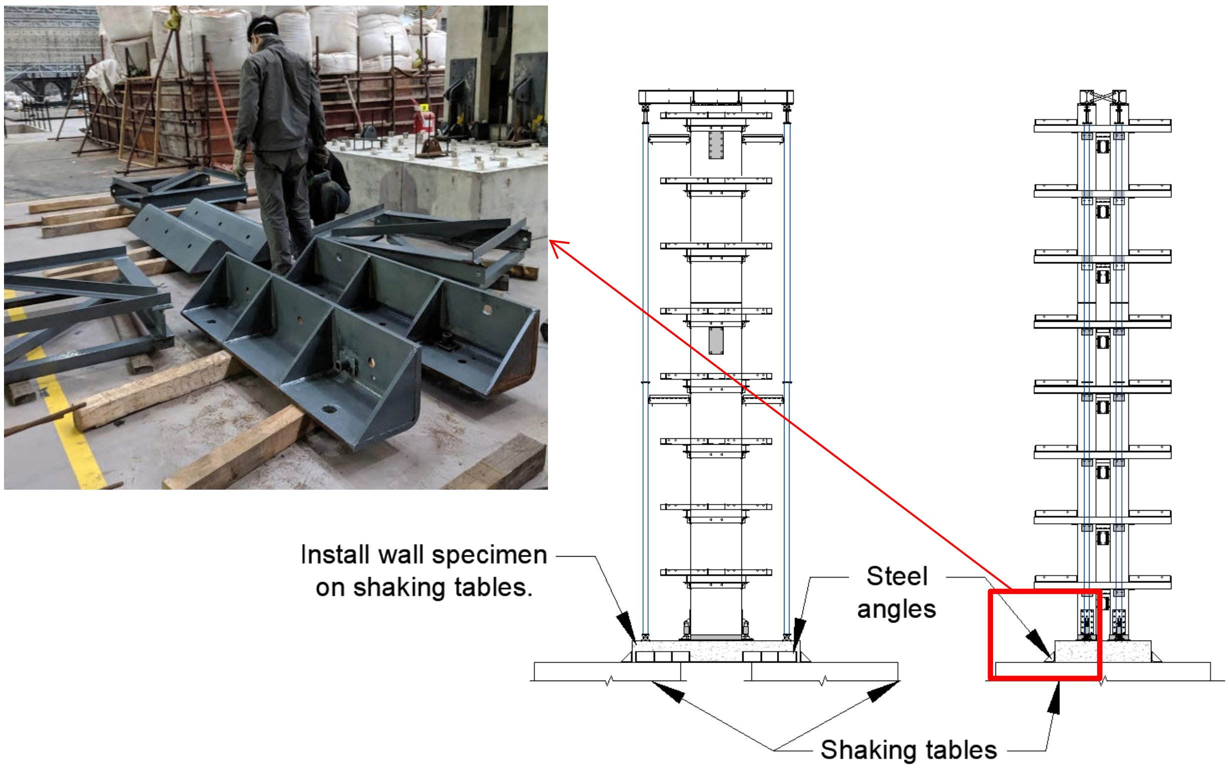

Step 11: Assemble the mass blocks

We will assemble the 32 mass blocks to the steel mass frame through screwed holes at all sides.

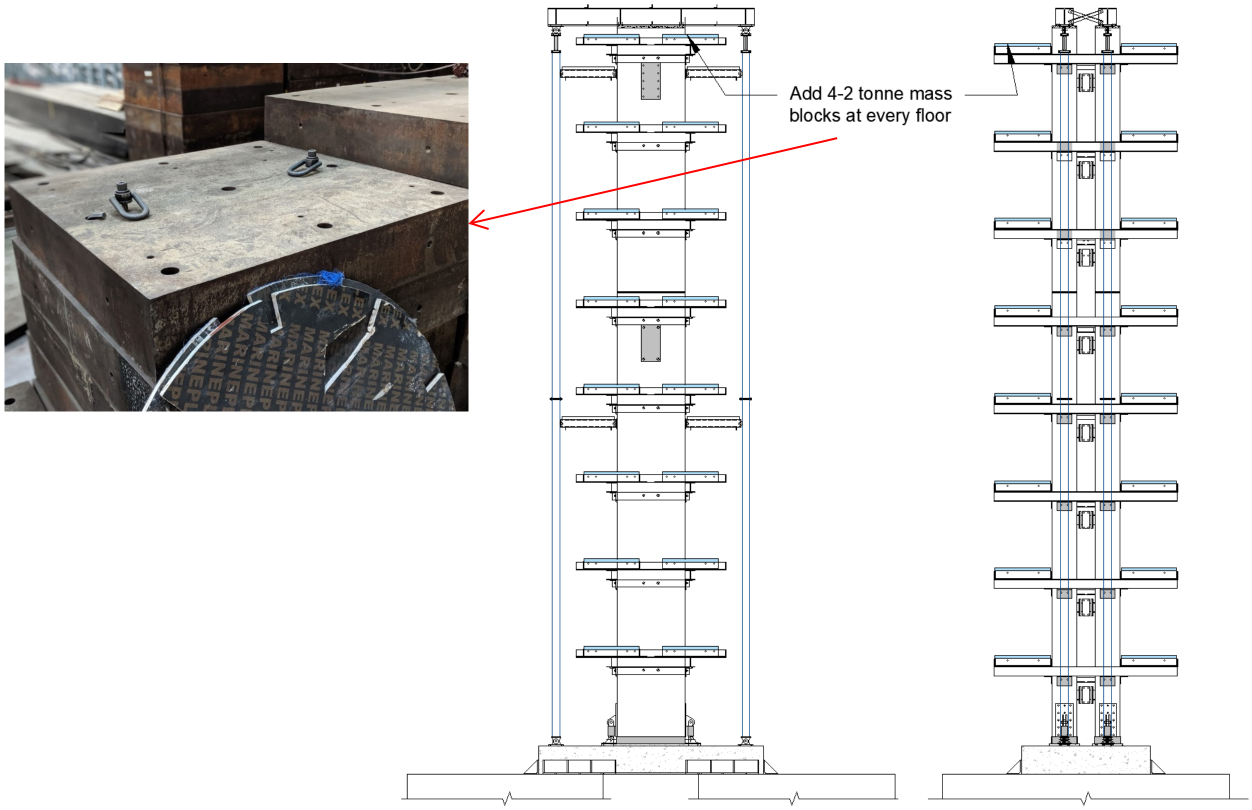

Step 12: Remove specimen from table, disassemble, and disposal.

After testing, remove specimen from table, disassemble and dispose specimen.